ICONST 2018

INTERNATIONAL CONFERENCE ON SCIENCE AND TECHNOLOGY

September 5 to 9, in Prizren, Kosovo

PROCEEDINGS & ABSTRACTS BOOK

iconst
www.iconst.org

www.iconst.org
info@iconst.org

KUTBİLGE
Association of Academicians
organized by

bilge sci

http://dergipark.gov.tr/bilgesci
kutbilgescience@gmail.com

ICONST 2018

International Conference on Science and Technology

September 5-9 in Prizren, Kosovo

PROCEEDINGS
&
ABSTRACTS BOOK

ICONST 2018

International Conference on Science and Technology

September 5-9 in Prizren, Kosovo

Editors

Dr. Kürşad Özkan
Dr. Mehmet Kılıç
Dr. Mustafa Karaboyacı
Dr. Kubilay Taşdelen
Dr. Hamza Kandemir
Dr. Halil Süel
MSc. Abdullah Beram
MSc. Serkan Özdemir
MSc. Doğan Akdemir
Ma. Fatih Mehmet Bakırtaş
Exp. Süleyman Uysal
Ma. Ergin Kala

Cover design & Layout

MSc. Tunahan Çınar

Copyright © 2018

Published by

Association of Kutbilge Academicians, Isparta, Turkey
E-Mail: kutbilgescience@gmail.com

ISBN: 978-605-68864-1-6

ICONST 2018

International Conference on Science and Technology

September 5-9 in Prizren, Kosovo

Organizig Committee

Dr. Kürşad Özkan
Dr. Mehmet Kılıç
Dr. Mustafa Karaboyacı
Dr. Kubilay Taşdelen
Dr. Hamza Kandemir
Dr. Halil Süel
MSc. Abdullah Beram
MSc. Serkan Özdemir
MSc. Doğan Akdemir
Ma. Fatih Mehmet Bakırtaş
Exp. Süleyman Uysal
Ma. Ergin Kala

Published by

Association of Kutbilge Academicians, Isparta, Turkey
E-Mail: kutbilgescience@gmail.com

ISBN: 978-605-68864-1-6

ICONST 2018

International Conference on Science and Technology

September 5-9 in Prizren, Kosovo

Scientific Committee

ICONST 2018

International Conference on Science and Technology

September 5-9 in Prizren, Kosovo

Participants Outside Turkey

Ahmed Al-Sarraj - IRANIAN
Ahmet Küçükkömürler - USA
Amani Bellahirech - TUNISIA
Artan Ahmeti - KOSOVO
Ayodeji Salau - NIGERIA
Bart Muys - BELGIUM
Cengiz Cesko - KOSOVO
Emna Ayari - HUNGARY
Ermira Idrızı - MACEDONIA
Giorgos Mallinis - GREECE
Iwona Klosak-Bazan - POLAND
Joanna Boguniewicz-Zablocka - POLAND
Mirjana Curlin - CROATIA
Miroslaw Kwiatkowski - POLAND
Nazar Mammedov - AZERBAIJAN
Noorjan Salahulddin Ibrahim - IRAQ
Steve Woodward - UNITED KINGDOM
Valdrin Beluli - KOSOVO
Vehebi Sofiu - KOSOVO
Vitor Rosao - PORTUGAL

ICONST 2018

International Conference on Science and Technology

September 5-9 in Prizren, Kosovo

Contents

International Conference on Science and Technology

ICONST 2018

5-9 September 2018 Prizren - KOSOVO

An Efficient Approximation to Numerical Solutions for Kawahara Equation via Modified Cubic B-spline Differential Quadrature Method

Ali Başhan[1]*

In this study, a Crank-Nicolson-Differential Quadrature Method based on utilizing modified cubic B-splines (MCBC-DQM) as a tool has been carried out to obtain the numerical solutions for the Kawahara equation. Firstly, the Kawahara equation has been discretized using both forward difference formula and Crank-Nicolson. Then, Rubin and Graves linearization technique has been utilized and differential quadrature method has been applied to obtain algebraic equation system. Four different test problems, namely single solitary wave, interaction of two solitary waves, interaction of three solitary waves and wave generation have been solved. Next, in order to be able to test the efficiency and accuracy of the newly applied method, the error norms L_2 and L_∞ as well as the three lowest invariants I_1, I_2, and I_3 have been computed. Besides those, the relative changes of invariants have been reported. Finally, the newly obtained numerical results have been compared with some of those available in the literature for similar parameters. The Crank-Nicolson-Differential Quadrature Method based on utilizing modified cubic B-splines (MCBC-DQM) as a tool has been carried out to obtain the numerical solutions for the Kawahara equation. The newly error norms L_2 and L_∞ are superior than earlier works. As one can see from the comparison between the obtained values of the error norms, invariants, and relative changes of the present method and those given in earlier works, MCBC-DQM results are undoubtedly better. Those newly obtained results obviously indicate that MCBC-DQM can also be used to produce numerical solutions of the Kawahara equation with high accuracy.

Keywords: Partial differential equations, Differential quadrature method, Modified cubic B-Splines, Kawahara equation.

[1]Bulent Ecevit University, Faculty of Science and Art, Dept. of Maths., 67100, Zonguldak, TURKEY
*Corresponding author: alibashan@gmail.com

International Conference on Science and Technology

ICONST 2018

5-9 September 2018 Prizren - KOSOVO

Bark Beetle Outbreaks in Forest due to Climate Change

Gonca Ece Özcan[1]*, Miraç Aydın[1], Korhan Enez[1]

Abstract: Today, changes in climate values occur as the greenhouse gases in the atmosphere increase significantly. These changes in climate values have many effects, such as increasing temperatures, changes in precipitation indexes, and rising sea levels. Such changes in the climate cause significant changes in the ecosystems and ecosystem elements in world. Particularly climate elements such as temperature and precipitation, which have vital importance for the livings in ecosystems, can have an impact on habitats and ecology. The effects of apparent changes in climate elements on livings in the ecosystems can cause differences in populations, living spaces and interactions of the livings in the ecosystems. Climate changes, and in particular increasing temperatures, can have an impact on the ecology, populations and spread of bark beetles, which are considered to be the main pests in forest ecosystems. Thousands of forestlands in Turkey are affected by bark beetles. Long-term climate changes such as global warming are highly likely to affect the forest ecosystem and forest dynamics. Although direct and indirect effects of climate change on insect populations are not exactly known, these adverse effects may trigger some bark beetle species, increase reproduction potential of species and thus increase the risk of insect outbreaks. The most important factors that may affect the ecosystem balance in a negative way and significantly weaken the resistance of host tree species to effective insect outbreaks and cause a significant increase in insect populations are those that arise out of in of climate elements such as increasing temperatures, seasonal droughts, and extreme summer temperatures. Population of species in the forests and their attacks against tree specifies increase especially in summer seasons when temperatures are high. Adverse effects of climate change on insect populations and ecologies that we need to consider as an undeniable threat today will be important in terms of identifying the potential areas where bark beetle outbreaks and subsequent deaths in forest ecosystems will take place, and taking necessary measures accordingly.

Keywords: Bark beetles, out breaks, forest, climate change

[1]Kastamonul University, Faculty of Forestry, 37100, Kastamonu, TURKEY
*Correspondingauthor: goncaece@kastamonu.edu.tr

International Conference on Science and Technology

ICONST 2018

5-9 September 2018 Prizren - KOSOVO

Hypermethylation of E-Cadherin (ECAD) Gene in Clear Cell Renal Cell Carcinoma (CCRCC)

Ayse Nur Pektas[1]*,Taner Dastan[2],Aytul Kitapci[3],Sevgi Durna Dastan[4],Sifa Turkoglu[5]

Abstarct: In every part of the world, many high-budget researches have been made for cancer, a disease cannot be totally enlightened despite great advancements in science and technology. However, this disease still causes deaths of many people nowadays. Clear cell renal carsinoma is one of the most common sub-type of renal celled cancer. Cancer, affected by environmental factors, is a process formed by the results of genetic and epigenetic changes. Methylation is the leading type of these epigenetic changes. Many researches in the field emphasized that some genes hypermethylation are efficient on the formation of many cancer types. In this study, the aim is to analyze the DNA methylation, one of the epigenetic changes on ECAD gene of renal cell carsinoma (RCC) patients and to determine the relations by comparing the present epigenetic features with clinic-pathologic parameters. Studies were organized in two groups; a control group with 153 individuals and a patient group with 113 individuals. The methylation of blood samples were determined by displaying in the gel after DNA isolation and methylation specific PCR (MSP) steps. Some descriptive statistics and Wilcoxon, Corelation and Lojistic Regression analyses were made with SPSS.

As the result of this analyzes, a statistically significant relationship has been determined and it is also found that the probability of occurance of this disease was 5 times more likely for the people who have methylation in their ECAD genes then those have not. According to the results of logistic regression analysis, it is seen that women are 4.253 times more likely to be ill compared to men. According to ECAD genes methylation analyzes for CCRCC disease, an increase in methylation of this gland is observed in the disease state, which is parallel to many studies in the literature. Although there is a significant increase in methylation for this gene, depending on the disease, it does not have a high percentage at which it could be a marker. However, it has been a very important and fundamental research for the diagnosis and treatment of CCRCC disease in terms of the effect of epigenetic mechanisms such as methylation analysis. By contributing to the existing literature in this area, it will be enlightening in planning new and different studies.

Acknowledgement:
We acknowledge with great pleasure the financial support provided by Cumhuriyet University Scientific Research Projects Coordination Unit (CUBAP), Project no:V-23

Keywords: Cancer, Hypermethylation, ECAD, MSP

[1] Cumhuriyet University, Advanced Techonology Research Center (CUTAM), 58140, Sivas, TURKEY
[2] Cumhuriyet University Yildizeli Vocational School, 58140, Sivas, TURKEY
[3] Bati Akdeniz Agricultural Research Institute, BATEM, 07100, Antalya, TURKEY
[4] Cumhuriyet University, Faculty of Veterinary Medicine, 58140, Sivas, TURKEY
[5] Cumhuriyet University, Faculty of Science, 58140, Sivas, TURKEY
*Corresponding author: aysenurpektas@cumhuriyet.edu.tr

International Conference on Science and Technology

ICONST 2018

5-9 September 2018 Prizren - KOSOVO

The Activities of Carbonic Anhydrase and Acetylcholinesterase Enzymes in Diffferent Tissues Related to Respiratory, Excretory and Reproductive Systems of Rats Under The Wireless Electromagnetic Fields Exposure

Ayse Nur Pektas[1]*, Umit Muhammet Kocyigit[2], , Taner Dastan[3],Sevgi Durna Dastan[4]
Parham Taslimi[5], Fatih Gurses[6], Ilhami Gulcin[5]

Abstract: The aim of our studies is to assist in understanding the effects of wireless electromagnetic waves on activities of carbonic anhydrase (CA) and acetylcholinesterase (AChE) enzymes in the different tissues related to respiratory, excretory and reproductive systems of the wistar albino rats. There are epidemiological studies in the literature regarding the effects of magnetic fields on cancer, reproduction, and neurobehavior. The global increase in the use of smartphones operating in exceeding radio frequencies (RF) mustered a significant focus on the possible health effects of electromagnetic radiation. Extensive use of wireless fidelity communication devices and their networks significantly increased the exposure of humans to RF fields. 2 different groups each of which contains 8 adult Wistar albino rats (180 ± 10 g body weight) were formed as control group and wireless electromagnetic wave administered groups. Rats were not in stress and housed in standart cages at temperature 24 ± 2°C with 12:12 h light/dark cycle with 60 ± 5 % humidity. The rats were necropsied and the different tissues of the rats were extracted. Activities of carbonic anhydrase and acetylcholinesterase enzymes were measured for each tissue by using the hydratase, esterase and acetylcholinioidide methods. All the experimental results were provided in mean ± standard deviation (±SD). Statistical significance was identified to be $p<0.05$.

It was observed that there were significant decreases of enzyme activities in wireless administered group in brain, spleen, kidney, and trachea tissues according to CA and AChE levels. There were significant difference between control group and WiFi-RF EMF groups with regard to the CA enzyme levels of trachea, spleen and kidney tissues ($p>0.05$). It was observed that there was a statistically significant difference ($p<0.05$) between the groups just for the brain tissue. We suggest that RF EMR from Wi-Fi can induce oxidative stress, change the CA and AChE enzyme activity and disturb the function and structure of these tissues in rats exposed to these Wi-Fi devices. Parameters in the present study and their relation to tissue damage is not concise, however, recently newer studies were stated the relationship to oxidative DNA damage.

Acknowledgement:
We thank Cumhuriyet University Advanced Research Center (CUTAM) for providing the laboratory during the experiments.

Keywords: Acetylcholinesterase, Carbonic anhydrase, Enzyme inhibition, Rat

[1] Cumhuriyet University, Advanced Techonology Research Center (CUTAM), 58140, Sivas, TURKEY
[2] Cumhuriyet University, Vocational School of Health Services, 58140, Sivas, TURKEY
[3] Cumhuriyet University, Yildizeli Vocational School, 58140, Sivas, TURKEY
[4] Cumhuriyet University, Faculty of Veterinary Medicine, 58140, Sivas, TURKEY
[5] Ataturk University, Faculty of Sciences, 25240, Erzurum, TURKEY
[6] Uludağ University, Faculty of Business, 16400, Bursa, TURKEY
*Corresponding author: info@iconst.org

International Conference on Science and Technology

ICONST 2018

5-9 September 2018 Prizren - KOSOVO

Safety Interactions Without Credit Credits Using Rfid Technology

Ümit Güven[1]*, Durmuş Özdemir[1]

Abstract: RFID (Radio Frequency Identification) technology; is one of the wireless communication technologies widely used in today's wide range of areas and sectors. This wireless communication technology mainly consists of reader, tag and antenna parts. Tags placed on various objects are read via Radio Frequency via the antenna. The information is transferred to the system by the reader by converting it into digital data and thus processes such as follow-up, information recording and control are performed. RFID technology; from the health sector to the agricultural sector, from education to security, to livestock used in many areas. In this study RFID technology used in contactless credit cards that becoming more prevalent today security vulnerabilities arising from the use of this technology, and methods for mitigating or preventing these risks have been identified. Credit card fraud is the biggest crime in the world that is showing no longer. In addition, contactless credit cards are becoming increasingly popular due to ease of use. Therefore, thanks to the acquired RFID reader device and software that can be easily downloaded from the internet, the data on contactless credit cards can be easily accessed. It is also a fact that the information can reach dangerous dimensions by reaching other personal information by means of social engineering methods that do not make any sense to themselves. Also, where people like public transportation and entertainment venues are very close to each other, those approaching with virtual POS devices can withdraw money from RFID credit cards.

2016 realized with contactless credit card transaction in Turkey, 45 million of them in 6300 reported that detected Saib. Moreover, when statistical data is viewed through the country contactless credit card with the purchase transaction of the Czech republic 72% Hungary 55% Poland 40% and the European Union overall average watched 13% of patients, which started to be used for the first time in the system in this case stated that remained 2% s level in Turkey. In this case, the RFID-enabled credit card that can be made is subject to a blockage. For this, RFID protected wallets or protective covers and information contained in our cards are prevented from transferring to people we do not want. It is possible to prevent the unauthorized collection of money from copying, copying or credit cards on this card. NFC (Near Field Communication) This service offered by banks is available on phones equipped with Android operating system, thanks to the bank application installed using the NFC features of the phones. Users can download the application, make a series of transaction steps according to the system of the banks, activate the NFC antenna and pay for the product price by touching the phones to the POS device. This method provides a very good security compared to the RFID system, but it does not offer as fast as RFID because it can cause speed loss due to operations such as activating the NFC antenna through the application on the phone.

Keywords: RFID, NFC, Credit Card, Data Security

[1] Dumlupınar University, Faculty of Engineering , 43000, Kutahya, TURKEY
* Corresponding author: umit.guven2@ogr.dpu.edu.tr

International Conference on Science and Technology

ICONST 2018

5-9 September 2018 Prizren - KOSOVO

A New Perspective for The Simulations of The Solitons of The Integrable mKdV Equation via Crank-Nicolson-Differential Quadrature Method

Ali Başhan[1]*

Abstract: In this study, approximate solutions of the mKdV equation have been obtained by using CN-DQM. Five famous test problems have been solved and compared with earlier works. The simulations of all test problems are given. The first order weighting coefficients are obtained by using modified cubic B-splines. Then second and third order weighting coefficients are obtained by Shu's recurrence relationship and matrix multiplication approach. After the discretization of mKdV equation with forward difference formulae and Crank-Nicolson scheme together, Rubin and Graves linearization technique is used. After the implementation of DQM linear equation system is obtained and solved by Gauss method easily. Present scheme gives better results than others when same time steps and less grid number i.e. large space steps are used. As a conclusion, it can be said that the present approximation is effective and efficient one for solving the mKdV equation and can also be used for numerical solutions of the other problems.

Keywords: Partial differential equations, differential quadrature method, mKdV equation, solitons, modified cubic B-splines.

[1]Bulent Ecevit University, Faculty of Science and Art, 67100, Zonguldak, TURKEY
*Corresponding author: alibashan@gmail.com

International Conference on Science and Technology

ICONST 2018

5-9 September 2018 Prizren - KOSOVO

Modelling Rate of Fire Spread in Stubble Fires in Turkey

Ömer Küçük[1]*, Hüseyin Cinko[2]

Abstract: Aim of the study was to developed regression models to estimate rate of fire spread in stubble fires. Stubble fires are an important rural environmental problem. Stubble fire on the products in neighboring agricultural lands, the orchards, the surrounding trees, nearby settlements and particularly in forests, is particularly damaging to the fuels. Uncontrolled burning also can be reason of the forest fire. The study was carried out in agricultural lands in central Anatolia in Turkey. After the agricultrutral harvests a total of 44 burning plots were prepared. Experimental surface fires were carried out between june ad september, under temperature, relative humidity, wind speed and fuel moisture conditions. During the experimental stubble fires, we used a drip torch for burning. Correlation and regression analysis was performed to investigate the relationships among fire behavior properties, weather conditions and fuel characteristics. To estimate rate of stubble fire spread, linear and non-linear regression equations were developed. A total of 44 experimental fires were carried out in the agricultural lands. During the experimenal stubble fires, air temperature ranged from 28 to 37 ºC Relative humidity ranged from 11 % to 37 %. The highest wind speed was recorded as 23 km sa^{-1} Fuel loadind of stubble ranged from 0.200 kg m^{-2} to 0.640 kg m^{-2}. Stubble moisture content ranged from, 3% to 19%. The rate of fire spread (ROS) ranged from 1 m min^{-1} to 30 m min^{-1}. Wind speed and fuel moisture content were the most important factors on the rate of spread. Wind speed alone explained 57% of the observed variation in the rate of spread. The addition of the fuel moisture content as the second independent variable improved slightly the percent variability explained (R^2= 0.723; $p<0.01$).

Keywords: Stubble fire, modelling, rate of fire spread, Turkey

Acknowledgement: This study supported by the Scientific Research Project Coordination Section of Kastamonu Universitiy (Project no: KUBAP -01/2013-58).

[1]Kastamonu University, Faculty of Forestry, 37100, Kastamonu, TURKEY
[2]General Directory of Forestry, 06000, Ankara, TURKEY
*Corresponding author: omerkucuk@kastamonu.edu.tr

International Conference on Science and Technology

ICONST 2018

5-9 September 2018 Prizren - KOSOVO

Determination of Product Losses in Harvesting of Wood Raw Material

Korhan Enez[1]*, Tuğrul Hodancı[2],

Abstract: Most of the country's forests are on mountainous and steep land. In order that, in this study conducted on in the Kastamonu district. The fact that Kastamonu is largely (74.6%) covered with mountains is, on one hand, reflected country-wide. It is known that in the forested regions with mountainous and steep land, there is a lot of damage and losses during the harvesting of the wood raw materials made under these circumstances. The harvesting of wood raw materials is at the top of the economic benefits of forests in forestry. Wood raw material harvesting is made of these stages; felling, skidding and transportation in conifers. In this study, it was aimed to determine the amount of product loss in production of wood raw materials at each stage. For this aim, after the felling operations are completed, the product types and quantities are determined. Afterwards, the products were quantified after they were removed from the forest. In this way, it will be possible to determine how much product loss has occurred as result of the production activity. The study was carried out with the observation of the production activities in the beech forest. While observed that there is a volume of loss 37, 68 % in the stamp made after cutting in a compartment forest; 28.43% volume loss was also observed in the products which were skidding and ready for transportation. Possible causes of the causes of the volume loss and suggested solutions are discussed and, proposals will be made to ensure that these losses can be withdrawn to a minimum level.

Keywords: Harvesting, wood raw material, product losses

[1]Kastamonul University, Faculty of Forestry, 37100, Kastamonu, TURKEY
[2]Kastamonul University Institute of Science, Forest Engineering Program 37100, Kastamonu, TURKEY
*Correspondingauthor: goncaece@kastamonu.edu.tr

International Conference on Science and Technology

ICONST 2018

5-9 September 2018 Prizren - KOSOVO

Investıgatıon on The Use of Thermal Capacities and Comfortable for Phase Changes

Ece Yılmaz[1]*, Fatih Yiğit[2], Ahmet Kabul[3], Mustafa Karaboyacı[3]

Abstract: Thermal comfort, which is an important need of people, provides a healthier life and a more efficient working environment. For this reason, it is of great importance to provide thermal conditions in which human life can be comforted in the life and working areas despite the seasonal weather conditions. In this study, the use of phase-change materials (PCM) to provide thermal comfort in residential and other living areas has been investigated. Various types of PCM were used in the examination and the room temperature was kept constant. In order to provide the desired thermal conditions, PCM were packed with different packing types and fixed to multiple points such as walls, curtains, flooring in the room and keeping the room temperature in balance. In addition, the heat retention capacity of the PCM has resulted in a reduction in the energy consumption for thermal comfort.

Keywords: Thermal comfort, Phase-Change Materials, Energy Efficiency

[2]Isparta University of Applied Sciences, Faculty of Thecnology, 32260, Isparta, TURKEY
*Corresponding author: fatihyigit@sdu.edu.tr

International Conference on Science and Technology

ICONST 2018

5-9 September 2018 Prizren - KOSOVO

Flower Recognition System based on Swarm Intelligence Based Image Segmentation and Neural Networks

Gürcan Yavuz[1], Ümit Güven[1], Doğan Aydın[1]*

Abstract: There are more than 250000 species of flowers on earth with a certain name, and many of the plant species are distinguished by their flowers. For botanists, detection of flower species is quite time-consuming and error-prone. Many non-specialists do not have a knowledge of flower species and their names, and information about flower species can only be obtained from books or the Internet (Hsu et al., In press). Therefore, powerful systems are needed that can automatically recognize flower species. In this study, an automatic flower recognition system has been implemented to overcome this problem. The system uses the IPSOAntK-mean algorithm which based on swarm intelligence for automatic flower part extraction from image. Then, the Artificial Neural Networks(ANN) used in the flower recognition process. Flower recognation task with the proposed system is done with three steps. First, we extract the flower part of the image from the background with a swarm intelligence based segmentation algorithm, IPSOAntK-means. IPSOAntK-means clustering algorithm was developed by combining incremental particle swarm optimization (IPSO), Ant Colony Optimization (ACO) and K-means in a hybrid manner. At second step, shape and color features of flowers (totally 12 features) were extracted from the extracted flower images. Finally, the obtained features are given as input to the different ANN models: Feed-Forward Neural Network (FFNN), Cascade-Forward Neural Network (CFNN) and Elman Neural Network (ENN).

The system was tested on 35 different flower species of the CAVIAR-Flower data set. 20 images were taken from data set for each flower type and 80% of them were used as training and 20% as test data.Although many flower types in the CAVIAR-Flower dataset are similar in shape and color, the successful recognition accuracy of the sysstem is 91,70% with FFNN, 92,18% with CFNN and 91,58% with ENN. In this study, IPSOAntK-means clustering algorithm, one of the first swarm-based approaches used for segmentation of color images, is used. The system achieved good results. Nevertheless, some work should be done to improve system performance. In the future, it is considered to perform parameter configuration tasks to improve the performance of the algorithm and to add powerful recognition models to the system.

Keywords: Swarm Intelligence, Particle Swarm Optimization, Color Image Segmentation, Flower Image Recognition

[1]Dumlupınar Uvniversity, Computer Engineering Department, 43100, Kütahya, TURKEY
*Corresponding author: doğan.aydin@dpu.edu.tr

International Conference on Science and Technology

ICONST 2018

5-9 September 2018 Prizren - KOSOVO

Wildfire Effects on Carbon Dynamics in an Oak-Pine Mixed Forest

Sepken Kaptanoglu Berber[1*], Ayten Namlı[2]

Abstract: CO_2 emission to the atmosphere is the main cause of global warming. Soil respiration originated from due largely to microbial activity is one of the most important CO_2 sources in the atmosphere. The present study was addressed to measure CO_2 evolution, microbial biomass carbon (Cmic), and β-D glucosidase activity playing essential roles into carbon cycle and, microbial respiration-microbial biomass carbon ratio (qCO_2), a good indicator in determining the soil fertility in a burned and adjacent unburned oak-pine mixed forest in Safranbolu region of Turkey.

ANOVA was applied to determine the statistically differences of the measured parameters among the burned-harvested soils, the burned-non-harvested soils and the unburned soil samples for each period and in total. Cmic increased with burning and harvesting the burned trees while CO_2 evolution decreased only after burning at months 4 and 7, which reversed into a year after the fire. However, there was no significant difference between the harvested (H) and non-harvested (NH) burned areas in terms of CO_2 evolution and the other parameters even though both areas were overall different from the unburned areas. The abundance of microbial biomass independent from the changes in CO_2 evolution and β-D glucosidase activity might be related to the substrate quality variation after burning and harvesting. Spring values of CO_2 evolution to the atmosphere were much higher in the unburned areas, which fell down in the last autumn likely due to the higher heat of the soil in the burned areas. Harvesting effect was not significant compared to fire as regards the parameters measured probably due to the rapid coverage of vegetation through sensitive area management and protection.

Keywords: CO_2 evolution, β-D glucosidase activity, qCO_2, soil microbial biomass carbon, wildfire.

[1*]General Directorate of Forestry, Research Institute for Forest Soil and Ecology, 26160 Eskisehir, Turkey.
[2] Ankara University, Soil Science Department, Ankara, Turkey
*Correspondingauthor: asepken@gmail.com

International Conference on Science and Technology

ICONST 2018

5-9 September 2018 Prizren - KOSOVO

Working and Applied Training Safety in Vocational Schools

Taner Karasoy[1]*, Kerem Asmaz[2]

Abstract: The Law on Occupational Health and Safety No. 6331 was adopted in 2012. This law covers industrial establishments, public institutions, primary and secondary schools which are affiliated to Ministry of National Education (MEB). The law also includes associate, undergraduate and graduate level of universities which are affiliated to Council of Higher Education (YOK). Informing all the personnel (academic and administrative) and the students who are educated in these units and execution of occupational health and safety work in these units have become a legal obligation. In addition to informing, in terms of work and education security, the academic and administrative working conditions of the personnel of the institution are appropriate to the safety of the work and the security of the education of the student is very important. In this study, a pilot vocational school was selected and the school was examined from the aspects of general fire safety, disaster risk and work hygiene. In addition, the most essential laboratories of applied education, which is very important for vocational colleges, have been examined in detail within the framework of the obligations of the Law on Occupational Health and Safety. The laboratories of the departments of Machinery, Electricity, Mechatronics, Aircraft Technologies, Cooking, Civil Aviation and Cabin Services have been examined in the analysis of the laboratories providing practical training. The results have been analyzed in detail.

Within the scope of the findings, it is observed that vocational schools are at the desired levels of disaster risk, fire safety and job hygiene but in the laboratories where practical education is given in terms of education security, it is observed that the concepts of occupational health and safety are not in the desired levels and measures are "partially" applied. Students of vocational schools in the field of education in occupational health and safety culture of assimilation in areas where they see the future of occupational health and safety culture in industry or education establishment is of great importance. For this reason, as the practices of these institutions are much more important than the oral trainings, the safety and health of the students and academic personnel are also very important for the quality of education to be desired.

Keywords: Occupational Health and Safety, Occupational Health and Safety in Vocational Schools, Applied Educational Security, Risk analysis in Vocational Schools, Fire security in Vocational Schools

[1] Okan University, Vacational School, Istanbul, TURKEY
[2] Yildiz Technical University, Faculty of Mechanical Engineering, 34349, Istanbul, TURKEY
*Corresponding author: taner.karasoy@okan.edu.tr

International Conference on Science and Technology

ICONST 2018

5-9 September 2018 Prizren - KOSOVO

Energy and Exergy Analysis of a Natural Gas Used Trigeneration System

Fatih Yiğit[1]*, Ahmet Kabul[1]

Abstract: In this study, tri generation system which is one of the in place energy generation methods is analyzed thermodynamically by using EES (Engineering Equation Solve) software. The electricity capacity, exergy losses, and exergy efficiency was calculated which of the case study of consuming of 1000 m3 natural gas. In the pre-determined conditions, it is calculated that a trigeneration system which consumes 1000 m3 of natural gas per month has a capacity of generating the electrical energy of 3.018 kW, heating capacity of 10.12 kW and cooling capacity of 6.574 kW. It is calculated that such a trigeneration system which has such capacities of production has a thermal efficiency of 24%, COP of 0.68 and total exergy loss of 8.49 kW. The total loss of exergy at each system component has a percentage of; 28% at the boiler, 24% at the condenser I, 14% at the absorber, 12% at the generator 11% at the condenser II, 11% at the evaporator and 2% at the turbine respectively. These results that are obtained have shown resemblance with the results that have been published previously

Keywords: In Place Energy Generation, Tri-generation Systems, Thermodynamic Analysis

[1]Suleyman Demirel University, Faculty of Thecnology, 32260, Isparta, TURKEY
*Correspondingauthor: fatihyigit@sdu.edu.tr

International Conference on Science and Technology

ICONST 2018

5-9 September 2018 Prizren - KOSOVO

Energy Efficiency in Cooling System with Variable Frequency Drive Control

Fatih Yiğit[1]*, Ahmet Kabul[1], Ahmed Al-Sarraj[2]

Abstract: In the recent years the industrial factories and buildings are used management system controllers in order to control the operations of heating, ventilation, air conditioning system, lighting systems, and some electrical equipment. The controlling systems are increased the ability to save energy and reduce an excessive energy consumption. The variable frequency drive (VFD) is one of the method that achieved to control the frequency of induction motors. This study presents the effect of installing variable frequency drive (VFD) for cooling systems to save energy by controlling frequency parameter using Arduino as a microcontroller board. During doing multi test with (VFD), the three phase AC compressor motor is tested on different frequencies and obtained different values of current at each frequency, at 50 Hz the current is 2A, at 45 Hz the current is 1.87A, finally at 40 Hz the current is 1.73A at the same voltage 380V. Assuming that a reference frequency is 50 Hz these measured values indicate that the consumption of electricity by the compressor is reduced by changing the frequency. The test approved that energy saving rates are 6.5% and 13.5% for 45 Hz and 40 Hz. Respectively. In addition, the test are noticed that with decreasing in the frequency the amount of time required to increase, to meet the total cooling load.

Depending on the perspective of meeting the total cooling load, the demand amount of energy for 45 Hz and 40 Hz are 5% and 27% respectiviley.as a result, the amount of energy most be decreased at 50Hz to meet the cooling load. Clearly, if the entire cooling load is operating in a single frequency directly the load will choose 50 Hz as a default frequency. Therefore, according to the fluctuations in the cooling load, the motor will operate at different frequencies in order to meet the instantaneous changing in loads, this facility gives a great advantages in the terms of energy efficiency.

Keywords: Variable Frequency Drive, Energy Efficıency, Cooling Systems, Energy Consumption, Variable Frequency Drive Control

[1]Suleyman Demirel University, Faculty of Technology, 32260, Isparta, TURKEY
University of Baghdad, College of Science, Baghdad, IRAQ
*Correspondingauthor: fatihyigit@sdu.edu.tr

International Conference on Science and Technology

ICONST 2018

5-9 September 2018 Prizren - KOSOVO

Performance of Brutian pine (*Pinus brutia* Ten.) Fibers Modified with Low Concentration NaOH Solutions in Fiberboard Production

Abdullah Beram*[1], Samim Yasar[1]

Abstract: The purpose of this study was to assess the changes in the chemical composition and thermal properties of Brutian pine (Pinus brutia Ten.) fibers treated with 0.25%, 0.50%, 0.75% and 1% NaOH solutions and their effects on the physical and mechanical properties of produced fiberboards. Main chemical components and Fourier transform infrared (FTIR) spectroscopy analyses revealed that the amount of extractive substances, lignin and hemicellulose decreased constantly as the NaOH concentration increased in alkali treatments, while the cellulose amount increased constantly. Thermogravimetric analysis (TGA) results showed that alkali treatment decreased the thermal resistance of the fibers. Alkali treatment of fibers increased the water absorption (WA) and thickness swelling (TS) of fiberboards. As the concentration of the alkali treatment increased, the mechanical properties of the fiberboards (the modulus of elasticity (MOE), the modulus of rupture (MOR) and internal bond strength (IB)) were also increased. The boards produced from untreated fibers and fibers treated with 0.25% and 0.50% NaOH were met the requirements of the standard TS EN 622-5 (2011) in terms of TS, MOE, MOR, and IB strength for load-bearing boards to be used under dry conditions.

Keywords: Brutian pine, alkali treatment, chemical composition, fiberboard, physical and mechanical properties.

Acknowledgement: This work was supported by the Suleyman Demirel University OYP Management under Grant OYP06088-DR-15. We would like to thank the Suleyman Demirel University OYP Management.

[1] Isparta University of Applied Sciences, Faculty of Forestry, 32260 Isparta, Turkey
*Corresponding author: beramabdullah@gmail.com

International Conference on Science and Technology

ICONST 2018

5-9 September 2018 Prizren - KOSOVO

The Volatile Compounds of Leaves from *Juniperus excelsa* Bieb.

Samim Yasar[1], Abdullah Beram[1*], Gurcan Guler[1]

Abstract: The leaves of Juniperus excelsa Bieb. were collected from Akdag-Aydogmus/Isparta in Mediterranean region of Turkey at an altitude of 1600 m in June 2017. The fresh materials were transported to laboratory in frozen bag and then stored at -20 ºC. The volatile compounds of fresh leaves from Juniperus excelsa Bieb. were determined using gas chromatography mass spectroscopy (GC-MS) after solid phase microextraction (SPME). The extract by SPME of fresh leaves is dominated by α- pinene, sabinene, limonene, β-thujone, 2-hexenal and β-myrcene with quantities of 36.19%, 16.07%, 12.02%, 9.03%, 7.01% and 5.81%, respectively. Thirty seven volatile compounds were identified in the fresh leaves of Juniperus excelsa Bieb.

Keywords: Juniperus excelsa Bieb., Fresh leaves, Volatile compounds, SPME, GC-MS.

[1]Isparta University of Applied Science, Faculty of Forestry, 32260, Isparta, TURKEY
*Correspondingauthor: beramabdullah@gmail.com

International Conference on Science and Technology

ICONST 2018

5-9 September 2018 Prizren - KOSOVO

Neonatal Isoflurane Exposure Acutely Increases Aquaporin-4 and Does Not Cause Long-Term Neurocognitive Impairment

Serdar Demirgan[1], Onat Akyol[1], Zeynep Temel[2], Aslıhan Şengelen[3], Murat Pekmez[3]*, Recep Demirgan[3], Mehmet Salih Sevdi[1], Kerem Erkalp[4], Ayşin Selcan[1],

Abstract: Isoflurane, an inhaled anesthetic, are widely used in daily clinical practice. The effect and action mechanism of isoflurane on neurocognitive functions is not completely understood. Aquaporin-4 (Aqp4), a tetrameric membrane-bound protein of the water-channel protein family, and plays an important role in the maintenance of synaptic plasticity and neurocognition. The aim of the presented study is to exhibit the effect of prolonged isoflurane anesthesia on brain Aqp4 expression and cognition of neonatal rats. Postnatal day (P) 10 rats randomized to the isoflurane group, exposed to 1,5% isoflurane in 50% oxygen for 6h. Rats in the control group, exposed to only 50% oxygen for 6h. In experiment one, P10 rats in isoflurane and control groups were sacrificed at 24 h later (P11). In experiment two, Morris Water Maze (MWM) test was performed to isoflurane and control groups at P28-P32 (acquisition phase) and at P33 (end of the probe trials) rats and then they were sacrificed. Whole brain samples were collected. Changes in Aqp4 levels were assessed by RT-qPCR and Western blotting, and cognitive functions were assessed by MWM (Morris Water Maze) test.

The results show that 1,5% isoflurane anaesthesia increases both mRNA and protein levels of the Aqp4 in P10 neonatal rats, which decreases over time. No cognitive dysfunction was observed due to isoflurane anaesthesia. The present study is the first to examine the effect of neonatal isoflurane exposure on the acute and long-term change in Aqp4 expression level was assessed. Our results indicated that 1.5% isoflurane inhalation for 6h markedly induced expression of Aqp4 protein as well as mRNA synthesis 24h after exposure, this increase might facilitate to preserve cognitive functions. Further studies should focus on the connection between neuroapoptosis with ROS markers and AQP4 expression after isoflurane exposure in neonatal rats**.**

Keywords: Aqp4, isoflurane, anesthesia, cognition, neonatal rat, neurotoxicity.

Acknowledgement: This research was supported by the Republic of Turkey Ministry of Health, University of Health Science, Bağcılar Training and Research Hospital, Research Funding (Grant no: 2016/109).

[1]University of Health Sciences, Bagcılar Training and Research Hospital, Department of Anesthesiology, 34000, Istanbul, TURKEY
[2]Istanbul Medipol University, Health Sciences Institute, Department of Neuroscience, 34000, Istanbul, TURKEY
[3]Istanbul University, Faculty of Science, Department of Molecular Biology and Genetics, 34134, Istanbul, TURKEY
[4]University of Health Sciences, Kanuni Sultan Süleyman Training and Research Hospital, Department of Anesthesiology, 34000, Istanbul, TURKEY
*Corresponding author: mpekmez@istanbul.edu.tr

International Conference on Science and Technology

ICONST 2018

5-9 September 2018 Prizren - KOSOVO

Blueberry Harvest Mechanisms

Ali Tekgüler[1]*, Tuğba Karaköse[2]

Abstract: Blueberry (*Vacciniumcorymbosum* L.) is a perennial plant that shed leaves in winter. It is from Ericaceae family and it is in the form of bushes. It grows in temperate climates and its motherland is America. It spread from American culture 110 years ago. It can grow in lightly textured and acidic soil. For this reason, the areas where agriculture can be done are limited. Because the production quantities are not enough, the selling prices are also high. Grape berries can be harvested by hand and machine. For the Blueberry harvest, harvesters with three different types of harvesting mechanisms were produced. The first blueberry harvester was manufactured in 1956, adapted from a mechanical cranberry picker. This machine had a mechanism consisting of a six-row scraper stick. These machines with high collection capacity reduce the need for labor and the cost of harvest. Blueberry manual harvesting hectare requires 1300 h of labor, while single row harvesting machine requires 25 h of labor/hectare. Thus, the cost of harvest falls from $ 2.8 per kg to $ 0.26 per kg. These machines are not economical for medium and small sized farms. In machine harvest, there are some problems for this plant. These problems are fruit falling on the ground during fruit harvest, the harvest of fruit that has not reached sufficient maturity, fruit and plant damage during picking. A lot of work has been done and continues to be done. However, sufficient harvesting efficiency has not yet been achieved. Blueberry should be harvested with a high quality and long shelf life that will appeal to the consumer.

Keywords: blueberry, harvest mechanism, machine.

[1]Ondokuz Mayis University, Samsun Vocational School, Department of Agricultural Machinery, İlkadım, Samsun, TURKEY
[2]Ondokuz Mayis University, Faculty of Agriculture, Department of Agricultural Machinery and Technologies Engineering, Atakum, Samsun, TURKEY.
*Correspondingauthor: atekgul@omu.edu.tr

International Conference on Science and Technology

ICONST 2018

5-9 September 2018 Prizren - KOSOVO

Structural Properties of Metamorphic Rocks of Tava Mount (Kütahya)

Meral Yılmaz[1]*, Ali Kamil Yüksel[2]

Abstract: The northern part of Anatolide-Tauride experienced regional high pressure/low temperature (HP/LT) metamorphism during the Alpine-Himalayan orogeny. By the type and age of the metamorphism, the metamorphic districts of Anatolides range from North to the South as Tavşanlı Zone, Afyon Zone, Menderes Massif and Lycian Nappes respectively. Metamorphism of these tectonic units is suggested by the contractional and extensional deformations during Alpine-Himalayan orogeny. The stratigraphy of the study area in the Afyon Zone starts at the base with the Middle-Upper Triassic İkibaşlı Formation. The Jurassic Çiçeklikaya Formation, composed of dolomitic carbonates, conformably overlies the İkibaşlı Formation. These two formations are overlain tectonically by an ophiolitic nappe of the Muratdağı Mélange along a thrust. The ophiolitic nappe movement direction which caused the metamorphism of İkibaşlı Formation, can be determined with kinematic studies along this tectonic contact zone. The methodology comprises systematic definitions and measurements of the mesoscopic shear criteria in outcrops oriented normal to the foliation and parallel to the associated stretching lineation. Mesoscopic structures which are used in kinematic studies, show that two different deformation phases (D_1 and D_2), while the initial deformation phase (D_1) is in ductile, the last phase (D_2) is brittle. The measured linear structures in the metamorphic rocks of İkibaşlı Formation trend in NE−SW direction. And also we define S shaped intrafolial fold and Z-shaped kink band in the tectonic contact zone. This S shaped intrafolial fold and Z-shaped kink band structures also show top-to-the-northeast shear during the tectonic transport. The tectonic contact between the İkibaşlı Formation and Muratdağı Mélange and their deformed rocks are unconformably overlied by Neogene aged sedimantery rocks in the field.

Keywords: Afyon Zone, Ophiolite emplacement, Kinematic indicators, Tava mount

Acknowledgement: This research has been supported by Balıkesir University Scientific Research Projects. Project Number: 2017/039

[1]Balıkesir University, Institute of Science and Technology, 10145, Çağış Campus, Balıkesir, TURKEY
[2]Balıkesir University, Faculty of Engineering, Department of Geology,10145, Çağış Campus, Balıkesir, TURKEY
*Corresponding author: meral-01-yilmaz@hotmail.com

International Conference on Science and Technology

ICONST 2018

5-9 September 2018 Prizren - KOSOVO

Habitat Selection, Population Densities and Activity Patterns of Jungle Cat (*Felis chaus* Scheberer, 1777) in Isparta/Egirdir (Hoyran) Lake.

Yasin Ünal[1], Abdülkadir Eryılmaz[2], Ahmet Koca[2], Osman Kürşat Bal[2]

Abstract: This research was conducted in the northern part of Lake Eğirdir (Hoyran Lake) between the years 2016-2017 within the borders of Isparta. In this study, presence-absence scanning and camera-trap method which are included in indirect observations from wildlife population inventory methods were used as integrated. As a result of the presence-absence studies, camera-trap sampling was carried out with opportunist methods in areas where trace-sign symptoms belonging to jungle cat. In addition, the spotlight counting method from direct inventory techniques is included to evaluate the results. At the end of the field studies, the jungle cat population density determination was performed by spotlit counting and camera-trap images. The habitat preferences were determined by using presence-absence inventories. In order to determine habitat types with high habitat preference and shares, starting from the reeds on the edge of Lake Eğirdir Hoyran, presence-absence screening method was applied to 50 counting line routes and 3 different habitat types (reed, agriculture, bush) systematically. In the counting process with the spotlight, at the same time start between the hours of 21.00-22.00 in the form of two vehicles, at the same time the counting process was ended. For each counting night, the 40 km road line was scanned with a spotlight. Spotlight counting method was carried out systematically in October-November. Kelker and Buckland Transect Density calculations were used to evaluating the results.

193 camera-trap stations were used in the study. In these stations, 4403 camera-trap days were reached and 83 camera-trap images of the jungle cat were obtained. A total of 2221 camera-trap recordings were obtained, 2128 of these belong to other mammalian species. The CAPTURE2 computer program was used to estimate population density with the maximum, minimum and average population size of the jungle cat. In order to estimate population size, Marking data, the results were analyzed by Jackknife-M (h), Removal-M (b), Chao-M (h) and Zippen-M (b) marking population density analysis models separately, then the results were recorded. Daily, seasonal and annual activity patterns of target species and other mammal species were obtained by using hourly data obtained from camera-trap records. The jungle cat was found to be the most active between 21:00 to 22:00 and 00:00 to 01:00. The jungle cat showed more activity in the spring season and it was found to be less active in summer. It was determined that the jungle cat has displayed/activity at the same time intervals as the wild hare. According to Kelker and Buckland Transekt method Population density were identified 0.25 individuals / 100 ha in 2015, and 0.17 individuals / 100 ha in 2016. According to the camera-trap method, the means population density values were 0.32 individuals / 100 ha by Jackknife-M (h).

Keywords: The jungle cat, Camera-trap, Marking, Lake Hoyran, Activity pattern, Isparta.

Acknowledgement: We would like to thank the 6th Regional Directorate of the Ministry of Agriculture and Forestry, General Directorate of Nature Conservation and National Parks for all kinds of support in the procurement and use of camera-traps in field works.

[1]Isparta University of Applied Sciences, Faculty of Forestry, 32260, Isparta, TURKEY
[2]Isparta University of Applied Sciences, The Institute for Graduate Education, 32260, Isparta, TURKEY
*Corresponding author: yasinunal@isparta.edu.tr

International Conference on Science and Technology

ICONST 2018

5-9 September 2018 Prizren - KOSOVO

Estimating of Caracal (*Caracal caracal* Schreber, 1776) Population Density, Activity Pattern and Interaction with The Ungulata Species in Antalya Duzlercamı Wildlife Development Area by The Camera-Trapping Method

Yasin ÜNAL[1], Ahmet Koca[2], Mevlüt ZENBİLCİ[2], Halil Süel[3]

Abstract: Caracal caracal, one of the 5 cat species of the Felidae family in our country, is one of the most important mammal species of our country in terms of biodiversity and gene value. Despite this, there is no inventory study for population size in Turkey and it is thought to be endangered. 8 of the 81 wildlife development areas in Turkey are located within the borders of Antalya. The Düzlerçamı Wildlife Development Area, which is the closest to the province of Antalya, has an important place in terms of wildlife and plant potential. Within the scope of TÜBİTAK ARDEB 214 O 248 project, a 30-month survey was conducted between April 15, 2015 and October 15, 2017 for the identification to target species (fallow deer) and other wildlife species. 30 camera-traps were purchased from the related project and made shooting at 445 stations for 17951 days. The camera-traps were placed on the field with an opportunist method and shot at the camera-trap station for a period of 30 days.

At the end of the fieldwork, one of the important species attached to the camera-trap was Caracal (Caracal caracal). 35 caracal photos were obtained in 22 camera-trap stations. From the obtained images, the Caracal caracal daily, yearly and seasonal activity patterns and relation with 4 different mammalian species determined in the region (Fallow deer-Dama dama, Wild boar-Sus scrofa, red fox-Vulpes vulpes and wild hare-Lepus europaeus) were examined and analyzed. As a result of examining the daily activity patterns, it was found that it was the most active between 24.00-01: 00 and it was active in 08: 00-09: 00, 16.00-17: 00 hours, respectively. It was found that the season with the highest monthly activity was in May (24%) and seasonal activity was in the spring (38%) season.

Keywords: Caracal (Caracal caracal), fallow deer (Dama dama), camera-trap, activity patterns, Antalya/Düzlerçamı.

Acknowledgement: We thank the Scientific and Technological Research Council of Turkey (TUBITAK, Project No: 214O248) to the achievement of the objectives of the study, primarily give financial support.

[1]Isparta University of Applied Sciences, Faculty of Forestry, 32260, Isparta, TURKEY
[2]Isparta University of Applied Sciences, The Institute for Graduate Education, 32260, Isparta, TURKEY
[3]Isparta University of Applied Sciences, Sutculer Dr. Hasan Gürbüz Vocational High School, 32950, Isparta, TURKEY
*Corresponding author: yasinunal@isparta.edu.tr

International Conference on Science and Technology

ICONST 2018

5-9 September 2018 Prizren - KOSOVO

Preferences for Use of Historic Streets: Kastamonu Şeyh Şabanı Veli Street

Nur Belkayalı [1]*, Elif Ayan[1]

Abstract: In today's cities, public life is moving from streets to shopping centers. The streets that are one of the areas where socialization is most seen in the social life are becoming one of the passing places. In the past, however, the streets are politically, economically, socially, and so on. places where many things have happened. The streets that contain the identity of the city and its history in various directions are drawing more attention today and the tendency to regain the sustainability politics by local governments is displayed. With the street improvement projects, more attention is paid to the preservation of the facade renovation works on today's historic streets as an accelerated cultural heritage.Kastamonu province center which hosts various civilizations today has many historical heritage. Şeyh Şabanı Veli Street, which is located in the city center and has an important place for religious tourism was conducted street improvement work in 2016. After this improvement work, many buildings on the street have become usable again. The scope of this study, it was investigated whether natural and artificial reinforcement elements and their effect on street preference in terms of cultural continuation and preference of the street after the facade renovation work. In the study, photographs of the streets were suggested on different plant arrangements and functions via CS Photoshop. The proposed suggestions were questioned to the users of the place and the visitors by photo survey method.The results of this study, Kastamonu especially the city of Turkey's making many of the city located in the historic streets of facade improvements after work by considering the reuse of the decisions in the fields users as well as visitors expectations for the cultural heritage of sustainability in landscape planning and design considering the criteria for application studies a precaution has emerged.

Keywords: Historic Street, Usage Preference, Kastamonu, Şeyh Şabanı Veli Street

[1] Kastamonu University, Faculty of Engineering and Architecture, Department of Landscape Architecture, Kastamonu, TURKEY
*Corresponding author: nbelkayali@kastamonu.edu.tr

International Conference on Science and Technology

ICONST 2018

5-9 September 2018 Prizren - KOSOVO

The Phenolic Contents and The Cytotoxic Effects Of Extracts From *Viscum album* (Mistletoe) Grown On Different Host Trees

Murat Pekmez[1]*

Abstract: Extracts of Viscum album (mistletoe) are commonly used for the cancer treatment. As a consequence of bioactive compounds of *Viscum album*, it has been used in many scientific researchs. Mistletoe and its active constituents possess cytotoxic effects on various cancer cell lines. In this study, methanolic and water extracts of *Viscum album*, grown on different host trees, were investigated for their potential cytotoxic activity and also phenolic contents of these extracts were measured. Cytotoxic activities were tested by MTT [3-(4,5-dimethylthiazol-2yl)-2,5-diphenly tetrazolium bromide)] method and phenolic contents were determined by HPLC. According to the results, the extracts prepared from Viscum album grown on locust tree has cytotoxic activity potential, since both the water and methanolic extracts showed the lowest EC_{50} values against HeLa, Vero and C6 glioma cell lines. According to HPLC results, the methanolic extract prepared from *Viscum album* grown on wild pear has the highest amount of phenolic content, especially for gentisic acid (24,000±3,100 mg / 100 g extract) and salysilic acid (25,700±6,930 mg / 100 g extract). The present study indicates that extracts from mistletoe growing on different trees inhibit the proliferation of cancer cell lines. The cytotoxic data obtained from the different extracts and cell lines, shows that cytotoxic doses differ and this depends on host tree, cell line, solvent of the extract and extract concentration.

Keywords: Viscum album, phenolic content, cytotoxic effects

Acknowledgement: This research was supported by the Research Foundation of Istanbul University, Project No: 27484

[1]* Istanbul University, Faculty of Science, Department of Molecular Biology and Genetics, 34134 Vezneciler-Istanbul TURKEY
*Corresponding author: mpekmez@istanbul.edu.tr

International Conference on Science and Technology

ICONST 2018

5-9 September 2018 Prizren - KOSOVO

The Assessment of Radioactivity and Radiological Hazards in Soil from Bolu Province, Turkey

Filiz Korkmaz Görür[1]*, Serdar Dizman[2], Recep Keser[2], Osman Görür[1]

Abstract: The natural radioactivity levels in soil samples of Bolu province of north-western Turkey have been determined. There is no information about radioactivity measurement reported in soil samples in Bolu province so far. For this reason, the activity concentrations of natural and artificial radionuclides (^{226}Ra, ^{232}Th, ^{40}K and ^{137}Cs) were measured in soil samples collected from 40 different points in Bolu province using gamma spectrometry with a high-purity germanium detector. The concentration of ^{226}Ra, ^{232}Th, ^{137}Cs and ^{40}K in the studied area has varied from 3.8 to 49.9 with an average of 18.2 Bq/kg, 4.1 to 37.9 with an average of 17.3 Bq/kg, 0.6 to 43.6 with an average of 7.5 Bq/kg and 64.6 to 518.9 with an average of 258.3 Bq/kg, respectively. At the end of the analysis, the radioactivity values were lower than the world average values reported by UNSCEAR. In order to evaluate the radiological hazards resulting from natural radioactivity, absorbed dose rate in air (D), radium equivalent activity (Raeq), external hazard index (Hex), gamma index (Iγ), the annual effective dose equivalent (AEDE), annual gonadal dose equivalent (AGDE) and excess life time cancer risk (ELCR) were calculated and the results were compared with international recommended values. Healthy effect due to natural radiation from soil samples of the Bolu provinces is low and thus, healthy hazards are insignificant.

Keywords: Natural radioactivity, soil, Bolu, radiological hazards.

[1]Abant İzzet Baysal University, Faculty of Sciences and Arts, Department of Physics, Bolu, Turkey
[2]Recep Tayyip Erdoğan University, Faculty of Sciences and Arts, Department of Physics, Rize 53100, Turkey
*Correspondingauthor: filizkorkmaz@yahoo.com

International Conference on Science and Technology

ICONST 2018

5-9 September 2018 Prizren - KOSOVO

Realization of *n*th-Order Current Transfer Functions Using Current-Feedback Amplifiers

Muhammet Cihat Mumcu[1]*, Fuat Anday[1]

Abstract: There are many synthesis method for the realization of nth-order voltage transfer function using active elements. However, these studies have many disadvantages such as slew rate limitation, narrow bandwith, constant gain-bandwith multiplication etc. In recent years, current-mode circuits are preferred over voltage-mode circuits due to their advantages such as high speed, wide bandwith, large dynamic range, low linear distortion, low power supply. Due to its advantages, current-mode circuits have been a significant research area for researchers. They have been widely applied in video signal processing, hard disk drive, communication integrated circuit, CDMA, ultra-wideband wireless access technology, etc. In this article, it is aimed to develop a new signal flow graph method which is one of active circuit synthesis procedures for realizing current mode transfer functions. Current-feedback amplifier (CFA) which has two major advantageous features such as very high slew rate and capability of realizing amplifiers displaying gain-bandwith decoupling, is used for this purpose. Then,two active circuits with a minimum number of passive and active elements has been given.AD844 is used as current-feedback amplifier in active circuits, because it is low cost active component providing an excellent combination of AC and DC performance. It is not affected slew rate limitations and rise-fall times are actually independent of output level. It combines high bandwith and very fast large signal response with excellent DC performance. It can be used as traditional opamps, but its current feedback achitecture results in much better AC performance and high lineartity.

According to the method used in this study, sub-CFA-circuit and corresponding sub-graph will be defined. Signal flow graphs composed of this sub-graph will be given in accordance with Mason gain formula for nth-order current transfer functions. Then, two active circuits will be obtained in accordance with the conversion rules using these signal flow graphs.

As a result of this study, two active CFA circuits for nth-order current mode transfer functions will be found using signal flow graph method. As an example, SPICE simulation of third order Butterworth low pass filter will be given. It should be noted that nth-order current-mode lowpass, highpass, bandpass, bandreject and allpass filter response can be easily obtained from the proposed method.

Keywords: AD844, Current transfer function, Signal flow graphs, Current feedback amplifier.

[1]Maltepe University, Faculty of Engineering and Natural Science, 34857, Istanbul, TURKEY
*Corresponding author e-mail: cihatmumcu@maltepe.edu.tr

International Conference on Science and Technology

ICONST 2018

5-9 September 2018 Prizren - KOSOVO

Investigating Knowledge Levels of People Living in Samsun Related to Radiation and Nuclear Power Plants

Recep Keser[1]*, Serdar Dizman[1], Adnan Yılmaz[2], Banu Çakır[3], Osman Görür[4]

Abstract: It is aimed to investigate knowledge levels of people living in Samsun related to radiation and nuclear power plants. This descriptive and cross-sectional study was conducted in September of 2015 by receiving responses of volunteer people living at random addresses determined by the Turkish Statistical Institute. The questionnaire consists of 12 multiple choice and open ended questions covering information on social and educational status, radiation and nuclear power plants. Of the 102 volunteers who participated in the survey, 47 (46.1%) are female and 55 (53.9%) are male. The ages of these volunteers range from 18 to 60. The answers to the question “Have you ever heard about radiation?” are as the following: 88 (%86, 3) of the participants said “yes”, 6 (%5, 9) said “no”, and 8 (%7, 8) stated that they had no ideas. While 55 participants (53.9%) defined radiation, 47 (%46, 1) did not give any description. 47 (%46, 1) of 88 participants who have heard about the word “radiation” did not define it. Some definitions of radiation suggested by the participants are “harmful rays”, “cancer”, “something that arises when you have an x-ray”, “something dangerous”, and “nuclear energy residue”. Of the participants, 89 (%87, 3) reported that they had heard about the word “nuclear power plant”, 5 (%4, 9) reported that they had not heard about the word, and 8 (%7, 8) reported that they had no ideas. The answers to the question “Do you know the function of nuclear power plants?” are as the following: %45, 1 (n=46) of the participants said “yes”, %20, 6 (n=21) said “no”, and %34, 3 (n=35) stated that they had no ideas. %51, 7 (n=46) of 89 participants who have heard about the word “nuclear power plant” reported that they knew the function of nuclear power plants, %18 (n=16) reported that they did not know their function, and %30,3 (n=27) reported that they had no ideas. 46 (%45, 1) participants answered to the last question “What is the function of nuclear power plants?”

The findings obtained from the study show a low level of knowledge of issues related to radiation and nuclear power plants and therefore public awareness of the issue should be raised in Turkey that will be soon acquainted with nuclear technology. Thus, some activities should be organized by Civil Society Organizations to raise awareness of the issues of radiation and nuclear power plants throughout the country.

Keywords: Radiation, Nuclear Power Plant, People, Samsun

[1]Recep Tayyip Erdogan University, Faculty of Sciences and Arts, 53100, Rize, TURKEY
[2]Recep Tayyip Erdogan University, Faculty of Medicine, 53100, Rize, TURKEY
[3]Hacettepe University, Faculty of Medicine, 06100, Ankara, TURKEY
[4]Abant Izzet Baysal University, Faculty of Sciences and Arts, 14030, Bolu, TURKEY
*Corresponding author: recep.keser@erdogan.edu.tr

International Conference on Science and Technology

ICONST 2018

5-9 September 2018 Prizren - KOSOVO

Determination of Correct Location of Chemical Attractant for Tropinota hirta (Poda, 1761) (Coleoptera: Cetoniidae)

Gökhan Aydın[1]*, Bülent Yaşar[2]

Abstract: The study was carried out in cherry orchard located in the boundaries of Atabey district in Isparta province. Totally ten chemical attractants approximately 2 m above from the ground were set up on branches of cherry trees. In the study conducted during the bloom period in which *T. hirta* was active on cherry trees, numbers of flowers and fruits were recorded daily to understand transformation of these flowers into fruits. As a result of the present study, fruit set was found out lower on branches with attractant than the branches without attractant 20.28 % and 30.86, respectively. This differences was found statistically significant. Therefore it is thought that the attractant hanging on the branches will increase the damage rate of Apple blossom beetle.

Keywords: Apple Blossom Beetle, Cherry, *Epicometis hirta*, Isparta, Turkey.

[1]Isparta University of Applied Science, Atabey Vocational School, 32670 Atabey, Isparta, TURKEY
[2]Isparta University of Applied Science,, Faculty of Agriculture, Department of Plant Protection, 32260, Isparta, TURKEY
*Corresponding author: gokhanaydin@sdu.edu.tr

International Conference on Science and Technology

ICONST 2018

5-9 September 2018 Prizren - KOSOVO

Getting Urban Children's and Landscape Architect's Oppinions About New Generation Natural Playground Proposals for Kastamonu City

Çiğdem Sakıcı[1]*, Türkan Sultan Yaşar Ismail[2]

Abstract: Most of the cities in Turkey, do not have enough outdoor playing spaces for children and parents often have security concers. These factors leed children to spend more time indoors. Today's urban children have to meet with their playing needs in interior spaces or modular playgrounds made of unnatural materials. The artificial modular playgrounds in Turkey mostly designed ignoring the user's needs and desires. In this regard, the essential relationship between designer and users is not felt in the most of playground designs in Turkey and these places are shaped with only the designer's predictions.

This research aims to analyze two main issues which are nature-child and designer-user relationships. Primarily, nature and child relationship is revealed, then the opinions of pupils between the age of 9-12 in Kastamonu City about existing modular playgrounds and natural playgrounds are determined. As a second step of the research, 11 playground options are designed with different concepts in the light of the critics and information from pupils. The 1/100 scaled models are made in order to make them perceptible for children. After that, these natural playground designs are presented with an exhibition for getting feedbacks and ideas from the potential users. After the critics from the children, the playground designs are also shown to professional designers and lastly, the differences and similarities between user's and designer's ideas are determined. A total of 105 children participated in the first survey conducted to determine the playing habits and preferences of the children living in Kastamonu city center. A total of 82 children and 39 specialists with the title of landscape architects participated in the second questionnaire for the evaluation of children's playground designs with different concepts suitable for children's wishes and needs.

Children playgrounds in Kastamonu city can not respond to the children's needs and requests. It is observed that children do not want to play much in these areas and they like to meet their play need more in digital environment. This situation has a negative impact on their development. It is revealed that if natural playgrounds are designed according to their wishes and needs, they like to play in these areas. With this way, more healthy, creative and environmentally conscious individuals can be trained. At the end of this research, it is revealed that landscape architects should design playgrounds not only with their perception, but also according to playground user's opinion and data.

This research aims to provide an insight to designers and initiate increasing number of natural playground designs which considers children's opinions and allowing them to discover nature by giving them the flexibility of play options.

Keywords: Nature and Child, Natural Playgrounds, User-Designer Relationship

[1]Kastamonu University, Architecture and Engineering Faculty, 37200, Kastamonu, TURKEY
[2] Kastamonu University, Architecture and Engineering Faculty, 37200, Kastamonu, TURKEY
*Correspondingauthor: csakici@kastamonu.edu.tr

International Conference on Science and Technology

ICONST 2018

5-9 September 2018 Prizren - KOSOVO

How New High Speed Railway Services Affect Existing Conventional Passenger Railway Services: Cases from Europe

Gökçe Aydın[1]*,Betül Değer Şitilbay[2],

Abstract: High speed rail is considered to be a big revolution in railway passenger transport. One of the most important quality measures for any transportation service is speed and high speed rail has an edge over road and in some cases air transport, in terms of speed. Although it is considered to be a revolution, high speed railway has never been introduced to a country where there had never been any railway passenger transport before. In all countries having high speed railway lines, conventional railway passenger lines had already existed and for most of the cases, the routes served by high speed railway lines were already being served by existing conventional lines. Under these conditions, some effects on the existing conventional railway services were unavoidable and they did occur. Introduction of high speed rail services affected the conventional passenger railway services sometimes positively and sometimes negatively. Examples to positive effects are generally limited to regional and local rail services that act as feeder lines to high speed rail services. These services have been improved to better feed the high speed train services and thus increase the ridership of them. This improvement was also beneficial to internal users of these lines. Examples to negative effects were experienced generally in the conventional lines that may compete with the high speed rail lines. Construction of high speed rail lines require huge investments and removal or weakening of the competition is often practiced to guarantee a better return of investment. The methods used for this include reducing the speed and frequency of the conventional trains, totally or partially cancelling the conventional services on some routes so rail passengers will be obliged to take the high speed trains, increasing the fares of conventional trains etc. This study will act as a survey of such cases across Europe, including Turkey. Both academic and non - academic publications (such as railway magazines and publications of civil society organizations in favour of conventional trains) will be surveyed to present the specific cases. Facts about the potential competition (in case it is really allowed) between high speed and conventional trains will also be emphasized.

Keywords: Rail transport, High-speed rail, Conventional Rail, Competition in Transport

[1]Aksaray University, Faculty of Engineering, 68100, Aksaray, TURKEY
[2]Yıldız Technical University, Faculty of Civil Engineering, 34220, İstanbul, TURKEY
*Corresponding author: info@iconst.org

International Conference on Science and Technology

ICONST 2018

5-9 September 2018 Prizren - KOSOVO

SiO_2 Nano Coating on Wooden Surface with Spray Technique

Oğuz Doğan[1]*

Abstract: Wettability of surfaces with liquids is an important property of materials that is controlled by the chemical composition and the geometry of the surface. Superhydrophobic surfaces that have a water contact angle 150° are attractive because of their importance in industrial applications. Because of the minimized contact with water, chemical reactions or bond formation through water are limited for a superhydrophobic surface. Thus, various phenomena are expected to be inhibited on such a surface, for example, snow sticking, contamination, disease transmission, and current conduction. Recently, with the increasing demands toward functionality of materials that cannot withstand high temperatures, such as textiles and plastics, the control of surface wettability via low-temperature processing is particularly significant. Surface modification with hydrophobic properties using the sol–gel method has been investigated during recent years. Although simple sol–gel reactions usually result in the formation of amorphous materials, self-organization of organosilane molecules offers an opportunity to create ordered hybrid materials with hydrophobic properties.

In this study, transparent and hydrophobic thin films are prepared on wooden surfaces. Liquid SiO_2 solutions produced by silicon-based nano- powder are covered on the fabric surface by using spray method. Wooden surfaces were coated at the room temperature in air with the different spray nozzles. Contact angle on the surface was measured by using with Drop Shape Analysis System contact angle meter. Scanning electron microscope (SEM) was used for investigating microstructure of the prepared surface. According to the Contact Angles measurements, the coated wooden surfaces showed hydrophobic character between 122 and 138 degrees, and the SiO_2 particles sticked to the wooden fibers as seen from SEM picture.

Keywords: SiO_2 nano glass, nano coating, nanotechnology, advanced materials, and wooden products.

[1]Necmettin Erbakan University, A.K. Education Faculty, Department of Physics, 42090, Konya/TURKEY,
*Correspondingauthor: odogan@konya.edu.tr

International Conference on Science and Technology

ICONST 2018

5-9 September 2018 Prizren - KOSOVO

Investigation of Natural Radioactivity Levels in Ceramic Tiles and Associated Radiological Hazards

Serdar Dizman[1]*, Recep Keser[1]

Abstract: All construction materials used in the construction of buildings contain natural radioisotopes at various rates. These radioisotopes are the main source of outdoor radiation to which people living in houses or workplaces are exposed. Therefore, it is important to determine the radioactivity levels in ceramic samples used in buildings. The natural radioactivity levels (^{226}Ra, ^{232}Th and ^{40}K) in the fifty-one ceramic tiles produced in Turkey were determined using high-purity germanium detector system (HPGe). In order to evaluate the radiological hazards originating from natural radionuclides of examined ceramic tiles, radium equivalent activity (Ra_{eq}), external hazard index (H_{ex}), representative level index ($I\gamma$), absorbed dose rate (D) and annual effective dose (AED) values was also calculated. The average activity concentrations of ^{226}Ra, ^{232}Th and ^{40}K radionuclides in the investigated ceramic tiles samples were found as 36.59 ± 2.64, 51.23 ± 2.81 and 420.81 ± 12.87 Bq/kg, respectively. These values are less than the world average values (50, 50, 500 Bq/kg) except the activity values of ^{232}Th. Again, the averages of radiological hazard parameters (Ra_{eq}, H_{ex}, $I\gamma$, D and AED) found for all ceramic tiles were found lower than the world averages. The present results was compared with the literature and the international reference values. This study show that the investigated ceramic tiles can be used safely in constructions and do not create significant radiological hazard when used in constructions.

Keywords: Ceramic tile, Natural radioactivity, Radiological hazard, Turkey

[1]Recep Tayyip Erdogan University, Faculty of Sciences and Arts, Department of Physics, 53100, Rize, TURKEY
*Corresponding author: serdar.dizman@erdogan.edu.tr

International Conference on Science and Technology

ICONST 2018

5-9 September 2018 Prizren - KOSOVO

Improvement of The Bleaching Process by Ultrasonic Applications in The Refining of Canola Oil

Necattin Cihat İçyer[1,2]*, Muhammet Zeki Durak[1]

Abstract: In bleaching phases, color pigments and other trace constituents formed during refining processes are removed by applying acid-activated earths. The goal of this study is to improve the bleaching process of canola oil using ultrasound method under various parameters, and then compare the results with the existing conventional methods. The response surface method (RSM) face centered central composite design (CCD) is created and the bleaching parameters for canola oil are optimized based on the spectrophotometric analysis at 446 nm and responses to the lovibond color scales. The neutral canola oil exposed to degumming was obtained from a local oil processing company (Besler Gıda, Turkey). All chemicals used were of an analytical grade and obtained from Merck (Germany). Acid-activated bleaching earth (Tonsil OPT 210 FF) was purchased from Süd Chemie A.G., Germany. The RSM face centered CCD was used to study the effects of three independent variables in the bleaching stage of the refining process for canola oil. The first of these parameters is the temperature (45°C - 75°C)/ ultrasonic power (20% - 60%), the second is the amount of bleaching earth (0.1% - 2% w/w), and the third is the contact time period range 2-15 min.

In the canola oil, the absorbance at the level 446 nm, yellow and red lovibond colors are 1.066, 70 and 3.4, respectively. In this study, the absorption of bleached canola oil at the level of 446 nm was observed to range from 0.071 to 0.905 and the highest color reduction was determined as 93.3%. On the other hand bleaching process resulted in the yellow and red ranging from 4.4 to 70 and from 1.0 to 3.4, respectively. The results show that by integrating the ultrasonic application into the bleaching process, it is possible to reduce the temperature applied to the oil by 25%, reduce the contact time by 50% and reduce the color value between 6 to 34%, when compared to the conventional methods. The results and analyses of this study suggested that the ultrasonic methods provide many advantages in oil bleaching processes, and offer many advantages for businesses in industrial oil productions.

Keywords: Bleaching, ultrasound, optimization, central composite design

[1] Yildiz Technical University, Chemical and Metallurgical Engineering Faculty, 34210, Istanbul, Turkey
[2]Mus Alparslan Univesity, Faculty of Engineering and Architecture, 49100, Muş, TURKEY
*Corresponding author: ncicyer@yildiz.edu.tr

International Conference on Science and Technology

ICONST 2018

5-9 September 2018 Prizren - KOSOVO

Synthesis and Charecterization of Benzimidazole-Derived New Azo Dyes

İzzet Şener*[1], Nesrin Şener, Merve Zurnacı, Mahmut Gür,

Abstract: It is known that azo dyes are the largest chemical class of industrial colorants. Their ease of preparation and economy of the reaction resulted in a large number of dyes. Azo dyes possessing an aromatic heterocyclic moiety increased the chromophoric strength and thus, have been reviewed comprehensively. Benzimidazole and its derivatives have been studied in anion and cation recognition systems that display color changes or fluorescence quenching or enhancement upon binding. In this study; benzimidazole derivative 1,3,4-thiadiazole compound was synthesized and this compound which is subsequently prepared was converted to azo dyes derivatives using coupling components. Obtained products were elucidated many spectroscopic methods such as FT-IR, ^{1}H-NMR and elemental analysis. 5-(1*H*-benzoimidazol-5-yl)-1,3,4-thiadiazol-2-amine compound was obtained by reaction of the benzimidazole carboxylic acid and thiosemararbazide in the presence of $POCl_3$. And then five new azo dyes were obtained from this synthesized compound by reaction with five different coupling components. The synthesized dyes were purified from DMSO/water mixture. The structures of azo dyes were analyzed by using spectroscopic methods such as FT-IR, ^{1}H-NMR and elemental analysis. It is seen that the spectral data obtained as a result of these analysis methods are compatible with the structures of the compounds. It was seen in the structure that the compounds obtained and the spectroscopic results are apparent.

Keywords: benzimidazole, heterocyclic, azo dye, 1,3,4-thiadizole.

Acknowledgement: The authors are grateful to the Scientific Research Projects Council of Kastamonu University (KUBAP01/2017-31).

[1]Department of Food Engineering, Faculty of Engineering and Architecture, Kastamonu University, Kastamonu, Turkey.
*Corresponding author: isener@kastamonu.edu.tr

International Conference on Science and Technology

ICONST 2018

5-9 September 2018 Prizren - KOSOVO

Synthesis and Charecterization of New Pyrazole Derivative Schiff Base Compounds

Nesrin Şener[1]*, Sevil Özkınalı, Mahmut Gür, Merve Zurnacı, İzzet Şener

Abstract: Schiff bases (RCH = NR') are condensation products of primary amines with aldehydes and ketones. The increasing interest in Schiff bases and metal complexes in various qualitative and quantitative determinations, enriching radioactive materials, in the paint industry, in the pharmaceutical and plastics industries, due to their biochemical activities, and especially in the synthesis of many Schiff bases, which can be used in liquid crystal technology in recent years. Schiff's complexes have gradually increased the importance of anticancer activity in the medical world and have enabled it to be used as a reactive reagent in cancers. Schiff base complexes of aromatic amines are used especially in the field of chemotherapy. Within the scope of this study, pyrazole derivative azo dyes were synthesized first from aromatic amines, then schiff bases were obtained from the reaction of aldehyde with azo compounds. The structures of final products were elucidated by spectroscopic methods such as FT-IR, ^{1}H-NMR, ^{13}C-NMR and elemental analysis. *p*-nitrobenzaldehyde and 3,5-diamino-4-phenylazo-1H-pyrazole compounds (1: 2 ratio) were dissolved in dry toluene at 250 mL of water and acetic acid was added dropwise until the pH was 4-5. It was then heated under reflux for 24 hours. Water was removed from the resulting product by distillation. This is followed by a further 3 hours of heating. The product cooled to room temperature was washed with the ethanol / water mixture and dried. The structures of final products were elucidated by some spectroscopic methods such as FT-IR, ^{1}H-NMR, ^{13}C-NMR and elemental analysis. It is seen that the spectral data obtained as a result of these analysis methods are compatible with the structures of the compounds. When the spectral data were examined, it was seen that the intended products were successfully synthesized.

Keywords: pyrazole, schiff base, azo dyes, aniline

Acknowledgement: The authors are grateful to the Scientific Research Projects Council of Kastamonu University (KUBAP01/2018-17).

[1] Kastamonu University, Faculty of Science-Arts, Department of Chemistry, Kastamonu, TURKEY
*Corresponding author: nsener@kastamonu.edu.tr

International Conference on Science and Technology

ICONST 2018

5-9 September 2018 Prizren - KOSOVO

Synthesis and Characterization of Novel Schiff Bases Including Benzimidazole Moiety

Mahmut Gür[1]*, Nesrin Şener, Sevil Özkınalı,Merve Zurnacı, İzzet Şener

Abstract: Despite numerous attempts to develop new structural prototypes in the search for more effective antimicrobials, benzimidazoles continue to remain a versatile compound against microorganisms and therefore, they are useful sub-structures for further molecular investigations. On the other hand, it has been shown in the literature that 1,3,4-thiadiazoles are related to pharmacological activities such as antimicrobial, antiviral, anesthetic, anticonvulsant. In this study; 1,3,4-thiadiazole compound derived from benzimidazole-5-carboxylic acid was synthesized and then, this compound was converted to schiff base derivatives using various aldehydes. Structures of final products were elucidated by spectroscopic methods such as FT-IR, ^{1}H-NMR and elemental analysis. First, 5-(1*H*-benzimidazol-5-yl)-1,3,4-thiadiazol-2-amine compound was obtained by reaction of the benzimidazole-5-carboxylic acid and thiosemacarbazide in the presence of $POCl_3$. Later, five new schiff base derivatives were obtained from 5-(1*H*-benzoimidazol-5-yl)-1,3,4-thiadiazol-2-amine by reaction with five different aldehydes in toluene. The structures of final products were determinated by some spectroscopic methods such as FT-IR, ^{1}H-NMR and elemental analysis. It is seen that the spectral data obtained as a result of these analysis methods are compatible with the structures of the compounds. Spectroscopic analysis showed that the compounds obtained were successfully synthesized.

Keywords: benzimidazole, heterocyclic, azo dye, schiff base.

Acknowledgement: The authors are grateful to the Scientific Research Projects Council of Kastamonu University (KUBAP01/2017-31).

[1]Kastamonu University, Faculty of Forestry, Department of Forest Industrial Engineering, Kastamonu, Turkey.
*Corresponding author: mahmutgur@kastamonu.edu.tr

International Conference on Science and Technology

ICONST 2018

5-9 September 2018 Prizren - KOSOVO

Investigation of Chemical Composition of *Thymus praecox* Opiz

Merve Zurnacı[1], İzzet Şener, Nesrin Şener, Mahmut Gür, Kerim Güney

Abstract: Thyme is the most commonly used fragrant plant with strong and slightly bitter flavor, known as spice and medicine, since ancient times among the population. Thyme plant is aromatically rich and has important bioactive molecules. Agriculture and trade of this plant are common in our country. For these reasons, the investigation of the chemical content of thyme has become important. In this study, it was aimed to determine the chemical composition of the *Thymus praecox Opiz* taxa which distributed in the Kastamonu region. The thyme plant, which is an economic valuable for the spice and essential oil industry, is mostly supplied from nature in our country. In this study, it was used the genus *Thymus praecox* distrubuted in the Kastamonu region Thyme was extracted with the soxhlet method using pure water, ethanol, methanol, methanol-water and ethyl acetate as solvents. The presence of flavonoids was investigated by normal phase HPLC. The essential oil of the thyme plant was analyzed by GC-FID / MS techniques GC-MS. Furthermore, the concentration of 18 elements found in the thixotropy was determined by ICP-OES.

In the HPLC analysis of thyme extracts extracted with different solvents, most of the samples were found to have flavonoids. Commonly found flavonoids in all extracts are eleutoroside, taxifolin, naringin, mircetin, quarcetin, butein, luteolin, campherol. The structure of a total of 50 compounds of the thyme essential oil is clarified. In the analysis by ICP-OES, it was determined that potassium (K) is the element with the highest concentration and Cobalt (Co) is the element with the lowest concentration in *Thymus praecox*. This study has contributed to the knowledge of the literature by determining the chemical composition of the thyme, which is a medicinal and aromatic plant, by various methods. It can be said that *Thymus praecox* has a potential as commercial resource for detected flavonoids.

Keywords: Thyme (*Thymus praecox* Opiz) , Thyme extract, Chemical composition, HPLC, GC-MS, ICP-OES.

Acknowledgement: The authors are grateful to the Scientific Research Projects Council of Kastamonu University (KUBAP03/2017-14).

[1]Kastamonu University, Institute of Science, Kastamonu, TURKEY
*Corresponding author: mzurnaci@kastamonu.edu.tr

International Conference on Science and Technology

ICONST 2018

5-9 September 2018 Prizren - KOSOVO

Investigation on Thermal and Mechanical Properties of Al_2O_3 Nanoparticle Reinforced Epoxy Nanocomposites

Şakir Yazman[1]*, Ahmet Samanci[2], Ahmet Akdemir[2]

Abstract: Epoxy polymers are become attractive due to their superior mechanical properties, good chemical and thermal resistance, versatile modifications, low viscosity, average curing temperature and easy producing. However, brittleness of epoxy polymers is a restriction for engineering applications. In recent years, production and researches on nanoparticle added epoxy composite are increased, in order to improve thermal and mechanical properties of epoxy polymers. Epoxy/ceramic nanocomposites are preferred greatly, owing to their high thermal conductivity, high strength and the most important due to their low costs. In this study, nanocomposites are produced through adding Al_2O_3 nanoparticles with different ratios(i.e0.5-2.0 wt%) by weight into epoxy matrix through applying solution mixing method. To determine shapes and dimensions of nanoparticles, images are taken by TEM. FTIR analysis of nanocomposites are conducted. Effects of nanoparticles on thermal properties are defined through DSC and TGA. In order to determine mechanical properties, 10 pieces of tensile specimens are produced for each reinforcement proportion and fractured surfaces are investigated by SEM images. The obtained results were evaluated statistically by means of Weibull approach.

Highest T_g value among the Al_2O_3 added nanocomposites was seen at 1.25% Al_2O_3 reinforced nanocomposites with 69.7 °C. Characteristic bands were formed and new peak formation wasn't observed on spectrum according to FTIR spectrums. According to tensile test results, in respect to UTS, elongation, Young modulus and static toughness, highest values compared to neat epoxy are gained from 1.0 wt % Al_2O_3 reinforced epoxy composite with 27.6, 75.6, 18.7 and 187.9 % increments respectively. Even though nanoparticle reinforcement increased the stress values, it is decreased stability and reliability of results. Well dispersed rigid nanoparticles in epoxy matrix decreases stress concentrations to minimum through providing homogenous dispersion of stress and improves mechanical properties. In addition to this, matrix/nanoparticle interaction and strong interface bonding provides more effective load transfer from epoxy matrix to nanoparticles, that is more rigid than the matrix, and it enhances mechanical properties. Nanoparticles, which is reinforced epoxy resin, changes epoxy resins' cure kinetic due to catalytic effect. As a result, cross-link density is increased and interaction between nanoparticles and functional groups of epoxy resin is increased as well. Agglomeration of nanoparticles increases stress concentration with decreasing surface area of nanoparticles, thus interaction between matrix and nanoparticles is decreased and a weak interface adhesion is formed, which can be reasons of decrement on mechanical properties.

Keywords: Nanocomposites, Thermal properties, Al_2O_3 nanoparticles, SEM, Weibull analysis

[1]Mechanical Department, Ilgın Technical Science College of SelcukUniversity, TURKEY
[2]Faculty of Aeronautical and Space Sciences, Necmettin Erbakan University, Konya, TURKEY
*Correspondingauthor: syazman@selcuk.edu.tr

International Conference on Science and Technology

ICONST 2018

5-9 September 2018 Prizren - KOSOVO

Effect of Different Ratios of Hungarian Vetch with Cereal Crop Mixtures on Hay Nutrient Value

Fırat Alatürk[1], Ahmet Gökkuş[1], Harun Baytekin[1]
Altıngül Özaslan Parlak[1], Selçuk Birer[2]

Abstract: This study has been conducted in order to determine the variations in digestibility and energy values of hay depending on the application of Hungarian vetch-cereal crop mixtures at different ratios. The research has been carried out in Canakkale in 2009–2011. The study has been designed according to randomized complete block design, and the plots were arranged as single and mixed (3:1, 2:2, 1:3 Hungarian vetch: cereal) crop sowing systems by using three replications with sowing Hungarian vetch mixing with barley, wheat, oats and triticale. Raw cellulose (RC), digestible dry matter (DDM), total digestible nutrients (TDDM), metabolic energy (ME), net energy (NEL) and relative feed value (RFV) like characteristics have been examined in this research. As the result of this research, the ratios of hay raw cellulose (RC) were not significantly important in accordance to different forms of sowing, while the values of DDM, TDDM, ME, NEL and RFV in hay were found higher in mixed sowing system than that of single sowing of cereal crops. In the study, it has been concluded that for being able to produce hay containing high nutrient value in the mixtures of Hungarian vetch with cereals then the mixture of wheat with Hungarian vetch with the ratio of 3: 1 would be suitable to sow

Keywords: Mixtures, forage, Hungarian vetch, barley, oat, wheat, triticale

International Conference on Science and Technology

ICONST 2018

5-9 September 2018 Prizren - KOSOVO

Effects of Different Ratios of Hungarian Vetch with Cereal Crop Mixtures on Hay Yield and Quality

Fırat Alatürk[a*], Ahmet Gökkuş[a], Altıngül Özaslan Parlak[a], Harun Baytekin[a], Selçuk Birer[b]

Abstract: This research has been conducted in Canakkale Province of Turkey with the aim of revealing the yield and quality of Hungarian vetch-cereal crop mixtures in 2009–2011. Hungarian vetch has been sown with the mixtures of barley, wheat, oat, and triticale using single and mixed cropping sowing methods (3:1, 2:2, 1:3 Hungarian vetch: cereal crops) according to the randomized complete block design by using three replications. Hay yield, species composition, ratios of crude protein (CP), NDF, ADF and crude ash (CA) were examined in this research. According to the results, the highest hay yield was obtained from the mixed sowing of oat and triticale by applying single and mixed cropping system. The highest ratio of weed (17.5%) in hay composition has been observed in single crop sowing of Hungarian vetch. The Hungarian vetch was mostly found in the mixtures with barley and wheat (30.6% and 24.2%) in the composition of hay. There was significantly important increase in the ratio of crude protein that correlated with the ratio of Hungarian vetch increased while the ratios of NDF and ADF decreased in case of mixed cropping. According to these results, sowing of Hungarian vetch with oats or triticale would be suitable for obtaining high yield and quality of hay using 3: 1 ratio of mixed cropping.

Keywords: Hungarian vetch, cereals, hay yield, species composition, hay quality..

a Canakkale Onsekiz Mart University Faculty of Agriculture Department of Field Crops–17100

bCanakkale Onsekiz Mart University, Vocational High School Bayramic, 17100 – CANAKKALE

*Corresponding author's e-mail: alaturkf@comu.edu.tr

International Conference on Science and Technology

ICONST 2018

5-9 September 2018 Prizren - KOSOVO

Relations Between Tree Height and Soil Properties in Semiarid Black Pine (*Pinus nigra* Arnold.) Afforestation

Yasin Karatepe[1]*, H. Oğuz Çoban[1], M. Ali Başaran[2]

Abstract: This study was carried out in black pine (*Pinus nigra* Arnold.) afforestation sites located in the southwest of Turkey (Burdur). The study area has a semi-arid climate type and has a transition climate characteristic between the Mediterranean climate and the continental climate.

The relationship between tree height and soil nutrient concentrations (P, K, Ca, Mg, Na, Fe, Mn, Zn and Cu), other soil characteristics (texture, pH, EC, lime and organic matter), and tree needle nutrient concentrations (N, P, K, Ca, Mg, Fe, Mn, Zn and Cu) were investigated in two different soil depths (0-30 cm and 30-60 cm) in 15 sample plots.

While there was statistically significant relationship between tree height and soil characteristics in five parameters for 0-30 cm soil depth (positive with clay and organic matter, negative with silt, pH and lime), a weaker correlation was found between the three parameters (positive with clay, negative with pH and lime) for the 30-60 cm depth. A positive significant relationship was determined between tree height and K, Mg, Mn and Cu concentrations at depths of 0-30 cm, and tree height and Na at depths of 30-60 cm. P, N and Cu concentrations of needle nutrients were found to have a significant positive correlation with tree height.

Keywords: Pinus nigra, afforestation, height, soil properties, nutrients

[1]Isparta Applied Science University, Faculty of Forestry, 32260, Isparta, TURKEY
[2]General Directorate of Forestry, East Anatolia Forest Research Institute, 25050, Erzurum, TURKEY
*Correspondingauthor: yasinkaratepe@sdu.edu.tr

International Conference on Science and Technology

ICONST 2018

5-9 September 2018 Prizren - KOSOVO

Drought Effects on Forests in Northwest Turkey

Yasin Karatepe[1]*, Mustafa Avcı[1], Nevzat Gürlevik[1], Akın Emin[2]

Abstract: In this study, the distribution of tree and shrub mortalities by species was examined after the drought in 2016 in northwestern Turkey, especially in forests of Istanbul, Çanakkale and Bursa Regional Directorates. Evaluations on climate data such as rainfall, relative humidity, high temperature values and average temperature values in the study area indicated that 2016 was in fact a very dry year.

Mortalities were common where the soil is generally shallow or where root development cannot be performed downward for some reason. When adjacent sites were evaluated, it has been determined that trees were rather healthy in the upper elevations or in the northern aspects, while tree mortalities were common in the lower elevations or in the southern aspects. The lack of mortality at the toeslopes and along the stream beds are also important signs that the mortality may have been caused by the drought in these areas. Although drought is believed to be the primary factor for the mortality, bark beetles have also been found and entomological problems have been observed in epidemic levels in some areas.

As a result of this field study, it was determined that Pinus nigra, Pinus brutia, Pinus pinaster, Juniperus oxycedrus, Erica arborea, Cistus creticus and Arbutus unedo were among the species commonly affected by the drought.

Keywords: Drought, Tree, Shrub, Mortallity, Mediterranean Climate.

Acknowledgement: We would like to thank the Republic of Turkey Ministry of Forestry and Water Affairs, General Directorate of Forestry for their support

[1]Suleyman Demirel University, Faculty of Forestry, 32260, Isparta, TURKEY
[2] General Directorate of Forestry, 06560, Ankara, TURKEY
*Corresponding author: yasinkaratepe@sdu.edu.tr

International Conference on Science and Technology

ICONST 2018

5-9 September 2018 Prizren - KOSOVO

Application of Smart Grid Technology in Electric Power Systems

Ahmet Karyeyen[1*], Ümit Albayrak[2], Barış Bakırcıoğlu[1], Fuat Şaylan[1]

Abstract: In recent years, it appears that the interest in smart grid technology has been increased by many countries in the world. The use of this technology as real time causes many problems. Many researches are being done for overcome this problem. Especially, smart grid technology has a great importance in solving problems such as power demand and power supply balancing and price disagreements in power systems. The main problem here is the demand forecast. Because of the minor mistakes in the forecasting, the supplier may face high costs. In this study, a compilation of researches on methods to provide economic balance between the demanded power and the supplier has been made. With these methods and studies, it is aimed to obtain the maximum profit for both the customers and the suppliers. In this research, recent studies on how smart grid technology is used in electric power systems have been investigated and compiled. As a result; the advantages and disadvantages of the methods used are investigated in the compilation of the researches about the solution of the pricing problems of power systems with smart grid technology. The studies were compared with supporting datas and presented. As a result of the study, the contributions of smart grid technology to the control of the power systems have been observed. It is proposed to increase the targeted profit by improving the more advantageous methods.

Keywords: Smart Grid, Electric Power System, Power Demand and Power Supply Balance, Maximum Profit for Customers.

[1]Selcuk University, Ilgın Vocational School, Department of Electronics and Automation, 42600, Konya, TURKEY
[2]Selcuk University, Ilgın Vocational School, Department of Computer Technology, 42600, Konya, TURKEY
*Corresponding author: akaryeyen@selcuk.edu.tr

International Conference on Science and Technology

ICONST 2018

5-9 September 2018 Prizren - KOSOVO

The Optimum Fuzzy Logic Controller For Load Frequency Control In Two-Area Power Systems

Ahmet Karyeyen[1*], Nurettin Çetinkaya[2]

Abstract: Electrical production control which is depending on the load of electric power systems is actually frequency control. In this paper, a fuzzy Proportional – Integral (PI) type controller is proposed for solving the load frequency control (LFC) problem. The fuzzy PI type controller is used in a two-area power system. The proposed fuzzy PI type controller has been compared with the other LFC techniques. The results show that the obtained optimal PI controller improves the dynamic performance of the power system especially in settling times (5% band). In interconnected power networks with two or more areas, the generation within each area has to be controlled so as to maintain scheduled power interchange. In this study, a fuzzy logic controller is proposed. In the proposed controller, K_p and K_i gains of each area are obtained with the help of fuzzy logic according to Area Control Error (ACE) signal of its own area. In the study, the simulation is implemented by using MATLAB Simulink Program and MATLAB Fuzzy Logic Toolbox (FLT). To damp out the oscillations due to instantaneous load perturbations as fast as possible, Automatic Generation Control (AGC) including the Fuzzy Logic Control (FLC) is used. The results obtained show that the controller improves effectively the damping of the oscillations after the load deviation in one of the areas in the interconnected system compared to conventional controllers. As a result; for two-area power system model; the data about maximum overshoot and settling time of 5% band in 0.01 pu step load variation which is occurred in the first area is given in study. As shown in the study; system have come the desired condition more quickly than the other studies with the proposed controller. The objective of this research is to design a fuzzy logic controller that can be solved the load frequency control problem in a shorter time. Therefore, a new controller structure is proposed to ensure load frequency control. In this proposed controller structure, K_p and K_i gains of each area are obtained with the help of fuzzy logic according to ACE signal of its own area. As a result of study the system is arriving to the desired condition in a shorter time than the other studies with the proposed controller. Also the maximum overshoot value is smaller than the other studies.

Keywords: Fuzzy Logic Controller, Load Frequency Control, Power System, Overshoot And Settling Time

[1]Selcuk University, Ilgın Vocational School, Department of Electronics and Automation, 42600, Konya, TURKEY
[2]Selcuk University, Faculty of Engineering, Department of Electrical and Electronics Engineering, 42075, Konya, TURKEY
*Corresponding author: akaryeyen@selcuk.edu.tr

International Conference on Science and Technology

ICONST 2018

5-9 September 2018 Prizren - KOSOVO

A Parametric Study of Header End-Plate Connections

Adem Karasu[1]*, Haluk Emre Alçiçek[1], Cüneyt Vatansever[1]

Abstract: In seismically active regions such as Turkey, the context of the nonlinearity provided by a building is based on the behaviors of structural components; beams, columns and their connections constituting the seismic force resisting system of the structure. Of these members, beam-to-column connections can play a considerably important role even if they have a capability of limited stiffness and flexural strength. Structural steel connections are mainly classified as a pinned or a moment connection. However, some beam-to-column connections having limited stiffness and flexural strength, which are called semi-rigid connections such as header end-plate connections designed so as to transmit only shear forces, can be characterized by moment-rotation relationship. For this characterization, the effect of some parameters such as thickness of the header end-plate, depth of the connection and number of the bolt rows on the behavior of header end-plate connections has been investigated by the help of finite element models. Analytical models that represent the header end-plate connections consist of IPE 300 beam, HEB 300 column, M20 bolts and end-plates with different thicknesses and heights.The finite element models include material, geometrical and contact nonlinearities. Because of reliable performance, the incompatible mode eight-node brick elements, denoted C3D8I, are used. Each material for each member is defined by true stress-true strain curve.

According to the analyses results, in addition to shear stresses, axial tensile stresses have been observed to occur in the bolts at the tension side. Thickness of the header end-plate, depth of the connection and beam web play a governing role in the development of initial rotational stiffness and the flexural strength of the header end-plate connections. However, for the equal connection depth, increasing the number of bolt rows has not influenced the connection behavior remarkably. The present study was performed to investigate the effect of different parameters on moment rotation behavior of header end-plate connections. Analyses results have shown that header end-plate connections have limited stiffness and flexural strength. However, they seem to be promising to provide the structural systems with additional stiffness, ductility and strength. Therefore, inter-story drifts can be limited and more energy imposed by earthquake can be dissipated.

Keywords: Steel structures, Semi-rigid connections, Header end-plate.

[1]Istanbul Technical University, Faculty of Civil Engineering, 34469, İstanbul, TURKEY
*Corresponding author: karasuad@itu.edu.tr

International Conference on Science and Technology

ICONST 2018

5-9 September 2018 Prizren - KOSOVO

Research on Shear Links with Perforated Web Sections

Haluk Emre Alçiçek[1]*, Adem Karasu[1], Cüneyt Vatansever[1]

Abstract: Eccentirally Braced Frame (EBF) system is one of the most desirable structural system in seismic design of steel structures. Many researchs show that EBF systems provide the high level of stiffness, ductility and energy dissipation capacity. Seismic energy is dissipated through shear or flexural yielding of link with large inelastic deformation in the link beam while columns, braces and beam outside of the link remain essentially elastic. To facilitate the large inelastic link rotation demand, link-to-column connection is exposed to large moments and shear forces. Due to the these forces stress concentrations developed in connection area are concluded fracture at low deformation level. Also depending on the overstrength ratio, design of all the other structural elements requests more effort. Using perforated web section concept in shear link beam may help to prevent difficulty design of connection and the other elements by limiting the link beam capacity without loss of stablity. Analytical models of W10×33 shear link beam with three different hole configuration are generated using ABAQUS software. Four-node shell element (S4R) was used and material nonlinearites taken into consideration through Von-Mises yield criterion with combined hardening. Geometric nonlinearities were accounted by employing the “nlgeom” option in ABAQUS. Link beam subjected to cyclic loading using the loading protocol specified in AISC seismic provision.

A series of analysis were performed to study the behavior of link beam with reduced web section. 10% of area reduction on web section with different hole arrangements were investigated. Shear force versus inelastic rotation curves show that increasing number of slots on web with same total open area has contributed to the reduction in shear force capacity at yielding point while inelastic link rotation capacity was increased. The present study was performed to determine the effect of perforated web on shear links in eccentrically braced frames. Finite element analysis have revealed that equally 6×4mm slots on web has stable hysteresis behavior whereas strength degredation was occured when 3×8mm slots were used on web section. The results of this study indicate that using high number of slots may help to limit forces that transmitting to the link-to-column connections and the other structural elements.

Keywords: Steel structures, Eccentrically braced frame, Shear link.

[1]Istanbul Technical University, Faculty of Civil Engineering, 34469, İstanbul, TURKEY
*Corresponding author: alcicek@itu.edu.tr

International Conference on Science and Technology

ICONST 2018

5-9 September 2018 Prizren - KOSOVO

Examination of the Possibility of Separation from Foreign Material in the Horizontal Wind Tunnel of Hazelnuts Collected from the Ground

K.Meriç Kalın[1*], M. Arif Beyhan[1], Hüseyin Sauk[1]

Abstract: A prototype horizontal wind tunnel was designed and produced in this study in order to research the possibility of separating materials such as stone and soil collected with hazelnut during mechanized hazelnut harvest. The trials were conducted with five different air velocitys (25, 30, 35, 40 and 45 m/s) and four different feed amounts (500, 750, 1000 and 1250 kgh^{-1}) by using stone-soil-hazelnut mixture which includes 8% stone and 8% soil. According to the results obtained, air velocity and product fall distance values which maximize the separating efficiency and minimize lost hazelnut ratio as were calculated as 25-30 m/s and 40 cm, respectively. For these values, stone separating efficiency was obtained between 50-96%, while soil separating efficiency was obtained between 8-73% and lost hazelnut ratio was obtained between 2-24%.

Keywords: Mechanized hazelnut harvest, horizontal wind tunnel, separation

[1] Ondokuz Mayıs University, Faculty of Agriculture Department of Agricultural Machinery and Technologies Engineering
*Correspondingauthor:

International Conference on Science and Technology

ICONST 2018

5-9 September 2018 Prizren - KOSOVO

The Influence of Urban Growth on Surroundıng Medıterranean Landscape Wıth Partıcular Reference to Degradatıon of Olıve Orchards

Derya Gülçin[1]*

Abstract: Monitoring Land Use/Land Cover (LULC) changes is important to make effective decisions in landscape planning and management. Quantifying the changing pattern of land helps us to understand how ecological impacts reveal and affect ecosystem services. The changes in landscapes can be assessed in different qualitative and quantitative ways. One of the aims of this study is to classify land cover using object-based image analysis and quantify the changes of the landscape patterns applying landscape metrics in Efeler district incorporating urban settlement of Aydin province during 25 years from 1986 to 2011. In this context, the combination of satellite imagery, geographic information systems (GIS), and landscape metrics were used. A Spot-1 image dated 1986 and a Worldview Ortoready Pan-sharpened satellite image dated 2011 respectively were processed for LULC classification. Six classes of land use including agriculture, bare soil, built environment, forest, main road, and river were identified. According to the overall accuracy assessment of 2 classified images, the accuracy values were computed as %85,6 (for LULC map dated 1986) and %89,8 (for LULC map dated 2011). The results of change-detection showed that during the whole study period, there was a remarkable increase in the built environment and the main road while bare soil decreased dramatically. It is also interesting that although urban expansion was higher, the total area of agricultural land almost remained the same. In fact, the location of agricultural land changed notably but the percentage of this area was unchanged. Within the boundary of urban settlement, agricultural areas, especially olive orchards were fragmented due to the developmental strategies of Aydin. Within the scope of change-detection analysis, degradation of olive orchards was highlighted. Heterogeneous structure and fragmented pattern of land cover were analyzed using several metrics at different levels.

Keywords: Land Use/Land Cover, change detection, GIS, olive orchards, landscape metrics

[1] Department of Landscape Architecture, Faculty of Agriculture, University of Adnan Menderes, 09010, Aydin, Turkey
*Correspondingauthor: derya.yazgi@adu.edu.tr

International Conference on Science and Technology

ICONST 2018

5-9 September 2018 Prizren - KOSOVO

Efficacy of Chlorpyrifos Ethyl on Mortality, Egg Hatching and Prey Consumption of the True Bug *Anthocoris nemoralis* (F.)

Baboo Ali[1]*, Avni Uğur[2]

Abstract: Chlorpyrifos ethyl is widely used in the chemical control program of different harmful insect pests in pear growing areas of Turkey. This insecticide also affects the population of the polyphagous predatory bug namely, *Anthocoris nemoralis* which is naturally found in pear orchards and particularly feeds on pear psylla, and this action is know as biological control. Biological control is the beneficial action of predators, parasitoids and pathogens in controlling different insect pests and their damges to the yield and quality of fruit and other agricultural crops. The main purpose of this study was to determine the effect of chlorpyrifos ethyl on mortality, egg hatching and prey consumption ratios of this polyphagous beneficial bug. Study has been conducted under laboratory conditions of 25±1°C, 70±10 R.H. and 16:8h (L:D). Different biological stages of the predatory bug, chlorpyrifos ethyl active ingredient insecticide, potter sprayer and fresh eggs of *Ephestia kuehniella* were used as the materials of this research work. Individuals of the predatory bug were fed by offering one third dose of chlorpyrifos ethyl contaminated *E. kuehniella* eggs in each treatment. The experiments were conducted by using 3 replications. Distilled water has been used in control treatments. Finally, the obtained data were analyzed by applying Tukey Test using the SPSS package program. As a result of this research work, the highest prey consumption (28.89±1.92) was observed in male treatments, while the lowest amount of *E. kuehniella* eggs (17.78±5.09) have been consumed by the 3rd nymphal stages of *A. nemoralis* within a time span of 24 h. As far as the egg hatching treatments are concerned, 36.67±0.03 eggs have been hatched after 120 hours of the conduction of experiments, but no egg hatching has been recorded within first 48 hours. The eggs started to hatch after 72 h of the conduction of experiment which was noted as 00.17±0.07. The highest mortality rate (67.77±4.04) has been recorded in 3rd nymphal instars followed by the female individuals of the true bug as 47.22±5.20, while the lowest mortality rate (42.22±5.48) was recorded in male individuals followed by the 5th nymphal stages of the polyphagous bug as 46.11±5.36. The application of chlorpyrifos ethyl active ingredient insecticide affected significantly the rate of egg hatching, mortality ratio of the 3rd nymphal instar and female individuals, and also the ratio of prey consumption of the 3rd immature stage of *A. nemoralis*.

Keywords: Mortality, egg hatching, chlorpyrifos ethyl, predatory bug, *Anthocoris nemoralis*

[1]Canakkale Onsekiz Mart University, Faculty of Agriculture, 17100, Canakkale, TURKEY
[2]Ankara University, Faculty of Agriculture, 06110, Ankara, TURKEY
*Correspondingauthor: babooali@comu.edu.tr

International Conference on Science and Technology

ICONST 2018

5-9 September 2018 Prizren - KOSOVO

Determination of Electromagnetic Field Levels in High School districts in Rize Province

Nilüfer As[1]*, Serdar Dizman[1], Yasin Karan[1]

Abstract: New technological products that are parts of our lives have become the main cause of electromagnetic pollution. International scientific organizations and communities have taken this issue under the spotlight; in this context, the limit values and standards were established. Especially in school districts, the use of mobile phones and wireless internet for education and communication has increased considerably. Given the intensity of students, teachers and staff in these regions, schools have become points of potential electromagnetic field pollution. Eleven high schools were identified in Rize city center and central province to determine the electromagnetic pollution in school regions. In these high schools, measurements were taken at the times when the students were in lectures in classes and in break times. Electromagnetic area (EMA) strength measurements were taken in the frequency band between 420 MHz and 2.6 GHz. Maximum and maximum average value are obtained during the six minutes measurements. A spectrum analyzer SRM 3006 (Narda Safety Test Solutions GmbH, Germany) operating in the 400 MHz to 6 GHz bandwidth was used to obtain these measurements. The results of these measurements have been compared with the limit values, which were declared by the International Commission on Non Ionizing Radiation Protection (ICNIRP) and Information and Communication Technologies Authority (ICTA). The maximum and maximum average of EMA strengths were determined as 1.72 V/m and 1.4 V/m, respectively. This measurement was taken from a high school in the city center during lecture time. The maximum and maximum average of EMA strength of break times was found 1.23 V/m and 0.86 V/m and they were taken from same school. Measurements taken from the schools away from city center were identified less than half of schools at the city center. All measurements were less than ICNIRP and ICTA limit values. The schools those are close to city center showed higher EMA strength compared to other schools those are away from city center. High density of electromagnetic sources such as mobile phones and Wi-Fi routers and the high concentration of base stations in these regions caused to these results. Also, measurements taken during the lectures were generally higher than the measurements in the breaks for the same schools.

Keywords: Electromagnetic area radiation, measurement, high school districts

[1]Recep Tayyip Erdogan University, Faculty of Sciences and Arts, Department of Physics, 53100, Rize, TURKEY
*Corresponding author: nilufer.as@erdogan.edu.tr

International Conference on Science and Technology

ICONST 2018

5-9 September 2018 Prizren - KOSOVO

Effects of Pomegranate Seed Oil on Blood Parameters and Egg Quality of Japanese (*Coturnix coturnix japonica*) Quail

Mustafa Öğütcü[1]*, Elif Dincer[2], Ali Karabayır[3]

Abstract: The aim of this study was to investigate the effects of pomegranate seed oil on blood parameters and egg quality of Japanese quails (Coturnix coturnix japonica). For this reason, a total of 120 quails at 5-7 day ages were divided into 4 groups (30 quails in each group) and placed in cages. For the feeding study, feed supplemented with 1, 3 and 5% pomegranate seed oil and control feed with no oil addition were prepared. Quail blood parameters and egg weight, shell strength, shell thickness, albumen and yolk index, colour, protein, fat, ash, Haugh unit, fatty acid and mineral compositions and combustion energy values were determined.

Keywords: Pomegranate seed oil, quail egg, quality, fatty acids

[1] Çanakkale Onsekiz Mart University, Faculty of Engineering, 17020, Çanakkale, TURKEY
[2] Çanakkale Onsekiz Mart University, Bayramic Vocational College, 17100, Çanakkale, TURKEY
[3] Çanakkale Onsekiz Mart University, Faculty of Agriculture, 17020, Çanakkale, TURKEY
*Corresponding author: mogutcu@comu.edu.tr

International Conference on Science and Technology

ICONST 2018

5-9 September 2018 Prizren - KOSOVO

Designing A Multipurpose Web-Based Terrain Robot Prototype

Ümit Albayrak[1], Barış Bakırcıoğlu[2*], Ahmet Karyeyen[2], Fuat Şaylan[2]

Abstract: One of the most important reasons for designing robots is to facilitate life tasks. This study aims to create a platform that is open for development by designing a prototype terrain robot that can fulfill more complicated tasks. This study is important in that if needed, this robot can be used for search and rescue, bomb disposal and discovery purposes for dangerous environments. In this study, the hardware and control design of a wheeled terrain robot, which has mobile cameras on it and 7-axis robot arm, was realized. The terrain robot can move with the help of six wheels that all have independent suspensions. Back-and-forth, left-and-right movements, robot arm control and camera navigation movements of the terrain robot can be controlled with a micro computer system attached on it. A web-based user control program was developed for the remote controlling of the terrain robot. This is because access can be provided this way from such platforms as smart phones, tables and PCs. In this study, a remote-controlled multipurpose terrain robot was designed and developed as a prototype. The terrain robot is the most advantageous in that it allows for a web-based control and it is oriented toward different purposes of use. However, it is disadvantegeous in that there is the problem of energy given its mobility. It is considered that in the future, with more efficient batteries, this problem could be eliminated. The terrain robot lends itself to multipurpose use thanks to its mechanical structure, equipments and easy controllability from different platforms. In case of need, it is planned that the robot could be used for a wide array of purposes which include military, space research, natural disasters and search and rescue activities in dangerous conditions for humanbeings.

Keywords: Terrain Robot, Mobile Robot, Web-Based Control, Embedded System.

[1]Selcuk University, Ilgın Vocational School, Departments of Computer Technology, 42600, Konya, TURKEY
[2]Selcuk University, Ilgın Vocational School, Departments of Electronics and Automation, 42600, Konya, TURKEY
*Corresponding author: umitalbayrak@selcuk.edu.tr

International Conference on Science and Technology

ICONST 2018

5-9 September 2018 Prizren - KOSOVO

Evaluating for Teacher Perceptions for Science, Technology, Engineering and Mathematics (STEM) Education in Secondary School

Hatice Akarsu[1*], Nevin Akarsu[2], Sefa Pekol[3], Nermin Akarsu[4], Ahmet Acarer[5]

Abstract: Science and technology are rapidly developing in the 21st century. Science, technology, engineering and mathematics are of great importance for people to continue their existence at this rate. The science, technology, engineering, mathematics (STEM) education system has also been developed by adding engineering and technology to science and mathematics courses for students to follow these developments. In this research, perceptions of the applicability of teachers' STEM education to secondary schools were investigated. The study group of the research is a secondary school of different disciplines. 20 teachers participated in the research as 4 Technology Design, 4 Mathematics, 4 Information Technologies, 4 Science and 4 Turkish Language disciplines voluntarily. The semi-structured interview technique was used as the data collection method and "content analysis" was performed. A simple coding system is used to identify the similarities and differences to describe the related themes. Teachers have stated that STEM education practices will make the lesson more interesting and fun, and that learning will be more permanent and continuous. In addition, research findings have shown that teachers need to be informed and given training seminars so that STEM applications can be better understood in schools. In order to provide teachers with equal educational opportunities for children, the work was done in this regard can be increased and teachers' information about STEM education can be increased. The number of students can be reduced in the classroom to increase success. Information and practices related to new up-to-date approaches can be integrated into training programs.

Keywords: STEM education, Teacher perception, Science, Education

[1]Kastamonu University, Faculty of Forest Engineering, 32260, Kastamonu, TURKEY
[2]Kastamonu University, Faculty of Education, 37200, Kastamonu, TURKEY
[3]Kastamonu University, Faculty of Education, 37200, Kastamonu, TURKEY
[4]Kastamonu University, Faculty of Forest Engineering, 32260, Kastamonu, TURKEY
[5]Suleyman Demirel University, Faculty of Forestry, 32260, Isparta, TURKEY
*Corresponding author: htce.akrsu@gmail.com

International Conference on Science and Technology

ICONST 2018

5-9 September 2018 Prizren - KOSOVO

Evaluation of Ecological Beliefs of 6th Grade Students by Using New Ecological Paradigm Scale

Hatice Akarsu[1*], Nevin Akarsu[2], Sefa Pekol[3], Nermin Akarsu[4], Ahmet Acarer[5]

Abstract: Science and technology have changed globalization and people's relations with nature. These changes made it necessary to re-examine nature and human relations. In this context, this study assessed the ecological beliefs of 6th grade students about living and living things. The research is designed with a quantitative pattern. The sample of the research was composed of 80 middle school 6th grade students who continued their education in the academic year of 2017-2018. The data were obtained with the "New Ecological Paradigm for Children Scale". The Crombach-alpha internal consistency coefficient and the correlation coefficient values of the scale were revised in this study. It has been determined that the analysis results are acceptable. New ecological paradigm scores of the students were evaluated using the SPSS 17.0 package program of the obtained data. Secondary school students; environmental beliefs, values ecological and environmental awareness levels were determined. The data obtained are presented in comparison with various properties. For secondary school students, training can be given to develop environmental awareness, attitudes and suggestions for solutions to environmental problems.. This study can be renewed in different sampling groups. Educational programs may include activities related to ecology. Research on how to improve the ecological paradigm values of secondary school students can be done.

Keywords: New ecological paradigm, Ecology, Environment, Attitude, Ecological belief

[1]Kastamonu University, Faculty of Forest Engineering, 32260, Kastamonu, TURKEY
[2]Kastamonu University, Faculty of Education, 37200, Kastamonu, TURKEY
[3]Kastamonu University, Faculty of Education, 37200, Kastamonu, TURKEY
[4]Kastamonu University, Faculty of Forest Engineering, 32260, Kastamonu, TURKEY
[5]Suleyman Demirel University, Faculty of Forestry, 32260, Isparta, TURKEY
*Corresponding author: htce.akrsu@gmail.com

International Conference on Science and Technology

ICONST 2018

5-9 September 2018 Prizren - KOSOVO

The Microencapsulation of Photochromic Dyes and Their Application to Cotton Fabric by Printing Method

A. Merih Sarıısık[1]*, Ozlem Topbas[2], Gokhan Erkan[1], Orhun Ek[3]

Abstract: In this study, two different photochromic dyes which include (1',3'-Dihydro-1',3',3'-trimethyl-6-nitro-spiro[2H-1-benzopyran-2,2'-(2H)-indole] and 1',3'-dihydro-8-methoxy-1',3',3'-tri-me-6 nitrospiro(1-benzopyran-indole) were microencapsulated by using coacervation and *in-situ* polymerization methods. Ethyl cellulose and melamine-urea-formaldehyde were used as polymers. The Fourier transform infrared spectroscopy (FTIR), X-ray diffractometry (XRD), particle size and size distribution analysis and scanning electron microscope (SEM) were utilized to characterize the structure, morphology and size distribution of phtochromic microcapsules. These microcapsules were applied to the 100% cotton fabric by printing method. Then, the activities of photochromic microcapsules on the fabric were analyzed by colour analysis under different light sources, washing and rubbing fastness tests.

Keywords: Photochromic microcapsules, ethyl cellulose, melamine-urea-formaldehyde, microencapsulation, cotton

[1]Dokuz Eylul University, Faculty of Engineering, Department of Textile Engineering, 35397, Izmir, TURKEY
[2]Dokuz Eylul University, The Graduate School of Natural and Applied Sciences, 35390, Izmir, TURKEY
[3]Soktas Weaving Industry Company, 09201, Aydın, TURKEY
*Corresponding author: merih.sariisik@deu.edu.tr

International Conference on Science and Technology

ICONST 2018

5-9 September 2018 Prizren - KOSOVO

InvestigatingMechanicalProperties of AdhesiveBondedJointswith MWCNT Reinforced Epoxy NanocompositeAdhesives

Şakir Yazman[1]*, Ahmet Akdemir[2],AhmetSamanci[2],Mahmut Özer[3]

Abstract: Adhesion can be defined as attractionthat is betweenmolecules and atomswhichare on the interface of adhesive and substrate. Processes of adhesionincludesadhesive, substratematerial, propersurfacetreatmentforsubstratematerial and interface/interphasebetweenadhesive and substratematerial.Aluminum and its' alloysareusedwidely in industriessuch as automotive and aerospace, since theyhavepropertieslikebeinglight, abilityforgoodplasticdeformation, goodmachinability and corrosionresistance. Weldingaluminumalloys is a difficultprocess and has disadvantages. Hence, adhesivelybondedjointsareused as alternatives. Mechanicalproperties of adhesivelybondedjointsareinvestigatedwhichmadewith epoxy nanocompositeadhesives, that is producedthrough MWCNT additionwithdifferentratios (0.5 – 2.0 %) byweight. In respect to this, Al 2024-T3 materials, which are used in aerospace industry commonly, single-lap joints were made according to standards. Surfaces of adhesively bonded aluminum specimens were prepared through subjecting firstly etching with sulfuric acid – sodium dichromate solution then anodizing with phosphoric acid according to standard. Roughness values of deformed surfaces were measured and occurred roughnesses' morphologies were investigated through AFM. To determine effect of nanoparticles on wettability, contact angles were measured for every addition amount. Shear stress, elongation and toughness values were identified through conducting tensile test on prepared single-lap joints. The obtained results were evaluated statistically by means of Weibull approach. Best results for MWCNT reinforced nanocomposite adhesives were achieved by 1.25 MWCNT reinforcement as increment in shear stress and elongation values in respect to adhesively bonded joints by neat epoxy, with 20.1 and 54.7 % increase respectively. Wetting angle of neat epoxy is measured as 32.8°. Minimum wettingangle (28.1°) is measured at 0.5% MWCNT reinforcedadhesives and wettingangle is increasingwithincrement in amount of reinforcement. Maximum wettingangle (38°) is measured at 2% MWCNT reinforcednanocomposite. Nanoparticleshave an importanteffect on mechanicalproperties of epoxy adhesives, especiallyincrements on toughnessproperties. Increases on mechanicalproperties of epoxy adhesiveaffectedstrength of adhesivelybondedjointspositively.
Homogenouslyaddednanoparticlesincreasedmechanicalproperties of bondedjointswithtoughnessmechanismssuch as pullout, crack deflection crack branching, pinning and bowing. Nanoparticlesimprovedwetting and increasedmechanicalinterlockingeffect. Also, nanoparticlesstrengthenedchemicalbondbetweensubstrate and adhesive and formedstrong interface betweenthem. Therefore, mechanicalproperties of adhesivelybondedjointsareincreased.

Keywords: Epoxy nanocompositeadhesives, MWCNT, single-lap joints, surface roughness, Weibull analysis, wettability

[1]Mechanical Department, Ilgın Technical ScienceCollege of SelcukUniversity, TURKEY
[2]Faculty of Aeronautical and Space Sciences, Necmettin Erbakan University, Konya, TURKEY
[3]Department of MechanicalEngineering, Faculty of Technology, Amasya University, Amasya, TURKEY
*Correspondingauthor: syazman@selcuk.edu.tr

International Conference on Science and Technology

ICONST 2018

5-9 September 2018 Prizren - KOSOVO

Temperature Control In Grain Drying Systems With Solid Fuel

Aydın GÜLLÜ[1]*, Emrah AYDIN[1], Hilmi KUŞÇU[2], Ozan AKI[1], Yusuf AVŞAR[1]

Abstract: In agricultural crops, the particulate cereals are harvested after they mature in the field. Harvesting occurs mostly in harvester machines, with the separation of the grain. it must be kept at a certain moisture value so that the grains can be stored. If the moisture level of the crop after harvest is too high, germination or decay may occur. For this unwanted situation, dehumidification is done with grain drying systems. Drying process is done by giving hot air on the grain. Different methods of heating the air are used. Electricity, liquid or gaseous fuels are the types of energy used to obtain hot air. The control of the boilers operating with these energy types counted is controlled by adjusting the fuel or energy level. However, the temperature control of a solid-fueled boiler is more complex. The heat energy generated as a result of the combustion of solid fuel heats the air. It is directly proportional to the amount of fuel and oxygen supplied for combustion. However, there is a large time delay in the system. In this study, temperature control of a solid fuel grain dryer was performed. After combustion starts for temperature control, fuel and oxygen are supplied to the combustion chamber. After the fuel and oxygen are supplied to the combustion chamber, a certain period of time is required to ignite the solid fuel. Following the end of the waiting period, a fuel boost is made according to the increase in temperature. In addition to fuel, oxygen entering the inside is also an important factor for combustion. In this study, both the amount of fuel was given for certain periods and the oxygen flow rate was controlled. The air temperature is kept constant by carrying out the control of this multi-input single-outlet system. The fuel supply is provided by a motor driven spiral. The air devise is controlled by the bellows. Motor operation time and speed are controlled to set two parameters. PLC is used as controller in the system. Control is provided by the developed software. The amount of hot air used in drying is measured and the amount of fuel and oxygen flow are set on the PLC side. When the airflow is controlled as PID, the amount of fuel is set by the feed and standby times. In this regard, the temperature is kept constant without being affected by the ambient conditions. The drying process is not affected by the ambient conditions. While the daytime ambient temperature is high, the amount of fuel and oxygen that is set for the incoming air temperature is not sufficient for cool air at night. For this reason, a control algorithm has been developed to keep the air temperature used in the dryer constant. The temperature of this system, which is a single inlet with multiple inputs, is automatically controlled.

Keywords: PLC, Temperature Control, Grain Drying Systems

[1] Trakya University, İpsala Vocational High School, 22400, Edirne, TURKEY
[2] Trakya University, Engineering Faculty, Edirne, TURKEY
*Corresponding author: aydingullu@trakya.edu.tr

International Conference on Science and Technology

ICONST 2018

5-9 September 2018 Prizren - KOSOVO

Production Cost of Potted Grapevine Sapling on Different Level of Clinoptilolite Mineral Applications

Fadime Ateş[1]*, Selçuk Karabat[1]

Abstract: Vine is one of the oldest fruited plant species in the world. The viticulture and wine culture began in the region covering the northeastern part of Anatolia thousands of years ago and is considered to have spread all over the world. Turkey is among the largest grapevine growing countries of the World. Turkey is among the most important countries with the area of vineyards and grape production in the World. Due to climate conditions and the suitability of growing conditions, viticulture is a source of livelihood for many producers throughout the country. In Turkey grapevine sapling production is made by the public and private sectors. The production of grapevine sapling is mostly done by the public sector. Both grafted rooted and potted grapevine sapling production was not enough in Turkey. This study was carried out during 2001-2002 in the production greenhouse of Manisa Viticulture Research Institute. Effect of different ratios of clinoptilolite minerals containing (15%, 30%, 100% and % 0 as control application) on production costs and revenue of potted sapling of Sultani Çekirdeksiz grape variety grafted on 1103 Paulsen (1103 P) and 41 B grapevine. At the result the highest per unit production cost was determined in the application of clinoptilolite minerals by 100% on Sultani Çekrdeksiz / 41 B with 6,71 TL, the lowest per unit production cost was determined in the application of clinoptilolite minerals by 30% on Sultani Çekrdeksiz / 1103 P with 2,61 TL. It was determined that the material expenses were the highest expenses in potted grapevine planting material (53,18 - 61,22 %). The most important factor affecting cost in sapling production is rate of sapling. Clinoptilolite mineral by 30% application has positive effects on the quality and rate of sapling on both Sultani Çekirdeksiz/41 B and Sultani Çekirdeksiz/1103 P. It's recommended that, for getting the best rate of sapling and growing parameters in potted grapevine sapling, using 30% clinoptilolite minerals for cv. Sultani Çekirdeksiz.

Acknowledgement: This research was supported by Directorate of Manisa Viticulture Research Institute. The authors Thank Enli Mining Industry and Trade Joınt Stock Company for their contribution to the project.

Keywords: Sultani Çekirdeksiz, 1103 Paulsen (1103 P) and 41 B grapevine rootstocks, Potted grapevine sapling production, Clinoptilolite mineral, Production cost

[1]Manisa Viticulture Research Institute, 45125, Manisa, TURKEY
*Corresponding author: fadime.ates@tarimorman.gov.tr

International Conference on Science and Technology
ICONST 2018
5-9 September 2018 Prizren - KOSOVO

Biological Activities of *Urginea maritima* L. Baker

Gulten OKMEN[1]

Abstract: Food-spoilage pathogens threaten human health. Moreover, these pathogens are resistant to antibiotics. Scientists are in search of a new path against these pathogens. In this study, biological activities of plant known as the "ada soğanı" in Turkey was studied and it contributed that to the literature. Studies on biological activities of *U. maritima* collected from Muğla province are very less. The aim of this study is to determine the antimicrobial, antioxidant and antimutagenic activities of *U. maritima*. *Urginea maritima* from Muğla province were collected for antimicrobial, antioxidant and antimutagenic studies. The antimicrobial activities were done by disc diffusion method. A total of 8 microorganisms were used in the study, seven of them are bacteria and the other is yeast. Non-enzymatic antioxidant activity tests were done by 1,1-diphenyl-2-picrylhydrazyl (DPPH) method. Antimutagenic activity studies were done by Ames Test. The antimicrobial activity of plant was found effective against food pathogens. The radical scavenging activity of plant was determined as 80 %. In addition to, antimutagenic activities of *U. maritima* were found 58,2% for *Salmonella* Typhimurium TA98 and 32,9% for *Salmonella* Typhimurium TA100. These values are high and important. As a result, *Urginea maritima* have antimicrobial, antioxidant and antimutagenic capacities. This plant is thought to be a good candidate for new agent searches.

Keywords: Antimicrobial activity, Antimutagenic activity, Antioxidant activity, *Urginea*

[1]Mugla Sitki Kocman University, Faculty of Science, 48000, Mugla, TURKEY
*Corresponding author: gultenokmen@gmail.com

International Conference on Science and Technology

ICONST 2018

5-9 September 2018 Prizren - KOSOVO

Determination of ACC Deaminase, Nitrogenase and Antagonistic Activities of Gram Negative Bacteria Isolated from Wheat Fields and their salt tolerance

Gulten OKMEN, Sukran KARDAS

Abstract: 1-aminocyclopropane-1-carboxylate (ACC) deaminase activity is an important marker for bacteria to support plant growth by lowering ethylene levels in plants. The enzyme has been found in limited number of bacteria and plays a important role in supporting plant growth and development under stress conditions by reducing stress induced ethylene production in plants. The aim of this study is to investigate strains with ACC deaminase, nitrogenase and antagonistic activities. In the present study, bacteria isolated from rhizosphere soils and wheat seedlings from Canakkale were screened for ACC deaminase activity and eight isolates were determined to be ACC deaminase positive. The results of traditional methods showed that eight bacteria were identified as *Pseudomonas*, *Enterobacter* and *Serratia* strains. These bacteria can utilize ACC as a sole nitrogen source because it contains ACC deaminase, which hydrolyzes ACC to ammonia and α-ketobutyrate. ACC deaminase activity was determined by measuring the production of α-ketobutyrate. Nitrogenase activity was based by Acetylene Reduction Assay (ARA). According to the results, there are some differences in ACC deaminase activities among all strains isolated from wheat fields. ACC deaminase activity were analyzed on eight bacteria. The highest ACC deaminase activity was found on *Pseudomonas* sp. CKB55 (2833 nmol α-ketobutyrate.$mg^{-1}.h^{-1}$). Whereas lowest activity was determined on *Enterobacter* sp. CKB17 (418 nmol α-ketobutyrate.$mg^{-1}.h^{-1}$). The highest nitrogenase activity was determined on *Pseudomonas* sp. CKB10 (808 nmol ethylene/ mg.h). In antagonistic activity studies, *Pseudomonas* sp. CKB52 was showed maximum inhibition zone against *Erwinia caratovora* ECC100, and the zone was 11 mm. Most of the isolates were showed tolerance to 1000 mM NaCl concentration. It is recommend that ACC deaminase- contaning bacteria could be a environment-friendly and promising potential strategy to promote plant growth, alleviate biotic and abiotic stresses and provide sustainable agriculture, especially for ethylene-sensitive plants production. As conclusion, Gram negative bacteria isolated from wheat fields have high ACC deaminase, nitrogenase and antagonistic activities. Additionally these bacteria have to high salt tolerance.

Acknowledgement: This work was supported by Mugla Sitki Kocman University Scientific Research Project (BAP /2015-034). Authors wish to thank Mugla Sitki Kocman University.

Keywords: Bacteria, ACC Deaminase Activity, Nitrogenase Activity, Antagonistic Activity, Salt Tolerance

Mugla Sitki Kocman University, Faculty of Science, 48000, Mugla, TURKEY
*Corresponding author: gultenokmen@gmail.com

International Conference on Science and Technology

ICONST 2018

5-9 September 2018 Prizren - KOSOVO

Antibacterial and Antioxidant Activities of *Vitex agnus-castus* L. against Mastitis Pathogens

Neslihan Balpınar[1*], Gulten Okmen[2], Mustafa Vurkun[2]

Abstract: It is widely reported that mastitis agents have developed resistance to antibiotics due to widespread use of antibiotics. The mastitis agents used in the study are 7 bacteria in total; 2 of them are *Staphylococcus aureus* and the another 5 bacteria are Coagulase-Negative *Staphylococci* (CNS). The plant material of *Vitex agnus-castus* was collected from Mugla-Turkey. Kirby-Bauer assay was used to screen the antibacterial activities. The other antibacterial activity test performed within the scope of the study was minimum inhibitory concentration (MIC) test. Antioxidant activities were carried out using 2,2′-azino-bis(3-ethylbenzothiazoline-6-sulfonic acid) (ABTS) technique. Results indicated that the extracts of *V. agnus-castus* had antibacterial activity against mastitis pathogens, and the range of inhibition zone was 8-10 mm. The largest zone was obtained from the methanol extract of *V. agnus-castus*. In the analysis conducted in order to determine the MIC value, no inhibition was observed in any of the tested concentrations. Among the extracts of the plant, the water extract had the highest antioxidant activity (78.95%). It was found that the extracts of *V. agnus-castus* have antibacterial activity against *Staphylococcus aureus* and CNS pathogens, and that the plant extracts can be used to treat mastitis caused by test bacteria.

Keywords: Antibacterial activity, Antioxidant activity, Mastitis, *Vitex agnus-castus*

[1]Burdur Mehmet Akif Ersoy University, Faculty of Arts and Science, 15030, Burdur, TURKEY
[2]Mugla Sitki Kocman University, Faculty of Science, 48000, Mugla, TURKEY
*Corresponding author: nerdogan@mehmetakif.edu.tr

International Conference on Science and Technology

ICONST 2018

5-9 September 2018 Prizren - KOSOVO

The Antibacterial Activities of *Ocimum basilicum* L. against Mastitis Pathogens and Its Antioxidant Activity

Neslihan BALPINAR[1]*, Gulten OKMEN [2], Mustafa VURKUN[2]

Abstract: In mastitis disease, *Staphylococci, Streptococci* and coliforms are the most common causative microorganisms. Today's new antibiotics attract a great deal of attention among researchers. This study aims to examine the antibacterial and antioxidant activities of the various extracts of *Ocimum basilicum* L. In the analysis, 7 mastitis agents are employed; 2 of them are *Staphylococcus aureus* and the remaining 5 bacteria are Coagulase-Negative *Staphylococci* (CNS). Disc diffusion method of Kirby-Bauer was used to determine the antibacterial activity. The other antibacterial activity test performed within the scope of the study was minimum inhibitory concentration (MIC) test. Antioxidant activity studies were carried out using 2,2-diphenyl-1-picrylhydrazyl (DPPH) radical scavenging technique. The results of the study indicated that *O. basilicum* had antibacterial activity against mastitis pathogens, and the largest zone of inhibition was 9 mm, which was obtained from the methanol extract of *O. basilicum*. The lowest MIC value was 3250 µg/mL. It was found that the water extracts have high antioxidant activity (72%). Consequently, it was found that the extracts of *O. basilicum* have antibacterial activity against mastitis pathogens. Besides, the plant extracts can be employed as natural antibacterial agent against mastitis pathogens. These results suggest that *O. basilicum* is a good candidate in developing new antibacterial and antioxidant agents.

Keywords: Antibacterial activity, Antioxidant activity, Mastitis, *Ocimum basilicum*

[1]Burdur Mehmet Akif Ersoy University, Faculty of Arts and Science, 15030, Burdur, TURKEY
[2]Mugla Sitki Kocman University, Faculty of Science, 48000, Mugla, TURKEY
*Corresponding author: nerdogan@mehmetakif.edu.tr

International Conference on Science and Technology

ICONST 2018

5-9 September 2018 Prizren - KOSOVO

Seasonal Effects on Heat Transfer for Exterior Wall: a Statistical Application

Tuğçe Pekdoğan[1]*

Özet: The temperature difference between the indoor and outdoor of the building is the primary cause of heat loss also heat gain in winter and summer months respectively. The greater this difference, the higher the rate of heat transfer. Most buildings have a higher heat loss when they are colder outside due to the controlled to a constant internal temperature. The effect of opaque wall surfaces of buildings which constitute a remarkable share in total energy consumption is depended upon by many factors, including annual climatic conditions, wall directions also locations. Improvements to building envelopes and systems depend on climatic conditions also the thickness of insulation. The objectives of the study were to develop a univariate framework for analyzing the seasonal effect of heat transfer from the opaque wall for low energy buildings and investigate changes in energy requirements all over the year for three cities in Turkey. The design of the methodology of the regression is applied to the opaque wall to determine the impact of four seasons according to selected parameters (city, orientation, insulation location). The responses of the design were analyzed using EViews software that offers statistical, forecasting and modeling tools. And the analytical tools of the software were used to confirm the best fit model. As a result, the main aspects of variance for each response variables are due to months of the year. City and orientation also insulation location of the building facade also are relevant for the heat transfer. The proposed regression methodology offers the correct identification of the seasons with the most effect on the external wall performance. The proposed model accounted that, energy output and insulation location are variables that interact mutually for different climates.

Keywords: Thermal insulation, Univariate Regression, Statistical Analysis, Low Energy Building, Insulation location, Wall orientation

International Conference on Science and Technology

ICONST 2018

5-9 September 2018 Prizren - KOSOVO

Using Carbon Dioxide Concentration to Determine Indoor Air Quality

Tugce Pekdogan[1]*, Mumine Gercek[1]

Abstract: It is important to analyze the ventilation performance of a building and to identify air leaks contributing to energy losses. Evaluating the carbon dioxide concentration based on the tracer-gas technique may be useful for obtaining air-tightness values. In addition, tracer gas measurements facilitate the determination of air exchange between indoor and outdoor environment under different ventilation conditions. In order to investigate the increasing quality of indoor air, the main objective of this study is to carry out an experimental study in the office room, considering the level of CO_2 as the indoor quality parameter in Izmir/Turkey. In this rectangular office building located in the northwest-southeast direction, the amount of indoor CO_2 is measured in this office unit facing the southeast direction. These measurements are made with the Testo 440 handheld CO_2 sensor. Measurements are taken at five-minute intervals when the office unit is not being used, increasing the amount of CO_2 by dry ice. In addition, in the outside environment, the device is controlled by measuring at the beginning. As the office is approximately 36 m^2, so there is only a single tracer injection point in its geometric center. The test is conducted according to the Standard ASTM E741. From the decay curve, two points decay calculation method is analyzed. The highest recorded concentration of CO_2 is 3267 ppm are provided, 430 ppm for outdoors and 3267 ppm for initial also the final point of the concentration is 527 ppm in 20 hours measurement. According to these parameters, the calculated ACR is 0.168 h^{-1}. Experiments are performed in an office room whose volume is 143.2 m^3 so the ventilation rate per m^3 per hour is 24.05 m^3/h which means 6.6 l/s (liter per second) and 13.98 cfm. It is found out that the most significant decay occurred between 01:11 and 06:11. This difference, which is considered influenced by changes in temperature, humidity, wind, etc. which occurs in outdoor measurements, also indicates the necessity of incorporating thermal comfort parameters into account. In this study, when the data are examined, the calculated speed is a singular value of a day and may show seasonal variability. Hence, measurements need to be repeated at different times of year to generate a comprehensive ventilation rate data. Also, a more detailed study is required to examine the effects of factors such as solar radiation, building envelope, type of heating system, number of users, existing furniture and equipment, etc. assumed to be effective on indoor air quality.

Keywords: Indoor environmental quality, Office, Carbon dioxide, Ventilation, Comfort.

[1]Izmir Institute of Technology, Faculty of Architecture, 35430, Izmir, TURKEY
*Corresponding author: tugcepekdogan@iyte.edu.tr

International Conference on Science and Technology

ICONST 2018

5-9 September 2018 Prizren - KOSOVO

Monte Carlo Modelling Of An Anti-Coincidence System For Gamma-Ray Spectroscopy

Necati Çelik[1]*, Selim Kaya[1], Uğur Çevik[2]

Abstract: Anti-Coincidence system consists of a detector shielded by generally NaI guard detectors to reduce the unwanted background signal produced as a result of Compton scattering of gamma-rays with the sample medium. An Anti-Coincidence system was designed using Monte Carlo simulation technique for gamma-ray spectroscopy. An HPGe detector was shielded by an annular and a plug NAI detectors in order to reduce the unwanted background signal that appear in gamma-ray spectroscopy. This system uses multiple detectors operated in anticoincidence mode to remove the scattering interactions that raise the Compton continuum from the spectrum. As a result of the suppression small peaks are allowed to be analyzed which might be deteriorated before the Compton continuum was suppressed. A disadvantage is that some real counts might be lost and hence the detection efficiency might be reduced in a certain extend.

Keywords: HpGe, NaI, Anti-Coincidence, Compton scattering.

[1] Gümüşhane University, Faculty of Engineering and Natural Sciences, Gümüşhane, Turkey
[2] Karadeniz Technical University, Faculty of Science, Department of Physics, Trabzon, Turkey
*Correspondingauthor: necati.celik@gumushane.edu.tr

International Conference on Science and Technology

ICONST 2018

5-9 September 2018 Prizren - KOSOVO

Numerical Solution of Momentum Equations for Newtonian Flow in Two Dimensional Cartesian Coordinate System

Ali Ateş[1]*, Eyub Canlı[1]

Abstract: Momentum equations and continuity equation obtained from general differential equations are solved by means of finite differences method that is one of the numerical solution methods, in two dimensional Cartesian coordinate system in this study. The governing equations organized according to laminar flow assumption at a channel flow considered for this purpose were discretized by means of the central difference and exponential schemes. Staggered grid was used during discretization and obtained algebraic equations were solved with PISO algorithm. The main aim of this work is to investigate the effects of central differences and exponential method that are members of discretization methods on solution results. Therefore results are discussed and compared by means of graphics formed using obtained outcomes-results. A computer software developed in DELPHI programming language was used in numerical solution. 3 different grid systems that are composed of 80x160, 160x320 and 320x640 nodes were used respectively for the solution. Additionally GCI analysis was done for the results that are obtained depending on the three different grid systems (coarse, medium and fine grids). The results of the present work are justified with graphical results from works on similar topics and they are found to be consistent. It is observed that exponential scheme is more successful than the central difference scheme when discretization methods are compared. 160x320 grid system is found sufficient according to conducted GCI analysis. Reynolds number appears to be an important parameter in this work. The effects of Reynolds number on the results are additionally discussed.

Keywords: Central Difference, CFD, Discretization, Exponential, GCI

[1] Selcuk University, Konya, Turkey
*Correspondingauthor: aates@selcuk.edu.tr

International Conference on Science and Technology

ICONST 2018

5-9 September 2018 Prizren - KOSOVO

In vitro Micropropagation of Endemic *Astragalus trifoliastrum* Species Native to Turkey

Mevlüde Alev Ateş*[1], Seher Karaman Erkul[2], Sevil Sağlam Yılmaz[1]

Abstract: *Astragalus* L. is the largest genus with 475 species and 64 sections in Turkey. Due to its general habitats 42% of these species are endemic to our country. These section species have been widely used in chinese traditional medicinal purposes. *Astragalus trifoliastrum* is one of these endemic species native to Eastern Anatolian Region of Turkey. Like all endemics, this species have difficulties in reproduction in nature. Where habitat management alone cannot conserve species threatened by human activity, micropropagation may advance species recovery. In this study we would like to try micropropagation of *Astragalus trifoliastrum* via its seeds that collected from its habitats in field studies. Seeds of *A.trifoliastrum* were used as materials. The seeds were cultured on MS media firstly for germination. After germination, two types of explants were used for micropropagation of the species. Hypocotyl and cotyledon explants were culture on MS media supplemented with kinetin (0.25, 0.50, 1.00, 2.00 mg/l) and their combinations with NAA (0.4 mg/l). After growth regulator treatment, propagated shoots were cultured in rooting media. MS media without growth regulators was very effective for seed germination in *in vitro* conditions (70%). Moreover hypocotyl explants and cotyledon explants gave different reactions for each different propagation media. Although there are some different studies on micropropagation of different species of *Astragalus* L. section, this is the first study on *A. trifoliastrum* species. This study may give up a point of view to the researchers for new studies due to use different plant growth regulators for propagation of the species. (This project was supported by Kirsehir Ahi Evran University Scientific Research Project Coordination Unit. with Project Number: ZRT.A4.18.016.)

Keywords: *Astragalus* L., micropropagation, *in vitro*, NAA, Kinetin

1 Departmant of Agricultural Biotechnology, Faculty of Agriculture, Kırşehir Ahi Evran University, 40200 Kırşehir, TURKEY

2 Department of Biology, Faculty of Arts and Sciences, Aksaray University, 68100 Aksaray, TURKEY

*Corresponding author: malev.ates@ahievran.edu.tr

International Conference on Science and Technology

ICONST 2018

5-9 September 2018 Prizren - KOSOVO

Molecular clock estimation on six *Astragalus L.* sections native to Turkey via cpDNA regions

Mevlüde Alev Ateş*[1], Seher Karaman Erkul[2], Zeki Aytaç[3], Zeki Kaya[4]

Abstract: *Astragalus* L. is the largest genus with 475 species and 64 sections in Turkey. Due to its general habitats 42% of these species are endemic to our country. In the current study six different sections (*Halicacabus, Megalocytis, Macrophyllium, Hymenostegis, Poterion and Hymenocoleous*) of *Astragalus* L. genus were used to estimate their divergence times. According to the nucleotide differences in DNA sequences, the molecular clock determines the times of species divergence. This gives us where and when the speciation start for this genus in evolutionary process. In the current study, cpDNA regions (*trn*L and *mat*K) were assessed to get molecular clock divergence time. For each region, the numbers calculated independently. Moreover, mutation rate was obtained as 2×10^{-3} of plant cpDNA as a constant value. Some *Astragalean* clade sequences were retrieved from NCBI database in order to interpret divergence time of *Astragalus* genus from others. Furthermore, new world *Astragalus* group species were included to understand the phylogenetic relationships between Turkish samples (Old World). The results indicate that estimated divergence time varied among geographic regions. Old World *Astragalus* diverged from other genus within Astragalean clade about 12.5 million years ago with respect to *trn*L intron and 14.5 million years ago regarding *mat*K regions of cpDNA. When the divergence times were estimated between available New world and Old world *Astragalus* species in the current study, the results indicated that New and Old world Astragalus species were diverged from each other about 7.3 million years ago with respect to *mat*K region. According to *trn*L and *mat*K regions, values of all six different sections were highly variable. Divergent time of *trn*L intron generally was later than it was *mat*K region. By using *trn*L non-coding region, value was 0.54 million years ago in the Pleistocene. Also, *Poterion* section was found to be diverged from other studied sections in same geological period as late Pleistocene based on *trn* L intron and *mat*K gene regions. Under the light of the results, it could be safe to say that *Poterion* section was younger than the other sections of *Astragalus* genus in evolutionary time.

Keywords: *Astragalus* L., molecular clock, cpDNA, *trn*L, *mat*K

1 Departmant of Agricultural Biotechnology, Faculty of Agriculture, Kırşehir Ahi Evran University, 40200 Kırşehir, TURKEY

2 Department of Biology, Faculty of Arts and Sciences, Aksaray University, 68100 Aksaray, TURKEY

3 Department of Biology, Faculty of Arts and Sciences, Gazi University, 06560 Ankara, TURKEY

4 Department of Biological Sciences, Faculty of Arts and Sciences, Middle East Technical University, 06800 Ankara, TURKEY

*Corresponding author: malev.ates@ahievran.edu.tr

International Conference on Science and Technology

ICONST 2018

5-9 September 2018 Prizren - KOSOVO

Effects of Different Chelated and Compost Fertilizer Doses on Digestion and Energy Values of Rangelands Hay

Fırat Alatürk[1]*, Ahmet Gökkuş[1]

Abstract: Rangelands is an important place in terms of quality and cheap feed production and animal fodder needs. But, in Turkey, rangelands have become in a condition that they cannot meet the needs of animals' fodder because of their improper way of manipulation. Therefore, in addition to enhancing rangelands improvement and fodder crops, the usage of rangelands in accordance with management principles and carrying out of development activities in rangelands such as fertilization in reduced yields will provide important contributions to cover up the gap of quality feed. This research has been carried out between 1st March, 2010 and 30th January, 2012 in Gerlengeç Village in Çanakkale Province, Turkey in order to determine the effect of fertilizing on rangelands hay chemical compositions. Experimental trails were established according to randomized complete block design using 4 replications. 5 and 10 kg 4M (organomineral, 5% N, 10% P, 25% organic matter) and 5 and 10 kg compost (N-P-K, 20:20:0) were used as fertilizer in this study. Plant samples were taken monthly from pasture four times from each plot of 0.5 m^2 area using cutting method. Hay samplings were done for the purpose to determine the chemical composition of rangelands hay once after every 10 days from 1st March to 1st May and from 1st May to 30th January once after every 30 days when plant growth was rapid. In this research, dry matter digestibility (DMD), consumption of dry matter (DMI), relative fodder value (RFV), total digestible nutrients (TDN), metabolic energy (ME) and net energy (NE_L) values of rangelands hay have been determined according to Moore (1994), Jahanzad et al. (2013), Lithourgidis (2006), Kaya (2008), Ball et al. (1996), Van Dyke and Anderson (2000). The obtained data were analyzed using SAS 9.0 statistical package program. Digestion and energy values of rangelands hay showed a significant increase depending on fertilizing, particularly, the doses of 5 and 10 kg of chelated fertilizer application were effective on DMD, TDN, ME and NE_L values, while the values of DMI and RFV increased with 10 kg 4M and 5 kg compost fertilizer applications. Digestion and energy values of the chelated and compost fertilizer applications of rangelands hay were increased significantly as compared to non-fertilized experimental plots. It is concluded that chelated or compost fertilizers would be suitable for the research area and similar ecologies as 10 kg/da N for obtaining high quality hay production.

Keywords: Chelated fertilizer, Compost fertilizer, Fertilizer dose, Digestible dry matter, Metabolic energy, Relative fodder value

[1]Department of Field Crops, Faculty of Agriculture, Çanakkale Onsekiz Mart University, Çanakkale, Turkey
*Correspondingauthor: agokkus@yahoo.com

International Conference on Science and Technology

ICONST 2018

5-9 September 2018 Prizren - KOSOVO

Effects of Some Herbicides on Upper and Subsoil Development of *Asphodelus aestivus* Brot. According to Different Dose and Seasonal Applications

Baboo Ali[1]*, Fırat Alatürk[1], Ahmet Gökkuş[1]

Abstract: Undesirable variations occurred in vegetation as the pasture is not manipulate in the lights of management principles. At the beginning of these, there are increases in the proportion of unwanted and toxic plant species. Amongst, *Asphodelus aestivus* Brot. is an important species and spreads in Mediterranean countries. This study was conducted aiming to increase the yield and quality of pasture and animal production subject to control this weed because it covers a huge area of pasture and it is also toxic to animals. Research has been carried out in Gerlengeç village of Biga District in Çanakkale, Turkey for a duration of 3 years from November 2014 to April 2015 and November 2017 to April 2018. Average number of *A. aestivus* per plot showed a variation from 20 to 30 plants/m^2. Research was established in three replications according to randomized complete block design. Research factors were consisted with five herbicides, their two different (applied and double) doses and two different seasonal (fall and spring) applications. Each plot was designed using 3 m^2 of area consisted of a total number of 60 experimental plots (5 herbicides x 2 doses x 2 seasons x 3 replications). Herbicide applications were done in autumn and early spring in November 15, 2014 - April 15, 2015 when newly emerged shoots of *A. aestivus* were starting to be appeared. Chlorosulfuron, glyphosate, dicamba+triasulphurine, methylsulphuron methyl+lodosulfuron methyl and tribenuron methyl+thifensulfuron methyl were used as active ingredients. Upper and sub soil developments of *A. aestivus* were examined. Data were analyzed using JMP 11 (SW) statistical package program. The number of plants significantly decreased from 30 plants/m^2 to 1-20 plants/m^2 depending on applied herbicides. Average plant height, leaf number, leaf width, leaf length and leaf weights decreased by 80-85%. Amongst the subsoil characteristics, average tuber weight per plant and average single tuber weight were recorded as 90-95%, tuber number and tuber length were 80-90% and a decrease of 68% was found in the average tuber diameter. Usage of different active ingredient herbicides along with their different doses in spring and autumn for the control of *A. aestivus* have weakened considerably the upper and subsoil development of plant. As a result, the most suitable active ingredients to be used to control this weed plant are glyphosate, methylsulfuron+lodosulfuron and tribenuron, the most suitable dose is two times of applied dose, and the most suitable season is spring.

Keywords: *Asphodelus aestivus*, herbicide, dose, season, chemical control

[1] Çanakkale Onsekiz Mart University, Faculty of Agriculture, 17100, Çanakkale, Turkey
*Corresponding author: alaturkf@comu.edu.tr

International Conference on Science and Technology

ICONST 2018

5-9 September 2018 Prizren - KOSOVO

The role of topography in the spatial distribution of tree species in the Mediterranean Region in the south of Turkey

Hüseyin Oğuz ÇOBAN[1]*, Süleyman ÇOŞGUN[2]

Abstract: Forest is an ecological system comprised of topography, climate, bedrock, soil and living organisms. These dynamic ecological variables have an impact on the existence of tree species that form forests and the structure of pure stands or other stands that they form with other tree species and the spatial distribution of stands. This study explored the impact of the topography on the spatial distribution of tree species that establish forests in areas under sea effect and areas that are not under see effect in the Mediterranean Region. A forest area of around 300,000 ha in Finike, Akseki and Elmalı forest directorates were explored. The association of the forests of Calabrian pine (*Pinus brutia* Ten.), Anatolian black pine (*Pinus nigra* Arnold.), Taurus fir (*Abies cilicica* Carr.), Taurus cedar (*Cedrus libani* A. Rich.), Juniperus spp. and Quercus spp. that are the main tree species in Turkey's forests with some variables which were elevation, slope and aspect were analysed. In this study, the digital elevation model of the study area was developed on the basis of the digital contour line data with a scale of 1/25000 with the help of the Geographic Information System (GIS). From those surface data, 3D analyses were conducted and the data on elevation, slope and aspect were driven. GIS-based spatial analyses were conducted to determine the spatial and areal distribution of the tree species in the study area. The results of the study demonstrated that *Pinus brutia* (Pb) was distributed up to 1700 m in Finike where Pb and and *Cedrus libani* (Cl) are the dominant tree species. It was observed that Pb could grow on the slopes of corridors that could transfer the sea effect into the inner parts in Elmalı and Akseki. In Akseki, *Pinus nigra* (Pn) and *Abies cilicica* (Ac) reached a certain size in the area and were mainly concentrated at elevations of 1100-1500 m and 1100-2000 m, respectively. Juniper species that were distributed mainly on the shady aspects (northwest, north, northeast and east) in Elmalı preferred sunny aspects (southeast, south, southwest and west) in other regions. Pb, Cl, Ac and Pn were distributed on shady aspects at lower elevations where their natural distribution started in each of the three regions while they are located mainly on sunny aspects at higher elevations. There is a similar situation also as regards juniper species in Elmalı. However, juniper and oak species are known to usually prefer sunny aspects. As regards the relation of forests with settlement and agricultural areas in the study sites, it was understood that forests were destroyed due to human impact, that's why they had to survive at higher slopes. It is suggested that information obtained from inquiries and analyses to be conducted through geographical information system should be used to protect the natural balance in forests and ensure their continuity while taking decisions that will affect the future of forests.

Keywords: Distribution of forests, Topography, GIS, Spatial analysis, Mediterranean Region

[1]Isparta University of Applied Sciences, Faculty of Forestry, 32260, Isparta, TURKEY
[2]Antalya Metropolitan Municipality, Antalya Water and Wastewater Administration, Antalya, TURKEY
*Corresponding author: hoguzc@gmail.com

International Conference on Science and Technology

ICONST 2018

5-9 September 2018 Prizren - KOSOVO

Road network analysis in Kovada Lake National Park in the south of Turkey based on Geographical Information System

Hüseyin Oğuz ÇOBAN[1]*, Seval ARSLAN[2]

Abstract: National parks are the areas that are allocated for the purpose of protecting the natural landscape, wild life and cultural assets. They enable people to feel the natural beauties and also create a strong bond between the uninterrupted wild life that could survive from past to present without artificial interventions, people and nature. Therefore, national parks are commonly preferred as recreational areas by people to get away from stress. Many national parks offer recreational and camping opportunities to visitors. It is important that visitors know how to access the parks, how they will walk around inside the park and the services it offers to them. Kovada Lake National Park located in Isparta province in the south of Turkey expect visitors with its unique natural beauties. Designated in 1970, this national park has a forest area of 4722,0 ha and lake area of 810,5 ha. The purpose of this study was to analyse the road network in Kovada Lake National Park. In this way, the baseline digital maps of transportation will be developed and contribute to further publicity of the park to visitors. The availability of the existing road map to pedestrians and vehicles was determined using the Geographical Information System. The entire road network available in the National park was toured on foot or by car. During these tours, the traces obtained by GPS were recorded in the geographical database and road data were classified. Furthermore, the possible location of the new pedestrian walkways was assessed, and new routes for pedestrian walkways were recommended for more efficient use of the park by visitors. The flora along the existing pathways or the proposed routes that the visitors will see was registered, photographed and uploaded to the geographical database. In this way, visitors to the national park will have advance information about the topographic structure of the pathway they will choose to follow in their tour and the flora they will observe along that route. Thus, recommendations for the planning of the road network required for effective use of natural resources in Kovada Lake National Park were proposed.

Keywords: Kovada Lake National Park, GIS, Road network analysis, Recreation

[1] Isparta University of Applied Sciences, Faculty of Forestry, 32260, Isparta, TURKEY
[2] Süleyman Demirel University, Graduate School of Natural and Applied Sciences, 32260, Isparta, TURKEY
*Corresponding author: hoguzc@gmail.com

International Conference on Science and Technology

ICONST 2018

5-9 September 2018 Prizren - KOSOVO

Investigation of the Effects of Land Cover Change on Wildlife, The Case Study of West Black Sea Region

Emre AKTÜRK[1], Ömer KÜÇÜK[1*], Özkan EVCİN[1], Kerim GÜNEY[1],

Abstract: Changes on land cover are one of the common topics in the literature currently, as they directly affect the habitat areas of plants and animals. Wildlife Development Areas (WDA) are important fields in the context of biodiversity, where hunting, wildlife and habitats are protected and sustainably developed by laws. Revealing both natural or man-made changes on vegetation cover in these areas is an important guide for current wildlife condition and future scenarios. For this reason, the land cover change of six wildlife development areas in the Western Black Sea Region was examined in this study. In this practice, it was aimed to determine the change of thirty years' land cover of the mentioned regions and to predict the effects on the wildlife existence in the regions according to the results. Geographical information systems (GIS) and remote sensing methods are used in the study. Three Landsat satellite images of vegetation-intensive periods were processed with the Supervised Pixel-Based classification method and control points were added to determine the accuracy of the results. In addition, the land cover was examined in four classes; wetlands, sparseley vegetated areas, areas with medium level vegetation and areas with dense vegetation. Finally, three land cover maps were created for the years 1986, 2000 and 2016 and used to illustrate the change from the past to the present day. According to the results obtained from the studies done, vegatation cover seems to increase significantly in all study fields. While the results generally showed a change to dense vegetation cover, in some areas an increase was observed in areas with medium level vegetation cover. In order to test the accuracy of the method used, 1340 control points were selected and a value of 0.85 kappa was obtained. An increase in openings in the forest could be an advantage for cervids who prefer these openings when considering about wildlife development. However, it should be noted that gaps in forests could also be a disadvantage for small mammals and species which are under the predator's pressure. For this reason such openings and land cover should be taken in the account by considering every species in the planning and management of wildlife. Thus, the results obtained with this study are thought to be important datasets for future management.

Keywords: Land cover, Wildlife Development Area, Wildlife, West Black Sea Region, GIS.

[1]Kastamonu University, Faculty of Forestry, 37150, Kastamonu, TURKEY
*Corresponding author: omerkucuk@kastamonu.edu.tr

International Conference on Science and Technology

ICONST 2018

5-9 September 2018 Prizren - KOSOVO

Medicinal Aromatic Plants Traditionally Used in Yenice YHGS (Karabük / Turkey)

Ayşe Öztürk[1]*, Kerim Güney[1], Erkan Babat[1]

Abstract: Forest ecosystems; besides the wood raw materials, it brings with it a variety of non-wood forest product (NWFP) services such as soil conservation, water production, biodiversity, recreation. Medical plants, edible plants, cosmetic plants, coloring plants, bulbous ornamental plants and mushrooms are also considered within the scope of Non-Wood Forest Products. Turkey is a very rich country in terms of natural resources such as geographical location, topographical diversity, climate, natural plant diversity, agricultural potential and so on. In this sense, it has significant potential in terms of NWFP, including aromatic plants by different ecosystems and rich flora owned primarily medicine. In the past, the local use of these plants has only been considered as traditional cultures, and today these plants have become an important source of national and international trade. In recent years, the importance given to NWFP and ethnobotanical studies in our country has increased and many studies have been carried out to reveal these values. The study area is located in Yenice district of Karabük. Karabük is located in the Black Sea region and it is represented by Europe -Siberian floristical and according to Turkey Grid System it also is in A4 square. In this study, the plants suitable for medicinal aromatic use from naturally grown plants in Yenice YHGS were determined by various literature researches. General information about the species, the part used, the way it is used and the area where it is used are given. Based on medicinal aromatic plants traditionally used and grown naturally in Yenice YHGS, evaluations have been made to determine the medicinal aromatic plant potential as well as to increase the medicinal aromatic uses of the species. Suggestions have been made on how to earn more income in the framework of sustainability without harming the nature by taking culture against unconsciously gathering and consumption of plants.

Keywords: Non-Wood Forest Products (NWFP), Karabük, Medicinal Plants, Aromatic Plants, Ethnobotany.

[1]Kastamonu University, Faculty of Forestry, 37150, Kastamonu, TURKEY
*Correspondingauthor: ayseozturk@kastamonu.edu.tr

International Conference on Science and Technology

ICONST 2018

5-9 September 2018 Prizren - KOSOVO

Evaluation of the Use of Natural Plants in Urban Habitats: Yenice Wildlife Development Area (Karabük/TURKEY) Example

Ayşe Öztürk[1]*, Kerim Güney[1], Erkan Babat[1]

Abstract: Although quite rich and has an important place in Turkey in terms of plant diversity, this wealth is not reflected in planting studies and the use of unnatural exotic plants is becoming widespread. Some of these alien species are threatening ecological balance by putting pressure on natural species due to their invasive nature, negatively affect the identity of the city and also harm the biodiversity. Yenice Wildlife Development Area selected as a study area has different vegetations such as forest, stream and pseudomaki due to its biogeographic location, climatic characteristics and size. It is possible to find plant taxa belonging to various phytogeographical regions at this region which is one of the most pristine and extensive forest areas of Turkey also gets into the Yenice Forests. This study aimed to make more use of natural richness and to guide the applications of planting in urban areas. Naturally grown plant species were identified in Yenice YHGS which contains plant species belonging to various forest habitats, aquatic habitats and arid habitats and the possibilities of use in planting different habitats according to urban ecology related to ground cover, rock gardens, aquatic, fence plants and climbing climber characteristics were evaluated. In addition to their visual qualities, natural plants are becoming increasingly important in planting studies because having more harmonious interaction with each other and with the environment they are in, and being more tolerant to environmental conditions, and providing shelter and food raw materials to living communities, and they are also economical. In addition, the use of natural plant species contributes to habitat continuity and ecosystem integrity. The use of plant species in natural habitats is also very important in terms of conservation and sustainability of genetic resources. In this sense, there is a need for planning and design studies to be carried out by considering natural species with high survival rates in urban and rural areas. By spreading the use of natural plant species, ecosystem balance and continuity can be provided by allowing passage corridors between natural vegetation and cities. In this context, it is necessary to determine the general properties and ecological requirements of the plant species to be used, as well as their visual and functional properties, and to determine their use potential in planting studies.

Keywords: Yenice, Use of Natural Species in Cities, Planting, Yenice Wildlife Development Area.

[1]Kastamonu University, Faculty of Forestry, 37150, Kastamonu, TURKEY
*Correspondingauthor: ayseozturk@kastamonu.edu.tr

International Conference on Science and Technology

ICONST 2018

5-9 September 2018 Prizren - KOSOVO

Usage Possibilities of Non-wood Forest Products of Forest Villagers (Eğirdir Province Case)

Ramazan Raimov[1], Hüseyin Fakir[1*]

Abstract: Recently, there has been increasing on demand for non-wood forest products. This demand increasing plays an important role in both commercial benefits and regional economic developments. For this reason, it is important to determine the availability and the usability of these non-wood products which are exist in Egirdir province for economic, social and environmental aspects.

Demographic and socio-economic structure of forest villagers in Egirdir, consumption purposes of non-wood forest products of the peasants consumption time, frequency of consumption, supply forms, consumed seen from vegetable products, benefits, and side effects, evaluations of influential factors in the consumption habits were put forwarded by this thesis study. A questionnaire which consist 25 questions was used for determining to consumer features.

In this study, 53 specimens belonging to 44 genera of 26 families were evaluated. In addition, a database includes scientific name, family, usable parts, usage of regional and determination of endemics, regional and national benefits were designed.

According to the results of this research; the consumers use these plants for general health, therapy and for pleasure. Consuming type is as infusion and decoction on large scale and also there is a big deficiency by means of using dose and side effect. Consuming of native plants is preferred as in form naturally collected from nature. Among the factors that affect consumption behaviors, recommendations of family and relatives are first place. In this regard, traditionalism dominates the formation of consumption habits.

Keywords: Forest Villagers, Non-Wood Forest Products, Eğirdir, Isparta.

[1]Isparta University of Applied Sciences, Faculty of Forestry, 32260, Isparta, TURKEY
*Correspondingauthor: huseyinfakir@isparta.edu.tr

International Conference on Science and Technology

ICONST 2018

5-9 September 2018 Prizren - KOSOVO

Relationships Between Forest Vegetation, Plant Diversity and Some Environmental Factors in Türkmen Mountain (Turkey)

Münevver Arslan[1]*, Serkan Gülsoy[2], Rıza Karataş[1], Ertan Şeref Koray[3], Aliye Sepken Kaptanoğlu[1], Ahmet Mert[2], Kürşad Özkan[2]

Abstract: In Turkey, many flora studies have been conducted on plant species richness. However, these studies reveal only plant species numbers. In some vegetation studies, some data are insufficient. The purpose of studying the diversity of plant species in Türkmen Mountain forest vegetation, which contains different plant communities; 1- To determine the species diversity of the study area by different indices (alpha, beta and gamma) and modelling the relationships between species diversty and some environmental factors. 2- To determinate the species diversity of plant groups and sample areas to compare the data obtained as a result of numerical analysis

The material of the work is the vascular plants in the forest of Türkmen Mountain which is between Eskişehir and Kütahya Provinces. The sampling plots belongs to vegetation were obtained by using Braun-Blanquet method. Two sub-sampling plots (totally 190) were taken under the plots (100 x 100 m^2). The size of per sub-sampling plot is 400 m^2 (20 x 20 m^2). The data of the sampling plots were stored in TURBOVEG Database Program and analyzed with Jaccard distance measure and flexible beta (-0,25) from group linkage method in PC-ORD software. The indicator taxa of plant groups were determined in the JUICE Program. The relationships between plant groups and bedrock formations which are in the form of presence and absence data were analyzed by Pearson Chi Square Test Statistic. The relationships between other variables (coverage of the tree layer and the shrub layer, radiation index (RI), altitude, slope and location) and plant groups were analyzed by Wilcoxon Rank Sum Test. Shannon H and Simpson 1-D from the alpha (α) diversity indices and beta (β_w) diversity index were calculated in Past Package Program. Gamma diversity (γ) was directly determined for plant groups as the sum of different species. The relations between α, βw and γ plant diversity values of the sample plots and environment variables were analyzed with regression tree method in DTREG software. As a result of the regression tree analysis, the model variables with the highest explanation value for the diversity indices were elevation, tree and shrub coverage, bedrock formations, slope and radiation index. Similar results were obtained as a result of the analysis for the distribution of plant groups. As a result, Türkmen Mountain forest vegetation is divided into 9 plant groups. When the three diversity indices are evaluated together, plant groups with the highest species diversity were Group 1 (*Pinus nigra* subsp. *pallasiana* – *Cistus laurifolius*), Group 2 (*Pinus nigra* subsp. *pallasiana* – *Dactylis glomerata* subsp. *hispanica*), Group 4 (*Pinus nigra* subsp. *pallasiana* – *Quercus petraea* subsp. *iberica*) and Group 8 (*Pinus sylvestris* – *Galium rotundifolium*). For the sustainability, monitoring and protection of species diversity, it will be appropriate the planning according to the factors affecting species diversity and species diversity of plant groups.

Key Words: Alpha, Beta and Gamma diversity, Species diversity, Forest vegetation, Türkmen Mountain (Turkey)

Acknowledgement: This study was supported by the research project "Relationships Among Plant Communities, Plant Diversity and Some Environmental Factors In Türkmen Mountain (ESK – 16 (6312) / 2013-2016)" from the Research Institute for Forest Soil and Ecology (Turkey)

[1]Research Institute for Forest Soil and Ecology, p.b. 61, 26160, Eskişehir, TURKEY
[2]Suleyman Demirel University, Faculty of Forestry, 32260, Isparta, TURKEY
[3]Regional Directorate of Forestry, 26010, Eskişehir, TURKEY
*Corresponding author: arslan28@yahoo.com

International Conference on Science and Technology

ICONST 2018

5-9 September 2018 Prizren - KOSOVO

Geometric Optimization of Elevator Motor Brake Disk by Finite Element Analysis

Semih Yüksel[1]*, Melih Küçükçalık[1], Zeki Alyanak[1], Selim Hartomacıoğlu[2]

Abstract: Electromagnetic brake for elevator is the most important component of elevator system due to safety. The brake system consists of disk, pad, springs, pressure plate, electromagnetic system, and other mechanic parts. The disks is the critical part of the brake. The disk must be able to withstand the moment due to elevator total capacity.

In this study, the disk was modelled by using computer aided design (CAD) software with parametric. Then the model convert to computer aided engineering (CAE) software. The finite element simulaiton was performend, and the parameters were optimized by using Response Surface Method (RSM). During the simulation, also, the mesh parameters were optimized. The output parameters of simulation are strain, von-misses stres, total deformatin, and fatigue life. The material properties of disk were determined by using experimental test methods. During this study, the hybrid methods named Finite Element Simulation (FEM) and Response Surface Method (RSM) wa used.

As a results of this study, optimal design parameters of disc were determined to be used in elevator electromagnetic brake system for an elevator of 800 Kg. The fatigue life, strin, total deformation and Von-Misses stress were determined and figured in the paper.

From this results, it was determined that the disk design parameters are important effects on the disk fatigue life and strength. The method used in this study can be used in optimization of design parameters of elevator system.

Keywords: Elevator brake disk, Finilet element simulation, Respon surface method, Optimization

1Department of Research &Development-Arkel Elektrik ve Elektronik San. ve Tic. A.Ş. 34885,Istanbul, TURKEY
2Bilig Yenileşim San. Tic. Ltd. Şti.34906, Istanbul TURKEY
*Corresponding author: semihyuksel@yandex.com

International Conference on Science and Technology

ICONST 2018

5-9 September 2018 Prizren - KOSOVO

Alpine Flora of Great Hacet Hill at the Ilgaz Mountain

Kerim Güney[1]*, Rüknettin Tekdemir[2]

Abstract: This study was carried out in 2001-2004 on the Alpine Flora of Ilgaz Mountains. The study area is located between Kastamonu and Çankırı provinces. The material of this study is plant species that distributed in Great Hacet Hill at the Ilgaz Mountain. The literature was searched and the existing plant species were determined. The Alpine region was observed for 4 years and plant samples were collected. The climate of the study area, the peak of the mountain, were estimated as an oceanic type by interpolation techniques, due to the lack of the meteorological data at this elevation (2000-2586 m). The flora of study area consists of 261 taxa which belong to 41 families and 139 genera.

Keywords: Ilgaz Mountain, Alpin Flora, Biodiversity.

Acknowledgement: This research was supported by Gazi University Scientific Research Projects Unit (32/ 2003-02).

[1]KastamonuUniversity, Faculty of Forestry, 31500, Kastamonu, TURKEY
[2]Gazi University, Graduate School of Natural and Applied Sciences, 06500, Ankara, TURKEY
*Corresponding author: kguney@kastamonu.edu.tr

International Conference on Science and Technology

ICONST 2018

5-9 September 2018 Prizren - KOSOVO

Floristic Diversity and EUNIS Habitat Types of Saros Gulf

Kerim Güney[1]*, Latif Kurt[2]

Abstract: This study was carried out between 2013 and 2014 in order to reveal the biodiversity of the Saros Gulf. In order to demonstrate biological terrestrial and nautical variety of Saros Gulf Special Environment Protection Area in this study has been performed for 720 days, biological components of Saros Gulf was researceh and physical and chemical properties of Saros Gulf registered with that report. The results are targeted to be basic for direction plan in Saros Gulf. The material of this study is plant species that distribute in Saros Gulf. Firstly, the literature was searched and the existing plant species were determined. Later habitats representing the research area were identified. EUNIS habitat types have been revealed by the identification of the plant species in the sampling areas representing the habitats. Finally, literature and field observations were combined to reveal floristic diversity. 1345 plant taxa were collected from the research area. In the year 2012-2014 for the 4 seasons as a result of the field studies; 5 different essential habitat types have been determined from the point of flora in the field. It is the most comprehensive biodiversity study to date in the field of research. This research has provided a basis for further work to be done in more detail.

Keywords: Saros Gulf, Turkey, Biodiversity

Acknowledgement: We would like to thank the Ministry of Environment and Urbanism for financial support for the project.

[1]KastamonuUniversity, Faculty of Forestry, 31500, Kastamonu, TURKEY
[2]Ankara University, Faculty of Science, 06100, Ankara, TURKEY
*Corresponding author: kguney@kastamonu.edu.tr

International Conference on Science and Technology

ICONST 2018

5-9 September 2018 Prizren - KOSOVO

Testing Daylight Performance In A Classroom In Terms Of Window-To-Wall Ratio And Glazing Transmittance Variations

Yasemin Öztürk[1]*, Arzu Cılasun Kunduracı[2], Tuğçe Kazanasmaz[1]

Abstract: Providing adequate amount of daylight helps students to increase their productivity and success. Well designed daylit spaces can be achieved by not only designing appropriate room and window geometries, but also considering material qualities. Window-to-wall ratio (WWR) is one indicators for the former criteria, glazing transmittance is the other indicator for the latter criteria. Both of them define the characteristics of façade and effective aperture. This study aims to present results of changes in glazing transmittance and WWR in a classroom to test the daylight performance at each proposed model.

A classroom having 55.8 m^2 floor area and a south facing façade is chosen for analyzing modifications in illuminance. Two desks, one is near to the wall side and another is near to window side are placed in Velux Daylight Visualiser 3 simulation software. Glazing transmittance is calculated as 78% during field measurements and existing WWR is calculated as 62.16%. The concern about proposed models are derived from the fact that at which ratio illuminance at the wall side can be increased and illuminance at the window side can be decreased when we use low-E glazing with lower transmittance values and glass curtain wall with higher window area. First model included a variation of glazing transmittance from 78% to 42%; since the main concern was to test a case corresponding to a low-E glazing with film coating having lower transmittance values. Second model is based on an increase of WWR from 62.16% to 83.93%. That modification correspond to how much illuminance on the wall side desk can rise referring to the glass curtain wall.

Illuminance on desks are 222.7 lx and 415.9 lx respectively for 21th June 09:00 simulation at clear sky condition at the existing conditions. So, the former illuminance is below the required work plane daylight illuminance, 300 lx according to IES. Illuminance on desks became as 121.3 lx and 220.3 lx respectively in the first model. When WWR increased at 21,77 % range and illuminance on desks are increased to 246.6 lx 491.5 lx respectively.

Illuminance on the wall side desk increased to 10.7 % on the first proposed model and illuminance on window side desk decreased by 47% with the second proposed model. Considering the proposed models, the most pleasant illuminance results are obtained for 09:00 simulation at the second model on 21th March, for 12:00 simulation at the first model on 21th September, and for 15:00 simulation at the second model on 21th December.

Keywords: Daylighting, Window-to-wall ratio, Glazing transmittance

[1]İzmir Institute of Techology, Faculty of Architecture, 35430, İzmir, TURKEY
[2]Yaşar University, Faculty of Architecture, 35100, İzmir, TURKEY
*Corresponding author: yaseminozturk@iyte.edu.tr

International Conference on Science and Technology

ICONST 2018

5-9 September 2018 Prizren - KOSOVO

Design and Overall Artificial Lighting Analysis of a Multifunctional Canteen

Yasemin Öztürk[1]*, Tuğçe Kazanasmaz[1] ,Arzu Cılasun Kunduracı[2]

Abstract: A space, which enables students to accomplish several activities at one place, helps to save time and increase their productivity. Therefore, the purpose of the study is to improve an existing multifunctional eating facility area in terms of its function, color and lamp choices.

A faculty canteen whose floor area is 236 m^2, is the case study to observe the effects of layout and luminaire changes to create a visually efficient and comfortable multifunctional place. To achieve this, existing artificial lighting conditions are determined. Within the space, there are two main areas: food preparation and eating area which illuminated by 20 suspended mounted luminaires for general lighting and 2 pendant luminaires for food preparation area. First, existing conditions are simulated in Dialux 4.13. Secondly, a new lighting design is proposed considering other relevant functions such as; drawing-eating area, reading area and exhibition area for the scale models. Food preparation area is redefined via cash point, juice center and kitchen area. Artificial lighting needs are arranged locally and analyzed for each of these functions individually. For general lighting, 12 LED ceiling recessed luminaire having 1400 lm are used while for kitchen and drawing-eating area 10 LED continuous row luminaire having 5260 lm, reading area has 4 LED recessed wallwasher having 4400 lm, and juice center contains 6 LED pendant luminaires having 2100 lm were used. In addition to those, localized lighting provided by 4 LED wallwasher spotlight having 1400 lm at exhibition area, and 2 recessed luminaire unit LED spotlights (having 499 lm) were applied over cash point and drawing desk.

Existing canteen's average illuminance level was simulated as 497 lx at eating area and 133 lx at kitchen area. With the proposed lighting design, average illuminance of 458 lx is obtained at drawing-eating and reading area, 338 lx at exhibition area and 196 lx at conversation area. New design's average illuminance is calculated as 277 lx and uniformity is 0.34, and illuminances ranging from 200 lx to 500 lx for the parts according to demands.

It is found that canteen's new lighting design gathers several functions such as eating, reading, drawing, exhibiting, and food preparation at one space, yet, each functions' visual requirements were provided locally. Thus, a multifunctional area where efficient and user friendly lighting design is proposed as a contribution to the practices.

Keywords: Artificial Lighting, Multifunctional spaces, Eating area lighting

[1]İzmir Institute of Techology, Faculty of Architecture, 35430, İzmir, TURKEY
[2]Yaşar University, Faculty of Architecture, 35100, İzmir, TURKEY
*Corresponding author: yaseminozturk@iyte.edu.tr

International Conference on Science and Technology

ICONST 2018

5-9 September 2018 Prizren - KOSOVO

Hydrodynamic Analysis of Rotational Printing in Fused Deposition Modelling

Ramazan Aslan[1], Osman Turan[1*]

Abstract: Nowadays, additive manufacturing (AM) known as 3D printing is one of the most popular method to create prototypes in many different engineering areas such as aerospace, automotive, biomedical and energy industries. Although there are several different methods of 3D printing, the most widely used is a process known as Fused Deposition Modeling (FDM), which is an extrusion based AM technique. FDM printers use a thermoplastic filament, which is heated to its melting point and then extruded, layer by layer, to create a three dimensional object. Thermoplastic metarials used in FDM exhibit shear thinning fluid behavior where the viscosity decrease with increasing shear rate. A number of empirical models have been proposed for describing the interrelation between shear stress and strain rate in shear thinning fluids, however, the power-law model is used, which is the simplest model, in current study as in many studies in the literature. This paper presents the hydrodynamic analysis of rotational printing in fused deposition modelling. The steady-state laminer flow of inelastic non-Newtonian fluids obeying a power law model in a rotating nozzle has been numerically analysed based on axisymmetric incompresibble flow conditions. It has been considered that the velocity components are identically zero due to the no-slip conditions and the impenetrability of the surface of the nozzle. A commercial package ANSYS-FLUENT, which has previously been utilised successfully for simulating non-Newtonian fluids, has been used in the numerical investigation. The governing equations are solved iteratively in the framework of the finite-volume methodology by applying the boundary conditions. The convective terms are discretized using a second-order upwind scheme, whereas the diffusive terms are discretized by a second-order central differencing scheme. The coupling between pressure and velocity is obtained using the well-known SIMPLE (Semi-Implicit Method for Pressure-Linked Equations) algorithm. The criterion of convergence was taken to be 10^{-6} for all the relative (scaled) residuals. In this study, the effects of nozzle rotation speed have been investigated on the velocity and pressure field for different nozzle diameters. It has been found that the pressure at the entrance of the nozzle die zone, which should be large enough to force material out through the nozzle for a good extrusion to be achieved in FDM, rises with increasing the nozzle rotation speed. It is also observed that the flow pattern in the rotating nozzle configuration is significantly different from those in the stationary nozzle configuration. A circulation appears at the entrance of nozzle in the rotating nozzle configuration and the size of this circulation increases with increasing the nozzle rotate speed. In addition to numerical investigation, thermodynamic and scale analysis have been carried out to elucidate the possible influence of the nozzle rotate speed on the pressure field. Both analysis also indicates that the pressure at the nozzle die zone increases with increasing the nozzle rotate speed as observed in the numerical analysis.

Keywords: 3D printing, Fused deposition modelling, FDM, Rotating nozzle, Extruder

[1]Bursa Technical University, Mechanical Engineering Department, 16310, Bursa, TURKEY
*Corresponding author: osman.turan@btu.edu.tr

International Conference on Science and Technology

ICONST 2018

5-9 September 2018 Prizren - KOSOVO

Investigation of Tool Wear and Delamination Factor for Lightweight Aerospcae AlSi10 Metal Foam Drilling Under CO_2 Based Cryogenic Cooling Conditions

Oguz COLAK[1]*, Lokman YUNLU[2]

Abstract: AlSi10 metal foam is a structural component used in the aerospace industry due to the lightweight based materials. These materials are known as discontinuous, and hard to machinability. In this study, cryogenic cooling technology was used to determine the effect of tool life on the drilling of the AlSi10 metal foam material. Tool wear progression was recorded for the following coolant options: cryogenic CO_2, under different drilling conditions. In this study CO_2 based sustainable coolant techonology is applied to drilling of AlSi10 metal foam materials. Tuguchi based L9 experimental drilling test was made under different drilling conditions (cutting speed Vc m/min and feed rade mm/rev) and different cooling condirions (Dry, 5 bar CO_2 coolant and 10 bar CO_2 coolant conditions). Cutting forces (Fx, Fy, Fz (N)), tool wear rates (µm) and drilling hole delamination factors were measured after each testing. Anova based analysis were carried out after drilling test of AlSi10 metal foam materials. 5 bar CO_2 coolant conditions show best tool wear results after drilling test. Lowest delamantion rates were exemined under dry coolant. Test results shows Cryogenic coolant technology was improve to tool life for AlSi10 foam metal drilling condition. But delamination factor were not effected coolant conditions.

Keywords: AlSi10 Metal Foam, Drilling, Tool Wear, Cryogenic Cooling, Aerospace Machining

Acknowledgement: This study were supported Suleyman Demirel University, CAD/CAM Research and Application Center.

[1] Eskişehir Teknical University, Engineering Faculty, Mechanical Engineerin Departmet, 2655 Tepebaşı, Eskişehir/TURKEY
[2] Mehmet Akif University, Engineering Faculty, Mechanical Engineerin Departmet, Burdur/TURKEY
*Corresponding author: oguzcolak@anadolu.edu.tr

International Conference on Science and Technology

ICONST 2018

5-9 September 2018 Prizren - KOSOVO

Drilling Force Modelling of Aerospace Carbon Fiber Rainforced Conposite Under Cryogenic Drilling Conditions

Oguz COLAK[1]*, Lokman YUNLU[2]

Abstract: Carbon Fiber Rainforced Composite (CFRP) mainly using in aerospace industry because lightweight strong materials. But these CFRP known as hard machinablity. Drillimg of this kind of materials is too hard. Expensive PCD based diomand drilling tool using for to get better tool life. Nowadays advanced coolant technology is applying to improve tool life. In this study CO2 based advanced cryogenic cooling is applied to machinig test for to get better tool life results. In this study CO_2 based sustainable coolant techonology is applied to drilling of CFRP materials. Tuguchi based L9 experimental drilling test was made under different drilling conditions (cutting speed Vc m/min and feed rade mm/rev) and different cooling condirions (Dry, 5 bar CO_2 coolant and 10 bar CO_2 coolant conditions). Cutting forces (Fx, Fy, Fz (N)), were modelled with experimental tests and drilling hole trust forcs were simulated for different tool geometrical conditions. Advanced analytical simulation based analysis of crayogenic drilling conditions were caried out after drilling test of CFRP materials. Suitable drill type were exemined under simulation conditions. Test results shows Cryogenic coolnat technology was improve to tool life for drilling of CFRP materials. The best drill tool geometry was found after simulation results.

Keywords: CFRP Drilling, Drilling, Drilling Simulation, Cryogenic Cooling, Aerospcae Composite Drilling

Acknowledgement: This study were supported Suleyman Demirel University, CAD/CAM Research and Application Center.

[1] Eskişehir Teknical University, Engineering Faculty, Mechanical Engineerin Departmet, 2655 Tepebaşı, Eskişehir/TURKEY
[2] Mehmet Akif University, Engineering Faculty, Mechanical Engineerin Departmet, Burdur/TURKEY
*Corresponding author: oguzcolak@anadolu.edu.tr

International Conference on Science and Technology

ICONST 2018

5-9 September 2018 Prizren - KOSOVO

Experimental Investigation of Mechanical and Tribological Properties of Traditional and Waste Reinforced Al6061 Metal Matrix Composites

Serkan ATES[1], Lokman YUNLU[2]*

Abstract: In this study Al6061 alloy as matrix material, SiC and Al_2O_3 ceramics which are frequently used in automotive industry as traditional reinforcements and blast furnace slag as waste reinforcement material. Blast furnace slag is a side product that is turned on during iron production in blast furnaces in iron and steel plants. Iron ore, limestone and coke are used as raw materials in demi production. Dual and triple hybrid composites were produced with single composites by using traditional and waste reinforcement materials. onolithic composites and hybrid composites were produced using the two-stage mixing casting method, which is liquid state production methods. In this method, the Al6061 alloy is first heated to 700ºC, then the alloy temperature is lowered to 600ºC and the alloy, which is semi-solid at this temperature, is preheated to 250ºC and added by hand. The microstructures of the produced composites were investigated by scanning electron microscopy. The porosity values obtained from EDS analyzes were calculated with Archimedes principle and the hardnesses were determined by Brinell hardness measurement method. It has been determined that the hardness of the composites increases with the increase of the weight ratio of the composites added in the hardness tests and the blast furnace slag powder is almost as effective as SiC and Al_2O_3 in increasing the hardness of the composites. The blast furnace slag we use as reinforcement element in the production of double and triple hybrid composites with monocomponent has increased the fatigue strength of Al6061 up to 11% by weight of reinforcement. Test results shows Blast furnace slag increased the fatigue strength of double and triple hybrid composites.

Keywords: Aluminum matrix composite, blast furnace slag, fatigue

[1,2] Mehmet Akif Ersoy University, Engineering Faculty, Mechanical Engineerin Departmet, Burdur/TURKEY
* Corresponding author: lyunlu@mehmetakif.edu.tr

International Conference on Science and Technology

ICONST 2018

5-9 September 2018 Prizren - KOSOVO

Investigation of Fatigue Behaviors of Traditional and Waste Reinforced Metal Matrix Composites

Serkan ATES[1], Lokman YUNLU[2]*

Abstract: In this study, Al6061 alloy as a matrix material, SiC and Al_20_3 ceramics which are frequently used in the automotive industry from traditional reinforced elements and marble dust obtained by powdering marble pieces. Besides single composites, Dual and triple hybrid composites were produced by using traditional and waste reinforced materials. powders with a powder size of 22-59 µm which will be used in our study were obtained by carrying out sieve analysis of the marble powder. For the fatigue strengths of the composites produced, 9 different stress value were measured until the samples were broken off by using the rotary curvature fatigue device. Three samples were produced from each sample and the prototype quantities and brinell hardness values were determined. Thus The reliability of the measurements is increased. The marble dust we used as reinforcements in the production of single and double composite and triple hybrid composites has increased the fatigue strength of A16061 to 11% by weight of reinforcement. Three samples were produced from each sample and the prototype quantities and brinell hardness values were determined. Thus The reliability of the measurements is increased. The marble dust we used as reinforcements in the production of single and double composite and triple hybrid composites has increased the fatigue strength of A16061 to 11% by weight of reinforcementIt has been determined that the hardness of composites increases with the weight ratio of the compound added in the hardness tests and that the marble powder is almost as effective as SiC and Al_2O_3 in increasing the hardness value of the composite. It has been determined that the increase in fatigue strength of marble dust Al6061, which we use in composite and hybrid composite production, increases as the weight ratio of marble powder used increases.

Keywords: Aluminum matrix composite, marble dust, fatigue, hardness, porozite

[1,2] Mehmet Akif Ersoy University, Engineering Faculty, Mechanical Engineerin Departmet, Burdur/TURKEY
* Corresponding author: lyunlu@mehmetakif.edu.tr

International Conference on Science and Technology

ICONST 2018

5-9 September 2018 Prizren - KOSOVO

Chemical Properties and Therapeutic Effects of Thermal Waters in Zilan Valley and Their Relations with Geological Units (Erciş -Van, Turkey)

Hacer Düzen[1]

Abstract: In this study, therapetic effects of thermal waters were investigated in Zilan valley, eastern part of the Turkey. Purpose of this study is determination of chemical properties of thermal waters and investigation of therapautic effects of them in terms of human health. Also relations between chemical properties of thermal waters and geological units were investigated in Zilan Valley. Samples were collected from five sample points and anion / cation analyses were carried out for five thermal water samples (from three thermal wells and two thermal springs). First well was drilled in 1988 by MTA (Mining Research Center in Turkey) and sample was collected by MTA in 1988. Also other two thermal wells were drilled by MTA and samples were collected in 2000 by MTA. Analyses were carried out by MTA in 1988 and 2000. Two thermal spring waters were collected in 2014 in content of this study. Anion / cation analyses were carried out in content of this study in ACME Analytical Laborataries. Also, geological map of the Zilan Valley was prepared in content of this study. As a result of the study, water types were detected as Na-Cl type for all thermal well waters (numbered ZG-1, ZG-2 and ZG-3 wells) and numbered 111 thermal spring. Water type was detected as Na-Cl-SO4 for numbered 112 thermal spring. Thermal waters with Na-Cl have a lot of therapeutic effects. Thermal waters with Na-Cl can be used in rheumatism, gynecologic diseases, neuritis, treatment of unconsolidated fractures and at the upper respiratory tract diseases. Geologically, all thermal waters are originated from marl (limestone with clay) units in Kızıldere Formation in the Zilan Valley. Cap rocks of the thermal system are Aladağ volcanics. Thermal waters in Zilan Valley are so important for human health and they should be use for treatments.

Keywords: Therapeutic, Chemical, Geological, Thermal, Zilan, Turkey

[1]İstanbul University, Faculty of Engineering, 34320, İstanbul, TURKEY
*Corresponding author: hcrduzen@gmail.com

International Conference on Science and Technology

ICONST 2018

5-9 September 2018 Prizren - KOSOVO

Computer analysis of the porous structure of activated carbons prepared from biomass

Mirosław Kwiatkowski[1]*, Jagoda Worek[1], Elżbieta Broniek[2]

Abstract: The activated carbons are amorphous graphitic carbon, consisting of SP2 hexagonal carbon layers with different sizes of pores ranging from micropores to macropores. The adsorption properties of the mentioned materials result from their significant surface and structural properties, in particularly high specific surface area and adsorption capacity. Activated carbons are produced from different raw materials of organic origin including biomass waste. The choice of raw material for the production of activated carbon is determined by the ultimate designation of the activated carbon as well as the availability and price of the raw material. Particularly wood processing industry and the carpentry industry as well as food processing industry have a huge potential of waste biomas, which can be successfully used for the production of active carbons. The arguments for the use of biomass waste for the production of activated carbons include relatively low cost of production, easy accessibility of the raw material and its renewability. In the present study, was considered the possibility of the production of activated carbon from biomass waste by means of chemical activation. In this study, in particular, the influence of the mass ratio of of activator's dry mass to the carbonizate mass, on the formation of the microporous structure of the obtained activated carbons was analysed. The new LBET method, was used for the calculations performed as part of this research. The LBET method is based on the original mathematical models of adsorption on heterogeneous surfaces, originating from an unique uniBET multilayer adsorption theory and the the fast multivariante identification numerical procedure of adsorption systems. Results of the research presented in this article highlighted the significant potential of the production of activated carbons with very high adsorption capacity and large specific surface area from wood, by means of activation with potassium hydroxide. Activated carbons obtained as part of the research are characterised, in fact, by adsorption properties virtually similar to those of the best carbon adsorbents obtained from homogeneous polymers. The presented research projects yielded a broad spectrum of information and shed a new light on the issues pertaining to the assessment of the effect of carbonaceous adsorbent production technology on the parameters of the microporous structure produced, which was also possible thanks to the application of LBET method to the analyses.

Keywords: Activated Carbons, Adsorption, Chemical Activation, Micropores, Numerical Methods.

Acknowledgement: The work was financed by the AGH University of Science and Technology in Krakow Grant No. 11.11.210.373, as well as a statutory activity subsidy from the Polish Ministry of Science and Higher Education for the Faculty of Chemistry of Wrocław University of Technology.

[1]AGH University of Science and Technology, Faculty of Energy and Fuels, al. A. Mickiewicza 30, 30-059 Krakow, POLAND
[2]Wrocław University of Technology, Faculty of Chemistry, Gdanska 7/9, 50-344 Wrocław, POLAND
*Corresponding author: kwiatkow@agh.edu.pl

International Conference on Science and Technology

ICONST 2018

5-9 September 2018 Prizren - KOSOVO

On Soft b-open Sets and Some New Seperation Axioms

Yunus Yumak[1]*, Aynur Keskin Kaymakcı[2]

Abstract: The notion of soft topological spaces introduced by Shabir and Naz. Also Shabir and Naz defined basic notions of soft topological spaces as soft open sets, soft closed sets, soft subspaces, soft closure and they established their several properties. Kandil et al. introduced new soft seperation axioms based on the soft semi open sets which are more general than the soft open sets. In this study, we define the notions of soft b-Di (for i = 0, 1, 2) spaces. We also obtained some properties and characterizations of these notations. Then, we gave the soft b-irresolute function notion by using soft b-open sets. Finally, we investigate above some soft separation axioms if they are preserved or not under soft b-irresolute functions. Soft topological spaces and general topological spaces. Some soft separation axioms are investigated if they are preserved or not under soft b-irresolute functions. The soft b-Di (for i = 0, 1, 2) spaces we defined maybe studied if they are transfered into the other areas of general topology.

Keywords: Soft open, Soft b-open, Soft bTi-spaces, Soft bDi-spaces.

[1]Selcuk University, Faculty of Science, 42100, Konya, TURKEY
[2] Selcuk University, Faculty of Science, 42100, Konya, TURKEY
*Corresponding author: yunusyumak@selcuk.edu.tr

International Conference on Science and Technology

ICONST 2018

5-9 September 2018 Prizren - KOSOVO

Plasma Enhanced Modified (Low Temperature and Shortened Time) Disperse Dyeings of Polyethylene Terephthalate Fabrics with Improved Fastness Properties

İbrahim Oğuz[1], Bengi Kutlu[1]*

Abstract: Regarding environmental issues, the effect of low temperature plasma treatment on dyeing of polyester fabrics with disperse dyes in terms of low temperature, short time and improved fastness were aimed in this study. Plain weave 100% polyester fabrics were subjected to low frequency plasma treatments under various power and durations using acrylic acid (AA) monomer. Plasma polymerization treatments was investigated by water absorption, ESCA and SEM analysis. Then dyeing was performed and color measurements were realized. Results were compared with dyed untreated fabrics. Washing and rubbing fastness were also examined. Were modified superficially by low frequency acrylic acid plasma polymerization technology. Water absorption test and ESCA (electron spectroscopy for chemical analysis) were applied to understand the effetcs of plasma treatments. Untreated and plasma treated fabrics were dyed by disperse dyestuffs by conventional method and also dyed at low temperature and at short time to obtain effects of plasma on dye uptake of fabrics. Color measurements, washing and rubbing fastness tests were used to investigate the effects of plasma on permanentness of short time (30minutes) and low temperature (110^{o}C) dyeings compared to coventional disperse dyeing. This study's general result was acrylic acid plasma polymerization technique was effective on dye uptake of polyester fibers in disperse dyeing. However, high impact result of the work was short time (30min) disperse dyeing of polyester fabrics can be an alternative to conventional long time dyeing (60min) when acrylic acid plasma polymerzation treatment with increased dry rubbing fastness. This results is promising for an ecological and energy saving alternative to conventional disperse dyeing.

Keywords: Plasma, XPS, acrylic acid, fabric, disperse dye, polyester

[1, 2]Dokuz Eylül University, Textile Engineering Department, 35390, Buca-İZMİR, TURKEY
*Corresponding author: bengi.kutlu@deu.edu.tr

International Conference on Science and Technology

ICONST 2018

5-9 September 2018 Prizren - KOSOVO

Energetic Assessment of A Transcritical Rankine Cycle Powered by Solar Energy

İsmail Özcan[1], Mehmet Altınkaynak[2], Ahmet Özsoy[2], Arif Emre Özgür[2*]

Abstract: Today, one of the most important environmental problems is global warming reality. So, clean energy resources gain more importance. The application of solar energy to electricity generation has received considerable attention. However cogeneration and trigeneration applications powered by solar energy have also been developed. In this study, an energetic assessment has been presented for a transcritical solar rankine cycle using CO2. In this study, a solar transcritical power cycle has been presented. Cycle components are CO2 pump, evacuated solar collector, CO2 turbine, CO2 condensing unit and pipe lines. CO2 has been selected cycle fluid. CO2 has excellent thermophsical properties. However, CO2 has unity global warming potential and zero ozone depletion potential. So, CO2 is a unique alternative cycle fluid for Rankine cycles. Pressure of liquid CO2 has been increased by CO2 pump. CO2 vaporizes in evacuated solar collectors at high pressure levels (9 MPa to 12 MPa). The temperature of CO2 can be increased 120 ^{o}C to 200 ^{o}C. At this condition, phase of CO2 is supercritical. Supercritic CO2 expands in the turbine to produce power. After turbine, pressure of CO2 is about 5.7 MPa. At this pressure, CO2 is cooled and condensed in the condensing unit. In this study, thermodynamical analysis has been applied transcritical CO2 solar power cycle. Analysis study has been made with various collector pressures. However, the temperature of CO2 has been selected as a variable parameter. Some assumptions have been defined to introduce analysis equations. Parametric analysis has been made using software (Engineering Equation Solver – EES). The analysis results have been presented with graphics. Power efficiency of cycle may exceed 20%. However, thermal efficiency of the system can be reaches higher than other solar thermal collecting units. Analysis results state that, transcritical CO2 power cycle can be feasible way to produce power from solar energy.

Keywords: CO2, transcritical, Rankine cycle, solar.

[1]Isparta Applied Sciences University, Graduate Institute, 32260, Isparta, TURKEY
[2]I sparta Applied Sciences University, Technology Faculty, 32260, Isparta, TURKEY
*Corresponding author: emreozgur@sdu.edu.tr

International Conference on Science and Technology

ICONST 2018

5-9 September 2018 Prizren - KOSOVO

Determination of Waste Heat Potential of A Cement Production Facility

Mehmet Altınkaynak[1*], Ali Kemal Yakut[1], Arif Emre Özgür[1]

Abstract: Cement is at the top of the building materials in the world. Therefore, there are high-level production facilities and capacities. Looking at the side of energy input, the cement sector, which takes place in the first place in terms of energy demand of the industry, is also in the top rank according to the amount of fuel used. Cement factories, mainly limestone, marble and clay mixture is milled in a mill to produce coal, natural gas, etc. from the raw material called farina type fuels to produce clinker. Fuel energy released during this clinker is used to preheat cyclones before entering the farina rotary kiln. It is possible to recover the waste heat in this preheating and in the chimney. There are a total of 52 cement factories in Turkey as of 2018. (http://www.tcma.org.tr/images/file/yeni%20haritamart2018_1.jpg). In this study, the potential of the energy of the burned gas circulating in the preheating process, namely cyclones and chimneys, will be presented in a point-by-point manner, taking into account the actual cement factory data. By placing steam exchangers in these potential points, it will be expressed that power generation can be done by Rankine cycle.

Keywords: Cement, Heat Recovery, Energy, Klinker, Farine.

[1]Isparta Applied Sciences University, Faculty of Forestry, 32260, Isparta, TURKEY
[2]Isparta Applied Sciences University, Faculty of Engineering, 32260, Isparta, TURKEY
*Corresponding author: mehmetaltinkaynak@sdu.edu.tr

International Conference on Science and Technology

ICONST 2018

5-9 September 2018 Prizren - KOSOVO

Efficiency Analysis of A Single Stage Transcritical Heat Pump

Arif Emre ÖZGÜR[1*], Hilmi Cenk BAYRAKÇI[2], Ahmet ELBİR[3], Özdemir DENİZ[3], Mehmet ALTINKAYNAK[2]

Abstract: Increased global warming and environmental damage will be much smarter to use environmentally friendly refrigerants in industrial cooling systems. In recent years, synthetic refrigerants have been seen much more damage to the environment in cooling technology, and the use of CO2 (R744), which is a natural refrigerant, has increased. The CO2 gas is a refrigerant with ODP = 1 and GWP = 0 properties. Transcritical CO2 has come into use effectively in heating and cooling systems. The costs of transcritical systems are considerably higher than those of traditional HFC- based systems. However, operating costs are less. There are more than four million installed transcritical CO2 household heat pumps throughout the world. CO2 has excellent thermophsical properties. However, CO2 has unity global warming potential and zero ozone depletion potential. So, CO2 is a unique alternative cycle fluid for heat pumps cycles. An experimental set up has been produced for analysis study. The system has different capilar tubes. It has been planned that experimental measurements will be presented. In this study, thermodynamic analysis of a transcritical CO2 heat pump has been presented. Analysis study has been made with various gas cooler pressures. However, the temperature of CO2 has been selected as a variable parameter. Some assumptions have been defined to introduce analysis equations. Parametric analysis has been made using software (Engineering Equation Solver – EES). In this study, the effectiveness of a single – stage CO2 transcritical heat pump cycle was presented graphically with different cycle analyses. The results have been stated that, system performance increases with decreasing temperature of CO2 after gas cooler. Analysis results state that, transcritical CO2 heat pump system can be feasible for water cooled gas cooling applications.

Keywords: CO2, transcritical, heat pump cycle, analysis.

[1]Isparta Applied Sciences University, Technology Faculty, Energy Syst. Eng. Dept., 32260, Isparta, TURKEY
[2]Isparta Applied Sciences University, Technology Faculty, Mechatronics Eng. Dept., 32260, Isparta, TURKEY
[3]Isparta Applied Sciences University, Graduate Institute, 32260, Isparta, TURKEY
*Corresponding author: emreozgur@sdu.edu.tr

International Conference on Science and Technology

ICONST 2018

5-9 September 2018 Prizren - KOSOVO

Spatial Distribution of Carbon Storage and Sequestration in Upper Seyhan Basin's Forest Biomass (2014-2025)

Merve Ersoy Mirici[1]*, Süha Berberoğlu[2]

Abstract: Forest ecosystem covers approximately 30% of terrestrial land surface and its major component is terrestrial carbon storage. Forests continuously accumulate large amount of atmospheric CO_2 by photosynthesis in vegetation, litterfall and soil layers. The carbon storage and sequestration of forests are important components not only for ecosystem good and services but also reducing effects of global climate change.

The study was aimed to determine the carbon storage and sequestration of forest biomass in the study area located at the Eastern Mediterranean Basin of Turkey. Analysis method includes; (i) producing current forest biomass carbon map (2014) using forest inventory based Growing Stock (GS), (ii) modelling future Land Use/Land Cover (LULC) by incorporating Multi-Layer Perceptron (MLP) and Markov Chain (MC) (2025), (iii) generation of future forest biomass carbon map with using InVEST model and (iv) estimating of potential forest carbon sequestration. The current forest biomass carbon has been determined by (i) stand types map, (ii) the amount of space covered by stand types, (iii) GS (Growing Stock) data, (iv) BEF (Biomass Expansion Factor), WD (Wood Density) and R (Root/Shoot Ratio) coefficients. It was also benefitted from percent tree cover data and ArcGIS 10.3 software.

Current and total above and below ground forest biomass carbon was found 6.85 TgC and 7.63 TgC, respectively. According to Business As Usual (BAU) scenario, the forest carbon sequestration was estimated as 0.78 TgC between 2014 and 2025.

The positive impact of carbon sequestration should be considered in reducing the global climate change effect. In this direction, monitoring of carbon sequestration in land/landscape planning studies plays a fundamental role for carbon offset. Additionally, possible carbon sequestration can be modelled on this basis of different LULC scenarios with this method.

Keywords: Carbon sequestration, Carbon storage, Forest, Multi-Layer Perceptron (MLP), Markov Chain (MC), Geographic Information System (GIS)

[1]Cukurova University, Faculty of Landscape Architecture, 01330, Adana, TURKEY
*Corresponding author: mrversoy@gmail.com

International Conference on Science and Technology

ICONST 2018

5-9 September 2018 Prizren - KOSOVO

Evaluation of Optimal Area Usage in Kastamonu City Center in terms of Landscape Planning

Sevgi Öztürk[1], Merve Kalaycı[1*], Kaan Meydan[1]

Abstract: Nowadays, natural and cultural resources are rapidly getting depleted. However, protection approaches that can be effective against this situation are not exhibited. Existing resources are at risk of extinction because of useing spaces incorrectly. In order to be able to make the right resource use and planning decisions, it is necessary to determine the optimal area uses considering the ecological basis.

The study was conducted at the border urban area of Kastamonu province. Natural and cultural resource values have been examined to determine area uses. In the first phase, the literature search is completed. Then field inventory studies were carried out. In the second phase; numerical suitability maps have been established for three different field types: agriculture, forest, settlement areas. Geographic Information Systems program, that ArcGIS 10.0 software, was used as a tool. Finally, the optimal fitness of the digitized areas has been determined.

Potential resource values of Kastamonu city center, due to incorrect use of areas and lack of planning, was determined not adequately assessed. To prevent incorrect use of space; local governments are required to make area utilization decisions in a short time. Making the environmentally sensitive planning studies, to provide tourism within the protection-utilization balance of resources and the promotion was found that very important economically.

It has been determined that there is misuse in the study where ecological conformities of existing natural and cultural resources are tested. It has been determined that resource values for these areas have deteriorated due to misuse. The reason behind all this is unconscious urbanization. It has been determined that sustainable resource use will not be possible due to this pressure.

Keywords: Landscape, Landscape Planning, Optimal Area Use, Compliance Map, Kastamonu.

[1]Kastamonu University, Faculty of Engineering and Architecture, 37200, Kastamonu, TURKEY
*Corresponding author: mkalayci@kastamonu.edu.tr

International Conference on Science and Technology

ICONST 2018

5-9 September 2018 Prizren - KOSOVO

The Effects of Irrigation with Reclaimed Wastewater on Heavy Metal Accumulation and Plant Development in Lettuce

Nuray Akbudak[1]*, Nafiz Biçen[2]

Abstract: Due to the increasing growth of the city, agricultural land has begun to take place in and around the living areas. This situation also increases the need for irrigation water available in agriculture. Recycled wastewater has become a global trend. This study assessed the impacts of lettuce irrigation with treated effluents, as compared to domestic water irrigation, on plant physiological structure and crop productivity. The treated effluents reused for irrigation were produced in two Municipal Wastewater Treatment Plants utilizing two discrete tertiary treatments (physical purification and biological treatment). The experiment was conducted for five months on the agriculture form by using lettuce leaf type ("Festival" and "Caipira") and head type lettuce ("Bombola"). In all plant groups (the productivity, weight, length, diameter, root fresh and dry weight, root diameter), quality characteristics (deformable and number of marketable leaves per plant, total chlorophyll) and heavy metal contents (Ni^{2+}, Pb^{2+}, Cd^{2+}, and Co^{2+}) were determined. Application of treated wastewater (TWW) increased marketable yield, number of leaves per plant, plant height and diameter. The highest yield of lettuce plants was obtained with the treated wastewater "Bombola". TWW irrigation also increased the growth parameters such as number of leaves, fresh root weight, dry weight and total chlorophyll. Results show a high influence of TWW in nitrate content of lettuce. Results on some heavy metal concentration (Ni^{2+}, Pb^{2+}) show higher values for "Festival" and "Bombola" plants irrigated with TWW than DW. Cd^{2+} and Co^{2+} values in the plants subjected to DW and TWW were similar. Values of total leaf chlorophyll content in all plants irrigated with TWW were higher than for those irrigated with DW. Results show that heavy metal accumulation, an important criterion for the use of treated waste water in agriculture, may differ in lettuce varieties. By choosing heavy metal tolerant varieties, treated wastewater can be used for long-term in sustainable agriculture.

Keywords: Heavy metal, *Lactuca sativa*, pollution, quality, wastewater

[1]Suleyman Demirel University, Faculty of Forestry, 32260, Isparta, TURKEY
[2]Suleyman Demirel University, Faculty of Engineering, 32260, Isparta, TURKEY
*Correspondingauthor: mevludeakkaya@gmail.com

International Conference on Science and Technology

ICONST 2018

5-9 September 2018 Prizren - KOSOVO

System Dynamıcs Modellıng for Determınıng Optımal Shıp Sızes and Types

Gizem Yüksel[1]*, Pelin Bolat[2], Muammer Kayişoğlu[3]

Abstract: With the specialization of industries, transit between continents, countries and regions has become an inevitable part of the industrial supply chain. At this point, multimodal transportation systems (MTS) is a type of shipment that allows optimal use of transport modes. The purpose of multimodal transport is to ensure that transport modes are used in the most appropriate and efficient manner.

This study aims to find multimodal transportation systems efficiency (MTS) and appropriate ship size and types according to the efficiency. For this purpose, it is developed a system dynamic modelling for a scenario in port of Turkey in a period of time.

In this context, this project underlines such as “what is the system dynamic modelling”, “which factors affect the MTS”, and “what is the equations of this dynamics”. In addition to this, it was determined that what will be the type and size of ships for specific scenario.

It is assumed that with 1000 TEU small feeder, with 2000 TEU feeder, with 5000 TEU feeder max values are used, 1 TEU value is assumed to be 14 TON and it is estimated aproximately 714 small feeders or 357 feeders or 142 feeder max vessels can be required to meet for demand in 2025.

Keywords: Multimodal transportation system, Maritime, System dynamic modelling

[1]Istanbul Technical University, Maritime Faculty, 34940, İstanbul, TURKEY
[2]Istanbul Technical University, Maritime Faculty, 34940, İstanbul, TURKEY
[3]Istanbul Technical University, Maritime Faculty, 34940, İstanbul, TURKEY
*Corresponding author: yukselg@itu.edu.tr

International Conference on Science and Technology

ICONST 2018

5-9 September 2018 Prizren - KOSOVO

Evaluatıng Cyber Securıty Awareness ın Marıtıme Domaın

Pelin Bolat[1]*, Gizem Yüksel[2], Selen Uygur[3]

Abstract: Maritime sector has a sophisticated, broad, open and integrated socio-technical structure that allows us to define itself as a maritime transport system. In today's age, the operation and management of such a complex system is directly provided by information and communication technologies (ICT). Accordingly, cyber security has taken to national and international agendas for maritime security as any attack to ICT in maritime domain can be resulted with economic and social damages. In the literature, most of cyber security attacks have reached their goal due to lack of realizing the risks and developing secure behavior by end users. Thus cyber security awareness has arisen as an important issue.

In the foregoing circumstances, in this study, it is aimed to investigate the perception of maritime employees for cyber security and understand the awareness level amongst them by a statistical approach via SPSS.

On the basis of literature review, the results and discussion of 183 maritime sector employees' feedback to our cyber security awareness questionnaire. Consequently, there is low cyber security awareness level among Turkish maritime employees.

Considering that International Maritime Organization (IMO) gave the maritime industry time for cyber security until 2021, we can say that companies need to start by increasing awareness of their staff.

Keywords Cybersecurity awareness, Maritime, Perception, Seafarers

[1]Istanbul Technical University, Maritime Faculty, 34940, İstanbul, TURKEY
[2][1]Istanbul Technical University, Maritime Faculty, 34940, İstanbul, TURKEY
[3]Istanbul Technical University, Maritime Faculty, 34940, İstanbul, TURKEY
*Corresponding author: yilmazp@itu.edu.tr

International Conference on Science and Technology

ICONST 2018

5-9 September 2018 Prizren - KOSOVO

Design of A Novel High Performance Aerator For Hydroponic Cultures and Its Numerical and Experimental Performance Analysis

Aliihsan Koca[1]*

Abstract: The concentration of dissolved oxygen in a culture solution is one of the most prominent factors affecting the growth of tops and roots of plants particularly for hydroponic systems. In these systems, there are different means of supplying oxygen into the culture solutions. One of them is using a water jet which feeds culture solution continuously. As it is well known, when a water jet plunges into a reservoir, after passing through an air layer, it entrains remarkable amount of air by forming a two-phase region in the reservoir. And hence, the oxygen transfer occurs between the bubbles and water reservoir. In this paper vertical plunging water jets particularly for use in hydroponic culture were studied. In the first part of this study, a new aerator nozzle has been designed numerically by comparing different geometries in order to maximize the aeration. To analyze the behavior of the device numerically, the governing equations were solved using the CFD commercial software of Ansys-Fluent©. The Volume of Fluid Model (VOF) was used to simulate the two-phase gas-liquid flow. In the second part an experimental system involving a complete re-circulation of water was installed. Transient behavior of the aeration device was observed with regard to dissolved oxygen concentration. Simulations have been conducted for jet heights of 0.1 and 0.4 m, while water flow rate varies between 0.4 and 1.4 m^3/h. For the new aerator; the effect of water flow rate on volumetric oxygen transfer coefficient for different aerator heights, the effect of jet velocity on penetration depth, the kinetic jet power per unit volume of water in the reservoir and volumetric oxygen transfer coefficient for different jet heights were evaulated. However, the change in dissolved oxygen concentration with time was measured. The effect of jet height is significant on the volumetric oxygen transfer coefficient and penetration depth in hydroponic media. The volumetric oxygen transfer coefficient and penetration depth increases with the increase in jet height, as a conclusion of enhanced spray characteristics of water jet.
The jet height has a significant effect on the penetration depth. For a given jet velocity penetration depth has been found to be maximum in case of the largest jet height. It has been observed that for fixed kinetic jet power per unit volume, better dissolved oxygen concentration can be achieved at larger plunging jet heights, which indicates a more efficient aeration system.

Keywords: CFD Simulation, Oxygen transfer, Hydroponic Culture, Volume of Fluid Model

[1] Fatih Sultan Mehmet Vakif University, Faculty of Engineering, 34445, Istanbul, TURKEY
*Corresponding author: akoca@fsm.edu.tr

International Conference on Science and Technology

ICONST 2018

5-9 September 2018 Prizren - KOSOVO

Usability Evaluation of Senaturk Academy Breast Health Monitoring Application

Fidan Kaya Gülağız[1]*, Hikmetcan Özcan[1], Suhap Şahin[1], Sertaç Ata Güler[2]

Abstract: Health monitoring applications are an important part of public healthcare. Through these applications, patients' identity information, disease information, treatment and treatment follow-up information are kept. These systems can either be designed to cover all of the medical units, or they can be designed specifically for different units. In this study, the usability evaluation of the developed breast health monitoring application for the Senaturk Academy, which has carried out long time studies in the field of senology, has been carried out.

For usability evaluation, a task list consisting of ten different tasks was first created for the purpose of health monitoring and a total of 13 participants (6 female, 7 male) at different levels of education were analyzed**.** The processing times and the number of clicks that participants spent in performing their tasks were recorded on the observation form. Times spent on tasks were rated with reference to a previous usability study. In addition, demographic characteristics such as age, gender, occupation, daily computer use of the participants were collected via user information survey. After the participants completed the assigned tasks, a Turkish short version (including 13 questions) of the Computer Systems Usability Questionnaire (T-CSUQ-SV) was used in order to ensure that the developed health monitoring application was evaluated in general. After obtaining the data, task completion rates and click counts were analyzed considering the processing time of the participants on tasks. Finally, through the applied questionnaire, the system usefulness, information quality, interface quality and overall satisfaction values of the developed application were obtained. The relationship between these values and the demographic data of the participants was determined using the Kruskal Wallis H Test and Mann Whitney U tests.

When the results obtained were examined, it was observed that the participants were successful in completing eight of the ten tasks. However, it has been observed that participants need a lot of time related to the task of creating a new patient record. Similarly, it has been observed that the average number of clicks is higher in unsuccessful tasks. When general survey results are examined, system usefulness, information quality, interface quality and general satisfaction values are obtained as respectively 2.07, 3.69, 2.513 and 2. According to the obtained results, the participants find the application satisfactory, but they think that the error messages should be more descriptive. When the relationship between demographic data and satisfaction parameters were examined, it was determined that there was a meaningful relationship between daily computer usage and system usefulness ($p = 0.028 < 0.05$) and interface quality ($p = 0.016 < 0.05$).

With this study, the deficiencies of breast health monitoring application developed for the Senaturk Academy have been determined. It is believed that the work performed is useful in determining the factors to be considered in the design of health monitoring applications to be developed for different units.

Keywords Health Monitoring Applications, T-CSUQ-SV, Usability, Usability Test.

Acknowledgement: We would like to thank the staff of Kocaeli University Medical Faculty Senaturk Academy for their contribution.

[1]Kocaeli University, Faculty of Engineering, Department of Computer Engineering, 41380, Umuttepe, TURKEY
[2] Kocaeli University, School of Medicine, Department of Surgery, 41380, Umuttepe, TURKEY
*fidan.kaya@kocaeli.edu.tr

International Conference on Social Science Research

ICONSR 2018

5-9 September 2018 Prizren - KOSOVO

Effect of UHT treatment on Liquid Egg Yolk

Emna Ayari[1]*, Németh Csaba [2], László Friedrich[3]

Abstract: Egg and its product are easily perishable items because of their high moisture content, although they have a very high amount of nutrients, especially protein. Many efforts have been channelled to increase the shelf-life of these products but Heat treatment according to literature is the most promising although egg and its products are heat-sensitive. Thus, a very low temperature is needed or a high temperature for a very short time. Ultra-Heat Treatment (UHT) is one of the known technology that we used for heat-sensitive products. The aim of the study, was to investigate the effect of UHT treatment (approximately 67°C for 190 seconds) on Liquid Egg Yolk (LEY). During twenty-one days, the colour was measured every seven days. We studied also the damage of proteins using DSC (Differential Scanning Calorimetry) and viscosity. On the 14th day of storage, the reference samples (raw LEY) showed high microbial contamination thus we stopped their tests while the UHT treated samples retained their properties until the 21st day. The Colour-difference (ΔE*ab) was upper than 3. The endothermic peak of treatement egg yolk had place after the the endothermic peak of raw egg yolk. İn the last day of storage, we can observe that the viscosity of egg yolk decreased. The effect of UHT treatment was clear on the DSC and viscosity graphs. And the Colour-difference (ΔE*ab) is very noticeable.

Keywords: Egg, Yolk, UHT, DSC....

[1] Department of Refrigeration and Livestock Products Technology, Faculty of Food Science, Szent Istvan University, Budapest, Hungary
[2] Department of Refrigeration and Livestock Products Technology, Faculty of Food Science, Szent Istvan University, Budapest, Hungary
[3] Capriovus Ltd., Szigetcsép, Dunasor, 073/72. hrsz., 2317 Hungary
*Corresponding author: ayari.mna@gmail.com

International Conference on Science and Technology

ICONST 2018

5-9 September 2018 Prizren - KOSOVO

Relationships Between Alpha Plant Diversity and Environmental Factors in the Dedegöl Mountain (Yenişarbademli) District

Esra Özge Aygül[1]*, Mehmet Güvenç Negiz[2]

Abstract: Biodiversity is the level of variation of life forms in a given ecosystem, biome or world, and is variable in terms of species, function, and structure among living things. This study was performed to investigate the relationships between environmental factors and alpha diversity (α) and woody plant species in the region of the Dedegöl Mountain (Yenişarbademli). The diversity components were calculated by the data obtained from 103 sample area of the field inventory method. During the field studies, coverage classes of woody plant species and environmental factors were recorded in each sample plot. The climate variables of sample plots are obtained from the worldclim.org. Then, the variability coefficients of some of the variables recorded in the sample plots were calculated and new variables were determined by using a digital elevation model (DEM). Principle component analysis (PCA) was applied to determine which of the indices used to calculate alpha species diversity could be used. Spearman correlation analysis and multiple regression analysis (MLR) were applied to determine the relationship between alpha species diversity and environmental factors. Interspecific Correlation Analysis was applied to determine the indicator species. In the study, regression analysis (RA), detrended correspondence analysis (DCA) and canonical compliance analysis (CCA) were applied to the vegetation matrix to determine the gradual distribution of sample plots over the ordination axes. The Shannon-Wiener index has been determined to have the highest coefficient as the PCA result. Spearman correlation analysis revealed that the alpha species variety had positive correlations with BIO1, BIO2, BIO4, BIO10, BIO11, ENLEM, YUZTAS, while the alpha species diversity had negative correlations with BIO12 and YKSLT. As a result of MLR, elevation variability was identified as the most important variable. ABICIL, CISLAU, EUPSPP, JUNEXC, JUNOXY, LAUNOB, POPTRE, ROSCAN, SAMEBU, THYSAM were identified as the most important indicator species. The combination of the most suitable environmental variables for RA, DCA, CCA result was obtained with surface roughness, BIO4 (temperature seasonality) and BIO12 (annual precipitation) variables. Shannon-Wiener index was found to be the most effective index, and surface roughness and elevation variables are the most important explanatory variables for alpha species diversity in the study area. With the help of the information obtained in this study, it is possible to plan the beta and gamma diversity studies in the following stages. Potential distribution models and mapping of species diversity components can be achieved.

Keywords: Alpha Species Diversity, Biodiversity, Dedegöl Mountain District, Environmental Factors

[1]Yozgat Bozok University, Boğazlıyan Vocational School, 66400, Yozgat, TURKEY
[2]Applied Sciences University of Isparta, Sütçüler Prof. Dr. Hasan Gürbüz Vocational School, 32950, Isparta, TURKEY
*Correspondingauthor: esra.ozge.aygul@bozok.edu.tr

International Conference on Science and Technology

ICONST 2018

5-9 September 2018 Prizren - KOSOVO

Analyzing the Growth Trade of Istanbul Ports According to Port Capacities

Firat Bolat[1]*

Abstract: Istanbul is a major port area for global commercial shipping. It comprises five administration maritime sectors; Ambarli, Istanbul, Sile, Silivri and Tuzla. All of these sectors has seaport areas. The activities of these seaports have been an economic indicator for national development. In this context the analysis of cargo throughput and vessel arrivals to these ports will show us trade growth and the level of port efficiencies and capacities. The aim of this paper is to analyse the variations of cargo throughput for eight years during 2010-2017 to develop effective port management strategies for Istanbul port area. The material and method used in the work should be clearly stated. Time series data of throughput of Istanbul port area. Data is analysed with statistical regressional analysis. Findings will include the shipping trade between 2010 and 2017 of Istanbul ports and regressional analysis. The growth trade that is found with statistical analysis can be used for effective port strategies and to understand the port capacities. These issues will be discussed in this part.

Keywords Port Capacity, Time Series Analysis, Istanbul Ports, Statistical Analysis

[1]Istanbul Technical University, Maritime Faculty, Istanbul, TURKEY.
*Corresponding author: firatbolat1@yahoo.com

International Conference on Science and Technology

ICONST 2018

5-9 September 2018 Prizren - KOSOVO

Reproducing a Component Diversity İndex for Regional Biodiversity Assessments

Mehmet Güvenç Negiz[1]*, Kürşad Özkan[2]

Abstract: The fact that there is no any rule in selection of a given diversity index concerning the measures of biodiversity means that utilization only one of these to define the diversity of living communities is insufficient. Different diversity indices have been used by many researchers. Even though diversity indices have different facets, they are also highly correlative with each other. That allows us to reproduce a component diversity index from the all diversity indices we have used. The present study was carried out to get a component diversity index for the Kuyucak mountain of the Mediterranean region, Turkey. In the study, the woody vegetation data obtained from 800 sample plots were used. The diversity indices (Species richness (S) Shannon entropy (H), Simpson 1–dominance (1–λ), Brillouin index (HB), reciprocal of Berker-Parker index (1/d), Menhinick (DMN) index, Margalef (DMG) index and Fisher' alpha (αF) were measured at each sample plot. The results of Pearson correlation analysis among the diversity indices showed that all indices are significantly correlated with each other at the level of 0.01. H has the strongest correlations with majority of the diversity indices whereas 1/d has generally weaker correlations with the indices compared to the other indices' inter-correlations.

Keywords: Biodiversity, Karst forests, Topographical heterogeneity, Diversity indices, Entropy

[1]S Süleyman Demirel University, Sutculer, Sütçüler Prof. Dr. Hasan Gürbüz Vocational School, 32950, Sütçüler-Isparta, Turkey
[2] Süleyman Demirel University, Faculty of Forestry, Department of Soil Science and Ecology, 32200, Isparta, Turkey
*Corresponding author: mehmetnegiz@sdu.edu.tr

International Conference on Science and Technology

ICONST 2018

5-9 September 2018 Prizren - KOSOVO

Assessment of Energy Saving Potential for Mehmet Akif Ersoy Unıversity Campus with Using a Co-Generation System

Sertaç Görgülü[1*], Arif Emre Özgür[2]

Abstract: Cogeneration technologies are a positive application in terms of environment as well as important in terms of energy economy. Especially when electricity energy is derived from fossil fuels, these matters are much more important. In 2014, avarage electricity generation efficiency from fossil fuels was 47,6% in the European Union. However this rate was 41,8% for our country and the other two non-EU countries (Iceland and Norway). These values indicate the importance of cogeneration applications. In this study, an assessment of energy saving potential for a University Campus is presented. All data has been obtained from İstiklal Campus of Mehmet Akif University. A system is modelled for heating and electricity requriements. Because of the campus geography diffuculties and distances from the faculty buildings suggested system capacity is limited. So heating energy requirement of some faculty buildings can be produced by the system. However the total electricity requirement can be obtained with the system. Economical and energetic evaluations are made for this strategy. Results are presented with tables.

Keywords: Co-generation, campus, energy assessment, Mehmet Akif Ersoy University.

[1] Mehmet Akif Ersoy University, Engineering and Architecture Faculty, 32260, Burdur, TURKEY
[2] Isparta Applied Science University,Technology Faculty, 32260, Isparta, TURKEY
*Corresponding author: sgorgulu@mehmetakif.edu.tr

International Conference on Science and Technology

ICONST 2018

5-9 September 2018 Prizren - KOSOVO

Determination of Extracellular Polymeric Matter Concentration in Different Types of Treatment Sludges

Nazlı Baldan Pakdil[1*], Murat Solak[2] Cemre Karslıoğlu[1], Yalçın İpek[1], Burcu Uzun[1]

Abstract:

In the study, extracellular polymeric substance (EPS) concentrations (protein, humic acid, polysaccharide, carbohydrate), one of the important parameters affecting flocking in the yeast production industry, potato chip processing industry and domestic wastewater treatment plant sludge were investigated. In addition, to determine the characterization of sewage sludge, the Capillary Suction Time (KES), Specific Filter Resistance (ÖFD), viscosity parameters were analyzed. While the highest amounts of humic acid, protein and carbohydrate were detected in domestic wastewater sludge, high levels of humic acid and polysaccharide (453 mg / L) were observed in potato chips processing sludge in terms of food sector.

Keywords: Sewage Sludge, Extracellular Polymeric Substances (EPS), Susuzlaştırma.

[1]Bolu Abant İzzet Baysal University, Faculty of Engineering, 14030, Bolu, TURKEY
[2]Düzce University, Faculty of Engineering, 81900, Düzce, TURKEY
*Corresponding author: nazlipakdil@gmail.com

International Conference on Science and Technology

ICONST 2018

5-9 September 2018 Prizren - KOSOVO

Estimating and Modelling of Plant Species Rarity in Yukarıgökdere District of Mediterranean Region

Ali Şenol[1], Serkan Özdemir[2]*

Abstract: Ecosystems are heterogeneous structures that consist of areas which have different characteristics. Living organisms are in equilibrium within these heterogeneous systems. But for different reasons (climate change, human activities, natural disasters, insects), the balance within ecosystems can be disrupted. At this point, it is important to classify the ecosystems and to identify the heterogeneous structure. In recent years, it is seen that different approaches are based on this topic. However, it was realized that the concept of rarity, which is an important criterion for ecosystems, was not sufficiently emphasized. Therefore, in present study the rarity values were estimated for each sample point using the rarity function in Yukarıgökdere district in Isparta. The sample point with the highest rarity value was found to be oa54 (0.861449) and the sample point with the lowest rarity value was oa88 (0.433060). Correlation analysis was performed between the environmental variables (site factors) and rarity values. The variables which were determined to be highly correlated were eliminated to avoid multicollinearity problem. Then, modeling was carried out between site factors and rarity values using regression tree technique. In next step, the obtained model was visualized and a rarity map was created. The variables that contributed to the model were determined as elevation, topographic position index, slope, index and heat index, respectively. As a result, it is considered that it is advantageous to consider the rarity map as a component together with the biodiversity calculations in the planning studies to be carried out in the present district.

Keywords: Ecosystem qualification components, mapping, rarity, regression modeling

[1] Isparta University of Applied Science, Faculty of Forestry, Isparta, TURKEY
[2] Isparta University of Applied Science, Sütçüler Prof. Dr. Hasan Gürbüz Vocational School, Isparta-Sütçüler, TURKEY

*Corresponding author: serkanozdemir@isparta.edu.tr

International Conference on Science and Technology

ICONST 2018

5-9 September 2018 Prizren - KOSOVO

Stress in Dairy Cattle

Onur Erzurum[1]*, Yasin Akkemik[2]

Abstract: Stress can be defined as the interaction between the internal or external factors in the organism or the interaction between the stress factors and the host defense responses. In animal breeding, from illness to death can lead to many undesirable consequences. Animals experience both psychological and physiological stress throughout their lives. In order not to be exposed to these stress factors, the factors that cause stress should be determined. If the stress factors affecting animals are managed correctly, the production will have a positive effect and increase the level of well-being. Determination of the stress can be done by determining the difference that will occur in measurable variables such as body temperature, respiration and pulse rate. The response to the stress factor begins with the central nervous system perceiving the stimulus as a threat. Physiological changes during stress and biological responses and responses to them can be examined as alarms and adaptations. Live is influenced by various internal and external factors (fear, noise, etc.). In organism, defensive effects are called stress factors. Excessive heat and cold, poor maintenance conditions (animal density, irregular nutrition etc.) and diseases are considered as important stress factors. Animals must be kept away from stress factors to ensure they are healthy and that they reach the desired product.

Keywords: Stress, Dairy Cattle, Milk yield

*[1,2]Selcuk University Karapinar Aydoganlar Vocational School

onurerzurum@selcuk.edu.tr

International Conference on Science and Technology

ICONST 2018

5-9 September 2018 Prizren - KOSOVO

Predicting Potential Distribution of Prickly Juniper (*Juniperus oxycedrus* L.) in The Mediterranean Region of Turkey

Serkan Gülsoy[1]*, Özdemir Şentürk[2], Alican Çıvğa[1], Kürşad Özkan[1]

Abstract: Forests have many functions. Thanks to these functions, which have forest areas on a global scale, they serve all living things, especially people. This leads to the protection of forest areas and the need to increase existing forest resources. Determination of the most suitable potential distribution areas of main forest trees is possible by increasing the forest areas as a result of proper afforestation. Therefore, there are many studies on this subject. However, studies on the determination of the potential distribution areas of other species with quite important functions in forest areas other than main forest tree species have been limited. In this sense, one of the species with quite important functions in the forest areas is Prickly juniper. It is aimed to model and map these potential distribution areas of this species in the mediterranean region. The study area is Sütçüler district within the boundaries of the Mediterranean Region of Turkey. Presence and absence data of this species were recorded in a total of 185 sample areas in the district. The data for climate and topographic variables are obtained from the digital map of the locality. Generalized Addittive Model (GAM) technique is used to determine the potential distribution areas of the species. The variables that constitute the representative model of the potential distribution areas are the elevation and the bedrock, respectively. Locations with elevations between 1000 m and 1500 m in the district have been the most suitable areas for potential distribution of the species. On the other hand, the conglomerate type rock has been found to play a more effective role for the potential distribution of the species than the other rock types. Prickly juniper is ecologically significant species in the sites with stony, rocky and shallow soil conditions with characteristic arid and semi-arid climatic properties of the Mediterranean basin. Especially in degraded forest areas, it has important functions such as preventing the soil from being exposed to erosion against the rainy waters. Apart from these, it is possible to enumerate many of these functions, such as global climate balance, industrial and firewood product and the medical-aromatic plant property. However, this species has been severely damaged in the natüre from past to day, especially in the ending of the human impact. The potential distribution maps obtained in the context of this study will be quite significant in order to ensure sustainability of this species in the natural areas in the future.

Keywords: Generalized Addittive Model, Mediterranean region, Prickly juniper, potential distribution

Acknowledgement: We would like to express our thanks to Republic of Turkey General Directorate of Forestry providing the opportunity to work in Sütculer forest areas.

[1] Isparta University of Applied Sciences, Faculty of Forestry, 32260, Isparta, TURKEY
[2] Burdur Mehmet Akif Ersoy University, Gölhisar Vocational High School, Department of Forestry, 15400, Burdur, TURKEY
*Corresponding author: srkngulsoy@gmail.com

International Conference on Science and Technology

ICONST 2018

5-9 September 2018 Prizren - KOSOVO

The Effect of Dietary Panax Ginseng Supplementation on Performance of Laying Quail

İsmail ÜLGER[1]*, Mahmut KALİBER[1], Fatih Doğan KOCA[2]

Abstract: This study was conducted to determine the effects of ginseng (GS, Panax ginseng) supplementation on performance parameters of laying quail. A total of 30 eight week old laying Japanese quail (Coturnix coturnix japonica) were divided into 3 treatment groups with 10 replicates in each. The treatments were as follows; the first group was fed with a control diet (GS0, no addition), while other two groups were fed with diets containing 5 (GS5) and 10 (GS10) g/kg dried GS root powder for 56 days. The egg yield (EY), feed consumption (FC) and egg weight (EW) of each quail were recorded daily; egg mass (EM) produced in 56 days and also feed conversion ratio (FCR) parameters were calculated from these data. The EY, FC, EM and FCR parameters of experimental quails were not significantly affected by dietary treatment ($P>0.05$). But there was a numerical increase in EY and EM parameters of GS5 (95.98% EY and 670.39 g EM in 56 d) and GS10 (96.68% EY and 682.54 g EM in 56 d) groups when compared with control (94.90% EY and 649.89 g EM in 56 d), and FC of GS supplemented groups was slightly lower than control group ($P>0.05$). Also, there were significant effects of dietary treatments on EW of quail ($P<0.01$) and EW of GS0, GS5 and GS10 groups were 12.02, 12.43 and 12.89 g/egg, respectively. As a result of all these significant and non-significant effects of GS supplementation, there has been a little improvement in FCR of quails which fed with GS supplemented diets ($P>0.05$). In conclusion, GS can be used as a feed additive in poultry diets to increase EW and to improve EY and FCR parameters.

Keywords: Egg yield, egg weight, feed additive, feed conversion ratio, poultry.

[1]Erciyes University, Agricultural Faculty, Department of Animal Science, Kayseri, Turkey.
[2]Erciyes University, Faculty of Veterinary Medicine
*Corresponding author: i_ulger@hotmail.com

International Conference on Science and Technology

ICONST 2018

5-9 September 2018 Prizren - KOSOVO

Sustainable Capitalization of Regulative Forest Ecosystem Services Related to Water Resources Management in BalkanMed Region: The BIOPROSPECT Project

Mallinis Georgios[1], Chrysafis Irene[1], Korakis Georgios[1], Pana Eleanna[1], Takavakoglou Vasileios[2], Dimitrios Zagkas[3]

Abstract: The Balkan Peninsula hosts a broad range of unique forest ecosystems. Forest Ecosystem Services (FESs) constitute the direct and indirect contributions of forest ecosystems to human wellbeing in the region and are usually generated by ecological processes within their area of influence such as catchments, habitats, or land use units.

Water-related services are the most important among the bundle of the provisional, regulating -maintenance and cultural services provided by forest ecosystems in many countries of the Mediterranean Rim. Regulating services encompass all benefits obtained from the regulation of ecosystem processes, including regulation of the chemical condition of freshwaters, attenuation of mass movement, hydrological cycle and water flow regulation, atmospheric composition and condition improvement, water supply and aquatic productivity. An important challenge in the domain of these forest ecosystem services, is the identification of the beneficiaries as well as in the quantification and valuation of the benefits. Quantification, economic and non-economic valuation of forest regulating ecosystem services is not only an approach for underpinning forest ecosystem services significance for beneficiaries' wellbeing. Furthermore, these tasks, are important for forest measures and actions prioritization, efficient allocation of finite resources when the demand exceeds the supply, avoiding unsustainable overuse and degradation of the forest resources.

Aim of this work, which is implement within the 2014-2020 INTERREG VB Balkan-Mediterranean BIOPROSPECT project, is to present an overview of forest regulative services related to water and propose a sustainability and capitalization framework in the Balkan-Mediterranean region. Specific objectives include a detail presentation of the EU and international water policies and directives, a review of the sustainable capitalization mechanisms for water-related forest ecosystem services, as well as forest management measures and practices that could ensure sustainability of forest ecosystem relating to water. In addition, hydrologic models, tools such as the Soil Water Assessment Tool (SWAT), the Integrated Valuation of Ecosystem Services and Tradeoffs (InVEST) and the WaterWorld that could be used for the quantification of the ecosystem services are presented. Finally, some key guidelines for the valuation and capitalization of forest ecosystem services related to water in order to ensure the sustainability of these regulating services in the BalkanMed region are presented.

Keywords Forest ecosystem service, Remote sensing, Systematic review

1 Department of Forestry and Management of Natural Resources, Democritus University of Thrace, Orestiada, 68200, Greece, gmallin@fmenr.duth.gr
2 Department of Agricultural Development, Democritus University of Thrace, Orestiada, Greece
3 HELLENIC FORESTS G.P.
Corresponding Author: gmallin@fmenr.duth.gr

International Conference on Science and Technology

ICONST 2018

5-9 September 2018 Prizren - KOSOVO

Usage Rates of Reed beds in Beyşehir Lake of Some Wild Mammals

Ahmet Mert[1]*, Ahmet Acarer[1]

Abstract: This study was carried out to reveal the usage rate of reed beds in the northwest region of Beyşehir Lake by some wild mammals. For this purpose, the locations of the reed beds in the study area have been primarily determined and mapped. As a result of the inventory in the field; sign, faeces and tracks of wild mammals were detected in a total of 462 points. Indirect census technique was applied to the whole area as a method in the study. Then, presence data plots belonging to wild mammals in which inventory made, were transferred to the digital domain. Density mapping for each species was made using these plots. ArcGIS 10.2 software was used for Hot spot analysis and mapping. Accordingly, in the study area, where for each species were never visited, rarely visited and frequently visited were identified. After then, areas preferred by species in the study area where reed beds intersected were detected. Spatial analyzes were performed using intersection ratios in order to reveal the relationships between these variables. In the result of study, Red fox (Vulpes vulpes), Wild boar (Sus scrofa), Beech marten (Martes foina), Coyote (Canis aureus), Jungle cat (Felis chaus), European hare (Lepus europaeus), Badger (Meles meles), Lynx (Lynx lynx) and Gray wolf (Canis lupus) were determined within area. According to the results of Hot spot analysis; reed beds showed effect on the distribution of wild mammals. In addition, it was detected that Jungle cat (%82), Lynx (%80), Coyote (%77), Red fox (%69), Wild boar (%69), Wolf (%67), Badger (%50), Beech marten (%38) and European hare (%5) were the most preferred species and the highest usage rate in these areas, respectively.

Keywords: Beyşehir Lake, reed beds, wildlife, density map

.

[1]Suleyman Demirel University, Faculty of Forestry, 32260, Isparta, TURKEY
*Correspondingauthor: ahmetmert@sdu.edu.tr

International Conference on Science and Technology

ICONST 2018

5-9 September 2018 Prizren - KOSOVO

Effects of Different Silicon Levels on Plant Growth and Fe Nutrition of Strawberry Cultivar "Camarosa"

Muzaffer İpek[1], Şeyma Arıkan[1], Lütfi Pırlak[1*], Ahmet Eşitken[1], Murat Şahin[2]

Abstract: The Fe deficiency is so important for plant nutrition especially strawberry plants in horticultural species. The high calcareous cause higher soil pH and Fe is not uptake sufficiently by plants. This causes low plant development, productivity and fruit quality. The aim of this research was to determine of silicon treatment effects on plant growth and Fe uptake of strawberry plant. The present study was conducted in greenhouse condition at University of Selçuk, Faculty of Agriculture and Horticulture Department. The effects of five silicon levels (1, 2, 3, 4, and 5mM) on plant growth and Fe uptake were investigated. The Camarosa strawberry cultivar was used as a plant material. The runner plant number, stem diameter, fresh plant and root weight, root length, leaf area, chlorophyll content, stomatal conductance, membrane permeability and Fe nutrient content was determined. The Fe and silicon (5mM) treatment both alone and mixed were found more effective than other treatment on plant growth and Fe uptake in strawberry plants. The runner plant number reached the highest number in silicon treatment (5mM) and Fe treatment with 2.31 and 2.25 runner plant per mother plant, respectively. The lowest runner plant number was obtained from control group with 1.48runner plant per mother plant. The highest Fe content was determined in silicon (5mM) treatment with 163.39mg kg^{-1}. The result of plant growth parameters and Fe uptake showed that silicon application promoted plant growth and Fe uptake in strawberry plants.

Keywords: Iron, Plant Growth, Silicon, Strawberry

[1]Selçuk University, Faculty of Agriculture, 42075, Konya, TURKEY
[2]Siirt University, Faculty of Agriculture, 56100, Isparta, TURKEY
*Corresponding author: pirlak@selcuk.edu.tr

International Conference on Science and Technology

ICONST 2018

5-9 September 2018 Prizren - KOSOVO

Development of Vocational Education Training for Students with Disabilities on Ecological Gardening

Mariana Ivanova[1], Nazan Arifoğlu[2]*, Mustafa Öğütcü[2], Selçuk Birer[2], Hacı Osman Mestav[2]

Abstract: Throughout the world one of the most important issues in education is continually becoming the education of students with disabilities. In this purpose, project entitled "Supporting access to training and qualification of people with disabilities through development of VET course on Ecological Vegetable Gardening based on ECVET learning outcomes", in which researchers from Bulgaria, Belgium, Slovenia and Turkey are involved, is supported by the European Union Erasmus+ Program. The aim of this project (ECOGARD-2017-1-BG01-KA202-036212) is to develop vocational education and training course and to support the improvement of the qualification level of people with learning difficulties in the field of ecological vegetable gardening. Within this project, syllabus, learning outcomes and methods of the course; training course to train the teachers how to train people with disabilities, after preparing the course materials application and practice will be elaborated and prepared. In this way, it is aimed that the students with learning disabilities are acquiring skills and competence as well as employment in the field of ecological agriculture and especially ecological vegetable gardening.

Keywords: people with dissabilities, ecological vegetable gardening, ECVET learning outcomes

[1] University of Agribusiness and Rural Development, Plovdiv, BULGARIA
[2] Canakkale Onsekiz Mart University, Canakkale, TURKEY
* Corresponding author's e-mail: n.arifoglu@comu.edu.tr

International Conference on Science and Technology

ICONST 2018

5-9 September 2018 Prizren - KOSOVO

Moss Gardening: Horticultural Uses

Özlem Tonguç Yayıntaş[1]*

Abstract: As the oldest living land plants, bryophytes, commonly called mosses, have been on Planet Earth for over 450 million years – that's 50 million years before ferns and other plants appeared. These pioneer plants can grow in places that other vascular plants can not grow – for instance, in locations that are too shady or the soil is inferior**.** Over the millennia, tiny mosses have developed features that make them immune to diseases, undesirable food for destructive insect pests, deer-resistant and tolerant of sub-freezing temperatures. In horticulture, position of mosses is almost incomparable in any other existing bryophyte industry (Nelson and Carpenter, 1965). Peat mosses have played a foremost task in horticulture for centuries (Perin, 1962; Arzeni, 1963; Adderley, 1965). Even if their application is a part of the background beautification, it has conventionally been used by Asians, they have frequently been utilized as soil additives and bedding for hothouse crops, potted decorative plants, and seedling beds (Cox and Westing, 1963; Sjors, 1980). Bryophytes are predominantly accepted as soil additives because of their remarkably high water holding capability and permeability to atmospheric air. Sphagnum sp. (peat) is an important soil conditioner and is commonly used for agricultural and horticultural purposes around the world. Many gardeners and landscapers rely on fertilizers, but as moss gardeners, you will need no soil supplements to encourage growth. In fact, too much nitrogen along with other macro, secondary, and trace nutrients could be harmful. Since mosses “eat” dust particles in such minute quantities, fertilizers could actually hamper moss growth. Even organic fertilizers might provide too much of a particular nutrient or micronutrient. For cultivation of mushroom (Agaricus bisporus), Sphagnum peat is the substrate of preference as sheathing/casing medium (Beyer, 1997). Bryophytes have also been used for green house crops, potted ornamental plants, seedlings and in garden soil. The use of mosses in the creation of hanging flower baskets is also common (Smith, 1996). In the USA, moss strips (Hypnum, Polytrichum and Sphagnum) of few centimeters wide are regularly used to construct hanging flower baskets. Another using the terrarium is a drier plant version of the aquarium. A terrarium is frequently set like an enclosed minuscule garden. Selection of moss taxa depends on the required moisture level and effect within the terrarium. For the farmer, landscaper or home gardener who wants to avoid the use of any chemicals such as pesticides, herbicides, and fertilizers, mosses are a natural choice.

Keywords: Bryophytes**,** Mosses, Gardening, Horticulture

[1]Çanakkale Onsekiz Mart University, Canakkale School of Applied Sciences, Fisheries Technology, 17100, Çanakkale, TURKEY
*Correspondingauthor:ozlemyayintas@hotmail.com

A printing error has occurred on this page.

International Conference on Science and Technology

ICONST 2018

5-9 September 2018 Prizren - KOSOVO

Extraction and Purification of Phycocyanin from *Arthrospira platensis* Gomont

Gülen Türker[1], İlknur Ak[2]*

Abstract: Phycocyanins are light-harvesting photosynthetic pigments in the algae such as: Rhodophyceae and Cyanobacteria and they participate in an extremely efficient energy transfer chain in photosynthesis. They consist of twomain groups which are phycocyanins and allophycocyanins. Phycocyanins are widley used in commercial applications as natural colorants for food and cosmetic. In addition, they could be used as a therapeutic agent in oxidative stress-induced diseases. C-phycocyanin (C-PC) mainly extracted from *Artrosphira* species which may contain 14 % (w/w) of this pigment within total cell protein. The aim of this study was to assess the phycocyanin content of dried *A. platensis* biomass using methanol solition. Dry biomass of *Arthrospira platensis* was obtained from İskoç Algae, Muğla, Turkey and stored at 5 ± 2 °C. In order to estimate the content of phycocyanin in dry biomass, repeated extraction was performed in the following manner. Dry biomass (0.5 g) was added 20 ml 70% methanol solution. The suspension was mixed and soaked at 4 °C for 1 hour. After extraction, the residue was centrifuged at 8900 rpm for 10 min. The supernatant was collected. This process was continued until the colorless supernatant was obtained. The phycocyanin content of the samples were determined according to Bennet and Bogard (1973). The collected phycocyanin solution was dried at 30 °C and milled into powder before antioxidant extraction. DPPH (2,2-diphenyl-1-picrylhydrasyl) radical scavenging activity was measured according to the Brand-Williams et al. (1995). The C-phycocyanin (C-PC) and allophycocyanin (A-PC) was determined as 0.08 mg/l and 0.21 mg/l, respectively. The total phycocyanin content was found 0.29 mg/g. The powdered phycocyanin, obtanied from dried *A. platensis*, showed antioxidant potential with a high IC50 (10.91 mg/g Ext.) and it is higher than Vitamin C (1.35 mg/g Ext.). In this study, phycocyanin was extracted from dried biomass of *A. platensis* by 70 % methanol solution. The results showed that phycocyanin production decreased with using methanol solution for extraction. The antioxidant acitivy of dried phycocyanin was lower than Vitamin C. According to our findings of this study that further investiagtions need to evaluate solvent extraction methods and physical form of the biomass to edevelop extraction process.

Keywords: *Arthrospira platensis*, C-Phycocyanin, A-Phycocyanin, Antioxidant activity

[1] Çanakkale Onsekiz Mart University, Çanakkale School of Applied Sciences, Department of Food Technology 17100, Çanakkale/Turkey
[2] Canakkale Onsekiz Mart University, Faculty of Marine Sciences and Technology, Department of Aquaculture, 17100, Çanakkale/Turkey
*Corresponding author: ilknurak@gmail.com

International Conference on Science and Technology

ICONST 2018

5-9 September 2018 Prizren - KOSOVO

Mapping Urban Green Spaces Based on an Object-Oriented Approach

Derya Gülçin[1]*, Abdullah Akpınar[1]

Abstract: The advent of technology and its implications on especially remote sensing image processing using High Resolution Satellite Images (HRSI) to map land cover provide researchers to monitor land changes, make landscape analyses, and manage land transformation. One of land dynamics that should be mapped for the sustainability of urban area is green spaces. Urban green spaces, such as parks, playgrounds, and residential greenery may promote both mental and physical health. Besides, they contribute to ecosystem services such as reducing heat island effect and carbon storage, aiding water regulation etc. Therefore, mapping urban green infrastructure from a high-resolution satellite image provides an important tool to conduct studies, researches, and projects for sustainable development of urban areas. As the material of this research, one of the orthophotos of Aydin urban area exemplifies the park, the green cover in the agricultural area, the playground, and the residential garden, was used. For classifying land cover from the orthophoto with Object-Based Image Analysis (OBIA), eCognition Developer 9.0 software was utilized. To combine spectral and shape features, multiresolution segmentation was implemented. Additionally, features as brightness and ratio green were used for the extraction of urban green areas. In this research, urban green areas were successfully extracted from the orthophoto and accuracy assessment was performed on the classified image. OBIA of high resolution imagery enables to extract detailed information of various targets on urban areas. The result of accuracy assessment of the classification achieved 84.68% overall accuracy. To increase the accuracy via manual interventions, manual classification tool of eCognition Developer 9.0 may be used if needed. .

Keywords: Urban green space, Green infrastructure, Object-based classification, Aydin

[1]Department of Landscape Architecture, Agricultural Faculty, University of Adnan Menderes, 09010, Aydin, Turkey

International Conference on Science and Technology

ICONST 2018

5-9 September 2018 Prizren - KOSOVO

The First Record of Egg Dimension and Breeding Biology of Collared pratincole (*Glareola pratincola*) from Southwest Turkey

Yasemin Öztürk[1]*, Leyla Özkan[2]

Abstract: As a result of its natural position, Turkey has different climate and rich habitat types besides lying on migration roads that are located between Eurasia and Africa. The aim of this study is to investigate the breeding biology of collared pratincole, a migratory bird species in Antalya/Boğazkent (Turkey). There are a lot of habitat types in this area of 200 ha. This speciality serves great biodiversity. Field work was carried out from March to October between 2016 and 2017. Every two years, from March to October, observations have been made as three days a week. In the study, direct observation method has been applied and the nests has been found by following the courting and copulating behaviours and incubating individuals from determined points that have been specified so as not to disturb the birds. The egg volume has been calculated according to the formulation V=0.51xLxW2 (Hoyt 1979) while egg index has been figured with regard to EI:100xW/L (Winkel 1970) formulation. 35 individuals and 16 nests were found in the first year and 25 individuals and 8 nests in the next year. According to the hatchling size, the breeding success of the species was 86.7% in 2016 and 85,7% in 2017.Considering the fledgling size, the figures were 46.4% in 2016 and 66.7% in 2017 respectively. Many factors affecting the breeding success of the species were specified in the region. Hooded crows (Corvus cornix), for example, was detected as being the natural predator of the species. Furthermore, the invasion of the breeding areas by humans and human-related activities such as construction, tourism and agriculture also harmfully affects the breeding success. According to our study Antalya/Boğazkent is a very important bird area in Turkey.

Keywords: Breeding success, Bogazkent, Egg index, *Glareola pratincola*, Marsh Migration, Productivity, Turkey .

[1]Burdur Mehmet Akif Ersoy University, Golhisar Vocational School Forestry Department, Golhisar, 15400, Burdur, TURKEY
[2]Duzce University, Faculty of Forestry, Wildlife Ecology and Management Department, Duzce, TURKEY
*Corresponding author: yyaseminozturk@gmail.com

International Conference on Science and Technology

ICONST 2018

5-9 September 2018 Prizren - KOSOVO

Long Term Bioaccumulation Monitoring of Chemical Contaminants in *Mytilus galloprovincialis*

Serhat Çolakoğlu[1], İbrahim Ender Künili[2*], Fatma Çolakoğlu[3]

Abstract: *Mytilus galloprovincialis* is an important shellfish species that constitutes major production and consumption among bivalve mollusks in Turkey. Shellfishes nutritive and well balanced diet stuffs for humans. However, they can be harmful to health, since they are filter feeding organisms and accumulate the toxic substances from the water in which they live. Thus, biomonitoring is an important preventative action in point of food safety. In this point, this study has designed to investigate the chemical contaminants in *M. galloprovincialis* from one of the most harvested place in Turkey. *Mytilus galloprovincialis* samples were collected from the Southern Coasts of Marmara Sea, Turkey, in the period of Winter 2014 - Summer 2017. After morphometric measurements, samples were prepared for analysis. Meat of mussels were cut into small pieces and then subjected to homogenization prior extraction of chemicals. Individual groups of dioxins (PCDDs, PCDFs, PCBs and TCDD) and the total dioxin concentrations were determined with using GC/HRMS, after samples prepared according to US EPA (1994). Benzopyrene with total PAHs were determined after extraction of samples with dichloromethane and using GC coupled with an ionization detector. Toxic metals (Pb, Cd, and Hg) in samples were determined after organic digestion constituted by solubilization of the 0.5 g portion of mussel meat with 10 ml concentrated nitric acid. Metal analysis was applied using Varian Liberty AX Sequential ICP-AES. Maximum levels of dioxins, PAHs, and toxic metals during monitoring period were determined as 0.30 pg/g, 2.52 mg/kg, and 0.43-0.34-0.76 (Pb-Cd-Hg) mg/kg, respectively. Dioxins, PAHs, and toxic metals were determined below the threshold levels enforced by European Commission. Results have shown that *M. galloprovincialis* samples were contaminated with toxic chemicals during 2014-2017 period. However, the determined levels of these chemicals were always lower than the threshold levels. Future researches should be maintained to ensure safety of this most harvested and consumed shellfish species for preventing consumer from health risks.

Keywords: *Mytilus galloprovincialis*, benzopyrene, polycyclic aromatic hydrocarbons, dioxin, toxic metals

[1]Canakkale Onsekiz Mart University, Vocational School of Technical Sciences, 17100, Canakkale, TURKEY
[2]Canakkale Onsekiz Mart University, Faculty of Marine Science and Technology, 17100, Canakkale, TURKEY
[3] Canakkale Onsekiz Mart University, School of Applied Sciences, 17100, Canakkale, TURKEY
*Corresponding author: enderkunili@yahoo.com

International Conference on Science and Technology

ICONST 2018

5-9 September 2018 Prizren - KOSOVO

Antıoxıdant and Antımıcrobıal Actıvıty of Sea Cucumber (*Holothuria tubulosa*) Exracts

İbrahim Ender Künili[1]*, Fatma Çolakoğlu[2]

Abstract: *Holothuria tubulosa* is an economic and most harvested sea cucumber species found in Turkey seas. Sea cucumbers are known to be sources of some of bioactive components which are plays important roles in human health. In this study, it was aimed to determine the antioxidant and antimicrobial activity of *H. tubulosa*. Total of 120 Holothuria tubulosa species were collected by scuba diving up to 15 meters depth from Southern Coasts of Çanakkale Strait in Marmara Sea, Turkey. Samples were cut into small pieces (<1 cm^2) and leave to oven (Nüve, FN 500) at 70°C for 20 hours for drying. Dried samples grinded into powder. Powders of samples mixed with water, water+methanol and acetonitrile at 1:10 (v/w) and % 0.1 trifloroacedic acid (6:4, v/v). The suspensions were mixed continuously at 25°C for 24 hours. At the end of continuous stirring, samples were centrifuged 6000 x g for 20 min. The supernatants of samples after centrifugation were collected and the solvents in supernatants were evaporated at 50°C. The remained extracts in flasks were rehydrated with distilled water, lyophilized and stored -20°C till used.For antioxidant activity, DPPH radical scavenging activity, Iron chelating, and Iron-Ferrozine Complex Reducing Capacity tests were performed and compared with Vitamin C, Butylated hydroxytoluene (BHT), and Ethylene Diamine Tetra Acedic Acid (EDTA). Antimicrobial activity of samples were determined the method of disk diffusion and tube dilution method described by CLSI (2006) and compared with reference antibiotic Amoxcyline-Cluvanaic acid. *H. tubulosa* extract has shown 60% DPPH activity, 60% Iron chelating activity and 0.7 absorbance at 700nm for Iron complex reducing activity. These percents were lower than reference antioxidants, but at highest concentration, they were closer to reference materials. Antimicrobial activity was observed as weak at all concentration in comparison with the reference antibiotic, Amoxcyline-Cluvanaic acid. Results have shown that there can be potantial antioxidant compounds in the extracts of *H. tubulosa*. Further reasearches sohuld be performed to clear this subject in point of exploring chemical structures of these components or utilization of these extracts in practical (e.g. food sector).

Keywords: *Holouthuria tubulosa*, sea cucumber, extract, antioxidant, antimicrobial, DPPH.

Acknowledgement: This work was supported by Scientific Research Fund of Canakkale Onsekiz Mart University under Grant Project No: FDK-2014-430.

[1]Canakkale Onsekiz Mart University, Faculty of Marine Science and Technology, 17100, Canakkale, TURKEY
[2] Canakkale Onsekiz Mart University, School of Applied Sciences, 17100, Canakkale, TURKEY
*Corresponding author: enderkunili@yahoo.com

International Conference on Science and Technology

ICONST 2018

5-9 September 2018 Prizren - KOSOVO

Assessing Teachers Digital Competency: Web-based tool

Ermira Idrizi[1], Andrea Kulakov[1], Sonja Filiposka[1], Vladimir Trajkovik[1]

Abstract: Even though there are several different frameworks and standards for proving the digital competencies expected from teachers, there is a need for a Web-based assessment tools that allow real, dependable and valid assessment of these competencies. This paper addresses the design challenges related to a software solution for self- and peer-assessment of teachers' digital competencies. In this system the competencies are assessed by a teacher his/herself or by his/her peers using the performance indicators that are based on the competency model for Teachers. Measuring digital competencies is a difficult task, which is seen in some attempts to develop frameworks and models. Evaluation methodology and instruments must be reliable, valid and flexible, but also affordable with respect to time and costs. Methodology together with assessment instrument must make sure that assessment decisions involve the evaluation of adequate evidence to judge the level of competency of the teacher. The methodology must express similar outcomes for teachers with equal competency at different times or places. The design challenge is to enable teachers to evaluate their educational technology competencies. In the first phase, we use personas as a method to describe the goals and motivations of archetypal users. We introduce five personas that cover our expected user groups: teacher training master student, novice teacher, experienced teacher, educational technologist of a school and training manager. Key concepts of this system will be the competency test which contains tasks that are mapped to performance indicators where users evaluate themselves by taking the competency test. In addition, a peer to peer review is established and the competency profile is created based on the complete input. This system is an inital work of how teachers can asses their digital competeny level, evaluate peers and also upgrade their level of competency. We hope this tool will not be a monolithic Web application, but as one component in a larger digital ecosystem of distributed tools that teachers are using in their everyday work in the digital age. Teachers' competency profiles created can be linked and embedded to other social media systems. In addition to supporting teachers' professional development the system will be used for collecting valuable data for further research on teachers' professional development. We foresee that this software can be also used as a generic competency assessment tool.

Keywords: Teachers digital competency, Web-based assessment tool, Peer review

Acknowledgement: The system will make it more easy for teachers to acccentate their digital competency level as well as open a communication channel between teachers to share their work and interchange materials for an specific competency level.

[1]Faculty of Computer Science and Engineering, Ss. Cyril and Methodius University, Skopje, R. Macedonia
*Corresponding author: ermiraidrizi@gmail.com

International Conference on Science and Technology

ICONST 2018

5-9 September 2018 Prizren - KOSOVO

Climate sensitivity of Pinus nigra trees from the Turkish lake district

Bart Muys[1]*,Ellen Janssen[1] , Kerstin Treydte[2], Nesibe Köse[3], Kürsad Özkan[4]

Abstract: The ancient city of Sagalassos, situated in the Turkish lake district, has been the subject of archaeological research for the last two decades, with a focus on nature-society interactions over times through interdisciplinary research. One of the points of interest is the study of climate in the past. Paleo-ecological records show a number of vegetation shifts since late Roman times that are suspected to be climate-driven. Tree-ring based climate reconstruction can provide additional insight into past climatic and environmental changes in the area. In this poster we present preliminary results of our dendroclimatological research in the region.

162 *Pinus nigra* and 200 *Juniperus excelsa* trees were sampled from 6 sites at tree-line altitude (1570-2130 masl), some dating back to 1300 AD. Tree ring width (TRW) was measured and samples were crossdated following standard procedures. As this work is still ongoing, we present preliminary results from two sites: YAK and SAN. Both time series were detrended with a negative exponential spline. The detrended series were averaged to form two site chronologies. The series were calibrated against contemporary climate data from Isparta, Seydisehir and Beysehir weather stations and from gridded data (CRU and EOBS). Pearson correlation coefficients between tree ring width and temperature, precipitation as well as drought indices (PDSI and SPEI) were calculated.

Tree ring width negatively correlates with June temperature, and positively correlates with May/June precipitation. TRW responds particularly strongly to May/June SPEI.

Comparison of tree ring width data with precipitation, temperature and drought indices indicates that black pine trees from the Turkish lake district respond well to late spring/early summer drought. Data from additional trees & sites will improve correlation coefficients and possibly point out other relevant climate signals in the trees. Stable isotope analysis and density measurements on a selection of samples may further support or improve the strength of the signal and make a reconstruction of drought incidence for the last five centuries.

Keywords: Dendrochronology, Dendroclimatology, Tree ring width

[1]KU Leuven, Department of Earth & Environmental Sciences, 3001 Leuven, BELGIUM
[2]WSL, 8903 Birmensdorf, SWITZERLAND
[3]University of Istanbul, Faculty of Forestry, TURKEY
[4]Suleyman Demirel University, Faculty of Engineering, 32260, Isparta, TURKEY
*Corresponding author: bart.muys@kuleuven.be

International Conference on Science and Technology

ICONST 2018

5-9 September 2018 Prizren - KOSOVO

The Importance of Root Rot Diseases in Forest Nurseries and The Usage of Mycorrhizal Fungi in Control

Ayşe Gülden Aday Kaya[1]*, Refika Ceyda Beram[2], H. Tuğba Doğmuş Lehtijarvi[2]

Abstract: *Phytophthora* and *Pythium*, two genera in the Pythiaceae, both include large numbers of soil-borne species responsible for root rot of herbaceous and woody plants, including forest trees. Many coniferous and deciduous tree species are susceptible to *Phytophthora* and *Pythium* infections. Moreover, when asymptomatic infected nursery plants are transported to planting sites, the pathogens, particularly *Phytophthora* spp., can cause considerable damage to other trees in the wider environment. Transfers of *Phytophthora* spp. from nurseries to the wider environment have frequently been reported, some resulting in severe dieback or death of the transplanted trees and shrubs, and irrevocable contamination of the planting sites. Approximately 496 million seedlings of 400 woody plant species, including *Pinus nigra*, *Cedrus libani*, *Juniperus excelsa* and *Castanea sativa*, are produced annually by forest nurseries in Turkey. Most of these plants are sold as 1- or 2-year-old bare root seedlings and are used for reforestation, although some are also used for amenity plantings. As to produce healthy seedlings, the role of mycorrhizal fungi which facilitate the uptake of water and nutrients, and increase plant resistance against draught, heavy metal toxicity and pathogens, is very important. In this review, the importance and the causal agents of the root rot diseases and its biological control with mycorrhizal fungi have been discussed.

Keywords: plantation, disease, oomycota, dieback

[1]Applied Sciences University of Isparta, Yenişarbademli Vocational School, 32850, Isparta, TURKEY
[2]Suleyman Demirel University, Faculty of Forestry, 32260, Isparta, TURKEY
*Corresponding author: guldenaday@sdu.edu.tr

International Conference on Science and Technology

ICONST 2018

5-9 September 2018 Prizren - KOSOVO

Population Structure of Wedge Clam, *Donax trunculus* (Bivalvia, Donacidae), in the Southern Sea of Marmara, Turkey

Serhat Çolakoğlu[1*], Pınar Yıldırım[2], Mine Çardak[2], Mukadder Arslan İhsanoğlu[3]

Abstract: The growth, reproduction, and density of wedge clam (*Donax trunculus*) were studied at a depth of 0.5-2 m in Denizkent in the Southern Sea of Marmara, Turkey. Samples were collected monthly between May 2017 and July 2018. The average density of the studied population ranged between 118 individuals m^{-2} (November) and 245 individuals m^{-2} (July). Von Bertalanffy growth parameters using the length–frequency distribution of Donax trunculus were estimated at L_∞ = 43.85 mm and the rate at which the asymptotic length (L_∞) is approached (K) = 0.73 y^{-1}. The slowest growth period was in January. Growth performance index, potential longevity and maximum length derived from seasonal parameters were calculated as 3.15, 4.11 y and 42 mm, respectively. The growth pattern showed negative allometric growth (slope [b] = 2.71), the spawning period occurred from April to July and peaked between May and June.

Keywords: *Donax trunculus*, growth, reproduction, density, Sea of Marmara.

[1]Canakkale Onsekiz Mart University, Vocational School of Technical Sciences, 17020, Canakkale, TURKEY
[2] Canakkale Onsekiz Mart University, School of Applied Sciences, 17020, Canakkale, TURKEY
[3]Canakkale Onsekiz Mart University, Faculty of Marine Science and Technology, 17020, Canakkale, TURKEY
*Corresponding author: serhat_colakoglu@comu.edu.tr

International Conference on Science and Technology

ICONST 2018

5-9 September 2018 Prizren - KOSOVO

Power Loss Optimization of Boost Power Factor Correction Inductor

Erkan Karakaş[1], Yusuf Öner[2], Selami Kesler[2] ,Metin Ersöz[3]

Abstract: Power factor is a very important parameter in power electronics because it gives a measure of how effective the real power utilization in the system. It also represents a measure of distortion of the line voltage and the line current and phase shift between them. Power Factor Correction (PFC) shapes the input current of the power supply to be in synchronization with the mains voltage, in order to maximize the real power drawn from the mains. Active power factor correction (APFC) techniques are popularly employed in many types of electronic equipments to increase the power factor and decrease the total harmonic distortion factor. Although APFC can be achieved by several topologies, the boost converter is the most popular topology used in PFC applications for simplicity and efficiency. The boost converter can operate in three modes: continuous conduction mode (CCM), discontinuous conduction mode (DCM), and critical conduction mode (CrCM). CCM operation requires a larger filter inductor compared to others. But it has several advantages like lower peak current, conduction loss and EMI. Boost Inductors play a critical role in Boost type PFC converters. It stores the energy that is transferred to the output and defines converter boundary. Also affects system efficiency through increasing or reducing semiconductor and magnetic losses depending on its value. In a typical boost PFC, inductor losses are %20 of total loss. Inductor losses include core and winding losses in AC and DC. There is a balance between core and winding losses. To obtain minimum inductor loss, number of turns (N) and current ripple (ΔI) of inductor must be selected properly. In this paper, an optimization has been applied to number of turns and current ripple in order to minimize the loss of the inductor in a typical boost PFC. Magnetics Company's 77439A7 Kool Mμ powder core is selected as the inductor core. For 500W output power, optimum results have been calculated and applied to an experimental setup.

Keywords: Boost PFC, Loss Optimization, PFC Inductor Design, Kool Mμ.

[2]Pamukkale University, Faculty of Engineering, 2100, Denizli, TURKEY
[3]Pamukkale University, Technical School Vocational High School, 2100, Denizli, TURKEY
[1]Senkron Ar-Ge mÜhendislik, Pamukkale Teknokent, 2100, Denizli, TURKEY
*Corresponding author: yoner@pau.edu.tr

International Conference on Science and Technology

ICONST 2018

5-9 September 2018 Prizren - KOSOVO

Investigation of the Effects of Rib on the Power Factor in Synchronous Reluctance Motor Rotor Design

Metin Ersöz [1], Yusuf Öner[2], Erkan Karakaş[3] , Selami Kesler[2]

Abstract: SynRMs are known as cold rotor motors. Since there are no copper bars in the rotors as in asynchronous motors, rotor copper losses are reduced to zero and rotor losses are minimized. In this way losses are reduced and motor efficiency improvements are ensured. At the same time, these studies show that the power factors of SynRMs are worse than those of asynchronous motors. SynRM's rotor geometry design has been realized. When the design was carried out, flux barriers were designed considering the Ld / Lq ratio. Parametric analyzes have been carried out on the lamination sheet, which is designed for the air / iron ratio on rotor lamination sheets to be important for motor performance. As a result of these parametric analyzes, it has been decided that the lamination sheet has 4 barriers. In the rotor design of SynRM, the measurements of H, W, Rb variables were analyzed and the values were taken into account. In the axial laminated rotor design, the rib widths must be thin so that the q axis inductance is low. The pelt is a factor that affects the power factor of the motor in its width. In this study, the rod-like and non- rib -like structure of the rotor structure of 11 kW SynRM was discussed and the effects of the rib on the power factor were investigated. The prototypes of the rotor geometries obtained as a result of the analyzes were investigated in terms of the effect on the power factor of the rib.

Keywords: Rib, Power Factor, Rotor Design

[1]Senkron Ar-Ge mÜhendislik, Pamukkale Teknokent, 2100, Denizli, TURKEY
[2]Pamukkale University, Faculty of Engineering, 2100, Denizli, TURKEY
[3]Pamukkale University, Technical School Vocational High School, 2100, Denizli, TURKEY
*Corresponding author: yoner@pau.edu.tr

International Conference on Science and Technology

ICONST 2018

5-9 September 2018 Prizren - KOSOVO

The Faintest and Closest Clusters in CFHTLS W4

Mukadder İĞDİ ŞEN [1]*

Abstract: Using T0007 version of CFHTLS Wide 4 (W4) field observations, photometric redshift values were calculated for $0.2 \leq z \leq 1.5$. Also the values of VIPERS spectroscopic catalog were used to control the obtained photometric redshifts. Using the galaxy SEDs in Le PHARE program the results obtained. The best results were found in $17.5 \leq i'_{AB} \leq 21.5$ as catastrophic error of 8.5% and accuracy value of 0.031. The catastrophic error and accuracy values in $17.5 \leq i'_{AB} \leq 24$ were determined as 4.1% and 0.030 respectively; the best correlation coefficient belongs to elliptical galaxies ($r = 0.929$). The relationship for elliptical galaxies between the photometric and spectroscopic redshift values was determined as $z_p = (0.953 \pm 0.008)\ z_s + (0.083 \pm 0.014)$. The detected clusters are in the range of $0.475 \leq z_s \leq 0.937$. In our calculations made by taking the Hubble constant value of 71 km s^{-1} Mpc^{-1}, the distance of the faintest cluster of (i´) 23.946 mag is 1.22×10^{23} km and the closest cluster is 0.61×10^{23} km.

Keywords: Photometric redshift, large scale structure, galaxies, CFHTLS

[1]Trakya Üniversity, Edirne Vocational College of Technical Sciences, 22020, Edirne, TURKEY
*Correspondingauthor: mukaddersen@trakya.edu.tr

International Conference on Science and Technology

ICONST 2018

5-9 September 2018 Prizren - KOSOVO

An Electrodeposition Method of Nickel–Graphene Composite Coatings on Ti–6Al–4V alloy

Osman Özkan[1], Harun Mindivan[2]*

Abstract: Titanium and its alloys are widely used in many applications such as marine, medical, chemical, automotive, architectural, and military sectors. Such a wide range of applications is related to high strength, low weight ratio and excellent corrosion resistance of titanium alloys. However, their poor wear resistance due to adhesive welds that are formed on their surface and the relatively high friction coefficient is one of factors limiting their widespread usage in load bearing applications. For this reason, it is usual to provide a protective surface treatment before their application in service. The main objective of this work has been the deposition of Nickel (Ni)–Graphene (Gr) composite coatings onto Ti–6Al–4V alloy plates via a pulse electrodeposition technique from a Watt's type electrolyte and characterization of their stuructural and tribological features. The characterization of the coatings were done by structural surveys, hardness measurements and wear tests. The addition of Gr nanosheets in a Ni plating solution not only imposed a higher hardness but also enhanced wear resistance. It can be seen from the EDS analyzes, pure Ni coating contains Ni and some rare amount of oxygen which is believed to form after removing from deposition bath. Ni/Gr composite coating similarly contains Ni and excessively carbon peak. According to the EDS results, no any impurity was detected and this show there was no reaction product between the reinforcement and Ni matrix. In this current work, as obtained in the XRD results, higher amount of Gr nanosheets also caused shifting 2θ angle to the right associated with peak broadening which is an evidence of grain refinement. This is also good evidence that Gr nanosheets cause to get heterogeneous nucleation, preferentially in the defect regions. Results showed that the incorporation of GNPs into the Ni matrix improved both hardness and wear behaviour of the composite coating compared to the pure Ni coating.

Keywords: Electrodeposition, Titanium, Surface modification, Wear

Acknowledgement: The financial support of the research foundation of Bilecik Seyh Edebali University (Project no.: 2017-02.BŞEÜ.03-01) is gratefully acknowledged.

[1]Bilecik Seyh Edeali University, Faculty of Engineering, 11210, Bilecik, TURKEY
[2] Bilecik Seyh Edeali University, Faculty of Engineering, 11210, Bilecik, TURKEY
*Corresponding author: hmindivan@gmail.com

International Conference on Science and Technology

ICONST 2018

5-9 September 2018 Prizren - KOSOVO

Tribocorrosion Behavior of Pulse Electrodeposited Nickel Coating on Ti–6Al–4V alloy in a Simulated Artificial Saliva Solution

Osman Özkan[1], Harun Mindivan[2]*

Abstract: Titanium and its alloys are generally preferred in marine, medical, chemical, automotive, architectural, and military sectors because of their high strength, low weight ratio and excellent corrosion resistance. However, the tribological performance of these alloys is inadequate in some engineering applications that include corrosive environments. For this reason, a surface treatment is required to overcome this disadvantage. Nickel coatings produced by electrodeposition are widely applied in different industrial fields because of ductility, excellent corrosion resistance and good wear resistance, with a hardness of between 150 and 700 HV. The coatings of electrodeposition can be performed by direct and pulse currents. Pulse electrodeposition provides a promising method to prepare metal and alloy coatings due to its independently controllable parameters and higher instantaneous current densities when compared with traditional direct current (DC) electrodeposition. In the pulse electrodeposition, the higher quality coating can be obtained by adjusting the plating parameters instead of additives. In the present investigation, pulse electrodeposition technique was used to deposit nickel on a Ti–6Al–4V alloy substrate. Coating of nickel was confirmed by X-Ray Diffractometer (XRD) and Energy Dispersive X-ray Spectroscopy (EDS) analysis. Light Optic Microscope (LOM) and Scanning Electron Microscopy (SEM) were used to assess the coating characteristics. The tribological tests were carried out in dry and open circuit potential conditions at 5 N normal force in an artificial saliva solution. XRD and EDS analyses confirmed the presence of nickel deposit. Pulse electrodeposition time of 1 h significantly improved the dry sliding ve tribocorrosion performance of the Ti–6Al–4V alloy. In this work, Ni coating was successfully deposited on a Ti–6Al–4V alloy substrate by pulse electrodeposition. The wear scar of Ti-6Al-4V alloy showed a combination of abrasive and adhesive wear mechanism as evidenced by the scratches with a very large plastic flow over the entire scar length and microcrack perpendicular to the sliding direction. In comparison, the worn surface topography of the Ni coating was characterized by a mild abrasive wear mechanism. Therefore, it can be said that the differences on the wear mechanisms of both samples could be attributed to the differences in hardness and repassivation kinetics inside the wear scar.

Keywords: Electrodeposition, Titanium, Surface modification, Tribocorrosion

Acknowledgement: The financial support of the research foundation of Bilecik Seyh Edebali University (Project no.: 2017-02.BŞEÜ.03-01) is gratefully acknowledged.

[1]Bilecik Seyh Edeali University, Faculty of Engineering, 11210, Bilecik, TURKEY
[2] Bilecik Seyh Edeali University, Faculty of Engineering, 11210, Bilecik, TURKEY
*Corresponding author: hmindivan@gmail.com

International Conference on Science and Technology

ICONST 2018

5-9 September 2018 Prizren - KOSOVO

Modifying the Properties of the HVOF Thermal Sprayed Inconel 625 Nickel Coating by Pulsed Plasma Nitriding Process

Ramazan Haldun Topçu[1], Harun Mindivan[2]*

Abstract: A new approach for the industrial applications involving high temperatures and aggressive environments of the steels, is by combining the processes of thermal spray with other surface engineering technologies, such as electroless coatings or nitriding. In recent years, literature data reported the nitriding process carried out on nonferrous alloys. In case of thermal sprayed nickel alloys, there is no study thus far on the effect of using pulse plasma nitriding together HVOF thermal spray. Steel plates were cut to the dimensions of 100 mm×50 mm×4 mm. Carbon steel substrates were High-Velocity Oxygen Fuel (HVOF) sprayed with Inconel 625 and then pulsed plasma nitrided at 793 K under 0.00025 MPa pressure for 43200 s in a gas mixture of 75 % N_2 and 25 % H_2. Structural characterization was made by Scanning Electron Microscopy (SEM) and X-Ray Diffraction (XRD) analysis. Mechanical characterization was made by hardness and reciprocating wear tests in dry sliding conditions. Microstructural characterization of the coatings was made by microscopic examinations, X-ray diffraction (XRD) and microhardness measurements. Microscopic examinations were performed on the cross-sections of the coatings by utilizing Nikon Eclipse LV150 light optic microscope (LOM). XRD analysis was carried out by utilizing CuK_α radiation with a Panalytical Empyrean diffractometer. The cross-sectional microhardness measurements were carried out using a Vickers microhardness tester (Shimadzu) with a load 50 g and a dwell time of 10 s. Dry sliding wear tests of the coatings were performed on a reciprocating wear tester operating in ball-on-disc configuration at room temperature. In this configuration, an Al_2O_3 ball with a diameter of 10 mm was sliding forward and backward against the coatings with a sliding speed of 1.7 cm s^{-1}. Normal load of the test, sliding amplitude (wear track length) of the reciprocating motion and overall sliding distance were 5 N, 10 mm and 50 m, respectively. Upon pulse plasma nitriding, surface hardness was significantly increased with a corresponding increase in wear resistance and a decrement in coefficient of friction. Nickel alloys are very expensive. Plating a steel part with nickel would cost much lesser than a part make of nickel alloy for large quantities. Producing a multilayer coating on the surface of the low carbon steel for sliding components under unlubricated conditions by sequential application of HVOF spray and pulsed plasma nitriding processes is the orginality of the study.

Keywords: Nitriding, HVOF spraying, Inconel 625, Wear

Acknowledgement: We would also like to express our thanks to Dr. Ersin. E. KORKMAZ for the support given in nitriding process.

[1]Bilecik Seyh Edeali University, Faculty of Engineering, 11210, Bilecik, TURKEY
[2] Bilecik Seyh Edeali University, Faculty of Engineering, 11210, Bilecik, TURKEY
*Corresponding author: hmindivan@gmail.com

International Conference on Science and Technology

ICONST 2018

5-9 September 2018 Prizren - KOSOVO

Dye Decolorization by Free and Immobilized Wild Thyme Polyphenol Oxidase Enzyme

Gulnur Arabaci[1]*, Ayse Usluoglu[2], Cengiz Cesko[3]

Abstract: Environmental pollution is becoming increased by textile waste waters as technology improves and poses a great threat to the health of humans and other living organisms around the world**.** For this reason, environmentally friendly and biotechnologically useful new methods have been developed**.** In this context, recent studies have focused on the development of immobilized enzymes and their applications for the removal of textile dye wastes from waste water. In this work, polyphenol oxidase enzyme (PPO) was extracted and partially purified from wild thyme (*Thymus serpyllum* L.) and immobilized on calcium alginate beads. Then, the free and immobilized enzymes were used for the removal of acid and metal complex dyes. 10 g**r**am of wild thyme plant from Sakarya region of Turkey was extracted with proper phosphate buffer solution (pH 7.0). The extract was mixed with different amounts of solid (NH4)2SO4 to reach 80% saturation in solution. This mixture was then centrifuged and dialyzed at 4°C in phosphate buffer for 24 h. The dialyzed enzyme was purified with Sephadex G-100 column. The purified enzyme was immobilized in sodium alginate beads with sodium alginate and $CaCl_2$ in distilled water. The free and immobilized enzymes were kinetically characterized by using 4-methylcatechol as a substrate at 420 nm. Telon Yellow ARB, Lanaset Bordo B, Lanaset Blue PA2R, Telon Red MGWN were used to determine the decolorization of dyes by the free and immobilized wild thyme PPO enzyme and the disappearance of color in the dye solutions by PPO enzyme was examined at prearranged λmax of the individual dye. Polyphenol oxidase enzyme was successfully partially purified from wild thyme and immobilized onto alginate beads. Immobilized wild thyme PPO enzyme had higher pH and temperature stability compare to free enzyme. Immobilized enzyme was considerably more effective for the decolorization of dyes as compared to free enzyme at pH 4.0. Purified and immobilized wild thyme enzyme was successfully characterized. Immobilization of the enzyme increased its stability to pH and temperature that can be more suitable for industrial applications especially decolorization of different textile dyes in wastewater.

Keywords: Polyphenol oxidase, wild thyme, alginate, immobilization, decolorization

Acknowledgement: This work was financially supported by Sakarya University Scientific Research Foundation (Project number: FBDTEZ- 2016-50-02-001).

[1]Sakarya University Science and Arts Faculty Chemistry Department 54187, Sakarya, TURKEY
[2]Sakarya University Science and Arts Faculty Chemistry Department 54187, Sakarya, TURKEY
[3]Sakarya University Science and Arts Faculty Chemistry Department 54187, Sakarya, TURKEY
*Corresponding author: garabaci@sakarya.edu.tr

International Conference on Science and Technology

ICONST 2018

5-9 September 2018 Prizren - KOSOVO

Forest Site Classification Acoording to The Distribution of Woody Plants in Gölhisar district

Özdemir Şentürk[1]*, Mehmet Güvenç Negiz[2], Serkan Gülsoy[3]

Abstract: Vegetation is a combination of plant species in a specific area that develops under certain site conditions has similar ecological requirements. From past to present day, a lot of research has been done on vegetation in different countries and / or regions. In recent years, many analytical methods for vegetation classification have been developed. In this study, it was aimed to classify and maping the forest sites using analytical methods according to the distribution of plant species in the Gölhisar district which hosts important vegetation communities. The study was carried out in 100 sample plots measuring 20x20 m in Gölhisar district. The woody plant species identified in these plots were recorded as presence and absence data. First, clustering analysis was applied to these data and vegetation groups were obtained on the basis of hierarchical clasification procedure. In the next step, environmental variables and vegetation societies are modeled using the classification tree technique. Models with statistically significant results as a result of the chi-square test were mapped and classification of forest sites in the district have been completed. At the last stage, indicator species were determined for each vegetation community using indicator species analysis. As a result of the clustering analysis and modeling stages which are performed depending on the woody plant species, a forest site classification for the district has been carried out. As a result, all environmental variables, mainly elevation, that are the most effective in distinguishing forest sites in the district have been identified. As a result of this study, basic forestry applications such as regeneration, afforestation and protection in the district can be implemented more successfully thanks to the map obtained from this study. In addition, these maps are of great importance in terms of observing the ecosystems against current threats such as climate change and environmental pollution.

Keywords: Cluster analysis, elevation, Gölhisar district, site factors, vegetation

Acknowledgement: We would like to express our appreciation to Burdur Mehmet Akif Ersoy University, Scientific Research Project Commission, which supported this study (0295-NAP-16)

[1]Burdur Mehmet Akif Ersoy University, Gölhsihar Vocational School, Forest Department 15400, Gölhisar, Burdur, TURKEY
[2]Isparta University of Applied Sciences, Sütçüler Prof.Dr. Hasan Gürbüz Vocational School, 32260, Isparta, TURKEY
[3]Isparta University of Applied Sciences, Faculty of Forestry, 32200, Isparta, TURKEY
*Corresponding author: ozdemirsenturk@gmail.com

International Conference on Science and Technology

ICONST 2018

5-9 September 2018 Prizren - KOSOVO

"Outside the Law" Acoustics

Vitor Rosão[1]*, Nazlı Yalçındağ[2], Mustafa Ece[3]

Abstract: Often Engineers, and other technicians, are faced with situations whose legal framework is not clear or up-to-date, given the latest scientific developments in the field. This situation also frequently occurs with Acoustical Engineers (here understood in a broad sense: all technicians who work and have responsibilities in the area of Acoustics). The aim of this communication it is analyse the "Outside the Law" (*Contra Legem*) acoustics situations and present, in a reasoned way, what actions are judged more appropriate, given the Engineer's ethical and deontological duties. The analysis and reasoning will be followed by practical examples for an easier understanding of the *Contra Legem* situations and of the recommended actions. The recommended actions should be understood only as an indication, according the authors experience and sensibility, and each Engineer/Technician, with responsibilities, should form his/her own opinion and define accordingly his/her steps. The authors hope this work can be useful, helping to make the difficult "out-of-law" decisions that need to be made. Typical law statments and autors experience. Useful recomendations for Acoustical Engineer's decisions. One example: when a given legislation, and/or national standard, has a methodology of characterization and penalization of noise due to the presence of tonalities, which is not in line with the latest scientific developments of the matter, should the Acoustic Engineer be restricted to the application of the national legislation/standard or apply the latest methods?

Keywords: Acoustics; Out-of-law.

[1]SCHIU, Vibration and Noise Engineering, Av. Villae de Milreu, Bloco E, Loja E, Estoi, 8005-466, Faro, PORTUGAL
[2]Suleyman Demirel University, Faculty of Engineering, 32260, Isparta, TURKEY
[3]Antalya Metropolitan Municipality, Department of Environmental Control and Protection, 07310, Antalya, TURKEY
*Corresponding author: vitor.schiu@gmail.com

International Conference on Science and Technology

ICONST 2018

5-9 September 2018 Prizren - KOSOVO

Mapping Habitat Suitability Of Game Animals in Sütçüler District, Isparta

Halil Süel[1]*, Kürşad Özkan[2], İdris Oğurlu[3]

Abstract: This study was carried out to create habitat suitability model of game animals associating by environmental, climatic factors and presence data of these species in Sütçüler-Isparta. For this purpose, 1090 sample plots on 218 transect were taken. All sings and footprints in total 6540 plots were determined and recorded to inventory cards to represent the species. Environmental variables were determined using by topographic and geological digital maps. Climatic variables were also supplied as climatic data using by the digital maps in http://www.worldclim.org data set. In the study, maximum entropy approach based on the presence data was considered. On this context, principal component analysis (PCA) was applied to reduce the climatic variables having high correlation each other. The main data on wild animals and environmental variables were subjected to modelling in MAXENT software. During the modelling stages, 10 times cross-validation test was applied to each species and ROC values of training and testing results for each iteration were recorded. The most appropriate model was chosen according to the average ROC and standard deviation values. The validity of this model was also tested Jacknife and Omission statistics. Finally, habitat suitability maps were generated using by the values of current models in Global Mapper 15 program. In this study, habitat suitability models for wild goat, hare, wild boar, badger, beech marten, gray wolf and red fox were obtained in Sütçüler district. According to habitat suitability maps, the altitude, bedrock, mean temperature of wettest quarter (BIO8), roads and streams were found as the most important environmental variables influencing the distribution of the species in the district.

Keywords: maximum entropy, MAXENT, environmental factors, mammals game species, habitat suitability models

[1]Isparta University of Applied Science, Sütçüler Prof. Dr. Hasan Gürbüz Vocational School, 32260, Isparta, Turkey
[2]Isparta University of Applied Science, Faculty of Forestry, Isparta, Turkey
[3]Istanbul Ticaret University, Istanbul, Turkey
*Correspondingauthor: halilsuel@isparta.edu.tr

International Conference on Science and Technology

ICONST 2018

5-9 September 2018 Prizren - KOSOVO

Predicting the Effect of Climate Change on the Potential Distribution of Crimean Juniper

Serkan Gülsoy[1], Ahmet Mert[1], Serkan Özdemir[2*]

Abstract: How climate change will affect the distribution of plant species in the future is an important topic in the ecological researches. Climate change scenarios are the most preferred parameters for revealing this uncertainty. The aim of this study is to determine the potential distribution areas for the present and future of the crimean juniper (*Juniperus excels* M. Bieb) that have significant distribution in Turkey. The present study was carried out in the Lakes district that covers Burdur, Isparta and Antalya provinces in the west of the Mediterranean region. During the study, the inventory data of 40 productive juniper stands in the region were collected. The future projections for the study area were made for the year 2070 with all Representative Concentration Pathways (RCPs) scenario (2.6, 4.5, 6.0, and 8.5) and 19 bioclimatic predictors from HadGEM2-ES. The bioclimatic variables were eliminated after a multicollinearity test, and their contributions were assessed using jackknife test. Modeling was performed by using the Maximum Entropy (MaxEnt) method. The AUC value of the acquired model was determined as 0.966 ± 0.028 (excellent accuracy). The model identified that Precipitation of Driest Month (bio14), Temperature Seasonality (bio4), Precipitation of Coldest Quarter (bio19), Max Temperature of Warmest Month (bio5), Mean Diurnal Range (bio2) was the major influenced variables in the current and future distributions of the species. According to the models acquired for the climate scenarios, there will be a dramatic decrease in the potential distribution of the crimean juniper in the Lakes district. Also, the potential distribution areas of the species will shift from the Mediterrenaen region to the inner parts of Western Anatolia and Western Black Sea. However, in present study, only data that acquire from the Lakes district were used. It is thought that the data to be collected from other districts together with this region can be present more precision results. Therefore, it is important to support this study with a more comprehensive inventory in the future. Consequently, the results from all these studies will be able to create an effective base for the biodiversity and ecosystem planning studies to be realized according to the climate change scenarios.

Keywords: Climate change, Crimean Juniper, Maximum Entropy, Representative Concentration Pathways (RCPs)

Acknowledgement: This study was financed by the TÜBİTAK (Project ID: 112O814). We would like to thank TÜBİTAK for their supports.

[1] Isparta University of Applied Science, Faculty of Forestry, Isparta, TURKEY
[2] Isparta University of Applied Science, Sütçüler Prof. Dr. Hasan Gürbüz Vocational School, Isparta-Sütçüler, TURKEY

*Corresponding author: serkanozdemir@isparta.edu.tr

International Conference on Science and Technology

ICONST 2018

5-9 September 2018 Prizren - KOSOVO

A Preliminary Investigation on the Earthworm (Clitellata, Megadrili) Distribution in Different Stands on Turkmen Mountain.

İbrahim Tavuç[1*], Mete Mısırlıoğlu[2], Aliye Sepken Kaptanoğlu[3], Nejat Çelik[3]

Abstract: Earthworms are defined as ecosystem engineer due to their possitive effects on the physical, chemical and biological properties of the soil. While the number of studies and interest in these organisms has been increasing all over the World, there have not been enough studies about the ecology of these organisms in our country. This study was carried out as a preliminary study to determine the status of different earthworm species on different stands in Turkmen mountain and to determine whether there is any difference in species richness between stands. The earthworms were gathered from the areas of 30x30x20 cm (Black Pine, Yellow Pine, Beech, Grassland, Black Pine + Yellow Pine) in 5 different stands in Turkmen Mountain located in the borders of Eskişehir and Kütahya. The earthworms were collected by combining the commercial mustard method with the hand sorting method. The earthworms were placed in plastic containers with % 70 ethyl alcohol and were taken to laboratory. Species and numbers were determined by stereo microscope in laboratory. With the data obtained, the species richness of each stand was calculated using Shannon Weiner diversity index in terms of earthworm. In the result of the study, 10 species and 74 individuals belonging to 4 genuses (*Aporrectodea, Dendrobaena, Lumbricus, Octolasion*) were found. The species with the highest frequency value is *Dendrobaena persimilis* (Omedeo & Rota, 1989). The area with the highest species richness was determined as grassland and the area with the least species was identified as Black Pine stands. When the earthworm abundance value is calculated for each stand in terms of earthworm, most individuals in yellowpine+blackpine, least individuals blackpine stands have been found. It has been observed that the combination of commercial mustard with handsorting method takes too much time. When eveluated in terms of yield, the commercial mustard method was not effective. Hand sorting method is effective and quick a method in terms of yield, but it requires intensive workload. In addition, there are not enough studies about this organism in our country. Therefore, there is a need for studies on relationships between vegetation and environmental factors with earthworms, their ecology and earthworms.

Keywords: Earthworms, Biodiversity, Ecology, Species richness, Shannon index

Acknowledgement: We thank Eskişehir Forest Soil and Ecology Research Institute for their valuable support in field-work. We would like to thank the Technological Research Council of Turkey (TÜBİTAK-2229): Biodiversity Measurement Processes - Inventory, Data Transfer and Calculation Techniques project and Project team.

[1] Suleyman Demirel University, Graduate of Natural and Applied Sciences, Department of Forest Engineering, 32260, Isparta ,TURKEY
[2] Eskişehir Osmangazi University, Faculty of Science and Letters, Department of Biology, 26480 Eskişehir, TURKEY
[3] Directorate of Forest Soil and Ecology Research Institute, Eskişehir, TURKEY
*Corresponding author: ibrahimtvc@gmail.com

International Conference on Science and Technology

ICONST 2018

5-9 September 2018 Prizren - KOSOVO

Green Electrospinning of Polyvinylpyrrolidone with Various Solvents

Funda Cengiz Çallıoğlu[1]*, Hülya Kesici Güler[1]

Abstract: In this study, it was achieved that Polyvinylpyrrolidone (PVP) nanofiber production with various solvents via green electrospinning approach. Green electrospinning is a type of electrospinning that clean and safe especially has vital importance for some application areas (medical, food etc.). The aim of the green electrospinning utilizes non-toxic, cheap, ecofriendly, mild, green solvents and materials. Optimum solvent selection and solvent quality are very important for electrospinnability of polymer solution and last product properties. Polyvinylpyrrolidone (PVP) is a water-soluble, hydrophilic and biocompatible polymer. PVP nanofiber-based materials have important biomedical application areas such as; wound dressing, drug delivery, tissue engineering etc. In this study, PVP was used as a polymer and non-hazardous solvents such as distilled water, rose water, lavender water, ethanol, acetone and acetic acid were used as a solvent. First of all, polymer solutitons were prepared with various solvents and then measurements of solutions conductivity and viscosity were completed. Then, nanofibers were produced with needle electrospinning and solvent effects on the spinnability were observed during the spinning process. Lastly, PVP nanofibers produced with various solvents were characterised with SEM to analyse solvent effects on the fiber morphology. According to the results; it was observed that solvent has an important effect on the spinnability and nanofiber morphology. In this study, green solvents effects were analysed and the best solvent for electrospinning of PVP was determined in terms of spinnability and fiber morphology (average fiber diameter, fiber diameter distrubition, fiber diameter coefficient, etc.). There are various reasons of solvent type effects on the electrospinnability and fiber morphology. It is possible to say that it can be related that solvents properties such as boiling point, dielectric constant, densiy, molecular wieght etc. Also another point which should be considered is various forces during the electrospinning (Coulombic force, viscoeleactic force etc.).

Keywords: Polyvinylpyrrolidone, green electrospinning, rose water, lavender water, green solvents

[1]Suleyman Demirel University, Faculty of Engineering, 32260, Isparta, TURKEY
*Corresponding author: fundacengiz@sdu.edu.tr

International Conference on Science and Technology

ICONST 2018

5-9 September 2018 Prizren - KOSOVO

Adsorption of Heavy Metals on Nano Zero-Valent Iron (NZVI) Surfaces: Thermodynamics and Kinetics

B. Ilker Harman[1]*, Noorjan S. Ibrahim[2]

Abstract: This work was conducted to synthesis of pumice supported nanoscale zerovalent iron (P-nZVI) P-nZVI was discovered as an excellent nanoadsorbent for the removal of heavy metals such as Ni(II), Zn(II) and Cd(II). The supporting of nZVI particles on pumice surface can help to eliminate the agglomeration of nZVI. nZVI particles were effectively dispersed on the surface of pumice. The impact of kinetic parameters such as reaction time, concentration, pH of solution, adsorbent dosage and solution temperature were studied. The Langmuir and Freundlich isotherm models have also been applied to the equilibrium adsorption data. The thermodynamic parameters indicated that the adsorption of Ni(II), Zn(II) and Cd(II) ions were spontaneous, endothermic. Highest heavy metal removals were obtained with P-nZVI particles. The results showed that P-nZVI can be considered as an important adsorbent in the removal of other metals from water.

Keywords: Adsorption kinetics, heavy metal, nZVI, pumice, thermodynamic.

[1]Isparta University of Applied Sciences, Technical Vocational School, 32260, Isparta, TURKEY
[2]Suleyman Demirel University, Faculty of Engineering, 32260, Isparta, TURKEY
*Correspondingauthor: ilkerharman@isparta.edu.tr

International Conference on Science and Technology

ICONST 2018

5-9 September 2018 Prizren - KOSOVO

In Vıvo Study ın Care of Dıabetıc Foot: The Effect of Geranıol Dressıng Obtaıned from Rose Oıl on Dıabetıc Wound Healıng

Sıddıka Ersoy[1]*, Aynur Türeyen[2], Ayşe Kocabıyık[3], Yeliz Karakaya[4]

Abstract: Diabetic foot problems in DM are accepted as a complication with special characteristics related to the mental, physical, social and economic aspects that restrict life and lead to organ loss. For effective wound care, developments in medicine, science and technology have allowed alternative wound care products to be developed and marketed. Investigations about wound care products have been directed to plants because of their antioxidant properties. Antioxidant, antibacterial, anti-HIV, anxiolytic, anti-inflammatory, analgesic, hypnotic, anti-spasmodic, antitumor, chemopreventive, antitussive and antidiabetic effects of rose oil have been determined in the previous researches. However, there is no specific research for diabetic individuals. In this study, to accelerate the wound healing, prevent the progression and worsening of the wound by providing cost effectiveness and to investigate the healing effect of dressing with geraniol material obtained from rose oil was aimed. The experimental period of the study was carried out between 2 and 27 June 2016 in Experimental Animal Production and Experimental Research Laboratory of University of Süleyman Demirel. 40 (male and female) adult Sprague-Dawley rats weighing 200-350 g were used Three experimental, two control group were formed. Except one of control group diabetes was induced by injecting streptozotocin. Group five was defined as nondiabetic group. For each animal three excisional ischemic wounds were created. Rose oil extract (geraniol) dressing, isotonic wet dressing and hydrocolloid wound dressing were applied topically once a day to first, second and third groups, respectively. No dressing was applied to the positive and negative control groups. Macro-level of follow-up of wound healing was assessed by wound scoring on days 3, 5, 7, 10, 13, 15. Micro-level of follow-up of wound healing was assessed by Immunohistochemical and histopathologic examinations. For this aim tissue samples were taken at 5th, 10th and 15th days. CD34, SMA and Vimentin were used, angiogenesis and tissues were investigated. Index of oxidative stress of wound healing was assessed by TAS / TOS measurements. Due to the macroscopic results of the study, it was determined that wound score was significantly decreased on day 3 in the first group (dressed with geraniol) and non diabetic groups compared with other groups. Significant decrease was observed in each macroscopic control. When the microscopic findings compared with day 0, in the first group, significant decrease of level of collagen density and epithelization were observed on day 10. Exept the positive control group, in all groups number of fibroblasts and infiltration of inflammatory cells were significantly decreased on day 10. In the positive control group significant decrease was observed on day 15. In the first group, increase in fat cells has become significant later than other groups. In all experimental groups, angiogenesis was started to increase from day 5 and get significance on day 15 compared to day 5 and 10. In the CD34, SMA and Vimentin staining, the first group showed superiority to other dressings. In biochemical measurements, initial measurements of OSI were similar in all groups. In the last measurements the highest drop was seen in geraniol dressed and negative control groups. According to the macroscopic and microscopic follow-up, geraniol dressed group provided similar wound healing with negative control group and showed superiority to the other products used as a standard in wound care. Our results suggest that clinical phase studies of geraniol dressing material should be studied and results should be present to clinic use.

Keywords: Diabetic Foot, Rat, Geraniol, Rose Oil, Hydrocolloid Cover.

[1]Suleyman Demirel University, Faculty of Health Sciences, Internal Medicine Nursing, Çünür, Isparta, TURKEY
[2]Ege University, Faculty of Nursing, Internal Medicine Nursing,Bornova, İzmir, TURKEY
[3]Suleyman Demirel University, Vocational College-Veterinary Medicine, Şarkikaraağaç, Isparta, TURKEY
[4]Isparta City Hospital, Merkez, Isparta, TURKEY

International Conference on Science and Technology

ICONST 2018

5-9 September 2018 Prizren - KOSOVO

A study on Suitability of Some Wood Species for Landscape Applications: Surface Color Changes at Autdoor Conditions

Candan Kus Sahin[1]

Abstract: Color changes of wood caused by weathering exposure in outdoor applications are a major down-grading factor and have a substantial economic impact on high-value wood products. In this study, each of the commonly used two types of woods (softwood and hardwood) from five species was looked at /studied. These species are: Scotch pine (Pinus sylvesteris), Calibrian pine (Pinus buritia), Black pine (Pinus nigra), Fir, (Abies bormülleriana), Spruce (Picea orientalis), Cherry, Chestnut, Beech (Fagus orientalis), Basswood, and Oak (Quercus). These were exposed to outdoor conditions and the wood surface discoloration and some property changes were analyzed. All wood species show a systematic trend to change to higher values of surface roughness with natural weathering progress. The Black pine, Calibrian pine and Beech wood samples show a more or less smooth trend, whereas Basswood gives/yields/assumes the highest surface roughness changes under all conditions. However, the hardwood species, except Basswood, have higher hardness properties both initially and at the end of weathering process when compared to softwoods. The surface discoloration that occurs is clearly visible as a natural texturing. However, the degree of, and the pattern of texturing, may vary with different kinds of woods; the color changes also vary to some extent. It was revealed that the discoloration is strongly dependent on the botanical origin of wood species. The lower lightness changes (DL %) were found for all three Pine species (16.2 to 37.2%) when compared to Fir (54.9%) and Spruce samples (91.8%). The Scotch pine wood showed highest values for the contribution of red color initially and low redness change on the surface after the weathering process, among the other softwood species.

Keywords: Wood, landscape practices, landscape material, color, weathering, discoloration, CIE system

[1]Suleyman Demirel University, Faculty of Architecture, Dept. of Landscape Architecture, 32260, Isparta, TURKEY
candansahina@sdu.edu.tr

International Conference on Science and Technology

ICONST 2018

5-9 September 2018 Prizren - KOSOVO

Evaluation of the Effects of Structural Measures on Noise Exposure, Antalya Konyaaltı Case

Nazlı S. Yalçındağ[1,2], Mustafa Ece[2*], Mehmet Kılıç[1]

Abstract: Assessment and Management of Environmental Noise Directive in 2005, the scope of the accession negotiations between the European Union and Turkey has entered the Turkish Legislation. Within the scope of this regulation, the administrations are obliged to make strategic noise map and noise action plan. In this context, the creation of noise action plans following the creation of noise maps is seen as a correct approach, but monitoring of the changes in the data over time is important. Dynamic and static data used in sound propagation models have changed with pedestrianization projects. In this reason sound has been moved. This means that the sound can not be eliminated, it can be moved from one point to another. At this point policies/choises about noise come to fore. The source of noise is human activities and social behaviors of human. Scientific and engineering approaches can not eleminate noise, this approaches can only manage noise. The most appropriate solution is to manage the noise. Because to change of human activities and social behavior of human is to troublesome. This study is based on a small part of doctoral thesis that is designed to develop a new tool for managing sound.

Keywords: Noise, GIS, Data Supply, Action plan

[1]SCHIU, Vibration and Noise Engineering, Av. Villae de Milreu, Bloco E, Loja E, Estoi, 8005-466, Faro, PORTUGAL
[2]Suleyman Demirel University, Faculty of Engineering, 32260, Isparta, TURKEY
*Corresponding author: mehmetkilic@sdu.edu.tr

International Conference on Science and Technology

ICONST 2018

5-9 September 2018 Prizren - KOSOVO

Modelling Potential Distribution of Turkish Oregano (*Origanum onites* L.) using Random Forest Method in Ovacık Mountain District

Serkan Özdemir[1]*, Musa Denizhan Ulusan[2]

Abstract: Non-wood forest products benefit people in many aspects (economic, environmental, social). As a consequence of this, there is an increasing demand. Therefore, sustainable use of non-wood forest products have importance. In this study, the potential distribution areas of *Origanum onites* L. (Turkish oregano) which are important for Turkey are determined. The study was carried out in the Ovacık Mountain District in Antalya. Data were collected in 92 sample areas. In the field studies, the presence-absence data of the origannum onites and the site factors were recorded. Potential distribution modelling of the target species was performed by using the random forest method on the R software. The model obtained as a result of potential distribution modeling is created by 4 different variables. These variables are topographic position index, elevation, annual average temperature and hillshade respectively according to the model contribution rates. The auc value of the model was determined as 0,95. The model obtained as a result of the study was visualized and a potential distribution of the Turkish oregano was mapping. It is known that the potential distribution maps are important for the sustainable using of the species which are particularly in demand. Consequently, it is thought that the obtained map will contribute to the plannings for Turkish oregano which is one of the important species for Turkey.

Keywords: Distribution modelling, mapping, random forest, Turkish oregano

[1]Isparta University of Applied Science, Sütçüler Prof. Dr. Hasan Gürbüz Vocational School, Isparta-Sütçüler, TURKEY
[2]Isparta University of Applied Science, Faculty of Forestry, Isparta, TURKEY
*Corresponding author: serkanozdemir@isparta.edu.tr

International Conference on Science and Technology

ICONST 2018

5-9 September 2018 Prizren - KOSOVO

Threats Ambrosia Beetles and Associated Fungi Pose to Forest Trees in Turkey

Amani Bellahirech[1], Funda Oskay[2], Asko Lehtijärvi [3*], R. Ceyda Beram[4], Mustafa Avci[4], Steve Woodward[5], Tuğba Doğmuş Lehtijärvi[4]

Abstract: Increases in outbreaks of pathogens and pests are evident in forests, plantations, nurseries and agricultural crop trees globally, resulting from increases in global trade, which plays a major role in the spread of invasive species. In recent years, there has been increasing interest in diseases caused by fungi vectored by ambrosia beetles. Ambrosia beetles in the families Scolytinae and Platypodinae typically infest weakened or dead trees and subsist entirely on symbiotic fungi they transfer into the xylem. Studies dealing with the relation between emerging fungal tree diseases and putative ambrosia beetle vectors were reviewed. Potential threats to Turkish forestry were discussed. Ambrosia beetle vectored diseases include laurel wilt disease and Japanese and Korean oak wilt diseases, all of which have caused significant economic losses. In the southeastern USA, Raffaelea lauricola transported by the exotic redbay ambrosia beetle, Xyleborus glabratus is currently causing lethal vascular wilt disease on Lauraceae members. The interaction between Raffaelea quercivora and Platypus quercivorus in Quercus spp. is another important case. R. quercivora has been responsible for mass mortality of fagaceous trees in Japan since the 1980s and is now widespread.
Species of Raffaelea are mycosymbionts of ambrosia beetles in the genus Platypus, and may pose health risks to trees in Europe, particularly Quercus spp. In Portugal, R. montetyi and R. canadensis were reported associated with Platypus cylindrus on cork oak. In Algeria, France and Tunisia, R. montetyi has been isolated in association with P. cylindrus. The same species has been reported to be primary for Xyleborus monographus and X. dryographus In Greece, P. cylindrus is a vector of canker stain disease which was recently found on plane trees also in Istanbul. In Turkish hazelnut orchards, Anisandrus dispar and Xylosandrus germanus associated with Ophiostoma spp. as well as Xyleborinus saxesenii were found. Xylosandrus germanus is an alien invasive species for Europe. A. dispar and X. saxesenii were also detected in İstanbul on forest tree species; Castanea sativa and Fagus orientalis. Recently, A. dispar infestation was observed on oak coppice stands in Thrace. Although diseases vectored by ambrosia beetles are rare there are several examples in the world. Spread of ambrosia beetles to new areas and effects of global climate change increase the probability of emergence of new harmful fungal-beetle associations.

Keywords: Ambrosia beetles, Turkey, forest, diseases

[1]Laboratoire de Gestion et Valorisation des Ressources Forestières, INRGREF, Université de Carthage, Rue Hédi Karray, BP 10, 2080 Ariana, Tunisia
[2]Çankırı Karatekin University, Faculty of Forestry, 18200, Çankırı, Turkey
[3]Bursa Technical University, Faculty of Forestry, 16310 Yıldırım-Bursa, Turkey
[4] Suleyman Demirel University, Faculty of Forestry, 32260, Isparta, Turkey
[5] University of Aberdeen, School of Biological Sciences, Cruickshank Building, Aberdeen AB24 3UU, Scotland, UK
*Corresponding author: asko.lehtijarvi@btu.edu.tr

International Conference on Science and Technology

ICONST 2018

5-9 September 2018 Prizren - KOSOVO

The Changes of Live Weight of Gökçeada Sheep Freely Grazed on Gökçeada Island (Turkey) Rangeland Reclaimed by Different Methods

Cemil Tölü[1]*, Fırat Alatürk[2], Ahmet Gökkuş[2]

Abstract: Native breeds that have been adapting to the local regions for many years are grown on near feral conditions in extensional and free systems in the world. Live weight losses and live weight tolerances of Gökçeada female sheep for 12 months and Gökçeada male sheep for 4 months were examined in *Sarcopoterium spinosum* dominated natural rangelands reclaimed by applying grubbing, burning and cutting methods in this research work. Grubbing, burning and cutting was carried out on selected rangelands to eliminate *Sarcopoterium spinosum* (Prickly Burnet) from the vegetative covering then forage crop seeds were sown to improve plant cover. Forty head of Gökçeada sheep were placed in 8 fenced plots on reclaimed and natural rangeland for two years. Each plot was arranged with a stocking rate of 0.15 ha/sheep and contained 5 sheep that grazed freely within their rearing plots. At the beginning of December, 3.32 aged females of Gökçeada sheep were placed in plots having live weight 31.08 kg (LW) and body condition scores (BCS) of 3.04, but at the end of experiment, average live weight was reduced to 28.70 kg LW and 2.93 BCS. LW and BCS reclamation methods varied considerably according to plots and seasons, but did not show any significant change in seeding plots. Average differences of LW among other plots have changed significantly, while non-significant between grubbing and burning as well cutting and natural plots. Average loss of LW in sheep was shown as 27.3%. WL and BCS losses in sheep were observed more severe, particularly, in sheep with higher lamb productions in cutting plots. LW values of Gökçeada sheep changed significantly in all seasons. Highest LW values were observed during winter only in pregnant sheep, while the lowest LW values in lambs in summer when they were started to be released from rangelands. The live weights of remained rams in rangeland plots started a downfall at the end of August, later they showed a slight increase in September and October, and then again a little bit decline was shown at the end of project ($P<0.0001$). It has been observed that the live weight loss tolerances of Gökçeada sheep were high in those rangeland plots which were formed for prickly burnet reclamation. However, in order to enable the Gökçeada sheep to survive on these conditions, additional feeding supplementation should be done especially during pregnancy, lamb enlargement and summer drought periods.

Keywords: *Sarcopoterium spinosum,* Reclamatior, Seeding, Climate, Body condition score

[1]Department of Animal Science, Faculty of Agriculture, Çanakkale Onsekiz Mart University, Çanakkale, Turkey
[2]Department of Crop Science, Faculty of Agriculture, Çanakkale Onsekiz Mart University, Çanakkale, Turkey
*Corresponding author: agokkus@yahoo.com

International Conference on Science and Technology

ICONST 2018

5-9 September 2018 Prizren - KOSOVO

The Potentıal Dıstrıbutıon of the Ecologıcal Features of Dog Rose (*Rosa canina* l.) ın Modelıng and Mappıng the Gazıantep Regıon of Nur Mountaın

Turgay Karakaya[1]*, Ersin Yücel[2]

Abstract: This study was carried out in order to make potential distribution modeling of dog rose (*Rosa canina* L.) species found naturally in Nur Mountain, Gaziantep. In this study Data obtained from 79 sample sites used. Interspecific correlation analysis (ICA) was applied to define indicator species of dog rose. The results of the applied ICA, showed that *Abies cilicica* Carr., *Pinus nigra* Arnold. and *Rubus caesius* L. were positively associated with dog rose whereas *Pinus brutia* Ten. became negative its indicator species. Classification and regression tree technique (CART) and maximum entropy approach (MAXENT) have been used to obtain the distribution models of the species. Binary data was used as a response data while applying CART. As for MAXENT, response data became presence-only data. Climatic, topographical variables and bedrock formation were used as explanatory data during the modeling processes. The optimum model obtained from CART was built by altitude, aspect and heat index. The variables found in the MAXENT model were altitude, slope % and topographical position index. According to the results of ten-fold cross validations, ROC values of the models were found more than 80 %. Geographical information systems were used for visualizations of the models. The obtained model based maps pointed out that habitat as the most suitable sites of dog rose are the lower and middle parts of the valleys found in the upper zone of the Nur Mountains. The results obtained by this study are fundamental for any kind of planning and implementation activities for the species of dog rose in Nur Mountain and its close environs.

Keywords: Distribution modelling, habitat suitability, non-wood forest products, profile techniques, discrimination methods, dog rose

[1] Republic of Turkey General Directorate of Forestry, Ankara, TURKEY
[2] Anadolu University, Faculty of Science, Department of Biology, Eskişehir, TURKEY
*Corresponding author: turgay26k@hotmail.com

International Conference on Science and Technology

ICONST 2018

5-9 September 2018 Prizren - KOSOVO

Bird Species of Ayazma Nature Park

Emrah Tagi Ertuğrul[1]*, Doğan Akdemir[2], Halil Süel[3], Serkan Özdemir[4]

Abstract: Anatolian geography, which is a bridge between Asia and Europe, has a rich diversity of habitat due to its different climate and topography features. Due to the diversity of habitats it has, this geography has become a frequent destination of different bird species. However, although it has an important position in terms of diversity of bird species, it is observed that the required importance are not given to the studies carried out in the field of ornithology in our country. In order to protect bird species and to ensure the continuity of their generations, inventory studies should be done firstly and the existence of bird species in every field is to be revealed. As a result of inventory studies conservation activities gain scientific character. This work was carried out in order to determine the bird species of the Ayazma Nature Park within the borders of Çanakkale. Ayazma Nature Park, which is determined as a study area, is located in the Kaz Mountains which is one of the rare areas that can protect their naturality in our country. Transect line counting technique is used for inventory. The transects that best represent the area were identified and bird observations were made. Observations were made early in the morning when bird species were most active. Binoculars and photographic camera were used to facilitate the identification of bird species. According to the results obtained, 21 birds belonging to 11 families belonging to 3 groups were observed in the study area. Bird species richness was determined high in areas near fruit gardens and water resources in the area. This study was carried out in order to get information about the bird species in Ayazma Nature Park. It is thought that the results obtained will be the source for the ornithological researches to be made in this field in the coming years. As a continuation of such studies, the ecological and biological requirements of observed bird species can be determined. In addition, environmental factors that are effective in the distribution of species of birds can be determined and potential distribution maps of bird species can be created and, they can be use to manage conservation-planning activities more effectively.

Keywords: Ayazma nature park, inventory, bird species richness, wildlife.

[1]Canakkale 18 Mart University, Bayramic Vocational School, Foresrtry Program, 17700, Çanakkale, TURKEY
[2]Balikesir University, Dursunbey Vocational School, Forestry Program, Balikesir, TURKEY
[3]Suleyman Demirel University, Faculty of Forestry, 32260, Isparta, TURKEY
[4]Suleyman Demirel University, Faculty of Engineering, 32260, Isparta, TURKEY
*Corresponding author: emrahertugrul@comu.edu.tr

International Conference on Science and Technology

ICONST 2018

5-9 September 2018 Prizren - KOSOVO

The Investigation of Aluminium Sulphate Influences with Double Components in Polyurethane Varnish Applications of Wood Materials

Sinan Sarı[1], Murat Özalp[1*]

Abstract: In this study, a different amount of aluminium sulphate is added into polyurethane varnish, which is used for upper surface treatments of wood materials. The pre-prepared polyurethane varnish is implemented on upper surfaces of beech wood (*Fagus orientalis* L.) and scotch pine (*Pinus sylvestris*) for wood materials. After that toughness, brightness and surface sticking resistance experiments are conducted over these varnish stratums. The effect of the aluminium sulphate added into the polyurethane varnish is determined. Consequently, it is determined that the aluminium sulphate added into the varnish increased the toughness on both wood types substantially; however, it also decreased the brightness and sticking resistance values of the varnish greatly.

Keywords: Aluminium sulphate, resistance of stick, hardness, brilliance, polyurethane varnish.

[1] Kütahya Dumlupinar University, Faculty of Simav Technology, 43500, Simav- Kütahya, TURKEY
*Correspondingauthor: murat.ozalp@dpu.edu.tr

International Conference on Science and Technology

ICONST 2018

5-9 September 2018 Prizren - KOSOVO

Preparation and Characterization of Composite Particleboard from Rose Wastes with Differen Polymer Adhesives

Mustafa Karaboyacı[1]*, Abdullah Beram[2]

Abstract: With the increasing demand for industrial forest products, terrestrial forests are far from meeting these usage demands. For this reason, wood-based industries have sought new sources. In order to meet the problem of raw material, it is advisable to grow rapidly developing tree species such as bamboo and to use annual plants. Besides annual crops, agricultural wastes also have an important potential in the world. Increased competition in the forest products sector and rising global raw material prices have forced producers to develop new products and production methods.

The purpose of this study was to investigate the usage of rose flower (*Rosa damascena* Mill.) wastes as a raw material for particleboard manufacturing. In the experimental design of particleboards, mixtures of rose pulp and brutian pine (*Pinus brutia* Ten.) particles were used. Particle boards are generally manufactured from dried lignocellulosic wood chips with synthetic resin adhesives under temperature and pressure. The Rosa damascena Mill flower grown around Isparta approximately 7,000 tons a year and after obtaining the oil, rose flowers lose their economic value and wastes are left to rot. The ratios of rose pulp and brutian pine were 0:100, 50:50 and 100:0. Composite particleboards was prepared with adding different amounts of urea formaldehyde resin and styrene acrylic copolymer**.**

In the study, physical and mechanical properties of the boards were evaluated. Physical properties values of produced particleboards were higher than the meeting of maximum values of the TS-EN 312 (2012) standard. Modulus of elasticity, modulus of rupture and internal bond strength values of the boards produced with 50% rose pulps satisfied the requirements for general-purpose particleboards used in dry conditions, as indicated by the TS-EN 312 (2012) standard. The increasing of rose pulps in the produced boards reduced the physical and mechanical values.

Keywords: Composite particleboard, Nanu PU, Styrene acrylic, Rose waste

[1]Suleyman Demirel University, Faculty of Engineering, 32260, Isparta, TURKEY
[2]Isparta University of Applied Science, Faculty of Forestry, 32260, Isparta, TURKEY
*Corresponding author: mustafakaraboyaci@sdu.edu.tr

International Conference on Science and Technology

ICONST 2018

5-9 September 2018 Prizren - KOSOVO

Alternative Wood Materials for Landscape Applications: Assessments of Woods From Fruit Trees For Playgrounds

Candan Kus Sahin[1]

Abstract: Playing games are important for children's development. Hence, it is important to select suitable materials for children's playgrounds. These materials should be comfortable, aesthetic, safe and environmentally friendly materials. It appears that there are clear variations on color properties of selected fruit-tree wood species. A number of orchard woods have been investigated for suitability of playgrounds in the view of responders. In this sense, the photos were taken of the specially prepared samples as stimuli, and there were three different groups of respondents. It was observed that the participants were effective in terms of age grouping and material preferences. For group A and C, majority of the participants preferred wooden elements for playground material, However, the majority of participants in group B (50.5%) preferred plastic elements, followed by wooden (31.5%), and then metal (18.0%). However, it was seen that the most significant factors for selection of material for a playground should be security for both Group A (79%), and C (76.5%), whereas it was aesthetic appearance for group B (71%). Similar results were found for color properties of wood -the majority of participants of all three groups preferred light colored wooden elements in playgrounds. The results for the aesthetic preferences of wood species judged one-by-one and judged together received similar results; the preference scores for fig wood is significantly higher than for other woods, *"wood color"* and *"aesthetic appearance"* are reliable positive predictors to aesthetic preferences. The majority of participants in these three groups preferred light colored wooden elements in playgrounds.

Keywords: children playground, landscape elements, wood, hardness, fruit-trees, fig, mulberry.

[1]Suleyman Demirel University, Faculty of Architecture, Dept. of Landscape Architecture, 32260, Isparta, TURKEY
candansahin@sdu.edu.tr

International Conference on Science and Technology

ICONST 2018

5-9 September 2018 Prizren - KOSOVO

The Malware Detection Based on Windows Api with Machine Learning Methods / Makine Öğrenme Yöntemleri İle Windows Api Tabanlı Kötü Amaçlı Yazılım Tespiti

Mahmut TOKMAK[1]*, Ecir Uğur KÜÇÜKSİLLE[2]

Özet: Günümüz internet çağında kötü amaçlı yazılımlar, bilgi güvenliği açısından ciddi ve gelişen bir tehdit olarak karşımıza çıkmaktadır. Bu nedenle kötü amaçlı yazılımların tespit edilmesi, kötü amaçlı yazılımın yol açabileceği zararların önlenmesi açısından son derece önem arz etmektedir. Bu çalışmada Windows Uygulama Programlama Arayüzü (API) çağrıları analiz edilerek kötü amaçlı yazılımlar tespit edilmeye çalışılmıştır. Kötü amaçlı ve kötü amaçlı olmayan çalıştırılabilir dosyalarından oluşan bir veri seti oluşturulmuştur. Veri setindeki her bir çalıştırılabilir dosya Windows uygulama programlama arayüzü çağrıları ele alınarak, Terim Frekansı-Ters Döküman Frekansı ağırlıklandırma yöntemi ile vektörel olarak ifade edilmiştir. Öznitelik vektörü üzerinde öznitelik seçimi yapılmıştır. Seçilen öznitelikler makine öğrenmesi metodları ile eğitilip test edilerek kötü amaçlı yazılım tespiti gerçekleştirilmiştir. Çalışmada oluşturulan veri setinde, 1.380 kötü amaçlı olmayan yazılım ve 2.754 kötü amaçlı yazılım olmak üzere 4.134 Windows çalıştırılabilir dosyası kullanılmıştır. Çalışmanın sonunda kullanılan makine öğrenme yöntemlerinden Destek Vektör Makineleri ile % 98.67, Rastgele Orman algoritması ile % 98.3 oranında başarım sağlanmıştır.

Anahtar Kelimeler: Kötü Amaçlı Yazılım Analizi, Bilgi ve Bilgisayar Güvenliği,Makine Öğrenmesi

Abstract: In today's internet age, malware emerges as a serious and growing threat in terms of information security. Therefore, detecting malware is extremely important in terms of preventing harm that malware may cause. In this study, by analyzing Windows Application Programming Interface (API) calls, it was tried to detect malware. A data set consisting of malware and benign executable files was created. Each portable executable file in the data set is expressed in vectors by the Term frequency-Inverse Document Frequency weighting method taking into account Windows application programming interface calls. Attribute selection was made on feature vector. The selected attributes were trained and tested by machine learning methods and detecting malware was achieved. In this study, 4.134 portable executable files were used, 1.380 of them are benign and 2.754 of them are malware. At the end of the study, it was achieved % 98.67 with Support Vector Machine that is one of the used machine learning methods, and % 98.3 with Random Forest algorithm.

Keywords: Malware Analysis,Information and Computer Security,Machine Learning

[1]Isparta University of Applied Sciences, Gelendost Vocational School, 32900, Isparta, TURKEY
[2]Suleyman Demirel University, Faculty of Engineering, 32260, Isparta, TURKEY
*Corresponding author: mahmuttokmak@sdu.edu.tr

Giriş

Bilgisayar teknolojileri her geçen gün daha da gelişmekte ve yaygınlaşmaktadır. Kişisel kullanımda ve kurumsal anlamda kullanımda yapılan işlemler elektronik platformlara aktarılarak kolaylık sağlanmaktadır. Elektronik ortamlara aktarılan bilgilerin güvenliğini sağlamak ise başlı başına bir önem derecesine sahip ve çözülmesi gereken bir problem olarak karşımıza çıkmaktadır. Çünkü kötü amaçlı yazılımların yarattığı tehditler sayısal olarak ve çeşitlilik olarak artmaktadır. Hatta tespit edilen kötü amaçlı bir yazılım şekil değişikliğine uğratılıp tekrar daha güçlü olarak karşımıza çıkabilmektedir. Bu tehditlerin başında kötü amaçlı yazılım (malware) ve casus yazılım (spyware) gelmektedir.

Kötü amaçlı yazılım (malware); İngilizce "malicious software" kelimelerinin kısaltmalarının kullanılması ile adlandırılmıştır. Girmiş olduğu sistemde zarar vermeyi amaçlayan bu yazılımlar bilgisayar virüsleri, solucanlar (worms), arka kapılar (backdoor) Truva atları (Trojan horse) ve casus yazılımlar(spyware) olarak çeşitlilik göstermektedir. Kötü amaçlı yazılımlar, hassas verilerin çalınması, şifrelenmesi, silinmesi, temel işlem işlevlerinin değiştirilmesi ve kullanıcıların izni olmadan bilgisayar faaliyetlerinin izlenmesi de dahil olmak üzere çeşitli işlevler gerçekleştirebilirler (Shabtai vd., 2009; Ye vd., 2008).

Kötü amaçlı yazılım türleri, belirli bir amaç için tasarlanmış işlevleri veya özellikleri içerir. Örneğin fidye virüsü (ransomware), bir kullanıcının sistemine bulaşarak verileri şifrelemek için tasarlanmıştır. Siber suçlular, sistem verilerinin şifresini çözmek karşılığında kurbandan fidye talep etmektedirler. Kök kullanıcı takımı (rootkit), mağdurun sistemine yönetici seviyesinde erişim sağlamak için tasarlanmış kötü amaçlı yazılımlardır. Yazılım kurulduktan sonra, tehdit aktörlerine, kök veya sisteme ayrıcalıklı erişim verirler. Arka kapı virüsü veya uzaktan erişimli Trojan (RAT), sistemde gizlice bir arka kapı oluşturur. Kullanıcıya veya sistemin güvenlik programlarına farkettirmeden tehdit aktörlerinin uzaktan erişmesine izin verirler (Ye vd., 2008; Basu vd. 2016; Bazrafshan vd. 2013).

Son zamanlarda, kötü amaçlı yazılımların daha da arttığı görülmektedir. McAfee Labs'ın 2018 yılının mart ayında yayınladığı rapora göre; 63,4 milyon yeni kötü amaçlı yazılım örneği ile tüm zamanların en yüksek rakamına eriştiği belirtilmiştir (McAfee, 2018). Microsoft Windows işletim sistemlerinin dünyadaki kullanım oranı 2018 mayıs ayı itibariyle % 76 olarak tespit edilmiştir (W3schools, 2018). Yüksek oranda kullanım oranına sahip olan Windows işletim sistemini hedef alan kötü amaçlı yazılımlar exe, com, dll gibi dosya uzantısına sahip olabilmektedirler (Belaoued ve Mazouzi, 2016). Böylesine yaygın kullanım oranına sahip olması ve gün geçtikçe artan kötü amaçlı yazılımların hedefi olması nedeniyle; Windows işletim sistemi ve çalıştırılabilir dosya formatı PE (Portable Executable) tipindeki kötü amaçlı yazılımların tespiti önemlidir ve çalışmamızın konusu olmuştur.

Kötü amaçlı yazılımların tespitinde iki tür analiz kullanılmaktadır. Bunlar; statik analiz ve dinamik analiz başlıkları altında incelenmektedir.

Statik analiz yaklaşımı, uygulamaların kötücül yazılım tespit ve korumalarını cihazlara yüklenmeden uygulamaların sundukları veriler aracılığıyla yapılmasını sağlamaktadır. Bu yaklaşımın en önemli avantajı, kötücül yazılımların cihaza yüklenmeden tespit ve korumasını sağlamasıdır. Böylelikle cihaz, kötücül yazılım içeriğinden etkilenmemektedir (Kabakuş vd., 2015). Kötü amaçlı yazılım analizi için yapılan bu çalışmada statik analiz yöntemi tercih edilmiştir.

Dinamik analiz yaklaşımının statik analiz yaklaşımından en önemli farkı, uygulama analizlerinin yürütme zamanında (runtime) yapılmasıdır. Dinamik analiz yaklaşımının en önemli avantajı, statik analiz aracılığıyla ortaya çıkartılamayacak karmaşıklıktaki eksiklik veya açıkların ortaya çıkartılmasını sağlamasıdır (Kabakuş vd., 2015).

Bu konuda literatürde yapılmış çeşitli çalışmalar mevcuttur. Bunlardan bazılarına çalışmanın devamında yer verilmiştir.

Wang vd. (Wang vd., 2009), Windows ortamlarında API dizilerinin sergilemiş olduğu şüpheli davranışların analizine dayalı bir virüs tespit etme yaklaşımı sunmuşlardır. Şüpheli davranışları saptamak ve virüsleri tespit etmek için Bayes algoritmasını uygulamışlardır.

Ďurfina vd. (Ďurfina vd., 2011) çalışmalarında güvenlik yazılım şirketlerinin hedef platformların çeşitliliği gibi konulara hazır olmadıklarını ve platform bağımsız malware analizi yöntemlerinin az olduğunu belirtmişlerdir. Geliştirmenin erken aşamasında, yeniden hedeflendirilebilir bir ters derleyici (decompiler) gibi bir kavram önermişlerdir. Bu kavram; retargetable decompiler platforma özgü, yüksek seviyeli dil (HLL) gösterimi için analiz edilebilir bir şekilde ikili uygulamalara dönüştürmektedir.

Yao vd. (Yao vd., 2013) kullanıcının izni olmadan tetiklenen işlemleri belirleyerek tespit işlemi yapan bir sistem geliştirmişlerdir. Önce uygulama java baytkodlara çevrilir. Sonra metot çağrıları ve kullanıcı tarafından tetiklenen işlemler çıkartılır. Daha sonra uygulamanın kontrol akış çizgesi çıkartılır ve bu kontrol akış çizgesi kullanılarak metot çağrıları ve kullanıcı tarafından tetiklenen işlemler arasında yollar bulunmaya çalışılır. Eğer metot çağrısı ile kullanıcı tarafından tetiklenen işlem arasında bir yol yoksa bu metot çağrısı risk içeren bir çağrı olarak etiketlenir. Kullanıcı tarafından tetiklenen metot çağrılarının tüm metot çağrılarına oranı güven yüzdesini verir. Bu yöntemi 708 zararsız, 482 zararlı yazılım üzerinde denemişlerdir. Zararlı yazılımların 313 tanesi %0 güven yüzdesine sahip olmuştur. Bunun nedeni bu uygulamaların hiç bir zaman kullanıcının tetiklemesine gerek olmayan metot çağrıları yapmalarıdır. Geriye kalan zararlı yazılımların güven yüzdesi ise oldukça düşük çıkmıştır. Sadece FakeNetFlix zararlı yazılımının güven yüzdesi %100 çıkmıştır. Bunun nedeni de bu yazılımın kullanıcıya sahte bir arayüz sağlamasından dolayıdır. Zararsız yazılımların ise %98'i %80 üstü güven yüzdesi sergilemiştir.

Rad vd. (Rad vd., 2012) kötücül yazılımın çalıştırılabilir ikili kodlarının çözümlenerek (disassembler), bu kodların işlem çağrılarının (opcode) sıklığını histogram üzerinde temsil ederek, histogram karşılaştırma temeline dayanan kötücül kodların sınıflandırmasını sağlayan bir yöntem geliştirmişlerdir.

Alkan vd. (Alkan vd, 2013) gelişen teknolojiyle birlikte siber saldırıların artması, hem kamu kurumlarının hem de özel kuruluşların daha güvenli sistemler kullanmasını zorunlu hale geldiğini belirtmişlerdir. Çalışmalarında sistemleri tehdit eden zararlı yazılımların tespit edilmesi, takip edilmesi ve müdahale edilmesine yönelik bir yazılım geliştirmişlerdir. Bu yazılım web sitelerinin takibini anlık yapan ve tamamen merkezi bulut tabanlı olarak çalışan, platform bağımsız kullanılıp yönetilebilen bir yazılım sistemidir. Çalışmalarında web sitelerini, sistemlerin DNS altyapılarını, SSL sertifikalarını, ağ erişim adımlarını, hem içeriğini hem de yapısal durumunu sürekli takip altında tutmuşlardır. Geliştirdikleri uygulama ile sitenin "hack" edilip edilmediğini, güvenlik zafiyeti barındırıp barındırmadığını, özellikle zararlı yazılım yayıp yaymadığını analiz ederek zararlı yazılımları tespit yoluna gitmişlerdir. Uygulama sayesinde sisteme kullanıcı tarafından girilen web sitelerini, yine kullanıcının belirlediği aralıklarla kontrolü gerçekleştirip güvenlik problemlerini tespit edip, bununla ilgili yetkili yöneticileri uyararak acilen müdahale edilmesine olanak sağlamayı hedeflemişlerdir.

Lösche vd. (Lösche vd., 2015) Birçok çalışmada görüldüğü gibi kötü amaçlı yazılımların bilgisayar platformları üzerinde kalıcı tehditler oluşturduğunu vurgulayarak başlamışlardır çalışmalarına. Her gün yayımlanan yeni tehditlere karşı güvenlik araştırmacılarının otomatik sistemler geliştirdiklerini belirtmişlerdir. Bu sistemlerin daha çok Windows platformuna yaygın şekilde entegre iken diğer Linux ve Mac OS X gibi birçok platformlarda geliştirilmesi gerekliliğine vurgu yapmışlardır. Analiz yaklaşımları 7 adımdan oluşmaktadır. Her adımın uygulanması platform bağımlı olmakla birlikte, genel analiz döngüsü platform bağımsızdır. Ayrıca uygulamada tüm büyük platformlar (Windows, Mac OS X, Linux) için kullanılabilir bir analiz aracı için Python kullanmışlardır.

Lim (Lim, 2016), API işlev çağrılarının bilgilerini analiz ederek yazılımın kötü amaçlı davranışlarını tespit etme yaklaşımını önermiştir. Tespit mekanizmasında dinamik API işlev çağrılarını analiz ederek, kötü niyetli yazılım davranışlarını saptamaya çalışmıştır. Analizin verimliliğini ve toleransını artırmak için, kötü amaçlı davranışları k-gram setleri olarak ayarlamış ve k-gram kümeleri ve API işlev çağrısı arasındaki benzerliği hesaplayarak tanımlama yapmıştır.

Gupta vd. (Gupta vd., 2016), kötü amaçlı yazılımları tespit etmek için Windows API çağrı dizileri kullanmışlardır. Win API çağrı dizilerini yakalamak için Microsoft'un Detours kütüphanesini kullanmışlardır. Toplam 534 API setini işlevlerine göre 26 kategoriye ayırmışlar ve bu kategorilere göre kötü amaçlı yazılımları tespit etmişlerdir. API çağrı modelini çıkarmak için n-gram analizi yapmışlardır.

Belaouded ve Mazouzi (Belaoued ve Mazouzi, 2016) API çağrıları ile birlikte PE Opsiyonel Başlık özniteliklerini kullanmışlar ve Ki kare özellik seçimine dayalı bir sistem önermişlerdir. Makine öğrenme yöntemlerini veri madenciliği yazılımı WEKA kullanarak yapmışlardır. Karar ağacı (J48), AdaBoostM1 algoritması ile Hızlandırılmış Karar Ağacı (Boosted Decision Tree), Döndürme Ağaç yapısı (Rotation Forest), Rastgele Orman (Random Forest) sınıflandırma algoritmalarının kötü amaçlı yazılımı tespit etme performanslarını değerlendirmişlerdir. En yüksek doğruluk oranını Hızlandırılmış Karar Ağacı yöntemi ile % 98.17 olarak belirtmişlerdir.

Yöntem

Önerilen yöntemde Windows tabanlı işletim sistemlerinin çalıştırılabilir dosyalar ve DLL'ler için kullandığı çalıştırılabilir dosya PE formatındaki dosyalar kullanılmıştır.

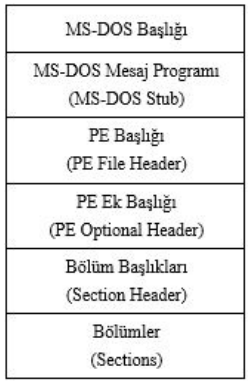

Şekil 1: PE dosya formatı

PE dosyaları, Şekil 1'de verildiği üzere, PE dosya başlığı, bölüm tablosu ve bölümlerin verilerini içerir. PE dosya başlığı, MS DOS stub, PE dosya imzası, COFF (CommonObject File Format) başlığı, ve diğer opsiyonel başlıkları içerir. Bölüm sayısı, yığıt ve yığın boyutu gibi dosya hakkında önemli bilgileri ihtiva eder. Bölüm tablosu, bölümlerin ismi, göreli konumu ve boyutu hakkında bilgi verir. Bu bölümlerde ise gerçek kod parçası, ilk değer atanmış veriler, dışarı aktarım (exports), içeri aktarım (imports) ve kaynaklar bulunmaktadır (Aydoğan ve Şen, 2014).

Yerel sistemde oluşabilecek zararları önlemek amacıyla oluşturulan sanal bir sistemde, Windows platformunun çalıştırılabilir PE formatındaki dosyaların, IAT (Import Address Table) bölümünden elde edilen Windows API çağrıları çalışmada kullanılmıştır. Elde edilen örnekler öznitelik çıkarma, öznitelik seçme gibi veri madenciliği yöntemleriyle işlendikten sonra bir veri seti oluşturulmuştur. Veri seti makine öğrenme yöntemleriyle eğitilip teste tabi tutulmuş ve sonuçları değerlendirilmiştir.

Veri Toplama

Çalışmada Windows işletim sistemini hedefleyen kötü amaçlı yazılım çalıştırılabilir dosyaları VX Heaven'dan toplanmıştır (VX Heaven, 2017). Alınan örnekler VirusTotal online virus tarayıcı sitesinde taranmış analiz sonuçları teyit edilmiştir (VirusTotal, 2017). Veri setimizde 2.754 kötü amaçlı yazılım bulunmaktadır. Elde dilen kötü amaçlı yazılım örnekleri 4 gruptan oluşmaktadır. Toplanan kötü amaçlı yazılımların %42'sini trojanlar, %20'sini wormlar, %20'sini backdoorlar, %18'ini virüsler oluşturmaktadır.
Kötü amaçlı olmayan örnekler ise; Windows işletim sisteminin sistem dosyalarından ve Malwr internet sitesinin son analiz edilen dosyalarından zararlı olmayan dosya örneklerinden alınmıştır (Malwr, 2017).Veri setimizde 1380 adet zararsız yazılım örneği bulunmaktadır.

Öznitelik Çıkarma Ve Öznitelik Seçme

PE dosyalarını okumak, API çağrılarını çıkarmak için yerel sistemden izole edilmiş sanal makine üzerinde, Python programlama dili kullanılmıştır. Python modülü olan Pefile'ı kullanan bir yazılım geliştirerek API çağrıları çıkarılmıştır. Elde edilen API çağrıları Microsoft'un MSDN kütüphanesinde paylaştığı çağrılarla kontrolü sağlanarak teyidi sağlanmıştır (Microsoft "Windows MSDN", 2017). Bu sayede farklı import çağrıları elimine edilmiştir.

Çıkarılan API çağrılarını kullanarak, her PE örneği için öznitelik vektörü oluşturulmuştur. Öznitelik vektörü oluşturulurken Tf-Idf ağırlıklandırma yöntemini kullanılmıştır.

Burada, Tf (Term frequency) terim sıklığını, Idf (Inverse term frequency) ters doküman sıklığını ifade etmektedir. Tf-Idf ise bu iki değerin çarpımı niteliğindedir.

Veri setini oluşturan yazılım örneklerinden toplanan API kelimelerinin kümesi Denklem (1)'de ifade edilmiştir;

$$W = \{w_1, w_2, \dots w_\Omega\} \tag{1}$$

İ'inci örneğe ait özellik vektörü Denklem (2) ile ifade edilmiştir.

$$x_i = \{\xi_i(w_1), \xi_i(w_2), \dots, \xi_i(w_\Omega)\} \tag{2}$$

ξ_i Denklem (3) ile ifade edilmiştir. M tüm örneklerin kümesi olarak kullanılmıştır.

$$\xi_i(w_j) = tf(i, w_j) \times idf(M, w_j) \tag{3}$$

Tf Denklem(4) ile Idf ise Denklem (5) ile ifade edilmiştir.

$$\mathrm{Tf}(i, w_j) = \frac{f(i, w_j)}{\sum j\, f(i, w_j)} \tag{4}$$

$$\mathrm{Idf}(\mathbf{M}, w_j) = log \frac{|\mathbf{M}|}{|\{m \in \mathbf{M} : w_j \in m\}|} \tag{5}$$

Burada $f(i, w_j)$, *i*'inci örneğe ait w_j API çağrısının frekansıdır (Manning vd., 2008; Akinori vd., 2015).

Oluşturulan öznitelik vektörleri için öznitelik seçim işlemi ile değerli öznitelikler seçilerek gereksiz, sınıflandırmaya katkısı olmayan öznitelikler filtrelenerek öznitelik sayısı daha da azaltılmaktadır. Öznitelik seçim işlemi için ReliefF özellik seçme modeli kullanılmıştır.

ReliefF modeli, Relief istatistiksel modelinin geliştirilmiş versiyonudur. Relief metodu, veri setinden bir örnek ele alarak ilgili örneğin, kendi sınıflarındaki diğer örneklerle yakınlığını ve farklı sınıflarla olan uzaklığına bağlı bir model oluşturarak öznitelik seçme işlemini gerçekleştirmektedir (Bolón -Canedo vd., 2014; Gümüşçü ve Aydilek, 2016).

Kötü amaçlı yazılımları tespit etmek için önerilen tespit mekanizması Şekil 2' de gösterilmiştir.

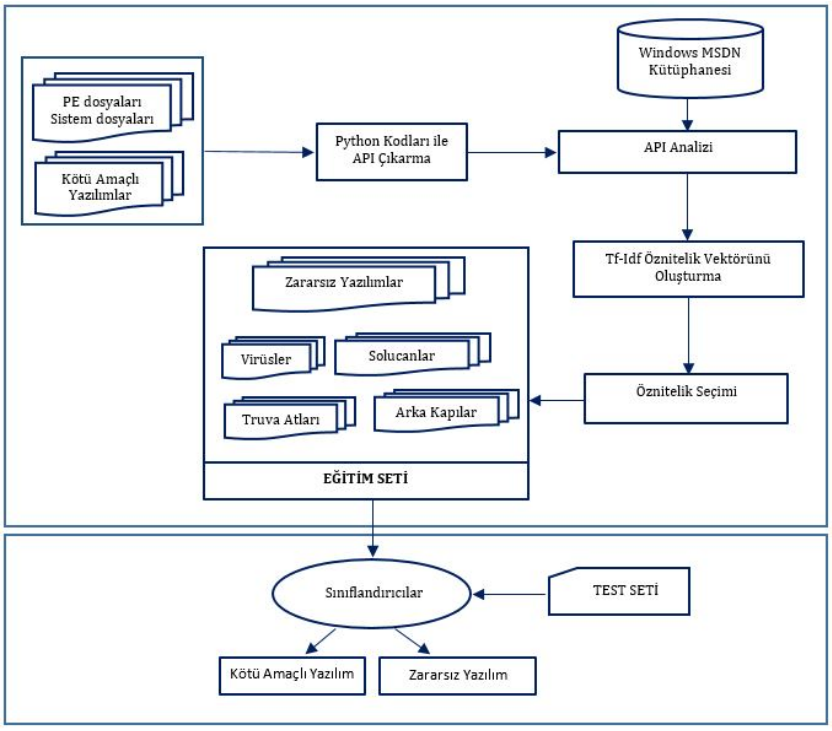

Şekil 2: Kötü Amaçlı Yazılım Tespit Sistemi

Bulgular

Çalışmalar Intel Core i5-4200 CPU 2.5 Ghz işlemci ve 8Gb bellek üzerinde çalışan 64 bit Windows işletim sistemi üzerinde gerçekleştirilmiştir. Özniteliklerin çıkarılması ve Tf-Idf ağırlıklandırılması Python ile öznitelik seçimi, sistemin eğitilmesi ve sınıflandırma algoritmaları ise veri madenciliğinde sıkça kullanılan Weka programı ile gerçekleştirilmiştir (Weka, 2015; Hall vd., 2009).

Çalışmada kullanılan makine öğrenme yöntemleri aşağıda sıralanmıştır;

- İstatistiksel tabanlı Navie Bayes (NB)
- C4.5 karar ağacını temel alan J48
- Karmaşık iş kurallarını sistematik bir şekilde modellenmesinde ve çözümlenmesinde kullanılan Decision Table (DT)
- Benzerlik yoluyla öğrenme teknikleri kullanan k-nearest neigbour (kNN)
- Birden fazla karar ağacı kullanarak sınıflandırma yapmayı hedefleyen Random Forest (RF)
- Perseptron algoritması tabanlı Voted Perceptron (VP)
- Regresyon tabanlı sınıflandırma yapan Logistic Regression Model (LRM)
- Destek vektör makineleri ile sınıflandırma yapan Sequential Minimal Optimization (SMO)
- Çok katmanlı perseptron algoritmasını kullanan Multi Layer Perceptron (MLP)

Deneylerimizde veri setinin %80'i eğitim için %20'si test için ayrılmıştır. Makine öğrenmesi algoritmaları performansının değerlendirilmesinde kullanılan, tespit oranının ölçütü Denklem (6)'da ifade edilen formül ile hesaplanmıştır (Duda vd., 2000).

$$\text{Tespit Oranı} = \frac{TP + TN}{TP + FN + TN + FP} \quad (6)$$

Tablo 1: Makine Öğrenmesi Yöntemlerinin Kötü Amaçlı Yazılımların Tespitindeki Oranları

	TP(%)	FP(%)	TN(%)	FN(%)	Tespit Oranı (%)
NB	0,809	0,191	0,989	0,011	92.745
J48	0,972	0,028	0,983	0,017	97.944
DT	0,898	0,102	0,925	0,075	91.536
kNN	0,936	0,064	0,976	0,024	96.252
RF	0,954	0,046	0,998	0,002	98.307
VP	0,866	0,134	0,991	0,009	94.801
LRM	0,912	0,088	0,956	0,044	94.075
SMO	0,968	0,032	0,996	0,004	98.670
MLP	0,951	0,049	0,993	0,007	97.824

Çalışmada kullanılan 9 adet makine öğrenme yöntemi yaklaşık olarak % 91.5 ile % 98.7 oranlarında tespit başarısı sergilemiştir. Tablo 1'de elde edilen sonuçlar verilmiştir. Tespit mekanizmasında en başarılı olan algoritma destek vektör makineleri ile sınıflandırma yapan SMO algoritması % 98.670'lik bir oranla yüksek oranda başarım sağlamıştır. Takip eden Random forest algoritması % 98.307, J48 algoritması % 97.944 oranında başarım sağlamıştır.

Tartışma ve Sonuçlar

Bu çalışmada, Windows PE kötü amaçlı yazılımların tespit edilmesinde Windows API çağrılarına odaklanılmıştır. Çalışmada kullanılan veri setinin farklı türden kötü amaçlı yazılım ihtiva etmesine dikkat edilmiştir. Toplanan ve analiz edilen örneklerin ve çeşitliliğinin literatürdeki bir çok araştırmadan nitelik ve nicelik olarak daha fazla olduğu görülmektedir. Günümüzde imza tabanlı analiz yapan uygulamaların tespit noktasında yetersiz kaldığı düşünüldüğünde kullanılan algoritamaların başarılı sonuçlar ürettiği görülmüştür. Kötü amaçlı yazılımları tespit etmek için dokuz farklı makine öğrenmesi yöntemi üzerinde araştırma yapılmıştır. Bunlardan tespit oranı açısından en iyi sonuç veren algoritma % 98.670'lik oranla SMO algoritması olmuştur. % 91.5'lik yüksek bir oran olmasına karşın çalışılan algoritmalar içinde en düşük tespit oranına sahip algoritma DT algoritması olmuştur.
Çalışmanın sonuçlarına bakıldığında, Windows PE kötü amaçlı yazılımların tespit edilmesinde, makine öğrenmesi yöntemleri ile önemli sonuçlar elde edilebildiği ve makine öğrenmesi yöntemlerinin kötü amaçlı yazılım tespiti noktasında etkin çözümler sunabildiği görülmüştür. Tespit oranındaki başarının artırılması ve PE dosyaları dışındaki kötü amaçlı yazılımların da tespit edilmesine yönelik olarak, sonraki çalışmalarda; daha fazla örnek toplayarak verisetinin artırılması, bunun yanı sıra bu çalışmada kullanılan makine öğrenmesi yöntemlerinin dışında literatürde yeralan diğer yöntemlerin kullanılması hedeflenmektedir.

Kaynaklar

Alkan M, Çifter B, Kılıç ET. (2013). Zararlı yazılım tespit, takip ve analiz yöntemleri geliştirilmesi. 6. Uluslararası Bilgi Güvenliği ve Kriptoloji Konferansı, Ankara, Türkiye, 20-21 Eylül 2013.

Akinori F, Murakami J, Mori T. (2014). Discovering similar malware samples using api call topics. Consumer Communications and Networking Conference (CCNC), 12th Annual IEEE, Nevada, USA, 9-12.January 2015.

Aydoğan E, Şen S. (2014). Kötücül Yazılımların Tespitinde Makine Öğrenmesi Yöntemlerinin Analizi, 2014 IEEE 22nd Signal Processing and Communications Applications Conference (SIU 2014), Trabzon, Turkey, 23-25 April 2014.

Basu, I., Sinha, N., Bhagat, D., Goswami, S., (2016). Malware Detection Based on Source Data using Data Mining: A Survey, American Journal Of Advanced Computing, Vol. 3(1). pp. 18-37.

Bazrafshan, Z., Hashemi, H., Fard, S. M. H., Hamzeh, A. (2013). A Survey on Heuristic Malware Detection Techniques, In Information and Knowledge Technology (IKT), 2013 5th Conference on, pp. 113–120, IEEE.

Belaoued, M., Mazouzi, S. (2014). Statistical Study of imported APIs by PE Type Malware, In Advanced Networking Distributed Systems and Applications (INDS), 2014 International Conference on, pp. 82–86, IEEE.

Bolón-Canedo V, Sánchez-Maroño N, Alonso-Betanzos A. (2014). A review of microarray datasets and applied feature selection methods. Information Sciences, 282:111–135.

Duda RO, Hart PE, Stork DG. (2000). Pattern Classification. 2nd ed, New York, USA, Wiley.

Ďurfina L, Křoustek J, Zemek P, Kolař D, Hruška T, Masařik K, Meduna A. (2011). Design of a retargetable decompiler for a static platform-independent malware analysis". International Journal of Security and Its Applications, 5 (4), 91-105.

Gupta S, Sharma K, Kaur S. (2016). Malware Characterization Using Windows API Call Sequences Security, Privacy, and Applied Cryptography Engineering. SPACE 2016. Lecture Notes in Computer Science, vol 10076. Springer, 271-280.

Gümüşçü A, Aydilek BA. (2016). 3 Farklı filtre modelli öznitelik seçme algoritmalarının kombine edilerek iyileştirilmesi. Afyon Kocatepe Üniversitesi Fen ve Mühendislik Bilimleri Dergisi D 16, Özel Sayı, 31-35.

Hall M, Frank E, Holmes G, Pfahringer B, Reutemann P, Witten IH. (2009). The weka data mining software: an update.ACM SIGKDD explorations newsletter,11.1, 10-18.

Kabakuş AT, Doğru İA, Aydın Ç. (2015). Android kötücül yazılım tespit ve koruma sistemleri. Erciyes Üniversitesi Fen Bilimleri Dergisi. 31, 9-16.

Lim H. (2016). Detecting malicious behaviors of software through analysis of apı sequence k-grams Computer Science and Information Technology, 4(3), 85-91.

Lösche U, Morgenstern M, Pilz H. (2015). A platform independent malware analysis framework. 2015 Ninth International Conference on IT Security Incident Management & IT Forensics, Magdeburg, Germany, 18-20 May 2015.

Machine Learning Group at the University of Waikato, "WEKA", http://www.cs.waikato.ac.nz/ml/weka (Erişim Tarihi: 01.03.2015)

Malwr, Claudio nex Guarnieri ve Alessandro jekil Tanasi, https://malwr.com/ (Erişim Tarihi: 12.07.2016-02.05.2017).

Manning CD, Raghavan P, Schutze, H. (2008). Introduction to Information Retrieval. New York, NY, USA, Cambridge University Press.

McAfee, https://www.mcafee.com/enterprise/en-us/threat-center/mcafee-labs/reports.html (Erişim Tarihi: 22.5.2018).

Microsoft, "Windows MSDN", https://msdn.microsoft.com/en-us/library/ (Erişim Tarihi: 10.05.2017).

Rad BB, Masrom M, Ibrahim S. (2012). Opcodes histogram for classifying metamorphic portable executables malware. E-Learning and E-Technologies in Education (ICEEE), 2012 International Conference on. IEEE, Lodz, Poland, 24-26 September 2012.

Shabtai, A., Moskovitch, R., Elovici, Y., Glezer, C. (2009). Detection of Malicious Code by Applying Machine Learning Classifiers On Static Features: A State-of-The-Art Survey, Information Security Technical Report, Vol. 14(1), pp. 16–29.

VirusTotal, https://www.virustotal.com/tr (Erişim Tarihi: 24.04.2017).

VX Heaven, http://vxheaven.org, (Erişim Tarihi: 09.02.2017).

Wang C, Pang J, Zhao R, Liu X. (2009). Using api sequence and bayes algorithm to detectsuspicious behavior, In Proceedings of International Conference on Communication Software and Networks (ICCSN '09), San Francisco, USA, 3-6 August 2009.

W3schools, https://www.w3schools.com/browsers/browsers_os.asp (Erişim Tarihi: 25.05.2018).

Yao DD, Ryder BG, Jiang X, Elish KO. (2013). A static assurance analysis of android applications, Technical Report: TR-13-03, 15p.

Ye, Y., Wang, D., Li, T., Ye, D., Jiang, Q. (2008). An Intelligent PE-Malware Detection System Based on Association Mining, Journal in Computer Virology, Vol. 4(4), pp. 323–334.

International Conference on Science and Technology

ICONST 2018

5-9 September 2018 Prizren - KOSOVO

Production and Characterization of Natural Lemonade Powder Using β-Cyclodextrin Particles

Yasemin İncegül[1], Mustafa Karaboyacı[2], Ebru Aydın[1], Mustafa Özçelik[1], Gülcan Özkan[1,*]

Abstract: Encapsulation of lipophilic food ingredients with cyclodextrin improves the stability of aromas, vitamins and coloring matter, as well as the prolongation of the product shelf life by preserving the product both physically and chemically. In this study, we aim to produce natural lemonade powder contains lemon peel oil, lemon juice, riboflavin and stevia with ß-cyclodextrin. Total moisture content, total oil content, pH, titration acidity, and color of the encapsulated lemonade were analysed. As well as total phenolic content, free radical scavenging activity, antidiabetic activity, volatile profile and sensory properties were determined. As a result total moisture content, total oil content as lemon oil, pH, titration acidity, and color (L*, a*, b*) of the encapsulated lemonade were 7.14 %, 8.3%, 3.79, 0.48 mg citric acid/g, and 56.6 (L*), -4.38 (a*), 10.93(b*). While total phenolic content and major volatile compound (limonene) of encapsulated lemonade sample were 5.69 GAE/g and 59.58 %, the activity of antidiabetic and free radical scavenging as antioxidant were not found. In assessing sensory characteristics, a hedonic scale was used in the range of 1 to 9, and that the samples are liked by taking points around 7.

Keywords: β-Cyclodextrin encapsulation, lemonade, antioxidant, antidiabetic, volatile, sensory

1. Introduction

Cyclodextrins (CD) are cyclic maltooligosaccharides consisting of α (1-4) glycosidic linked glucose unit. Cyclodextrins are named according to the number of glucose units and most preferred are α -CD, β -CD and γ-CD, respectively, consisting of the 6, 7 and 8 glucose units. Cyclodextrins are biological compounds that act as hosts for the enzymatic cleavage of starch (Eastburn & Tao, 1994). Most of the interactions that occur in the molecule are host and guest types (Szejtli, 1998). The internal geometry of cyclodextrins, which are geometrically in the form of 3-dimensional conical cylinders, is hydrophobic and their outer surfaces are hydrophilic. Cyclodextrins can be used in many industrial fields such as food, pharmacy, cosmetics, chemistry, agriculture and textile (Avcı & Dönmez, 2010).

Cyclodextrins are formed as a result of treatment of starch with cyclodextrin glycosyltransferase enzyme (Singh, Sharma & Banerjee, 2002). Cyclodextrins are composed of at least six glycopyranose units. Due to the sterically hindered cyclodextrins containing less than six glucopyranose units are not formed. Alpha (α) cyclodextrin contains six, beta (β) cyclodextrin contains seven, and gamma (γ) cyclodextrin contains eight glycopyranose units (Crini & Morcellet, 2002). The chemical structure of cyclodextrin (α), (β) and (γ) is as shown in Figure 1 (Szejtli, 2004).

[1]Suleyman Demirel University, Faculty of Engineering, Department of Food Engineering, Isparta, TURKEY
[2]Suleyman Demirel University, Faculty of Engineering, Department of Chemical Engineering, Isparta, TURKEY
[*]Corresponding author: gulcanozkan@sdu.edu.tr

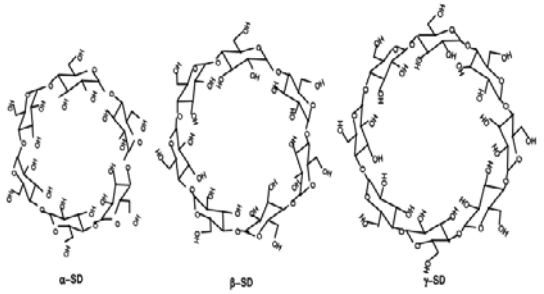

Figure 1. Chemical structure of α, β and γ-cyclodextrins, (Szejtli, 2004)

The three-dimensional shapes of cyclodextrins are conical cylinders (Magnusdottir, Mason, & Loftsson, 2002). All hydroxyl groups are on the outer surface of the molecule, and the presence of hydroxyl groups on the outer surface of the molecule provides CD water solubility (hydrophilic). The molecule is apolar in nature, providing C3 and C5 hydrogen atoms and glycosidic oxygen bridges (Song, Bai, Xu, He, & Pan, 2009). The molecular apolar property allows CD's to form inclusion complexes with many hydrophobic molecules (Valle, 2004).

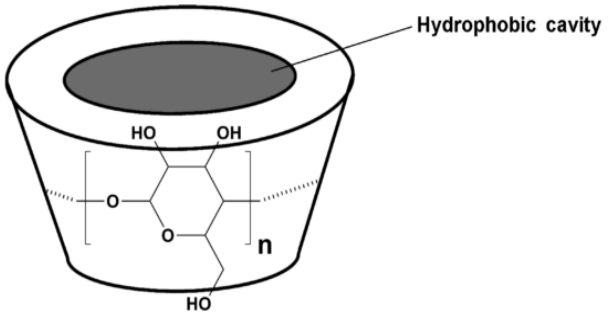

Figure 2. Schematic 3D representation of a cyclodextrin molecule (Vermonden, Nostrum, Hennink, & van de Manakker, 2009)

Cyclodextrins are organic substances with the capacity to form inclusion complexes. The inclusion complex is the component that occurs when the host molecule keeps the guest molecule in its cavity without forming any covalent bonds (Astray & Mejuto, 2009). The 3D structure of CD's is an important parameter for interacting with hydrophobic compounds or functional groups (Valle, 2004). CD's can be taken as empty capsules, however compared to the traditional encapsulation methods they are used effectively to protect each encapsulated molecule and thus find many uses in the food industry (Szente & Szejtli, 2004).

CD's are used in the food industry to increase the solubility of various vitamins and colorants, to protect heat, light and oxygen sensitive food components, to suppress undesirable flavors and odorants, to stabilize aromas, vitamins and essential fatty acids, to achieve controlled release of certain food ingredients, such as the removal of cholesterol can be used as a supporting and process assistant in the direction of goals (Szente & Szejtli, 2004), (Astray & Mejuto, 2009), (Mourtzinos, Kalogeropoulos, Papadakis, Konstantinou, & Karathanos, 2008).

Aroma ingredients are important components that influence the preference of the product in the mind of consumers. Cyclodextrins are one of the methods used in the encapsulation of flavor substances (G. A. Reineccius & Risch, 1986); (T. A. Reineccius, Reineccius, & Peppard, 2006).

Cyclodextrins can be used in the removal or masking of undesired compounds (Astray & Mejuto, 2009). Bitter taste is an important criterion in rejecting most food. CD's were found to interfere with the bitter taste

compound and reduce the perception of the taste buds in our slice (Górnas, Neunert, Baczyński, & Polewski, 2009). They can be used for the purpose of reducing the ache in coffee, fruit juices, and alcoholic beverages (Szente & Szejtli, 2004). Narinjin and lemon are components that cause pain in orange and grapefruit waters and can be reduced by β-SD (T. Reineccius, Reineccius, & Peppard, 2008). CD's have been used to improve flavor as used to stabilize and eliminate bitterness in sweeteners such as stevioside and rubicide (Singh vd., 2002).

Cyclodextrin molecules can also be used to protect against oxidative, thermal and light-induced degradation. The phenolic compounds that cause enzymatic browning are removed from the medium by CD treatment and the reaction is inhibited. As a result of the work carried out, apples (J. M. López-Nicolás, Núñez-Delicado, Sánchez-Ferrer, & García-Carmona, 2006); pear (J. M. López-Nicolás & García-Carmona, 2007); peach (J. López-Nicolás, Perez-Lopez, Carbonell-Barrachina, & García-Carmona, 2007); banana (J. M. López-Nicolás, Pérez-López, Carbonell-Barrachina, & García-Carmona, 2007); pomegranate (Deshaware & Gupta, 2018) was added with β-CD polymer to remove the polyphenols from the medium. In addition, cyclodextrins were successfully used to stabilize the components of rosemary (Mercader-Ros, Luca-Abellan, Fortea, Gabaldón, & Delicado, 2010) similar to thermal and gastrointestinal stabilization of blackberry (Fernandes vd., 2018) anthocyanins. Another use of cyclodextrins is on the assessment of waste and by-products. The use of organic solvents in the assessment of waste causes environmental pollution and personnel health risks. In this context, it is important to replace organic solvents with green extraction agents. In the recovery of phenolic compounds such as catechin and epicatechin from red grape leaf (López-miranda vd., 2016); (Ratnasooriya & Rupasinghe, 2012); it has been reported that the use of CD for the recovery of epigallocatechin from tea leaves (Cui vd., 2017) provides a better yield than using a 50% ethanol solution. Extraction with β-CD can be said to be more economical and safer than extraction with organic solvents (Santos, Buera, & Mazzobre, 2017).

One of the most important application areas of CD's food industry is the removal of cholesterol from animal products. CD is added at the appropriate temperature by adding cholesterol to the removal medium and the complex is obtained and the resulting complex is removed from the medium by filtration and centrifugation. The CD-cholesterol complex isolated from the medium is separated from the cholesterol CD by heating in water. CD can be reused after removal of cholesterol (Hedges, 1998). Cholesterol reduction studies were carried out using cyclodextrin in milk (H. S. Kwak, Kim, Kim, Choi, & Kang, 2004); mayonnaise (T.-H. Jung, Ha, Ahn, & Kwak, 2008); butter (T. H. Jung, Kim, Yu, Ahn, & Kwak, 2005); cheese (S. H. Kwak, Jung, Shim, & Ahn, 2002) and cream (Shim, Ahn, & Kwak, 2003) products.

2. Material and Method

2.1. Material

Materials used in this study are lemon juice, lemon peel oil, riboflavin, stevia and beta cyclodextrin. Cold-pressed 100 % lemon peel oil obtained from Botalife, β-cyclodextrin (Cavamax W7 pharma), and lemon juice were used as raw materials in the microencapsulation process. After encapsulation citric acid monohydrate (Sigma), riboflavin-5-phosphate sodium (DSM) and stevia powder (Takita) were added to the paste.

2.2. Encapsulation Method

Microencapsulation method is designed similar to Bhandari and colleagues' (1999) method. They use 70 ml of distilled water for 100 grams of β-cyclodextrin. In this research, we used 9 mL of lemon juice for preparing 10 grams of β-cyclodextrin for to obtain more taste and flavor. If the liquid is used at a lower rate, the dough becomes solid too quickly and after that the additional components can not be dissolved in the dough solution. The ratio of β-cyclodextrin to lemon oil was 88:12 in dry basis like Bhandari and colleagues (1998). They found this ratio as an optimum amount (Bhandari, Arcy, Le, & Bich, 1998). For preparing 10 grams of encapsulated lemon oil 8.8 grams of β-cyclodextrin dissolved in 9 mL of lemon juice and stirred in mechanical stirrer at 60 rpm. After dispersion of β-cyclodextrin than 1.2 mL of lemon oil added to mixture

and stirred 15 minutes. Bhandari and colleagues (1999) found that 15 minutes is optimum kneading time for microencapsulation of lemon oil. After 15 minutes, 0.0125 g (12.5 ppm) of riboflavin-5-phosphate sodium added to the mixture. Followed by 1.2 g (6,000 ppm) citric acid and 6 g (30,000 ppm) stevia were added to dough mixture. The mixture was stirred until it becomes dense. The resulting dough mixture was dried at 70 °C for 24 hours in oven. Hardened dough is ground in the mortar and sieved from a 100 mesh sieve (Bhandari, Arcy, & Padukka, 1999). And thus instant lemonade powder is obtained.

2.3. Total Moisture Content Analysis

The total moisture contetn of lemon oil filled cyclodextrin powder complexes was determined by AOAC 925.45 method (AOAC, 1996). 2 g of samples was weighed into aluminum weighing container and dried in a at 70 C. After drying, the conteiner was covered and cooled to 25 C in a desiccator with silica gel for about 20 min before weighing. This process was repeated every hour until the mass change was less than 2 mg.

2.4. Total Oil Extraction Analysis

For determination of total oil content of the cyclodextrin inclusion complexes, 2 grams of encapsulated cyclodextrin with constant weighing was boiled in hexane (powder hexane ratio is 1 to 20) for 30 minutes by using modified method of Bhandari et al. (1992) and Anandaraman and Reineccius (1987). After 30 minutes 100 mL destilled water was added to the solution and filtered. Filtrate was rinsed with hexane again and this process was repeated for 3 times. The last filtrate was analyses with GCMS to be sure about there are no oil in the filtrate. Obtaioned residue was dried in an oven at 70 °C over a night. The amount of mass lost by the cyclodextrin was calculated as the oil ratio of the complex.

2.5. Determination of pH value

Lemonade pH values were determined using a pH meter (Hanna Instruments USA). The liquid product was read by directly immersing the probe.

2.6. Determination of Titration Acidity

5 g of lemonade at room temperature is removed and titrated with 0.1 N NaOH adjusted to pH 8.1. The result is expressed as citric acid.(Cemeroğlu, 2007)

2.7. Color Analysis

Lemonade color values are determined by automatic color device (3nh, nh310). L*, a*, b* values were determined with the device.

2.8. Total phenolic content

Total phenolic content (TPC) of the extracts was determined according to the method of Li, Guo, Yang, Wei, Xu & Cheng (2006). Briefly, 0.4 mL of diluted extracts were mixed with 2 mL of 10-fold diluted Folin–Ciocalteu's phenol reagent and 1.6 mL of 7.5% Na2CO3 was added. The mixture was allowed to stand for 1 hour. The absorbance versus prepared blank was read at 760 nm. Six different concentrations of gallic acid solutions (20– 200 mg/L) were used for calibrations. The final results were expressed as mg gallic acid equivalent (GAE) g of dry lemonade.

2.9. Free radical scavenging activity

Free radical scavenging activity as antioxidant properties is under the influence of holding free radicals and it's been determined by using 1, 1-diphenyl-2-picrilhidrazil (DPPH) method (Dorman, Koşar, Kahlos, Holm, & Hiltunen, 2003). The powder of lemonade (2 g) was solved in 250 mL water. The solved lemonade in water were added 450 lL of Tris-HCL solution (50 mM - pH 7.4) and 1 ml DPPH (0.1 mM) and were incubated for 30 minutes. The absorbance of the standard and the samples were measured at 517 nm. Before

calculating IC_{50} value, antiradical activity % of the extracts at different doses was determined using the following formula:

Free radical scavenging activity % = 100 x (absorbance of the control - absorbance of the sample/absorbance of the control)

2.10. Determination of antidiabetic activity

The initial steps of method development involved determining the activities of sucrase, in an acetone-extract of rat intestinal tissues and improving a previously published method (Aydin., 2015) by analysing glucose production from sucrose with the hexokinase assay.

2.11.Volatile compounds analysis

The 2 g lemonade sample is transferred to a 15 ml volumetric vial that is sealed with a silicone septum. The sample is placed in a 45 °C heater block with stirring by means of a magnetic stirrer. Balancing was performed for 15 minutes and then, a Carboxen/polydimethylsiloxane manual SPME fibre (75 mm Fused Silica, Supelco Ltd., Bellefonte, PA, USA) was inserted into the vial and maintained in the head-space for 30 min at 45 C to extract volatile compounds from the lemonade. Finally, the fiber was placed in the injection block of the gas chromatograph at 250 °C for 5 minutes to determine the flavor compounds obtained from lemonade (Cevik, Ozkan, & Mustafa, 2016).

2.12. Sensory analysis

Sensory analysis was carried out at Süleyman Demirel University Faculty of Engineering Department of Food Engineering. A hedonic scale was used between 1 and 9. The number 1 on the scale is very bad, 5: the middle and 9 were expressed in perfect form.

3. Results and Discussion

3.1. Physicochemical properties of encapsulated lemonade

The moisture content of the β-cyclodextrin inclusion complex was calculated 7.14 % by the vacuum-drying method (AOAC, 1990). Bhandari et. al. (1999) used this method and the calculate moisture content of the β-cyclodextrin 9.94%. Results are similar and the moisture content of a sample is influenced by the climate of the studied area and the humidity in the air.

The resulting total oil extraction results can also be evaluated as inclusion efficiency. As a result of the analysis, it was determined that the cyclodextrin inclusion complex contains 8.3% lemon oil. Bhandari et. al. (1998) used the same method and they reported that 94.51 mg of volatiles/g of cyclodextrin, that is 9.451 g of oil volatiles (or 9.68 g of lemon oil) per 100 g of β-cyclodextrin. Our total oil content is smilar to this result. In our method we used hexane for to remove all lemon oil from hydrofobic cavity. Because hexan is an apolar solvent and apolar cavity wants to take this solvent inside. Out side of the cyclodextrin is polar so after boiling with hexane we add water to the flask for to solve cyclodextrin and than solution can be filter easly.

The lemonade pH and titration acidity values obtained by dissolving 2 g of lemonade preparation in 200 ml water were found to be 3.79 ± 0.01 and 0.48 ± 0.02 mg citric acid/g sample respectively. Lemon by-product characteristics were investigated and the pH value was found to be 3.80. This value was found in the literature between 3.14-3.96 (M'hiri, Ghali, Nasr, & Boudhrioua, 2018). Lemon peel oil is a by-product of lemon and is encapsulated in the production of lemonade and re-dissolved by dissolution in water. The pH value of lemonade produced by using lemon juice and lemon peel oil was found in the current range in the

literature. It may be due to the presence of organic acids such as citric, ascorbic and malic acids in the lemon by-product and lemonade high acidity.

Lemonade L*, a*, b* values were found to be 56.6 ± 0.56, -4.38 ± 0.16 and 10.93 ± 0.22 respectively. When the color values of lemon wastes are examined, L *, a * and b * values are found as 43.78, 4.13 and 12.72 respectively (M'hiri vd., 2018). When we compare our results withthe study, the value of a* is very low, which can be explained by the greening of the resulting color of the lemonade enriched with riboflavin.

3.2. Total phenolic compounds and funtional properties of encapsulated lemonade

As a result of total phenolic substance amount analysis performed, the phenolic content of lemonade was determined as 5.69 ± 0.18 mg GAE/g. In the study conducted by M'hiri et al. (2018) the composition of lemon waste products was investigated and the total amount of phenolic substance was found to be 55.2 mg GAE / g. The waste consists of lemon peel, lemon seed, dough and water. In our work, only lemon oil and lemon juice are used. The phenolic content we found could be found to be lower because of the use of only lemon oil and water and because of the encapsulation process.

Free radical scavenging and antibiabetic activities as functional properties of powder lemonade produced in the study have been reviewed. It is determined that, as a result of the analysis carried out, the antidiabetic and antioxidant properties of the lemonade are not important due to the lowest content of lemonade oil and phenolic in encapsulated product. Also it was found that prepared lemonade did not inhibit the sucrase activity. Therefore it could conclude that lemonade does not have any antidiabetic activity.

3.3. Volatile properties of encapsulated lemonade

The oil obtained from the colored parts of the citrus peels consists of more than 100 compounds. Composition of these oils was terpenecarbons, oxygenated compounds and non-volatile compounds. Some important compounds in citrus oils found as alpha-pinene, beta-pinene, myristine, lemonine, gamma-terpinene, valencene, sabinen, neral and geranial (Karhan, 2006). The main component was determined that as limonene in proportion to one of the most important components of essential oil (37.63-69.71%) of sour lemon peel by Bourgou, Rahali, Ourghemmi, and Sa (2012). In another study also conducted on lemon oil, it was stated that volatile oil predominates mainly of Limonen (61.64%), β-pinene (13.85%) and γ-terpinene (9.95%) (Hasani, Mahdi, & Ghorbani, 2018). In our study, limonene, β-pinene and γ-terpinen and fractions encapsulated with β-cyclodextrin were determined as 59.58% and 12.29% and 4.39% respectively. When these ratios are examined it can be concluded that the essential components of lemon oil are successfully encapsulated with CD's. The main constituents encapsulated in the study were limonene (59.58%), γ-terpinene (12.29%), β-pinene (4.39%), β-pisabolene (3.89%) and β-myrcene (2.59) %. The results of analysis of the lemonade volatile compounds are given in the following Table 1.

Table 1. Lemonade volatile components

Name of Volatile compounds	Area	Area%
α-Thujene	193910	0.06
α-Pinene	3328894	1.00
Camphene	532726	0.16
Sabinene	340410	0.10
β-Pinene	14591282	4.39
β-Myrcene	8627343	2.59
l-Phellandrene	704094	0.21

α-Terpinene	1765288	0.53
p-Cymene	6160958	1.85
Limonene	198119060	59.58
Z-Ocimene	492894	0.15
β-Ocimene	1020180	0.31
γ-Terpinene	40880843	12.29
Isolimonen	176928	0.05
α-Terpinolene	5277306	1.59
p,α-Dimethylstyrene	7506035	2.26
Nonanal	127328	0.04
E-Sabinene hydrate	262164	0.08
β-Fenchyl alcohol	364244	0.11
Decanal	89169	0.03
Z-Citral	1266660	0.38
E-Citral	4044566	1.22
δ-Elemene	121603	0.04
Citronellyl acetate	84169	0.03
Neryl acetate	5133534	1.54
Linalyl acetate	4729812	1.42
β-Elemene	232858	0.07
Caryophyllene	1828104	0.55
α-Bergamotene	6030590	1.81
(E)-β-Farnesene	640090	0.19
β-Santalene	210499	0.06
β-Himachalene	157143	0.05
Curcumene	137105	0.04
Isocaryophyllene	297755	0.09
β-Selinene	120377	0.04
Valencene	191172	0.06
α-Selinene	208172	0.06
α-Bisabolene	1610211	0.48
(E,E)-α-Farnesene	958931	0.29
β-Bisabolene	12941173	3.89

α-Cedren	373112	0.11
Cadinene	173281	0.05
α-Patchoulene	136253	0.04
α-Humulene	365568	0.11
TOTAL	332553794	100.00

3.4. Sensory properties of encapsulated lemonade

The color, odor, flavor, sweetness, bitterness, sourness lemon flavor, taste of lemonade and overall appreciation were evaluated sensory using hedonic scale. It is expressed that the smell and aroma of the lemonade evaluated by the panelists is likes and resembles the classical lemonade. Likewise, it was determined that lemon flavor was sufficient and liked. These results show us that the encapsulation process using cyclodextrin particles is successful in lemonade odor, taste and aroma. Lemonade has parallel scores when assessed for bitterness and sourness originating from phenolics, and this value is around 7. So the product is liked by bitter taste and sourness taste. The results obtained are given in Figure 3.

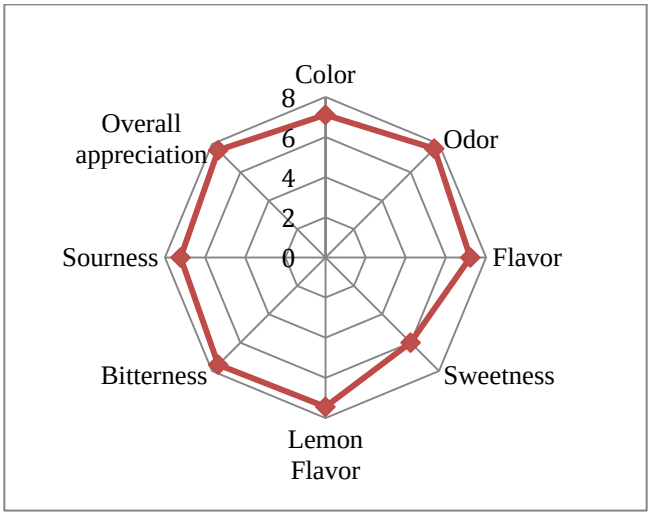

Figure 3.Sensory properties of lemonade

Conclusions

In summary, the mixure of lemon oil, lemon juice, citric acid, stevia and riboflavin was succesfully encapsulated by using beta cyclodextrin to produce the powder of natural lemonade. Also the volatile subtances of lemon oil was encapsulated succesfully and the sensory properties of the last product were highly liked by the panelist. However the functional properties as radical scavenging activity and antidiabetic activity of the powder of natural lemonade were not determined. As a result, the encapsulated lemonade product could be using home appliances and industry as natural powder formulation in practical.

References

Anandaraman, S., and Reineccius, G. (1987). Analysis of encapsulated orange peel oil. Perfumer & Flavorist 12, 33-39.

AOAC. In Official Methods of Analysis of the Association of Official Analytical Chemists, 5th ed.; Helrich, K., Ed.; AOAC International: Arlington, VA, 1990; p 1010.

Astray, G., & Mejuto, J. C. (2009). A Review on The Use of Cyclodextrins in Foods, Food Hydrocolloids 23, 1631-1640.

Avcı, A., & Dönmez, S. (2010). Cylodextrins and Their Usage In The Food Industry. Gıda Dergisi, 35, 305-312.

Aydin, E., 2015. Effects of Natural Products on Sugar Metabolism and Digestive Enzymes (Doctoral dissertation, University of Leeds).

Bhandari, B. R., Arcy, B. R. D., Le, L., & Bich, T. (1998). Lemon Oil to β-Cyclodextrin Ratio Effect on the Inclusion Efficiency of β-Cyclodextrin and the Retention of Oil Volatiles in the Complex. J. Agric. Food Chem., 46, 1494-1499.

Bhandari, B. R., Arcy, B. R. D., & Padukka, I. (1999). Encapsulation of Lemon Oil by Paste Method Using β-Cyclodextrin: Encapsulation Efficiency and Profile of Oil Volatiles. J. Agric. Food Chem., 47, 5194-5197.

Bhandari, B. R., Dumoulin, E. D., Richard, H. M. J., Noleau, I., and Lebert, A.M. (1992). Flavour encapsulation by spray drying: Application to citral and linalyl acetate. J. Food Sci. 57, 217-221.

Bourgou, S., Rahali, F. Z., Ourghemmi, I., & Sa, M. (2012). Changes of Peel Essential Oil Composition of Four Tunisian Citrus during Fruit Maturation. The cientific World Journal, 1-10.

Bourgou, S., Rahali, F. Z., Ourghemmi, I., & Sa, M. (2012). Changes of Peel Essential Oil Composition of Four Tunisian Citrus during Fruit Maturation. The cientific World Journal, 1-10.

Cemeroğlu, B. (2007). Gıda Analizleri (Gıda Tekno). Bizim Büro Basımevi, 535s, Ankara.

Dorman, H. J. D., Koşar, M., Kahlos, K., Holm, Y., & Hiltunen, R. (2003). Antioxidant Properties and Composition of Aqueous Extracts from Mentha Species, Hybrids, Varieties, and Cultivars. Journal of Agricultural and Food Chemistry, 51(16), 4563-4569.

Hasani, S., Mahdi, S., & Ghorbani, M. (2018). International Journal of Biological Macromolecules Nanoencapsulation of lemon essential oil in Chitosan-Hicap system . Part 1 : Study on its physical and structural characteristics. International Journal of Biological Macromolecules, 115, 143-151.

M'hiri, N., Ghali, R., Nasr, I. Ben, & Boudhrioua, N. (2018). Effect of different drying processes on functional properties of industrial lemon byproduct. Process Safety and Environmental Protection, 116, 450-460.

Cevik, S., Ozkan, G., & Mustafa, K. (2016). Optimization of malaxation process of virgin olive oil using desired and undesired volatile contents LWT 73.

Crini, G., & Morcellet, M. (2002). Synthesis and applications of adsorbents containing cyclodextrins. J. Sep. Sci., (25), 789-813.

Cui, L., Liu, Y., Liu, T., Yuan, Y., Yue, T., Cai, R., & Wang, Z. (2017). Extraction of Epigallocatechin Gallate and Epicatechin Gallate from Tea Leaves Using β-Cyclodextrin. Journal of Food Science, 82(2), 394-400.

Deshaware, S., & Gupta, S. (2018). Debittering of bitter gourd juice using β-cyclodextrin: Mechanism and effect on antidiabetic potential, 262 (November 2017), 78-85.

Eastburn, S., & Tao, B. (1994). Application of modifiyied cyclodextrins. Biotechnol Adv., 12, 325-339.

Fernandes, A., Rocha, M. A. A., Santos, L. M. N. B. F., Brás, J., Oliveira, J., Mateus, N., & Freitas, V. De. (2018). Blackberry anthocyanins: β-Cyclodextrin forti fi cation for thermal and gastrointestinal stabilization. Food Chemistry, 245, 426-431.

Górnas, P., Neunert, G., Baczyński, K., & Polewski, K. (2009). β-cyclodextrin complexes with chlorogenic and caffeic acids from coffee brew: Spectroscopic, thermodynamic and molecular modelling study. Food Chemistry, 114(1), 190-196.

Hasani, S., Mahdi, S., & Ghorbani, M. (2018). International Journal of Biological Macromolecules Nanoencapsulation of lemon essential oil in Chitosan-Hicap system. Part 1: Study on its physical and structural characteristics. International Journal of Biological Macromolecules, 115, 143-151.

Hedges, A. R. (1998). Industrial Applications of Cyclodextrins. Chem Rev., (98), 2035-2044.

Jung, T.-H., Ha, H.-J., Ahn, J., & Kwak, H.-S. (2008). Development of cholesterol- reduced mayonnaise with crosslinked b-cyclodextrin and added phytosterol. Korean Journal of Food Science Ani. Resource, 28(2), 211-217.

Jung, T. H., Kim, J. J., Yu, S. H., Ahn, J., & Kwak, H. S. (2005). Properties of cholesterol-reduced butter and effect of gamma linolenic acid added butter on blood cholesterol. Asian-Australasian Journal of Animal Sciences, 18(11), 1646-1654.

Karhan, M. (2006). Turunçgil Kabuk Yağlarının Elde Edilmesi ve Gıda Endüstrisinde Kullanımı. Gıda Teknolojileri Elektronik Dergisi, 3, 71-77.

Kwak, H. S., Kim, S. H., Kim, J. H., Choi, H. J., & Kang, J. (2004). Immobilized β-Cyclodextrin as a Simple and Recyclable Method for Cholesterol Removal in Milk. Arch Pham Res, 27(8), 873-877.

Kwak, S. H., Jung, C. S., Shim, Y. S., & Ahn, J. (2002). Removal of Cholesterol from Cheddar Cheese by β-Cyclodextrin. J. Agric. Food Chem., 50, 7293-7298.

Li, Y., Guo, C., Yang, J., Wei, J., Xu, J., & Cheng, S. (2006). Evaluation of antioxidant properties of pomegranate peel extract in comparison with pomegranate pulp extract. Food Chemistry, 96, 254-260.

López-miranda, S., Serrano-martínez, A., Hernández-sánchez, P., Guardiola, L., Pérez-sánchez, H., Fortea, I., Núñez-delicado, E. (2016). Use of cyclodextrins to recover catechin and epicatechin from red grape pomace. Food Chemistry, 203, 379-385.

López-Nicolás, J. M., & García-Carmona, F. (2007). Use of Cyclodextrins as Secondary Antioxidants to Improve the Color of Fresh Pear Juice. Journal of Agricultural and Food Chemistry, 55(15), 6330-6338.

López-Nicolás, J. M., Núñez-Delicado, E., Sánchez-Ferrer, Á., & García-Carmona, F. (2006). Kinetic model of apple juice enzymatic browning in the presence of cyclodextrins: The use of maltosyl-β-cyclodextrin as secondary antioxidant. Food Chemistry, 101(3), 1164-1171.

López-Nicolás, J. M., Pérez-López, A. J., Carbonell-Barrachina, Á., & García-Carmona, F. (2007). Kinetic Study of the Activation of Banana Juice Enzymatic Browning by the Addition of Maltosyl-β-cyclodextrin. Journal of Agricultural and Food Chemistry, 55(23), 9655-9662.

López-Nicolás, J., Perez-Lopez, A., Carbonell-Barrachina, A., & García-Carmona, F. (2007). Use of Natural and Modified Cyclodextrins as Inhibiting Agents of Peach Juice Enzymatic Browning. Journal of agricultural and food chemistry (C. 55).

Magnusdottir, A., Mason, M., & Loftsson, T. (2002). Cyclodextrins. J Inclusion Phenom Macrocyclic Chem., 44, 213-218.

Mercader-Ros, M., Luca-Abellan, C., Fortea, M. I., Gabaldón, J. A., & Delicado, E. (2010). Effect of HP- β-cyclodextrins complexation on the antioxidant activity of flavonols. Food Chemistry, 118(3), 769-773.

M'hiri, N., Ghali, R., Nasr, I. Ben, & Boudhrioua, N. (2018). Effect of different drying processes on functional properties of industrial lemon byproduct. Process Safety and Environmental Protection, 116.

Mourtzinos, I., Kalogeropoulos, N., Papadakis, S. E., Konstantinou, K., & Karathanos, V. T. (2008). Encapsulation of Nutraceutical Monoterpenes in β-Cyclodextrin and Modified Starch. Sensory and Food Quality, 73(1), 89-94.

Ratnasooriya, C. C., & Rupasinghe, H. P. V. (2012). Extraction of phenolic compounds from grapes and their pomace using β-cyclodextrin. Food Chemistry, 134(2), 625-631.

Reineccius, G. A., & Risch, S. J. (1986). Encapsulation of artificial flavors by β-cyclodextrin. Perfumer and Flavorist, 11(4), 1-6.

Reineccius, T. A., Reineccius, G. A., & Peppard, T. I. (2006). Flavor Release from Cyclodextrin Complexes: Comparison of Alpha, Beta, and Gamma Types. Journal of Food Science (68).

Reineccius, T., Reineccius, G., & Peppard, T. (2008). Utilization of β-Cyclodextrin for Improved Flavor Retention in Thermally Processed Foods. Journal of Food Science (69).

Santos, C., Buera, P., & Mazzobre, F. (2017). Novel Trends in Cyclodextrins Encapsulation Applications in Food Science. Current Opinion in Food Science, 16, 106-113.

Shim, S. Y., Ahn, J., & Kwak, H. S. (2003). Functional Properties of Cholesterol-Removed Whipping Cream Treated by β-Cyclodextrin. Journal of Dairy Science, 86(9), 2767-2772.

Singh, M., Sharma, R., & Banerjee, U. C. (2002). Biotechnological Aplications of Cyclodextrins. Biotechnol Advances, 20, 341-359.

Song, X. Le, Bai, L., Xu, M. X., He, J., & Pan, Z. S. (2009). Inclusion Complexation, Encapsulation Interaction and Inclusion Number in Cyclodextrin Chemistry, 253, 1276-1284.

Szejtli, J. (1998). Introduction and General Overview of Cyclodextrin Chemistry. Chem Rev., 98, 1743-1753.

Szejtli, J. (2004). Past, present, and future of cyclodextrin research *. Pure Appl. Chem., 76(10), 1825–1845.

Szente, L., & Szejtli, J. (2004). Trends in Food Science & Technology, 15, 137-142.

Valle, E. M. M. Del. (2004). Cyclodextrins and their uses: a review. Process Biochemistry, 39, 1033-1046.

Vermonden, T., Nostrum, C. F. Van, Hennink, W. E., & van de Manakker, F. (2009). Cyclodextrin-Based Polymeric Materials: Synthesis, Properties and Pharmaceutical/Biomedical Applications. Biomacromolecules, 10(12), 3157-3175.

[1]*International Conference on Science and Technology*

ICONST 2018

5-9 September 2018 Prizren - KOSOVO

Evaluation of Textural and Some Physical Properties of Oleomargarine Formulated with Sunflower and Sesame Oil

Serife Cevik[1], Gülcan Özkan[2,*], Erkan Karacabey[2]

Abstract: Recently structuring liquid oils has become an interesting research area, mainly due to reduction in saturated fat intake and elimination of trans fats from our diets. The goal of current study was to examine detailed textural characterization and some physical properties of oleomargarine to gain new insights about the gelation behavior of natural waxes and edible oils. In this study, it was aimed to investigate oleomargarine formation by mixing refined sunflower oils with bees and carnauba wax and enrichment with addition of functional sesame oil into formulas. Sunflower oil was in the formulas as refined oil whereas sesame was used as functional oil, refined carnauba wax was used as gel formation agent. Oleomargarine production was performed according to central composite design including parameters of oil and wax concentrations. During oleomargarine production, refined oil was enriched with functional oil at different concentration (0-30%) and then mixed with wax at different levels (5-10.0% of carnauba concentration). In order to investigate the effects of process parameters on oleomargarine formation, response surface methodology (RSM) was used. Textural properties, oil binding capacity (OBC), crystal formation time (CFT), and color of oleomargarine were responses.

As textural properties, hardness (g force) and stickiness (g force) were measured with a Texture Analyzer TA.XT.plus (Stable Micro System, England) equipped with suitable probe. The hardness and stickiness values provide information about the spread ability of the samples. As the wax concentration increased in SSC oloegel samples, hardness and stickiness value increased. L* (luminosity). a∗ (+ redness/ – greenness). and b∗ (+ yellowness/ – blueness) values of the oleomargarine samples are the color parameters.. Oil binding capacity of oleomargarine samples were found to be in the range of 64.14 (%) to 97.16(%) and the time required for crystallization was at least 7.40 minutes. Briefly, this study served for margarine sector of food industry by providing basic information about oleomargarine formulation with the effects of parameters.

Keywords: Oleomargarine, textural and some physicochemical properties, response surface method (RSM).

1. Introduction

In recent years, some health problems especially heart disease obesity and some kind of cancer depend on fat consumption in diet (Berasategi vd., 2014; Grasso vd., 2014). Saturated and trans fats are perceived negatively due to their possible links to cardiovascular disease and other undesirable health effects (Singh vd., 2017). It is known that consuming saturated fats and cholesterol more than the specified percentage cause increase of the amount of LDL known as "bad cholesterol'' (Co ve Marangoni, 2012; Patel and Dewettinck, 2016). Therefore, there is a relation between high cholesterol level and unsaturated / saturated fat ratio, the effects of this relationship on the increase of coronary heart disease are emphasized (Youssef ve Barbut, 2009; 2011). Consumers' demand tents to healthy products having reduced saturated fat content. Recently, a new approach called as organogelation or oleogelation has been developed in order to prepare

[1]IspartaUniversity of Applied Science, Gelendost Vocational School, Department of Food Processing, Isparta, TURKEY
[2]Suleyman Demirel University, Faculty of Engineering, Department of Food Engineering, Isparta, TURKEY
[*]Corresponding author: gulcanozkan@sdu.edu.tr

healthier products. Organogels are defined as 3-dimensional networks of an organic phase produced by adding some organogelators into the liquid phase. When the organic phase is edible oil, the structure is sometimes called as oleogel. Organogels have some advantages such as not changing the fatty acid composition; therefore, no trans and saturated fatty acids are produced (Toro-Vazquez and others 2007; Marangoni and Garti 2011; Co and Marangoni 2012).
In literature, many different kinds of gelator such as waxes have been used for organogelation. Carnauba wax is a plant wax obtained from the leaves of the Brazilian palm *Copernicia prunifera*. Carnauba wax approximately contains 1% of hydrocarbons with 40% of aliphatic esters. Carnauba wax has a unique structure containing a high proportion of ‘‘unusual’’ chemical constituents such as unesterified alcohols (12 %), x-hydroxy esters (14 %) and esters of hydroxylated cinnamic acid (30 %), with the remainder being unidentified impurities (Patel and Dewettinck, 2016). Bees wax is a complex mixture of chemical compounds predominantly based in straight-chain monohydric alcohol compounds with carbon chains from C24 to C36 and straight-chain acids with carbon skeletons of up to C36, including some C18 hydroxyl acids that can be esters, diesters and triesters (Yilmaz & Dagdemir, 2012).

In this study, it was aimed to investigate oleomargarine formation by mixing sunflower oil as refined oil with carnauba wax and enrichment with addition of sesame oil. Oleomargarine production was performed according to experimental design by the central composite design including parameters of oil and wax concentrations.

2. Material and Method

2.1. Material

Refined sunflower oil was purchased from Komili A.Ş. Sesame oil was purchased from Oneva A.Ş. Carnauba wax was provided by BMT Chemical Company. Carnauba wax is classified as GRAS (generally recognized as safe) status food.

2.2. Method

Oloeogel Preperation

In order to form the oleomargarine, previously weighed refined and functional oils and wax were placed into glass beaker and heated in a water bath previously set at 90°C. After melting of wax was completed, mixture was stirred at 400 rpm for - 5 min. Some analysis such as crystal formation time and oil binding capacity were immediately determined. Afterwards, the hot gel was allowed to cool down at room temperature (20 °C). Following the crystallization sample was stored at +4 °C in refrigerator for one night, and then its texture properties and color parameters were measured.

Oil binding capacity

The method of Da Pieve and others (2010) was adapted for this analysis. The method was modified. Firstly, empty eppendorf tubes were carefully weighed (a). Approximately, 10 mL of oleomargarine sample was placed into an empty eppendorf tube from the completely melted mixture and the tube was left for 1 h 15 min for gel formation in refrigerator (+4°C). When the organogel was completely formed in the refrigerator, the tube was carefully weighed (b) and centrifuged at 9100 × g for 25 min. Then, the tube was turned over and left for 5 min for drainage of excess oil and then the tube was re-weighed (c). Finally, the oil binding capacity (% OBC) was calculated by

Eq. (1). $\%\text{Released Oil} = [(b - a) - (c - a)] / (b - a) \times 100$

$\%\text{OBC} = 100 - \%\text{ Released Oil}$ (1).

Crystal formation time

Approximately 10 mL of oleomargarine sample (completely melted mixture) was placed into glass tube and the tube was left in a water bath for 2 hours at 90 °C for equal temperature setting. Afterwards, the tube was left at room temperature to cool down for gel formation (Dassanayake and others 2009). Total time required for gel formation was recorded as gelation time.

Color measurement

Color parameters (L*, a*, and b*) of oleomargarine samples were measured at three locations of each sample by using a colorimeter (NH310, 3nh Tech. Co., Ltd. China) (Robertson, 1977). The equipment was standardized each time with white and black references. Mean values were reported.

Textural properties

The textural properties of the oleomargarine s were measured with a Texture Analyzer TA.XT.plus (Stable Micro System, England) equipped with 45° conic probe. The oleogels were allowed to set up in the lower cone holders at room temperature in advance of testing. The probe proceeded to penetrate 23 mm into the gel at a rate of 3.0 mm/s and then was pulled out from the sample at 10mm/s speed. The values of hardness and stickiness were calculated by using instrument software (Texture Exponent v.6.1.4.0, Stable Microsystems).

Experimental design

A central composite design was selected for the optimization of process conditions (refined / functional oil ratio and wax concentration), each at five levels with 13 runs including five central points. Optimization of independent variables of oil addition ratio (X1) and wax concentration (X2) was carried out to achieve the best performance of texture (Z1), color (Z2), oil binding capacity (Z3), and crystal formation time (Z4). Experimentally determined responses for each corresponding trial were given in Table 1. Response surface methodology (RSM) was used for optimization using Minitab Software (Minitab 18.1.1). Full quadratic second order regression model including the linear, quadratic and two factor interaction effects was proposed for the prediction of responses (Eq. 1).

$$Z = \beta_0 + \sum_{i=1}^{2} \beta_i X_i + \sum_{i=1}^{2} \beta_{ii} X_i^2 + \sum_{i=1}^{1} \sum_{j=i+1}^{2} \beta_{ij} X_i X_j \quad \text{Eq. (1).}$$

where Z was the dependent variable, the X was the independent variables β_0 was the constant coefficient, β_i was the linear coefficient (main effect), β_{ii} was the quadratic coefficient, and β_{ij} was the two factors interaction coefficient. Model adequacy was evaluated by considering parameter of R^2 value of regression.

SSC= Sunflower oil enriched by sesame oil mixed with carnauba wax

Table 1. Central Composite Design for SSC oleomargarine samples

Run Order[a]	Refined/Functional Oil Ratio (g/g)	Carnauba Wax Rate (%)
1	15.00	7.50
2	15.00	7.50
3	0.00	7.50
4	15.00	5.00
5	25.61	9.27
6	15.00	7.50
7	4.39	9.27
8	15.00	10.00
9	15.00	7.50
10	30.00	7.50
11	25.61	5.73
12	4.39	5.73
13	15.00	7.50

[a]Randomized

3. Results and Discussion

Corresponding textural properties of SSC oleomargarine samples were given in Table 2.

Table 2. Textural properties of SSC oleomargarine samples

run order[a]	Hardness[b] SSC	Stickiness[b] SSC
1	255.49	-58.61
2	245.97	-58.94
3	253.75	-56.34
4	62.77	-13.16
5	521.37	-99.36
6	248.30	-54.51
7	510.90	-101.35
8	623.19	-107.59
9	242.77	-54.92
10	232.91	-59.49
11	102.64	-22.69
12	94.27	-22.20
13	227.64	-56.56

[a]Randomized; [b] g, force

As the wax concentration increased, hardness and stickiness values of oleomargarine samples were seen to rise (Table 2). Results of regression analysis was reported in Table 3, where it is clear that model shows high prediction ability to guess the textural properties of resulted samples. Parameter of R^2 value of regression was also in furtherance this fact, since it is more than 0.9 for both textural properties (hardness and stickiness) of SSC. In other words, model could explain the more than 90% of variation in responses as a function of process conditions (Table 3).

Table 3. Regression coefficients of proposed models for the investigated textural properties of SSC oleomargarine samples

variables[a]	Hardness SSC	Stickiness SSC
β0	244.03***	-56.71***
β1	-1.88ns	-0.52ns
β2	287.78***	-51.15***
β11	6.4ns	-2.33ns
β22	106.0***	-4.79ns
β12	1.1ns	1.24ns
Model	***	***
R^2	99.35	98.49

[ns],not significant ($p > 0.05$); [*]significant at $p \leq 0.05$, [**],significant at $p \leq 0.01$; [***],significant at $p \leq 0.001$

Color parameters (L*; luminosity. a∗;+ redness/ – greenness. and b∗; + yellowness/ – blueness) of oleomargarine samples were measured and corresponding mean values were given in Table 4.

Table 4. Color Values (L*, a*and b*) of SSC Oleomargarine Samples

run order[a]	SSC		
	L*	a*	b*
1	45.07	0.34	7.67
2	46.09	0.38	8.00
3	43.89	0.50	8.08
4	43.19	0.20	7.04
5	44.68	0.45	9.43
6	46.13	0.30	7.95
7	45.82	0.42	8.65
8	45.89	0.60	9.53
9	45.28	0.33	8.09
10	43.41	0.35	8.80
11	42.24	0.41	8.07
12	41.66	0.67	7.84
13	45.37	0.35	8.18

[a]Randomized

Table 5. Regression coefficients of proposed models for the investigated responses of SSC oleomargarine color value (L*. a*and b*)

variables[a]	SSC		
	L*	a*	b*
β0	45.20***	0.31	8.00***
β1	-0.27ns	-0.03	0.32*
β2	1.77***	0.09	0.94***
β11	-1.62***	0.12	0.51*
β22	-0.88*	0.10	0.46*
β12	-0.56ns	0.01	0.39ns
Model	***	ns	***
R^2	91.35	34.74	85.21

Table 6. Oil Binding Capacity (%) and Crystal formation Time of SSC Oleomargarine Samples

run order[a]	OBC(%)	CFT(min)
	SSC	SSC
1	85.29	8.00
2	86.25	8.02
3	84.61	8.28
4	64.14	14.15
5	96.93	7.50
6	86.73	8.05
7	91.51	8.10
8	97.16	7.40
9	86.97	8.10
10	86.51	8.30
11	70.69	9.57
12	73.51	13.30

13	85.70	8.05

[a]Randomized

SSC oleomargarine samples oil binding capacity (%) and crystal formation time were presented in Table 6. Oleomargarines were found to bind liquid oil more than 64.14 (%) and the time required for crystallization was found to require equal or more than 7.40 minutes. The highest oil binding capacity (97.16%) and the least crystal formation time (7.40 min) were achieved in the formulation examined at trial 5, in which the highest gel formation agent concentration (10%) was used in formulation. Corresponding developed models were presented in Table 7. It can be seen from Table 7 that, both models had high prediction performance (explaining the more than 90% of variation). Thus, both models could be used to evaluate process dependent variation in OBC (%) and CFT (min), when sunflower oil, sesame oil and carnauba wax were used together, but at varied ratios for formation of oleomargarine.

Table 7. Regression coefficients of proposed models for the investigated responses (oil binding capacity (%) and crystal formation time) of SSC oleomargarine

variables[a]	OBC(%) SSC	CFT SSC
β0	86.19***	8.04***
β1	0.93*	-0.76ns
β2	16.08***	-2.97***
β11	-0.60ns	0.29ns
β22	-5.51***	2.77***
β12	4.12***	1.57*
Model	***	***
R^2	99.58	90.78

[ns].not significant ($p > 0.05$); [*].significant at $p \leq 0.05$. [**].significant at $p \leq 0.01$; [***].significant at $p \leq 0.001$.

Acknowledgements

This work was supported by Suleyman Demirel
University Scientific Research Projects Coordination Unit (grant number 4849-D1-17).

References

Berasategi. I.. Garcia-Iniguez de Ciriano. M.. Navarro-Blasco. I.. Calvo. M.I.. Cavero. R.Y.. Astiasaran. I.. Ansorena. D. (2014). Reduced-fat Bologna sausages with improved lipid fraction. J Sci Food Agric. 94: 744-751.

Co. E.D.. Marangoni. A.G. (2012). Organogels: An alternative edible oil-structuring method. J Am Oil Chem Soc. 89: 749-780.

Da Pieve S. Calligaris S. Co E. Nicoli MC. Marangoni AG. 2010. Shear nanostructuring of monoglyceride organogels. Food Biophys 5:211–7.

Dassanayake LSK. Kodali DR. Ueno S. Sato K. 2009. Physical properties of rice bran wax in bulk and organogels. J Am Oil Chem Soc 86:1163–73.

Grasso. S.. Brunton. N.P.. Lyng. J.G.. Lalor. F.. Monahan F.J. (2014). Healthy processed meat products-Regulatory. reformulation and consumer challenges. Trends Food Sci Technol. 39: 4-17.

Marangoni A. Garti N. 2011. Food oil gels: new strategies for structuring edible oils. INFORM 22(5):317–20.

Patel. A.R.. Dewettinck. K.. 2016. Edible oil structuring: an overview and recent updates. Food & Function. 7(1). 20-29.

Robertson A.R. (1977). The CIE 1976 Color- Difference Formulae. Color Research and Application. 2(1). 7-11.

Singh. A.. Auzanneau. F.I.. Rogers. M.A.. 2017. Advances in edible oleogel technologies – A decade in review. Food Research International. 97. 307-317.

Toro-Vazquez JF. Morales-Rueda JA. Dibildox-Alvarado E. Charo´-Alonso M. Alonzo-Macias M. Gonza´lez-Cha´vez MM. 2007. Thermal and textural properties of organogels developed by Candelilla wax in safflower oil. J Am Oil Chem Soc 84:989–1000. E1738 Journal

Yilmaz, F., & Dagdemir, E. (2012). The effects of beeswax coating on quality of Kashar cheese during ripening. International Journal of Food Science and Technology, 47(12), 2582–2589 doi: 10.1111/j.1365 2621.2012.03137.x.

Youssef. M.K.. Barbut. S. (2009). Effects of protein level and fat/oil on emulsion stability. texture. microstructure and color of meat batters. Meat Sci. 82: 228-233.

Youssef. M.K.. Barbut. S. (2011). Fat reduction in comminuted meat products-effects of beef fat. regular and pre-emulsified canola oil. Meat Sci. 87: 356-360.

International Conference on Science and Technology

ICONST 2018

5-9 September 2018 Prizren - KOSOVO

Finite Elemant Method Modeling Of Clamped Masonry Walls / Kenetli Yığma Duvarların Sonlu Elemanlar Metoduyla Modellenmesi

Tulin Celik[1], Sukran Tanriverdi[1*], Ali Ural[1], Fatih Kursat Firat[1]

Özet: İlk çağlardan bu yana insanlar barınma alanları yapmak için yığma birimler olan taş, tuğla, briket ve kerpiç gibi malzemeler kullanmışlardır. Depremler, yangınlar, zeminden kaynaklanan problemler, çeşitli çevresel faktörlerin oluşturduğu fiziksel ve kimyasal bozulmalar sonucu tarihi yapılarda büyük hasarlar meydana gelmiştir. Bu hasarlar yığma yapıların kayma ve çekme gerilmelerinin düşük olmasından kaynaklanmaktadır. Yapı sisteminin birlikte hareket etmesi ve yapının bütününde sünek bir davranış görülmesi için genellikle bağlantı elemanları olarak kenetler ve zıvanalar kullanılmıştır.

Bu çalışmada, kenetlerin batma noktası ile taşın kenarı arasındaki mesafe dikkate alınmış ve kenetlerin duvarın kayma dayanımı üzerindeki etkisi incelenmiştir. Çalışmada 3 boyutlu sayısal modeli oluşturmak için sonlu elemanlar yöntemini (FEM) esas alan LUSAS yazılımından yararlanılmıştır. Analiz sonuçları doğrultusunda, taş kenarı ile batma noktası arasındaki mesafe incelenmiş ve bunların taş birimler üzerindeki etkileri karşılaştırmalı olarak gösterilmiştir.

Anahtar Kelimeler: Tarihi Yapılar, LUSAS, Kenet Elemanlar, Çekme Gerilmesi, Yığma Birim

Abstract: Since the early ages, people have used materials which are masonry units such as stone, brick and adobes to make areas for sheltering. Historical structures have been occurring great damage arising from earthquake, fire, soil problems, various environmental factors are caused physical and chemical deterioration These damages are arised from low shear and tensile stresses in masonry walls. Clamps and dowels are often used as connections in many historical buildings. These elements move together with the structural system and the whole structure shows ductile behavior with these elements.

In this study, distance to the edge of the stone was taken into account with immersion point of the clamps and the influence of the clamps on the shear strength of the wall was investigated. The LUSAS software based on the finite element method (FEM) was used to create a 3D numerical model. In direction with the results of analysis, the distance between the edge of the stone and the immersion point is examined and the effects of those on the stone units are comparatively illustrated.

Keywords: Historical Structures, LUSAS, Clamp Elements, Tensile Stress, Masonry Unit

Giriş

Tarihi yapılar, geçmişten günümüze kadar gelebilen eski uygarlıkların kültürünü, yaşantısını, inançlarını ve bulunduğu dönemin dokusunu bizlere anlatan eserlerdir. Ülkemizdeki tarihi yapıları cami, tekke, imaret, medrese, han, hamam, köprü, su kemeri, kale vb. gibi yapılar oluşturmaktadır. Bu tarihi yapıların büyük çoğunluğu taş, tuğla ve briket gibi malzemelerden yapılmıştır. Bu tür malzemeler kullanılarak yapılan yığma yapılar düşük çekme dayanımına sahiptir ve bunlar birçoğu deprem, sel, yangın gibi doğal afetler karşısında zarar görür ya da yıkılır.

Donatısız yığma sistemler düşük çekme dayanımına sahiptir. Bu yapılara gelen deprem kuvvetiyle birlikte yapılar ağır hasar görür ya da yıkılır. Bu yapılarda sünekliği artıracak herhangi bir malzeme kullanılmadığı için dinamik etkiler altında gevrek bir davranış sergileyerek hasar görürler (Ural, 2009). Bu sebeplerden dolayı birçok donatısız yığma yapı onarım ve güçlendirmeye ihtiyaç duymaktadır.

[1]Aksaray University, Faculty of Engineering, 68100, Aksaray, TURKEY
*Corresponding author: sukran_tugrulelci@hotmail.com

Gelen yatay kuvvetler karşısında yığma yapı sisteminin bir bütün halinde hareket etmesi oldukça önemlidir. Fakat gelen yatay kuvvetlere karşı yığma yapı sisteminin kayma kuvvetine karşı dayanımı oldukça düşük olduğu için yapı bütünlüğü korunamamaktadır. Bu yapıların stabilitesini sağlamak için yığma yapılarda kenet ve zıvana gibi metal bağlantı elemanları kullanılmaktadır. Günümüzde bu konuyla ilgili yapılmış literatürde yapılan çalışmalar incelendiğinde kenetlerin yığma sistem üzerine olumlu sonuçlar doğurduğu görülmüştür.

Papadopoulos (2006), yaptığı çalışmada Apollo Epikourius Tapınağında taş bloklar arasında bulunan metal bağlantı elemanlarını incelenmiştir. Kenet alanlarının taş blokların taşıma kapasitelerine etkisini üç boyutlu analizler yardımıyla hesaplanmıştır. Sonuçta, yığma yapının maksimum dayanımı sağlaması için taş blokları birbirine bağlayan yeni kenet bağlantı alanları araştırmıştır. Toumbakari (2008), Parthenon Tapınağındaki kuzey duvarı üzerine bir araştırma yapmıştır. Söz konusu tapınak duvarlarında taşları birbirine bağlamak amacıyla kenet uygulamalar kullanılmıştır. Bu kenet uygulamalarının duvarın davranışına etkileri araştırmıştır. Demir, (2012) yaptığı çalışmada ana değişkenin çok tabakalı tarihi duvarların kayma davranışına etkisini incelemiştir. Değişken olarak, eksenel gerilme düzeyi, kenet ve zıvana kullanımı ve dış tabakalar arasında iç moloz dolguyu kullanmıştır. Deneysel çalışma, yerdeğiştime kontrollü olarak etkitilen tekrarlı kesme kuvvetlerine maruz bırakılmış duvar numunelerinden meydana gelmektedir. Gerçekleştirilen deneysel çalınma ile kenetlerin kullanılması çatlak dağılımını etkilemekle birlikte, kullanılan küfeki taşının çekme dayanımının sınırlı olması nedeniyle taşlar çatlamış ve kenetlerin etkinlikleri sınırladığı sonucuna varılmıştır. Koçak, (2013), çalışmasında düşük kayma dayanımına sahip yığma taş duvarların kayma dayanımını arttırmak amacıyla birçok teknik geliştirmiştir. Yaptığı deneysel çalışmada taş yığma duvarların kayma dayanımını arttırma için metal bağlantı elemanları kullanmıştır. Deneysel çalışmasında 3 farklı metal bağlantı elemanı (kenet) geliştirilmiştir. 10 farklı deney numunesi üretilerek kayma dayanımları araştırılmıştır ve bunların kayma dayanımları deneysel denklemlerle desteklenmiştir. Çalışmanın sonunda, geliştirilen yeni metal bağlantı elemanlarının yığma yapıların kayma dayanımlarını ve sünekliğini etkili bir şekilde arttırdığı ortaya koymuştur. Uslu, (2013), Yaptığı çalışmada, tarihi yığma yapılarda kullanılan metal bağlantı elemanları irdelemiştir. Metal bağlantı elemanları kullanılarak örülen taş yığma duvarlar üzerinde deneysel çalışmalar yapmıştır. Metal bağlantı elemanları olarak kenet ve zıvana kullanılmıştır. Deneysel çalışmada, taş yığma duvar numunelerinin diyagonal basınç etkisine tabi tutarak duvarların kesme etkisindeki davranışlarını incelemiştir. Numunelerin kırılma yüklerine ve kesme dayanımlarına göre değerlendirme yapmıştır. Kenet ve zıvanalar ile yapılan taş yığma duvarların bağlantı elemanı kullanılmayan taş yığma duvara göre daha yüksek dayanım gösterdiği sonucuna varılmıştır. Ural vd., (2015), Deneysel çalışmasında farklı kenet-zıvana sistemlerine sahip aynı ebattaki yığma duvar numuneleri üzerinde gerçekleştirilen deneyler sonucunda sistemlerin yığma duvarların kesme (kayma) kapasitesine ne tür bir etkisi olduğu incelenmiş ve fotoğraflar yardımıyla çeşitli yorumlarda bulunulmuştur. Çalışma sonucunda, günümüzde yapılacak olan restorasyon çalışmalarına ışık tutabilecek önemli bazı sonuçlara ulaşmıştır. Kurugöl ve Küçük (2015), Çalışmasında tarihi süreç içerisinde demir malzemenin geleneksel mimarideki genel uygulama yer ve biçimleri ele alınarak, üretim teknikleri ve şekil verme yöntemleri açıklamışlar ve aynı zamanda demir malzemede zaman içerisinde ortaya çıkan çeşitli problemler ortaya koymuşlardır.

Şekil 1. Mevlana Müzesinde bulunan yığma taş bloklar üstündeki kenet uygulamaları

2. Malzeme ve Metot

Bu çalışmada, kenetin batma noktasının taşın kenarına olan mesafesi ve yığma taş bloklar üzerindeki kayma dayanımına etkisi incelenmiştir. Değişken olarak kenetin batma noktasının taşın kenarına olan mesafesi ele alınmıştır. Kenetin kenara olan mesafesi 20, 40, 60, 80 ve 100 mm ‘dir. Bütün modellerde kenet elemanlarının genişliği 20 mm ve batma derinliği 40mm olarak alınmıştır. Yığma taş blokların ortalama basınç dayanımı 4 MPa olarak belirlenirken

Elastisite Modülü 4000 MPa ve Poisson Oranı 0,2 olarak bulunmuştur. Yığma taş bloklar 200x100x100 mm^3 ebadında, metal bağlantı elemanları olarak kullanılan kenet elemanlar ise 200x20x2 mm^3 boyutundadır (Şekil 2). Sonlu elemanlar metodu kullanılarak yığma birimler ve kenetler LUSAS programında modellenmiştir. Analizlerde malzemenin doğrusal olmayan özelliklerinden faydalanılmış, geometrik olarak ikinci mertebe etkileri dikkate alınmamıştır. Şekil 3'de yapılan modelin aşamaları sırası ile gösterilmiştir.

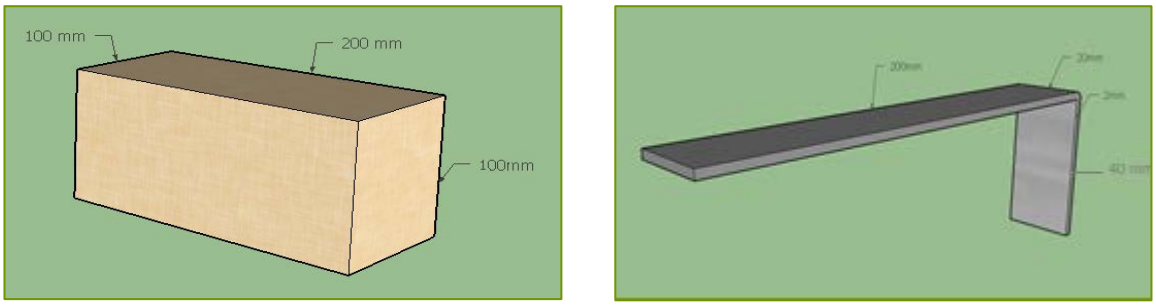

(a) (b)

Şekil 2. (a) Yığma taş blok modelinin boyutları, (b) Kenet modelinin boyutları

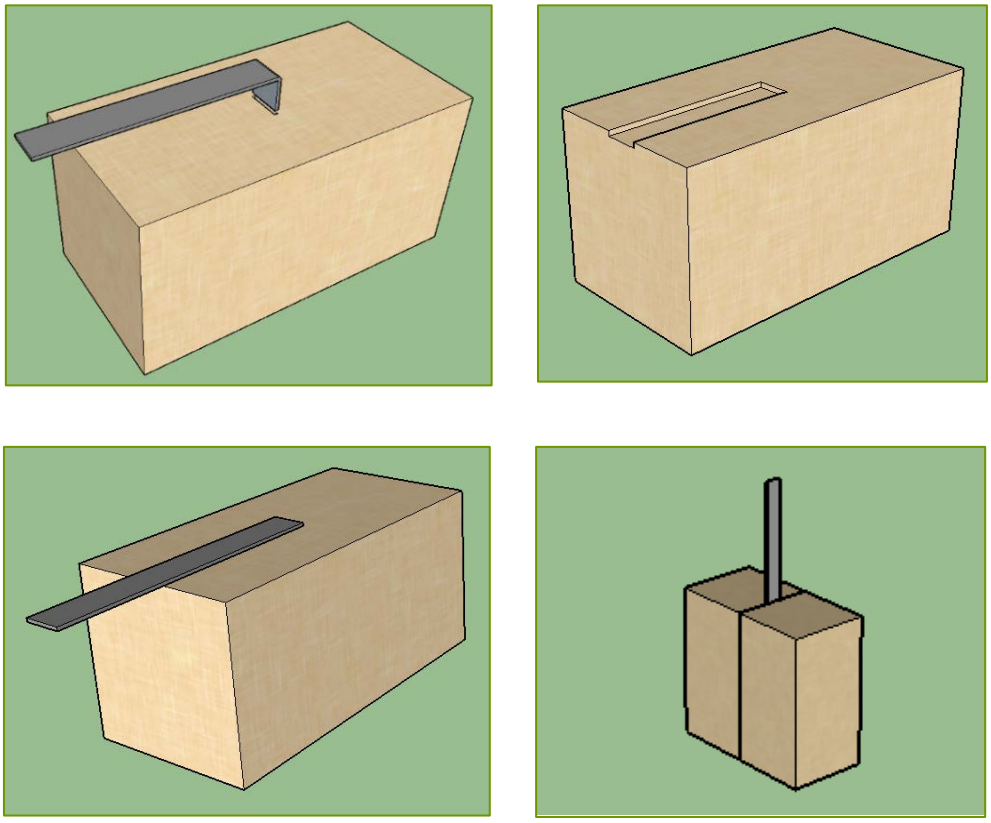

Şekil 3. Kenetin yığma taş bloklar arasına yerleştirilmesi

Birinci taş blok üzerinde kenetin içine girebilmesi için 40x20x2 mm^3 ebadında bir dikdörtgen delik açılmıştır. Kenet taş blok üzerinde bu deliğe yerleştirilmiştir. İkinci taş blok üstünde kenetin üstünü kapatacak şekilde 100x20x2 mm^3 boyutlarında dikdörtgen oyuklar açılmıştır. Bu oyukların uzunluğu, kenetin kenarına olan mesafesine göre 20 mm, 40 mm,60 mm,80 mm,100 mm olarak değişmektedir. Kenet iki tane taş blok arasına yerleştirilmiştir. Şekil 4' de sayısal modellerinin ve kenetin yerleştirilmesi gösterilirken Tablo 1'de modellerin geometrik özellikleri verilmiştir.

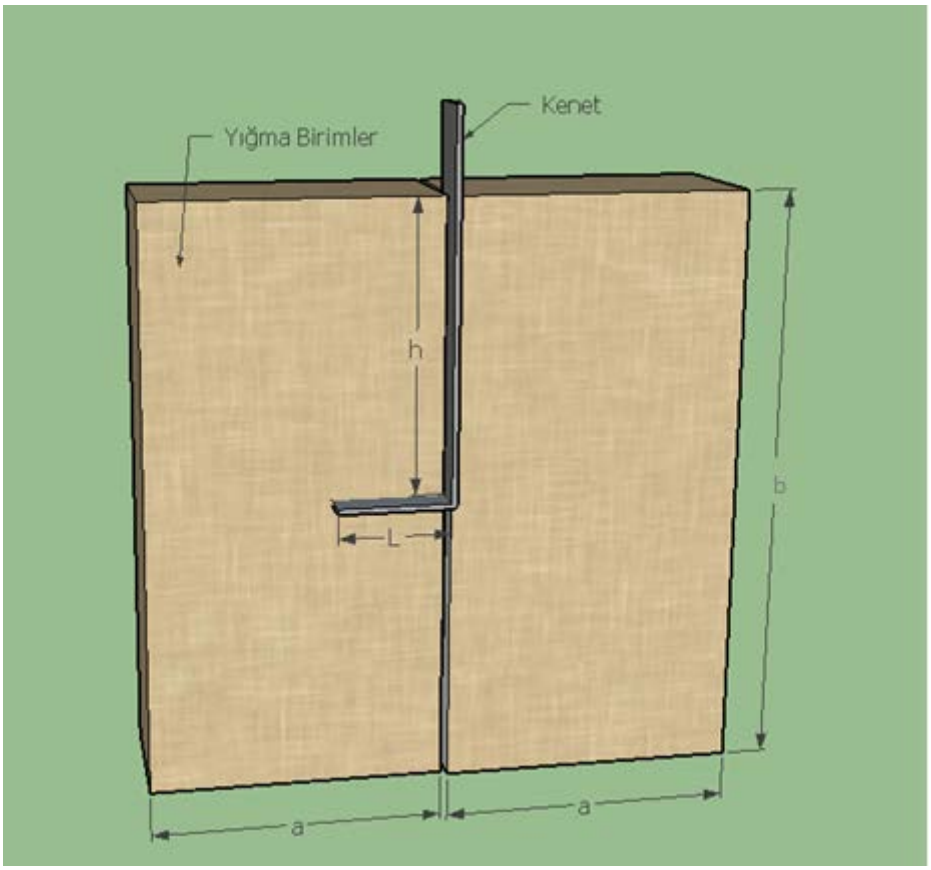

Şekil 4. Sayısal model ve kenetin yerleştirilmesi

Tablo 1. Hazırlanan modellerin geometrik özellikleri

Model No	L (mm)	a (mm)	b (mm)	h (mm)
1	40	100	200	20
2				40
3				60
4				80
5				100

3. Kenetlerin Sonlu Elemanlar Yöntemiyle Analizi

3 boyutlu sayısal kenet modelini oluşturmak için sonlu elemanlar yöntemini esas alan LUSAS (2013) yazılımı kullanılmıştır. Bu çalışmada kenetin taş blokların kenara olan mesafesi incelenmiştir. Sayısal modellemede kenetin, Elastisite Modülü 210000 MPa, Poission Oranı 0,3 olduğu kabul edilmiştir. Bunun yanında taş blokların, Elastisite Modülü 4000 MPa ve Poission Oranı 0,2 olduğu varsayılmaktadır. Bu çalışmada taş blokların doğrusal olmayan davranışını temsilen Drucker- Prager kriteri kullanılmıştır. Drucker- Prager kriteri elastik-tam plastik bir davranışı temsil ettiğinden dolayı model plastik aşamaya geçtiğinde yatay bir seyir izlemektedir. Şekil 5'de sayısal modellerin analiz sonucunda deplasman ve çekme gerilmesi renklendirmeleri görülmektedir. Renklendirmeler 4 kN' luk yük altındaki görüntülerdir. Bu aşamada taş bloklarda doğrusal ötesi davranış başlamıştır.

	Deplasman	Çekme gerilmesi
Analiz 1 **(100 mm)** Maksimum deplasman= 0.0795 mm Maksimum çekme gerilme=0.3889 MPa	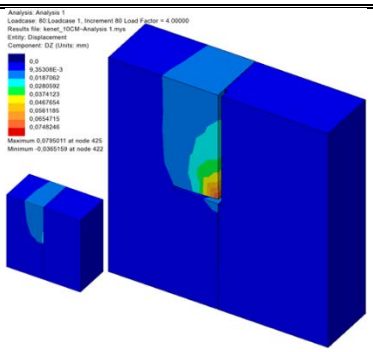	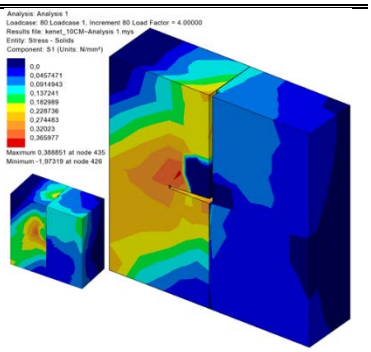
Analiz 2 **(80 mm)** Maksimum deplasman= 0.0876 mm Maksimum çekme gerilme=0.4046 MPa	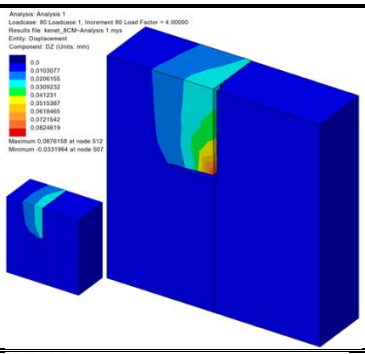	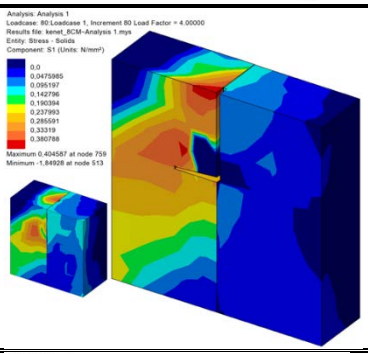
Analiz 3 **(60 mm)** Maksimum deplasman= 0.1125 mm Maksimum çekme gerilme=0.4016 MPa	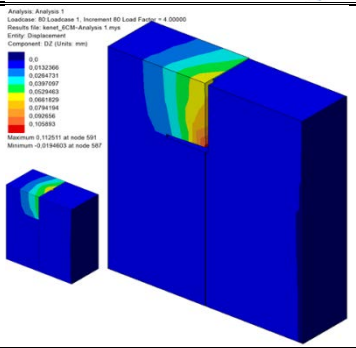	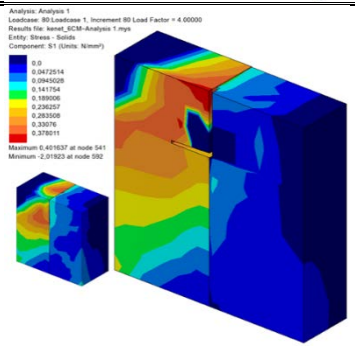
Analiz 4 **(40 mm)** Maksimum deplasman= 0.2370 mm Maksimum çekme gerilme=0.4029 MPa	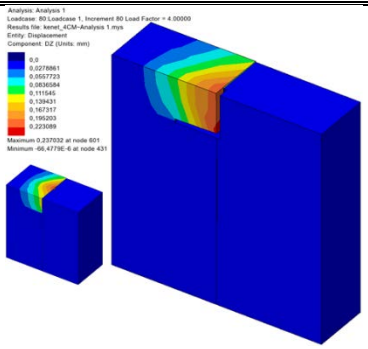	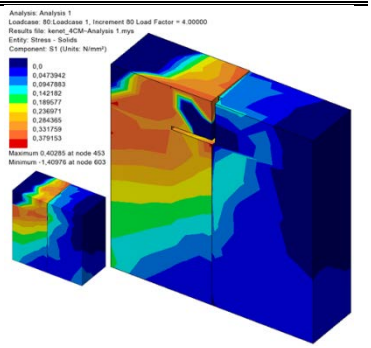
Analiz 5 **(20 mm)** Maksimum deplasman= 0.05979 Maksimum çekme gerilme=0.4043 MPa	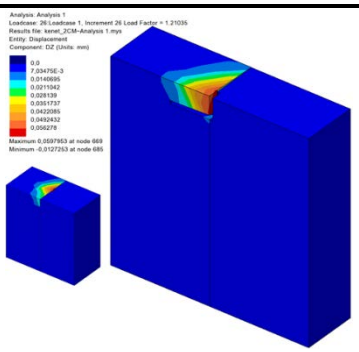	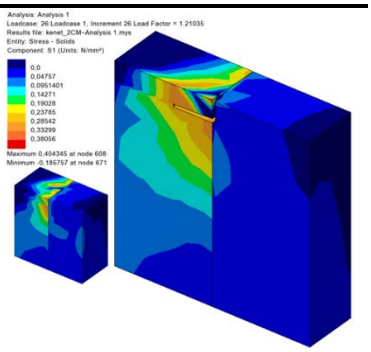

Şekil 5. Sonlu eleman analiz sonuçları

Sonlu elemanlar modelleriyle yapılan analizler neticesinde modellerin maksimum noktadaki çekme gerilme-çekme şekil değiştirme, yük-deplasman ve kayma gerilme-kayma şekil değiştirme grafikleri Şekil 6'da verilmiştir. Şekil 6 (a) ya bakıldığında batma mesafesi 20 mm ve 40 mm olan modellerin çekme gerilme değerleri birbirine yakınlık gösterirken diğer modellere oranla çekme gerilme değerleri düşüktür. Batma mesafesi 60 mm, 80 mm ve 100 mm olan modellerin çekme gerilme-çekme şekil değiştirme grafikleri birbirine çok yakın çıkmıştır. Yine aynı şekilde Şekil 6 (b) incelendiğinde 20 mm'lik model çok fazla yük taşıyamamıştır. Yük- deplasman grafiğinde de 60 mm, 80 mm ve 100 mm'lik modeller benzer davranış gösterirken 40 mm'lik model farklı bir davranış sergilemiştir. Şekil 6 (c)'de batma mesafesi 20 mm olan model diğer modellere göre çok düşük kayma gerilmesi değerine sahiptir. Diğer modellerin kayma gerilme-kayma şekil değiştirme grafikleri birbirlerine oldukça yakın çıkmıştır.

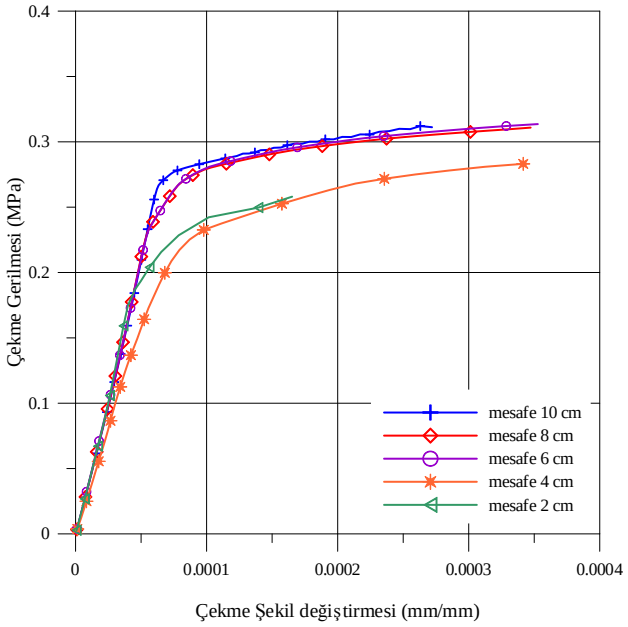

a) Çekme gerilmesi-çekme şekil değiştirmesi grafikleri

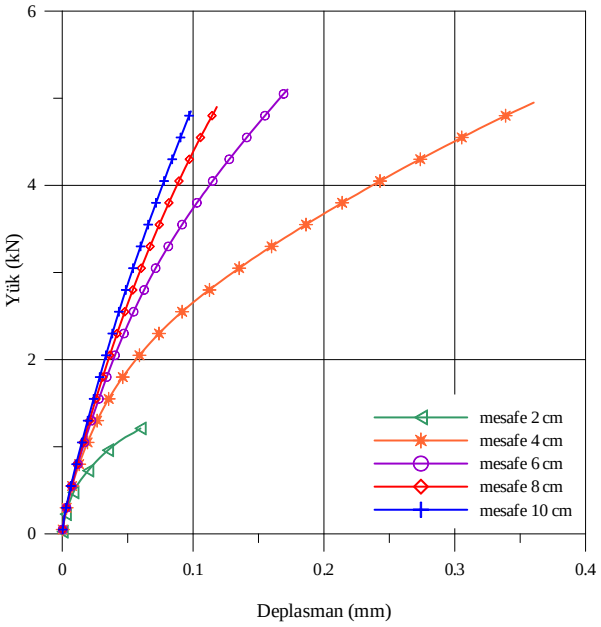

b) Yük-deplasman grafikleri

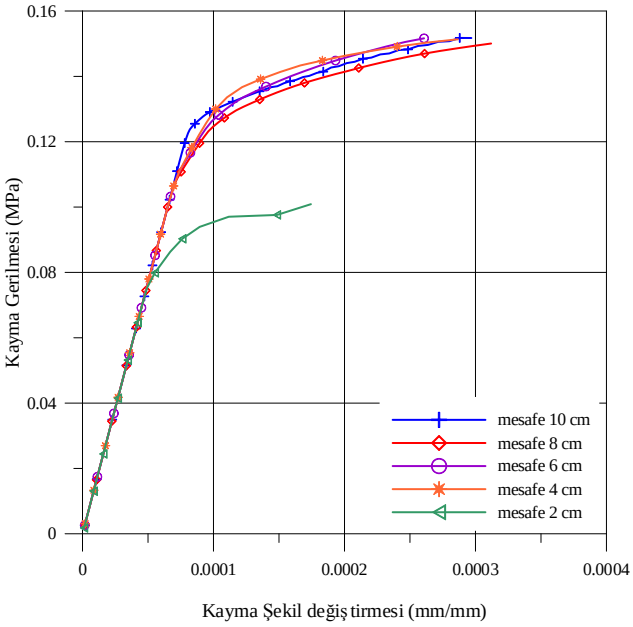

c) Kayma gerilmesi-kayma şekil değiştirmesi grafikleri

Şekil 6. Sonlu elemanlar modelleriyle yapılan analizler neticesinde elde edilen a) çekme gerilmesi- çekme şekil değiştirmesi grafikleri, b) yük-deplasman grafikleri ve c) kayma gerilmesi- kayma şekil değiştirmesi grafikleri modelleri

4. Sonuçlar

Kenetlerin batma noktasının taşın kenarı arasındaki mesafe dikkate alınarak yapılan analizlere ait sonuçlar Tablo 2'de verilmektedir. Yapılan analiz sonuçları kenetin, taşın kenarına olan mesafesine göre değişkenlik göstermektedir. Bu analizlerden elde edilen sonuçlar karşılaştırılarak, restorasyon çalışmaları için bazı önerilerde bulunulmuştur.

Tablo 2. Kenet uygulamalarının analiz sonuçları

Analiz Durumu	Maksimum Çekme Gerilmesi (MPa)	Maksimum Çekme Şekil Değiştirmesi (mm/mm)	Maksimum Kayma Gerilmesi (MPa)	Maksimum Kayma Şekil Değiştirmesi (mm/mm)	Maksimum Yük (kN)	Maksimum Deplasman (mm)
Analiz 1 (10 cm)	0.312	0.000272	0.152	0.000297	4.85	0.098
Analiz 2 (8 cm)	0.311	0.000347	0.150	0.000312	4.90	0.116
Analiz 3 (6 cm)	0.314	0.000353	0.151	0.000261	5.10	0.172
Analiz 4 (4 cm)	0.299	0.000342	0.151	0.000287	4.95	0.360
Analiz 5 (2 cm)	0.258	0.000165	0.101	0.000174	1.21	0.059

Tarihi yapılarda zaman içerisinde bozulmalar meydana gelmekte ve yapı elemanları dayanımlarını kaybetmektedir. Bu yapıları gelecek nesillere daha sağlam ve güvenilir bir şekilde ulaştırmak için güçlendirmek gerekmektedir. Güçlendirme çalışmalarında metal bağlantı elemanı olan kenet ve zıvanalar kullanılmaktadır. Bu metal bağlantı elemanlarının nasıl tasarlanacağı ve ne şekilde uygulanacağı önemli bir çalışma konusudur.

- Kenetin batma noktasının taşın kenarına olan mesafesi hakkında literatürde yapılan bir çalışma bulunmamaktadır. Yapılan çalışmada batma mesafesi 40 mm, 60 mm, 80 mm ve 100 mm olan modeller 20 mm batma mesafesine sahip modele göre daha fazla yük taşımışlardır. 40 mm'lik model fazla yük taşısada gerek yük- deplasman grafiğinde gerekse çekme gerilmesi-çekme şekil değiştirmesi grafiğinde batma mesafesi 60 mm, 80 mm ve 100 mm olan modellere göre farklı bir davranış sergilemiştir.

- Analiz sonucunda batma mesafesi 20 mm olan modelde çekme ve kayma gerilmeleri diğer modellere göre oldukça azdır. 60 mm, 80 mm ve 100 cmm batma mesafesine sahip modellerin çekme gerilme değerleri birbirlerine oldukça yakın çıkmıştır. Bunun yanında maksimum yüke karşılık gelen şekil değiştirme miktarları en fazla sırası ile 60 mm, 80 mm ve 100 mm batma mesafesine sahip modellerde görülmektedir.

- Yapılan analiz sonucunda 200x100x100 mm^3 ebatındaki taşlar için kenetin batma noktasının taşın kenarı arasındaki mesafenin 40 mm den küçük olmaması gerektiği sonucuna varılmıştır.

- Bu çalışma ile kenetin batma noktasının taşın kenarına olan mesafesinin, taşın uzunluğuna oranı (h/b) 0.2 değerinden küçük olmayacağı önerilmektedir. Yapılan bu çalışmanın onarım ve güçlendirme amacıyla yapılacak olan restorasyon uygulamalarına iyi bir referans olacağı düşünülmektedir.

- İleriki çalışmalarda, yapılan sayısal analizin deneysel çalışması yapılacak ve sonuçlar birbirleri ile karşılaştırılarak kıyaslanacaktır.

Kaynaklar

Demir, C. (2012). Seismic behaviour of historical stone masonry multi-leaf walls. Phd thesis, Istanbul Technical University, Graduate School of Science Engineering and Technology, Istanbul.

Kurugöl, S., Küçük, S.G. (2015). Tarihi eserlerde demir malzeme kullanım ve uygulama teknikleri. 5. Tarihi Eserlerin Güçlendirilmesi ve Geleceğe Güvenle Devredilmesi Sempozyumu, Erzurum, 521-536.

Koçak, Y. (2013). Yığma yapılarda kayma dayanımının artırılması amacıyla farklı bağlantı elemanı uygulamaları. Yüksek Lisans Tezi, Aksaray Üniversitesi, Fen Bilimleri Enstitüsü, Aksaray.

Lusas, Finite element analysis software products, Finite Element System FEA Ltd, 2013.

Papadopoulos, K.A. (2006). The restoration study of the connections between the stone blocks in the steps of the temple of Apollo Epikourios. Proceedings of Structural Analysis of Historical Construction, Eds with D'Ayala & Fodde, New Delhi.

Toumbakari, E.E. (2008). The Athens Parthenon: Analysis and interpretation of the structural failures in the ortho state of the northern wall. Proceedings of the Structural Analysis of Historical Construction, Eds with D'Ayala & Fodde, New Delhi.

Ural vd., (2015). Kenet ve zıvanaların yığma duvarların kesme (kayma) davranışına etkisi. 5. Tarihi Eserlerin Güçlendirilmesi ve Geleceğe Güvenle Devredilmesi Sempozyumu, Erzurum, 537-548.

Ural, A. (2009). Yığma yapıların doğrusal ve doğrusal olmayan davranışlarının incelenmesi. Doktora Tezi, Karadeniz Teknik Üniversitesi, Fen Bilimleri Enstitüsü, Trabzon.

Uslu, S. (2013). Tarihi yığma yapılarda kullanılan metal bağlantı elemanlarının deneysel metotlarda incelenmesi. Yüksek Lisans Tezi, Aksaray Üniversitesi, Fen Bilimleri Enstitüsü, Aksaray.

International Conference on Science and Technology

ICONST 2018

5-9 September 2018 Prizren - KOSOVO

Batma Derinliği Farklı Olan Kenetlerin Yığma Duvarların Davranışına Etkisinin Araştırılması / Investigation of The Effect of The Clamps with Different Immersion Depth on The Masonry Wall's Behaviour

Sukran Tanriverdi[1], Tulin Celik[1*], Ali Ural[1], Fatih Kursat Firat[1]

Özet: Tarih boyunca insanlar barınma ihtiyacını karşılamak amacıyla birçok yığma yapı inşa etmiştir. Yığma yapılar deprem, sel, rüzgâr gibi doğal afetler nedeniyle ağır hasar almıştır. Bunun temel nedeni taş yığma yapıların düşük çekme dayanımına sahip olmasıdır. Tarihte yığma yapıların çekme dayanımını arttırmak için çeşitli bağlantı elemanları kullanılmıştır. Bu bağlantı elemanları ilk olarak ahşap malzemeden üretilmesine rağmen daha sonra teknolojinin gelişmesiyle birlikte metal malzemelerden yapılmaya devam edilmiştir.
Bu çalışmada metal bağlantı elemanı olarak kullanılan kenetlerin, yığma taş blokların davranışlarına etkisi deneysel metotlarla incelenmiştir. Yapılan deneysel çalışmada değişken olarak kenet demirlerinin yığma taş blok üzerindeki batma derinliği dikkate alınmıştır. Bu konu hakkında literatür de yapılmış çalışma yok denecek kadar azdır ve bu çalışmayla literatürdeki bu eksiklerin giderilmesi amaçlanmaktadır.

Anahtar Kelimeler: Tarihi Yapılar, Yığma Yapılar, Kenet, Bağlantı Elemanı, Çekme Gerilmesi

Abstract: Throughout history, people have built many masonry structures to meet the need for shelter. Masonry structures has taken heavy damage due to natural disasters such as earthquakes, floods, wind. The main reason is that it has low tensile strength of stone masonry structures. Various connectors have been used to increase tensile strength of the masonry structure in the history. Although these connectors were manufactured from the first wood material and then they continued to be made from metal materials with the development of technology.
In this study, the effects of the clamps used as metal connection elements on the behavior of the masonry stone blocks were investigated by experimental methods. In the experimental study, immersion depth of clamps on the masonry stone block are taken into consideration as a variable. It is almost no studies in the literature on this topic and the study is aimed to overcome these short comings of the literatüre.

Keywords: Historical Buildings, Masonry Constructions, Clamp, Connection Element, Tensile Stress

Giriş

Yığma yapılar briket, taş, kerpiç, tuğla gibi birimlerin harçlar ile oluşturdukları taşıyıcı sistemlerdir. İlk çağlardan günümüze kadar insanoğlu barınma amacıyla çeşitli yığma yapılar yapmışlardır. Yapılan araştırmalar neticesinde yığma yapıların ilk örnekleri M.Ö. 1500 yıllarında Mısırlılara ait yer altı mezarlarında görülmüştür.

Yığma yapılar aynı eksende birbirine ters yönde yüklemelere maruz kaldığı zaman kayma (kesme) etkisiyle, yığma yapılarda büyük deformasyonlar oluşmaktadır. Bu deformasyonu önlemek ve kesme kuvvetine karşı dayanımı arttırmak amacıyla bu yapıları oluşturan tuğla, taş, briket, kerpiç gibi malzemelerin yanında düşey doğrultudaki yığma birimleri birbirine bağlayan eleman olarak bilinen zıvana ve yatayda iki yığma birimi bağlayan kenet elemanları kullanılmaktadır. Selçuklu ve Osmanlı döneminde yapılan cami, han, hamam, minare gibi yapılarda bunun örnekleri görülmektedir. Metal bağlantı elemanı olarak kullanılan kenetler U, Z, T, I, ve kırlangıç kuyruğu şeklinde olup, yapıda bir bütünlük sağlayarak taş blokların hareket etmesine ve kaymasına engel olmaktadır. Literatürde yapılan çalışmalar incelendiği zaman bağlantı elemanı olarak kullanılan kenet ve zıvana demirlerinin sistemin sünekliğini ve dayanımını önemli derecede artırdığı ortaya çıkmaktadır.

[1]Aksaray University, Faculty of Engineering, 68100, Aksaray, TURKEY
*Corresponding author: tulinsandikci@gmail.com

(Ural, 2017) yaptığı çalışmada değişken olarak ele aldığı zıvana demirlerinin çapının yığma duvarın kayma davranışına etkisini deneysel metotlarla incelemiştir. Deney sonucunda zıvanalı numunelerin kayma dayanımlarının, zıvanasız referans numunenin kayma dayanımından daha büyük olduğu ve en uygun zıvana oranının %0,49 civarında olduğu ortaya koymuştur. (Uslu, 2013) yüksek lisans tez çalışmasında, kenet ve zıvanaların yığma duvarın kayma mukavemetini yaklaşık olarak 4 kat artırdığını yapmış olduğu deneyler sonucunda ortaya çıkarmıştır. (Yılmaz, 2013) yaptığı çalışmada çeşitli metal bağlantı elemanları kullanarak taş yığma duvarlarını güçlendirmiş ve bu numunelerin kayma dayanımlarını araştırmıştır. Çalışma sonucunda metal bağlantı elemanlarının yığma yapıların kayma dayanımlarını ve sünekliğini etkili bir şekilde arttırdığını ortaya koymuştur. (Demir, 2012) yaptığı doktora tezi çalışmasında çok tabakalı tarihi duvarın kayma davranışına etkisini incelemiştir. Değişken olarak eksenel gerilme yüzeyi, kenet ve zıvana kullanımı ve dış tabakalar arasındaki iç moloz dolguyu kullanmıştır. Bu deneysel çalışma ile kenetlerin kullanılması çatlak dağılımını etkilemek ile birlikte, kullanılan taşın çekme dayanımının sınırlı olması nedeniyle taşlar çatlamış ve kenetlerin etkinlikleri sınırladığı sonucuna varılmıştır. (Kourkolis ve Pasiou, 2009) çalışmasında yığma yapı elemanı olan mermer bloklar ile bu blokları birbirine bağlayan metal bağlantı elemanların ve harcın etkisini araştırmıştır. Yığma yapıya etki edecek yüklere karşın malzemelerin uygun davranışı için kenet sistemlerinin mermer bloklara doğru yerleştirilmesinin önemini vurgulamıştır. (Toumbakari, 2008) çalışmasında Parthenon Tapınağındaki kuzey duvarı üzerine bir araştırma yapmıştır. Yaptığı çalışmada tapınak duvarlarında taşları birbirine bağlayan kenetlerin, duvarın davranışına etkisini incelemiştir. (Papadopoulos, 2006) çalışmasında, Apollo Epikourius Tapınağında taş bloklar arasındaki kenet bağlantı elemanları araştırılmıştır. Taş blokların kapasiteleri 3 boyutlu analizleri ile kenet alanları dikkate alınarak hesaplanmıştır. Çalışma sonucunda yığma yapının maksimum direnci sağlaması için taş blokları birbirine bağlayan yeni kenet bağlantı alanları incelenmiştir. Şekil 1'de gösterildiği gibi kenet elemanlarını, yığma yapılarda sütunlarda, duvarlarda, mezar başlıklarında, köprü korkuluklarında, anıtlarda birçok yerde kullanılmıştır.

(a)

(b)

(c)

(d)

(e)

(f)

Şekil 1. Kenet uygulama örnekleri, a) Köprü korkuluklarında kenet uygulaması, (b) Mezar başlıklarında görülen kenetler, (c) Truva antik kentindeki anıtlarda görülen kenetler, (d) Sütun ayaklarında, (e) Duvarlarda görülen kenet uygulamaları, (f) Cami minarelerinde kenet uygulamaları (Kuşüzümü, 2010)

Materyal ve Yöntem

Bu çalışmada kullanılan taş, Aksaray iline bağlı Sevinçli kasabasında çıkarılan ve yaygın olarak kullanılan volkanik kökenli tüf taşıdır. Deneysel olarak yapılan bu çalışma Aksaray Üniversitesi, Mühendislik Fakültesi, İnşaat Mühendisliği, Yapı Mekaniği laboratuvarında gerçekleştirilmiştir. Bu çalışma ile farklı batma derinliğine sahip 2 mm kalınlığındaki kenet demirlerinin yığma taş blokların davranışlarına etkisi incelenmiştir. Toplam 21 adet deney numunesi üzerinde kayma (kesme) testleri yapılmıştır. Deney sonucunda elde edilen sayısal veriler birbirileri ile karşılaştırılarak tablo ve grafik halinde sunulmuştur.

Deneyde kullanılan, 100x100x200 mm^3 ebadındaki tüf taşının mekanik özelliklerini belirlemek amacıyla basınç dayanımı testleri ve eğilmede çekme testleri gerçekleştirilmiştir. Taşın basınç dayanımını test edebilmek için (TS EN 771-6, 2007)' ye uygun olarak hazırlanan taşın ebatı 50x50x50 mm^3 kesilerek oda sıcaklığında kuruması sağlanmıştır. (TS EN 772-1, 2012) (Kagir birimlerin basınç dayanımının tayini)'de belirtildiği gibi 6 adet taşın basınç dayanım testleri yapılmıştır. Elde edilen basınç dayanım değerleri, maksimum yükün uygulanan alana oranı ile elde edilmiştir. Tek numune dayanımlarının aritmetik ortalaması hesaplanarak yığma birimlerin basınç dayanımı elde edilmiştir. Deneylerde kullanılan tüf taşının basınç dayanım sonuçları Çizelge 1'de verilmiştir.

Çizelge 1. Yığma taş birimler için basınç dayanım test sonuçları

Numune No	En kesit boyutları (mm)		Kırılma Yükü (N)	Basınç Dayanımı (MPa)
	a	b		
A1	52	51	12650	4,77
A2	50	50	10850	4,34
A3	50	50	8570	3,43
A4	50	48	9970	4,15
A5	52	50	11450	4,40
A6	51	53	8450	3,13
			Ortalama	4,04
			Standart Sapma	0,63

Yığma taş birimlerin yarmada çekme testleri (TS EN 772-6, 2004) (Beton kagir birimlerin eğilmede çekme dayanımının tayini) 'ya uygun olarak hazırlanan taşın ebatı 40x40x160 mm^3 (B1-B6 numuneleri) ve 50x100x150 mm^3 (C1-C6 numuneleri) kesilerek toplam 12 adet numune üzerinde gerçekleştirilmiştir. Taş numunelerinin eğilmede çekme dayanımları Denklem 1 ile hesaplanmıştır.

$$R_{tf} = \frac{PL}{bd^2} \quad (1)$$

Burada R_{tf}; eğilmede çekme dayanımı (N/mm^2), P; maksimum yükleme (N), b; taşın genişliği (mm), L; taşın boyu ve d; taşın yüksekliğini (mm) temsil etmektedir. Çizelge 2'de tüf taşının eğilmede çekme dayanım sonuçları verilmiştir. Yapılan çalışma sonucunda taşın eğilmede çekme dayanımı ortalama 0,65 N/mm^2 olarak tespit edilmiştir.

Çizelge 2. Yığma taş birimler için eğilmede çekme dayanım test sonuçları

Numune No (MPA)	P (N)	L (mm)	b (mm)	d (mm)	R_{tf}
B1	490	100	44	38	0,77
B2	490	100	39	45	0,62
B3	560	100	40	40	0,88
B4	570	100	41	44	0,72
B5	500	100	44	41	0,68
B6	450	100	45	41	0,59
C1	3300	100	49	99	0,69
C2	3990	100	54	97	0,79

C3	2500	100	48	99	0,53
C4	2860	100	51	99	0,57
C5	2570	100	51	99	0,51
C6	2450	100	50	99	0,50
				Ortalama	0,65
				Standart Sapma	0,12

Deneylerde kullanılan metal bağlantı elemanı olan kenet 20 mm kalınlığında metal bir sac seçilmiştir. Kenet ile ilgili çekme testleri (TS EN ISO 6892-1, 2011) (Metalik malzemeler çekme deneyi) standardında belirtilen şekilde Denklem 2 ile hesaplanmıştır.

$$R_m=F_m \quad (2)$$

Burada; R_m çekme dayanımı (MPa), F_m deney sırasında akma noktası geçildikten sonar deney numunesinin dayandığı en büyük yüktür. Yapılan deney sonucunda kenetlerin çekme dayanımı 290 MPa civarında bulunmuştur.

Deneysel Çalışma

Bu çalışma Aksaray Üniversitesi Mühendislik Fakültesi Yapı Laboratuarında bulunan, (TS EN 1052-3, 2004)'e uygun olarak hazırlanan deney düzeneğinde gerçekleştirilmiştir. 15 mm kalınlığında 300x400 mm^2 ebadındaki üç adet çelik plaka Şekil 2'de gösterildiği gibi köşelerinden 50 mm uzaklıkta delikler delinerek 16 mm'lik tij demirleri ile birbirlerine bağlanmıştır. Bu tij demirlerine yerleştirilen bulonlar sayesinde çelik levhalar hareket edebilmektedir. Eksenel yükü okuyabilmek için 10 tonluk bir yük hücresi iki çelik plaka arasına sabitlenmiştir. (TS EN 1052-3)'e göre üç ayrı eksenel basınç yükünün her birisi için en az üç adet numunenin deneye tabi tutulması zorunludur. Standard da belirtildiği gibi basınç dayanımı 10 MPa'dan küçük olan yığma birimlerde eksenel basınç yükleri 0,1 MPa, 0,3 MPa ve 0,5 MPa dayanım sağlayacak şekilde uygulanmalıdır. Yaptığımız deneysel çalışmada basınç dayanımı yaklaşık 4 MPa civarında olduğu için eksenel basınç yükü 0,3 MPa alınmıştır. Tijlere bağlı bulonlar sıkılarak çelik plakaların hareketiyle eksenel basınç yük verilmektedir. Yük hücresinde okunan eksenel yük seviyesi istenen noktaya geldiğinde bulonlar sabitleştirilip, deney düzeneğinin üst kısmına bir adet hidrolik pompa ve üzerine 50 ton kapasiteli bir yük hücresi konularak kayma yükü verilmektedir.

Şekil 2. Deney Düzeneği

Bağlantı elemanı olarak kullanılan kenetlerin, yığma taş blokların davranışına etkisini incelemek amacıyla batma derinlikleri değişken olarak alınmıştır. 2 cm genişliğinde, 2 mm kalınlığındaki kenetin batma derinliği, 10x10x20 cm^3 ebatındaki taşın ortasından 1,2,3,4,5,6,7 cm alınarak her bir numuneden 3'er adet olmak üzere toplamda 21 adet numune teste tabii tutulmuştur. Deney numunesine yerleştirilen kenet elemanları, hidrolik pompa yardımı ile yukarıya doğru çekilerek maksimum kayma yükü elde edilmiştir.

Bulgular

Deney sonuçları grafik ve resimler ile karşılaştırmalı olarak sunulup, açıklanmıştır. Numunelerin deney öncesi ve deney sonrası resimleri Şekil 3'de gösterilmiştir.

(a)

(b)

(c)

Şekil 3. Numunelerin (a) Deney öncesi ve (b), (c) Deney sonrası hali

Farklı batma derinliğine sahip kenetlerden 21 adet yapılarak herbiri için ayrı ayrı Şekil 4'de gösterildiği gibi yük- zaman grafikleri çizilmiştir. Deney sırasında 1 cm ve 2 cm batma derinliği ile yapılan kenet elemanlarında sıyrılmalar gözlemlenmiştir ve bundan dolayı fazla yük taşıyamamışlardır. Şekil 4 ve Şekil 5 de görüldüğü gibi batma derinliği 1 cm ve 2 cm olan kenet elemanlarının taşıdığı yük diğer deney numunelerine göre düşük olup, sırası ile yaklaşık olarak ortalama 1,48 kN ve 2,33 kN değerindedir. Maksimum yük taşıyan, batma derinliği 6 cm olan deney numunesinin ortalama taşıdığı yük 3,31 kN'dur. 3 cm batma derinliğine sahip kenet ile yapılan testler sonucunda ortalama taşınan yük 2,75 kN olarak bulunmuştur. Batma derinliği 4 cm, 5 cm ve 7 cm olan kenet elemanları ile yapılan deneyler sonucunda ortalama taşıdıkları yük sırası ile 2,98 kN, 3,13 kN ve 3,22 kN olarak tespit edilmiştir. Batma derinlikleri 6 cm ve 7 cm olan kenetlerin ortalama taşıdığı yükler birbirine oldukça yakın çıkmıştır. Benzer şekilde 4 cm ve 5 cm batma derinliğine sahip olan kenet uygulamaları ile yapılan deney elemanları, birbirine oldukça yakın değerde yük taşımışlardır.

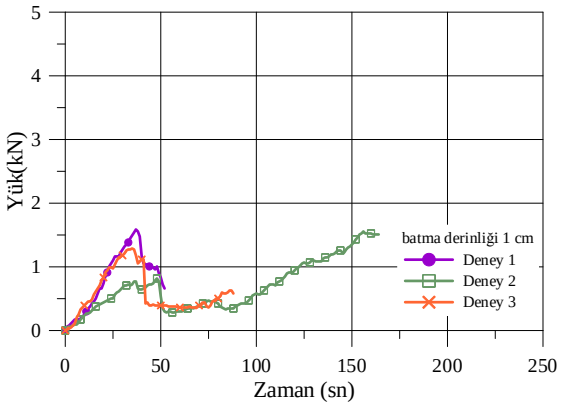

(a) 1 cm'lik numuneler

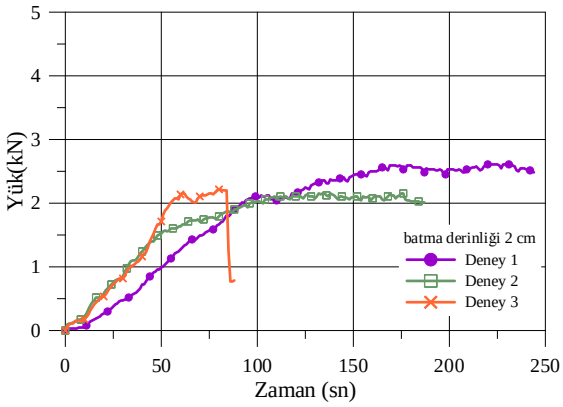

(b) 2 cm'lik numuneler

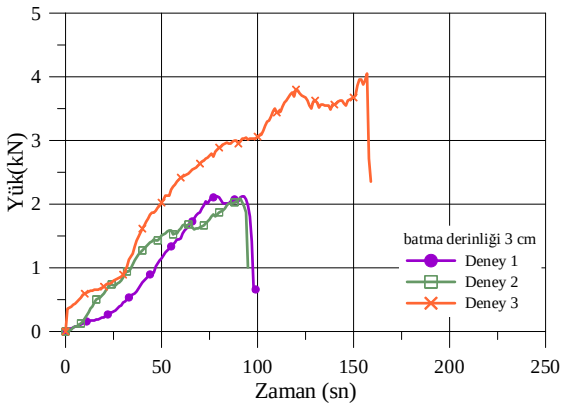

(c) 3 cm'lik numuneler

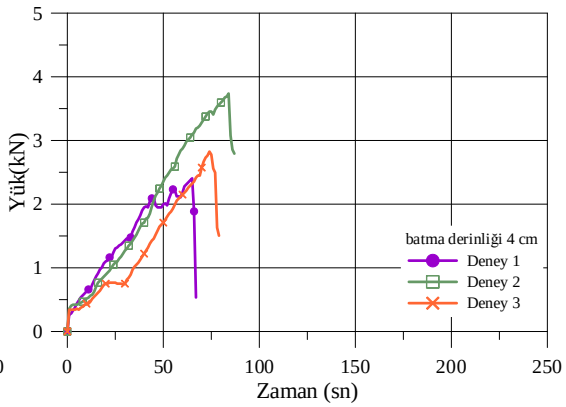

(d) 4 cm'lik numuneler

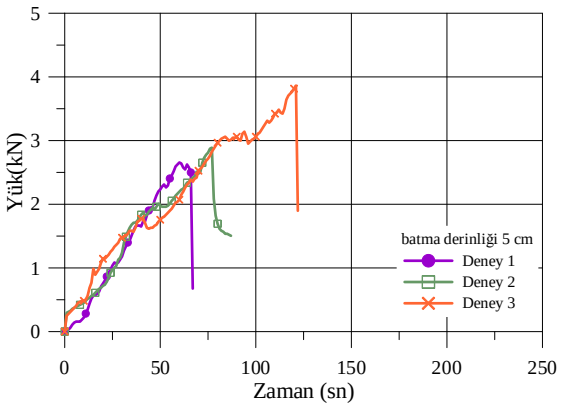

(e) 5 cm'lik numuneler

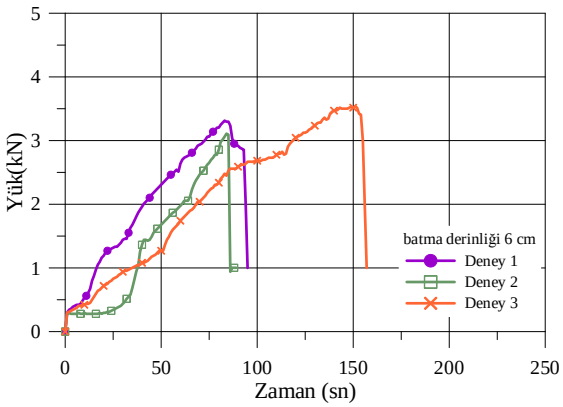

(f) 6 cm'lik numuneler

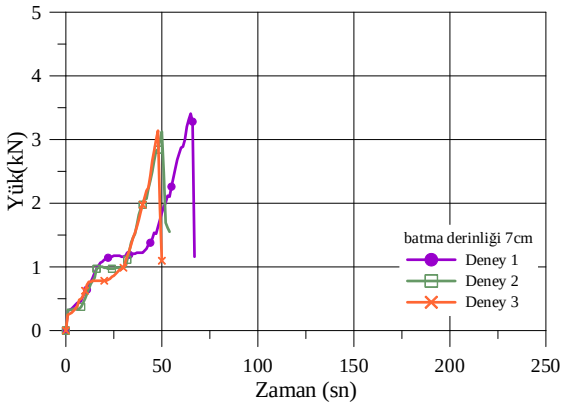

(g) 7 cm'lik numuneler

Şekil 4. Yük-Zaman Grafiği (a) 1 cm, (b) 2 cm, (c) 3 cm, (d) 4 cm, (e) 5 cm, (f) 6 cm, (g) 7 cm 'lik numuneler

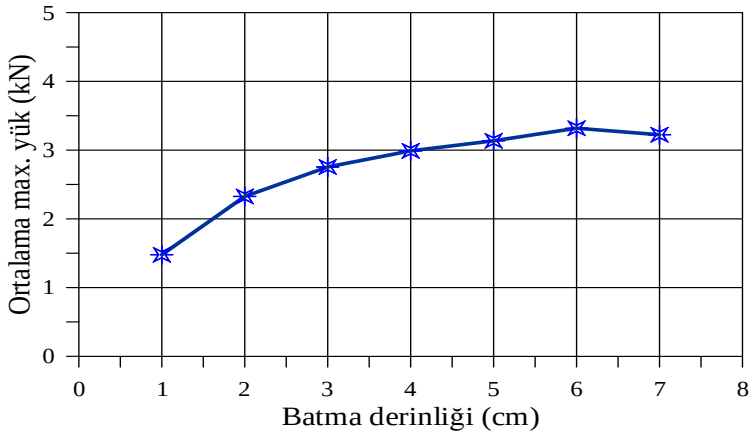

Şekil 5. Ortalama maksimum yük- batma derinliği grafiği

Tartışma ve Sonuçlar

Bu çalışmada metal bağlantı elemanı olarak kullanılan kenetlerin, yığma taş blokların davranışlarına etkisi deneysel metotlarla incelenmiştir. Batma derinliği değişken olarak alınan deneysel çalışmada her bir numuneden 3'er adet, toplamda 21 adet deney numunesi kayma testine tabi tutulmuştur. Aşağıda bu çalışmadan elde edilen sonuçlar maddeler halinde sıralanmıştır.

- Batma derinliği uygulanan yük ile orantılı olarak değişmektedir. Maksimum taşınan yük batma derinliği 6 cm olan deney elemanında görülürken, 7cm'lik kenet uygulaması yapılan numunelerde taşınan ortalama yükte azalmalar gözlenmiştir. Bunun nedeni, kenetin taşın üzerindeki etkidiği yüzey alanının azalmasından kaynaklanmaktadır.

- Kenetin batma derinliğinin 3 cm'den daha düşük olduğu numunelerde sıyrılmalar meydana gelmiştir. Bu sebeple minimum batma derinliğinin 3 cm olması sonucuna varılmıştır. Farklı taş numuneleri içinde benzer sonuçların elde edilebileceği düşünülmektedir.

- İleride bu çalışma daha da kapsamlı hale getirilebilir. Örneğin genişliği farklı metal bağlantı elemanlarının yığma duvarın kayma dayanımına etkisi araştırılabilir.

- Bu çalışma tarihi yapılarda özellikle restorasyon ve güçlendirme uygulamalarında iyi bir referans olarak bu konu üzerine yapılacak olan diğer bilimsel çalışmalara önemli bir katkı sağlaması beklenmektedir.

Kaynaklar

Demir, C. (2012). Seismic behaviour of historical stone masonry multi-leaf walls. Phd thesis, Istanbul Technical University, Graduate School of Science Engineering and Technology, Istanbul.

Koçak, Y. (2013). Yığma yapılarda kayma dayanımının artırılması amacıyla farklı bağlantı elemanı uygulamaları. Yüksek Lisans Tezi, Aksaray Üniversitesi, Fen Bilimleri Enstitüsü, Aksaray.

Kourkoulis, S.K., Pasiou, E.D. (2009). Epistyles connected with "I" connectors under pure shear. Journal of the Serbian Society for Computational Mechanics, 2, 2, 81- 99.

Kuşüzümü, K.H. (2010). İstanbul minareleri, restorasyon konservasyon arkeoloji ve sanat yıllığı. Vakıflar Genel Müdürlüğü, 1, 57-66.

Papadopoulos, K.A. (2006). The restoration study of the connections between the stone blocks in the steps of the temple of Apollo Epikourios. Proceedings of Structural Analysis of Historical Construction, Eds with D'Ayala & Fodde, New Delhi.

TS EN 1052-3, (2004). Kâgir-deney metodları-bölüm 3: Başlangıç kayma dayanımının tayini, Türk Standartları Enstitüsü, Ankara.

TS EN 772-1, (2012). Kâgir birimler-deney yöntemleri-bölüm 1: Basınç dayanımının tayini, Türk Standartları Enstitüsü, Ankara.

TS EN 772-6, (2004). Kâgir birimler-deney metotları-bölüm 6: Beton kâgir birimlerin eğilmede çekme dayanımının tayini, Türk Standartları Enstitüsü, Ankara.

TS EN ISO 6892-1, (2004). Metalik malzemeler-çekme deneyi-bölüm 1: Ortam sıcaklığında deney metodu, Türk Standartları Enstitüsü, Ankara.

Toumbakari, E.E. (2008). The Athens Parthenon: Analysis and interpretation of the structural failures in the ortho state of the northern wall. Proceedings of the Structural Analysis of Historical Construction, Eds with D'Ayala & Fodde, New Delhi.

Ural, A. (2017). Zıvana demirlerinin yığma duvarların kayma davranışına etkisinin incelenmesi. Uluslararası Katılımlı 6. Tarihi Yapıların Korunması ve Güçlendirilmesi Sempozyumu, Trabzon.

Uslu, S. (2013). Tarihi yığma yapılarda kullanılan metal bağlantı elemanlarının deneysel metotlarda incelenmesi. Yüksek Lisans Tezi, Aksaray Üniversitesi, Fen Bilimleri Enstitüsü, Aksaray.

International Conference on Science and Technology

ICONST 2018

5-9 September 2018 Prizren - KOSOVO

Investigation of Antioxidant Resistance in Walnut Oil Emulsions by ''Area Under Curve'' Method

Temel Kan BAKIR[1]*

Abstract: The area under curve (AUC) approach is the first quantitative method to measure the antioxidant protection against lipid oxidation in a slightly different order than the antioxidative activity from the reductive analyzes due to interface effects. In this study, peroxidation kinetics of walnut oil emulsion was performed using a new method of AUC approximation based on Fe(III)- thiocyanate and TBARS colorimetry. In copper-catalyzed walnut oil emulsions aerated at 37 ° C and pH 7, the absorbance values obtained as a function of the incubation time gave sigmoidal curves and the formation of oxidation products followed a pseudo first order kinetic. In addition, the area under the kinetic curves obtained by the addition of gallic acid at different concentrations to walnut oil was calculated and used for the Net AUC ($AUC_{sample} - AUC_{blank}$) values. The results were expressed as inhibition (%) according to Fe (III) SCN and TBARS methods. For both methods, walnut oil oxidation was observed to be reduced by the addition of 5, 10, 20, 40 and 80 µM gallic acid. The equations of the curves obtained with net AUC against concentration were $y = 1.61x10^6c + 106.06$ for Fe (III) SCN method and $y = 0.37x10^6c + 13.12$ for TBARS method. Pseudo first order kinetic equation and AUC method were used comparatively in evaluating the results. Both methods confirmed that the rate of oxidation was reduced in antioxidant-added walnut oil. These results show that the AUC approach is a successful method that can be easily adapted to analytical methods and measure antioxidant protection against lipid oxidation.

Keywords: Area under curve (AUC) method, Ferric Thiocyanate Method, TBARS Method, Walnut Oil, Lipid peroxidation kinetics

Introduction

Oils and fats, which are essential fatty acid sources, are an important part of the human diet (Rohman et al.,2011). While some vegetable oils are rich in monounsaturated fat-rich fatty acid compounds, they play a role in the prevention of many diseases and also contain antioxidants that prevent the attack of free radicals (Aguilera et al.,2003).The positive health effects of some vegetable oils are due to fatty acid-rich mono-unsaturated fatty acids. This is due to antioxidants that prevent the attack of free radicals and biomolecules by various mechanisms (Ramadan et al., 2006; Tripoli et al., 2005). Bipin and Jong-Bang reported that walnut oil contains linoleic acid and antioxidants in high amounts and contributes to reducing the risk of hypertriglyceridemia due to its extraordinary nutritional value (Vaidya and Eun, 2013). The effect of free radical scavenging of walnut, peanut, hazelnut and almond oils, was studied a lot of times with DPPH (2,2-diphenyl-1-picrylhydrazyl) method by using different solvents such as ethyl acetate or hexane / ethyl acetate (Li et al.,2007; Arranz et al.,2008) .

Especially walnut oil is highly susceptible to oxidation due to high levels of polyunsaturated fatty acids. This is why oil oxidation destroys the chemical, nutritional properties and reduces the storage life. Lipid oxidation is probably the most important factors affecting the shelf life of edible oils. The hydroperoxides produced by lipid oxidation can decompose into various smaller molecules such as aldehydes, ketones, alcohols, and carboxylic acids (Rohman et al.,2011). Unrefined oils, like natural antioxidants, may contain many health-

[1] Kastamonu University, Faculty of Science and Letters, Department of Chemistry, 37150, Kastamonu, TURKEY
*Corresponding author: temelkan@kastamonu.edu.tr, temelkan@hotmail.com

promoting supplements. Some free fatty acids and pro-oxidants such as hydroperoxides, or tocopherols, phenols and possibly other substances may act as antioxidants, possibly containing phospholipids. Nutritionally important antioxidants, such as tocopherols and carotenoids, often increase fat stability and therefore naturally rich oils are preferred (Miraliakbari and Shahidi, 2008).

In this study, it was aimed to measure the antioxidant protection against lipid oxidation by the area under the curve (AUC) method, a new quantitative approach to gallic acid availability of copper catalysed walnut oil aerated at 37 ° C and pH 7.

Materials And Methods

Chemicals which were analytical grade provided from Sigma-Aldrich Co. LLC. and the walnut oil was bought fresh from Doğavita Pharmaceutical Food Industry and Trade Co. (Çiftcizade, Turkey). In each stage deionized purity water was used. Absorbents was measured using a SHIMADZU the UVM-1240 UV-Visible spectrophotometer (Shimadzu Corp.,Kyoto, Japan manufactures) and The pH measurements were made using a Metrohm 632 Digital pH-meter (Metrohm AG, CH-9100 Herisau, Switzerland). All the experiments were carried out at 37 ◦C by means of a thermostated system (±0.1 ◦C) which contained an immersion circulator (NUVE BM 30 Circulation Water Bank, Ankara, Turkey).

Analysis of oxidation products by using ferric thiocyanate and TBARS method

The production of hydroperoxides were analysed by using Fe(III)-SCN method. The primary oxidation grade was measured by sequentially adding ethanol (4.7 mL, 75% v/v), ammonium thiocyanate (0.1 mL, 30% w/v), sample solution (0.1 mL), and ferrous chloride (0.1 mL of 0.02 M in 3.5% v/v HCl). The Fe(III)-SCN complex was determined at 500 nm and peroxide concentration was analysed by reading against a blank containing identical components without walnut emulsion (Bakır et al.,2013).

The secondary oxidation products, symbolized as malondialdehyde (MDA), were analysed by using TBARS method. For these measurements, 0.1 mL sample solution was transferred to test tubes containing 0.15 mL of trichloroacetic acid (TCA, 2.8%), 0.1 mL of thiobarbituric acid (TBA, 1%) and 2.65 mL of distilled water to make a total volume of 3 mL was added. The mixture was stored for 15 min in a water bath at 95-100 °C and then cooled in an ice bath for 5 min. The absorbance was measured against the control blanks at 532 nm (Ohkawa et al.,1979).

Measurement of lipid oxidation kinetic

Lipid peroxidation can be explained kinetically by monitoring the formation of primer and secondary products. From a general point of view, reaction rates were calculated (k) by observing the so-called first-order reactions. Lipid peroxidation can be explained kinetically by monitoring the formation of primer and secondary products. As a general overview, the reaction rates (k) were given by observing the pseudo-first order reactions (Bakır et al.,2014). The equation (1) proposed by Yıloğan-Beker *et al.* (2011) allows the kinetic evaluation of the primary and secondary products of walnut oil oxidation.

$$\mathrm{Ln}\left(\frac{1-A_t}{A_t}\right) = \mathrm{Ln}\left(\frac{1-A_0}{A_0}\right) - k.t \qquad (1)$$

Here, A_0 is the initial absorbance, A_t is the absorbance at time (t) proportional to the total concentration of hydroperoxides or aldehydes measured by ferric-thiocyanate (Fe(III)-SCN) and TBARS colorimetric methods, respectively.

Preparation of emulsion system solution walnut oil emulsions and antioxidant solutions were prepared freshly every day and all other solutions stored at degree of 4 ºC. Walnut oil emulsion was prepared by mixing 0.3 gram walnut oil with 3 mL (Tween 80 + Span 80, HLB: 10) system. Then, the emulsion was slowly homogenized by adding 90 mL of NH_4Ac (1M, pH = 7) buffer solution.

Statistical analysis

All experiments were performed in triplicate and the statistical analyses were investigated using MICROCAL ORIGIN 8.5.1 (Origin Lab Corp., Northampton, MA, USA) for calculating the final AUC values.

Results

In this study lipid oxidation was monitored by recording the absorbance against time. Formation of primary products (hydroperoxides) Fe (III) - thiocyanate method and secondary products (aldehyde, ketone, etc.) were investigated by TBARS method. The absorbance changes measured by both methods as a function of the incubation time showed sigmoidal curves depending on the gallic acid concentrations(Figure 1 ve 2).

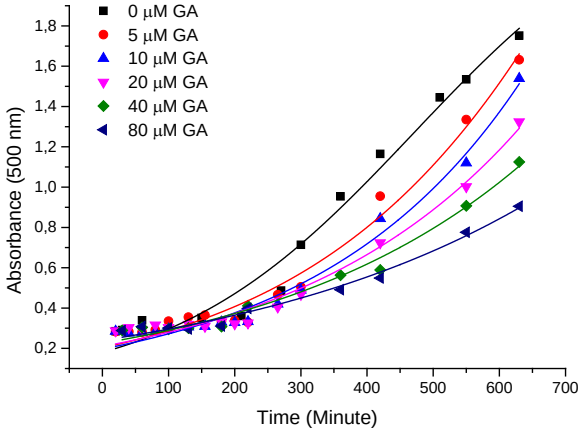

Figure 1. Changes in absorbance over time in walnut oil oxidation system for gallic acid (GA) measured by Fe(III)-SCN method.

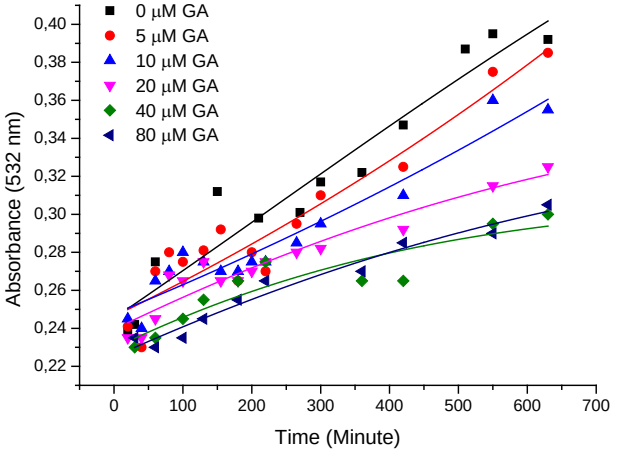

Figure 2. Changes in absorbance over time in walnut oil oxidation system for gallic acid (GA) measured by TBARS method

The formation of primary and secondary oxidation products from the walnut oil-Cu (II) system followed the pseudo-first order kinetic. The calculated rate constants for both methods are given in Table 1. According to this, it was observed that the rate constants of primer and secondary product occurrences decrease with increasing gallic acid concentration, but not regular order.

Table 1. The effect of gallic acid on the rate constants of primary and secondary oxidation products formation from walnut oil–Cu(II) system.

	Fe(III)SCN Method		TBARS Method	
GA Conc. (μM)	$k \pm S_k$ (min $^{-1}$) x 10^{-2}	R^2	$k \pm S_k$ (min $^{-1}$) x 10^{-2}	R^2
0	0.85±0.24	0.620	0.12±0.01	0.919
5	0.75±0.16	0.637	0.10±0.01	0.880
10	0.54±0.10	0.724	0.08±0.007	0.910
20	0.39±0.07	0.730	0.06±0.006	0.875
40	0.55±0.08	0.844	0.05±0.008	0.803
80	0.48±0.06	0.890	0.06±0.005	0.947

k: pseudo-first order rate constant with respect to hydroperoxides formation (measured by Fe(III)-SCN and TBARS method).

The results were expressed as inhibition (%) according to Fe (III) SCN and TBARS methods. For both methods, walnut oil oxidation was observed to be reduced by the addition of 5, 10, 20, 40 and 80 μM gallic acid (Figure 3).

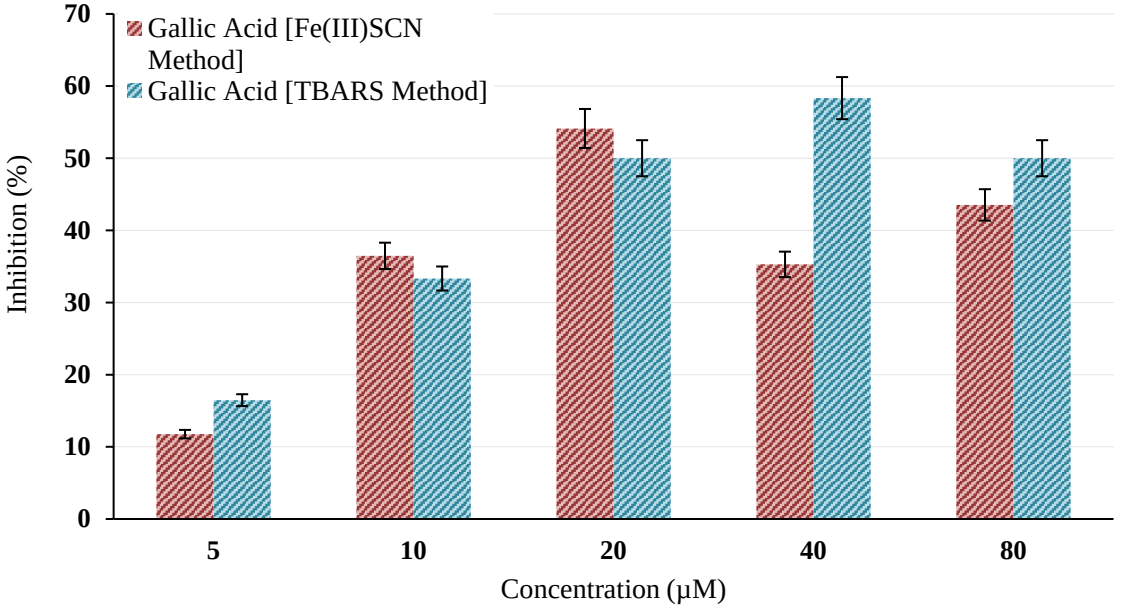

Figure 3. Inhibition (%) of walnut oil autoxidation induced by Cu(II) (as measured by the Fe(III)-SCN and TBARS assays) as a function of differant gallic acid concentrations. The calculated results are given as mean % 95 confidence interval.

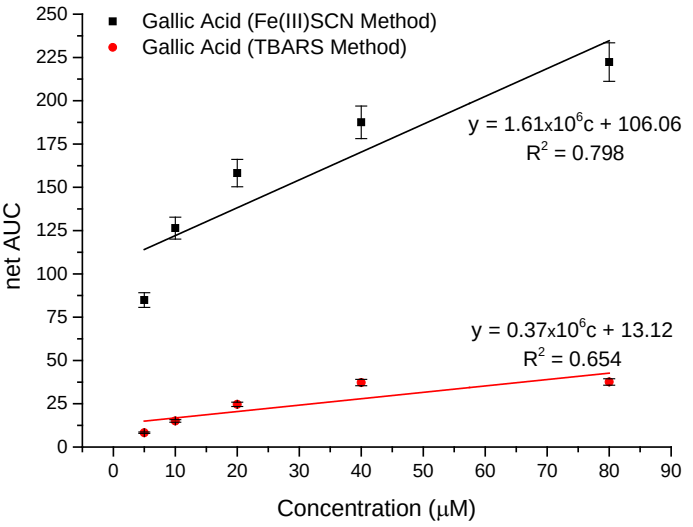

Figure 4. Net AUC versus concentration of Gallic Acid (GA) in walnut oil oxidation induced by copper(II) and oxygen [measured by Fe(III)- SCN (a) and TBARS (b) assays]

In addition, from the absorbance/time curves, AUC values of antioxidants as a function of antioxidant concentration were found. The area under the kinetic curves obtained by the addition of gallic acid at different concentrations to walnut oil was calculated and used for the Net AUC (AUCsample – AUCblank) values (Figure 4). Standard calibration lines were obtained by plotting net AUC against the concentration of gallic acid (net AUC= ax ± b , where b is the intercept, a is the slope, and x is the concentration of antioxidant). The equations of the curves obtained with net AUC against concentration were $y = 1.61x10^6c + 106.06$ for Fe (III) SCN method and $y = 0.37x10^6c + 13.12$ for TBARS method.

Discussion

Many studies that have used the AUC approach earlier have been limited to the antioxidant capacity assays based on the TBARS method (Kerrihard et al.,2016; Schisterman et al.,2001). Monitoring of lipid oxidation products requires very complex and laborious work. Substance concentrations with protective antioxidant activity against lipid peroxidation can be defined both as a measure of the area under the absorbance time curves as well as in the thermodynamic sense of the kinetic lag time (Huang et al.,2005). The AUC method is an indication of the simultaneous measurement of thermodynamic quantities such as a measure of the area under the absorbance time curves and a lag time (Bakır et al.,2017).

In this study, antioxidant protection was measured using gallic acid in walnut oil oxidation. The results were evaluated with reaction kinetics and the area under curve approach (AUC). Oxidation studies on walnut oil and similar oils have been made by many researchers for a long time (Miraliakbari and Shahidi, 2008; Crowe and White, 2003; Beveridge et al.,2005; Lutterodt et al.,2011). To the best of our knowledge, studies investigating antioxidant behavior in a walnut oil emulsion environment are very limited. However, walnut oil has been studied in oxidation studies like many industrial oils. Bipin and Jong Bang reported that secondary oxidation products formed by the decomposition of p-anisidine (p-AV) and hydroperoxides of walnut oil increased mainly due to the formation of aldehydes in oil as the oxidation duration and temperature increased (Vaidya and Eun, 2013).

Jianhua Yi *et al.* observed the formation times of primary and secondary oxidation products in the walnut oil emulsion system by examining the change of free fatty acids. As a result, they have reported that unsaturated fatty acids are effective in the formation of oxidation products (Yi et al., 2013). In our work, we preferred to use walnut oil in order to shorten the oxidation time and to make it easy to follow. These studies in the

emulsion environment can be followed by individual evaluation of each fatty acid. However, lipid oxidation makes it difficult to assess the reaction rates separately and to monitor the activity of antioxidant in the whole fat emulsion environment, because it is a complex reaction. Nevertheless, the AUC approach enables the assessment of antioxidant activity by monitoring the initiation, propagation and termination stages of lipid oxidation. The pseudo-first order kinetic equation and the AUC method were used comparatively to evaluate the results in our study. Both methods confirmed that the oxidation rate in walnut oil added with antioxidant decreased. These results demonstrate that the AUC approach is a successful method that can be readily adapted to analytical methods and can detect antioxidant protection against lipid oxidation.

Acknowledgements

The author gratefully acknowledge to Kastamonu University Center Research Laboratory and Doğavita İlaç Gıda Sanayi ve Ticaret A.Ş. (Çiftcizade, Türkiye) for the technical assistance and the oil used.

References

Aguilera, C. M., Mesa, M. D., Ramírez-Tortosa, M. C., Nestares, M. T., Ros, E. and Gil, A. (2003) Sunflower oil does not protect against LDL oxidation as virgin olive oil does in patients with peripheral vascular disease. Clinical Nutrition. 23, 673–681.

Arranz S., Cert R., Pérez-Jiménez J., Cert A. and Saura-Calixto F. (2008) Comparison between free radical scavenging capacity and oxidative stability of nut oils.Food Chemistry. 110, 985–990.

Bakır, T., Sönmezoğlu, İ., İmer, F. and Apak, R. (2013) Polar paradox revisited: analogous pairs of hydrophilic and lipophilic antioxidants in linoleic acid emulsion containing Cu(II). J Sci Food Agric. 93, 2478–2485.

Bakır, T., Sönmezoğlu, İ., İmer, F. and Apak, R. (2014) Antioxidant/prooxidant effects of a-tocopherol, quercetin and isorhamnetin on linoleic acid peroxidation induced by Cu(II) and H2O2. Int J Food Sci Nutr. 65(2), 226–234.

Bakır, T., Sönmezoglu, I. and Apak, R. (2017) Quantification of Antioxidant Ability Against Lipid Peroxidation with an 'Area Under Curve' Approach. Am Oil Chem Soc. 94,77– 88.

Beveridge, T.H.J., Girard, B., Kopp, T. and Drover, J.C.G. (2005) Yield and composition of grape seed oils extracted by supercritical carbon dioxide and petroleum ether: Varietal effects. J. Agr. Food Chem. 53,1799-1804.

Crowe, T.D. and White, P.J. (2003) Oxidative Stability of Walnut Oils Extracted with Supercritical Carbon Dioxide. Journal of the American Oil Chemists' Society. 80,575-577.

Huang, D., Ou, B. and Prior, R.L. (2005) The chemistry behind antioxidant capacity assays. J Agric Food Chem. 53,1841- 56.

Kerrihard, A.L., Nagy, K., Craft, B.D. and Pegg, R.B. (2016) Correlations among differing quantitative definitions of lipid oxidative stability in commodity fats and oils. European J Lipid Sci and Tech. 118(5):724-734.

Li, L., Rong, T., Yang, Y., Kramer, J. K. G. and Hernández, M. (2007) Fatty acid profiles, tocopherol contents and antioxidant activities of hearnut (Juglans ailanthifolia Var cordiformis) and Persian walnut (Juglans regia L.). Journal of Agricultural and Food Chemistry. 55, 1164–1169.

Lutterodt, H., Slavin, M., Whent, M., Turner, E. and Yu, L. (2011) Fatty acid composition, oxidative stability, antioxidant, and antiproliferative properties of selected cold-pressed grape seed oils and flours. Food Chem. 128, 391-399.

Miraliakbari, H. and Shahidi, F. (2008) Antioxidant activity of minor components of tree nut oils. Food Chemistry. 111,421–427.

Miraliakbari, H. and Shahidi, F. (2008) Oxidative Stability of Tree Nut Oils. J.Agric. Food Chem. 56,4751–4759.

Ohkawa H., Ohishı N. and Tagi K. (1979) Assay for Lipid Peroxides in Animal Tissues by Thiobarbituric Acid Reaction. Anal Biochem. 95, 351-358.

Ramadan, M. F. and Moersel, J. T. (2006) Screening of the antiradical action of vegetable oils. Journal of Food Composition and Analysis. 19, 838–842.

Rohman, A., Che Man, Y. B., Ismail, A. and Hashim, P. (2011) Monitoring the oxidative stability of virgin coconut oil during oven test using chemical indexes and FTIR spectroscopy. International Food Research Journal. 18,303-310.

Schisterman, E.F., Faraggi, D., Browne, R., Freudenheim, J., Dorn, J., Muti, P., Armstrong, D., Reiser, B. and Trevisan, M. (2001) TBARS and cardiovascular disease in a population-based sample. J Cardiovascular Risk. 8(4):219-225.

Tripoli, E., Giammanco, M., Tabacchi, G., Di Majo, D., Giammanco, S. and La Guardia, M. (2005) The phenolic compounds of olive oil: Structure, biological activity and beneficial effects on human health. Nutrition Research Reviews. 18, 98–112.

Vaidya, B. and Eun J.B. (2013) Effect of Temperature on Oxidation Kinetics of Walnut and Grape Seed Oil. Food Sci. Biotechnol. 22: 273-279.

Yıldoğan-Beker, B., Bakır, T., Sonmezoğlu, İ., İmer, F. and Apak, R. (2011) Antioxidant protective effect of flavonoids on linoleic acid peroxidation induced by copper(II)/ascorbic acid system. Chem Phys Lipids. 164, 732-739.

Yi, J., Zhu, Z., Dong, W., David Julian McClements, D.J. and Decker, E.A. (2013) Influence of free fatty acids on oxidative stability in water-in-walnut oil emulsions. Eur. J. Lipid Sci. Technol. 115,1013–1020.

International Conference on Science and Technology

ICONST 2018

5-9 September 2018 Prizren - KOSOVO

Measurement Of Work Safety And Occupational Health Perceptions of Chemical Sector Employes

Mustafa Karaboyacı[1]*, Hamza Kandemir[2], Egemen Uysal[3]

Abstract: Occupational accidents that occur in working life is the one of the major problems of working life. Today, despite many developments in the field of occupational health and safety, occupational accident statistics are still high. A safe and healthy working environment by providing occupational health and safety practices, plays an important role in the prevention of occupational accidents, increasing operational productivity and profitability, promotion of corporate image, customer satisfaction and employees to feel good about themselves in the physical and spiritual aspects.

Chemical industry is accepted as a risky sector in terms of occupational health and safety. For this reason, if the necessary corrective and preventive actions are taken, it helps not only strengthen the workers health and safety conditions but also prevents economic losses due to the temporary and permanent workforce loss or deadly work accidents, improving productivity. For this reason, enterprises performance of occupational health and safety performance measures helps to collect information on the current status or success of business health and safety-related strategies and activities. The scientific criteria for measuring these performances are summarized within the scope of this study.

Keywords: Worker's Health, Job Safety, Job Safety Culture, Job Safety Performance, Risk Analysis

1. Introduction

The human factor which are the most important source of enterprices exposed to occupational accidents and occupational diseases, and that has led to the development of various practices and strategies on occupational health and safety. Although nowadays there are many developments in the area of occupational health and safety, but occupational accident statistics are still high. Therefore, it needs to focus more and more on occupational health and safety all over the world and develop new strategies (Alli, 2008). Nowadays, the enterprises implement the practices related to occupational health and safety in accordance with the legal regulations of the country in which they operate in accordance with various standards or models. The main legal regulation on occupational health and safety in Turkish Labor Law is the OHS Law No. 6331. According to article 4 of Law No. 6331. the employer should monitor compliance with occupational health and safety measures and ensure that any non-conformities are eliminated. According to this provision, the employer's obligation not only consists of taking precautions, but also consistently monitoring, controlling and supervising whether the employees comply with the legislation and the occupational health and safety regulations laid down in the workplace. This monitoring process can be done by various methods and tools. In the law or regulations, it is not clear how to perform this monitoring task, and has been given flexibility to the employer in this regard. Within this framework, the development of the occupational health and safety performance scale may be an important tool to help the employer to fulfill its monitoring and audit obligation

[1]Suleyman Demirel University, Faculty of Engineering, Chemical Eng. Dpt. 32260, Isparta, TURKEY
[2]Isparta University of Applied Sciences, Atabey Vocational High School, Isparta, TURKEY
[3]Suleyman Demirel University, Faculty of Engineering, Chemical Eng. Dpt. 32260, Isparta, TURKEY
*Correspondingauthor: mustafakaraboyaci@sdu.edu.tr

(Üngören and Koç, 2015). Occupational health and safety, which has become more important with each passing day and has become a determinant of the country's development levels, is defined as systematic work to protect workers from work accidents and occupational diseases and to provide them with a healthy and safe working environment (Tozkoparan and Taşoğlu, 2011). There are two concepts that are frequently used in daily life at the base of occupational health and safety. These concepts are health and safety. Health as word meaning; expresses the state of being completely physical, spiritual and social (Larson, 1996). It is not a correct approach to express the concept of health as the absence of pathological findings. As seen in the definition above, the psychological and social aspects of human being are evaluated within the concept of health. Health is the most important element necessary for the continuation of life and is one of the fundamental rights to be protected within the legal system (Susser, 1993). Another concept that is at the base of occupational health and safety is security. Security can describe as "being in a safe" or "being away from danger" (Harms-Ringdahl, 2005). More precisely, the individual or social well-being, whether by being away from any physical, spiritual, material and spiritual dangers or keeping them under control, constitutes the definition of security (Maurice et al., 2001: 238).

It is almost impossible to find a workplace where there are no chemical factors in the business world. This could be a car repair shop with old oils, a carpentry workshop using paints, a chemical production facility, or an office which including toner powder. In all these establishments, the health of workers should be guaranteed. Millions of different products are produced for daily use from the known average of 100,000 chemicals. Many of the chemical products are used in many different processes in order to achieve the most appropriate effect of the substances according to their usage areas. In this way, the paint can be applied to the material by hand brush, or sprayed. The redundancy and use of products raises a fundamental question in this context. What kind of necessary regulation and condition should be presented to determine the appropriate measure for the responsible employer and supervisor. Chemicals exposed to workplaces and routes of transmission to the body come into contact with the human body through breathing, absorption (skin or eye) and digestive systems. Accordingly, these routes of transmission should be considered and necessary measures taken. In this way, not only the organs infected which are exposed directly from chemicals, the organs that are not exposed directly from this chemicals can be infected. Also through the placenta can pass to the baby in the womb. When chemicals enter the body they can cause local or systemic effects (if they pass into the bloodstream and thus distribute all parts of the body). The toxic effects of chemicals are not the same in all organs. Usually they affect 1-2 organs. These organs, which show the toxic effects of chemicals, are defined as the target organ. Various factors affect occupational diseases in the chemical industry. These are economic factors, technologies (low automation, batch production), business plan, environmental conditions and human factor. Technological advances in the chemical industry cause increase in productivity, decrease in occupational diseases and increase working safety (Fabiano et al., 2010).

Diseases that are caused by chemicals, physical agents and biological factors that are harmful to human health in the workplace are called occupational diseases. Chemical factors are the most common factors among the workplace environment factors. The number of chemicals used in various work sectors are very high. These substances are dangerous for human health and cause various occupational diseases. Heavy metals (lead, mercury, arsenic, cadmium, chromium and aluminum etc.), solvents (benzene, toluene, hexane, trichlorethylene, etc.), toxic gases (carbon monoxide, methane, sulfurous hydrogen, hydrogen cyanide, etc.), pesticides (organic phosphorous compounds, arsenic compounds, chlorinated hydrocarbons, etc.), acid and alkaline substances seems to cause discomfort such as dependence, behavioral disorder, toxicologic. Physical factors such as temperature, noise, radiation, vibration and pressure cause musculoskeletal disorders. It is seen that some chemicals that irritate the respiratory tract cause asthma and lung disease, and that the substance called silica (SiO2) settles into the lungs, resulting in the occurrence of silicosis, a type of lung disease. It is also seen that some toxic chemicals such as asbestos used in the chemical industry cause lung, stomach, intestine, larynx cancers and cancer disease called mesothelioma. The substances used in the chemical industry such as mercury vaporize and cause industrial poisoning, benzene leads to blood cancer. Diseases caused by chemical substances include anemia, liver and kidney disorders. It is seen that organic solvents used in the chemical industry create damage in the functional units of the central nervous system, liver and blood of the workers. In the chemical industry, headache, fatigue (weakness), skin problems and burns, eye irritation are seen. And also, lung and skin are the main organs of occupational diseases in chemical industry workers. It has been observed that compounds such as carbon disulfide and organic

nitrogen used in the chemical industry affect the cardiovascular system and blood pressure. Carbon monoxide is strongly induced in cardiac spasm (Stellman and Ilo, 1998). Chemical vapors and gases enter the body through inhalation and these vapours and gases mix with blood and accumulates in the organs, damages the organs and causing poisoning. These toxic substances appear to adversely affect the digestive system, lungs and pancreas (Stellman and Ilo, 1998). Solvents are typical substances that cause acute effects. These affect the body in a short time and often have a short duration. However, the solvents have both acute and chronic effects on the nervous system. Chronic exposure is caused by prolonged exposure to hazardous substances. Lung disease called asbestosis is an example of chronic disease. Examples of pneumoconiosis occupational disease caused by accumulation of chronic dust in the lungs includes silicosis that caused by quartz powder and asbestosis that caused by asbestos dust. Silicosis disease is observed in patients exposed to quartz dust for a long time. This disease manifests itself in the difficulty of breathing due to damage to lung tissue over time. Zinc and some other metals are known to cause metal gas fever when inhaled in large quantities (ISAG, 2006). Chemical gases are examples of chlorine and sulfur dioxide irritant gases. Their high concentration in the air can damage the lungs. One of the most common health risks in working life is caused by vapors and solvents. Many metal and metal alloys are used in the chemical industry. Lead and mercury vapors can easily condense in the air when these metals heated. When these metals are absorbed in the body for a period of time, it appears to cause lead or mercury poisoning and also damage the nervous system. Chromium, cobalt and nickel are examples of other dangerous metals. These metals cause respiratory diseases and cancer. Some chromium and nickel alloys pass into the blood through the lungs and cause damage to the internal organs and allergies (ISAG, 2006).

Necessary importance should be given to occupational diseases. Unless this importance is given, both labor force loss and inefficient working conditions will make production difficult. Occupational diseases can be prevented by measures to be taken in the workplace environment. In addition, in terms of worker health and work safety, the inspection and controls must be carried out continuously during the processing, transportation and storage of chemicals (Ayanoğlu, 2007). Health acts as a driving force in economic development. Because occupational diseases cause economic losses due to the health expenses of the people who work or because of the health expenses. There is an opposite relationship between occupational diseases and job performance. It is seen that organizations that invest in occupational disease and safety have increased productivity and have a stronger economy (Korkmaz, 2011). In addition to legal requirements, there are also risk analysis methods obtained by sectoral experiences in order to ensure the health safety of the employees of the chemical sector. Businesses can apply many methods to measure safety performance. This can be done by examining past accidents, observing employees safe behaviors and deficiencies of the system, measuring perceptions or observing employees at certain times.

Risk analysis methods are basically examined in two groups:

a) Qualitative Methods: The risk assessment is done verbally and the expert assesses the risks and risk priority values based on his / her own experience and intuition. When calculating the forecasted risk, descriptive values such as high and very high are used instead of numerical values. This prediction is entirely based on subjective evaluations and often does not show a systematic quality. In such methods, the intuition and reasoning ability of the evaluating expert is important for the reliability of the method. Therefore, it is not correct to make a risk assessment in qualitative systems only by qualitative methods (Uslu, 2014).

b) Quantitative Methods: Numerical values are used in the definition and calculation of risks. In addition to simple techniques such as probability and reliability theorems, complex techniques such as simulation models are used in the calculation of these numerical values (Uslu, 2014).

In the risk analysis:
(Preliminary Hazard Analysis (PHA)
Hazard and Operability Studies (HAZOP)
Failure mode and effects analysis (FMEA)
Fault tree analysis (FTA)
Job safety analysis (JSA)
Matrix method

Multivariate X type matrix method
Fine Kinney method, risk scoring method
“What If” Technique
Preliminary Risk Analysis (PRA)
Risk Assessment Checklist
Cause-Consequence Analysis
Event tree analysis (ETA)
Hazard analysis and critical control points (HACCP)
qualitative and quantitative methods are used.

Within the scope of the risk analysis process, persons related to the subject such as workers, engineers, department managers, factory managers should be informed about the identified risk and the measures to be taken. The prevention of occupational accidents by electrical, chemical and mechanical controls requires an engineering approach, but identifying sources of danger in terms of work-related health problems and occupational diseases, and assessing risks require physician sensitivity and preventive medicine methodology. For this reason, employees who have knowledge about different subjects, who have experience in operations, managers, maintenance staff, health personnel etc. should be able to participate in the process (Akadam, 2010)

2. Material and Method

The population and sample of the study: The study was carried out on 102 employees at 4 factories in Denizli Organized Industrial Zone where chemical substances were used extensively. There are 128 companies operating in Denizli OIZ, 176 firms operating in construction, interrupting production, and firms in construction. The region is leading in textile production in Turkey. Scale of study:

Scale of study:
The scale which is improved by Üngüren and Koç (2015) at their "Occupational Health and Safety Application Performance Evaluation Scale: Validity and Reliability Study" was used as a data collection tool.

In this study, the scale was developed by adding the globally accepted rules of the chemical industry in terms of worker health and safety, taking into account the dimensions of the scale to measure the occupational health and occupational safety developed by Üngüren and Koç (2015).

The following questions were added to the"Administrative measures and precaution related to occupational health and safety" dimension. These questions include legal measures to be taken by management. The implementation of the measures will mean that the administration is aware of the situation and applies them.

These questions are:
”In the factory where I work, we hang the material safety data sheets of chemicals next to chemicals.“
“The company I work in has a current inventory of chemicals.”
“At the factory where I work, the chemicals are labeled according to the regulations.”

Following question is added to the "Employees works according to occupational health and safety criteria" dimension.

“When workers see a new chemical in the company where I work in, they examine the safety data sheet and labels.”

Because this attitude is a behavior that workers who work in accordance with occupational health and safety criteria should naturally do. The answers to this question will show employess occupational safety consciousness levels and and whether they work in accordance with this consciousness.

Following question were adeed to the “Awareness and consciousness about occupational health and safety of employees”dimension.

"When in contact with chemicals, I use protective clothing and equipment according to the hazard symbols on it."

"Before working with a chemical, I check the symbols on the label."

"I know the meaning of the R and S phrases on the labels of chemicals, if I do not know, I will learn from the authorities."

Following question were added to the "Occupational health and safety training practices" dimension.

"In the company I work with, employees are informed about the hazards and safe use of chemicals."

"Employees are trained about the meanings of the R and S phrases and the hazard symbols in the company I work."

The first question was asked to understand whether there was a real training in the company. In the second question, only those persons who are trained in this subject can know what the R and S phrases and hazardous symbols are. So this is the verifier of the first question.

Following question were added to the "Collaboration and communication between management and employees on occupational health and safety" dimension.

"When working with chemicals in the factory, there are strict measures on the use of protective clothing and equipment."

"Instead of chemicals that have high risks for the employees, if possible it is preferable that have less risky ones."

The first question was asked to understand how much care is given to the safety of the workers. This question was raised because the managers, who care about their workers and who have strong communication with them, tend to use the least risky chemicals.

Statistical Analysis: Data analysis of the study was done by using SPSS 22. package program. Descriptive and descriptive statistical analyzes were applied to the data. Applied analyzes are single and multiple ANOVA, POST HOC tests, t tests.

3. Results and Discussion

The frequency distribution of the demographic variables of the study is given in Table 1 below.

Table 1: Demographic Variables Frequency Distribution

Graduation	***n***	***%***
High School	68	%68
Associate degree	17	%17
Bachelor degree	12	%12
Graduate	3	%3
Total		
Work experience	***n***	***%***
0-1 years	9	%9
2-5 years	13	%13
6-10 years	24	%24
11 years and more	54	%54

Age range	*n*	*%*
18-24	13	%13
25-31	23	%23
32-38	30	%30
39-45	24	%24
46-52	9	%9
53-59	1	%1

Work Experience at Present Job	*n*	*%*
0-2 years	20	%20
2-5 years	31	%31
6-10 years	20	%20
11 years and more	29	%29

Gender	*n*	*%*
Female	25	%25
Male	75	%75

The firms in which the research is conducted have more than 10 years of activity in the sector. Firms are big companies according to Denizli sector scale. 22 out of 124 questionnaires were excluded from the analysis because, they were not able to use. When Table 1 is interpreted, the ratio of high school graduates is quite high, (68%) in terms of education level of chemical workers. The proportion of those working in the sector with a total work experience of more than 11 years (54%) is higher than the others. In terms of total work experience, it can be said that experienced employees are more intense. The percentage of employees in the 25-45 age group is 77%. This age range can be interpreted as a dynamic time frame where employees are most efficient. This is an advantageous view of the sector. In terms of work experience in the present companies, those who are between 2-5 years are at the highest level with 31%. In terms of gender distribution, there is a male dominated structure (75%) is seen in the chemical sector.

The statements in the questionnaire form consist of 5 factors. These are :
"Administrative measures and precaution related to occupational health and safety"
"Employees works according to occupational health and safety criteria"
“Awareness and consciousness about occupational health and safety of employees”
“Occupational health and safety training practices”
“Collaboration and communication between management and employees on occupational health and safety”

There are 41 statements in the questionnaire. Difference tests, (One Way Anova and T-test) were performed between demographic variables and dimensions. As a result of the analyzes, a significant difference was found between the awareness and consciousness of the employees about occupational health and safety with total work experience. It is statistically significant that the level of awareness and consciousness between the workers which have 2-5 years work experience is higher than those of 11 and more. Table 2 shows the difference between groups with POST HOC (LSD and Games Howell) tests.

Table 2. POST HOC (LSD and Games Howell) tests and difference between the groups in the size variable of occupational health and safety training practices.

Multiple Comparisons Dependent Variable: Awareness	(I) Total Work Experience	(J) Total Work Experience	Mean Difference (I-J)	Std. Error	Sig.	95% Confidence Interval	
						Lower Bound	Upper Bound
LSD	1	2	-0.47388	0.28909	0.104	-1.0477	0.0999
		3	-0.12346	0.26058	0.637	-0.6407	0.3938
		4	0.03909	0.24003	0.871	-0.4374	0.5155
	2	1	0.47388	0.28909	0.104	-0.0999	1.0477
		3	0.35043	0.22958	0.130	-0.1053	0.8061
		4	0.5129*	0.20596	0.014	0.1042	0.9218
	3	1	0.12346	0.26058	0.637	-0.3938	0.6407
		2	-0.35043	0.22958	0.130	-0.8061	0.1053
		4	0.16255	0.16355	0.323	-0.1621	0.4872
	4	1	-0.03909	0.24003	0.871	-0.5155	0.4374
		2	-0.51298*	0.20596	0.014	-0.9218	-0.1042
		3	-0.16255	0.16355	0.323	-0.4872	0.1621
Games-Howell	1	2	-0.47388	0.32576	0.491	-1.4329	0.4851
		3	-0.12346	0.30969	0.977	-1.0570	0.8101
		4	0.03909	0.30095	0.999	-0.8851	0.9633
	2	1	0.47388	0.32576	0.491	-0.4851	1.4329
		3	0.35043	0.19618	0.303	-0.1885	0.8893
		4	0.51298*	0.18207	0.046	0.0067	1.0193
	3	1	.12346	0.30969	0.977	-0.8101	1.0570
		2	-0.35043	0.19618	0.303	-0.8893	0.1885
		4	0.16255	0.15143	0.707	-0.2394	0.5645
	4	1	-0.03909	0.30095	0.999	-0.9633	0.8851
		2	-0.51298*	0.18207	0.046	-1.0193	-0.0067
		3	-0.16255	0.15143	0.707	-0.5645	0.2394
* The mean difference is significant at the 0.05 level.							

A significant difference was reached with the difference tests between the dimension of occupational health and safety and educational practices. It is statistically significant that the occupational health and safety training practices are more effective than those who have a total work experience of 2-5 years, between 0-1 years and more than 11 years. Table 3 shows the difference between groups with POST HOC (LSD and Games Howell) tests. The efficiency of the training of highly experienced employees and inexperienced employees is not as effective as the employees with a total work experience of 2 to 5 years. In other words, trainings are effective on employees with a maximum of 2-5 years of experience.

It can be understood that education is less effective in those with less work experience. However, it should be considered carefully to be less effective in people with more than 11 years of work experience. People who do the same work for a long time, due to vocatioonal blindness or nonchalance are starting to ignore work safety measures. These results suggest that we need to pay more attention people who have many years of experience as well as novice workers, during their work safety training.

Table 3. Different between groups in effectiveness of training of employees according to their level of experince with POST HOC (LSD and Games Howell) tests.

Multiple Comparisons							
Dependent Variable: Training							
	(I) Top_İş_Tec	(J) Top_İş_Tec	Mean Difference (I-J)	Std. Error	Sig.	95% Confidence Interval	
						Lower Bound	Upper Bound
LSD	1	2	-0.65201*	0.30972	0.038	-1.2668	-0.0372
		3	-0.17857	0.27918	0.524	-0.7327	0.3756
		4	-0.23545	0.25716	0.362	-0.7459	0.2750
	2	1	0.65201*	0.30972	0.038	0.0372	1.2668
		3	0.47344	0.24597	0.057	-0.0148	0.9617
		4	0.41656	0.22066	0.062	-0.0214	0.8546
	3	1	0.17857	0.27918	0.524	-0.3756	0.7327
		2	-0.47344	0.24597	0.057	-0.9617	0.0148
		4	-0.05688	0.17523	0.746	-0.4047	0.2909
	4	1	0.23545	0.25716	0.362	-0.2750	0.7459
		2	-0.41656	0.22066	0.062	-0.8546	0.0214
		3	0.05688	0.17523	0.746	-0.2909	0.4047
Games-Howell	1	2	-0.65201	0.35210	0.307	-1.7318	0.4277
		3	-0.17857	0.36711	0.961	-1.2743	0.9172
		4	-0.23545	0.34665	0.902	-1.3095	0.8386
	2	1	0.65201	0.35210	0.307	-0.4277	1.7318
		3	0.47344	0.19109	0.081	-.0419	0.9888
		4	0.41656*	0.14803	0.040	.0150	0.8181
	3	1	0.17857	0.36711	0.961	-0.9172	1.2743
		2	-0.47344	0.19109	0.081	-0.9888	0.0419
		4	-0.05688	0.18086	0.989	-0.5410	0.4272
	4	1	0.23545	0.34665	0.902	-0.8386	1.3095
		2	-0.41656*	0.14803	0.040	-0.8181	-0.0150
		3	0.05688	0.18086	0.989	-0.4272	0.5410
* The mean difference is significant at the 0.05 level.							

The correlation test between the dimensions is given in Table 4. There are significant correlations between dimensions according to the results. The correlation values have 0.548 ($p < 0.05$) and 0.734 ($p < 0.05$) betweeen the dimensi1ons. According to this, the highest correlation is between "Administrative measures and precaution related to occupational health and safety" and Occupational health and safety training practices"(0.734, $p<0.05$).

Table 4. Correlation test between dimensions

Correlations						
	Administrative	Criterion	Awareness	Training	Communication	
Administrative	Pearson Correlation	1	0.548**	0.627**	0.734**	0.694**
	Sig. (2-tailed)		0.000	0.000	0.000	0.000
	N	100	100	100	100	100
Criterion	Pearson Correlation	0.548**	1	0.638**	0.501**	0.626**
	Sig. (2-tailed)	0.000		0.000	0.000	0.000
	N	100	100	100	100	100
Awareness	Pearson Correlation	0.627**	0.638**	1	0.767**	0.789**
	Sig. (2-tailed)	0.000	0.000		0.000	0.000
	N	100	100	100	100	100
Training	Pearson Correlation	0.734**	0.501**	0.767**	1	0.853**
	Sig. (2-tailed)	0.000	0.000	0.000		0.000
	N	100	100	100	100	100
Communication	Pearson Correlation	0.694**	0.626**	0.789**	0.853**	1
	Sig. (2-tailed)	0.000	0.000	0.000	0.000	
	N	100	100	100	100	100
**. Correlation is significant at the 0.01 level (2-tailed).						

In addition, there were no differences in the scores of the expressions included in the scale and the scores of the expressions included in the original scale. This shows that the dimensions of the measurement tool do not contradict internationally accepted chemical sector applications.

References

Alli, B. O. (2008), "Fundamental Principles of Occupational Health and Safety", International Labor Office, Geneva.

Akadam, A. (2010). "The Relatıonshıp Between The Perceptıon Of The Job Safety Performance And The Job Safety Culture: A Research On The Metal Sector", Eskişehir Osmangazi University Institute of Social Sciences, Unpublished Master Thesis.

Ayanoğlu, C., (2007), "Ergonomics and Stress at Work", Journal of Occupational Health and Safety, Sayı 34, s. 29-36.

Fabiano, B., Fabio C., Andrea P. R., Pastorino R., (2010), "Port Safety and The Container Revolution: A Statistical Study on Human Factor and Occupational Accidents over The Long Period", Safety Science, Cilt 48, s. 980990.

Gerek, N. (2006). Occupational Health and Safety, Anadolu University, Eskişehir, WEBOSFET.

Harms-Ringdahl, L. (2005), “Safety Analysis: Principles and Practice in Occupational Safety”, (CRC Press), New York.

ISAG (2006), Safe and Healthy Working Conditions, Ankara.

Korkmaz, O. (2011). Occupational Health and Safety Chemical Industry in Turkey. Zonguldak Karaelmas University Journal of Social Sciences, 7(14).

Larson, J. (1996), “The World Health Organization’s Definition of Health: Social Versus Spiritual Health”, Social Indicators Research, No. 38: 181-192

Maurice, P.; Lavoie, M., L. Laflamme, L. Svanström, C. Romer ve R. Anderson (2001), “Safety and Safety Promotion: Definitions for Operational Developments”, Injury Control and Safety Promotion, 8(4): 237-240.

Stellman, J. M., ILO (1998), Encyclopaedia of Occupational Health and Safety, 4th Edition, International Labour Organization, U.S.A.

Susser, M. (1993), “Health as a Human Right: An Epidemiologst’s Perspective on the Public Health”, American Journal of Public Health, 83(3): 418-426

Tozkoparan, G. ve J. Taşoğlu (2011), “A Study on Determining the Attitudes of Employees on Occupational Health and Safety Practices”, Uludag Journal of Economy and Society, 30(1): 181-209.

Uslu, V. (2014). The Relatıonshıp Between The Perceptıon Of The Job Safety Performance And The Job Safety Culture: A Research On The Metal Sector, (Master's thesis, Eskişehir Osmangazi University).

Üngören, E., Koç, T. S. (2015). Occupational Health and Safety Application Performance Evaluation Scale: Validity and Reliability Study, Journal Of Social Security, 5 (2), 124-144.

International Conference on Science and Technology

ICONST 2018

5-9 September 2018 Prizren - KOSOVO

Ti_3SiC_2 MAX Phase From TiC-Si-Ti Mixture

Ahmet Atasoy[1]*, Emre Saka[1]

Abstract: There are more than ten MAX phase systems and more than fifty MAX phases. This work is focused to produce Ti_3SiC_2 MAX phase using Si, C, TiC powders. On the DTA curve of the mixture showed two exothermic peaks at temperature 970 and 1250 ˚C which were related with the formation of the MAX structure on the carbide layer. TiSi, SiC, TiC and Ti_3SiC_2 phases were detected in the sintered samples at temperature above 1300 ˚C for 3 h sintering time. At higher temperature and longer reaction time, SiC decomposes depending on the holding and reaction temperature. The silicon to titanium carbide and carbon ratios should be in stoichiometric but the silicon content of the starting composition requires more than 20% excess.

Keywords: TiC, silicon, carbide, machinable ceramic,

Introduction

Max phase was discovered by Nowontny and co workers(Noontny 1970, 1982), but these new discovered phases did not receive much attention until pure Ti_3SiC_2 phase purely produced(Barsoum 1996). MAX phase, M is early group of 2 elements, A is transition elements and X is C or N in the system. There are more than ten discovered MAX phase systems can be classified according to the stoichiometric structure of the phases which are 211, 312, 431, 523 and 735(Hu 2013). There are growing interests on the MAX materials family at the last two decades because of the MAX phase materials combine metal and ceramic material properties(Rodovic 2013, Barsoum 2001). The materials are very stable and desired at high temperature applications(Chen 2001, Sunberg 2004). They have unique mechanical, thermal and chemical properties which are used wide range of applications from cutting tools (Gilbert 2000), to as a radiation shielding material in nuclear reactants(Hoffman 2012). These materials are new generation materials which replaced with the advanced ceramics in the near future. The decomposition temperatures of the materials change between 850-2300˚C, depending upon the type and number of impurities present(Li 2003, Bao 2004, Zhen 2005). Preparation and processing methods of MAX phase include solid state synthesis[15], mechanical alloying (Raoult 1994, Orthner 2002), arc melting (Gupta 2004), hot pressing (Zhou 2000[a]), chemical vapor deposition(Zhou 2000[b]), spark plasma sintering(Zhou 2000[c]), pulse discharge sintering(21), pressureless sintering(Sun 2002) and self propagation (Merzhanov 2004, Mishra 2011). Among the MAX phase ceramics, Ti_3SiC_2 is one of the most attraction material which is half of the published papers were about it(Barsoum 2001, Raoult 1994). It is usually processed from pure Ti, Si, SiC and TiC powders or combinations at high temperature(Barsoum 2000, Etzkorn 2007, Sun 2004, Pampunch 1989, El Saeed 2012).

In our previous studies, high purity and composite powders were synthesized successfully using a number of different starting materials and compositions by pressureless and thermic processes. Depending on the starting composition, the desired MAX phase was obtained by the aluminothermic reduction and carburizing of $TiO_2/SiO_2/C/Al$ powders at 1400 ˚C for 2h(Atasoy 2016). A series of experimental studies have been carried using high purity Ti, Si and graphite powders at a time temperature schedule of 1350 ˚C for 2 and 4 h. Addition of the Ti_3SiC_2, SiC and TiC phases were formed. The formation of the MAX phase is more

[1]Sakarya University, Faculty of Technology, Sakarya, TURKEY
*Corresponding author: aatasoy@sakarya.edu.tr

favorable at lower temperature. It was found that, the carbon content has significant effect on the formed MAX phase in which it decomposes to the carbides of Ti and Si at higher temperatures(Atasoy 2017). Based on our experimental studies, the aim of the work presented here is to investigate the processing and formation of 312 TiSiC MAX phase from the mixture of TiC, Ti and Si.

Materials and Method

In the present study, high purity TiC, Tiand Si powders were used as starting materials to synthesis Ti_3SiC_2 phase. The characteristic of the powders are given in Table 1.Titanim and silicon powders were provided from the Alfa Aesarcompany. TiC powder was provided from.

Table 1. Some properties of the starting powders.

	Mp ˚C	D ($g.cm^{-3}$)	Par. size	Purity (%)
TiC	3200	4.93	5-20μm	99.99
Ti	1668	4.506	5-7 μm	99.99
Si	1412	2.33	2-5 μm	99.5

To prepare homogeneous mixture corresponding to the desired stoichiometric, the powders were ball milled with silicon carbide balls for 6 h. After the mixing operation, green compacts were obtained from the cold compaction of mixture with a uniaxial pressure of 300 MPa. After words the green compacts were placed in a graphite crucible and sintered at temperatures between 1300-1500 ˚C under Ar atmosphere for various holding times. The density of the green and the sintered samples were measured by Archimedes method. For the determination of mineral in the starting mixtures and the obtained phases in the products, X-ray diffraction method (D/max Rigaku, Japan) was used at the condition of Cu Kα radiation (λ=0.15418 nm) with a step size of 0.02˚ (2θ) and a scanning rate of 2˚ min^{-1}. Energy dispersive analytical X-ray (EDAX) was also used for basic chemical analysis. Thermal analysis of the mixture was performed on a simultaneous thermal analyser (Netzsch STA 400, Germany). TG/DTA was performed in an alumina crucible, under nitrogen atmosphere in the temperature range of 20-1450 ˚C and heating rate of 10 ˚C/min. For microstructure and morphology of the starting and the reduced samples were investigated by scanning electron microscopy (SEM) coupled energy dispersive X-ray spectroscopy (EDX).

For the preparing of ternary compound Ti_3SiC_2in a single stage, the solid-state reaction method was chosen. Overall reaction to produce Ti_3SiC_2 by given reactions.

$$2TiC_{(s)} + Ti + Si_{(s)} + \rightarrow Ti_3SiC_2 \qquad (1)$$

To prepare homogeneous mixture corresponding to the desired stoichiometric, to minimize any contaminations, the powders were ball milled with SiC balls for 6 h. After the mixing stage, green compacts were obtained from the cold compaction of mixture with a uniaxial pressure of 300 MPa. After words the green compacts were placed in a graphite crucible and sintered at temperatures between 1300-1500 ˚C under argon atmosphere for various holding times.

For the determination of crystalline of the starting mixtures and the obtained phases in the products, X-ray diffraction method (D/max Rigaku, Japan) was used at the condition of Cu Kα radiation (λ=0.15418 nm) with a step size of 0.02˚ (2θ) and a scanning rate of 2˚ min^{-1}. Energy dispersive analytical X-ray (EDAX) was also used for basic chemical analysis.

Thermal analysis of the mixture was performed on a simultaneous thermal analyser (Netzsch STA 400, Germany). TG/DTA was performed in an alumina crucible, under nitrogen atmosphere in the temperature range of 20-1450 ˚C and heating rate of 10 ˚C/min.

For microstructure and morphology of the starting and the reduced samples were investigated by scanning electron microscopy (SEM) coupled energy dispersive X-ray spectroscopy (EDX).

Results

For the preparing of ternary compound Ti_3SiC_2in a single stage, the solid-state reaction method was chosen. The first step is the preparation of TiC, Ti and Si powder according to the reaction 1 in a stoichiometric ratio. A green compact is prepared with this homogeneousmixture and put in an graphite crucible. They were sintered at temperatures between 1300-1500 ˚C for various holding times under Ar.

In Figure 1 shows the X-ray diffraction pattern of the starting composition (at the bottom line). As expected it consisted TiC, Si and Ti. This figure also presents the X-ray diffraction patterns of the sintered samples at 1300 ˚C for various holding times. depending on the sintering time, it was clear that the figure displays different patterns and different newly formed phases such as SiC, TiSi inter metallic and Ti_3SiC_2. At this sintering temperature, the sintering time has key role on the formation of the desired structure which needs more than 2 h. At the experimental condition, the high percentage of the MAX phase was formed in 4 h. holding time.

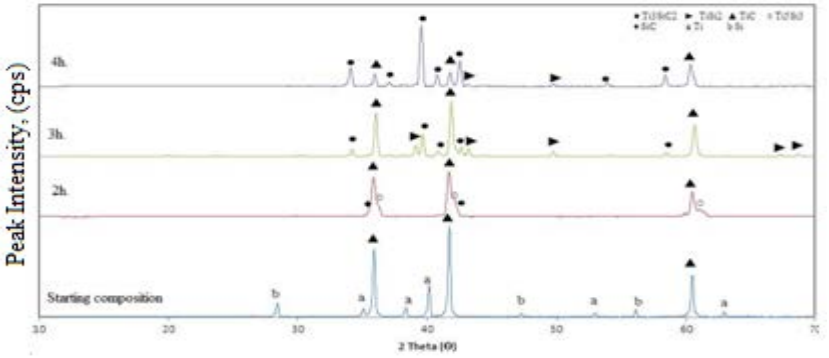

Figure 1.XRD pattern of the sintered sample at 1300 ˚Cfor various times.

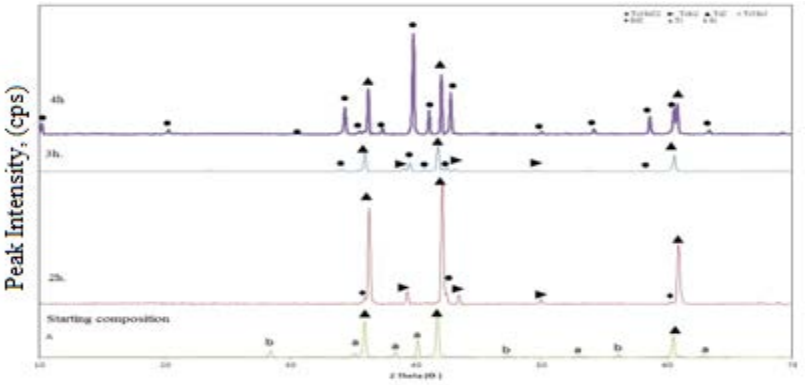

Figure 2.XRD pattern of the sintered sample at 1400 ˚C for various times.

Figure 2 shows the sintered samples at 1400 ˚C which displays different patterns and the new formed phases. At this temperature, the first reaction products were inter metallic phases of Ti-Si system where were TiSi, $TiSi_2$ and Ti_5Si_3. When the sintering time increases they were converted into the carbides and Ti_3SiC_2phases. This observation and the results suggests that the formation of the phase starts with inter metallic and carbide phases both depending on the sintering temperature and holding time.

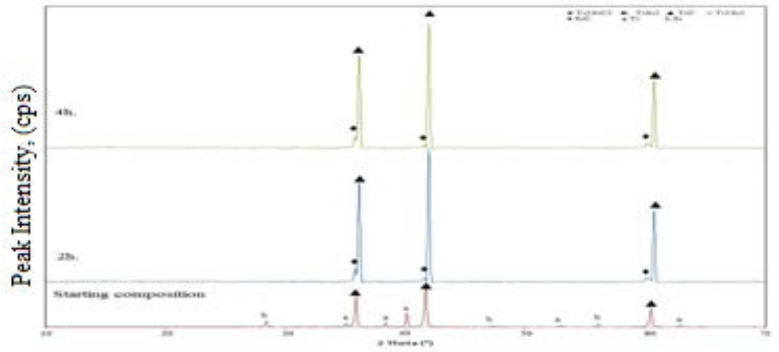

Figure 3.XRD pattern of the sintered sample at 1500 ˚C for various times.

Final X-ray diffraction patterns of the sintered samples at 1500 ˚C for various holding times were presented in Figure 3. As seen from it, TiC phase was increased and SiC was formed. It was very amazing results that at his temperature, the formed MAX phase was disappeared. Our experiments showed that, the formed Ti_3SiC_2 phase was decomposed to TiC and SiC at both holding time. It was also assumed that the type of the used crucible was important that when graphite crucible was used the formation of carbide phases was accelerated as well as it decomposes the formed Ti_3SiC_2 phase to carbides at higher temperatures. Our results showed that, the stability of Ti_3SiC_2 phase was related with the carbon content of the initial composition and the type of crucible used.

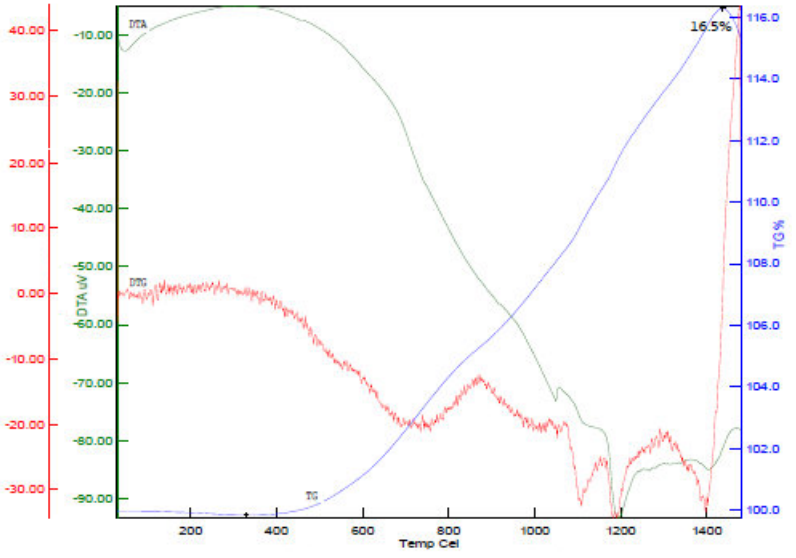

Figure 4. TG/DTA curves of mixture powders of Ti, TiC, Si and C powders.

Thermal analysis of the mixture of TiC, Ti and Si powder was presented in Figure 4. As seen from the TG curve of the mixture, there is weight gain during the experiment. It can be seen that the weight gaining starts at temperature above 400 ˚C and continuous with sintering temperature. Under the experimental conditions, both of the starting powders were stable and the experiment was carried out in argon flow. This kind of weight gaining can be explained by the oxidation of carbide or metallic portion of the starting composition. More investigations are necessary to clarify the weight gaining of the mixture. On the other, three endothermic and one exothermic peaks are observed on the DTA curve of the mixture. When compared them, they were resulted in conflicting conclusions. Again, in presence of Ar flow, any oxidation reaction should not take place in the mixture. However, some oxide content may come from the ball which was used for milling stage. This kind of contamination may resulted weight gain in the sintered samples.

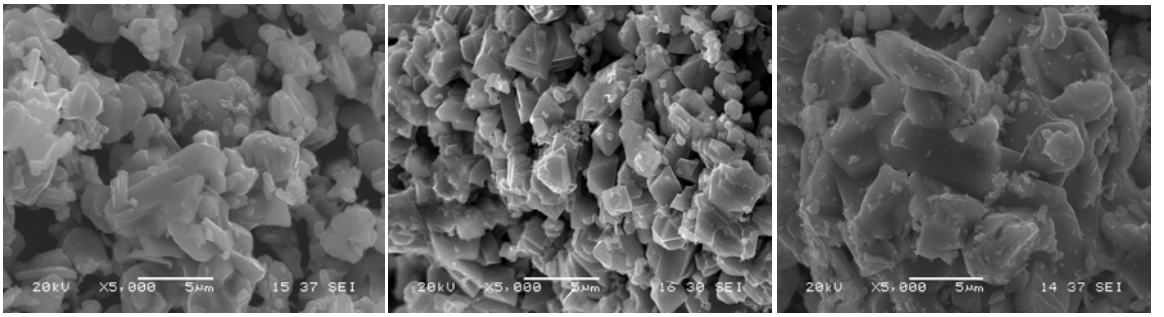

Figure 5.SEM micrograph of the sintered samples at 1300, 1400 and 1500 ˚C for 2h holding times.

Figure 5 shows the selected SEM micrograph after heat treating at different sintering temperatures for 2h. The particles were composed of TiC, SiC and Ti_3SiC_2. At 1400 ˚C, the structure seems to be layered and has more Ti_3SiC_2 particles than the right and left side pictures. As confirmed by the X-ray diffraction patterns (Figure 3) the particles on the right side of the Figure 5 belongs to TiC and SiC.

The reaction mechanism of the Ti_3SiC_2 phase depends on the used powders. When thermo chemically stable powders were used the reaction mechanism controls by diffusion model with solid state reaction between the reactants. In the case of TiC-Ti and Si powders, the formation of Ti_3SiC_2 phase rate controlling by the overall reaction. The first nucleation of the Ti_3SiC_2 starts on the surface of TiC and grows epitaxial.

Discussion and Conclusions

Many attempts have been reported the formation of the 312 phase. It was reported the phase composition and the reaction mechanism of the MAX phase depends on the starting powders, the sintering conditions and parameters and even depends on used crucible. When TiC and Si were used as starting powders, the Ti_3SiC_2 forms on the TiC phase. The wet ability of Si is more feasible and covers all around TiC particles during the sintering stage. The growth mechanism of theTi_3SiC_2 is epitaxial.

It was very interesting results that there was no MAX phase at sintering temperature of 1500 ˚C for the shorteror the longer holding times. The phase was decomposed into the carbides of Si and Ti. The tendency of decomposition reaction may be related with the used crucible which was graphite where creates carbon source that plays critical point in the system. The DTA curve showed a big exothermic peak nearly the same temperature as those determined by the XRD analysis.

The results of X-Ray diffraction analysis were presented in Fig 1-3 showing the relative intensity of the newly formed phases of the sintered samples. As the sintering time was increased, the formation of the desired phase increased linearly except the highest sintering temperature of the mixture.

The results of TG/DTA experiments were reported in Fig 4 showing the relative mass variations and its derivative as a function of temperature with a heating rate of 10 ˚Cmin^{-1}. A significant mass gaining was observed at temperature between 400-1500˚C.

Ti_3SiC_2 is a bridge material between ceramics and metals. It is also new generation ceramics. TiC, Ti and Si powders used for synthesis of Ti_3SiC_2MAX phase by solid state method at a time-temperature schedule of 1300-1500 ˚C in Ar atmosphere condition. Depending on the reaction temperatures and the sintering time, TiSi, SiC and Ti_3SiC_2 phases were formed. TiC and SiC with elongated or equiaxed shape distributed in Ti_3SiC_2matrix. The formation of Ti_3SiC_2depends on Ti-Si binary phases. Silicon content plays an important role in the wetting of TiC particle and the formation of Ti_3SiC_2phase.Ti_3SiC_2 phase was successfully obtained at 1300 ˚C for 3 h sintering time, and it was decomposed into TiC and SiC at higher temperature. The further work should be performed to optimize the sintering process parameters and to investigate the mechanical properties of the sintered samples.

Acknowledgements

The study was financially supported by the Scientific Research Project Unit of Sakarya University under the project number of 2016-50-01-005. EmreSaka has a scholarship of the Scientific and Technological Research Council of Turkey (TÜBİTAK) on the priority researchareas program (2210-C) with the project no of 1649B021508867.

References

Atasoy A, Saka E. (2016) Synthesis of the MAX phase of Ti_3SiC_2 ceramic from oxide. 18. Inter Metall and Metarials Congr. (IMMC 2016) Istanbul, 71-74

Atasoy A. (2017) Synthesis and characterisation of Ti_3SiC_2 based composite', Fresenius Environmental Bulletin, 26 (8), 5163-5169

Bao YW, Zhou YC. (2004) Mechanical properties of Ti_3SiC_2 at high temperature. Acta Metall 17: 4 65-70

Barsoum MW, El-Raghy T. (1996) Synthesis and characterization of a remarkable Ceramic: Ti_3SiC_2. J Amer Cer Soc. 79;1953-1956

Barsoum MW. (2000) The $M_{N+1}AX_N$ phases: a new class of solids; thermodynamically stable nano laminates. Prog Solid State Chem. 28.201-81

Barsoum MW, El-Raghy T. (2001) The max phases: unique new carbides and nitride materials. Amer Scientific. 89: 334-343

Chen D, Shirato K, Barsoum MW, El-Raghy T, Ritchie RO. (2001) Cyclic fatigue-crack growth and fracture properties in Ti_3SiC_2 ceramics at elevated temperatures. J Am Ceram Soc. 84(12): 2914-2920

El Saeed MA, Deorsola F A, Rashad RM. (2012) Optimization of the MAX phase synthesis. Int J Ref Metals Hard Mat. 35: 127-131

Etzkorn J, Ade M, Hillebrecht H. (2007) Ta_3AlC_2 and Ta_4AlC_3-single-crystal investigations of two new ternary carbides of tantalum synthesized by the molten metal technique. Inorg Chem. 46: 1410-1418

Gilbert CJ, Bloyer DR, Barsoum MW, El-Raghy T, Tomsia AP, Ritchie RO. (2000) Fatigue-crack growth and fracture properties of coarse and fine grained Ti_3SiC_2. Scripta Mat. 238:761-767

Gupta S. Barsoum MW. (2004) Syntheses and oxidation of V_2AlC and $(Ti_{0.5}V_{0.5})_2AlC$ in air. J Electro Chem Soc. 151: 24-29

Hoffman EN, Vinson DW, Sindelar RL, Tallman DJ, Kohse G, Barsoum MW. (2012) MAX phase carbides and nitrides: Properties for future nuclear power plant in-core applications and neutron transmutation analysis. Nuc Eng & Design. 244: 17-24

Hu C, Xhang H, Li F, Huang Q, Bao Y. (2013) New phases discovery in MAX family. Int J Ref Metals Hard Mat. 36: 300-312

Li SB, Chang LF, Zhang LT. (2003) Oxidation behavior of Ti_3SiC_2 at high temperature in air. Mat Science Eng Struc Mat Prog Microstructure Process. 341:112-120

Merzhanov AG. (2004) The chemistry of self-propagating high-temperature synthesis. J Mat Chem. 14: 1779-1786

Mishra SK, Khusboo A, Sherbokov V. (2011) Fabrication of in-situ Ti-Si-C fine grained composite by the self propagating high temperature synthesis. Int J Ref Met Hard Mat. 29: 209-213.

Noontny H. (1970) Struktuchemiteeinigerverbindungen der ubergangsmetallemit den elementen C Si GeSn. Prog Solid State Chem. 2: 27-62.

Noontny H, Schuster JC, Rogl P. (1982) Structural chemistry of complex carbides and related compounds, J Solis State Chem. 44: 126-133

Orthner HR, Tomasi R, Botta FWJ. (2002) Reaction sintering of titanium carbide and titanium silicide prepared by high energy milling. Mater Sci Eng. 336:202-208

Pampunch R, Lis J, Stobierski L, Tymkiewicz M. (1989) Solid combustion synthesis of Ti_3SiC_2S. J Eur Ceram Soc. 5: 283-287

Raoult C. Langlais F, Naslain R. (1994) Solid state synthesis and obtain and characterization of the ternary phase Ti_3SiC_2. J Mat Sci. 29: 3384-3394

Rodovic M, Barsoum MW. (2013) Max phases: Bridging the gap between metals and ceramics. Amer Ceram Soc. 92(3):20-27

Sun ZM, Zhang ZF, Hashimoto H, Abe T. (2002) Tannery compound Ti_3SiC_2: Part 1.Pulse discharge sintering synthesis. Mat Trans. 43: 428-431

Sun ZM, Yang S, Hohimoto H. (2004) Ti_3SiC_2 powder synthesis. Ceram Int. 30: 1873-1877.

Sunberg M, Malmgvist G, Magnusson A, El-Raghy T. (2004) Alumina forming high temperature silicides-carbides, Ceram Inter. 30: 899-1904

Yoo HI, Barsoum MW, El-Rabhy T. (2000) TiSiC; A material with negligible thermo power over an extended temperature. Natura. 407:581-582

Zhang ZF, Sun ZM, Hashimoto H, Abe T. (2004) Effect of sintering temperature and Si content on the purity of Ti_3SiC_2 synthesis from Ti/Si/TiC powders. J Alloy Comp. 352:283-288.

Zhen T, Barsoum MW, Kalidindi SR. (2005) Effect of temperature, strain rate and grain size on the compressive properties of Ti_3SiC_2. Acta Mater 53: 4163-71.

Zhou Y, Sun Z. (2000) Temperature fluctuation/hot pressing synthesis of Ti_3SiC_2. J Mat Sci. 35: 4343-46

Zhou Y, Sun Z. (2000)) Pulsed electro spark deposition of MAX phase Cr_2AlC based coating on titanium alloy. Surf Coat Tech. 235:454-460.

Zhou Y, Sun Z. (2000) Low temperature thermal expansion, high temperature electrical conductivity and mechanical properties of Nb_4AlC_3 ceramic synthesized by spark plasma sintering. J Alloys Compd. 487:675-81.

International Conference on Science and Technology

ICONST 2018

5-9 September 2018 Prizren - KOSOVO

A New Descriptor for 3D Object Detection using RGB-D

Erkut Arıcan[1]*, Tarkan Aydın[1]

Özet: Nesne algılama, bilgisayarla görü için çok önemli bir çalışma alanıdır. Bir çok araştırmada nesne bulmak için yalnızca RGB görüntüleri kullanılmıştır. Bu çalışmada, RGB derinlik görüntü verisini kullanarak nesne algılama için yeni bir tanımlayıcı vektör önerilmektedir. Yeni bir özellik vektörü oluşturmak için RGB görünütüsü derinlik görüntüsü ile birleştirilmiştir. Ayrıca, çalışmamızda K-ortalama kümeleme ve histogram kullanılmıştır. Yöntemimizi eğitmek ve test etmek için makine öğrenme algoritmaları kullanılmıştır. RGB-D görüntülerinin RGB görüntüleri ile kıyaslandığında daha doğru sonuçlar verdiği görülmüştür.

Anahtar Kelimeler: RGB-D, Derinlik Görüntüsü, Makine Öğrenmesi, K-Ortalama

Abstract: Object detection is a very important study area in computer vision. Many research use only RGB images to find objects. In our work, we present new descriptor for object detection using RGB-D's Depth image data. We combine RGB image with depth image to create new feature vector. We also use K-means cluster and histogram in our work. We use machine learning algorithms to train and test our method. Result shows us to RGB-D images are given better accuracy results to comparing with RGB image.

Keywords: RGB-D, Depth Image, Machine Learning, K-Means

Introduction

There are many fields in computer vision and object detection is the most popular one. A long time ago, finding object was a challenging process. In last decades, many works show that finding object became an easy process for computer vision but mostly RGB information without depth is used. In literature, you can find many studies using descriptor which are very preferred in computer vision (Bay et al. 2006; Lowe 2004; Calonder et al. 2010; Rublee et al. 2011; Shechtman & Irani 2007)

Nowadays, technology is going better and cheaper therefore you can find and access 3D image easily. You can create dataset using Microsoft Kinect (Microsoft n.d.) , Intel RealSense 3D Camera (Intel n.d.) , etc. or you can download many 3D image dataset like SUN3D (Xiao et al. 2013), Berkeley 3D Object Dataset (Janoch et al. 2011), RGB-D Object Dataset (Lai et al. 2011) and NYU Dataset (Silberman et al. 2012) . In literature, you can find some 3D descriptors such as Huang's study (Huang & You 2012) and (Arıcan & Aydın 2017). In (Huang & You 2012), authors propose 3D local descriptor using self-similarity and point cloud information while in (Arıcan & Aydın 2017), authors used depth oriented gradients for object detection.

In this paper, we propose a new descriptor for 3D object detection using RGB and Depth image together. We combine 3 important information and create a new descriptor. Bag of Visual Word (Csurka et al. 2004) algorithm is our base algorithm and we add Local Self Similarity (Shechtman & Irani 2007) and Depth information to create a new 3D descriptor for object detection.

[1]Bahçeşehir University, Faculty of Engineering and Natural Sciences, Computer Engineering Department 34353, İstanbul, TÜRKİYE
*Correspondingauthor: erkut.arican@eng.bau.edu.tr

Our paper continue as follows: background information about Bag of Visual Words and Local Self-Similarity is given in Background Section. Then proposed method is explained in Section Material and Method. Results are showed in Result Section. Finally, in the last section, we summarized our study and mention future works.

Background

In this section, we explain Bag of Visual Words (BoW) and Local Self Similarity (LSS) methods which compose base method with Depth information to our study.

- **Bag of Visual Words**

Csurka and et. all (Csurka et al. 2004) developed a descriptor for identifying the object. Authors define 4 main steps for Bag of Visual Words. These steps are; 1) determining of image patches; 2) creating a vocabulary; 3) creating bag of keypoints and 4) using multi-class classifier for determining categories for input images.

- **Local Self Similarity**

In Local Self Similarity (Shechtman & Irani 2007), they use self-similarities for same object but different image characteristics. They create image patch and region part to create correlation surface. When they create the correlation surface, they use binned log-polar representation and create a descriptor. In Figure 1, you can see LSS method.

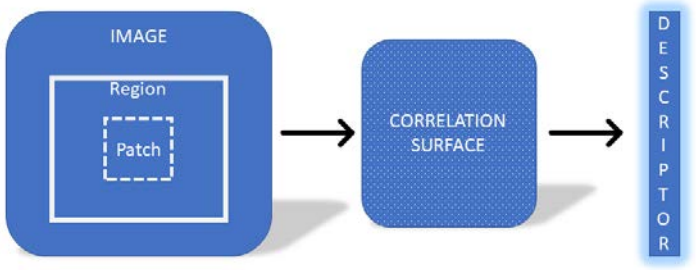

Figure 1 Local Self Similarity

Authors used Sum of Squared Distance method for creating correlation surface, these part is another key point to our work.

Material and Method

We explained background information about our work in previous section. Now, we will explain our method. Bag of Visual Words selected as a base method and it uses SURF points (Bay et al. 2006) for feature extraction which we modified in our study.

In the first step, we read RGB image in grayscale format and found SURF points. We selected each SURF points as a center point and extracted 4x4 patch matrix and 12x12 region matrix. We use template matching algorithm for these 2 matrices with Sum of Square Distance (Eq.1) and create SSD matrix in the size of 9x9. This size will also define Depth image matrix's size. In Figure 2, you can see an example of template matching.

$$d_i(I_j, T) = \sum_{i=1}^{n} |I_{i,j} - T_i| \quad (1)$$

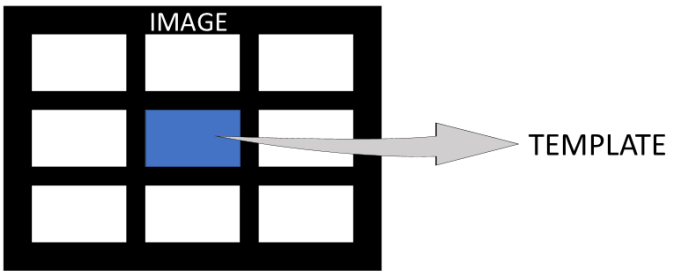

Figure 2 Template Matching Example

Afterwords, we need to convert Depth image to grayscale, then we select same SURF points as a center points and create 9x9 matrix. From now on depth matrix is called DM. An important part of our study is combining this depth information to local self-similarity method. For the combining process, firstly we normalize DM and convert SSD matrix as a double and then create a new matrix using Equation 2 as follows

$$DS = (SSD * e^{DM})^T \tag{2}$$

We convert this matrix in a single row to create our new descriptor.

In Algorithm 1, we explain our method step by step.

Algorithm 1 Our Method

1. Read RGB image in grayscale
2. Detect SURF points
3. For each SURF points selected as a center
    a. Extract 4x4 patch matrix from image
    b. Extract 12x12 region matrix from image
    c. Calculate SSD
    d. Read Depth image in grayscale
    e. Extract 9x9 matrix from depth image (DM)
    f. Create new matrix using SSD and DM
    g. Convert matrix to 1-D vector
    h. Return new descriptor

Results

We use RGB-D Object Dataset (Lai et al. 2011) to test our algorithm. In this Kinect style dataset, there are 300 common household objects, 51 categories. We create implementation to our algorithm using MATLAB (MATLAB n.d.). In Table 1, you can see comparison between our method and BoW + SSD results for different number of labels.

Table 1 Comprasion Methods Different Number of Labels

	Accuracy		
Method	4 Labels	5 Labels	6 Labels
BoW + SSD	61%	48%	46%
Our Method	**64%**	**51%**	**57%**

It is clear that our algorithm gives better performance than Bag of Visual Words + SSD algorithm.

Discussion and Conclusions

Using RGB is very popular and often preferred in object detection. On the other hand, depth images are becoming easily accessible information, so we contribute literature as proposing a new descriptor for object detection using RGB-D images. Adding depth image gives better accuracy than using only RGB. For future work, we will try to improve our method to give much better performance.

Acknowledgements

This study is a part of Bahcesehir University Doctoral Programme's PhD Dissertation.

References/Kaynaklar

Arıcan, E. & Aydın, T., 2017. Object Detection With RGB-D Data Using Depth Oriented Gradients. In Book of Proceedings - International Conference on Engineering and Natural Sciences.

Bay, H., Tuytelaars, T. & Van Gool, L., 2006. SURF: Speeded up robust features. In Lecture Notes in Computer Science (including subseries Lecture Notes in Artificial Intelligence and Lecture Notes in Bioinformatics). pp. 404–417.

Calonder, M. et al., 2010. BRIEF: Binary robust independent elementary features. Lecture Notes in Computer Science (including subseries Lecture Notes in Artificial Intelligence and Lecture Notes in Bioinformatics), 6314 LNCS(PART 4), pp.778–792.

Csurka, G. et al., 2004. Visual categorization with bag of keypoints. International Workshop on Statistical Learning in Computer Vision.

Huang, J. & You, S., 2012. Point cloud matching based on 3D self-similarity. In Computer Vision and Pattern Recognition Workshops (CVPRW), 2012 IEEE Computer Society Conference on. pp. 41–48.

Intel, Intel RealSense. Available at: https://www.intel.com.

Janoch, A. et al., 2011. A category-level 3-D object dataset: Putting the Kinect to work. Proceedings of the IEEE International Conference on Computer Vision, pp.1168–1174.

Lai, K. et al., 2011. A large-scale hierarchical multi-view RGB-D object dataset. In Proceedings - IEEE International Conference on Robotics and Automation. pp. 1817–1824.

Lowe, D.G., 2004. Distinctive image features from scale-invariant keypoints. International Journal of Computer Vision, 60(2), pp.91–110.

MATLAB, MATLAB. Available at: https://www.mathworks.com/products/matlab.html.

Microsoft, Kinect. Available at: https://dev.windows.com/en-us/kinect.

Rublee, E. et al., 2011. ORB: An efficient alternative to SIFT or SURF. Proceedings of the IEEE International Conference on Computer Vision, pp.2564–2571.

Shechtman, E. & Irani, M., 2007. Matching local self-similarities across images and videos. In Proceedings of the IEEE Computer Society Conference on Computer Vision and Pattern Recognition. IEEE, pp. 1–8.

Silberman, N. et al., 2012. Indoor segmentation and support inference from RGBD images. Lecture Notes in Computer Science (including subseries Lecture Notes in Artificial Intelligence and Lecture Notes in Bioinformatics), 7576 LNCS(PART 5), pp.746–760.

Xiao, J., Owens, A. & Torralba, A., 2013. SUN3D: A database of big spaces reconstructed using SfM and object labels. Proceedings of the IEEE International Conference on Computer Vision, pp.1625–1632.

International Conference on Science and Technology

ICONST 2018

5-9 September 2018 Prizren - KOSOVO

Investigation of Chemical Components of Spartium junceum Branches by Polar and Apolar Solvents

Özlem Karaboyacı[1]*, Semra Kılıç[2]

Abstract: In this study, metabolites of spartium junceum branches were investigated after set seed season. As it is known, the secondary metabolites in the plants vary according to the seasonal conditions and seasons. Branches were extracted with ethyl acetate and hexane to determine the different components. The yields of the extracts obtained were analyzed and their contents were analyzed by GC MS and TOF LC / MS.

Keywords: Spartium junceum, branch metabolites, extraction

Introduction

The Spartium junceum is the Mediterranean basin and is naturally found on the northern and southern sides of the Mediterranean Sea. In our country, Çanakkale, Istanbul, Kocaeli, Kastamonu, Sinop, Samsun, Trabzon, Izmir, Mugla, Antalya, Mersin, Adana, Hatay grows in a very common environment. In the literature, it has been reported that the flowers of the mulberry flowers have a calming, antiulcer, diuretic, analgesic, antiinflammatory and antitumor effect (Cerchiara et al. 2013). The stems of the plant are also used in fiber production. The fiber obtained is of interest because of its high mechanical strength as well as a biodegradable fiber. Gabriele et al. 2010 obtained a high-yield fiber material, Cerchiara et al. 2014, which proved to be much more durable than linen. This plant, which is valuable for each component from its branches to its essential oil, will turn into a medical product for neck, back and joint pain and sports injuries.

According to scientific studies on Spartium junceum, Bezic et al. 2003 reported that spartein was found to have an analeptic effect on the body of the plant. Menghini et al. In 2006 in their study on mice, spartium junceum blossom extract has proven pain relief and anti-inflammatory effects. Ghasemi et al. In their study in 2015, they have shown that Spartium junceum flowers in the region of Iran contain high levels of linalool and camphor. In addition to their pleasant odor, these compounds provide the fast absorption of the active ingredients from the skin in cosmetics.

In the literature, It is raported that there in no growth of Spartium junceum plant in Turkey after sea level is above 650 meters. But the plants which we used in this study was collected somewhere around the Kazak tunnels which have altitude ober 1100 meters. Even the plant is seen on the coast of the Gölcük lake with an altitude of 1387.

Material and Method

Spartium Junceum branches were collected after the set seed season. The collected branches were milled in the mill. In order to determine the chemical composition, 10 g of plant samples were taken and extraction

[1]Suleyman Demirel University, Faculty of Engineering,Bioengineering Dpt. 32260, Isparta, TURKEY
[2]Suleyman Demirel University, Faculty of Arts and Science, Biology Dpt. 32260, Isparta, TURKEY
*Correspondingauthor: ozlemkaraboyaci@gmail.com

was carried out in 100 µl of hexane and ethyl acetate solvents for 1 night. After the extraction time, the resulting mixture was taken to the rotary evaporator to remove it from the solvent. The obtained yield ratio of the samples was calculated and saples sent to GC-MS and TOF LC / MS for analysis.

Results

After evaporation, the rest mass of the extract is called the extraction efficiency. In this study, the mass obtained from ethyl acetate extract is 40 mg / g. The mass obtained from the hexane extract is 10 mg / g. The yield of ethyl acetate extraction is 4 times higher than that of hexane extraction.

Figure 1 and 2 shows the GC MS spectrum of extractes. In the GC MS analysis DB 5 MS column was used with mass detector. Figure 3 and 4 shows the TOF LC / MS analysis of the extracts.

As seen from figure 1 nothing was detected with GC MS in hexane extract. But Two compenets was detected in ethy acetate extract as seen in Table 1. Accourding to Pub Chem records Acetyl tributyl citrate is a flavouring ingredient and plasticiser used in packaging films for food. Other component is the Pentatriacontane and pentatriacontane is considered to be a hydrocarbon lipid molecule use in food sector.

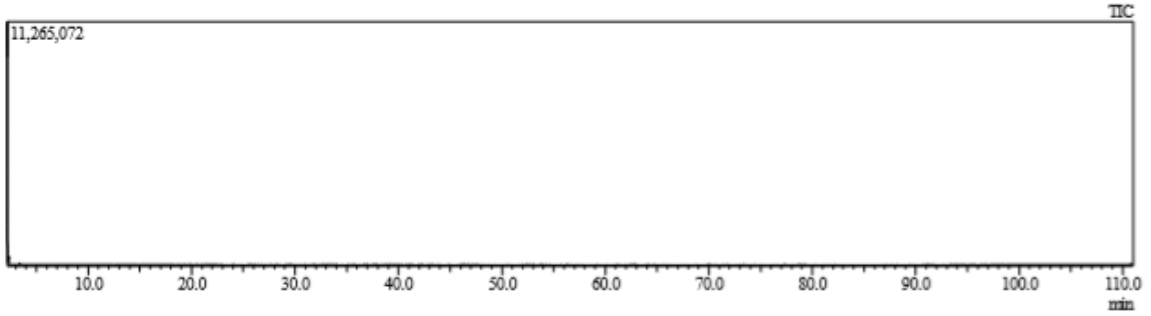

Figure 1. GC MS results of hexane extracted Spartium Junceum branches

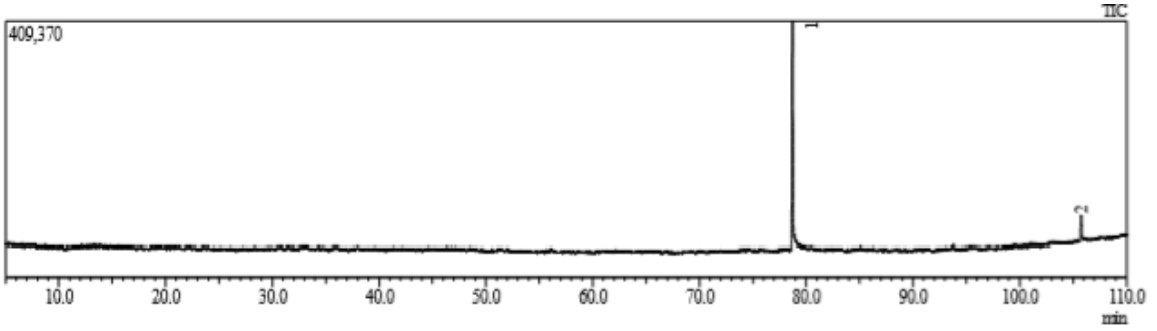

Figure 2. GC MS results of ethyl acetate extracted Spartium Junceum branches

Table 1. GC MS library screening of ethyl acetate extract

Peak#	R.Time	Name	Area	Area%
1	78.724	Citrate <tributyl-> acetate	1955566	88.20
2	105.768	Pentatriacontane (CAS) n-Pentatriacontane	261530	11.80
			2217096	100.00

Table 2. TOF LC / MS library screening of hexane extract

m/z	z	Abund	Name	Formula	Ion	Score (DB)	Hits (DB)
230.2481	1	91907.45	Xestoaminol C	C14 H31 N O	(M+H)+	95.99	1
231.2498	1	15802.24		C14 H31 N O	(M+H)+		
242.2479		4511.2					

As seen from table 2 TOF LC / MS detect Xestoaminol C in the hexane extract. Also TOF LC / MS results of ethyl acetate extract is smilar. TOF LC / MS detect only Xestoaminol C in the ethyl acetate exctract to. According to Pubchem records Xestoaminol C (1-deoxytetradecasphinganine) is a sphingoid that is tetradecasphinganine in which the terminal hydroxy group has been replaced by a hydrogen. It has a role as a metabolite. It is a sphingoid and an amino alcohol. It derives from a tetradecasphinganine.

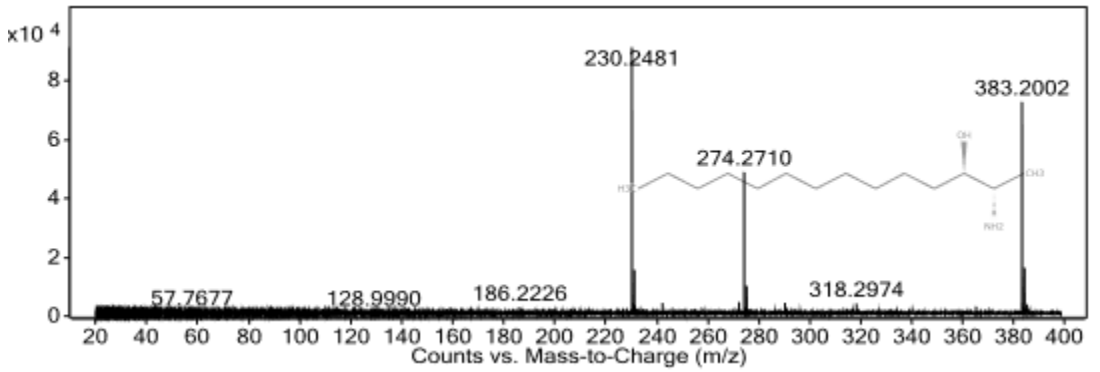

Figure 3. TOF LC / MS results of hexane extracted Spartium Junceum branches

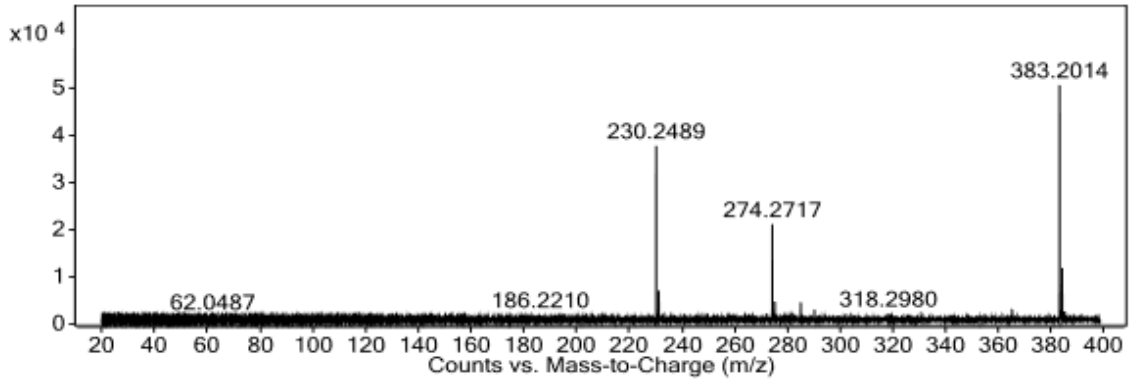

Figure . TOF LC / MS results of ethyl acetate extracted Spartium Junceum branches

Discussion and Conclusions

In this study spartium junceum branches were investigated after set seed season. Three useful components were detected with two different analysis method. The exact presence of these components should be verified by analyzing on the HPLC instrument against the standard.

But there is no spartein in the branches like Bezic et al. 2003 reproted before. Therefore, the plant will be re-analyzed during flowering. The presence of secondary metabolites may vary depending on the ambient conditions and season.

References

Bezic, N., Dunkic, V., Radonic, A. (2003). Anatomical and chemical adaptation of Spartium junceum L. in arid habitat.Acta Biologica Cracoviensia Series Botanica, 45(2), 43-47.

Cerchiara, T., Blaiotta, G., Straface, V. S., Belsito, E., Liguori, A., Luppi, B., ... & Chidichimo, G. (2013). Biological Activity of Spartium junceum L.(Fabaceae) Aromatic Water. Natural Resources, 4(3), 229. 99

Cerchiara, T., Gallucci, M. C., Gattuso, C., Luppi, B., & Bigucci, F. (2014). Chemical Composition, Morphology and Tensile Properties of Spanish Broom (Spartium junceum L.) Fibres in Comparison with Flax (Linum usitatissimum L.). Fibres & Textiles in Eastern Europe.

Gabriele, B., Cerchiara, T., Salerno, G., Chidichimo, G., Vetere, M. V., Alampi, C., ... & Cassano, A. (2010). A new physical–chemical process for the efficient production of cellulose fibers from Spanish broom (Spartium junceum L.). Bioresource technology, 101(2), 724-729

Ghasemi, Y., Abedtash, H., Morowvat, M. H., Mohagheghzadeh, A., & Ardeshir-Rouhani-Fard, S. (2015). Essential oil composition and bioinformatic analysis of Spanish broom (Spartium junceum L.). Trends in Pharmaceutical Sciences, 1(2), 97-104.

Menghini, L., Massarelli, P., Bruni, G., & Pagiotti, R. (2006). Anti-inflammatory and analgesic effects of Spartium junceum L. flower extracts: a preliminary study. Journal of medicinal food, 9(3), 386-390.

International Conference on Science and Technology

ICONST 2018

5-9 September 2018 Prizren - KOSOVO

Sokak Aydınlatmalarında Kullanılan Yüksek Güçlü LED'lerin Farklı Türbülans Modeli ve Farklı Duvar Yaklaşımlarında Termal Analizi / Thermal Analysis of Various High Power Leds with Different Turbulance Models and Wall Approaches Using Cfd for Street Lights

Burcu Çiçek[1]*, Necmettin Şahin[2]

Özet: Işık yayan diyotlar (LED'ler) elektrik enerjisini doğrudan ışık enerjisine dönüştüren yarı-iletkenler cihazlardır. Bununla birlikte LED'ler kendisine uygulanan elektrik enerjisinin yaklaşık %20'sini ışık enerjisine dönüştürebilmektedir. Geri kalan enerji ısı enerji enerjisine dönüşürek LED çiplerinde yüksek sıcaklığa sebep olmaktadır. LED'lerde oluşan yüksek ısı akısı, LED'lerin ömür, kararlılık ve güvenirliğini etkilemektedir. Özellikle yüksek güçlü LED'lerde jonksiyon sıcaklığını izin verilen sınırın altında tutmak gerekir. Bu yüzden LED paketlerinin efektif termal yönetimi LED'lerin performansını geliştirmek açısından önemlidir. Son yıllarda birçok araştırmacı ve yüksek güçlü LED üreticisi LED çiplerini soğutmak için farklı metotlar üzerinde durmuştur. LED'lerde meydana gelen yüksek ısı akısını çözmek için kullanılan başlıca yöntemlerden biri LED paketini oluşturan bileşenlerde optimum malzeme seçimidir. Bunu yanı sıra yüksek güçlü LED paket tasarımında maliyetin kontrol edilmesi LED'in etkili soğutulması kadar önemlidir. Bu yüzden fan veya sıvı soğutma gibi pahalı soğutma yöntemlerinden kaçınmak gerekir. Faz değişimi yüksek ısı akısı üreten elektronik cihazlar için umut verici bir soğutma yöntemidir. Bu bağlamda yüksek ısı transfer katsayısına sahip, karmaşık parçalar içermeyen ve dolayısıyla bakım gerektirmeyen ısı boruları, LED'lerde ısı problemini çözmek için uygun ve düşük maliyeti bir soğutma yöntemi olarak görülmektedir. Literatürde, elektronik cihaz soğutması için ısı borularının kullanımı ile ilgili çalışmalar mevcuttur.

Bu çalışmada, sokak aydınlatmalarında kullanılacak yüksek güçlü LED'lerden ısı yayılımını sağlamak amacıyla U-şekilli silindirik bakır ısı boruları kullanılmıştır. Sistemin termal analizi ANSYS Fluent yazılımında sayısal olarak gerçekleştirilmiştir. İlk olarak dört farklı yüksek güçlü LED modeli kullanılan sistem, LED çip hacminin maksimum sıcaklık üzerindeki etkisini belirlemek için termal olarak analiz edilmiştir. Daha sonra sürekli rejimde yapılan ve sıkıştırılamaz akış koşulları varsayılarak her bir LED modeli için farklı türbülans modellerinin ve duvar yaklaşımlarının etkileri değerlendirilmiştir.

Anahtar Kelimeler: Yüksek güçlü LED, termal analiz, HAD, türbülans modeli

Abstact: Light emitting diodes (LEDs) are solid state semiconductor devices that directly convert electrical energy into light energy, however, LEDs convert only about 20% of the applied electric energy to light energy. The remaining energy is converted into heat energy, causing high temperatures in the LED chips. High heat fluxes in the LEDs limit the reliability, stability and lifetime of them. Especially in high power LEDs, it is necessary to keep the junction temperature below the allowable limit. So, effective thermal management of the LED package is critical to improve LED performance. In recent years, many researchers and high-power LED manufacturers have used different cooling methods for LED chips. One of the main methods is to select optimum materials of LED components to solve high heat flux problem

[1,2]Aksaray University, Department of Mechanical Engineering, 68100, Aksaray, TURKEY
*Corresponding author: cicekb@aksaray.edu.tr

that occurs on the LEDs. Besides, controlling the cost in high power LED package design is equally important as effective cooling. It is necessary to avoid expensive cooling methods such as fan or liquid cooling. Phase change is a promising cooling method for electronic devices that produce high heat flux. In this regard, heat pipes, which have high effective heat transfer coefficients, no complicated parts and are therefore maintenance free, are seen as a suitable and cost - effective cooling method for solving the heat problem in LEDs. In literature, studies related tu usage of heat pipes for electronic device cooling are available.

In this study, in order to provide heat dissipation of the high power LEDs to be used for street illumination, U-shaped cylindrical copper heat pipes are used. Thermal analysis of this system was carried out numerically in the ANSYS Fluent software. Firstly, thermal analysis was performed for different models of high power LEDs for determination of the effect of LED chip volume on maximum temperature. Afterwards, in the analyses performed in continuous regime and under the assumption of incompressible flow, the effects of different turbulence models and wall approaches on the solution were evaluated for each LED model.

Keywords: High power LEDs, thermal analysis, CFD, turbulence models

Giriş

LED'ler geleneksel akkor ve flüoresan lamba ile karşılaştırıldığında yüksek ışık akısı, uzun ömür ve güvenirlik gibi birçok avantaja sahip olmasına rağmen LED çiplerinde oluşan yüksek ısı akıları LED'in verimliliğini önemli ölçüde etkilemektedir. Bu nedenle LED performansını artırmak için LED çipinde meydana gelen yüksek sıcaklığı LED'den uzaklaştırmak gerekmektedir. Literatürde elektronik cihazların soğutulması ile ilgili çalışmalar mevcuttur(Shen vd., 2013, Tang vd., 2014 ve Moon vd., 2016). Özellikle ısı borusu simülasyonlarını hesaplamalı akışkanlar dinamiğinde gerçekleştiren de birçok çalışma bulunmaktadır.

Ashish vd.,(2016), düz ısı borulu termal yayıcının termal davranışı 3D-quasi matematiksel model tarafından tanımlamış ve sayısal olarak modellemişlerdir. Buhar fazındaki hesaplamalar için açık (explicit) sonlu hacimler metodu kullanılmıştır. Isı yayıcının ön ve arkası için geçici sıcaklık dağılımları elde edilmiştir. Aynı zamanda buhar çekirdeğindeki hız dağılımı da elde edilmiştir. Sayısal sonuçlar buhar fazının yüksek ısı yayılımının, buhar çekirdeğindeki sıcaklık dağılımını hızlandırdığı ve proses boyunca sıcaklık dağılımını uniform hale gelmesini sağladığı görülmüştür. Suresh ve Bhramara (2013) ise evaporatör bölgesinden ısıyı alıp kondenser bölgesine gönderen iki fazlı bir ısı değiştirici olan salınımlı ısı borusu ANSYS CFX'de sayısal olarak modellemiştir. Çalışma akışkanı olarak aseton kullanılan ısı borusunda doluluk oranı %60 olarak belirlenmiştir. Evaporatör sınırında 9 W'dan 15 W'a kadar ısı girişi sağlanmış ve kondenser girişinde sınır şartı olarak ise yaklaşık 7945 W/m^2 aralığında ısı akısı girilmiştir. Adyabatik kısmında ise ısı akısı sıfır alınmıştır. Buharlaştırıcıdaki aseton sıcaklığındaki düşüş ısının konderser bölümüne taşındığını göstermiştir. Isı borusunun evaporatör, kondenser ve adyabatik bölgelerindeki hava ve aseton oranlarındaki hacimsel oranın PHP'nin içindeki akış modeline yansıdığı görülmüştür.

Lin vd., (2013) minyatür oscillating ısı borularının ısı transfer mekanizmalarını incelemek ve ısı transfer kapasitelerini tahmin etmek amacıyla MOPH'un kapsamlı bir fiziksel ve matematiksel modeli inşa edilmiştir. Çalışma akışkanı olarak su kullanılmış olup simülasyonları karşılaştırmak için Volume of Fluid (VOF) ve Mixture Model Fluent'te kullanılmıştır. Sonuçlar MOPH'da, mixture modelininin iki fazlı akış simülasyonları için daha uygun olduğunu göstermiştir. Wang vd., (2015) yaptıkları çalışmada iki boyutlu tekli loop closed-loop pulsating heat pipe (CLPHP) CFD'de incelemişlerdir. VOF metodu, farklı evaporatör ve kondenser uzunluk oranları için CLPHP'nin termal performansı belirlenmiştir. Analizler, 10 W'dan 40 W'a kadar ısı girişi ve %30'dan %60'a doluluk oranı için gerçekleşmiştir. Elde edilen nümerik sonuçlar deneysel sonuçlarla karşılaştırılmış ve birbirlerine uygun olduğu görülmüştür.

Asmaie vd., (2016) iki fazlı akış ile ısı transferi sağlayan termosifonun simulasyonu için hesaplamalı akışkanlar dinamiği (HAD) modeli geliştirmiştir. Çalışma akışkanı olarak de-iyonize su ve CuO/Su

nanoakışkan kullanılmıştır. Sonuçlar nanoakışkandaki ısı akısının suya göre yaklaşık yüzde 46 daha yüksek olduğunu göstermiştir. Ayrıca nanoakışkan konsantrasyonunu artırılarak duvar sıcaklığının azaldığı ve optimum konsantrasyonun ağırlıkça %1 olduğu görülmüştür. Chaudhari vd., (2016) ısı borusunun farklı işletme koşulları altında termal davranışını çalışmak için deneysel çalışma gerçekleştirmişlerdir. Deneysel çalışmanın doğrulanması için ANSYS programında sayısal olarak simülasyon yapılmış ve sonuçlar karşılaştırılmıştır. Isı borusu damıtılmış su ve 40 nm ve 70 nm çapındaki CuO + BN hibrit nanoparçacıkları ile yüklenmiştir. Güç girişleri, ısı borusu eğim açısı ve nanopartikül konsantrasyonunun ısı borusu termal dirence etkileri araştırılmıştır. Sonuçlar % 2'lik hacimsel konsantrasyona sahip CuO+BN / H2O hibrit nanoakışkanların maksimum ısı transferi sağlamak için oldukça etkili olduğu görülmüştür.

Elnaggar vd., (2011) PC-CPU soğutması için U şeklinde ısı borusu kullanmışlardır. Isı borusuna kanatçıklar entegre edilmiştir. Deneyler, sistemi dikdörtgensel bir tünel içinde yer alan bir ısı kaynağı üzerine dikey olarak monte ederek gerçekleştirilmiştir ve bir üfleyici vasıtasıyla zorlanmış taşınım şartları oluşturulmuştur. Toplam termal direnç ve ısı transfer katsayısının tahmini için hem doğal hem zorlanmış taşınım modları kararlı koşullar altında yürütülmüştür. Deneysel sonuçların doğrulanması için ANSYS 10 yazılımında simülasyonlar yürütülmüş ve elde edilen sonuçların deneysel sonuçlarla uygun olduğu görülmüştür. Dev ve Budania (2016), ısı borusunun kararlı hal performanslarını analiz etmek için iki boyutlu sonlu elemanlar metodunu geliştirmişlerdir. Isı borusu boyunca sıcaklık dağılımını tahmin etmek için sonlu elemanlar modelini ANSYS yazılımında kullanmışlardır. Bu çalışmada farklı ısı borusu duvar malzemesi, farklı fitil efektif ısıl iletkenliği, evaporatörde farklı ısı akısı ve farklı çalışma akışkanı kullanılmıştır. Isı borusu duvarı ve fitil malzemesi için uygun malzeme ve termal iletkenlikler seçilmiştir. Schmid vd., (2017)150W'lık LED sokak aydınlatmaları için aktif bir hava soğutma sisteminin parçası olarak çift borulu bir ısı değiştiricisi kullanımını incelemişlerdir. Havanın bir fan yardımı ile lambanın içinde kapalı bir döngü oluşturacak şekilde sirkülasyonu ayarlanmıştır. Isının dış ortama olan ısı dağılımı doğal konveksiyon ile gerçekleşmektedir. Deneyler 5 m yüksekliğindeki prototiple gerçekleşmiş ve nümerik modelden elde edilen verileri doğrulamak için kullanıştır. Deneysel sonuçlardan LED'teki fazla sıcaklığın 42 °C'ye kadar düşürülebildiği görülmüştür. İki boyutlu aksi-simetrik nümerik bir çalışma ile boru uzunluğu, malzeme iletkenliği, akış yönü, boru çapı oranı, kütle akış hızı ve ısı aktarım hızı gibi değişen parametrelerin performans üzerindeki etkisi incelenmiştir. Sonuçlar lamba direğinin uzatılma oluşan ısı kaybının büyük oranda akış hızına bağlı olduğunu gösteriyor.

Bu çalışmada yol, sokak ve cadde aydınlatmaları için 4 adet 25 W'lık yüksek güçlü COP LED çipi bulunan LED paketleri tasarlanmıştır (Şekil 1). LED paketi sırasıyla InGaN LED çipi, ötektik malzemesi, kalıp, kalıp bağlantı malzemesi, elektronik devre kartı ve termal ara yüzey malzemesinden oluşmaktadır. Tasarlanmış LED paketinin boyutları ve termal iletkenlikleri Tablo 1'de verilmiştir. Soğutucu plakanın hemen altına yerleştirilen ısı borularının özellikleri de Tablo 2'de verilmiştir. Sistemde kullanılan U şeklinde bakır ısı borularında çalışma akışkanı olarak su tercih edilmiştir. Dış ortam sıcaklığı ise 35°C olarak alınmıştır. İlk olarak tasarlanan modelde farklı hacimlerde LED çipleri kullanılmış ve aynı güç girişi için termal analizleri yapılmıştır. Buna göre LED çip hacmi arttıkça birim hacim başına üretilen ısı miktarı azalacağından modelin maksimum sıcaklığında bir miktar düşme görülmüştür. İkinci olarak da analizlerde 6 farklı türbülans modeli ve 3 farklı duvar yaklaşımı kullanılmıştır. Hesaplamalar sonunda, analizlerde farklı türbülans ve duvar yaklaşımları kullanılmasının elde edilen maksimum LED değerlerinde görülür şekilde farklılıklar oluşturduğu görülmüştür.

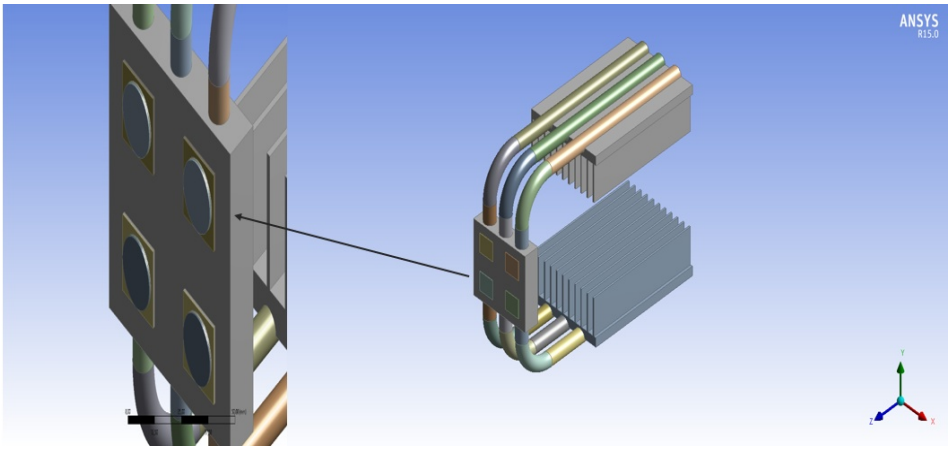

Şekil 1. Tasarlanan Modelin Geometrisi

Materyal ve Metot

Hesaplamalı Akışkanlar Dinamiği (HAD), akışkanlar mekaniğinin sayısal analiz ve algoritmalarını kullanan bir dalıdır; akışkan akışları içeren problemleri hesaplar ve analiz eder. Bu çalışmada nümerik hesaplamalar için ANSYS Fluent 15.0 programı kullanılmıştır. Tasarlanan model ANSYS Fluent'te 3 aşamada nümerik olarak çözülmüştür.

Ön İşlemci: Ön işlemcide sistem Ansys Workbench'te modellenmiş ve oluşturulan modelin verileri Mesh'e aktarılarak ağ yapısı oluşturulmuştur. Ağ yapısı oluşturulurken skewness faktörü 0.96'dan daha düşük ve trapez (üçgen) yapıda olması dikkat edilmiştir. Sistemde iç içe iki akış alanı modellenmiş ve dıştaki akış alanının ağ yapısı içtekinden daha seyrek oluşturulmuştur. Model üzerinde her bir analiz için yaklaşık 5000000 eleman ve 1300000 düğüm noktası elde edilmiştir. Ağ yapısının detayları Şekil 2'de verilmiştir.

Tablo 1. Tasarlanan LED paketinin yapısal boyutları ve termal iletkenlikleri.

	Genişlik (mm)	Boyut (mm)	Malzeme	Termal İletkenlik (W/m.K)
LED Çipi	0.6	R=17	GaN	130
Metalizasyon Malzemesi	0.01	"	Au-Si ötektik bağlama	27
Kalıp	0.375	"	Silikon	124
Kalıp Bağlantısı	0.05	"	Au-20Sn	57
Elektronik Devre Kartı	0.3/ 0.38 / 0.3	19×19	Al_2O_3 DBC	24
TIM	0.05	"	Termal ara yüzey malzemesi	3
Soğutucu Plaka	-	-	Alüminyum	202

Tablo 2. Isı borusunun özellikleri

Parametreler	
Toplam ısı borusu uzunluğu	0.58 m
Isı borusu kondenser uzunluğu	0.20 m
Isı borusu evaporatör uzunluğu	0.10 m
Isı borusu çapı (D)	0.010 m
Isı borusu malzemesi	Bakır
Toplam ısı girişi (Her bir LED için)	25 W
Isı borusu termal iletkenliği	20000 W/m.K
Çalışma akışkanı	Su

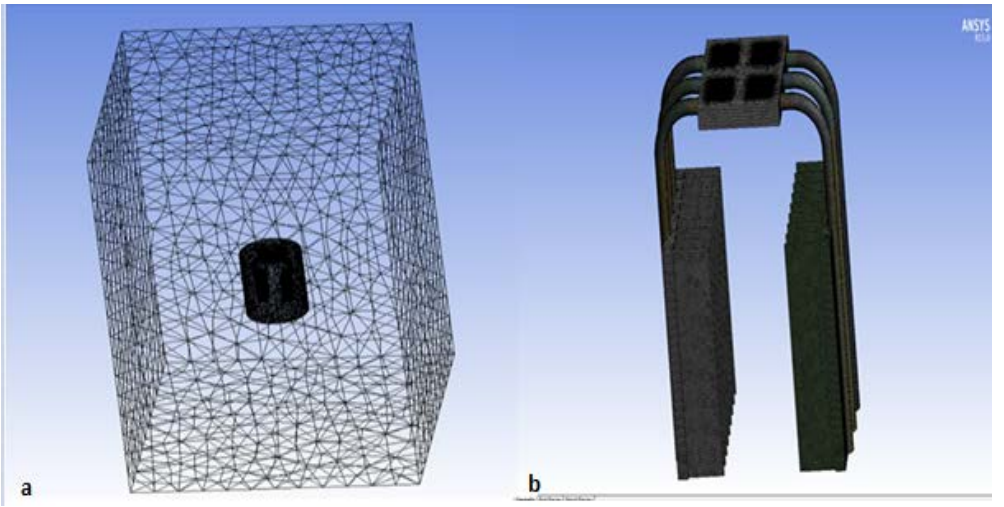

Şekil 2. Tasarlanan sistemin ağ yapısı

Çözücü: Çözücüde sınır şartları girilmiş ve Navier-Stokes denklemleri kullanılarak hesaplamalar yapılmıştır. Navier Stokes denklemleri süreklilik, momentum ve enerji olmak üzere üç denklemden oluşur. Bunlar, denklem (1-5)'de verilmiştir. Nümerik hesaplamalar için Simple Method ve Turbulent Mixing Length modeli kullanılmıştır.

Süreklilik Denklemi

$$\frac{\partial u}{\partial x}+\frac{\partial v}{\partial y}+\frac{\partial w}{\partial z}=0 \tag{1}$$

Momentum Denklemi

x- momentum

$$\rho\left(u\frac{\partial u}{\partial x}+v\frac{\partial u}{\partial y}+w\frac{\partial u}{\partial z}\right)=-\frac{\partial \rho}{\partial x}+\mu\left(\frac{\partial^2 u}{\partial x^2}+\frac{\partial^2 u}{\partial y^2}+\frac{\partial^2 u}{\partial z^2}\right) \tag{2}$$

y- momentum

$$\rho\left(u\frac{\partial v}{\partial x}+v\frac{\partial v}{\partial y}+w\frac{\partial v}{\partial z}\right)=-\frac{\partial \rho}{\partial y}+\mu\left(\frac{\partial^2 v}{\partial x^2}+\frac{\partial^2 v}{\partial y^2}+\frac{\partial^2 v}{\partial z^2}\right) \quad (3)$$

z- momentum

$$\rho\left(u\frac{\partial w}{\partial x}+v\frac{\partial w}{\partial y}+w\frac{\partial w}{\partial z}\right)=-\frac{\partial \rho}{\partial z}+\mu\left(\frac{\partial^2 w}{\partial x^2}+\frac{\partial^2 w}{\partial y^2}+\frac{\partial^2 w}{\partial z^2}\right) \quad (4)$$

Enerji Denklemi

$$\left(u\frac{\partial T}{\partial x}+v\frac{\partial T}{\partial y}+w\frac{\partial T}{\partial z}\right)=\frac{1}{\alpha}+\mu\left(\frac{\partial^2 w}{\partial x^2}+\frac{\partial^2 w}{\partial y^2}+\frac{\partial^2 w}{\partial z^2}\right) \quad (5)$$

Son İşlemci: Son işlemcide elde edilen bulgular görselleştirilmiştir. Sistemin sıcaklık dağılımları elde edilmiştir.

Nümerik Analiz

Bu çalışmada, sokak aydınlatmalarında kullanılacak LED paketlerinin soğutulması için tasarlanan modelde 3 adet U-şeklinde bakır silindirik ısı borusu kullanılmıştır. Isı boruları evaporatör, adyabatik ve kondenser olmak üzere 3 bölgeden oluşmaktadır. Sıcak ortamdan ısı çekip kondensere ileten evaporatör bölgesi ısı üretiminin maksimum olduğu LED çipinin altındaki soğutucu plakanın içine entegre edilmiştir. Kondenser bölgesinde çalışma akışkanının yoğunlaşıp ortama daha fazla ısı vermesi için soğutucu plakalar yerleştirilmiştir. Isı transfer yüzey alanını artırmak için de kanatçıklı yapı oluşturulmuştur. Verilen çalışma koşulları altında modelin termal analizi ANSYS Fluent programında yapılmıştır. Şekil 3'te analizin yakınma diyagramı verilmiştir. Yaklaşık 4400 iterasyon sonucu programın yakınsadığı görülmüştür. Son işlemci kısmında ise verilen geometri ve sınır şartlarında tüm modelin sıcaklık dağılımı elde edilmiştir (Şekil 4).
Tasarımda her biri 25 W'lık Luxeon COB 1208 LED çipi kullanılmıştır. Analiz sonuçlarına göre her bir LED'te oluşan maksimum sıcaklık 78.2 °C olarak belirlenmiştir.

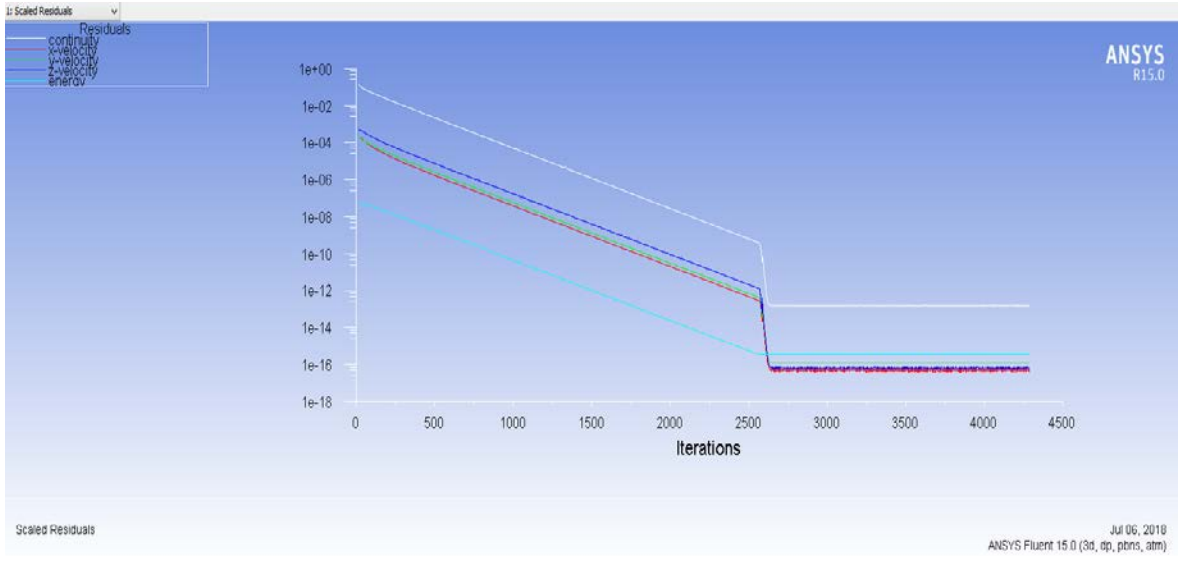

Şekil 3. Fluent programı çözücü kısmında analizin yakınsama diyagramı.

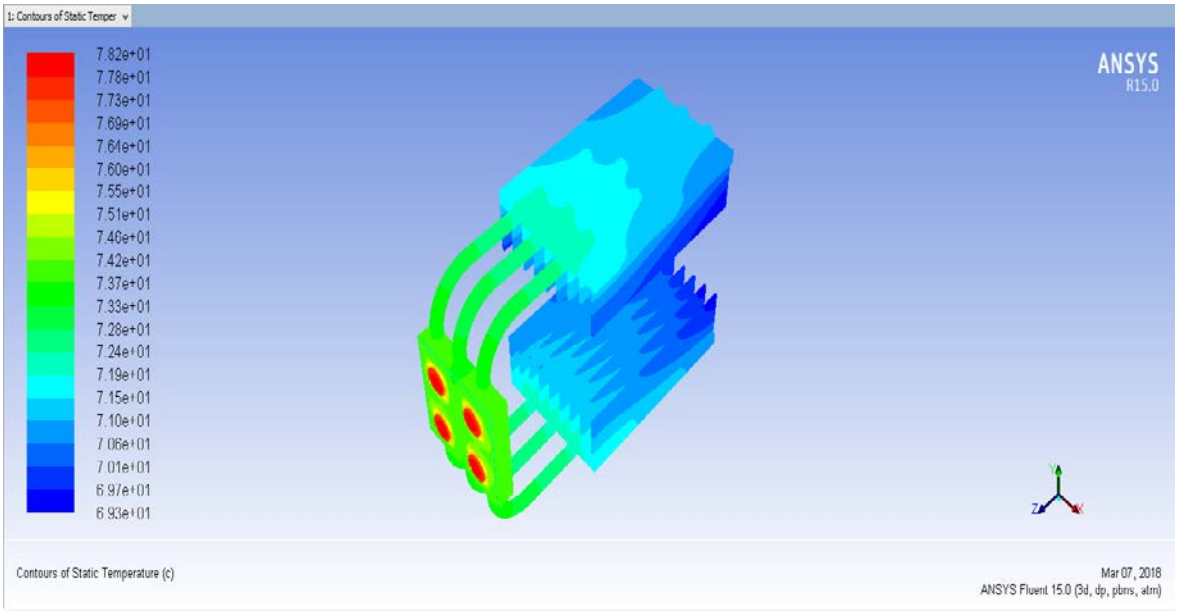

Şekil 4. Tasarlanan sistemin verilen geometri ve sınır şartlarında sıcaklık dağılımı.

LED Hacminin Maksimum Sıcaklığa Etkisi

Elektronik cihazların minyatürleştirilmesi birim hacim başına üretilen ısı miktarında artışa neden olur. Şekil 4'de sıcaklık dağılım grafiği verilen sistemde LED çipi olarak 25 W gücünde 4 adet eş LED çipi kullanılmıştır. Bu çalışmada Lumiled Luxeon COP LED'e ek olarak LED çip hacminin maksimum sıcaklığa etkisini incelemek için farklı boyutta 4 LED çipi daha ele alınmıştır. Şekil 1'de verilen model üzerine bu LED çipleri entegre edilmiş ve aynı sınır koşulları altında ANSYS Fluent yazılımıyla analizler gerçekleştirilmiştir. Cree-Xlamp, Osram ve Sequl gibi farklı markalardan oluşan LED'lerin boyutları ve özellikleri her bir LED'in kataloğundan bulunmuştur. Şekil 5'te tasarımda kullanılan LED çiplerinin boyutları verilmiştir. Buna göre her bir LED'e 25 W'lık güç verilerek benzer sınır şartlarında analizler yapılmıştır. Elde edilen sıcaklık dağılımları ve optik özellikleri karşılaştırılmıştır. Tablo 3'de analiz sonucu elde edilen LED'lerin modeli, LED hacmi, birim başına üretilen ısı miktarı ve izin verilen maksimum jonksiyon sıcaklıkları verilmiştir.

Tablo 3. LED çip modelleri ve özellikleri

LED Markası	Modeli	LED çip hacmi	Birim başına üretilen ısı miktarı	İzin verilen maksimum Jonksiyon Sıcaklığı
Cree® XLamp®	CXA1520 LED	47.625mm^3	3.83e+08W/m^3	150°C
OSRAM	SOLERIQ® S 13	77.299mm^3	2.36+08W/m^3	125°C
SEQUL	ZC25 – Z-Power COB	183.98 mm^3	9.97+07 W/m^3	125°C
Cree® XLamp®	CXA2530 LED	190.5 mm^3	9.58+07 W/m^3	150°C

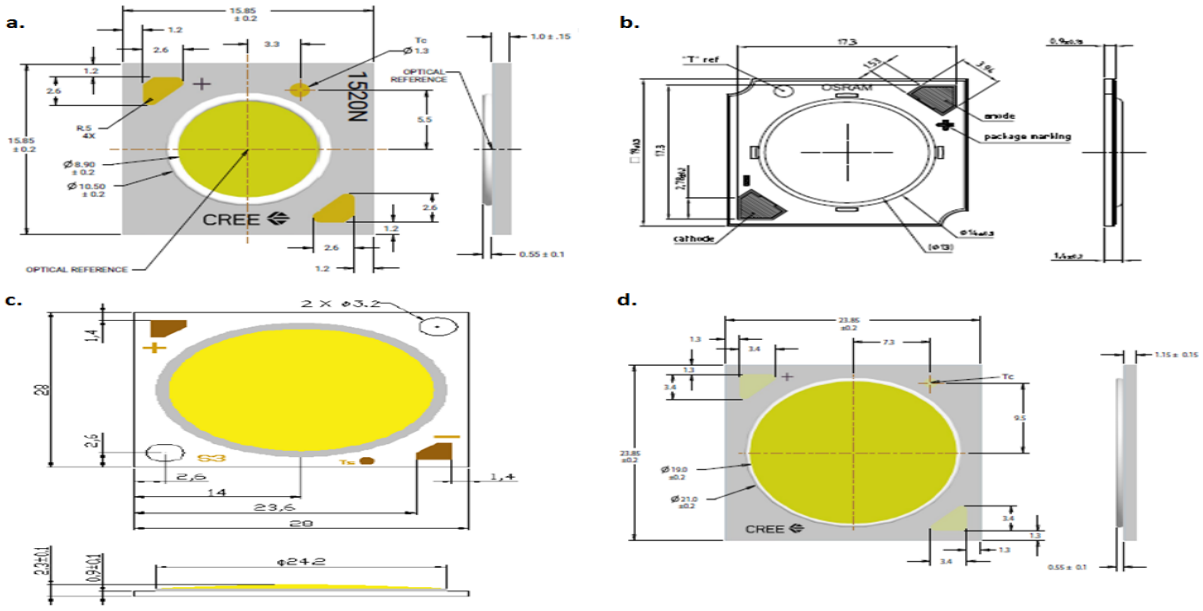

Şekil 5. a. Cree® XLamp® CXA1520 LED (Cree, 2018a), b. OSRAM SOLERIQR S 13 (Sarnikon, 2018), c. SEQULZC25 – Z-Power COB (Mouser, 2018), d. Cree® XLamp® CXA2530 LED (Cree, 2018b).

Tasarlanan mevcut modelin diğer tüm geometrik özellikleri ve sınır şartları aynı kalmak suretiyle, Şekil 5'de boyutları verilen 4 farklı LED çipi tasarımda kullanılarak ANSYS Fluent programında sıcaklık değerleri elde edilmiştir (Şekil 6-9).

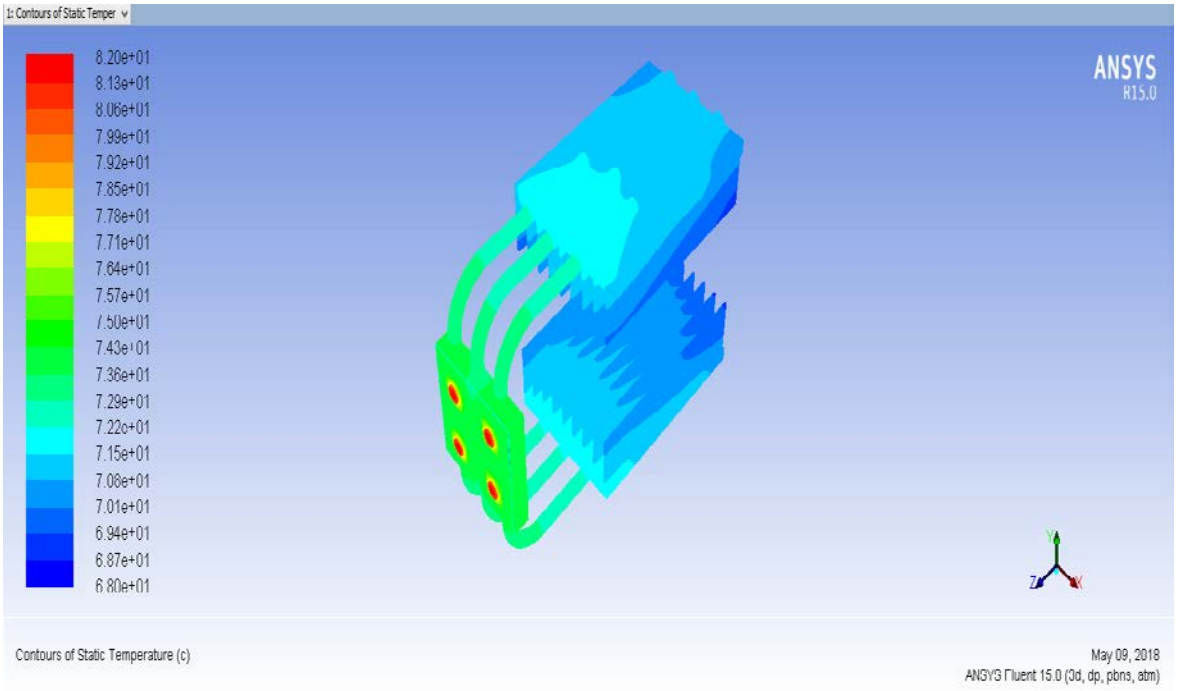

Şekil 6. Cree® XLamp® CXA1520 LED çipi ile tasarlanan modelin sıcaklık dağılım grafiği

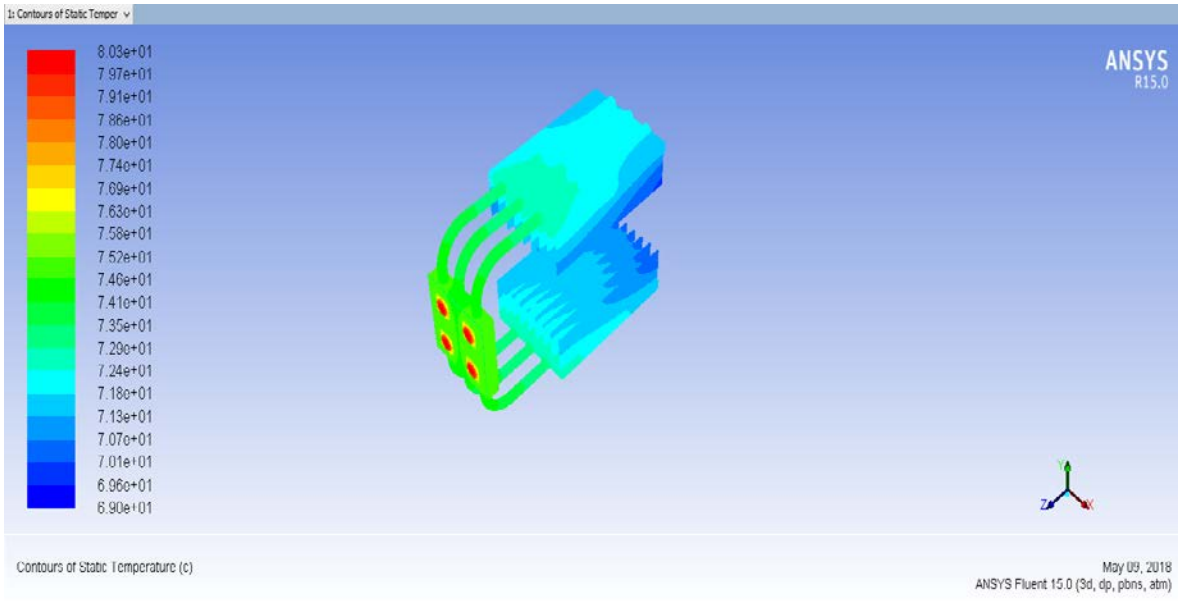

Şekil 7. OSRAM SOLERIQR S 13 LED çipi ile tasarlanan modelin sıcaklık dağılım grafiği

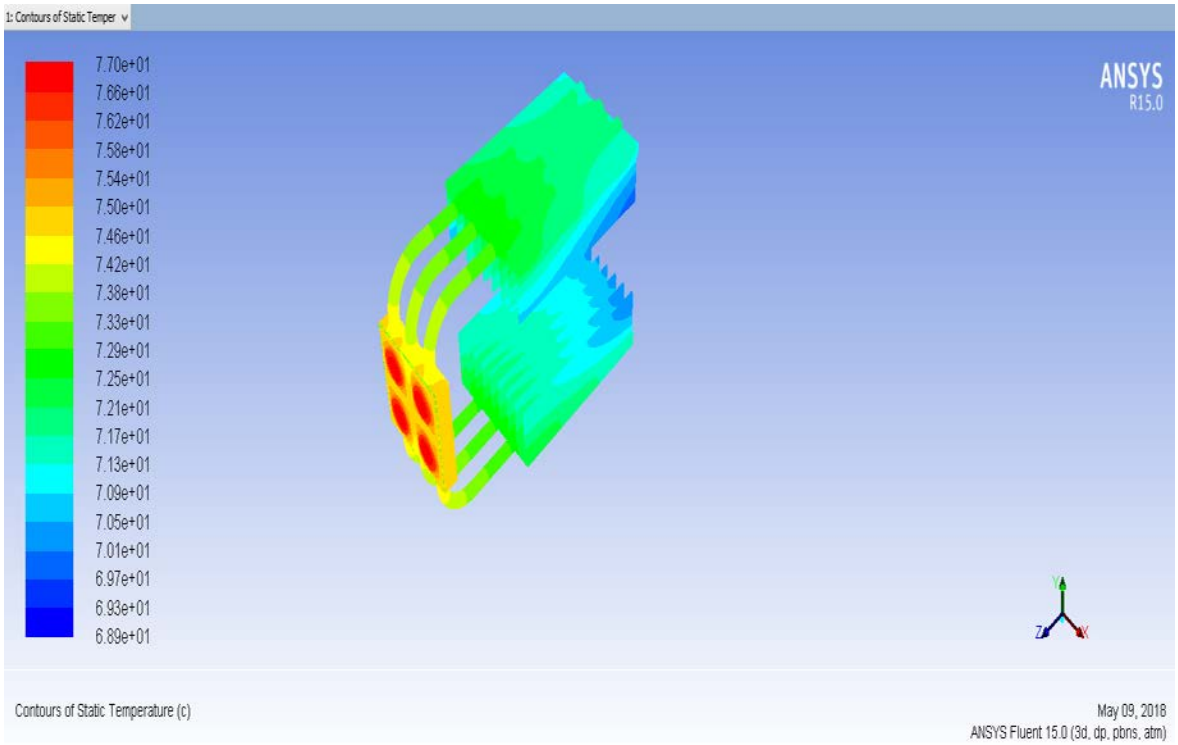

Şekil 8. SEQULZC25– Z-Power COB LED çipi ile tasarlanan modelin sıcaklık dağılım grafiği

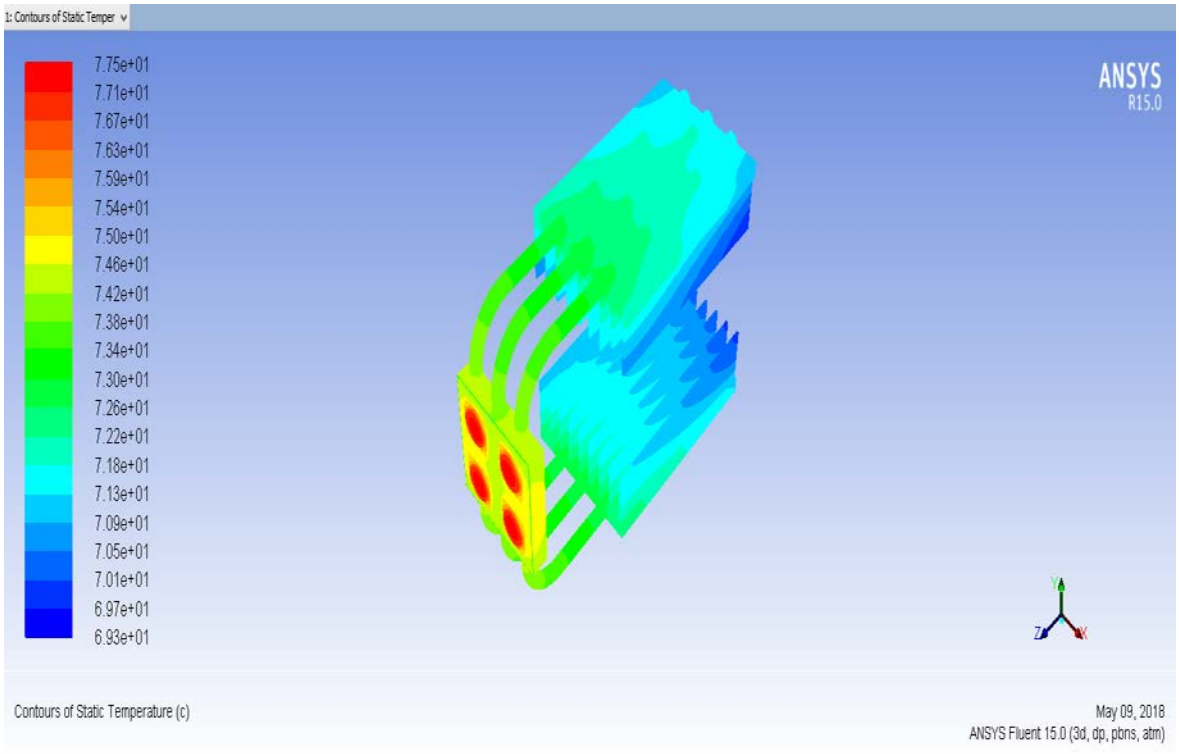

Şekil 9. Cree® XLamp® CXA2530 LED çipi ile tasarlanan modelin sıcaklık dağılım grafiği

Farklı Türbülans Modelleri ve Duvar Yaklaşımlarının Maksimum Sıcaklığa Etkisi

Duvar fonksiyonları hesaplamalı akışkanlar dinamiğinde yaygın olarak kullanılır ve hesaplamalarda oldukça kolaylık sağlar. Tasarlanan sistemin termal analizlerinde türbülans modeli olarak Turbulent Mixing Lengh modeli ve duvar yaklaşımı olarak da Standart Wall Function fonksiyonları kullanılmıştır. Bu çalışmada ek olarak Standart k-ε, Rng-k- ε, Realizable k- ε, Standart k-w ve SST-k-w gibi türbülans modelleri Standart Wall Function, Enhanced Wall Treatment ve Non Equilibrium Wall Function gibi farklı duvar yaklaşımlarıyla birlikte uygulanmış ve maksimum LED sıcaklık değerleri elde edilmiştir. Birim başına üretilen ısı miktarı farklı 4 LED çipi için, farklı türbülans modelleri ve duvar yaklaşımları ile birlikte sayısal analizler yapılmış ve elde edilen maksimum LED sıcaklıkları Tablo 4'te verilmiştir.

Tablo 4. Farklı türbülans modeli ve duvar yaklaşımlarına göre maksimum LED sıcaklık değerleri

Türbülans Modeli	Duvar Yaklaşımı	Maksimum LED Sıcaklığı (°C)			
		Cree® XLamp® CXA1520 LED	OSRAM SOLERIQR S 13	SEQULZC25 – Z-Power COB	Cree® XLamp® CXA2530 LED
Turbulent Mixing Length	-	82.0	80.3	77	77.5
Standart k-ε	Standard Wall Function	84.9	83.04	79.8	80.4
	Enhanced Wall Treatment	87.2	85.42	82.1°C	82.7
	Non Equilibrium Wall Function	78.9	77.1	73.9	74.4
Rng-k- ε	Standard Wall Function	87.1	85.32	82	82.6
	Enhanced Wall Treatment	87.8	86.02	82.7	83.3
	Non Equilibrium Wall Function	87.3	85.52	82.2	82.8
Realizable k-ε	Standard Wall Function	87.4	85.6	82.3	82.7
	Enhanced Wall Treatment	87.33	85.5	82.2	82.6
	Non Equilibrium Wall Function	80.2	78.4	75.1	75.7
Standart k-w	-	87.25	85.4	82	82.5
SST-k-w	-	88.13	86.3	82.9	83.55

Sonuç ve Tartışma

Bu çalışmada Şekil 1'de görüldüğü gibi 4 adet 25W'lık LED çipinin sistemin soğutulması için U-tipi silindirik bir ısı borusu kullanılmıştır. Isı borusu 3 adet bileşenden oluşmaktadır. Bunlar evaporatör, adyabatik ve kondenser bölgesidir. Evaporatör bölgesi ısıyı alıp kondensere iletmek için kurulan bir mekanizmadır bu yüzden ısı üretiminin maksimum olduğu LED çipinin hemen altındaki bakır levhaya yerleştirilmiştir. Sistemden taşınım yoluyla maksimum ısı atılabilmesi için kondenser bölgesine alüminyum soğutucu plaka entegre edilmiştir. Soğutucu plakanın üzerine ısı transfer yüzey alanını genişletmek amacıyla kanatçıklı yapı kullanılmıştır.

İlk olarak tasarlanan modelde farklı hacimlerde LED çipleri kullanılmış ve aynı güç girişi için termal analizler yapılmıştır. Buna göre LED çip hacmi arttıkça birim hacim başına üretilen ısı miktarı azalacağından LED çipinin maksimum sıcaklığında bir miktar düşme görülmüştür. LED çip hacmi 47.625 mm^3 olan Cree® XLamp® CXA1520 LED ile 190.5 mm^3 olanCree® XLamp® CXA2530 LED'e aynı güç uygulandığında oluşan maksimum sıcaklık farkının yaklaşık 5°C olduğu belirlenmiştir. Bunun yanı sıra SEQUL ZC2–Z-Power COB'un birim hacim başına üretilen ısı miktarının Cree® XLamp® CXA2530 'den daha büyük olmasına rağmen elektronik devre kartı boyutunun etkisinden dolayı SEQUL ZC2–Z-Power COB'un analizde elde edilen maksimum sıcaklığı daha düşük bulunmuştur. Buradan da elektronik devre kartı boyutunun da maksimum sıcaklığa etkili olduğu görülmüştür.

İkinci olarak da analizlerde 6 farklı türbülans modeli ve 3 farklı duvar yaklaşımı kullanılmıştır. Hesaplamalar sonunda, analizlerde farklı türbülans ve duvar yaklaşımları kullanılmasının, elde edilen maksimum LED değerlerinde görülür şekilde farklılıklar oluşturduğu görülmüştür. Aynı türbülans modelinde farklı duvar yaklaşımları kullanıldığında maksimum LED sıcaklık değerleri arasında yaklaşık 6-7 °C'ye kadar değişme gözlenmiştir.

Kaynaklar

Asmaie, L., Haghshenasfard, M., Mehrabani-Zeinabad, A., Esfahany, M. N. (2013). Thermal performance analysis of nanofluids in a thermosyphon heat pipe using CFD modeling, Heat and Mass Transfer, 49(5), 667-678.

Ashish R., Chaudhari , Bhosale S. Y. (2016). CFD Validation and experimental investigation of circular heat pipe using hybrid nanofluid, International Journal of Innovative Research in Science, Engineering and Technology, Vol. 5, Issue 9, September.

Carbajal, G., Sobhan, C. B., Queheillalt, D. T., Wadley, H. N. (2007). A quasi-3D analysis of the thermal performance of a flat heat pipe", International Journal of Heat and Mass Transfer, 50(21-22), 4286-4296.

Cree, (2018a). http:// www.cree.com/led-components/media/documents/ds-CXA1520.pdf / (Erişim tarihi: 12.04.2018).

Cree, (2018b). http://www.cree.com/led-components/media/documents/ds-CXA2530.pdf / (Erişim tarihi: 12.04.2018).

Dev, K., Budania, B. (2016). Sımulatıon And Modelıng Of Heat Pipe, International Journal of Technical Research (IJTR),Vol. 5, Issue 1, Mar-Apr.

Elnaggar, M. H., Abdullah, M. Z., Mujeebu, M. A. (2011). Experimental analysis and FEM simulation of finned U-shape multi heat pipe for desktop PC cooling, Energy Conversion and Management, 52(8-9), 2937-2944.

Lin, Z., Wang, S., Shirakashi, R., Zhang, L. W. (2013). Simulation of a miniature oscillating heat pipe in bottom heating mode using CFD with unsteady modeling, International Journal of Heat and Mass Transfer, 57(2), 642-656.

Mouser, (2018). Mouser Electronics. https:// www. mouser.com.tr/datasheet /2/363/ZC25%20SDW04F1C%20or%20SDW84F1C%20 [7-2013]-1202857.pdf./(Erişim tarihi: 13.08.2018).

Moon, S. H., Park, Y. W., Yang, H. M. (2016). A single unit cooling fins aluminum flat heat pipe for 100W socket type COB LED lamp. Applied Thermal Engineering.

Sarnikon, (2018). Sarnikon Metal Ve Elektronik San. Tic.Ltd.Şti. http://www.sarnikon.com/led-led-aydinlatma-cozumleri/osram-led-chip/osram-led-soleriq-s13/ (Erişim tarihi: 12.04.2018).

Schmid, G., Huang, Z. L., Yang, T. H., Chen, S. L. (2017). Numerical analysis of a vertical double-pipe single-flow heat exchanger applied in an active cooling system for high-power LED street lights. Applied Energy, 195, 426-438.

Shen, S.C., Huang, H.J., Shaw, H.J. (2013). Design and estimation of a MCPCB-Flat Plate heat pipe for LED array module, Proceedings of 2013 IEEE International Conference on Mechatronics and Automation August 4 - 7, Takamatsu, Japan.

Suresh, Z. V., Bhramara, B. (2016). CFD analysis of single turn pulsating heat pipe, International Journal of Scientific & Engineering Research, Volume 7, Issue 6, June-2016 238 ISSN 2229-5518 IJSER.

Tang, Y., Ding, X., Li, Z., Li, B. (2014) A high power LED device with chips directly mounted on heat pipes, Applied Thermal Engineering 66- 632-639.

Wang, J. C., Huang, H. S., Chen, S. L. (2007). Experimental investigations of thermal resistance of a heat sink with horizontal embedded heat pipes, International Communications in Heat and Mass Transfer, 34(8), 958-970.

International Conference on Science and Technology

ICONST 2018

5-9 September 2018 Prizren - KOSOVO

A Comparison of the Multivariate Calibration Methods with Feature Selection for Gas Sensors' Long-Term Drift Effect

Gulnur Begum Cangoz*[1], Selda Guney

Abstract: In many electronic nose applications where gas sensors utilizing for a long time, there is an undesirable drift effect on the sensors, which affects the classification quality negatively. Although the sensor drift is inevitable, it is possible to reduce this effect with the calibration transfer methods. This paper presents a comparison study of various multivariate standardization methods to facilitate an effective calibration way on a comprehensive dataset, which is reachable on-line. In this study, three methods applied: direct standardization (DS) orthogonal signal correction (OSC) and piecewise direct standardization (PDS). In addition, these three methods are applied data, which consisted of selected features. The results have shown that the classification success has increased with multivariate calibration technique applied to the selected features.

Keywords: calibration transfer; feature selection; gas sensors; multivariate drift correction; standardization methods

Introduction

In the last few decades, there has been significant improvement of electronic nose (e-nose) devices, which are consisting of gas sensor arrays. Whilst gas sensors are operating in a long time, the sensors' responses change in time without any control, and it is called sensor drift. There are two types of sensor drift: short-term (also called second order drift) and long-term drift (also called first order or real drift). The short-term drift occurs because of vicinity factors. For instance, temperature, humidity, thermal, and memory effects cause the short-term drift. These factors can keep under control. On the other hand, long-term drift cannot. The long-term drift is inevitable, because it occurs at sensors' internal structures. As we know, the chemical processes are not reversible. For robust measurements, sensors' responses need to stabilize over time. Hence, the calibration methods are propose to cope with drift effect [1].

Different ways have been tried for getting rid of sensor drift with a calibration model in the literature so far. To correct the drift effects, some of studies are utilized the univariate calibration techniques, some of them are utilized the multivariate calibration techniques. For the univariate technique, every variables of the master instrument matches the variables of the slave instrument for fitting a curve. After calculating two variables of the curve slope and intercept point, the univariate calibration can be used to get the results. However this technique seems easy for usage, it does not appropriate solution considering gas sensors' applications. So, we focused on the multivariate calibration techniques in this study.

So many studies with different ways and proposed methods had been done in the literature before. However, a reviewed article [2] is one of the most comprehensive one. Several methods reviewed in this article, and some of the methods were studied with near infrared (NIR) data. They investigated direct standardization (DS), piece-wise direct standardization (PDS), artificial neural network (ANN), maximum likelihood principal component

[1] Department of Electrical and Electronic Engineering, Baskent University, Ankara, Turkey
Correspondingauthor: gbcangoz@baskent.edu.tr

analysis (MLPCA), and positive matrix factorization (PMF). According to the work, PDS may be the best solution for complex systems. Moreover, ANN can be easily applied, but it suffers from overfitting problem. As a result of this article, for choosing the best technique there is no perfect guideline.

Another study about calibration transfer methods is [3]. In this study, in order to specify some ingredients in gasoline three NIR spectrometers are studied. DS, PDS, orthogonal signal correction (OSC), reverse standardization (RS), piecewise reverse standardization (PRS), slope and bias correction (SBC), and model updating (MU) methods are compared to each other and researchers claimed that RS is the best method. Furthermore, MU is the best way, when the transfer samples cannot storage practically.

Although some methods are using for interpreting the signals, e.g., principal component analysis (PCA) and partial least squares (PLS), they also are using for the component correction [4]. It is because; component correction is based on OSC. With using 39 gas sensors for four gases, and after logging the recordings for two months, multiplicative drift correction (MDC), PCA and PLS based component correction methods are compared, and the best root mean square error prediction (RMSEP) value could get by PLS based component correction method [5].

According to the literature, the most successful and the popular methods seem DS, PDS and OSC [6-10]. Just as the former literature's works, we followed the trend in our study, and compared their classification successes for different features.

Material and Methods

A.Dataset

We used a comprehensive dataset, which is freely reachable on-line for our study [11]. The dataset was consisted by A. Vergara and his team. They collected data from sixteen metal-oxide gas sensors' for three years, and they got 13,910 recordings. Their aim is to distinguish the six different components: ammonia, acetaldehyde, acetone, ethylene, ethanol, and toluene regardless of their concentration. They extracted eight features: the steady-state response of the sensors (the differentiation maximum value and minimum value of sensor response), normalized version of steady-state response, exponential moving average of both rising, and decaying portion of the sensor response for three different smoothing parameters.

The data they collected for 36 months are not distributed uniform month by month. That is why, they composed 10 batches instead of categorizing 36 measurement sets. In our study, we used batch 7 and batch 10. It is because that month 21, which means batch 7, has 3613 total recordings. On the other side, month 36, batch 10, has 3600 total recordings with every kind of gas. We intent to build a calibration model via these samples. Our goal is to train the model on batch 7 and to test it on batch 10. Because, the time interval between two batches is 15 months and it is enough to investigate drift effect on sensors' surface. We assumed that the data of batch 7 is obtained from master instrument, and the data of batch 10 is obtained from slave instrument.

B. Feature Selection

Feature selection has an important role for the machine learning systems. The main aim of the feature selection is that neglect some input features that effecting output minor. In other words, the feature selection is applied to reduce the dimension of the data. It also means that data become more understandable. Furthermore, the irrelevant input features cause greater computational cost. Namely, the feature selection is essential.

There are many ways to select the features from the data. In our work, we used the sequential selection algorithm. It starts with computing all feature subsets, which consist of only one input feature. So, it measures the Leave-One-Out Cross Validation error of the one-component subsets [12].

C. Methods

The need of the calibration model discussed earlier. The general idea of all the calibration methods is that modelling variations between two instruments and diminish it. Creating a calibration model consisting of four fundamental steps.

1. Selecting the transfer samples from both master and slave instruments. D optimal, E optimal, and Kennard-Stone (KS) algorithm can be performed to choose the transfer samples.
2. Generating a mathematical model via transfer samples.
3. Transform the slave instrument's transfer samples to the master instrument's responses.
4. Eventually, the prediction model is trained on master instrument's transfer samples, and it is ready for mathematical manipulating in order to reduce drift effect.

Among the different calibration models, we select the above model and we used DS, PDS and OSC methods to transform the slave instrument's samples to the master instrument's response. These methods applied to the slave instrument's data for the correction. An illustration of this correction can be seen in the Fig. 1 [13].

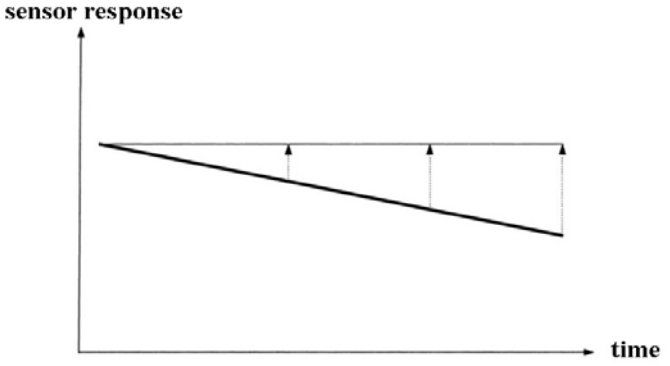

Fig. 1. Drift affect on a sensor

Direct standardization (DS) is one of the multivariate calibration techniques, proposed by Wang et. al. [14]. This method uses a transformation matrix, T, provides a linear relationship between two instruments' responses. As Y1 is a master instrument's standardized samples matrix and Y2 is the slave samples matrix, which is consisting of samples that was going to manipulate in order to adjust drift effect. T transformation matrix can be calculated as (1).

$$T = Y_2^{+} Y_1 \qquad (1)$$

where Y_2^{+} is a pseudo-inverse of Y_2. After calculating T, instrument responses can be predicted by multiplying new samples transpose matrix with T. As we can see, this method presents a linear relationship. Therefore, it is not an excellent technique. Besides, it has over-fitting problem, unless there is enough transfer samples.

Piecewise direct standardization (PDS) is an also the multivariate calibration technique [14]. This method is similar to DS except it uses windowing technique. Every transfer samples of the master instrument correspond to slave instrument's transfer samples, which are located in a sliding window.

For example, the number of the sensors be n, *i* be the any sensor, and r be the response of the standardization samples measured on the master instruments is corresponding to the sensors located in the window around *i*th sensor. For getting a sub-transformation matrix of *i*th sensor t*i*, (2) is applied where R is the response matrix of the transfer samples.

$$r_i = R_i t_i \qquad (2)$$

Afterwards, for all the sensors, sub-transformation matrices compiled in one big matrix, which is illustrated as symbol T.

$$T = \mathrm{diag}\,(t_1^T, t_2^T, t_3^T, \ldots, t_n^T) \qquad (3)$$

With calculated matrix T, the calibration model can be applied in order to remove differences between two devices.

Orthogonal Signal Correction (OSC) is another method, and it generally uses for pre-processing [15]. The reason is that its objective is to remove the noise by finding the components, which are orthogonal to the data. Nowadays, OSC is also using for the multivariate calibration and the idea is the same: to remove vectors, which are orthogonal to both instruments to make the model more transferable [2].

The algorithm used in OSC is very much alike NIPALS algorithm, which used in PCA and PLS. In this algorithm, the weight vector (w) is updating, in accordance with the score vector (t). The score vector can be calculated as (4), and the standardized data's expression of X is given as (5).

$$t = X \cdot w \quad (4)$$

$$X_{osc} = X - \sum_{i=1}^{n} T_i P_i' \quad (5)$$

where T is the classes of gases, P is the loadings matrices, and n is the OSC factors, which means that how many time this procedure is applied.

In our work, we made a comparison of some calibration methods and we tried a different way for standardization process. We assumed that if the best features selected, the classification success may increase regardless of which calibration model is applied or unapplied. We attempted to select best features, which means that the highest classification success with chosen features. We applied DS, PDS and OSC to the comprehensive dataset. Besides, we tried these three different methods, and the raw data with the best features. Like mentioned, feature selection process is employed by the sequential selection algorithm.

To achieve our goal, we considered two batches: batch 7 and batch 10. For the analogy, the batch 7 is the master and the batch 10 is the slave instrument. Therefore, we analyzed two groups. Group 1 is consisting of chosen training and chosen test data from batch 10. Group 2 is consisting of chosen training data from batch 7 and chosen testing data from batch 10.

Results and Disscussion

Our attempt to increase the classification success began with finding the success of raw data, the direct standardized data, the standardized data by orthogonal signal correction, and the piece-wise direct standardized data. Afterwards, we determined the finest features and same methods applied again, but this time along with the selected features. The classification successes of the raw data, the direct standardized data, the standardized data by orthogonal signal correction and the piece-wise direct standardized data are given in Table 1. As shown in Table 1, the most efficient calibration method is PDS for both groups.

On the other hand, the classification successes of same adjustment with selected best features of data are given in Table 2. As shown in Table 2, the most effective calibration method is again PDS for two groups.

According to outcomes of the tables, it can be said that selecting features has a great impact on datasets, especially for group 2. The performance is improved for all adjustments except PDS. However, the success of PDS's and PDS with selected features' percentages are 95,41 and 94,81 in a row, and the difference between them seems minor.

For representing classification successes more clear, confusion matrices for raw data, and PDS with selected features technique for all six gases are demonstrated in Table III and Table IV respectively. By these results, Table V and Table VI are created, and they illustrate the sensitivity vs. specificity of the six gases. The most drifted data according to Table III and V, belongs to ammonia and toluene gas. It can be seen clearly from Table IV and VI, the correction of this data, and selected features increase the sensitivity success of the data.

Table 1. Classıfıcatıon Success For Calıbratıon Methods

Dataset		**Success (%)**			
Train Data Set	***Test Data Set***	***Success 1[a]***	***Success 2[b]***	***Success 3[c]***	***Success 4[d]***
Batch10	Batch10	87,68	60,83	95,41	87,73
Batch7	Batch10	64,12	63,33	67,91	64,12

Success of Raw Data, [b.] Success of Direct Standardization, [c.]Success of Piece-wise Direct Standardization, [d.]Success of Orthogonal Signal Correction

Table 2. Classıfıcatıon Success For Calıbratıon Methods wıth Selected Features

Dataset		**Success (%)**			
Train Data Set	***Test Data Set***	***Success 4[e]***	***Success 5[f]***	***Success 6[g]***	***Success 7[h]***
Batch10	Batch10	88,14	88,70	94,81	88,14
Batch7	Batch10	72,87	77,17	75,69	72,87

[e.]Success of Raw Data with selected feature, [f.]Success of Direct Standardization with selected feature, [g.]Success of Piece-wise Direct Standardization with selected feature, [h.]Success of Orthogonal Signal Correction with selected feature

Table 3. A Confusion Matrix For Raw Data

	Predicted Values						
		A[i]	***B[j]***	***C[k]***	***D[l]***	***E[m]***	***F[n]***
Actual Values	***A[i]***	358	0	0	22	0	0
	B[j]	0	331	0	0	1	0
	C[k]	0	51	118	0	0	0
	D[l]	51	40	0	444	0	3
	E[m]	0	0	2	0	324	2
	F[n]	0	0	0	38	65	323

Table 4. A Confusion Matrix For Pds Wıth Selected Features

	Predicted Values						
		A[i]	***B[j]***	***C[k]***	***D[l]***	***E[m]***	***F[n]***
Actual Values	***A[i]***	296	0	0	22	0	0
	B[j]	0	338	2	0	0	0
	C[k]	0	21	357	0	0	0
	D[l]	64	0	0	337	0	0
	E[m]	0	0	0	0	360	0
	F[n]	0	1	1	1	0	360

[i.]Ethanol, [j.]Ethylene, [k.]Ammonia, [l.]Acetaldehyde, [m.]Acetone, [n.]Toluene

Table 5. Sensitivity and Specificity for Raw Data

Gas	***Specificity (%)***	***Sensitivity (%)***
Ethanol	97,16	94,21
Ethylene	95,06	99,70
Ammonia	99,90	69,82
Acetaldehyde	96,33	82,53
Acetone	96,42	98,78
Toluene	99,71	75,82

Table 6. Sensitivity and Specificity for Pds Wıth Selected Features

Gas	***Specificity (%)***	***Sensitivity (%)***
Ethanol	96,52	93,08
Ethylene	98,79	99,41
Ammonia	99,83	94,44
Acetaldehyde	98,69	84,03
Acetone	100	100
Toluene	100	99,17

Conclusıon

Although gas sensors' drift is unavoidable, it has multiple solutions to eliminate this problem. The calibration transfer methods are useful to get rid of this drift effect. Moreover, these calibration methods can be more accurate by utilizing our study. In this context, we have got a significant improvement using the raw data, DS, OSC and PDS with the sequential selection algorithm. The results of our study have pointed out that selecting the best features also can be a technique for calibrating alone. The important point here is to select the features, which are least effected from the drift. This may be the motivation for the future works. On the other side, when it is combined with DS, OSC and PDS methods, the best classification success value can get with PDS. Once and for all, our comparison with or without feature selection, has a potential to use in many machine learning applications.

References

[1] T.C. Pearce, S.S. Schiffman, H.T. Nagle, and J.W. Gardner, Handbook of Machine Olfaction. 1st ed., Wiley-VCH, Weinheim, 2002, pp.79.

[2] R.N.Feudale, N.A.Woody, H.Tan, A.J.Myles, S.D.Brown, and J.Ferre, "Transfer of mulivariate calibration models: A review," Chemomet. Intell. Lab. Syst., 2002, vol. 64, pp. 181-192.

[3] C.F.Pereira, M.F.Pimentel, R.K.H.Galvao, F.A.Honorato, L Stragevitch, and M.N.Martins, "A comparative study of calibration transfer methods for determination of gasoline quality parametres in three different near infrared spectrometers," Anal. Chim. Acta, 2008, vol. 611, pp. 41-47.

[4] O.Tomic, H.Ulmer, and J.Haugen, "Standardization methods for handling instrument related signal shift in gas-sensor array measurement data," Anal. Chim. Acta, 2002, vol.472, pp. 99-111.

[5] T.Artursson, T.Eklöv, I.Lundström, P. Martensson, M.Sjöström, and M.Holmberg, "Drift correction for gas sensors using multivariate methods," J. Chemomet., 2000, vol. 14, pp. 711-723.

[6] L.Fernandez, S.Guney, A.Gutierrez-Galvez, and S.Marco, "Calibration transfer in temperature modulated gas sensor arrays," Sensors and Actuat. B, Chem., 2016, vol.231, pp. 276-284.

[7] R.K.H.Galvãoa, S.F.C.Soares, M.N.Martins, M.F.Pimentel, and M.C.U. Araújo, “Calibration transfer employing univariate correction and robust regression,” Anal. Chim. Acta, 2015, vol. 864, pp. 1-8.

[8] B.Malli, A.Birlutiu, and T.Natschläger, “Standard-free calibration transfer - An evaluation of different techniques,” Chemomet. Intell. Lab. Syst., 2017, vol.161, pp. 49-60.

[9] V.Panchuk, D.Kirsanov, E.Oleneva, V.Semenov, A.Legin, “Calibration transfer between different analytical methods,” Talanta, 2017, vol. 170, pp. 457-463.

[10] F.Zhang, W.Chen, R.Zhang, B.Ding, H.Yao, J.Ge, L.Ju, W.Yang, and Y.Du, “Sampling error profile analysis for calibration transfer in multivariate calibration,” Chemomet. Intell. Lab. Syst., 2017, vol. 171, pp. 234-240.

[11] A.Vergara, S.Vembu, T.Ayhan, M.A.Ryan, M.L.Homer, R.Huerta, “Chemical gas sensor drift compensation using classifier ensmbles,” Sensors and Actuat. B, Chem., 2012, vol. 166-167, pp. 320-329.

[12] G.Chandrashekar, and F.Sahin, “A survey on feature selection methods,” Computers and Electrical Engineering, 2014, vol. 40, pp. 16-28.

[13] J.Haugen, O.Tomic, K.Kvaal, “A calibration method for handling the temporal drift of solid state gas-sensors,” Anal. Chim. Acta, 2000, vol. 407, pp. 23-39.

[14] Y.Wang, D.J.Veltkamp, and B.R.Kowalski, “Multivariate instrument standardization,” Anal. Chem., 1991, vol. 63, pp. 2750–2756.

[15] S.Wold, H.Antti, F.Lindgren, J.Öhman, “Orthogonal signal correction of near-infrared spectra,” Chemomet. Intell. Lab. Syst., 1998, vol. 44, pp. 175-185.

International Conference on Science and Technology

ICONST 2018

5-9 September 2018 Prizren - KOSOVO

Experimental and Numerical Verification of Drying Kinetics of Different Foodstuffs and Investigation of Shrinkage Effects

Burak Turkan[1], Yakup Sen[1], Akin Burak Etemoglu[1]*, Ahmet Serhan Canbolat[1]

Abstract: The present study describes shrinkage effects and the numerical modelling of the drying process. The governing equation of heat and mass transfer in food were presented. Drying kinetics of the carrot, cucumber and eggplant was investigated experimentally. Experimental data were applied to five different drying models. The model which gives the closest results to the experimental data was predicted as the Midilli model for each food. The temperature and moisture values obtained from the experimental study were compared with numerical analysis and found to be a considerable agreement. The shrinkage effect in the drying process was studied by using the ALE (Arbitrary Lagrangian Eulerian) method. Using this method, it was examined the variation in the moisture content of shrinkage effect.

Keywords: Convective drying, shrinkage, numerical and experimental study, thin drying models.

Introduction

Carrot is a food product containing nutrient minerals rich in vitamins B1, B2.B6 and B12. It also contains carotene and carotenoids. Carrots have a good taste and must be consumed fresh. It is used as raw material in food processing industries (such as baby food and instant soups) (Singh and Gupta, 2007, Lima et al. 2004). Eggplant is grown in North America, Asia and the Mediterranean region. It is important to keep the eggplant fresh for a long time in terms of shelf life. Cucumbers are scientifically categorized in the family Cucumbaceae, a family of melon fruit, Cucumis sativus. Drying is required to provide more stable food products and to be used all year round (Puig et al. 2012). Water that fruits and vegetables contain causes chemical degradation. Therefore, the drying process is used for the long-term conservation of agricultural products. With the drying process, the long-term healthy storage of seasonally produced foods is ensured without losing their vitamin value. Thus, the economic waste is prevented, and a long-term quality product is presented to the consumer (Alibas, 2006).

The drying process is a complex process consisting of simultaneous heat and mass transfer mechanisms. The air drying process usually consists of a period of constant rate, followed by a period of falling rate. In the constant rate period, the surface is covered with water. As the water evaporates, the mass transfer from the surface occurs. Air velocity, air temperature, and relative humidity are factors affecting the drying rate in this process. In the falling rate period, moisture transfer is controlled by internal mass transfer mechanisms such as capillary flow, liquid and vapour diffusion. One or more of these mechanisms may have a simultaneous effect in the falling rate period. Air temperature, chemical composition, physical structure and thickness of the product affect the drying rate. Two falling rate periods occur in hygroscopic materials. The wet surface area decreases as the product moisture mixes with the air in the 1st falling rate period. After the surface dries, the 2nd falling rate period begins, and evaporation occurs inside of the product (Heldman and Hartel, 1999; Geankoplis, 1993; Rizvi, 1995; Toledo, 1999).

Fick's law of diffusion is used to describe the drying kinetics. The thin layer drying models obtained by using this law are frequently encountered in the literature. The Lewis model (Lewis, 1921); Henderson and Pabis model (Henderson and Pabis, 1961); Two Term model (Madamba et al. 1996); Wang and Singh model (Wang and Sing, 1978); Midilli model (Midilli et al. 2002) can be given as examples. These models are classified as theoretical, semi-theoretical, and experimental (Midilli and Küçük, 2003; Demiray and Tulek, 2012; Wam, 2006). The drying process and kinetics of agricultural products have been investigated by many researchers in the literature (Doymaz, 2016; Guiné et al. 2014; Madhiyanon et al. 2009; Kaya et al. 2010; Baini and Langrish, 2007; Zlatanovic et al. 2013; Torki-Harchegani et al.

[1]Bursa Uludag University, Faculty of Engineering, Mechanical Engineering Department, TR-16059, Bursa, TURKEY
*Corresponding author: aetem@uludag.edu.tr

2016). The mathematical modelling of the drying process is important in terms of the performance of drying systems (Cihan et al. 2007).

The drying of agricultural products such as fruits and vegetables containing high moisture usually creates a remarkable deformation effect. The shrinkage effect occurring in food products has a strong effect on the drying rate and the structure of the dried product and is observable (Lima et al. 2002; Queiroz and Nebra, 2001). However, if the study is not focused on drying kinetics, the mechanical deformation effect may be neglected (Ketelaars et al. 1992).

In this study, it was aimed to obtain the drying characteristics of carrot, cucumber and eggplant. For this purpose, the characteristics were obtained experimentally and the drying conditions were modelled and compared with the numerical study including shrinkage effect (ALE method). Five drying model was used to find the closest result to experimental data. Finally, the compatibility of the results obtained with the drying models in the literature was investigated.

Material and Methods

Carrot, eggplant and cucumber were used in the experiments. Drying processes were accomplished by a convective tunnel type drier. The experimental schematic diagram was demonstrated in Figure 1.

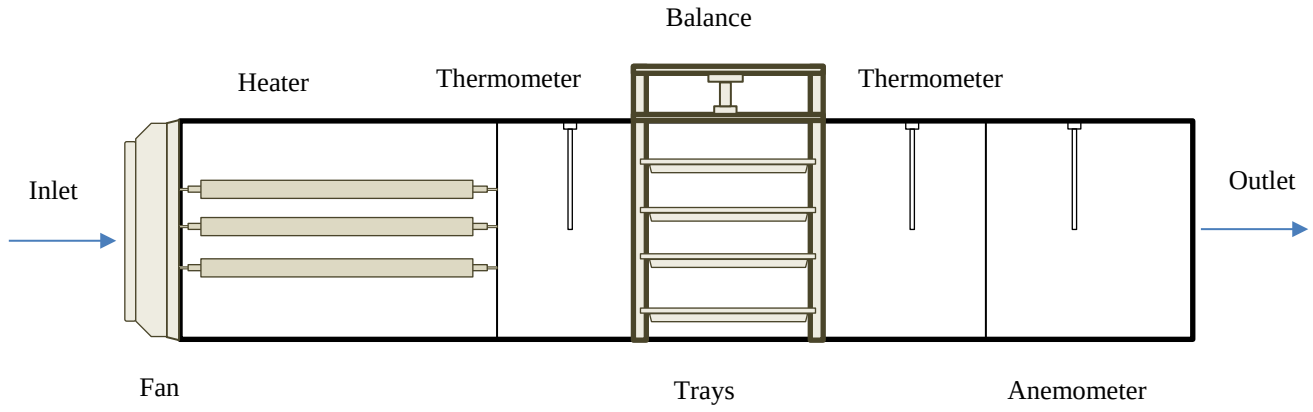

Figure 1. Schematic diagram of the tunnel type convective dryer

Carrot, eggplant and cucumber slices weighing 93±0.05 g were placed in a dryer for the determination of the initial moisture and dried at an air temperature of 60±0.3°C for 24 hours. Drying was carried out until the difference between the last two amount became 1%. The average initial moisture content (on wet basis) of the foodstuff (carrot, eggplant and cucumber) was worked out to be 79.51%, 92.3% and 88.56%, respectively. The air temperature of 60±0.3°C and 0.7 m/s air velocity was used during experiments. Carrot, eggplant and cucumber were sliced to 1 cm thickness. The change in the weight of the foods was registered with a digital scale with a sensitivity of 0.05 g during the experiment.

Calculation of Moisture Content

Eq.1 and Eq.2 dry and wet basis expressions are defined as:

$$M_{DB} = \left(\frac{W_w}{W_{dr}}\right) = \left(\frac{W\_ W_{dr}}{W_{dr}}\right) \quad (1)$$

$$\%M_{WB} = \left(\frac{W_w}{W_w + W_{dr}}\right) \times 100 \quad (2)$$

where W is initial weight (g) of the product, W_w is the mass (g) of the water in the product, and W_{dr} is the mass (g) of the dry product (Doymaz et al. 2006).
Dimensionless moisture ratios (MR) is related to moisture content as:

$$\mathrm{MR} = \frac{M_t - M_e}{M_i - M_e} \quad (4)$$

where M_e [g water /(g dry matter)] is the equilibrium moisture content at the end of drying, and M_i [g water /(g dry matter)] is the initial moisture content.

Mathematical Modelling for the Numerical Analysis

The energy conservation equation in solids based on Fourier's law can be given as follows;

$$\rho c_p \left(\frac{\partial T}{\partial t}\right) + \nabla(-k\nabla T) = 0 \quad (5)$$

where c_p is specific heat of food [J /(kg K)], k is the thermal conductivity of food [W /(mK)], ρ is the density of food [kg /m^3] and the mass conservation equation in solids based on Fick's law can be given as follows (Sabarez, 2012):

$$\frac{\partial M}{\partial t} + \nabla\left(-D_{eff}\nabla M\right) = 0 \quad (6)$$

where D_{eff} is an effective diffusion coefficient (m^2 /s) and M is the moisture content (g water /g material).

Initial and Boundary Conditions

The initial moisture content (on wet basis) of the carrot, eggplant and cucumber was obtained to be 79.51%, 92.3% and 88.56%, respectively and initial temperature of food is 15 °C.

Heat transfer boundary conditions

The surface boundary condition for heat transfer is given by:

$$-\mathrm{n}(-k\nabla T) = h_t(T - T_s) \quad (7)$$

where h_t is heat transfer coefficient [W /(m^{2}K)] and T_s is the drying air temperature (°C).
Symmetry boundary condition for heat transfer is given by:

$$\mathrm{n}(k\nabla T) = 0 \quad (8)$$

Mass transfer boundary conditions

The surface boundary condition for mass transfer is given by;

$$-\mathrm{n}(D\nabla M) = h_m(M - M_s) \quad (9)$$

where h_m is mass transfer coefficient (m/s) and M_s is the equilibrium moisture content (g water/g material).
Symmetry boundary condition for mass transfer is given by:

$$\mathrm{n}(D\nabla M) = 0 \quad (10)$$

Calculation of the Heat and Mass Transfer Coefficients

The heat and mass transfer coefficients are calculated with well-known correlations in the literature. (Cengel, 2002; Kumar et al. 2015; Karim and Hawlader, 2005).

$$\mathrm{Nu} = \frac{h_T L}{k} = 0.664\ \mathrm{Re}^{0.5} Pr^{0.33} \quad (11)$$

$$\mathrm{Sh} = \frac{h_M L}{D_{AB}} = 0.664\ \mathrm{Re}^{0.5} Sc^{0.33} \quad (12)$$

Data Analysis

Five different experimental, semi-experimental, and theoretical thin layer drying models (Lewis model, Henderson and Pabis model, Two Term model, Wang and Sing model and Midilli model) used in the literature were applied. (see Table 1)

Table 1. Constants and coefficients of the drying models

Model No	Name of Model	Model	Reference
1	Lewis	MR=exp(-kt)	(Lewis, 1921)
2	Henderson and Pabis	MR=aexp(-kt)	(Henderson and Pabis,1961)
3	Two Term	MR=aexp(-k_0t)+bexp(-k_1t)	(Madamba et al. 1996)
4	Wang and Singh	MR=1+at+bt^2	(Wang and Sing, 1978)
5	Midilli	MR=aexp(-kt^n)+bt	(Midilli et al. 2002)

MR: moisture ratio, k, k_0, k_1: drying constant (min^{-1}), a, b: coefficient, n: drying constant

Statistical conclusions were calculated using the Sigma Plot program. The drying coefficients (a, b, k, k_0, k_1, n) and the coefficients of determination (R^2), standard error of estimate (SEE), and chi-square (x^2) expressions, which are statistical parameters are calculated as (Goyal et al. 2007):

$$\text{SEE} = \sqrt{\frac{\sum_{i=1}^{N}\left(MR_{exp} - MR_{pred}\right)^2}{N - z}} \tag{13}$$

$$x^2 = \frac{\sum_{i=1}^{N}\left(MR_{exp} - MR_{pred}\right)^2}{N - z} \tag{14}$$

where $MR_{experimental}$ is experimental moisture ratio, $MR_{predicted}$ is the predicted moisture ratio, N is the number of experimental data points and z is the number of parameters in the model.
It is difficult to figure out the shrinkage effect experimentally. In this study, the linear distribution method of the shrinkage rate was used. The shrinkage rate at any point of the food is defined as;

$$u(x) = u(b)\frac{x}{b} \tag{15}$$

The rate value on the surface is given in Eq. (15)

$$u(b) = \frac{b - b(old)}{\Delta t} \tag{16}$$

where, b (old) is the half-thickness of the food at the next time, and b is the initial half-thickness (Karim and Hawlader, 2005). In order to figure out the half-thickness of the food at any time, the following expression obtained depending on the moisture content of the food at that time is used (Desmorieux and Moyne, 1992).

$$b = b_0\left[\frac{\rho_w + M\rho_s}{\rho_w + M_0\rho_s}\right] \tag{17}$$

Uncertainty Analysis

It is necessary to determine the total error by performing the uncertainty analysis of the measurement results. Overall uncertainity can be calculated using the following expressions;

$$W_r = \left[\left(\frac{\partial R}{\partial x_1}w_1\right)^2 + \left(\frac{\partial R}{\partial x_2}w_2\right)^2 + \cdots + \left(\frac{\partial R}{\partial x_n}w_n\right)^2\right]^{\frac{1}{2}} \tag{18}$$

$$e = \frac{W_r}{R} \tag{19}$$

where, R (x_1,x_2,x_3….x_n) a function of independent variables, Wr overall uncertainty, w_1,w_2,w_3….w_n error value of independent variables and e relative uncertainty (Moffat, 1988; Kumar et al. 2015).
Uncertainty analysis of moisture content was calculated using Eq. 18-19. The relative uncertainties for cucumber, eggplant and carrot was obtained as ± 0.5%, 0.7% and 0.3%, respectively.

Results

Experimental Drying Kinetics

The experimental variation of moisture content (dry basis) and temperature with time at air velocity of 0.7 m/s with 60°C air temperature are shown in Figure 2. As shown in Figure 2a, at the end of the 3 hour drying period, the moisture content of each foodstuff (cucumber, carrot and eggplant) decreased by 61% , 66% and 83%, respectively. The surface temperatures are also shown in Figure 2b. Measured surface temperature values vary in an extensive range of 14.5°C to 57°C. Surface temperature values for cucumber are higher than carrot and eggplant. The surface temperature values for cucumber, carrot and eggplant are calculated as 55.6°C, 52.5°C and 47°C at the end of the 3 hour drying period. Since the moisture content in the product decreases throughout the drying process, The obtained data are also compatible with the results of some studies in the literature (Pakowski and Adamski, 2007; Maskan, 2000; Nguyen and Price, 2007; Motevali et al. 2010; Srikiatden and Roberts, 2006; Gogus and Maskan, 1999; Baini and Langrish, 2008; Thuwapanichayanan et al. 2011; Madamba et al. 1996; Demirel and Turhan, 2003; Hawlader et al. 1991; Karim and Hawlader, 2005; Agarry and Owabor, 2012; Afolabi and Agarry, 2014; Hadrich and Kechaou, 2009; Mirzaee et al. 2009).

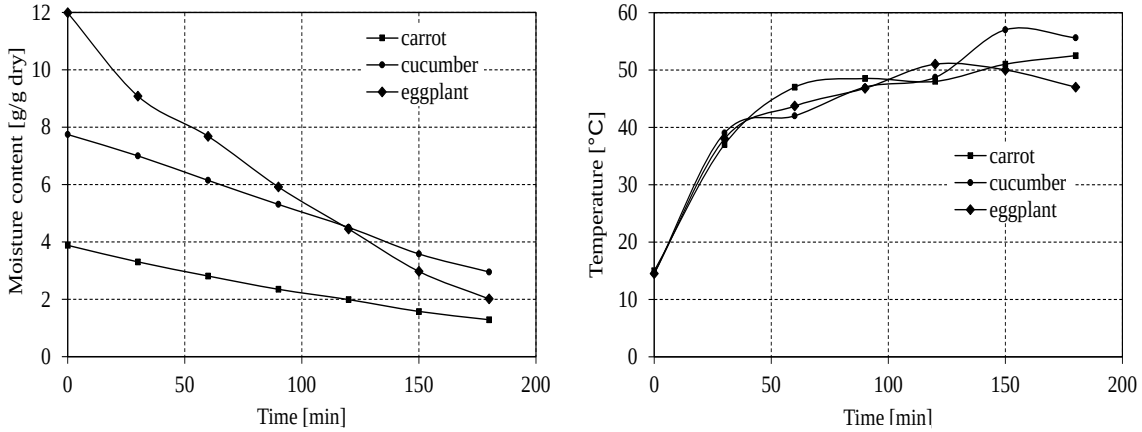

(a) (b)

Figure 2. (a) Moisture content (b) temperature (c) weight versus drying time for different foodstuff (carrot, cucumber and eggplant) at drying temperatures 60°C and the air velocity of 0.7 m/s

Moisture content obtained the experimental data at drying air temperature of 60°C was executed for five well-known semi-empirical models were given in Table 1. The statistical results (a, b, k, k_0, k_1, n, R^2, SEE, and x^2) obtained from these models coefficients were presented collectively in Table 2. In order to describe the most appropriate model using the dimensionless moisture content obtained from the experiment, the R^2 value should be close to 1 and SEE and x^2 values should be close to 0 (Pangavhane et al. 1999). R^2 , SEE and x^2 values in the Midilli model were calculated to be 0.99, 0.0061, and 3.71×10^{-5} for the carrot. R^2 , SEE and x^2 values in the Midilli model were calculated to be 0.99, 0.0077, and 6.00×10^{-5} for the cucumber. R^2 , SEE and x^2 values in the Midilli model were calculated to be 0.99, 0.0169 and 0.0003 for the eggplant. According to this results, it can be said that the Midilli model gives better predictions among the other models and is the most appropriate model.

Table 2 . Statistical parameter values and coefficients obtained for carrot, cucumber and eggplant

	Carrot Constants and coefficients			Cucumber Constants and coefficients			Eggplant Constants and coefficients		
Model	R^2	SEE	x^2	R^2	SEE	x^2	R^2	SEE	x^2
1	0.99	0.0149	0.0002	0.97	0.0345	0.0012	0.98	0.0320	0.0010
2	0.99	0.0148	0.0002	0.98	0.0321	0.0010	0.98	0.0347	0.0012
3	0.99	0.0191	0.0004	0.98	0.0415	0.0017	0.98	0.0448	0.0020
4	0.99	0.0054	2.95×10^{-5}	0.99	0.0086	7.42×10^{-5}	0.99	0.0230	0.0005
5	0.99	0.0061	3.71×10^{-5}	0.99	0.0077	6.00×10^{-5}	0.99	0.0169	0.0003
1	k=0.0058			k=0.0047			k=0.0086		
2	k=0.0059	a=1.0123		k=0.0050	a= 1.0345		k=0.0087	a=1.0099	
3	a=0.47	b=0.85		a=0.49	b=0.53		a=0.49	b=0.51	
	k_0=0.0059	k_1=0.0059		k_0=0.0050	k_1=0.0050		k_0=0.0087	k_1=0.0087	
4	a=-0.005	$b=7.23\times10^{-6}$		a=-0.0035	$b=5.88\times10^{-8}$		a=-0.0069	$b=1.26\times10^{-5}$	
5	a=0.99	b=-0.0007		a=0.99	b=-0.0008		a=0.99	b=-0.0025	
	n=0.97	k=0.0049		n=1.22	k=0.0012		n=0.59	k=0.0224	

R^2, the coefficient of determination; SEE, standard error of estimate; x^2, chi-square; k, k_0, k_1, drying constant (min^{-1}); a ,b, coefficients; n, drying constant

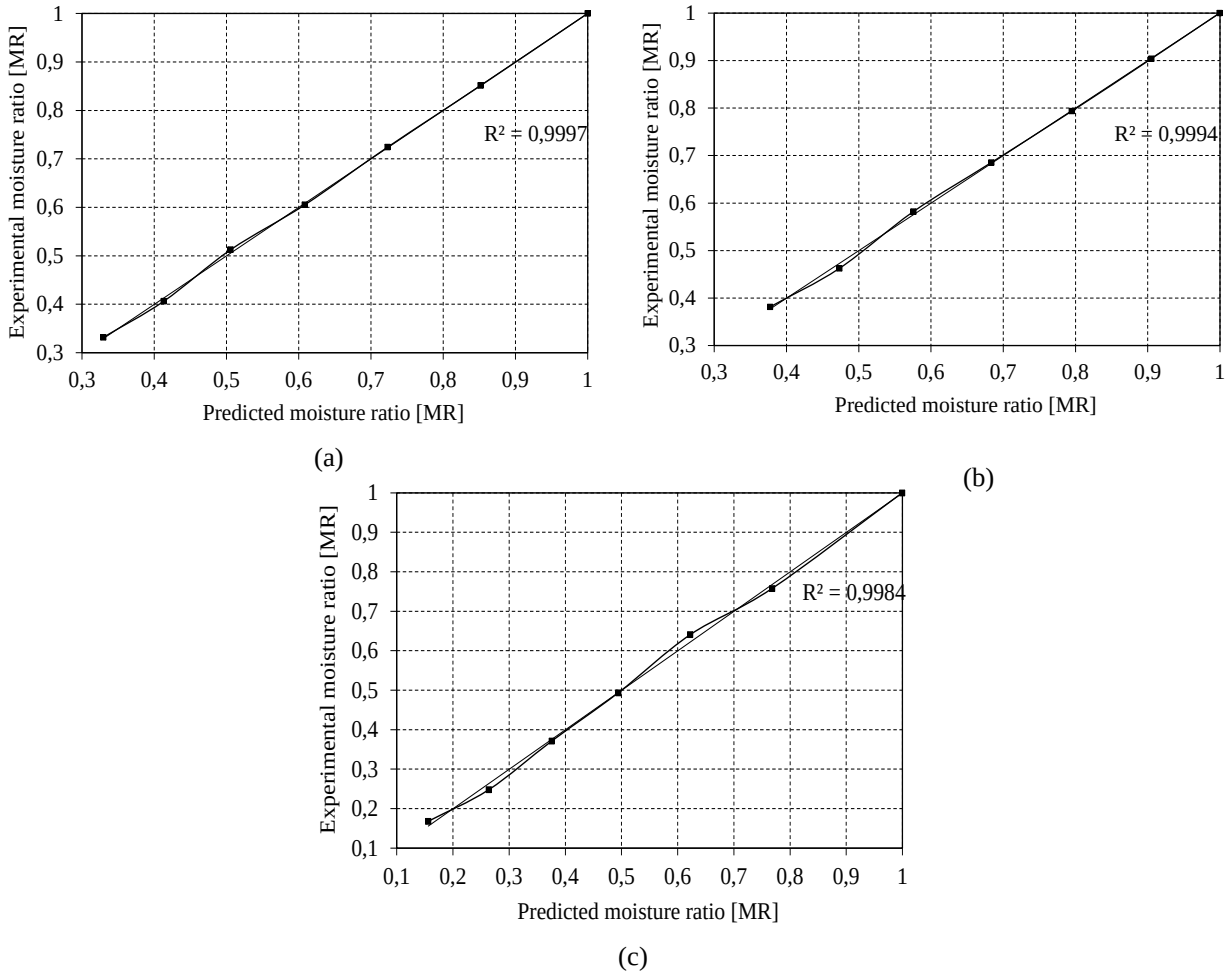

Figure 3. The relationship between experimental moisture rate and predicted moisture ratio for different foodstuffs (a-carrot, b-cucumber, c-eggplant)

Using the sigma plot programme, predicted moisture ratio values for the Midilli Model are calculated for each food. Validation of the Midilli model is evaluated by comparing the computed moisture ratio with observed moisture ratio. The performance of the model at different foodstuffs is shown in Figure 3. Regression coefficients (R^2) of each food (carrot, cucumber and eggplant) are obtained from 0.9997, 0.9994 and 0.9984, respectively. The 45° straight line between experimental and predicted ratios provide that the Midilli model is a good predictor. Midilli model has also been found suitable by various researchers (Wang et al. 2009; Amiri et al. 2011; Sadi and Meziane, 2015; Mihindukulasuriya and Jayasuriya, 2013). In some studies conducted in the literature, the Midilli model (Vega-Galvez et al. 2012) in strawberry drying; the Logarithmic model (Zhu and Shen, 2014) in peach drying; the Two term model (Zielinska and Markowski, 2010) in carrot drying, and the Midilli model (Taheri-Garavand et al. 2011) in tomato drying were found to be the best defining models for drying.

Numerical study and verification

A two-dimensional axisymmetric model was used to describe the simultaneous heat and mass transfer equations in the hot air convection drying process. Due to the axisymmetry of the food slabs, only one-quarter of the planer intersection was taken into consideration in the numerical method. It is observed in the literature that this model approach has been used in some numerical drying studies (Sabarez, 2012; Kumar et al. 2015).

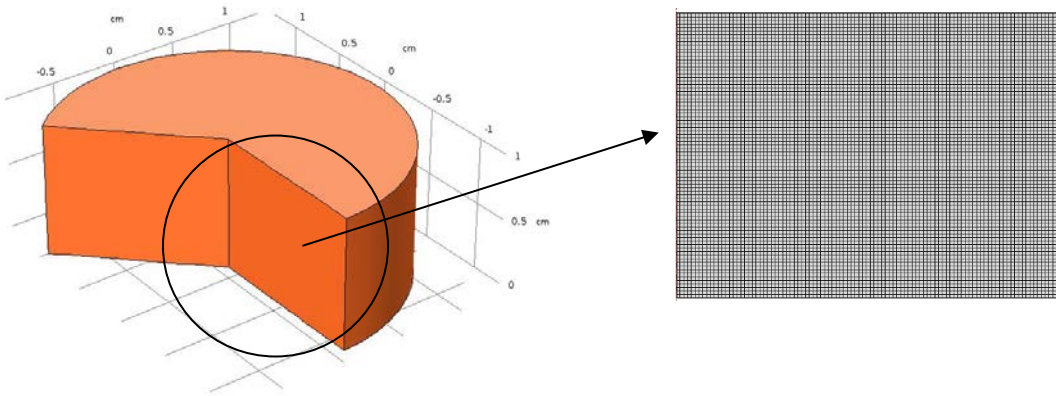

Figure 4. The model used in analyses and mesh structure

To simplify the model, the following assumptions were made;
• There is no heat production inside the food.
•The heat transfer in the food was considered by conduction (Fourier's Law), and mass transfer occured with diffusion (Fick's Law).
•The shrinkage effect was considered during the drying period.
•The thermophysical properties of the air and food were constant during the drying process.
•The temperature and velocity of drying air are constant.

Solution Methodology

Non-linear simultaneous heat and mass transfer equations are solved numerically by COMSOL Multiphysics using appropriate initial and boundary conditions and assumptions to obtain the temperature and moisture distributions in the apple during drying. The main steps of the solution process are as follows:

•Heat and mass transfer coefficients calculation
•Defining geometry
•Creating a mesh structure
•Realizing the physical conditions (initial, boundary conditions etc.)
•Integrating and solving the governing equations (Comsol Multiphysics™ 5.3. 2018).

Table 3. Thermophysical properties and experimental drying conditions of the carrot, cucumber and eggplant

Parameter	Value	Reference
Air velocity (m/s)	0.7	
Food temperature (°C)	15	
Food density (kg/m^3)	1029-950-571	(Adams 1975; Fasina and Fleming 2001;Ali et al. 2002)
Air temperature (°C)	60	
Food moisture content (% w.b.)	79-88-92	
Air relative humidity (%)	79	
Thermal conductivity of food (W/mK)	0.569-0.62-0.356	(Adams 1975; Fasina and Fleming 2001;Ali et al .2002)
Specific heat (J/kgK)	3849-4030-3900	(Adams 1975; Fasina and Fleming 2001;Ali et al .2002)
Heat of vaporization (kJ/kg)	2466	(Cengel, 2002)
Water density (kg/m^3)	999.1	(Cengel, 2002)
Heat transfer coefficient (W/m^{2}K)	20.33	
Mass transfer coefficient (m/s)	0.0190	
Shrinkage velocity (m/s) ×10^7	2.481-2.527-3.370	
Moisture diffusivity (m^2/s) ×10^{10}	9.374-8-9.6883	(Togrul 2006; Shahari et al 2014, Guine et al 2017)

Food materials were modelled for numerical simulation. Mesh independence study of moisture content was investigated and the maximum difference was found at 1 %. Different mesh structures were applied to foods (Figure 4). Finally, for the accurate solution, grid structure which consists of 8000 quadrilateral elements, 360 edge elements and 4 vertex elements was selected. The time-dependent problem was solved by using implicit time stepping method. The nonlinear PDE (partial differential equations) were solved using Newton's method with relative tolerance 0.001 and absolute tolerance 0.0001 using the commercial Comsol Multiphysics 5.3. The parameters and thermophysical properties used in the analyses are presented in Table 3. Non-linear partial differential transport equations were solved by the numerical method in order to determine the temperature and moisture content values of the air and food material. Deformed mesh was used to consider the volume change due to the fluid transfer. Therefore an Arbitrary Lagrange Eulerian (ALE) was applied in the Comsol Multiphysics 5.3. The ALE method is used as an application between the Lagrangian and Eulerian approaches that allow the identification of moving boundaries. The Laplace smoothing type was defined as the deformed mesh.

Figure 5 shows the change in moisture content of carrot under shrinkage effect with time. Increasing shrinkage effect was obtained during drying. After 1, 2 and 3 hours, the amount of decrease in the volume of the food was determined as 22.8%, 42% and 55.7%. Similarly, the shrinkage effect in cucumber during drying is given in Figure 6. After 1, 2 and 3 hours, the percentage change in product volume was calculated as 21.6%, 41% and 55.7%.

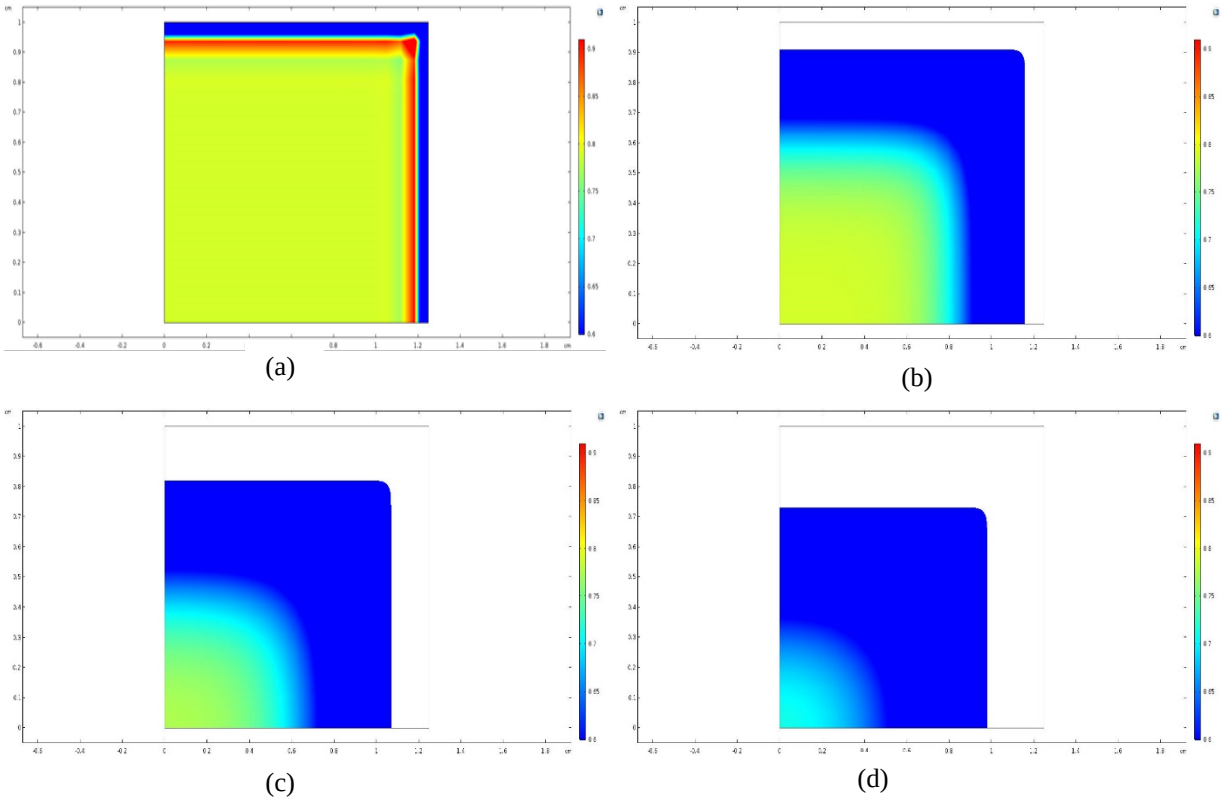

Figure 5. Evolution in the moisture content of the carrot over time during drying process considering the shrinkage effect (a-Start of drying, b-First hour, c- Second hour, d- Third hour)

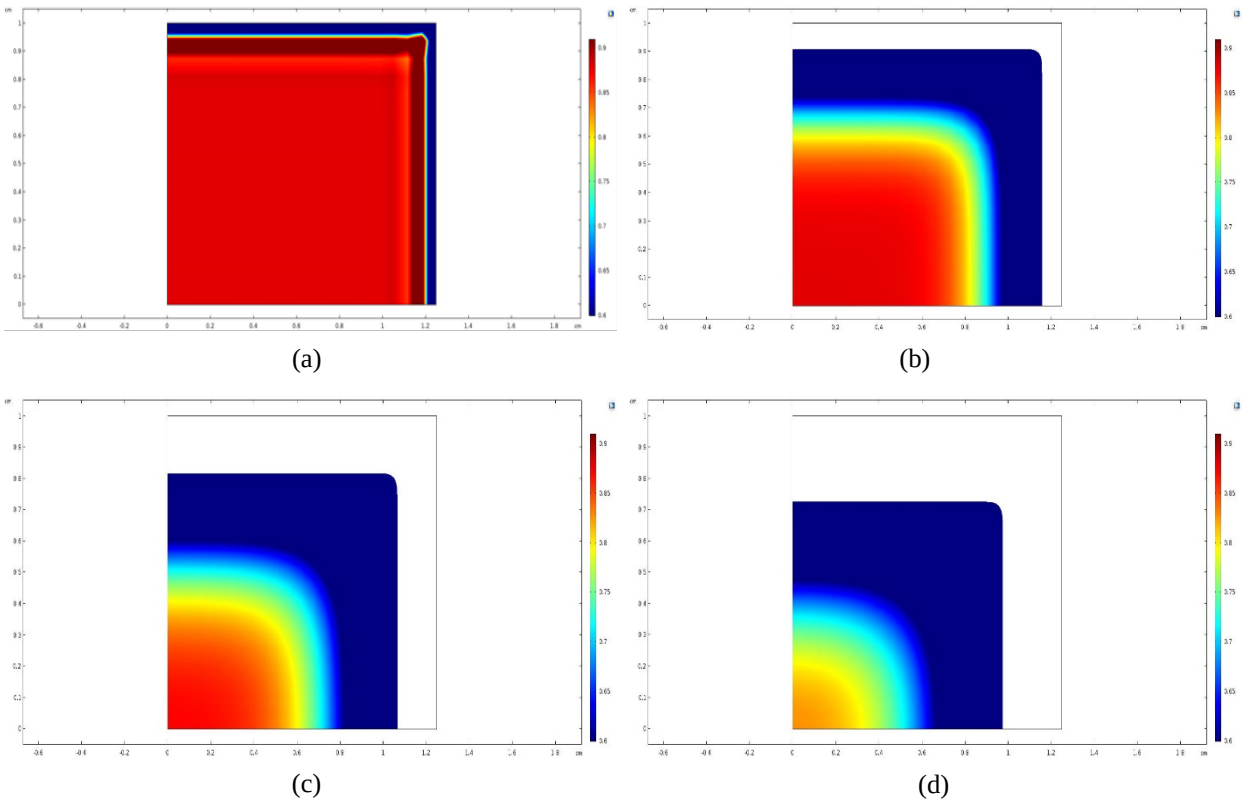

(a) (b)

(c) (d)

Figure 6. Evolution in the moisture content of the cucumber over time during drying process considering the shrinkage effect (a-Start of drying, b-First hour, c- Second hour, d- Third hour)

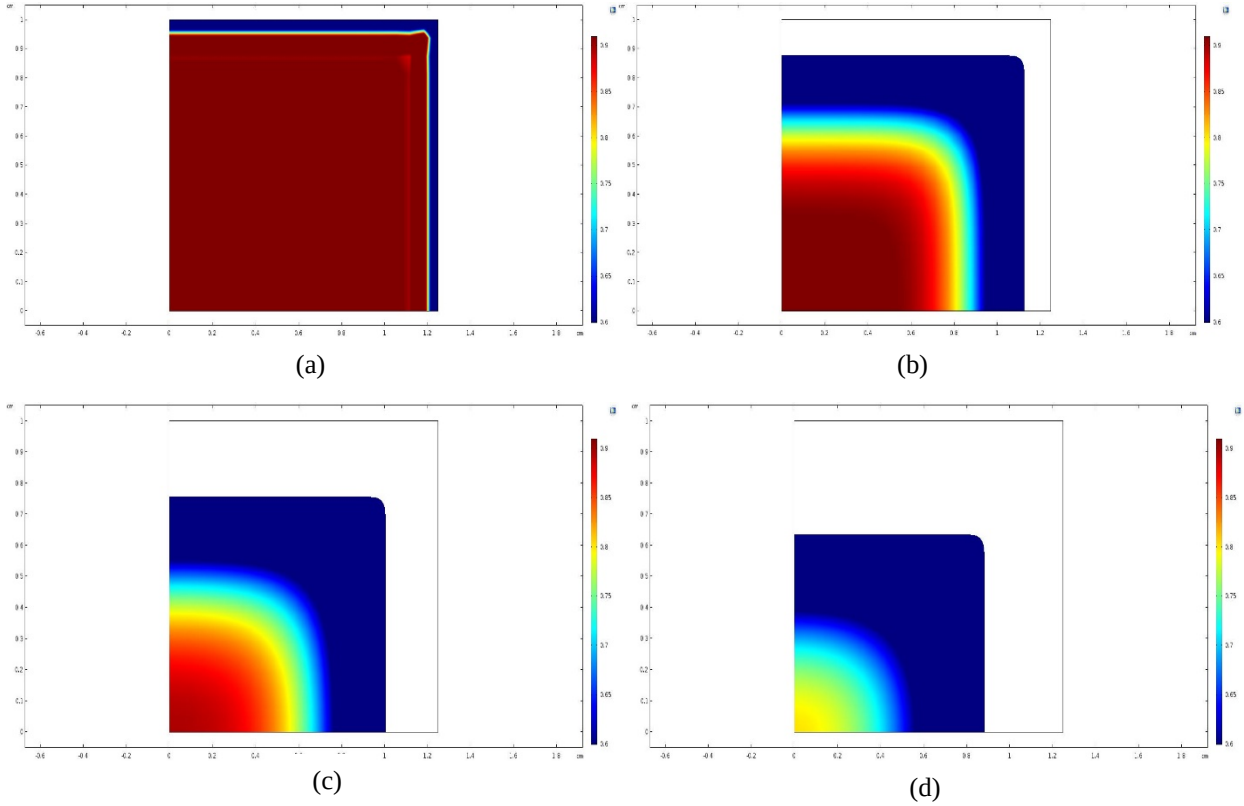

(a) (b)

(c) (d)

Figure 7. Evolution in the moisture content of the eggplant over time during drying process considering the shrinkage effect (a-Start of drying, b-First hour, c- Second hour, d- Third hour)

The percent change in volume of eggplant was obtained 37.8%, 51.4% and 68.7%, at the end of 1st, 2nd and 3rd hours of drying. Figure 8 shows the volume changes of different foodstuffs during the drying time. At the end of 3 hours, the

volume of carrot and cucumber was 2.17 $\times 10^{-6}$ m^3 while the volume of eggplant was calculated as 1.53 $\times 10^{-6}$ m^3. According to the results obtained from Figure 5-8, it can be said that the effect of shrinkage appeared most in the eggplant. The volume changes of carrot and cucumber are almost too close together.

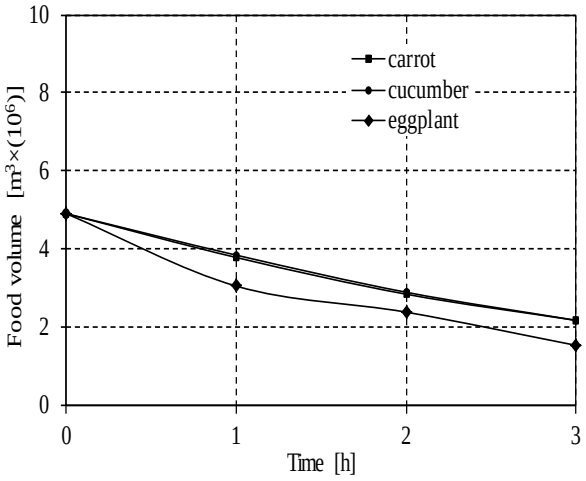

Figure 8. Volume change profile for carrot, cucumber and eggplant

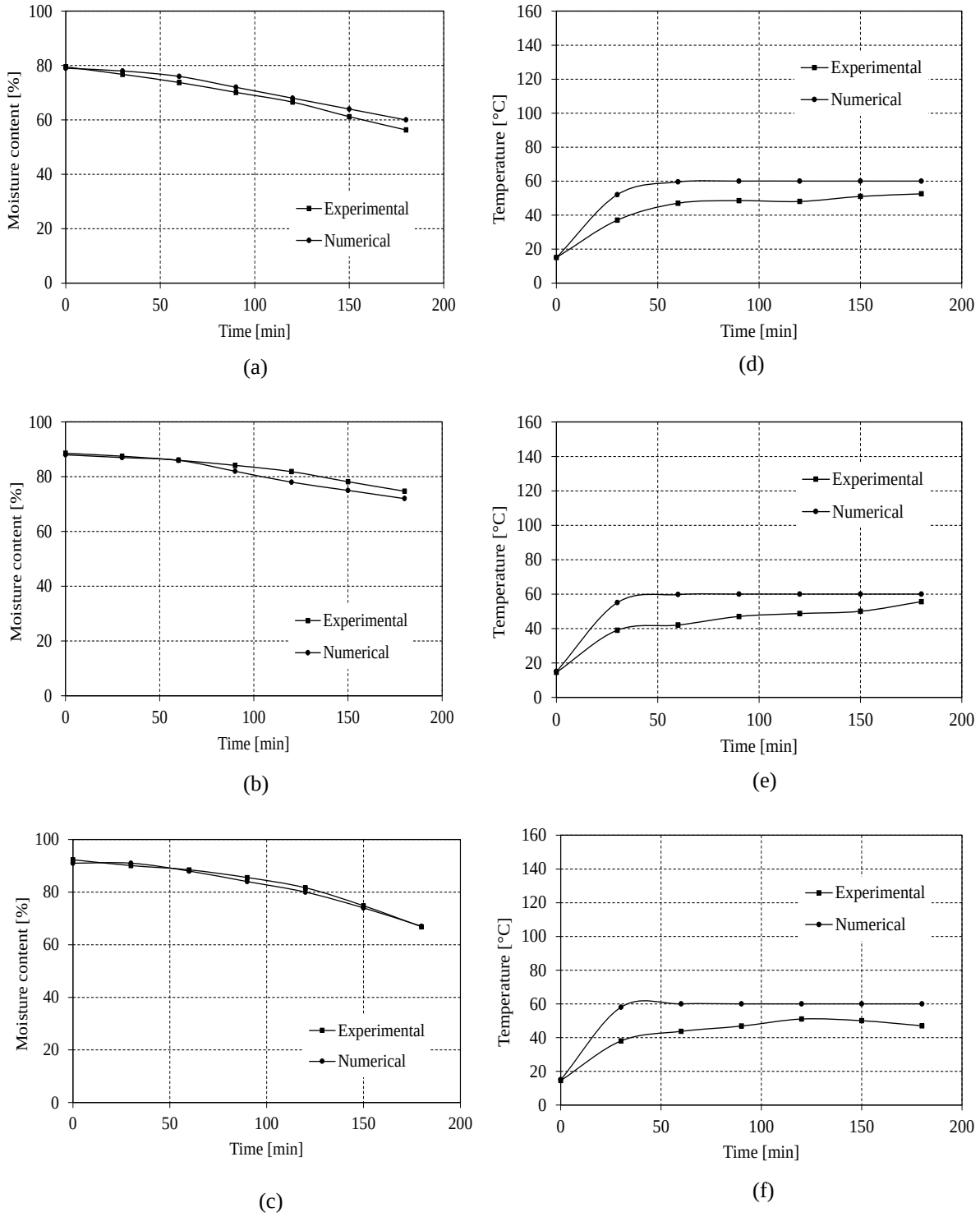

Figure 9. Variation numerical model with shrinkage and experimental study (a-d carrot, b-e cucumber, c-f eggplant)

The numerical model was verified by comparing the moisture content (on wet basis) and temperature values obtained from experiments. Figure 9 (a-b-c) shows the variation of the moisture content (on wet basis) values obtained from the experiment with the average moisture content (on wet basis) values obtained from the analysis for different foodstuffs. A difference of approximately 2.7%, 2.4%, and 0.8% was found between the values obtained from the experiments and analyses for carrot, cucumber and eggplant. The temperature values of the product center were experimentally measured and numerically calculated during drying. Figure 9 (d-e-f) shows the temperature changes of the product center obtained experimentally and numerically for each food.. The average difference between the temperature values of the product obtained from the experiments and numerical simulation was found to be 16%, 18%, and 20%, respectively, for the carrot, cucumber and eggplant. As a result, it can be said that there is a very good agreement between numerical and experimental results.

Discussion and Conclusions

In this study, firstly, drying kinetics of the carrot, cucumber and eggplant was investigated experimentally. In order to find the most suitable model for the data obtained from the experiment, five different film drying models which are widely used in the literature have been used. Models which considering shrinkage effect was developed in order to define the drying characteristics (temperature and moisture distributions). The volumetric shrinkage rates of food products were examined. Finally, the numerical results were compared with the experimental results. The numerical results were found to be in considerable agreement with experimental results. The conclusions can be summarized as follows:

•According to obtained results it was determined that the fastest drying occurred in the eggplant at the air temperature of 60 °C and the air velocity of 0.7 [m/s] . Therefore, eggplant should be preferred to carry out a faster-drying process.

• As a result of the nonlinear regression analysis, it can be said that the best model in describing the drying kinetics of carrot, cucumber and eggplant is the Midilli model.

•The remaining moisture content may cause deterioration in the food and formation of microorganisms. For this reason, minimizing the moisture content is vital. It is difficult to determine how much moisture remains at any point in the food during drying, experimentally. Therefore, numerical analysis for the drying process is very important. By using the numerical method, the temperature and moisture distributions of the food can be easily estimated depending on the time.

•The shrinkage effect was calculated for the change in the product volume and the maximum volumetric change was realized for eggplant with 68.7%.

•The data obtained by experimental and numerical solutions were compared, and the results were found to be compatible with each other. According to this result, the mathematical model (including shrinkage effect) expressing simultaneous heat and mass transfers can be used to estimate the moisture and temperature distribution in the product during drying.

References

Adams, C. (1975). Nutritive Value of American Foods. Agriculture Handbook,No. 456. Agricultural Research Service, U.S. Department of Agriculture,Washington, DC.

Afolabi, T. J., Agarry, S. E. (2014). Mathematical modelling and simulation of the mass and heat transfer of batch convective air drying of tropical fruits. Chemical and Process Engineering Research, 23: 9-19.

Agarry, S. E., Owabor, C. N. (2012). Modelling of the drying kinetics of banana under natural convection and forced air drying. Journal of Nigerian Society of Chemical Engineers, 27(1), 101 – 115.

Ali, S. D., Ramaswamy, H. S., Awuah, G. B. (2002). Thermo-Physical Properties of Selected Vegetables as Influenced by Temperature and Moisture Content. Journal of Food Process Engineering, 25, 417-433.

Alibas, I. (2006). Characteristics of chard leaves during microwave, convective, and combined microwaveconvective drying. Drying Technology, 24(1):1425-1435.

Amiri, C. R., Amiri, P. J., Esna-Ashari, M. (2011). Modeling of moisture diffusivity, activation energy and specific energy consumption of high moisture corn in a fixed and fluidized bed convective dryer. Spanish Journal of Agricultural Research, 9(1) 28-40.

Baini, R., Langrish, T. A. G. (2007). Choosing an appropriate drying model for intermittent and continuous drying of bananas. Journal of Food Engineering, 79(1) 330–343.

Baini, R., Langrish, T. A. G. (2008). An assessment of the mechanisms for diffusion in the drying of bananas. Journal of Food Engineering, 85: 201–214.

Cihan, A., Kahveci, K., Hacıhafızoğlu, O. (2007). Modelling of intermittent drying of thin layer rough rice. Journal of Food Engineering, 79:293-298.

Comsol Multiphysics 5.3. (2018). Heat Transfer Model Library, Heat Transfer Module User's Guide, Chemical Reaction Engineering Module User's Guide.

Çengel, Y.A. (2002). Heat Transfer : A Practical Approach; McGraw-Hill: Boston.

Demiray, E., Tulek, Y. (2012). Thin-layer drying of tomato (Lycopersicum esculentum Mill. cv. Rio Grande) slices in a convective hot air dryer. Heat Mass Transfer, 48(5):841–847.

Demirel, D., Turhan, M. (2003). Air-drying behavior of Dwarf Cavendish and Gros Michel banana slices. Journal of Food Engineering, 59, 1–11.

Desmorieux, H., Moyne, C. (1992). Analysis of dryer performance for tropical foodstuffs using the characteristic drying curve concept, in Drying A.S. Mujumder, Editor, 834-843.

Doymaz, İ., Tugrul, N., Pala, M. (2006). Drying characteristics of dill and parsley leaves. Journal of Food Engineering, 77: 559-565.

Doymaz, I. (2016). Drying kinetics, rehydration and colour characteristics of convective hot-air drying of carrot slices. Heat Mass Transfer, DOI 10.1007/s00231-016-1791-8.

Fasina, O.O., Fleming. H.P. (2001). Heat transfer characteristics of cucumbers during blanching. J Food Eng, 47:203–10.

Geankoplis, C. J. (1993). Transport Processes and Unit Operations. New Jersey: Prentice-Hall.

Gogus, F., Maskan, M. (1999). Water adsorption and drying characteristics of okra (Hisbiscus esculentus L.). Drying Technology, 17: 883–894.

Goyal, R. K., Kingsly, A. R. P., Mainkanthan, M. R., Ilyas, S. M. (2007). Mathematical modeling of thin- layer drying kinetics of plum in a tunnel dryer. Journal of food Engineering, 79(1): 176-180.

Guine, R. P. F., Brito, M. F. S., Ribeiro, J. R. P. (2017). Evaluation of Mass Transfer Properties in Convective Drying of Kiwi and Eggplant, International Journal of Food Engineering, DOI: 10.1515/ijfe-2016-0257.

Guine, R. P. F., Serio, S. I. A., Correia, P. M. R., Barroca, M. J. (2014). Effect of pre-treatment on some physical–chemical properties of dried carrots. J Hyg Eng Des, 6:187–191.

Hadrich, B., Kechaou, N. (2009). Mathematical modeling and simulation of shrunk cylindrical material's drying kinetics, Approximation and application to banana. Food and Bioproducts Processing, 87:96–101

Hawlader, M. N. A., Uddin, M. S., Ho, J. C., Teng, A. B. W. (1991). Drying characteristics of tomatoes. Journal of Food Engineering, 14, 259–268.

Heldman, D. R., Hartel, R. W. (1999). Principles of food processing. Gaithersburg: Aspen Publishers, Inc..

Henderson, S. M., Pabis, S. (1961). Grain drying theory I: temperature effect on drying coefficient . J. Agr. Eng. Resource, 6(3): 169–174.

Karim, M. A., Hawlader, M. N. A. (2005). Mathematical modelling and experimental investigation of tropical fruits drying, International Journal of Heat and Mass Transfer, 48:(23) 4914-4925.

Kaya, A., Aydın, O., Kolaylı, S. (2010). Effect of different drying conditions on the vitamin C (ascorbic acid) content of Hayward kiwifruits (Actinidia deliciosa Planch). Food and Bioproducts Processing, 88:(2-3) 165–173.

Ketelaars, A.A.J., Jomaa, W., Puigalli, J.R., Coumans, W.J. (1992). Drying Shrinkage and stress. In A.S. Mujumdar, Drying'92(pp.293-303), Amsterdam:Elsevier.

Kumar, C., Millar, G,J., Karim, M. A. (2015). Effective Diffusivity and Evaporative Cooling in Convective Drying of Food Material. Drying Technology,33:227-237.

Lewis, W. K. (1921). The rate of drying of solid materials. J. Ind. Eng. Chem., 13(5): 427–432

Lima, A.G.B., Queiroz, M.R., Nebra, S.A. (2002). Simultaneous moisture transport and shrinkage during drying solids with ellipsoidal configuration. Chemical Engineering Journal, 86: 83–85.

Lima, K. S., Cople, A.L.S., Lima, L.C., Freitas, R.C., Della-Modesta, R.L., Godoy, O. (2004). Effect of Low Doses of Irradiation on the Carotenoids in Read-to-Eat Carrots. Food Science and Technology (Campinas), 24(2): 183–193.

Madamba, P. S., Driscoll, R. H., Buckle, K. A. (1996). The thin layer drying characteristics of garlic slices. Journal of Food Engineering, 29(1): 75-97.

Madhiyanon, T., Phila, A., Soponronnarit, A. (2009). Models of fluidized bed drying for thin-layer chopped coconut. Appl Therm Eng, 29:2849–2854.

Maskan, M. (2000). Microwave/air and microwave finish drying of banana. Journal of Food Engineering, 44:71–78.

Midilli, A., Kucuk, H., Yapar, Z. (2002). A new model for single layer drying. Drying Technology, 20(7):1503-1513.

Midilli, A., Kucuk, H. (2003). Mathematical modeling of thin layer drying of pistachio by using solar energy. Energy Conversion and Management, 44(7): 1111-1122.

Mihindukulasuriya, S. D. F., Jayasuriya, H. P. W. (2013). Mathematical modeling of drying characteristics of chilli in hot air oven and fluidized bed dryers. Agricultural Engineering International: CIGR Journal, 15(1): 154-166.

Moffat, R.J. (1988). Describing the uncertainties in experimental results, Experimental Thermal and Fluid Science, 1(1): 3-17.

Nguyen, H. M., Price, E. W. (2007). Air drying of banana: Influence of experimental parameters, slab thickness, banana maturity and harvesting season. Journal of Food Engineering, 79(1): 200-207.

Pakowski, Z., Adamski, A. (2007). The comparison of two models of convective drying of shrinking materials using apple tissue as an example. Drying Technology, 25: 1139-1147.

Pangavhane, D. R., Sawhney, P. N., Sarsavadia, P. N. (1999). Effect of various dipping pretreatments on drying kinetics of thompson seedless grapes. J Food Eng., 39: 211-216.

Puig, A., Perez-Munuera, I., Carcel, J.A., Hernando, I., Garcia-Perez, J.V. (2012). Moisture loss kinetics and microstructural changes in eggplant (Solanum melongena L.) during conventional and ultrasonically assisted convective drying. Food and Bioproducts Processing, 90: 624–632.

Queiroz, M. R., Nebra, S. A. (2001). Theoretical and experimental analysis of the drying kinetics of bananas. Journal of Food Engineering, 47:127–132.

Rizvi, S. S. H. (1995). Thermodynamic properties of foods in dehydration. In M. A. Rao & S. S. H. Rizvi (Eds.), Engineering properties of foods (pp. 223–309). New York: Marcel Dekker, Inc.

Sabarez, H. T. (2012). Computational modelling of the transport phenomena occurring during convective drying of prunes. Journal of Food Engineering, 111(2), 279–288.

Sadi, T., Meziane, S. (2015). Mathematical modelling, moisture diffusion and specific energy consumption of thin layer microwave drying of olive pomace. International Food Research Journal, 22(2), 494-501 .

Shahari, N., Hussein, S.M., Nursabrina, M., Hibberd, S. (2014). Mathematical modelling of cucumber (cucumis sativus) drying, Proceedings of the 21st National Symposium on Mathematical Sciences (SKSM21) AIP Conf. Proc. 1605, 307-312, doi: 10.1063/1.4887607.

Singh, B., Gupta, A.K. (2007). Mass transfer kinetics and determination of effective diffusivity during convective dehydration of pre-osmosed carrot cubes. J. Food Eng., 79, 459 470.

Srikiatden, J., Roberts, J. S. (2006). Measuring moisture diffusivity of potato and carrot (core and cortex) during convective hot air and isothermal drying. Journal of Food Engineering, 74:143-152.

Taheri-Garavand, A., Rafiee, A., Keyhani, A. (2011). Mathematical Modeling of Thin Layer Drying Kinetics of Tomato Influence of Air Dryer Conditions. Int. Trans. J Eng. Manag& Applied Sci&Technol., 2: 147-160.

Thuwapanichayanan, R., Prachayawarakorn, S., Kunwisawa, J., Soponronnarit, S. (2011). Determination of effective moisture diffusivity and assessment of quality attributes of banana slices during drying. LWT - Food Science and Technology, 44(6), 1502-1510.

Togrul, H. (2006). Suitable drying model for infrared drying of carrot, Journal of Food Engineering, 77, 610–619.

Toledo, R. T. (1999). Fundamentals of food process engineering (2nd ed.). Gaithersburg: Aspen Publishers, Inc..

Torki-Harchegani, M., Ghasemi-Varnamkhasti, M., Ghanbarian, D., Sadeghi, M., Tohidi, M. (2016). Dehydration characteristics and mathematical modelling of lemon slices drying undergoing oven treatment. Heat Mass Transfer, 52 (2) 281–289.

Vega-Galvez, A., Puente-Diaz, L., Lemus-Mondaca, R., Miranda, M., Torres, M.J. (2012). Mathematical Modelling of Thin-layer Drying Kinetics of Cape Gooseberry (Physalis peruviana L.). J Food Process Preservation, 38, 728-736.

Wam, M. (2006). Thin-layer modeling of the convective, microwave, microwave-convective and microwave-vacuum drying of lactose powder. J Food Eng, 72:113–123.

Wang, C. Y., Singh, R. P. (1978). A single layer drying equation for rough rice. ASAE Paper No: 78-3001, ASAE, St. Joseph, MI.

Wang, Z. F., Fang, S. Z., Hu, X. S. (2009). Effective diffusivities and energy consumption of whole fruit Chinese jujube (Zizyphus jujuba Miller) in Microwave Drying. Drying technology, 27(10) 1097-1104.

Zhu, A., Shen, X. (2014). The model and mass transfer characteristics of convection drying of peach slices. Int J Heat and Mass Trans, 72: 345-351.

Zielinska, M., Markowski, M. (2010). Air drying characteristics and moisture diffusivity of carrots. Chem Eng Process: Process Intensification, 49, 212-218.

Zlatanovic, I., Komatina, M., Antonijevi, D. (2013). Low-temperature convective drying of apple cubes. Applied Thermal Engineering, 53:114-123.

International Conference on Science and Technology

ICONST 2018

5-9 September 2018 Prizren - KOSOVO

Thermoeconomic Analysis of Regenerative Gas Turbine Based Heat And Power System

Yakup Sen[1]*, Burak Turkan, Recep Yamankaradeniz, Omer Kaynakli

Abstract: Analysis of power generation systems is important for the efficient utilization of energy sources. The most used method for analysis of the energy conversion process is the first law of thermodynamics - especially for computation of work and heat exchanges as well as thermal efficiency. However, there is increasing interest in combined utilization of both the first and second laws, using such concepts as exergy and exergy destruction in order to evaluate the efficiency with which the available energy is utilized. In this study, a thermodynamic analysis and performance of regenerative gas turbine based heat and power system was carried out using the first, second laws of thermodynamics and thermoeconomic concepts. Exergetic and thermoeconomic analyses were conducted to determine the exergy destruction and exergy efficiency of each major component of power plant. Thermoeconomic analysis showed amount of the cost of exergy destruction in the all components. The exergy costing analysis revealed that the unit cost of fuel and product.

Keywords: Thermoeconomic analysis, Power plant, Thermodynamic modelling.

Introduction

An exergoeconomic analysis consists of an exergetic analysis, an economic analysis, and an exergoeconomic evaluation, all conducted at the level of plant components. The primary contribution of an exergy analysis to the evaluation of an energy system comes through a thermoeconomic evaluation which considers not only the inefficiencies but also the costs associated with these inefficiencies and the investment expenditures required to reduce them. The objective of a thermodynamic optimization is to minimize the thermodynamic inefficiencies within the system, whereas the objective of a thermoeconomic optimization of a system is to estimate the cost-optimal structure and the cost optimal values of the thermodynamic inefficiencies in each component.

Although other authors conduct pioneering studies in the field of thermoeconomics during the 1960s, the effort to apply thermoeconomics systematically to the analysis of energy systems flourished only after 1980s and 1990s, when a group of specialists in the field (C. Frangopoulos, G. Tsatsaronis, A. Valero, and M. von Spakovsky, 1994) decided 211 / Vol. 17 (No. 4) Int. Centre for Applied Thermodynamics (ICAT) to compare their methodologies by solving a predefined and simple problem (CGAM Problem) of optimization in order to unify the thermoeconomic methodologies

When depletion of fossil fuels, global warming and other environmental factors are considered together, reducing energy costs only is not adequate for future generations of humanity and for a sustainable Earth. Thus, studies in the field of energy efficiency and distributed generation systems are encouraged by the idea of cheaper electricity generation with lower carbon emission systems, and utilization of energy on-site with lesser losses (EPA, 2010).

Misra et al. (2002) have reported that the optimization of thermal systems is generally based on thermodynamic analysis. However the systems so optimized often are not viable due to economic constraints. The theory of exergetic cost is a thermoeconomic optimization technique, combines the thermodynamic analysis with that of economic constraints to obtain an optimum configuration of a thermal system.

Kwak et al. (2003) have done the exergetic and thermodynamic analyses of a 500MW combined cycle plant. Mass and energy conservation laws were applied to each component of the system. Quantitative balances of the exergy and exergetic cost for each component and for the whole system was carefully considered. The exergoeconomic model, which represented the productive structure of the system considered, was used to visualize the cost formation process

Uludag University, Faculty of Engineering, Mechanical Engineering Department, TR-16059, Bursa, Turkey,
*Corresponding Author (sorumlu yazarı):yakupsen@uludag.edu.tr

and the productive interaction between components. Cogeneration is the simultaneous production of electric power and usable heat from a single fuel input (Çakir et al., 2012).

Guarinello et al. (2000) have investigated application of thermoeconomic concepts to a projected steam injected gas turbine cogeneration system, which aims at providing the thermal and electrical demands of an industrial district. The power plant is evaluated on the basis of the first and second laws of thermodynamics. A thermoeconomic analysis using the theory of exergetic cost, was performed in order to determine the production cost of electricity and steam.

Bilgen (2000) has investigated the exergetic and engineering aspects of gas turbine based cogeneration plants. The exergy analysis is based on the first and second laws of thermodynamics. The engineering analysis is based on both the methodology of levelized cost and the pay back period. To simulate these systems, an algorithm was developed. Two cogeneration cycles, one consisting of a gas turbine and the other of a gas turbine and steam turbine to produce electricity and process heat were analyzed.

When studies on the cogeneration and trigeneration systems are examined, Zheng and Furimsky (2003) have identified a model using the ASPEN simulation program for their cogeneration plants in their work. The calculated values were compared with the power plant data of 43.6 MW gas turbine and 28.6 MW steam turbine and their results were examined. This program is also used by Shell, Texaco, KRW and BGL oil companies in combined cycle power plants. Bilgen (2000) studied the simulation of exergy and engineering analysis in cogeneration plants operating with gas turbine, waste heat boiler and steam turbine. Examine the exergy analysis according to the first and second laws of thermodynamics. Engineering analysis has been examined according to investment and repayment costs. Algorithm was created for the simulation of the analysis which was made. Toral et al. (2000) developed the SQP package program for the optimization and simulation of cogeneration plants. This program offers an economic optimization model for investment and production costs in a combined cycle power plant.

Material and Methods

The schematic diagram of the CHP system in this study is shown in Fig. 1. ambient air enters the air compressor at point (1) and, after isentropic compression at point (2), it leaves compressor and comes to air pre-heater to preheat the combustion air used in a fuel-burning. This hot air enters combustion chamber at point (3) which is fed by fuel injected into the combustion chamber at point (10). After combustion reaction, hot exhaust gas is produced at point (4). Next, the hot gases leaving combustion chamber are expanded through a gas turbine to produce power. At point (5) hot flue gases leave gas turbine and enter heat recovery steam generator in which energy of flue gases are being utilized to produce steam that has 35 MW heat capacity, 12.994 kg/s and 2MPa saturated steam flow rate capacity in this system. Flue gases are utilized in HRSG to generate steam.

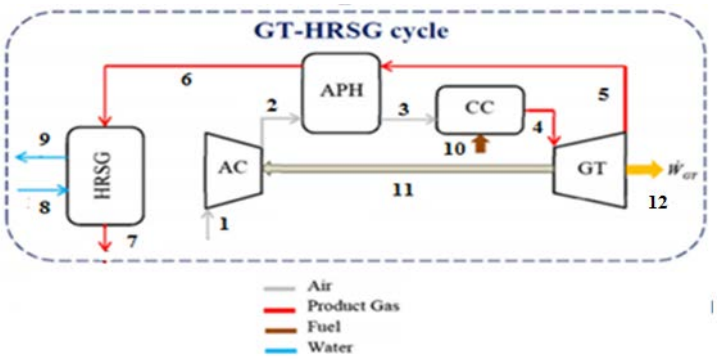

Figure 1 Designed cogeneration system

1. Construction of the system

Figure 1 shows the schematic diagram of a regenerative gas-turbine based heat and power plant (CHP) and shows the exergy flows and the state points which we accounted for in this analysis. In this model, the compressor pressure ratio r_p=8 isentropic efficiency of the compressor η_{sc}=80%. The net maximum power generated by the system is 30 MW and 35 MW heat capacity, 12.994 kg/s and 2MPa saturated steam flow rate capacity. This model's values of the decision variables r_p=8, η_{sc} =80%, T_4=1453.15 K and η_{gt} =85% are taken. For the purpose of analysis the following assumptions are made:

Environmental conditions of the air at the inlet are: P_0=1.013 bar and T_0 =25 °C.

The power plant operates at steady state.

Fuel is assumed to be pure methane (CH_4).

Air and the combustion gases are considered ideal gases with constant specific heats.

The exit temperature is above the dew point temperature of the combustion product.

The pressure drop in the air preheater and combustion chamber is 5%.

The effectiveness of the air preheater is 85%.

2. Economic Analysis of Cogeneration System

All costs due to owning and operating a plant depend on the type of financing, required capital, expected life of a component, etc. The levelized cost method of Moran (1982) is used here. Using the capital recovery factor CRF(i/n) and present worth factor, the annual levelized cost may be written as:

$$\dot{C}\left(\$/\text{year}\right)=\left[\text{PEC}-\left(\text{SV}\right)\text{PWF}\left(\text{i},\text{n}\right)\right]\text{CRF}\left(\text{i},\text{n}\right) \tag{1}$$

$$SV=0.1, CRF(i,n)=i/1-(1+i)^{(-n)}$$
$$PWF(i,n)=(1+i)^{(-n)} \tag{2}$$

and PEC is the purchased-equipment cost.

$$\dot{C}_k=\left(\text{PEC}-\frac{0.1}{\left(1+\text{i}\right)^{\text{n}}}\right)\left(\frac{\text{i}}{1-\frac{1}{\left(1+\text{i}\right)^{\text{n}}}}\right) \tag{3}$$

i is the interest rate and n, the time period.

Equations for calculating the purchased-equipment costs for the components of the power plant are as follows (Bejan et al., 1996):

Table 1. Economic data and cost functions for economic modelling

Properties	
Yearly time of operation (h)	8000
Interest rate (i) %	6
Lifetime of system (n) year	10
Capital recovery factor (CRF)	0.147
Maintenance factor (ϕ_k)	1.06
Price for fuel (USD/GJ)	4.55

System components and capital investment cost functions;

Air compressor (AC);

$$\text{PEC}_{\text{AC}}=\left(\frac{C_{11}\dot{m}_{\text{air}}}{C_{12}-\eta_{\text{sc}}}\right)\left(\frac{p_2}{p_1}\right)\ln\left(\frac{p_2}{p_1}\right)=\left(\frac{71.1*\dot{m}_{\text{air}}}{0.9-\eta_{sc}}\right).\left(\frac{p_2}{p_1}\right).\ln\left(\frac{p_2}{p_1}\right) \tag{4}$$

Combustion Chamber (CC);

$$PEC_{CC} = \left(\frac{C_{21}\dot{m}_{air}}{C_{22} - \frac{p_4}{p_3}}\right)\left[1 + \exp\left(C_{23}T_4 - C_{24}\right)\right] = \left(\frac{46.08 * \dot{m}_{air}}{0.995 - \frac{p_4}{p_3}}\right)\left(1 + \exp\left(0.018 * T_4 - 26.4\right)\right) \quad (5)$$

Gas Turbine (GT);

$$PEC_{GT} = \left(\frac{C_{31}\dot{m}_{gas}}{C_{32} - \eta_{st}}\right)\ln\left(\frac{p_4}{p_5}\right) * \left(1 + \exp\left(C_{33}T_4 - C_{34}\right)\right) = \left(\frac{479.34 * \dot{m}_{gas}}{0.92 - \eta_{st}}\right)\ln\left(\frac{p_4}{p_5}\right)\left(1 + \exp\left(0.036 * T_4 - 54.4\right)\right) \quad (6)$$

Air Pre-Heater (APH);

$$PEC_{APH} = C_{41}\left(\frac{\dot{m}_{gas}\left(h_5 - h_6\right)}{U\Delta T_{lm,aph}}\right)^{0.6} = 4122 * \left(\frac{1.01958 * \left(h_5 - h_6\right)}{18 * \Delta T_{lm,aph}}\right)^{0.6} \quad (7)$$

Heat Recovery Unit (HRU);

$$PEC_{HRU} = 6570\left[\left(\frac{Q_{ec}}{\Delta T_{LMTD_{ec}}}\right)^{0.8} + \left(\frac{Q_{ev}}{\Delta T_{LMTD_{ev}}}\right)^{0.8}\right] + 21276.m_{steam} + 1184.4m_{gas}^{1.2} \quad (8)$$

Dividing the levelized cost by 8000 annual operating hours, we obtain the following capital cost rate for the k component of the plant:

$$\dot{Z}_k\left(\$/h\right) = \frac{\phi_k \dot{C}_k}{H} \quad (9)$$

The maintenance cost is taken into consideration through the factor $\phi_k = 1.06$ for each plant component whose expected life is assumed to be 10 years with an interest rate of 6%, H is the plant operating hour. The number of hours of plant operation per year and the maintenance factor utilized in this study are the typical numbers employed in standard exergoeconomic analysis.

3. Exergy Costing Principles for the System

The exergoeconomic costs of all the flows that appear in the system's schematic diagram are obtained through exergy costing principles. In exergy costing, a cost is associated with each exergy stream. Exergy costing involves cost balances usually formulated for each component separately. For a component receiving a heat transfer and generating power, the cost balance equation may be written as follow (Bejan et al., 1996):

$$\sum_e \dot{C}_{e,k} + \dot{C}_{w,k} = \dot{C}_{q,k} + \sum_i \dot{C}_{i,k} + \dot{Z}_k \quad (10)$$

Where the variable $\dot{C}$ denotes a cost rate associated with an exergy stream and the variable $\dot{Z}$ represents non-exergy-related costs which are calculated by economic analysis.

F-Principle: The cost of exergy removal from a stream must be equal to the cost of supplying the exergy to the same stream in a component located upstream.

P-Principle: Associates the same average cost to any exergy unit supplied to any stream that is related to the product.

The formulations of cost balance for each component and the required auxiliary equations are as follows:

Air compressor:

$$\dot{C}_2 = \dot{C}_1 + \dot{C}_{11} + \dot{Z}_{ac} \tag{11}$$

Where the subscript 11 denotes the power input to the compressor.

Air preheater:

$$\dot{C}_3 + \dot{C}_6 = \dot{C}_2 + \dot{C}_5 + \dot{Z}_{aph} \tag{12}$$

$$c_5 = c_6 \quad or \quad \frac{\dot{C}_5}{\dot{E}_5} = \frac{\dot{C}_6}{\dot{E}_6} \quad (F - Rule)$$

Combustion chamber:

$$\dot{C}_4 = \dot{C}_3 + \dot{C}_{10} + \dot{Z}_{cc} \tag{13}$$

Gas turbine:

$$\dot{C}_5 + \dot{C}_{12} + \dot{C}_{11} = \dot{C}_4 + \dot{Z}_{gt} \tag{14}$$

$$c_4 = c_5 \; or \quad \frac{\dot{C}_4}{\dot{E}_4} = \frac{\dot{C}_5}{\dot{E}_5} \quad (F - Rule)$$

Heat Recovery Unit:

$$\dot{C}_9 + \dot{C}_7 = \dot{C}_6 + \dot{C}_8 + \dot{Z}_{HRU} \tag{15}$$

$$c_8 = 0 \quad c_6 = c_7$$

Where the subscript 12 denotes the net power generated by the turbine. Auxiliary equations are written assuming the same unit cost of incoming and outgoing fuel exergy streams.

Zero unit cost is assumed for air entering the air compressor:

$$\dot{C}_1 = 0$$

An additional auxiliary equation is formulated assuming the same unit cost of exergy for the net power exported from the system and power input to the compressor:

P-Rule:

$$c_{12} = c_{11} \quad or \quad \frac{\dot{C}_{12}}{\dot{W}_{net}} = \frac{\dot{C}_{11}}{\dot{W}_{ac}}$$

The information of the cost streams help in exergoeconomic evaluation of the system. In exergoeconomic evaluation of thermal systems certain quantities, known as exergoeconomic variables, play an important role. These are the average unit cost of fuel ($c_{F,k}$), average unit cost of product ($c_{P,k}$), the cost rate of exergy destruction $\left(\dot{C}_{D,k}\right)$ and the exergoeconomic factor (f_k):

Mathematically, these are expressed as (Bejan et al., 1996):

$$c_{F,k} = \dot{C}_{F,k} / \dot{E}_{F,k}$$

$$c_{P,k} = \dot{C}_{P,k} / \dot{E}_{P,k}$$

$$\dot{C}_{D,k} = c_{F,k}\dot{E}_{D,k}$$

$$f_k = \frac{\dot{Z}_k}{\dot{Z}_k + \dot{C}_{D,k}} \tag{16}$$

Results

Table 1. Results from thermodynamic and economic analysis for 30 MW net power, 35 MW Heat Recovery Unit capacity and 2MPa saturated steam flow rate capacity Cogeneration Heat and Power Plant (CHP)

	Fluid	$\dot{m}$ mass flow rate (kg/s)	Temperature (°K)	Pressure (bar)	Exergy Flow Rate (MW)	Cost Flow Rate ($/h)	Cost per Exergy Unit ($/GJ)
1	Air	111.515	298.15	1.013	0	0	0
2	Air	111.515	589.91	8.104	30.216	2138.799	19.662
3	Air	111.515	893.15	7.691	51.708	3552.311	19.083
4	Combustion Products	113.134	1453.15	7.306	111.042	4946.187	12.373
5	Combustion Products	113.134	998.045	1.013	43.405	1933.388	12.373
6	Combustion Products	113.134	716.398	1.013	19.315	860.341	12.373
7	Combustion Products	103.56	405.892	1.013	1.713	76.292	12.373
8	Water	12.994	298.15	20	0.025	0	0
9	Water	12.994	486.15	20	11.872	1213.82	28.401
10	Methane	1.619	350.414	12.691	81.044	1333.339	4.57
11	Power to air compressor	--	--	--	33.601	1779.985	14.715
Net Power					30	1589.248	14.715

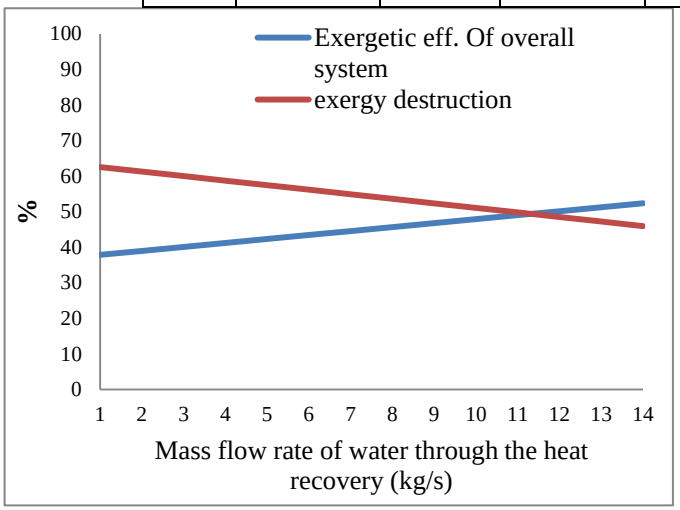

(a)

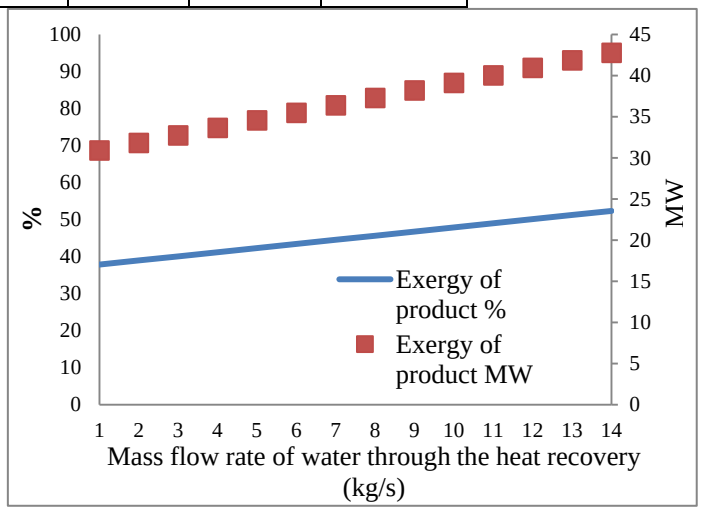

(b)

Figure 2 **For 14 kg/s mass flow rate of water through the heat recovery** (a) exergetic efficiency of overall system and exergy destruction ratio of overall system (b) exergy of product ratio for overall system and amount of exergy of product

Figure 2 shows that the higher mass flow rate of water through the heat recovery influences exergy of product of Heat recovery unit and exergy destruction, exergetic efficiency of overall system. A higher mass flow rates of water through the heat recovery are favorable for exergy efficiency of system.

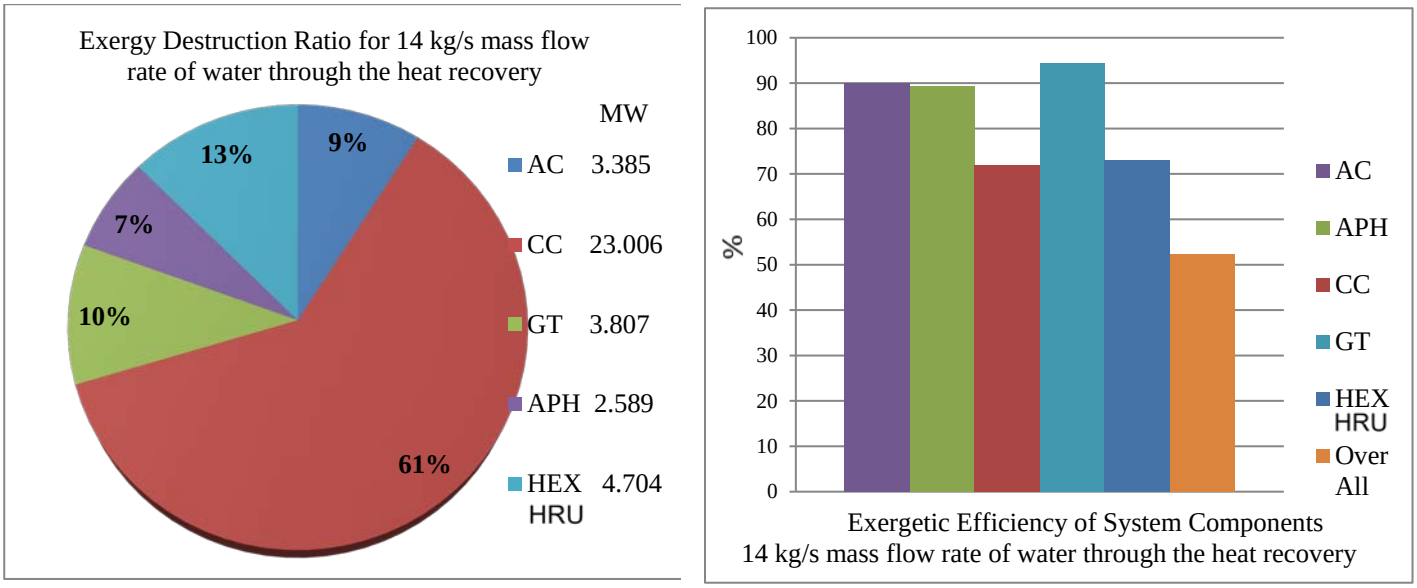

(a) (b)

Figure 3 **For 14 kg/s mass flow rate of water through the heat recovery** (a) exergy destruction ratio and exergy destruction amount of system components (b) exergetic efficiency of system components

The effects of mass flow rate of water through the heat recovery (14 kg/s) on exergy destruction ratio, amount and exergetic efficiency of the system components represented in Figure 3.

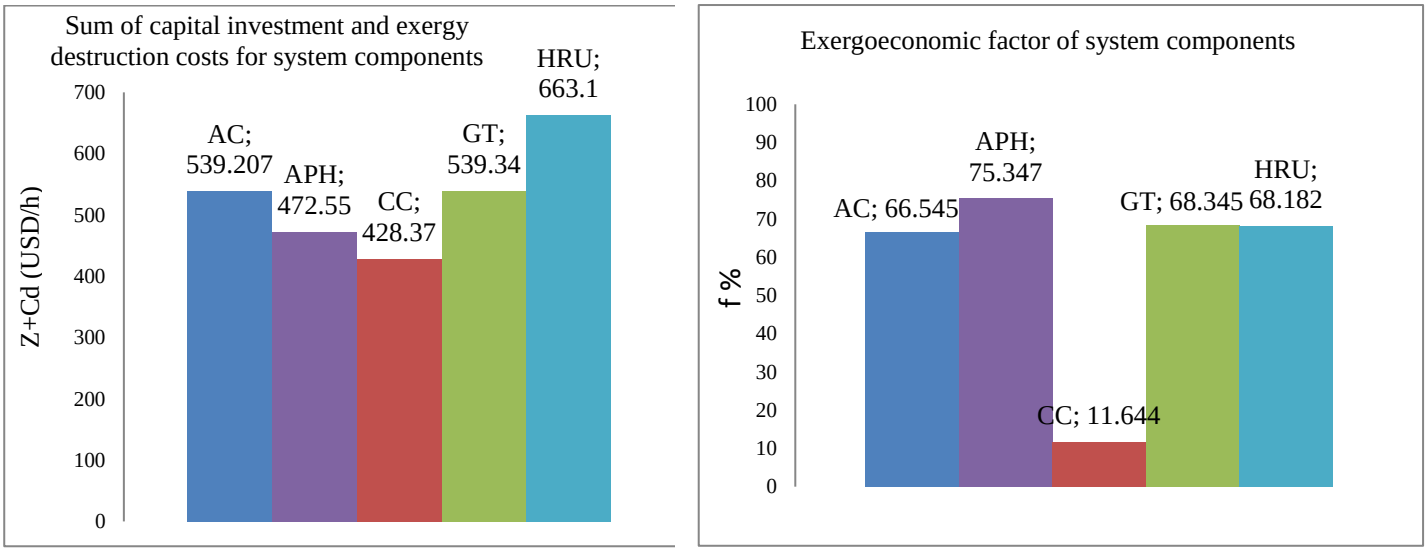

(a) (b)

Figure 4 (a) sum of capital investment and exergy destruction costs for system components (b) exergoeconomic factor of system components

The components having the highest value of the sum of $\dot{Z}_k + C_{D,k}$ are the most important components from the exergoeconomic viewpoint. As seen in Figure 4 the Heat Recovery Unit (HRU) has the highest value of $\dot{Z}_k + C_{D,k}$ and relatively high value of exergoeconomic factor f, and this suggests that the capital investment cost dominates. Hence,

the component efficiency should be improved by decreasing the capital investment cost. This can be achieved by increased gas slide pressure drop. High value of the exergoeconomic factor in the air pre-heater suggests a reduction in the investment cost of this component. A relatively high value of the exergoeconomic factor in the air compressor suggests a reduction in the investment cost of this component. This may be achieved by reducing the pressure ratio and the isentropic efficiency. In the case of gas turbine, sum of the exergy destruction and investment cost are high. The system performance may be improved by increasing the investment cost of this component. Capital investment of the gas turbine depend on temperature T_4 ,pressure ratio P_2/P_1, and isentropic efficiency η .To increase the capital investment $\dot{Z}_k$, we should consider an increase in the value of at least one of these variables.

Analysis for Different Heat Capacities of Heat Recovery Unit

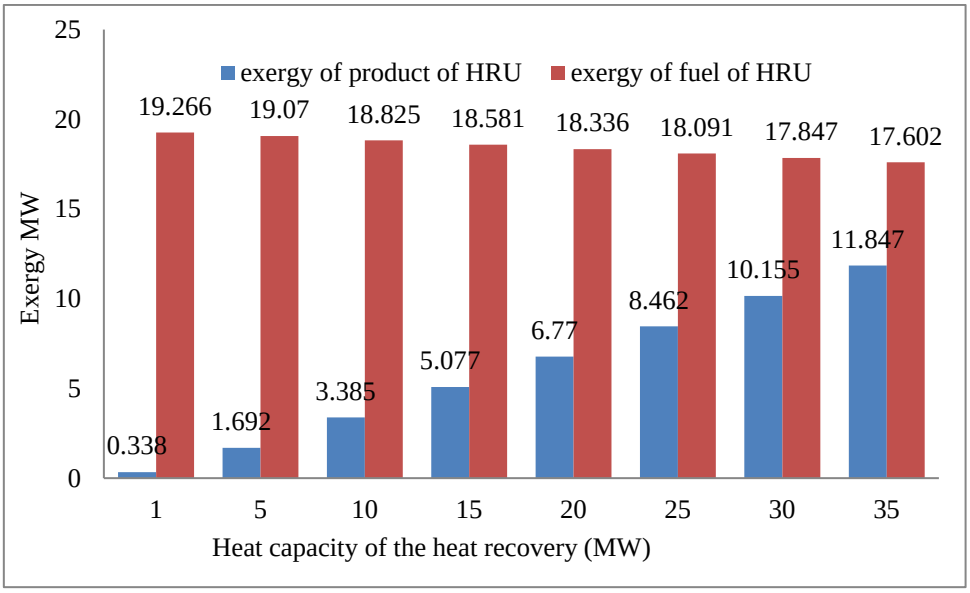

(a)

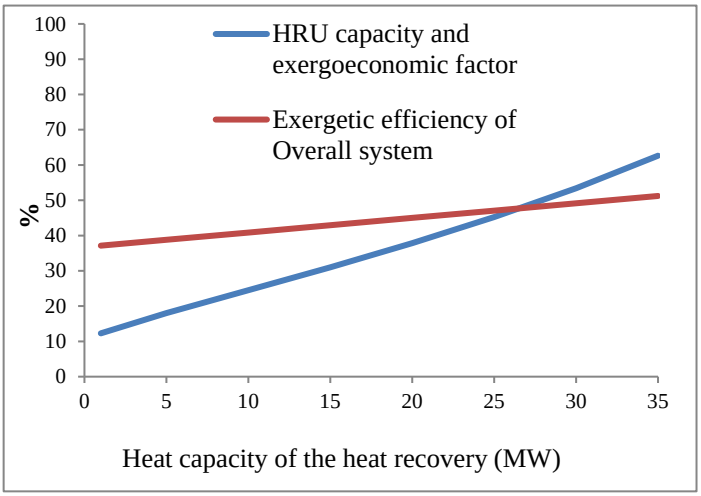

(a)

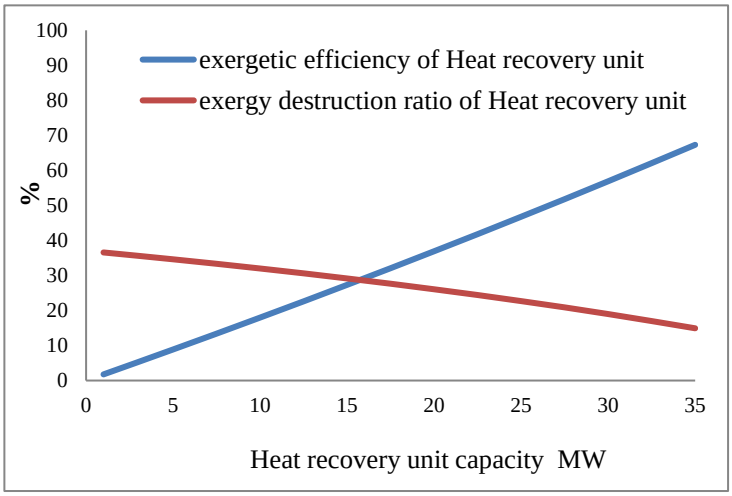

(c)

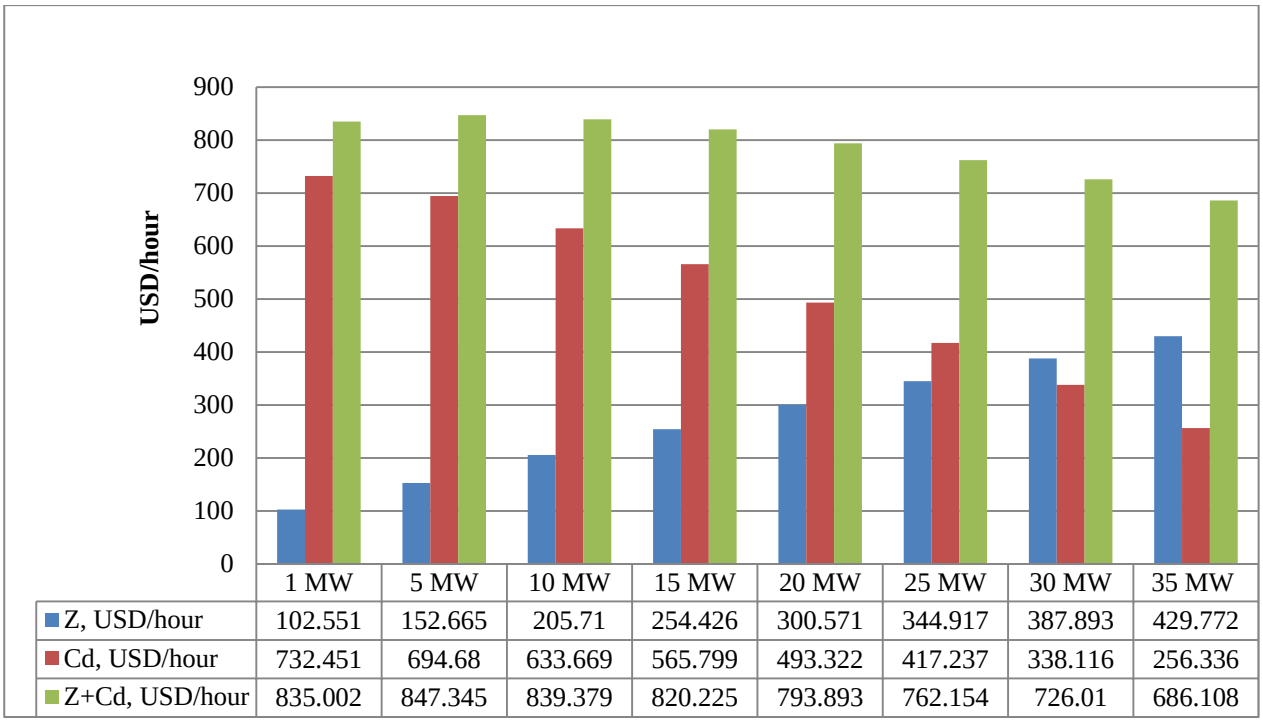

	1 MW	5 MW	10 MW	15 MW	20 MW	25 MW	30 MW	35 MW
Z, USD/hour	102.551	152.665	205.71	254.426	300.571	344.917	387.893	429.772
Cd, USD/hour	732.451	694.68	633.669	565.799	493.322	417.237	338.116	256.336
Z+Cd, USD/hour	835.002	847.345	839.379	820.225	793.893	762.154	726.01	686.108

(d) Different heat recovery capacities and costs of capital investment, exergy destruction and total

Figure 5 **For different HRU capacities** (a) exergy of product of HRU and exergy of fuel of HRU (b) exergoeconomic factor of HRU and exergetic efficiency of overall system (c) exergetic efficiency of HRU and exergy destruction ratio of HRU (d) Different heat recovery capacities and costs of capital investment, exergy destruction and total**.**

Analysis of different pressure of water at the heat recovery intlet (MPa) at 35 MW Heat Recovery Capacity

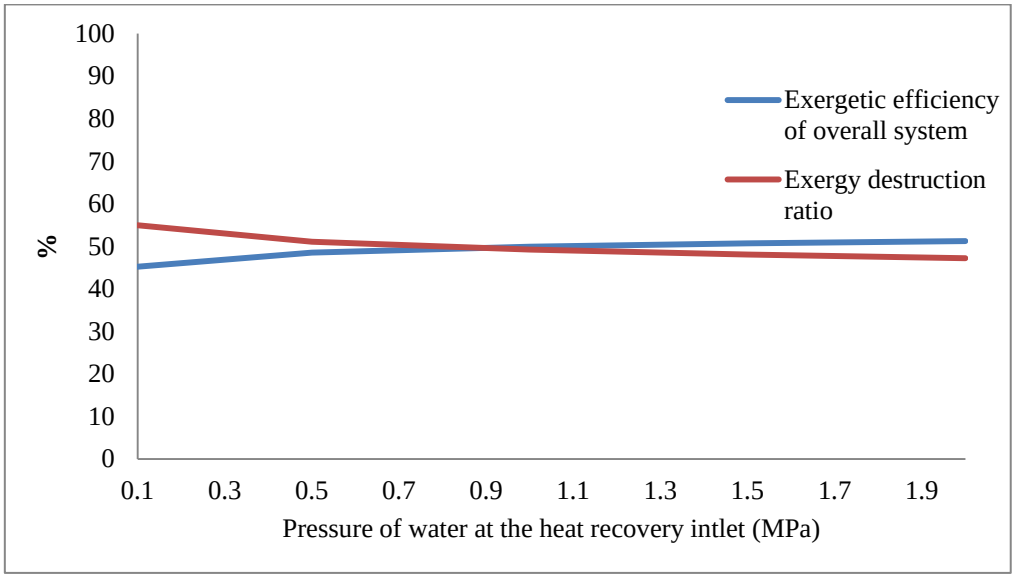

(a)

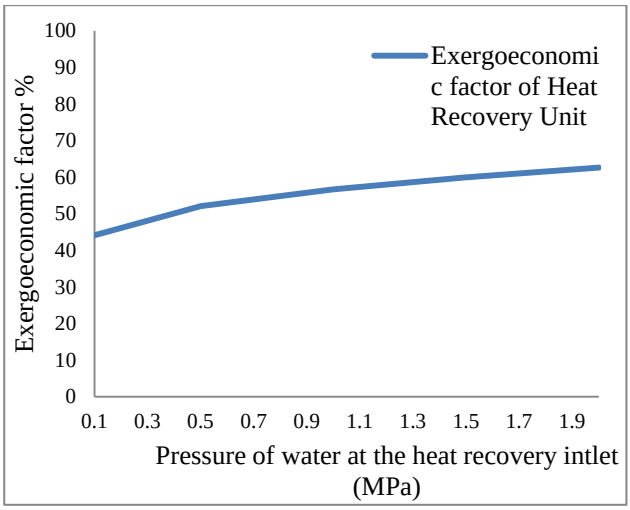

(b)

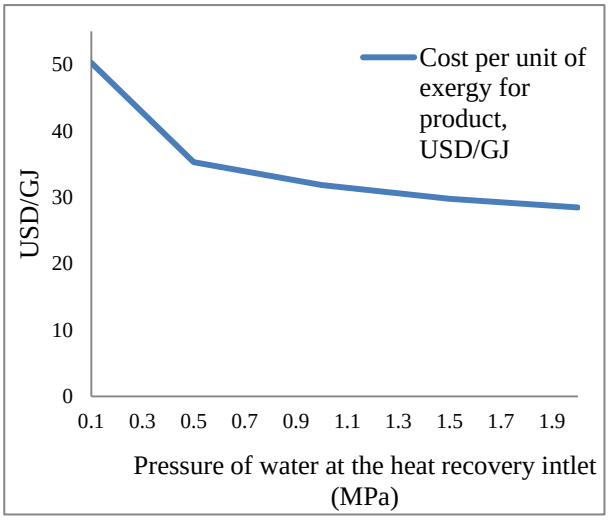

(c)

Figure 6 **For different pressure of water at HRU inlet** (a) exergetic efficiency of overall system and exergy destruction ratio of overall system (b) exergoeconomic factor of HRU (c) cost per unit of exergy for product (USD/GJ)

Figure 6 shows that the higher pressure of water at the heat recovery inlet influences different system parameters.
As pressure increases, the exergy destruction ratio of overall system and cost per unit of exergy for product decreases for HRU (heat recovery unit) and increases exergoeconomic factor of HRU and exergetic efficiency of overall system up to %51.225 at 2MPa HRU operating pressure.

Discussion and Conclusions

Combining the second law of thermodynamics with economics, thermoeconomics using availability of energy, exergy for cost purposes provides a powerful tool used to evaluate the cost effectiveness of thermal systems, with the intent of evaluating and enhance the system performance from both economic and thermodynamics point of view. The analysis assists in the understanding of the cost value associated with exergy destroyed in a thermal system, and hence provides energy system's designers and operators with the information, necessary for operating, maintaining, and evaluating the performance of energy systems.

Thermoeconomic optimization considers how the capital investment in one part of the system effects other parts of the system. The optimization of energy system design consists of modifying the system structure and component design parameters according to one or more specified design objectives. In this paper, thermoeconomic optimization and analysis has been performed for a 30 MW regenerative gas turbine based cogeneration heat and power plant. The two objectives are involved in the optimization process: thermodynamic (maximum efficiency and minimum fuel consumption), economic (minimum cost per unit of time and maximum profit per unit of production).

Nomenclature

c – average cost per unit exergy ($/kJ);
f - exergy economic factor,
CHP - combined heating and power
CRF - capital recovery factor
$\dot{C}$- cost rate with exergy stream , ($/h);
$\dot{C}_D$- cost rate with exergy destruction, ($/h);
$\dot{E}$- exergy, (W);
i - interest rate
n - total operating period of the system (year);
PEC - purchase cost, ($);
PWF - present worth factor
r_p- pressure ratio
SV - salvage value
T - temperature, K;

Subscripts

AC - air compressor.
APH - air pre-heater.
CC - combustion chamber.
GT - gas turbine.
HRSG - heat recovery steam generator.
HRU - heat recovery unit.
HEX - heat exchanger
D - destruction
F - fuel
k - component “k”
P - product
w - water
W- work

$\dot{Z}$ - equipment cost rate, ($/h) ;

$\dot{Z}_k$ - capital cost rate of unit k, ($/h) ;

Symbols

ϕ_k - maintenance factor

n_{st} - isentropic turbine efficiency

n_{sc} - isentropic compressor efficiency

References

A. Valero, M. Lozano, L. Serra, G. Tsatsaronis, J. Pisa, C. Frangopoulos, M. Spakovski,(1994). CGAM Problem: Definition and Conventional Solution. Energy The International Journal, Vol. 19, pp. 279-286.

A. Bejan, G. Tsatsaronis, M. Moran,(1996). Thermal design and optimization. New York: Wiley.

E. Bilgen, (2000). Exergetic and Engineering Analyses of Gas Turbine Based Cogeneration System. Energy, Vol. 25, pp 1215-1229.

Guarinello, F., Cerqueira, S. and Nebra, S., (2000). Thermodynamic Evaluation of a Gas Turbine Cogeneration System. Energy Convers. Mgmt. Vol, 41, pp 1191-1200.

Kwak, H., Kim, D. and Jean, J., (2003). Exergetic and Thermodynamic Analyses of Power Plants. Energy, Vol. 28, pp 343-360.

L. Zheng, E, (2003). Furimsky. ASPEN Simulation of Cogeneration Plants. Energy Conversion & Management, 44: 1845-1851.

Mısra, R., Sahor, P. and Gupta, A.,(2002). Application of the Exergetic Cost Theory to the LiBr / H2O Vapour Absorption System. Energy, Vol. 27, pp1009-1025.

Moran, M. J., (1982). Availability analysis: A guide to efficient energy use. Englewood Cliffs, NJ: Prentice-Hall.

R. Toral, W. Morton, D.R. Mitchell, (2000). Using New Packages for Modelling, Equation Oriented Simulation and Optimization of a Cogeneration Plant. Computers and Chemical Engineering, 24: 2667-2685.

Y. Cengel, M.A. Boles, (2008). Thermodynamics an Engineering Approach.

International Conference on Science and Technology

ICONST 2018

5-9 September 2018 Prizren - KOSOVO

The Study on Pre-Prototype Manufacturing of a Beta Type Stirling Engine by Using Three Dimensional Printing Technologies

Derviş Erol[1]*, Sinan Çalışkan[2]

Abstract: Nowadays, three-dimensional printing technologies have become widespread with the developing technology, and they have reached a significant level in many developed countries with their use in the manufacturing of prototypes almost in every field. Pre-prototypes of all kinds of parts designed three dimensionally in computer-aided design programs can be made faster and cheaper compared to the traditional methods of manufacturing of a prototype by using three-dimensional printing technologies. Thus, they provide great advantages in terms of time and cost for designers before the manufacturing of the actual prototype of complex systems and provide great convenience in research and design studies. Since the manufacturing of the prototype of Stirling engines involves important and detailed processes, the manufacturing of the prototype of these engines is very time-consuming and overcosting. Before the manufacturing of the prototype of Stirling engines, numerical analyses are carried out to determine the working parameters of the engine and their designs are made three dimensionally with the help of computer aided design programs. Errors in designs made in the computer environment are often not noticed during design and appear during manufacturing. Due to these errors of design, significant losses in terms of time and cost are experienced. In this study, the pre-prototype of a beta type Stirling engine was manufactured before the manufacturing of the actual prototype using three-dimensional printing technologies. As a result of the study, it was checked whether the system works mechanically and visually with the manufacturing of the pre-prototype obtained without spending high costs. With the help of this study, unexpected errors of design were prevented during manufacturing and unnecessary time and cost losses were avoided.

Keywords: 3D prototype, 3D printing technology, Stirling engines, Rhombic drive mechanism

Introduction

Three-dimensional printing technologies, also known as rapid prototyping technology, are one of the most significant rapid developments in terms of technology increasing with the industrialization in 21st century (Al-Ahmari et al. 2018; Jaiganesh, 2014). Californian designer Charles, W. Hull designed and manufactured the first machine that could produce a three-dimensional prototype of an item in the 1980's. This design registered as Stereolithography method in 1986 with the original patent number US4575330, has started a new process in the manufacturing sector (Hull, 1986; Ngo et al. 2018). In three-dimensional printing technology, any item designed as three-dimension in computer-aided design programs is virtually divided into layers by the help of a special computer software. This item is manufactured from the three-dimensional design directly by overlapping these virtual layers to the melted layer material. This manufacturing method is also known as additive manufacturing as it is the exact opposite of the traditional manufacturing methods. Macro-sized items are produced by the micro-sized items through this method. The devices that carry out this process are called three-dimensional printer (Singh et al. 2017).

[1] Kırıkkale University, Department of Automotive Technology, Yahşihan, Kırıkkale, TURKEY
[2] Hitit University, Department of Mechanical Engineering, Çorum, TURKEY
*Corresponding author: derol40@gmail.com

In the three-dimensional printing technologies, various raw materials are used as a production material from plastics to metals and ceramic to wax. Three-dimensional printing technology is a new technology widely used and developed in recent years especially in the fields of Medicine, Space-Aeronautics, Automotive, Military, and Architecture. It is observed that the majority of the academic studies that have been carried out by using three-dimensional printing technologies were realized in engineering and medicine fields (Pucci et al. 2017; Lee et al. 2017).

Three-dimensional printing technology offers many advantages such as saving time and cost compared to traditional prototype manufacturing methods, facilitating the prototype manufacture of complex parts and causing less harmful waste to the environment. In addition to these advantages, it provides great conveniences to the designers for the research and development works (Munaz et al. 2016).

Nowadays, the manufacturing of Stirling engine parts is generally carried out by using conventional manufacturing methods such as turning, milling and other machining processes. Stirling engines are structurally very complicated systems.

Therefore, the operating parameters of the engine are determined by numerical analyzes and three-dimensional designs are created by the help of computer-aided design programs before the prototype manufacture of the engine developed by the designers. Errors in computer-generated designs are often unrecognizable in the process of designing and appear during the manufacturing process. Great losses are faced in terms of time and cost due to these design flaws.

In this study, it is planned to manufacture a preliminary prototype of beta type Stirling engine before the actual prototype by using three-dimensional printing technologies. It will be checked whether the system works mechanically and visually without spending high costs by means of the preliminary prototype manufacture obtained as a result of the study. With the help of this work, It is predicted to prevent unexpected design errors during manufacturing and avoid unnecessary time and cost losses.

Material and Method

In the scope of this study, the drawings and assembling of the items whose preliminary prototypes to be manufactured in three-dimensional printer have been realized in a computer-aided design program called as SolidWorks. Figure 1. shows schematic views of the Stirling engine with the rhombic drive mechanism in SolidWorks environment. The engine block, expansion cylinder and piston, power cylinder and piston, connecting rods of expansion and power piston, rhombic gears and flywheel are the major components of the engine.

Following the designs of the items to be prototype manufactured, the related design folders must be converted into a suitable software language that three-dimensional printers can use. This software language is described as STL (Stereo Lithography). Each item on Solidworks environment has been rebuilt separately in STL format.

In the scope of this study, the pre-prototype manufacture of Stirling engine with the rhombic drive mechanism has been carried out by using Zortrax M200 model printers as seen in Figure 2. The maximum print dimension of the Zortrax M200 model is 200 x 200 x 180 mm. The Zortrax M200 model can conveniently use wide range of filament materials. The engine parts, whose print dimensions exceed this limit, are manufactured in multi-parts. These parts have been then assembled using a suitable adhesive. Filament materials, as known as Z-ABS, the product of Zortrax, are used in the manufacturing of the parts. Z-ABS filament materials are preferred for the manufacturing of the parts where mate and smooth surfaces are obtained and are mainly used for testing purposes. Three-dimensional parts with high quality, smooth and high resistance strength are produced with Zortrax M200 model.

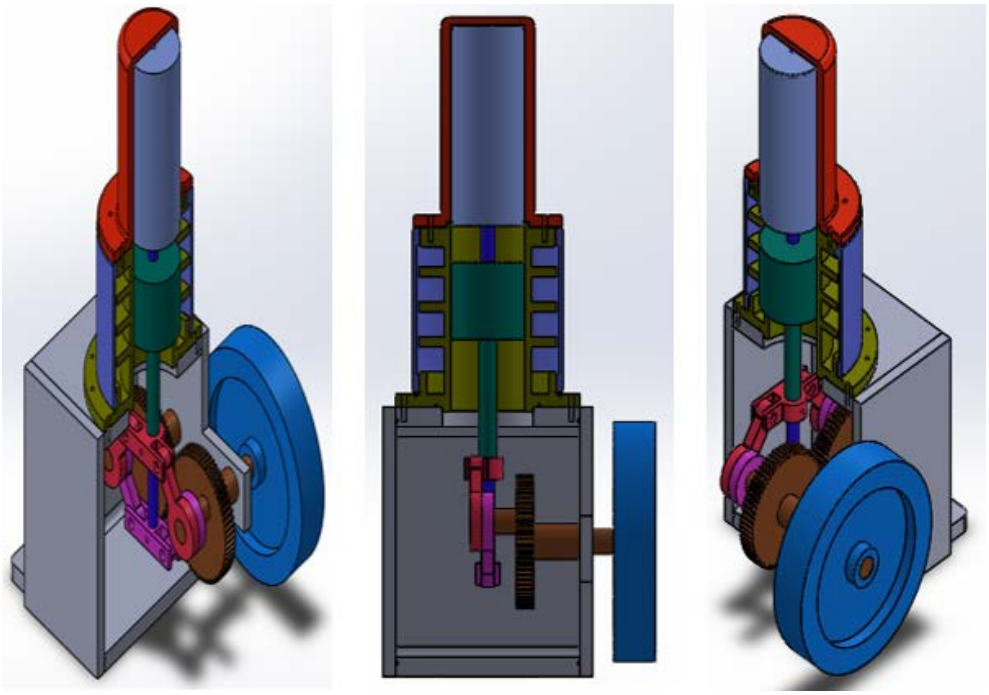

Figure 1. Schematic views in the SolidWorks environment of pre-prototype Stirling engine

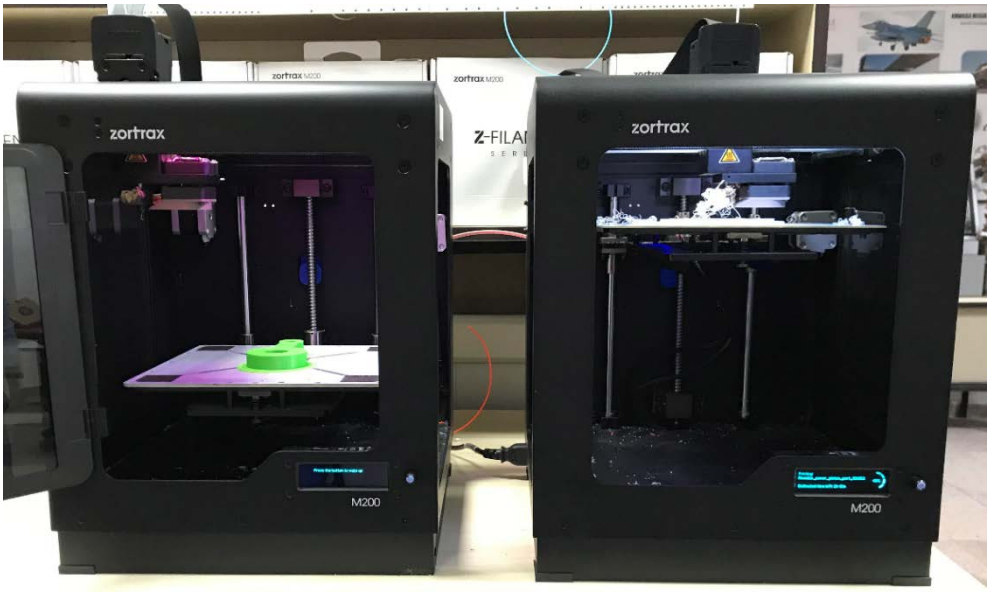

Figure 2. Zortrax M200 model three-dimensional printers

The layering of the parts of Stirling engine to be manufactured and print settings are made via Z-Suite software as seen in Figure 3. For the entire geometry of the part in layering process, it is necessary to create a manufacturing sequence from the bottom to the top of the layer. Furthermore, printing parameters such as the type of the material to be printed, printing thickness, printing quality and material occupancy structure can be adjusted in different shapes upon the requests of the user through the Z-Suite software. Following these basic adjustments, the three-dimensional manufacturing process is initiated by transferring to printer via USB or SD card in the file format that can be used by the three-dimensional printer. Figure 4. shows some of the basic parts of the Stirling engine which has been manufactured pre-prototype such as expansion cylinder, power cylinder, engine block, flywheel and rhombic drive mechanism gears.

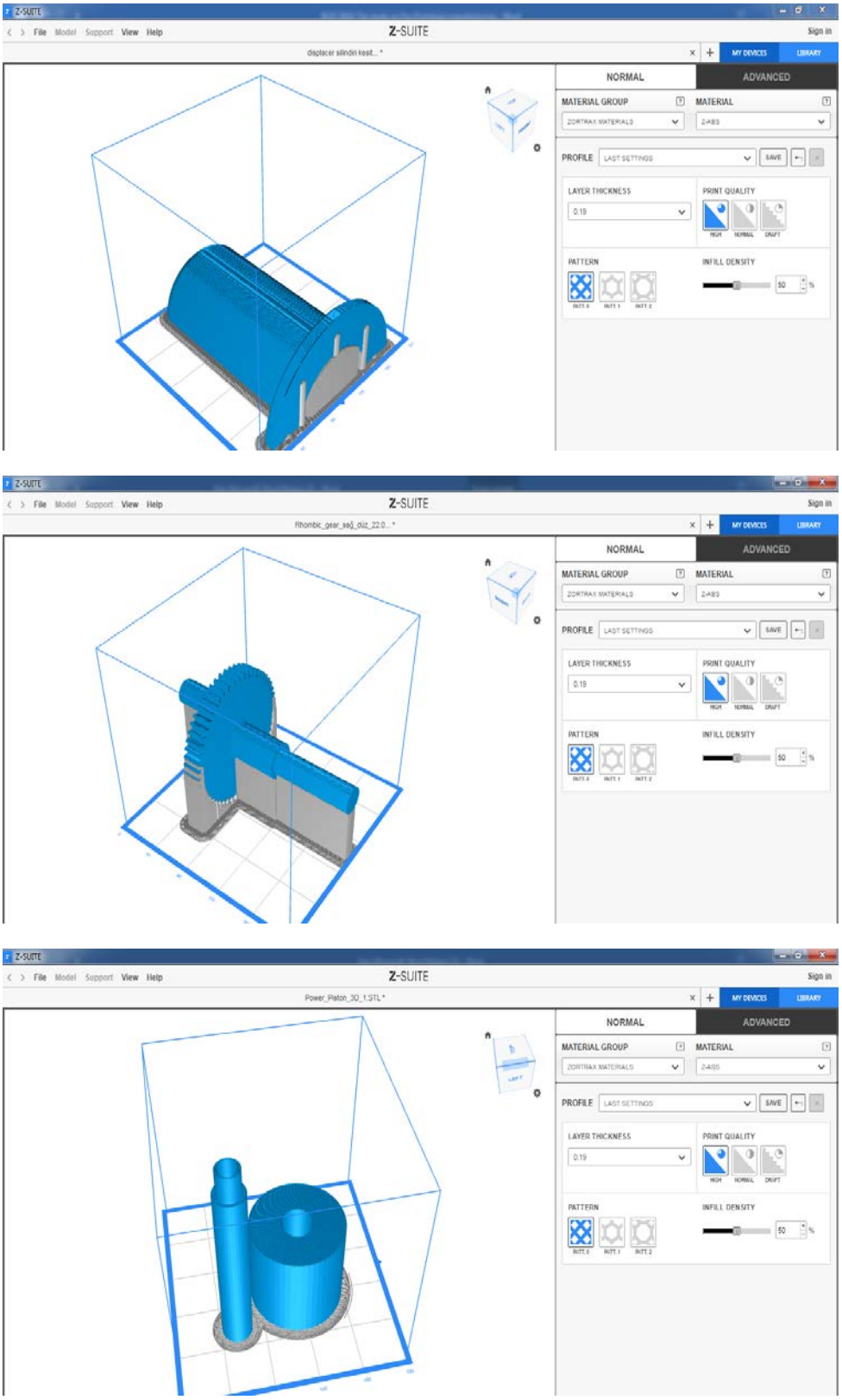

Figure 3. Schematic views of engine parts in Z-Suite software on the computer

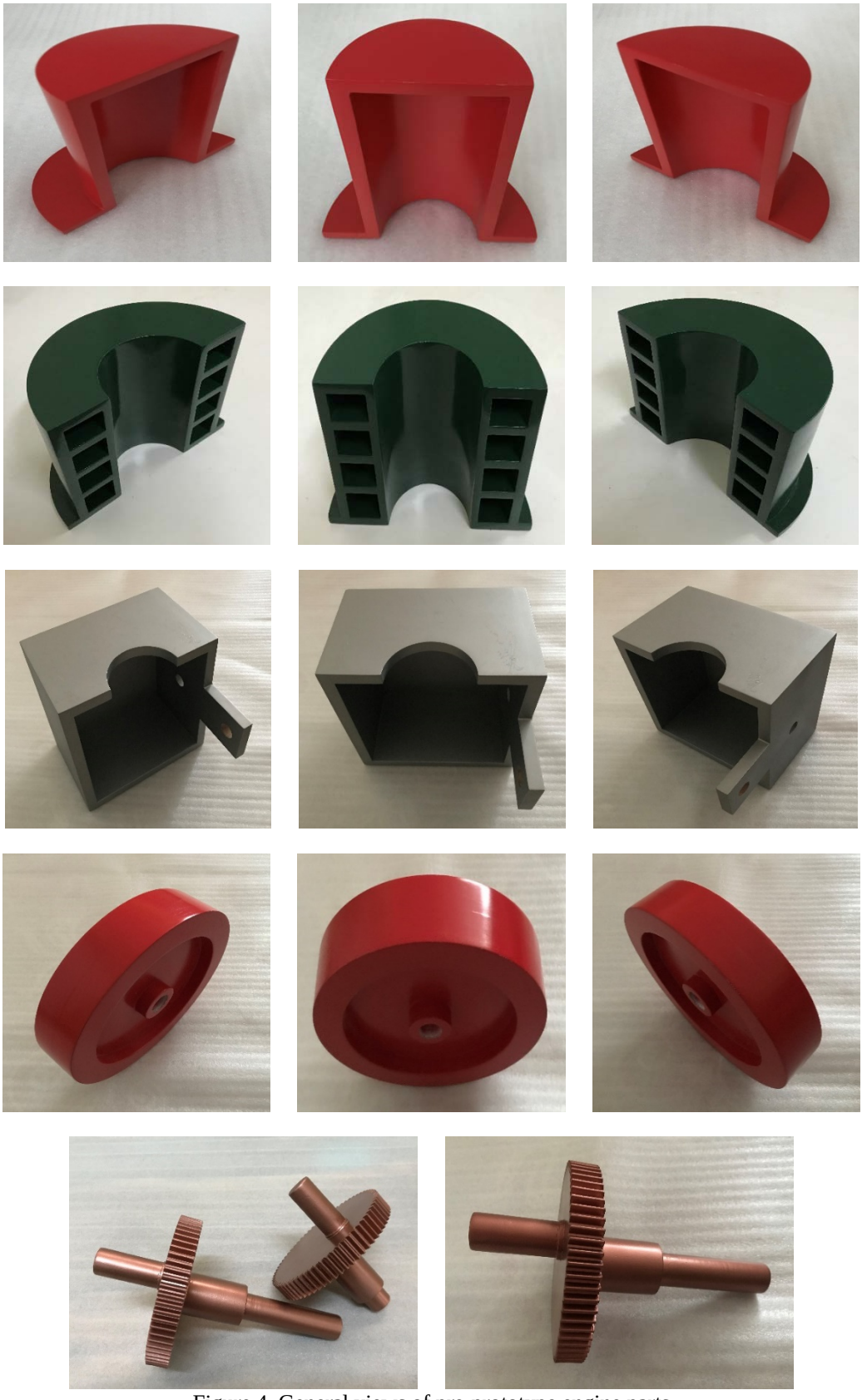

Figure 4. General views of pre-prototype engine parts

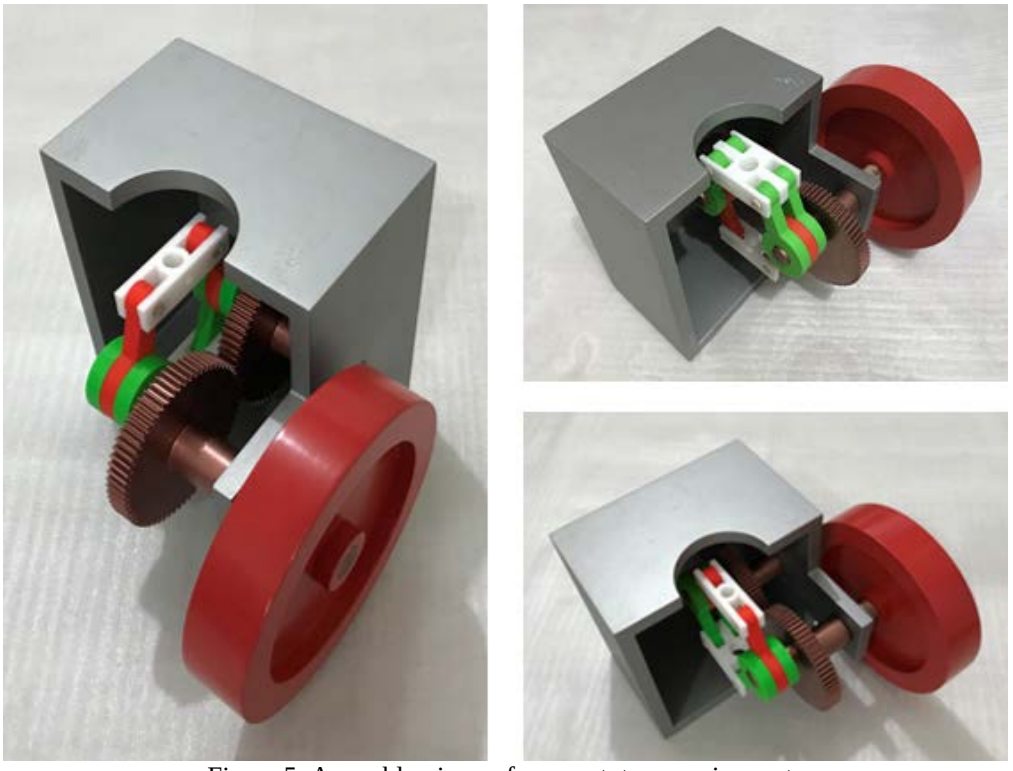

Figure 5. Assembly views of pre-prototype engine parts

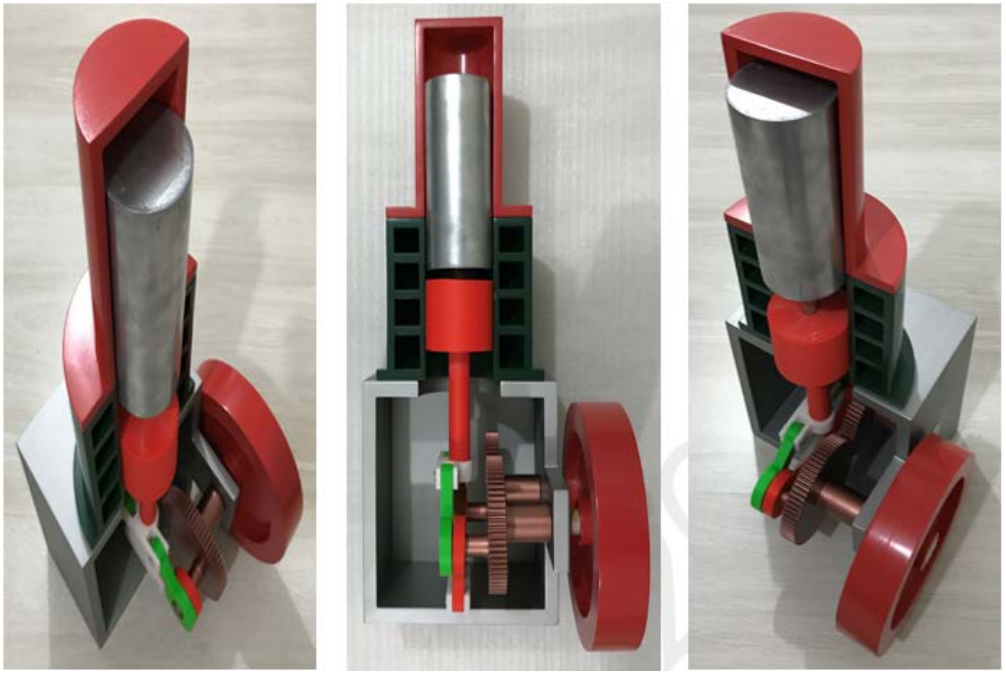

Figure 6. Assembly views of pre-prototype Stirling engine with rhombic drive mechanism

Figure 7 shows rhombic drive mechanism, power and displacer pistons of the Stirling engine which has been manufactured pre-prototype.

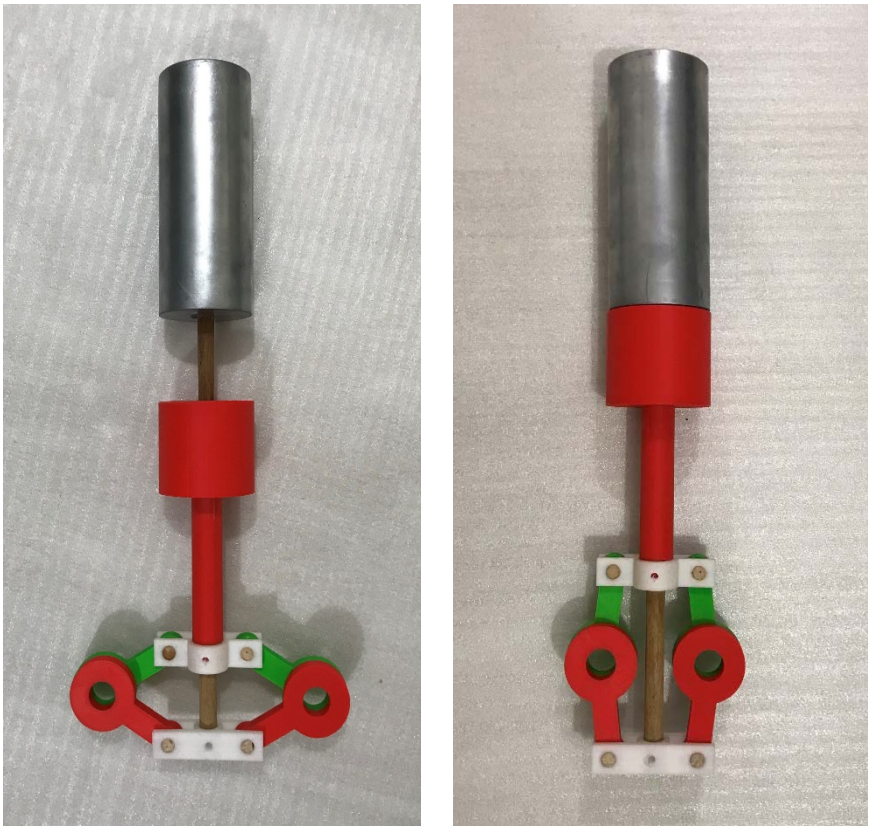

Figure 7. Assembly views of pre-prototype rhombic drive mechanism

Results and Discussions

In this study, the manufacture of preliminary prototype has been carried out before the actual prototype of a beta type Stirling engine with rhombic drive mechanism by using three-dimensional printing technologies. As a result of the researches and studies, the following evaluations are listed for the benefits of the preliminary prototype manufacturing of Stirling engine that has been manufactured by using three-dimensional printers.

- ❖ It has been checked whether the system works mechanically and visually without spending high costs by means of the preliminary prototype manufacture obtained as a result of the study.

- ❖ Unnecessary losses of time and cost are prevented by avoiding unexpected design errors during manufacturing process.

- ❖ Prior to the start of the actual prototype manufacturing, significant contributions have been provided to the development of the design of Stirling engine. Thus, the actual prototype manufacturing process becomes more productive and efficient.

Acknowledgment

This study was supported within scope of the project numbered MUH19002.18.001. by the Hitit University Scientific Research Projects Coordination Unit. We would like to thank Hitit University Scientific Research Projects Coordination Unit for their financial support.

References

Al-Ahmari, A., Ameen, W., Abidi, M. H., and Mian, S. H., (2018). Evaluation of 3D printing approach for manual assembly training. International Journal of Industrial Ergonomics, 66(1), 57-62.

Hull, C. W., (1986). Apparatus for production of three dimensional objects by stereolithography. United States Patent No: US4575330

Jaiganesh, V., and Mugilan, E., (2014). Manufacturing of PMMA cam shaft by rapid prototyping. Procedia Engineering 97(1), 2127-2135.

Lee, J. Y., An, J., and Chua, C. K., (2017). Fundamentals and applications of 3D printing for novel materials. Applied Materials Today, 7(1), 120-133.

Munaz, A., Vadivelu, R. K., John, J. S., Barton, M., Kamble, H., and Nguyen, N. T. (2016). Three dimensional printing of biological matters. Journal of Science: Advanced Materials and Devices, 1(1), 1-17.

Ngo, T. D., Kashani, A., Imbalzano, G., Nguyen, K. T., and Hui, D. (2018). Additive manufacturing (3D printing): A review of materials, methods, applications and challenges. Composites Part B: Engineering, 143(1), 172-196.

Pucci, J. U., Christophe, B. R., Sisti, J. A., and Connolly Jr, E. S., (2017). Three dimensional printing: technologies, applications, and limitations in neurosurgery. Biotechnology advances, 35(5), 521-529.

Singh, S., Ramakrishna, S., and Singh, R., (2017). Material issues in additive manufacturing: a review. Journal of Manufacturing Processes, 25(1), 185-200.

International Conference on Science and Technology

ICONST 2018

5-9 September 2018 Prizren - KOSOVO

Encouraging Factories to Process Innovation: A Game Theory Approach

Burcu Kubur Özbel[1]*, Adil Baykasoğlu[2]

Abstract: Competitiveness of companies often depends process design, which considerable influence cost factors. From this motivation, this work studies the affects of process-innovation incentives in factories. A case study is presented to illustrate the importance of cooperation in process innovation between different factories. It is aimed to reduce the cost of the workstation for all cooperating factories. One of the way to attain this aim is to improve the efficiency of the manufacturing process in assembly line by merging the assembly line systems of different factories so that their joint costs are reduced. Therefore, after innovative process design, instead of solving two different single-model assembly line balancing problem, a mixed-model assembly line balancing problem is solved. For this reason, a novel single assembly line balancing model is proposed by making some adaptations on the known models in the literature. After getting profits from the cooperation, the next question is to determine how to share profit among partners. The Shapley value approach is used to allocate the profit obtained from process innovations. The Shapley value considers the marginal contribution of each participant in a collaborative system and provides a unique allocation solution. Results show that, significant profit increment can be obtained across the factories through cooperation. The following future work can be considered to further improve the present study. First of all, the assembly line balancing problem can be tackled for different objectives. Another issue is related to the negotiation power of factories, which is assumed to be same for all factories. Relaxation of this assumption may be more realistic for some circumstances. Finally, this research can be extended by employing and comparing other solution concepts for cooperative games.

Keywords: Process innovations, Assembly lines, Game theory, Shapley value, Profit sharing

Introduction

For dynamic and competitive environment collaboration generates important advantages. The increasing need for manufacturing due to resources shortages, environmental deterioration and new regulations, requires companies to organize their activities in order to explore and take full advantage of the cooperation. The plants decide to participate collaborative networks to minimize their individual costs. In this study, process-innovation incentives denote the guarantee of joint gains among the network plants whenever the total efficiency of the network increases. Game theoretical modelling is used to study the design of process-innovation incentives for plants network. In general, earlier literature concerning innovation-incentive mechanisms is mostly concerned either with the national level (Jaffe, 2000; Conceição et al. 2003, Kuhlmann and Edler, 2003) or with the intra-firm level (Leptien ,1995 ; Nerkar et al. 1996; Bester and Petrakis, 2004).

[1]Dokuz Eylül University, Faculty of Engineering, Departmnent of Industrial Engineering, 35397, Buca, İzmir, TURKEY
[2]Dokuz Eylül University, Faculty of Engineering, Departmnent of Industrial Engineering, 35397, Buca, İzmir, TURKEY
*Corresponding author: burcu.kubur@deu.edu.tr

However, the research on innovation incentives for company networks has been scarce. In addition to this, game theory applications to innovation systems have been few.

Three levels of innovation games exist in the literature. These are intra-organizal games, inter-organizational games and meta-organizal games (Baniak, 2012). For a detailed analysis between innovation and game theory the work which is done by Baniak (2012) is recommended. During the last decade, game theoretic applications on inter-organizational relationships have become popular. For example, Wolters and Schuller (1997), Lim (2001), Corbett and DeCroix (2001) and Cousins (2002). However, all of this work is presented game theoretic model which analysis strategic relationships between suppliers. Still, it is very scare overlapping area of game theory and innovation approach. Mostly, they focus on non-cooperative game models instead of cooperative game models. Therefore, in the considered case, cooperative game model within inter-organizational case is taken into account from the assembly line perspectives. In the literature, there exist only one work Amasaka (2007) which makes innovation in the working environment. This study selects vehicle assembly line models and investigates a production line that employes a comprehensive analysis of incorporated ergonomics, physiology and psychology. Results show that, measures for an aging workplace developed by this activity yielded practical results and are being applied to both domestic and overseas operations to improve productivity.

This paper contributes to the existing literature in several ways. First, it presents the explicit design of process- innovation incentives for plants. Based on the game theory, utility sharing strategy namely Shapley value approach is used to encourage the plants to be innovate. Second, proposed binary integer programming formulation for mixed model assembly line balancing problem by Gökcen and Erel (1998) is adjusted for single assembly line balancing problem.

Material and Method

The motivation for the game theoretic study of process innovations in plants networks is presented. The advantages of horizontal cooperation is indicated especially in terms of reduction on assembling cost of plants. First, plants' individual (before the coalition case) assembling cost are determined by solving single assembly line balancing problem. After that, the coalitional costs are obtained by solving mixed model assembly line balancing problem which is given by Gökcen and Erel (1998). To allocate coalitional costs, Shapley value approach is used. The Shapley value considers the marginal contribution of each participant in a collaborative system and provides a unique allocation solution.

Cost estimation models

In a single model assembly line balancing problem, one homogeneous product is continuously manufactured in large quantities. The set of tasks and the set of precedence relations which specify the permissible orderings of the tasks are given and the problem is to assign the tasks to an ordered sequence of stations such that the precedence relations are satisfied and some performance measure is optimized. In this paper, the work of Gökcen and Erel (1998) is adjusted for single assembly line balancing problem to calculate no coalitional case of plant's cost.

The assumptions of the model are listed below:

1. Task performance times are known.
2. Precedence relations between tasks are known.
3. Parallel stations are not allowed.

Before explaining the proposed model, index sets, parameters and decision variables are given.

Notation

N	=total number of tasks	
K	=number of stations	
t_i	=processing time task *i*	*i*=1..*N*
P_i	=subset of all tasks that precede task *i*	*i*=1..*N*
F_i	=subset of all tasks that follow task *i*	*i*=1..*N*
C	=cycle time	
E_i	=earliest station task *i* can be assigned to, given the precedence relations	*i*=1..*N*
L_i	=latest station task *i* can be assigned to, given the precedence relations	*i*=1..*N*
V_{ik}	=1 If task *i* is assigned to station *k*, 0 otherwise	
X_k	=1 If station *k* is utilized, 0 otherwise	
W_k	=subset of all tasks that can be assigned to station *k*	
$\|\|W_k\|\|$	=number of tasks in set W_k	

Patterson and Albracht (1975) firstly developed a model for the single-model assembly line balancing problem. Expressions for the earliest and latest station of task i are modified for the single-model assembly line balancing problem as follows:

$$E_i=\left[\frac{t_i+\sum_{j\in P_i} t_j}{C}\right]^+ \quad \text{for} \quad i=1,...,N, \tag{1}$$

$$L_i=k+1-\left[\frac{t_i+\sum_{j\in F_i} t_j}{C}\right]^+ \quad \text{for} \quad i=1,...,N, \tag{2}$$

Constraints

The constraints of the model can be grouped into four sets and are explained below.

Assignment constraints:

This set of constraints assures that tasks of each model are assigned to at most one station and can be written as follows:

$$\sum_{k=E_i}^{L_i} V_{ik}=1 \quad \text{for} \quad i=1,...,N, \tag{3}$$

Precedence constraints:

In the combined precedence diagram, the precedence relation between task *a* and task *b*, where *b* is an immediate follower of *a*, can be expressed as follows:

$$\sum_{k=E_a}^{L_a} k.V_{ak}-\sum_{k=E_b}^{L_b} k.V_{bk}\le 0 \ \ where \ \ L_a\ge E_b \ \text{ and } \ E_b\ge E_a \tag{4}$$

Cycle time constraints:

The sum of the task performance times within a station must be less than or equal to the cycle time and this can be expressed as follows:

$$\sum_{i\in W_k}^{L_a} t_i V_{ik}\le C \quad \text{for} \quad k=1,...,K, \tag{5}$$

Stations constraints:

If the work content of station *k* for a model is zero, then the work content of this station must also be zero. This can be accomplished by introducing the following constraints:

$$\sum_{i\in W_k} V_{ik}\text{-}\|W_k\|X_k\le 0 \ \text{ for } \ k=1,...,K, \tag{6}$$

Objective function:

The objective is to minimize the number of stations utilized:

$$Min\sum_{k=1} X_k \tag{7}$$

Note that, to estimate the assembling cost of plants of coalition which is mixed model assembly line balancing problem is solved via Gökcen and Erel (1998)'s binary integer programming formulation.

Cost savings allocation

This section deals with the problem of how to share the benefits of that collaboration among the different partners. This is not an easy question, since it is not obvious what the contribution of each company to the

total cost savings is. It may be first thought that some rule, such as sharing the cost savings proportional to the participated company. However, in general, this type of simple proportional rule does not guarantee that a fair and equitable distribution of the benefits of the collaboration is attained (Cruijssen et al. 2007; D'Amours et al. 2010; Shapley, 1950). Therefore, a more theoretically-grounded approach is needed and one of the most appropriate alternatives seems to be cooperative game theory (CGT). Game theory generally defined as the study of mathematical models of conflict and cooperation between intelligent rational decision-makers. CGT provides a natural framework within joint cost savings allocation problems. A cooperative game is the branch of game theory which has two elements. These are a set of players N = {1,2, …, |N|} and a characteristic function c. In short, a game (Γ) is defined by the pair (N, c). Players are decision makers and we call every subset S ⊆ N cooperating players of a coalition. If two players are not cooperating, they belong to different coalitions; i.e., there is only one occurrence of cooperation. N is called the grand coalition. The number of coalition ($2^{|N|}$) rising exponentially with the increasing number of players. The set of players is assumed finite. The characteristic function:

$$c : 2^N \rightarrow R \tag{8}$$

assigns a cost or profit value (representing the total amount of transferable utility) to each coalition S ⊆ N which determines the best outcome for the coalition S if the players in S cooperate without the players in N\S. Empty set c(Ø)=0. The characteristic function can be interpreted as profits or costs. Although there are many CGT solution concepts, we will concentrate on the Shapley value method.
Shapley (1958) aims to develop an allocation method that yields a unique solution for every game in coalitional form. The cost allocated to the company *j* is equal to

$$y_j = \sum_{S \subset N : j \in S} \frac{(|S|-1)!(|N|-|S|)!}{|N|!} [c(S) - c(S - \{j\})] \tag{9}$$

The Shapley value is based on four axioms formulated by Shapley (1958). These axioms express that a cost allocation computed according to this solution concept satisfies the properties of efficiency, symmetry, dummy property and additivity. Symmetry property states that if two arbitrary participants, *i* and *j*, have the same marginal cost with respect to all coalitions not containing *i* and *j*, the costs allocated to these two participants must be equal. The dummy property states that if participant is a dummy, in the sense that he or she neither helps nor harms any coalition he or she may join, then his or her allocated cost should be zero. Finally, additivity property expresses that, given three different characteristic cost functions c_1, c_2 and $c_1 + c_2$ for each participant, the allocated cost based on $c_1 + c_2$ must be equal to the sum of the allocated costs based on c_1 and c_2, respectively Frisk (2010).

Results

This section applies the results of innovation network coalition of two plants and these plants produce different products. In the considered example, all the numerical values are fictitious. In plant 1, product X is produced and in plant 2, product Y is produced. There exists 7 tasks in the model of product X and 9 tasks in the model of product Y. Also, 5 tasks are common for both models. In coalitional case, these 5 tasks are manufactured together by plants which participate the coalition on a mixed model assembly line. Thus, we will utilize the similarity between the precedence relations of different models in our model. Thomopoulos (1970) used the concept of a combined precedence diagram to join the precedence relations of different models on a single diagram. The combined precedence diagram can be constructed straightforward with precedence matrices. A precedence matrix is an upper-triangular matrix with an *ab*th entry of 1 if the processing of task *b* requires the completion of task *a*. Otherwise, the entry is zero. The precedence matrix of the combined precedence diagram is constructed as follows: the *ab*th entry of the matrix is 1 if the *ab*th entry of any of precedence matrices of the models is 1. Furthermore, if there are any implied precedence relations, then the related entries in the combined precedence matrix should also be 1. Note that there should be no conflict in the precedence relations across the models. The combined diagram reduces the number of variables and constraints of the model significantly. The individual precedence diagram of each model that exist in plants can be depicted as in Figure 1. In Figure 1, the numbers next to the nodes represent task

performance times. Cycle time is taken as 10 minutes for each model and the number of stations is limited to 4.

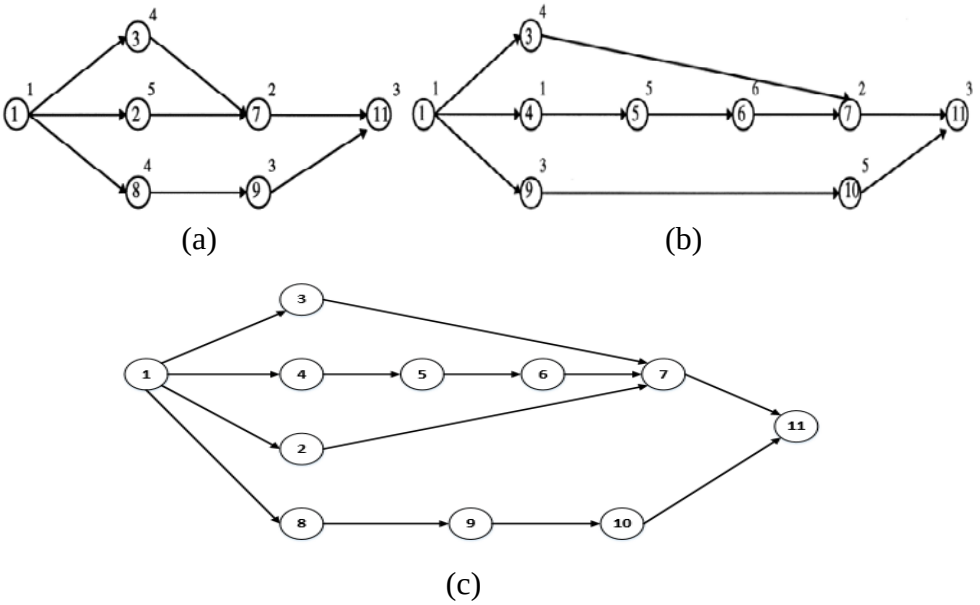

Figure 1 Precedence diagrams of (a) product X model, (b) product Y model and (c) combined.

Formulation of Product X model

The earliest and latest stations to which the tasks can be assigned to are given in Table 1.

Table 1 The earliest and latest stations to which the tasks can be assigned

Tasks	Earliest station	Latest station
1	1	3
2	1	4
3	1	4
7	2	4
8	1	4
9	1	4
11	3	4

Following solution is obtained by applying the above model to a single-model assembly line balancing problem for the product X model of plant 1. Solution of the product X model is given in following Table 2.

Table 1 Result of product X model

Station	Task	Station Time
1	1,8,9	8
2	3	4
3	2,7,11	10

Formulation of Product Y model

The earliest and latest stations to which the tasks can be assigned to are given in Table 3.

Table 3. The earliest and latest stations to which the tasks can be assigned

Tasks	Earliest station	Latest station
1	1	2
3	1	4
4	1	3
5	1	3
6	2	3
7	2	4
9	1	3
10	1	4
11	3	4

Following solution is obtained by by applying the above model to a single-model assembly line balancing problem for the product Y model of plant 2. Solution of the product Y model is given in following Table 4.

Table 4. Result of product Y model

Station	Task	Station Time
1	1,4,5,9	10
2	3,6	10
3	7,10,11	10

Gökcen and Erel (1998) proposed the mixed-model assembly line balancing problem by using following notations:

Notation

N	=total number of tasks	
K	=number of stations	
P	=number of models (products)	
PR_i	=subset of all tasks that precede task *i*	*i*=1..*N*
S_i	= subset of all tasks that follow task *i*	*i*=1..*N*
t_{im}	=performance time of task *i* of model *m*	*i*=1..*N*; *m*=1,...,*P*
C_m	=cycle time of model *m*,	*m*=1,...,*P*
E_{im}	=earliest station task *i* of model *m* can be assigned to, given the precedence relations	*i*=1..*N*; *m*=1,...,*P*
L_{im}	=latest station task *i* of model *m* can be assigned to, given the precedence relations	*i*=1..*N*; *m*=1,...,*P*

$E_{im}=\left[\frac{t_{im}+\sum_{j\in PR_i} t_{jm}}{C_m}\right]^+$ for *i*=1,...,*N*, *m*=1,...,*P*

$L_{im}=k+1-\left[\frac{t_{im}+\sum_{j\in S_i} t_{jm}}{C_m}\right]^+$ for *i*=1,...,*N*, *m*=1,...,*P*

where $[x]^+$ denotes the smallest integer greater than or equal to *x*. The earliest and latest stations task *i* on the combined precedence diagram can be assigned to are max_m=1…P$\{E_{im}\}$ and min_m=1…P$\{L_{im}\}$ respectively. The earliest and latest stations to which the tasks can be assigned to are given in Table 5.

Table 5 The earliest and latest stations to which the tasks can be assigned

Tasks	Earliest station	Latest station
1	1	2
2	1	4
3	1	4
4	1	3
5	1	3
6	2	3
7	2	4
8	1	4
9	1	3
10	1	4
11	3	4

By using Gökcen and Erel (1998) formulation, the solution of the combined model is given in Table 6. All results are obtained by using LINGO and conducted on a PC with Intel Core i5-4210U CPU 1.7 GHz processor and 4 GB RAM.

Table 6 The optimal solution

	Combined	Model 1		Model 2	
Station	**Tasks**	**Tasks**	**Station time**	**Tasks**	**Station time**
1	1,4,5,8,9	1,8,9	8	1,4,5,9	10
2	3,6	3	4	3,6	10
3	2,7,10,11	2,7,11	10	7,10,11	10

Each individual case: {Model1}, {Model2} must be solved 2 times, so that for coalition S: {Model1 Model2} the minimum total cost C(S) can be computed. These values are shown in Table 7.

Table 7. The corresponding optimal transportation cost C(S) for each of the possible coalitions

S	C(S)
{Model1}	3
{Model2}	3
{Model1, Model2}	3

After the coalitional cost is calculated, allocational costs are computed according to Shapley value method. For both models, it is equal to 1.5. In this case, final allocation 1.5 meaning that three stations should be allocated to each plant fairly and exactly the half cost is saving.

Discussion and Conclusions

The expectation from cooperation is to reduce the network cost in accordance with non-cooperative situation. In this paper, an example of cooperation of two plants that produce two products which necessitate common tasks is considered. The objective of the problem is to obtain minimum cost for all plants (in this case there exist two plants). For this reason, a mathematical programming model is used to measure the benefits of merging the assembly line systems of different plants so that their joint costs are reduced. Plants in the same business line is merged and the coalition cost arising from their horizontal cooperation is allocated among plants using cooperative game theory approach. Although there are many cost savings allocation solution concepts, it is concentrated here on only one of them, namely the Shapley value based solution approach. To gain insight into the problem, an example problem is presented. In this case, we have a maximum two plants

in the coalition. Since in real life, there is a limit on the number of partners in the coalition due to the increasing transaction costs, complexity of managing the collaboration etc. Results show that significant cost reduction (in this study exactly half) is obtained due to the cooperation within the plants. The following future studies can be considered to further improve the present study. First of all, the assembly line balancing problem (both single and mixed) can be tackled for different objectives and constraints instead to minimize the number of stations. Since there is no universal approach to cover all of the variations of the problem and majority of the proposed models seem to be problem dependent. Another issue is related to the negotiation power of plants which is assumed to be same for all plants. Relaxation of this assumption may be more realistic for some circumstances. Finally, this research can be extended by employing and comparing other solution concepts for cooperative games.

References

Amasaka, K. (2007). Applying New JIT—Toyota's global production strategy: Epoch-making innovation of the work environment. Robotics and Computer-Integrated Manufacturing, 23(3), 285-293.

Baniak, A., Dubina, I. (2012). Innovation analysis and game theory: A review. Innovation, 14(2), 178-191.

Bester, H., Petrakis, E. (2004). Wages and productivity growth in a dynamic monopoly. International Journal of Industrial Organization, 22(1), 83-100.

Corbett, C. J., DeCroix, G. A. (2001). Shared-savings contracts for indirect materials in supply chains: Channel profits and environmental impacts. Management Science, 47(7), 881-893.

Cousins, P. D. (2002). A conceptual model for managing long-term inter-organisational relationships. European Journal of Purchasing & Supply Management, 8(2), 71-82.

Conceição, P., Heitor, M. V., Veloso, F. (2003). Infrastructures, incentives, and institutions: Fostering distributed knowledge bases for the learning society. Technological Forecasting and Social Change, 70(7), 583-617.

Cruijssen, F., Bräysy, O., Dullaert, W., Fleuren, H., Salomon, M. (2007). Joint route planning under varying market conditions. International Journal of Physical Distribution & Logistics Management, 37(4), 287-304.

D'Amours, S., Rönnqvist, M. (2010). Issues in collaborative logistics, In: Energy, natural resources and environmental economics. Springer Berlin Heidelberg, 395-409.

Frisk, M., Göthe-Lundgren, M., Jörnsten, K., Rönnqvist, M. (2010). Cost allocation in collaborative forest transportation. European Journal of Operational Research, 205(2), 448-458.

Gökcen, H., Erel, E. (1998). Binary integer formulation for mixed-model assembly line balancing problem. Computers & Industrial Engineering, 34(2), 451-461.

Jaffe, A. B. (2000). The US patent system in transition: policy innovation and the innovation process. Research Policy, 29(4), 531-557.

Kuhlmann, S., Edler, J. (2003). Scenarios of technology and innovation policies in Europe: Investigating future governance. Technological Forecasting and Social Change, 70(7), 619-637.

Knight, K. E. (1967). A descriptive model of the intra-firm innovation process. The Journal of Business, 40(4), 478-496.

Leptien, C. (1995). Incentives for employed inventors: an empirical analysis with special emphasis on the German law for employee's inventions. R&D Management, 25(2), 213-225.

Lim, W. S. (2001). Producer-supplier contracts with incomplete information. Management Science, 47(5), 709-715.

Macaskill, J. L. C. (1972). Production-line balances for mixed-model lines. Management Science, 19(4-part-1), 423-434.

Nerkar, A. A., McGrath, R. G., MacMillan, I. C. (1996). Three facets of satisfaction and their influence on the performance of innovation teams. Journal of Business Venturing, 11(3), 167-188.

Patterson, J. H., Albracht, J. J. (1975). Assembly-line balancing: zero-one programming with Fibonacci search. Operations Research, 23(1), 166-172.

Shapley, L. S., 1950, "Quota solutions of n-person games", in H. W. Kuhn and A. W. Tucker, eds., Contributions to the Theory of Games, vol. II (Annals of Mathematics Study No. 28), Princeton, pp. 343-59.

Thomopoulos, N. T. (1970). Mixed model line balancing with smoothed station assignments. Management Science, 16(9), 593-603.

Thomopoulos, N. T. (1970). Mixed model line balancing with smoothed station assignments. Management Science, 16(9), 593-603.

Van der Meulen, B. (1998). Science policies as principal–agent games: Institutionalization and path dependency in the relation between government and science. Research Policy, 27(4), 397-414.

Wolters, H., Schuller, F. (1997). Explaining supplier-buyer partnerships: a dynamic game theory approach. European Journal of Purchasing & Supply Management, 3(3), 155-164.

International Conference on Science and Technology
ICONST 2018
5-9 September 2018 Prizren - KOSOVO

Investment Rısk Evaluatıon Of Siirt Madenköy Copper Mine in Turkey

Merve Karaabat Varol[1]*, İbrahim Uğur[2], Selamet G. Erçelebi[3]

Abstract: Mining investments are high-risky investments due to mineral deposit uncertainties. Therefore, before any investment decision is given, an economic assessment should be performed and several risk situations must be taken into consideration. In this study, it was examined whether or not an investment made in a copper mine in Siirt, Turkey is economical by using Sensitivity Analysis and Monte Carlo Simulation. The aim of this study is to construct cash flows for this copper mine with an average grade of 2.35% Cu and 39.821.000 tons reserve throughout 25 years for two different situations. In the first case, it was assumed that the total investment amount will be covered by 100% equity, while in the second case the total investment amount was assumed to be 30% equity and 70% bank loan. In the Sensitivity Analysis, mineral processing and operating costs, the average grades and ore concentrate sale prices were evaluated over optimistic and pessimistic forecasts. Changes in the net present value and internal rate of return were examined without risk. Monte Carlo Simulation was run by using computer software program @Risk 6.0 and applied to investment criteria for this copper mine field. The analysis of the output modelling situations where decisions were made under uncertainty gave reliable results by quantifying the degree of risk for this mining project. Consequently, if the investment was provided with 100% equity, NPV was 136.369.150,7 $ and IRR was 32% with a discount rate of 15%, probably as likely to harm the project was about 0,018. If the investment was provided with 30% equity, NPV was 111.742.245,4 $, IRR was 28% with a discount rate of 15%, probably as likely to harm the project was about 0,05. In accordance with the results, the investment can be said to be a profitable project in both assumptions.

Keywords: Mining Investment, Uncertainty, Risk Analysis, Monte Carlo Simulation Method, Sensitivity Analysis, Investment Appraisal

1. Introduction

The evaluation of a mining project is a long and complicated process from exploration to exploitation stages. Many decisions involve too many influential risk factors with different kinds of uncertainties since mining investments are potentially carrying high risks.

To evaluate mining project, it is necessary to make certain assumptions considering production rate range, reserve, characteristic of mineral deposit, capital cost, cash flow, mine life, return of capital, inflation, discount rate, unit sales price, operating cost per ton, operating methods and jeometallurgy (Hartman and Mutmansky, 2002). Climatic conditions, environmental factors, ore dressing, market condition, productivity and rate of growth are essential to consider other parameters (Hartman and Mutmansky, 2002).

[1]Suleyman Demirel University, Faculty of Engineering, 32260, Isparta, TURKEY
[2]Suleyman Demirel University, Faculty of Engineering, 32260, Isparta, TURKEY
[3]İstanbul Technical University, Faculty of Mining, 34469, Istanbul, TURKEY
*Corresponding author: info@iconst.org

At the evaluation of the mine investment, there are a number of risks arising from some uncertainties. These uncertainties are classified as exploration uncertainties, economic uncertainties and engineering uncertainties (Dehghani and Ataee-pour, 2012). Economic uncertainties as future metal prices and operating costs are the most important factors affecting the value of the project. Exploration uncertainties occur during the resource evaluation stages such as geologic uncertainty, data collection, modelling, classification and reporting of the deposit (Dehghani and Ataee-pour, 2012). Engineering uncertainties include determination of bench heights, control of grade, minimum production width, choice of production process, dilution factor, geotechnical and hydrological factors, recovery factors and metallurgical recovery (Hartman and Mutmansky, 2002).

Risk analysis is the compulsory factor for all stages of mine feasibility studies, planning and production (Simonsen and Perry, 1999). To evaluate the risk of a considered mining risk, firstly economic model must be generated. Determining the economic value of a project is based on several investment approaches and cash flows such as net present value, payback period, internal rate of return and accounting rate. After calculating these values, risk analysis methods such as Sensitivity Analysis and Monte Carlo simulation are generally used to investigate the changes and measure the risk (Wei et al., 2011; Pincock Consulting Service, 2012).

Literature on Sensitivity Analysis was limited in the past. Morley et al. (1999) proposed a financial model of a project significant effort was expended on capital and operating cost estimation, commodity price forecasts, and choice of discount rates while uncertainty in the primary input, the reserve, was overlooked. Iloiu and Csiminga (2009) was based on IRR and NPV criteria. They presented the purpose of sensitivity analysis and the steps that must be followed in order to perform a sensitivity analysis as well as a numeric example. Sabour and Wood (2009) proposed the economy of a gold mine over cash flow model. Aryafar et al. (2011) estimated the capital costs and present value of revenue and costs and then assessed the operating costs by considering total production at Basalt-Andesite Mine in Persian.

Literature on Monte Carlo Simulation is more than literature on Sensitivity Analysis. Kreuzer et al. (2008) showed that how the potential mining project formation was formed, how the expected average value was computed and net present value's possible distribution. As discussed by Bastante et al. (2008) suggested a simple method for introducing price and cost increases into the risk analysis via the Monte Carlo method and show how geological, technical and economic uncertainty could be integrated in risk analysis. Sabour and Dimitrakopoulos (2011) conducted a survey by the open pit mine design that combines the flexibility of operating with uncertainty in the selection of a method. Oraee et al. (2011) pointed out the project on the basis of several economic variables. These economic variables have been estimated under the conditions of uncertainty. The net present value was obtained under these uncertainties. As described in Wei et al. (2011) proposed that the Monte Carlo simulation was performed in computer and applied to an iron ore mine investment. Based on the simulating results, this project's investment was analyzed.

In this study, the importance of estimation of NPV of orebody with risk and without risk was underlined. This study summarizes the preliminary results of a research project supported by Teaching Staff Training Program (OYP). A copper mine was investigated through Sensitivity Analysis and Monte Carlo simulation and the difference was compared in terms of economic under risk and without risk situations. Cash flow was constructed by two assumptions, 100% equity and 30% equity and 70% bank loan. The investment was evaluated with Sensitivity Analysis and Monte Carlo Simulation Analysis. In accordance with the results, the investment can be said to be a profitable project in both assumptions.

2. Material and Methods

2.1. Description of the Project Site

Project site is located near the village of Madenköy, 40 km north-east of the town of Siirt. Resource estimation and classification results were obtained and calculated for three domains. Three orebody were created for the Madenköy deposit. Domain 1, the largest orebody, is located in the eastern part of the study

area with a volume calculated by almost 10 million m3. Domain 2, the small orebody above orebody 3, is located in the eastern part of the study area with a volume calculated by around 120.000 m3. Domain 3, the other small orebody below orebody 2, is located in the south-west of the area with a volume calculated by around 500.000 m3 (Figure 1).

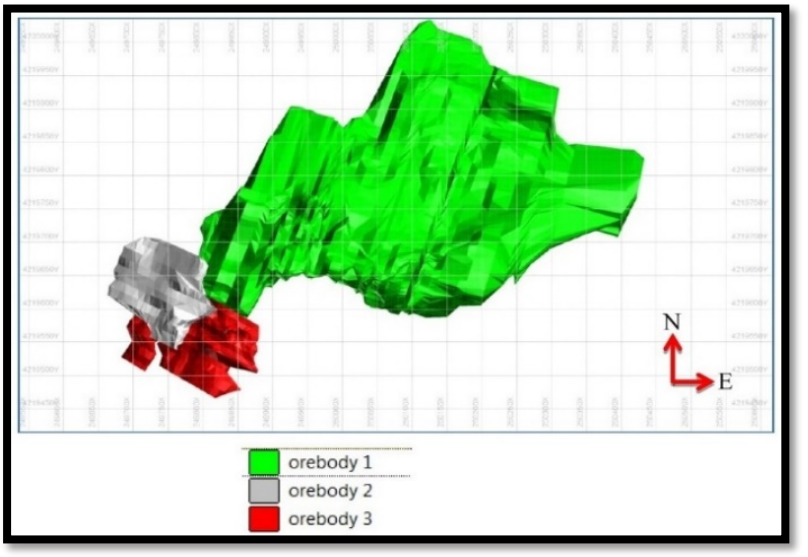

Figure 1. Plan view of the Park Electric wireframes (Park Electric Technical Report)

2.2. Operating Method

Park Elektrik Üretim Madencilik Sanayi ve Ticaret A.Ş has turned underground mining to open pit mining method in Madenköy. It was tried in 2 shifts of 8 hours per day and 300 days per year. According to Park Electric technical report, copper reserves on the mine's total measured, indicated and inferred are 39.821.000 tonnes. In this study, the evaluation was made out of copper reserves of 37.572.183 tonnes by considering measured and indicated reserves (Table 1). It was of an average grade of 20% copper concentrate. Concentrate recovery of 90%, the average ore grade was calculated as 2.40% Cu and concentration ratio was calculated 9,46 ton ore/ ton concentrate.

Table 1. Resource Estimation and Classification

Resource Category	Tonnes(t)	Cu(%)	SG(t/m3)
Measured + Indicated	37.572.183	2,35	4,05
Total Resources	39.821.000	2,40	

1.500.000 tonnes of ore was operated and returned to about 160.000 tonnes of concentrate at plant per year from mine.

2.3. Equipment Selection

It was planned to product 1.500.000 tonnes ore per year. Ore production and overburden were done with 5 m3 capacity excavators and 40 tonnes capacity trucks. Average density of stripping material was 2,5 ton/m3, average density of ore was 4,05 ton/m3.

2.3.1. Selection of drilling machine

Considered in the design of drilling and blasting, hole diameters, slice thickness and the distance between holes were selected as 6 inches (15,24 cm), 5 m and 5 m respectively. It has been decided to select 6

drilling machines and 5 of them were for overburden and the other one was for ore production.

2.3.2. Selection of excavator and truck

The excavated overburden material was conveyed to the dump site in approximately 2,5 km distance. The produced ore was transferred to 2 km away. According to the amount of overburden and production, the number of required trucks and excavators was calculated as 9 excavators and 45 trucks for overburden, 1 excavator and 5 trucks for ore production.

2.3.3. Costs Analysis

Total Investment Expenditures for 5 m3 excavators and 40 tonnes trucks were shown in Table 2. Investigation project costs of 65.502 $, land arrangement expenses of 78.603 $, communication systems of 131.004 $, fuel oil storage and drainage systems of 131.004 $ was expected.

Table 2. Total Investment Costs

	Value (TL)	Value ($)
Studies Project Costs	150.000	65.502
Land Regulation Costs	180.000	78.603
Mineral Processing Machinery Equipment Expense	4.995.000	2.181.223
Overburden Machinery Equipment Expense	39.625.000	17.303.493
Fuel Tank-Drainage Systems	300.000	131.004
Communication Systems	300.000	131.004
Foundation Expense	450.000	196.506
Unexpected Expenses (%4)	1.840.000	803.493
General Expenses (%2)	953.800	416.506
Physical Growth (%2)	975.876	426.147
Total Fixed Investment (TL)	49.769.676	21.733.483

2.3.4. Operating Cost

As a result of the data, for 5m3 excavator and 40 tonnes truck, stripping cost was 4,93 $/m3, ore production costs was 3,53 $/m3 (Table 3)

Table 3. Total Operating Costs

Expenses	Overburden (TL/m3)	Ore (TL/ton)
Drilling	0.7903	0.1951
Blasting	1.7165	0.4238
Loading	1.5333	0.7667
Transport	5.1633	4.4200
Repair and Maintenance	0.1769	0.1130
Personel Expenses	0.7568	1.4040
Spare Part	0.1397	0.0943
General Expenses (%2)	0.2055	0.1483
Unexpected Expenses (%2)	0.2096	0.1513
Depreciation	0.5885	0.3735
TOTAL (TL)	11.28	8.09
TOTAL ($)	4.93	3.53

2.3.5. Cash Flow

Cash flow was formed as a result of cost calculations. In the case of investment with 100% equity investment, NPV was 136.369.150,7 $ with a reduction rate of 15% and IRR was 32% (Table 4). When the project was invested with 30% equity + 70% bank loan, NPV was calculated as 111.742.245,4 $, and IRR was 28% (Table 5). In both cases, the project investment was paid back about 2 years.

Table 4 Annual Cash Flow (100% equity investment)

Year	Annual Cash Flow($)	Year	Annual Cash Flow($)	Year	Annual Cash Flow($)	Year	Annual Cash Flow($)
0	-73.342.107	7	53.329.655	14	53.329.655	21	42.524.415
1	-36.943.231	8	53.329.655	15	53.184.677	22	53.184.677
2	14.191.524	9	53.329.655	16	47.258.040	23	53.329.655
3	53.329.655	10	53.329.655	17	53.329.655	24	53.329.655
4	53.329.655	11	38.157.603	18	53.329.655	25	76.665.791
5	53.329.655	12	53.329.655	19	53.329.655		
6	47.258.040	13	53.329.655	20	53.329.655		

Table 5 Annual Cash Flow (30% equity investment + 70% bank loan)

Year	Annual Cash Flow($)	Year	Annual Cash Flow($)	Year	Annual Cash Flow($)	Year	Annual Cash Flow($)
0	-73.342.107	7	48.038.429	14	53.329.655	21	42.524.415
1	-42.216.879	8	48.262.606	15	53.184.677	22	53.184.677
2	10.499.971	9	48.776.740	16	47.258.040	23	53.329.655
3	46.561.808	10	49.145.895	17	53.329.655	24	53.329.655
4	46.930.963	11	34.342.998	18	53.329.655	25	76.665.791
5	47.300.119	12	49.884.206	19	53.329.655		
6	41.597.658	13	53.329.655	20	53.329.655		

2.3.6. Sensitivity Analysis

In this research, in the sensitivity analysis, mineral processing and operating costs, the average grade and ore concentrate sale prices were evaluated ±% changes over optimistic and pessimistic forecasts with Excel, changes in the net present value and internal rate of return were examined.

In the case of 100% equity investment, in cases where price fell below 30%, NPV fell to negative values. If the grade was down around 36%, the project NPV value was to be negative. It was observed that the cost of operating and mineral processing projects did not have much impact on NPV.

Similarly, when results of price and grade showed a 20%-30% decline, IRR fell below the target of 20% (Figure 3 and Figure 4).

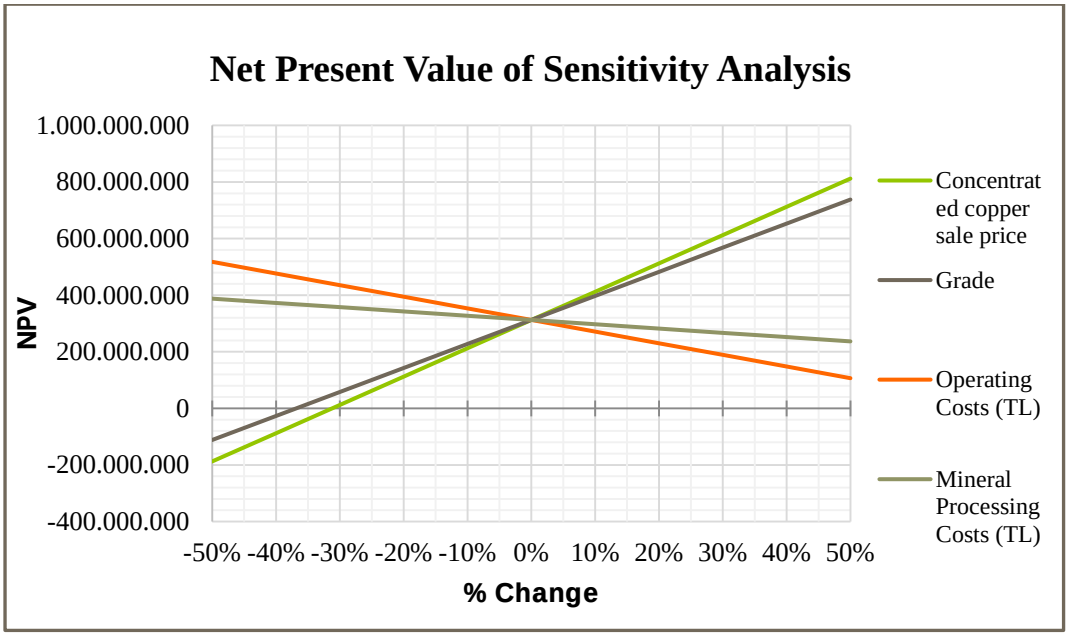

Figure 3. Effects of change on NPV

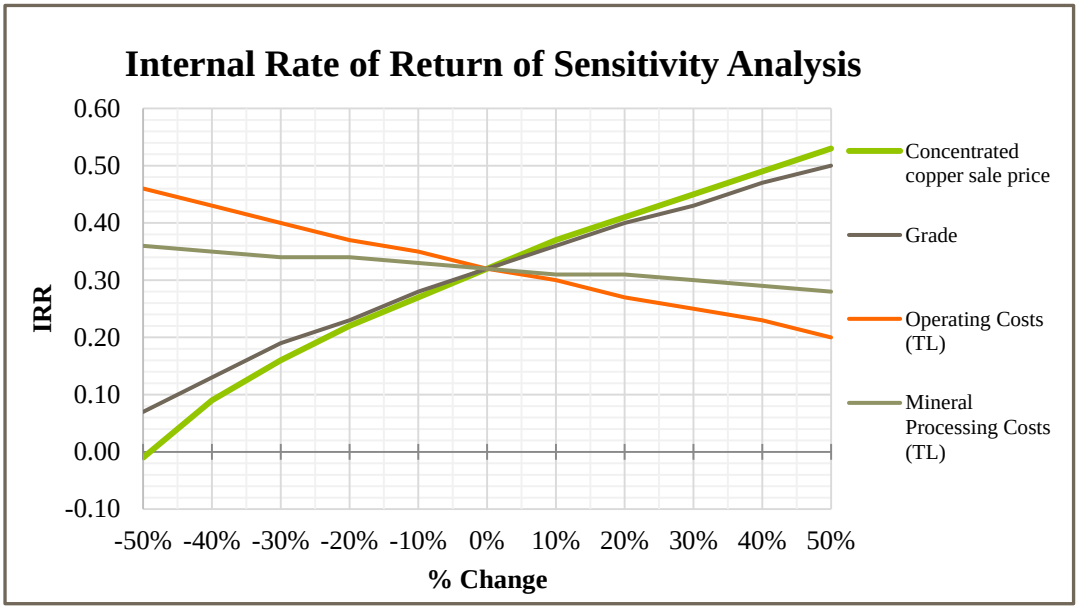

Figure 4. Effects of change on IRR

In the case of 30% equity investment, in cases where price fell below 25%, NPV fell to negative values. If the grade was down around 30%, the project NPV value was to be negative. It was observed that the cost of operating and mineral processing projects did not have much impact on NPV.

Similarly, when results of price and grade showed a 20%-30% decline, IRR fell below the target of 20%. It is shown as below (Figure 5 and Figure 6).

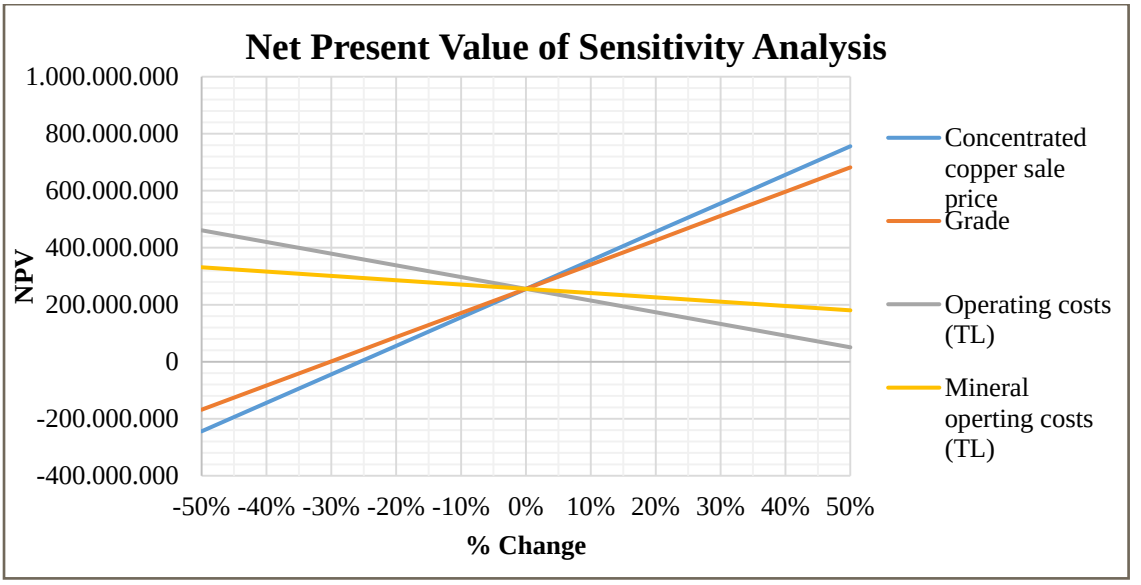

Figure 5. Effects of change on NPV

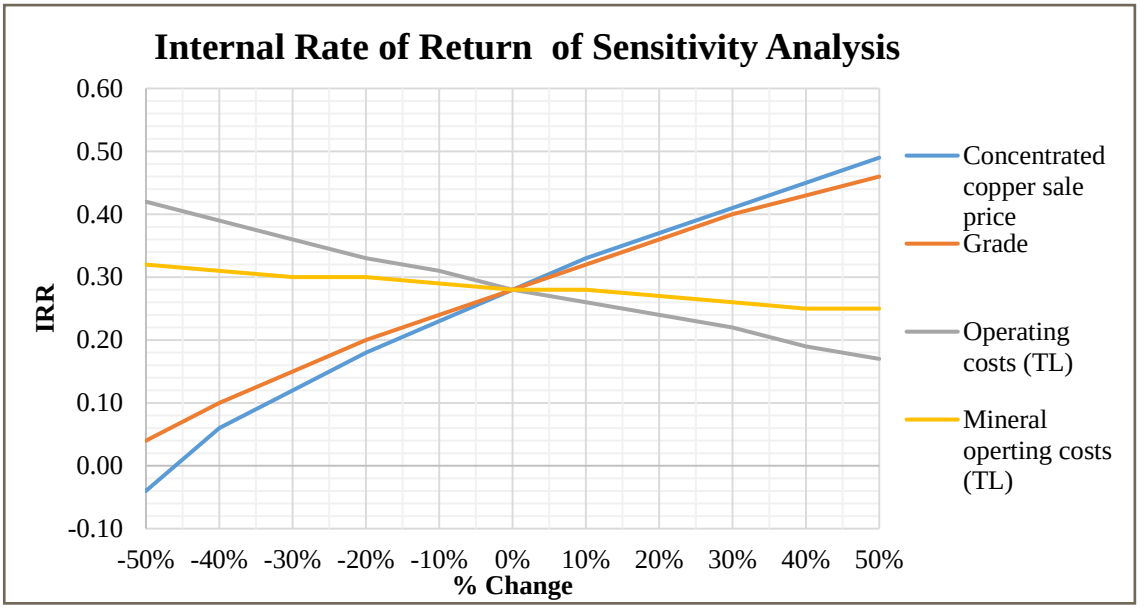

Figure 6. Effects of change on IRR

2.3.7. Probability Analysis - Monte Carlo Simulation

Monte Carlo simulation is one of the powerful and commonly used techniques for risk analysis.
When the net cash flow was prepared by considering risks and uncertainties, NPV and IRR were calculated by performing 100,000 iterations in @RISK software programme. Concentrated ore sales price, average grade, overburden and operating costs, mineral processing costs and initial investments were considered as risky situations.

Some probability distributions were defined to evaluate the uncertainties in this study. These uncertainties were;
Mine operating costs and overburden costs outcome differed in scale parameters, the mean and standart

deviation. Thus, the distribution was normal (Figure 7).

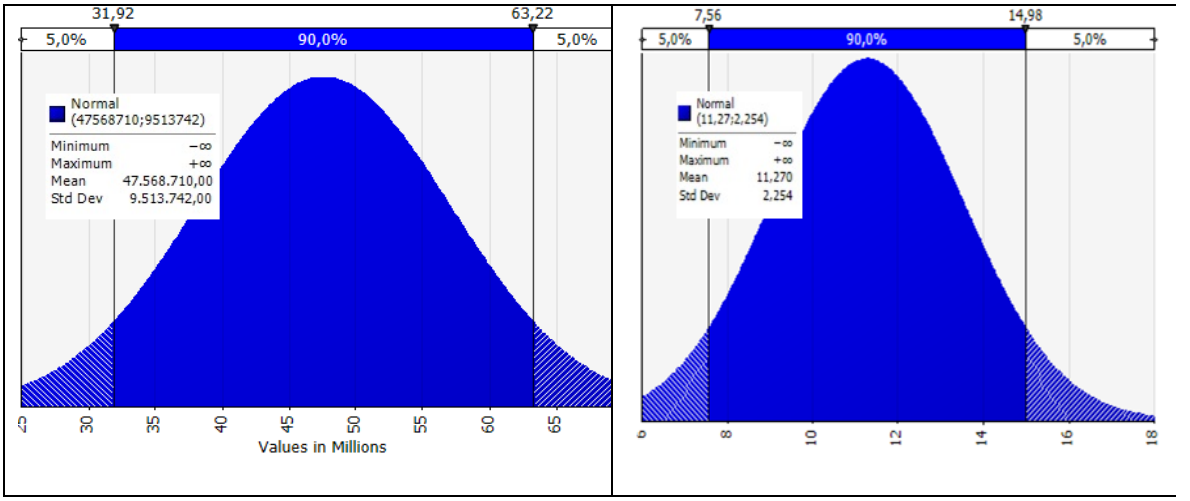

Figure 7. Distribution of operating costs: Normal(47.568.710, 9.513.742), and Distribution of the overburden costs:
Normal (11.27,2.254).

- Mineral processing costs outcomes were similar as operating costs, so the distribution was normal, and the average
  grade outcome was the constant average rate, so the distribution was exponential (Figure 8).

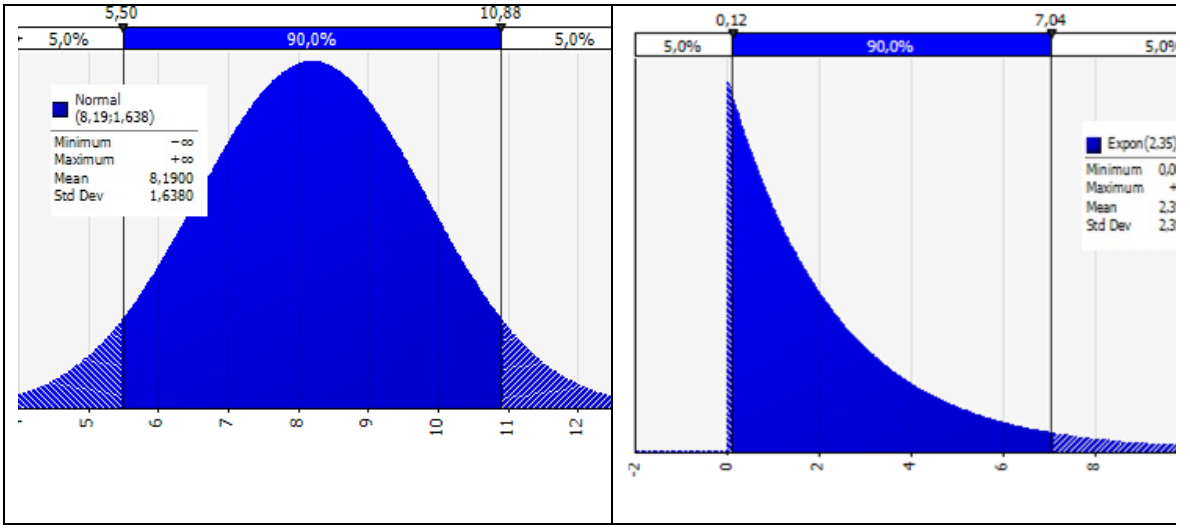

Figure 8. Distribution of the ore costs: Normal(8.19,1.638), and Distribution of average grade: Expon(2,35).

Total initial investment outcome was based on knowledge of minimum, maximum and most likely, so the distribution was was triangular, and concentrated ore sales price outcomes were equally probable, so the distribution were uniform (Figure 9) .

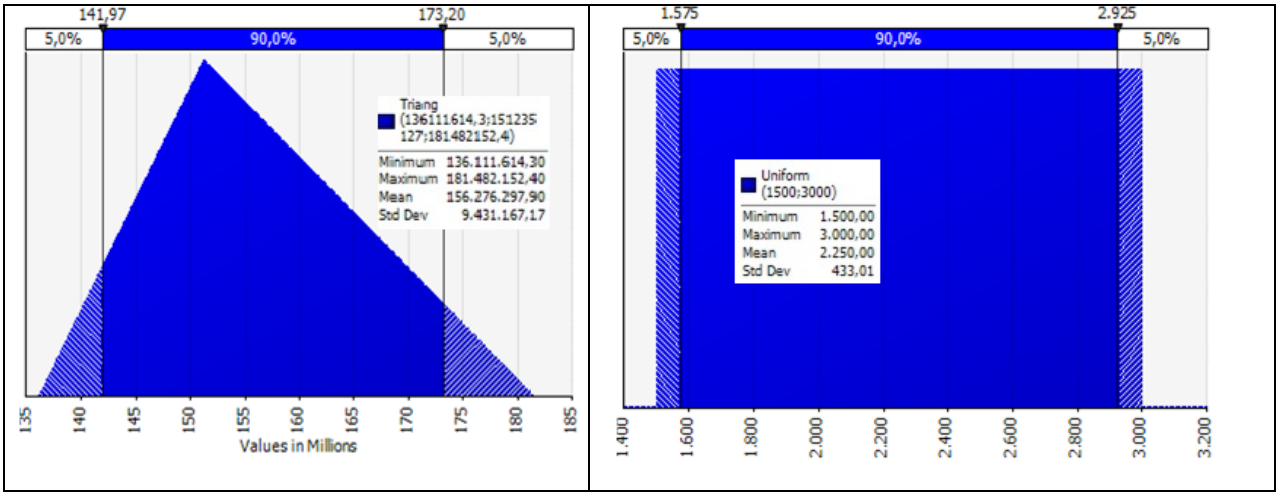

Figure 9. Distribution of Total initial investment: Triang(129.392.708, 143.769.676, 172.523.611), and Distribution of Concentrated ore sales price: Uniform (1500-3000)

By using these probability distributions, risk simulation studies on net cash flow were made. If the investment was provided with a 100% equity, NPV was as 481.068.971 TL, IRR was 36% average(Figure 10 and Figure 11).

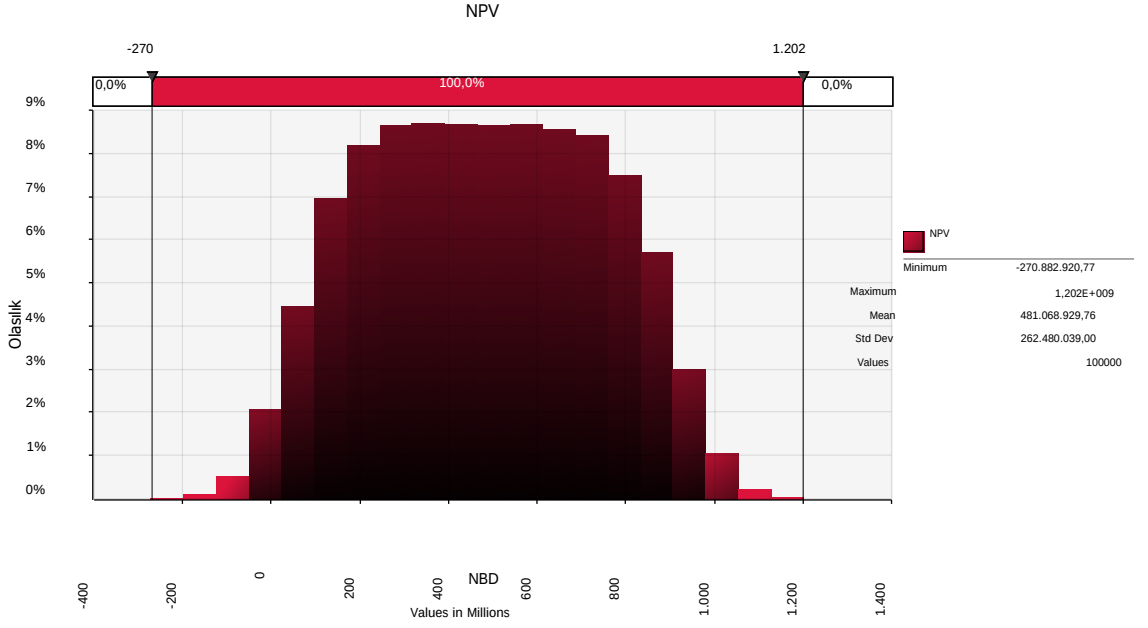

Figure 10. Probability distribution of NPV

PV

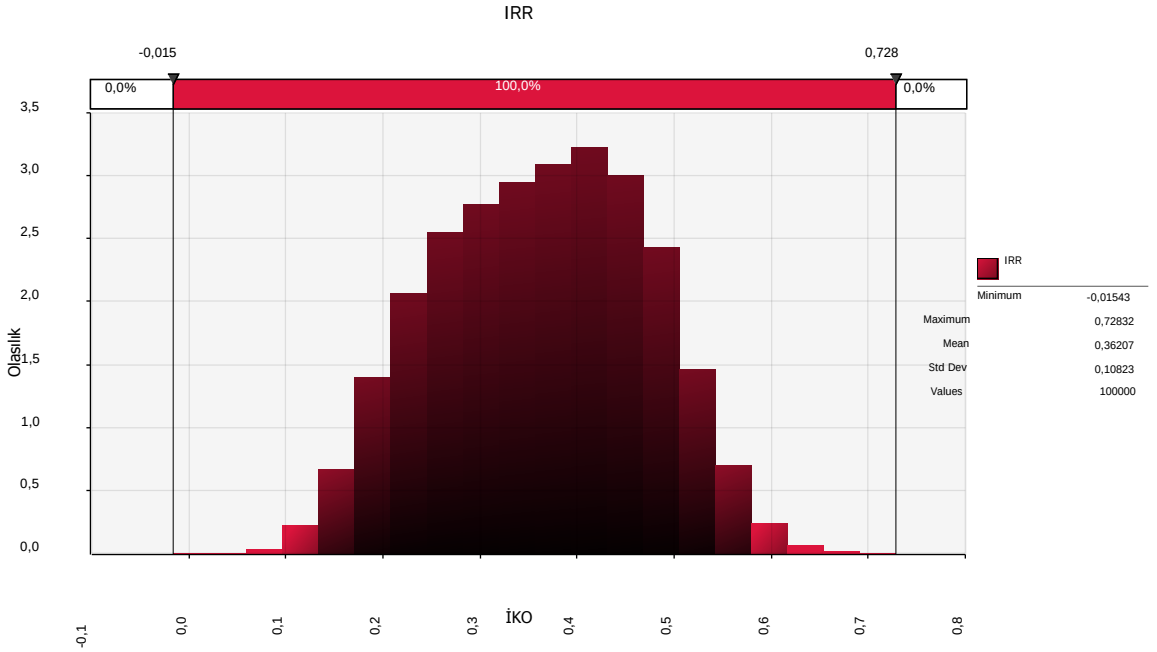

Figure 11. Probability distribution of IRR

By using these probability distributions, risk simulation studies on net cash flow were made. If the investment was provided with a 30% equity, NPV was as 414.052.307 TL, IRR was 32% average (Figure 12 and Figure 13).

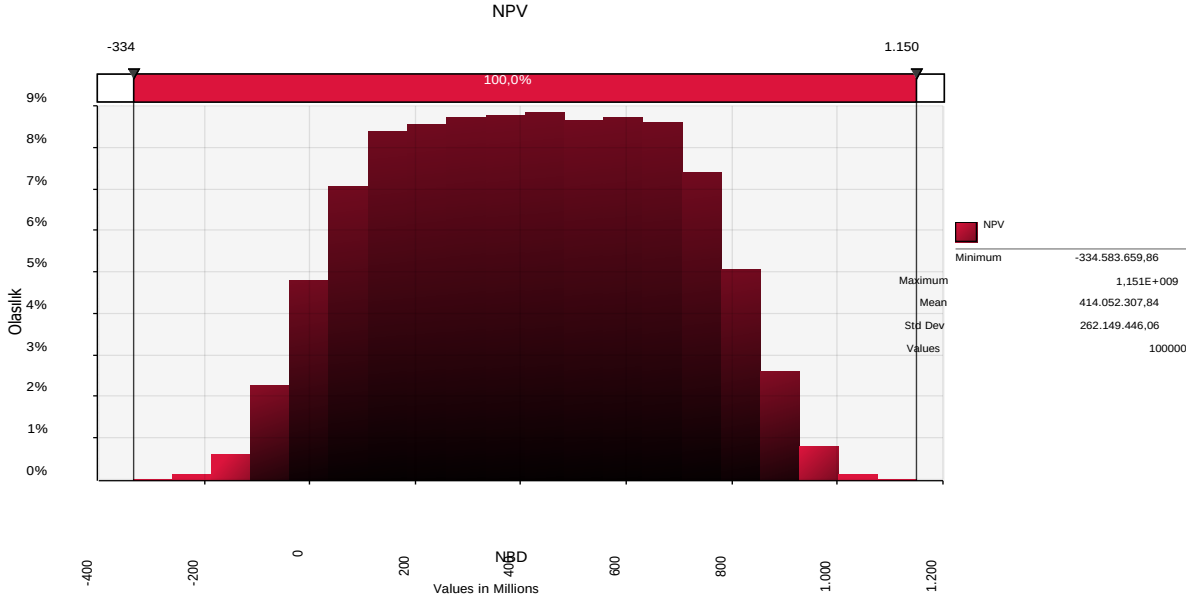

Figure 12. Probability distribution of NPV

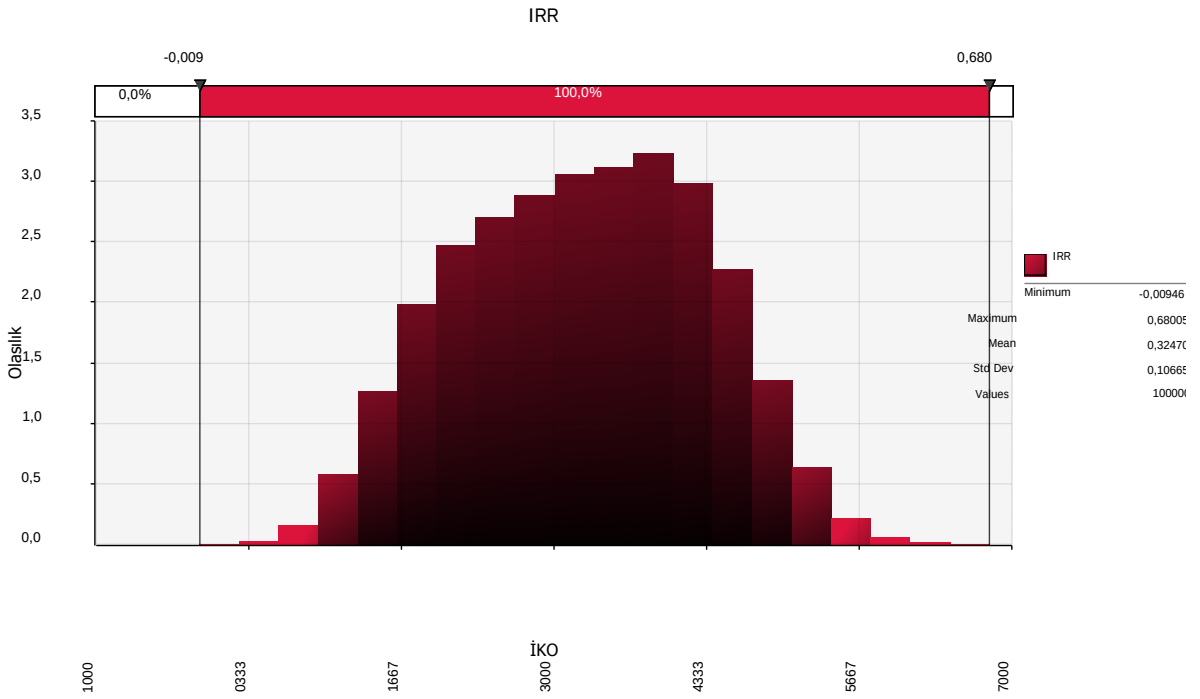

Figure 13. Probability distribution of IRR

3. Results

Considering all data, total initial investment of 62.781.518 $, overburden cost of 4.93 $/m3, ore cost of 3.53 $/tonnes and concentrate cost of 131 $/tonnes were calculated. Firstly, the net cash flow has been established by ignoring the uncertainty and risk. In this case, if the investment was provided with 100% equity, NPV was 136.369.150,7 $ and IRR was 32% with a discount rate of 15%. If the investment was provided with 30% equity, NPV was 111.742.245,4 $, IRR was 28% with a discount rate of 15%.

When the net cash flow was formed, the net present value and the internal rate of return were taken into consideration without risk. Uncertainties such as concentrated ore sales price, grade, costs of operating and mineral processing were taken into account over optimistic and pessimistic predictions with ± % changes. In case the price fell below 25-30%, NPV fell into negative. If grade fell below 30-35%, NPV would be negative. It was observed that the cost of operating and mineral processing projects did not have much impact on NPV. If sales price and grade fell below 20-30%, IRR would reach the lower value than the target rate.

Simulation results in the case of 100% equity investment;

- Average net present value was about 210 million $, internal rate of return was 36%.
- Net present value was higher than probability of 0,90 from 56.33 million $; probability of 0,50 from 210 million $.
- The probability of NPV any higher chance than net present value with risk-free was 0,69.
- A little probable as 0,018 of net present value took negative project.
- Internal rate of return was high probably of 0,90 from 21,5%; probably of 0,50 from 36,6%;
- Internal rate of return was high probably of 0,927 from 20%;
- Internal rate of return likely to be lower than selected rate of 15% was 0,018.

Simulation results in the case of 30% equity investment;

- Average net present value was about 181 million $, internal rate of return was 32%.
- Net present value was higher than probability of 0,90 from 27 million $; probability of 0,50 from 181

million $.

- The probability of NPV any higher chance than net present value with risk-free was 0,686.
- A little probable as 0,05 of net present value took negative project.
- Internal rate of return was high probably of 0,90 from 17,9%; probably of 0,50 from 32,9%;
- Internal rate of return was high probably of 0,856 from 20%;
- Internal rate of return likely to be lower than selected rate of 15% was 0,05.

4. Discussion

Assessing the all simulations if the investment was provided with 100% equity, probably as likely to harm the project was about 0,018. In accordance with the above results, the investment can be said to be a profitable investments of all kinds. In the other case, assessing the all simulations if the investment was provided with 30% equity, probably as likely to harm the project was about 0,05. In accordance with the above results, the other investment alternative can be said to be a profitable investments of all kinds. NPV and IRR values resulting from the simulation have been found to be consistent with the net present value and internal rate of return of cash flow in evaluation of risk-free. Consequently, the overall mining investment in economic evaluation techniques was assessed and risk parameters were calculated. While the risk analysis was carried out, sensitivity analysis and Monte Carlo simulation can be selected as risk analysis. Uncertainties that are selected during the sensitivity analysis of the parameters are not understood how they affect each other, because it is considered separately. But Monte Carlo simulation is done if the uncertainties are taken into consideration at the same time. Monte Carlo simulation of the investment risk assessment is carried out as a result of the probability distribution.

References

Abdel Sabour, S.A., Wood, G., 2009. Economic Evaluation of Gold Mining Projects: From Static Discounted Cash Flow to Real Options. In Corral, M.D., Earle, J.L. (Ed.), Gold Mining: Formation and Resource Estimation (91-109). Nova Science Publisher, Inc., 227p, New York.

Abdel Sabour, S.A., Dimitrakopoulos, R., 2011. Incorporating Geological and Market Uncertainties and Operational Flexibility into Open Pit Mine Design. Journal of Mining Science, 47(2), 191-201.

Aryafar, A., Giv, M.J., Motlagh, S.Z., 2011. Sensitivity Analysis of Investment in Sarbisheh Basalt-Andesite Mine, Birjand, Using of Monte Carlo Simulation. International Multidisciplinary Scientific GeoConferences, 1, 927.

Bastante, F.G., Taboada, J., Alejano, L., Alonso, E. 2008. Optimization Tools and Simulation Methods for Designing and Evaluating a Mining Operation. Stochastic Environmental Research and Risk Assessment, 22, 727-735.

Dehghani, H., Ataee-pour, M., 2012. Determination of the Effect of Operating Cost Uncertainty on Mining Project Evaluation. Resources Policy, (37), 109-117.

Hartman, H.L., Mutmansky, J.M., 2002. Introductory Mining Engineering. John Wiley & Sons, Inc., 570p, ABD.

Iloiu, M., Csiminga, D., 2009. Project Risk Evaluation Methods-Sensitivity Analysis. Annals of the University of Petroşani, 9, 33-38.

Kreuzer, O.P., Etheridge, M.A., Guj, P., McMahon, M.E., Holden, D.J., 2008. Linking Mineral Deposit Models to Quantitative Risk Analysis and Decision-Making in Exploration. Economic Geology, 103, 829-850.

Morley, C., Snowden, V., Day, D., 1999. Financial Impact of Resource/Reserve Uncertainty. The Journal of the South African Institute of Mining and Metallurgy, 293-301.

Oraee, K., Sayadi, A.R., Tavassoli, S.M.M., 2011. Economic Evaluation and Sensitivity-Risk Analysis Of Zarshuran Gold Mine Project, SME Annual Meeting.

Park Elektrik A.Ş. Jeoloji Raporu, 2012.

Park Elektrik A.Ş. İşletme Raporu, 2012.

Pincock Allen and Holt Consulting Service, 2012. Mineral Project Evaluation. 115.

Simonsen, H., Perry, J., 1999. Risk Identification, Assessment and Management in the Mining and Metallurgical Industries. The Journal of the South African Institute of Mining and Metallurgy, 321-332.

Wei, J., Jian, Z., Jianglan, L., 2011. Mining Investment Risk Analysis Based on Monte Carlo Simulation. Management of e-Commerce and e-Government (ICMeCG), 2011 Fifth International Conference on pp. 72-75. Hubei.

International Conference on Science and Technology

ICONST 2018

5-9 September 2018 Prizren - KOSOVO

Forecasting Annual Electricity Consumption of Turkey via Grey Prediction Approach

Burcu Kubur Özbel[1]*, Adil Baykasoğlu[2]

Abstract: Energy is an important source of economic development. It is also used as an economic index to show the industrial development of a country. Therefore, many countries are concerned with energy issues. Due to the high-tech industries and rapid changes occuring in developing economies, prediction of energy consumption is important for all countries in the world. Forecasting of the energy consumption is generally difficult task. Since, many factors affects its prediction. Therefore, developing more accurate prediction models is always welcome. In this study, electricity consumption of Turkey between 1970 and 2014 is analyzed. Using the past data, the amount of total electricity consumption of Turkey is predicted for the period until 2025. The statistical method for the forecasting electricity consumption is generally need to make some assumptions on the data such as normal distribution etc. However, collected data may not truly fit normality assumptions. Therefore, in this study first-order and one-variable grey differential equation model (GM(1,1)) is used for predicting electricity energy consumption. In this work, an auto-regressive moving average (ARIMA) model is also used. Since data contain non-stationary component. Different performance measures are used to determine the accuracy of the prediction results of the models. These measures are mean squared error (MSE), mean absolute deviation (MAD) and mean absolute percentage error (MAPE). Results show that the employed methods are efficient. According to MSE metric, the accuracy of the prediction values based on AR(1) model is the highest. In addition, GM(1,1) with different horizontal adjustment coefficient parameters generate different prediction values. From these results, it is easy to see the important effect of horizontal adjustment coefficient parameter. Therefore, performance measure metrics can be reduced with finding the optimized value of horizontal adjustment coefficient parameter.

Keywords: Electric energy consumption, Forecasting, GM(1,1) model, ARIMA model

Introduction

The growing human population increases energy demand. Therefore, the forecast of energy consumption has become a crucial need for the development of countries and the environment. Moreover, energy consumption forecasting plays a vital role in decision-making and future planning. Especially, when limited information on data exists. In real-world problems, for a variety of reasons some of the input parameters (capacities, costs etc.) exhibit different types of uncertainty due to the inadequateness of data (Dantzig et al. 1955). Thus researchers try to find efficient methods for coping with different types of uncertainty in data, which can be probabilistic, possibilistic, and/or interval. Important tools for decision making in fuzzy set theory was proposed by Bellman et al. (1970). This concept was adopted to interval grey numbers for the first time in early 1980s as interdisciplinary scientific area and interval grey number's parameters may be specified as

[1]Dokuz Eylül University, Faculty of Engineering, Departmnent of Industrial Engineering, 35397, Buca, İzmir, TURKEY
[2]Dokuz Eylül University, Faculty of Engineering, Departmnent of Industrial Engineering, 35397, Buca, İzmir, TURKEY
*Corresponding author: burcu.kubur@deu.edu.tr

lying certain lower and upper bound limits (Deng, 1982). The theory can handle poor information systems which have partially unknown parameters and/or involving small samples. Grey models express unknown system's behavior by using small number of data. Having this property, it has many application areas and has become quite popular. For instance, social, economical, financial, technological, and industrial applications etc., systems are some of the systems in the real world that grey models are encountered. Herewith, new mathematical theories arose in the grey set field. This theory, include five main parts namely grey prediction system, grey relational analysis (GRA) approach, grey decision making approach, grey-based programming, and grey control methods. Grey forecasting model (GM), which is based on grey theory, can be constructed with at least four observations (Chiang et al. 1998). This leads to the suggestion that the grey forecasting model is suitable for forecasting in the competitive environment where decision makers can reference only limited historical data. One of the competitive environment is electricity energy consumption. The statistical methods for the forcasting electricity consumption is generally need large sample size. However, collected electricity energy consumption data are often small sample size. Hence, assumption of normal data can not validated. In this cases, grey forecasting models are easily adopted due to working well with small data. Therefore, in this study grey model (GM) is used. Grey forecasting models can be divided into two categories (Liu et al. 2010). These are single-variable and multi-variable models. Specifically, in this work first order one-variable grey model GM(1,1) is used to predict total electricity energy consumption. In these models, only single time sequence is variable and related system' factors are not considered. Therefore, these models get benefits of simple modeling process. Also, this property puts an important limitation on the model. The reason is model does not include outside effects. Therefore, in the considered study, also an auto-regressive moving average (ARIMA) model is used, since total electricity energy consumption data contain non-stationary component.

Recently, grey forecasting models are commonly used. Especially, Grey prediction model GM (1,1) which is a time series prediction model covering a group of differential equations adapted for finding the parameter of variance and solution of first order differential equation. In real life, GM (1,1) is used to predict the several values in different areas. For instance, it is used to predict the vegetable production quantities (Sun, 1991), number of airline passengers (Hsu et al. 1998), risks of mortal accidents (Mao et al. 2006), value of stock prices (Wang, 2002) and so on. Apart from these areas, GM is also widely used in energy forecasting. For example, in one study, electricity demand of Twain is predicted (Al-Shobaki et al. 2008). In this paper two models are presented, one model is based on the generated energy data and the other one is based on the consumed energy data. In another study, integrated grey model and markov model is used to forecast China's electric-power demand by using historical data of the electric-power requirement from 1985 to 2001 in China (Huang et al. 2007). Also, grey rolling prediction model is used in order to forecast Turkey's electricity demand of industrial sector and total electricity demand (Akay et al. 2007). The electricity consumption data is used for Turkey from 1970 to 2004 for modeling the GP with Rolling Mechanism (GPRM) and the rolling mechanism rise forecasting accuracy of GP with chaotic data. Also Turkey's electricity consumption is forcested by using data of total electricity consumption from 1945 to 2010 (Hamzacebi et al. 2014). In this study, Optimized Grey Modelling (1,1) is used. In this model parameters of GM (1,1), namely θ and k, is tried to be optimized and it is founded that these parameters generally fixed to θ=0.5 and k=4. Also, effects of these parameters on prediction performance is investigated and results showed that Optimized Grey Modelling (1,1) are better than the results obtaining in the literature. In a different study, Turkey's electricity consumption related with CO_2 emission is forecasted by using grey prediction model with data of 1965 to 2012 of energy-related CO_2 emissions (Hamzacebi et al. 2015). Another important factor for prediction performance of GM (1,1) is the residual series. These series, mostly linked with the number of data points with the same sign. To increase the effectiveness of the residual sign, there exist integrated residual modification and residual genetic programming (GP) sign estimation study which is aimed to increase the precision of the residual sign estimator (Lee et al. 2011). They applied the proposed forecasting model on a real life energy consumption case of China by using historical annual energy consumption data from 1990 to 2003. Results showed that proposed method has higher predictive power of precision than the existing models in the literature. As it can be seen from the literature, integrated methods widely used since they give better results. One example of these integrated methods, GM (1, 1) and ratio-to-moving-average deseasonalization method is used for purifying of the seasonality characteristic data (Tseng et al. 2001). This method is used to predict the total production value of Taiwan's machinery industry. In another example, the forecasting performance of grey prediction models on educational attainment vis-à-vis that of exponential

smoothing combined with multiple linear regression used by the National Center for Education Statistics (NCES) is aimed (Tang et al. 2016).

Material and Method

In the considered problem, Turkey' electricity consumption data from period of 1970-2014 is used. The data have been collected from TEDC, Electricity Distribution and Consumption Statistics of Turkey. Figure 1 illustrates the data graphically.

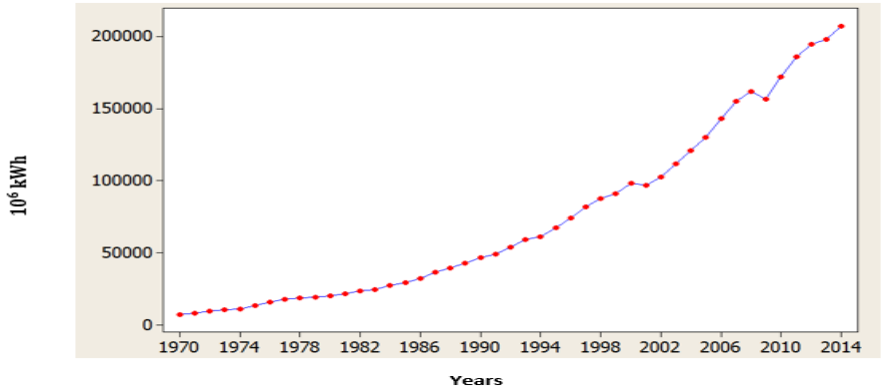

Figure 1. Historical data of total electricity consumption in Turkey for the period of 1970-2014

In addition, numeric data of electricity consumption of Turkey from 1970 to 2004 were given in Table 1.

Table 1. Total electricity consumption by years

Year	Total(GWh)	Year	Total(GWh)
1970	7.308	1993	59.237
1971	8.289	1994	61.401
1972	9.527	1995	67.394
1973	10.530	1996	74.157
1974	11.359	1997	81.885
1975	13.492	1998	87.705
1976	16.079	1999	91.202
1977	17.969	2000	98.296
1978	18.934	2001	97.070
1979	19.633	2002	102.948
1980	20.398	2003	111.766
1981	22.030	2004	121.142
1982	23.587	2005	130.263
1983	24.465	2006	143.071
1984	27.635	2007	155.135
1985	29.709	2008	161.948
1986	32.210	2009	156.894
1987	36.697	2010	172.051
1988	39.722	2011	186.100
1989	43.120	2012	194.923
1990	46.820	2013	198.045
1991	49.283	2014	207.375
1992	53.985		

Employed methods, GM(1,1) and ARIMA are briefly explained as follows:

Basic GM(1,1)

GM(1,1) is a time series forecasting model which implies a first order single variable prediction model. GM(1,1) is based on the following three essential steps (Julong, 1989):

1) Accumulated generating operation (AGO)
2) Grey modeling
3) Inverse accumulated generating operation (IAGO)

The steps of GM(1,1) are shown as follows:

Step 1: For the initial time sequence

$X^0 = \{X_1^0, X_2^0, X_3^0, \ldots\ldots, X_n^0\} = (X_t^0; \quad t = 1,2,3,\ldots,n; \quad n \geq 4)$ (1)

where X_t^0 is a non-negative sequence and n is the number of the data.

Step 2: When this sequence is subjected to AGO, the following sequence X^1 is obtained. It is obvious that X_k^1 is monotonically increasing.

$X^1 = \{X_1^1, X_2^1, X_3^1, \ldots\ldots, X_n^1\} = (X_t^1; \quad t = 1,2,3,\ldots,n; \quad n \geq 4)$ (2)

where

$X_k^1 = \{ \sum_{t=1}^{k} X_t^0, \quad t=1,2,\ldots,n; \quad k=1,2,\ldots,n\}$ (3)

Step 3: Form grey modeling by establishing a first order grey differential equation

$X_t^0 + aZ_t^1 = b, \quad t=2,\ldots,n$ (4)

where

$Z_t^1 = \theta X_t^1 + (1- \theta) X_{t-1}^1, \quad t=2,\ldots,n$ (5)

Here θ denotes a horizontal adjustment coefficient, and $0<\theta<1$. The selecting criterion of θ value is based on the smallest forecasting error rate. In Eq. (4), a is called the development coefficient and b is called driving coefficient. Applying least square method coefficients, $[a, b]^T$ can be estimated as follows:

$A=\begin{bmatrix} a \\ b \end{bmatrix} = (B^T B)^{-1} B^T Y_n$ (6)

where

$B=\begin{bmatrix} -Z_2^1 & 1 \\ -Z_3^1 & 1 \\ \ldots & \ldots \\ -Z_n^1 & 1 \end{bmatrix} \quad Y=\begin{bmatrix} X_2^0 \\ X_3^0 \\ \ldots \\ X_n^0 \end{bmatrix}$ (7)

$Y=BA$

Step 4: The whitenization processes is defined as follows:

$\frac{dX_t^1}{dt} + aX_t^1 = b$ (8)

Hence, using a and b coefficients, the AGO grey prediction model can be obtained.

$\hat{x}_{t+1}^1 = [X_1^0 - \frac{b}{a}]e^{-at} + \frac{b}{a}, \quad t = 0,1,2,\ldots n$ (9)

Step 5: Obtain the prediction value of original sequence by IAGO operation. IAGO operation can be defined as follows:

$X_{t+1}^0 = X_{t+1}^1 - X_t^1$ (10)

If Eq. (9) is substituted in Eq. (10) then Eq. (11) is obtained as follows:

$\hat{x}^0_{t+1}$ =(1-e^a)[X^0_1- $\frac{b}{a}$]e^{-at} (11)

Auto Regressive Integrated Moving Average (ARIMA)

The ARIMA (*p, d, q*) is a model with three parameters:
d=number of differences for stationarity,
p=order of the AR component,
q=order of the MA component.
In an ARIMA model, the future value of *a* variable is assumed to be a linear function of several past observations and random errors. That is, the underlying process that generates the time series with the mean μ has the form (Khashei et al. 2009):

$\Phi(B)\nabla^d(y_t$- μ) =θ(B)a_tm, (12)

Where y_t and a_t are the actual value and random error at time period *t*, respectively:
$\Phi(B)=1-\sum_{i=1}^{p}\Phi_i B^i$, $\theta(B)=1-\sum_{j=1}^{q}\theta_j B^j$ are polynomials in *B* of degree *p* and *q*, Φ_i(i=1,2,….,*p*) and θ_j(j=1,2,….,*q*) are model parameters, ∇=1-*B*, *B* is the backward shift operator, *p* and *q* are integers and often referred to as orders of the model, and *d* is an integer and often referred to as order of differencing. Random errors,a_t, are assumed to be independently and identically distributed with a mean of zero and a constant variance of σ^2.

Box and Jenkins (Box et al. 1976) proposed to use the autocorrelation function (ACF) and the partial autocorrelation function (PACF) of the sample data as the basic tools to identify the order of the ARIMA model. The Box and Jenkins (Box et al. 1976) methodology includes three iterative steps of model identification, parameter estimation, and diagnostic checking. The basic idea of model identification is that if a time series is generated from an ARIMA process, it should have some theoretical autocorrelation properties. By matching the empirical autocorrelation patterns with the theoretical ones, it is often possible to identify one or several potential models for the given time series.

Results

Basic mathematical model of grey system GM(1,1) is coded by using MATLAB software. The modeling data set is total electricity consumption rates for the years 1970-2014. Using GM(1,1) the amount of total electricity consumption of Turkey are predicted for the period until 2025. In the literature, different performance measures have been used in order to determine the accuracy of the prediction models. In this study, three performance measures such as Mean Absolute Deviation (MAD), Mean Square Error (MSE) and Mean Absolute Percentage Error (MAPE) are used. Since the θ parameter affect the prediction performance of GM(1,1), different values of these parameters (θ=0.1 and θ=0.5 and θ=0.9) are used to investigate the prediction performance of GM (1,1). The prediction values of GM(1,1) for the given electricity consumption data of Turkey is given in Table 2. The performance values of GM(1,1) with different θ is also given in Table 2. The comparison results show that GM(1,1) with θ=0.9 performs more accurate predictions than the others.

Table 2. Prediction values of Turkey's total electricity energy demand until 2025

Year	Forecasted Value, θ=0.1	Forecasted Value, θ=0.5	Forecasted Value, θ=0.9
a	-0.065923	-0.064658	-0.063044
b	15.2276	14.9198	14.528
MAD	17.0452	11.7441	6.2191
MSE	497.4002	227.749	57.9173
MAPE	32.7781	26.9659	20.6102
2015	295.3033	273.5012	247.8703
2016	315.4265	291.7693	264
2017	336.921	311.2576	281.1793

2018	359.8802	332.0477	299.4766
2019	384.4039	354.2264	318.9645
2020	410.5988	377.8864	339.7206
2021	438.5787	403.1269	361.8273
2022	468.4653	430.0532	385.3726
2023	500.3885	458.778	410.45
2024	534.4871	489.4215	437.1593
2025	570.9093	522.1117	465.6067

The prediction of Turkey's total electricity energy demand until 2025 is shown in Figure 2.

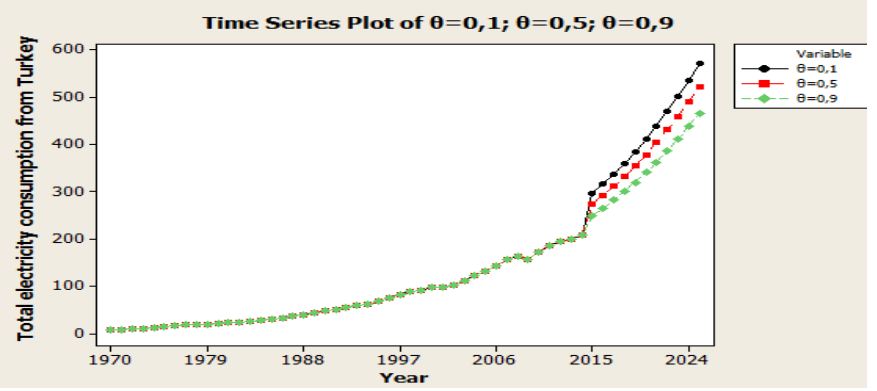

Figure 2. Turkey's total electricity energy demand prediction until 2025 by using GM(1,1) with different θ

The plot of GM(1,1) with parameter θ=0.9 residuals versus time is shown in Figure 3. It looks no seasonality appears and residual distribution has a random pattern.

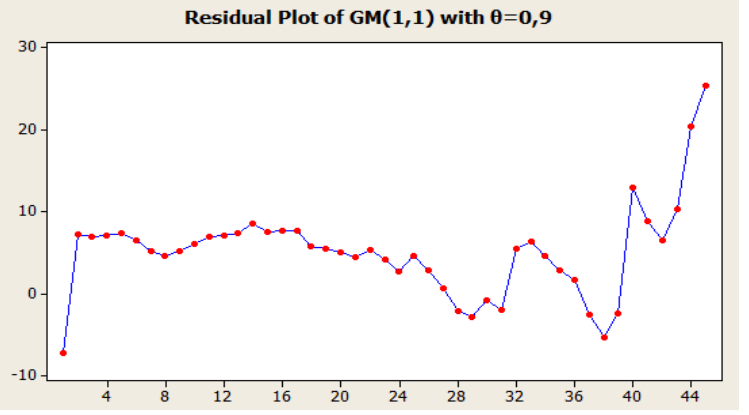

Figure 3. Plot of residuals versus time for the GM(1,1) model with θ=0.9

Figure 1 shows the data used for the electricity consumption of Turkey for the period of 1970-2014. From this data, it is suspected that there should be some relationship (i.e., autocorrelation) between the electricity consumption in the current year and the electricity consumption in the previous years. As always, we start our analysis with the time series plot of the data, which is shown in Figure 1. After year 2006, the process shows sign of nonstationarity with changing mean and possibly variance. Therefore, features of ACF and PACF should be examined for the given data. Figure 4 shows the ACF of given data.

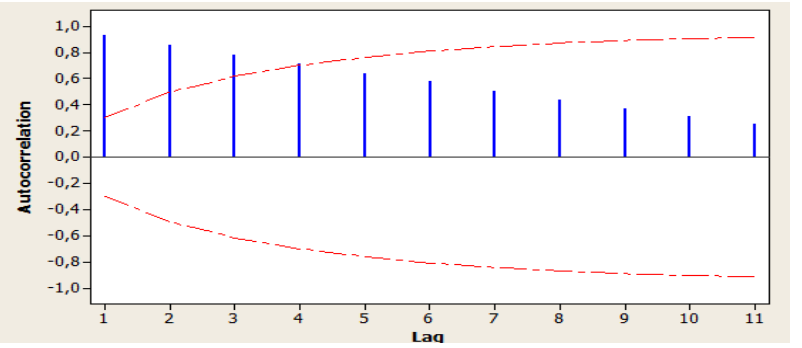

Figure 4. ACF plot

ACF plot shows that it cuts off after lag 3 (or maybe even 4), suggesting a MA(3) model. Also, it has an (or a mixture of) exponential decay(s) pattern suggesting an AR(p) model. For resolving the conflict, sample PACF plot is considered. Figure 5 shows the PACF plot of given data.

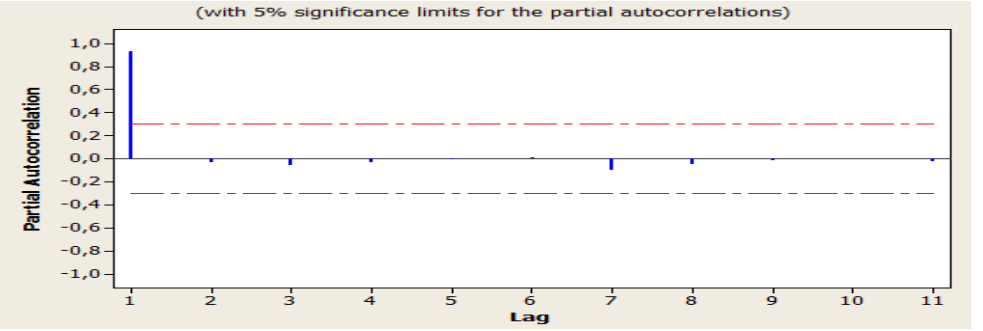

Figure 5. PACF plot

PACF plot shows that it cuts off after lag 1. Hence, it is assumed that the appropriate model to fit is the AR(1) model. Because, the slowly decreasing sample ACF and sample PACF with significant value at lag 1, which is close to 1 that confirm the process can be deemed nonstationary. Figure 6 shows the Minitab Output for the AR(1) model for the data used for electricity consumption of Turkey for the period of 1970-2014.

```
Final Estimates of Parameters

Type      Coef  SE Coef       T      P
AR   1  1,0193   0,0079  129,44  0,000

Number of observations:  45
Residuals:    SS =  1008,89 (backforecasts excluded)
              MS =  22,93  DF = 44

Modified Box-Pierce (Ljung-Box) Chi-Square statistic

Lag            12     24     36  48
Chi-Square   17,1   21,1   41,3   *
DF             11     23     35   *
P-Value     0,105  0,576  0,215   *
```

Figure 6. Minitab Output for the AR(1) model for the data used for electricity consumption of Turkey

From Figure 6, it is concluded by using the modified Box-Pierce test that there is no autocorrelation left in the residuals. The parameter estimates are φ1= 1,0193 and it turn out to be significant. Because p value is significant. Also, MSE is calculated to be 22,93. The modified Box-Pierce (ljung-box) test also significant.

Since, p value is greater than 0.05. We can also see that there is no autocorrelation left in the residuals from the residual plots of the ACF and PACF which is shown in Figure 7 and Figure 8 respectively.

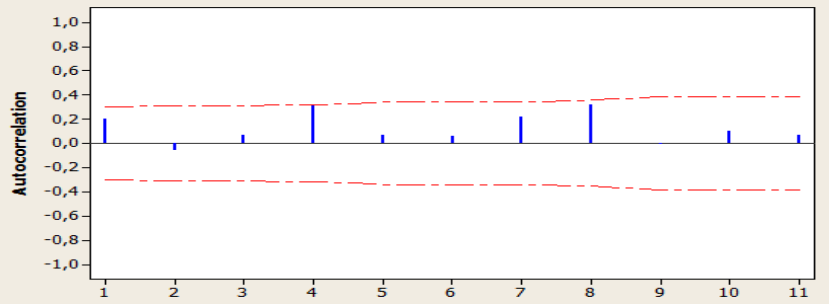

Figure 7. ACF of residuals

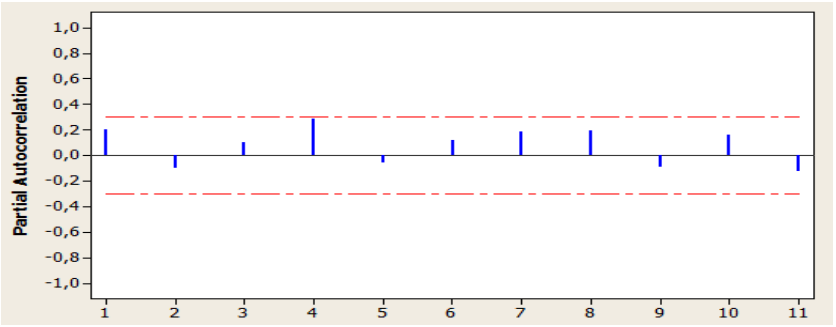

Figure 8. PACF of residuals

As the last diagnostic check, we have the 4-in-1 residual plots provided by Minitab which is shown in Figure 9: Normal Probability Plot, Residuals versus Fitted Value, Histogram of the Residuals, and Time Series Plot of the Residuals. This figure indicates that the fit is indeed acceptable.

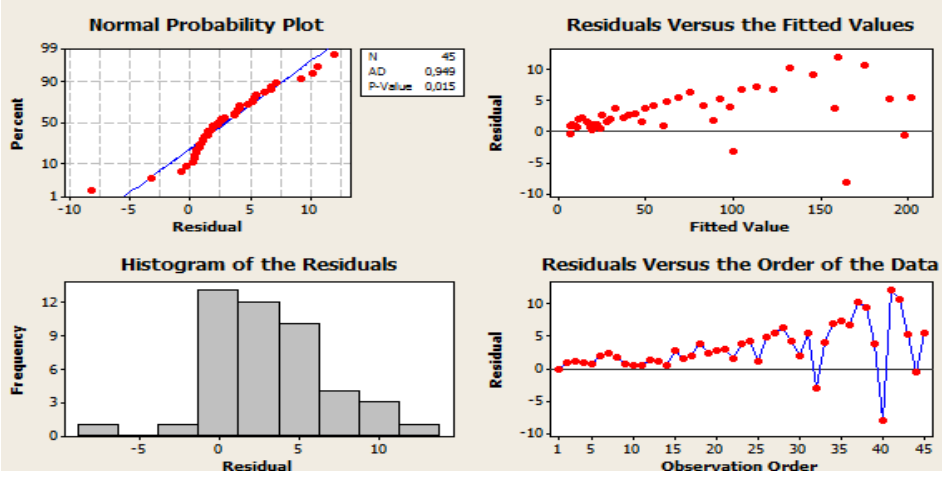

Figure 9. 4-in-1 residual plots

Finally, total electricity consumption of Turkey were forecasted for the period until 2025 by using the AR(1) model and Table 3 shows the predicted results until 2025.

Table 3. Forecasted values of total electricity consumption of Turkey by using the AR(1) model.

Year	Forecasted Value
2015	211,382
2016	215,466
2017	219,629
2018	223,873
2019	228,199
2020	232,608
2021	237,102
2022	241,684
2023	246,354
2024	251,114
2025	255,966

Discussion and Conclusions

Forecasting the energy consumption is generally thought as a difficult task. Since, there exist many factors that affect. Some of them are rapid development of technology, governmental issues etc. Therefore, to develop an accurate prediction model plays a critical role. In this study, electricity consumption of Turkey is tried to be predicted based on Grey modelling system and Auto-Regressive Integrated Moving Average (ARIMA) model. Results are compared according to the MAD, MSE and MAPE metrics. Finally, AR(1) model's MSE is calculated as 22,93 which the smallest one. Also GM(1,1) with different θ parameter generate different MSE values. For example, in case of θ=0.1 GM(1,1) has 497.4002 MSE value, θ=0.5 GM(1,1) has 227.749 MSE value and θ=0.9 GM(1,1) has 57.9173 MSE value. From this results it is easy to see the important effect of θ parameter. Therefore, it is coclueded that MSE metric can be reduced by finding the optimized value of θ parameter. Although MSE metric show that accuracy of the prediction result is based on AR(1) model is the highest. However, generally ARIMA models have one important disadvantage that models require a large amount of historical data in order to produce accurate results. Hence, GM(1,1) model can be suggested when limited data exist. Finally, based on the predicted values of this study, required resources can be calculated for the future periods.

References

Akay, D., Atak, M. (2007). Grey prediction with rolling mechanism for electricity demand forecasting of Turkey. Energy, 32(9), 1670-1675.

Al-Shobaki, S., Mohsen, M. (2008). Modeling and forecasting of electrical power demands for capacity planning. Energy Conversion and Management, 49(11), 3367-3375.

Bellman, Richard E., Lotfi Asker Zadeh. (1970). Decision-making in a fuzzy environment. Management Science 17(4), B-141.

Chiang, J. S., Wu, P. L., Chiang, S. D., Chang, T. J., Chang, S. T.,Wen, K. L. (1998). The Introduction of Grey System Theory. Gao-Li Publication, Taiwan.

Dantzig, George B. (1955). Linear programming under uncertainty. Management Science 1(3), 197-206.

Deng, J. (1982). Control problems of grey system. Systems & Control Letters, 1(5), 288–294.

Hamzacebi, C., Es, H. A. (2014). Forecasting the annual electricity consumption of Turkey using an optimized grey model. Energy, 70, 165-171.

Hamzacebi, C., Karakurt, I. (2015). Forecasting the Energy-related CO2 Emissions of Turkey Using a Grey Prediction Model. Energy Sources, Part A: Recovery, Utilization, and Environmental Effects, 37(9), 1023-1031.

Hsu, C. I., Wen, Y. H. (1998). Improved grey prediction models for the trans -pacific air p Transportation Planning and Technology, 22(2), 87-107.

Huang, M., He, Y., Cen, H. (2007). Predictive analysis on electric-power supply and demand in China. Renewable Energy, 32(7), 1165-1174.

Julong, D. (1989). Introduction to grey system theory. The Journal of Grey System, 1(1), 1-24.

Khashei, M., Bijari, M., Ardali, G. A. R. (2009). Improvement of auto-regressive integrated moving average models using fuzzy logic and artificial neural networks (ANNs). Neurocomputing, 72(4), 956-967.

Lee, Y. S., Tong, L. I. (2011). Forecasting energy consumption using a grey model improved by incorporating genetic programming. Energy Conversion and Management, 52(1), 147-152.

Liu, S., Forrest, J. Y. L. (2010). Grey Systems: Theory and Applications. Springer.

Mao, M., Chirwa, E. C. (2006). Application of grey model GM (1, 1) to vehicle fatality risk estimation. Technological Forecasting and Social Change, 73(5), 588-605.

Box, P., Jenkins, G.M. (1976). Time Series Analysis: Forecasting and Control, Holdenday Inc., San Francisco, CA.

Sun, G. (1991). Prediction of vegetable yields by grey model GM (1, 1). Journal of Grey System, 2(2), 187-197.

Tang, H. W., Chou, T. C. R. (2016). On the fit and forecasting performance of grey prediction models for projecting educational attainment. Kybernetes, 45(9).

Tseng, F. M., Yu, H. C., Tzeng, G. H. (2001). Applied hybrid grey model to forecast seasonal time series. Technological Forecasting and Social Change, 67(2), 291-302.

Wang, Y. F. (2002). Predicting stock price using fuzzy grey prediction system. Expert Systems with Applications, 22(1), 33-38.

International Conference on Science and Technology

ICONST 2018

5-9 September 2018 Prizren - KOSOVO

Bioengineering Methods in the Production, Development and Metabolism of Essential Oil in Plants

Özlem Karaboyacı[1]*, Semra Kılıç[2]

Abstract: Essential oils are odorous oily liquids derived from plant material. Essential oils have been used extensively from pre-history times as, bactericidal, fungicide, insecticidal, and medical purposes. Many of these components are produced as secondary metabolites in plants. Therefore, the development of production of these components are important in terms of medicine and industry. In this study, bioengineering methods used in the production, development and metabolism of essential oils in plants were investigated. Recent developments on this issue have been summarized and reported.

Keywords: Essential oils, bioengineering, seconder metabolites

Introduction

People use plants to obtain an important portion of the essential foods they need to survive. Plants are a crucial source of nutrients such as carbohydrates, protein, fat, minerals and vitamins. They also contain highly important chemicals for pharmaceutical, chemical, cosmetic and agricultural control industries. These chemicals are referred to as “secondary metabolites” and some plant products are considered under this category. High diversity in the number and structure of secondary metabolites is a specific characteristic of secondary metabolites. They are understood to have a very complicated mechanism specific to plants for defence, protection, adaptation, survival and continuation of next generations. The available written historical sources mention that ancient humans used plants for the treatment of various diseases. It is doubtless that this type of usage was not based on the secondary products that are active substances but on the plant itself or its extracts obtained through different means. Today, plants are used as pharmaceutical active ingredients. Medical and aromatic plants are those ones that are used to prevent diseases, maintain health or treat diseases. Medicinal plants are used in nutrition, cosmetics, body care, incense or religious ceremonies while aromatic plants are used for good smell and taste (Bayram et al., 2010).

Essential oils are mixtures that are extracted from plant roots, bodies, leaves, fruits, barks and flowers by different methods; are in liquid form at room temperature, volatile with a strong scent, can be easily crystalized, are usually colourless or light yellow, give the plant its characteristic smell and flavour, contain several compounds, have lipoid structure that can be drifted with water, contain oxygenated terpenoit derivatives, benzoid compounds, nitrogen or sulphur and are usually comprised of terpens (Adams, 2004;, Bayrak, 2006;, Çalikoğlu et al., 2006;, Evren and Tekgüler 2011;, Yaylı, 2013;, Kaya and Ergönül 2015). They exist in the glandular hair, secretion pocket, secretory canals or secretory cells depending on the family of the relevant plant (Çelik and Çelik, 2007).

[1]Suleyman Demirel University, Faculty of Engineering,Bioengineering Dpt. 32260, Isparta, TURKEY
[2]Suleyman Demirel University, Faculty of Arts and Science, Biology Dpt. 32260, Isparta, TURKEY
*Correspondingauthor: ozlemkaraboyaci@gmail.com

1.1. What is Essential Oil?

Essential oil is a natural, usually colourless or light yellow product with a strong scent that is obtained from plant leaves, fruits, barks or roots, is in liquid form at room temperature and can be easily crystalized.

It is also referred to as essence or etheric oil because of its nice scent. It does not mix with water, which makes it different from the fatty oil although it is defined as oil (Ceylan, 1983).

1.1.1. Chemical Characteristics of Essential Oils

Terpenes constitute the largest group in the chemical structure of essential oils. Some compounds also contain low amount of alcohols, aldehydes, esters, phenols, nitrogen and sulphur. The oxygenated derivatives that are formed due to the oxidation of terpenes give plants their scent and flavour while they are also therapeutic (Linskens, 1997).

1.1.2. Pharmacological Properties of Essential Oils

The activity of an essential oil is confused with the action of the plant from which it is extracted. For example, the essential oil of Rosmarinus is antimicrobial while the infusion of the plant has an antispasmodic and choleretic effect.

The activities found in some essential oils are as follows;

Antiseptic activity: They are often antiseptic against strains that are resistant to antibiotics. Some essential oils are also effective against fungi and yeasts. Almost all of them are used as preservative. Melisa officinalis, Rosamarinus officinalis, Mentha piperita, Lavandula, Eucalyptus, Eugenia... vs. Sitral, Geraniol, Linalol and Timol are more antiseptic than phenols.

Spasmolytic and sedative effect: They reduce and suppress GIS (gastro intestinal system) spasms. They often increase gastric secretion and have “digestive” and “stomachic” effect. They are effective in various psychosomatic problems. Thymus, Ocimum, Angelica, Matricaria, Eugenia, Melisa, Mentha are spasmolytic. O.Anisi is used internally as spasmolytic. O. Menthae shows spasmolytic effect by preventing calcium entry into cells .

Irritant properties: Products such as turpentine increase blood flow in capillary vessels, local rash, sense of burn and show slightly local anaesthetic effect in some cases if used externally. Oils such as Eucalyptus, Pinus and O.Niaouli stimulate the cells in the mucosa and increase the mobility of the epithelium of the bronchi (expectorant). Essential oils that are used in various sectors such as cosmetic, perfumery, pharmacology and food industries have been extracted by different methods since the Romans.

Essential oils are used as spasmolytic, irritant, antiseptic, antimicrobial, antifungal, antiviral, antimutagenic and antibiotic agents in the pharmacology (Evren and Tekgüler, 2011).

2. Bioengineering Methods for Essential Oil Production and Metabolism

Increased industrial interest in plant-based chemicals has also been increasing the attention to the plants’ secondary metabolisms and the physiology and biochemistry of plant products. ıt is important to change the phytochemical production positively through conventional and non-conventional biotechnological methods. Most of the plants’ secondary metabolites (SM) depend directly and indirectly on the plants’ reactions to various environmental factors and stimuli. They are usually produced at baseline level in their normal course that is triggered by cell damage or as a reaction to external factors, and function as phytopharmaceuticals. Secondary metabolites are usually produced in their normal course. They are triggered in case of cell damage or as a reaction to external factors and

start functioning as phytopharmaceuticals. Moreover, bioactive compounds are used widely directly in cosmetics, aroma and perfumery industries, as paint and pigment, food additives, insecticides or as an important component in various formulations. The use of plant-based bioactive compounds in modern medicine has successfully focused the global attention on the research of medicinal plants at global level. The need for plant-based therapeutic molecules in the pharmaceutical industries across the world has increased. The main ways of obtaining such components include extraction from natural resources and chemical synthesis. Non-environmental friendly nature of conventional extraction method that is non-renewable, uneconomical and time-consuming has increased the interest of global scientific community in the biotechnology-based production systems (Dubey et al. 2017).

2.1. Plant Tissue Culture

It refers to the process of obtaining new tissues, plant or plant products (such as metabolites) from the whole plant, plant parts such as cells (meristematic cells, cell concentration or callus cells), tissues or organs (apical meristem, root etc.) under aseptic conditions (in an environment free from any kind of microorganisms) in an in vitro medium. The main objectives of tissue culture are to develop a new variety and create genetic diversity in the existing varieties. Furthermore, various tissue culture methods are routinely used to save and endangered species and production of species that are difficult to propagate (Babaoğlu et al. 2001).

2.2. Secondary Metabolites

They are produced by a very complicated mechanism that plants develop for defence, protection, adaptation, survival and continuation of next generations. Secondary metabolites have important functions such as resistance to various abiotic agents such as drought, salinity, UV beams; defence against herbivores and microorganisms; attracting animals and other carriers for pollination and seed distribution. Moreover, they also have an economic value. For example; they are used as pharmaceutical ingredients, food supplements and in perfumes and agricultural control products. Since they are important not only for plants' defence against pathogens but also in economic and medical aspects, plant tissue culture techniques have become one of the most important means for their production. (Atar and Çölgeçen 2013)

Plants are used as pharmaceutical active ingredients for most of the world population. Particularly in the developing countries, 80% of the population meet their health requirements primarily through medicinal products. Given that 80% of the world population live in the developing countries, 64% of the total world population use plants for therapeutic purposes. In the developed countries, however, 25% of the prescribed drugs are plant-based chemicals. There is no doubt that the exploration and assessment of plants used by people for the treatment of various diseases, which are named as folk remedy, have played an important role in their discovery (Babaoğlu et al. 2001).

Today, secondary metabolites have a huge potential for use. There are some challenges and disadvantages in extracting them from plants under natural conditions. Plants are raised in small quantities and at certain development stages under natural conditions, during which they occupy agricultural fields; constant collection of some plant species from the nature may pose extinction threat, while it is difficult and expensive to collect some of them. Furthermore, the amount and quality of secondary metabolites are influenced by the climate conditions. They can be produced in desired quantities at the desired time through biotechnological means, extinction danger is also eliminated, while they can be produced in abundant amounts at standard quality.

There are basically 3 systems to produce secondary metabolites through plant cell and tissue culture, which can be summarized as follows.

2.2.1. Metabolite Production through Differentiated and Organized Cultures

Root Cultures: With this method, in cases where metabolites are synthesized in the root, the parts taken from it are cultured in an appropriate medium. Moreover, adventive root cultures (root formed in another organ of a plant apart from its normal root growth region) that are obtained by stimulating different tissues of the plant (laves, body, nodes etc.) for root growth are preferred to produce secondary metabolites from some plants (Erkoyuncu and Yorgancılar 2016).

2.2.2. Metabolite Production through Non-Differentiated and Non-Organized Cultures

Callus is a stack of differentiated cells formed by plant cells or tissues placed in in vitro culture media. Callus is usually formed on the surfaces of injured or cut tissues (Babaoğlu et al. 2001). Callus cultures can be described as masses with morphological irregularities formed by in vitro culturing of organs or tissue pieces excised from the main plant that still retain their mitotic capabilities. The origin of the tissue where callus culture is initiated plays an important role for the production of secondary metabolites (Erkoyuncu and Yorgancılar 2016.).

2.2.3. Micro Propagation Method

Micro propagation is a tissue culture technique used to propagate high number of genetically similar plants quickly from the plant parts (embryo, seed, body, shoot etc.) that have the potential to form a whole plant in the in vitro media under microorganism-free conditions (Özkaynak nd Samancı 2005).

Micro propagation also enables the vegetative propagation of several medicinal and aromatic plants fast and in high quantities. If the nutrient requirements of plants, growth regulator and culture requirements are known very well, all plant species can be produced using the micro propagation technique. The micro propagation of medicinal and aromatic plants has considerable advantages such as availability of plants at any time in a year, shorter culturing time, protection of endangered medicinal plants, phenotypic and genotypic homogeneity of plants produced, easier production of challenging species in addition to the benefits ot in vitro propagation methods (Erkoyuncu and Yorgancılar 2016).

Cell concentration is another non-differentiated and non-organized culture method for metabolite. The difference in the culture medium of cell concentration from that of callus culture is that a thickening agent is added to the callus culture medium whereas it is not added in the concentration medium. Therefore, concentration medium is liquid. Callus cultures are used in order to get a good result from cell concentration cultures, which is technically more advantageous. Parts taken from callus culture that has adapted to in vitro medium can adapt to liquid medium more easily than those parts taken from the main plant (Atar and Çölgeçen 2013).

Micro propagation is a production method that also allows vegetative propagation of medicinal and aromatic plants fast and in high quantities. It is defined as obtaining new plants under in vitro conditions from the plant parts that have the potential to form a whole plant (embryo, seed, body, shoot, root, callus, one cell or pollen grain etc.). If the nutrient requirements of plants, growth regulator and culture requirements are known very well, all plant species can be produced using the micro propagation technique. (Erkoyuncu and Yorgancılar 2016).

Hairy root method can be suggested as the most effective method of all the abovementioned ones. Hairy root culture is more advantageous for secondary metabolite production compared to other culture systems because of its various characteristics such a high growth rate and genetic and biochemical stability. Hairy root cultures form model systems for plant metabolism and physiology. Plant cell concentration is one of the culture stages of manufacturing special chemical substances and pharmaceuticals. Hairy roots are also used as a source in transgenic plant regeneration (Atar and Çölgeçen 2013)

Biotechnological intervention makes it possible to remove the time, cost and geopolitical constraints of crop production and overcome the challenging issues such as climate and disease without compromising the sustainability of the nature. Majority of the biotechnology-based production systems include "the production of plant-based therapeutic molecules using in-vitro plant cultures". As regards the reasons of the of plants for therapeutic purposes, we thing that any plant-based metabolite has a significant medicinal value or it act as a precursor to start the medicinal action. Components that provide medicinal effect are usually the products of secondary metabolites and thus they are produced in small quantities as they are not essentially required for plant growth. Besides, production of plants that have medicinal metabolites may take several months or years for the maturation of plants. Moreover, they are vulnerable to environmental and seasonal changes and thus cannot strike the supply and demand equilibrium. Due to their complex chemical complexes, their chemical synthesis is boring and complicated. (Dubey et al. 2017)

In vitro plant culture under selective and nutritional conditions is a promising production technique, through which is bioactive compounds are produced using isolated cells and/or organs. This technique is divided into two categories as production based on cell concentration cultures and production based on roots/ hair roots. As regards the comparison of cell concentration culturing method with plant root cultures and hairy root cultures, the former has some limitations such as metabolite production in specialized cells at different development stages and genetic instability of these cells. Features such as high growth rate and low culture cost make hairy root cultures be superior to plant root cultures. Hairy root culture method have distinctive features such as high growth potential, genetic and biochemical binding, low doubling time and etc. Moreover, when optimized for liquid cultures, they can display their final growth and metabolite production capabilities even at large-scale productions. There are research reports and reviews in the literature regarding therapeutic SM production by hairy root culture method (Dubey et al. 2017).

3. Haıry Root Culture Method

Hairy root is indeed a plant disease. It is caused by Agrobacterium bacteria that are gram-negative bacteria in the family of Rhizobiaceae which lives in the soil. Agrobacterium tumafaciens causes root collar tumours while Agrobacterium rhizogenes leads to hairy root formation. This disease manifests itself as small and excessive enlargements in the parts of trunks and roots that are closer to the soil surface. At early development stages, tumours are more or less globular, white or nude coloured and very soft. At later stages, external tissues become brown or black due to cell death and decay. They transfer their own DNA region to the plant’s genome through the genes they carry in both their own genomes and plasmids, which leads to hairy root disease (Hooykaas and Schilperoort 1984).

Hairy root culture has the following advantages: easy to apply, affordable, high genetic transformation rate, stable metabolite yield as the stable settlement of the transferred gene in the genome, fast root growth without need for external auxin use, same and even higher potential to produce secondary metabolites compared to the main plant, allowing genetic manipulations targeted in the metabolic pathway where the synthesis realized. Therefore, it is preferred for the production of several root-driven or non-root driven metabolites in cases when other cell and tissue culture techniques are not appropriate (Erkoyuncu and Yorgancılar 2016).

Low production rate and high production costs are the main reasons why there is failure at industrial scale as regards the production of secondary metabolites. Various strategies have been used to make hairy root culture technology affordable for the production of therapeutic molecules. They include ambient optimization, precursor feeding, elicitation and metabolic engineering. They have been extensively explored at a global scientific platform for not only secondary metabolite production but also better understanding of natural gene transfer and its physiological, molecular and biochemical results.

3.1. Ambient Optimization

Hairy root formation is followed by medium optimization. Hairy roots can basically grow in any basal tissue culture medium as underlined in the studies of Murashige and Skoog, Gamborg's B5, Nitsch and Nitsch. Nutritional requirements may vary depending on the plant system and purpose of establishing the roots. Hairy roots of some plant species grow well in a medium enhanced with additional vitamin while those of some other plant species require half and even a quarter of regular growth environment. Furthermore, the amount of both carbohydrate source and nitrogen source and its type play an important role in growth and SM production. Sometimes ambient optimization is needed to assess the relation between food supplement and desired metabolite flow. The presence of a certain nutrient in the medium of hairy root cultures of some plant species is important for not only growth but also accumulation of the desired metabolite (Murthy et al. 2014) (Pudersell et al. 2012). Media are optimized with hairy roots; while they are also considered as a preliminary strategy to optimize metabolite production using hairy root cultures (Sung et al. 2000) .

3.2. Elicitation

Elicits are compounds that stimulate any kind of plant defence. A wider definition of elicits includes exogenous elicitors and compounds released by plants due to the movement of pathogenic substances (pathogen (endogenous elicitors). Plants display a wide range of defence strategies against pathogen attacks. Resistance to pathogens is realized by the existing (founder) and evoked defence systems. Induction defence reactions are triggered after the recognition of a series of chemical factors named 'elicitors'. Indeed, the term elicitor is used for molecules that can induce phytoalexin but it is currently used for compounds that stimulate any kind of plant defence (Angelova et al. 2006).

Elicitation is the induced and/or extended biosynthesis of SMs due to the initiation of a physical, chemical or biological elicitor (information molecule) in a plant system (Namdeo A. 2007). Information molecule activates the inducible defence variables in a plant system and leads to the activation of its various protection mechanisms. The biosynthesis of the same or new SMs in the sstem is induced or extended through such mechanisms. As in robust plants, physical, chemical and biological factors trigger quantitative and qualitative change in the biochemical profile of hairy roots due to the induced enzymatic pathways. Therefore, elicitation is a widely acknowledged strategy applied to increase the production of therapeutic SMs that are preferred to hairy root culture of medicinal plants. Root tissue's response to the elicitor molecule requires a well-defined signal transmission network on cell surface and inside cells. The interaction between signal transducers and regulation of the next SMs' biosynthetic pathway genes is the main reason for the changes in the biochemical profiles of the hairy roots obtained (Goel et al. 2011) .

3.3. Precursor feeding, Biotransformation and Co-Culture Systems

Limitation of precursor molecules in the system is one of the main reasons for low SM yield of hairy roots. Addition of metabolic pathway precursors to the medium may induce or improve the deired metabolite synthesis or accumulation. In most of the cases, enzyme machine is available to proceed the desired metabolites but the system cannot achieve optimum or sufficient yield due to the lack of close and remote precursors. To solve this problem, biotransformation of precursors required to obtain the desired metabolite has been explored for several plants (Murthy et al. 2014) .

Plant-based pharmaceutical compounds that grow naturally acquire better therapeutic properties due to the changes introduced to their molecular structures. There is an increasing commercial demand for these analogues of natural compounds due to decreased toxicity, sufficient resolution and better pharmacokinetics. Hairy root based biotransformation creates compounds with better therapeutic potential in which any substrate transforms to the analogue of its molecule. It is known that there are remarkable therapeutic compounds produced using the method of enzymatic transformation of medicinal plants' hairy roots and chemical reactions such as hydroxylation, glycosylation,

glucosylation, oxidoreduction, hydrogenation and hydrolysis caused by the enzymatic reactions (Srivastava V. 2015) .

3.4. Metabolic Engineering

Every biological system has a well-regulated information flow from genes to metabolites. At molecular level, the activated regulatory network causes defined physiological and biochemical changes to keep the system balanced during the initiation of excitatory signals. Due to their proximity to local plants, hairy root cultures are globally used to investigate various aspects of plant behaviour and its regulation at molecular level under variable conditions. Production of therapeutic SMs and their regulation by way of genetic manipulation attract scientists. Metabolic engineering of hairy root based SM pathways can be manipulated through the following ways.

3.4.1. Engineering of Metobolic Pathway Genes

Under this method, genetic manipulation directly leads to the desired metabolic shift. The concerned gene may go through early or late /final biosynthesis step but engineering at the late/final steps results in more satisfactory production. Target genes are usually on the rate-limiting step, which is followed by reactions catalysed by non-limiting enzymes. Multiple gene engineering is also a common trend. This approach has been used to increase therapeutic molecules in tropane alkaloids (TA) and terpenoid indole alkaloids (TIA) (Moyano et al. 2003).

3.4.2. Transcription Factor Engineering

Plant SMs are primarily involved in plant-environment interactions. Such interactions are mediated by a series of gene expression modulations through hormonal signalling followed by transcription factors (TF). The reason why hairy root cultures produce high amount of SMs is because stress-related hormones that regulate TFs are identified and used (Yang et al. 2012) .

3.4.3. Simultaneous Engineering of Metabolic Pathway Genes and Transcription Factors

Sometimes overexpression of TFs does not result in an increase in distinct metabolites. This is the result of the regulation of multiple metabolic pathways which does not change the overall result significantly (Li et al. 2015) .

3.5. Addition and Expression of a Relevant Gene Isolated from a Different Source

Under this method, an unwanted molecule can only be produced by transferring a relevant gene segment to the hairy root cells of host plants from a non-plant source. This approach is considered to be a logical action to suppress the activity of unwanted genes related to the concerned property or metabolite. In general, this strategy is used to define the significance of a gene in a biosynthetic pathway. Moreover, in hairy root culture based SM production, the strategy is also used to produce unnatural metabolites or manipulate a metabolic pathway (Runguphan et al. 2009) .

3.6. Changing Chromosome Number

The purpose of this method is to increase the metabolite production potential by doubling or multiplying the number of basal chromosomes, thereby increasing the overall plant potential. This method may originate from the of conventional breeding which has a high productivity potential in polyploid plants. This superiority also applies to the other properties of the plant including SM production. There is a correlation between Changing Chromosome Number and enhancement of phytopharmaceuticals (Lavania et al. 2005).

4. Bıotransformatıon

Biotransformation is an important implementation area for the production of secondary metabolites using plant tissue and cell cultures. It has is a technology with the same synthesis cycle and applied to transform less-beneficial to more-beneficial.

For example, digitoxin and digoxin are isolated from Digitalis lanata, which are the most important ingredients of drugs that regulate heart rhythm. Although digitoxin is more available, digoxin is preferred more commonly for treatment purposes. For that reason, transformation is realized via chemical synthesis (Baydar and Telci 2015)

References

Adams R.P., (2004). Identification of essential oil components by gas, quadrupole spectroscopy. Allured publishing Co, Carol Stream, IL, USA, pp.1-456

Angelova, Z., Georgiev, S., Roos, W. 2006. Elicitation of plants. Biotechnology & Biotechnological Equipment, 20(2), 72-83.

Atar, H., Çölgeçen, H., 2013. Bitki doku kültüründe iridoit glikozitler. Marmara Fen Bilimleri Dergisi, 25(3), 115-133.

Babaoğlu M, Gürel E ve Özcan S (2001) Bitki Biyoteknolojisi I. Doku Kültürü ve Uygulamaları. Selçuk Üniversitesi Basımevi, 374.

Baydar, H., Telci, İ., 2015. Tıbbi ve aromatik bitkilerde ıslah, tohumluk, tescil ve sertifikasyon. Türktop Dergisi 5(15): 12-21

Bayrak, A. 2006. Gıda Aromaları. Gıda Teknolojisi Derneği Yayın no: 32. 497 s., Baran Ofset, Ankara.

Bayram, E., S. Kırıcı, S. Tansı, G. Yılmaz, O. Arabacı, S. Kızıl, İ. Telci , Tıbbi Ve Aromatik Bitkiler, 2010.

Ceylan, A. 1983. Tıbbi Bitkiler-II. Ege Üniversitesi Ziraat Fakültesi Yayını No:481, Bornova-İzmir.

Çalikoğlu, E., Kıralan, M., Bayrak, A., (2006). Uçucu Yağ Nedir, Nasıl Üretilir ve Türkiye'deki Durumuna Genel Bir Bakış Türkiye 9. Gıda Kongresi, 24-26.

Çelik, E., Çelik, G.Y., 2007. Bitki uçucu yağlarının antimikrobiyal özellikleri. On-Line Mikrobiyoloji Dergisi, 5(26).

Dubey, S. K., Pandey, A., & Sangwan, R. S. Current Developments in Biotechnology and Bioengineering. ISBN: 978-0-444-63661-4 pages 2017, Pages 259–282. 2017 Elsevier B.V Amsterdam, Netherlands.

Erkoyuncu, M. T., Yorgancılar, M. 2016. Bitki Doku Kültürü Yöntemleri İle Sekonder metabolitlerin Üretimi. Selçuk Tarım Bilimleri Dergisi, 2(1), 66-76.

Evren M., Tekgüler B., (2011). „Uçucu Yağların Antimikrobiyel Özellikleri" Mikrobiyoloji Dergisi , 9(3), 28-40.

Goel M.K. ,Mehrotra S. ,Kukreja A.K. , Elicitor-induced cellular and molecular events are responsible for productivity enhancement in hairy root cultures: an insight study, Applied Biochemistry and Biotechnology 165 (5-6) (2011) 1342-1355.

Hooykaas P. J. J., Schilperoort R. A., 1984. The moleculer genetics of crown gall tumorigenesis. In: Scandalios Jg, Caspari EW (eds), Advances in Genetics, Volume 22, Molekuler Genetics of Plants., pp. 209-283.

Kaya, D, Ergönül, PG. (2015). Obtaining methods of volatile oils. GIDA-Journal of Food, 40(5), 303-310.

Lavania, U. C. "Genomic and ploidy manipulation for enhanced production of phyto-pharmaceuticals." Plant Genetic Resources3.2 (2005): 170-177.

Linskens, H. F., Jackson, J.F, b Modern Methods of Plant Analysis, Vol. 12: Essential Oils and waxes, Springer, Germany, 1997.

Li B., Wang B. ,Li H. , Peng L. , Ru M. , Liang Z., et al., Establishment of Salvia castanea Diels f. tomentosa Stib. hairy root cultures and the promotion of tanshinone accumulation and gene expression with Ag, methyl jasmonate, and yeast extract elicitation, Protoplasma 253 (1) (2015) 87-100.

Mehrotra, S., Srivastava, V., Rahman, L. U., & Kukreja, A. K. (2015). Hairy root biotechnology—indicative timeline to understand missing links and future outlook. Protoplasma, 252(5), 1189-1201.

Moyano E. , Jouhikainen K. , Tammela P. , Palazo´n J. , Cusido R. M. , Pin ol M. T. , et al., Effect of pmt gene overexpression on tropane alkaloid production in transformed root cultures of Datura metel and Hyoscyamus muticus, Journal of Experimental Botany 54 (381) (2003) 203-211.

Murthy, H. N., Lee, E. J., & Paek, K. Y. (2014). Production of secondary metabolites from cell and organ cultures: strategies and approaches for biomass improvement and metabolite accumulation. Plant Cell, Tissue and Organ Culture (PCTOC), 118(1), 1-16.

Namdeo, A. G. "Plant cell elicitation for production of secondary metabolites: a review." Pharmacogn Rev 1.1 (2007): 69-79.

Özkaynak, E., Samancı, B. 2005. Mikroçoğaltımda Alıştırma. Selçuk Tarım Ve Gıda Bilimleri Dergisi, 19(36), 28-36.

Pudersell, Katrin, et al. "Inorganic ions in the medium modify tropane alkaloids and riboflavin output in Hyoscyamus niger root cultures." Pharmacognosy magazine 8.29 (2012): 73.

Runguphan, Weerawat, Justin J. Maresh, and Sarah E. O'Connor. "Silencing of tryptamine biosynthesis for production of nonnatural alkaloids in plant culture." Proceedings of the National Academy of Sciences 106.33 (2009): 13673-13678.

Sung L.S. , Huang S.Y. , Medium optimization of transformed root cultures of Stizolobium hassjoo producing L-DOPA with response surface methodology, Biotechnology Progress 16 (6) (2000) 1135-1140.

Yang C.Q., Fang X., Wu X.M., Mao Y.B., Wang L.J., Chen X.Y., Transcriptional regulation of plant secondary metabolism, Journal of Integrative Plant Biology 54 (2012) 703-712.

Yaylı, N., (2013). Uçucu Yağlar ve Tıbbi Kullanımları. 1. İlaç Kimyası, Üretimi, Teknolojiisi, Standardizasyonu Kongresi, Kimyagerler Derneği, 29-31 Mart 2013, Antalya

International Conference on Science and Technology

ICONST 2018

5-9 September 2018 Prizren - KOSOVO

The Pisum Sativum Based Magnetic Biocomposite Preparation, Characterization And Using of Biosorbent

Aslıhan Arslan Kartal[1*], Cem Gök[2], Abdullah Akdoğan[3]

Abstract: In this study, describes magnetic biocomposite that use natural renewable resources and reduce adverse effects on the environment. The *Pisum Sativum* leaves powder and magnetite was encapsulated into alginate beads in aqueous calcium chloride solution to prepare a biocomposite material. Surface properties and the possible binding sites of the biocomposite were evaluated by instrumental analysis using Fourier Transform Infrared Spectroscopy- Attenuated Total Reflection (FTIR-ATR) and Scanning Electron Microscope (SEM). Biosorption, the process of passive cation binding by dead or living biomass, represents a potentially cost-effective way of eliminating metal ions from water samples. In this work, biosorption of some metal ions using magnetic biocomposite were investigated. Different sorption and thermodynamic parameters have been tested from sorption results by batch technique. The report of *biocomposite* on the biosorption studies was presented.

Keywords: Biosorption, *Pisum Sativum* leaves, alginate, metal ions

Introduction

Heavy metal pollution is one of the major environmental problems today. For this reason, most of the researchers have used various adsorbents to remove heavy metal ions over the past few decades. Most of heavy metal ions are toxic to living organisms. These metal ions are non-degradable and are persistent in the environment. Therefore, the elimination of heavy metal ions from wastewater is important to protect public health. Industrial effluents are a major cause of heavy metal concentration, these effluents are coming from many industries such as corrosion of water pipes, waste of dumping, electroplating, electrolysis, electro-osmosis, mining, surface finishing, energy and fuel producing, fertilizer, pesticide, iron and steel, leather, metal surface treating, photography, aerospace and atomic energy installations etc. Thus the removal and recovery of heavy metals from effluent streams are essential to the protection of the environment (Salman et al., 2014; Wang and Chen 2009; Sağ, Y. 2001). Biosorption has substituted to traditional methods for treatment of diluted, large volume industrial effluents such as precipitation, adsorption, coagulation etc. and is quite economical, safe with consent of their recovery from the sorbing biomass (Aytaş et al., 2016; Baig et al., 2012; Basha and Jha, 2008;). Biosorption is a term that describes metals removal by passive binding in living and dead biomass from aqueous solutions in a mechanism that is not controlled by metabolic steps (Oliveira et al., 2011).Several researchers proposed numerous biomass types as excellent metal biosorbents including bacteria, fungi, algae, industrial wastes etc., which offer active sites such as carbonyl (–CO), carboxyl (–COOH), hydroxyl (–OH), amino (–NH2) and sulfhydryl (–SH) groups for binding of metal cations and make them popular for efficient removal of metals from contaminated waters (Aftab et al., 2013).

In this study, biocomposite adsorbent obtained from the *Pisum Sativum*, magnetite and alginate was used as an alternate low-cost biosorbent for heavy metal ions removal from aqueous solutions. Moreover the biocomposite functional groups implicated in the biosorption process were studied using FTIR-ATR spectral analysis.

[*1] Pamukkale University, Faculty of Arts and Science, Department of Chemistry, Denizli, TURKEY
[2] Pamukkale University, Faculty of Technology, Department of Metallurgical and Materials Engineering, Denizli, TURKEY
[3] Pamukkale University, Faculty of Engineering, Department of Chemical Engineering, Denizli, TURKEY
*Corresponding author: aslihank@pau.edu.tr

Scanning Electron Microscopy is also used for characterizing the fundamental physical properties of the sorbent materials as the particle shape, surface morphology and texture, appropriate size distribution of the biosorbent.

Materials and Methods

Materials and Instrumentation

All chemicals (calcium chloride, sodium alginate, iron (II-III) oxide, acetic acid and sodium acetate) were of analytical reagent grade, used without further purification, and supplied from Aldrich, Germany. Pure water was obtained by using a Human Power purification system resistivity of 18 MΩ cm^{-1}(Human Corporation, Seoul, Korea). Metal stock standards (1000mg L^{-1}) were prepared by dissolving appropriate amount of nitrate salts of metals (Merck, Germany) Fourier Transform Infrared Spectroscopy-Attenuated Total Reflection (Agilent FTIR-ATR) was used to determine the vibration frequency changes in the functional groups in the prepared biosorbent within the range of wave-number of 4400-400 cm^{-1}. Surface properties were evaluated using Scanning Electron Microscope (Zeıss Supra 40VP, FESEM, Germany). The pH measurements were performed with a pH meter (WTW-pH-meter-720, Weilhemim, Germany). A Perkin Elmer Model AAnalyst 700 flame atomic absorption spectrometer (FAAS) was used for the determination of target metals. During the experiments, Precias XB 220A analytical scale and Socorex Acura Manual micropipette were used.

Preparation of Composite

Harvested fresh *Pisum Sativum* leaf samples were extensively washed with tap and distilled water to remove impurities. Then, samples were dried at room temperature. The leaf samples were transferred to oven and dried at 50°C for 24 hours using an oven. The dried samples were ground in a mortar with pestle and sieved using a standard mesh (<120 µm) sieve. *Pisum Sativum* leaves powder and magnetite was encapsulated into sodium alginate beads in aqueous calcium chloride solution to prepare a biocomposite material. For this purpose, a required amount of sodium alginate (%2) was dissolved in 10 ml distilled water with constant stirring at 50ºC until a gelous solution was obtained. *Pisum Sativum* leaves powder (0.1 g) and magnetite (0.05 g) were mixed carefully under continuous stirring until the mixture became homogeneous. The suspension was injected drop wise into a 0.5 M solution of calcium chloride with the help of injection syringe. Fine biocomposite beads of alginate-*Pisum Sativum* leaves powder were formed. The hydrogel beads were separated from the solution by filtration and dried for overnight in an oven maintained at 50 ºC (Figure 1). Dried mass of the beads was used as adsorbent for metal ions removal.

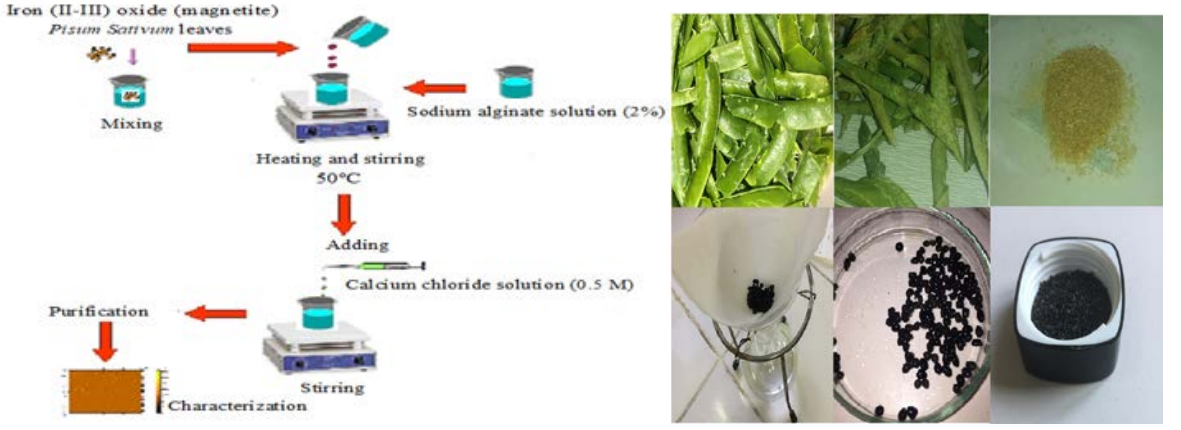

Figure 1. General procedure of biocomposites preparation

Results and Discussion

Characterization of Biocomposite

Infrared spectroscopy was used to characterize functional groups in biocomposite before and after biosorption. Figure 2 shows the change in availability of functional groups of biosorbent and the changes in the functional groups and surface properties after biosorption process. The presence of different characteristics peaks demonstrated the possible presence of various functional groups such as carboxylic, hydroxyl, amino and carbonyl groups. The wavenumber of the peak at 3289 cm^{-1} have disappeared after biosorption process, probably because of metal ions binding with amino and hydroxyl groups on the surface of the biosorbent. After biosorption, the new peaks around 2000-2250 were shown, which might be due to complexing or electrostatic interaction. In the FT-IR spectrums, the region<800 cm^{-1} is awarded the name finger print zone. The peaks in this region are related to the phosphate and sulphur functional groups. A change in the peak shape and a decrease in the peak intensity are observed after biosorption in this region.

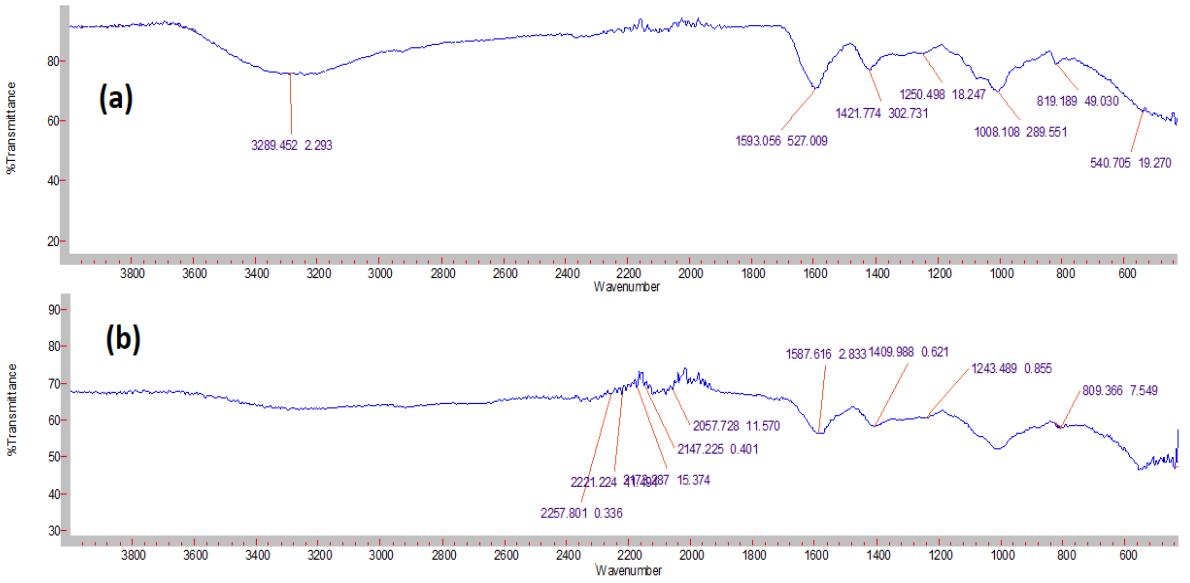

Figure 2. Infrared spectra of biocomposite (a) before and (b) after biosorption

Scanning electron microscopy (SEM) was employed to characterize the sorbent materials, including the particle shape, surface morphology, texture, and appropriate size distribution. The SEM analysis provides the direct observation of the surface microstructures and morphology of the biomasses. The changes in surface structure of after biosorption were elucidated as shown in Figure 3 at 5000 magnifications. The biomass had stable morphology after biosorption process. It can be seen from Figure 3 that the surface of biomass was porous and irregular. This morphology is indicated by the increases in surface area and pore volume that provided higher capacity for the metal ion biosorption. Metal ions can penetrate easily to these pores and channels.

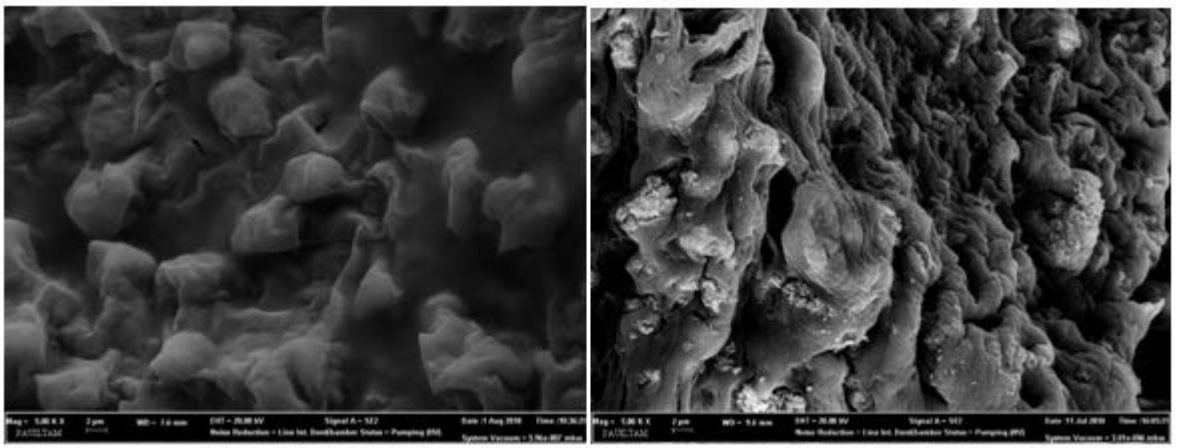

(a) (b)

Figure 3. SEM images of biocomposite (a) before and (b) after biosorption

Biosorption

The biosorption experiments for metal ions with biocomposite *Pisum Sativum* leaves were carried out by using batch measurements using a thermostated shaker bath as a function of solution pH, extraction time, biocomposite amount, and temperature. Most biosorption experiments were performed using the 125 mg of biosorbent suspended in 25 mL of metal ion solutions in a polyethylene (PE) flask at pH 4 (CH_3COOH/CH_3COONa), 50^0C and 180 min extraction time. The solution was separated from the solids by decantation after biosorption. Unadsorbed metal ions were determined by flame AAS.

The amount of adsorbed metal ions was calculated from the difference of the concentration in aqueous solution before and after biosorption. The percent biosorption (%) were calculated using the following equations:

$$\text{Biosorption (\%)} = \frac{C_i - C_e}{C_i} \text{x100}$$

where C_i and C_e are the concentrations of the metal ion in initial and final solutions respectively. All experiments were always performed in duplicates. ±5% was the limit of experimental error of each duplicate. The bioremoval efficiencies of biomasses for metals ions are investigated by cadmium (Cd), chromium (Cr), and lead (Pb). Uptakes of Cd, Cr and Pb ions were recorded as 65±2%, 54±5% and 90±4%, respectively. The bioremoval efficiency of biocomposite for lead ions is higher than other metal ions.

It is necessary to understand the mechanism of biosorption to clarify the process. The uptake of the metal ion by biomaterials is a complicated physico-chemical process. Absorption, adsorption, ion exchange, surface complexation and precipitation are the potential biosorption mechanisms. The uptake of the metal ions by biocomposite mainly takes place in passive mode which is independent of energy, mainly through chemical functional groups of the material.

The FT-IR and SEM analysis indicated that metal ions mainly adsorbed on the binding sites of surface of biosorbents. It contains lots of organic groups. The potential binding groups of biomposite are carboxylates, amines, imidazoles, phosphates, sulfhydryls, sulfates, and hydroxyls. Magnetite has not taken an active role in the process. The biocomposite combining magnetic separation by magnetite are one of the most promising technologies. These adsorbents provide an efficient, fast and economical method for separation and remediation studies. Mass of wastewater can be disposed in a short time without producing further contaminants by this technique.

Conclusion

Abundantly available local and natural materials have much potential as a biosorbent material for the removal and recovery of heavy metals ions. When metal intake capacities are compared, prepared biocomposite has great attention to lead with 90% percent removal rate. The results of the biosorption studies show biocomposite is viable sorbent material for application in the treatment of water.

Biosorption of heavy metals occurs as a result of ionic interactions between metal ions and functional groups such as carboxyl (-COOH), hydroxide (-OH) and amide ($-NH_2$) associated with the polysaccharides of the biocomposite surface. Morphological analysis is indicated that high surface area and pore volume that provided higher capacity for the metal ion biosorption. Metal ions can penetrate easily to these pores and channels.
Biosorption capacities of biosorbents are comparable with many other adsorbents and biosorbents in the literature. The *Pisum Sativum* based magnetic biocomposite appeared to be an effective and alternative technique for the removal and recovery of heavy metals ions.

Acknowledgement

The authors would like to thank the Scientific Research Projects (SRP) Coordination Unit of Pamukkale University for financially supporting this research and conference with project number 2018 KKP181(2018KRM002).

References

Aftab, K., Akhtar, K., Jabbar, A., Bukhari, I. H., Noreen, R. (2013). Physico-chemical study for zinc removal and recovery onto native/chemically modified *Aspergillusflavus* NA9 from industrial effluent, Water Research, 47, 13, 4238-4246.

Aytaş, Ş., Sezer, H., Gök, C. (2016). Characterization of *Cystoseira sp*. for the isolation of Uranium. Analytical Letters, 49 (4), 523-540.

Baig, J.A., Kazi T.G., Elci, L. (2012). Biosorption characteristics of indigenous plant material for trivalent arsenic removal from groundwater: equilibrium and kinetic studies.Separation Science and Technology, 47(7), 1044-1054.

Basha, S., Jha, B. (2008). Estimation of isotherm parameters for biosorption of Cd(II) and Pb(II) onto brown seaweed, *Lobophorawariegata*, Journal of Chemical & Engineering Data, 53, 449-455.

Oliveira, R.C., Jouannin, C., Guibal, E., Garcia, Jr. O. (2011). Samarium(III) and raseodymium(III) biosorption on Sargassum sp.: Batch study. Process Biochemistry, 46, 3, 736-744.

Sağ, Y. (2001). Biosorption of heavy metals by fungal biomass and modeling of fungal biosorption: a review. Separation and Purification Methods, 30 (1), 1-48.

Salman, H. A., Ibrahim, M. I., Tarek M. M., Abbas H. S. (2014). Biosorption of Heavy Metals: A Review, Journal of Chemical Science and Technology, 3, 4, 74-102.

Wang, J.L. and Chen, C. (2009). Biosorbents for heavy metals removal and their future a review. Biotechnology Advances, 27, 195-226.

International Conference on Science and Technology

ICONST 2018

5-9 September 2018 Prizren - KOSOVO

Road Pavement Management System for Economic Sustainability of Road Transport: YTU Davutpaşa example / Karayolu Taşımacılığının Ekonomik Sürdürülebilirliği için Üstyapı Yönetim Sistemi: YTÜ Davutpaşa Örneği

Betül Değer Şitilbay[1]*, Gökçe Aydın[2]

Özet: İnsanların ulaşım ihtiyaçlarını karşılamak, hizmet sağlayıcılarının öncelikli sorumlulukları arasında yer almaktadır. Ulaştırma sektörü de bu ihtiyaçları karşılamak için gerekli olan yapıdır. Sahip olunan gelişmiş yol ağları ise bu sektöre yapılan büyük yatırımlar ve harcanan büyük kaynaklar sonucunda elde edilmektedir. Bu nedenle, bu alanda yapılan her yenilikçi çalışmanın ve verimlilik adına sağlanan her katkının aynı zamanda ülke ekonomisine de büyük fayda sağlayacağını söylemek mümkündür. Ulaştırma yatırımları hep büyük harcamalar gerektirmiştir ve bu şekilde olmaya devam edecektir. Özellikle mevcut yolların sürekli harcama gerektiren ihtiyaçlarının olduğu bir gerçektir. Bu nedenle, yolların mevcut durumlarının detaylı bir şekilde analiz edilebilmesi ve yapılan bu analizlerin de doğru ve hızlı bir şekilde değerlendirilmesiyle birlikte en uygun 'Yol Üstyapı Yönetim Sistemi"nin oluşturulması önem kazanmaktadır. Yol üstyapı yönetim sistemiyle sağlanması beklenen faydalar arasında, kullanımda olan yolların, hizmet düzeyi açısından sürdürülebilirliklerinin daha düşük bir maliyet ile sağlanması ve beraberinde kaynak tüketiminin minimize edilmesi sayesinde yeni yatırımların önünün açılması da sayılabilir. Yollar hizmete ilk açıldıklarında, üstyapıları, kusursuz olmamakla birlikte, çok yüksek bir performansa sahiptir. Ancak zaman içerisinde çeşitli sebeplerle bu performanslarda azalmalar meydana gelmektedir. Bu sebeplerden bazıları; çevresel koşullar, trafik yükleri ve malzeme özellikleri olarak sayılabilir. Ancak, mevcut üstyapının ömrünü uzatmak mümkündür. Bunun için, öncelikle, geniş kapsamlı olarak hazırlanan bir üstyapı yönetim sistemine ihtiyaç vardır. Çünkü iyi bir üstyapı yönetim sistemi sayesinde doğru zamanda doğru bakım yöntemleri uygulanabilmekte ve üstyapı performansları arttırılabilmektedir.

Bu çalışma kapsamında üstyapı yönetim sistemine ilişkin örnek bir uygulama gerçekleştirilmiştir. Bu uygulama için, belirlenen bir yol ağında saha incelemeleri yapılarak bozulma tipleri belirlenmiştir. Elde edilen verilerden yararlanılarak, üstyapının mevcut durumu belirlendikten sonra performans yönetiminin yapılabilmesi için gerekli bozulma tahminleri gerçekleştirilmiştir. Seçilen örnek ağ, Yıldız Teknik Üniversitesi Davutpaşa Kampüsü sınırları içinde bulunan bir yol ağıdır. Bu yol ağına ait üstyapı durumunun belirlenmesi çalışmalarında, yerinde gözlem ve ölçümlerle elde edilen veriler kullanılarak, ağın çeşitli kısımları için PCR (Pavement Condition Rating) derecelendirilmesi yapılmıştır. Daha sonra, mevcut durumdaki bozulmaların zaman içerisinde ilerleyişinin belirlenmesi için bir tahmin modeli kullanılmıştır. Elde edilen sonuçlar, kampüs içerisinde yoğun olarak kullanılan bu yol ağının belirli kesimlerinde mevcut durumun zaman içerisinde kötüleşerek bakım gerektireceğini göstermektedir. Bu uygulamalı örnekte görülebileceği gibi, iyi bir üst yapı yönetim sisteminin gerekli aşamalarının geleceğe yönelik olarak

[1]Yıldız Technical University, Faculty of Engineering, 34220, İstanbul, TURKEY
[2]Aksaray University, Faculty of Engineering, 32260, Aksaray, TURKEY
*Correspondingauthor: gokceaydin@aksaray.edu.tr

değerlendirilmesi mümkün olmaktadır. Çalışma sonucunda, seçilen bu yol ağının, üniversite kampüsüne ait olması ve dolayısıyla yaya öncelikli olması ve düşük hızlarda araç seyirlerine maruz kalmasına rağmen, özellikle iklimsel koşulların etkisiyle üstyapı performansının olumsuz etkilendiği ve zamanla kötüleştiği belirlenmiştir.

Anahtar Kelimeler: Yol kaplamaları, yol üstyapıları, bakım ve onarım, yol üstyapı yönetim sistemi

Abstract: Meeting the transportation needs of communities is among the principal responsibilities of the service providers. Highly developed national road networks are formed by huge investments with a huge resource consumption. Therefore, it is possible to say that, any innovative study for improving a national road network's efficiency will also be beneficial for the national economy. Transportation structures always demanded big investments and it will be so in the future. Especially, it is an undeniable fact that, existing roads have needs that force continuous expenditures. Therefore, it becomes important to analyze the current situation of the existing roads and development of the "Road Pavement Management System" (RPMS) by the accurate and rapid evaluation of those analyses. Among the benefits expected from the application of RPMS is provision of sustainability of the service level of road pavement with a lower cost (therefore minimized resource consumption) and thus creating budget for new investments.

The performance of a road pavement just after it is put into service is, although not excellent, very high. However, performance deteriorates over time for several reasons, such as traffic loads, ambient conditions and material properties. Fortunately, it is possible to extend the life of the pavement. To achieve this, an extensive pavement management system is needed. Because, by means of a good pavement management system, correct maintenance methods can be applied at the correct time and thus pavement performance can be enhanced.

This study contains an example application of a RPMS. In the selected road network, which lies within the Yıldız Technical University Davutpaşa Campus, field studies were performed and types of deteriorations were determined. The current situation of the pavement were specified by using the data obtained and estimations for future deteriorations were done. Using the data obtained by in - situ observations and measurements, comprehensive PCR (Pavement Condition Rating) scales were formed for the network. Afterwards, an estimation model was used for the future progress of the deteriorations. Results indicate that, some parts of the network, which have a high traffic load will continue to deteriorate over time and will need maintenance. Thanks to this practical example, it is possible to evaluate the stages of a RPMS. As the result of the study, it was determined that, although this network is one with pedestrian priority and low vehicle speeds, its performance is adversely affected by climatic conditions.

Keywords: Road pavement, maintenance, road pavement management system

Giriş

Günümüzün zorunlu ihtiyaçlarından biri olan ulaşım, modern dünyanın yeniliklerinin de gerektirdiği şekilde günden güne önemini arttırmaktadır. Bu durum, ulaşım sektörünün her alanına farklı biçimlerde yansımaktadır. Özellikle, trafik sorunları, kirlilik ve gürültü problemleri, güvenlik ve konfor koşullarının iyileştirilmesi ihtiyacı ve kaynak tüketiminin azaltılması gerekliliği (geri dönüştürülebilir kaynak tüketimi) gibi konular öne çıkmaktadır. Yollardaki bu gibi problemlerin çözümü ise büyük maliyetler gerektirmektedir. Bu nedenle, yol uygulamalarında maliyeti azaltmaya yönelik çalışmalar yürütülmesi oldukça anlamlıdır.
Yol uygulamalarında, yüksek maliyetlere sebep olan bir etken de üstyapı çalışmalarıdır. Üstyapılar, sadece ilk yapım aşamasına ait harcamaları gerektirmekle kalmayıp, zaman içerisinde çeşitli sebeplerle meydana gelen bozulmaların giderilmesi için de bakım ve onarım gerektirdiği için ilave büyük maliyetlere ihtiyaç duymaktadır.

20 yıllık bir hizmet ömrüne sahip olması için tasarlanmış bir üstyapının, bakım ve onarım yapılmadan ancak 10-12 yıl (bazen daha da az) arasında istenen performans, konfor ve güvenlik şartlarında hizmet verebildiği

belirtilmektedir (Haas vd., 1994). Servis ömrü boyunca bir yoldan beklenen performansın sağlanması ve korunması için planlı ve programlı bir şekilde bakım-onarım çalışmaları yapılmak zorundadır.
Üstyapı yönetimi, ilk yapıldığında yüksek bir performansa sahip olan yolun, gerek trafik, gerekse iklim koşullarından dolayı performansının düşmesini geciktirmek ve böylece üstyapının ömrünü uzatmak için yapılacak olan bakım ve onarım işlemlerinin planlı ve programlı olarak uygulanması anlamına gelmektedir. İyi bir üstyapı yönetim sistemi aşağıda listelenen öğeleri içermelidir (Kırbaş, 2007):

- Planlama
- Programlama
- Tasarım
- Yapım
- Bakım
- Onarım
- Yenileme

Üstyapı yönetimi kavramı, ilk olarak 1960'lı yıllarda, mevcut kaynakların en uygun biçimde değerlendirilebilmesi amacıyla ortaya atılmıştır. İlk başlarda göz ile yapılan değerlendirmeler, daha sonra yerini tahribatlı deneylere bırakmıştır. Üstyapı bozulmalarını ve taşıma kapasitesini belirlemek amacıyla yapılan bu deneylerin verdiği zararlar ve uygulama zorlukları ise tahribatsız deney uygulamalarının geliştirilmesini sağlamıştır.

"Yol Üstyapı Yönetim Sistemi" terimi, ilk defa 1960'ların sonu ile 1970'lerin başlarında kullanılmaya başlanmış ve geliştirilmiştir. Geliştirilen ilk sistemlerden en büyük ölçekli olanının "Project 123" adıyla Teksas Yollar İdaresi (Texas Highway Department), Teksas A&M Üniversitesi (Texas A&M University) ve Teksas Üniversitesi'nin (University of Texas) ortaklaşa çalıştığı ve yönettiği sistem olduğu belirtilmektedir (Kırbaş, 2007). Günümüzde ise, yol üstyapı yönetim sisteminde kullanılan iki önemli bozulma etüdü olarak PAVER ve MTCO (Municipal Transportation Commission of Ontario) verilebilir. Shahin ve Becker, 1984 yılında PAVER sisteminin kullandığı üstyapı durum indeksi (PCI) adında bir model geliştirmişlerdir.
Abaza vd. (2004) yaptıkları bir çalışmada, Markov tahmin modeli ile entegre edilmiş bir üstyapı yönetim sisteminin, yol bakım ve onarım çalışmalarındaki karar verme süreçlerine olan etkilerini araştırmıştır. Sonuçlar, geliştirilen modelin bakım ve onarım kararlarının verilmesinde optimum koşulların sağlanabilmesine olanak sağladığını göstermektedir.

Cline vd. (2003), yaptıkları çalışmada, üstyapı mühendislerinin yol bozulmalarını belirlemek için yaptıkları ölçüm ve görsel değerlendirmelerden elde edilen verilerin bilgisayar teknolojileriyle işlenebilirliğini ve PAVER sisteminde kullanılan PCI değerini belirlemek için uygunluğunu araştırmıştır. Çalışmanın sonucunda her iki yöntemle elde edilen PCI verilerinin benzer sonuçları verdiği saptanmıştır.

Bandara ve Gunaratne (2001) tarafından geliştirilen bir modelde, bulanık mantık yöntemi kullanılarak, Sri Lanka yol ağına ait kesimlerin mevcut üstyapı durumlarına göre bakım öncelikleri belirlenmiştir. Elde edilen bu sonuçlarla, geliştirilen modelin Markov tahmin yöntemi ile entegre edilmesi durumuna ait sonuçlar karşılaştırılmıştır.

Karim vd. (2016) yaptıkları bir çalışmada, Yemen'in ticari başkenti olan Aden şehrini kuzey bölgesinde yer alan diğer büyük şehirler ile bağlayan yol ağına ait bakım ve rehabilitasyon çalışmalarının değerlendirilmesi ve önerilmesi amacıyla bir üstyapı durum analizi gerçekleştirmiştir. Çalışmada, (Pavement Condition Index) PCI'ye dayanarak hazırlanan Teknik El Kitabı TM 5-623'dan yararlanılarak, PAVER ™ (1982) sistemi ile üstyapı analizi yapılmıştır. Çalışma sonuçlarından faydanılarak, Yemen için yük taşımacılığı ve seyahat açısından çok fazla kullanılan bu yolun, bakım ve rehabilitasyon durumu analiz değerlendirilmiştir.
Terzi (2004), bulanık mantık yöntemini kullanarak, sathi kaplamalar ve asfalt betonu kaplamalar için hem üstyapıda oluşabilecek tüm bozulmaları, hem de bu bozulmalara neden olabilecek tüm etkenleri göz önüne alan hizmet düzeyi tahmin modelleri geliştirmiştir.

Bu çalışma kapsamında ise üstyapı yönetim sistemine ilişkin örnek bir uygulama gerçekleştirilmesi amaçlanmıştır. Bunun için öncelikle, Yıldız Teknik Üniversitesi Davutpaşa kampüsü sınırları içinde bulunan

bir yol ağı seçilmiştir. İnceleme yapılacak ağ seçimi için kampüs içi yol ağının en büyük trafik hacmini gören kesimi olma özelliği göz önünde bulundurulmuştur. Seçilen yol ağına ait üstyapı durumunun belirlenmesi için ise arazide/yerinde gözlem ve ölçümler yapılmıştır. Elde edilen bu ölçümlere ait veriler kullanılarak, ağın çeşitli kısımları için PCR (Pavement Condition Rating) derecelendirilmesi yapılmıştır. Daha sonra, mevcut durumdaki bozulmaların zaman içerisinde ilerleyişinin belirlenmesi için bir tahmin modeli kullanılmıştır.

Yöntem

Karayolu üstyapı yönetim sistemi çalışmalarında, belirli bir kesim için en uygun bakım yöntemine/zamanına karar verme ve uygulama işlemi, belirli veriler ışığında yapılmaktadır. Yol boyunca yapılan gözlem ve ölçümler karar vericiye en uygun çözüm yöntemini seçtirecek doğrultuda kolaylık sağlamaktadır. Üstyapı durumunun belirlenmesi çalışmasında, yerinde gözlem ve ölçümlerle elde edilen verilerin, ilgili hesap aşamalarından geçirilmesi ile, PCR derecelendirilmesinin yapılması amaçlanmaktadır. PCR derecesi aralıklarına göre üstyapıya ait performansı belirten sözel ifadeler Şekil 1'de yer almaktadır.

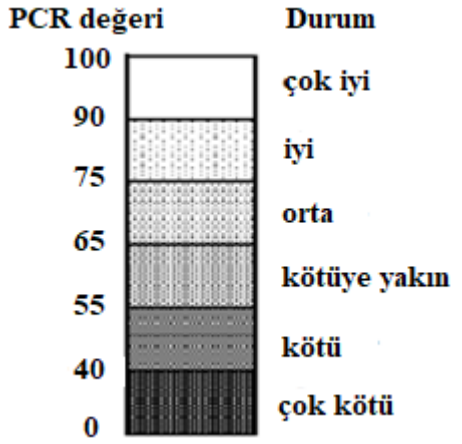

Şekil 1. PCR Göstergesi ve Derecelendirilmesi (Karaşahin, 2014)

Uygulama Örneği: YTÜ, Davutpaşa Kampüsü

Çalışma kapsamında seçilen yol ağı *İstanbul*, bölüm *Davutpaşa* ve kesim ise *Yıldız Teknik Üniversitesi Davutpaşa Kampüsü* İnşaat Fakültesi arkasından başlayan ve Elektrik-Elektronik Fakültesi binası önüne kadar olan yol olarak belirlenmiş, yol üstyapı mevcut durumu incelemesi yapılmıştır. Çalışılan yol kesimine ait uydu görüntüsü Şekil 2'de yer almaktadır.

Şekil 2. Çalışılan Yol Kesimi (Uydu Görüntüsü)

Üstyapı bilgisi edinilmek istenen yol, benzer bozulma cinsleri ve yol karakteristikleri (kavşak giriş ve çıkışları, diğer yollarla bağlantı noktaları) dikkate alınarak kesimlere ayrılmıştır (Şekil 3). Toplam 15 adet kesim (2x1 şeritli) bulunmaktadır. Seçilen yol ağının başlangıç noktası (yol kilometresinin 0+000 olduğu nokta)Şekil 3'te gösterildiği gibi kabul edilmiştir. Kesimlere ait platform genişliği ise 14,5 m'dir.

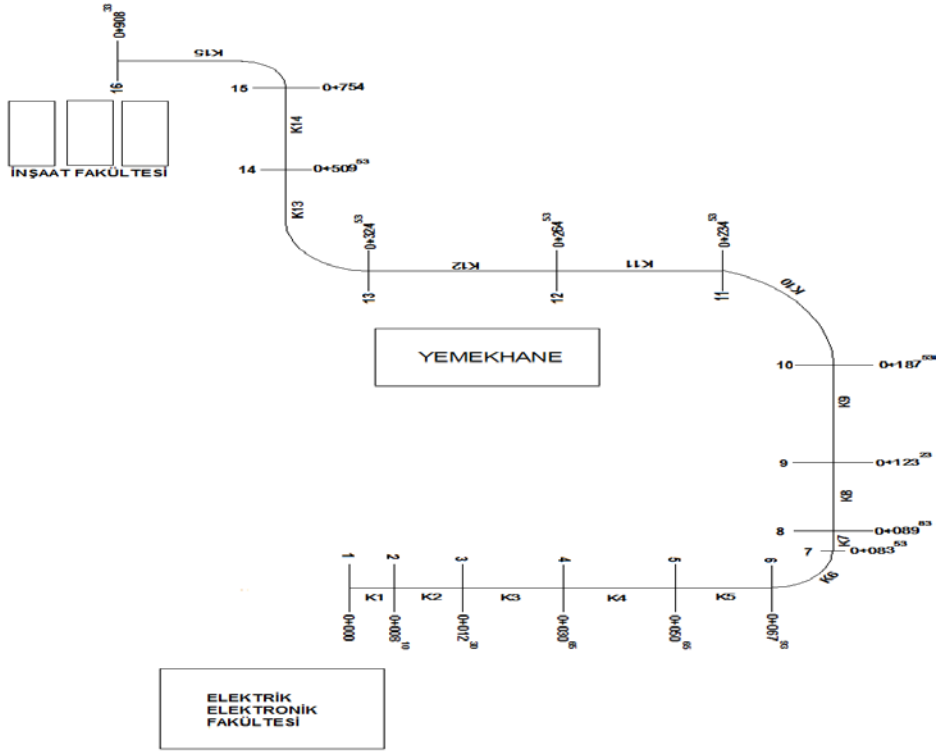

Şekil 3. Çalışılan yol ağı ve kesimler

Her bir kesime ait bozulma cinsleri ve miktarları gözle muayene ve ölçüm teknikleri kullanılarak belirlenmiştir. Karşılaşılan bozulma tiplerine ait örnekler Şekil 4'te yer almaktadır.

Şekil 4. Kesimlere ait bozulma örnekleri

PCR değerinin belirlenmesi

Yerinde gözlem ve ölçümlerle her bir bozulma tipinin ağırlığının, şiddetinin ve yoğunluğunun tespit edilmesinin ardından, yine her bir bozulma tipi için ayrı ayrı azaltma faktörü değerleri belirlenmiştir. Bunun için Tablo 1'den yararlanılmıştır. Burada yapılan işlem şu şekilde özetlenebilir;

Bozulma tiplerine ait ağırlık değerleri birbirinden farklı olduğu gibi, bozulmanın şiddeti ve yoğunluğu da farklı seviyelerde olabilmektedir. Bu nedenle, öncelikle kesimlere ait bozulma tipleri belirlenerek, gruplandırılmaktadır. Daha sonra ilgili kesime ait bozulma grubunda yer alan her bir bozulma tipi için Tablo 1'de yer alan ağırlık değerleri, şiddet ve yoğunluk derecesine ait katsayılarla çarpılarak ilgili kesimin azaltma faktörü olarak belirlenmektedir. Şiddet derecesinin göstergesi olan katsayının seçimi, sahada bozulma miktarının ölçülmesi (m^2 veya uzunluk cinsinden bozulma miktarı) neticesinde yapılır. Bozulma şiddeti, sırasıyla "az", "orta" veya "çok" olarak isimlendirilerek, her birine denk gelen toplam üç adet katsayıdan birinin seçilmesi şeklinde elde edilir. Yoğunluk derecelendirmesine ait katsayının seçimi ise göz ile muayene sonucunda yapılır. İlgili katsayı seçiminde, benzer şekilde, üç adet sözel ifade yer almaktadır. Bunlar; "nadir", "sık" veya "aşırı" olarak isimlendirilir. Bu sözel ifadelerden seçilen derecelendirmeye karşılık gelen yoğunluk katsayısı da, Tablo 1'den faydanılarak elde edilir. Son olarak, ağırlık değeri, şiddet katsayısı ve yoğunluk katsayısı çarpılarak, ilgili kesime ait bozulma grubunda yer alan her bir bozulma tipi için ayrı ayrı azaltma faktörü hesaplanmış olur.

Tablo 1. PCR değeri belirleme kriterleri (Karaşahin, 2014)

Bozulma Tipi	Bozulma ağırlığı	Şiddeti	Yoğunluğu	Toplam
sökülme	10	.3 .6 1	.5 .8 1	---------
kusma	5	.8 .8 1	.6 .9 1	---------
oluklanma	5	.4 .8 1	.5 .8 1	---------
timsah sırtı çatlak	10	.3 .7 1	.6 .8 1	---------
çukur/ayrılma	10	.4 .7 1	.5 .8 1	---------
yama	5	.3 .6 1	.6 .8 1	---------
çökme	10	.5 .7 1	.5 .8 1	---------
çatlak kaplama kusuru	5	1 1 1	.5 .8 1	---------
tekerlek izi	15	.4 .7 1	.5 .7 1	---------
boyuna derz çatlağı	5	.4 .7 1	.5 .7 1	---------
boyuna çatlak	5	.2 .6 1	.4 .8 1	---------
köşe çatlağı	5	.4 .7 1	.5 .7 1	---------
rastgele çatlak	5	.4 .7 1	.5 .7 1	---------
blok/enine çatlak	10	.4 .7 1	.5 .7 1	---------
enine çatlak	15	.4 .7 1	.5 .8 1	---------
pompalama	15	.7 .7 1	.3 .7 1	---------
faylanma	10	.4 .7 1	.5 .8 1	---------
yüzey bozulması	10	.4 .7 1	.6 .8 1	---------
Toplam bozulma				---------
100 - Toplam Bozulma = PCR				---------

Her kesimde, her bir bozulma tipi için belirlenen azaltma faktörlerinin toplamı alınarak, söz konusu kesim için toplam azaltma faktörü değerleri hesaplanmıştır.
PCR = 100 – Σ azaltma faktörleri
Azaltma Faktörü = ağırlık x şiddet x yoğunluk (bozulma tipine ve miktarına bağlı)
Örnek Kesim 1 için ; PCR = 100 – (5 x 1 x 0,8) – (10 x 0,7 x 0,8) = 90,4 çok iyi olarak bulunmuştur.

Bulgular

Çalışma kapsamında söz konusu tüm kesimlere ait PCR değerleri Tablo 2'de görülmektedir. Seçilen yol kesimlerinde, farklı bozulma tiplerinin yer alması sebebiyle, ölçülen PCR değerleri değişkenlik göstermektedir. Kesimlere ait elde edilen PCR değerleri genel olarak üstyapının iyi durumda olduğunu göstermekle birlikte, iki kesim için aynı durum söz konusu olamamaktadır. Bunlardan biri, "Kesim 12"'dir. Bu kesim için hesaplanan PCR değerinin 59,1 olması, üstyapı durum derecelendirmesindeki sözel ifade olarak "kötüye yakın" bölgesinde yer almaktadır. Bir diğeri ise, "Kesim 15'tir. Bu kesimde hesaplanan PCR değeri ise 30,6'dır. Bu değer, üstyapı durum derecelendirmesinde "çok kötü" durumda olan bölgeyi işaretlemektedir. Kesimlerdeki bu farklılıkların, üstyapıda meydana gelen bozulma tiplerinin farklı olmasından ve dolayısıyla hem bozulma cinsinin PCR değeri hesaplamadaki etkisi (ağırlığı) hem de yoğunluk/şiddet oranlarının farklı olması gibi sebeplerden kaynaklandığı söylenebilmektedir.

Tablo 2 Kesimlere Ait PCR Değerlerinin Hesabı

Kesim Adı	Bozulma Tipi	Ağırlık	Şiddet		Yoğunluk		PCR =100-Σ(TA*Ş*Y)
Kesim 1	Yama Bozulması	5	Tİ > 12mm (çok)	1	Sık	0,8	90,4
	Oyuk	10	25mm<Derinlik<50mm	0,7	Sık	0,8	
Kesim 2	Yama Bozulması	5	Tİ > 12mm (çok)	1	Sık	0,8	91
	Boyuna Kırılma	5	ÇG >19 mm (40mm) (çok)	1	Aşırı	1	
Kesim 3	Yama Bozulması	5	Tİ > 12mm (çok)	1	Aşırı	1	88
	Oyuk	10	25mm<Derinlik<50mm	0,7	Aşırı	1	
Kesim 4	Yama Bozulması	5	Tİ > 12mm (çok)	1	Aşırı	1	94
	Boyuna Kırılma	5	ÇG<6 mm (5 mm) (az)	0,4	Nadir	0,5	
Kesim 5	Gözlenmedi	-	-	-	-	-	100
Kesim 6	Blok Kırılma	10	Çok	1	Aşırı	1	75
	Enine Çatlak	15	ÇG >19 mm (60mm) (çok)	1	Aşırı	1	
Kesim 7	Yorulma Çatlağı	10	Çok(3 adet)	1	Aşırı	1	70
Kesim 8	Çukur	10	ÇD>50 mm (60 mm) (çok)	1	Aşırı	1	90
Kesim 9	Çukur	10	ÇD>50 mm (60 mm) (çok)	1	Aşırı	1	70
Kesim 10	Yama Bozulması	5	Tİ <6mm (az)	0,3	Nadir	0,6	79,1
	Çukur	10	ÇD>50 mm (60 mm) (çok)	1	Aşırı	1	
Kesim 11	Enine Çatlak	15	ÇG >19 mm (60mm) (çok)	1	Aşırı	1	71,5
	Boyuna Kırılma	5	ÇG >19 mm (40mm) (çok)	1	Sık	0,7	
	Yorulma Çatlağı	10	Çok	1	Aşırı	1	
Kesim 12	Enine Çatlak	15	ÇG >19 mm (60mm) (çok)	1	Aşırı	1	59,1
	Boyuna Kırılma	5	ÇG<6 mm (5 mm) (az)	0,4	Nadir	0,5	
	Yorulma Çatlağı	10	Çok	1	Aşırı	1	
	Çukur	10	ÇD? 25 mm (25 mm) (orta)	0,7	Aşırı	1	
	Yama Bozulması	5	Tİ <6mm (az)	0,3	Nadir	0,6	
Kesim 13	Gözlenmedi	-	-	-	-	-	100
Kesim 14	Yüzey Bozulması	10	Az	0,4	Nadir	0,6	84,6
	Çukur	10	ÇD? 50 mm (50 mm) (çok)	1	Aşırı	1	
	Sökülme	10	Orta	0,6	Nadir	0,5	
Kesim 15	Yorulma Çatlağı	10	Çok	1	Aşırı	1	30,6
	Çukur	10	ÇD? 50 mm (50 mm) (çok)	1	Aşırı	1	
	Yama Bozulması	5	Tİ > 12mm (çok)	1	Sık	0,8	
	Yüzey Bozulması	10	Az	0,4	Nadir	0,6	
	Tekerlek İzi	15	6mm<Derinlik<12mm (az)	0,4	Nadir	0,5	

Yola Ait Performans Tahmin Modelinin Oluşturulması ve Değerlendirilmesi

Çalışmada, tüm kesimlere ait mevcut PCR değeri sonuçlarından yararlanarak, performans tahmini için 'Lineer Azalan Tahmin Modeli' kullanılmıştır. Modelin kullanım kolaylığı tercih sebebi olarak görülmektedir. Bu modelde iki ölçüm noktasından azalan bir doğru ile gelecekteki durum tahmin edilebilmektedir. Bu model oluşturulurken her kesim için ayrı ayrı uygulanmıştır ve genelleştirme yapılmamıştır. Modeli oluştururken, geçmişteki trafik yükleri ve bakım düzeylerinin gelecekte de değişmeyeceği varsayımı yapılmaktadır.

Model, şu andan sonraki her iki yılda bir, tüm kesimlerin PCR değerlerinin 40'ın altına düştüğü zamana kadar oluşturulmuştur. Her kesime ait PCR tahmin değerleri Tablo 3'te verilmiştir. Modeli gösteren grafik ise Şekil 5'te yer almaktadır.

Tablo 3. Tüm kesimlere ait PCR değeri tahminleri

Kesim No	İlk durum	Mevcut Durum	2 yıl sonra	4 yıl sonra	6 yıl sonra	8 yıl sonra	10 yıl sonra	12 yıl sonra	14 yıl sonra	16 yıl sonra	18 yıl sonra	20 yıl sonra
1	100	90,4	80,8	71,2	61,6	52	42,4	32,8	--	–	--	--
2	100	91	82	73	64	55	46	37	--	–	--	--
3	100	88	76	64	52	40	28	--	--	–	--	--
4	100	94	88	82	76	70	64	58	52	46	40	34
5	100	100	100	--	--	--	--	--	--	–	--	--
6	100	75	50	25	--	--	--	--	--	–	--	--
7	100	70	40	10	--	--	--	--	--	–	--	--
8	100	90	80	70	60	50	40	30	--	–	--	--
9	100	70	40	10	--	--	--	--	--	–	--	--
10	100	79,1	58,2	37,3	--	--	--	--	--	–	--	--
11	100	71,5	43	14,5	--	--	--	--	--	–	--	--
12	100	59,1	18,2	--	--	--	--	--	--	–	--	--
13	100	100	100	--	--	--	--	--	--	–	--	--
14	100	84,6	69,2	53,8	38,4	--	--	--	--	–	--	--
15	100	30,6		--	--	--	--	--	--	–	--	--

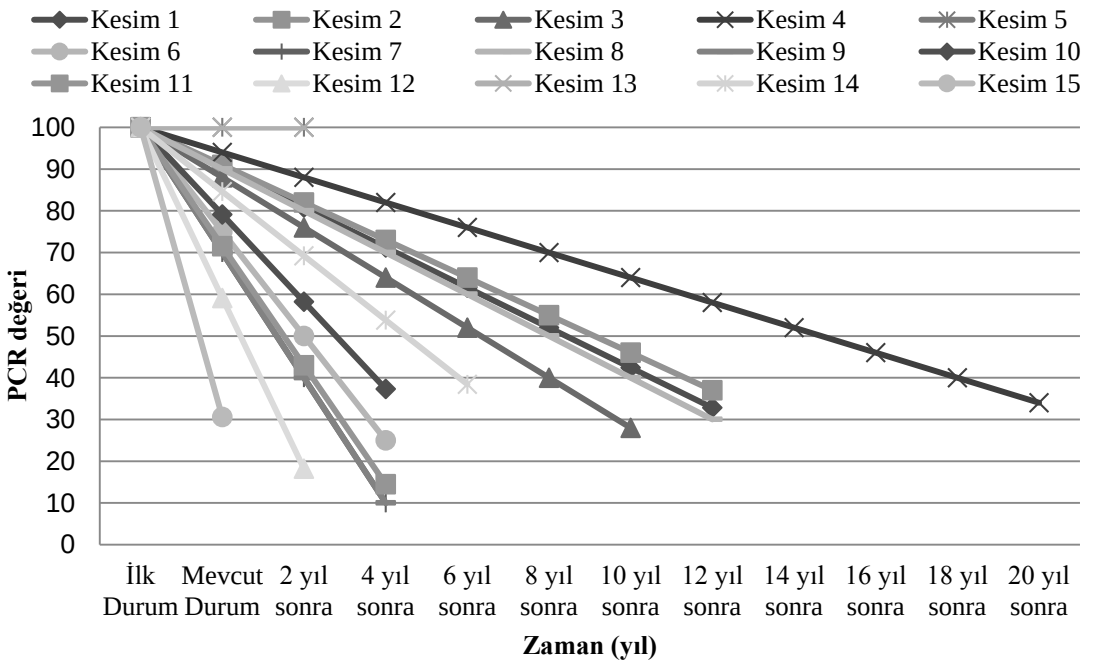

Şekil 5. Tahmin sonuçları

Modele ait tahmin sonuçları, mevcut durumda PCR değerleri 80'in üzerinde olan kesimlerin kısa vadede bakım gerektirmediğini, ancak, 70 - 80 aralığında PCR değerine sahip kesimler için ise 2-4 yıl aralığında, bakım-onarım çalışmasının gerekli olacağını göstermektedir. Mevcut durumda PCR değeri 60 ve altında değerlere sahip kesimlerin (kesim 12 ve kesim 15) ise kısa vadede bakımlarının yapılmaması durumunda trafik güvenliği için olumsuz koşullara sebebiyet verme olasılığının bulunduğu görülmektedir.

Yol kesiminin bütünü için PCR değerini hesaplamak için Formül 1'de yer alan ifade kullanılmaktadır (ilave örneklem kullanılmadığından ortalama PCR değeri bulunur):

$$\mathrm{PCR_S} = \frac{\mathrm{PCR_1}+\mathrm{PCR_2}+\cdots+\mathrm{PCR_N}}{\mathrm{N}} \qquad \text{(Formül 1)}$$

Burada, $\boldsymbol{PCR_S}$: Yol kesimi PCR değeri,
$\boldsymbol{PCR_1}$: Kesim 1'in PCR değeri,
$\boldsymbol{PCR_2}$**:** Kesim 2'nin PCR değeri,
$\boldsymbol{PCR_N}$**:** Son (*N'inci*) kesimin PCR değeri,
$\boldsymbol{N}$**:** Kesimdeki toplam kesim sayısı,

Buna göre bu çalışmadaki kesim için:

$$\boldsymbol{PCR_S} = \frac{PCR_1 + PCR_2 + \cdots \ldots\ldots\ldots\ldots + PCR_{14}}{N}$$
$$= \frac{90{,}4 + 91 + 88 + 94 + 100 + 75 + 70 + 90 + 70 + 79{,}1 + 71{,}5 + 59{,}1 + 100 + 84{,}6 + 30{,}6}{14}$$

$\boldsymbol{PCR} = 79{,}55 \cong 80 \Rightarrow$ Şekil 6'da yer alan bozulma seviyesi- üstyapı tamir yöntemi ilişkisine bakıldığında, çalışılan yol kesimine ait üstyapının durumu **iyi** olarak belirlenmektedir.

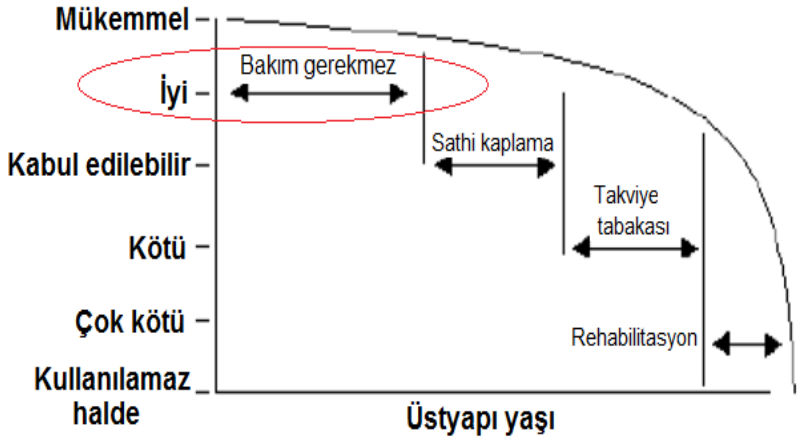

Şekil 6. Bozulma Seviyeleri – Üstyapı Tamir Yöntemi Grafiği (Karaşahin, 2014)

Tartışma ve Sonuçlar

PCR (Pavement Condition Rating) derecelendirmesi yöntemi, yol yüzeyinin performansını belirlemek ve bakım-rehabilitasyon ihtiyaçlarını tespit etmek için kullanılabilen basit ve düşük maliyetli bir uygulamadır. Bu yöntem sayesinde, yol bakım ve oranımı için gerekli olan bütçe, planlı olarak ve maksimum fayda sağlayacak şekilde kullanılabilmektedir.

Çalışma kapsamında üstyapı yönetim sistemine ilişkin örnek bir uygulama gerçekleştirilmiştir. Bunun için, belirlenen bir yol ağında saha incelemeleri yapılarak bozulma tipleri belirlenmiştir. Elde edilen verilerden

yararlanılarak, üstyapının mevcut durumu belirlendikten sonra performans yönetiminin yapılabilmesi için gerekli bozulma tahminleri gerçekleştirilmiştir.
Elde edilen sonuçlar, kampüs içerisinde yoğun olarak kullanılan bu yol ağının belirli kesimlerinde mevcut durumun zaman içerisinde kötüleşerek bakım gerektireceğini göstermektedir. Bu uygulamalı örnekte görülebileceği gibi, iyi bir üst yapı yönetim sisteminin gerekli aşamalarının geleceğe yönelik olarak değerlendirilmesi mümkün olmaktadır. Çalışma sonucunda, seçilen bu yol ağının, üniversite kampüsüne ait olması ve dolayısıyla yaya öncelikli olması ve düşük hızlarda araç seyirlerine maruz kalmasına rağmen, özellikle iklimsel koşulların etkisiyle performansının olumsuz etkilendiği ve zamanla kötüleştiği belirlenmiştir.

Yolun mevcut üstyapı durumuna ait PCR değerlerine göre hesaplanan tahmini PCR değerleri ışığında, kesimlerin ayrı ayrı değerlendirilmesi de mümkündür. Buna göre;

- PCR değerlerine bakılarak "iyi" durumda olduğu belirlenen kesimlerden, Kesim 1, Kesim 2, Kesim 4, Kesim 5 ve Kesim 13 için, bakım gerekmediğini ancak, çatlak dolgusu ile mevcut az problemli kesimlerin kolaylıkla iyileştirilebileceği söylenebilir.
- PCR değerlerine bakılarak "kabul edilebilir" durumda olduğu belirlenen kesimlerden, Kesim 3, Kesim 8, Kesim 10 ve Kesim 14 için, ince takviye tabakası uygulanabileceği görülmüştür.
- Yine PCR değerlerine bakılarak "orta- kötü" durumda olduğu belirlenen kesimlerden, Kesim 6, Kesim 7, Kesim 9 ve Kesim 11 için, kalın takviye tabakası gerekmektedir.
- Son olarak, PCR değerlerine bakılarak "çok kötü" durumda olduğu belirlenen kesimler olan, Kesim 12 ve Kesim 15 için iyileştirme gereksinimi bulunmaktadır.

Çalışmanın ilerleyen aşamalarında, kampüsün yoğun olarak kullanılan diğer kesimlerini de kapsayan, daha geniş içerikli bir saha çalışmasının yapılması planlanmaktadır. Böylelikle, yapılan tahminlerin gerçekleşme durumları analiz edilebilirken, yapılan bakım çalışmları ve bunların zamanlamalarının etkisiyle üstyapı performansında meydana gelecek iyileşmeler de belirlenebilecektir. Planlanan geniş kapsamlı gelecek çalışmalarda, kampüs yollarına ait üstyapı yönetim planlamasına ilişkin önerilerin yapılmasının oldukça anlamlı olacağı düşünülmektedir.

Kaynaklar

Abaza, K. A., Ashur, S. A., Al-Khatib, I.A. (2004). Integrated Pavement Management System with a Markovian Prediction Model. Journal of Transportation Engineering, 130(1): 24-33.

Bandara, N. ve Gunaratne, M., (2001). Current and Future Pavement Maintenance Priorization Based on Rapid Visual Condition Evaluation. Journal of Transportation Engineering, 127(2):116-123.

Cline, D. G., Shahin, M. Y., Burkhalter, J. A., (2003). Automated Data Collection for Pavement Condition Index Survey. Transportation Research Board, Annual Meeting CD-ROM.

Haas, R., Hudson, W. R., Zaniewski, J. (1994). Modern Pavement Management, Krieger Publishing Company, Florida.

Karaşahin, M. (2014). Yol Üstyapı Yönetim Sistemleri Ders Notları, İnşaat Mühendisliği Doktora programı, İstanbul Üniversitesi.

Karim, F. M.A., Rubasi, K.A.H., Saleh, A.A. (2016). The Road Pavement Condition Index (PCI) Evaluation and Maintenance: A Case Study of Yemen. Organization, Technology and Management in Construction, 8: 1446-1455.

Kırbaş, U. (2007). Üstyapı Yönetim Sistemi ve Beşiktaş İlçesi Örneğinde Uygulama Olanaklarının Araştırılması. Yüksek Lisans Tezi, Yıldız Teknik Üniversitesi FBE, İstanbul.

Terzi, S. (2004). Coğrafi Bilgi Sistemi Yardımıyla Karayolu Üstyapı Bakım Yönetim Modeli Geliştirilmesi. Doktora Tezi, SDÜ Fen Bilimleri Enstitüsü.

International Conference on Science and Technology

ICONST 2018

5-9 September 2018 Prizren - KOSOVO

Analysis of NH_3-H_2O Absorption Systems Using Data Mining Process

Ecir Uğur Küçüksille[1], Arzu Şencan Şahin[2], Önder Kızılkan[2*]

Abstract: In this paper, as a new approach, thermodynamic analysis with data mining process of ammonia-water absorption refrigeration systems (ARS) was carried out. Performance analysis of the ARS is very complex because of analytic functions used for calculating the properties of fluid couples and simulation programs. Therefore, it is extremely difficult to perform analysis of this system. It is well known that the generator temperature, evaporator temperature, condenser temperature, absorber temperature, weak and strong solution concentration affect the ARS's coefficient of performance (COP) and circulation ratio (f). In present study, Linear Regression and M5'Rules models are applied within Data Mining Process for determining variation of COP and f values related to system temperatures. Furthermore, variations of COP and f values were graphed depending on different system parameters.

Keywords: Data mining, Ammonia-water, Absorption system, COP, Performance analysis

Introduction

ARS is technology based on extensive development and experience in the early years of the refrigeration industry, in particular for ice production. From the beginning, its development has been linked to periods of high energy prices. In the last years, nevertheless, there has been a great resurgence of interest in this technology not only because of the rise in the energy prices but mainly due to the social and scientific awareness about the environmental degradation. Contrary to compression refrigeration machines, which need high quality electric energy to run, ammonia-water absorption refrigeration machines use low quality thermal energy. Moreover, as the temperature of the heat source does not usually need to be so high (80-150 °C), the wasted heat in many processes can be used to power absorption refrigeration machines. In addition, the AWRS use natural substances, which do not cause ozone depletion as working fluids. For all these reasons, this technology has been classified as environmentally friendly (Herold, et al., 1996; Alefeld and Radermacher, 1994)

Theoretical and experimental works on the performance characteristics and thermodynamic analysis of ARSs are available in the literature (Fernandez and Vazquez M, 2001; Francisco, et al., 2002; Ghaddar, et al., 1997; Chen and Schouten, 1998; Chow, et al., 2002; Wu and Eames, 2000; Sun, 1998; Xu and Dai, 1997; Jelinek, et al., 2002). Theoretical performance analysis of the ARS is complex due to the equations of thermodynamic properties of working fluid and simulation programs. In this study, in order to simplify performance analysis of the ARS, data mining process was used. Linear Regression and M5'Rules models are applied within Data Mining Process for determining variation of COP and f values related to system temperatures. The best result was obtained by using M5'Rules Model. Furthermore, variations of COP and f values were graphed depending on different system parameters.

[1]Suleyman Demirel University, Faculty of Engineering, Department of Computer Engineering, 32260, Isparta, TURKEY
[2]Isparta University of Applied Sciences, Faculty of Technology, Department of Energy Systems Engineering, 32260, Isparta, TURKEY
*Corresponding author: onderkizilkan@isparta.edu.tr

Theoretical Analysis

The single-stage ammonia-water ARS cycle consists of four main components, namely the condenser, evaporator, absorber and generator, as shown in Figure 1.Other auxiliary components include the expansion valves, pump, rectifier and heat exchanger. Low pressure, weak solution from the absorber is pumped through the solution heat exchanger to the generator operating at a high pressure. The generator separates the binary solution of water and ammonia by causing the ammonia to vaporize, and the rectifier purifies the ammonia vapor. High pressure ammonia gas is passed through the expansion valve to the evaporator as low pressure liquid ammonia. The high pressure transport fluid, water, from the generator is returned to the absorber through the solution heat exchanger and the expansion valve. The low pressure liquid ammonia in the evaporator is used to cool the space to be refrigerated. During the cooling process, the liquid ammonia vaporizes and the transport fluid, water, absorbs the vapor to form a weak ammonia solution in the absorber (Herold et al., 1996; ASHRAE, 1997).

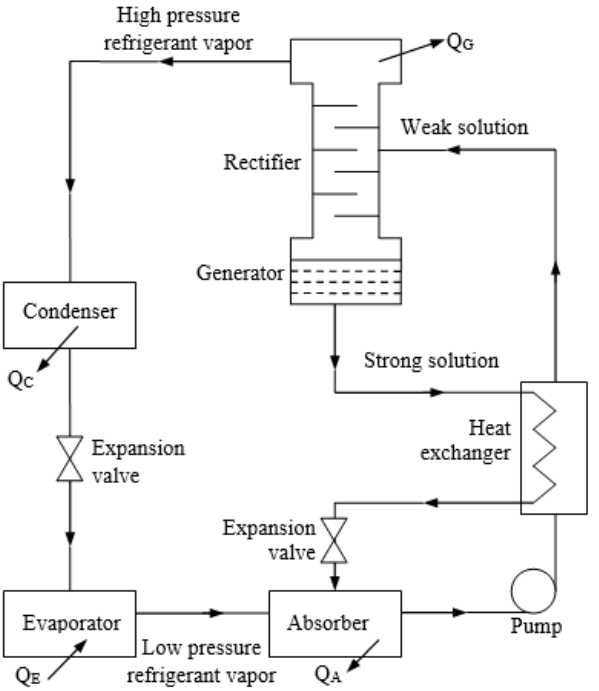

Figure 1. The schematic of ARS cycle

The cycle performance is measured by the coefficient of performance (COP), which is is defined as the heat load in the evaporator per unit of heat load in the generator and can be written as:

$$\mathrm{COP} = \frac{\dot{Q}_E}{\dot{Q}_g} \tag{1}$$

The circulation ratio (f) is defined as the mass flow rate of solution from the absorber to the generator (weak solution) to the mass flow rate of working fluid (refrigerant), that is:

$$f = \frac{\dot{m}_w}{\dot{m}_{re}} \tag{2}$$

Data Mining Process

Knowledge discovery uses data mining and machine learning techniques that have evolved through a synergy in artificial intelligence, computer science, statistics, and other related fields (Goodwin, et al., 2003). Data Mining is often defined as the process of extracting valid, previously unknown, comprehensible information

from large databases in order to improve and optimize business decisions (Braha and Shmilovici, 2002). In others definition Data mining is defined as the identification of interesting structure in data, where structure designates patterns, statistical or predictive models of the data, and relationships among parts of the data (Fayyad and Uthurusamy, 2002).

This creative process generally involves phases of data understanding, data preparation, modeling, and evaluation. It is a hybrid disciplinary that integrates technologies of databases, statistics, machine learning, signal processing, and high performance computing. This rapidly emerging technology is motivated by the need for new techniques to help analyze, understand or even visualize the huge amounts of stored data gathered from business and scientific applications. The major data mining functions that are developed in commercial and research communities include summarization, association, classification, prediction and clustering as shown in Figure 2 (Li and Shue, 2006).

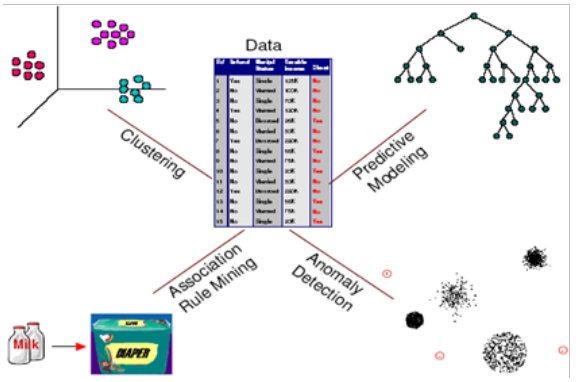

Figure 2. Data Mining Tasks

Data understanding starts with an initial data collection and proceeds with activities to get familiar with the data, to identify data quality problems, and to discover first insights into the data. Data preparation covers all activities that construct the final data set to be modeled from the initial raw data. The tasks of this phase may include data cleaning for removing noise and inconsistent data, and data transformation for extracting the embedded features (Zhou, 2003). Successful mining of data relies on refining tools and techniques capable of rendering large quantities of data understandable and meaningful (Mattison, 1996). The modeling phase applies various modeling techniques, determines the optimal values for parameters in models, and finds the one most suitable to meet the objectives. The evaluation phase evaluates the model found in the last stage to confirm its validity to fit the problem requirements. No matter which areas data mining is applied to, most of the efforts are directed toward the data preparation phase (Li and Shue, 2006). The process of knowledge discovery in databases can be seen in Figure 3.

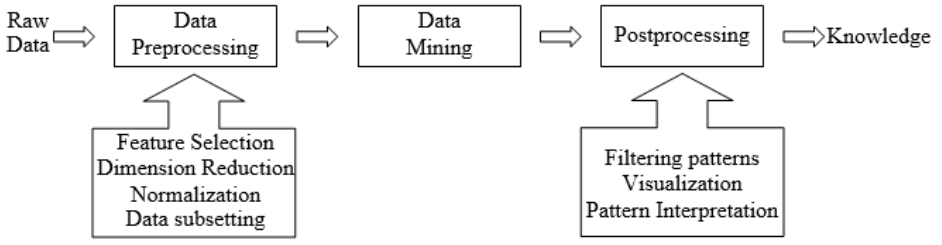

Figure 3. The process of knowledge discovery in databases

A good relational database management system will form the core of the data repository, and adequately reflect both the data structure and the process flow, and the database design will anticipate the kind of analysis and data mining to be performed. The data repository should also support access to existing

databases allowing retrieval of supporting information that can be used at various levels in the decision making process (Rupp and Wang, 2004).

Data mining is a powerful technique for extracting predictive information from large databases. The automated analysis offered by data mining goes beyond the retrospective analysis of data. Data mining tools can answer questions that are too time-consuming to resolve with methods based on first principles. In data mining, databases are searched for hidden patterns to reveal predictive information in patterns that are too complicated for human experts to identify (Hoffmann and Apostolakis, 2003; Lee, et al., 2006; Yuan, et al., 2000). Data mining is applied in a wide variety of fields for prediction, e.g. stock-prices, customer behavior, production control. In addition, data mining has also been applied to other types of scientific data such as bioinformatical, astronomical, and medical data (Li and Shue, 2006). In this study, different data mining algorithms (Linear Regression and M5'Rules) were used.

Linear Regression (LR)

Linear regression is a well-known method of mathematically modeling the relationship between a dependent variable and one or more independent variables (Schikora and Godfrey, 2003). Regression uses existing values to forecast what other values will be. In the simplest case, regression uses standard statistical techniques such as linear regression. Unfortunately, many real-world problems are not simply linear projections of previous values. For instance, sales volumes, stock prices, and product failure rates are all very difficult to predict because they may depend on complex interactions of multiple predictor variables. Therefore, more complex techniques (e.g., logistic regression, decision trees, or neural nets) may be necessary to forecast future values.

M5'Rules

The method for generating rules from model trees, which it is called M5'Rules, is straightforward and works as follows: a tree learner (in this case model trees) is applied to the full training dataset and a pruned tree is learned. Next, the best leaf (according to some heuristic) is made into a rule and the tree is discarded. All instances covered by the rule are removed from the dataset. The process is applied recursively to the remaining instances and terminates when all instances are covered by one or more rules. This is basic separate-and-conquer strategy for learning rules; however, instead of building a single rule, as it is done usually, we build a full model tree at each stage, and make its "best" leaf into a rule. This avoids potential for over-pruning called hasty generalization. In contrast to PART, which employs the same strategy for categorical prediction, M5'Rules builds full trees instead of partially explored trees. Building partial trees leads to greater computational efficiency, and does not affect the size and accuracy of the resulting rules (Hall et al., 1999).

Performance Analysis Using Data Mining Process

Equations used for the analytical performance of ammonia-water absorption refrigeration system were presented by Sun (1997). As can be seen from literature, complex equations are required in order to carry out the performance analysis of ARS and the whole procedure is fairly difficult and time consuming. In order to simplify this analysis, Data mining is used in the present work. The computer program was performed under WEKA-3-4.4. As seen Table 1, the inputs of the network are the temperature at various components of the system and concentration values, whereas output is the COP and f. In order to achieve the optimal result, different data mining algorithms (Linear Regression and M5'Rules) were used. R2 values of these different algorithms are given in Table 2 for circulation ratio (f) and COP calculations.

Table 1. Input and output parameters

Input parameters	Output parameters
Generator temperature	
Evaporator temperature	
Condenser temperature	Circulation ratio (f)
Absorber temperature	COP
Weak solution concentration	
Strong solution concentration	

Table 2. Comparison of R^2-values between different algorithms for circulation rate and COP

Method	Output value	
	f	COP
LR	0.828	0.953
M5'Rules	0.962	0.953

Results and Discussion

The generator temperature, evaporator temperature, condenser temperature, absorber temperature, weak and strong solution concentration effect the coefficient of performance (COP) and circulation ratio (f) of ARS. Theoretical performance analysis of the ARS is complex due to the equations of thermodynamic properties of working fluid and simulation programs. Therefore, in order to simplify performance analysis of the ARS, data mining process was used. In study, different data mining algorithms (Linear Regression and M5'Rules) were used. As seen Table 2, the optimal result from these algorithms was obtained using the M5'Rules. Variations of COP and f values with different operating parameters of ARS have been theoretically calculated and presented in Figs. 4-9. Figure 4 shows the variation of COP of ARS with generator temperature and evaporator temperature. In Figure 4, it is seen that COP increases with increasing generator temperature and evaporator temperature. It should be noted that the COP at higher generator temperature decreases. This behavior may be explained by the fact that further increase in generator temperature will lead to the increase in irreversibility. This results in a decrease in the COP.

Figure 5 shows the variation of COP of ARS with condenser temperature and evaporator temperature. COP of system increase with increasing evaporator temperature. COP decreases when condenser temperature increases. The reason of this, an increase in the condenser temperature will result in a higher temperature condensate having a greater enthalpy. This condensate, upon its return to evaporator, has a reduced refrigerant effect. The result of an increase in condenser temperature is a reduction in capacity, and an increase in the energy input requirements.

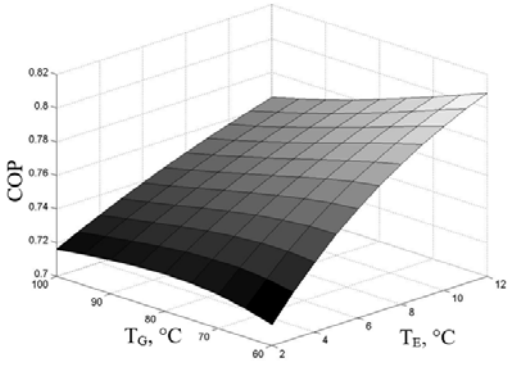

Figure 4. Variation of the COP of ARS with generator temperature and evaporator temperature

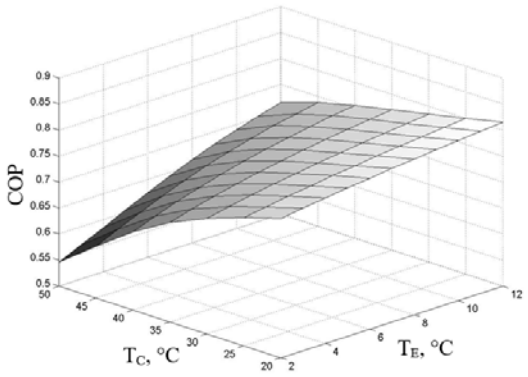

Figure 5. Variation of the COP of ARS with condenser temperature and evaporator temperature

Figure 6 shows the variation of COP of ARS with absorber temperature and evaporator temperature. Similarly in Figure 5, COP value of the system increases with increase of evaporator temperature and decreases with increase absorber temperature. As seen Figure 6, the influence on performance of ARS of absorber temperature is higher than condenser temperature. Variation flow rate, which is an important design and optimization parameter of ARS, is given in Figure 7 in relation to generator and evaporator temperatures. With the increase of generator and evaporator temperatures, flow rate of the system decreases. In absorption systems, increase of flow rate is unfavorable case, because, it causes circulation losses and reduces coefficient of performance (COP).

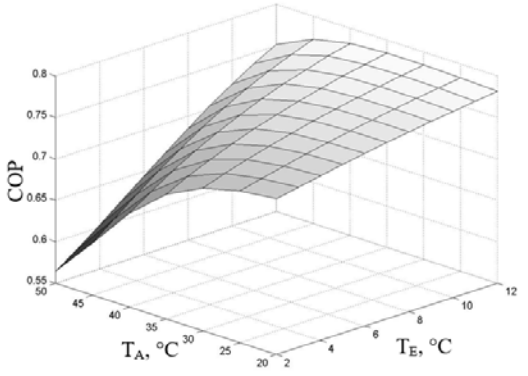

Figure 6. Variation of the COP of ARS with absorber temperature and evaporator temperature

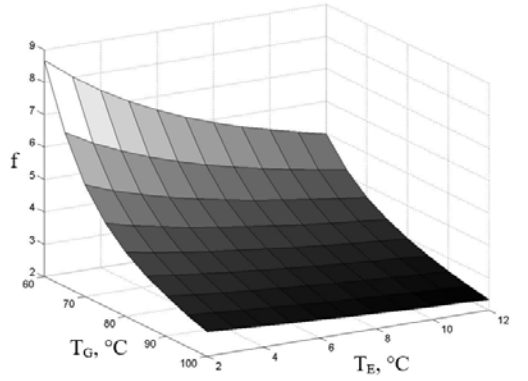

Figure 7. Variation of the f value of ARS with generator temperature and evaporator temperature

Variation of flow rate in relation to condenser and evaporator temperatures is given in Figure 8. As seen from the figure, with the increase of evaporator temperature, flow rate decreases, in contrary to this, with the increase of condenser temperature, flow rate increases. Variation of flow rate with absorber and evaporator temperatures is given in Figure 9. With the increase of evaporator temperature, flow rate decreases and with increase of absorber temperature, flow rate increases.

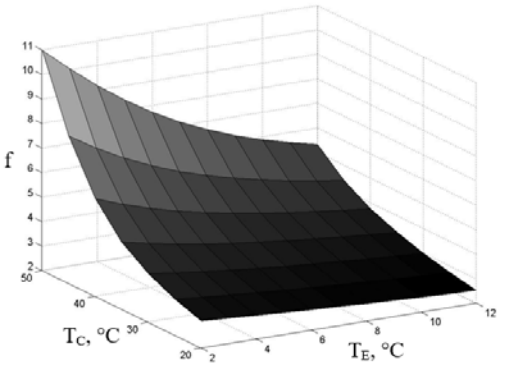

Figure 8. Variation of the f value of ARS with condenser temperature and evaporator temperature

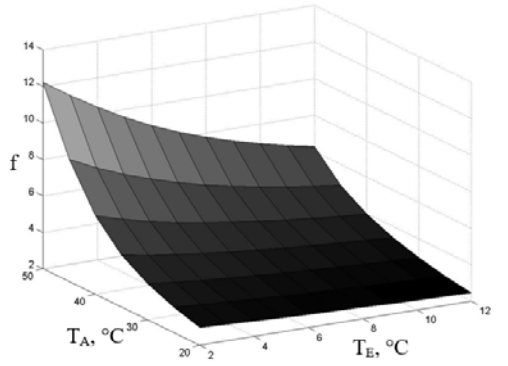

Figure 9. Variation of the f value of ARS with absorber temperature and evaporator temperature

The effect on COP and f values of weak solution ammonia mass fraction is shown in Figure 10. As seen from the figure, with the increase of weak solution concentration, mass flow rate of refrigerant increases. Thus, COP value of the system increases. In contrary to COP, with the increase of weak solution concentration, the value of f decreases. The effect on COP and f values of strong solution ammonia mass fraction is given in Figure 11. From the figure, with the increase of strong solution concentration, the value of f increases, additionally, with the decrease of mass flow rate of refrigerant, the system performance decreases. This means the value of COP decreases.

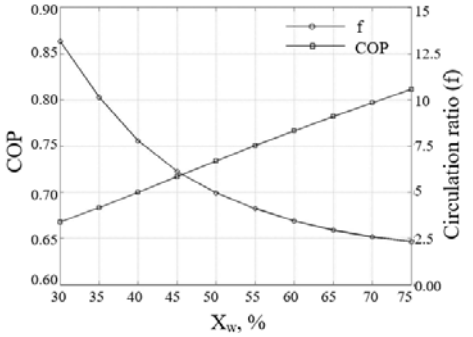

Figure 10. Effect on COP and f values of weak solution ammonia mass fraction

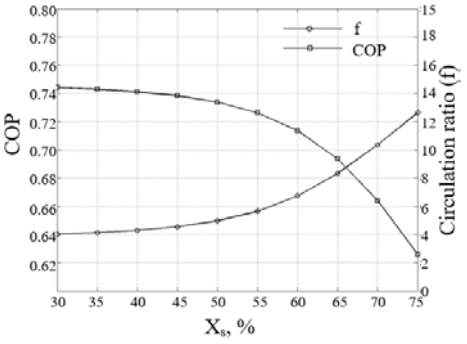

Figure 11. Effect on COP and f values of strong solution ammonia mass fraction

Conclusions

In this paper, data mining process is successfully applied to determine of COP and f values of ARS. The optimal result from different data mining algorithms was obtained using the M5'Rules. R^2-value for circulation ratio values is 0.962 and the R2-value for COP values is 0.953 which can be considered as very satisfactory. The new methodology provides faster and simpler solutions instead of complex equations. In the analysis of ARS, it was found out that COP increased with increasing evaporator, generator temperature and with decreasing absorber and condenser temperature. It was found out that f values decreased with increasing evaporator, generator temperature and with decreasing absorber and condenser temperature. Additionally, with the increase of weak solution concentration, f value decreases and COP value of the system increases. With the increase of strong solution concentration, f value increases and COP value of the system decreases.

References

Alefeld, G., Radermacher, R. (1994). Heat Conversion Systems, CRC Press.

ASHRAE, (1997). Fundamentals handbook, American Society of Heating Refrigerating and Air Conditioning Engineers Inc.

Braha, D., Shmilovici, A. (2002). Data Mining for Improving a Cleaning Process in the Semiconductor Industry. Semiconductor Manufacturing, 15(1), 91-101.

Chen J., Schouten J.A. (1998). Optimum performance characteristics of an irreversible absorption refrigeration system. Energy Conversion and Management, 39(10), 999-1007.

Chow T.T., Zhang G.Q., Lin Z., Song C.L. (2002). Global optimization of absorption chiller system by genetic algorithm and neural network. Energy and Buildings, 34,103-109.

Fayyad, U.M., Uthurusamy, R. (2002). Evolving data mining into solutions for insights. Communications of the ACM, 45(8), 28-31.

Fernandez S., Vazquez M. (2001). Study and control of the optimal generation temperature in NH3-H2O absorption refrigeration systems. Applied Thermal Engineering, 21, 343-357.

Francisco A., Illanes R., Torres J.L., Castillo M., Blas M., Prieto E., Garcia A. (2002). Development and testing of a prototype of low-power water–ammonia absorption equipment for solar energy applications. Renewable Energy, 25, 537–544.

Ghaddar N.K., Shihab M., Bdeir F. (1997). Modeling and simulation of solar absorption syastem performance in Beirut. Renewable Energy, 10(4), 539-558.

Goodwin, L., Van Dyne, M., Lin, S., Talbert, S. (2003). Data Mining Issues and Opportunities for Building Nursing Knowledge. Journal of Biomedical Informatics, 36, 379-388.

Hall, M., Holmes, G. and Frank, E. (1999). Generating Rule Sets from Model Trees, Proceedings of the Twelfth Australian Joint Conference on Artificial Intelligence, 1-12.

Herold, K.E., Radermacher, R., Klein, S.A. (1996). Absorption Chillers and Heat Pumps, CRC Press.

Hoffmann, D., Apostolakis, J. (2003). Crystal Structure Prediction By Data Mining. Journal of Molecular Structure, 647, 17-39.

Jelinek M., Levy A., Borde I. (2002). Performance of triple-pressure-level absorption cycle with R125-N,N-dimethylethylurea. Applied Energy, 71, 171-189.

Lee, TS., Chiu, C.C., Chou, Y.C., Lu, C.J. (2006). Mining The Customer Credit Using Classification And Regression Tree And Multivariate Adaptive Regression Splines. Computational Statistics and Data Analaysis, 50(4), 1113-1130.

Li, S.T., Shue, L.Y. (2006). Data mining to aid policy making in air pollution management. Expert Systems with Applications, 30(1), 50-58.

Mattison, R. (1996). Data Warehousing: Strategies, Technologies and Techniques Statistical Analysis, SPSS Inc. WhitePapers.

Rupp, B., Wang, J. (2003). Predictive Models For Protein Crystallization. Methods, 34(3), 390-407.

Schikora, P.,F., Godfrey, M.,R. (2003). Efficacy Of End-User Neuralnetwork And Data Mining Software For Predicting Complex System Performance. International Journal of Production Economics, 84, 231-253.

Sun D.W. (1997). Thermodynamic Design Data and Optimum Design Maps for Absorption Refrigeration Systems. Applied Thermal Engineering, 17(3), 211-221.

Sun D.W. (1998). Comparison of the performances of NH3-H2O, NH3-LiNO3 and NH3-NaSCN absorption refrigeration systems. Energy Conversion and Management, 39(5/6), 357-368.

Wu S., Eames I.W. (2000). Innovations in vapour-absorption cycles. Applied Energy, 66, 251-266.

Xu G.P., Dai Y.Q. (1997). Theoretical analysis and optimization of a double-effect parallel-flow-type absorption chiller. Applied Thermal Engineering, 17(2), 157-170.

Yuan, B., Wang, X.,Z., Morris, T. (2000). Software Analyser Design Using Data Mining Technology For Toxicity Prediction Of Aqueous Effluents. Waste Management, 20, 677-686.

Zhou, Z.H. (2003). Three perspectives of data mining. Artificial Intelligence, 143(1), 139–146.

International Conference on Science and Technology

ICONST 2018

5-9 September 2018 Prizren - KOSOVO

An Explanation About Negative Absorbance Readings Performed for the Measurement of Low Concentration Chemical Oxygen Demand

Hüseyin Yazıcı[1]*, Mehmet Kılıç[2]

Abstract: In environmental engineering applications such as wastewater treatment operations, determination of chemical oxygen demand (COD) concentration is an important and routine analysis method since this determination provides an insight into evolution of pollution level of wastewaters. According to the Standard Methods (APHA), determination of COD concentration is performed by several procedures that are categorized under the title 5220. Among these methods, 5220D Closed Reflux Colorimetric Method is considered more economical and environmental-friendly method since this method generates smaller quantities of hazardous wastes such as mercury, hexavalent chromium, sulfuric acid, silver, and acids. The principle of the method is based on absorbance measurements of samples at selected wavelengths. In the method, absorbance readings should be performed at two different wavelength regions: (i) at 600-nm wavelength for COD values between 100 and 900 mg/L, and (ii) at 420-nm for COD values of 90 mg/L or less, thus demanding preparation of two different calibration curves. Unlike obtaining positive results from absorbance readings at 600 nm, absorbance readings at 420 nm yields negative results. If this difference is not carefully taken into account, negative absorbance results yielded from the calibration curve prepared for the low range COD concentration may cause confusions. It is thought that the main underlying causes of obtaining negative absorbance readings are not understood well and that, therefore, the method has not been drawn considerable interest by researchers. In this study, results of obtaining negative absorbance readings during measurement of low range COD concentrations with the method 5220D are explained.

Keywords: Chemical oxygen demand, standard method, low-range concentration determination, absorbance reading, negative result.

Introduction

Water is, since ancient times, the most strictly managed resource of sedentary human societies. The impact of water quality on the environment and on public health justifies the investment in managing and controlling the safety of its domestic, public and industrial use. The sustainable management of water resources must be supported on the production of safe and adequately abundant drinking water and on the treatment of wastewaters (Silva et al., 2011). If untreated wastewater containing contamination enters into the surface and ground water resources, it leads to a serious environmental and human health risk (Tchobanoglous and Burton, 1991; Alam, 2015). To minimize the potential risks from untreated wastewater entering freshwater resources, water quality professionals assess water quality by monitoring and measuring the concentrations of several parameters and comparing with their standards (Mancy, 1971; Mor et al., 2006; Alam, 2015). Some of the unique analytical parameters of the water pollution control industry are biochemical oxygen demand (BOD), chemical oxygen demand (COD), taste, odor, color, chlorine demand, hardness, alkalinity and

[1]Suleyman Demirel University, Vocational School of Aksu Mehmet Süreyya Demiraslan, Department of Environmental Protection Technologies, 32510 Isparta, TURKEY
[2]Suleyman Demirel University, Faculty of Engineering, Department of Environmental Engineering, 32260, Isparta, TURKEY
*Correspondingauthor: huseyinyazici@sdu.edu.tr

biodegradability tests (Tchobanoglous and Burton, 1991; Henze, 2002; Alam, 2015). Finding excessive levels of one or more of these parameters can serve as an early warning of potential pollution problems (Alam, 2015). The most relevant pollution impact of domestic wastewaters results from organic matter (Silva et al., 2011). For assessing the concentration of organic matters in water resources, oxygen demand is an important parameter (Domini et al., 2006). If domestic or industrial wastewater is discharged into a receiving stream without proper treatment, wastewater organic matters increase the activity of microbes in the stream resulting in consumption of dissolved oxygen and consecutively an increase in oxygen demand. Therefore, wastewater treatment plant operators are often interested in knowing the amount of organic content in wastewater (Kim et al., 2007). COD, BOD and total organic carbon (TOC) are three main indexes used to assess organic pollution in aqueous systems (Domini et al., 2006). Among these, COD is the main parameter widely used to estimate the organic content of wastewater (Vyrides and Stuckey, 2009) because, as a pollution monitoring parameter, COD has the advantage of speed and simplicity compared with BOD, and requires less equipment than to TOC determination (Domini et al., 2006). The ability of testing wastewaters in a couple of hours, instead of the five days required for BOD_5, makes this analytical evaluation of COD most popular and useful despite the fact that it also involves the oxidation of inorganic matter (Silva et al., 2011). Thus, COD is preferred for estimating organic pollution (Jones et al., 1985; Dasgupta and Petersen, 1990; Kim et al., 2000; Domini et al., 2006).

COD is defined as the amount of oxygen equivalents consumed in oxidizing the organic compounds of samples by strong oxidizing agents such as dichromate or permanganate (Alam, 2015). It is used to measure the total quantity of oxygen consuming substances in the complete chemical breakdown of organic substances in water, thus measuring the quality and determining what organic load is present in the water (Verma and Singh 2013; Emamgholizadeh et al., 2014). COD values are also used to monitor wastewaters before (influent) and after (effluent) treatment (Alam, 2015). [1] In fact, the cost of wastewater treatment contracted by the polluting industry is frequently settled in terms of the pollution charge quantified by its COD value. Likewise, the management of wastewaters facilities, such as the schedule of maintenance activities or the use of parallel treatment units, is also frequently based on COD values (Silva et al., 2011). Therefore, reliability of COD values is important to protect the environment and to guarantee the economical sustainability of the treatment facility (Wu et al., 2011; Alam, 2015).

COD measurements are commonly made on samples of wastewater treatment facility or of natural waters contaminated by domestic and industrial wastes. It is measured as a standardized laboratory assay in which a closed water sample is incubated with a strong chemical oxidant under specific conditions of temperature and for a particular time (Alam, 2015). In the conventional COD evaluation methods, a known excess of oxidant is added to a sample and the mixture is boiled. After the oxidation has proceeded for a finite period of time, the initial concentration of organic species can be calculated by determining the amount of the remaining oxidizing agent commonly by titration (APHA, 1999; (Domini et al., 2006). The conventional methods, however, require the time consuming process (about 3 h) of refluxing samples to achieve more complete oxidation plus additional time for titration, and the reproducibility of the results are dependent upon the skill of the operator. Moreover, the conventional methods consume some expensive (Ag_2SO_4) and toxic (Cr and Hg) chemicals (Appleton et al., 1986; Hejzlar and Kopacek, 1990; Domini et al., 2006). Consequently, secondary pollution is unavoidable when these methods are employed (Han et al., 2011; Yao et al., 2014). For these reasons, many efforts have been made to improve the procedure focusing mainly on digestion and quantitation steps. A few engineers have carried out research to improve the COD analyzing method; mainly to reduce or eliminate digestion time and/or to automatically determine residual $Cr_2O_2^{7-}$ to quantify wastewater COD. Instead of a reflux apparatus used in Standard Methods, a pressurized sterilizer (Ryding and Forsberg, 1977), a glass tube filled with quartz and sand (Rozenberg, 1993), a microwave (Cuesta et al., 1998) and ultrasound (Canals et al., 2002) have been applied to digest water samples (Kim et al., 2007). Photocatalytic oxidation using nano-TiO_2 (Ai et al., 2004) or ozone aided by UV radiation (Jin et al., 2004) was also used to oxidize organics without providing heat (Kim et al., (2007). Although these methods have been shown to have a number of advantages over the traditional COD determination methods, they are far from perfect (Yao et al., 2014).

The Standard Methods (APHA, 1999) is well established and is used by the majority of researchers and plant operators in the waste–wastewater field to express the polluting ability of a wastewater. According to the

Standard Methods, determination of COD concentration is performed by several methods that are categorized under the title 5220. In the COD determinations with the open reflux method (5220B) and the closed reflux methods (5220C and D), silver, hexavalent chromium and mercury salts are used and these additives create hazardous wastes. The closed reflux methods (C and D) are more economical in the use of metallic salt reagents and generate smaller quantities of hazardous waste. Beside the cost and environmental aspects of any of these three methods, selection of the method should also be done depending on the concentration measurement range of the method. In these three methods, the dichromate ion ($Cr_2O_7^{2-}$) is the specified oxidant and it is reduced to the chromic ion (Cr^3). The extend of reduction in the chromic ion changes depending on the COD concentration of the examined sample, Therefore, selection of the appropriate method should be done according to this phenomenon. COD concentration of a sample having >50 mg O_2/L can be measured by all three methods. It is also possible to determine for low-range COD values by either performing a titration procedure as described in the open reflux method (5220B) or the closed reflux method (5220C) or measuring absorbance of the treated sample in a spectrophotometer as described in the closed reflux method (5220D). In the titration procedure, the titration is terminated when the solution color changes from greenish to reddish brown. Therefore, titration results may vary as the color perception ranges vary among analysts. In addition, color-blind analysts cannot perform the titration. Additionally, it is reported in the Standard Methods (APHA, 1999) that COD values of 5 to 50 mg O_2/L can be measured by the open reflux method with lesser accuracy and determinations of COD values <100 mg O_2/L by the closed reflux titrimetric method (5220C) require a more diluted dichromate digestion solution or a more dilute FAS titrant (Kim et al., (2007).

Low-range COD values can alternatively be measured by the closed reflux method 5220D without performing the titration procedure. In this method, absorbance measurements must be performed in two different visible spectrum regions at 600 and 420 nm in spectrophotometer depending on the predicted COD concentration of the examined sample. For COD values between 100-900 mg/L and COD values of 90 mg/L or less, absorbance measurements are performed at 600-nm and 420-nm wavelenght region, respectively. Therefore, a researcher has to prepare two different calibration curves if low-range COD values are also needed to be examined. When doing this, it should be considered that absorbance readings at 420 nm might yield negative absorbance results on the spectrophotometer while readings at 600 nm yield positive absorbance results even if the standard test solutions or samples are well prepared. If this difference is not carefully taken into account, negative absorbance results yielded from the calibration curve prepared for the low range COD concentration may cause confusions. In the literature, there are several studies where COD measurements were carried out by the method 5220D (GilPavas et al., 2018; He et al., 2018; Montalvo et al., 2018; Pantziaros et al., 2018; repinc et al., 2018). However, since no detailed information was supplied, it is not clearly understood from studies that if absorbance readings for low-range COD values were actually performed at the requiring absorbance region. It is thought that the main underlying causes of obtaining negative absorbance readings are not understood well and that, therefore, the method has not been drawn considerable interest by researchers. In this study, results of obtaining negative absorbance readings during measurement of low range COD concentrations with the method 5220D are explained. For this purpose, COD results of an enhanced biological phosphorus removal (EBPR) system were utilized. Detailed information for reactor operation, operating conditions, feeding solution and experimental studies can be found in the study of Yazıcı and Kılıç (2016).

2. Material and Method

2.1. Seeding sludge, experimental setup and EBPR reactor operation

The seeding sludge was collected from oxic zone of an activated sludge tank in Lara Advanced Wastewater Treatment Plant (Antalya, Turkey). After the sludge was collected, it was almost immediately transported to the laboratory, homogenized, and then 2.5 L sludge was transferred into the sequencing batch reactor (SBR). A laboratory-scale SBR (BioFlo 110, New Brunswick Scientific Co., U.S.A.) having 7.5 L of total volume was operated with a working volume of 5.0 L and four 6-h cycles per day under alternating anaerobic-aerobic conditions. Schematic representation of operational components of the SBR is shown in Figure 1.

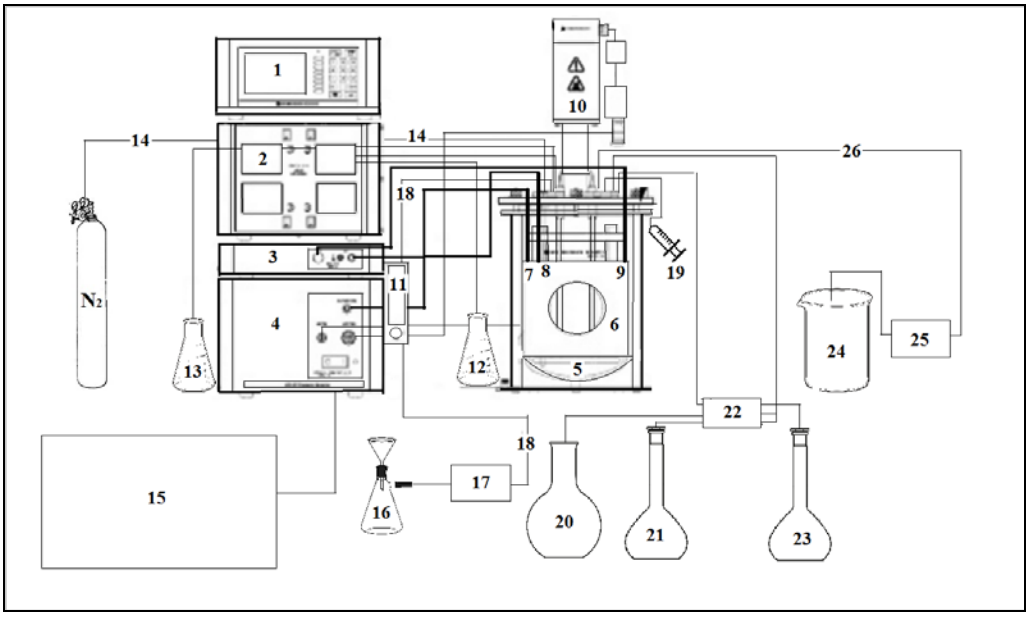

Figure 1. Schematic representation of operational components of the SBR (**1:** Primary control unit, **2**: Pumps, **3**: dO2/pH control module, **4**: Power controller, **5**: Glass vessel, **6**: Heat blanket, **7**: Thermowell, **8**: pH sensor, **9**: dO2 sensor, **10**: Agitation motor, **11**: Rotameter, **12**: Acid addition, **13**: Base addition, **14**: Nitrogen gas stream, **15**: Electrical supply, **16**: Vacuum filtration unit, **17**: Air compressor, **18**: Air stream, **19**: Sampling syringe, **20**: Solution A, **21**: Solution B, **22**: Two-sided peristaltic pump, **23**: Waste sludge withdrawal stream, **24**: Effluent collection beaker, **25**: One-sided peristaltic pump, **26**: Effluent stream)

2.2. Feeding solution

The solution was fed to the reactor as two separate solutions named Solution A and Solution B at the beginning of the feeding phase with a total volume of 2.5 L. The solution A was included sodium acetate as the sole carbon source. The initial COD concentration in the Solution A was adjusted to 500 mg/L.

2.3. COD measurements

COD concentrations were determined according to the Standard Methods as described in the section 5220D. The absorbance readings for the standard solution, blank solutions and samples were performed at 600 nm for COD concentrations higher than 100 mg/L and at 420 nm for COD concentrations <90 mg/L in a spectrophotometer (WTW, SpektroFlex 6100). High-range COD measurements were carried out for anaerobic cycles, whereas low-range COD measurements were carried out for aerobic cycles. Heating of culture tubes was carried out in a thermoreactor (WTW, CR2200) at 150 °C for 2 h. The standards were prepared from potassium hydrogen phthalate solution with a known COD equivalent ranging between 100 to 1000 mg/L for the high-range values and 10 to 90 mg/L for the low-range values. Absorbance value of each standard solution was yielded from three separate solutions and the mean values were used to prepare calibration curves. 16 mm glass tubes were used for all absorbance readings.

3. Results

The prepared calibration curves for high- and low-range COD measurements are shown in Fig 2. As seen from Fig 2, the calibration curve for high-range COD measurements yielded positive absorbance results and a coefficient of determination (R^2) value of 0.9995 (Fig 2a). However, the curve for low-range COD measurements yielded negative absorbance results, and the R^2 value was found to be 0.985 (Fig 2b).

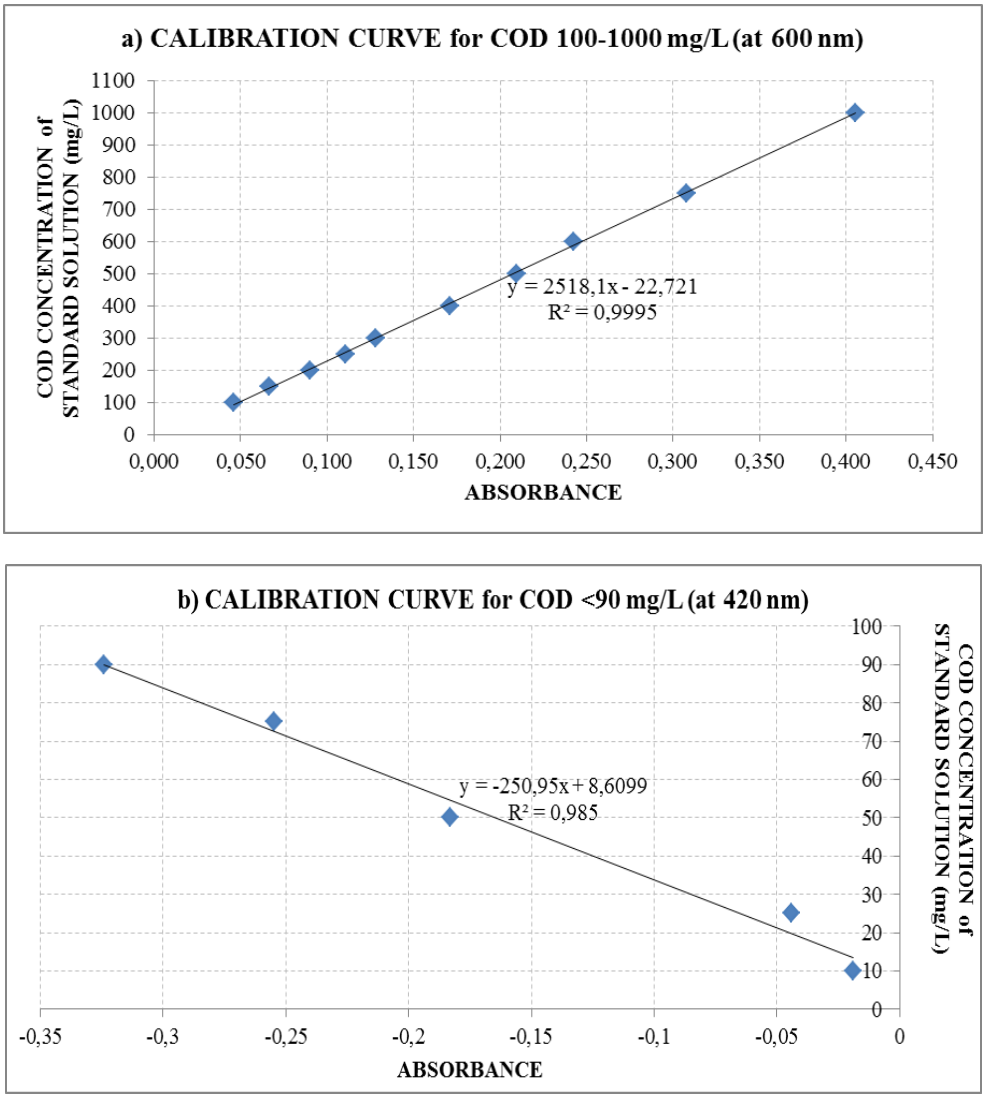

Figure 2. The prepared calibration curve **a)** for high-range COD measurements, and **(b)** for low-range COD measurements.

Table 1 shows the experimental results that were obtained from the EBPR study (Yazıcı and Kılıç, 2016). The results imply that a great portion of the initial COD concentration removed at the end of the aerobic cycle during the first 10 days. After this period, the COD removal took place during the anaerobic cycle and a slight removal occurred during the aerobic cycle. As can be seen from Table 1, positive absorbance readings were obtained for the high-range COD values where the measurements were performed at 600-nm region. However, the low-range COD measurements yielded negative absorbance readings where the measurements were performed at 420-nm region. Although obtaining the negative absorbance results, these results were successfully converted to the positive concentration values.

Table 1. Experimental results for high- and low-range COD measurements

Reactor Operation Time	**High-range COD Results (at the end of anaerobic cycle)**		**Low-range COD Results (at the end of aerobic cycle)**	
Days	Absorbance	Concentration	Absorbance	Concentration
0	0,231	558.9	-0,278	78.3
2	0,177	422.9	-0,223	64.5
4	0,121	281.9	-0,204	59.8
6	0,18	430.5	-0,131	41.4
8	0,114	264.3	-0,133	41.9
10	0,133	312.1	-0,137	42.9
12	0,092	208.9	-0,117	37.9
14	0,074	163.6	-0,135	42.4
16	0,066	143.4	-0,14	43.7

4. Discussions and Conclusions

Unlike obtaining positive results from absorbance readings at 600 nm wavelength, obtaining negative absorbance results at 420 nm wavelength may lead a researcher to think that there is something wrong with the prepared standard and/or blank solutions or the spectrophotometer used if the main underlying causes of obtaining such results are not well known by the researcher. Such dissimilarity between obtaining positive and negative absorbance results may eventually cause giving up the idea of using the method for low-range COD measurements even if several attempts have already been performed in order to obtain positive absorbance readings.

As explained in the Standard Methods, the dichromate ion oxidizes organic matters in the sample when the sample is digested, resulting in the change of chromium from the Cr^{6+} state to the Cr^{3+} state. Both of these chromium species absorb in the visible region of the spectrum. The dichromate ion ($Cr_2O_7^{2-}$) absorbs strongly in the 400-nm region, where the Cr^{3+} absorption is much less. The Cr^{3+} ion absorbs strongly in the 600-nm region, where the dichromate has nearly zero absorption. The Cr^{3+} ion has a minimum in the region of 400 nm. Thus a working absorption maximum is at 420 nm. If a COD determination is required for the high-range values, increase in the change of chromium from the Cr^{6+} to Cr^{3+} in the 600-nm region is determined. That means the amount of the resultant Cr^{3+} ion increases at the end of the digestion procedure if the given COD concentration of a sample increases since the conversation of the Cr^{6+} state to the Cr^{3+} state increases. If a COD determination is required for the low-range values, the decrease in $Cr_2O_7^{2-}$ ion concentration at 420 nm is determined since the corresponding generation of Cr^{3+} gives a small absorption increase at this absorbance region, but this is compensated for in the calibration procedure.

Based on the above explanations and experimental results, it can be briefly concluded that absorbance readings for COD concentrations less than 90 mg/L should be measured at 420-nm region at the spectrophotometer when COD measurements are performed according to the standard method 5220D. Then, the corresponding concentration values can be successfully converted to positive values through negative absorbance results by using the linear equation of the calibration curve.

Acknowledgements

This study was funded by the Scientific Research Project Commission of Süleyman Demirel University, Isparta, Turkey (project no. 2202-D-10). The financial assistance of the study is thankfully acknowledged by the authors.

References

Ai, S., Li, J., Yang, Y., Gao, M., Pan, Z., Jin, L. (2004). Study on photocatalytic oxidation for determination of chemical oxygen demand using a nano-TiO_2-$K_2Cr_2O_7$ system. Analytical Chimica Acta, 509, 237-241.

Alam, T. (2015). Estimation of chemical oxygen demand in wastewater using UV-VIS spectroscopy (MASc). School of Mechatronic Systems Engineering Faculty of Applied Sciences, Simon Fraser University, British Columbia, Canada.

APHA (1999). Standard Methods for the Examination of Water and Wastewater. American Public Health Association, Washington DC.

Canals A., Cuesta, A., Gras, L., Hernandez, M.R. (2002). New ultrasound assisted chemical oxygen demand determination. Ultrasonic Sonochemistry, 9, 143-149.

Cuesta, A., Todoli, J.L., Mora, J., Canals, A. (1998). Rapid determination of chemical oxygen demand by a semi-automated method based on microwave sample digestion, chromium(VI) organic solvent extraction and flame atomic absorption spectrometry. Analytica Chimica Acta, 372, 399-409.

Dasgupta, P.K., Petersen, K. (1990). Kinetic approach to the measurement of chemical oxygen demand with an automated micro batch analyzer. Analytical Chemistry, 62, 395-402.

Daughton,C.G., Jones, B.M., Sakaji, R.H. (1985). Organic nitrogen determination in oil shale retort waters. Analytical Chemistry, 57, 2326-2333.

Domini, C.E., Hidalgo, M., Marken, F., Canals, A. (2006). Comparison of three optimized digestion methods for rapid determination of chemical oxygen demand: Closed microwaves, open microwaves and ultrasound irradiation. Analytica Chimica Acta, 561, 210-217.

Emamgholizadeh, S., Kashi, H., Marofpoor, I. (2014). Prediction of water quality parameters of Karoon River (Iran) by artificial intelligence-based models. International Journal of Environmental Science and Technology, 11, 645-656.

GilPavas, E., Dobrosz-Gómez, I., Gómez-García, M.A. (2018). Optimization of sequential chemical coagulation - electro-oxidation process for the treatment of an industrial textile wastewater. Journal of Water Process Engineering, 22, 73-79.

Guoqing, W., Weihong, B., Jiaming, L., Guangwei, F. (2011). Determination of chemical oxygen demand in water using near-infrared transmission and UV absorbance method. Chinese Optics Letters, 9:s10705–310709.

Han, Y., Qiu, J., Miao, Y., Han, J., Zhang, S., Zhang, H., Zhao, H. (2003). Robust TiO2/BDD heterojunction photoanodes for determination of chemical oxygen demand in wastewaters. Analytical Methods, 3, 2003-2009.

He, Q., Zhang, D., Main, K., Feng, C., Ergas, S.J. (2018). Biological denitrification in marine aquaculture systems: A multiple electron donor microcosm study. Bioresource Technology, 263, 340-349.

Henze, M., Harremoes, P., Jansen, C., Arvin, E. (2002). Wastewater treatment: Biological and chemical processes. Springer Science & Business Media, 422 p.

Jin, B., He, Y., Shen, J., Zhung, Z., Wang, X., Lee, F.S.C. (2004). Measurement of chemical oxygen demand (COD) in natural water samples by flow injection ozonation chemiluminescence (FI-CL) technique. Journal of Environmental Monitoring, 6, 673-678.

Kim, Y., Lee, K., Sasaki, S., Hashimoto, K., Ikebukuro, K., Karube, I. (2000). Photocatalytic sensor for chemical oxygen demand determination based on oxygen electrode. Analytical Chemistry, 72, 3379-3382.

Kim, H., Lim, H., Colosimo, M.F. (2007). Determination of chemical oxygen demand (COD) using ultrasound digestion and oxidation-reduction potential-based titration. Journal of Environmental Science and Health Part A, 42(11), 1665-1670.

Mancy, K.H. (1971). Instrumental analysis for water pollution control. Ann Arbor Science Publishers Inc., 331 p

Montalvo, S., Vielma, S., Borja, R., Huili, C., Guerrero, L. (2018). Increase in biogas production in anaerobic sludge digestion by combining aerobic hydrolysis and addition of metallic wastes. Renewable Energy, 123, 541-548.

Mor, S., Ravindra, K., Dahiya, R.P., Chandra, A. (2006). Leachate characterization and assessment of groundwater pollution near municipal solid waste landfill site. Environmental Monitoring and Assessment, 118(1-3), 435-456.

Pantziaros, A.G., Jaho, S., Karga, I., Iakovides, I.C., Koutsoukos, P.G., Paraskeva, C.A. (2018). Struvite precipitation and COD reduction in a two-step treatment of olive millwastewater. Journal of Chemical Technology & Biotechnology, 93, 730-735.

Repinc, S.K., Sket, R., Zavec, D., Miku, K.V., Fermoso, F.G. Stres, B. (2018). Full-scale agricultural biogas plant metal content and process parameters in relation to bacterial and archaeal microbial communities over 2.5 year span. Journal of Environmental Management, 213, 566-574.

Rozenberg, M. (1993). The fast method of the COD determination. Analytical Letters, 26(9), 2025-2030.

Ryding, S.O., Forsberg, A. (1977). A mercury-free accelerated method for determining the chemical oxygen demand of large numbers of water samples by autoclaving them under pressure with acid-dichromate. Water Research, 11(9), 801-805.

Silva, A.M.E.V., Silva R.J.N.B., Camões, M.F.G.F.C. (2011). Optimization of the determination of chemical oxygen demand in wastewaters. Analytica Chimica Acta, 699, 161-169.

Tchobanoglous, G., Burton, F.L. (1991). Wastewater engineering: Treatment, disposal and reuse. McGraw Hill Inc., 1334 p.

Verma, A.K., Singh, T.N. (2013). Prediction of water quality from simple field parameters. Environmental Earth Sciences, 69(3), 821-829.

Vyrides, I., Stuckey, D.D. (2009). A modified method for the determination of chemical oxygen demand (COD) for samples with high salinity and low organics. Bioresource Technology, 100, 979-982.

Yao, N., Wang, J., Zhou, Y. (2014). Rapid determination of the chemical oxygen demand of water using a thermal biosensor. Sensors, 14, 9949-9960.

Yazıcı, H., Kılıç, M. (2016). Effect of the concentration balance in feeding solutions on EBPR performance of a sequencing batch reactor fed with sodium acetate or glucose. Water, Air and Soil Pollution, 227:389.

International Conference on Science and Technology

ICONST 2018

5-9 September 2018 Prizren - KOSOVO

Sundial as Urban Furnishings

Nur Belkayalı [1]*, Elif Ayan[2]

Abstract: Ever since the day of human existence, he has examined the everyday change in the world and has made various inventions to determine the cycle of time. Clocks have been produced in order to know the time using the tools of the age. The most reliable of these inventions is the solar watches built with the help of a stick on the ground using solar rays. It is seen that the sun clocks that were used by the Egyptians were used to determine the times of prayer in the Muslim world. Firstly, horizontally used clocks were created later on oblique and vertical planes. By the beginning of the use of mechanical clocks, solar clocks became unusable and only remained for visual purposes.
Today, the sundials that are traced in various places are protected as part of the cultural heritage. Nowadays, the sundials that attract attention as a member of urban renaissance are used in different designs and in the square, mosque courts, urban parks.
Within the scope of this study, examples of different forms and contemporary sundials were examined. Samples of Kastamonu city, which can be used in urban park, were questioned with the help of questionnaire. According to the survey, it is suggested that the most preferred form of the solar clock form, which will reflect Kastamonu identity, be used in urban parks.

Keywords: Sundial, Urban Furnishings, Kastamonu

Introduction

The time comes from the word "khronos" in Greek is one of the basic dimensions of the world of movement and change, which is constantly flowing in the same way, which is thought to be measurable quantity at any moment (Unat, 2004; Kaplan, 2009). Time is an uninterrupted process in which events come from past to present and follow each other towards the future, and it is the basic element that gives meaning to action. Time is a concept that exists in nature, which can be perceived and measured by our sense organs, and is defined as the time required to change position according to each other during the motions of all the objects in the universe (Gürbüz and Aydın, 2012). Ever since the day of human existence, he has examined the everyday change in the world and has made various inventions to determine the cycle of time. Clocks have been produced in order to know the time using the tools of the age. The most reliable of these inventions is the sun dial built with the aid of a bar on the ground using solar rays. The sun dial using The sun's rays, which form the basis of time measurement, were invented for the first time in 1500 BC by the Egyptians, later by the Chinese, Greeks and Romans (Dönmez and Kabaş, 2005). Due to the important place of worship in Islam due to the time, the sun has been worked on in more detail and continued its existence by developing in the Seljuk and Ottoman periods which were used extensively in the region of Mesopotamia where the sun was seen abundantly. It also provides the opportunity to learn about the movement of the world.
The working principle of the sun dial is realized by the world itself and the turning movement around the sun. It is astronomical devices that show the time of day with the help of a shadow created by the Sun and it

[1]Kastamonu University, Faculty of Forestry, 37100, Kastamonu TURKEY
*Correspondingauthor: nbelkayali@kastamonu.edu.tr

enables to measure in the daytime that the sun is the time according to the movement of the shadow on the specially prepared marble, stone or metal floor (dial) (Kabaş 2004). The Earth appears to be moving exactly in every 24 hours, with a spinning sun, 15 degrees clockwise, and the sun's shadow moves in the same direction. With this return, the shadows are formed at different lengths (URL 1, 2018). This principle basically depends on the marking of the shadows of the pointed metal writing instruments as the sun covers the entire sky. The best known of these are the columns of the church fronts or church hunts, and one of them is in the Kirkdale Church in Yorkshire, which was built in the Old English period (Figure 1).

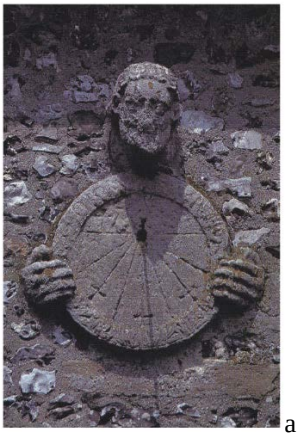
a


b

Figure 1a. Sun clock at Kirkdale Church (Ronald, 1997 Transcribed by Korkmaz, 2010)
Figure 1b. Limestone sundial dating from the 13th century Egyptian civilization (Url 2, 2018)
Figure 1. The oldest known solar watches

Sundials vary according to the level in which they are located. Fixed or portable solar clocks are available in spherical, horizontal and vertical planes (Korkmaz, 2010), horizontal quadrants, southward vertical quadrants, westward vertical quadrants, eastward vertical quadrants, northward vertical quadrants, randomly oriented vertical quadrants, quadrants, equatorial quadrants, meridian sundials, polar sundials. Horizontal quadrant solar clocks are generally parallel to the horizon, and they are seen as circular, square, rectangular or polygonal quadrants on small columns or in squares in the gardens and squares. Vertical quadrants are placed squarely on the building facades perpendicular to the horizon (Kabas, 2004). Each of the horizontal and vertical sundials consists of a rectangular plane with clock lines written on it with a triangular gnomon (shadow of the shadow) perpendicular to it. The length of the sun spilled by the gnomon of a sun clock depends on the position of the earth relative to the time of year, the latitude of the quadrant and its daily rotation. Correcting for daylight saving time is a simple renumbering of clock lines (Jhonston and Anneberg, 2002; URL-3, 2018). Sun dials, which have become increasingly inevitable with the invention of mechanical clocks, used in the agora, temple surroundings and city centers during the Ancient Greek period (Kaplan, 2009) and in the mosque walls in Ottoman period (Salman, 2003) are now being used as an artistic object. As Western societies begin to give importance as cultural heritage, there are sun clocks in different types redesigned today in parks, squares and campus areas of western countries (Kabas, 2004). Different recreational parks are designed with different sundials in mind (Figure 2). Solar watches used in residential gardens are usually designed in simple or detailed form from bronze, brass, iron, stainless steel or other durable, long-lasting materials. Most are bolted onto a stone or on attached bases (URL-4, 2018).

Figure 2. Sundial (URL2)

In Buscot Park, Oxfordshire country cottage, the third public of Lord Faringdon's public use, a special sundial was designed to draw attention to the temporal variability of Buscot Obelisk, the focal point of an Egyptian garden (Figure 3).

Figure 3. Buscot Park sundial (Url-5, 2018)

Sundials, which are mostly seen in parks, can also be created directly in educational institutions using their own shadows (Figure 4).

Figure 4. Human use sundial (Url 6, 2018)

The aim of this study is to examine the effects of the use of aesthetic and functional use of the city clocks in different dimensions of the city in different dimensions of the city in the urban identity and the cultural heritage in the context of Kastamonu city and to determine in which areas the residents of Kastamonu want to use the sundial and that is to design an appropriate sundial.

Material and Method

This study was carried out in order to design a sundial for Kastamonu city in accordance with the preferences of open space users so that the sun clock can be made part of today's city experience. Kastamonu is a city dominated by various civilizations throughout history and dominated by the terrestrial climate in the Western Black Sea region, which houses many different historical monuments. Although there is no information about sundial in the historical information of the city, there is a historical sundial in a mosque on the neighboring town of Safranbolu, Karabük province. Historical and cultural areas such as Nasrullah Square, Cumhuriyet Square, Ismail Bey Complex and Yakup Ağa Complex, which are important places in the past of the city, are attracted to tourism. When you look at the open spaces in the city, it is seen that most of them have similar uses and some monuments are attracting attention. In this study, the user preferences of the sun clocks which can be used in park, square and historical circles in Kastamonu city center were investigated in terms of material, application form and form and a sundial design was tried to be presented in this direction.
In the study, firstly literature researches have been done and examples of sundials used in different fields in the world have been examined. Later, people who had seen Kastamonu before, or who live in this city, had a questionnaire work through Google Form. In the questionnaire study, it was asked which areas they would like to see in their sunshine, which form, application form and material they would prefer, and examples of sun clock design for the area / fields preferred in the obtained information light.

Results

A total of 109 people living in the city of Kastamonu participated in the study and 60.6% (n = 60) of the participants and 39.4% (n = 43) of the participants were male and 51.4% of the participants were between 21 and 30 years of age and 56.9% Those who have undergraduate education. The socio-demographic characteristics of the participants are shown in Table 1. According to Table 1, 38.5% of the participants are less than 5 years old. Kastamonu is also living in 36.7% (n = 40) more than 10 years.

Table 1. Socio-Demographic Structures of Participants

		n	%
gender	female	66	60,5
	male	43	39,4
age	15-20	7	6,4
	21-30	56	51,3
	31-40	28	25,7
	41-50	13	11,9
	50 and over	5	4,6
education	primary education	1	0,9
	pre-license	14	12,8
	license	13	11,9
	graduate	62	56,9
	literate	19	17,47
dwelling	Less than 5 years	42	38,57
	5 years	19	17,47
	10 years	8	7,37
	Over 10 years	40	36,7

In the study, 96.2% (n = 102) of the participants prefer to have the clock in the environment where they have the clock, while 83.3% of the participants (n = 90) say that it is necessary to know the time of day.

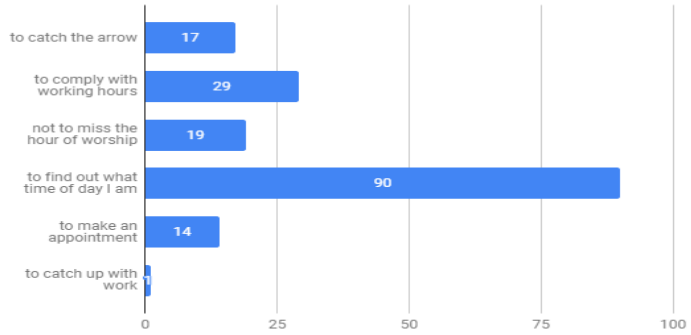

Figure 5. The Need for Time Learner

If you want to see the sundial in Kastamonu city, you will see 82.6% (n = 90) of the participants, 30.3% are mosque courts, 29.4% are in parks, 12.8% are in the school garden and 3.7% they wanted to see in the home garden. The results of the application of the solar hours and the materials are shown in Table 2.

Table 2. Preferred Sun Clock Times for Kastamonu City

		n	%
material	Metal	27	24,8
	bronze	46	42,2
	iron	8	7,3
	rice	24	22,0
	marble	34	31,2
	rock	33	30,3
	wooden	22	20,2
form	horizontal quadrant	21	19,3
	vertical south oriented	6	5,5
	vertical north-oriented	6	5,5
	vertical western oriented	8	7,3
	vertically orientated	6	5,5
	randomly oriented vertical quadrant	6	5,5
	randomly oriented oblique quadrant	15	13,8
	equatorial quadrant	16	14,7
	polar sun clock	15	13,8
	meridian sun clock	10	9,2

According to Table 2, 71.6% (n = 68) of the participants prefered a sundial shape with 52.3% (n = 57) in global form, while 83.5% (n = 91) preferred constant sundial. While 19.3% (n = 21) prefer to use horizontal quartz sundials, 5.5% (n = 6) prefer to see Kastamonu with vertical southward, vertical northward, vertical eastward and randomly oriented vertical quadrants . According to Table 3, it was found that 42.2% (n = 46) of participants were bronze, while 7.3% (n = 8) preferred iron-coated sundials.

Discussion and Conclusions

Many inventions have been produced in order to learn the time, which has been a subject of wonder since the days when human beings existed. Mechanical clocks are still in use today with the progress of technology from the most primitive non-mechanical sun, water and sand clocks. While non-mechanical solar clocks are

used for religious ceremonies in many civilizations, they remain in courtyards or on walls today, with many functions lost and only for visual purposes. In many European cities it is seen that sun clocks are an important symbol of the city in parks and squares, and that many are available. In Mesopotamia, the sun clocks that were built in the regions where the sun was seen for a long time were used in the mosque hunters during the Ottoman period. This study for the sundial suggestion in Kastamonu, one of the settlement areas of the Ottoman Empire, prefered to see the participants in fixed spherical form mostly on the square and on the ground in the sundial preferences. In Nasrullah Square, where the sun clock to be proposed for Kastamonu city is located, Nasrullah Caminin can be positioned on the square in the square as a horizontal quadrant with a fixed bronze material on its floor (Figure 6). Nasrullah Square is an important landmark of the city with its historical background, which is popularly used by the public and shows great interest in tourists.

Figure 6. Suggest Sundial

In this direction, it is necessary to form the form by considering the sundial to be proposed for this place as a cultural heritage item. Sundials, which can address past, present and future, should be assessed in appropriate areas according to the climatic conditions of the city in planning and design work as urban rehabilitation staff.

In this study, it is emphasized that the visual features of the solar clocks, which will be evaluated as one of the city's symbolic texts, as well as the continuity of its usability as a function, must be given to the cities as a heritage item.

References

Gürbüz, M., Aydın, A. H. (2012). Zaman kavramı ve yönetimi.

Dönmez, A., Kabaş, A. (2005). Düzlem Kadranlı Yatay Güneş Saati.

Johnston, R., Anneberg, L. (2002). Sundials Make Interesting Freshman Design Projects. *age*, *7*, 1.

Kabaş, A. (2004). Güneş Saatleri. *Çanakkale Onsekiz Mart Üniversitesi Fen Bilimleri Enstitüsü Fizik Anabilim Dalı, Yüksek Lisans Tezi*, 1-3

Kaplan, D. (2009). Antik Çağ'da Zaman, Konik Güneş Saatleri Ve Smıntheıon Örneği. Anatolia 35.

Korkmaz, A. (2010). *Zamanı ölçen tasarım araçları ve kişisel saatler* (Doctoral dissertation, DEÜ Güzel Sanatlar Enstitüsü).

Salman, B. (2003). Antik Çağda Güneş Saatleri ve Zaman Kavramı. *Dokuz Eylül Üniversitesi Sosyal Bilimler Enstitüsü Arkeoloji Anabilim Dalı, Yüksek Lisans Tezi*

Unat, Y. (2004). İslam'da ve Türklerde Zaman ve Takvim. *Türk Dünyası Nevruz Ansiklopedisi*, 15-25.

Url1. http://www.westernexplorers.us/sundial-designs-skwier-2010.pdf

Url2. https://www.archaeology.org/issues/99-1307/artifact/935-egypt-limestone-sundial-valley-kings

Url3. http://streamla.com/project/great-lawn-park-6th-avenue-sundial/nggallery/thumbnails

Url4. https://www.gardenvisit.com/garden_products/garden_ornaments/sundials_garden

Url5.https://www.gardeningknowhow.com/garden-how-to/design/lideas/using-sundials-in-gardens.htm

Url6. https://www.architecturaldigest.com/story/sir-mark-lennox-boyd-sundials

Url7. https://www.crayola.com/lesson-plans/human-sundial-lesson-plan/

International Conference on Science and Technology

ICONST 2018

5-9 September 2018 Prizren - KOSOVO

Diversity and Biotechnological Potential of Dominated Culturable Bacteria Isolated From Acidic Tea Wastes

Ramazan Çakmakçı[1]*, Atefeh Varmazyari[2]

Abstract: Information about the composition and diversity of the bacterial community characteristics in tea waste is scarce. Functions, production and sustainability of ecosystem depend on the diversity and distribution of the importance of microorganisms in ecological processes. Microorganisms provide the circulation of plant nutrients and convert organic wastes into useful resources. Therefore, it is important to investigate the effect of microorganisms in the composting process and to ensure their use in agriculture. This research was carried out with the aim of developing a bacteria which can be used as a biological fertilizer in plant growing and composting of vegetable wastes by determining its characteristics such as identify, characterization, nitrogen fixation and phosphate dissolution and promoting plant development by isolating Eastern Black Sea region from acidic tea wastes. In order to isolate bacteria, 51 natural tea wastes samples were taken from 17 different localities. It is taken into consideration in the sample, whether the plant grows or not in tea wastes, the decomposition and decay of the wastes, the duration to stay in natural conditions, the color and odor-like parameters. Over 180 bacteria were randomly selected from nitrogen-free solid malate-sucrose and nonselective agar-solidified trypticase soy broth (TSBA) medium, and identified based on fatty acid methyl esters (FAMEs) analysis using the MIDI system. Phosphate solubilization and N_2-fixing activity of the bacterial isolates was detected on NBRIP-BPB and N-free malate sucrose medium, respectively. In the study, 124 bacterial strains were isolated, which belonged to 31 genera and 54 species, from 51 natural tea waste samples from 17 locations, and characterize them for plant growth promoting attributes. Isolated on the basis of nitrogen fixation and phosphate solubilizing activity, the most common cultivated bacterial community from with the tea waste represented 31 different known bacterial genera were *Bacillus* (41.9%), *Pseudomonas* (12.9%), *Paenibacillus* (6.5%), *Stenotrophomonas* (4.8%) and *Burkholderia* (3.2%) genus comprised many different species, with the most abundant being *Bacillus licheniformis, Bacillus pumilus, Bacillus laevolacticus, Pseudomonas fluorescens, Bacillus subtilis, Paenibacillus polymyxa and Pseudomonas putida.* Among the 124 bacterial strains, 103 strains exhibited N_2-fixing activity and 85 were efficient in phosphate solubilisation; 76 strains were efficient in N_2-fixation and P-solubilisation. Investigating the bacterial diversity of tea wastes and evaluating them as composts can provide additional income, increase productivity in tea enterprises and reduce environmental pollution. In this study demonstrated the bacteria isolated from the acidic tea wastes, which have potential industrial applications. With this research, also be able to accelerate composting process, and identified the bacterial population can be used to enrich the compost.

Keywords: Tea waste, Isolation, Nitrogen fixation, Phosphate solubilization, Biodiversity.

Introduction

In recent years, tea factory waste has also gained popularity due to its potential to remove heavy metal pollutants (Wasewar et al., 2008) and to adsorb heavy metals in wastewater has become the focus of attention as well as a very broad application prospects (Febrianto et al.,2009). Tea pruning litter and tea waste are commonly available in and around tea garden. An average of 18 kg of tea is packed for the market and 4 kg of

*[1]Çanakkale Onsekiz Mart University, Faculty of Agriculture, Department of Field Crops, 17100, Çanakkale, TURKEY;
[2]Atatürk University, Faculty of Agriculture, Department of Field Crops, 25240, Erzurum, TURKEY
Corresponding author: rcakmakci@comu.edu.tr

waste are produced from 100 kg of green tea leaves. Tea waste contains a large number of useful components including cellulose, hemicellulose, lignin, polyphenols (such as catechin, epicatechin gallate and epigallocatechin gallate), structural proteins, condensed tannins, amino acids, vitamin, major elements and trace elements and so on (Yamamoto et al., 1997; Kondo et al., 2004; Ng et al., 2013). Also tea leaves contain large amounts of potentially metal-chelating substances (Morikawa and Saigusa, 2008).

In the rhizosphere, plant-microbe associations play critical part in major ecosystem processes. Most of the vast amounts of wastes not dispose generated poises public health concerns and adds strain on diminishing land space in emerging urban centers. Because of the increased production of waste in the world, the source of great concern at different levels of population (Woulters *et al*., 2005); various alternatives are exercised to diminish this increase by elimination, purification and/or recycling it. The modern concept of environmental management is based on the recycling of wastes (Ashraf et al., 2007). In this context, composting appears to be a safe form of treatment of some wastes and the reclamation of the nutrients contained in them (Iranzo et al., 2004). Tea gardens are usually grown as a monoculture and receive considerable amounts of fertilization, root exudates, and leaf litter (Çakmakçı et al., 2010). Since tea pruning litter, leaf litter and tea wastes are not mixed into the soil by composting, they are not effective in nutrition the tea plants. A large quantity of tea leaf waste remains unutilized.

Microorganisms convert organic waste into useful resources and investigation the effect of microorganisms in the composting process is an important issue. Microbial management of organic waste is a promising, environment-friendly approach to manage the large quantities of organic waste due to its recycling potential. Composting is a biotechnological process by which different microbial communities play a key role in biotransformation of complex organic substrates into useful decomposed residues (Patchaye et al., 2018). Previous studies on the composting of agricultural wastes have focussed on the relationship between the microbial diversity or succession and the change in the compost's physicochemical properties (Huang et al 2010; Partanen et al., 2010¸Zainudin et al., 2014).

Knowledge of the true microbial diversity in tea waste is fundamental to effective utilization of this waste. A sustainable efficient way of waste management is needful, to which end, enhanced composting through the employment of appropriate bio preparations offers environmentally safe strategy. One of environment-friendly intervention is effective management of wastes, particularly as it concerns agricultural and food processing wastes. Composting is one of the more economical and environmentally safe methods of recycling waste generated by the consumer society. Although composting is a microbiological process, little is known about microorganisms involved and their activities during specific phases of the composting process (Rebollido et al., 2008). Processing of wastes and prevention of environmental pollution require difficult and expensive methods. Biotechnology is a process that raw materials are converted to new products by living organisms and the composting process of wastes depends on the composition and diversity of the bacterial community characteristics in tea waste.

The simultaneous treatment of different kinds of biomass in the tea industry through composting is a good practice for promoting recycling and zero waste strategies. Investigating the bacterial diversity of tea wastes and evaluating them as composts can provide additional income, increase productivity in tea enterprises and reduce environmental pollution. It is important to use renewable tea waste to maximize crop yields and minimize the environmental hazards. Selection of natural microorganisms which can be used for quality compost production and shortening of composting period and which will be applied to composted material is important for promoting plant nutrition and also for preventing environmental pollution.

Due to the resident microbial community, the active component mediating the biodegradation and conversion processes during composting; optimization of compost quality was directly linked to the composition and

succession of microbial communities in the composting process (Peters et al., 2000). Degradation of wastes and the occurrence or realization of new products requires the use living organisms. Characterizing and understanding of microbial community structure and diversity may provide information needed to improve and evaluate compost processing. Although composting is a microbiological process, little is known about microorganisms involved and their activities of the starting materials in the composting process and during specific phases of the composting process. It has therefore become highly imperative to develop an alternative technique for the needed good quality compost in a shorter period and identify the specific microorganisms promoting plant growth involved in the degradation with the aim of improving the biodegradation process. Therefore, the objective of this study is to isolate and identify PGPR from the tea wastes, and characterize them for N_2-fixation, P-solubilisation.

Material and Method

In order to isolate bacteria, 51 natural tea wastes samples were taken from 17 different localities. It is taken into consideration in the sample, whether the plant grows or not in tea wastes, the decomposition and decay of the wastes, the duration to stay in natural conditions, the color and odor-like parameters. Ten grams of waste from each sample was aseptically weighed and transferred to an Erlenmeyer flask with 100 ml sterile water, and was shaken for 30 min at 150 rpm. Immediately after shaking, a series of ten-fold dilutions of the suspension was made for each sample by pipetting 1 ml aliquots into 9 ml sterile water. The final dilution was 10^5-fold; 0.1 ml of each dilution of the series was placed onto a Petri dish. Three replicate dishes were made for each dilution. Dishes were placed in an incubator at 28°C for seven days (aerobically). Over 180 bacteria were randomly selected from nitrogen-free solid malate-sucrose and nonselective agar-solidified trypticase soy broth (TSBA) medium, and identified based on fatty acid methyl esters (FAMEs) analysis using the MIDI system.

Cells were streaked in a quadrant pattern and grown overnight on TSBA. Approximately 50 mg of bacterial cells, harvested from the third and fourth quadrant streak of growth, were used for the extraction using standard extraction techniques (Çakmakçı et al., 2010). FAME profiles were obtained by running samples on a Hewlett Packard Agilent GC 6890 GC fitted with a microprocessor containing the Sherlock Microbial Identification System (MIDI) Software (V.A. 06. 03). The FAME profiles were compared with the TSBA40 aerobe library. FAME profiles were routinely used to identify genera, species, and strains of bacteria (Caesar-TonThat et al. 2007). Only strains with the similarity index (SIM) ≥0.3 were considered a good match (Oka et al. 2000). The bacterial strains were characterized by morphological, biochemical and physiological tests including pigment production on nutrient agar medium, the Gram reaction, catalase, oxidase, amylase, sucrose, starch hydrolysis, nitrate reduction activities and growth at 36°C on N-free basal medium (Forbes et al. 1998). The identified bacterial strains at the genus level were maintained in nutrient broth (NB) with 30% glycerol at −86°C for further tests.

Phosphate solubilization and N_2-fixing activity of the bacterial isolates was detected on National Botanical Research Institute's phosphate growth medium (NBRIP-BPB) and N-free malate sucrose medium, respectively. For the P-solubilization, 5 ml of NBRIP-BPB medium was transferred to a sterile test tube and autoclaved. Autoclaved, uninoculated broth medium served as controls. The sterile liquid medium was inoculated with 500µl suspension of the tested bacterial strains. The test tubes were incubated for 14 days at room temperature. At the end of the incubation period, change in pH of the culture broth was recorded (Çakmakçı et al., 2010).

Bacteria isolates were selected from N-free solid malateesucrose medium (NFMM) modified from Döbereiner (1989). Modified NFMM medium per liter distilled water (sucrose, 10.0 g; L-malic acid, 5.0 g; $MgSO_4 \cdot H_2O$, 0.2 g; $FeCl_3$, 0.01 g; NaCl, 0.1 g; $CaCl_2 \cdot 2H_2O$, 0.02 g; K_2HPO_4, 0.1 g; KH_2PO_4, 0.4 g; $Na_2MoO_4 \cdot H_2O$,

0.002 g) with 18 g agar for solid medium was used for isolation. The medium adjusted to pH 7.2 with 1 N NaOH prior to agar addition and was then sterilized at 121°C for 20 min in an autoclave (Xie et al., 2003). N-free medium was used in order to obtain nitrogen fixing PGPR (Piromyou et al., 2011; Karagöz et al., 2012).

Results

Most of the N_2-fixing and P-solubilizing bacteria isolated were Gram-positive (55.3 and 58.8%), and Gram-negative constituted only 44.7 and 41.2%. Bacteria belonging to the phylum Firmicutes were found to be predominant in all tea wastes, except in 6 natural tea wastes samples. Based on the fatty acid methyl ester profiles, 31 bacterial genera were identified with a similarity index of >0.3, but 66.1% of the identified isolates belonged to four genera: *Bacillus*, *Pseudomonas*, *Paenibacillus* and *Stenotrophomonas* (Table 1). The most common N_2-fixing and P-solubilizing bacteria associated with tea wastes were *Bacillus* (41.9%) and *Pseudomonas* (12.9%). Based on the FAME profiles, the bacilli group comprised many different species, with the most abundant being *Bacillus licheniformis* (14 strains), *B. cereus* (8 strains), *B. pumilus* (6 strains), *B. laevolacticus* (6 strains), *B. subtilis* (5 strains), and *B. megaterium* (4 strains).

Among the Gram-positive N_2-fixing and P-solubilizing *Firmicutes, Actinobacteria* and *acteroidetes*, 12 isolates of *Bacillus licheniformis*, 6 isolates of *Bacillus pumilus*, 5 isolates of *Bacillus laevolacticus*, 4 isolates each of *Bacillus cereus, Bacillus subtilis*, 3 isolates each of *Paenibacillus polymyxa and Bacillus megaterium*, 2 isolates each of *Bacillus atrophaeus, Bacillus coagulans* and *Micrococcus luteus* and a single isolate of other 7 genera were confirmed as P- solubilizing bacteria. Among the Gram negative N_2-fixing and P-solubilizing Pseudomonas, the dominant ones were *P. fluorescens* (6 strains), followed by *P. putida* (5 strains) and *P. alcaligenes* (Table 1).

Among the other γ-proteobacteria, four isolates of *Stenotrophomonas maltophilia*, 3 isolates each of *Acinetobacter calcoaceticus* and *Proteus vulgaris*, 2 isolates each of *Pseudomonas alcaligenes* and *Photorhabdus luminescens* and single isolate each of *Lysobacter enzymogenes enzymogenes, Stenotrophomonas acidaminiphila, Pseudomonas stutzeri, Cedecea davisae, Hafnia alvei, Rahnella aquatilis, Serratia fonticola* and *Serratia marcescens* were confirmed as nitrogen fixing bacteria. 15 phosphate-solubilizing and/or nitrogen-fixing α- and β-proteobacterial strains were isolated from the waste of tea; 2 isolates each of *Burkholderia cepacia, Burkholderia pyrrocinia* and *Alcaligenes faecalis* and 9 isolates of other genera. The number of cultivable N_2-fixing bacteria expressed as colony-forming units (CFU) ranged between $4.4\pm0.5\times10^5$ and $4.6\pm1.5\times10^7$ CFU g^{-1} dry tea wastes in the sampled the various agro climatic regions in Eastern Black Sea region.

Table 1. Diversity and biotechnological potential of the dominant culturable bacteria from the acidic tea wastes

Taxonomic identification	Order	Bacterial strain FAME identification	Number of isolates*
Alphaproteobacteria	*Rhizobiales*	*Rhizobium radiobacter*	1 (1,1)
		Ochrobactrum anthropi	1 (1,1)
		Phyllobacterium myrsinacearum	1(1,0)
		Methylobacterium mesophilicum	1(ND)
		Methylobacterium radiotolerans	1(ND)
		Roseomonas fauriae	1 (1,1)
	Rhodobacterales	*Paracoccus denitrificans*	1 (1,0)
		Rhodobacter sphaeroides	1(1,0)
Betaproteobacteria	*Burkholderiales*	*Burkholderia cepacia*	2 (2,1)
		Burkholderia pyrrocinia	2 (2,1)
		Alcaligenes faecalis	2 (2,1)
		Acidovorax facilis	1 (0,1)
Gammaproteobacteria	*Xanthomonadales*	*Lysobacter enzyme.. enzymogenes*	1 (1,1)
		Stenotrophomonas acidaminiphila	2 (1,2)

		Stenotrophomonas maltophilia	4 (4,3)
	Pseudomonadales	*Pseudomonas alcaligenes*	2 (2,1)
		Pseudomonas fluorescens	6 (6,6)
		Pseudomonas mucidolens	1(1,0)
		Pseudomonas putida	5 (5,4)
		Pseudomonas pseudoalcaligenes	1 (0,1)
		Pseudomonas stutzeri	1 (1,0)
		Acinetobacter calcoaceticus	3 (3,2)
	Enterobacteriales	*Cedecea davisae*	1 (1,1)
		Hafnia alvei	1 (1,1)
		Photorhabdus luminescens	2 (2,2)
		Proteus vulgaris	3 (3,2)
		Rahnella aquatilis	1 (1,0)
		Serratia fonticola	1 (1,1)
		Serratia marcescens	1 (1,1)
Firmicutes	*Clostridiales*	*Clostridium* sp.	1(1,0)
	Bacillales	*Bacillus amyloliquefaciens*	2 (1,0)
		Bacillus atrophaeus	2 (2,2)
		Bacillus cereus	8 (6,4)
		Bacillus coagulans	2 (0,2)
		Bacillus laevolacticus	6 (5,5)
		Bacillus licheniformis	14 (11,12)
		Bacillus megaterium	4 (3,3)
		Bacillus pumilus	6 (6,6)
		Bacillus thuringiensis	1 (1,0)
		Bacillus thuringiensis israelensis	1 (ND)
		Bacillus thuringiensis kurstaki	1 (ND)
		Bacillus subtilis	5 (5,4)
		Paenibacillus macquariensis	1 (1,1)
		Paenibacillus polymyxa	5 (4,3)
		Paenibacillus validus	2 (2,1)
		Brevibacillus parabrevis	3 (2,1)
		Geobacillus stearothermophilus	1 (1,1)
Actinobacteria	*Actinomycetales*	*Arthrobacter globiformis*	1 (1,1)
		Cellulomonas turbata	1 (1,0)
		Cellulomonas fimi	1 (ND)
		Microbacterium chocolatum	1 (1,1)
		Micrococcus luteus	2 (1,2)
		Rhodococcus erythropolis	1 (1,1)
Bacteroidetes	*Flavobacteriales*	*Flavobacterium johnsoniae*	1(1,0)
No library match			12
Unidentified**			44
Total			180 (103,85)

*Numbers in parentheses indicate the number of N_2- fixing and P-solubilizing strains where bacterial genera were detected, ND: not determined, **Isolates named with a similarity index <0.3

Discussion and Conclusions

This study has shown that tea vaste is an important microbial resource, considering its rich bacterial diversity. Gram-positive bacteria of the genus Bacillus were found in abundance in acidic tea wastes of the present study. Bacilli and other spore-forming bacteria are the predominant culturable bacteria found in tea wastes. The results indicated that N_2-fixing and P-solubilizing *B. licheniformis, B. cereus, B. pumilus, B. laevolacticus, B. subtilis, and B. megaterium* are the dominant bacterial species in tea waste, while *P. fluorescens, P. putida,* and *S. maltophilia* are the dominant Gram-negative bacterial species in tea wastes. The data obtained show a greater abundance of Gram-positive bacteria in the tea wastes, in agreement with previous studies (Xue et al. 2008; Çakmakçı et al., 2010) that show a higher level of Gram-positive *Bacillus* and *Paenibacillus* species in the tea rhizosphere and orchard soil. Several strains of bacilli, mainly species of the genera *Bacillus* and *Paenibacillus*, displaying important plant growth promoting characteristics were isolated from tea wastes. Among the strains isolated in the present study have also been isolated from the rhizosphere as N_2-fixers and/or P-solubilizers (Xie et al., 2003; Poonguzhali et al, 2006; Rau et al., 2009; Çakmakçı et al., 2010; Karagöz et al., 2012). It is

well established that microorganisms play a key role in the composting process as they transform the solid organic material into usable end products such as biomass, CO_2, heat and humus-like. Also end waited in natural conditions for different periods in tea waste products revealed that the both the total number of bacteria and their diversity were clearly related to the different phases of tea wastes. In this study demonstrated the bacteria isolated from tea wastes in the natural environment, which have potential industrial applications. With this research, also be able to accelerate composting process, and identified the bacterial population can be used to enrich the compost. Thus, these results should be effective measures for future in using tea garden waste materials for the preparation of valued eco-friendly compost. This will be helpful to prepare eco-friendly compost and its application for sustainable tea cultivation.

References

Ashraf, R., Shahid, F., Ali, T.A. (2007). Association of fungi, bacteria and actinomycetes with different composts. Pakistan Journal of Botany, 39, 2141-2151.

Caesar-TonThat, T.C., Caesar, A.J., Gaskin, J.F., Sainju, U.M., Busscher, W.J. (2007). Taxonomic diversity of predominant culturable bacteria associated with microaggregates from two different agroecosystems and their ability to aggregate soil in vitro. Applied Soil Ecology, 36, 10–21.

Çakmakçı, R., Dönmez, M.F., Ertürk, Y., Erat, M., Haznedar, A., Sekban, R. (2010). Diversity and metabolic potential of culturable bacteria from the rhizosphere of Turkish tea grown in acidic soils. Plant and Soil, 332 (1-2), 299-318.

Döbereiner, J. (1989). Isolation and identification of root associated diazotrophs, in: F.A. Skinner (Ed.), Nitrogen Fixation with Non-Legumes, Kluwer Academic Publishers, Dordrecht, Boston, London, 103-108.

Febrianto, J., Kosasih, A.N., Sunarso, J., Ju, Y.H., Indraswati, N., Ismadji, S. (2009). Equilibrium and kinetic studies in adsorption of heavy metals using biosorbent: a summary of recent studies. The Journal of Hazardous Materials, 62, 616–645.

Forbes, B.A., Sahm, D.F., Weissfeld, A.S. (1998). Bailey and Scott's diagnostic microbiology, 11th edn. Mosby Inc, St. Louis, p 1068.

Huang, D.L., Zeng, G.M., Feng, C.L., Hu, S., Lai, C., Zhao, M.H., Su, F.F., Tang, L., Liu, H.L (2010). Changes of microbial populations structure related to lignin degredation during lignocellulosic waste composting. Bioresource Technology, 101, 4062-4067.

Iranzo, M., Canizares, J.V.. Roca-Perez, L., Sainz-Pardo, I., Mormeneo, S., Boluda, R. (2004). Characteristic of rice straw and sewage sludge as composting materials in Valencia (Spain). Bioresource Technology, 95(1), 107-112.

Wasewar, K.L., Atif, M., Prasad, B., Indra Mani Mishra, I.M. (2008). Adsorption of zinc using tea factory waste: kinetics, equilibrium and thermodynamics. Clean, 36, 320- 329.

Karagöz, K., Ateş, F., Karagöz, H., Kotan, R., Çakmakçı, R. (2012). Characterization of plant growth-promoting traits of bacteria isolated from the rhizosphere of grapevine grown in alkaline and acidic soils. European Journal of Soil Biology, 50, 144-150.

Kondo, M., Kita, K. and Yokota, H. (2004). Effects of tea leaf waste of green tea, oolong tea, and black tea addition on sudangrass silage quality and in vitro gas production. Journal of the Science of Food and Agriculture, 84, 721-727.

Morikawa, C. K., Saigusa M. (2008). Recycling coffee and tea wastes to increase plant available Fe in alkaline soils. Plant and Soil, 304,249–255.

Ng, I.S., Wu, X.O., Yang, X.M., Xie, Y.P., Lu, Y.H., Chen, C. (2013). Synergistic effect of Trichoderma reesei cellulases on agricultural tea waste for adsorption of heavy metal Cr (VI). Bioresource Technology, 145, 297–301.

Oka, N., Hartel, P.G., Finlay-Moore, O., Gagliardi, J., Zuberer, D.A., Fuhrmann, J.J., Angle, J.S., Skipper, H.D. (2000). Misidentification of soil bacteria by fatty acid methyl ester (FAME) and BIOLOG analyses. Biology and Fertility of Soils, 32, 256–258.

Partanen, P., Hultman, J., paulin, L., Auvenin, P., Romantschuk, M. (2010). Bacterial diversity at different stage of the composting process. BMC Microbiolooogy, 10, 94.

Patchaye, M., Sundarkrishnan, B., Tamilselvan, S., Sakthivel, N. (2018). Microbial management of organic waste in agroecosystem. In: Panpatte D., Jhala, Y., Shelat, H., Vyas, R. (Eds), Microorganisms for Green Revolution. Microorganisms for Sustainability, vol. 7. 45-73, Springer, Singapore.

Peters, S., Koschinsky, S., Schwieger, F., Tebbe, C.C. (2000). Succession of microbial communities during hot composting as detected by PCR–single-strand-conformation polymorphism-based genetic profiles of small-subunit rRNA genes. Applied and Environmental Microbiology, 66, 930-936.

Piromyou, P., Buranabanyat, B., Tantasawat, P., Tittabutr, P., Boonkerd, N., Teaumroong, N. (2011). Effect of plant growth promoting rhizobacteria (PGPR) inoculation on microbial community structure in rhizosphere of forage corn cultivated in Thailand. The European Journal of Soil Biology, 47, 44-54.

Poonguzhali, S., Madhaiyan, M., Sa, T. (2006). Cultivation-dependent characterization of rhizobacterial communities from field grown Chinese cabbage *Brassica campestris* ssp *pekinensis* and screening of traits for potential plant growth promotion, Plant and Soil, 286, 167-180.

Rau, N., Mishra, V., Sharma, M., Das, M.K., Ahaluwalia, K., Sharma, R.S. (2009). Evaluation of functional diversity in rhizobacterial taxa of a wild grass (*Saccharum ravennae*) colonizing abandoned fly ash dumps in Delhi urban ecosystem, Soil Biol. Biochem. 41, 813-821.

Rebollido, R., Martínez, J., Aguilera, Y., Melchor, K., Koerner, I.., Stegmann, R. (2008). Microbial populations during composting process of organic fraction of municıpal solid waste. Applied Ecology and Environmental Research, 6(3), 61-67.

Wouters, I.M., Spaan, S., Douwes, J., Doekes, G., Heederik, D. (2005). Overview of personal occupational exposure levels to inhale dust, endotoxin, β (1-3)-glucan and fungal extracellular polysaccharides in the waste management chain. Annals of Occupational Hygiene, 47, 1-15.

Xie, G.H., Cai, M.Y., Tao, G.C., Steinberger, Y. (2003). Cultivable heterotrophic N_2-fixing bacterial diversity in rice fields in the Yangtze River Plain. Biology and Fertility of Soils, 37, 29-38.

Xue, D., Yao, H.Y., Ge, D.Y., Huang, C.Y. (2008). Soil microbial community structure in diverse land use systems: a comparative study using Biolog, DGGE, and PLFA analyses. Pedosphere, 18, 653–663.

Yamamoto, T., Juneja, L.R., Chu, D.-C., Kim, M. (1997). Chemistry and applications of green tea, CRC Press, Florida, USA.

Zainudin, M.H.M., Hassan, M.A., Shah, U.K.M., Abdullah, N., Tokura, M., Yasueda, H., Shirai, Y., Sakai, K., Baharuddin, A.S. (2014). Bacterial community structure and biochemical changes associated with composting of lignocellulosic oil palm empty fruit bunch. Bio Resources, 9, 316-335.

International Conference on Science and Technology

ICONST 2018

5-9 September 2018 Prizren - KOSOVO

Influence of a Plant Growth-Promoting Rhizobacteria on Birdsfoot Trefoil Growth

Ramazan Çakmakçı[1]*, Halit Karagöz[2], Fırat Alatürk[1], Baboo Ali[1], Ahmet Gökkuş[1]

Abstract: Birdsfoot trefoil hay is the important for fodder components of feed to dairy and farm animals. It is a potentially valuable forage species for grassland agriculture, and adapts well to less suitable growing areas. Organic farming and the use of microorganisms in agriculture are becoming a major tool for sustaining the soil quality degraded by intensive use of synthetic chemicals for increasing crop production. Therefore, use of plant growth promoting rhizobacteria (PGPR) as biofertilizers is an integral part of sustainable farming, hold promising future for agriculture and obtain importance in forage-type grasses.This study was conducted with birdsfoot trefoil *(Lotus corniculatus* cv. Leo) in greenhouse conditions in order to investigated inoculation with 4 different N_2-fixing and P-solubilizing bacterial species (*Bacillus megaterium* RC3D, *Paenibacillus polymyxa* RC12, *Pantoea agglomerans* RC58, and *Bacillus subtilis* RC63) in in comparison to control and mineral fertiliser (40 mg N and 30 mg P kg^{-1} soil) application. The experiment was arranged as a completely randomized design with seven treatments and five replicates (each having ten seedlings). The experiment was repeated twice. For this experiment, pure cultures were grown in 50% strength tryptic soy broth on a rotary shaker (120 rpm; 25 °C) for 3 days. Bacteria were then harvested by centrifugation (ca. 3000 x g for 10 min), washed and re-suspended in 10 mM sterile phosphate buffer (SPB), pH 7 to a density of 10^9 cfu ml^{-1} for the bacterial strains. The single bacterial inoculation involved dipping the root system of the seedling into a suspension of each PGPR strains for 60 min, prior to planting. Inoculation of birdsfoot trefoil seedling with RC3D, RC12, RC58, and RC63 increased aerial dry weight per plant by 7.1, 10.0, 21.3 and 22.7% as compared to the control, plant height by 6.7, 9.9, 18.2 and 21.2%, and root dry weight by 11.0, 15.1, 19.9 and 21.3%, respectively. N and P application increased plant height, aerial and root dry weight up to 16.7 and 12.6%, 16.8 and 16.2%, and 12.4 and 15.6%, respectively. Except for PGPR strains RC3D and RC12, other treatments significantly increased fresh and dry weight aerial part of per plants.The experiment revealed that the PGPR inoculation, and N and P supply were an effective treatment to improve the parameters measured of birdsfoot trefoil, especially with reference to the increase in dry weight of both the root system and the upper plant parts. Of the effective bacteria tested consistently gave growth, and total biomass yields equal to chemical fertilizes applied. PGPR strains tested have a potential to be used as a bio-fertilizer in the sustainable and environmentally friendly birdsfoot trefoil production

Keywords: Plant growth-promoting rhizobacteria, Hay weight, Birdsfoot trefoil, Root dry weight.

Introduction

Lotus corniculatus (bird's-foot trefoil) is a potentially valuable species for grassland agriculture. Bird's foot trefoil species are an important perennial leguminous plant which can be utilized in forage production due to its high agronomic properties. It is a perennial legume, natural tetraploid, cross-pollinated, and with a taproot (Grant and Niizeki, 2009) that gives it the capacity to adapt to soils with poor drainage in winter and restricted water supply in summer. Due to its wide adaptability, high nutritional value and resistance to grazing, extreme heat, cold, humid conditions, and poor and acidic soils, it is an important forage plant which can be used as for

[1]Çanakkale Onsekiz Mart University, Faculty of Agriculture, Department of Field Crops, 17100, Çanakkale, TURKEY.
[2]Atatürk University, Faculty of Agriculture, Department of Field Crops, 25240, Erzurum, TURKEY.
*Corresponding author: rcakmakci@comu.edu.tr

pasture, hay, silage, pasture rehabilitation and forage crops agriculture. Birds foot trefoil is a valuable forage crop because it adapts well to less suitable growing areas where Gramineae predominate and where alfalfa and others legumes do not grow (Agnusdei, 1991; Leon & Bertiller, 1982). It is therefore, the most suitable legume for enhancing soil nitrogen, and is also highly digestible, with a forage quality comparable to alfalfa and white clover (Beuselinck and Grant, 1995; Clua et al., 2012). Birdsfoot trefoil thrives in the same soils and climate favored by alfalfa, but is more tolerant of low fertility, especially phosphorus, low pH, and poorly drained soils than alfalfa, and it also holds its quality better compared too many other legumes (Brummer et al., 2016). It has the capacity to efficiently absorb P in conditions of low P and water supply (Russelle et al., 1991) and to adapt to soils that are marginal for growing other crops. Also, bird's foot trefoil is preferred to alfalfa for its higher tolerance to unsutitable environmental conditions, and resistance to cuscuta attacks (Nicolic ve ark., 1997, 2006; Raikar et al. 2008; Aydın et al., 2009). In recent studies, Lotus spp. were shown to possess a great potential to adapt to a number of abiotic stresses, making them suitable candidates for phytoremediation of degraded environments (Escaray et al. 2012; Yousaf et al. 2010a, b). Living mulches of *L. corniculatus* are permanent cover crops that can fix atmospheric N and improve soil quality **(**Duiker and Hartwig, 2004**).** Research with *Lotus* species has shown relatively high levels of forage production in low-input systems (Hopkins et al., 1996). Also *Lotus corniculatus* is a early-succession plant, pioneering the colonization of post-mining landscapes (Felderer et al 2013), and takes important place in grass-legume mixtures for establishing artificial grasslands in the hilly-mountainous regions (Petrović et al., 2011).

The two temperate forage legumes containing condensed tannins that promote ruminant production are birdsfoot trefoil and sainfoin (MacAdam and Villalba, 2015). Birds foot trefoil is a high quality forage and a legume containing condensed tannin that does not cause bloat in ruminants when freshly grazed as green, it is include the potential to decrease ruminal protein degradation through binding protein and to reduce ruminal methane production (Heuzé et al., 2016; Christensen et al., 2017). Also condensed tannins, present in birds foot, have benefited ruminant animal nutrition through protein protection and thus preventing formation of the stable foam which causes bloat and decrease suppression of internal parasites loads and enteric methane anv ammonia emissions (MacAdam and Villalba, 2015; Reynolds et al., 2005). Also they prevent bloat by binding to and precipitating proteins, which reduces protein concentration in the rumen and increases rumen bypass or "undegradable" protein (Barry et al., 1986). Birdsfoot trefoil also contains higher concentrations of non-fibrous carbohydrates than alfalfa (MacAdam and Griggs, 2013), meaning that its ratio of protein-to carbohydrates is more evenly matched for better ruminant nutrition (Brummer et al., 2016). *Lotus* species are normally used to improve the quality of pastures because of their high content of condensed tannins.

Changing from a conventional livestock production system, based on fertilized grass swards, to an organic management system requires the establishment of legume-based swards to replace the purchased fertilizer nitrogen. In this context, the lotus can produce higher profits than grass-based systems using high levels of nitrogen fertilizer, as are potential plants such as red clover, white clover, lucerne and galega (Doyle and Topp, 2004). Strongly developed root system of birdsfoot trefoil binds well and protects soil against erosion, and takes significant place in sustainable agricultural and organic production (Tomić et al., 2007).

Also, high use of inorganic N and other fertilizers on grasslands contribute primarily to a number of environmental problems such as emissions of N to the environment and pollution of surface and ground water, runoff and leaching to contaminate the atmosphere and water bodies, deterioration of soil structure and fertility, consumption of fossil fuels and greenhouse gas emissions associated with fertilizer manufacture and its distribution and application. In view of the continuing increase in cost and scarcity of mineral fertilizers resulting from the use of high-cost fossil energy, there is renewed interest in organic recycling and biological nitrogen-fixation to improve soil fertility and productivity. On the other hand, nitrogen fertilizers increase the growth of legume crops but considerably reduce the amount of nitrogen fixed, and the innovative view of agricultural production attracts the growing demand of biological fertilizers exclusive of alternative to agro-chemicals. And also, organic management system requires the establishment of legume-based swards to replace the purchased fertilizer nitrogen. Plant-associated N_2-fixing and P-solubilizing bacteria are regarded as a possible alternative to inorganic nitrogen fertilizers, and PGPR strains have previously attracted the attention of agriculturists as soil inoculums to improve plant growth and yield (Şahin et al., 2004, Çakmakçı et al., 2006, 2014; Bhattacharyya and Jha, 2012; Chauhan et al., 2015; Maksimov et al., 2015). Therefore, a study was

conducted in order to investigate the effect of single inoculations with N_2-fixing and P-solubilizing bacterial species on birdsfoot trefoil *(Lotus corniculatus* cv. Leo) growth.

Material and Method

This study was conducted with birdsfoot trefoil *(Lotus corniculatus* cv. Leo) in greenhouse conditions in order to investigated inoculation with 4 different N_2-fixing and P-solubilizing bacterial species in comparison to control and fertiliser application. The experiment was arranged as a completely randomized design with seven treatments and five replicates (each having ten seedlings). The following treatments with five replicates were investigated: (1) control (without bacteria inoculation and mineral fertilizers), (2) N fertilizer (40 mg N kg^{-1} soil), (3) P fertilizer (30 mg P kg^{-1} soil), (4) *Bacillus megaterium* RC3D, (5) *Paenibacillus polymyxa* RC12, (6) *Pantoea agglomerans* RC58 and (7) *Bacillus subtilis* RC63, The pots were arranged in a completely randomized factorial design in the greenhouse. For this experiment, pure cultures were grown in 50% strength TSB on a rotary shaker (120 rpm; 25 °C) for 3 days. Bacteria were then harvested by centrifugation (ca. 3000 x g for 10 min), washed and re-suspended in a 10 mM sterile phosphate buffer (SPB) pH 7 to a density of 10^9 cfu ml^{-1} for thebacterial strains. The bacterial inoculation involved dipping the root system of the saplings into a suspension of each PGPR strain for 60 min, prior to planting. Control plants received 5 ml of diluted SPB with no bacteria.

Birds foot trefoil seeds were germinated in a seed trays containing garden soil/peat/sandy (2:1:1 [v/v]) at 24±5°C with 60% relative humidity, with 16 h day, and 8 h night conditions in greenhouse. Seedlings were removed from seed trays after one month. Prior to planting, the root system of the seedlings was dipping into a suspension of each PGPR strain for 60 min. İn 5 ml diluted SPB without bacteria, control plants stayed. Later three uniform 30-day-old inoculated seedlings were transferred into each pots containing virgin garden soil, and seedlings were thinned to one after 2 weeks. All plants were grown in a greenhouse under a day/night cycle of 16/8 h natural light and 60/70% relative humidity. Watered pots up to 60% water holding capacity were maintained at this moisture content by watering to weight every 4 d. Weed control was done by hand when required. About 110 days after planting, the birdsfoot trefoil plants were harvested. At harvest, the following were measured: plant height, root and aerial fresh and dry weights, obtained by drying the plant matter in an oven at 80ºC until their weight became constant.

Results

Of the 7 treatments, the maximum aerial fresh and dry weight in birdsfoot trefoil was seen in *Bacillus subtilis* RC63 inoculation, followed by *Pantoea agglomerans* RC58, N fertilizer, and P fertilizer. In this study, inoculation with *Bacillus megaterium* RC3D and *Paenibacillus polymyxa* RC12 bacteria had no significant effect on aerial fresh and dry weight in birdsfoot trefoil compared with control. Differences in terms of aerial dry weight were, however, not significant between *Paenibacillus polymyxa* RC12 and *Bacillus megaterium* RC3D inoculation with control. Among the treatments tested, inoculation with *Bacillus subtilis* RC63 and *Pantoea agglomerans* RC58 bacterial strains and NPK fertilizer application increased aerial fresh weight, earial dry weight and root dry weight of birds foot trefoil plants signifcantly compared with the control; the maximum yield and growth parameters in this plant found with the *Bacillus subtilis* RC63 inoculations (Table 1). Plant growth promoting bacterial inoculation and mineral fertilizer applications increased root fresh and dry weight compared wit uninoculated control, whereas there were no significant differences in root weight between inoculation and fertilizer treatments. Inoculation with N2-fixing *Bacillus subtilis* RC63 and *Pantoea agglomerans* RC58, and application N fertilizer significantly increased plant height by birdsfoot trefoil plants compared to the uninoculated control. In contrast, there was no significant difference in the plant height among the other treatments.

Table 1. Effect of plant growth promoting bacteria and mineral fertilizer on root and aerial weight and plant height on *Lotus corniculatus* plants, 110 days after sowing

Treatments*	Aerial fresh weight**	Aerial dry weight	Root fresh weight	Root dry weight	Plant height (cm)
Control	34.0±3.0 c	8.85±0.78 c	10.59±0.82 c	3.17±0.26 b	24.5±2.1 c
N fertilizer	39.6 ±3.4 ab	10.33± 1,8 ab	10.93± 1.48 bc	3.56± 0.18 a	28.5± 3.4 ab
P fertilizer	39.5 ±3.2 ab	10.28±0.91 ab	12.20 ±1.03 a-c	3.66 ±0.31 a	27.5 ±2.5 a-c
B. megaterium RC3D	36.5 ±3.8 bc	9.48±0.99 bc	11.47±1.71 a-c	3.52±0.30 ab	26.1±2.7 bc
P. polymyxa RC12	37.4±3.7 a-c	9.73±0.97 a-c	12.48±1.54 a-c	3.64±0.31 a	27.1±2.7 a-c
P. agglomerans RC58	41.5± 3.9 a	10.73±1.01 ab	11.96±1.50 ab	3.80±0.38 a	28.9±2.8 ab
B. subtilis RC63	41.6±2.5 a	10.86±0.43 a	13.07± 1.60 a	3.84± 0.13 a	29.7± 1.4 a

*Control: without bacteria inoculation or mineral fertilizers; N fertilizer (40 mg N kg^{-1} soil), P fertilizer (30 mg P kg^{-1} soil); **Values are means ±SE; averages of the same column values (each section separately) followed by the same letter did not differ significantly in Duncan's multiple range tests at 0.05% significance

Discussion and Conclusions

Greenhouse trials showed that treatments including bacterial strains and fertilizer application signi¿cantly affected the parameters investigated compared with the control, depending on strains, N and P fertilizers and growth parameter evaluated. The early growth and development of bird's foot trefoil is slow in control and seedling vigor is poor and establishment of new stands is difficut. All bacterial inoculations caused significant differences on the tested plant parameters such as root and shoot dry weight a plant height, with respect to the control, and these parameters of plants inoculated with the nitrogen fixing and phosphate solubilizing bacteria were equal to those of plants receiving N and P fertilizers. The screening of rhizobacteria that show multiple plant growth-promoting traits such as IAA production, P solubilization, and N_2 fixation suggests that they have good potential for testing and applications in improving the growth *Lotus corniculotus.* It is particularly interesting that shoot and root weight, and plant height of bird's-foot trefoil grown was significantly enhanced by PGPR equal to or higher than N and P applied plots. Inoculation with P-solubilizing bacteria increased the root and shoot development in Lotus corniculatus equally close to mineral N and P applications. Although it is well known that phosphorus fertilization improves the competitive ability of legumes, *Lotus corniculatus* has demonstrated a greater response to lower doses P and P-solubilizing bacteria. These findings were very important in that they showed that this plant could be grown without the use of P and N fertilizers, using the bacteria tested in this study.

The phenotypic in vitro characterization presented in this paper highlighted significant differences in terms of shoot and root growth performances in bird's-foot trefoil grown in different mixed IAA-producing, N_2-fixing, and/or P-solubilizing bacteria. Treatment of *Lotus corniculatus* seeds by nitrogen-fixing and phosphate-solubilizing bacteria in saline environment stimulated germination rate and increased growth and length of seedlings, and caused favorable effect on population of agrovaluable microbial species (Aleschenkova et al., 2017). Root-colonizing growth-promoting rhizobacteria *Pseudomonas putida* increased birdsfoot trefoil plant growth, shoot mass and nodulation (Staley et al., 1992). Phosphorus fertilization improves the implantation and competitive ability of legumes. *L. corniculatus* has been shown to respond better to lower doses of phosphorus than other legume species, such as *Trifolium pratense* (Ayala Torales et al., 1992). An increased phosphorus absorption per unit of root biomass has been already reported for *Lotus corniculatus* (Valkov and Chiurazzi, 2016**).** Phosphate fertilization may also increase cool-season grass production by promoting the density of herbaceous legumes *Lotus tenuifolius* and *Trifolium repens* that enrich soil nitrogen through fixation (Suttie et al., 2005). Dry weight of the *Lotus* cultivars after sowing was significantly increased by increasing levels of phosphorus, and also condensed tannin content of perennial in *L. corniculatus* (Kelman 2006). Pasture

legumes have a relatively high requirement for phosphorous and normally adequate application of phosphate fertilizer is a primary requirement for legumes to succeed (Valkov and Chiurazzi, 2016**).** The ability to respond to locally increased P availability with enhanced root proliferation has been shown that low soil P was limiting the growth of L. corniculatus in the unfertilized soil and responds with root proliferation into P-enriched soil (Felderer et al., 2013). However, to fully exploit the potential benefits of introducing pasture-based grass-legume systems, an increased scientific knowledge of biological fertilizers and useful microorganisms and legume agronomy for screening of favourable traits is needed. Thus, the growth and yield parameters of bird's-foot trefoil could be enhanced by PGPR treatment due to high nutritive value combined with ruminant-friendly tannins will support livestock production without risk of bloat, while it fixes nitrogen to increase production in the entire pasture.

References

Agnusdei, M. (1991). Análisis de gradiente de vegetación, suelo y uso en pastizales de áreas bajas de la depresión del Salado. *Tesis M Sc*. Facultad de Ciencias Agrarias, UNMdP.

Aleschenkova, Z, Naumovich, N., Uladzislau, K. (2017). Nitrogen-fixing and phosphate-solubilizing bacteria resistant to technogenic soil salinization. 4th World Congress and Expo on Applied Microbiology, November 29-December 01, 2017 Madrid, Spain, Journal of Microbial & Biochemical Technology, 9,6.

Ayala Torales, A., Acosta, G., Deregibus, V., Cabrini, S. (1992). Efectos de la modalidad de defoliación y de la fertilización fosforada en pasturas integradas por *Lotus corniculatus L*. Revista Argentina de Producción Animal, 15(1), 77-80.

Aydın, M., Haliloğlu, K., Uysal, P., Tosun, M., Şahin, E. (2009). Micpropagation of Birds Foot Trefoil (*Lotus Corniculatus* L.) under *In Vitro* Conditions. Türkiye VIII Tarla Bitkileri Kongresi Bildiriler Kitabı Cilt 2, 19-22 Ekim,753-756.

Barry, T.N., Manley, T.R. (1986). Interrelationships between the concentrations of total condensed tannin, free condensed tannin and lignin in Lotus sp. and their possible consequences in ruminant nutrition. The Journal of the Science of Food and Agriculture, 37, 248–254.

Beuselinck, P. R., & Grant, W. F. (1995). Birdsfoot trefoil. Forages and Introduction to Grassland Agriculture, 1, 237-248.

Bhattacharyya, P, Jha, D. (2012). Plant growth-promoting rhizobacteria (PGPR): emergence in agriculture. World Journal of Microbiology and Biotechnology, 28(4), 1327–1350.

Brummer, J.E., MacAdam, J.W., Shewmaker, G., Islam, M.A. (2016). Establishing Birdsfoot Trefoil in the Mountain West. Utah State University, Plants, Soils and Climate, September 2016 Bulletin 1.

Cakmakci, R, Turan, M, Gulluce, M, Sahin, F. (2014). Rhizobacteria for reduced fertilizer inputs in wheat (*Triticum aestivum* spp. *vulgare*) and barley (*Hordeum vulgare*) on Aridisols in Turkey. International Journal of Plant Production, 8,163-182.

Chauhan, A., Shirkot, C., Kaushal, R., Rao, D. (2015). Plant growth-promoting rhizobacteria of medicinal plants in NW Himalayas: Current Status and Future Prospects. Plant-GrowthPromoting Rhizobacteria (PGPR) and Medicinal Plants: Chapter 19. Soil Biology, Springer International Publishing Swetzerland, 381–412.

Christensen, R.G., Eun, J.-S., Yang, S.Y., Min, B.R., MacAdam, J.W. (2017). In vitro effects of birdsfoot trefoil (*Lotus corniculatus* L.) pasture on ruminal fermentation, microbial population, and methane production, The Professional Animal Scientist, 33, 451–460.

Clua, A., Conti, M., Beltrano, J. (2012). The Effects of glyphosate on the growth of birdsfoot trefoil (*Lotus corniculatus)* and its interaction with different phosphorus contents in soil. Journal of Agricultural Science, 4 (7), 208-218.

Çakmakçı, R., Dönmez, F., Aydın, A., Şahin, F. (2006). Growth promotion of plants by plant growth-promoting rhizobacteria under greenhouse and two different field soil conditions. Soil Biology & Biochemistry, 38 (6), 1482-1487.

Doyle, C.J., Topp, C.F.E. (2004). The economic opportunities for increasing the use of forage legumes in north European livestock systems under both conventional and organic management. Renewable Agriculture and Food Systems, 19,15-22.

Duiker, S.W., Hartwig, N.L. (2004). Living mulches of legumes in imidazolinone-resistant corn. Agronomy Journal, 96, 1021-1028.

Escaray, F.J., Menendez, A.B., Garriz, A., Pieckenstain, F.L., Estrella, M.J., Castagno, L.N., Carrasco, P., Sanjuan, J., Ruiz, O.A. (2012). Ecological and agronomic importance of the plant genus *Lotus*. Its application in grassland sustainability and the amelioration of constrained and contaminated soils. Lant Science, 182,121–133

Felderer, B., Boldt-Burisch, K. M., Schneider, B. U., Hütll, R.F.J., Schulin, R. (2013). Root growth of *Lotus corniculatus* interacts with P distribution in young sandy soil. Biogeosciences, 10, 1737–1749.

Grant, W. F., Niizeki, M. (2009). Birdsfoot trefoil *(Lotus corniculatus* L.) Chapter 6. p. 153-205. In Singh, R.J. (ed.), Genetic Resources, Chromosome Engineering, and Crop İmprovement: Forage Crops. CRC Press, Boca Raton, Florida, USA.

Heuzé V., Tran G., Nozière P., Lebas F. (2016). Birdsfoot trefoil (*Lotus corniculatus*). Feedipedia, a programme by INRA, CIRAD, AFZ and FAO. https://www.feedipedia.org/node/280 last updated on February 8, 2016, 13:52.

Hopkins A., Martyn T.M., Johnson R.H., Sheldrick R.D., Lavender R.L. (1996). Forage production by two Lotus species as influenced by companion grass species. Grass and Forage Science, 51, 343–349.

Kelman, W.M. (2006). The interactive effects of phosphorus, sulfur and cultivar on the early growth and condensed tannin content of greater Lotus (*Lotus uliginosus*) and birdsfoot trefoil (*L. corniculatus*). Australıan Journal of Experımental Agrıculture, 46, 53-58.

Leon, R. J. C., Bertiller, S. (1982). Aspectos fenológicos de dos comunidades de un pastizal de la Depresión del Salado (provincia de Buenos Aires). Boletin de la Sociedad Argentina de Botanica, 20(3-4), 329-347.

MacAdam, J.W., Villalba, J.J., 2015. Beneficial Effects of Temperate Forage Legumes that Contain Condensed Tannins Agriculture, 5, 475-491.

MacAdam, J.W.; Griggs, T.C. (2013). Irrigated Birdsfoot Trefoil Variety Trial: Forage Yields; Utah State University Cooperative Extension Service: Logan, UT, USA.

Maksimov, I, Veselova, S, Nuzhnaya, T, Sarvarova, E, Khairullin, R. (2015). Plant growth-promoting bacteria in regulation of plant resistance to stress factors. Russian Journal of Plant Physiology, 62(6), 715–26.

Nicolic, R., Mitic, N., Ninkovic, S., Neskovic, M. (1997). Evaluation of agronomic traits in tissue culture derived progeny of bird's _foot trefoil. Plant Cell, Tissue and Organ Culture, 48, 67-69.

Nikolic, R., Mitic, N., Miletic, R., Neskovic, M. (2006). Effects of cytokinins on in vitro seed germination and early seedling morphogenesis in *Lotus corniculatus* L. The Journal of Plant Growth Regulation, 25(3), 187-194.

Petrović, S., Vučković, S., Simić, A., 2011. Stand densıty effects on bırdsfoot trefoıl herbage yıeld grown for combıned usage. Biotechnology in Animal Husbandry 27 (4), 1523-1530.

Raikar, S.V, Braun, R. H., Bryant, C., Conne,r A.J., Christey, M.C. (2008). Efficient isolation, culture and regeneration of *Lotus corniculatus* L protoplasts. Plant Biotechnology Reports, 2, 171-177.

Reynolds, S.G., Suttie, J.M., Staberg, P. (2005). Country Pasture Profiles, CDROM, FAO, Rome, Italy.

Russelle, M., McGraw, R., Leep, R. (1991). Birdsfoot trefoil response to phosphorous and potassium. Journal of Production Agriculture 4,114-120.

Staley, T.E., Lawrence, E.G., Nance, E.L. (1992). Influence of a plant growth-promoting pseudomonad and vesicular-arbuscular mycorrhizal fungus on alfalfa and birdsfoot trefoil growth and nodulation. Biology and Fertility of Soils, 14,175-180.

Suttie, J.M., Reynolds, S.G., Batello, C. (2005). Grasslands of the World. Food and Agriculture Organization of the United Nations ROME.

Şahin, F., Çakmakçı, R, Kantar, F. (2004). Sugar beet and barley yields in relation to inoculation with N_2-fixing and phosphate solubilizing bacteria. Plant and Soil, 265 (1-2), 123-129.

Tomić, Z., Lugić, Z., Radović, J., Sokolović, D., Nešić, Z., Krnjaja, V. (2007). Perennial legumes and grasses stable source of quality livestock fodder feed. Biotechnology in Animal Husbandriy, 23, 559-572.

Valkov, V.T., Chiurazzi, M. (2016). An in vitro procedure for phenotypic screening of growth parameters and symbiotic performances in *Lotus corniculatus* cultivars maintained in different nutritional conditions. Plants 5, 40, 1-11.

Yousaf, S., Andria, V., Reichenauer, T.G., Smalla, K., Sessitsch, A. (2010a). Phylogenetic and functional diversity of alkane degrading bacteria associated with Italian ryegrass (*Lolium multiflorum*) and Birdsfoot trefoil (*Lotus corniculatus*) in a petroleum oil-contaminated environment. The Journal of Hazardous Materials, 184 (1-3), 523–532

Yousaf, S., Ripka, K., Reichenauer, T.G., Andria, V., Afzal, M., Sessitsch, A., (2010b). Hydrocarbon degradation and plant colonization by selected bacterial strains isolated from Italian ryegrass and birdsfoot trefoil. Journal of Applied Microbiology, 109 (4), 1389–1401.

International Conference on Science and Technology

ICONST 2018

5-9 September 2018 Prizren - KOSOVO

An Investigation About Performance Properties of Camouflage Fabrics

Merdan Arnaovezov[1], Ayşe Merih Sarıışık[1], Gizem Ceylan Türkoğlu[1]*

Abstract: The production of technical textiles is becoming widespread with developments on technology and electronics. The military clothing and equipment in technical textiles have great importance in terms of their protective features. Recent developments have forced soldiers to wear camouflage uniforms. Properly selected camouflage patterns and equipment in the military provide a strategic advantage substantially. The main aim of this study is to give information about camouflage fabrics and to investigate the situation in recent developments. In this study, physical and performance properties of five different types of commercial woven camouflage fabric were investigated. Fabric properties and washing, perspiration, light and rubbing fastness of these fabrics were examined. Resistance to surface wetting (spray test) and water vapor permeability of fabrics were determined. The fabrics were exposed to sunlight to investigate changes in performance characteristics. Tensile properties and color changes on fabrics before and after sun exposure were specified.

Keywords: Camouflage, military textiles, performance tests

Introduction

Camouflage clothing is widely used among nature lovers, hunters and fishermen beside military purposes and very useful dress that can be worn in all weather conditions. With the progress of the technology, the importance of camouflage fabrics in the military has steadily increased. A person hidden in an area can be seen by other people or animals when they are stationary or mobile. The reason for decryption in the first case is that there is no consistent contrast with the environment. In the second case, the movement causes to be noticed. Outlines of figurines that do not match the surrounding and colors that do not look like an element of the environment are decrypted. Camouflage is active in both cases. It changes the color of the object, removes the symmetry from the middle, unifies with the environment, prevents blurring and proportionality of the figurine. In short, the task of camouflaging is to ensure that a person looks like part of a plant, swamp or rock. That is to transform it into an object that does not constitute a danger. The properties expected from camouflage fabrics are primarily comfortable, durable, environmentally compatible and fit for purpose (Adanur, 2017; Kovacevic et al., 2012; Schutz et al., 2005). The purpose of this study is; to determine the structural characteristics of different military camouflage fabrics, to evaluate their performances in open air conditions and to give information about recent developments.

Material and Method

In this study, five different commercial camouflage fabrics were used. Two of the fabrics were obtained from a foreign and the other three from companies based in Turkey. Mass per unit area of woven fabrics were specified by TS 251. To determine the characteristics of fabrics, washing, perspiration, light and rubbing fastnesses are examined according to TS EN ISO 105- C06; E04; B02 and X12 respectively by using multifiber. TS EN ISO 4920 was performed to determine the resistance to surface wetting (spray test) and water vapor permeability features were analyzed with regarding to BS 7209.

[1] Dokuz Eylul University, Department of Textile Engineering, İzmir, TURKEY
*Corresponding author: gizem.turkoglu@deu.edu.tr

To see the performance changes of the fabrics in the open air, they were exposed to sunlight in a glass frame for 33 days between December to January in Izmir province (Figure 1). Changes in tensile properties before and after sun exposure were examined by TS EN ISO 13934-1. Color changes were measured by Minolta spectrophotometer; the L, a, b and DE values were calculated.

Results

The patterns of fabrics are given in Figure 1. On the right of Figure 1, experimental setup for sun exposure is represented. The setup was covered with window class in both sides and placed where it can take direct sunlight.

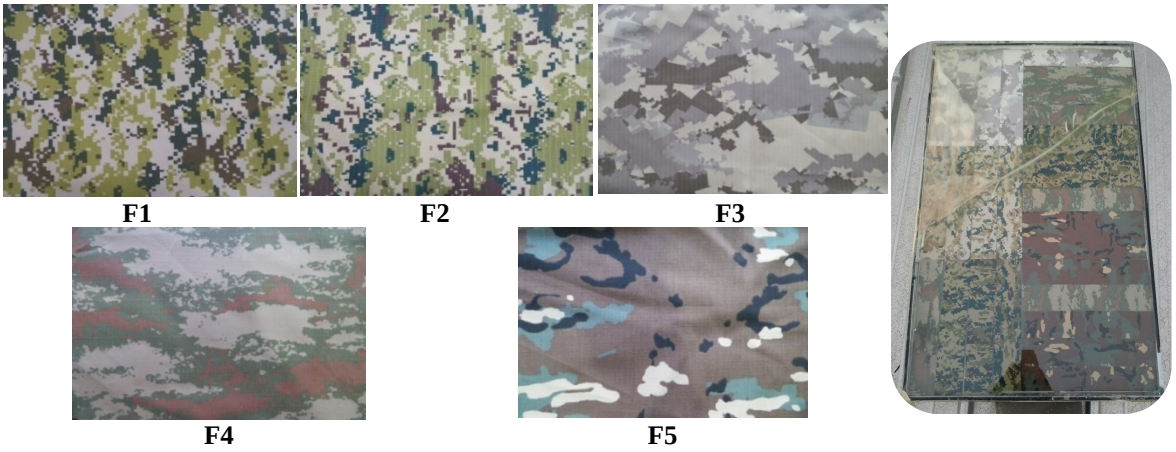

Figure 1. Fabrics and experimental setup for sun exposure

Fabric properties are examined in Table 1. Staining on multifiber and color change on the fabric was also performed on washing and perspiration fastness tests. It was determined that the color fastness values of all the fabrics against washing and artificial light were close to each other and the fabrics had passing grades. It is anticipated that samples subjected to wet rubbing tests in the rubbing fastness have lower values than those subjected to dry rubbing. In the experiments against acidic and alkali perspiration solution, moderate values were obtained in all fabrics. It has been determined that F4 gives better results than other fabrics on a general fastness assessment. However, F1, F2 and F4 show no water repellency. The water vapor permeability values of all fabrics were found to be similar.

Color changes on fabrics after fastness tests were examined on camouflage fabrics. When all the colors on the fabric are evaluated together, it is understood that the fading value of the F3 is better than the F1, F2 and F5. All the colors on F4 fade less than all other fabrics.

Table 1. Fabric properties

Fabrics	Fiber Composition	Weight (g/m^2)	Fastness									Water Repellency	Water Vapor Permeability ($g/m^2/day$)
			Light	Washing		Rubbing		Perspiration					
								Acid		Alkali			
				CO	PET	Dry	Wet	CO	PET	CO	PET		
F1	50% PET 50% CO	235	6	5	5	4/5	4/5	5	3/4	5	3/4	ISO 0	842.68
F2	50% PET 50% CO	225	7	5	4/5	4	3/4	4/5	5	4/5	5	ISO 0	820.51
F3	15% PET 85% CO	200	7	5	4/5	4/5	4	5	4/5	5	4/5	ISO 5	838.25
F4	20% PET 80% CO	240	7	5	5	5	4	5	5	5	5	ISO 0	833.81
F5	50% PET 50% CO	228	7	5	4	4/5	4	4/5	4	4/5	4	ISO 5	833.81

Table 2. Effect of sun exposure on tensile strenght, breaking elongation and color change

Fabrics		Tensile Strenght (kgf)		Breaking Elongation (%)		Color Change (ΔE)	
		Before Sun Exposure	After Sun Exposure	Before Sun Exposure	After Sun Exposure	Colors	Before & After Sun Exposure
F1	Warp	127.08	91.045	89.638	58.895	Dark Green	8.414
	Weft	67.706	47.875	68.742	40.95	Cream	1.605
						Light Green	15.349
F2	Warp	124.94	124.93	35.838	35.86	Dark Green	12.006
	Weft	92.804	94.243	66.17	68.693	Cream	2.317
						Light Green	6.062
F3	Warp	177.94	175.733	20.742	20.35	Gray	4.164
	Weft	60.49	62.655	25.08	24.875	Brown	0.744
						Cream	1.809
F4	Warp	150.52	146.366	26.282	27.66	Light Brown	2.278
	Weft	97.206	101.25	31.714	29.395	Dark Brown	1.340
						Green	1.429
F5	Warp	141.78	137.9	43.088	43.146	Green	12.687
						Brown	1.778
	Weft	72.904	70.153	44.134	43.086	Cream	10.559
						Black	4.538

In Table 2, tensile strength change on warp direction after sun exposure was 28%, 0.1%, 1.2%, 2.8% 2.7%, F1 to F5, respectively. The resistance of the first fabric to sunlight is found to be quite low, where F1 decreased 127.08 to 91.045 and F4 150.52 to 146.366 kgf on warp direction. Breaking elongation was also examined after sun exposure. It was noted that the most affected fabric was found to be F1.

Color changes on main colors after sun exposure was evaluated by spectrophotometer and ΔE values are calculated according to CIE Lab (Table 2).

Discussion and Conclusions

The most important features on clothes of the new century soldiers are having communication equipment inside the clothes, able to follow the physical condition and give constant location notification, ability to perceive the surrounding light and accordingly perceive the camouflage pattern, having protection against firearms, radiation, chemical and biological agents. Certainly, beside all these features, military clothes should be light as possible so that they will not restrict the ability of maneuver.

References

Adanur, S. 2017. Wellington Sears handbook of industrial textiles.

Bilgi, M., Kalaoğlu, F., 2010. Özel apre tekniklerinin askeri kumaşların performans ve konforu üzerindeki etkileri, Tekstil ve Konfeksiyon, 20(4), 343-348.

Fortuniak, K., Redlich, G., Obersztyn, E., Olejnik, M., Bartczak, A., Król, I. 2013. Assessment and verification of the functionality of new, multi ;component, c
21,5(101):73-79.

Kovacevic S., Schwarz I., Durasevic, V. 2012. Analysis of printed fabrics for military camouflage clothing. Fibres &Textiles in Eastern Europe; 20,3(92): 82-86.

Schutz G., Cardello V., Winterhalter C. 2005. Perceptions of fiber and fabric uses and the factors contributing to military clothing comfort and satisfaction. Textile Research Journal, 75(3), 223-232.

Wilusz, E. (ed) 2010 Military Textiles in Applicationsof nonwovens intechnical textiles, Woodhead Publishing in Textiles: Number 73, s 26-33

International Conference on Science and Technology

ICONST 2018

5-9 September 2018 Prizren - KOSOVO

A New Outlook for Numerical Simulations of Solitons of Schrödinger Equation via Quartic B-spline Based Crank-Nicolson-Differential Quadrature method

Ali Başhan [1*]

Abstract: The present manuscript dwells on quartic B-splines based Crank-Nicolson-Differential Quadrature Method (CN-DQM) in order to find out the numerical solutions for the nonlinear Schrödinger (NLS) equation. For this purpose, first of all, Schrödinger equation is going to be converted into a system of coupled real value differential equations. After that, they have been discretized using important type of finite difference method namely Crank-Nicolson scheme. Next, Rubin and Graves type linearization techniques have been applied and differential quadrature method has been used. After all those processes, these partial differential equations result in an algebraic equation system. As a further step, in order to be able to test the accuracy of the newly hybrid method, the error norms L_2 and L_∞ as well as the two lowest invariants I_1 and I_2 have been calculated. In addition to those test tools, the relative changes in those invariants have been given. As a final step, those newly obtained numerical results have been compared with some of those available in the literature using similar parameters. This comparison has clearly indicated that the currently utilized method, namely CN-DQM, is an effective and efficient numerical scheme and allow us to propose it to solve a wider range of nonlinear equations.

Keywords: Partial differential equations, Differential quadrature method, Quartic B-Splines, Schrödinger equation.

Introduction

In nature, many of the physical phenomena can easily be described by NLS equation such as propagation of optical pulses, waves in water, waves in plasmas, and self focusing in laser pulses. As a result of this, among others, many researchers have tried hard to present analytical solutions of NLS (Karpman and Krushkal, 1969; Scott et al., 1973; Zakharov and Shabat, 1972) and numerical solutions have been studied (Delfour et al., 1981; Thab and Ablowitz; 1984; Argyris and Haase, 1987; Gardner et al., 1993; Robinson,1997). NLS equation has a nature of attracting the attention of many researchers to show the accuracy of the numerical methods. Thus, particularly in recent decades, many applications of various methods for the NLS equation can be seen in the literature (Dag, 1999; Dereli et al.,2009; Saka, 2012).

First of all, we are going to take into consideration the NLS equation given in the following form

$$iz_t + z_{xx} + q\,|z|^2 z = 0, \quad x \in [a, b], \quad t \in [0, T] \tag{1}$$

together with the boundary conditions

[1]Zonguldak Bulent Ecevit University, Faculty of Science and Art, Deparment of Maths, 67100, Zonguldak, TURKEY
*Correspondingauthor: alibashan@gmail.com

$z(a, t) = z(b, t) = 0,$

where $i = \sqrt{-1}$, q is a real parameter. Also the subscripts x and t denote partial derivatives with respect to space and time, respectively.

In order to be able to compute the complex value of function z, we have to convert it into the coupled real value functions by rewriting

$$z(x, t) = u(x, t) + iv(x, t) \quad (2)$$

in which both of u(x, t) and v(x, t) are real functions. Upon substituting (2) into the Eq.(1) it yields coupled real value partial differential equation system

$$u_t + v_{xx} + q[u^2v + v^3]= 0, \quad (3)$$
$$v_t - u_{xx} - q[v^2u + u^3]= 0. \quad (4)$$

Just after application of boundary conditions to (2) newly obtained boundary conditions can be given in the following form

$$u(a, t) = u(b, t) = 0,$$
$$v(a, t) = v(b, t) = 0. \quad (5)$$

Recently, DQM, first introduced by Bellman et al. in 1972, has had wide application areas thanks to its considerably less number of grid points usage. In the literature, it can be seen that many researchers have developed various types of DQM using different base functions (Bellman et al., 1976; Zhong, 2004; Cheng et al., 2005; Korkmaz et al.,2011).

Quartic B-spline DQM

DQM can be defined as an approximation to a derivative of a given function by using the linear summation of its values at specific discrete grid points over the solution domain of a problem. Let us take the grid distribution $a = x_1 < x_2 < \cdots < x_N = b$ of a finite interval [a, b] into consideration. Provided that any given function U(x) is enough smooth over the solution domain, its derivatives with respect to x at a grid point x_i can be approximated by a linear summation of all the functional values in the solution domain, namely,

$$U_x^{(r)}(x_i) = \sum_{j=1}^{N} w_{ij}^{(r)} U(x_j), \text{ i = 1, 2, ...,N, r = 1, 2, ...,N − 1} \quad (6)$$

where r denotes the order of the derivative, $w_{ij}^{(r)}$ represent the weighting coefficients of the r−th order derivative approximation and N denotes the number of grid points in the solution domain. Here, the index j represents the fact that $w_{ij}^{(r)}$ is the corresponding weighting coefficient of the functional value U (x_j).
In this study, we need the first order and the second order derivative of the function U(x). So, firstly we will find value of the equation (6) for the r = 1.

Using the quartic B-splines as test functions in the fundamental DQM equation (6) leads to the equation

$$\frac{d^{(r)}Q_m(x_i)}{dx^{(r)}} = \sum_{j=m-1}^{m+2} w_{ij}^{(r)} Q_m(x_j), \text{ m = −1, 0, . . . ,N + 1, i = 1, 2, ...,N.} \quad (7)$$

When DQM methodology is applied, the fundamental equality for determining the corresponding weighting coefficients of the first order derivative approximation is obtained as (Korkmaz et al., 2011) used:

$$\frac{dQ_m(x_i)}{dx} = \sum_{j=m-1}^{m+2} w_{ij}^{(r)} Q_m(x_j), \text{ m = −1, 0, . . . ,N + 1, i = 1, 2, ...,N.} \quad (8)$$

After the using the value of quartic B-splines for the first grid point, the equation systems consist of N + 6 unknowns and N + 3 equations are obtained. For this system to have a unique solution, it is required to add three additional equations to the system. By the derivations of the equations

$$\frac{d^{(2)}Q_m(x_1)}{dx^2} = \sum_{j=-2}^{1} w_{1j}^{(1)} Q'_{-1}(x_j) \quad (9)$$

$$\frac{d^{(2)}Q_N(x_1)}{dx^2} = \sum_{j=N-1}^{N+2} w_{1j}^{(1)} Q'_{N}(x_j) \quad (10)$$

$$\frac{d^{(2)}Q_{N+1}(x_1)}{dx^2} = \sum_{j=N}^{N+3} w_{1j}^{(1)} Q'_{N+1}(x_j) \quad (11)$$

is obtained. By using the equations (9), (10) and (11) which we obtained by derivations, three unknown terms will be eliminate from equation system. So the rearranged system is solved via Thomas algorithm. Same process implemented to the remained grid points.

By the matrix multiplication approach, the second order weighting coefficients are determined as below (Shu, 2000):

$$[A^2] = [A^1]\,[A^1] \quad (12)$$

where

$[A^1]$, $[A^2]$ are the weighting coefficients matrices of the first order and the second order derivatives, respectively (Shu, 2000).

Discretization Process

One can implement Crank-Nicolson scheme to Eq. (3) and obtain

$$\frac{u^{n+1}-u^n}{\Delta t} + \frac{v_{xx}^{n+1}+v_{xx}^n}{2} + q\left[\frac{(v^3)^{n+1}+(v^3)^n}{2}\right] + q\left[\frac{(u^2v)^{n+1}+(u^2v)^n}{2}\right] = 0 \quad (13)$$

Then, the rearrangement of Eq. (13) yields the following form

$$2u^{n+1} + \Delta t[v_{xx}^{n+1} + q((v^3)^{n+1} + (u^2v)^{n+1})] = 2u^n - \Delta t[v_{xx}^n + q((v^3)^n + (u^2v)^n)]. \quad (14)$$

After the using linearization techniques of Rubin and Graves [35] in Eq. (14) to eliminate the nonlinear terms, and using the differential quadrature method the system obtained of the form

$$[2 + 2q\Delta t U_i^n V_i^n]U_i^{n+1} + \left[\Delta t\left(w_{ii}^{(2)} + q(3(V_i^n)^2 + (U_i^n)^2)\right)\right]V_i^{n+1} + \sum_{j=1,i\neq j}^{N}(\Delta t w_{ij}^{(2)})V_j^{n+1} = \varphi_i^n \quad (15)$$

where

$$\varphi_i^n = 2U_i^n + \Delta t[-V_{xxi}^n + q(V_i^n)^3 + q(U_i^n)^2 V_i^n].$$

Same process obtained to Eq. (4) and algebraic equation system solved via Gauss elimination method.

Numerical example

In this section, test problem has been considered as the motion of single soliton of which analytic solution is given of the form

$$z(x,t) = \alpha\left(\frac{2}{q}\right)^{1/2} \exp i\{0.5Sx - 0.25(S^2-\alpha^2)t\}\,\mathrm{sech}\,\alpha(x-St) \quad (16)$$

where S denotes the speed of the single soliton whose amplitude depends on. We have chosen the values of q = 2, S = 4, α = 1, 2 and the region $-20 \leq x \leq 20$ just to be able to compare with earlier works. When $\alpha = 1$ is taken, the envelop soliton

$$|z| = \operatorname{sech}(x - 4t)$$

moves toward the right having unchanged properties such as speed S = 4, shape, and amplitude $\alpha = 1$

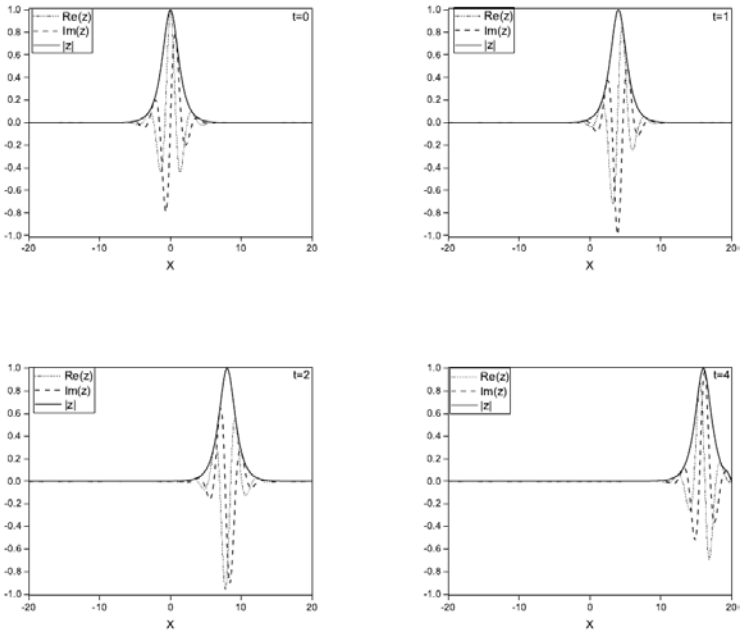

Figure 1 Motion of single soliton: $\Delta t = 0.005$ and N=291

Table 1. L_2 and L_∞ error norms and invariants: $\Delta t = 0.005$

	Present(CN-DQM) N=291				Quad. FEM[13] N=800			
t	I_1	I_2	L_2	L_∞	I_1	I_2	L_2	L_∞
0.0	2.00000	7.33370	0.00000	0.00000	2.0	7.3537736	0.0000	0.0000
0.5	2.00000	7.33371	0.00012	0.00008	2.0	7.3537756	0.0002	0.0002
1.0	2.00001	7.33373	0.00023	0.00015	2.0	7.3537778	0.0004	0.0003
1.5	2.00001	7.33374	0.00032	0.00021	2.0	7.3537793	0.0007	0.0004
2.0	2.00001	7.33375	0.00040	0.00026	2.0	7.3537802	0.0008	0.0005
2.5	2.00001	7.33377	0.00047	0.00029	2.0	7.3537803	0.0009	0.0006

Results

For visual representation, the simulations of single soliton for values of Δt=0.005, N = 291 at times t = 0, 1, 2, and 4 are illustrated in Figure 1. As one can see clearly from Figure 1, the both components of z which are the real and imaginary parts and the module |z| is shown. For comparison purpose, the values of the error norms L_2 and L_∞, and two lowest invariants I_1 and I_2 are presented in comparison with quadratic FEM (Dag, 1999) for values of Δt=0.005 and N = 291 at various times in Table 1. As one can see straightforwardly from Table 1, by using the same parameters and less number of the grid points than earlier work [13] the present results are better than quadratic FEM (Dag, 1999) solutions.

Discussion and Conclusions

In the present manuscript, we have successfully implemented CN-DQM for the numerical solution of nonlinear Schrödinger equation. In the solution process, to be able to compute the complex value of function z, we have converted it into the coupled real value functions. In order to obtain the second order derivative approximation, quartic B-spline differential quadrature method has been utilized. Then, test problem has been investigated. The performance and accuracy of the method have been tested by calculating the error norms L_2 and L_∞, and two lowest invariants I_1 and I_2. As one can see from the comparison between the obtained values of the error norms of the present method and given in earlier work (Dag, 1999), CN-DQM results are undoubtedly better then given in earlier work (Dag, 1999). Those newly obtained results obviously indicate that CN-DQM can also be used to produce numerical solutions of the NLS equation with high accuracy.

References

Argyris, J. and Haase M., (1987) . An engineer's guide to soliton phenomena: Application of the finite element method, Comput. Methods Appl. Mech. Engrg. 61, 71-122.

Bellman, R., Kashef, B.G. and Casti, J. (1972). Differential quadrature: a tecnique for the rapid solution of nonlinear differential equations, Journal of Computational Physics, Vol. 10,pp. 40-52.

Bellman, R., Kashef, B., Lee, E.S. and Vasudevan, R. (1976). Differential Quadrature and Splines, Computers and Mathematics with Applications, Pergamon, Oxford, pp. 371-6.

Cheng, J., Wang, B. and Du, S. (2005). A theoretical analysis of piezoelectric/composite laminate with larger-amplitude deflection effect, Part II: hermite differential quadrature method and application, International Journal of Solids and Structures, Vol. 42, pp. 6181-201.

Dag, I. (1999). A Quadratic B-Spline Finite Element Method for Solving the Nonlinear Schrödinger Equation, Comp. Methods Appl. Mech. Eng. 174, 247-258.

Delfour, M., Fortin, M. and Payre, G. (1981). Finite-difference solutions of a non-linear Schrödinger equation, J. Comput. Phys. 44 277-288.

Dereli, Y., Irk, D. and Dag, I. (2009). Simulations of Solitons Using Radial Basis Functions for NLS Equation," Chaos, Solitons and Fractals. 42, 1227.

Gardner, L.R.T., Gardner, G.A., Zaki, S.I. and El Sharawi, Z. (1993). A leapfrog algorithm and stability studies for the non-linear Schr¨odinger equation, Arabian J. Sci. Engrg. 23-32.

Karpman, V.I. and Krushkal, E.M. (1969). Modulated waves in non-linear dispersive media, Soviet Phys. JEPT 28 277.

Korkmaz, A., Aksoy, A.M. and Dag, I. (2011). Quartic B-spline Differential Quadrature Method", International Journal of Nonlinear Science, Vol.11 No.4,pp.403-411.

Robinson, M.P., (1997). The solution of nonlinear Schrödinger equations using orthogonal spline collacation, Comput. Math. Applic. 33(7) 39-57.

Saka, B. (2012). A quintic B-spline finite-element method for solving the nonlinear Schrödinger equation, Physics of Wave Phenomena, Vol. 20, No. 2, pp.107–117.

Scott, A.C., Chu, F.Y.F. and Mclaughlin, D.W., (1973). The soliton: A new concept in applied science, Procc. IEEE 61 1443.

Shu, C. (2000). Differential Quadrature and its application in engineering, Springer-Verlag London Ltd.

Thab, T.R. and Ablowitz, MJ. (1984). Analytical and numerical aspects of certain nonlinear evolution equations. II, Numerical, nonlinear Schrodinger equations, J. Comput. Phys. 55 203-230.

Zakharov, V.E. and Shabat, A.B., (1972). Exact theory of two dimensional self focusing and one dimensional self waves in non-linear media, JEPT 34 62.

Zhong, H. (2004). Spline-based differential quadrature for fourth order equations and its application to Kirchhoff plates", Applied Mathematical Modelling, Vol. 28, pp. 353-66.

International Conference on Science and Technology

ICONST 2018

5-9 September 2018 Prizren - KOSOVO

Comparison of the TCT and Hybrid TCT PV Array Configurations Under Partial Shading Conditons

Okan Bingöl[1], Burçin Özkaya[1]*, Serdar Paçacı[2], Onur Mahmut Pişirir[3]

Abstract: As the demand for energy is increasing day by day and the fossil fuels are getting depleted at a faster rate. Among the renewable energy sources, the use of solar or photovoltaic (PV) energy is increasing day by day due to freely available, pollution-free, low maintenance cost, reliable, and infinite. The efficiency of the PV system mainly depends on the solar irradiance and temperature. Especially, partial shading has negative effect on the PV system. Therefore, in the literature, many approach have been presented for this problem and one of them is PV array configurations. In this study, in order to examine the efficiency of PV array configurations, total cross tied (TCT), series parallel–total cross tied (SP-TCT), and bridged link–total cross tied (BL-TCT) configurations are carried out for 4×6 size of PV array under partial shading. The simulation of the PV array configurations was done for various shading patterns such as, short and narrow (SN), short and wide (SW), long and narrow (LN), long and wide (LW), and randomly distributed (RD) patterns. The results for each shading patterns were compared according to mismatch loss and fill factor. TCT has the best performance than the other configurations. Moreover, performance of the configurations are compared in terms of mismatch loss and fill factor. With reference to this, TCT has less mismatch loss and high fill factor by comparison with the others.

Keywords: Photovoltaic array configuration, partial shading, shading loss, fill factor.

Introduction

Solar energy is the most promising renewable energy resources due to its advantages such as freely available, pollution-free, low maintenance cost, reliable, and infinite (Rani et al., 2013; Reisi et al., 2013; Rao et al., 2014; Parlak, 2014; Malathy and Ramaprabha, 2015; Saravanan and Babu, 2016; Bingöl and Özkaya, 2018). Despite its advantages, it has a very significant drawback, which is low energy efficiency. The most important environmental factors that affect the operating performance of the PV modules are full or partial shading (Belhachat and Larbes, 2015; Bana and Saini, 2017). Full or partial shading over a PV array can cause adverse effects (Nguyen and Lehman, 2008; Dos Santos et al., 2011; Sanseverino et al., 2015). These are;

- The power obtained from the PV array is lower than the maximum power value.
- The hot spot problem, which will be happening in the shading PV module, can damage PV cells.

Under partial or full shading conditions, the solar radiation values of the modules in the PV array are different from each other. In this case, bypass diodes are connected parallel to the PV modules to prevent the hot spot problem. Due to the usage of the bypass diode, there is multiple peaks in the P-V characteristic. In this case, it must be provided that the PV system is operated at maximum power point or maximum power is obtained. In order to increase the efficiency of PV systems, one of the recommended method is PV array configurations in the literature (Rao et al., 2014; Belhachat and Larbes, 2015; Yadav et al., 2017; Bana and Saini, 2017).

[1]Applied Sciences University of Isparta, Faculty of Technology, Electrical and Electronics Engineering Department, 32260, Isparta, TURKEY
[2]Suleyman Demirel University, Department of Information Technologies, 32260, Isparta, TURKEY
[3]Applied Sciences University of Isparta, Vocational School of Distance Learning, 32260, Isparta, TURKEY
*Corresponding author: burcinozkaya@sdu.edu.tr

In the literature, different PV array configurations are proposed. These are series (S), parallel (P), series-parallel (SP), total-cross-tied (TCT), bridged-link (BL) and honeycomb (HC) (Malathy and Ramaprabha, 2015; Belhachat and Larbes, 2015). In addition to these configurations, hybrid configurations are proposed that are series-parallel-total-cross-tied (SP-TCT) and bridged-linked-total-cross-tied (BL-TCT) (Yadav et al., 2016; Yadav et al., 2017). Rao et al. (2014) proposed a fixed configuration to increase the efficiency of PV array under partial shading conditions. The proposed configuration was applied on 3×3 and 5×5 PV sequences and the results were compared with SP, TCT and BL configuration. According to the simulation results, the proposed configuration has higher power than the others. Belhachat and Larbes (2015) analyzed the performance of S, P, SP, TCT, BL and HC configurations for all possible shading scenarios on a 6×4 PV array. According to the results, the highest power was obtained in most of the shading scenarios from the TCT. Malathy and Ramaprabha (2015) analyzed the performance of PV array configurations under different shading scenarios for different size of PV arrays. In addition, S, P, SP, TCT, HC and BL, as well as a new configuration was proposed. The proposed new connection scheme achieved higher efficiency than the TCT configuration. Bana and Saini (2017) proposed a new PV array configuration. The maximum power value obtained from the proposed configuration was compared with SP, TCT, BL and HC configurations for 14 different shading scenarios. Mishra et al. (2017), a new PV array was proposed. They compared the performance of the proposed configuration with TCT, SP-TCT, BL-TCT and BL-HC in terms of power loss and fill factor for various shading scenarios. Yadav et al. (2017) were compared the performance of TCT, SP-TCT, HC-TCT, magic square (MS), rearranged TCT (RTCT), rearranged SP-TCT (RSP-TCT), and rearranged BL-TCT (RBL-TCT) configurations under different partial shading conditions to improve the efficiency of PV array.

In the study, the performance of TCT, SP-TCT, and BL-TCT configurations was evaluated under different shading scenarios. In order to test the performance of the configurations, a 4×6 size PV array was used and simulations were conducted with MATLAB/Simulink. According to the simulation results, the maximum power value obtained from the PV array varied for the configurations. Generally, TCT has the best performance than the other configurations. Moreover, performance of the configurations are compared in terms of mismatch loss and fill factor. With reference to this, TCT has less mismatch loss and high fill factor by comparison with the others.

2. PV System Description

2.1. Model of a PV cell

In the literature, various equivalent circuit model of PV cell is given. Among them, the most commonly used is single diode equivalent circuit and it is given in Fig. 1. In Fig. 1, I_{ph} is a cuurent source, D is diode, R_s and R_{sh} are a series resistance and a parallel resistance, respectively (De Soto et al., 2006; Tsai et al., 2008; Villalva et al., 2009; Tsai, 2010; Chouder et al., 2010; Bingöl and Özkaya, 2018).

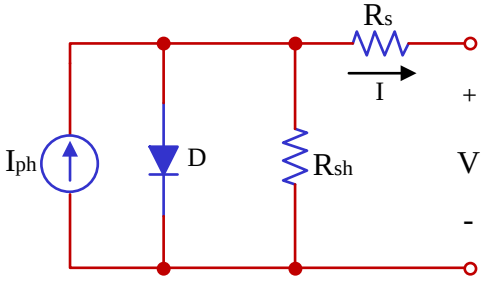

Figure 1. The equivalent circuit of a PV cell

The voltage-current characteristic equation of a PV cell is given as follows:

$$I = I_{ph} - I_s\left(e^{\frac{q(V+IR_S)}{kT_cA}} - 1\right) - \frac{V+IR_S}{R_{sh}} \quad (1)$$

Here,

I_{ph}: Light generated current,
I_s : the cell saturation of dark current,
T_c : the cell's operating temperature in Kelvin (K),
k : Boltzmann constant (1.381x10^{-23} J/K),
q : Electron charge (1.602 x 10^{-19} C),
A : Diode ideality constant.
The photo-current (I_{ph}) mainly depends on the solar irradiation and temperature and is given in Eq. (2).

$$I_{ph} = G\left(I_{sc} + K_I.\left(T_c - T_{ref}\right)\right) \quad (2)$$

Here,
G: Solar irradiation level (kW/m^2),
I_{sc}: The short circuit current of the cell at 25°C and 1000 W/m^2,
K_I: The short-circuit current temperature coefficient of the cell,
T_{ref}: The reference temperature of the cell.
The PV module parameters used in the study is given in Table 1.

Table 1. PV module parameters

Parameter	Label	Value
Maximum power	P_{max}	100 W
Maximum power point voltage	V_{mpp}	18.9 V
Maximum power point current	I_{mpp}	5.29 A
Open circuit voltage	V_{oc}	22.5 V
Short circuit current	I_{sc}	5.75 A
Number of series cell	N_S	36
Temperature coefficient of Isc	K_I	0.04%/ °C

2.2. The Effect of Partial Shading on PV Array

Partial shading is the most important environmental factors adversely affecting the performance of PV array. It is caused by several factors such as cloud, building, tree, and snow. Under uniform conditions, all modules of PV array have same electrical characteristics and output power. When partial shading occurs, output power of the PV module decreases. In this case, shaded cell generates the current less than the non-shaded cell and the shaded PV cells carry the negative voltage and behave as a load. Therefore, the heat of the PV cells will increase and this may damage the PV cells. This is called "hot spot" problem. In order to prevent the "hot spot" problem, bypass diodes are connected the PV module in parallel. Thus, the current flows over the bypass diode instead of PV module (Belhachat and Larbes, 2015; Bana and Saini, 2017). Usage of bypass diode solves this problem, but it causes multiple peaks in the P-V characteristic. In order to observe the effect of the partial shading and bypass diode, a 3×1 series connected PV array is used. Test are conducted for uniform condition, without bypass diode, and with bypass diode and are shown in Fig. 3 respectively. In Fig. 4 (a) and (b), PV and I-V characteristics of test cases are given. According to Fig. 4 (a), there is one maximum power point for uniform condition and without bypass diode. However, PV array with bypass diode has three maximum power point and one of them is global maximum power point.

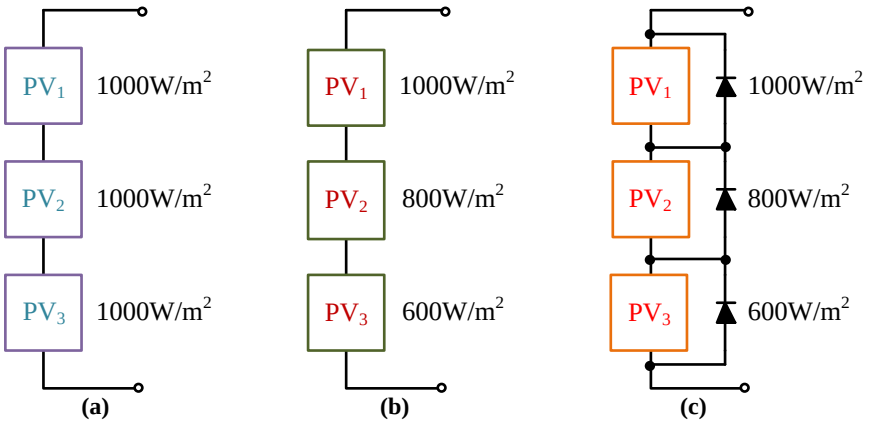

Figure 3. A 3×1 series connected PV array under **(a)** Uniform condition, **(b)** without bypass diode, and **(c)** with bypass diode.

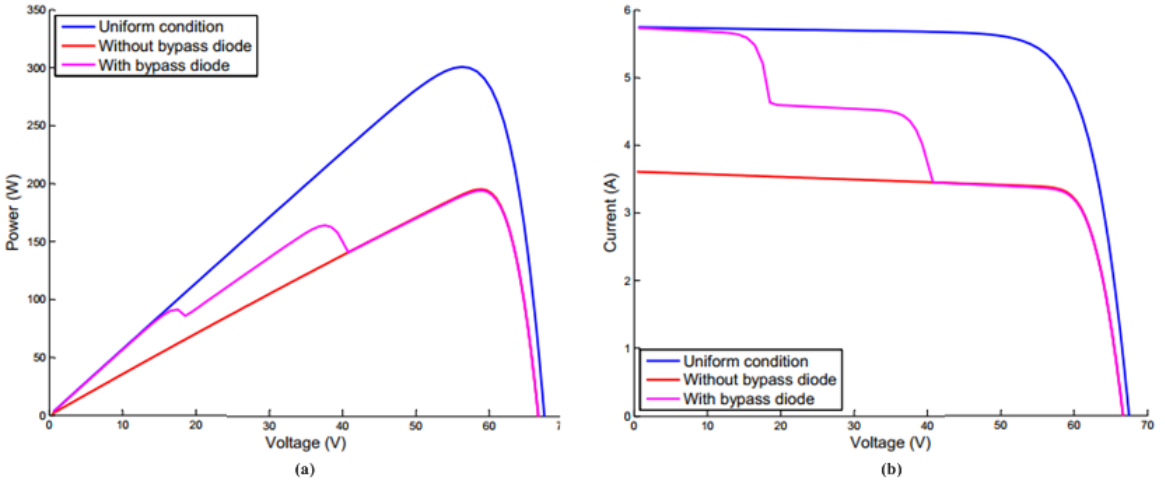

Figure 4. (a) P-V and **(b)** I-V characteristics of a 3×1 size series connected PV array under uniform condition, without bypass diode and with bypass diode.

2.3. PV Array Configurations

In the literature, different PV array configurations are proposed. These are series-parallel (SP), total-cross-tied (TCT), and bridged-linked (BL) (Belhachat and Larbes, 2015; Malathy and Ramaprabha, 2015; Bana and Saini, 2017). Except these configurations, series-parallel-total-cross-tied (SP-TCT) and bridged-linked-total-cross-tied (BL-TCT) array configurations are also proposed (Yadav et al., 2016; Yadav et al., 2017).

In SP configuration, all modules are first connected in series form and then these series connection are connected in parallel. It is given in Fig. 5 (a).

TCT configuration is created by cross-connecting modules in each row of the serial-parallel configuration and is given in Fig. 5 (b).

In BL configuration, there is a bridged unit consisting of four modules. The two modules in this bridge are connected in series and then connected in parallel. Bridges are connected to each other by cross ties. It is given in Fig. 5 (c).

SP-TCT is a hybrid configuration of the SP and TCT. In this configuration, number of bridge is less than TCT ann it is given in Fig. 5 (d).

BL-TCT is a hybrid configuration of the BL and TCT. In this configuration, number of bridge is less than TCT ann it is given in Fig. 5 (e).

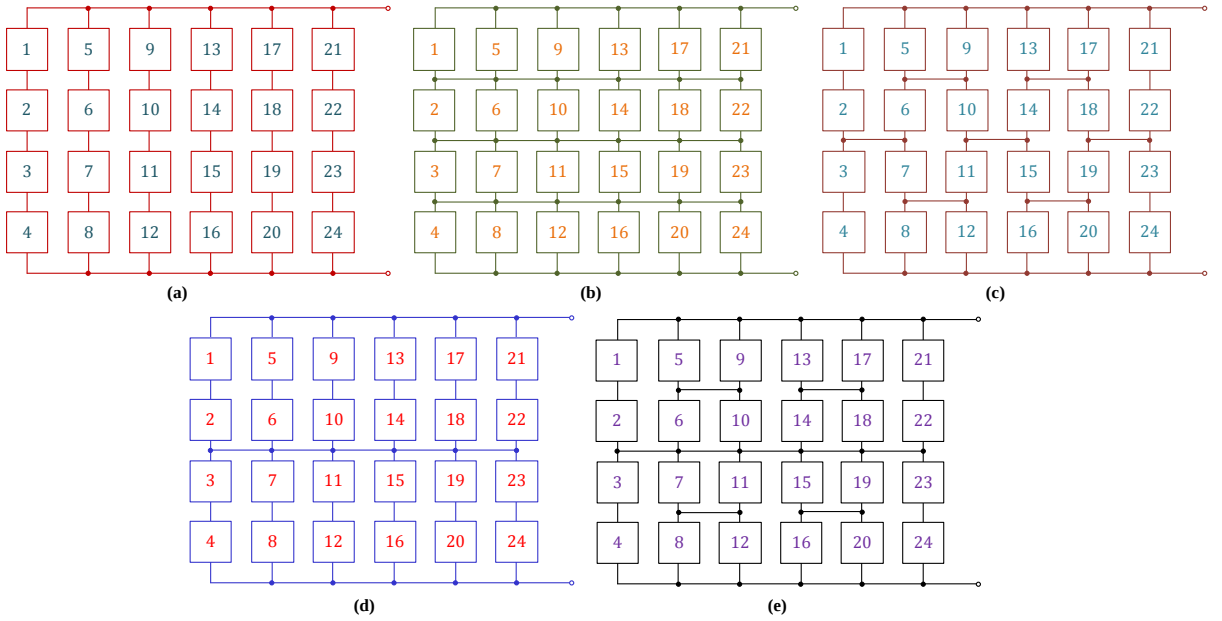

Figure 5. PV array configurations **(a)** SP, **(b)** TCT, **(c)** BL, **(d)** SP-TCT, **(e)** BL-TCT

3. Shading Scenarios

In order to efficiency of the PV array configurations, a 4×6 size PV array are simulated for 5 shading scenarios and shading scenarios are given in Fig. 6.

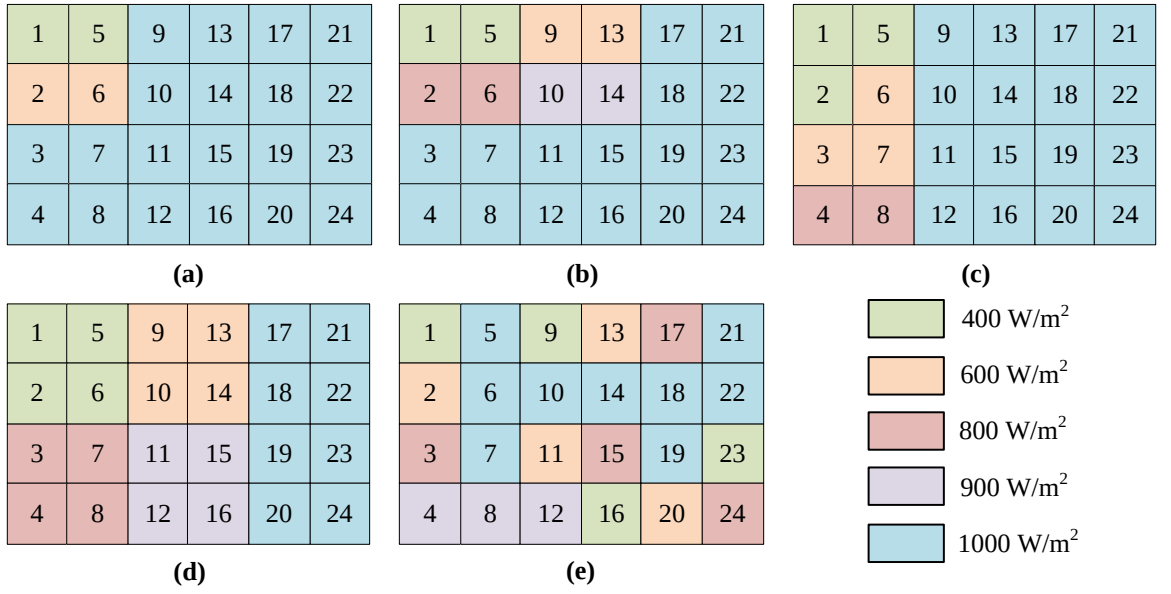

Figure 6. Shading (a) Scenario 1, (a) Scenario 2, (a) Scenario 3, (a) Scenario 4 ve (a) Scenario 5

Scenario 1: Shading is short and narrow on the PV array and given in Fig. 6 (a).

Scenario 2: Shading is short and wide on the PV array and given in Fig. 6 (b).

Scenario 3: Shading is long and narrow on the PV array and given in Fig. 6 (c).

Scenario 4: Shading is long and wide on the PV array and given in Fig. 6 (d).

***Scenario 5*:** In this case, the solar irradiance values PV array is randomly distributed and given in Fig. 6 (e).

4. Simulation Results

A 4×6 size PV array for TCT, SP-TCT, and BL-TCT configurations are tested under uniform condition (1000 W/m^2 and 25°C) and results are given in Table 2. Also, P-V and I-V characteristics of the configurations are given in Fig. 7 (a) and (b), respectively.

Table 2. Simulation results under uniform condition

Configuration	Pmax (W)	Vmax (V)	Imax (A)
TCT	2398,3	75,54	31,75
SP-TCT	2398,3	75,54	31,75
BL-TCT	2398,3	75,54	31,75

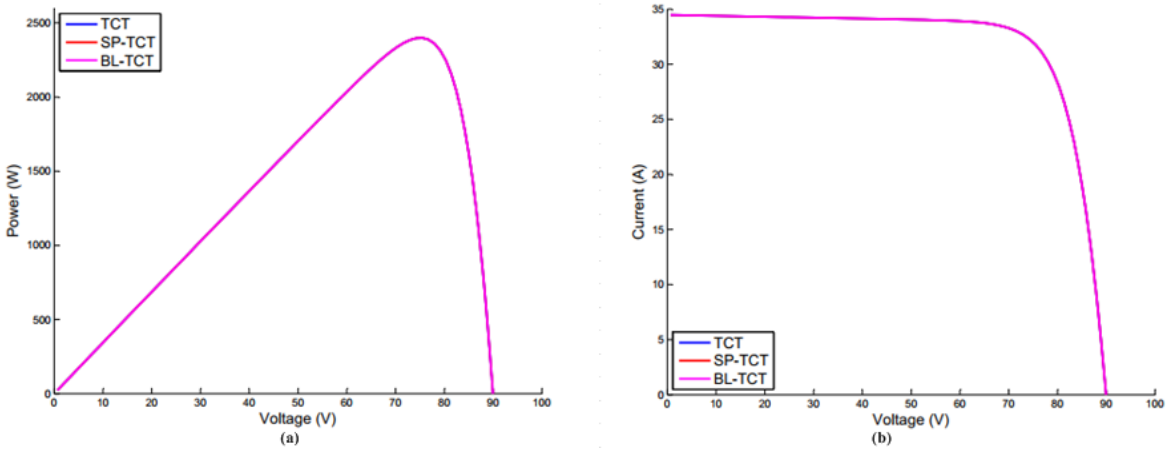

Figure 7. (a) P-V and **(b)** I-V characteristics of PV array configurations under uniform condition

Simulation results of five shading scenarios are given in Table 3. According to Table 3, the global maximum power values of TCT configuration are higher than other configurations for all shading scenarios. The values obtained from the Scenario 1, 2, 3, 4, and 5 are respectively 2047,9 W, 1749,5 W, 1994,3 W, 1667 W, and 1760 W. However, from Scenario 4, the maximum power is same for all configurations.

Table 3. Simulation results of shading scenarios

Shading Scenario	Configuration	Pmax (W)	Vmax (V)	Imax (A)
1	**TCT**	**2047,9**	**89,58**	**26,59**
	SP-TCT	2021,9	89,58	26,35
	BL-TCT	2021,9	89,56	26,14
2	**TCT**	**1749,5**	**79,27**	**22,07**
	SP-TCT	1720,7	78,26	21,99
	BL-TCT	1720,7	78,26	21,99
3	**TCT**	**1994,3**	**75,91**	**26,27**
	SP-TCT	1972,2	75,96	25,97
	BL-TCT	1977,9	75,94	26,05
4	**TCT**	**1667**	**77,24**	**21,58**
	SP-TCT	**1667**	**77,24**	**21,58**
	BL-TCT	**1667**	**76,37**	**21,83**
5	**TCT**	**1760**	**76,25**	**23,08**
	SP-TCT	1576,6	77,31	20,39
	BL-TCT	1746,3	76,32	22,88

5. Results and Discussion

The maximum power values obtained from TCT, SP-TCT, and BL-TCT configurations under five shading scenarios are compared. As a result, excepting Scenario 4, TCT has the highest maximum power. Moreover, the results of shading scenarios are compared in terms of mismatch loss and fill factor.

5.1. Mismatch Loss

Mismatch loss is the difference between the sum of individual maximum power of the modules ($P_{\max\_individual}$) and the global maximum power point (P_{GMMP}) under partial shading conditions (Vijayalekshmy, et al., 2014; Vijayalekshmy, et al., 2016; Bingöl and Özkaya, 2018). It is calculated with Eq. (3).

$$P_{mismatchloss} = P_{\max\_individual} - P_{GMMP} \quad (3)$$

Mismatch loss values for all shading scenarios are given in Fig. 8. According to Fig. 8, for Scenario 1 and 2, TCT has the lowest mismatch loss value and SP-TCT and BL-TCT has the same mismatch loss value. For Scenario 3 and 5, TCT has the lowest mismatch loss value and SP-TCT has the highest mismatch loss value. For Scenario 4, all scenarios have the same mismatch loss value.

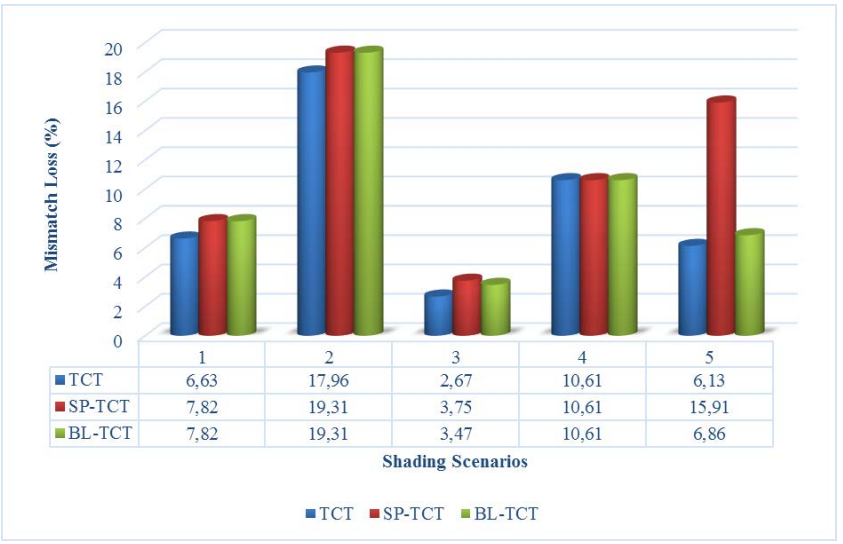

Figure 8. Mismatch loss values for shading scenarios

5.2. Fill Factor

Fill factor is the ratio of the global maximum power (P_{GMMP}) obtained from partial shading to product of the open circuit voltage and short circuit current of the array configuration (Vijayalekshm et al., 2014; Vijayalekshmy et al., 2016; Bingöl and Özkaya, 2018). The fill factor is calculated with Eq. (4)

$$FF = \frac{P_{GMMP}}{V_{oc} \times I_{sc}} \tag{4}$$

For five shading scenarious, the fill factor values are given in Fig. 9. According to Fig. 9, fill factor value of TCT configuration is the highest for all shading scenarios excepting Scenario 4. For Scenario 4, all configurations has the same fill factor value.

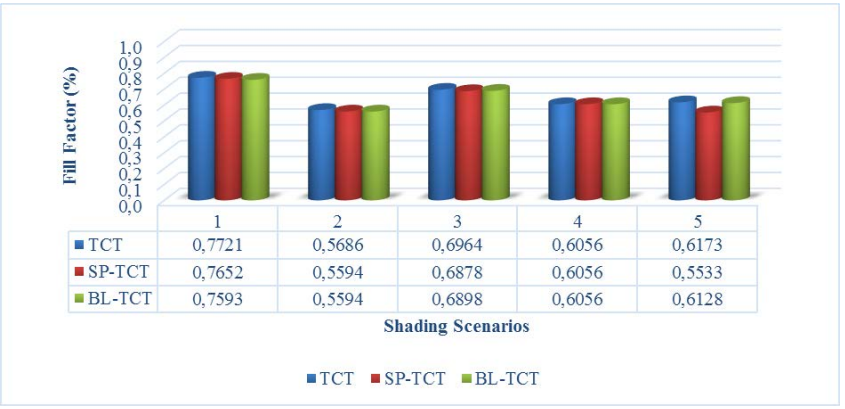

Figure 9. Fill factor values for shading scenarios

6. Conclusion

In the study, the performance of the TCT and hybrid TCT PV array configurations were tested on a 4×6 PV array for five different shading scenarios in terms of mismatch loss and fill factor. For Scenario 1, TCT provides the highest maximum power (2047,9 W) and SP-TCT and BL-TCT give the same maximum power (2021,9 W). For Scenario 2, TCT provides the highest maximum power (1749,5 W) and SP-TCT and BL-TCT give the same maximum power (1720,7 W). For Scenario 3, when TCT provides the highest maximum power (1994,3 W), SP-TCT gives the lowest maximum power (1972,2 W). For Scenario 4, all array configurations give the same maximum power (1667 W). For Scenario 5, when TCT provides the highest

maximum power (1760 W), SP-TCT gives the lowest maximum power (1576,6 W). According to these results, TCT provides the best performance for all shading scenarios and it increases the maximum power compared to other configurations. Moreover, a TCT configured PV array has the lowest mismatch loss value and highest fill factor for all shading scenarios.

References

Bana, S., Saini, R. P., 2017. Experimental investigation on power output of different photovoltaic array configurations under uniform and partial shading scenarios. Energy, 127, 438-453.

Belhachat, F., Larbes, C., 2015. Modeling, analysis and comparison of solar photovoltaic array configurations under partial shading conditions. Solar Energy, 120, 399-418.

Bidram, A., Davoudi, A., & Balog, R. S., 2012. Control and circuit techniques to mitigate partial shading effects in photovoltaic arrays. IEEE Journal of Photovoltaics, 2(4), 532-546.

Bingöl, O., & Özkaya, B., 2018. Analysis and comparison of different PV array configurations under partial shading conditions. Solar Energy, 160, 336-343.

Chouder, A., Silvestre, S., Sadaoui, N., Rahmani, L., 2012. Modeling and simulation of a grid connected PV system based on the evaluation of main PV module parameters. Simulation Modelling Practice and Theory, 20(1), 46-58.

De Soto, W., Klein, S. A., Beckman, W. A., 2006. Improvement and validation of a model for photovoltaic array performance. Solar energy, 80(1), 78-88.

Dos Santos, P., Vicente, E. M., & Ribeiro, E. R., 2011. Reconfiguration methodology of shaded photovoltaic panels to maximize the produced energy. In Power Electronics Conference (COBEP) IEEE, 700-706.

Malathy, S., & Ramaprabha, R., 2015.Comprehensive analysis on the role of array size and configuration on energy yield of photovoltaic systems under shaded conditions. Renewable and Sustainable Energy Reviews, 49, 672-679.

Malathy, S., & Ramaprabha, R., 2017. Reconfiguration strategies to extract maximum power from photovoltaic array under partially shaded conditions. Renewable and Sustainable Energy Reviews.

Mishra, N., Yadav, A. S., Pachauri, R., Chauhan, Y. K., & Yadav, V. K., 2017. Performance enhancement of PV system using proposed array topologies under various shadow patterns. Solar Energy, 157, 641-656.

Moballegh, S., & Jiang, J., 2014. Modeling, prediction, and experimental validations of power peaks of PV arrays under partial shading conditions. IEEE Transactions on Sustainable Energy, 5(1), 293-300.

Nguyen, D., &Lehman, B., 2008, February. A reconfigurable solar photovoltaic array under shadow conditions. In Applied Power Electronics Conference and Exposition (APEC), Twenty-Third Annual IEEE, 980-986.

Parlak, K. Ş., 2014. PV array reconfiguration method under partial shading conditions. International Journal of Electrical Power & Energy Systems, 63, 713-721.

Rani, B. I., Ilango, G. S., & Nagamani, C., 2013. Enhanced power generation from PV array under partial shading conditions by shade dispersion using Su Do Ku configuration. IEEE Transactions on sustainable energy, 4(3), 594-601.

Rao, P. S., Ilango, G. S., & Nagamani, C., 2014. Maximum power from PV arrays using a fixed configuration under different shading conditions. IEEE journal of Photovoltaics, 4(2), 679-686.

Reisi, A. R., Moradi, M. H., & Jamasb, S., 2013. Classification and comparison of maximum power point tracking techniques for photovoltaic system: A review. Renewable and Sustainable Energy Reviews, 19, 433-443.

Saravanan, S., & Babu, N. R., 2016. Maximum power point tracking algorithms for photovoltaic system–A review. Renewable and Sustainable Energy Reviews, 57, 192-204.

Tsai, H. L., Tu, C. S., Su, Y. J., 2008. Development of generalized photovoltaic model using MATLAB/SIMULINK. In Proceedings of the world congress on Engineering and computer science, 22-24 October, San Francisco, USA, 1-6.

Tsai, H. L., 2010. Insolation-oriented model of photovoltaic module using Matlab/Simulink. Solar Energy, 84(7), 1318-1326.

Vijayalekshmy, S., Bindu, G. R., Iyer, S. R., 2014. Estimation of Power Losses in Photovoltaic Array Configurations under Moving Cloud Conditions. Advances in Computing and Communications (ICACC), 2014 Fourth International Conference on. IEEE, 366-369.

Vijayalekshmy, S., Bindu, G. R., Iyer, S. R., 2016. A novel Zig-Zag scheme for power enhancement of partially shaded solar arrays. Solar Energy, 135, 92-102.

Villalva, M. G., Gazoli, J. R., Ruppert Filho, E., 2009. Comprehensive approach to modeling and simulation of photovoltaic arrays. IEEE Transactions on power electronics, 24(5), 1198-1208.

Yadav, A. S., Pachauri, R. K., & Chauhan, Y. K. , 2016. Comprehensive Investigation of PV arrays with puzzle shade dispersion for improved performance. Solar Energy, 129, 256-285.

Yadav, A. S., Pachauri, R. K., Chauhan, Y. K., Choudhury, S., & Singh, R., 2017. Performance enhancement of partially shaded PV array using novel shade dispersion effect on magic-square puzzle configuration. Solar Energy, 144, 780-797.

International Conference on Science and Technology

ICONST 2018

5-9 September 2018 Prizren - KOSOVO

Stochastic Fractal Search Algorithm for ANFIS Training

Okan Bingöl[1*], Serdar Paçacı[2], Onur Mahmut Pişirir[3], Burçin Özkaya[4]

Abstract: Adaptive network fuzzy inference system (ANFIS) is a very efficient modeling method by combining the attributes of both of fuzzy inference system and neural network. The ANFIS structure must be trained before it can be used. The training process is actually the process of adjusting the ANFIS parameters. In this study, we considered that the ANFIS training process as an optimization problem. So, we apply stochastic fractal search algorithm for training the ANFIS structure. The antecedent and consequence parameters are adjusted by using this algorithm in ANFIS. Finally, the method is applied to the classification of wine dataset and showed satisfactory results.

Keywords: ANFIS, stochastic fractal search, classification, neuro-fuzzy.

Introduction

Adaptive network-based fuzzy inference system (ANFIS) can be thought of as a combination of fuzzy logic and multilayered perceptrons in the artificial neural network. The parameters must be set before the ANFIS structure can be used. The training process is actually the process of adjusting the ANFIS parameters. These parameters are devided into two parts, antecedent and consequence. ANFIS must be trained to determine these parameters since it contains artificial neural network components. Training is the process of determining parameter values. Methods have been developed that use with and without using derivative knowledge for training. We see that methods without using the derivative information are generally heuristic algorithms in the literature.

In 2007, modified particle swarm optimization algorithm is applied for training of all parameters of ANFIS structure and the method is simulated for complex nonlinear systems (Ghomsheh et al., 2007). In 2011, differential evolution algorithm is used for training the antecedent parameters of ANFIS structure. The consequent part parameters are learned by a gradient descent algorithm. Moreover, the method has been applied to predict of the chaotic signal under both noise-free and noisy conditions and simulation of the two-dimensional sinc function (Zangeneh et al., 2011). In 2013, Karaboga and Kaya apply the artificial bee colony algorithm for training ANFIS parameters (Karaboga and Kaya, 2013). Furhermore, they have used the algorithm for identifying the nonlinear dynamic system (Karaboga and Kaya, 2014). Haznedar and Kalinli optimize ANFIS parameter using genetic algorithm in 2013. They apply ANFIS to the nonlinear dynamic system identification problem. In 2018, the whale optimization algorithm is applied for training of ANFIS structure. The method has been applied to nonlinear system identification problem and predict of chaotic time series mackey-glass (Canayaz and Özdağ, 2018).

Optimization is the process of choosing the best solution from among the alternatives possible under certain conditions in a problem. Heuristic algorithms are algorithms that can give optimal solutions for large size optimization problems in acceptable time. In 2015, Salimi has been developed the stochastic fractal search (SFS) algorithm by inspiring the diffusion properties of fractals (Salimi, 2015). The property of an object or quantity, which explains self-similarity on all scales, in a somewhat technical sense, is called fractal. When

[1,4] Applied Sciences University of Isparta, Faculty of Technology, Electrical and Electronics Engineering Department, 32260, Isparta, TURKEY
[2]Suleyman Demirel University, IT Department, Software Development, 32260, Isparta, TURKEY
[3] Applied Sciences University of Isparta, Vocational School of Distance Learning, 32260, Isparta, TURKEY
*Correspondingauthor: okanbingol@sdu.edu.tr

you look closely at any part of the fractals, that part and whole part has the same features (Mandelbrot and Pignoni, 1983).

The aim of this study is to adjust the antecedent and consequence parameters of ANFIS using the SFS algorithm. The wine data set was used to test this method. The 13 attributes in this dataset were used for input and the information about which class the wine belongs to was obtained. So, ANFIS structure modeled as 13 input and a single output.

Stochastic Fractal Search Algorithm

The SFS algorithm has been developed inspiring from the diffusion properties of the fractals in nature. When the structure of algorithm is examined, it appears that it consists of two main functions. The first is a diffusion function that simulates the diffusion of fractals and the second is the update process. Diffusion process is used to generate new solutions in search space. Update process is a process updates the position of the point according to the positions of the other points in the group. The best particle generated in the diffusion process is thought to be a single particle and the particles whose energy decreased are discarded. For an effective search in problem space, SFS uses random methods such as process update (Bingöl et al., 2017).

Gaussian walks are used in the diffusion process. The two functions used in the algorithm for this process are as shown in Eq. (1) and (2). Here, ε and ε' are uniformly distributed random values between 0 and 1. BP shows the position of best point and P_i is the ith position in the group.

$$GW_1 = Gaussian(\mu_{BP}, \sigma) + (\varepsilon \, x \, BP - \varepsilon' \, x \, P_i) \tag{1}$$

$$GW_2 = Gaussian(\mu_P, \sigma) \tag{2}$$

σ is the step length of the Gaussian walk and is calculated as shown in Eq. (3). Here, when g represents the generation value, the value of the log(g) / g function decreases as the generation value increases and this reduces the step length in the walk. Thus, the reduction in step length provides more local search and obtaining results which are closer to solution.

$$\sigma = \left| \frac{\log(g)}{g} x(P_i - BP) \right| \tag{3}$$

When diffusion process of all fractals finished, each solution point is sorted by the fitness value. While the fitness value is calculated, each solution is sent as a parameter to the fitness function. The return value of the fitness function is taken as the fitness value. The fitness function is a function chosen to give the magnitude of optimal solution proximity. After the sorting process, a probability value is given so that these solution points are uniformly distributed. This process is carried out according to Eq. (4). Here, N is the number of points in the group and rank (P_i) is expressed as the rank of the of the P_i point in group.

$$Pa_i = \frac{rank(P_i)}{N} \tag{4}$$

After the calculation of the sequence and probability values, if the $P_{ai} < \varepsilon$ condition is satisfied, the first update is performed as shown in Eq. (5) for each Pi point in the group. Here, the calculated value is the new position point. P_r and P_t are randomly selected points in the group. The ε variable obtained from uniform distribution is a random value between 0 and 1 and j expresses the jth dimension in solution point.

$$P_i'(j) = P_r(j) - \varepsilon \, x \, (P_t(j) - P_i(j)) \tag{5}$$

After the evaluation on the components of the relevant point in the first update process, the second update process is performed. Here, the positions of the points are evaluated taking into consideration the positions of the other solution points in the group. This feature increases the quality of exploration of search space. In the second updating process, first the probability values are recalculated according to Eq. (4). If $P_{ai} < \varepsilon$, the

second update calculations are made for the corresponding solution point. Otherwise, update is not performed on the corresponding point. In the second update process, according to the value that ε has received the process according to Eq. (6) and (7) is performed.

$$P_i^{"} = P_i^{'} - \hat{\varepsilon}\, x\,(P_t^{'} - BP) \;\Big|\; \varepsilon^{'} \le 0.5 \tag{6}$$

$$P_i^{"} = P_i^{'} - \hat{\varepsilon}\, x\,(P_t^{'} - P_r^{'}) \;\Big|\; \varepsilon^{'} > 0.5 \tag{7}$$

The basic steps of SFS algorithm as follows:

```
1   Initialize a population of N fractals
2   While (generation < maximum generation or (stop criterion)) Do
    {
3       For each fractal Pi in the population Do
        {
4           Call Diffusion Process
            {
    1           For i=1 to maximumDiffusion Do
                {
    2               Apply gaussian walk
    3               Calculate fitness value
    4               Replace fractal if better fitness value
                }
            }
        }
5       Call First Updating Process
        {
    1       Rank all fractal using fitness values
    2       For each fractal Pi in the population Do
            {
    3           For each dimension j in Pi Do
                {
    4               If rand[0 , 1] ≥ Pai
                    {
    5                   Update the value
                    }
                }
            }
        }
6       Calculate fitness values
7       Call Second Updating Process
        {
    1       Rank all fractal using fitness values
    2       For each fractal Pi in the population Do
            {
    3           If rand[0 , 1] ≥ Pai
                {
    4               Update position of the fractal
                }
            }
        }

    }
```

ANFIS

The ANFIS emerged by combining the decision-making ability of fuzzy logic and the learning ability of the artificial neural network. It uses the Sugeno type fuzzy model and itsstructure has two main parts which are

the antecedent part and the consequence part. Each part is connected to each other by the fuzzy rules in network form (Jang, 1993). A five-layer ANFIS structure is shown in Fig. 1.

Layer 1 is called fuzzification layer and it executes a fuzzification process. Membership functions used for fuzzification processes are in this layer. In this study, the membership functions are gaussian membership function so, it depends on two parameters μ and σ. μ and σ denote the center and standard deviation, respectively. The parameters in this layer are called antecedent parameters. The node outputs are given in Eq. (8).

$$O_i^1 = \mu_{Ai}(x) \tag{8}$$

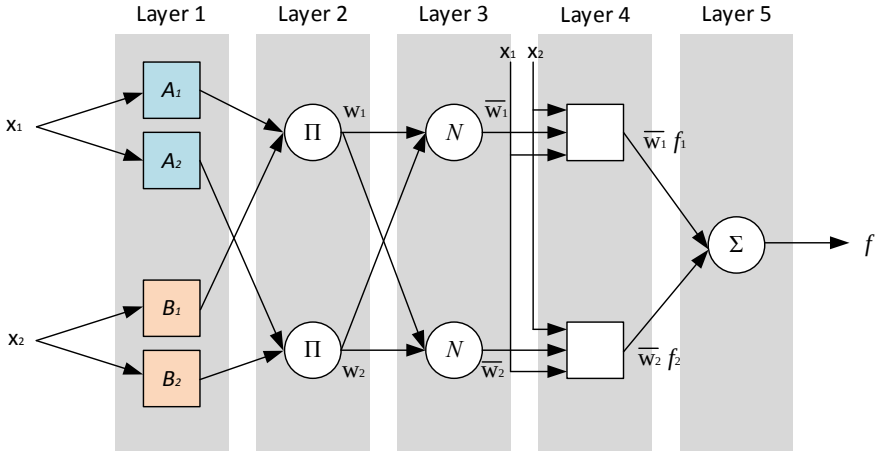

Figure 1. A five-layer ANFIS structure

Layer 2 is called rule layer. The nodes in this layer represent the firing strength of a rule. The output of the rule nodes according to Eq. (9) is performed.

$$O_i^2 = \omega_i = \mu_{Ai}(x_1)\mu_{Bi}(x_2) \tag{9}$$

Layer 3 is called normalization layer. This layer calculates the normalized firing strength for each of the inputs. Eq. (10) shows that how calculation the normalized value.

$$O_i^3 = \varpi_i = \frac{\omega_i}{\omega_1 + \omega_2} \tag{10}$$

Layer 4 is called defuzzification layer. In this layer weighted output values of each rule are calculated. The output this layer calculates using Eq. (11). p_i, r_i and q_i are parameters and that are referred to as consequence parameters.

$$O_i^4 = \varpi_i f_i = \varpi_i (p_i x_1 + q_i x_2 + r_i) \tag{11}$$

Layer 5 is called output layer. This layer computes the overall as the summation of input values. Eq. (12) shows the output of this layer.

$$O_i^5 = \sum_i \varpi_i f_i = \frac{\sum_i \omega_i f_i}{\sum_i \omega_i} \tag{12}$$

Training ANFIS using SFS Algorithm

When we look at the ANFIS structure, we need to set the parameters of membership functions in the first layer and the parameters p, q, r, etc. in the fourth layer used for defuzzification. In this study, the Gaussian

membership function is used and therefore, it is necessary to set 2 parameters which are center and the standard deviation for each membership function. Moreover, for each output function, 3 parameters must be set. For example, we suppose that in a two-input and one-output system, 3 membership functions are defined for each input and 3 output functions are defined for output. In this case, it is necessary to set 12 parameters for membership functions and 9 parameters for output functions, so a total of 21 parameters must be set. It can also be considered as a 21-dimensional optimization problem. These parameters are expressed by the position values of the fractal in the SFS algorithm. Fig. 2 shows that the explanation of parameter array.

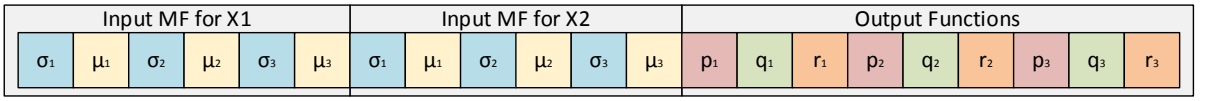

Figure 2. Explanation of parameter array

For the fitness function the RMSE error function shown in Eq. (13) is used. $\overline{y}_i$ represents the output obtained by ANFIS, y_i represents the desired output and N represents the number of data in the dataset.

$$RMSE = \sqrt{\frac{\sum_{i=1}^{N}(y_i - \overline{y}_i)^2}{N}} \tag{13}$$

In this study, wine dataset is used to test ANFIS training with SFS algorithm. Wine dataset has 13 features, 3 classes, and 176 samples. Thus, ANFIS for this data set is modeled as having 13 inputs and single output. In this case, it is necessary to set 78 (6 x 13) parameters for membership functions and 42 (14 x 3) parameters for output functions. So, a total of 120 parameters must be adjusted.

Simulation Results

Wine dataset is the results of a chemical analysis of wines grown in the same region in Italy, but they are derived from three different cultivars. The analysis determined the quantities of 13 constituents found in each of the three types of wines. These 13 constituents are alcohol, malic acid, ash, the alkalinity of ash, magnesium, total phenols, flavonoids, nonflavonoid phenols, proanthocyanins, color intensity, hue, OD280/OD315 of diluted wines, and proline, respectively (Dua and Karra Taniskidou, 2017).

In the ANFIS training process, the number of fractals, the number of diffusions, the selection of diffusion function value, and maximum number of generation are taken as 100, 2 and 0.9, 250, respectively. The SFS algorithm used in training the ANFIS structure has run 20 times independently of each other and the average classification error was found. According to the results obtained, with the use of SFS algorithm in the training of ANFIS showed 98.32% correct classification. Classification result of the wine dataset with ANFIS is shown in Fig. 3. As can be seen in the Fig. 3, three samples are incorrectly classified in the dataset. These are samples 44, 122 and 131.

For example, if the 82nd sample values in the dataset are given as input to the trained ANFIS structure, the graph of the results obtained is shown in Fig. 4. As can be seen in the Fig. 4, the output value of ANFIS structure is 1.64. When we round the value, we get the result that the corresponding data belongs to the second class, which is the same as the class given in the dataset.

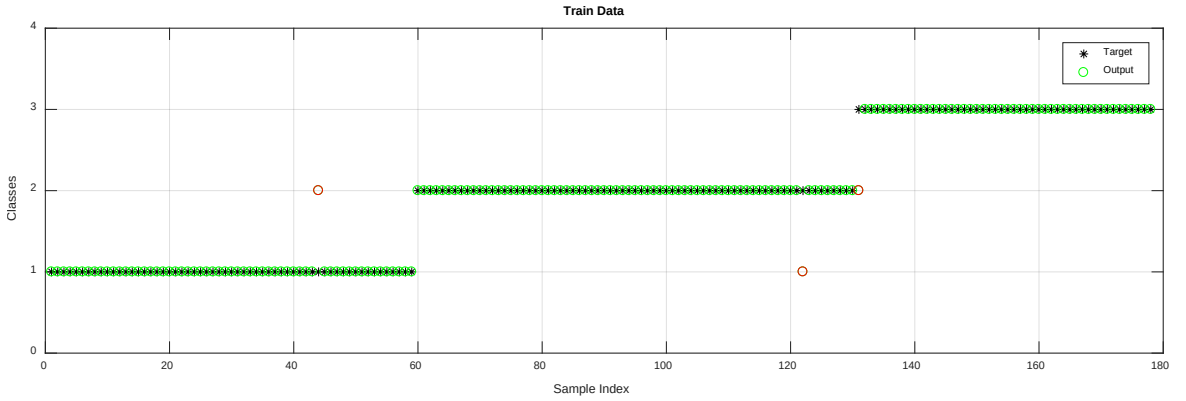

Figure 3. Classification result of the wine dataset

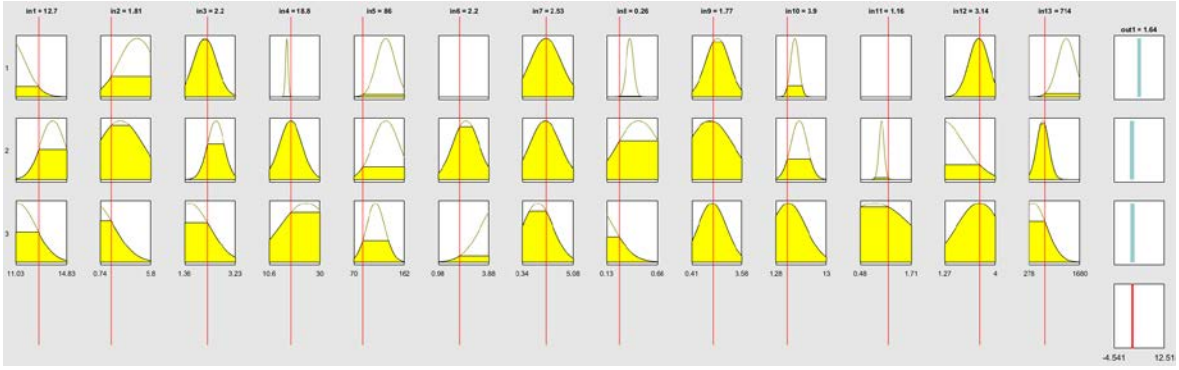

Figure 4. Classification result of the wine dataset

Conclusions

In this study, the SFS algorithm is used for the training of ANFIS structure. The antecedent and consequence parameters in the ANFIS structure is adjusted by this algorithm. The results show that the SFS algorithm can be used in the training of ANFIS. However, when maximum number of generations in the SFS algorithm increases, it has been observed that the success rate of the training of the ANFIS increases. For example, when the maximum number of generations is increased to 2000 values, the correct classification rate for the wine data set is up to 99.44%.

References

Bingöl, O., Güvenç, U., Duman, S., Paçacı, S. (2017). Stochastic fractal search with chaos. In Artificial Intelligence and Data Processing Symposium (IDAP), 2017 International, 1-6.

Canayaz, M., Özdağ, R. (2018). Training ANFIS using The Whale Optimization Algorithm. International Conference on Advanced Technologies, Computer Engineering and Science (ICATCES'18), 409-414.

Dua, D., Karra Taniskidou, E. (2017). UCI Machine Learning Repository [http://archive.ics.uci.edu/ml]. Irvine, CA: University of California, School of Information and Computer Science.

Ghomsheh, V.S., Shoorehdeli, M.A., Teshnehlab, M. (2007). Training ANFIS structure with modified PSO algorithm. In Proceedings of Mediterranean Conference on Control and Automation. 1-6.

Haznedar, B., Kalinli, A. (2016). Training ANFIS using genetic algorithm for dynamic systems identification. International Journal of Intelligent Systems and Applications in Engineering, 4 (Special Issue-1), 44-47.

Jang, J.S. (1993). ANFIS: adaptive-network-based fuzzy inference system. IEEE transactions on systems, man, and cybernetics, 23(3), 665-685.

Karaboga, D., Kaya, E. (2013). Training ANFIS using artificial bee colony algorithm. In Innovations in Intelligent Systems and Applications (INISTA), 2013 IEEE International Symposium on. 1-5.

Karaboga, D., Kaya, E. (2014). Training ANFIS using artificial bee colony algorithm for nonlinear dynamic systems identification. In Signal Processing and Communications Applications Conference (SIU), 2014 22nd 493-496.

Mandelbrot B.B., Pignoni R. (1983). The fractal geometry of nature.

Salimi, H. (2015). Stochastic fractal search: a powerful metaheuristic algorithm. Knowledge-Based Systems, 75, 1-18.

Zangeneh, A.Z., Mansouri, M., Teshnehlab, M., Sedigh, A.K. (2011). Training ANFIS system with DE algorithm. In Advanced Computational Intelligence (IWACI), 2011 Fourth International Workshop on. 308-314.

International Conference on Science and Technology

ICONST 2018

5-9 September 2018 Prizren - KOSOVO

Bluetooth Based Smart Vacuum Design and Implementation

Aydın Güllü[1]*, Musa Çağlar[2]

Abstract: The number of smart devices that are developed to facilitate people's everyday tasks is increasing day by day. The devices presented to the end user can communicate with each other through the concept of Industry 4.0. This process, known as the internet of things (IoT), allows devices to be controlled over the Internet. A vacuum cleaner designed in the scope of this study can connect to the internete and fulfill the assigned tasks. Autonomous home sweeping can be performed in accordance with given tasks. The autonomous electric vacuum cleaner developed in this study; body, vacuum part, sensors, battery, motors that provide movement consists of battery and electronic circuit. It can sweep itself autonomously without touching the surrounding objects by means of the absorbers on the broom which is a small design. In addition, the Bluetooth wireless communication technology that you use can be commanded via smart phone / tablet. A home plan can be defined by means of developed software. At this point, the robot can be instructed which parts to clean. In this respect, self-autonomously assigned tasks can be successfully replaced. The system also allows remote control over the internet with the help of wi-fi. Routine home sweeping is performed autonomously with the developed smart vacuum cleaner. With the developed mobile software, it is possible to choose which environment and how much the robot can work. In addition, the robot measures its own charge and can go to the charging station and the need. It has been seen that the robot fulfills the assigned tasks in a three-room home plan. With the developed Android application, the robot can be controlled automatically and manually. With the concept of internet of objects, the developing trend made it possible to produce many smart devices. When combined with economical electronics, mechanical hardware and software, a lot of innovations come into play that will make human life easier. In this developed work, it was ensured that the routine work of the people was done by means of an intelligent broom (autonomous robot). With improved hardware and software, people will save time and work power. As a result, human life will greatly facilitate

Keywords: IoT, Smart Vacuum Cleaner, Otonom Robot

Introduction

Mechatronic systems consist of mechanical parts, electronic circuitry and software (Carryer, Ohline, & Kenny, 2011). The equipment that makes up these systems is easy to reach in recent years. With the used 3d printing machines, mechanical parts designed in the desired structure are produced(Kesner & Howe, 2011). The software developed for microcontrollers used in electronic circuit design can be controlled quickly and flexibly. All these components form the mechatronic system. Sensor technology is used for intelligent mechatronic systems. Autonomous operation can be achieved by processing the information from the environment with the used sensors.(Mahalik, 2003) The number of intelligent devices produced by utilizing these opportunities is increasing day by day.

In recent years, the development of electronic circuits and communication protocols used in wireless communications have brought autonomous and intelligent work to another dimension. In this way, the machines can be remotely controlled and communicated with each other to be able to function. This period, called Industry 4.0, offers many conveniences(Lasi, Fettke, Kemper, Feld, & Hoffmann, 2014). During this period, studies such as speed safety came to the forefront in studies on machines communicating with one

[1]Trakya University, Ipsala Vocational School 22400, Edirne, TURKEY
[2] Trakya University, Ipsala Vocational School 22400, Edirne, TURKEY
*Correspondingauthor: aydingullu@trakya.edu.tr

another. In this period, which is called the internet of things, a lot of new algorithm algorithms are presented (Gubbi, Buyya, Marusic, & Palaniswami, 2013).

In this study, a remote controlled mobic robot was designed to allow autonomous motion. In the next sections, mechanical, electrical and software designs will be mentioned. The findings and usefulness of the robot's work will be explained.

Material and Method

This section is explained in three parts. Firstly, the visual design is described by mechanical design. Electrical equipment used later is mentioned. Lastly, the software is mentioned. The software is microcontroller control software and developed mobile application.

Mechanical Hardware

The autonomous mobile vacuum cleaner is mounted on a mechanical chassis. A 12V powered vacuum cleaner is mounted on the designed chassis. In addition, battery, electronic card, sensors, bluetooth module, motor and wheels are mounted on the chassis.

The robot is able to move in the environment with information from sensors that perceive it. Differential driving model is used for the design which takes center of gravity of the robot. There is one free-moving passive wheel on the front. Figures 1 and 2 are shown robot images.

Figure 1. Smart Vacuum Robot

Figure 2. Smart Vacuum Robot

Electronic Hardware

Modules have been used in electronic circuit design. Arduino platform is used in control part of this prototype robot. The Atmega328p 8bit microcontroller is used. With the L298 h-bridge integration, two motors are independently controlled.

Motor speed control is done by PWM signals. The control of the vacuum cleaner motor is controlled on / off. The wheels are equipped with a hall effect sensor for position information. The estimated position is determined by the distance on this sensor. In addition, at certain distances, position verification and reference were made with RF-ID tags. An RF-ID sensor was used for this (RC522). In this way, the robot can correctly detect the location information. Optical sensors are used to detect the environment. Three sensors surround the peripherals. With these enhancements, the robot can work autonomously. The location selection uses the Bluetooth module for functions such as manual control. A protocol has been written for module communication with the robot. It is controlled via an application developed for mobile devices. This allows remote control.

Software and Mobil App

The software is made in two stages. First; microcontroller software. This is the main control software. This software, which communicates all of the electronic hardware, is encoded in the micro controller. The software running in conjunction with the mobile application controls the robot's hardware according to the received commands. The second one is mobile application software. The software developed on http://appinventor.mit.edu platform is used by being installed on the android device. The device that communicates via the Bluetooth platform can connect to the Internet via a server. Local control was carried out within the scope of this study. Designed mobile application screens are shown in Figures 3 and 4.

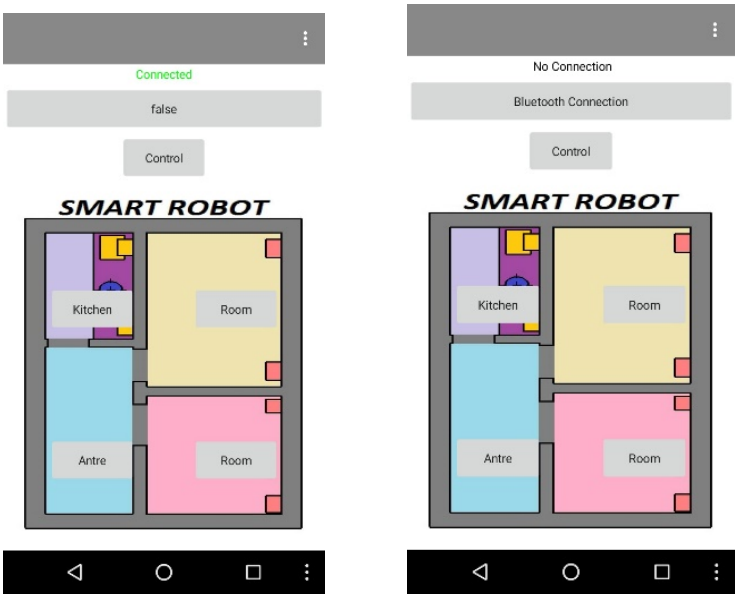

Figure 2. Mobile Application Screen (Home Sketch)

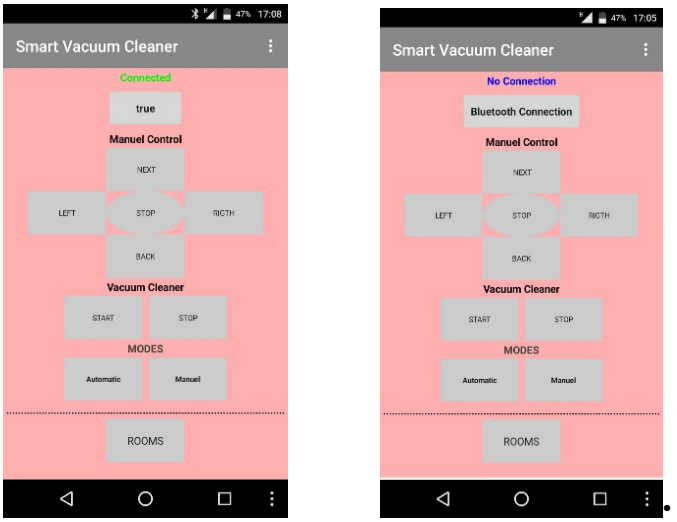

Figure 3 Mobile Application Screen (Control Screen)

Results

In this study, an autonomous vacuum cleaner was designed. The design will be able to self-clean by sensing the objects around it. In addition, the robot communicates with bluetooth and can execute commands that are given wirelessly. The mobile app has been developed for this process. This will make it easier for people to do daily tasks. It also provides remote control via a network connection that can be set up. Location information is perceived on the robot side on the sketch side of the wheel and the previously defined sketch. The developed work can work more functionally with commercial facilities with limited opportunities.

Discussion and Conclusions

The common reasoning of different people by accessing information through internet technology has led to a rapid solution in practice. Another advantage is the availability of many sensor hardware with internet shopping. Open source microcontrollers also provide flexible control. In this study, an assistant mobile robot was designed by taking advantage of these advantages and it was operated more functional with the concept of objects' internet. A range of functions have been added to facilitate the human life, such as sensing the environment, working at the locale where self-charging is desired, and the area scanning function developed for equipment control. Tests made have given successful results for limited location.

References

Carryer, J. E., Ohline, R. M., & Kenny, T. W. (2011). *Introduction to mechatronic design*: Prentice Hall Boston.

Gubbi, J., Buyya, R., Marusic, S., & Palaniswami, M. (2013). Internet of Things (IoT): A vision, architectural elements, and future directions. *Future generation computer systems, 29*(7), 1645-1660.

Kesner, S. B., & Howe, R. D. (2011). Design principles for rapid prototyping forces sensors using 3-D printing. *IEEE/ASME Transactions on mechatronics, 16*(5), 866-870.

Lasi, H., Fettke, P., Kemper, H.-G., Feld, T., & Hoffmann, M. (2014). Industry 4.0. *Business & Information Systems Engineering, 6*(4), 239-242.

Mahalik, N. P. (2003). *Mechatronics*: Tata McGraw-Hill.

International Conference on Science and Technology

ICONST 2018

5-9 September 2018 Prizren - KOSOVO

Investigation of the Effects of Salubrinal on ER Stress in Experimental PCOS Model

Aslı Emincik[1]*, Zeynep Banu Güngör[2], Elif Güzel Meydanlı[1]

Abstract: Polycystic ovary syndrome (PCOS) is a disease characterized by hyperandrogenism and ovary dysfunction. In various physiological and pathological conditions, unfolded and misfolded proteins result in endoplasmic reticulum (ER) stress and induce unfolded protein response (UPR). Salubrinal (SAL) inhibits dephosphorylation of α-subunit of eukaryotic initiation factor 2 (eIF2α) which functions in UPR pathway, resulting in inhibition of ER stress. In the present study, it was aimed to investigate the role of ER stress in PCOS and the effect of SAL on this role. Thirty 25 day-old Balb/c mice were divided into four groups as control, PCOS, PCOS+SAL and SAL. The animals were weighted at the beginning and end of study. Serum testosterone (T), luteinizing hormone (LH) and activating transcription factor 4 (ATF4) were analyzed by ELISA. Light microscopic and electron microscopic analysis of ovarium were performed. 78-kDa glucose-regulated protein (GRP78/BiP), p-eIF2α and poli ADP riboz (PAR) expressions in granulosa cells were evaluated immunohistochemically. All data were compared statistically.At the end of experiments, weights and serum T levels of the animal increased in PCOS group while serum LH and ATF4 expressions decreased. Morphometrically, number of follicles with a diameter in between 150-300 µm declined, number of follicles larger than 300 µm and the percentage of cystic follicles increased. Immunoreactivities of ER stress markers, GRP78/BiP and p-eIF2α decreased, whereas oxidative stress (OS) dependent PAR expression increased. Ultrastructurally, PCOS group had no ER enlargement which was observed in control group while there were disjunctions between granulosa and theca cells and mitochondrial damage in granulosa cells.In experimentally established PCOS, we showed that elevated OS levels did not induce but rather decreased ER stress levels in granulosa cells, and SAL injection in PCOS model was ineffective on searched parameters in this study. Since ER stress play roles in certain physiological processes, we consider that inhibitors of ER stress may not be always feasible for reproductive tissues and more studies concerning this issue are needed.

Keywords: ER Stress, PCOS, Oxidative Stress, Ovary.

Introduction

Polycystic ovary syndrome (PCOS) is an endocrine disorder with a prevalence of 4-11% among women with reproductive age [1]. According to 2009 diagnosis criteria of Androgen Excess and PCOS Society, woman showing both of two criteria of clinical and/or biochemical hyperandrogenism and ovary disfunction is PCOS patient [2]. Clinically, diagnosing a woman as having PCOS implies an increased risk for infertility, dysfunctional bleeding, endometrial carcinoma, obesity, type 2 diabetes mellitus (DM), dyslipidemia, hypertension, and possibly cardiovascular disease [3, 4]. One of PCOS criteria, hyperandorgenism, i.e. elevated level of androgens like testosterone (T) and androstenedione causes disordered secretion of gonadotropin releasing hormone, resulting in ovulatory defects and formation of follicle cysts[5, 6].

It has been known that oxidative stress (OS) and inflammation markers increase in PCOS women in direct proportion to androgen levels [7]. Poly ADP ribose polymerase (PARP) is a protein family functioning in many cellular events such as DNA repair, genomic stability, chromatin functions and cell death [8].

[1]İstanbul Üniversitesi, Cerrahpaşa Tıp Fakültesi, Histoloji ve Embriyoloji Anabilim Dalı, İstanbul
[2]İstanbul Üniversitesi, Cerrahpaşa Tıp Fakültesi, Biyokimya Anabilim Dalı, İstanbul
*Correspondingauthor: ang0986@gmail.com

Depending on ROS mediated cellular stress and single strand DNA damage, the most expressed isoform of PARP, nuclear PARP-1 is activated. Active PARP-1 cleaves the substrate nicotinamide adenine dinucleotide (NAD^+) into nicotinamide and ADP to generate PAR structure, allowing repair of single strand DNA damage [9]. Elevated stress signals increase PARP-1 activation and PAR synthesis[10]. Excessive PARP activation causes a rapid depletion of intracellular NAD^+ and ATP which are important for cellular energy metabolism and healthy mitochondria function, resulting in cellular functional defects and necrosis [11].

Endoplasmic reticulum (ER) is a prominent perinuclear organelle for synthesis and folding of secretory proteins and membrane proteins. Due to hypoxia, oxidative damage, variation in calcium homeostasis, viral infections, protein inclusion bodies, elevated synthesis of secretory proteins, failure in cellular energy and/or nutritional homeostasis, unfolded or misfolded proteins are accumulated in ER, resulting in ER stress. As a result of ER stress, unfolded protein response (UPR) is induced to protect the cell [12, 13,14].

Taking part in PERK pathway of ER stress induced UPR downstream pathways, the eukaryotic translation-initiation factor 2α (eIF2α) is phosphorylated by activated PERK to attenuate the rate of general translation initiation and prevent further protein synthesis. Salubrinal (SAL) is a molecular compound which inhibits eIF2α dephosphorylation, allowing constant phosphorylated eIF2α, thereby, inhibiting protein translation and leading to decrease in protein synthesis [15]. Thus, ER homeostasis is protected and prevent the cell against apoptotic fate [16].

Considering that OS induces ER stress and is enhanced in PCOS pathogenesis, in this study, we assumed the presence of ER stress in a model of experimental PCOS established in female Balb/c mice and aimed to investigate the effect of SAL, an ER stress inhibitor, in PCOS. Starting from this point of view, this study targeted to evaluate serum T, LH and ATF4 levels biochemically and expressions of PAR, GRP78/BiP and eIF2α immunohistochemically in ovarium, as well as to examine the ovarium granulosa cells by light microscopic and electron microscopic techniques.

Material and Method

Study Design

30 female 25 days old Balb/c mice (Istanbul University Aziz Sancar Institute of Experimental Medicine, İstanbul, Turkey) were maintained on 12-h light, 12-h dark cycles and given food and water *ad libitum*. The animals divided into four groups as control, PCOS, PCOS+SAL and SAL. Control group (n:6) injected with 0.1 ml sesame oil (sc) for 20 days, then injected with salin (ip) for 5 days. PCOS group (n:8) injected (sc) with DHEA (6mg/100g) for 20 days, then injected with salin (ip) for 5 days. PCOS+SAL group (n:8) injected (sc) with DHEA for 20 days, then injected with SAL (1mg/kg) (ip) for 5 days. SAL group (n:8) injected with 0.1 ml sesame-oil for 20 days, then injected with SAL (ip) for 5 days. The animals were weighted at the beginning and end of study. Monitoring of estrous cycles by daily vaginal lavage began at 40 days of age and continued through the end of the study.

Biochemical Analysis of Serum

After 25 consecutive days of treatments, blood samples were obtained by cardiac puncture from each mouse before sacrifice. Serum T (Mouse Testosterone ELISA Kit, Yehua Biological Technology, Shanghai, China), LH (Mouse Luteinizing Hormone ELISA Kit, Yehua Biological Technology, Shanghai, China) and ATF4 (Mouse Activating Transcription Factor-4 ELISA Kit, Yehua Biological Technology, Shanghai, China) levels were determined by ELISA.

Morphological and Morphometrical Evaluation of Ovaries

Ovarian tissue was fixed overnight in 10% neutral formalin and then dehydrated in a graded series of ethanol and cleared with xylene, for embedding in paraffin using an automated tissue processor (Spin Tissue Processor STP-120, Thermo Scientific, Germany). Sections with thickness of 5 μm were obtained using a sliding microtome (HM 430; Thermo Fisher Scientific, Munich, Germany). The tissue sections were stained

with hematoxylin and eosin and evaluated using a light microscope (BX61; Olympus, Tokyo, Japan) attached with a computerized digital camera (DP72; Olympus, Tokyo, Japan).

Immunohistochemistry

The sections were immunostained with GRP78/BiP antibody (1:200; Cell Signaling Technology, Beverly, MA), p-eIF2α antibody (1/100, rabbit monoclonal, Cell Signaling Technology, Beverly, MA,USA) and PAR antibody (1/100, Enzo Life Sciences, Farmingdale, NY, USA).

Ultrastructural Analysis by Transmission Electron Microscopy

Sections were analyzed and photographed using a transmission electron microscope (Jeol-1011, Tokyo, Japan) with an attached digital camera (Olympus-Veleta TEM Camera, Tokyo, Japan).

Statistical Analysis

Statistical analyses were performed using Sigma Plot 13 (Systat Software, San Jose, USA). All Data were analyzed by one-way ANOVA.

Results

At the beginning of study, weights of animals were adjusted in equal mean in each groups (P=0.873). At the end of experiment, weights of mice in PCOS and PCOS + SAL groups were significantly higher than the control and SAL groups (P<0.001) (Figure 1).

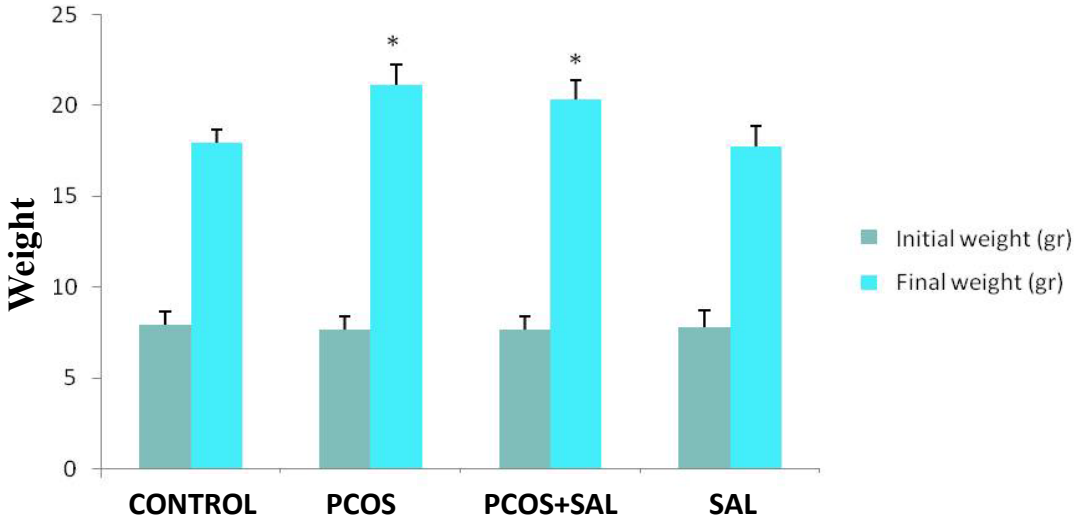

Figure 1:Initial and final body weight of mice.

Biochemical Findings

Comparing serum T levels of the groups, animals in PCOS and PCOS+SAL groups showed significantly increased levels with respect to the control group (P=0.002 and P=0.004, respectively) and to SAL group (P=0.002 and P=0.005, respectively). Other groups showed no significant differences.
Comparing serum LH levels of the groups, PCOS group revealed significantly decreased levels in comparison with the control and SAL groups (P=0.045 and P=0.016, respectively).
Comparing serum ATF4 levels of the groups, PCOS mice showed significantly lower levels in comparison with the control, PCOS+ SAL and SAL groups (P=0.007, P=0.005 and P<0.001, respectively).

Vaginal Smear Findings

Mice in the control and SAL groups had regular estrous cycle whereas PCOS and PCOS+SAL groups had irregular and prolonged cycles. Normal estrous cycle of the mice is approximately 4-5 days.

Light Microscopic Findings

Sections from PCOS group showed a large number of cystic follicles (Figure 2B). The granulosa cell layer around follicle cyst was determined to be quite thinner. Corpus luteum was rarely observed. This was evaluated as an indicator of anovulation or oligoovulation in PCOS group.

Sections of PCOS+SAL group shared similar features with PCOS group. In a similar manner, the follicle cysts and degenerated oocytes, zona pellucida and granulosa cells (Figure 2C).

SAL group showed similar images to the control group. Healthy preantral and antral follicles in ovarium cortex was detected to have a granulosa cell layer composed of 8-9 cell layers (Figure 2D).

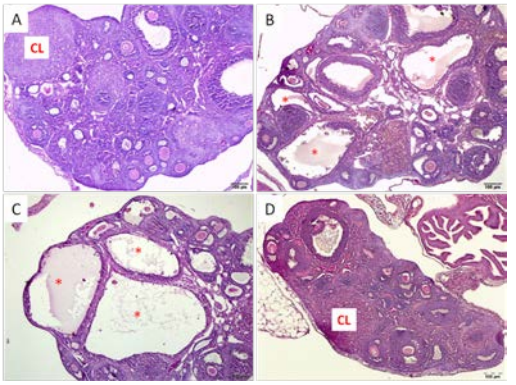

Figure 2: Control (A), PCOS (B), PCOS+SAL (C), SAL (D) groups. Corpus Luteum (CL), follicular cyst (*). H+E, X10.

The Number and Diameters of Follicles

Primordial, primary, secondary and tertiary follicles of all groups were counted and compared statistically. The follicle number of PCOS group declined significantly as compared with the control group (P=0.002). The number in PCOS + SAL group also declined significantly in comparison to both control and SAL groups (P<0.001, P=0.038, respectively).

In addition to follicle number, follicles were divided into groups and calculated with their sizes as 150-300 µm (early small antral follicles), >300 µm (large antral follicles) and cystic follicles. The number of follicles measured as 150-300 µm in ovaries of mice in PCOS and PCOS+SAL groups declined significantly in comparison to the number of control and SAL group. The number of follicle with a diameter > 300 µm in PCOS and PCOS+SAL groups increased significantly compared with the control SAL groups. Comparing the percentages of cystic follicles calculated by the ratio of number of cystic follicles in ovarium to the total number of follicles, PCOS and PCOS+SAL groups had statistically significant higher ratio in comparison to the ratio of control and SAL groups.

Immunohistochemical Findings

GRP78/BiP staining intensity and distribution in the cytoplasm of total granulosa cells of all follicles were evaluated immunohistochemically by using H-Score method and compare statistically. Negative control sections did not show any immunoreaction. GRP78/BiP immunoreactions in normal non-cystic granulosa cells of PCOS and PCOS+SAL groups decreased significantly in comparison to the immunoreactions in

control and SAL groups. No statistically significant difference was found between other groups in terms of GRP-78/BiP immunoreactivity (Figure 3A) .

p-eIF2α immunoreactivities in PCOS and PCOS+SAL groups decreased markedly compared with the control and SAL groups (P<0.001). Other groups showed no statistically significant difference. The decreased immunoreactivity of ER stress marker, GRP-78/BiP, was consistent with the decrease in immunoreactivity of p-eIF2α induced by ER stress in granulosa cells of PCOS and PCOS+SAL groups (Figure 3B).

PAR immunoreactivity in granulosa cells of PCOS and PCOS+SAL groups was observed to be enhanced compared with the control and SAL groups (P<0.001). Other groups showed no statistically significant difference (Figure 3C).

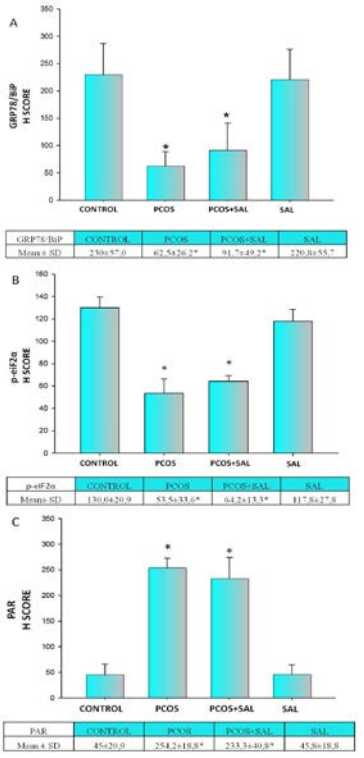

Figure 3: Expression of GRP78/BiP (A), p-eIF2α (B), PAR (C) in groups. GRP78/BiP and p-eIF2α expression decreased while PAR expression increased in PCOS and PCOS+SAL groups.

Electron Microscopical Findings

In PCOS group, there was no dilatation in GER cisternae as in the control group. Mitochondria dilated, swelled and lost their cisternae, with myelin-like structures inside mitochondria. There were local disjunctions between granulosa cells and theca cells. In PCOS+SAL group, cystic follicles as in PCOS group and granulosa cells with thinner layers around the cysts were detected. Cytoplasmic and nuclear invagination were observed in nuclei of granulosa cells. As in PCOS group, chromatin margination was observed. GER had no dilatation. Granulosa cells of SAL group showed similar ultrastructural morphology to granulosa cells in the control group.

Discussion and Conclusions

By as-yet-unknown mechanism regarding PCOS, environmental, epigenetic and hormonal factors are considered to be crucial in the course of disease [17]. To confirm establishment of PCOS model, hyperandrogenism and ovary dysfunction were tested in the present study. Serum T levels and vaginal smear findings indicate successful establishment of experimental PCOS model.

Increased weights of the animals injected subcutaneous DHEA are consistent with the obesity which is characteristic of patients with PCOS [18] and with increased weights of animals in experimental PCOS models [19]. Non-significant change in weights of PCOS+SAL groups compared with PCOS group suggests that SAL has not any effect on weights in our PCOS model.

In this study, LH levels were measured biochemically. A large number of studies have shown that LH levels are higher in PCOS women [20, 21] and experimental PCOS animal models [20, 22]. However, Tessaro et al. reported for the first time that LH level was lower in mice of PCOS model injected by DHEA in comparison to the control mice [23, 24]. Excessive LH secretion results in surplus of T levels [25]. Thus, in this study, we suggest that subcutaneous injection of DHEA externally in PCOS model may inhibit LH through a negative feedback mechanism, resulted in decreased LH levels.

In the present study, GRP78/BiP and p-eIF2α immunoreactivities were examined to evaluate ER stress in granulosa cells. GRP78/BiP immunostaining in PCOS group was lower than the control and SAL groups. Previous studies have reported that androgens are able to induce [26, 27] and inhibit [28] follicular development and these effects depend on type, dose and usage duration of androgens [28, 29]. Androgens can induce atresia and apoptosis, allowing inhibition of follicular development and ovulation. In the light of these information, our study suggests that follicular development in granulosa cells may arrest due to the increase in serumT levels by DHEA injection, thereby cellular protein load decreases because of the decreased protein synthesis depending on arrest of follicular development; thus, ER stress related GRP78/BiP immunoreactivity decreases in PCOS group. p-eIF2α immunoreactivity in ovarium tissues of mice were significantly lower in PCOS group compared with the control group. This finding is parallel with GRP78/BiP immunoreactivity and supports the fact that ER stress decreased in PCOS group.

In PCOS patients, high levels of OS and low antioxidant concentration suggesting this oxidative condition are observed [30]. Hyperandrogenism causes increase of ROS levels in ovarium As a result of enhanced OS, a nuclear enzyme PARP is activated [31]. The main enzyme of PARP family PARP-1 is responsible of 90% of PAR production [32]. In our study, PAR activity in granulosa cells of PCOS group was statistically higher than the control group. In light of these results, we concluded that OS may not always increase ER stress parameters.

The data for SAL, not a common apoptotic inhibitor and not providing any protection against signals not related to ER stress [33, 34] are consistent with our findings, supporting not inducing ER stress. ER stress is characterized by dilatation of ER lumens due to protein accumulation in electron microscopic examinations [35, 36]. In our study, there was a dilatation of ER lumen of granulosa cells in the control and SAL groups while PCOS and PCOS+SAL groups had no dilatation; this supported our immunohistochemical findings and showed that ER stress in granulosa cells of PCOS and PCOS+SAL groups were lower than the control and SAL groups.

As a conclusion, we elucidated by light and electron microscopical methods that OS increases but ER stress decreases in the PCOS model established by DHEA injection. According to these results, we identified that OS may not always induce ER stress. Since ER stress and relevant UPR mechanisms are needed for normal functions of reproductive tissues such as normal oocyte development, follicular growth and maturation, endometrial menstrual cycle, preimplantation embryo development, ER stress inhibitors like SAL may not be always appropriate for reproductive tissues in terms of treatment of related diseases and we suggest that this issue needs to be searched further by dose and time dependent studies.

Acknowledgements

This study was supported by the Scientific Research Projects Coordination Unit of Istanbul University.

References

1. Dashti, S., et al., *A Review on the Assessment of the Efficacy of Common Treatments in Polycystic Ovarian Syndrome on Prevention of Diabetes Mellitus.* Journal of family & reproductive health, 2017. **11**(2): p. 56.
2. Azziz, R., et al., *The Androgen Excess and PCOS Society criteria for the polycystic ovary syndrome: the complete task force report.* Fertility and sterility, 2009. **91**(2): p. 456-488.
3. Jamilian, M., et al., *Metabolic response to selenium supplementation in women with polycystic ovary syndrome: a randomized, double-blind, placebo-controlled trial.* Clinical endocrinology, 2015. **82**(6): p. 885-891.
4. Thethi, T.K., et al., *Role of insulin sensitizers on cardiovascular risk factors in polycystic ovarian syndrome: a meta-analysis.* Endocrine Practice, 2015. **21**(6): p. 645-667.
5. Masszi, G., et al., *Reduced estradiol-induced vasodilation and poly-(ADP-ribose) polymerase (PARP) activity in the aortas of rats with experimental polycystic ovary syndrome (PCOS).* PloS one, 2013. **8**(3): p. e55589.
6. Moore, A.M., et al., *Enhancement of a robust arcuate GABAergic input to gonadotropin-releasing hormone neurons in a model of polycystic ovarian syndrome.* Proceedings of the National Academy of Sciences, 2015. **112**(2): p. 596-601.
7. Yang, Y., et al., *Is interleukin-18 associated with polycystic ovary syndrome?* Reproductive Biology and Endocrinology, 2011. **9**(1): p. 7.
8. Herceg, Z. and Z.-Q. Wang, *Functions of poly (ADP-ribose) polymerase (PARP) in DNA repair, genomic integrity and cell death.* Mutation Research/Fundamental and Molecular Mechanisms of Mutagenesis, 2001. **477**(1): p. 97-110.
9. Cseh, A.M., et al., *Poly (adenosine diphosphate-ribose) polymerase as therapeutic target: lessons learned from its inhibitors.* Oncotarget, 2017. **8**(30): p. 50221.
10. Luo, X. and W.L. Kraus, *On PAR with PARP: cellular stress signaling through poly (ADP-ribose) and PARP-1.* Genes & development, 2012. **26**(5): p. 417-432.
11. Horvath, E., et al., *Rapid 'glycaemic swings' induce nitrosative stress, activate poly (ADP-ribose) polymerase and impair endothelial function in a rat model of diabetes mellitus.* Diabetologia, 2009. **52**(5): p. 952-961.
12. Liu, A.-X., et al., *Sustained endoplasmic reticulum stress as a cofactor of oxidative stress in decidual cells from patients with early pregnancy loss.* The Journal of Clinical Endocrinology & Metabolism, 2011. **96**(3): p. E493-E497.
13. Kim, I., W. Xu, and J.C. Reed, *Cell death and endoplasmic reticulum stress: disease relevance and therapeutic opportunities.* Nature reviews Drug discovery, 2008. **7**(12): p. 1013.
14. Michalak, M. and M.C. Gye, *Endoplasmic reticulum stress in periimplantation embryos.* Clinical and experimental reproductive medicine, 2015. **42**(1): p. 1-7.
15. Choy, M.S., et al., *Structural and functional analysis of the GADD34: PP1 eIF2α phosphatase.* Cell reports, 2015. **11**(12): p. 1885-1891.
16. Boyce, M., et al., *A selective inhibitor of eIF2α dephosphorylation protects cells from ER stress.* Science, 2005. **307**(5711): p. 935-939.
17. Selen, E.S., et al., *NMR metabolomics show evidence for mitochondrial oxidative stress in a mouse model of polycystic ovary syndrome.* Journal of proteome research, 2015. **14**(8): p. 3284-3291.
18. Chen, X., et al., *Adipokines in reproductive function: a link between obesity and polycystic ovary syndrome.* Journal of molecular endocrinology, 2013. **50**(2): p. R21-R37.
19. Rajan, R.K. and B. Balaji, *Soy isoflavones exert beneficial effects on letrozole-induced rat polycystic ovary syndrome (PCOS) model through anti-androgenic mechanism.* Pharmaceutical biology, 2017. **55**(1): p. 242-251.
20. Franks, S., S. Robinson, and D.S. Willis, *Nutrition, insulin and polycystic ovary syndrome.* Reviews of Reproduction, 1996. **1**(1): p. 47-53.

21. Blank, S., C. McCartney, and J. Marshall, *The origins and sequelae of abnormal neuroendocrine function in polycystic ovary syndrome.* Human reproduction update, 2006. **12**(4): p. 351-361.
22. Manneras, L., et al., *A new rat model exhibiting both ovarian and metabolic characteristics of polycystic ovary syndrome.* Endocrinology, 2007. **148**(8): p. 3781-3791.
23. Tessaro, I., et al., *Effect of oral administration of low-dose follicle stimulating hormone on hyperandrogenized mice as a model of polycystic ovary syndrome.* Journal of ovarian research, 2015. **8**(1): p. 64.
24. Solorzano, C.M.B., et al., *Neuroendocrine dysfunction in polycystic ovary syndrome.* Steroids, 2012. **77**(4): p. 332-337.
25. Diamanti-Kandarakis, E. and A. Dunaif, *Insulin resistance and the polycystic ovary syndrome revisited: an update on mechanisms and implications.* Endocrine reviews, 2012. **33**(6): p. 981-1030.
26. Hillier, S.G. and G.T. Ross, *Effects of exogenous testosterone on ovarian weight, follicular morphology and intraovarian progesterone concentration in estrogen-primed hypophysectomized immature female rats.* Biology of Reproduction, 1979. **20**(2): p. 261-268.
27. Yang, M. and J. Fortune, *Testosterone stimulates the primary to secondary follicle transition in bovine follicles in vitro.* Biology of Reproduction, 2006. **75**(6): p. 924-932.
28. Conway, B., V. Mahesh, and T. Mills, *Effect of dihydrotestosterone on the growth and function of ovarian follicles in intact immature female rats primed with PMSG.* Journal of reproduction and fertility, 1990. **90**(1): p. 267-277.
29. Drummond, A.E., *The role of steroids in follicular growth.* Reproductive biology and endocrinology, 2006. **4**(1): p. 16.
30. Agarwal, A., et al., *The effects of oxidative stress on female reproduction: a review.* Reproductive biology and endocrinology, 2012. **10**(1): p. 49.
31. Chiu, J., et al., *Oxidative stress-induced, poly (ADP-ribose) polymerase-dependent upregulation of ET-1 expression in chronic diabetic complications.* Canadian journal of physiology and pharmacology, 2008. **86**(6): p. 365-372.
32. Wyrsch, P., et al., *Cell death and autophagy under oxidative stress: roles of poly (ADP-ribose) polymerases and Ca2+*. Molecular and cellular biology, 2012. **32**(17): p. 3541-3553.
33. Li, R.J., et al., *Salubrinal protects cardiomyocytes against apoptosis in a rat myocardial infarction model via suppressing the dephosphorylation of eukaryotic translation initiation factor 2α.* Molecular medicine reports, 2015. **12**(1): p. 1043-1049.
34. Sui, T., et al., *Mitomycin C induces apoptosis in human epidural scar fibroblasts after surgical decompression for spinal cord injury.* Neural regeneration research, 2017. **12**(4): p. 644.
35. Oslowski, C.M. and F. Urano, *Measuring ER stress and the unfolded protein response using mammalian tissue culture system*, in *Methods in enzymology*. 2011, Elsevier. p. 71-92.
36. Akiyama, M., et al., *Increased insulin demand promotes while pioglitazone prevents pancreatic beta cell apoptosis in Wfs1 knockout mice.* Diabetologia, 2009. **52**(4): p. 653-663.

International Conference on Science and Technology

ICONST 2018

5-9 September 2018 Prizren - KOSOVO

The Investigation of Technological Developments and Innovations in Vehicle Tires

Derviş Erol[1]*, Battal Doğan[2]

Abstract: Vehicle tires produced with some binding and strengthening components under passenger and cargo vehicles effect directly driving comfort and performance due to the fact that it is the only contact point between the vehicle and the road. In this study, technological developments and innovation studies on fuel consumption, driving safety and noise effects of vehicle tires are examined. Tires effect fuel consumption based on rolling resistance in vehicles. In recent years, great innovations in tire technology have come to the forefront in the automotive industry in terms of fuel economy. Providing driving safety besides the performance of a vehicle is important in terms of reducing loss of life and property. Most tire failures, especially those that cause traffic accidents, are caused by a damaged tire that has partially or completely lost air. Therefore, the latest technological developments in tires have been examined in terms of driving safety in study. Noise is a physical risk factor that effects human health adversely. The noise in vehicles mostly is made by the tires. In the present study, the latest technological developments and methods that used to reduce tire noise in vehicles have been investigated.

Keywords: Tire technology, Tire innovations, The History of tire, Vehicle safety, Passenger safety, Tire noise

1. Introduction

Vehicle tire is made up of carbon black, silica, cord fabric, steel wires, oils and various chemical substances besides rubber which is the main raw material. Tires, designed to hold compressed air inside, are one of the most important parts that provide contact between road and vehicle. Thanks to the R & G work carried out by tire manufacturers, today's vehicle tires have reached very important levels in terms of excellent handling, superior braking performance, comfort and steering even under extreme conditions (Erol, 2011).

Depending on the developing technology and changing needs, technological developments have been taking place in vehicle tires as well as in every sphere of life. In 1839, the American chemist Charles GOODYEAR transformed the mixture of natural rubber with sulfur by changing the chemical structure by the effect of temperature, and succeed to transform the rubber from plastic to elastic form to make it possible for the commercial use (Erol, 2011; Goodyear, 2018a). Robert William THOMSON patented pneumatic tires in France in 1846 and in the United States in 1847 (Erol, 2011). In 1887, Scottish veterinarian John Boyd DUNLOP developed the first pneumatic tires with his son's three-wheeled bicycle, a simple tire model obtained by attaching a rubber solution impregnated canvas fabric to wooden wheels and inflating it with air, and lead the development of today's vehicle tires (Dunlop, 2018a). In 1888 Edouard MICHELIN and his brother Andre MICHELIN founded the Michelin tire company. In 1891, Edouard MICHELIN developed the first detachable bicycle tire and in 1895, he had produced the first pneumatic vhicle tire successfully by adapting the concept to the vehicles (Michelin, 2018a).

[1] Kırıkkale University, Department of Automotive Technology, Yahşihan, Kırıkkale, TURKEY
[2] Kırıkkale University, Department of Mechanical Engineering, Yahşihan, Kırıkkale, TURKEY
*Corresponding author: derol40@gmail.com

August SCHRADER developed the valve system used in pneumatic bicycle tires in 1891 and patented this system by adapting it for vehicle tires in 1896 (Schrader, 2018). In 1892, Continental tire company has started manufacturing pneumatic tires for bicycles. In 1898 Continental started mass production of pneumatic tires to provide high-speed travel opportunity. In 1904, Continental tire company has made mass production of pneumatic tires with tread pattern which is more durable by using carbon black, and launched to the market (Continental, 2018a). In 1903, the Goodyear tire company patented the first Tubeless tire. In 1909, Goodyear developed the first pneumatic aircraft tire (Goodyear, 2018a). In 1926, the Continental tire company began using carbon black as a raw material in rubber production as a reinforcing filler material to obtain more resistance for abrasion besides characteristic color of tires. In 1936, the company began to use synthetic rubber in tire production to reduce dependence on natural rubber (Continental, 2018a). In 1937, Goodyear tire company made the first tire production and tests using synthetic rubber (Erol, 2011; Goodyear, 2018a). In 1946, Michelin tire company patented the first radial tire technology. In 1952, the company has started to use radial tire technology in truck tires (Michelin, 2018a). The United Stated Department of Transport made the use of DOT number obligatory in 1968 (Erol, 2011).

In the 1970's, Dunlop launched the world's first non-failing tire, Denovo, to the market, providing long-distance and high-speed control to drivers, even in tire puncture or air leaks situations (Dunlop, 2018b). In 2005, Michelin developed the first airless tire called X-Tweel-consists of the abbreviation of the words "tire" and "wheel" in English- and compressed air is not used in this tire. Flexible arms provide the necessary support for undertaking a shock-absorbing role (Michelin, 2018b). Since 2012, it has been compulsory for automobiles and light commercial vehicles to have special labels indicating some basic performance values such as tire fuel consumption, wet road handling and tire noise. In this respect, it is aimed to give correct and impartial information to the users (Bridgestone, 2018a; Continental, 2018b; Goodyear, 2018b).

In tire technology, company mergers in the world, their search on new technologies and market, big companies thoughts of having a wider market and the whishes of vehicle manufacturers has given acceleration to the development of tire technology since the invention of the tire. In the present study, technological developments and innovation studies on fuel consumption, driving safety and noise effects of vehicle tires have been examined.

2. Innovation studies on vehicle tires

2.1 The effects of tires on fuel comsumption

Depending on the rolling resistance of the tires, the vehicle has negative effects on fuel consumption. Significant works has been done by tire manufacturers to reduce this resistance. Driving safety and comfort are directly associated to the condition of the tires. It effects handling on wet ground in a negative way to pump the tires insufficiently and it also increases the rolling resistance.

The tires are responsible for the fuel consumption so that it cannot be ignored. Since 2012, For cars and light commercial vehicles, It has been a compulsory to have special labels in all tires sold in Europe. Each lables inform the driver about that tire regards to some basic performance values such as tire consumption, wet road handling and tire noise (Bridgestone, 2018a; Continental, 2018b; Goodyear, 2018b). As shown in Figure 1, grading is done in seven different ways (from green to red) from highest fuel efficiency to lowest fuel efficiency rating based on tire rolling resistances. Briefly, tires with high fuel efficiency provide less rolling resistance between the road and the tire during travel, resulting in less energy consumption. And this means that less fuel is consumed. Choosing tires with high fuel efficiency allows for more mileage with the same tank, while also reducing CO2 emissions. On the wet road, the braking performance label measures how well a tire brakes in wet conditions. The performance range is between A (safest, short-haul stop) and G (most unsafe, long-haul stop) as on the fuel consumption label.

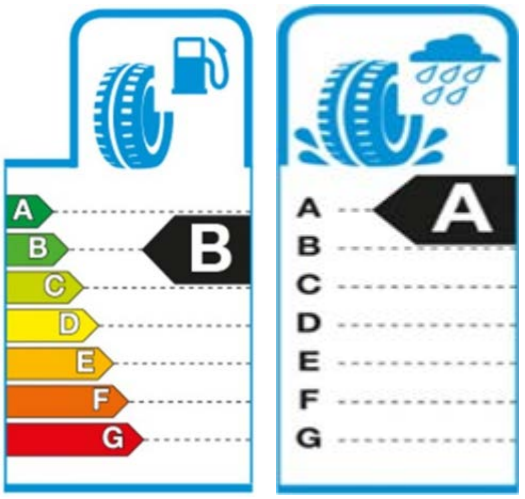

Figure 1. Fuel efficiency and wet road braking performance labels

2.2. The effects of tires on driving safety

Most tire malfunctions are caused by tires with low/no air pressure. Tires, completely free of the air, cannot function task of steering a vehicle traveling at high speeds and cause the vehicle to get out of control during driving period. Even in such unfavorable adverse situations, the safety of the driver and the passengers is brought to the highest levels with Run-flat technology, while maintaining the handling performance of the tires. Run-flat technology prevents a failed tire, has partially or completely lost air, from being squeezed between the rim and the road and prevents the tire from detachment, allowing the driver to go on safely without losing control of the vehicle. At the present time, this technology is divided into three groups: Support Ring Run-flat tire systems, Self Sealing Run-flat tire systems and Self Supporting Run-flat tire systems (Bridgestone, 2018b; Continental, 2018c; Hutchinson, 2018).

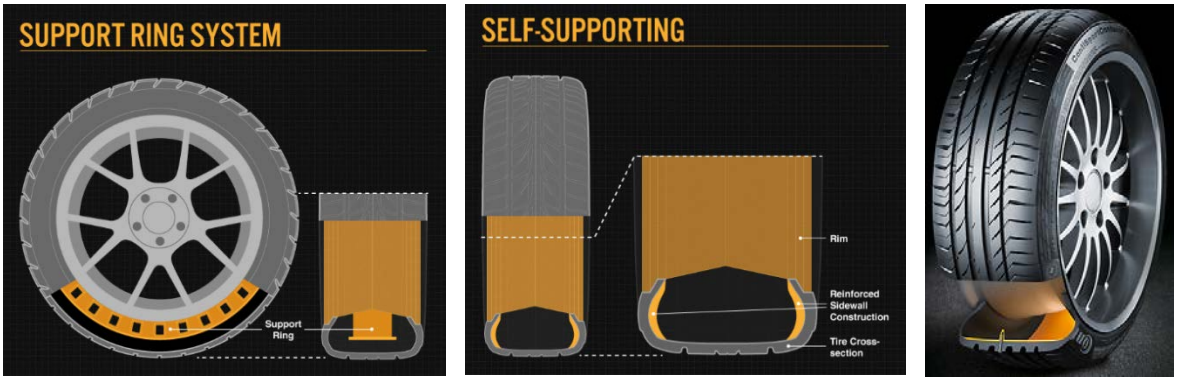

Figure 2. Classification of Run-flat technology (Bridgestone, 2018c; Continental, 2018d; Tyrestop, 2018).

Vehicles with run-flat technology do not have spare tires. Special spare tires, take a small space, have been developed for saving place and other alternative in-car systems in the trunk of vehicles that do not have run-flat technology (Mini Stepne, 2018; Continental, 2018e). Some vehicle manufacturers launch the vehicle they produced to the market without spare tires and equipment. Moreover, some drivers, especially whose trunks are small, do not keep the standart spare tyres in their trunk. So the use of mini spare tyres is increasing day by day.

Figure 3. Mini spare tire and a vehicle with mini spare tire

The tire air pressure effects many important parameters such as driving comfort, fuel consumption, rolling resistance, safe steering of the vehicle, cornering, braking, general handling characteristics and the life of the vehicle tire. The correct air pressure reduces the risk of losing the control of vehicle and prevents the tire from wearing and irreversible damage to its interior. If the tire pressure is too low or too low, it will shorten the life of the tire because it creates more stress or crush on the tire sidewalls. The conditions of tires with Low, High and Normal air pressures has given in Figure 4. A tire with insufficient air pressure causes the tire's sidewalls parts to be damaged. This can lead the tire to break down or even disintegrate. As the air pressure decreases, the rolling resistance of the tire increases and causes more fuel to be consumed so that the resulting energy loss is balanced by the engine. A tire with extreme air pressure causes the tread to reduce contact with the road, reduces driving comfort and leads more wear on the middle of the tire as shown in Figure 4 (Continental, 2018e; Tirebuyer, 2018; Tyroola, 2018).

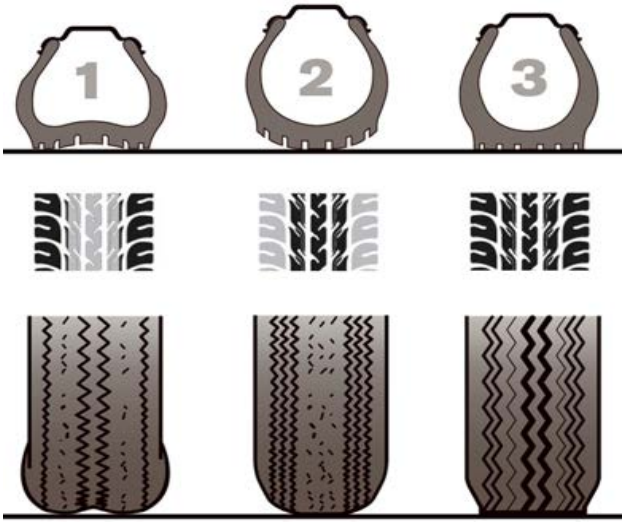

Figure 4. Road contact conditions of tires with Low, High and Normal air pressure

Since a tire with the correct air pressure provides full contact with the road, it reduces the risk of losing handling at high speeds. The correct air pressure reduces the risk of losing the control of vehicle and prevents the tire from wearing and irreversible damage to its interior. Providing the correct air presure is one of the necessary conditions for optimum fuel consumption and economical driving. By the help of new systems developed, the tire air pressure is electronically controlled by a special sensor and the amount of air lost by

the tires for any reason is reported as a warning to the drivers during the travel (Bridgestone, 2018d; Continental, 2018f; Kal Tire, 2018).

Today's tire pressure control systems have two different modes of operation. One of them is known as a direct tire pressure control system and the other is known as an indirect tire pressure control system. In tire pressure control systems that measure directly, the air pressure in the tire is constantly measured and controlled by a sensor placed in the car's air valves. Some type of air valves with tire pressure sensor are shown in Figure 5. (Bridgestone, 2018d; Continental, 2018f; Kal Tire, 2018).

Figure 5. Air valves with tire pressure sensor

In the systems controlling the tire pressure indirectly, measure the data transmitted by the wheel speed sensors used by the ABS system in automobiles. So the air pressure inside the tire is not measured directly. Instead, how long the tire completes a round is measured.and reported as a warning to the drivers when the value measured is other than what it should be (Bridgestone, 2018d).

In addition to these pressure control systems, the Trelleborg Tire Company has developed a new tire pressure control system by the help of special equipment placed on harvester. And it can reduce or increase the amount of air pressure in the tire, depending on the harvester's load. It is stated thet this new generation tire pressure control system is still in operation to be used in vehicles in the upcoming years (Trelleborg, 2018).

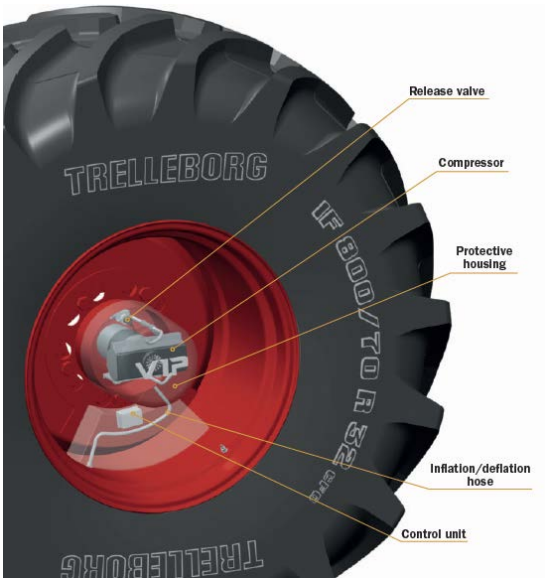

Figure 6. New generation tire pressure control system developed by Trelleborg Company (Trelleborg, 2018).

The Mitas Tire Company has developed a new generation of agricultural tires called “Pneutrac” for use in tractors and harvester, providing fuel economy and driving safety. The fuel consumption is reduced by maintaining the air pressures on harvester and tractor tires at minimum levels where it can safely carry the load, allowing the wheel to reach the maximum contact area with the ground by the help of these new technologies. Thus, the grip surface of the tire is increased and it provides an advandage for traction performance and soil productivity preventing wheel spinning (Mitas, 2018; Mitasag, 2018).

Figure 7. New generation agricultural tire developed by Mitas Company

Michelin, one of the leading companies in the tire industry, developed a new generation airless tire called X-Tweel in 2005. The air inside the tire is replaced by highly durable and highly flexible rods. If the tire encounters any obstacles on the road, the bouncing and jolt that normally occurs is reduced to a lower level by acting as a kind of suspension. The grip on the tires is provided by a rubber layer placed on the back of the tire as on standard tires. This rubber can easily be replaced with new ones in case of aging. The most substantial advantage of this new tire technology is that the tires are completely airless which allows them to function successfully on the worst-case scenario. Objects that will damage or puncture a standard tire are ineffective against this tire produced using special techniques (Michelin, 2018b).

Figure 8. X-Tweel tires developed by Michelin (Michelin, 2018b).

2.3. The effects of tires on vehicle noise

It is known that the tire noise is caused by the air trapped as a result of the contact between the tire and the road. The tire noise is a very important parameter to long-distance drivers for their driving comfort and attention. This noise can be disturbing not only for the driver but also for the people around.

The tire noise performance label measures how much noise a tire makes in decibels (dB). The performance range is shown between three black waves (highest volume) and one black wave (lowest volume). The noise comes from automobiles is partially generated by tires. By using proper tire in terms of noise, annoyance noise level exposed to the surrounding area can be reduced (Bridgestone, 2018a; Continental, 2018b; Goodyear, 2018b).

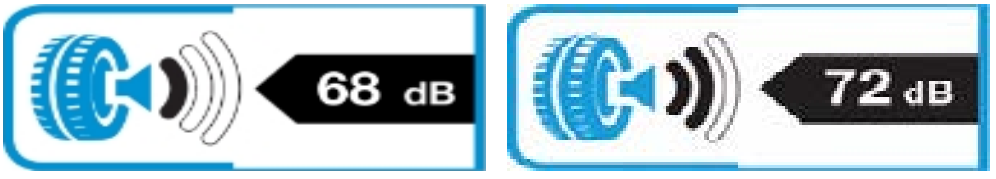

Figure 9. Tire noise performance labels at different volumes

Nowadays, new design and innovation studies are in progress to reduce the noise caused by tires while driving. Within this scope, dominant tire firms such as Pirelli, Continental and Michelin have done a new study to reduce tire noises (Continental, 2018g; Michelin, 2018c; Pirelli, 2018). In this study, it has been stated that a special sound insulation material placed inside the tire helps to reduce the internal noise about 4-9 dB, depending on the vehicle, speed and road surface, as shown in Figure 9. It has been explained that the noise a human can hear, could be reduced by 50% with the help of this newly developed system called “Noise Cancelling System”.

Figure 10. System developed by Pirelli, Continental and Michelin Companies

3. Conclusions

Tire is a very important part of a vehicle contact with the ground. Tires carry out many tasks from carrying stationary vehicle to resisting the forces generated in the moments of take-off and break. Keeping the vehicle in a safe way is related to the tires in all weather and road conditions. For this reason, vehicle tires directly effect driving comfort and performance. In this study, technological developments and innovation studies on fuel consumption, driving safety and noise effects of vehicle tires are examined. Rolling resistance forces resulting from the strain on tires and road effect the fuel comsumption. There are many factors that have an effect on the rolling resistance as tire structure and conditions. Driving without harming the enviroment can be possible by reducing fuel consumption.

The tire air pressure effects many important parameters such as driving comfort, fuel consumption, rolling resistance, safe steering of the vehicle, cornering, braking, general handling characteristics and the life of the vehicle tire. The correct air pressure reduces the risk of losing the control of vehicle and prevents the tire from wearing and irreversible damage to its interior. If the tire pressure is too low or too low, it will shorten the life of the tire because it creates more stress or crush on the tire sidewalls. As the air pressure decreases, the rolling resistance of the tire increases and causes more fuel to be consumed so that the resulting energy loss is balanced by the engine. It is the tire's duty to steer vehicle at driving. Losing the control of the vehicle resulting from tire failure cause the loss of life and property. Run-flat technology prevents a failed tire, has partially or completely lost air, from being squeezed between the rim and the road and prevents the tire from detachment, allowing the driver to go on safely without losing control of the vehicle.

The noise generated by road and tire contact during the movement of vehicles influences human health physiologically and psychologically. Nowadays, special noise insulation materias have been developed to

reduce tire noise in vehicles. The noise level is reduced by 50% with the help of these newly developed noise cancelling systems.

References

Bridgestone, (2018). Bridgestone Tire Company, Tire Label. https://www.bridgestone.com.tr/lastik-etiketi-uygulamasi (Erişim Tarihi:07.06.2018).

Bridgestone, (2018). Bridgestone Tire Company, Bridgestone's Run Flat Technology. https://www.bridgestone.com/technology_innovation/run-flat_tire/ (Erişim Tarihi:07.06.2018).

Bridgestone, (2018). Bridgestone Tire Company, Extended Mobility Technology, Run Flat Tires Technology. https://www.bridgestonetire.com/tread-and-trend/drivers-ed/run-flat-tires (Erişim Tarihi:07.06.2018).

Bridgestone, (2018). Bridgestone Tire Company, Tyre Pressure Monitoring System Technology. https://www.bridgestonetire.com/tread-and-trend/drivers-ed/tire-pressure-monitoring-system-how-tpms-works (Erişim Tarihi:07.06.2018).

Continental, (2018). Continental Tire Company, History. https://www.continental-corporation.com/en/company/history (Erişim Tarihi:07.06.2018).

Continental, (2018). Continental Tire Company, Tire Label. https://www.continental-tyres.co.uk/car/technology/eu-tyre-label (Erişim Tarihi:07.06.2018).

Continental, (2018). Continental Tire Company, Extended Mobility Technology. https://www.continental-tyres.co.uk/car/technology/extended-mobility-main (Erişim Tarihi:07.06.2018).

Continental, (2018). Continental Tire Company, Contiseal Technology. https://www.continental-tires.com/car/technology/extended-mobility-main/contiseal (Erişim Tarihi:07.06.2018).

Continental, (2018). Continental Tire Company, Sparetyres Technologies. https://www.continental-tyres.co.uk/car/technology/extended-mobility-main/sparetyres (Erişim Tarihi:07.06.2018).

Continental, (2018). Continental Tire Company, Tyre Pressure Monitoring System Technology. https://www.continental-tyres.co.uk/car/technology/tpms (Erişim Tarihi:07.06.2018).

Continental, (2018). Continental Tire Company, New Technologies. https://www.continental-tires.com/car/technology/contisilent (Erişim Tarihi:07.06.2018).

Dunlop, (2018). Dunlop Tire Company History. https://www.dunloptires.com/en-US/company/tire-history (Erişim Tarihi:07.06.2018).

Dunlop, (2018). Dunlop Tire Company, Research and Development Studies. https://www.dunlop.eu/dunlop_euen/_header/about_us/research_and_development/ (Erişim Tarihi:07.06.2018).

Erol D., (2011). Vehicle Tires. Electronic Journal of Vehicle Technologies, (3) 37-50.

Goodyear, (2018). Goodyear Tire Company History. https://corporate.goodyear.com/en-US/about/history.html (Erişim Tarihi:07.06.2018).

Goodyear, (2018). Goodyear Tire Company, Tire Label. https://www.goodyear.eu/tr_tr/consumer/learn/eu-tire-label-explained.html (Erişim Tarihi:07.06.2018).

Hutchinson, (2018). Hutchinson Tire Company, Extended mobility technology, Run Flat. http://www.hutchinsoninc.com/CMS/index.php?page=Runflats (Erişim Tarihi:07.06.2018).

Kal Tire, (2018). Kal Tire Company, Tyre Pressure Monitoring System Technology. https://info.kaltire.com/what-is-a-tpms-tire-pressure-monitoring-system-and-why-do-i-need-it/ (Erişim Tarihi:07.06.2018).

Michelin, (2018). Michelin Tire Company History. https://www.michelin.com/eng/michelin-group/profile/History-of-Michelin (Erişim Tarihi:07.06.2018).

Michelin, (2018). Michelin Tire Company, Tweel. https://www.michelintweel.com/ (Erişim Tarihi:07.06.2018).

Michelin, (2018). Michelin Tire Company, Tire Noise Control System and Acoustic Technology. https://www.michelinman.com/US/en/why-michelin/michelin-acoustic-technology.html (Erişim Tarihi:07.06.2018).

Mini Stepne, (2018). Mini Stepne Company. http://www.ministepne.com.tr/Gallery.aspx (Erişim Tarihi:07.06.2018).

Mitas, (2018). Mitas Tire Company, Innovation. http://www.mitas-tyres.com/gb/about/mitas-innovation/ (Erişim Tarihi:07.06.2018).

Mitasag, (2018). Mitas Tire Company, Pneutrac Tire Technology. http://www.mitasag.com/about/press-releases/mitas-aims-to-launch-pneutrac-in-two-years/ (Erişim Tarihi:07.06.2018).

Pirelli, (2018). Pirelli Tire Company, Tire Noise Control System. https://www.pirelli.com/tyres/en-ww/car/pncs-technology (Erişim Tarihi:07.06.2018).

Schrader, (2018). Schrader Company History. http://www.schraderinternational.com/Schrader-Past-To-Present/Schrader-History (Erişim Tarihi:07.06.2018).

Tirebuyer, (2018). Tire Pressure and Performance. https://www.tirebuyer.com/education/tire-pressure-and-performance (Erişim Tarihi:07.06.2018).

Trelleborg, (2018). Trelleborg Tire Company. https://www.trelleborg.com/trelleborg-variable-inflation-pressure-brochure (Erişim Tarihi:07.06.2018).

Tyrestop, (2018). Extended mobility technology, Run Flat Technology. http://www.tyrestop.ie/runflat-tyres.aspx (Erişim Tarihi:07.06.2018).

Tyroola, (2018). Tyre Pressure. https://www.tyroola.com.au/guides/tyre-pressure/ (Erişim Tarihi:07.06.2018).

International Conference on Science and Technology

ICONST 2018

5-9 September 2018 Prizren - KOSOVO

Research on Shear Links with Perforated Web Sections

Haluk Emre Alçiçek[1]*, Adem Karasu[1], Cüneyt Vatansever[1]

Abstract: In eccentirally braced frames (EBFs), link-to-column connections and the structural elements outside of the links must resist the internal forces generated by fully yielded and strain-hardened links. Using slotted perforated web section concept in shear link may help to prevent difficulty in design of link-to-column connections and all other frame members by limiting the link capacity without loss of its stability. For this, a shear link beam with a section of W10×33 was selected and three different slot hole pattern were generated in its web to form three different specimens. Finite element models of these specimens were developed using ABAQUS software. Material of link beam was ASTM A992 steel. A series of analyses were performed under quasi-static cyclic loading to study the behavior of link beam with reduced web section. 10.6% of area reduction in the web section with different hole arrangements were investigated and the effect of slotted perforated web on shear links was examined. Finite element analyses have revealed that equally spaced 6×4mm slots in the web had stable hysteresis behavior whereas strength degredation was occured when equally spaced 3×8mm slots were used in the web. The results of this study indicate that using high number of slot holes may help to limit forces transmitting to the link-to-column connections and all other frame members.

Keywords: Steel structures, eccentrically braced frame, shear link, reduced web.

Introduction

Eccentirally Braced Frame (EBF) system is one of the most desirable structural system in seismic design of steel structures. Many researchs state that EBF systems provide the high level of stiffness, ductility and seismic energy dissipation capacity by combining benefits of moment frames and concentrically braced frames (Azad and Topkaya, 2017). In eccentirally braced frames, seismic energy is dissipated through shear, flexural or both shear and flexural yielding of link with large inelastic deformation in the link beam while columns, braces and beam outside of the link remain essentially elastic (Liao and Goel, 2006; Yiğitsoy et al., 2014). To facilitate the large inelastic link rotation demand, link-to-column connection is exposed to large moments and shear forces. Due to these forces, stress concentrations develop in connection area, resulting in fracture at low deformation level (Azad and Topkaya, 2017). In addition, depending on the overstrength ratio calculated by considering expected yield strength of the link, design of all other frame members is required to remain essentially elastic.

Link beams attached to the columns have less inelastic rotation capacity due to the tendency of fracture in the flange at connection area (Prinz and Richards, 2009). In bolted web connection, bolt slippage was occurred because of the large shear force. The bolt slippage lead to flange fractures (Malley and Popov, 1984; Okazaki, 2004; Popov, 1983). Extensive analytical and experimental researches on link beam with link-to-column connection have shown that promising connection details very limited and researches are on-going (Okazaki 2004; Okazaki et al., 2015; Okazaki and Engelhardt, 2006). Also there is no any prequalified link-to-column connection according to the AISC 341-16 (2016).

[1]Istanbul Technical University, Faculty of Civil Engineering, 34469, İstanbul, TURKEY
*Correspondingauthor: alcicek@itu.edu.tr

In order to prevent brittle failure of eccentrically braced frames, link-to-column connections and all other frame members must be proportioned following the capacity design principles considering the forces developed by the fully yielded and strain hardened link, nominal forces must be amplified by overstrength factor. In previous study on overstrength, overstrength value of 1.5 has been suggested (Popov, 1989). Ji at. al. (Ji et al., 2016) stated that this value underestimate the maximum forces for short links, especially links with link length ratio lower than unity. Capacity design concept in EBFs may lead to overdesign in some cases (Hauksdottir, 2008). If link beam capacities are reduced as much as possible, this may allow link-to-column connections and all other frame members to be designed in more economical way.

The present research investigates the effects of removing some portion of web area in link beam on cyclic behavior of link. Several finite element analyses were done to reveal that the behavior of link beam with reduced sections. The next section describes the finite element modelling, model verification study and analyses considering investigated parameters. The third section presents the results of the analyses. In the last section, results were discussed.

Material and Method

Reference model

W10×33 wide-flange American profile with length of 584 mm was considered as a reference model based on (Okazaki et al. 2004). The depth, flange width, web and flange thicknesses of the W10×33 section were 247mm, 202mm, 7.4mm and 11mm, respectively. Material of the profile was ASTM A992 steel, the yield stress and tensile strength values that determined by coupon testing are given in Table 1 (Okazaki et al., 2004).

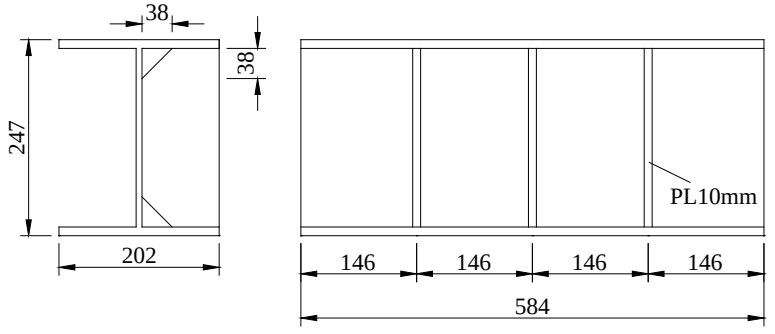

Figure 1: Reference model (Okazaki et al., 2004).

Table 1: The measured yield stress and tensile strength values.

Yield Stress F_y [MPa]		Tensile Strength F_u [MPa]	
Flange	Web	Flange	Web
356	382	507	503

Shear Link Prototypes

Three slot hole arrangements with 10.6% of area reduction in web section were implemented on reference profile. Fig 2. summarize the details of the investigated slot hole patterns and properties of slotted perforated links are given in Table 2. The prototypes are classified into three groups according to the slot hole geometry. For example, tag of 3×8 defines the slot hole pattern which have three slots placed along the depth with the height of 8mm. In the longitudinal direction of the web, each row has two slot-shaped perforations.

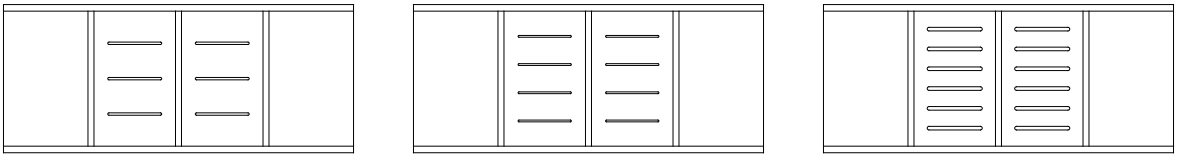

Figure 2: Slot hole patterns.

Table 2: The details of the investigated slot hole patterns.

Tag	n [Quantity]	h_h [mm]	h_s [mm]	l_s [mm]	Ratio of reduced area [%]	Width-to-thickness ratio of portions between two slits
3×8	3	8	51	86	10.6	6.89
4×6	4	6	41	86	10.6	5.54
6×4	6	4	29.5	86	10.6	3.99

n : quantity of the removed portions in vertical direction, h_h: height of the removed portions, h_s : height of the portions between slot holes , l_s : length of the slits.

Finite element modeling

Finite element models of W10×33 shear link beam with three different slot hole patterns were developed by using ABAQUS/CAE 2017 (HKS, 2017) software. Four-node shell element (S4R) was utilized to define the link beam and stiffeners. Material nonlinearites was taken into consideration through Von-Mises yield criterion with combined hardening. To capture second order effects, geometric nonlinearities were accounted for by employing the “nlgeom” option in ABAQUS. Finite element model of typical link beam is shown in Fig. 3.

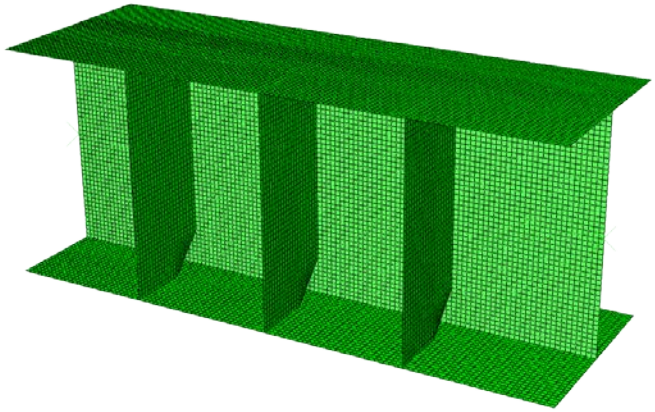

Figure 3: Finite element model of typical link beam.

Rigid body constraint was employed at both ends of the link. Motions of the end surfaces were constrained to the motion of a single reference point in the middle of the web at each end. As illustrated in Fig. 4, node on left end was constrained against all three rotations and translation except for horizontal translation. On the other hand, node on right end was free to vertical translation, but all other rotations and translations were fixed at this node.

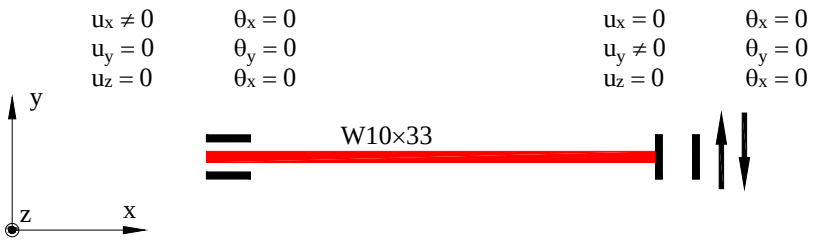

Figure 4: Boundary conditions.

Cyclic displacement history was applied on the right end reference node which is vertically free end of the shear link. Revised loading protocol for shear links, which developed by Richards and Uang (Richards and Uang, 2003), was followed (see Fig. 5). Displacement was determined by trigonometric tangent rule (link length times link end rotation angle) for each step. Maximum link rotation was 0.13 rad (76mm in drift). The expected link rotation was 0.08 rad without any strength and stiffness degradation.

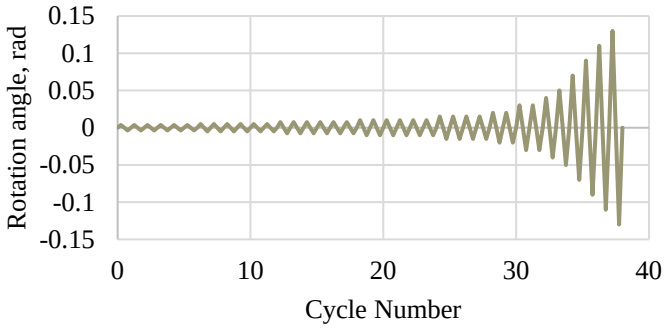

Figure 5: Loading protocol.

Model verification

Reference model adopted from Okazaki et. Al. (Okazaki et al., 2004) was subjected to quasi-static cyclic loading, to verify the accuracy of the finite element modeling assumptions in this study, then results were compared to those from experimental research (Okazaki et al., 2004). Specimen denoted as 4A-RLP was examined out of 24 specimens. Link geometry, material properties and loading protocol were explained above sections. The inelastic rotation versus link shear force curves from the experimental test and finite element analysis are illustrated in Fig. 6. The results of the test and model analysis demonstrated a good agreement. Similar behavior was observed both experimental and model study.

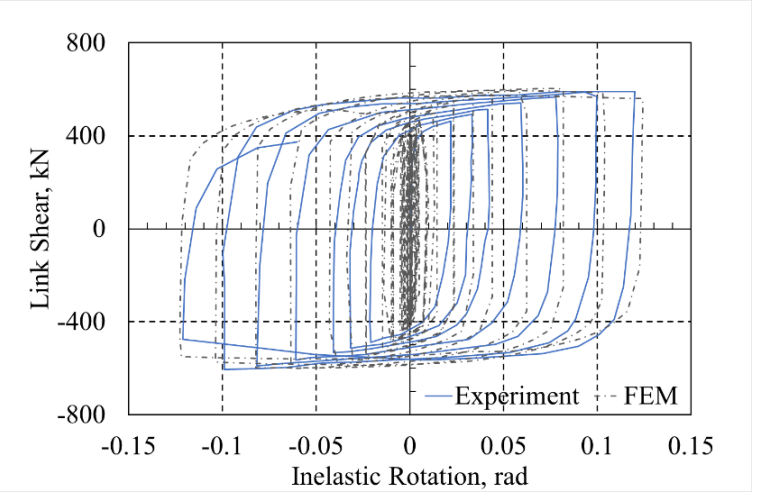

Figure 6: Link shear versus inelastic rotation hysteresis curves from experimental and model study.

Results

Link shear versus link inelastic rotation curves for sample models are shown in Figs. 8, 9 and 10. Introducing the slot holes to the web of the link beam substantially reduces the shear capacitiy as expected. However, all models do not give a promising behavior to reduce the shear capacity due to the tendency of losing stability by means of inelastic web buckling.

As shown in Fig.7, for 3×8 slot hole arrangement, the graph reveals that inelastic web buckling has started at rotation 0.04 rad, after that there has been a gradual strength degradation in link shear. Plastic rotation capacity was defined by which the link shear force was equivalent to 80% of maximum shear force value. According to this approach, plastic link rotation capacity for 3×8 slot hole arrangement was 0.06 rad. which was less than the required plastic link rotation specified as a 0.08 rad. for shear links. The reduced capacity of model 3×8 can be explained by which the inelastic buckling of web plate around slots occur. The curve of model 4×6 in Fig. 8 exhibits a slight decrease in link shear capacity after the rotation level of 0.08 rad. In this case, plastic rotation capacity was achieved at a link rotation of 0.10 rad. As can be seen from the Fig. 9, when 6 slot holes were incorporated into the web, strength degredation was not observed. All cycles were successfully completed and stable hystereses were achieved.

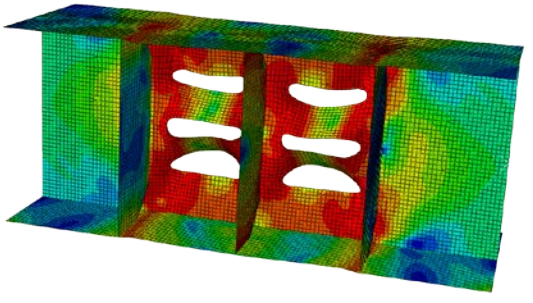

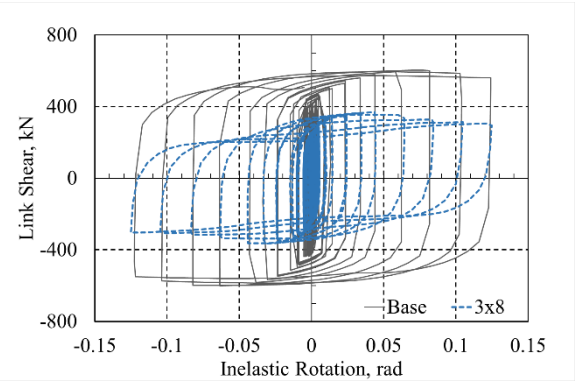

Figure 7: Deformed shape and link shear versus inelastic rotation hystereses loops for 3×8.

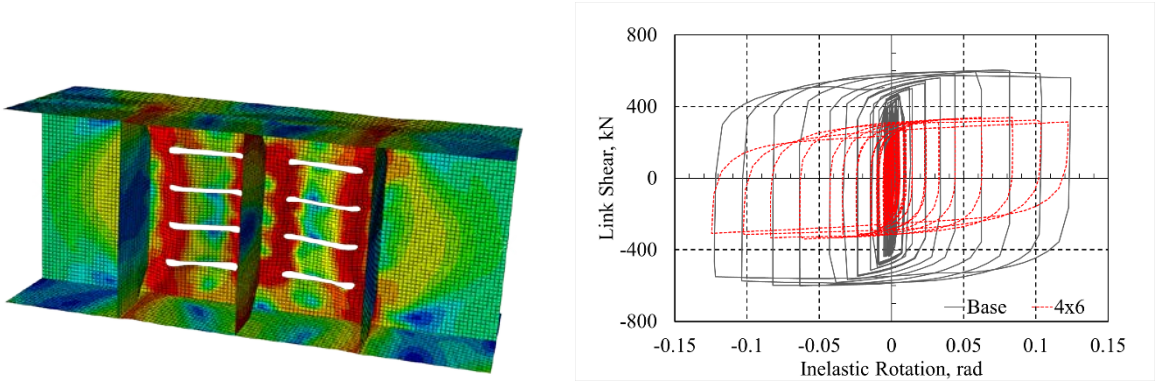

Figure 8: Deformed shape and link shear versus inelastic rotation hystereses loops for 4×6.

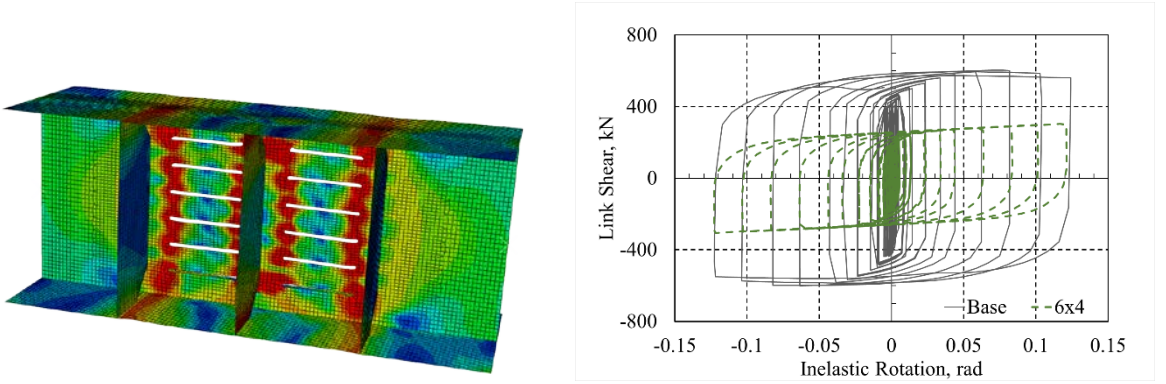

Figure 9: Deformed shape and link shear versus inelastic rotation hystereses loops for 6×4.

Discussion and Conclusions

An objective of this research was to investigate the effectiveness of the slotted perforated web section on shear links. In this study, three different slot hole patterns were taken into account with 10.6% of total area reduction. Shear force versus inelastic rotation curves show that increasing number of slots in the web with the same reduced area has contributed to the reduction in shear force capacity at yielding point while inelastic link rotation capacity was increased. A comparison of the results reveals that width-to-thickness ratio of the portions had a significant influence on the inelastic link rotation. As width-to-thickness ratio of the portions between slot holes increases, the portions reach their strength because they lose their stability.

The research has also shown that stress concentration was moved closer to the edges of the holes. If there is no buckling failure was observed, shear yielding dominated plastic mechanism transforms into the flexural yielding at the two sides of the strips.

Further research is continuing by the authors to develop exact correlation between the slot hole dimensions and link behavior to provide design basis for shear links with reduced web section. In this paper, a preliminary study was presented, the finite element study and experimental investigation have been in progress.

References

AISC 341-16, (2016). Seismic provisions for structural steel buildings, American Institute of Steel Construction, Chicago, Illinois, USA.

Azad, K. and Topkaya, C. (2017). A review of research on steel eccentrically braced frames. Journal of

Constructional Steel Research, 128, 53–73.

Chao, S. and Goel, S. (2006). Performance-based seismic design of eccentrically braced frames using target drift and yield mechanism as performance criteria. Engineering Journal, 3.

Engelhardt, M. D. and Popov, E. P. (1989). Behavior of long links in eccentrically braced frames. Earthquake Engineering Research Center. Report No: UCB/EERC-89/01. (January)

Hauksdottir, H. O. (2008). Application of the reduced beam section concept for improving the ductility of certain eccentrically braced frames. Ph.D. Thesis. University of Washington.

HKS, (2017). ABAQUS/Standard CAE, Hibbit Karlsson Sorenson Inc., Version 2017

Ji, X., Wang, Y., Ma, Q. and Okazaki, T. (2016). Cyclic behavior of very short steel shear links. Journal of Structural Engineering. 142(2), 1–10.

Malley, J. O. and Popov, E. P. (1983). Design considerations for shear links in eccentrically braced frames. Earthquake Engineering Research Center. Report No: UCB/EERC·83/24. (November)

Malley, J. O. and Popov, E. P. (1984). Shear links in eccentrically braced frames. Journal of Structural Engineering, 110(9), 2275–2295.

Okazaki, T., Arce, G., Ryu, H.-C. and Engelhardt, M. D. (2004). Recent research on link performance in steel eccentically braced frames. 13th World Conference on Earthquake Engineering. 1-6 August. Vancouver, B.C., Canada

Okazaki, T. (2004). Seismic performance of link-to-column connections in steel eccentrically braced frames. Ph.D. Thesis. The University of Texas.

Okazaki, T. and Engelhardt, M. D. (2006). Finite element simulation of link-to-column connections in steel eccentrically braced frames. 8th U.S. National Conference on Earthquake Engineering. 18-22 April. San Francisco, California, USA.

Okazaki, T., Engelhardt, M. D., Hong, J.-K., Uang, C. and Drolias, A. (2015). Improved link-to-column connections for steel eccentrically braced frames. Journal of Structural Engineering. 10(8), 1–8.

Prinz, G. S. and Richards, P. W. (2009). Eccentrically braced frame links with reduced web sections. Journal of Constructional Steel Research. 65(10–11), 1971–1978.

Richards, P. W. and Uang, C.-M. (2003). Development of testing protocol for short links in eccentrically braced frames. AISC. Report No: SSRP-2003/08. (May)

Yiğitsoy, G., Topkaya, C. and Okazaki, T. (2014). Stability of beams in steel eccentrically braced frames. Journal of Constructional Steel Research, 96, 14–25.

International Conference on Science and Technology

ICONST 2018

5-9 September 2018 Prizren - KOSOVO

Determination of Optimum Frames in Frames in Hangar Type Steel Industry Structures / Hangar Tipi Çelik Endüstri Yapılarında Optimum Çerçevenin Belirlenmesi

Sadrettin SANCIOĞLU [1]*, Abdulkerim İLGÜN [2]

Özet: Günümüzde inşaat mühendisleri tarafından yapılan yapının tasarım ve projelendirilmesinde temel olarak (Emniyet– Ekonomik- Estetik) kuralı esas alınmaktadır. Emniyetli taşıma gücü, dijital ortamlarda belirli yönetmelik ve yöntemlerle kolaylıkla sağlanmaktadır. Fakat en emniyetli yapı, her zaman en ekonomik yapı olmayabilir. Burada inşaat mühendisi, emniyet ve maliyet dengesini optimum düzeyde kurmalıdır. Özellikle maliyetin yüksek olduğu çelik yapı sistemlerinin, ülkemizde yaygın olarak uygulandığı yapılar genellikle endüstri yapılarıdır. Bu çalışmadaki amaç ülkemizdeki çelik yapıların kullanımının arttırılmasına katkı sağlamak ve uygulayıcılara çerçeve seçiminde, ekonomik açıdan karşılaştırmada yardımcı olmaktır. Çalışmada tasarım parametreleri; makas açıklığı, çerçeve aralığı ve çatı eğimi olarak öngörülmektedir. Sabit kolon yüksekliğinde 7 farklı makas açıklığı (15m, 16m, 17m, 18m, 19m, 20m ve 21m), 7 farklı çerçeve aralığı (5m, 5.5m, 6m, 6.5m, 7m, 7.5m, 8m) ve 5 farklı çatı eğiminin (%5, %6, %7, %8, %9), hangar tipi endüstri yapısının maliyetine etkisi araştırılmıştır. Analizde kullanılacak yükler Yapı Elemanlarının Boyutlandırılmasında Alınacak Yüklerin Hesap Değerleri (TS498)[1]'e göre Konya ili için belirlenmiştir. Analiz "2016- Çelik Yapıların Tasarım, Hesap ve Yapım Esaslarına Dair Yönetmeliği (ÇYHY)[2]" ne göre 6 farklı kombinasyonda SAP 2000 programı ile yapılmıştır. Toplam 245 çerçeve analiz edilmiştir. Emniyet ve maliyet dengesi kurulduğunda optimum çerçeve tasarımının %6 çatı eğiminde, 15 m makas açıklığında ve 7.5 m çerçeve aralığında olduğu görülmüştür.

Anahtar Kelimeler: Çelik Yapılar, Maliyet, Optimum Çerçeve Tasarımı

Abstract: Today, the rule of Safety-Economic-Aesthetic is mainly based on in the design and construction of the structure built by civil engineers. Safe transport power is easily provided in digital environment with certain regulation and methods. However, the safest structure may not always be the most economical structure. Here, civil engineer should set the safety and cost balance to the optimum level. Particularly, the structures, which costly steel building systems are widely applied in our country, are generally industrial structures. The aim of this study is to contribute to the increase of the use of steel structures in our country and to help applicants compare economically in choosing frameworks. Design parameters in the study are foreseen as truss span, frame spacing and roof slope. The impact of fixed-column long 7 different truss spans (15m, 16m, 17m, 18m, 19m, 20m and 21m), 7 different frame spacings (5m, 5.5m, 6m, 6.5m, 7m, 7.5m, 8m) and 5 different roof slopes (5%, 6%, 7%, 8%, 9%) on the cost of hangar type industry structure was researched. The loads to be used in the analysis were determined for the province of Konya according to Calculation Values of the Loads to be taken in the dimensioning of the structural elements (TS498)[1]. The analysis was carried out with SAP 2000 program in 6 different combinations according to "2016- Regulation on the Design, Calculation and Construction Principles of Steel Structures (ÇYHY)[2]". Totally, 245 frames were analyzed. When the safety and cost balance were set, the optimum frame design was found to be 6% roof slope, 15 m truss span and 7.5 m frame spacing.

Keywords: Steel Structures, Cost, Optimum Frame Design

[1]Suleyman Demirel University, Faculty of Forestry, 32260, Isparta, TURKEY
[2]Suleyman Demirel University, Faculty of Engineering, 32260, Isparta, TURKEY
*Correspondingauthor: mevludeakkaya@gmail.com

Giriş

Emniyet– Ekonomik- Estetik kuralı, inşaat mühendisliğinin genel çalışma prensibini tanımlamaktadır. Bir çelik projenin tasarımı aşamasındaki emniyetli taşıma gücü hesapları belirli yönetmelik ve yöntemlerle sağlanmaktadır. Tekla Structures, SAP 2000, ETABS gibi kullanılan programlar bu yönetmelik ve yöntemlerin kullanıldığı programlara örnektir. İlerleyen teknoloji ve beyin gücü ile en zorlu uygulamalar bile hayata geçirilebilmektedir.

Bu sürecin projelendirme aşamasında faydalanılan üç boyutlu yapı modelleme programlarından biri de SAP2000 programıdır[3]. Türkiye'de yapı tasarımında kullanılan kar ve rüzgâr yükleri TS498'e göre belirlenmektedir. Birçok çelik yapı, üzerine etkiyecek kar ve rüzgar yüklerinin yetersiz alınması, proje, imalat ve bakım aşamalarındaki eksiklikler sebebiyle hasar görmekte hatta çökmektedir[4].

Şekil 1. İş yerinin çatısı çöktü[4, 2014].

Emniyeti arttırırken, yapıdaki kesit ve boyutlar büyüyeceğinden maliyet yükselmektedir. Bu nedenle en önemli kriterlerden biri olan ekonomik boyut minimum düzeyde kalmaktadır.

Ülkemizde çelik yapı yönetmeliği olarak kullanılan ÇYHY, AISC 360-16 yönetmeliği esas alınarak hazırlanmıştır. Dolayısıyla SAP 2000 programı ile yapılan analizlerde AISC 360-16 tanımlanmış, tasarım yöntemi olarak güvenli dayanım yöntemi seçilmiştir. Tasarımda kullanılan kar ve rüzgâr yükleri ÇYHY'nin kabul ettiği TS498 yönetmeliğinden Konya iline göre belirlenmiştir. Analizde ÇYHY de belirtilen yük kombinasyonlarından 6 tanesi kullanılmıştır. Hangar tipi endüstri yapısının kolon yüksekliği 8 m de sabit tutulup 7 farklı makas açıklığı, 7 farklı çerçeve aralığı ve 5 farklı çatı eğimine göre tasarımı yapılmıştır.

Materyal ve Yöntem

Kolonlar HEA – HEB – IPE profillerden; kirişler IPE (guseli) profillerden, aşıklar ve kuşaklar C ve Z profillerden seçilmiştir.

Tasarım ve analiz; aşık ve kuşaklar için L/2'den gergili basit kiriş olarak; 1,5 m aralıklı şekilde tasarlanmış olup, elle yapılacak hesaba göre tip ve kesiti belirlenmiştir. Malzeme tipi S235R'dir. Aşık ve kuşaklar belirlenirken rüzgâr yükü, aşıklar üzerinde emme kuvveti uygulandığından ihmal edilmiştir. Aşık ve kuşaklar için maksimum gerilmenin %90' ı ve sehim tahkikininde L/300 boyunun geçmemesi sağlanmıştır. Bu değerle kıyaslandığında maksimum sehim sınırı %99 olarak kabul edilmiştir. Belirlenen aşık ve kuşakların zati yükleri SAP 2000 arayüzünde çizgisel yük olarak çerçevelere aktarılmıştır.

Tasarım ve analiz; kolonlar ve kirişler için SAP 2000 programına göre belirlenmiştir. Kolonlar ve kirişler için malzeme tipi S275R'dir. ÇYHY ye göre R katsayısı '5' ve omega Ω katsayısı '1.63' olarak belirlenmiştir. Kirişler IPE tipi profilden, guseli (değişken kesitli) olarak çözülmüş (0.2L; 0.6L; 0.2L) ve guse boyu kiriş boyunun 1/5' i kadar belirlenmiştir. Dayanım için gerekli kombinasyonlar ÇYHY ye göre

- 0.6G + W
- G
- G + 0.75K
- G + 0.75K + 0.75W
- G + K
- G + W

olarak belirlenmiştir. Yapılan hesaplarda dayanımın %90' ı geçmemesi istenmektedir. SAP 2000 arayüzünde tasarım tipi "Emniyet Gerilmeleri Yöntemi" olarak belirtilmiştir.

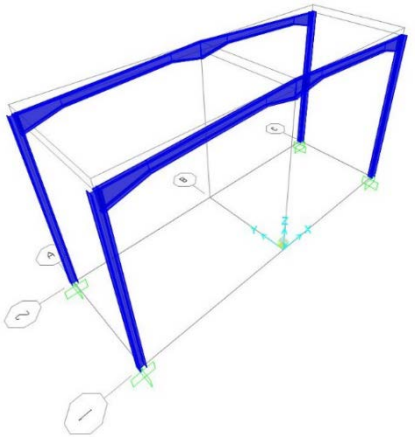

Şekil 2. Çerçevelerin tasarımı (Örnek: 15m, 5m, %5)

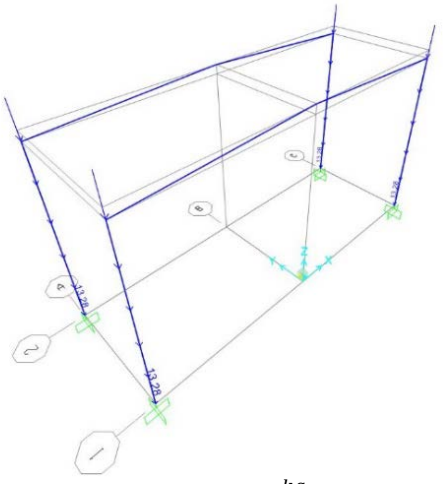

Şekil 3. Kuşak yükü ($\frac{kg}{m}$)

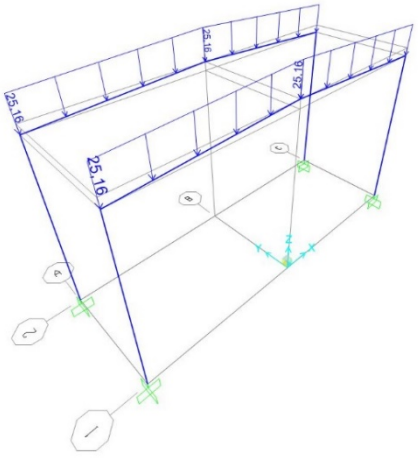

Şekil 4. Aşık yükü ($\frac{kg}{m}$)

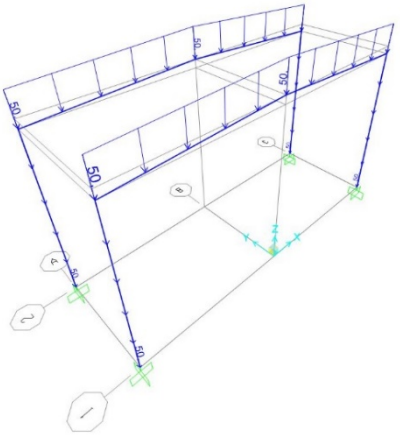

Şekil 5. Kaplama yükü ($\frac{kg}{m}$)

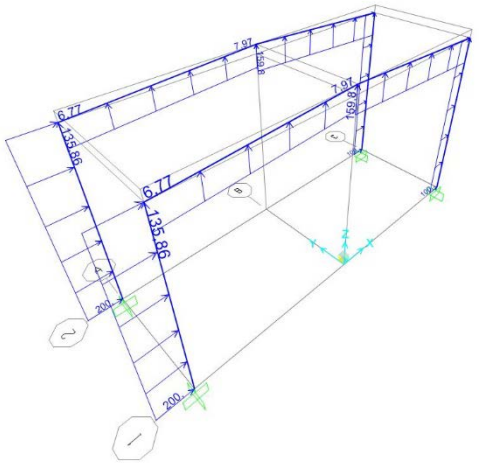

Şekil 6. Rüzgâr yükü ($\frac{kg}{m}$)

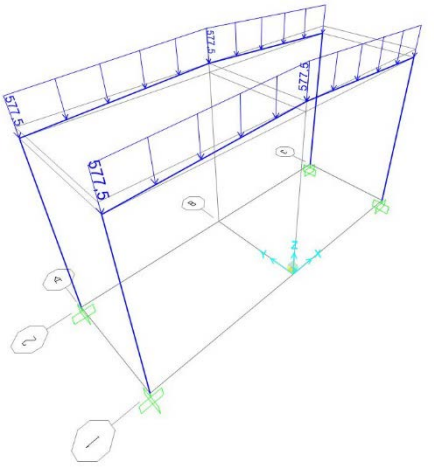

Şekil 7. Kar yükü ($\frac{kg}{m}$)

Bulgular

Bu çalışmada (Emniyet– Ekonomik- Estetik) kuralına göre sabit kolon yüksekliğinde 7 farklı makas açıklığı (15m, 16m, 17m, 18m, 19m, 20m ve 21m), 7 farklı çerçeve aralığı (5m, 5.5m, 6m, 6.5m, 7m, 7.5m, 8m) ve 5 farklı çatı eğiminin (%5, %6, %7, %8, %9), hangar tipi endüstri yapısının maliyetine etkisi araştırılmıştır. Analizde kullanılacak yükler Yapı Elemanlarının Boyutlandırılmasında Alınacak Yüklerin Hesap Değerleri (TS498)'e göre Konya ili için belirlenmiştir. Analiz "2016- Çelik Yapıların Tasarım, Hesap ve Yapım Esaslarına Dair Yönetmeliği (ÇYHY)[2]" ne göre 6 farklı kombinasyonda SAP 2000 programı ile yapılmıştır. Yapılan analizler sonucunda elde edilen grafikler incelendiğinde; çatı eğimi ve makas açıklığı sabit tutulup çerçeve aralığı değiştirildiğinde, kesitin değişmediği varsayılırsa, en büyük çerçeve aralığında metrekare başına düşen kilogramın en aza indiği görülmektedir. Bunun sebebi kesrin bölen kısımda yer alan metrekarenin, lineer olarak artmamasından kaynaklanmaktadır. Kesitin değiştiği varsayılırsa, en optimum sonucun 6.5 m – 7.5 m olduğu görülmektedir[6].

Çatı eğimi ve çerçeve aralığı sabit tutulup makas açıklığı değiştirildiğinde, kolon ve kiriş kesitlerinin büyümesinden dolayı, metrekare başına düşen ağırlığın arttığı görülmektedir.

Makas açıklığı ve çerçeve aralığı sabit tutulup çatı eğimi değiştirildiğinde, kullanılan kiriş boyunun artmasından dolayı, metrekare başına düşen ağırlığın az da olsa arttığı görülmektedir.

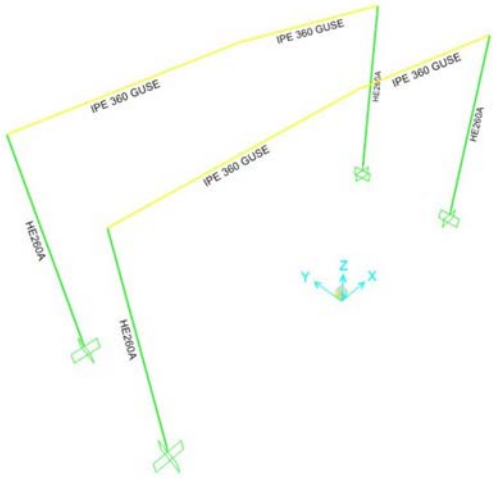

Şekil 8. SAP 2000 Analiz sonucu

Tartışma ve Sonuçlar

Tüm grafiklerden ve bulgulardan yola çıkarak en ekonomik kesite; çatı eğiminin azaldığı, makas açıklığının azaldığı ve çerçeve aralığının arttığı yerlerde ulaşılabilir. Emniyet ve maliyet dengesi kurulduğunda optimum çerçeve tasarımının %6 çatı eğiminde, 15 m makas açıklığında ve 7.5 m çerçeve aralığında olduğu görülmüştür (Şekil13).

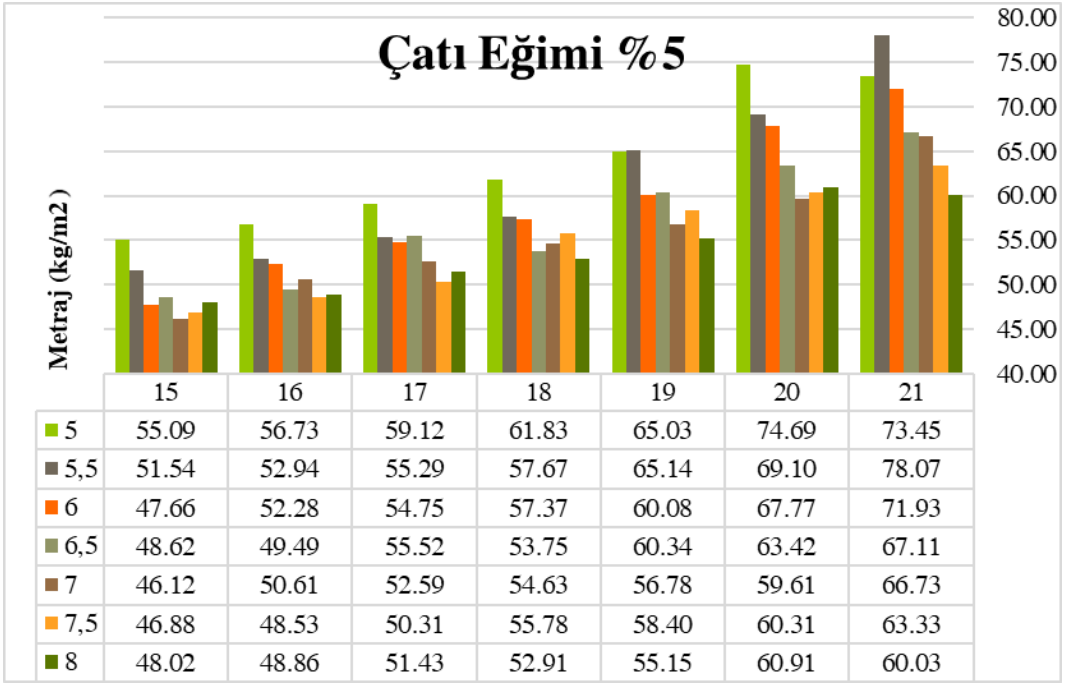

	15	16	17	18	19	20	21
5	55.09	56.73	59.12	61.83	65.03	74.69	73.45
5,5	51.54	52.94	55.29	57.67	65.14	69.10	78.07
6	47.66	52.28	54.75	57.37	60.08	67.77	71.93
6,5	48.62	49.49	55.52	53.75	60.34	63.42	67.11
7	46.12	50.61	52.59	54.63	56.78	59.61	66.73
7,5	46.88	48.53	50.31	55.78	58.40	60.31	63.33
8	48.02	48.86	51.43	52.91	55.15	60.91	60.03

Şekil 9. Çerçeve aralığı ve makas açıklığının metraj ilişkisi (%5 eğim)

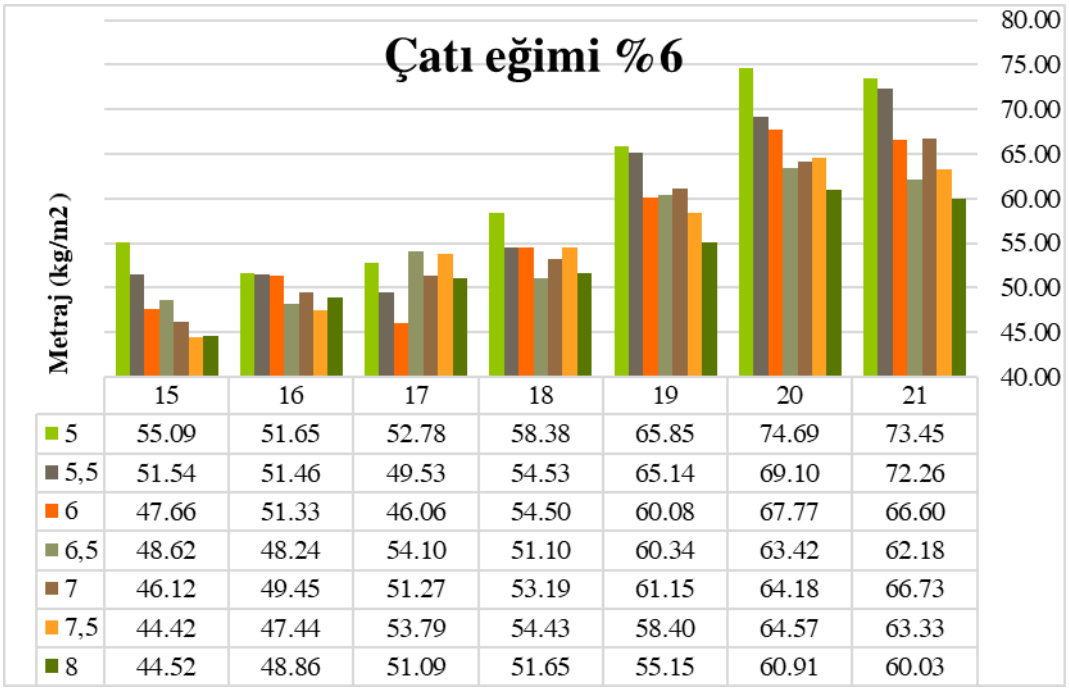

	15	16	17	18	19	20	21
5	55.09	51.65	52.78	58.38	65.85	74.69	73.45
5,5	51.54	51.46	49.53	54.53	65.14	69.10	72.26
6	47.66	51.33	46.06	54.50	60.08	67.77	66.60
6,5	48.62	48.24	54.10	51.10	60.34	63.42	62.18
7	46.12	49.45	51.27	53.19	61.15	64.18	66.73
7,5	44.42	47.44	53.79	54.43	58.40	64.57	63.33
8	44.52	48.86	51.09	51.65	55.15	60.91	60.03

Şekil 10. Çerçeve aralığı ve makas açıklığının metraj ilişkisi (%6 eğim)

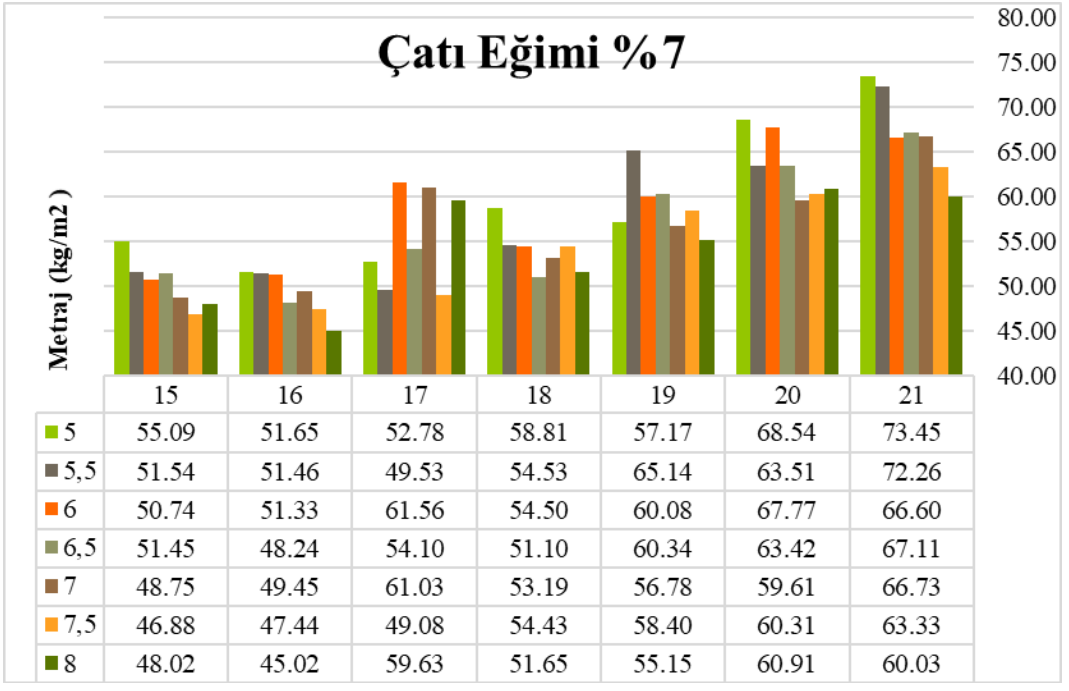

	15	16	17	18	19	20	21
5	55.09	51.65	52.78	58.81	57.17	68.54	73.45
5,5	51.54	51.46	49.53	54.53	65.14	63.51	72.26
6	50.74	51.33	61.56	54.50	60.08	67.77	66.60
6,5	51.45	48.24	54.10	51.10	60.34	63.42	67.11
7	48.75	49.45	61.03	53.19	56.78	59.61	66.73
7,5	46.88	47.44	49.08	54.43	58.40	60.31	63.33
8	48.02	45.02	59.63	51.65	55.15	60.91	60.03

Şekil 11. Çerçeve aralığı ve makas açıklığının metraj ilişkisi (%7 eğim)

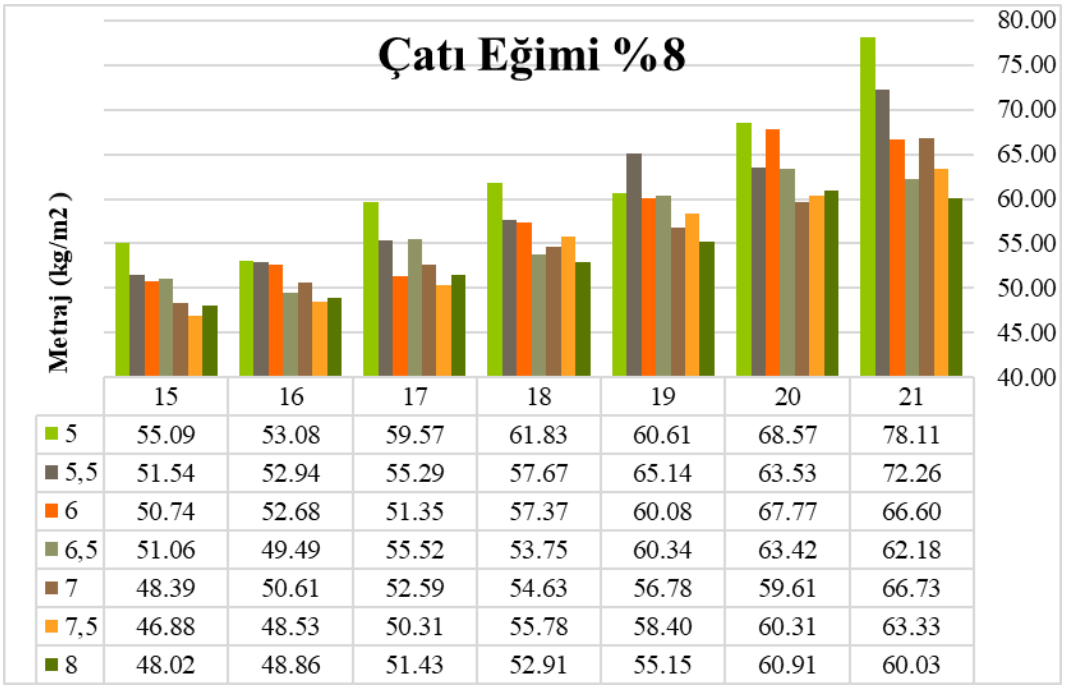

	15	16	17	18	19	20	21
5	55.09	53.08	59.57	61.83	60.61	68.57	78.11
5,5	51.54	52.94	55.29	57.67	65.14	63.53	72.26
6	50.74	52.68	51.35	57.37	60.08	67.77	66.60
6,5	51.06	49.49	55.52	53.75	60.34	63.42	62.18
7	48.39	50.61	52.59	54.63	56.78	59.61	66.73
7,5	46.88	48.53	50.31	55.78	58.40	60.31	63.33
8	48.02	48.86	51.43	52.91	55.15	60.91	60.03

Şekil 12. Çerçeve aralığı ve makas açıklığının metraj ilişkisi (%8 eğim)

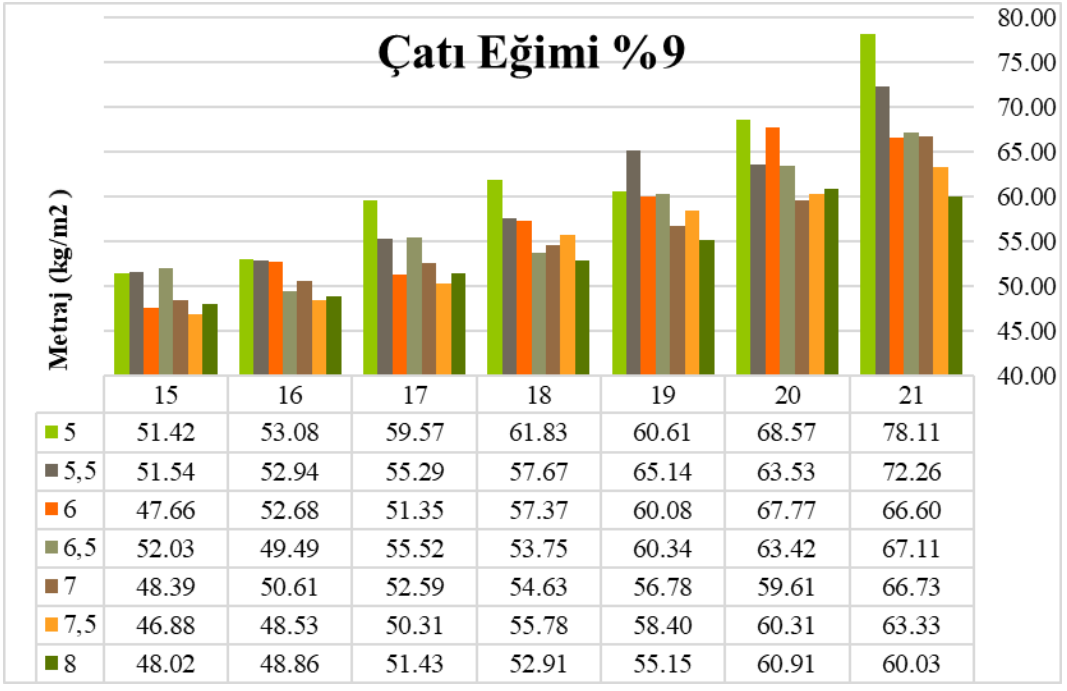

	15	16	17	18	19	20	21
5	51.42	53.08	59.57	61.83	60.61	68.57	78.11
5,5	51.54	52.94	55.29	57.67	65.14	63.53	72.26
6	47.66	52.68	51.35	57.37	60.08	67.77	66.60
6,5	52.03	49.49	55.52	53.75	60.34	63.42	67.11
7	48.39	50.61	52.59	54.63	56.78	59.61	66.73
7,5	46.88	48.53	50.31	55.78	58.40	60.31	63.33
8	48.02	48.86	51.43	52.91	55.15	60.91	60.03

Şekil 13. Çerçeve aralığı ve makas açıklığının metraj ilişkisi (%9 eğim)

Bu çalışmanın uygulamaya katkı sağlaması açısından makas açıklığı değerleri 25 m ye kadar ve çatı eğimi değerleri %30 a kadar çıkarılabilir. Uygulama yapacak mühendislere ön boyutlandırma için abaklar hazırlanabilir. Bu şekilde ülkemizdeki çelik yapıların kullanımının arttırılmasına katkı sağlanabilir ve uygulayıcılara çerçeve seçiminde, ekonomik açıdan karşılaştırmada yardımcı olunabilir.

Teşekkür

Çalışma boyunca her türlü tecrübesini ve bilgisini esirgemeyen Danışman Hocam Dr. Abdulkerim İLGÜN'e ve destekleri ile her zaman yanımda olan KTO Karatay Üniversitesi Mühendislik Fakültesi İnşaat Mühendisliği Bölümü Öğretim Elemanlarına teşekkür ederim.

Kaynaklar

[1] A. Ve, B. Mukavemet, and T. İ. B. Metot, TS498, vol. 2012, no. 112. Türkiye, 2013.

[2] 2016- Çelik Yapıların Tasarım, Hesap ve Yapım Esaslarına Dair Yönetmeliği (ÇYHY). Türkiye.

[3] K. Sinem, "ÇELİK YAPILARIN SAP2000 PROGRAMI İLE ANALİZ VE TASARIMI," 2005.

[4] C. Terzi, A. Gürbüz, V. Süme, and İ. Ustabaş, "Kar Yükünün Tetiklemesi Sonucu Çöken Örnek Bir Çelik Çatının İncelenmesi," 2015, pp. 363–372.

[5] www.yenimeram.com.tr, "http://www.yenimeram.com.tr/konyada-8-yerinin-catisi-kar-nedeniyle-coktu-44563.htm," Konya.

[6] S. Sadrettin, "İNŞAAT MÜHENDİSLİĞİ CIE 492 İnşaat Mühendisliğinde Tasarım ve Projelendirme (Bitirme Projesi)," KTO Karatay Üniversitesi, 2017.

International Conference on Science and Technology

ICONST 2018

5-9 September 2018 Prizren - KOSOVO

Anadolu Kara Çamının (*Pinus nigra* J. F. var. *şeneriana*) Bazı Mekanik Özelliklerine Isıl İşlemin Etkileri ve Yetişme muhiti Toprak Özellikleri

The Effects of Heat Treatment on Some Mechanical Properties of Anatolian Black Pine (*Pinus nigra* J. F. var. *şeneriana*) Wood and Soil Characteristics of Growing Area

Murat Akman[1]*, Murat Özalp[2], Melis Çerçioğlu[3]

Özet: Bu çalışmada, Anadolu Karaçamının (*Pinus nigra* J. F. var. *şeneriana*) eğilme direnci ve basınç direncine ısıl işlemin etkileri araştırılmıştır. Bu amaçla, bu çalışmada kullanılan Karaçam odun örnekleri 250 ° C'de 2 saat süre ile ısıl işleme tabi tutulmuştur. Isıl işlem görmüş ve görmemiş odun örneklerinin test sonuçları karşılaştırılmıştır. Isıl işlem, basın direnci ve eğilme direnci değerlerini düşürerek olumsuz etkilemiştir. Toprak analizleri Kütahya Dumlupınar Üniversitesi Simav Meslek Yüksek Okulu'nun toprak laboratuvarında yapılmıştır. Analiz sonucunda toprağın alkali, kumlu ve organik maddenin humus bakımından zengin olduğu görülmüştür.

Anahtar Kelimeler: Eğilme Direnci, Isıl İşlem, Ebe Karaçam, Toprak Analizi, Basınç Direnci

Abstract: In this study were investigate the effects of heat treatment on bending strength and compression strength of anatolian black pine (Pinus nigra J. F. var. seneriana). For this purpose, black pine wood samples used in this study were kept in temperature of 250 °C for 2 hours. The test results of heat-treated black pine wood and control samples showed that mechanical properties including compression strength and bending strength effected negatively with heat treatment. In additional, soil characteristics of anatolian black pine growing area were investigated. Analysis were conducted in the soil laboratory of Kutahya Dumlupinar University Simav Vocational High School. As a result of the analysis, it was observed that the the soil alkaline, sandy and organic matter were rich in humus.

Keywords: Bending strength, Heat treatment, Anatolian black pine, Soil analysis, Compression strength.

Giriş

Ağaç malzeme, yapısal özelliklerine göre farklı kullanım yerlerinde kullanılmaktadır. Doğal bir malzeme olan ağaç malzemenin özellikleri türlerine göre farklılık gösterir. Odun modifikasyon yöntemlerinin uygulanış şekli, iklim, toprak vb. gibi faktörlerin etkisiyle aynı tür ağaçlardan elde edilen malzemeler bile farklı özellikler gösterebilir. Bu nedenle ağaç malzemenin kullanıma uygunluğunun belirlenmesi için öncelikle mekanik özelliklerinin çok iyi irdelenmesi ve bu özelliklerin geliştirilmesinde hangi yönteminin tercih sebebi olduğunun

[1] Kütahya Dumlupınar Üniversitesi, Fen Bilimleri Enstitüsü, 43000, Kütahya/Türkiye
[2] Kütahya Dumlupınar Üniversitesi, Simav Teknoloji Fakültesi, 43500, Simav- Kütahya/Türkiye
[3] Kütahya Dumlupınar Üniversitesi, Simav Meslek Yüksekokulu, 43500, Simav- Kütahya/Türkiye
*Correspondingauthor: murat.ozalp@dpu.edu.tr

iyi tespit edilmesi ve bunun yanı sıra yetişme mühitinin iklim ve toprak özelliklerinin de iyi bilinmesi önem arz etmektedir. Günümüzde ısıl işlem (Thermo Wood) uygulanışı Avrupa'nın birçok ülkesinde değişik isimlerle anılmakta ve değişik yöntemlerle icra edilmektedir. Bu yöntemlerden bazıları, ağaç malzemenin ısıtılması için buhar kullanılan Finlandiya (Thermowood) yöntemi, Hollanda buhar ve sıcak havanın birlikte kullanıldığı Plato yöntemi, Fransız (Reftification) inert gaz kullanılan yöntem ve sıcak yağ kullanılan Alman (OHT) yöntemleridir (Mayes ve Oksanen, 2002).

Basınç direncine, ağaç malzemeye uygulanan ısıl işlemin etkisinin araştırıldığı bir çalışmada, *Quercus suber* odunu 100 °C ve 300 °C'de ısıl işleme tabi tutulmuştur. Çalışma sonucunda, 300 C'de su buharı ortamında ısıl işleme maruz bırakılan örneklerde kontrol örneklerine göre direnç kayıplarının fazla olduğu, bununda ısıya maruz kalan ağaç malzemenin termal bozunmasıyla ilişkili olduğu belirtilmiştir. (Rozsa ve Fortes, 1989).

Çam odunları kullanılarak yapılan çalışmada 180 °C ile 250 °C sıcaklıklarda su buharı koruması altında ısıl işleme tabi tutulmuşlardır. Sonuç olarak ısıl işleme maruz kalan örnekler kontrol örnekleri ile karşılaştırıldığında belli oranlarda eğilme direncinde kayıplar yaşandığı belirtilmiştir (Viitaniemi, 1997).

Farklı sıcaklıklarda ve sürelerde ısıl işleme maruz bırakılan çam ve kayın diri odunlarında yapılan deneysel incelemelerde, özellikle her iki ağaç türünde 150 C ve üzerindeki sıcaklıklarda eğilmede elastikiyet modülünde bir azalmanın meydana geldiği belirtilmiştir. Bununla beraber basınç direnci az miktarda etkilenirken şok direnci daha fazla etkilenmiştir (Schneider, 1971).

Isıl işlem uygulamasının Okaliptus (*Eucalyptus saligna*) odununda direnç özelliklerine etkisi araştırılmıştır. Örnekler 105 °C ile 155 °C sıcaklıklarda 10 ile 160 saat arasında değişen sürelerde ısıl işleme tabi tutulmuştur. Deney sonucunda sıcaklığın ve sürenin artmasıyla, eğilme direncinde, eğilmede elastikiyet modülünde, liflere paralel basınç ve makaslama dirençlerinde ciddi oranlarda düşüşlerin yaşandığı belirtilmiştir (Vital ve Lucia, 1983).

Eğilme direncindeki ilk kayıplardan ısıl işlem süresince lignin ve selülozun bozunması veya depolimerizasyonu değil hemiselülozun modifikasyonu ve/veya bozunması öncelikli olarak sorumlu tutulmaktadır. Eğilme direncindeki daha fazla azalma ısıl işlem süresi ve sıcaklığına bağlı olarak artmaktadır. Lignin-hemiselüloz matriksi içerisinde hemiselülozun yan zincirlerinin kırılması neticesinde yük paylaşma kapasitesinin bozulduğunu ve bu sebeple direnç kayıplarından sorumlu tutulabileceğini ifade etmiştir. Diğer bir sebep ise hemiselülozun omurgasının bozulması nedeniyle hemiselülozun polimerizasyon derecesinin azalmasıdır (LeVan, vd., 1990). Hemiselülozların bozunması malzeme bileşenleri arasında çapraz bağlanma reaksiyonlarına, mikrofibrillerin kristalizasyonuna ve mikrofibrillerde biriken gerilimin azalmasına neden olur (Dwianto, vd., 1996). Farklı ağaç türleri ve ısıl işlem şartlarına bağlı olarak %4 ile %49 arasında değişen oranlarda eğilme direnci azalışı bildirilmiştir (Esteves, vd., 2007; Shi, vd., 2007).

Basınç değerindeki değişiklikler ısıl işlemin yöntemine ve uygulama parametrelerine ve bunlara bağlı olarak değişen kimyasal yapıyla ilişkilidir. Isıl işlem uygulaması yapılmış ağaç türlerinde normal malzemeye göre daha fazla lignin oranına ve daha az asit sayısına sahiptir ki bu durum hemiselülozların ve bazı ekstraktiflerin bozunduğunu gösterir (Nuopponen et al., 2005). Ağaç malzemenin yapısını teşkil eden hemiselüloz 180 °C'de, lignin 200 °C'de ve selüloz ise 210 °C'de değişime uğrayarak, yapısında bozunma başlar. Buradanda görüleceği üzere ağaç malzemede ilk bozulan yapı yine asetil grubu içeren hemiselüloz, akabinde lignin ve en son olarak da selüloz yapı takip eder (Jeske et al., 2012; Ndiaye and Tidjani, 2012; Tufan ve ark, 2015).

Çalışmanın amacı; ülkemizde doğal olarak yetişen ve endemik tür kabul edilmiş olan Ebe Karaçamı (*Pinus nigra* J. F. var. *şeneriana*) ağaç malzemesinin eğilme ve basınç direnç değerlerini tespit ederek, bu türün ısıl işlem uygulaması neticesinde; eğilme ve basınç dirençleri üzerindeki etkisini araştırılarak, bu türün yetişme mühiti toprak tespitini yapmaktır.

Materyal ve Yöntem

2.1. Ağaç malzeme

Bu çalışma da kullanılan Ebe Karaçamına ait örnekler Kütahya'nın Domaniç ilçesine bağlı Domaniç Orman İşletme Müdürlüğü Ala göz Orman İşletme Şefliği 104 nolu bölmesi, 1025 rakımlı Karakıran tepenin kuzeyindeki mevkiinden temin edilmiştir.

2.2. Eğilme direnci

Eğilme direnci denemeleri TS 2474 sayılı standarda uygun olarak üniversal deney cihazında yapılmıştır. Eğilme direnci aşağıdaki formül ile hesaplanmıştır.

$$\sigma_e = \frac{3 \cdot F_{max} \cdot P}{2 \cdot m \cdot n^2} \quad (N/mm^2) \qquad (2.1)$$

Burada;

σ_e : Eğilme direnci (N/ mm^2) ,
F_{max} : Kırılma anındaki maksimum kuvvet (N),
P : Dayanak noktaları arsındaki açıklık (mm),
m : Deney parçasının genişliği (mm),s
n : Deney parçasının kalınlığı (mm) olarak alınmıştır.

2.3. Basınç direnci

Basınç direnci denemeleri TS 2595 sayılı standarda uygun olarak üniversal deney cihazında yapılmıştır. Basınç direnci ($_{B//}$) aşağıdaki formül yardımıyla hesaplanmıştır;

$$\sigma_{B//} = \frac{F_{max}}{k.s} \quad (N/mm^2) \qquad (2.2)$$

Burada;

F_{max} : Kırılma anındaki kuvvet (N),
k : Deney parçası enine kesit kenar uzunluğu (mm),
s : Deney parçası enine kesit kenar uzunluğu (mm).

2.4. Toprak örneklerinin analize hazırlanması

Ebe Karaçamı (*Pinus nigra* J. F. var. *şeneriana*) yetişme ortamından tekniğe uygun olarak alınan toprak örnekleri, laboratuvarda hava kurusu haline getirilip 2 mm'lik elekten geçirildikten sonra analizlerde kullanılmak üzere hazır hale getirilmiştir (Soil Survey Staff, 1951). Toprakların dane büyüklüğü dağılımı yani % kum, % mil ve % kil fraksiyonları hidrometre yöntemi uygulanarak belirlenmiştir (Bouyoucos, 1962). Her fraksiyon için bulunan veriler bünye üçgenine uygulanarak toprak örneklerinin bünyeleri belirlenmiştir (Black, 1965). Toprak pH'sı, sature toprak macununda cam elekrotlu pH-metre ile belirlenmiştir (Jackson, 1967). Toprağın elektriksel iletkenliği (EC) U.S. Salinity Lab. Staff'a göre cam elektrotlu EC-metre ile analiz edilmiştir (U.S. Salinity Lab. Staff., 1954). Kireç yüzdesi (% $CaCO_3$) Scheibler kalsimetresi ile analiz edilmiştir (Tüzüner, 1990). Organik madde, modifiye Walkley-Black yöntemine göre belirlenmiştir (Nelson ve Sommer, 1982). Toprak örneklerinin toplam azot (N) miktarı, modifiye makro Kjeldahl yöntemi ile, alınabilir potasyum (K) içerikleri ise değeri 7 olan 1 N NH_4OAc ile çalkalanarak elde edilen süzüklerde fleymfotometre ile tayin edilmiştir (Kacar, 1995). Alınabilir fosfor (P) miktarları, Olsen yöntemine göre kolorimetrik olarak tayin edilmiştir (Olsen ve Sommers, 1982).

Bulgular

Ebe Karaçamı (*Pinus nigra ssp. Pallasiana var. Şeneriana*) ağaç malzemesinin mekaniksel özelliklerinden eğilme ve basınç dirençleri tespiti ile yine aynı ağaç malzemesine ısıl işlem yöntemi uygulanarak mekanik özelliklerden eğilme ve basınç dirençlerine olan etkisini incelemek ve bu türün yetişme muhitinin toprak özelliklerinin belirlenmesi için araştırmalar yapılmıştır. Elde edilen bulgular aşağıda verilmiştir.

3.1. Mekanik özelliklere ait bulgular

Ebe Karaçamı örneklerinin eğilme ve basınç direnci deneyleri yapılmıştır. Elde edilen veriler ve analizleri aşağıda verilmiştir.

3.1.1. Eğilme direncine ait bulgular

Ebe Karaçamı ısıl işlem uygulanmayan örnekleri 20℃ ve %65 bağıl nem şartlarında 3 hafta süre ile iklimlendirme dolabında, klimatize edilip hava kurusu hale getirilmiştir. 250℃ sıcaklıkta 2 saat süre ile ısıl işlem uygulanan örneklerle birlikte deney öncesi genişlik ve kalınlıkları belirlendikten sonra eğilme direnci deneyleri, 4 tonluk universal deney cihazında, dayanak açıklığı 140 mm olarak ve 20 mm/dk deneme hızında ayarlanarak yük örneklerin tam ortasından yıllık halkalara paralel, liflere dik yönde yapılmıştır.

Ağaç malzemenin eğilme dirençlerinin tespiti için 10 ar adet kontrol örnekleri ve ısıl işlem uygulanmış örnekler eğilme direnci testine tabi tutulmuştur. Hesaplanmış olan eğilme direnci değerleri Çizelge 3.1'de verilmiştir.

Çizelge 3.1. Liflere dik yönde eğilme direnci değerleri (Bending strength values)

Örnek	Kontrol Örnekleri	Isıl İşlem Uygulanmış Örnekler
No	Eğilme Direnci (N/mm^2)	
1	165,22	100,28
2	142,62	71,71
3	174,70	83,40
4	107,15	69,24
5	116,88	76,45
6	98,81	65,15
7	108,33	62,11
8	69,91	82,00
9	150,86	81,09
10	163,50	72,65

Isıl işlem uygulamasının eğilme direnci üzerinde ki etkisinin belirlenmesi amacı ile elde edilen eğilme direnci değerlerine Design-Expert® 7.0.3 istatistik programı kullanılarak istatistik analiz gerçekleştirilmiştir. Elde edilen etkileşim grafiği Şekil 3.1' de verilmiştir.

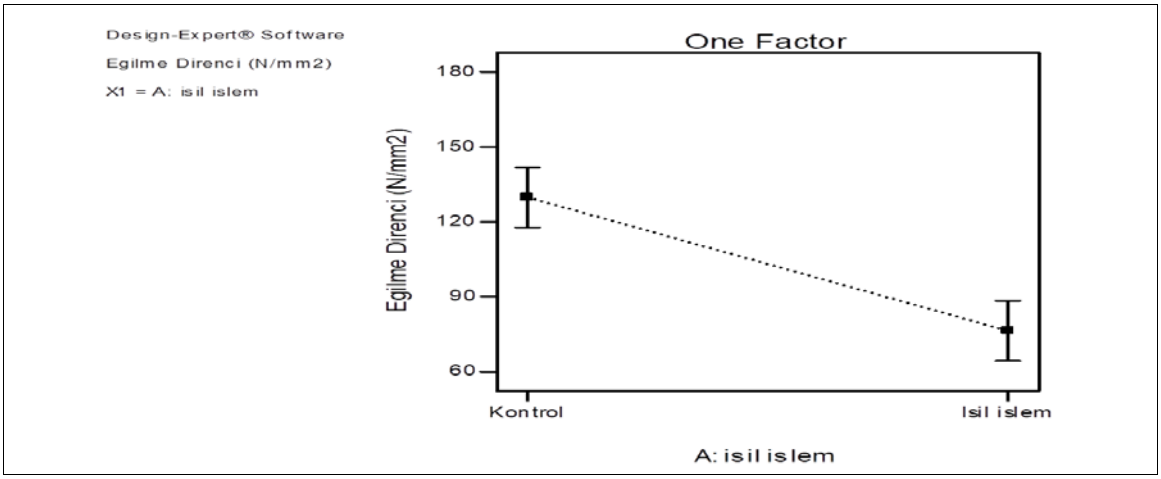

Şekil 3.1. Eğilme direnci etkileşim grafiği (Bending strength interaction graph)

Şekil 3.1'deki etkileşim grafiği incelendiğinde ısıl işlem uygulanması ile eğilme direnci değerlerinin keskin bir şekilde düştüğü belirlenmiştir. Yapılan istatistik analiz sonucunda ısıl işlem uygulamasının eğilme direnci üzerinde istatistiksel olarak önemli derecede etkili olduğu belirlenmiştir (P=0,0002). Ebe Karaçamına ait elde edilen eğilme direnci değerlerinin özeti Çizelge 3.2'de verilmiştir.

Çizelge 3.2. Ebe Karaçam ağaç malzemesine ait özet eğilme direnci değerleri. (Bending strength values belong to black pine wood)

Tespitler	**Odun Malzeme Örneklerinin**	
	Kontrol Eğilme Direnci (N/mm^2)	**Isıl İşlem Uygulaması Sonucu Eğilme Direnci (N/mm^2)**
	Değerler	
$\bar{e}$	129,80	76,41
δ_x	34,48	11,01
Min	69,91	62,11
Max	174,70	100,28
N	10	10

Isıl işlemi uygulanmayan kontrol örneklerinin ortalama eğilme direnci değerinin 129,80 N/mm^2 olduğu ve ısıl işlem uygulanmış örnek gruplarında ise ortalama 76,41 N/mm^2 eğilme direnci değeri ölçülmüştür. Isıl işlem uygulanan örneklerde sıcaklık ve sürenin etkisiyle eğilme direnci değerinde %41 oranında bir azalma olduğu belirlenmiştir. Isıl işlem uygulanmamış kontrol örneklerinde en yüksek ve en düşük eğilme direnci değerleri sırası ile 174,70 N/mm^2 ve 69,91 N/mm^2 belirlenirken, ısıl işlem uygulanmış örneklerde en yüksek ve en düşük eğilme direnci değerleri sırasıyla 100,28 N/mm^2 ve 62,11 N/mm^2 olarak belirlenmiştir. Ayrıca ısıl işlem uygulaması süresince reçine kanalları etrafındaki epitelyum hücrelerin ve özışınlarındaki paranşim hücrelerinin zarar görmesi de etkili olmaktadır.

3.1.2. Basınç direncine ait bulgular

Isıl işlem uygulanmayan kontrol örnekleri 20°C ve %65 bağıl nem koşullarında 3 hafta süre ile iklimlendirme dolabında, klimatize edilip hava kurusu hale getirilmiştir. 250°C sıcaklıkta 2 saat süre ile ısıl işlem uygulanan örneklerle birlikte deney öncesi genişlik ve kalınlıkları belirlendikten sonra basınç direnci deneyleri, 4 tonluk universal deney cihazında örneklerin en kesitine homojen ve örnekleri 0,5-1,0 dakika içinde ezecek şekilde numuneler kırılıncaya kadar 20 mm/dk bir kuvvet uygulanmıştır.

Ağaç malzemenin basınç dirençlerinin tespiti için 15 er adet kontrol örnekleri ve ısıl işlem uygulanmış örnekler basınç direnci testine tabi tutulmuştur. Hesaplanmış olan basınç direnci değerleri Çizelge 3.3'de verilmiştir.

Çizelge 3.3. Basınç direnci değerleri (Compression strength values)

Örnek	Kontrol Örnekleri	Isıl İşlem Uygulanmış Örnekler
No	Basınç Direnci (N/mm^2)	
1	52,68	36,06
2	42,14	46,57
3	56,95	47,36
4	55,85	42,20
5	56,61	47,44
6	62,92	46,02
7	56,56	38,78
8	54,17	42,26
9	58,23	41,38
10	54,24	49,21
11	57,05	37,05
12	48,64	47,70
13	57,60	34,06
14	39,63	50,68
15	55,08	48,91

Isıl işlem uygulamasının basınç direnci üzerinde ki etkisinin belirlenmesi amacı ile elde edilen basınç direnci değerlerine Design-Expert® 7.0.3 istatistik programı kullanılarak istatistik analiz gerçekleştirilmiştir. Elde edilen etkileşim grafiği Şekil 3.3' te verilmiştir.

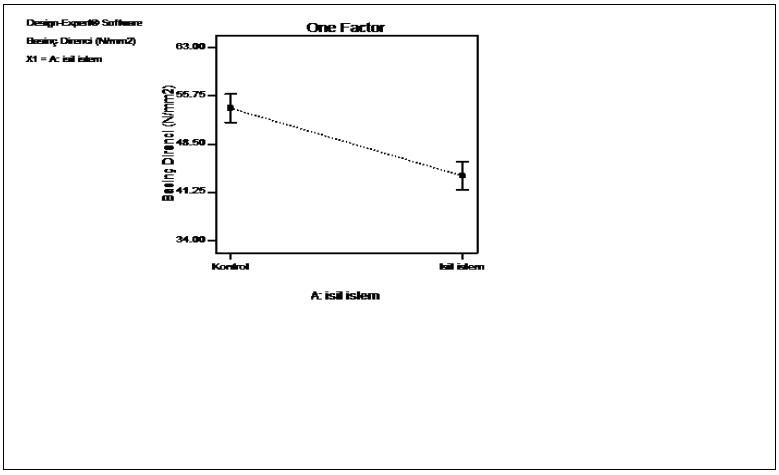

Şekil 3.2. Basınç direnci etkileşim grafiği (Compression strength Interaction Chart)

Şekil 3.2'de ki etkileşim grafiği incelendiğinde ısıl işlem uygulanması ile basınç direnci değerlerinin belirgin bir şekilde düştüğü belirlenmiştir. Yapılan istatistik analiz sonucunda ısıl işlem uygulamasının basınç direnci üzerinde istatistiksel olarak önemli derecede etkili olduğu belirlenmiştir (P< 0,0001). Ebe Karaçamına ait elde edilen basınç direnci değerlerinin özeti Çizelge 3.4'te verilmiştir.

Çizelge 3.4. Ebe Karaçam ağaç malzemesine ait özet basınç direnci değerleri (Compression strength values belong to black pine wood)

Tespitler	Odun Malzeme Örneklerinin	
	Kontrol Basınç Direnci (N/mm^2)	Isıl İşlem Uygulaması Sonucu Basınç Direnci (N/mm^2)
	Değerler	
$\bar{e}$	53,89	43,71
δ_x	6,12	5,30
Min	39,63	34,06
Max	62,92	50,68
N	15	15

Isıl işlemi uygulanmayan kontrol örneklerinin ortalama basınç direnci değerinin 53,89 N/mm^2 olduğu ve ısıl işlem uygulanmış örnek gruplarında ise ortalama 43,71 N/mm^2 basınç direnci değeri ölçülmüştür. Bu datalar ışığında ısıl işlem uygulanan örneklerde sıcaklık ve sürenin etkisiyle basınç direnci değerinde %19 oranında bir azalma olduğu belirlenmiştir. Isıl işlem uygulanmamış kontrol örneklerinde en yüksek ve en düşük basınç direnci değerleri sırası ile 62,92 N/mm^2 ve 39,63 N/mm^2 belirlenirken, ısıl işlem uygulanmış örneklerde en yüksek ve en düşük basınç direnci değerleri sırasıyla 50,68 N/mm^2 ve 34,06 N/mm^2 olarak belirlenmiştir.

3.2. Toprak özelliklere ait bulgular

Toprak laboratuvarında yapılan kimyasal analiz sonuçlarından da görüleceği üzere, sahanın toprak yapısının kontrolünde kumlu toprak olduğu, kireç oranı iyi sınıfında olmasına rağmen, çok hassas bitkilerin zarar görebileceği tuzluluk oranına sahip olduğu görülmüştür.

Toprağın verimliliğini etkileyen önemli bir faktörlerden olan toprak reaksiyonu normal verimli toprakların p^H değerleri 4.5 ile 8.5 arasında değişir. Analiz sonucuna göre yetişme mühiti p^H 8,87 derecesi idealin altındadır ve kuvvetli alkalidir.

Topraktaki bitki besin maddelerinin bitkilere yarayışlıkları o toprağın reaksiyonu ile çok yakından ilgilidir. Gerek bitki besin maddelerinin yarayışlılıkları ve gerekse topraktaki mikrobiyal faaliyetler için en uygun p^H değerleri 6-7 civarındadır. Toprak içerisinde bitki ve hayvan kalıntılarının mikroorganizmalar tarafından parçalanması ile oluşan humus bakımından çok zengin yapıdadır. Bu özellik toprağın fiziksel özelliklerine olumlu etki ederken, organik madde terkibindeki besin maddeleri de bitkilere fayda sağlar. Ayrıca besin maddelerinin ve suyun toprakta tutulmasına yardımcı olur, toprak kırıntılı bünyesine yararlı olur.

Bitkilerin yapraklarında, kök uçlarında ve tomurcuk gibi genç ve çabuk büyüyen kısımlarında bulunan, bitkinin olgunlaşmasına, kalitesine ve miktarına olumlu katkı sağlayan, aynı zamanda renk, tat ve koku gibi özellikleri düzenleyen potasyum bakımından yeterli seviyededir. Bu yüzden ağaç türünde herhangi bir tepe ve kenarlarında kurumalar görülmemiştir.

Bu ağaç türünün normal büyümelerine katkı sağlayan fosfor oranı çok az miktarda bulunmasına rağmen herhangi bir renk değişikliğine rastlanılmamıştır.

Genel anlamda orman ağaç türlerinin yetişmesine uygun yapıda olduğu tespit edilmiştir. Ebe Karaçamı yetişme mühitinin toprak analizine ait kimyasal analiz sonuçları Çizelge 3.5'te verilmiştir.

Çizelge 3.5. Toprak analiz sonuçları (Soil analysis results)

Yapılan Analizler	**Sonuç**	**Değerlendirme**
P^h	8,87	Kuvvetli Alkali
EC(mScm)	0,04	Tuzsuz
Kireç(%)	3,15	Kireçli
Kum(%)	64,72	
Mil(%)	18,00	
Kil(%)	17,28	
Bünye(%)		Kumlu Tın
Organik Madde(%)	5,24	Humuslu
Alınabilir Fosfor(%)	0,06	ÇokAz
Alınabilir Potasyum(ppm)	66,30	Yeterli

Tartışma ve Sonuçlar

Ebe Karaçamı ağaç malzemesine ısıl işlem uygulaması sonrası sıcaklık ve süreyle orantılı olarak, eğilme direnci değerlerinde düşüşler görülmüştür. Bu azalma, ısıl işlem uygulamasında malzemenin en hassas bileşeni hemiselülozun yapısının ve bünyesindeki meydana gelen değişmelerden kaynaklanmaktadır. Yük paylaşımı dengesinin bozulmasına neden olan lignin ve hemiselüloz matriksi içeriğindeki hemiselüloz yan zincirlerinin kırılmasıdır. Isıl işlem uygulaması sonucu meydana gelen direnç azalmasının bir sebebinin de hemiselülozların polimerizasyon derecesindeki azalışlarından kaynaklanır. Kısa polimerizasyon derecesi ve amorf selüloz mikrofibrilleri çevresine yerleşmiş bir polimerin malzeme liflerinin direnci üzerine katkı edeceği çok fazla hipotetiktir.

Isıl işlem uygulaması yapılmış ağaç malzemelerinde basınç direncine anizotropik etki görülmeye değerdir. Liflerine paralel basınç yönünde %41 oranında azalma eğilimi göstermektedir. Bunun nedeni hücre çeperindeki su miktarının azalmasından kaynaklanır. Isıl işlem uygulaması sonucu amorf selülozun bozulması ve kristalleşmesi, malzemenin yapısındaki kristalimsi selüloz miktarının önemli ölçüde azalmasına neden olur. Kristalimsi selülozun yapısı anizotropik yapı ihtiva ettiğinden katı ve rijit yapısı liflere paralel yönde basınç direncini azaltır. Yine lignin ve polimer ağının çapraz bağlanmasındaki azalmalar, orta lamel direncini azaltır ve hücre çeperinin direnç özelliklerine negatif etki ederek, basınç direncinin azalmasına vesile olur.

Topraktaki besin maddelerinin bitkiye yarayışlılığı, o toprağın p^H'sı ile çok yakından ilgilidir. Gerek bitki besin maddelerinin yarayışlılıkları ve gerekse topraktaki mikrobiyolojik faaliyetler için en uygun p^H değerleri 6-7 arasındadır. Toprakların organik madde içeriği ise toprağın üretkenlik kapasitesini etkileyen önemli bir parametredir. Toprağın fiziksel, kimyasal ve biyolojik özellikleri üzerine pozitif etkileri olan organik madde, toprak organizmaları için de bir besin kaynağıdır. Bitkilere besin maddesi sağlayarak doğrudan bitki gelişimini ve verimini etkiler. Ayrıca dolaylı olarak toprağın fiziksel özelliklerini modifiye ederek kök bölgesinde gelişme sağlayarak bitki büyümesini teşvik etmektedir.

Araştırma alanının toprağı kumlu tın bünyeli, az kireçli, tuzsuz, kuvvetli alkali, organik madde ve toplam azot içeriği bakımından zengin, alınabilir fosfor ve potasyum içerikleri bakımından ise az miktardadır. Genel olarak toprak özelliklerinin orman ağaç türlerinin yetişmesine uygun yapıda olduğu belirlenmiştir.

Bu çalışmada elde edilen veriler ışığında; Ebe Karaçamından elde edilen masif ahşabın büyük boyutlu ve kavisli elemanlarda tek parça olarak kullanılma olanağının zor olduğu, bu yüzden ağaç malzeme kullanılma tercihinin kısa ve küçük boyutlarda olması verimliliği arttıracaktır. Isıl işlem uygulaması gören malzemeden oymacılık sanatı geliştirilerek estetik ürünler elde edilebilir. Bunun yanında oyuncak sektörü başta olmak üzere masif sandalye, kapı sereni, masif panel yapımı, iç ve dış mekan mobilyaları üretiminde sağlıklı ürünler ortaya çıkarabileceği düşünülmektedir.

Kaynaklar

Black, C.A. (1965). Methods of Soil Analysis, Part 1: Physical and Mineralogical Properties, including statistics of measurement and sampling. Agronomy Ser. 9. American Society of Agronomy, Inc. Publisher, Madison, Wisconsin, USA.

Bouyoucos, G.J., (1962). Hydrometer method improved for making particle size analysis of soils. Agronomy Journal, 54, 464-465.

Dwianto, W., Tanaka, F., Inoue, M., Norimoto, M. (2005). Fagus orientalis changes of wood by heat or steam treatment. Wood Research, 83, 47-49.

Esteves, B.M., Domingos, I. J., Pereira, H. M. (2007). Pine wood modification by heat treatment in air. Biroresources, 3, 1, 142-154.

Jackson, M.L, (1967). Soil Chemical Analysis, Prentice-Hall of India Private Limited, NewDelhi.

Jeske, H., Schirp, A., Cornelius, F. (2012). Development of a thermogravimetric analysis (TGA) method for quanti analysis of wood flour and polypropylene in wood plastic composites (WPC), Thermochimica Acta 543. 165-171.

Kacar, B. (1995). Bitki ve Toprağın Kimyasal Analizleri III: Toprak Analizleri. 3, Ankara Üniversitesi Ziraat Fakültesi Eğitim Araştırma ve Gelişme Vakfı

LeVan, S.L., Ross, R.J., Winandy, J.E. (1990). Effects of Fire Retardant Chemicals on Bending Properties of Wood at Elevated Temperatures, Res. Pap. FPL-RP498, USDA Forest Service Forest Products Laboratory, Madison, WI-USA, 24 pp.

Mayes, D., Oksanen, O., (2002). Thermo wood Hanbook, Finnforest, 3, Finland.

Ndiaye, D., Tidjani, A. (2012). Effects of coupling agents on thermal behavior and mechanical properties of wood flour/polypropylene Composites, Journal of Composite Materials, 46 (24), 3067–3075.

Nelson, D.W., Sommer, L.E, (1982). Total carbon, organic carbon and organic matter. In: Methods of Soil Analysis, Part II: Chemical and microbiological properties. (Eds: A.L. Page, R.H. Miller and D.R. Keeney), American Society of Agronomy, Madison, WI, pp 539-579.

Nuopponen, M., (2005). FT-IR and UV Raman spectroscopic studies on thermal modification of scotch pine wood and its extractable compounds. Helsinki University of Technology, Espoo, Finland.

Olsen, S.R., Sommers, E.L. (1982). Phosphorous availability indices, phosporus soluble in sodium bicarbonate. In: Methods of Soil Analysis, Part II: Chemical and microbiological properties. 2nd ed. (Eds: A.L. Page, P.H. Miller and D.R. Keeney), American Society of Agronomy, Madison, WI, pp. 404-430.

Rozsa, M.E., Fortes, M.A, (1989). Effects os Water Vapour Heatin on Structure and Properties of Cork, *Wood Science Technology*, 23, 2, 27-34.

Schneider, A, (1971). Investigations on the Influence of Heat Treatment in the temperature Range 100-200 ℃ on modulus of Elasticit. *Holz Roh-u Werkstoff*, 29, 11, 431-440.

Shi, J.L., Kocaefe, D., Zhang, J. (2007). Mechanical behaviour of Québec wood species heat-treated using ThermoWood process. *Holz als Roh-und Werkstoff*, 65, 255-259.

Soil Survey Staff. (1951). Soil survey manual, USDA Agriculture Handbook 18, U.S. Government Printing Office, Washington, DC.

Tufan, M., Güleç, T., Çukur, U., Akbaş, S., İmamoğlu, S. (2015). Atık Bardaklardan Üretilen Odun Plastik Kompozitlerin Bazı Özellikleri, *Kastamonu Üniversitesi Orman Fakültesi Dergisi*, 15, 2, 176-182.

Tüzüner, A, (1990). Toprak ve Su Analiz Laboratuvarları El Kitabı. Tarım Orman ve Köy İşleri Bakanlığı Köy Hizmetleri Genel Müdürlüğü Yayın No: 279, 375 s.

U.S. Salinity Laboratory. (1954). Diagnosis and Improvement of Saline and Alkali Soils, USDA Handbook 60. U.S. Government Printing Office, Washington, DC, pp.1-160.

Viitaniemi, P. (1997, 12 December). Decay resistant wood created in a Heating process, Industrial Horizons.

Vital, B.R., Lucia, M.D. (1983). Effect of heating on some properties of *Eacalyptus saligna* Wood, Revista-Arvore, 7, 2, 136-146.

International Conference on Science and Technology

ICONST 2018

5-9 September 2018 Prizren - KOSOVO

Investigation of The Effects of Heat Treatment on Varnished Wood Material

Beytullah Kazan[1]*, Murat Özalp[1]

Abstract: In this study, the effects of the heat treatment applied varnished wood materials on hardness, brightness and varnishes' surface sticking resistance were investigated. For this purpose, firstly Pinus Sylvestris L., Fagus Orientalis L. and Castanea Sativa M. wooden samples were varnished by the water based varnish and after that they were kept in temperatures of 100 ˚C, 125 ˚C and 150 ˚C for times of 2, 4 and 6 hours. According to test results it was determined that while the hardness and varnishes' surface sticking resistance were improved for all samples which were processed 2 hours in temperatures of 100 ˚C, the brightness, surface sticking resistance and brightness of the samples which were processed 4 and 6 hours in 100 ˚C and 2, 4 and 6 hours in 125 ˚C and 150 ˚C were deteriorated. Furthermore, it was observed that the hardness resistance of all samples which processed for 2, 4 and 6 hours in 100 ˚C, 125 ˚C and 150 ˚C were high. In all varnished wood species, the dual-component varnish gave better results than the single-component varnish.

Keywords: Heat treatment, hardness, brightness, resistance of sticking, water-based varnish

1. Introduction

Top surface processes have been applied since time immemorial in order to provide protecting against external effects, to increase esthetical value, and to eliminate negative properties of wood material [1]. A range of chemical changes and reactions resulting in degradation of components such as wood hemicellulose, lignin etc. by the effect of high temperature during heat treatments occur, and changes in wood structure are formed. It is applied temperatures over 150 C^{o} for places of use desired high durability, and under 150 C^{o} for indoor usages generally [2]. Water vapor and high temperatures in heat treatment processes are used in principle. Therefore, process conditions have corrosive properties and water and various components are dissociate from wood and are evaporated [3]. Budakci, investigated the effect of layer thickness on hardness, brightness, and surface sticking resistance in wood varnishes. He determined that third layer varnish applications don't have any effect on hardness and increasing layer thickness increases surface sticking resistance in polymeric-based varnishes [4]. Highley and Kicle, reported that coating with different varnish layer on the purpose of protecting surface of wood materials against external effects is a method used as most commonly [5]. Atar, performed bleaching with 6 group solutions in impregnated and natural scotch pine, oriental beech, chestnut and sessile oak woods. It was applied water-based and synthetic varnish to their surfaces, and it was specified that bleaching tools decrease surface sticking resistance of varnishes by 3-5% averagely, and the best results were obtained with water-based varnish [6]. Sogutlu, determined that wood material high density is also have a high surface sticking resistance, as a result of regression analysis performed to specify relation between density and adhesive resistance [7]. The pentahydrate added into the varnish increased toughness and sticking resistance; however, it decreased the brightness rate of varnish on the other side [8]. It is observed that as the rate of the pentahydrate added into the water-based varnish increased from 0 % to 30 %, the varnishes' sticking rate increased 50.46 % in Chesnut wood and 37.04 % in Scotch pine wood. Toughness rate increased 55.79 % in Chesnut wood and 41.98 % in Scotch pine, Brightness rate decreased 68.52 % in Chesnut wood and 58.88 % in Scotch pine [9].

The purpose of the study is to determine effects of heat treatment applied to varnished wood material on properties of varnish.

[1]Kutahya Dumlupinar University, Faculty of Simav Technology, Department of Wood Products Industrial Engineering, 43500 Simav-Kütahya/Turkey
*Correspondingauthor: murat.ozalpl@dpu.edu.tr

2. Material and Method

2.1. Wood Material

First-class and flawless wood samples obtained from scotch pine (Pinus silvestris L.), beech wood (Fagus orientalis L.), chestnut (Castanea sativa M.) woods were used in all experiments. Experiment samples were prepared according to ASTM-D 358 and TS 801 principals [10]. After samples in air-dry moisture were brought to 100x100x8 dimension, they were sanded with 100 numbered sandpaper first,and 120 numbered sandpaper after. 300 samples were prepared as 5 experiments for every tree species, varnish species, and heat treatment method in the study.

2.2. Varnish

In varnishing of experiment samples, (A) single component belong to Trimetal company and (B) dual component belong to Hemel company (Sayerlack VS 5341+ AH 1547 hardener) water-based varnishes were used. It was corresponded to ASTM D-3023 principals in varnishing of samples. Properties of varnishes used in experiments were given in Table1.

Table 1. Technical specifications of varnishes

Specifications	Varnish type	
	Single components	Dual components
Amounts of solids (%)	30±2	36±1
P^H (25°C)	8,8	9,2
Layer thickness (µm)	85	130

2.3. Heat Treatment Application

Heat treatment was applied to varnished materials and in air-dry conditions. Experiments were subjected to heat treatment inside oven in 100 C°, 125 C° and 150 C° for times of 2, 4, 6 hours in conformity with the purpose of experiment.

2.4. Adhesive

In experiments, 404 Steel Adhesive, which doesn't have solver effect on two-component epoxy-resinous varnish layers according to ASTM D-4541 and TS EN-24624 and have high adhesive force was used [11,12].

2.5. Surface Sticking Test

Surface sticking resistance of varnish layers was determined in adhesion test device working with air system by adapting to ASTM D-4541 and TS EN 24624 principals in the research [12,13]. The equation given below was used while calculating the resistance of sticking.

$$X = 4F / \pi.d^2 \quad (1)$$

Where;

F: Splitting force (Newton), d: Sample cylinder's radius (mm), X: Sticking resistance (MPa).

2.6. Pendulum Hardness Measurement

Hardness values of varnish layer specifying durability to external factors were determined with pendulum hardness measurement device according to könig method by adapting to principals specified in ANS/ISO 1522 [13].

2.7. Surface Brightness Measurement

Measurements were performed with brightness measurement device (Glossmeter) by taking advantage of shining capability of varnish surfaces within the frame of principals specified in TS 4318 EN ISO 2813 [14].

3. Results

3.1. Hardness Resistance Measurements

Obtained hardness resistance values belong to scotch pine wood were given in Table 2.

Table 2. Hardness resistance values belong to scotch pine wood

Hardness measurement values (Pendulum)										
Wood type	Temperature (°C)	Time (hour)	Varnish Type	Values					n	Average
SCOTCH PINE	Non-treatment	-	A	33	35	35	31	34	5	33,6
			B	48	37	44	44	39	5	42,3
	100	2	A	30	36	36	34	37	5	34,6
			B	48	42	47	43	41	5	44,2
		4	A	31	35	34	36	38	5	34,8
			B	47	45	44	45	46	5	45,4
		6	A	38	36	39	36	35	5	36,8
			B	48	48	47	46	46	5	47
	125	2	A	34	36	35	35	38	5	35,6
			B	46	48	47	47	49	5	47,4
		4	A	35	35	36	38	39	5	36,6
			B	48	48	50	51	49	5	49,2
		6	A	36	38	36	37	38	5	37
			B	50	51	48	49	52	5	50
	150	2	A	36	38	36	34	38	5	36,4
			B	50	51	49	49	52	5	50,2
		4	A	38	38	40	36	38	5	38
			B	48	51	52	52	54	5	51,4
		6	A	39	38	36	39	40	5	38,4
			B	54	52	50	54	51	5	52,2

After single and dual component varnish applications of scotch pine tree; lowest hardness values were seen in specimens subjected to non-heat-treated single component varnish application, while highest hardness values were seen in specimens subjected to dual component varnish application and waited for 6 hours in 150 C° as a result of comparing hardness values of non-heat-treated specimens and heat-treated specimens according to heat treatment temperature and time. As a result of comparing hardness values of non-heat-treated specimens subjected to single component varnish application and heat-treated specimens, it was seen that heat-treated specimens have higher hardness values compared with specimens varnished without heat-treatment. As a result of comparing dual component varnished non-heat-treated specimens and heat-treated specimens, it was observed that hardness values of heat-treated specimens have higher than specimens varnished without heat-treatment.

Obtained hardness resistance values belong to beech wood were given in Table 3.

Table 3. Hardness resistance values belong to beech wood

Hardness measurement values (Pendulum)										
Wood type	Temperature (°C)	Time (hour)	Varnish type	Values					n	Average
BEECH WOOD	Non-treatment	–	A	49	53	60	60	54	5	55,2
			B	61	58	66	61	63	5	61,8
	100	2	A	54	58	53	58	57	5	56
			B	68	66	65	60	59	5	63,6
		4	A	56	58	59	57	58	5	57,6
			B	65	66	65	63	63	5	64,4
		6	A	56	59	60	58	57	5	58
			B	65	63	68	64	67	5	65,4
	125	2	A	56	59	60	59	59	5	58,6
			B	65	64	65	67	68	5	65,8
		4	A	58	60	61	59	58	5	59,2
			B	68	64	69	67	68	5	67,2
		6	A	60	61	59	61	58	5	59,8
			B	68	65	70	69	68	5	68
	150	2	A	58	61	60	58	58	5	59
			B	69	69	65	68	68	5	67,8
		4	A	58	61	62	58	60	5	59,8
			B	68	69	71	68	68	5	68,8
		6	A	59	60	62	62	63	5	61,2
			B	68	70	70	71	71	5	70

After single and dual component varnish applications of beech wood; lowest hardness values were seen in non-heat-treated specimens, while highest hardness values were seen in dual component varnished specimens waited for 6 hours in 150 C° according to heat treatment temperature and time conditions. As a result of comparing hardness values of non-heat-treated specimens subjected to single component varnish application and heat-treated specimens, it was seen that heat-treated specimens have higher hardness values compared with specimens varnished as non-heat-treated. As a result of comparing dual component varnished non-heat-treated specimens and heat-treated specimens, it was observed that hardness values of heat-treated specimens have higher than specimens varnished without heat-treatment.

Obtained hardness measurement values belong to chestnut wood were given in Table 4.

Table 4. Hardness measurement values belong to chestnut wood

Hardness measurement values (Pendulum)										
Wood type	Temperature (°C)	Time (hour)	Varnish type	Values					n	Average
CHESNUT	Non-treatment	-	A	43	39	51	38	42	5	42,6
			B	59	63	52	49	53	5	55,2
	100	2	A	49	45	40	40	44	5	43,6
			B	60	58	58	56	59	5	58,2
		4	A	45	47	48	46	41	5	45,4
			B	59	64	60	60	57	5	60
		6	A	46	48	48	47	46	5	47
			B	61	62	59	63	61	5	61,2
	125	2	A	48	44	45	47	48	5	46,4
			B	63	61	59	62	62	5	61,4
		4	A	46	48	47	48	46	5	47
			B	62	64	62	62	63	5	62,6
		6	A	48	49	48	50	47	5	48,4
			B	65	63	63	62	65	5	63,6
	150	2	A	45	48	47	50	51	5	48,2
			B	65	62	63	66	64	5	64
		4	A	50	48	49	51	47	5	49
			B	65	62	67	67	64	5	65
		6	A	51	49	50	50	50	5	50
			B	68	69	63	65	67	5	66,4

After single and dual component varnish applications of chestnut wood; lowest hardness values were seen in non-heat-treated single component specimens, while highest hardness values were seen in dual component varnished specimens waited for 6 hours in 150 C° according to heat treatment temperature and time conditions. As a result of comparing hardness values of non-heat-treated specimens subjected to single component varnish application and heat-treated specimens, it was observed that heat-treated specimens have higher hardness values compared with specimens varnished as non-heat-treated. As a result of comparing dual component varnished non-heat-treated specimens and heat-treated specimens, it was seen that hardness values of heat-treated specimens have higher than specimens varnished without heat-treatment.

3.2. The results of varnishes' surface sticking resistance

Obtained varnishes' surface sticking resistance values belong to scotch pine wood were given in Table 5.

Table 5. Varnishes' surface sticking resistance values belong to scotch pine wood

Surface sticking resistance (MPa)											
Wood type	Temperature (°C) (°C)	Time (hour)	Varnish type	Values					n	Average
SCOTCH PINE	Non-treatment	–	A	3,82	3,56	3,63	3,37	3,43	5	3,56
			B	4,14	3,94	4,14	3,75	3,82	5	3,95
	100	2	A	3,82	3,69	3,56	3,63	3,75	5	3,69
			B	4,33	4,33	4,39	4,14	4,20	5	4,27
		4	A	3,63	3,63	3,56	3,69	3,69	5	3,64
			B	4,33	4,26	4,20	4,07	4,14	5	4,20
		6	A	3,63	3,56	3,56	3,69	3,43	5	3,57
			B	4,07	4,07	4,33	4,14	4,01	5	4,12
	125	2	A	3,43	3,37	3,56	3,63	3,56	5	3,51
			B	4,20	4,14	4,01	3,88	4,01	5	4,04
		4	A	3,37	3,43	3,56	3,43	3,37	5	3,43
			B	3,94	4,07	3,82	3,94	4,01	5	3,95
		6	A	3,50	3,31	3,50	3,37	3,31	5	3,39
			B	3,75	4,01	3,82	3,88	4,01	5	3,89
	150	2	A	3,56	3,37	3,43	3,31	3,31	5	3,39
			B	3,94	3,82	3,75	4,01	3,94	5	3,89
		4	A	3,43	3,31	3,24	3,18	3,43	5	3,31
			B	3,69	3,82	3,88	3,75	3,94	5	3,81
		6	A	3,05	3,18	3,31	3,24	3,12	5	3,18
			B	3,82	3,69	3,75	3,63	3,88	5	3,75

After single and dual component varnish applications of scotch pine wood; lowest adhesive resistance was seen in specimens performed single component varnish application and waited for 6 hours in 150 C°, while highest adhesive resistance was seen in specimens performed dual component varnish application and waited for 2 hours in 100 C° according to heat treatment temperature and time conditions. As a result of comparing adhesive resistance values of non-heat-treated specimens subjected to single component varnish application and heat-treated specimens, specimens waited for 2, 4, 6 hours in 100 C° have higher adhesive resistance than specimens varnished as without heat treatment, and it was seen that adhesive resistance values decreased in other heat treatment temperatures and times. As a result of comparing dual component varnished non-heat-treated specimens and heat-treated specimens, specimens waited for 2, 4, 6 hours in 100 C° and waited for 2 hours in 125 C° have higher adhesive resistance, and it was observed that adhesive resistance values decreased in other heat treatment temperatures and times.

Obtained varnishes' surface sticking resistance values belong to beech wood were given in Table 6.

Table 6. Varnishes' surface sticking resistance values belong to beech wood

Surface sticking resistance (MPa)										
Wood type	Temperature (°C)	Time (hour)	Varnish type	Values					n	Average
BEECH WOOD	Non-treatment	–	A	5,28	4,96	5,35	5,09	5,09	5	5,14
			B	5,73	5,54	5,60	5,79	5,54	5	5,64
	100	2	A	5,47	5,41	5,28	5,41	5,54	5	5,42
			B	5,86	5,73	5,47	5,60	5,47	5	5,62
		4	A	5,47	5,41	5,35	5,35	5,28	5	5,37
			B	5,60	5,41	5,66	5,54	5,41	5	5,52
		6	A	5,35	5,28	5,35	5,28	5,15	5	5,28
			B	5,35	5,47	5,54	5,41	5,35	5	5,42
	125	2	A	5,15	5,09	5,28	5,28	5,03	5	5,16
			B	5,35	5,41	5,35	5,54	5,47	5	5,42
		4	A	5,22	5,03	5,03	4,96	5,28	5	5,10
			B	5,35	5,28	5,47	5,15	5,22	5	5,29
		6	A	4,96	4,96	4,84	5,09	5,03	5	4,97
			B	5,28	5,15	5,28	5,09	5,28	5	5,21
	150	2	A	4,90	4,96	5,09	4,96	5,03	5	4,98
			B	5,09	5,28	5,15	5,35	5,28	5	5,23
		4	A	4,84	4,77	4,96	4,84	4,96	5	4,87
			B	5,22	5,15	5,03	5,09	4,96	5	5,09
		6	A	4,77	4,96	4,84	4,84	4,71	5	4,82
			B	5,03	4,96	5,09	5,03	4,96	5	5,01

After single and dual component varnish applications of beech wood; lowest adhesive resistance was seen in specimens performed single component varnish application and waited for 6 hours in 150 C°, while highest adhesive resistance was seen in specimens performed dual component varnish application and waited for 2 hours in 100 C° according to heat treatment temperature and time conditions. As a result of comparing adhesive resistance values of non-heat-treated specimens subjected to single component varnish application and heat-treated specimens, specimens waited for 2, 4, 6 hours in 100 C° and waited for 2 hours in 125 C° have higher adhesive resistance compared to specimens varnished as without heat treatment. As a result of comparing dual component varnished non-heat-treated specimens and heat-treated specimens, specimens waited for 2, 4, 6 hours in 100 C° and waited for 2 hours in 125 C° have higher adhesive resistance, and it was observed that adhesive resistance values decreased in other heat treatment temperatures and times.

Obtained varnishes' surface sticking resistance values belong to chestnut wood were given in Table 7.

Table 7. Varnishes' surface sticking resistance values belong to chestnut wood

Surface sticking resistance (MPa)											
Wood type	Temperature (°C) (°C)	Time (hour)	Varnish type	Values					n	Average
CHESNUT	Non-treatment	–	A	3,88	3,69	3,82	3,88	3,94	5	3,84
			B	4,14	4,20	4,45	4,33	4,39	5	4,30
	100	2	A	4,07	4,14	4,07	4,01	4,14	5	4,08
			B	4,65	4,65	4,52	4,58	4,71	5	4,62
		4	A	4,14	4,07	4,01	3,82	3,88	5	3,98
			B	4,65	4,58	4,52	4,33	4,45	5	4,50
		6	A	3,82	3,82	3,94	3,88	3,88	5	3,86
			B	4,52	4,33	4,26	4,33	4,39	5	4,36
	125	2	A	3,82	3,82	3,88	3,94	3,75	5	3,84
			B	4,52	4,52	4,26	4,20	4,33	5	4,36
		4	A	3,69	3,82	3,82	3,75	3,69	5	3,75
			B	4,39	4,45	4,26	4,14	4,20	5	4,28
		6	A	3,69	3,75	3,82	3,63	3,63	5	3,70
			B	4,33	4,26	4,07	4,07	3,94	5	4,13
	150	2	A	3,69	3,63	3,69	3,75	3,69	5	3,69
			B	4,20	4,07	4,26	4,14	4,07	5	4,14
		4	A	3,63	3,56	3,69	3,43	3,63	5	3,58
			B	4,14	4,01	3,94	4,07	3,94	5	4,02
		6	A	3,24	3,69	3,31	3,63	3,37	5	3,44
			B	4,07	3,94	3,94	4,01	3,88	5	3,96

After single and dual component varnish applications of chestnut wood; lowest adhesive resistance was seen in specimens performed single component varnish application and waited for 6 hours in 150 C°, while highest adhesive resistance was seen in specimens performed dual component varnish application and waited for 2 hours in 100 C° according to heat treatment temperature and time conditions. As a result of comparing adhesive resistance values of non-heat-treated specimens subjected to single component varnish application and heat-treated specimens, specimens waited for 2, 4, 6 hours in 100 C° have higher adhesive resistance than specimens varnished as without heat treatment, and it was seen that adhesive resistance values decreased in other heat treatment temperatures and times. As a result of comparing dual component varnished non-heat-treated specimens and heat-treated specimens, specimens waited for 2, 4, 6 hours in 100 C° and waited for 2 hours in 125 C° have higher adhesive resistance, and it was observed that adhesive resistance values decreased in other heat treatment temperatures and times.

3.3. Brightness Measurements

Obtained brightness measurement values belong to scotch pine wood were given in Table 8.

Table 8. Brightness measurement values belong to scotch pine wood

Brightness measurement values (60°)										
Wood type	Temperature (°C)	Time (hour)	Varnish type	Values					n	Average
SCOTCH PINE	Non-treatment	–	A	69,8	68,7	67,7	65,4	70,8	5	68,48
			B	74,8	74,9	74,5	74,2	74,3	5	74,54
	100	2	A	68,6	69,7	70,1	71,3	68,4	5	69,62
			B	76,4	75,8	76,8	77,3	76,9	5	76,64
		4	A	68,3	69,7	65,9	68,3	69,1	5	68,26
			B	76,4	75,3	76,3	75,1	75,9	5	75,8
		6	A	68,4	65,9	68,7	68,5	67,2	5	67,74
			B	73,8	74,6	73,9	75,2	76,2	5	74,74
	125	2	A	68,5	67,2	68,5	65,4	68,6	5	67,64
			B	74,6	75,3	73,4	75,3	73,6	5	74,74
		4	A	68,5	64,2	68,1	65,5	66,2	5	66,5
			B	73,8	75,1	73,5	74,3	72,9	5	73,92
		6	A	66,4	67,7	67,1	65,2	64,3	5	66,14
			B	73,4	72,1	73,	71,2	70,9	5	72,18
	150	2	A	66,4	65,2	67,1	67,2	66,3	5	66,44
			B	73,1	73,1	74,3	72,9	73,4	5	73,36
		4	A	65,7	68,1	63,4	64,8	65,8	5	65,56
			B	70,6	72,2	69,8	71,3	73,2	5	71,42
		6	A	64,5	61,8	66,3	65,2	65,8	5	64,72
			B	71,3	67,9	72,6	71,5	70,6	5	70,78

After single and dual component varnish applications of scotch pine wood; lowest brightness values were seen in pieces performed single component varnish application and waited for 6 hours in 150 C°, while highest brightness values were seen in specimens performed dual component varnish application and waited for 2 hours in 100 C°. As a result of comparing brightness values of non-heat-treated specimens subjected to single component varnish application and heat-treated specimens, brightness values of specimens waited for 2 hours in 100 C° have higher than specimens varnished as without heat treatment, and it was seen that brightness values decreased in other heat treatment temperatures and times. As a result of comparing dual component varnished non-heat-treated specimens and heat-treated specimens, specimens waited for 2, 4, 6 hours in 100 C° have higher brightness values, and it was observed that brightness values decreased in other heat treatment temperatures and times.

Obtained brightness measurement values belong to beech wood were given in Table 9.

Table 9. Brightness measurement values belong to beech wood

Brightness measurement values (60°)										
Wood type	Temperature (°C)	Time (hour)	Varnish type	Values					n	Average
BEECH WOOD	Non-treatment	–	A	68,3	66,4	68,1	64,9	66,4	5	66,82
			B	74,8	73,9	75,5	74,4	74,1	5	74,54
	100	2	A	67,9	66,4	67,2	68,1	65,5	5	67,02
			B	75,9	75,6	76,1	76,3	77,1	5	76,2
		4	A	68,2	63,8	66,1	63,7	63,5	5	65,06
			B	77,6	76,5	75,5	75,2	74,6	5	75,88
		6	A	63,5	68,2	64,8	63,5	63,2	5	64,64
			B	75,2	75,6	76,1	73,4	73,8	5	74,82
	125	2	A	63,4	66,2	65,2	64,8	63,3	5	64,58
			B	75,3	73,4	72,2	74,3	75,6	5	74,16
		4	A	65,2	65,4	63,9	64,5	61,3	5	64,06
			B	75,5	71,3	70,6	71,2	73,1	5	72,34
		6	A	63,2	60,8	61,8	62,4	61,1	5	61,86
			B	71,9	70,6	71,2	70,6	68,9	5	70,64
	150	2	A	62,4	62,8	59,1	59,7	63,8	5	61,56
			B	71,5	70,7	69,1	70,5	71,5	5	70,66
		4	A	61,6	61,8	60,7	59,9	59,2	5	60,64
			B	71,3	68,3	69,8	69,1	67,3	5	69,16
		6	A	59,7	61,2	62,8	58,3	58,4	5	60,08
			B	70,4	67,8	68,8	65,9	67,8	5	68,14

After single and dual component varnish applications of beech wood; lowest brightness values were seen in pieces performed single component varnish application and waited for 6 hours in 100 C°, while highest brightness values were seen in specimens performed dual component varnish application and waited for 2 hours in 100 C°. As a result of comparing brightness values of non-heat-treated specimens subjected to single component varnish application and heat-treated specimens, brightness values of specimens waited for 2 hours in 100 C° have higher than specimens varnished as without heat treatment, and it was seen that brightness values decreased in other heat treatment temperatures and times. As a result of comparing dual component varnished non-heat-treated specimens and heat-treated specimens, specimens waited for 2, 4, 6 hours in 100 C° have higher brightness values, and it was observed that brightness values decreased in other heat treatment temperatures and times.

Obtained brightness measurement values belong to chestnut wood were given in Table 10.

Table 10. Brightness measurement values belong to chestnut wood

Brightness measurement values (60°)										
Wood type	Temperature (°C)	Time (hour)	Varnish type	Values					n	Average
CHESNUT	Non-treatment	–	A	64,4	63,3	63,6	64,3	63,9	5	63,9
			B	73,4	73,1	72,3	72,3	72,5	5	72,72
	100	2	A	65,2	64,5	62,1	66,1	64,3	5	64,44
			B	72,6	75,3	74,3	75,1	74,2	5	74,3
		4	A	68,3	64,2	63,5	64,2	63,1	5	64,66
			B	73,2	72,6	71,8	74,3	72,2	5	72,82
		6	A	63,5	65,3	64,8	61,2	63,5	5	63,66
			B	73,5	74,	71,5	70,6	71,3	5	72,24
	125	2	A	65,2	64,3	63,8	62,5	62,8	5	63,72
			B	71,3	72,6	68,9	70,6	72,2	5	71,12
		4	A	65,3	62,4	60,4	61,3	61,1	5	62,1
			B	73,2	68,7	69,5	68,9	70,5	5	70,16
		6	A	61,3	59,9	63,2	58,7	58,9	5	60,4
			B	68,3	70,8	69,7	71,2	70,1	5	70,02
	150	2	A	60,5	61,3	61,2	61,2	60,2	5	60,88
			B	70,8	69,8	70,5	68,8	71,6	5	70,3
		4	A	59,4	60,8	61,3	58,6	60,5	5	60,12
			B	70,4	68,9	68,8	68,9	69,4	5	69,28
		6	A	57,9	57,7	58,4	58,2	58,1	5	58,06
			B	68,5	67,3	67,3	68,7	68,2	5	68

After single and dual component varnish applications of chestnut wood; lowest brightness values were seen in pieces performed single component varnish application and waited for 6 hours in 150 C°, while highest brightness values were seen in specimens performed dual component varnish application and waited for 2 hours in 100 C°. As a result of comparing brightness values of non-heat-treated specimens subjected to single component varnish application and heat-treated specimens, brightness values of specimens waited for 2 and 4 hours in 100 C° have higher than specimens varnished as without heat treatment, and it was seen that brightness values decreased in other heat treatment temperatures and times. As a result of comparing dual component varnished non-heat-treated specimens and heat-treated specimens, specimens waited for 2 and 4 hours in 100 C° have higher brightness values, and it was observed that brightness values decreased in other heat treatment temperatures and times.

4. Discussion and Conclusions

Hardness resistance values; increase heat treatment temperature degree and time in all tree species caused an increase of hardness values in single component and dual component varnish type.

Varnishes' surface sticking resistance values; while it was seen improvements in Varnishes' surface sticking resistance in all tree species specimens subjected to heat treatment in 100 C° for 2, 4, and 6 hours in all tree species, it was seen negativities in adhesive resistances in specimens waited 2, 4, and 6 hours in 125 C° and 150 C°.

Brightness values; it was seen negativities in brightness values in specimens waited 4, and 6 hours in 100 C° , and waited 2, 4, and 6 hours in 125 C° and 150 C°, while it was seen improvements in brightness values in all tree species specimens subjected to heat treatment in 100 C° for 2 hours in all tree species.

References

[1]Sanıvar, N.,Woodworking Surface Finishing, National Education Printing House, İstanbul 2001.

[2] Kantay R.; Kartal N; Heat process practices and properties of heat treated wooden material. Wooden Magazine, 33:36-42 (2007).

[3] Thermoodwood Handbook 2003. Finnish Thermowood Association, Helsinki , Finland .

[4] Budakçı, M., "The eefects of layer thickness in varnish to brillance, hardness and resistance of stick, Master thesis, *Gazi University, Graduate School of Natural and Applied Sciences,* Ankara,(1997).

[5] Highley, T.L., Kıcle, T.K., Phytopsthology (Blanchette, R.A., et al.,), (1990).

[6] Atar, M., "Effects on the surface treatment of Color-opening chemical substances in wooden material, Ph. D. Thesis, *Gazi University, Graduate School of Natural and Applied Sciences,* Ankara,15-17 (1999).

[7] Sogutlu, C, "The using of some native wood species in kundekari construction. Ph. D. Thesis, *Gazi University, Graduate School of Natural and Applied Sciences,* 101-102 (1504) (2004), Ankara.

[8] Ozalp, M. (2008) The investigation of borax pentahydrate influences with double components in varnish applications of wood materials'', Wood Res.,53(4): 121-128.

[9] Ozalp, M., Korkut, S. (2011) The research of borax pentahydrate effects with water-based double components in varnish applications of wooden materials'', Wood Res., 56(1), : 105-114.

[10] ASTM D 358 ''Standard Specification for Wood to Be Used as Panels in Weathering Tests of Coatings'' *American Society for Testing and Materials,* 5-9 (1998).

[11] ASTM D-4541., "Standard Test Method for Pull-Off Strength of Coatings Using Portable Adhesion Testers", *American Society for Testing and Materials,* 12-15 (1995).

[12] TS EN 24624., "Paints and varnishes - Pulling Test", Ankara, (1996)

[13] ANS/IS01522., "Paints and Varnishes-Pendulum Damping Test Approved as an American National Standard by ASTM International", (1998).

[14] TS 4318 EN ISO 2813, Paint and varnishes- nonmetallic paint films determining the brillance in 20°, 60° and 85°, *TSE,* Ankara, (2002).

International Conference on Science and Technology

ICONST 2018

5-9 September 2018 Prizren - KOSOVO

Optical Pickups for String Musical Instruments

Ibrahim Atakan KUBILAY[1]*

Abstract In this paper, the optical pickup transducers for musical instruments are examined. The concept of using optical pickups for musical instruments is a new and open research area with many challenges and opportunities. The background on optical pickups, their introduction to musical instrument design, their advantages and disadvantages compared to the commonly used magnetic pickups are presented, along with basic concepts and technical details. A brief historical background on electric guitars is given, along with the development of the new optical pickup, followed by a study of the physical instrument setup and the necessary processing steps involved. Finally the opportunities and challenges facing this new technology are discussed, and possible roads for further research explored.

Keywords: optical pickup; string musical instrument; line camera; audio processing; image processing

Introduction Optical pickup is a new and exciting technology that allows string motion detection in stringed electric musical instruments. It has many advantages over the magnetic pickups, but it also has some drawbacks associated with being a relatively young and emerging technology. This technology is based on a very simple concept and developed over time by various entrepreneurs, engineers and researchers. This paper aims to give a brief introduction to this new technology, and discuss some of the trade-offs, challenges and issues concerning this new subject.

In this study the term optical pickup is used in a very broad sense, including setups that use only one photo-sensitive element like a photo-transistor, photo-diode or photo-resistor, and more advanced setups that use image-sensors such as line-cameras and possibly even conventional 2D image sensors. Optical guitar is used as a general term simply referring to a guitar that uses any optical pickup.

This paper is organized as follows; the fundamental concepts behind optical pickup technology and its historical background are presented in Introduction, the physical setup of an optical pickup is discussed in Material and Methods as well as the processing of the acquired image and its conversion into sound, the challenges and opportunities of optical pickups are presented in Results, and finally future work necessary for the optical pickup to be a commercially viable product is detailed in Conclusion.

The magnetic pickups are briefly discussed below only to allow the reader the ability to realize how the optical pickups differ from magnetic pickups. After this short introduction the optical pickups are discussed.
The relevant chapter in the book The Science of String Instruments [1] gives a good overview of the development of the electric guitar. Early acoustic recordings relied on mechanical devices that cut grooves on cylinders and discs. When recording an orchestra, the louder wind and bass instruments obstructed and masked the weaker string instruments, making them almost inaudible. Therefore there were various attempts at obtaining a louder string sound. These attempts included the use of steel-cored strings and attachments of horns and resonators to the string instruments [1].

[1]Dokuz Eylul University, Faculty of Engineering, 35160, Izmir, TURKEY
*Corresponding author: atakan@cs.deu.edu.tr

Early attempts at what we would today call electric guitars started in early 1920s. In early 1930s George Beauchamp invented a compact magnetic pickup that directly sensed vibrations of metallic strings and was granted several patents on this technology [2]. He also successfully commercialized and sold this new technology starting from 1932, and by 1936 was manufacturing all kinds of electric string musical instruments. Les Paul, himself a famous guitar performer, introduced the solid body concept, which discarded the sound cavity and used a slim, solid body, allowing more energy to be conserved for the strings, because the strings no longer transferred most of their energy to the sound hole which was rendered unnecessary by the magnetic pickup. Leo Fender also contributed to the magnetic pickup based electric guitar we know today, launching the guitar model known by his name [3].

The magnetic pickup, also called the inductive electro-magnetic pickup uses a magnet wrapped inside a coil to convert the change in the magnetic field caused the vibration of a metallic string into a varying voltage signal. This voltage variation depends on the amplitude and velocity of string vibration. In this setting the poles of a magnet are connected by invisible field lines. When a metallic string moves perpendicular to these lines, a corresponding voltage will appear on the coil surrounding the magnet as dictated by Faraday's Law. Note that the motion of the string parallel to the field lines will not be adequately detected. The voltage generated will increase proportionally with increasing number of coil turns, again in accordance with Faraday's Law. Typical pickups may have more than 6000 turns of wire in a coil. A thin wire is preferred to increase the number of turns without increasing size. Most electric guitars use six cylindrical magnets, one for each string, even though some guitars feature more magnets. In Stratocaster type guitars there are three sets of magnets for using different locations along the string for a different tonal quality. These magnet sets are attached to the guitar by screws, allowing adjustment of the distance between the string and the magnet, again allowing more control over tonal quality [1]. Moreover, many guitars allow the mixing of outputs from any of these pickups selected by the user, resulting in a vertical or horizontal shift in the resonant peak of the output, giving the user more freedom in choosing the desired effect [4].

The disadvantages of the magnetic pickup are as follows:

1. It should be apparent from the discussion above that magnetic pickups can't work with any string material other than metal.

2. The pickup position causes some standing wave harmonics to be lost, as they may have nodes near the pickup position[4]. This problem is not specific to magnetic pickups, however optical pickups with their reduced cost and size may be placed at more positions on the guitar, partially alleviating this problem.

3. Magnetic pickups, like optical pickups, have a non-linear response to string motion, usually modelled by a simple or generalized Hammerstein Model where an S-shaped curve relating string displacement and voltage produced at the output of the pickup may be constructed [5].

4. They can't adequately detect string motion parallel to the magnetic field lines of the pickup magnets. Actual string motion is rarely restricted to a single plane of oscillation and the oscillation moves from one plane to another over time. The finite element simulation published in [4] shows a magnetic flux change of about 4 μT for the vertical string motion while only 0.7 μT for the horizontal string motion.

5. The coil of wire around the magnets act as an antenna, responding to electro-magnetic noise in the environment. The most common source of such noise is the wall outlet hums at 60Hz (in the US, 50Hz in Europe) [6]. Humbucker type magnetic pickups partially solve this problem by using two sets of magnets with one coil wrapped in a different direction than the other, making the noise cancel out at the cost of using double number of magnets, and a tone difference resulting from the fact that the magnets are now a small distance away from each other relative to the string, producing a different tone color [6].

6. The pickup output is not uniform across all frequencies, it peaks at a resonant frequency determined by the inductive and capacitive characteristics of the pickup, or more specifically the thickness of wire used, the number of turns and even the insulation material [4].

7. Magnetic pickups are not only sensitive at a single point, but over a small strip of the string, and this causes a low-pass filter effect [4]. The optical pickup also has a strip of a view, but this strip is much narrower than in the case of a magnetic pickup.

8. Magnetic pickups are heavy and it's difficult to place them on the soundboard, this additional weight reduces the amplitude of string motion, as well as changing the tone of the sound [6].

Piezo pickups are mostly used for fitting existing stringed musical instruments which have an acoustical cavity and convert them easily into electric instruments. They are much less common than magnetic pickups, so are not discussed in this study.

Even though the optical pickups go as far back as 1970s, the number of academic papers about them is not large due to the fact that businesses which manufactured such pickups were more interested in taking commercial patents than publishing academic papers, so it's from these patents that the early history of optical pickups may be traced.

The year 1973 is when optical pickups were formally born. Dennis A. Ferber's patent application for an optical pickup transducer was accepted [7], and Ronald R. Hoag was granted his patent in Canada[8]. Hoag's design appeared in many publications, including August 1977 issue of Musician's Guide. Hoag would go on to produce the K-max optical guitars based on his patent. The basic idea suggested both patents is very similar, and will be discussed in more detail in Material and Methods. Both were designed with an eye to convert existing acoustical guitars into optical guitars, so their designs were not aimed at an optical guitar built from the ground up. In fact, both magnetic and optical guitars may be constructed with a solid body, allowing savings in materials, cost and weight. These first patents both used a single photo-sensitive element to detect the motion of each string. The setups were also quite big, and they both needed an enclosed box to block ambient light interfering with the photo-sensitive element. This box also prevented performers from using their fingers on the strings near the pickup location.

Similar patents proposing improvements over optical pickups were granted in late 1980s [9][10]. In 1991, Timothy J. Barnard introduced the important idea of using two photo-sensitive elements and two light sources to capture string motion in both vertical and horizontal polarizations [11]. Even though the string motion is mostly taken as the vertical motion, it also oscillates horizontally, and some energy goes back and forth between these two transverse polarizations after string excitation. By using two photo-sensitive elements, Barnard was able to get two signals from the same string, one for each transverse polarization.

In 1993, Bradley W. Curtis, Bruce L. Kennedy and Christopher R. Willcox were granted the patent [12] which later became the basis for the Lightwave Systems optical guitars. It consisted of three walls enclosing the string with two photo-sensitive elements and a single light source. Lightwave Systems would use infrared source-detector pairs in its commercial products, alleviating the noise problem from ambient light that would have arisen if a simpler, visible-light-sensitive pickup element were used.

Material and Methods:

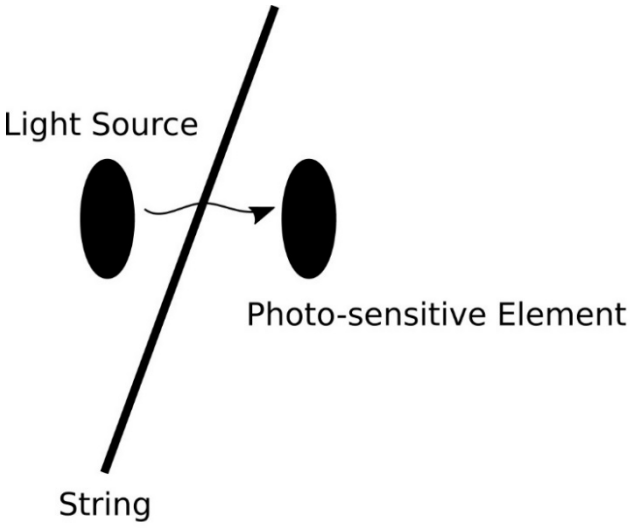

Figure 1. The basic concept of an optical pickup. The photo-sensitive element may be realized by a variety of electronic components ranging from photo-resistors to 2D imaging sensors.

All optical pickups are made up of at least one light source and one photo-sensitive element. The string is between these two components so as to obstruct the path of the light source to the photo-sensitive element. As the string vibrates, it cuts the light coming in from the light source in various ways, this change in light intensity is captured by the photo-sensitive element and converted to a varying voltage signal, which represents a modulated version of the original string oscillation.

The resulting signal is much weaker than the case of the magnetic pickup so an internal pre-amp circuit is necessary before hooking the optical guitar up to the external guitar amp. This is setup can be easily built and experimented with, even using a simple photo-resistor as the light-sensitive element and a preferably brighter than normal LED as the light source. By now, it must be clear that optical pickups are active pickups, they need both a constant light source, and a voltage supply that would be modulated by the string motion. This implies that there must be a battery or DC adapter socket in the optical guitar.

The photo-sensitive element in an optical guitar can take on a variety of different forms, from primitive photo-resistors to conventional 2D image sensor chips. Using simple sensors allows the use of simpler circuits, simplifies instrument body design and causes less power consumption, and reduces cost. However the information about the actual string motion is largely lost in such setups due to the fact that we are using only one light-sensitive element. There are improvements proposed as discussed in the Introduction, such as using multiple sensors for measuring both horizontal and vertical string oscillation. Using more advanced image sensors such as line cameras result in much more accurate representations of string motion, at the cost of increased size, power consumption, heat generation and expense.

Photo-resistor is the most primitive light-sensitive element that can be used in an optical-pickup setup. It has the property of offering a varying resistance depending on the light impinging upon it. It may be used in a voltage divider setup to yield a time-varying voltage modulated by the motion of the string blocking light from a light source such as a bright LED. The result is an analog signal modulated directly by the motion of the string. It's quite easy to design an optical pickup using a photo-resistor. They are also quite cheap. However, photo-resistors are sensitive to a large spectrum of wavelengths, so ambient light can easily interfere with their operation. Photo-resistors are also sensitive to heat fluctuations. An example of an optical pickup circuit that uses a photo-resistor is given in Figure 2.

Photo-diodes and photo-transistors operate more like switches turning on and off as it becomes light and dark.

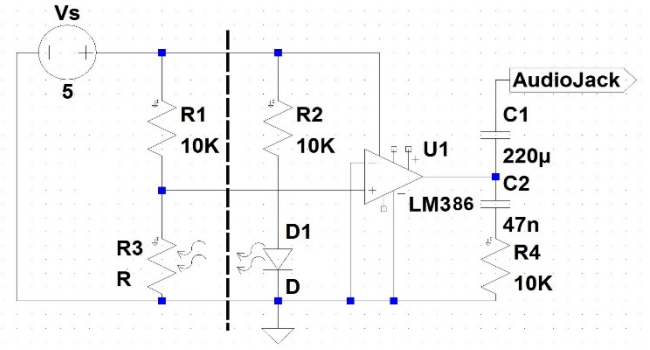

Figure 2. A very simple optical pickup circuit diagram using an off-the-shelf photo-resistor as the light-sensitive element. It was used in a simple voltage-divider configuration, and much of the other components to the right of the circuit are used to operate the amplifier as advised in its data sheet. The physical guitar string, represented by a dashed line, is placed between the LED and the photo-resistor. Diagram created using LTSpice.

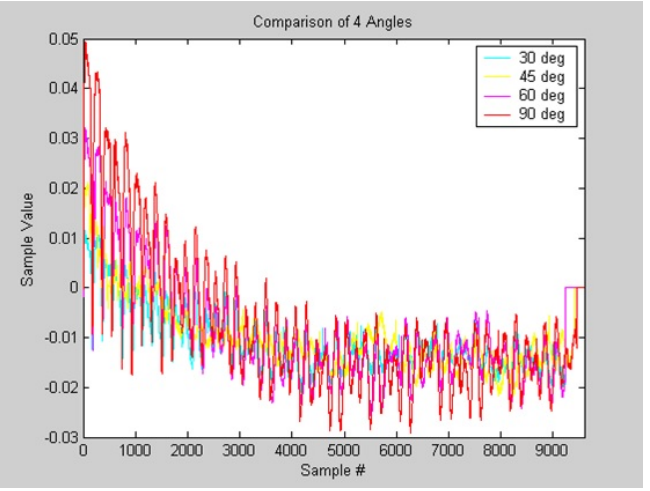

F**igure 3.** The digital signal created by a vibrating guitar string obstructing the light of a photo-resistor at different angles to the string. The voltage from the photo-resistor was amplified using an LM-386 chip, using a circuit layout similar to the one given in Fig. 3. Image adapted from [13].

The requirements for the light source are as follows; It must be small enough so it may be placed close to the string without touching other strings and use the small space available on the bridge of the guitar, it must be brighter than the ambient light, it must not excessively flicker as that would interfere with string motion detection, and it must not consume excessive power so it may be fed by a portable battery for a reasonable amount of time. Unfortunately, most light sources don't have a constant brightness output. This variation of brightness output in a light source is called flicker. There are many causes of flicker in light sources, those directly fed from a wall outlet are especially prone to this problem. Flicker is also problematic for room and vehicle lighting [14], so it was extensively studied [15] [16], with proposals on its reduction[17]. Without dwelling any further on this subject, we must mention that the optical pickup must either use dedicated circuitry connected to the light source to reduce flicker, or obtain a test case of pure flicker for the light source so it may be corrected with digital signal processing techniques.

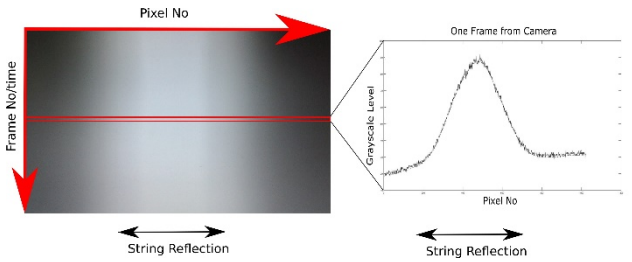

Figure 4. The line-camera view of a string. In this case the light source is placed above the line-camera so that light reflected from the string reaches the imaging sensor. The lightest pixels (the peak in the graph to the right) correspond to the string. As the string moves up and down, the peak's location moves to left and right, informing us about the location of the string at minute intervals in time. Time scale in seconds may be directly calculated by simply dividing the frame number by number of frames captured per second (fps).

We can't use the output of the light-sensitive element directly. Even in the case of the simple photo-resistor, the modulated signal must be pre-amplified before it can be sent to the external guitar amp. Moreover, the response of the photo-sensitive element itself to luminance may not be linear. We may have to compensate for this non-linearity using hardwired circuits or by programming an on-board DSP chip. We definitely need to calibrate string motion with respect to the actual voltage change produced at the output. For these simple photo-sensitive elements, the output is still analog.

When we progress into line and 2D imaging sensors, there are different requirements. The output of these elements are now a vector for the line-camera , and a matrix for the conventional 2D imaging sensor which contains digital data representing the light intensity falling on the pixel elements. Of course, the pixels where the light source is obstructed by the string will have values corresponding to less light intensity, however there are cases when the string is so thick (like a piano string) that light source is reflected off the string and into the image sensor, in which case the string position will correspond to lighter areas and the background to darker areas, like the case in Figure 3. Please see [18] for a more detailed explanation of the subject.

By early 2018, most advanced consumer grade video applications use 60 fps (frames per second) capture rates. High frequency strings such as those used in the violin can vibrate with a frequency in excess of 3.5 KHz. Therefore, the Nyquist Sampling Frequency must be at least 7 KHz, and often a higher sampling rate is desirable. Therefore it may be recommended that at a sampling rate of at least 10 KHz for capturing string motion in such instruments. In applications that require high frame rates, such as those needed to capture string motion, heat generated by the camera becomes a major problem. Heat sinks must be added to cool the camera, but this conflicts with the tight space constraints on the musical instrument for positioning the camera. Therefore, there must be a compromise between using a high enough frame rate to capture string motion, and keep it low enough so as not to produce excessive heat and require large heat sinks. Liquid cooling may be mulled as a potential solution.

Line Cameras have the advantage of faster fps rates due to the presence of less pixels and produce relatively less heat than their 2D counterparts. They also usually use only grayscale values to allow for the required high frame rates. The resolution of the line camera determines how accurately the string shadow cast on the imaging sensor array represents the actual string motion. It's desirable that the entire span of string motion be represented by the entirety of the imaging sensor array without clipping. The custom design of optical lens elements to focus string motion onto the imaging sensor array can help effective utilization of the entire sensor length.

Results

The optical detection of string motion has many challenges and opportunities. Like all new technologies, it is expensive, bulky and cumbersome at the beginning. This new technology is like the first large and expensive digital cameras that used floppy disks to store their low-resolution images. Optical pickup technology is at a

similar point in its history. There is a lot of research and work ahead to make it a commercially viable product, but there is little doubt that it's the future of electrical string musical instruments.

The field of musical instrument design is a notoriously conservative one. The magnetic pickup itself only goes as far back as 1937[2], and before that the guitar took centuries to evolve. Therefore it's not easy to convince many musicians who still believe there is no place for optical pick-ups in the music industry, just as there were those who thought digital cameras would never be used for serious photographic work. There are many guitar performers who like the magnetic feel of the sound.

Single-element optical pick-ups can be manufactured in very small sizes that easily fit into the tight space around the string, but for more advanced high-fps line and 2D cameras, size is still a limiting factor. Even when all the electronic chips are moved inside the guitar body, the line image sensor takes up considerable space. Moreover, as discussed in Materials and Methods, line cameras used in high-fps applications generate considerable heat, which makes it necessary to use large heat sinks around the camera body. This is yet another factor that adds to the size of the imaging unit.

High-speed cameras with a capture rate of more than 1000fps are quite expensive, often costing thousands of US Dollars. This means that optical pickup technology using high-speed sensor micro-cameras would cost at least as much, if not more. Therefore, at present cost remains a major obstacle against the affordability and thus commercial success of the optical pickup. However, as the technology progresses and more research is made by scientists and engineers, cost will come down, as has been the case with all emerging technologies. Especially materials science and nano-technology may enable the shrinking of the imaging unit as well as the heat sink components, allowing them to be easily placed on the guitar.

The new pioneering technology of the optical pickup promises many new opportunities and advantages for the music industry. Musicians are artists, and they like new technologies like other consumers. The optical pickup is an interesting new technology which will certainly appeal to those always seeking the cutting edge technology. The optical pickup which employs a dedicated imaging sensor will provide direct digital output which may be manipulated at will by DSP microchips directly installed on the guitar. The result will be a fully computerized guitar which the performer can hook up to his/her notebook computer with a USB cable. The inputs from all strings, and even from different polarizations of the same string may be mixed at will for the output, or even transmitted as separate channels. Gibson Guitar Company already started selling guitars with automatic tuning and other electronic tools [1]. Such guitars can make good use of the digital output provided by the optical pickup.

Discussion

The subject of the optical pickup constitutes a new, exciting research subject with many opportunities for development. The main problems were outlined in Results. In this Section, we will examine development areas and possible future work for interested researchers.

The physical setup of the optical pickup offers great room for improvement. The photo sensing element, its corresponding detector and the heatsink required to cool the setup, as well as a power supply limit the compactness of an optical guitar system. Use of less space-consuming cooling methods such as liquid cooling may be employed.

As discussed in Material and Methods, it's desirable to project the entire oscillation of the string onto the length of the imaging sensor with narrow margins. This can be achieved by using micro-lenses that can also be used to accurately focus the string shadow for the sensor. This focusing process provides better background and string distinction for the sensor. In small distances, focus can be disturbed by even the slightest movement of the light source or the imaging sensor, so incorporation of auto-focus technology may be required. These lenses may be also coated for filtering of ambient light coming from directions other than the light-source, much like a polarized filter commonly used in photography. There must be a compromise between the complexity of the light sensing element and the resolution required to accurately distinguish motion of the string.

Optical pickups require power in order to:

- Provide source voltage for the pickup circuitry
- The light source
- On-board DSP chip
- Operating and cooling the imaging sensor/camera

Therefore it's imperative to use power-efficient strategies to conserve the very precious source of power. Battery usage is a must for stand-alone performance. One way to replenish the battery could be using a system converting mechanical energy created by the performer playing the strings into electricity.
Shrinking in size and price of the imaging element is necessary if the optical guitar is to be realized as a commercially feasible musical instrument. And when it does, it will create a revolution in music industry, much like the electric guitar did about 80 years ago.

References

[1] C. Gough, "Electric Guitar and Violin," in *The Science of String Instruments*. New York, NY, USA:Springer, 2010, ch. 22, pp.393-399.

[2] G. D. Beauchamp, "Electrical stringed musical instrument," U.S. Patent: 2 089 171, Aug. 10, 1937.

[3] C. L. Fender, "Electromagnetic pickup for lute-type musical instrument," U.S. Patent: 2 968 204, Jan. 17, 1961.

[4] Paiva, R.C.D., Pakarinen, J., Välimäki, V., "Acoustics and modeling of pickups," *J. Audio Eng. Soc.*, vol. 60, no. 10, pp. 768-780, Oct. 2012.

[5] A. Novak, L. Guadagnin, B. Lihoreau, P. Lotton, E. Brasseur, L. Simon, "Measurements and modeling of the nonlinear behavior of a guitar pickup at low frequencies," *Appl. Sci.*, vol. 7, no. 50, Jan. 2017.

[6] R. M. French, "Guitar Electronics," in *Engineering the Guitar*. New York, NY, USA: Springer, 2009, pp.209-221.

[7] D. A. Ferber, "Stringed musical instrument with optoelectronic pickup sound amplifier," U.S. Patent: 3 733 953, May 22, 1973.

[8] R. R. Hoag. "Light responsive transducer for musical instruments," Canada Patent: 921 738, Feb. 27, 1973.

[9] Mc Coy, Bing, "Optical pickup for use with a stringed musical instrument," U.S. Patent: 4 688 460, Aug. 25, 1987.

[10] D. J. Christian, "Photonic pickup for use with a stringed musical instrument," U.S. Patent: 4 815 353, Mar. 28, 1989.

[11] T. J. Barnard, "Optoelectronic pickup for stringed instruments," U.S. Patent: 5 012 086, Apr. 30, 1991.

[12] B. W. Curtis, B. L. Kennedy and C. R. Willcox, "Optoelectronic transducer system for stringed instruments", U.S. Patent: 5 237 126, Aug. 17, 1993.

[13] I. A. Kubilay, "3D modeling of string motion", M.S. Thesis, Dept. of Electrical and Computer Engineering, Missouri University of Science and Technology, Rolla, MO, 2006.

[14] A. J. Wilkins, B. Lehman, “Designing to mitigate effects of flicker in LED lighting: reducing risks to health and safety,” *IEEE Power Electronics Magazine,* vol. 1, no. 3, pp. 18-26, September 2014.

[15] L. Arexis-Boisson, Y. Zhang, G. Zissis, S. Kitsinelis, “LED flicker: a drawback or an opportunity?,” *Optics and Photonics Journal,* vol. 3, no. 1, pp. 63-66, 2013.

[16] M. Rylander, E. J. Powers, and T. Kim, “LED lamp flicker caused by interharmonics,” in *Instrumentation and Measurement Technology Conference Proceedings, 2008. IMTC 2008*, Victoria, Canada, 2008.

[17] X. Ruan, K. Yao, S. Tan, Y. Yang, Z. Ye, S. Wang, “A flicker-free electrolytic capacitor-less AC–DC LED driver,” *IEEE Transactions on Power Electronics,* vol. 27, no. 11, pp. 4540-4548, 2012.

[18] I. A. Kubilay, D. Kartofelev, M. Mustonen, A. Stulov, V. Välimäki, M. Pàmies-Vilà, “High-speed line-camera measurements of a vibrating string,” in *Proceedings of BNAM 2014* , Tallinn, ESTONIA, 2014.

International Conference on Science and Technology

ICONST 2018

5-9 September 2018 Prizren - KOSOVO

Chemical Composition and Metal Contents of Five Edible Mushroom Species from Kastamonu, Turkey

Mertcan Karadeniz[1]*, Mansor Boufars[2], Temel kan Bakır[3], Sabri Ünal[1]

Abstract: Edible mushrooms commonly used in traditional medicines and alternative medicine studies due to their chemical content are widely consumed all over the world. In this work, chemical composition and metal contents were analyzed for *Boletus edulis* (Bed), *Hydnum repandum* (Hre), *Ramaria fennica* (Rfe), *Cratellus cornucopioides* (Cco) and *Cantharellus cibarius* (Cci) collected from Kastamonu in the West Black Sea region of Turkey. The determination of mushroom chemical compositions was performed using GC / MS (Agilent Technologies 7890A) instrument. Natural compounds of mushroom classified as Carboxylic acids, Flavonoids, Polyphenols, Flavor and taste components were given as g / 100 g of dry matter. In addition, all samples were analyzed by a SpectroBlue ICP-OES to obtain the concentration of Co,Cu,Cd,Pb,Ni,Cr, Na, Ca,Al,Fe,Zn,Ba,P,Mg,As,Mn and B. The polyphenolic substance content was found to be the richest in *Ramaria fennica* and the richest flavonoid, phenolic acid and carboxylic acid content was in *Cantharellus cibarius*. In *Boletus edulis* and *Cratellus cornucopioides*, flavor and aroma substances were found to be much higher than other mushroom species examined. While maximum and minumum metal contents of mushrooms were found as mg/g for Mg (1.90-0.65), P (5.00-2.99), Zn (0.11-0.03), Ca (2.49-0.39) and Fe (0.91-0.03), the maximum and minumum trace metal contents of mushrooms were found for as mg/kg for Cr (13.06-2.19), Ni (12.02-1.38), Cu (39.06-12.01), Co (4.16-0.79), Pb (5.74-0.82). Chemical contents of five mushroom species grown in the Kastamonu region were determined. Organic compounds contained in these edible mushroom species have been found to be very valuable in terms of human health.

Keywords: Edible Mushrooms, Chemical compositions, Metal Contents, Kastamonu, *Boletus edulis*, *Hydnum repandum*, *Ramaria fennica*, *Cratellus cornucopioides* and *Cantharellus cibarius*

Introduction

Wild mushrooms are widely consumed in our country, especially in Anatolian cities due to their wide variety of aromatic flavors. They are also used in conventional medicines due to their chemical properties. Mushrooms are rich in protein and carbohydrates and are low in fat and calories.

Mushrooms are rich in carbohydrate, protein, ascorbic acid, tocopherol, iron, zinc, selenium, sodium, chitin, fibers and minerals. These functional properties of fungi are mainly due to their chemical composition.Many wild edible mushroom species are known to accumulate high levels of heavy metals. Therefore, many studies have been conducted on the metal content.

It is known that the chemical composition of mushrooms causes some changes in their antioxidant properties and the metal contents are effective in changing these properties. Mineral accumulation in mushrooms is

[1]Kastamonu University, Faculty of Forestry, Department of Forest Engineering, 37150, Kastamonu, Turkey
[2]Kastamonu University, Institute of Science (PhD Student), 37150, Kastamonu, Turkey
[3]Kastamonu University, Faculty of Science and Letters, Department of Chemistry, 37150, Kastamonu, Turkey
*Corresponding author: mkaradeniz@kastamonu.edu.tr

usually dependent on the metabolism of the species, and is also strongly influenced by the chemical composition of the mushroom from the substrate.

In this work, chemical composition and metal contents were analyzed for Boletus edulis (Bed), *Hydnum repandum* (Hre), *Ramaria fennica* (Rfe), *Cratellus cornucopioides* (Cco) and *Cantharellus cibarius* (Cci) collected from Kastamonu in the West Black Sea region of Turkey.

Materials and Methods

All analytically pure chemicals were purchased from Sigma-Aldrich Co. LLC. Deionized water (18.2 MX / cm) was taken from the Milli-Q system (Human Power I Plus, Korea) and used to prepare all aqueous solutions. All mineral acids that used, have the highest quality (Merck, Darmstadt, Germany). All plastic and glass products were cleaned by immersion in a 10% nitric acid liquid solution overnight and cooling with deionized water. In this study, a SpectroBlue ICP-OES (spectrometer) was also used for basic analysis. Also CEM Mars 5 closed microwave system was used in the research.

Collection and Preparation of Mushroom Samples

The main material of the study is five different species of mushroom (*Hydnum repandum*, *Cantharellus cibarius*, *Ramaria fennica*, *Boletus edulis* and *Craterellus cornucopioides*) collected from the forest areas of Kastamonu.

All fresh mushrooms (*Hydnum repandum*, Cantharellus *cibarius*, *Ramaria fennica*, *Boletus edulis* and *Craterellus cornucopioides*) were collected from Kastamonu İnebolu, Taşköprü, Araç, Azdavay and Devrekani at August –October 2016-2017 (Figure 1, Table 1). Species of mushrooms were identified by Prof. Dr. Sabri ÜNAL at Mushroom Research and Application Center of Kastamonu University.

The collected mushrooms were dried at 30ºC. for 48 hours after the pieces were weighed in a weight of 100 g each. Dried mushrooms are homogenously powdered for use in analyzes.

Figure1. Localities where fungi are collected..

Table 1. Collection points for each fungus species

Mushroom	Registration Number	Collection point
Boletus edulis	370012	Araç
Cantharellus cibarius	370013	Azdavay
Craterellus cornucopioides	370015	Devrekani
Hydnum repandum	370018	İnebolu
Ramaria fennica	370019	Taşköprü

***** Registration number given for each mushroom species at Kastamonu University Mushroom Research and Application Center.

Determination of Organic Compounds of Mushrooms

The chemical composition of the samples was determined at the Regional Center For Food & Feed - RCFF (Residues Lab) laboratory in Egypt / Giza. GC-MS analysis was performed using a GC (Agilent Technologies 7890A) coupled with a mass selective detector (MSD, Agilent 7000) equipped with an apolar Agilent HP-5ms (5% phenyl methyl poly siloxane). The column (30m 0.25 mm id and 0.25 um film thickness), carrier gas, helium with a linear velocity of 1 ml / min was used. Identification of the components was done by comparing the mass spectra and retention times with the NIST and WILEY libraries on the computer, as well as by comparing the fragmentation model of mass spectral data with those reported in the literature.

Determination of Metal Content of Mushrooms

The dried samples were homogenized and stored in polyethylene bottles. To obtain the mushroom extracts, 0,5 g of the sample in the microwave extraction system was removed with 7 mL HNO_3 (65%) and 1 mL H2O2 (30%) for 30 min and finally diluted with 50 mL of deionized water. The microwave system was used for 15 minutes at a temperature of 200°C and held constant for 15 minutes. For element analysis (ICP plasma), the sources of the stimuli have facilitated their use in this investigation (Yamac ve ark., 2007).

Statistical analysis

Statistical significance levels were calculated using SPSS 13 software (SPSS Inc., Chicago, IL, USA) and for table and graphical calculations for all mushroom species were performed using Microcal Origin Pro 8.5.1. (Origin Lab. Corp., Northampton, MA, USA).

Result and Discussion

Chemical Composition of Mushrooms

Although species of mushrooms are effective on the chemical compounds they contain, the environment and climate in which they grow also affects it (Mattila et al., 2002; Stojkovic et al., 2014). Studies on mushroom compositions have shown interesting results in many compounds with biological activity. Mushrooms which are superior to many foods with their aminoacid contents are low fat free diet sources. In particular, phenolic compounds such as antioxidants, antitumor, antiinflammatory, sterols, terpenes and sesquiterpenes have been the subject of many medical researches (Reis et al. 2011, Vamanu and Nita 2014).

Polyphenolic Compounds and Flavonoids

In this study, the phenolic content that support a healthy life is given in Table 2 for 5 fungal species. Enterodiol is a substance that is formed as a result of the oxidation of lignans which is rich in grains, beans, strawberries and pistachios and is a protective against many chronic diseases (Wang, 2002; Corsini, 2010). Particularly it was found mostly in Cci content and then Bed, Cco and Rfe content in this study. Hydroquinone, which is an aromatic organic compound of phenol type, used as an antioxidant in cosmetic products and mostly in oils, has been found mostly in the Bed and least in Hre (Table 2). Papaveroline found Cco, Hre, Bed and Rfe are also

abundant. Hexestrol which acts as a cancer receptor and diuvaretin which inhibits the growth of cancer cells are present in mushrooms (Table 2). Especially, in Hre, Rfe and Cci diuvaretin values were found to be higher. Coniferyl alcohol is a class of phenylpropanoid which is involved in the biosynthesis of eugenol and stilbane and coumarin. Salbutamol and salmeterol used in the treatment of chronic bronchitis, chronic obstructive pulmonary disorder and asthma attacks were found to be close to all fungal species. All mushroom species were found to contain polyphenolics, especially effective on allergic disorders. Resveratrol exhibits antioxidant, antiaging, antiinflammatory, antiallergic and similar activities thanks to its ability to bind many biomolecules easily (Ergin and Yaylalı, 2013). It is estimated that the antioxidant properties of resveratrol are found in certain levels especially in Hre and Cci. Lignin biosynthesis is initiated by an enzyme-catalyzed phenol dehydrogenation of the mixture of coniferyl, sinapil and p-covalil alcohols (Quideau and Ralph). Coniferil has the highest rate of Hre content.

Table 2. Poliphenolics as health-promoting constituents of *Boletus edulis (Bed)***,** *Hydnum repandum (Hre)***,** *Ramaria fennica (Rfe)***,** *Cratellus cornucopioides (Cco)* and *Cantharellus cibarius (Cci)* (g/100 g of dry matter)

Poliphenolics	**Bed**	**Hre**	**Rfe**	**Cco**	**Cci**
Enterodiol	4.91	0.67	3.92	4.71	10.30
Hydroquinone	2.30	0.56	0.92	1.01	1.44
Papaveroline	15.83	17.16	12.30	21.41	1.21
Pyrocatechol	2.90	1.86	0.56	0.99	0.79
Hexestrol	0.53	0.27	0.38	0.44	0.24
Salbutamol	0.28	0.20	0.33	0.58	0.23
Salmeterol	0.43	0.59	0.56	0.42	0.86
Diuvaretin	0.25	4.28	2.36	0.99	1.65
Resveratrol	0.57	2.92	0.71	0.49	1.08
p-Cresol	0.27	0.55	2.45	0.32	0.43
Coniferyl alcohol	0.33	0.54	0.33	0.41	0.22
2,6-di-tert-butylphenol	0.68	0.25	0.29	0.31	0.18
2-(2-hydroxyethoxy) phenol	2.72	1.14	2.53	1.27	3.53
4-Methylcatechol	0.85	0.34	0.73	0.86	1.20
Cannabigerol	-	3.17	26.14	0.66	3.39
Eugenol	-	-	0.86	-	-
6-hydroxy-4,4,5,8-tetramethyl hydrocoumarin	0.37	0.29	0.40	0.27	0.66
5,7-dihydroxy-8-propionyl-4-propylcoumarin	0.31	1.41	0.67	0.61	1.17
7,7-methoxy 4,4-dimethyl-3,6-bicoumarin	1.21	1.54	0.87	3.08	9.71
S-(2,5-Dihydroxyphenyl) cyclohexylthiocarbamat	0.29	0.42	0.41	0.37	1.34

2,6-Di-tert-butylphenol is used as UV stabilizers and antioxidants for hydrocarbon based products ranging from industrial to petrochemicals to plastics (Shpakovsky et al, 2018). 2,6-Di-tert -butylphenol was found to be present in the Bed content, followed by Cco, Rfe, Hre and Cci, respectively. Antioxidant activities of mushrooms are closely related to polyphenolic and flavanoid contents according to many studies (Reis et al. 2012, Smolskaite et al. 2015). In this study, flavanoid and phenolic acid values of 5 fungi species are shown in Table 3.

2- (2-Hydroxyethoxy) phenol, which is used in the preparation of macrocyclic lipophilic benzodendered ethers, is not uncommon for the five mushroom species studied, compared to many fungal compositions. In particular, Rfe Cci and Hre of the fungal species examined include the cannabigerol compound with anti-inflammatory action. Studies have shown that there are many cannabinoids such as cannabigerol that can work as a "team" with cannabidiol to achieve the best therapeutic results (Tortora and Derrickson, 2008; Borelli et al., 2013).

Coumarins are abundant in the class of substances with both flavoring and flavoring properties and phenolic properties in the fungal species studied. Coumarins contain various benzo-alpha-pyrrole compounds that are found naturally and together with significant and diverse physiological activities. Coumarins are found

naturally in many plants such as tonka beans, cinnamon, melilot, green tea, mint, celery, blueberries, lavender, blueberries. Coumarin is used as an additive in detergents with its fragrant and fragrant donor properties (Felter at el., 2006; Poumale et al., 2013). In the studied mushrooms, 6-hydroxy-4,4,5,8-tetramethyl hydrocoumarin and 7,7-methoxy 4,4-dimethyl-3,6-bicoumarine were most commonly found in Cci, 5,7-dihydroxy-8-propionyl-4 propylcoumarin was found in Hre at most.

Table 3 shows some of the flavonoid species found in mushroom species. Isoflavones, which are part of the human diet all over the world, are abundant in soy protein (Esch et al., 2016). In this study, genistin which is a type of isoflavones, were found mostly in Hre, Rfe and Cci. Genistine has been used in some cancer research in vivo (Da et al., 2015). Fisetin is a plant polyphenol like quercetin, kaempferol and myricetin. As a coloring agent, it is found in many fruits and vegetables such as strawberries, apples, onions and cucumbers (Esselen and Barth, 2014; Paluszczak and Baer-Dubowska, 2014). Of these flavanols, fisetin and myrcetin was found in Cci, querrcetin was found in Hre and keampferol was found in Rfe at the highest rate.

The antioxidant hydroxyflavone (Erenler et al., 2017) was found in Cco with the rate of 0.44%. Esculetin, known for its anti-inflammatory and antioxidant properties (Kok et al., 2009; Park et al., 2010; Witaicenis et al., 2010) and the radicine (Aldrich et al., 2015), which has phytotoxic properties, has been found to be the highest in Rfe. Genkwanin (Gao et al., 2014), one of the leading non-glycosylated flavonoids in many plants with anti-inflammatory activities, was found in the bed with the rate of 2.97%. Kaempferol (Chen et al., 2013), which inhibits cancer cell growth and angiography by enhancing the body's antioxidant defenses, has been most commonly seen in Rfe. Quercetin, an effective antioxidant with strong radical scavenging activities (Srivastava et al., 2016), was the highest in Rfe among the examined fungi with a rate of 11.72%.

Table 3. Flavanoids and phenolic acids as health-promoting constituents of *Boletus edulis* (Bed)**,** *Hydnum repandum* (Hre)**,** *Ramaria fennica* (Rfe)**,** *Cratellus cornucopioides* (Cco) and *Cantharellus cibarius* (Cci) (g/100 g of dry matter)

Flavanoids	**Bed**	**Hre**	**Rfe**	**Cco**	**Cci**
Hydroxyflavone	0.27	0.27	0.34	0.44	0.28
Hesperetin	0.38	0.22	0.45	-	0.91
Myricetin	0.27	0.17	0.41	0.35	0.81
Esculetin	0.34	0.22	0.39	0.32	0.27
Radicinin	0.25	0.31	0.43	0.28	0.20
Genkwanin	2.97	0.83	0.29	-	-
Kaempferol	0.57	0.76	1.46	0.30	1.29
Quercetin	0.55	11.72	7.76	0.64	0.15
Quercetin 3,4,7-trimethyl ether	-	0.19	1.09	0.32	024
4,7-dihydroxy flavone,	1.07	4.91	1.17	3.80	6.85
4,7-dimethoxy isoflavone	0.96	0.36	1.74	2.71	4.59
Genistin	0.31	2.08	2.10	1.35	2.35
Fisetin	-	2.76	1.69	0.70	5.82
Fustin	-	3.65	1.29	0.69	4.23
Phenolic Acids					
3,4-dimethoxy cinnamic acid	0.25	0.22	-	-	0.35
Caffeic acid phenethyl ester	0.30	1.73	0.46	0.81	0.68
Sinapic acid	0.29	0.20	-	0.34	0.23
γ-resorcylic *acid*	0.26	0.28	0.50	0.29	0.25

Flavor and Taste Components

Mushrooms contain bioactive micronutrient contents, such as proteins, as well as antioxidant potential, such as phenolics and carboxylic acids, as well as phenytoids. In addition to this, because of its unique aroma and flavors, it has been an interesting subject by many researchers to have fungus as a food additive. (Miles and Chang, 2004; Zawirska-Wojtasiak, 2004; Fernandes et al., 2013). Du et al. (2010), , found that abundant aroma composition was alcohols, aldehydes and ketones, similar to this study. Other important compounds include terpenes, eight carbon compounds and derivatives thereof. (Cheng et al. 2012, Malheiro et al. 2013).

Thomas (1973) reported more than 60 compounds in the content of dried *Boletus edulis*. However, some compounds are believed to be the product of the drying process. In Agaricus bisporus, low boiling volatiles (acetaldehyde, acetone, ethanol and ethyl acetate) and short-chain fatty acids (acetic, isobutyric, isovaleric and n-butyric acids) were also detected in ethylene.

The major odorants of Agaricus bisporus and other fungal flavors were defined as compounds such as 1-octanol, 3-octanol, 3-octanone, 1-octen-3-ol and 2-octen-1-ol, and were found to be the major contributors to fungus flavor (Dudareva 1975). ; Chambers et al., 1998; Combet et al., 2006; Melinda et al., 2017).

Methylmalonic acid is a compound that reacts with vitamin B-12 to produce coenzyme A (CoA). Coenzyme A is required for normal cellular function. When deficiencies in vitamin B-12 occur, the levels of methylmalonic acid increase. Thus, methylmalonic acid is determined as an indicator of B12 deficiency in the body. In this study, it was found in all mushrooms except Cco (Klee et al., 2000; Fenton et al., 2014).

The taste and aroma donors for the 5 fungal species examined are given in Table 4. According to this, carvacrol compounds were found in Bed which gave the highest sweetness to 4-hydroxy-2-methoxybenzaldehyde, zearalenone, 2-phenyl-1-pyrroline and thyme. For Cco, 4-hydroxy-2-methoxy benzaldehyde, zearalenone, carvacrol, terpinol and borneol compounds were determined higher. Zearalenone and farnesol are the most common compounds in the Cci and Hre. The fact that these compounds are dispersed in different fractions in mushrooms is an indication of the fact that the mushrooms have a lot of taste and aroma (Mukonyi et al., 2001; Chami et al., 2005; Can Baser, 2008; Arunasree, 2010).

Table 4. Carboxilic acids and natural compounds of *Boletus edulis (Bed)*, *Hydnum repandum (Hre)*, *Ramaria fennica (Rfe)*, *Cratellus cornucopioides (Cco)* and *Cantharellus cibarius (Cci)* (g/100 g of dry matter)

Carboxilic acids	**Bed**	**Hre**	**Rfe**	**Cco**	**Cci**
Salicylic acid	-	-	-	-	1.76
Methyl malonic acid	1.12	1.12	0.43	-	1.40
Salicyluric acid	0.42	0.26	0.28	0.31	0.24
Flavor and taste components					
2-phenyl-1-pyrroline	2.32	0.88	-	0.34	-
2,6-dihydroxyacetophenone	0.41	0.22	0.53	0.30	0.58
Eucalyptol	0.59	0.18	0.30	0.49	0.36
Terpineol	0.29	0.31	0.27	1.03	0.38
Borneol	-	2.08	2.80	1.73	2.79
2-allyl-p-cresol	0.62	0.29	0.92	0.83	1.20
Carvacrol	1.74	1.51	1.38	1.91	3.27
Cyanidin	0.68	0.50	0.45	0.39	0.47
Zearalenone	13.72	0.87	1.77	10.83	6.05
Farnesol	-	6.02	2.73	0.95	4.51
β-Citronellol	-	0.89	-	-	-
4-hydroxy-2-methoxybenzaldehdye	25.08	5.82	4.50	26.93	4.84
7,8-dihydro-α-ionone	-	-	1.76	-	-
2-methyl-1-naphthol	-	0.77	-	-	-
2-hydroxy-6-methoxyacetophenone	-	2.38	-	-	-

Mineral Composition of Mushrooms

Minerals are inorganic nutrients. The basic mineral elements including macro elements (Ca), Mg (Mg) and Sodium (Na) are the main mineral elements and the minor elements are Iron (Fe), Zinc (Zn), Manganese Mn), and Aluminum, Al, Cobalt, Cu, Cadmium, Lead, Nickel and Cr (Table 5).

Major Elements

Magnesium Essential to good health, magnesium helps to maintain normal muscle and nerve function, keeps heart rhythm steady, supports a healthy immune system and keeps bones strong. As illustrated in Table 5 the lowest mean and highest mean levels of average manganese contents in the present study were measured as 6.454 and 18.982 mg/kg dry matter in *Boletus edulis* and *Cantharells cibarius*, respectively. Magnesium levels ranged in the literature between 180-1900 mg/kg (Uzun et al., 2011) , 23.1 to 40.7 mg/100 g dry. (Mallikarjuna et al., 2012),330 - 6560 mg/kg (Demirbaş, 2001), 61.8 – 65.22 mg/kg(Abdullah et al., 2017),688 - 1150 mg/kg dw (Tuzen, Sesli, & Soylak, 2007). Compared to earlier published reports the determined levels of magnesium is relatively low.

According to the results of this study, as Table 5 the maximum mean aluminium content was 10.55 mg/kg in Hre. The reported aluminium concentrations in previous studies for wild-growing mushrooms were : 8.5–365 mg/kg DM (Rudawska & Leski, 2005), 4.25 to 285.92 µg g–1 dry matter (Gezer et al., 2015),4.8–42.7 for aluminium (Akyuz et al., 2010), 34 and 112 mg kg (Kalač, 2010). According to World Health Organisation (WHO) the permissible aluminum dose for an adult is quite high (60mg per day) (WHO, 1989).

Calcium is an alkaline earth metal, Calcium is an essential mineral required for optimal bone formation and skeletal Growth, calcium provides the structure for our teeth and bones and is needed for muscle contraction (Del valle ve ark., 2011). The preceding Table 5 shows the minimum and maximum mean levels of calcium were measured as 3.91 mg/kg dry matter and 24.88 mg/kg dry matter in *Boletus edulis* and *Cantharells cibarius*. Most results of calcium levels are agreement with that reported by (Konuk et al., 2007). The values are also very low when compared with 170 - 8800 mg/kg (Gençcelep et al., 2009).

Sodium is an essential macro element, especially in animals and the human organism. The concentration of Na has an important physiological effect on different organs and cellular mechanisms and especially on the K/Na pump of cell membranes.(Wani et al., 2010; Yusuf et al., 2007). The results are given in Table 5 showes that the mean concentration of sodium in mushrooms were 0.814 mg/kg dry matter in Rfe to 411.97 mg/kg dry matter in Cci. Generally, previous studies show that sodium concentrations of mushrooms were higher than our results, The average sodium content of the different mushroom taxa varies between 100 and 400 mg/kg(Vetter, 2003) and (14.9-96 mg/kg)(Bakır, Ünal, Karadeniz, & Bakır, 2015).

Iron is highly required physiologically formation and to enhance oxygen carrying capacity of red blood cells.Fe is necessary for the formation of haemoglobin and also plays an important role in oxygen and electron transfer in human body. Its deficiency causes gastrointestinal infection, anaemia, nose bleeding and myocardial infection (Ullah et al., 2012). The results show that the mean content of iron of the mushrooms studied was found higher in Rfe (9,09 mg/kg) (Tablo 5). Compared with (Bakır et al., 2015) to a published report, the determined levels of iron is relatively high (0,128-0,099 mg/kg). Not all results were compatible (Gezer et al., 2015) 7,12 – 300 mg/kg and (Uzun et al., 2011) 5-1930 mg/kg. The iron concentrations in edible plants the WHO (WHO, 1989) limit has not yet been established for iron, but in in edible plants was 20 ppm.(Kalač & Svoboda, 2000) reported iron content was found to vary between 30.0 and 150.0 mg/kg. The range of iron in selective medicinal herbs of Egypt in the study carried out was between 261 ppm to 1239 ppm (Jabeen, Shah, Khan, & Hayat, 2010). Previous studies indicate that iron concentrations was as follows: 31,3–1190 mg/kg (Sesli and Tüzen, 1999), 30–150 mg/kg (Kalač & Svoboda, 2000), 56,1–7162 mg/kg(Miles & Chang, 2004). Compared to previous studies, our result is very low.

Table 5. Mean Mineral Element Composition of Five Wild Edible Mushrooms Growing in Kastamonu (mg/kg)

Sample (ppb)	Co	Cu	Cd	Pb	Ni	Cr
Boletus edulis	37,39±0,2	180,75±0,6	4,48±0,1	8,17±0,2	28,58±0,3	21,90±0,1
Cantharellus cibarius	41,60±69.24	120,09±0.98	3,37±4.66	57,43±14.19	120,20±182.82	27,44±29.87
Craterellus cornucopioides	7,94±0,10	228,90± 0,61	5,53±0,09	14,27±0,38	13,74±0,11	24,81±0,18
Hydnum repandum	23,65±0,05	390,64±0,95	6,27±0,13	23,52±0,81	59,50±0,31	130,61±0,74
Ramaria fennica	20,50±0,08	322,03±0,42	14,34±0,10	14,81±0,08	73,14±0,70	44,20±0,15

Sample (ppm)	Na	Ca	Al	Fe	Zn	P	Mg	Mn
Boletus edulis	6,98±0,05	3,91±0,03	2,72±0,02	2,40±0,01	0,64±0,00	35,66±0,19	6,45±0,02	0,37±0,00
Cantharellus cibarius	411,97±1,68	24,88±0,29	0,97±0,01	0,33±0.01	0,28±0,07	0,06±0,33	18,98±0,33	0,27±0,30
Craterellus cornucopioides	6,61±0,04	12,94±0,19	5,03±0,01	4,06±0,02	0,39±0,00	48,61±0,06	11,56±0,02	0,14±0,00
Hydnum repandum	6,29±0,06	14,85±0,08	10,55±0,04	9,01±0,06	1,15±0,01	29,92±0,10	12,00±0,04	1,73±0,01
Ramaria fennica	0,81±0,00	14,99±0,15	6,54±0,02	9,09±0,03	0,64±0,00	50,09±0,01	13,62±0,04	1,19±0,01

Minor Elements

Cobalt is required for all animals, including humans. It is also an important component of cobalamin, also known as vitamin B12. The cobalt content of our mushroom samples were determined as C.cibarius (4.1), B. edulis (3.73), H. repandum (2.3), R.fennica (2.04) and C. cornucopioides (0.79) mg / kg (Table 5). All published papers agree that the cobalt content generally exceeds 0.5 mg / g or less than about 0.1 mg / g (Ouzouni et al., 2009; Kalač et al., 2000; Kalač, 2010; Falandysz et al. , 2017).

Lead is the third risky trace element in mushroom after cadmium and mercury,. Lead is toxic and non-essential metals and they are toxic (Unak et al. 2007, García, 2009). The results in Table 5 show the amounts of lead recorded for mushroom species: Cci (5.74), Hre (2.35), Rfe (1.48), Cco (1.42), Bed (0.81) mg / kg. The lead results of all mushroom species in the study showed compatibility with the literature. The lead concentrations in the literature were reported to be 0.67 to 12.9 mg / kg (Zhu, 2011), 0.75 - 7.77 mg / kg (Tüzen et al. 1998), 0.40 -2.80 mg / kg (Svoboda et al., 2000), respectively.

Copper is the third richest element in the human body and has a vitamin-like effect on living systems. A small amount of copper is present in the human body (50-120 mg), but plays a critical role in various biochemical processes (Yaman and Akdeniz 2004). As shown in Table 5, the contents of Copper obtained from fungi are H.repandum (39), R.fennica (32.2), C. cornucopioides (22.8), B. edulis (18.0) and Cantharells cibarius (12) mg / kg. These levels are below the permissible limits of WHO in food at 40 mg / kg (Bahemuka and Mubofu 1999). Daily dietary standards for copper have been determined by various health institutions in the world (Sarıkurkcu, 2011, Solak et al., 2012). Copper concentrations accumulated in mushrooms are generally 100 edilme300 mg / kg and are not considered as health risks (Soylak et al. 2005).

Chromium can be considered as a trace element, but it is toxic for overdose health. Chromium in mushrooms is mainly affected by ecosystem and soil acidic and organic matter content (Gast et al., 1988). Mushrooms have much more chromium content than other foods (Barancsi, 2002). In this study, chromium contents obtained from fungi were determined as Hre (13), Rfe (4.42), Cci (2.7), Cco (2.48) and Bed (2.19) mg / kg, respectively (Table 5). In studies conducted in the literature, chromium values in mushroom samples are 7.0–11.0 mg / kg (Sivrikaya et al., 2002). 1.95tedir73.8 mg / kg (Yamaç et al., 2007).
Nickel plays an important role in the biology of microorganisms and plants (Sigel et al. 2008). Nickel is useful as an activator of some enzyme systems, but is harmful if found at high levels (Zhu, 2011). According to the results obtained in this study, Cci (12) was found to be Rfe (7.31), Hre (5.94), Bed (2.85) Cco (1.37) .mg / kg

(Table 5). It is reported that the recommended daily nickel intake according to the WHO is between 100 and 300 mg / kg. Values are reported in the literature in the range of 8.2 - 21.6 mg / kg (Handkerchief, 2004) and 1.22 - 58.60 mg / Kg (Yamac, 2007). The results showed that the nickel content of the samples of mushrooms examined was consistent with those reported in the literature.

References

Abdullah, K., Kiliçel, F. & Karapinar, H. S. (2017). Mineral Contents of Some Wild Edible Mushrooms.

Akyuz, M., Onganer, A. N., Erecevit, P., Kirbag, S. (2010). Antimicrobial activity of some edible mushrooms in the eastern and southeast Anatolia region of Turkey. Gazi University Journal of Science, 23(2), 125-130.

Aldrich, T. J., Rolshausen, P. E., Roper, M. C., Reader, J. M., Steinhaus, M. J., Rapicavoli, J., Vosburg, D. A. & Maloney, K. N. (2015). Radicinin from Cochliobolus sp. inhibits Xylella fastidiosa, the causal agent of Pierce's Disease of grapevine. Phytochemistry, 116, 130-137.

Arunasree, K. M. (2010). Anti-proliferative effects of carvacrol on a human metastatic breast cancer cell line, MDA-MB 231. Phytomedicine, 17(8-9), 581-588.

Bahemuka, T. E., & Mubofu, E. B. (1999). Heavy metals in edible green vegetables grown along the sites of the Sinza and Msimbazi rivers in Dar es Salaam, Tanzania. Food Chemistry, 6

Bakır, T., Ünal, S., Karadeniz, M., Bakır, A. S. (2015). A Comparative Study on Antioxidant Properties and Metal Contents of Some Edible Mushroom Samples From Kastamonu, Turkey. Journal of Food and Health Science, 3(4), 132-140.

Barancsi, A. (2002). Evaluation of the chrome content of some wild-living and cultivated mushrooms from a human nutritional aspect. Elelmezesi Ipar Hungary.

Borrelli, F., Fasolino, I., Romano, B., Capasso, R., Maiello, F., Coppola, D. & Izzo, A. A. (2013). Beneficial effect of the non-psychotropic plant cannabinoid cannabigerol on experimental inflammatory bowel disease. Biochemical pharmacology, 85(9), 1306-1316.

Can Baser, K. H. (2008). Biological and pharmacological activities of carvacrol and carvacrol bearing essential oils. Current pharmaceutical design, 14(29), 3106-3119.

Chambers IV, E., Smith, E. C., Seitz, L. M., & Sauer, D. B. (1998). Sensory properties of musty compounds in food. In Developments in food science (Vol. 40, pp. 173-180). Elsevier.

Chami, N., Bennis, S., Chami, F., Aboussekhra, A., & Remmal, A. (2005). Study of anticandidal activity of carvacrol and eugenol in vitro and in vivo. Oral microbiology and immunology, 20(2), 106-111.

Chen, A. Y., & Chen, Y. C. (2013). A review of the dietary flavonoid, kaempferol on human health and cancer chemoprevention. Food chemistry, 138(4), 2099-2107.

Cheng, Y., Sun, J., Ye, X. Q., Lv, B. B., Chu, Y., & Chen, J. C. (2012). Advances on flavor substances of edible mushrooms. Science and Technology of Food Industry, 10, 412-414.

Combet, E., Henderson, J., Eastwood, D. C., & Burton, K. S. (2006). Eight-carbon volatiles in mushrooms and fungi: properties, analysis, and biosynthesis. Mycoscience, 47(6), 317-326.

Corsini, E. (2010). Overview of alternative methods in immunotoxicology. Toxicology Letters, (196), S29.

Da, H., Gu, X. J., & Xiao, P. G. (2015). Medicinal plants: Chemistry, biology and omics. Woodhead Publishing.

Del Valle, H. B., Yaktine, A. L., Taylor, C. L., Ross, A. C. (Eds.). (2011). Dietary reference intakes for calcium and vitamin D. National Academies Press.

Demirbaş, A. (2001). Concentrations of 21 metals in 18 species of mushrooms growing in the East Black Sea region. Food Chemistry, 75(4), 453-457.

Du, P., Zhang, X., He, S., & Sun, H. (2010). Flavor and elementary analysis of the wild Tremellodon gelatinosum from Yunnan. Chemistry and Industry of Forest Products, 30(3), 97-102.

Dudareva, N. T. (1975). Aromatic substances of fresh and sublimation dried mushrooms. Prikladnaia biokhimiia i mikrobiologiia.

Erenler, R., Demirtas, I., Karan, T., Altun, M., & Gul, F. (2017). Inhibitory Effect of 6, 7-dimethoxy-5-hydroxyflavone on Human Cervix Carcinoma in Vitro. International Journal of Secondary Metabolite, 4(3, Special Issue 2), 512-516.

Ergin, K., & Yaylalı, A. (2013). Resveratrol ve etkileri üzerine bir gözden geçirme. Medical Journal of Suleyman Demirel University, 20(3).

Esch, H. L., Kleider, C., Scheffler, A., & Lehmann, L. (2016). Isoflavones: Toxicological Aspects and Efficacy. In Nutraceuticals (pp. 465-487).

Esselen, M., & Barth, S. W. (2014). Food-Borne Topoisomerase Inhibitors: Risk or Benefit. In Advances in Molecular Toxicology (Vol. 8, pp. 123-171). Elsevier.

Falandysz, J., Sapkota, A., Dryżałowska, A., Mędyk, M., & Feng, X. (2017). Analysis of some metallic elements and metalloids composition and relationships in parasol mushroom Macrolepiota procera. Environmental Science and Pollution Research, 24(18), 15528-15537.

Felter, S. P., Vassallo, J. D., Carlton, B. D., & Daston, G. P. (2006). A safety assessment of coumarin taking into account species-specificity of toxicokinetics. Food and Chemical Toxicology, 44(4), 462-475.

Fenton WA, Gravel RA, Rosenblatt DS (2014). Disorders of Propionate and Methylmalonate Metabolism. The Online Metabolic and Molecular Basis of Inherited Disease (OMBBID).

Fernandes, Â., Barreira, J. C., Antonio, A. L., Santos, P. M., Martins, A., Oliveira, M. B. P., & Ferreira, I. C. (2013). Study of chemical changes and antioxidant activity variation induced by gamma-irradiation on wild mushrooms: comparative study through principal component analysis. Food research international, 54(1), 18-25.

Gao, Y., Liu, F., Fang, L., Cai, R., Zong, C., & Qi, Y. (2014). Genkwanin inhibits proinflammatory mediators mainly through the regulation of miR-101/MKP-1/MAPK pathway in LPS-activated macrophages. PloS one, 9(5), e96741.

Gast, C. H., Jansen, E., Bierling, J., & Haanstra, L. (1988). Heavy metals in mushrooms and their relationship with soil characteristics. Chemosphere, 17(4), 789-799.

Gençcelep, H., Uzun, Y., Tunçtürk, Y., Demirel, K. (2009). Determination of mineral contents of wild-grown edible mushrooms. Food Chemistry, 113(4), 1033-1036.

Gezer, K., Kaygusuz, O., Eyupoglu, V., Surucu, A., Doker, S. (2015). Determination by ICP/MS of Trace Metal Content in Ten Edible Wild Mushrooms from Turkey. Oxidation Communications, 38(1A), 398-407.

Jabeen, S., Shah, M. T., Khan, S., Hayat, M. Q. (2010). Determination of major and trace elements in ten important folk therapeutic plants of Haripur basin, Pakistan. Journal of Medicinal Plants Research, 4(7), 559-566.

Kalač, P. (2010). Trace element contents in European species of wild growing edible mushrooms: a review for the period 2000–2009. Food Chemistry, 122(1), 2-15.

Kalač, P. (2010). Trace element contents in European species of wild growing edible mushrooms: a review for the period 2000–2009. Food Chemistry, 122(1), 2-15.

Kalač, P., Svoboda, L. r. (2000). A review of trace element concentrations in edible mushrooms. Food Chemistry, 69(3), 273-281.

Klee, G. G. (2000). Cobalamin and folate evaluation: measurement of methylmalonic acid and homocysteine vs vitamin B12 and folate. Clinical chemistry, 46(8), 1277-1283.

Kok, S. H., Yeh, C. C., Chen, M. L., & Kuo, M. Y. P. (2009). Esculetin enhances TRAIL-induced apoptosis through DR5 upregulation in human oral cancer SAS cells. Oral oncology, 45(12),1067-1072.

Konuk, M., Afyon, A., Yagiz, D. (2007). Minor element and heavy metal contents of wild growing and edible mushrooms from western Black Sea region of Turkey. Fresenius Environmental Bulletin, 16(11A), 1359.

Malheiro, R., de Pinho, P. G., Soares, S., da Silva Ferreira, A. C., & Baptista, P. (2013). Volatile biomarkers for wild mushrooms species discrimination. Food Research International, 54(1), 186-194.

Mallikarjuna, S., Ranjini, A., Haware, D. J., Vijayalakshmi, M., Shashirekha, M. & Rajarathnam, S. (2012). Mineral composition of four edible mushrooms. Journal of Chemistry, 2013.

Mattila, P., Salo-Väänänen, P., Könkö, K., Aro, H., & Jalava, T. (2002). Basic composition and amino acid contents of mushrooms cultivated in Finland. Journal of Agricultural and Food Chemistry, 50(22), 6419-6422.

Melinda, N. A. G. Y., Socaci, S., Tofana, M., Biris-Dorhoi, E. S., Țibulcă, D., Petruț, G., & Salanta, C. L. (2017). Chemical Composition and Bioactive Compounds of Some Wild Edible Mushrooms. Bulletin of University of Agricultural Sciences and Veterinary Medicine Cluj-Napoca: Food Science and Technology, 74(1), 1-8.

Mendil, D., O.D. Uluozlu, M. Tuzen, E. Hasdemir and H. Sari, 2005. Trace metal levels in mushroom samples from Ordu, Turkey. Food Chem., 91: 463-467.

Miles, P. G., & Chang, S. T. (2004). Mushrooms: cultivation, nutritional value, medicinal effect, and environmental impact. CRC press.

Mukonyi, K. W., & Ndiege, I. O. (2001). 2-Hydroxy-4-methoxybenzaldehyde: aromatic taste modifying compound from Mondia whytei skeels. Bulletin of the Chemical Society of Ethiopia, 15(2), 137-142.

Ouzouni, P. K., Petridis, D., Koller, W.-D., Riganakos, K. A. (2009). Nutritional value and metal content of wild edible mushrooms collected from West Macedonia and Epirus, Greece. Food Chemistry, 115(4), 1575-1580.

Paluszczak, J., & Baer-Dubowska, W. (2014). DNA Methylation as a Target of Cancer Chemoprevention by Dietary Polyphenols. In Polyphenols in Human Health and Disease (pp. 1385-1392).

Park, C., Jin, C. Y., Kwon, H. J., Hwang, H. J., Kim, G. Y., Choi, I. W., Kwon, T. K., Kim, B. W., Kim, W. J. & Choi, Y. H. (2010). Induction of apoptosis by esculetin in human leukemia U937 cells: roles of Bcl-2 and extracellular-regulated kinase signaling. Toxicology in Vitro, 24(2), 486-494.

Poumale, H. M. P., Hamm, R., Zang, Y., Shiono, Y., & Kuete, V. (2013). Coumarins and related compounds from the medicinal plants of Africa. In Medicinal Plant Research in Africa (pp. 261-300).

Quideau, S., & Ralph, J. (1992). Facile large-scale synthesis of coniferyl, sinapyl, and p-coumaryl alcohol. Journal of agricultural and food chemistry, 40(7), 1108-1110.

Reis, F. S., Barros, L., Martins, A., & Ferreira, I. C. (2012). Chemical composition and nutritional value of the most widely appreciated cultivated mushrooms: an inter-species comparative study. Food and Chemical Toxicology, 50(2), 191-197.

Rudawska, M., Leski, T. (2005). Macro-and microelement contents in fruiting bodies of wild mushrooms from the Notecka forest in west-central Poland. Food Chemistry, 92(3), 499-506.

Sarikurkcu, C., Copur, M., Yildiz, D., Akata, I. (2011). Metal concentration of wild edible mushrooms in Soguksu National Park in Turkey. Food Chemistry, 128(3), 731-734.

Shpakovsky, D. B., Shtil, A. A., Kharitonashvili, E. V., Tyurin, V. Y., Antonenko, T. A., Nazarov, A. A., & Ott, I. (2018). The antioxidant 2, 6-di-tert-butylphenol moiety attenuates the pro-oxidant properties of the auranofin analogue. Metallomics, 10(3), 406-413.

Sivrikaya, H., Bacak, L., Saraçbaşı, A., & Eroğlu, H. (2002). Trace elements in Pleurotus sajor-caju cultivated on chemithermomechanical pulp for bio-bleaching. Food Chemistry, 79(2)

Smolskaitė, L., Venskutonis, P. R., & Talou, T. (2015). Comprehensive evaluation of antioxidant and antimicrobial properties of different mushroom species. LWT-Food Science and Technology, 60(1), 462-471.

Soylak, M., S. Saracoglu, M. Tuzen and D. Mendil, 2005. Determination of trace metals in mushroom samples from Kayseri, Turkey. Food Chem., 92: 649-652.

Srivastava, S., Somasagara, R. R., Hegde, M., Nishana, M., Tadi, S. K., Srivastava, M., Choudhary, B. & Raghavan, S. C. (2016). Quercetin, a natural flavonoid interacts with DNA, arrests cell cycle and causes tumor regression by activating mitochondrial pathway of apoptosis. Scientific reports, 6, 24049.

Stojković, D. S., Barros, L., Calhelha, R. C., Glamočlija, J., Ćirić, A., Van Griensven, L. J., ... & Ferreira, I. C. (2014). A detailed comparative study between chemical and bioactive properties of Ganoderma lucidum from different origins. International journal of food sciences and nutrition, 65(1), 42-47.

Thomas, A. F. (1973). Analysis of the flavor of the dried mushroom, *Boletus edulis*. Journal of Agricultural and Food Chemistry, 21(6), 955-958.

Tortora, G. J., & Derrickson, B. H. (2008). Principles of anatomy and physiology. John Wiley & Sons.

Tüzen, M., Sesli, E. & Soylak, M. (2007). Trace element levels of mushroom species from East Black Sea region of Turkey. Food Control, 18(7), 806-810.

Tüzen, M., Özdemir, M., & Demirbaş, A. (1998). Study of heavy metals in some cultivated and uncultivated mushrooms of Turkish origin. Food Chemistry, 63(2), 247-251.

Ullah, R., Khader, J. A., Hussain, I., Talha, N. M. A., Khan, N. (2012). Investigation of macro and micro-nutrients in selected medicinal plants. African Journal of Pharmacy and Pharmacology, 6(25), 1829-1832.

Vamanu, E., & Nita, S. (2014). Bioactive compounds, antioxidant and anti-inflammatory activities of extracts from Cantharellus cibarius. Revista de Chimie, 65(3), 372-379.

Wang, L. Q. (2002). Mammalian phytoestrogens: enterodiol and enterolactone. Journal of Chromatography B, 777(1-2), 289-309.

Wani, B. A., Bodha, R., Wani, A. (2010). Nutritional and medicinal importance of mushrooms. Journal of Medicinal Plants Research, 4(24), 2598-2604.

WHO (1989). Health through oral health: guidelines for planning and monitoring for oral health care: Quintessence Pub Co.

Witaicenis, A., Seito, L. N., & Di Stasi, L. C. (2010). Intestinal anti-inflammatory activity of esculetin and 4-methylesculetin in the trinitrobenzenesulphonic acid model of rat colitis. Chemico-biological interactions, 186(2), 211-218.

Yamaç, M., Yıldız, D., Sarıkürkcü, C., Celikkollu, M., Solak, M. H. (2007). Heavy metals in some edible mushrooms from the Central Anatolia, Turkey. Food Chemistry, 103(2), 263-267.

Yaman, M., & Akdeniz, I. (2004). Sensitivity enhancement in flame atomic absorption spectrometry for determination of copper in human thyroid tissues. Analytical Sciences, 20(9), 1363-1366.

Yusuf, A., Mofio, B., Ahmed, A. (2007). Proximate and mineral composition of Tamarindus indica Linn 1753 seeds. Science world journal, 2(1).

Zawirska-Wojtasiak, R. (2004). Optical purity of (R)-(−)-1-octen-3-ol in the aroma of various species of edible mushrooms. Food Chemistry, 86(1), 113-118.

Zhu, F., Qu, L., Fan, W., Qiao, M., Hao, H., Wang, X. (2011). Assessment of heavy metals in some wild edible mushrooms collected from Yunnan Province, China. Environmental monitoring and assessment, 179(1), 191-199

International Conference on Science and Technology

ICONST 2018

5-9 September 2018 Prizren - KOSOVO

Drone Design for Abiding Legal Guidelines

Ibrahim Atakan KUBİLAY[1]*, Huriye KUBİLAY[2]

Abstract: In the recent years, drones have found widespread usage in many diverse applications. Many governments have imposed legal guidelines to enable a safe operating environment for the drones, avoid their usage for crime and other activities harmful to human beings and animals. The limitations imposed by the governments should be closely matched by the technical design and development of drone hardware and software. In this paper, the technical basics of drone operation and the legal frameworks in several countries that have imposed drone regulations are discussed, and possible recommendations for designing drones that abide by legal guidelines are made. The paper concludes with proposals for future research.

Keywords: drone, quadcopter, UAV, legal framework, aerospace law

Introduction:

As of 2018, it's unnecessary to elaborate on the drone craze in our increasingly technologically driven World. Drones are used in applications that span every aspect of our lives. It's plausible that within a few years drones will be as integral as smart phones in our lives. Moreover, governments, institutions an deven criminal organizations utilize drone technology for a variety of applications (Valente, 2017;,Sathyamoorti, 2015). Placing drone use inside a legal framework has proven difficult because of the rapidity of advancements in drone technology. In this paper we aim to outline some major problems with regard to illegal and unethical uses of drones, analyze the legal and technical aspects of the problem, and finally make some recommendations that will enable law-enforcement to prevent attacks using drones while at the same time respecting privacy concerns of drone users.

The paper is organized as follows; We make formal definitions in Introduction, examine the legal and technical fundamentals of drone operation, discuss some recent incidences involving drones and the ways in which a drone may poise a threat in Materials and Methods, a snapshot of the current situation and the reasons behind the vulnerabilities will be presented in Results and finally recommendations for making the drones conformant to legal guidelines will be presented in Discussion.

Definitions

Drone the general name given to any flying object flown without a crew inside, either in real-time by an operator, by using a pre-defined set of waypoints, or autonomously by interpreting data from its sensors according to its pre-installed software. Miriam Webster Dictionary defines drone broadly as "an unmanned aircraft or ship guided by remote control or onboard computers" (Webster, 2018) even though in this study we will exclude sea-born vehicles. In daily usage drone usually implies a multi-copter vehicle while Unmanned Aerial Vehicle (UAV) is commonly used for fixed wing unmanned vehicles.

Illegal Activity means the usage of drones to physically (eg. Assassination) or psychologically (eg. Capturing private photos of a citizen) harm human beings, animals, livestock, plants, foodstuffs, goods or anything of value to human beings and society (eg. An attack on a wheat store to cause famine), as well as any activity that produces an illegal profit (eg. Remote broadcasting of a football match without paying royalty fees).

Attacker is a human being or a team of human beings who wish to use one or more drones to cause harm or unwarranted profit as described above.

[1]Dokuz Eylul University, Faculty of Engineering, 35160, Izmir, TURKEY
[2]Izmir University of Economics, Faculty of Law, 35330, Izmir, TURKEY
*Corresponding author: atakan@cs.deu.edu.tr

Defender is a human being, a group of human beings, or a facility that is vulnerable to a drone attack.

Material and Methods

The technical details of drone operations, as well as the legal frameworks in several countries are examined.

Legal Status of Drones

Drones are "*movable property*" (Ertaş, 2011) in the context of property law. So, they are governed by the provisions of Civil Law. All legal transactions, such as purchase and sale, leasing, unless otherwise specified, may be realized by an oral or a written contract. As an exceptional example, pledging of a drone is realized by transfer of its actual possession. A drone may be pledged in context of a business enterprise pledge, by a pledge contract, in written or electronic form and registration in Mortgage Movable Registry (Art.2 (1) k and Art.8 of Act on Movable Mortgage in Commercial Transactions). Pledge contract in written form, signatures of the parties should be ratified by Notary or pledge contract should be signed in the presence of Register Authorised. Pledge contract in electronic form should be ratified by secured electronic signature.

When a drone would be transferred as an element of a business enterprise, transfer contract should be in written form (Art.11 of Turkish Commercial Code, 6102).

The civil liability of drone operator is regulated by the general provisions of Turkish Code of Obligations, numbered 6098, and the civil liability of insureds, sourced from compulsory third-party insurance is regulated by Turkish Commercial Code, numbered 6102, Turkish Civil Aviation Act, numbered 2920 and Insurance Law, numbered 5684. Drone operators can also insure their interests; as hull insurance and third-party insurance, voluntarily.

In case of illegal usage of drones, criminal sanctions, regulated by Criminal Law, numbered 5237 may be applied.
Drones' usage has been regulated by Administrative Law, in national level.
They may be subject of national and/or international law, because of their transnational nature.

International Conventions

Although, the unmanned air vehicles technology has arisen recently, the rules of some international conventions, have been accepted to be applied in this field, entered into force in previous years.

It is controversial if the Rome Convention, which has been promulgated before planning the usage of drones intensively, may be applied to drone incidents or not. It is suggested that the definition in Chicago Convention (Convention on International Civil Aviation, Chicago, December 7 1944), so as the concept of "*aircraft*" hasn't been defined in Rome Convention. To Annex: 7 (Aircraft Nationality and Registration Marks) added to Chicago Convention, aircraft is defined as *"Any machine that can derive support in the atmosphere from the reactions of the air other than the reactions of the air against the earth's surface."* As seized in Technical View on Introduction to Legal Frame on Operation of Unmanned Aircrafts, dated 18 December 2015, prepeared by European Department of Aircraft Security, this definition shoud include drones, designed to be operated without a pilot in craft or operated, pursuant to general understanding (Sözer, 2009).

Turkey signed the Montreal Convention 1999/Convention for the Unification of Certain Rules for International Carriage by Air (Montreal, 28 May 1999), with the following reservation and was become a Contracting State in 26 March, 2011;

"*The instrument of ratification by Turkey contains the following declaration in accordance with Article 57:*
The said Convention shall not apply to international carriage by air performed and operated directly by the Republic of Turkey for non-commercial purposes in respect to its functions and duties as a Sovereign State and to the carriage of persons, cargo and baggage for Turkish military authorities on aircraft registered in or leased by the Republic of Turkey, the whole capacity of which has been reserved by or on behalf of such authorities."

Convention on Compensation for Damage Caused by Aircraft to Third Parties, Montréal, 02.05.2009) and Convention on Compensation for Damage to Third Parties Resulting from Acts of Unlawful Interference Involving Aircraft, Montréal, 02.05.2009. They aren't in force anymore. So, today there isn't an assurance account in international law.

European Union Law

In European Union, "*Regulation (EC) No 785/2004 of The European Parliament And Of The Council Of 21 April 2004 On Insurance Requirements For Air Carriers And Aircraft Operators"* was published.

Model aircrafts, of which maximum take-off mass are smaller than 20 kg. are not in the scope of the Regulation. Maximum take-off mass of aircrafts is special to each aircraft and it is a weight written in certificate of airworthiness.

Turkish Law

In Turkish Law, "*Unmanned aircraft*" is defined as any aircraft, which can fly without a man and and can cruise on air (Art. m.4 (1), c, ç of By-Law[1]). Pursuant to the Art.8 of By-Law, the minimum assurance amount is between 750.000 SDR and 700.000.000 SDR.

"*Guideline on Unmanned Air Vehicle Systems*" was published in 22 February 2016, based on Turkish Civil Aviation Act, numbered 2920, because of some security concerns such as spying, theft and terror. According to the Guideline, by taking into consideration the types of unmanned air vehicles, the liability and the necessity to make compulsory insurance contract have been determined. The unmanned aircrafts, over minimum 25 kg., must be insured against third party liability risk.

The concept of "*Privacy of private life*" hasn't been explicitly defined in Turkish Law, but it has been protected by Art.20 of the Constitution of the Republic of Turkey and Art.134 of Turkish Criminal Act, numbered 5237.

Technical Fundamentals of Drone Design

A drone, regardless of its size, is a system of components that must work in harmony to operate the drone. There are three main components:

1) Airframe (Fuselage, landing gear, duct, etc…)
2) Propulsion System (Motors, Propellers, Electronic Speed Controller (ESC), etc…)
3) Command and Control System (RC Transmitter\Receiver, Radio Telemetry, Ground Control Station (GCS), Autopilot, etc…)

The motors are arranged in various configurations such as quad, quadx (4 motors), hexa, y6 (6 motors), octo, x8 (8 motors), etc modes, with quadx being the most common where the motors are arranged as if at the endpoints of letter x. Propulsion system is very important in a drone system and it must be targeted for any successful attack on the drone itself. Usually brushless DC motors driven by a star type three phase bridge circuit are used for running the propellers. The Electronic Speed Controller (ESC) is used to control the speed of the propellers based on the pulse width modulation (PWM) signals coming from the autopilot which are too weak to directly run the propellers. Battery used impacts the endurance (ie. Flight time) of the drone. Considerations of performance and cost have made Lithium Polymer (LiPo) and Nickel Metal Hydride (NiMH) batteries very popular for powering drone motors. An RC transmitter may be used to directly communicate with the drone and control it in short range (Quan, 2017).

A controller frequency of 2.4 GHz is commonly used and the controlling signal is created by a microcomputer rather than a crystal, and as a result power consumption is reduced, channel interference is avoided and a smaller antenna becomes possible. This frequency requires the controller to be in direct line of sight connection with the drone, so the drone is very difficult to control from behind an obstacle such as a hill (Quan, 2017). This is an important consideration, because it forces a potential attacker to be in direct visual contact with the drone, making him/her vulnerable to visual detection (Rodday, 2016).

An autopilot module uses data from various sensors such as GPS, height sensor, Inertial Measurement Unit (IMU) to control flight parameters of a drone. It can be semi or fully automatic, taking commands directly from an operator in real time, or flying according to a predefined flight pattern, respectively. Radio telemetry refers to a digital RS-232 radio interface that works at 19.2 Kbps that allows long distance reliable data transmission. While direct control of the drone by a controller is limited to a range of about 100mm, radio telemetry that connects the drone to a GCS (see below) can have a range of several kilometers (Rodday, 2016).Finally, a Ground Control Station (GCS) is a software on a personel computer which allows the drone pilot to predefine a flight path for the drone using waypoints, and recording flight data for later analysis (Quan, 2017).
Prevention of an attack by a drone involves moving the drone away from the dangerous area and then disabling it for a safe landing without hurting anybody on the ground. If the drone is just disabled at will, there is the risk that it will collide with the object (eg. an airplane) or fall on humans. Therefore it's imperative that the following sequence is followed in disabling it:

[1] By Law on Third Party Liability Insurance of Civil Aircrafts, see OJ 27 July, 2017, 30136. For the previous By-Law, entered into force on 01 January, 2006, see OJ 15 November, 2005, 25994.

1-Move drone away from danger area
2-Find a safe landing zone (LZ)
3-fall in a safe place by disabling the propulsion system, without wandering away from the LZ

The main issue to be discussed in this paper is the prevention of a deliberate act of harm by a drone rather than an accident.

Recent Incidences Involving Drones

Drones are known to be involved in several incidences of illegal activity. Threats posed by drones are categorized by several studies [Valente, 2017; Sathyamoorti, 2015). Dropping contraband such as weapons and drugs into prisons seems to be very common (Valente, 2017; Sathyamoorti, 2015). They are also used by criminals who carry them in backpacks to livestream video of law enforcement officers, so they can escape capture by them (Murdoch, 2018). Carrying drugs is another popular application of drones by criminals. Illegal livestreaming sports matches is another interesting, less harmful but none-the-less illegal drone application. Hacking smart phones and sending unsolicited advertisements to nearby smart phones are also observed (Sathyamoorti, 2015).

Landing drones near political figures for protest is reported in (Sathyamoorti, 2015). Most recently, on August 5th, 2018 an assassination attempt on Venezuelan president Nicholas Maduro involved two DJI Matrice 600 drones carrying C4 explosives of 1kg each (Mogollon, 2018). The drone model was a high-end model costing several thousands of dollars designed for use by professional film makers, capable of carrying more than 5kg and a flight time of more than 15 minutes powered by its 6 motors (Barrett, 2016).

Drones pose serious dangers for commercial airliners. There are several reports of drones getting dangerously close to airplanes (Zhong, 2018), as well as the threat of a drone being intentionally driven into the engine of an airplane. Dutch police used trained eagles to intercept drones until December 2017 (Hillen, 2017) and other drones with catching nets are commonly used to capture and disable malicious drones [Sathyamoorti, 2015; Hillen, 2017].

Even military grade drones are known to have been vulnerable to possible attack, with a US surveillance drone video feed was captured over Iraq, and a GCS for Predator and Reaper armed drones was infected by a virus. Unlike commercially available drones, military grade drone command links are encrypted and are thus more resilient to an attacker taking control of the drone, but this is not the case for consumer grade drones (Sathyamoorti, 2015). In this context, it's worth noting that US Army, previously using drones manufactured by Chinese company DJI in military operations, has suspended their use due to suspicions of drone operations being relayed back to China, underlying the effect of international political rifts in technological considerations (Valente, 2017).

In an interesting study (Rodday, 2016), an undisclosed professional drone which can carry a large payload and has relatively long flight time was successfully hacked using a Man-in-the-Middle (MitM) style attack and its control taken over. This study shows that even advanced civilian drones are possible to hack in theory. Advantages of using consumer grade drones for illegal activities is listed in (Sathyamoorti, 2015).

Results

In this chapter, a snapshot of the current situation is presented. The main vulnerability of a drone is that it must communicate by its pilot or a GCS over a wireless network. Therefore any possible attack on a drone is fundamentally a wireless network attack. Wireless networks are well-known for their security vulnerabilities and the situation becomes only worse in the context of drones. In a study, three types of drones were successfully hacked using their open access points using unencrypted data links and two were actally brought down (Valente, 2017). Using the lack of password protection of ftp and telnet on a drone link, an attacker can gain access to it as root, enabling them to take control of the drone as well as accessing its video stream. Using root access, the SSID of the drone's wireless network is changed, disconnecting the legitimate pilot of the drone and allowing the attacker to take control. The file system permissions may be altered for gaining access as root. Such vulnerabilities are part of a more general security problem with respect to the communaction between IoT devices and mobile apps (Valente, 2017).

It was discussed in (Rodday, 2016) that many serial link parameters such as network ID, baud rate and channel are set to default values for all drones and so are easy to find by a simple online search, while variable parameters such as destination low and high addresses may be obtained by inciting an acknowledge message by the IoT chip on the drone. The mobile apps used to control the drones pose another problem. These apps are not properly obfuscated, and may be easily reverse engineered as shown in (Valente, 2017) to discover the commands used for control of the drone which may be used by an attacker.

See (Wei, 2016) for a hardware solution that can take control of any radio controlled device using the DMSx protocol.

Current Safeguards Against Illegal Use of Drones

The most promiant safeguard against drone misuse is what is known as geofencing, implemented most notably by drones built by DJI Company. It consists of a database of points over the globe such as civilian and military airports, power plants, city squares and other sensitive locations where the drone is not permitted to operate. The flight control module prevents the drone from flying in these areas, however it must be noted that it's possible to by-pass this safeguard by modifying the software of the drone (Sathyamoorti, 2015).

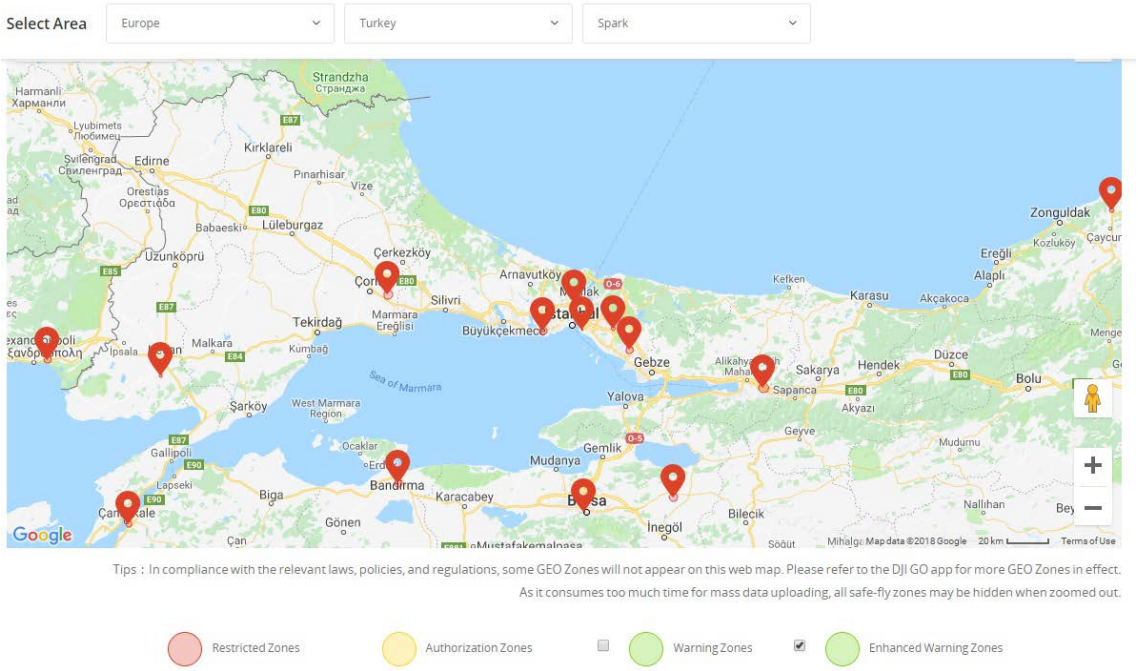

Figure 1. DJI geofencing restricted zones in the Marmara Region of Turkey (DJI, 2018).

Methods to detect a drone are radar which needs dedicated personnel and hardware, acoustic sensing where the motor noise of the drone is picked up by a microphpne and drone type and location detected by audio processing methods, RF sensing where the radio control signals for the drone are detected, Electro Optical (EO) Sensing (ie. Conventional and/or thermal cameras that detect the drone or its remote pilot visually). The possible defenses against a drone attack are jamming or taking control of the drone's command link, jamming or spoofing the Global Navigation Satellite System (GNSS) on the drone, or kinetic defense, which basically means capturing and moving away an attacker drone by a net (Sathyamoorti, 2015).

Discussion

In this section, several legal and technical proposals for improving drone security will be discussed.

Recommendations

The identity, nationality and compulsory third party insurance policy of a drone should be recorded on the drone, registered by a dedicated government authority and those documents should be kept physically by the operator of the drone.

Wireless network over which the drone pilot and the drone system communicates is the weakest link in the context of hacking a drone. Therefore, it's imperative that the standard wireless networking protocols are password protected with different passwords and their filesystem permissions must be set up appropriately.

A very important step that would considerably enhance drone security is to encrypt the command links that operate between the drone pilot and the drone. Subject to the type and sophistication of the chosen encryption method, such a step is bound to reduce response times for the drone, therefore ways to further accelerate command response must be researched, if necessary using dedicated accelerator hardware, even though in flight theory we wish to have as little extra weight as possible.

The most important contribution we propose in this paper is the creation of a golden key, a combination of hardware and software modules that allows government employees such as law enforcement officers, firefighters and commercial airline pilots access to the command link of the drone and steer it away to a safe location and if necessary bring it down by disabling its propulsion system. Such a system should employ both short range and long range communication protocols using a variable frequency scheme so it can't be jammed by the attacker. Great care must be taken that the golden key does not interfere with the conventional flight avionics of commercial airliners. It must provide immediate access to the drone and clear it away from the danger zone, if necessary using its own video feed for this purpose. In technical terms, this is hacking the drone, but done for legitimate purposes by authorized personnel and through an easier hacking route. The golden key system must be embedded in all drones that are legally allowed to fly in a country by the manufacturer. The details and operating parameters of a golden key system must be kept secret within the confines of the government community such as in the case of emergency access doors in commercial airliners that may be used in the event of hijacking to gain access to the plane. Moreover different implementations across different countries will actually be an advantage because there will be no single system that once hacked would compromise the entire golden key concept.

We believe that the rights of the drone owner may be protected against frivolous use of the golden key as follows. When a law enforcement agency uses a fail/abort command on a drone, they will submit a standard report to a specialized court that includes the location (GPS coordinates) and time of the event, type of danger present, and possible outcomes had the fail/abort was not used.

This will enable a drone owner to challenge a fail/safe command if the proper filing is not made by the law enforcement agency, and/or if the reasoning in the report is contestable. Therefore both the privacy of the drone owner and his/her protection against monetary damage will be protected.

References

Barrett, B., https://www.wired.com/2016/04/dji-m600-drone/ [Accessed: 05-Aug-2018].

DJI, 2018. https://www.dji.com/flysafe/geo-map [Accessed: 05-Aug-2018].

Ertaş, Ş.**,** Eşya Hukuku, 9. Baskı, İzmir 2011.

Fingas, J., https://www.engadget.com/2018/08/04/venezuela-says-maduro-was-target-of-drone-assassination-attempt/ [Accessed: 05-Aug-2018].

Hillen, B., https://www.dpreview.com/news/5429354776/the-dutch-police-have-shut-down-their-drone-catching-eagle-program [Accessed: 05-Aug-2018].

J. Valente and A. A. Cardenas, "Understanding Security Threats in Consumer Drones Through the Lens of the Discovery Quadcopter Family," in *Proceedings of the 2017 Workshop on Internet of Things Security and Privacy*, New York, NY, USA, 2017, pp. 31–36.

Mogollon, M., http://www.latimes.com/world/la-fg-venezuela-drone-attack-20180805-story.html [Accessed: 05-Aug-2018].

Murdock, J., https://www.newsweek.com/drone-swarm-used-criminals-disrupt-fbi-hostage-rescue-operation-910431 [Accessed: 05-Aug-2018].

Rodday, N. M., "Exploring security vulnerabilities of unmanned aerial vehicles - IEEE Conference Publication." [Online]. Available: https://ieeexplore.ieee.org/document/7502939/. [Accessed: 14-Aug-2018].

Sathyamoorti, D., "A Review of Security Threats of Unmanned Aerial Vehicles and Mitigation Steps." [Online]. Available:https://www.researchgate.net/publication/282443666_A_Review_of_Security_Threats_of_Unmanned_Aerial_Vehicles_and_Mitigation_Steps. [Accessed: 14-Aug-2018].

Sözer, B., Türk Hukukunda ve Uluslararası Hukukta Hava Yolu İle Yük Taşıma Sözleşmesi, Genişletilmiş 2. Bası,İstanbul 2009.

Q. Quan, "Introduction to Multicopter Design and Control", Singapore:Springer, 2017, p. 31.
Wei, W., https://thehackernews.com/2016/10/how-to-hack-drone.html [Accessed: 05-Aug-2018].

WEBSTER, 2018. https://www.merriam-webster.com/dictionary/drone [Accessed: 05-Aug-2018].

Zhang, M., https://petapixel.com/2018/07/18/this-drone-hovered-dangerously-close-to-an-airliner-takeoff/ [Accessed: 05-Aug-2018].

International Conference on Science and Technology

ICONST 2018

5-9 September 2018 Prizren - KOSOVO

Haşhaş Hasat Makinası Geliştirilmesi / Development of Poppy Harvester

Cengiz Özarslan[1]*, Türker Saraçoğlu[1], A. Fatih Hacıyusufoğlu[2]

Özet: Haşhaş tarımında ekim, bakım ve hasat işlemlerinin yoğunluğu ve zorluğu haşhaş tarımını sınırlandırmaktadır. Haşhaşın el ile tarladan toplanıp, sonrasında parçalanıp ayrılması işlemleri yoğun emek ve zaman tüketimi gerektirmekte, bu ise maliyeti çok artırmaktadır. Bu çalışmada, hasat zamanında çalışma koşullarının ağırlığı, hasat için işgücü gereksiniminin fazlalığı, hasat zamanında işçi bulmanın zorluğu, yüksek işçi ücreti, el ile hasatta ürünün fazla yer kaplaması, ürünün araziden taşınma koşulları, birim zamanda hasat veriminin düşük olması gibi nedenlerden dolayı ülkemiz koşulları, mevcut uygulamalar ve sorunlar dikkate alınarak haşhaş kapsüllerini hasat edip kapsüllerini parçalayabilecek ve parçalanmış materyal içinden sap, tohum ve kapsül parçalarını ayırabilecek bir haşhaş hasat makinası prototipinin geliştirilmesi amaçlanmıştır. Çalışma tasarım ve imalat aşamalarından oluşmaktadır. Prototip makine; ana şase, dolap, biçme düzeni, iletim ünitesi, harmanlama ünitesi ve ayırma ünitesinden oluşmaktadır. Şase makinanın bağlantı elemanları, yürüme organları, hasat ünitesi, iletim ünitesi, harmanlama ünitesi, ayırma ünitesi ve güç aktarım organların üzerinde toplandığı yapıdır. Makine ana şasesi üzerinde 4 adet tekerlek bulunmaktadır. Dolap, biçilecek sapları bıçak ağzına yatırmakta ve biçilen sapları makinaya aktarmaktadır. Dolap, devir ayar imkanı da tanıyan hidrolik motor ile tahrik edilmektedir. Prototip makinada 150 cm iş genişliğinde normal bıçak tipinde ve keskin kenarları dişli yapıda olan parmaklı üçgen yapraklı biçme düzeni kullanılmıştır. Biçme düzeni 1.69 m/s ortalama bıçak hızını sağlayacak şekilde 600 min^{-1} ortalamada olmak üzere hidromotordan ayarlanabilmektedir. Dolap tarafından yatırılan ve biçme düzeni tarafından biçilen ürünün harmanlama ünitesine iletimi için bantlı tip konveyörlerin kullanılmıştır. Bunun için tasarımı yapılan konveyör, biçme düzeninin hemen arkasında biçilen ürünü yatay olarak taşımakta, daha sonra harmanlama ünitesinin besleme ağızına yükseltecek şekilde iki kademeli imal edilmiştir. Konveyör 2 m/s ortalama iletim hızı sağlayacak şekilde hidromotordan ayarlanabilmektedir. Makinada saplı haşhaş kapsüllerinin parçalanması için bir çift 300 mm çap ve 900 mm uzunluk ölçülerinde yivli merdaneli harmanlama ünitesi tasarımlanarak imal edilmiştir. Merdanelerin üzerinde kapsüllerin tutularak araya çekilmesini kolaylaştırmak amacıyla 45° eğimli 2.5 mm derinliğe sahip yivler bulunmaktadır. Merdanelerden birisi 100 min^{-1}, diğeri 200 min^{-1} devirlerde dönecek şekilde kuyruk milinden tahrik edilmektedir. Ayırma ünitesinde yer alan elek kasasında üst üste üç elek yer almaktadır. Üst elek, sap parçalarını tarlaya dökecek ve kapsül parçaları ile tohumu alta geçirecek; orta elek kapsül parçalarını üzerinde toplayacak ve alt elek ise tohumu üzerinde tutup, tozu alta indirecek yapıdadır. Elek eğimi 5°, elek ivmesi 11 m/s^2, eksantrik yarıçapı 2.5 cm olacak şekilde eksantrik devir sayısı 200 min^{-1} devirde dönecek şekilde kuyruk milinden tahrik edilmektedir.

Anahtar Kelimeler: Haşhaş, Hasat, Harmanlama, Ayırma

Abstract: The intensification and difficulty of cultivation, maintenance, and harvesting in poppy cultivation limit the poppy cultivation. The processes of disintegration and separation after poppy collected by hand from the field are required labor intensive and time-consumption; this increases the cost as well. It is aimed that the development of poppy harvester prototype which harvest of poppy capsules, disintegrate of capsules, separate

[1]Aydın Adnan Menderes University, Faculty of Agriculture, 09100, Aydın, TURKEY
[2] Aydın Adnan Menderes University, Aydın Vocational School, 09100, Aydın, TURKEY
*Correspondingauthor: ozarslanc@yahoo.com

seed, capsule and stem that is consider our country's conditions, existing applications and problems therefore the reason as the hard working conditions, the surplus of labor requirements for harvesting, the difficulty of finding workers at harvest period, high labor costs, occupying much of the product in the harvesting, transport conditions from the field, low harvest yield. The study consists of design and manufacturing stages. The prototype machine consists of mainframe, reel, cutter bar, transmission unit, threshing unit and separation unit. The mainframe is the structure that the machines are assembled on. The machine mainframe has 4 wheels. The reel tilts the poppy stalks to the knife mouth and transfers to the conveyor. The reel is driven by a hydraulic motor which also allows the setting of the speed. In the prototype machine, triangular knife type with 150 cm work width and sharp edges with threaded construction was used. The cutter bar can be adjusted to a mean speed of 600 min^{-1} to provide a mean knife speed of 1.69 m/s. Belt type conveyors have been used for conveying to the threshing unit of the product laid by the reel and harvested by the cutter bar. The conveyor has been manufactured in two stages so as to transport the harvested product horizontally just behind the cutter bar, then to raise it to the feed mouth of the threshing unit. The conveyor can be adjusted by a hydraulic motor to provide an average conveying speed of 2 m/s. The threshing unit which has a pair of 300 mm dia. and 900 mm length grooved surfaced roller was designed for breaking into pieces of the poppy capsules. There are grooves with a depth of 2.5 mm inclined by 45° to facilitate gripping the capsules by the rollers. One of the rollers is driven by the PTO, turning at 100 min^{-1} and the other at 200 min^{-1}. There are three sieves in the separation unit. The upper sieve transfers the parts of the stalk to the field and the capsules parts and seeds to the middle sieve. The middle sieve holds the capsule parts. The lower sieve holds the seeds and transfers the dust to bottom. Sieve inclination is 5º, sieve acceleration is 11 m/s^2 and the eccentric radius is 2.5 cm. The eccentric is driven by the PTO to turn at 200 min^{-1} revolutions.

Keywords: Poppy, Harvest, Threshing, Separation

Giriş

Ülkemizde geleneksel olarak tarımı yapılan haşhaş, Papaver somniferum L. türü olan tek yıllık bir kültür bitkisidir. Bilimsel sınıflandırmaya göre Papaver somniferum L., Rhoedales takımının Papaveraceae familyasındandır. Bu familya da Papaver cinsi içerisinde yer almaktadır. Haşhaş bitkisi 700–1200 metre yükseklikte, organik maddece zengin topraklarda en iyi şekilde yetişmektedir. Toprak yorgunluğu olmaması, hastalık ve zararlılardan olumsuz etkilenmemesi için haşhaş tarımında münavebe uygulanmaktadır (Anonim, 2015).

Haşhaşın tohumundan, yağından, küspesinden, afyonundan, saplarından ve çiçeklerinden yararlanılmaktadır. Özellikle yağ bitkileri arasında önemli bir yere sahiptir. Tohumları %44-54 yağ içeriği ile bir besin maddesi olarak kullanılmaktadır. Değişik ve cazip renkli tohumları ekmek ve pastalar üzerine süs ve besin maddesi olarak konulmaktadır. Yağı çıkarıldıktan sonra geriye kalan küspesi hayvan yemi olarak değerlendirilmektedir. Bu sayede sütteki yağ oranını yükseltmektedir. Kapsüllerden elde edilen afyon, içeriğindeki 20 çeşit alkoloidden dolayı tıpta birçok ilacın hazırlanmasında kullanılmaktadır. Dekardan ortalama 350 kg artık sap elde edilmektedir (Erdurmuş ve Öneş, 1990). Haşhaş tohumları gri-mavi, sarı, beyaz, çiğ kahve ve pembe renklerde olabilmektedir. Türkiye'de en fazla yetiştirilen haşhaşlar sırasıyla mavi, beyaz ve sarı tohumlu çeşitlerdir. Üretilen haşhaş tohumlarından bir kısmı üretici ihtiyaçları için ayrılmakta, geri kalan kısmı ise serbest piyasada işlem görmektedir. Tohumları ayrıca, kozmetik ve boya sanayinde de kullanıldığı bilinmektedir.

Haşhaştan ekonomik değeri olan tohum ve kapsül kabuğu olmak üzere iki önemli ürün elde edilmektedir. Bunların dışında henüz alkaloid oluşmamış bitkiler; yeşil salata, bitki artığı sapları ise yakacak olarak ülkemizde değerlendirilmektedir.

Dünyada haşhaş ekimi Birleşmiş Milletler Teşkilatı denetiminde yasal ana üretici olarak Türkiye, Hindistan, Avustralya, Fransa, İspanya, Macaristan'da yapılmaktadır. Ayrıca Hindistan ve Kuzey Kore'de afyon üretim amaçlı; Avusturya, Almanya, Çekya, Hollanda, Polonya ve Ukrayna'da gıda ve süs bitkisi amaçlı haşhaş ekimi yapılmaktadır. Son beş yıllık verilerin ortalamasına göre ülkemiz dünya yasal haşhaş ekim alanları içerisinde %48'lik bir paya sahiptir (Şekil 1) (Anonim, 2018).

Ülkemizde haşhaş ekimi 3298 Sayılı Uyuşturucu Maddelerle İlgili Kanun ve Yönetmelik çerçevesinde lisansa tabi, kontrollü ve çizilmemiş haşhaş kapsülü üretimi şeklinde yapılmaktadır.

Bakanlar Kurulu tarafından haşhaş ekimine müsaade edilen yerlerde, Toprak Mahsulleri Ofisi (TMO) Genel Müdürlüğünce yapılan planlama çerçevesinde, Birleşmiş Milletler Teşkilatının ülkemize verdiği 70.000 hektar limit dâhilinde haşhaş ekimi ve çizilmemiş kapsül üretimi yaptırılmaktadır.

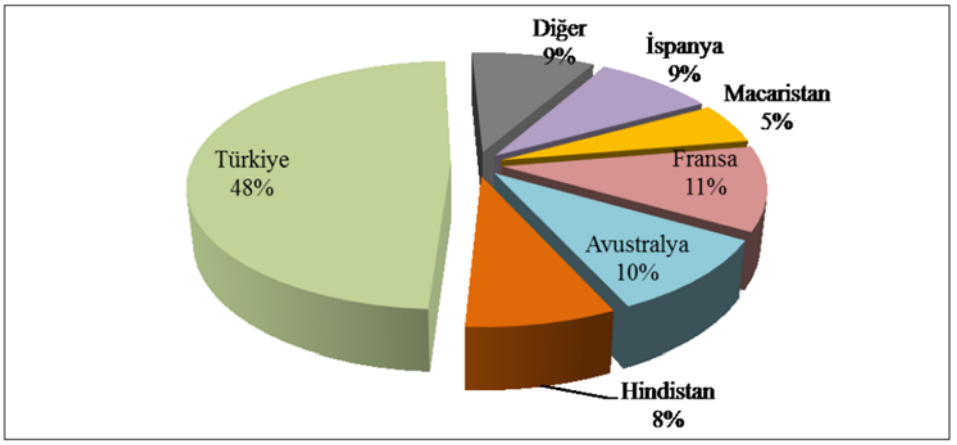

Şekil 1. 2013-2017 yılları ortalamalarına göre Dünya yasal haşhaş ekim alanlarının dağılımı

Söz konusu 70.000 hektar ekim limiti, ekiliş ve üretim potansiyelleri dikkate alınarak yerleşim birimlerine dağıtılmaktadır. Yerleşim birimi bazında verilen haşhaş ekim limitleri çiftçilere paylaştırılarak bu limit çerçevesinde bir çiftçiye en fazla 3 tarlasında haşhaş ekim izni verilmektedir (Anonim, 2018).

Haşhaş hassas bir bitki olduğundan olumsuz iklim koşullarından (don, kuraklık, aşırı sıcaklıklar vs.) etkilenmesi nedeniyle uzun yıllar ortalamasına göre %33 civarında kayıp oluşmaktadır. Ayrıca haşhaş ekim izni alıp ekim yapmayan çiftçilerden kaynaklanan beyan kayıpları ise %14 civarında bulunmaktadır. Üretim kaybının bazı yıllarda %70'lere ulaştığı görülmüştür. 2017 yılında ülkemizde yasal haşhaş ekim alanı 23.731 hektar olmuştur. Bu alandan 13.836 ton kapsül ve 15.244 ton tohum elde edilmiştir (TÜİK, 2017). Haşhaş ekim izni verilip yukarıda belirtilen kayıplardan arta kalan alanlarda haşhaş kapsülü üretimi gerçekleştirilmektedir. Haşhaş kapsülünün uyuşturucu madde içermesi nedeniyle tek ve zorunlu alıcısı TMO Genel Müdürlüğüdür. Çiftçiler, ürettikleri haşhaş kapsülünü izin belgelerinde belirtilmiş olan miktarın üstünde de olsa o yılın en geç Eylül ayı sonuna kadar tespit edilen bedeli karşılığında TMO iş yerlerine teslim etmek zorundadırlar. Satın alınan kapsüller işlenmek üzere Afyon Alkaloidleri Fabrikası İşletme Müdürlüğüne sevk edilmektedir. Haşhaş tohumu gıda amaçlı kullanıldığından serbest piyasada işlem görmektedir (Anonim, 2015).

Modern tarım tekniklerinin uygulanmasıyla üretici şartlarında 150 kg kapsül kabuğu ve bundan daha fazla tohumun dekardan alındığı görülmüştür. Haşhaş ülkemizde genel olarak güzlük ekilmekle birlikte, kıştan zarar görülmesi halinde ya da kışın çok sert geçtiği yörelerde yazlık olarak da ekilebilmektedir. Güzlük ekim zamanı, haşhaş ekim bölgelerine göre bazı farklılıklar göstermekle birlikte Ekim ayının ilk haftasıdır. Yazlık ekim zamanı ise Mart sonu Nisan başıdır (Erdurmuş ve Öneş, 1990).

Üretim girdilerinde tasarruf, üretimin her aşamasında ürün kayıplarının önlenmesi, ekim metotları ve mekanizasyonu, saf ve temiz ürün elde etme yöntemleri haşhaş üretimi ve mekanizasyonu sorunlarının başında gelmektedir (Karaca, 1996).

Ülkemizde haşhaş ekimi genel olarak elle serpme şeklinde yapılmakla birlikte son yıllarda makina ile ekim yöntemine (30-40 cm sıra arası mesafelerde) geçiş yapılmaya başlanmıştır. Elle ekimde tohum yalnız, bazen de yarı yarıya ince kumla karıştırılıp tarlaya serpilmektedir. Serpme ekimde dekara verilen tohum 1-5 kg arasında değişmektedir. Makinalı ekimde ise dekara verilen tohum miktarı 300 grama kadar düşmektedir.

Makinalı ekimde çıkışlar üniform olmakta, özellikle çapalama ve ilaçlamada büyük oranda işçi tasarrufu sağlanmaktadır.

Haşhaş hasadı Temmuz-Ağustos ayları içinde yapılmaktadır. Haşhaş kapsülleri kuruduğu zaman zarlar üzerinde dizilen tohumlar kapsül dibine dökülmektedir. Bir bitki üzerindeki ya da bir tarladaki tüm kapsüller aynı zamanda olgunlaşmamaktadır. En son oluşan kapsüller en son olgunlaştığından hasada karar vermek için en alt kapsüllere bakmak gerekmektedir. Kapsüllerin açık ve kapalı oluşu bir çeşit özelliği olmakla birlikte, olgunlaştığı halde hasat edilmeyen ve güneşe maruz kalan, diğer bir ifadeyle aşırı derecede kuruyan kapsüllerde de açılma görülebilmektedir. Bu yüzden, hasatta tohum dökülmesine ve kayba neden olduğundan hasat zamanının geciktirilmemesi gerekmektedir (Hacıyusufoğlu, 2013). Ayrıca hasat sezonundaki olası yağış tehdidi kapsüllerin açılmasına, kapsüllerin kararmasına, tohumların dökülmesine ve tohumun çimlenme kabiliyetinin azalmasına yol açabilmektedir. Bu da kapsül ve tohumun değerinin düşmesine neden olmaktadır. Dolayısıyla haşhaş hasadının kısa sürede tamamlanma zorunluluğu bulunmaktadır.

Hasat işlemleri Dünya'da çeşitli şekillerde yapılmaktadır. Afganistan, Hindistan, Pakistan gibi bazı ülkelerde haşhaş kapsülleri çizilerek (afyon sakızı çıkartılarak) yapılmaktadır. Avustralya, Romanya, Macaristan ve Avusturya gibi ülkelerde ise haşhaş hasadı makina ile yapılmaktadır.

Uygulamada hasat mekanizasyonunda 2 yöntem vardır:

1-) Küçük arazilerde kullanılmak üzere Macaristan'da sapları 10–20 cm uzunluktan kapsülle birlikte kesen ve biçme makinelerine monte edilebilir özel bir hasat adaptörü geliştirilmiştir. Kesim sonrasında, kapsül ve tohum ayırma, çiftlik merkezinde gerçekleştirilmektedir. Burada ürün öbekler halinde işleme zamanına kadar saklanabilmektedir.

2-) Büyük arazilerde modifiye edilmiş biçerdöver ile haşhaş kapsülleri 10–20 cm uzunluğunda saplardan kesilmektedir. Bu yöntemin başarısı temiz ve yabancı ottan arındırılmış tarla koşullarına bağlıdır. Ayrıca biçerdöverle hasatta üniform bitki yüksekliği gerekmektedir. Bu ise tarlada yüksek bitki yoğunluğu ile başarılabilmektedir. Bu durumda da bitki başına kapsül sayısı düşmektedir. Ilıman iklimlerde optimum bitki yoğunluğu 450,000 bitki/ha olmakta ve bitki başına 1-2 kapsül düşmektedir. Ülkemiz koşullarında bu değerler sırasıyla 25,000 bitki/ha ve 5-8 kapsüldür.

Mekanize hasadın, işgücü gereksinimini ve maliyeti azaltması gibi avantajları olmasına karşın, hasat işlemi sırasında kapsül-tohum kaybı ve tohuma yüksek oranda zarar vermesi ise dezavantajlarının bulunduğu ifade edilmektedir (Németh, 1998). Bu tip kullanılan makinaların bir diğer büyük dezavantajı ise hasat edilen haşhaş kapsülü ile birlikte oldukça fazla miktarda haşhaş sapını karıştırmasıdır. Bu olumsuzluğun elde edilen birim hammaddede alkaloid oranını düşürdüğü belirtilmiştir (Földesi, 1992). Bu tip makinalar Avustralya gibi günlük ışıklanma süresi yüksek olan ülkelerde tercih edilmektedir. Bu bölgelerde yetişen haşhaş bitkisinde, ışıklanma süresi fazla olduğu için kapsüldeki alkaloid oranının daha yüksek değerlerde bulunması ve ayrıca haşhaş bitki boylarının homojen olması bu gibi ülkelerde bu makinaların kullanımına olanak sağlamıştır. Ancak ülkemizde işletmelerin küçük ölçekteki yapıları, bitki sap uzunluklarının heterojen olması ve hasat sonrası kapsül parçaları içinde istenmeyen materyal olarak sap parçalarının karışması bu makinaların kullanımı için dezavantajları oluşturmaktadır.

Afganistan, Çin ve Hindistan gibi ülkelerde ise kapsül yeşil iken kurumadan özel aletlerle çizilerek baz morfini toplanmaktadır. Daha sonra kapsüller el ile toplanıp çuvallara doldurulmaktadır (Hacıyusufoğlu, 2013). Türkiye'de haşhaş hasadı ise doğrudan kapsüllerin elle kırılması ile yapılmaktadır (Şekil 2). Elle hasatta, kapsüller sapa birleşme noktasındaki boğumdan kırılarak toplanmaktadır (Şekil 3). Kopartılan kapsüller büyük çuvallarda toplanarak depolanmaktadır.

Şekil 2. Türkiye'de elle haşhaş hasadı

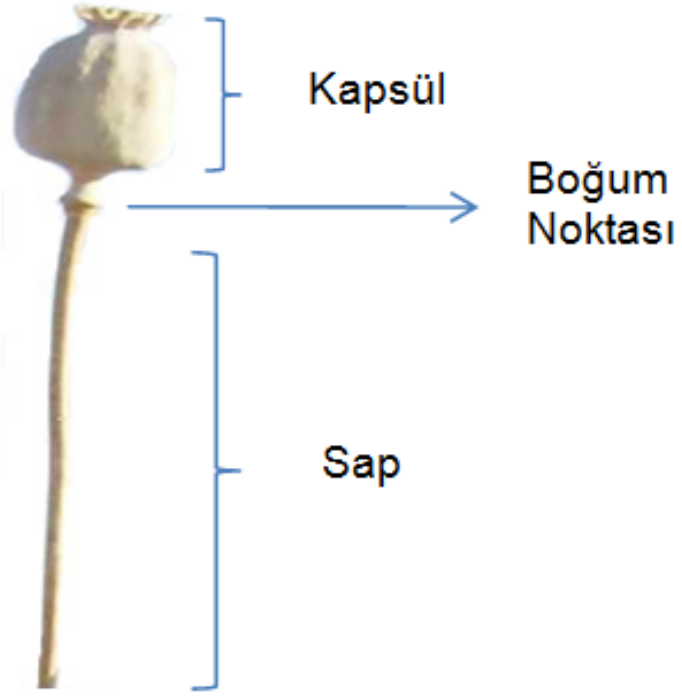

Şekil 3. Haşhaş bitkisinin kapsül, boğum ve sap kısmı

Hasat sonrası toplanan ürün kapsül kırma makinasından geçirilmekte veya tahta tokaçlarla kırılmaktadır. Ülkemizde elle hasat sonrası kullanılan kapsül kırma makineleri genellikle traktör kuyruk milinden hareket almakta ya da elektrik motoru ile çalıştırılmaktadır. Bu makinelerin iş kapasite ise yaklaşık 2 ton/h'dir.

Kapsül kırma makinelerinin besleme haznesine elle doldurulan haşhaş kapsülleri, yedirme düzeni vasıtasıyla parçalama bölmesine aktarılmakta ve kapsüller parçalanmaktadır. Buradan eleklere düşen kapsül kırıkları ve haşhaş tohumları elenmektedir. Ayrılan haşhaş ve kapsülleri ayrı ayrı çuvallara doldurulmaktadır. Üst eleğin delik çapı ortalama olarak 3-5 mm, alt eleğin ise delik çapları 2-3 mm civarındadır. Alt elek kapsül ve kavuz parçalarını haşhaştan iyi ayırmalıdır. Aksi durumunda yemeklik haşhaşın tadı acılaşarak, kalitesizleşmektedir. Karaca (1996), Afyon yöresinde imal edilen haşhaş kapsülü kırma-ayırma makinasının bazı yapısal ve işletme özelliklerinin belirlenmesi ve geliştirilmesi olanaklarını araştırmıştır. Bu amaçla kırıcı ünite devri, elek stroku ve besleme ağzı kesit alanının özgül enerji tüketimi, iş kapasitesi ve temizleme etkinliği üzerine etkilerini tespit etmiştir. Sonuç olarak 270 min^{-1} kırıcı ünite devri, 58 mm elek strokuna karşılık 361 cm^2'lik besleme ağzı kesit alanının en uygun çalışma durumu olduğunu saptamıştır.

Haşhaşın tarladan toplanıp, sonrasında parçalanıp ayrılması işlemleri yoğun emek ve zaman tüketimi gerektirmekte, bu ise maliyeti çok artırmaktadır.

Haşhaş hasadında karşılaşılan sorunlar göz önünde tutulduğunda ülkemizdeki haşhaş tarımı yapılan ve çoğu küçük ölçekteki (ortalama 7 dekar) işletmelerde kullanılabilecek özgün makinalara ihtiyaç olduğu görülmektedir. Bu kapsamda, ülkemiz koşullarına uygun haşhaş kapsüllerini hasat edip kapsüllerini parçalayabilecek ve parçalanmış materyal içinden sap, tohum ve kapsül parçalarını ayırabilecek bir haşhaş hasat makinası prototipinin geliştirilmesi oldukça yararlı olacaktır.
Bu çalışmanın amacı; ülkemiz koşulları, mevcut uygulamalar ve sorunlar dikkate alınarak haşhaş kapsüllerini hasat ederek parçalayan ve sapından ayrılmış haşhaş kapsülü ve tohumunun elde edilmesini sağlayan haşhaş hasat makinası tasarım ve imalatının gerçekleştirilmesidir.

Materyal ve Yöntem

Çalışma iki aşamadan oluşmaktadır. Birinci aşamada haşhaş hasat makinasının tasarımı gerçekleştirilmiş olup ikinci aşamada ise imalatı gerçekleştirilmiştir. Tasarım parametreleri ana hatlarıyla belirlenen prototip makinanın tasarım aşamasında, bilgisayar destekli tasarım programlarından yararlanılmıştır. Makinanın çizimleri bilgisayar ortamında oluşturulmuş ve makinanın katı modeli ve teknik resimleri ortaya konulmuştur.

Makinanın genel yapısı

Prototip makina, hasat ünitesi, iletim ünitesi, harmanlama ünitesi, ayırma ünitesi, çuvallama ve güç aktarım sistemi olmak üzere altı ana kısımdan oluşacaktır. Bu altı ana kısım bir şasi üzerine monte edilecek olup şasi taşıma tekerlekleri vasıtasıyla desteklenecektir.

Hasat ünitesi

Hasat ünitesi, makinanın fonksiyonlarının yerine getirilmesinde birincil öncelikli ünitedir. Uygun yapılan hasadın, harmanlama ve ayırma işlemlerinin başarısı ile ürün kayıpları üzerinde önemli etkileri bulunmaktadır. Dolayısıyla hasat ünitesi için; kullanılacak kesme yöntemi, bıçak tipi, bıçak hızı, kesme genişliği, biçilecek sapların bıçağa yönlendirilmesi ve biçilen sapların makinaya aktarılması (dolap düzeni) işlemlerinde uygun parametrelerin seçimi önem kazanmaktadır. Makinanın önünde bulunan hasat ünitesinde yer alan elemanlar ve özellikleri aşağıda yer almaktadır.

Sap ayırıcılar: Biçilen ürünle biçilmemiş ürünü birbirinden ayırmak, biçme düzeni kenarına gelen ürünün yatmasını veya dolap pervazına sarılmasını önlemek amacıyla biçme düzeninin her iki ucuna sap ayırıcılar yerleştirilmesi kararlaştırılmıştır.
Dolap: Hasat ünitesi içinde biçme kalitesini en çok dolap performansı etkilemektedir. Biçme düzeninin üstünde ve önünde dönerek çalışan dolap, biçilecek sapları bıçak ağzına yatırmakta ve biçilen sapları makinaya aktarmaktadır.

Dolapta iki farklı ayar imkanı bulunmaktadır. Bunlardan ilki dolabın yükseklik ayarıdır. Dolabın yüksekliği, anız yüksekliği ve tarladaki bitki boyu göz önüne alınarak aşağıdaki eşitlikten bulunmaktadır (Ülger, 1982).

$$C = \frac{D}{2} + \frac{2}{3}(H - h)$$

Bu eşitlikte; C, bıçaklardan itibaren dolap merkezi yüksekliği; D, dolap çapı; H, sap yüksekliği; h, biçme (anız) yüksekliğidir. Dolabın yükseklik ayarı, hasat ünitesinin şase üzerine yerleştirilen üç adet manivela düzeni ile sağlanmaktadır.

Dolap ayarlarından ikincisi de dolabın devir ayarıdır. Dolabın biçilecek sapları bıçak ağzına yatırabilmesi için pervazlardaki çevre hızının makina ilerleme hızından büyük olması (%10-25) gerekmektedir (Kadayıfçılar, 1991). Dolabın tahriki, kolay devir ayar imkanı da tanıyan hidrolik motor ile sağlanmaktadır.
Biçme düzeni: Kombine kesme yapan parmaklı üçgen yapraklı biçme düzeni kullanılmıştır. Biçme düzeni normal bıçak tipinde ve keskin kenarları dişli yapıdadır. Bu tip bıçak kuru ve sert yapıdaki ürünlerin başarıyla kesilmesinde kullanılmaktadır. Bu tip materyaller için uygun bıçak ortalama hızı 1.3-1.9 ms^{-1} önerilmektedir (Kadayıfçılar, 1991). Biçme düzeni, hidrolik motor ile bağlantılı bir eksantrik düzen (Group Schumacher, Germany) aracılığıyla tahrik edilmektedir.

İletim ünitesi

Dolap tarafından yatırılan ve biçme düzeni tarafından biçilen ürünün harmanlama ünitesine iletimi için bantlı tip konveyörün kullanılmıştır. Konveyör tek parça banttan, fakat iki bölümden oluşmaktadır. Konveyörün ilk bölümü biçme düzeninin hemen arkasında yer alan kısım olup ilerleme yönüne dik çalışan pervazlı tip yatay konumda olup diğer kısmı ise materyali harmanlama ünitesine yükseltecek eğimli yönde hareket etmektedir. Konveyöre ait iletim kapasitesi aşağıdaki eşitliğe göre belirlenmiştir (Ayık, 1985).

$$K = 3.6 \cdot k \cdot V$$

Bu eşitlikte; K, konveyör kapasitesi (t/h); k, birim konveyör boyuna düşen özgül yük miktarı (kg/m); V, iletim hızıdır (m/s).

$$k = F \cdot \gamma$$

Bu eşitlikte; F, yükün enine kesit alanı (m^2); γ, yükün yığma ağırlığıdır (kg/m^3).

Harmanlama ünitesi

Belirli bir sap uzunluğunda kapsüllerin kesilmesi durumunda, kapsül kırma ve ayırma aşamasında bu artıkların (sap) uzaklaştırılması gerekmektedir. Bu sorunun ortadan kaldırılması amacıyla belirli uzunlukta kesilmiş sapa sahip kapsüllerin kırılması için uygun parçalama ünitesi kullanılması oldukça önemlidir. Bu çalışmada saplı haşhaş kapsüllerinin parçalanmasına imkân tanıyacak bir çift yivli merdaneli parçalama ünitesi tasarlanmıştır. Çalışmanın hazırlık sürecinde bu ünitenin etkinliğini ortaya koymak amacıyla bir model parçalama ünitesi (Şekil 4) ile yapılan ön denemelerde saplı kapsüllerin boğum noktasından parçalandığı, sapların ise genellikle tek parça halinde üniteyi terk ettiği ortaya konulmuştur. Dolayısıyla parçalama ünitesinden sonraki ayırma ünitesinde farklı boyutlardaki kapsül parçaları, tohumlar ve sapların birbirlerinden ayrılmasının daha kolay olacağı düşünülmektedir.

Şekil 4. Model haşhaş kapsülü parçalama ünitesi

Ayırma ünitesi

Harmanlama ünitesinin altına konumlandırılan ayırma ünitesinde farklı boyutlardaki kapsül parçaları, tohumlar ve saplar birbirlerinden ayrılmaktadır. Karaca (1996) çalışmasında kullandığı haşhaş kapsülü kırma-ayırma makinasında yer alan ayırma sisteminde elek eğimini 0-3º, üst elek numarasını ø5, alt elek numarasını ø2, elek alanlarını 0.54 m^2 olarak vermiştir. Geliştirilen prototip makinada bu ölçüler esas alınarak, harmanlama ünitesinden gelecek materyal dağılımları da göz önünde bulundurularak ölçülendirme yapılmıştır. Ayırma ünitesi elek kasasından oluşmaktadır. Elek kasasında üst üste üç elek yer almaktadır. Üst elek iki kademeli delik çapına sahip yuvarlak delikli sac elektir. Orta elek ise kapsül parçaları ile tohumu birbirinden ayırmaktadır. Karışımın içindeki parçalanma sırasında ortaya çıkan toz ise alt eleğin altında toplanmaktadır.

Çuvallama

Ayırma ünitesinden çıkan kapsül parçaları ve tohumlar makinanın arkasına konumlandırılacak çuvallama üniteleri aracılıyla ayrı ayrı çuvallanacaktır.

Güç aktarım sistemi

Geliştirilen prototip makina üzerinde güç transferi yapılacak 6 nokta bulunmaktadır. Bunlar; dolap, biçme düzeni, konveyör, parçalama ünitesi ve elek kasasıdır. Çeki aracı olan traktörün kuyruk milinden alınan hareketin parçalama ünitesi ve elek kasasına ihtiyaç duyulan devir kademelerinde iletiminde uygun

redüksiyona sahip mekanik güç aktarım sistemleri (kayış-kasnak) kullanılmıştır. Dolap, biçme düzeni ve konveyör tahriki ise traktör hidrolik sisteminden beslenen hidrolik motorlarca sağlanmaktadır.

Bulgular

Tasarım aşamasında prototip makinanın ana kısımlarına ilişkin belirlenen parametreler aşağıda verilmiştir. Ülkemizdeki haşhaş üretim alanlarının küçük ölçekte olması nedeniyle prototip makinanın iş genişliğinin 1500 mm olması planlanmıştır. Prototip makinada 1000 mm çapında, 6 adet düz pervaza ve her pervazda 12 adet parmağa sahip dolap kullanılmıştır. Biçme düzeni 1.69 m/s ortalama bıçak hızını sağlayacak şekilde 600 min^{-1} ortalamada olmak üzere hidromotordan ayarlanabilecek şekilde tasarımı gerçekleştirilmiştir. Ancak bu hız değeri traktör hidrolik çıkışlarına yerleştirilen bir kısma valfi yardımıyla istenilen değerlerde ayarlanabilmektedir.

Konveyör 2 m/s ortalama iletim hızı sağlayacak şekilde 380 min^{-1} ortalamada olmak üzere hidromotordan ayarlanabilmektedir. Biçme ünitesinde olduğu gibi konveyör hızı da traktör hidrolik çıkışlarına yerleştirilen bir kısma valfi yardımıyla istenilen değerlerde ayarlanabilmektedir.

Model parçalama ünitesi ile yapılan ön denemelerde merdanelerin 300 mm çap ve 900 mm uzunluk ölçülerinin etkin bir parçalama için yeterli olduğu görülmüştür. Merdanelerin üzerinde kapsüllerin tutularak araya çekilmesini kolaylaştırmak amacıyla 45º eğimli 2.5 mm derinliğe sahip yivler bulunmaktadır. Merdanelerden birisi 100 min^{-1}, diğeri 200 min^{-1} devirlerde dönecek şekilde kuyruk milinden tahrik edilmektedir.

Elek kasasındaki üst eleğin harmanlama ünitesinin hemen altındaki bölümü ø5 mm deliklere sahip olup, daha sonraki bölümde delik çapları ø27 mm'dir. Bu bölümde kapsül parçaları ve tohum alt eleğe geçerken saplar elek üzerinde ilerleyerek tarlaya sevk edilmektedir. Kapsül parçaları orta eleğin üzerinde hareket ederek elek sonundaki çuvallama ünitesine, tohumlar ise alt elek üzerinden bir diğer çuvallama ünitesine ulaşmaktadır. Elek eğimi 5º, elek ivmesi 11 m/s^2, eksantrik yarıçapı 2.5 cm ve eksantrik devir sayısı 200 min^{-1} devirde dönecek şekilde kuyruk milinden tahrik edilmesi planlanmıştır.

Prototip makinanın tasarım aşaması sonucu oluşturulan görünüm Şekil 5'de sunulmuştur.

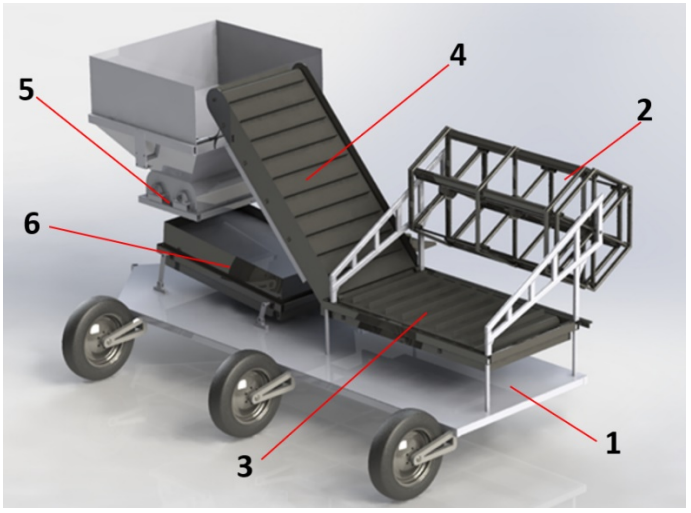

Şekil 5. Makinanın genel şematik görünümü (1: Şasi, 2: Dolap, 3: Yatay konveyör, 4: Eğimli konveyör, 5: Harmanlama ünitesi, 6: Ayırma ünitesi)

Çalışmada tasarım sonucu imalatı gerçekleştirilen haşhaş hasat makinasının genel görünümü Şekil 6'da verilmiştir.

Şekil 6. İmal edilen prototip makinanın genel görünümü

Teşekkür

Bu çalışma, Türkiye Bilimsel ve Teknolojik Araştırma Kurumu (TÜBİTAK) tarafından desteklenmiştir.

Kaynaklar

Anonim (2015). 2014 Yılı Haşhaş Sektör Raporu. TMO Genel Müdürlüğü, Ankara.

Ayık, M. (1985). Ürün İşleme Tekniği ve Makinaları. Ankara Üniversitesi Ziraat Fakültesi Yayınları: 957, Ders Kitabı: 277, Ankara.

Erdurmuş A, Öneş Y. (1990) Haşhaş. T.M.O. Alkasan Yayınları Mesleki Kitaplar, Ankara.

Földesi D. (1992). Poppy. V: Cultivation and processing of medical plants. Hornok L. (ed.). Budapest, Akadémiai Kiadó: 119-128.

Hacıyusufoğlu, A.F. (2013). Laboratuar Koşullarında Haşhaş Kapsül Toplama Sisteminin Geliştirilmesi. Doktora Tezi, Adnan Menderes Üniversitesi Fen Bilimleri Enstitüsü Tarım Makinaları Anabilim Dalı, Aydın.

Kadayıfçılar, S. (1991). Biçer-Döverlerin Tasarım Esasları. Türkiye Zirai Donatım Kurumu Mesleki Yayınları No: 54, Ankara.

Karaca, H. (1996). Afyon Yöresinde Kullanılan Haşhaş Kapsülü Kırma-Ayırma Makinasının Bazı Yapısal ve İşletme Özelliklerinin Belirlenmesi ve Geliştirilmesi. Yüksek Lisans Tezi, Selçuk Üniversitesi Fen Bilimleri Enstitüsü Tarım Makinaları Anabilim Dalı, Konya.

Németh, É. (1998). Raw material production: cultivation of poppy in the temperate zone. In: Bernáth J (ed) Poppy: the genus Papaver. Harwood Academic, pp: 219-255, Amsterdam.

TÜİK, (2017). Bitkisel Üretim İstatistikleri Veri Tabanı; http://www.tuik.gov.tr (Erişim Tarihi: 06.08.2018).

Ülger, P. (1982). Tarımsal Makinaların İlkeleri ve Projeleme Esasları. Atatürk Üniversitesi Yayınları No: 605, Ziraat Fakültesi Yayınları No: 280, Ders Kitapları Serisi No: 43, Erzurum.

International Conference on Science and Technology

ICONST 2018

5-9 September 2018 Prizren - KOSOVO

Acute Stent Thrombosis (Kounis Syndrome?)

Artan Ahmeti[1,2]*, Enis Gerbovič[3], Vigan Mahmutaj[3], Taulant Sadriu[3], Jetmir Sejdiu[3], Sami Gjoka[1], Mahmut Cakmak[3]

Abstract: Stent thrombosis is an uncommon but life-threatening complication after percutaneous coronary intervention (PCI) often manifesting as acute coronary syndrome or even cardiac death (1) (2) (3). The mechanism of thrombosis is multifactorial, hence various procedure, lesion and patient related factors have been associated with its occurrence (4), (5), (6). Potential causes include stent length, complex lesions, suboptimal stent insertion, withdrawal of anti-dual antiplatelet therapy, and hypersensitivity to stent components (7), (8). Beside these factors the role of adjunctive antithrombotic therapy remains unchallenged. Traditional classification categories the complication into early (24h – 30 days), late (30 days to one year), and very late (after one year) (9). The incidence of stent thrombosis ranges between 0.6 and 4.4% (10).

Anahtar Kelimeler: Stent thrombosis, Kounis syndrome

Case Report

A 40-year-old female admitted with complains of typical chest pain. She was smoker for last 15 years and she had positive family history for coronary artery disease (CAD). All findings on physical examination resulted normal: blood pressure 130/80mm mmHg, heart rate 80/minute, and no pathological findings on auscultation. Blood tests resulted: red blood cells = 4.04 x 106/mm3, white blood cells = 10.2 x 103/mm3, hematocrit = 30.7 %, hemoglobin = 9.4 g/dl, Platelets: 341 x 103/mm3, glycemia (not fasting) = 5.1 mmol/L, creatinine = 73 mmol/L, blood urea nitrogen-BUN = 7.2 mmol/L, aspartate transaminase = 10 IU/L, alanine aminotransferase = 19 IU/L, CKMB: 23 U/L, LDH: 408U/L. Troponin HS: 79.1 pg/ml

Her first 12-lead ECG showed no change (Fig nr.1). But, after more than 12-hour observation in the emergency department, were note dynamic ECG change (the inverted T wave in precordial lead), (Fig. nr 2). and elevation of Troponin more than ten-fold (cTn: 815.3 pg/ml). Patient was referred to the Catheterization Laboratory for Primary Percutaneous Coronary Intervention (PCI). Coronary angiography revealed sub occlusive left anterior descending (LAD) in distal segment and had normal left main, right coronary artery and circumflex artery. The LAD was treated with primary PCI with DES 2.75x23 mm (Xience Pro). In control angiography there was TIMI flow III without residual stenosis. The patient was transferred to coronary care unit where here ECG and hemodynamic status was monitored.

Second session (26.02.2017, 02:07 h): Next day about 02:07 she complained for chest pain. ECG was performed and it showed ST segment elevation in V1-V6. She was taken immediately to cath. lab. and coronary angiography revealed thrombus from the ostial segment of LAD to the distal part where stent was implanted. It was predilated with balloon 2.5x 12 mm and then stented with stent 2.75 x 20 mm (Promus) in distal segment and 3.0 x 18 mm (Xience) in proximal segment. 3 ml of Tirofiban and 15 ml of Alteplase was given intracoronary. In control angiography there was TIMI flow III without residual stenosis. Post procedure ECG was done and ST segment begun to decline. 4 hours later another ECG was performed and there were negative

[1]Clinic of Cardiology, University Clinical Centre of Kosova, Prishtina, Kosovo;
[2]Medical Faculty, University of Prishtina, Prishtina, Kosovo;
[3]Istanbul Medicine Hospital, Prishtina, Kosovo;
*Correspondingauthor: artan.ahmeti@uni-pr.edu

T waves with persistent ST elevation about 1 mm in V1-V6. She was transferred to coronary care unit where we began therapy with Tirofiban and heparin continuously and we switched from clopidogrel to prasugrel.

Third session (26.01.2017, 10:17 minute): 8 hours later the chest pain started again. ECG was done and it revealed elevation of ST segment in V1-V6 about 6 mm. Coronary angiography was repeated and it showed proximal stent thrombosis. The cardiosurgeon was consulted for the possibility to perform CABG surgery. Because the first stent was deployed in the distal part of the vessel it was considered as non graftable so we had to continue to do revascularization with PCI. Firstly, the vessel was predilated with balloon 3.0 x 20 mm and then stented with stent 2.5 x 15 mm (Xience). 15 ml of Alteplase was given intracoronary. In control angiography there was TIMI flow III without residual stenosis.

Fourth session: (26.01.2017, 16:50 minute). Patient complained for chest pain and there were ECG changes. Coronary Angiography was repeated and it revealed stent thrombosis in proximal segment. PTCA was performed with balloon size of 3.0 x 20 mm and 3.0 x 30 mm. Due to suspicion on metal allergy we started therapy with Diphenhydramine tab 500 mg 1x1. P.O

Fifth session (27.01.2017 14:58 min). Patient complained for chest pain and there were ECG changes. Coronary angiography was repeated and it revealed proximal stent thrombosis. It was predilated with balloon NC 3.0 x 20 mm, 3.0 x 27 mm and then it was stented with BMS stent of size 3.0 x 12 mm. In control angiography there was TIMI flow III with residual thrombus in distal part of stent. We decided to switch from Prasugrel to Ticagrelor and methylprednisolone IV was given.

Sixth session (27.01.2017, 20:09 min). Patient complained for chest pain and there were ECG changes. Coronary angiography was repeated and it revealed proximal stent thrombosis. PTCA was performed with balloon NC 3.0 x 27 mm. In control angiography there was TIMI flow III with residual thrombus in distal part of stent.

Seventh session (28.01.2017). Patient complained for chest pain and there were ECG changes. Coronary angiography was repeated and it revealed proximal stent thrombosis. Thrombus aspiration was performed and then PTCA with balloon 3.0 x 20 mm. The patient condition got worsen. She experienced cardiorespiratory arrest. CPR was performed, normal sinus rhythm (NSR) was returned but she remained in respirator.

Eighth session: (28.01.2017). Coronary angiography was repeated and it revealed LMCA occlusion. A stent was deployed in LMCA to LCX. In control angiography there was TIMI flow 0 in LAD and TIMI flow III in LCx. Patient was transferred to Coronary Care unit where she experienced another episode of Cardiac arrest and despite CPR she could not survive and died.

Laboratory tests : urea: 17.0..23.9 mg/dl, creatinine: 0.65…0.50…1.30 mg/dl, Glucose: 105.4…126.5 mg/dl, Cholesterol Total: 146.5 mg/dl, Triglycerides: 164.4 mg/dl, ALT: 11.4 U/I, AST: 29.0U/I, CK: 220.6U/L, CK-MB: 14.9 U/L, Troponin T: 955.0 µg/L, Sodium: 145mEg/L, Potassium: 4.1 mmol/L, WBC: 8.9..15.1…13.6 x 103/mm3, RBC: 4.73…4.17..3.87 106/mm3, HGB: 9.6…8.7..7.7 g/dl, HCT: 30.1…27.2…24.3 , PLT: 340…216…191 x 103/mm3, HBSAG: neg., Anti-HIV: neg., Anti HCV: neg.

Discussion

The pathophysiology of early stent thrombosis it's not still fully understood, but combination of factors may be involved, including procedural factors, such insufficient expansion of the stent, inadequate post-procedural lumen dimensions, residual dissection, slow flow and location of the lesion in bifurcation (4), (11), (12). In most cases stent thrombosis present as acute myocardial infarction (MI), and mora than 60 > with ST elevation MI (STEMI) (13).

Early stent thrombosis

When the thrombosis occurs within 30 days after stent implantation. In this case the technical and procedural factors are important. Early stent thrombosis has higher incidence when the result of procedural is suboptimal (e.g. slow flow, stent under expansion and malposition, coronary dissection and tissue prolapse) (4), (11), (16). Because the arterial segment of stenting has not reendothelialized, discontinuation of dual antiplatelet therapy drugs (DAPT) will provoke stent thrombosis.

Stent allergy (Kounis Syndrome): Several important papers have been published concerning hypersensitivity toward metallic stent failure such as restenosis-thrombosis. The polymer coating fragment and expose metal struts (17). The elements like nickel, cobalt, and molybdenum are known to cause contact allergy (18), (19), (20). Studies of related polymers have demonstrated local and systemic hypersensitivity responses to intravascular and locally applied polymers, usual a type IV hypersensitivity mediated by allergen-specific T lymphocytes (21). Because of paucity of Langerhans cells compared to the skin, the stents of coronary vessels triggers a weak immunological response (22), (23). The systemic administration of anti-inflammatory therapy might be appropriate when a metal allergy is confirm or strongly suspected (24), (25).

Heparin-induced thrombocytopenia (HIT)

When acute coronary thrombosis occurs during PCI, HIT should always be strongly considered. HIT is a critical cause of severe thrombotic complications associated with PCI. HIT may develop in two distinct forms: type I and type II (26). Type 1 HIT is a nonimmune disorder that results from the direct effect of heparin on platelet activation and presents within the first 2 days after exposure to heparin. Type 2 HIT is an immune-mediated disorder that typically occurs 4-10 days after exposure to heparin and has life-threatening thrombotic complications (27), (28).

Since seroconversion of anti-PF4/heparin antibodies can occur in approximately 10% of patients after PCI with heparin use (19). HIT should be considered in patients who will undergo PCI, especially if they underwent PCI within the past month. HIT antibodies can develop five days after the initiation of heparin administration or later (29), (30).

Protein S deficiency

Protein S is a plasma protein that serves as a cofactor for the anticoagulant effect (31). A protein S deficiency is a well-known genetic tendency to the thromboembolism (32). However, protein S deficiency was not generally considered as a risk factor for intervention. While several reports indicated coronary thrombosis in patients with protein S deficiency, their coronary arteries did not have organic stenosis or evidence of plaque rupture (33), (34).

Treatment of stent thrombosis

Primary PCI is the treatment of choice. It seems reasonable to post dilation correct stent under expansion and malposition with high pressure balloons (NC). Intravascular ultrasonography (IVUS) and Optical Coherence tomography (OCT) might have value to guide coronary reintervention.

Conclusion

Although Early Stent Thrombosis is a rare complication after PCI but are associated with high morbidity and mortality rate. Our patient had frequent stent thrombosis and she underwent 8 procedures of coronary angiography and PCI. Our concern is to determine the etiology of frequent stent thrombosis. Taking into consideration that we have tried many types of antiaggregation therapy as clopidogrel, prasugrel, tikagrelor, tirofiban we can exclude drug resistance as a possible cause.

The patient was not known to have used UFH recently. Immune-mediated HIT usually occurs between 5 to 14 days after first beginning heparin therapy so occurence of stent thrombosis, many hours after it was implanted,

excludes HIT as a possible cause of stent thrombosis. Genetic causes of hypercoagulability were not tested but in patient's history we did not find any event of systemic thrombosis. It is worth noting that the patient told us for possible allergy to gold, metal as she had some skin changes on finger and ear due to ring and earring. Allergic acute coronary syndrome (Kounis Syndrome) may be a cause of stent thrombosis. There were no systemic allergic reaction and we did not do blood testing for allergies. By excluding other possible causes, even though not proven by any test, we can consider Kounis Syndrome to be the cause of frequent stent thrombosis in the case of our patient. Antihistamine and steroids was included in the therapy, in the second day, but it was not proven successful to prevent stent thrombosis.

References/Kaynaklar

1. Vlachojannis GJ, Postdoctoral Research Fellow, Interventional Cardiovascular Research, Mount Sinai Medical Center, Claessen BE, Cardiology Fellow, Academic Medical Centre Amsterdam, Dangas GD, Professor of Medicine, Mount Sinai School of Medicine; Director of Cardiovascular Innovation, Zena and Michael A Weiner Cardiovascular Institute, Mount Sinai Medical Center, One Gustave L Levy Place (Box 1030), New York, NY 10029, US. E: george.dangas@mountsinai.org. Early Stent Thrombosis after Percutaneous Coronary Intervention for Acute Myocardial Infarction. Interv Cardiol Rev. 2012;7(1):33.

2. Cutlip DE, Baim DS, Ho KK, Popma JJ, Lansky AJ, Cohen DJ, et al. Stent thrombosis in the modern era: a pooled analysis of multicenter coronary stent clinical trials. Circulation. 2001 Apr 17;103(15):1967–71.

3. Lemesle G, Delhaye C, Bonello L, de Labriolle A, Waksman R, Pichard A. Stent thrombosis in 2008: Definition, predictors, prognosis and treatment. Arch Cardiovasc Dis. 2008 Nov;101(11–12):769–77.

4. van Werkum JW, Heestermans AA, Zomer AC, Kelder JC, Suttorp M-J, Rensing BJ, et al. Predictors of Coronary Stent Thrombosis. J Am Coll Cardiol. 2009 Apr;53(16):1399–409.

5. Généreux P, Stone GW, Harrington RA, Gibson CM, Steg PG, Brener SJ, et al. Impact of intraprocedural stent thrombosis during percutaneous coronary intervention: insights from the CHAMPION PHOENIX Trial (Clinical Trial Comparing Cangrelor to Clopidogrel Standard of Care Therapy in Subjects Who Require Percutaneous Coronary Intervention). J Am Coll Cardiol. 2014 Feb 25;63(7):619–29.

6. Nakano M, Yahagi K, Otsuka F, Sakakura K, Finn AV, Kutys R, et al. Causes of Early Stent Thrombosis in Patients Presenting With Acute Coronary Syndrome. J Am Coll Cardiol. 2014 Jun;63(23):2510–20.

7. Claessen BE, Henriques JPS, Jaffer FA, Mehran R, Piek JJ, Dangas GD. Stent Thrombosis. JACC Cardiovasc Interv. 2014 Oct;7(10):1081–92.

8. Farb A. Pathological Mechanisms of Fatal Late Coronary Stent Thrombosis in Humans. Circulation. 2003 Oct 7;108(14):1701–6.

9. Tyczyński P, Karcz MA, Kalińczuk Ł, Fronczak A, Witkowski A. Editorial Early stent thrombosis. Aetiology, treatment, and prognosis. Adv Interv Cardiol. 2014;4:221–5.

10. Buchanan GL, Basavarajaiah S, Chieffo A. Stent Thrombosis: Incidence, Predictors and New Technologies. Thrombosis. 2012;2012:1–12.

11. Moussa I, Di Mario C, Reimers B, Akiyama T, Tobis J, Colombo A. Subacute stent thrombosis in the era of intravascular ultrasound-guided coronary stenting without anticoagulation: frequency, predictors and clinical outcome. J Am Coll Cardiol. 1997 Jan;29(1):6–12.

12. Lüscher TF, Steffel J, Eberli FR, Joner M, Nakazawa G, Tanner FC, et al. Drug-eluting stent and coronary thrombosis: biological mechanisms and clinical implications. Circulation. 2007 Feb 27;115(8):1051–8.

13. Armstrong EJ, Feldman DN, Wang TY, Kaltenbach LA, Yeo K-K, Wong SC, et al. Clinical Presentation, Management, and Outcomes of Angiographically Documented Early, Late, and Very Late Stent Thrombosis. JACC Cardiovasc Interv. 2012 Feb;5(2):131–40.

14. Morice M-C, Serruys PW, Sousa JE, Fajadet J, Ban Hayashi E, Perin M, et al. A Randomized Comparison of a Sirolimus-Eluting Stent with a Standard Stent for Coronary Revascularization. N Engl J Med. 2002 Jun 6;346(23):1773–80.

15. Biondi-Zoccai GGL, Agostoni P, Sangiorgi GM, Airoldi F, Cosgrave J, Chieffo A, et al. Incidence, predictors, and outcomes of coronary dissections left untreated after drug-eluting stent implantation†. Eur Heart J. 2006 Mar 1;27(5):540–6.

16. Cheneau E. Predictors of Subacute Stent Thrombosis: Results of a Systematic Intravascular Ultrasound Study. Circulation. 2003 Jun 23;108(1):43–7.

17. Virmani R, Guagliumi G, Farb A, Musumeci G, Grieco N, Motta T, et al. Localized hypersensitivity and late coronary thrombosis secondary to a sirolimus-eluting stent: should we be cautious? Circulation. 2004 Feb 17;109(6):701–5.

18. Aliağaoğlu C, Turan H, Erden İ, Albayrak H, Özhan H, Başar C, et al. Relation of Nickel Allergy with in-Stent Restenosis in Patients Treated with Cobalt Chromium Stents. Ann Dermatol. 2012;24(4):426.

19. Konishi T, Yamamoto T, Funayama N, Yamaguchi B, Sakurai S, Nishihara H, et al. Stent thrombosis caused by metal allergy complicated by protein S deficiency and heparin-induced thrombocytopenia: a case report and review of the literature. Thromb J [Internet]. 2015 Dec [cited 2018 Jun 21];13(1). Available from: http://www.thrombosisjournal.com/content/13/1/25

20. Wataha JC, O'Dell NL, Singh BB, Ghazi M, Whitford GM, Lockwood PE. Relating nickel-induced tissue inflammation to nickel release in vivo. J Biomed Mater Res. 2001;58(5):537–44.

21. van der Giessen WJ, Lincoff AM, Schwartz RS, van Beusekom HM, Serruys PW, Holmes DR, et al. Marked inflammatory sequelae to implantation of biodegradable and nonbiodegradable polymers in porcine coronary arteries. Circulation. 1996 Oct 1;94(7):1690–7.

22. Romero-Brufau S, Best PJM, Holmes DR, Mathew V, Davis MDP, Sandhu GS, et al. Outcomes After Coronary Stent Implantation in Patients With Metal Allergy. Circ Cardiovasc Interv. 2012 Apr 1;5(2):220–6.

23. Nebeker JR, Virmani R, Bennett CL, Hoffman JM, Samore MH, Alvarez J, et al. Hypersensitivity Cases Associated With Drug-Eluting Coronary Stents. J Am Coll Cardiol. 2006 Jan;47(1):175–81.

24. Farb A, Weber DK, Kolodgie FD, Burke AP, Virmani R. Morphological predictors of restenosis after coronary stenting in humans. Circulation. 2002 Jun 25;105(25):2974–80.

25. Rogers C, Welt FG, Karnovsky MJ, Edelman ER. Monocyte recruitment and neointimal hyperplasia in rabbits. Coupled inhibitory effects of heparin. Arterioscler Thromb Vasc Biol. 1996 Oct;16(10):1312–8.

26. Rice L. Heparin-Induced Thrombocytopenia: Myths and Misconceptions (That Will Cause Trouble for You and Your Patient). Arch Intern Med. 2004 Oct 11;164(18):1961.

27. Warkentin TE, Greinacher A. Heparin-induced thrombocytopenia: recognition, treatment, and prevention: the Seventh ACCP Conference on Antithrombotic and Thrombolytic Therapy. Chest. 2004 Sep;126(3 Suppl):311S–337S.

28. Greinacher A. CLINICAL PRACTICE. Heparin-Induced Thrombocytopenia. N Engl J Med. 2015 Jul 16;373(3):252–61.

29. Williams RT. Anti-Platelet Factor 4/Heparin Antibodies: An Independent Predictor of 30-Day Myocardial Infarction After Acute Coronary Ischemic Syndromes. Circulation. 2003 May 13;107(18):2307–12.

30. Warkentin TE, Sheppard J-AI, Moore JC, Cook RJ, Kelton JG. Studies of the immune response in heparin-induced thrombocytopenia. Blood. 2009 May 14;113(20):4963–9.

31. Lipe B, Ornstein DL. Deficiencies of Natural Anticoagulants, Protein C, Protein S, and Antithrombin. Circulation. 2011 Oct 4;124(14):e365–8.

32. Mateo J, Oliver A, Borrell M, Sala N, Fontcuberta J. Laboratory evaluation and clinical characteristics of 2,132 consecutive unselected patients with venous thromboembolism--results of the Spanish Multicentric Study on Thrombophilia (EMET-Study). Thromb Haemost. 1997 Mar;77(3):444–51.

33. Carrié D, Béard T, Sié P, Boudjemaa B, Delay M, Bernadet P. [Simultaneous thrombosis of the left anterior interventricular and right coronary arteries in a 27 year-old patient with protein S deficiency]. Arch Mal Coeur Vaiss. 1993 Jun;86(6):921–4.

34. Manzar KJ, Padder FA, Conrad AR, Freeman I, Jonas EA. Acute myocardial infarction with normal coronary artery: a case report and review of literature. Am J Med Sci. 1997 Nov;314(5):342–5.

International Conference on Science and Technology

ICONST 2018

5-9 September 2018 Prizren - KOSOVO

Trialeurodes vaporariorum Westfood (Hom.: Aleyrodidae) Üzerinde Bazı Böcek Gelişim Düzenleyicilerin (IGR) Etkisi / Effects of some IGRs on Greenhouse whitefiles (*Trialeurodes vaporariorum* Westfood (Hom.: Aleyrodidae)

Hasan Sungur Civelek[1]*, Oktay Dursun[2], Mert Kosovaeri

Özet: Bu çalışma 09.04.2007 ve 18.06.2007 tarihleri arasında laboratuar koşullarında, sera beyazsineği, *Trialeurodes vaporariorum* (Hom.: Aleyrodidae) mücadelesinde böcek gelişim düzenleyicisi (IGR) etkiye sahip bileşiklerin etkilerinin ortaya konulabilmesi amacıyla gerçekleştirilmiştir. Ortaca (Muğla) seralarından Mart 2007 döneminde temin edilen sera beyazsineği erginleri laboratuarda yetiştirilmekte olan domates fidelerinin üzerine salınmıştır. Saksılarda yetiştirilen bitkilerden, her bir uygulama için beşer saksı tesadüfi olarak seçilmiştir. Dört çeşit IGR(Böcek Gelişim Düzenleyicisi) etkiye sahip insektisitler Lufenuron (Lufenox, Sygenta, 100cc/100 L); Diflubenozuron (Dimilin, Cansa, 20gr/100 L); Pyriproxyfen (Admiral, Sumitomo, 50cc/100L) ve Neem Azal T/S (Trifolio-M, Lahnau/ Germany, 4 L/100 L) önerilen dozlarda kullanılmıştır. Ardarda iki uygulama şeklinde gerçekleştirilen bu çalışmada, ilaçlamalar haftada bir tekrar edilerek toplam 5 ilaçlama yapılmıştır. Sayımlar ilaçlama öncesi populasyonu (T+0), ilaçlamadan bir gün sonraki canlı nimf sayısı (T+1), ilaçlamadan üç gün sonraki canlı nimf sayısı (T+3) ve ilaçlamadan yedi gün sonraki canlı nimf sayıları (T+7) tespit edilmiştir. Birinci uygulama sonucunda kullanılan preparatların etkisi önemsiz bulunmuş, ikinci uygulamada ise sadece Admiral'in etkisi diğerlerine göre önemli ama kontrole yakın bulunmuştur. Dolayısıyla her 2 uygulamada da beklenen etki elde edilememiştir.

Sera beyazsineği kısa zamanda döl veren yüksek üreme gücüne sahip bir zararlıdır. Bu nedenle bulunduğu ortamda dölleri kısa zamanda iç içe geçebilmekte ve her biyolojik dönemi bir arada bulunabilmektedir. Kullanılan preparatlar zararlıların ergin öncesi dönemleri üzerinde etkili olup ergin öldürücülük yetenekleri son derece kısıtlıdır. Bu nedenle böcek gelişim düzenleyicilerinin, sera beyazsineği gibi üreme gücü çok yüksek olan bir zararlının kontrolünde eğer zararlının ilaçlama başlangıcındaki populasyonu da yüksekse etkili olamadıkları düşünülmektedir. Dolayısıyla sera beyazsineği gibi zararlılara karşı böcek gelişim düzenleyicileri kullanılacağı zaman, baskı altına alınabilme süreçlerini daha kısa ve ekonomik hale getirebilmek amacıyla başlangıçta etki süresi kısa, seçici bir sentetik insektisitin en düşük dozunda uygulanması ve sonraki uygulamalarda böcek gelişim düzenleyicilerin programa alınması son derece yararlı olacaktır.

Anahtar Kelimeler: *Trialeurodes vaporariorum*, Beyazsinek, IGR, Türkiye

Abstract: The study was conducted in laboratory conditions between 09.04.2007 and 18.06.2007 as to find out the effects of IGRs at greenhouse whitefly control. It was implemented as two trials. Whitefiles collected from greenhouses around Ortaca in March 2007 were let in tomato seedlings grown in laboratory. Five vases of tomato seedling were chosen randomly for each insectiside and some IGR effecting insecticides (Lufenuron, Lufenox, Sygenta, 100cc/100 L; Diflubenozuron, Dimilin, Cansa, 20gr/100 L; Pyriproxyfen, Admiral, Sumitomo, 50cc/100L ve Neem Azal T/S (Trifolio-M, Lahnau/ Germany, 4 L/100 L) were applied at offered doses. At controls of both 2 periods, totally five weekly applications were done. Counts of living larva were a day before the treatment (T+0), after a day (T+1) and after three days (T+3) and after seven days (T+7). In the

[1] Muğla Üniversitesi, Fen Fakültesi, Biyoloji Bölümü, Kötekli/ Muğla, TURKEY
*Correspondingauthor: chasan@mu.edu.tr

first application effects of the IGRs were not significant, in the second one, effect of Admiral was more significant compared to the others but it was just at a similar level to control. So the expected result couldn't be reached at both application processes.
Greenhouse whitefly is a pest having a high reproduction rate and giving generations in a short period, so it's overlap generations from each biological period can be found. Pereparats have effects in immature stages but so limited on adult whiteflies. So IGRs are not effective on a pest having a high production potential like whitefly if the population is much when the application starts. In conclusion,when IGRs are used; to make the pressure period shorter and cheaper, applying a low-dose synthetic insecticide having a short effect at the begining and including IGRs in following applications will be more useful.

Keywords: *Trialeurodes vaporariorum*, Whitefly, IGR, Turkey

Giriş

Trialeurodes vaporariorum Westfood (Hom., Aleyrodidae) (Sera Beyazsineği) serin bölgelerde seralarda yetiştirilen pek çok bitkide zararlı bir türdür (Lodos 1986). Daha önce yapılan araştırmalarda serada domates ve hıyar bitkilerinde zararlı olan sera beyazsineğine yalnızca ilkbaharda, sonbahar üretim döneminde ise hakim tür olarak pamuk beyazsineği *Bemisia tabaci*' ye rastlanıldığı belirtilmektedir. (Öncüer et al, 1994). Yaşarakıncı ve Hıncal (1997), tarafından *T. vaporariorum'* un tüm seralarda domatesin çiçeklenme dönemi öncesinde görülmeye başladığı; çiçeklenme ve meyve dönemi olan Haziran- Temmuz aylarında maksimum yoğunluğa ulaştığı bildirilmiştir.

Beyazsinekler seralardaki sebzelerde, ortamın sıcaklığına ve nemine bağlı olarak mevsim boyunca yaşamlarını sürdürebilmektedir.. Erginler 14°C' nin altında yumurta bırakmakta ve 10°C' nin altında ise faaliyetlerini yavaşlatmaktadır. . Yılda ortalama 9–10 döl verebilen bu türün dişileri ortalama 200–300 yumurta bırakmaktadır. Beyazsinek türlerinin en iyi gelişme gösterdiği sıcaklık aralığı 25°C, en iyi nem oranı ise %60'ın üzerindeki orantılı nem koşullarıdır. Bu koşullarda bazı türler 4–5 hafta gibi çok kısa bir sürede zarar yapacak populasyon yoğunluğuna ulaşabilirler (Ulusoy, 2001). Polifag bir zararlı olup, özellikle domates, hıyar, biber, fasulye ve patlıcanda önemli zararlara neden olmaktadır. Beyazsinek erginleri gerek beslenme ve yumurta bırakma gerekse dinlenme için yaprakların alt yüzeyini ve bitkilerin alt kısımlarını tercih ederler. Sera beyazsineği *T. vaporariorum* bitkiye doğrudan ve dolaylı olarak zarar vermektedir. Larva ve erginlerin bitki özsuyunu emerek beslenmeleri ve buna bağlı olarak da bitkinin zayıflaması, yaprakların sararması beyazsineğin doğrudan meydana getirdiği zararlardandır. Ayrıca beslenme sırasında tatlı ve yapışkan bir madde salgılayarak, fumajin oluşturması; bitkide fotosentezin sekteye uğramasına, bitkinin görünümünün bozulmasına ve pazar değerinin düşmesine neden olarak dolaylı zararlara da yol açarlar. Erginlerin bazı virüslere vektörlük etmesi ise bitkiye verdiği en önemli dolaylı zarardır. Bu zarar, zaman zaman direkt zararından daha önemli olabilmektedir (Anonymous, 2007).

Seralar taşıdığı uygun fiziksel koşullar nedeniyle kimyasal savaş dışındaki diğer savaş yöntemlerinin daha geniş olarak uygulanabileceği ve başarılı olabileceği ortamlardır. Bunların arasında biyolojik savaş çalışmaları da yer almaktadır (Yoldaş, 1995). *T. vaporariorum* populasyonun yaprak başı 5 nimf olduğunda, yaprak başına 1 adet olacak şekilde *Encarsia formosa* (Gahan) (Hymenoptera, Aphelinidae)' nın düzenli olarak salınımıyla ***baskı*** altında tutabileceğini bildirmektedir.

T. vaporariorum'a karşı kimyasal savaşta yoğun olarak sentetik insektisitler kullanılmaktadır. Fakat son yıllarda sentetik insektisitlerin bilinçsizce kullanımı sonucu zararlılarda oluşan dayanıklılık, insan, çevre ve hedef dışı organizmalara olumsuz etkileri, bilimsel çalışmalarla kanıtlanmış ve bu zararlıyla savaşta eğilim, biyolojik savaş etmenleri ve doğal organik insektisitlerin kullanılması yönünde artmıştır (Miller and Uetz,1998).

Söz konusu doğal organik insektisitlerden en önemlisi ve en çok kullanılanı *Azadirachta indica* Juss. (Melliceae)'dan elde edilen azadirachtin etkili maddesidir (Schmutterer, 1990; Copping and Menn, 2000). Bunun yanında yurtdışında doğal yağ asitlerinin potasyum tuzlarından elde edilmiş maddeler de örtü altı zararlılarından yaprakbitleri, tripsler ve beyazsineklere karşı savaşta kullanılmaktadır (Copping, 2001). Neem

azal ve neem oil tarımsal savaşta zararlı mücadelesinde en yaygın kullanılan bitkisel kökenli insektisittir. Beyazsinekler, yaprak bitleri, kırmızı örümcekler, larvalar, galerisineği, thripsler gibi zararlılara etkili olduğuna dair bir çok çalışma bulunmaktadır (Awad ve ark.,1998). Neem' in tarlalarda yaygın olarak kullanıldığı dozlar ya da düşük dozları uygulandığında parazitoitler üzerindeki etkisi de oldukça düşüktür. Sulu neem süspansiyonlarının neem yağı ekstraktlarından daha az toksik olduğu bildirilmiştir (Condor, 2007).

Böcek gelişim düzenleyicileri (IGR) ve böcek gelişim engelleyicileri (IDI), seçici ve özel etki şekilleri ile hem çevre kirlenmesi hem de dayanıklılığı önlemesi gibi olumlu yönleriyle günümüzün en aktüel konusunu oluşturmuştur. Böceklerin kendi gelişmeleri için vücutlarında salgılanan bu bileşikler kullanılarak özellikle böceklerin doğal hormon dengeleri bozulmakta ve böylece büyüme ve gelişme engellenerek veya durdurularak zararlarının önlenmesi bu tekniğin ana prensibidir. Böceklerde hormon dengesini etkileyen ve uygulamalı entomoloji de pratiğe geçmiş olan en önemli maddeler Juvenil Hormon ve Benzoylurea türevleridir (Derinbay, 2008). Benzoylurea türevi içerisinde en yaygın bilinen, Diflubenzuron, böceklerde kitin oluşumunu engelleyen ve larvaların gömlek değiştirmeyerek ölümlerine neden olan bir bileşiktir (Zeki et al., 1999). Potansiyel bir kitin sentezi engelleyicisi olarak kabul edilen cryomazin' in etki mekanizması tam olarak açıklığa kavuşturulmamakla beraber yapılan çalışmalarda hücre turgor basıncını arttırdığı, kütikuladaki keselerin sıvı ile dolmasına neden olduğu sonuçta kütikulada lezyonlar oluşturmakta bunun sonucu olarak da deri değiştirmeesnasında anormalliklere neden olmaktadır (Ünal &Gürkan, 2001).

Mart ve ark. (2001), *Bemicia tabaci* üzerinde yaptıkları çalışmada, buprofezin ve pyriproxyfen etkili maddeli IGR' ların, zararlının yoğunluğunun düşük olduğu ilk ilaçlamalarda kullanılması hem yararlı türlerin korunması açısından hem de direnç oluşumunun geciktirilmesi yönünden faydalı olacağını belirtmişlerdir. Aynı çalışmanın sonucu olarak etkileri araştırılan böcek gelişim düzenleyicilerinden buprofezin ve pyriproxyfen içeren preparatların beyazsinek erginlerine etkisi, karşılaştırma ilaçlarına oranla düşük bulunurken, larva ve pupalara karşı etkisi yüksek bulunmuş ve pamuk alanlarında *B. tabaci*' ye karşı kullanılabileceği belirlenmiştir.
Bu çalışma sera beyazsineği, *T.vaporariorum'* un mücadelesinde sentetik insektisitlere alternatif olarak 4 farklı IGR özellikte preparatın etkilerinin ortaya konulabilmesi amacıyla gerçekleştirilmiştir.

Material and Method / Materyal ve Yöntem

Bu çalışmanın ana materyalini *Lycopersicum esculentum* var. M–16 ve *L. esculentum* var. Jaledo cinsi domatesler, domatesin ana zararlıları arasında bulunan sera beyazsineği *T. vaporariorum* ve üç çeşit böcek gelişim düzenleyicisi (IGR) ve yine aynı etkiye sahip bitkisel kökenli bir preparat oluşturmuştur.

Bu çalışma 09.04.2007 ve 18.06.2007 tarihleri arasında 22^0C±2 sıcaklık, % 49±5 oransal nem ve 14:10 (A:K) aydınlanma koşullarına sahip laboratuvar koşullarında ardı ardına iki deneme olarak Muğla Üniversitesi Fen Edebiyat Fakültesi Biyoloji Bölümü Entomoloji Laboratuvarı' nda gerçekleştirilmiştir.

Bitki Yetiştirme

Antalya'dan getirilen, *L. esculentum* var. M–16 cinsi domates fideleri birinci denemede, *L. esculentum* var. Jaledo cinsi domates fideleri ise ikinci denemede kullanılmıştır. Bu fideler 25x15 cm ebatlarındaki plastik saksılara dikilerek laboratuvar ortamında yetiştirilmiştir.

Trialeurodes vaporariorum' un Üretimi

Ortaca (Muğla) seralarından Mart 2007 döneminde temin edilen sera beyazsineği erginleri, yetiştirilmekte olan domates fidelerinin üzerine salınmıştır. Kısa zamanda üreyen beyazsinek bireyleri IGR' ların etkisi üzerine yapılacak denemelerde kaynak olarak kullanılmıştır.

İnsektisit Uygulamaları ve Sayımları

Her iki denemede de IGR etkili olan Lufenuron (Lufenox, Sygenta, 100cc/100 L); Diflubenozuron (Dimilin, Cansa, 20gr/100 L); Pyriproxyfen (Admiral, Sumitomo, 50cc/100L) ve Neem Azal T/S (Trifolio-M, Lahnau/ Germany, 4 L/100 L) önerilen dozlarda kullanılmıştır. Admiral, *T. vaporariorum* üzerinde ruhsatlı olup pozitif

kontrol ilacı olarak kullanılmıştır. Ayrıca sadece su uygulaması yapılan bitkiler ilaçsız kontrol örnekleri olarak kullanılmıştır.

Yetiştirilen bitkilerden, her bir uygulama için beşer saksı olmak üzere toplam 25 saksı rastgele seçilmiştir. Böylece deneme her bir karakter için beşer tekerrürde kurulmuştur. İlaçlamalardaki sayım yöntemi Tarım Bakanlığı Koruma Kontrol Genel Müdürlüğü ilaçlama yönetmeliğine uygun olarak gerçekleştirilmiştir (Anonymus, 2007). Bu amaçla, *T. vaporariorum* nimflerinin ilaçlama öncesi populasyonu (T+0), ilaçlamadan bir gün sonraki canlı nimf sayısı (T+1), ilaçlamadan üç gün sonraki canlı nimf sayısı (T+3) ve ilaçlamadan yedi gün sonraki her bitki için canlı nimf sayısı (T+7) sayılarak kaydedilmiştir.

İlaçlamalar 1 litrelik el pülverizatörleriyle yapılmıştır. Beyazsinek nimfleri yaprağın alt kısmında olduğundan ilaçların yaprağın alt kısmına temas edecek şekilde püskürtülmesine özen gösterilmiştir.

Birbiri ardı sıra kurulan her 2 denemede de ilaç uygulamaları haftada 1 tekrar edilmiştir. Böylece 1. denemede toplam 5 ilaçlama ve 15 sayım, 2. denemede de toplam 5 ilaçlama ve 16 sayım sayım yapılarak sonuçlar elde edilmiştir.

Sayımlarda her saksıdaki bitki üzerinden rastgele 5 yaprak seçilmiş ve bu yapraklardaki sera beyazsinek nimfleri sayılarak kaydedilmiştir.

Data Analizi

Yapılan çalışmada kullanılan insektisitlerin *T. vaporariorum* nimflerinin populasyonuna etkilerini belirlemek için SPSS (15.0) Software paket programı kullanılarak tek yönlü varyans analizi yapılmıştır. Gruplar arası farklılığın $p < 0.05$'e göre istatistiksel anlamda farklı çıkması halinde bu farklılıkların gruplar arasındaki önemi için LSD (en küçük önemli fark) testi kullanılmıştır.

Bulgular

3 farklı IGR özellikteki insektisit ve bitkisel kökenli insektisit etkisi bilinen Neem Azal-T/S ile domatesteki beyazsinek *T. vaporariorum* populasyonuna etkisi üzerine yapılan çalışmanın sonuçları Şekil 1, 2 ve Çizelge 1 de verilmiştir.

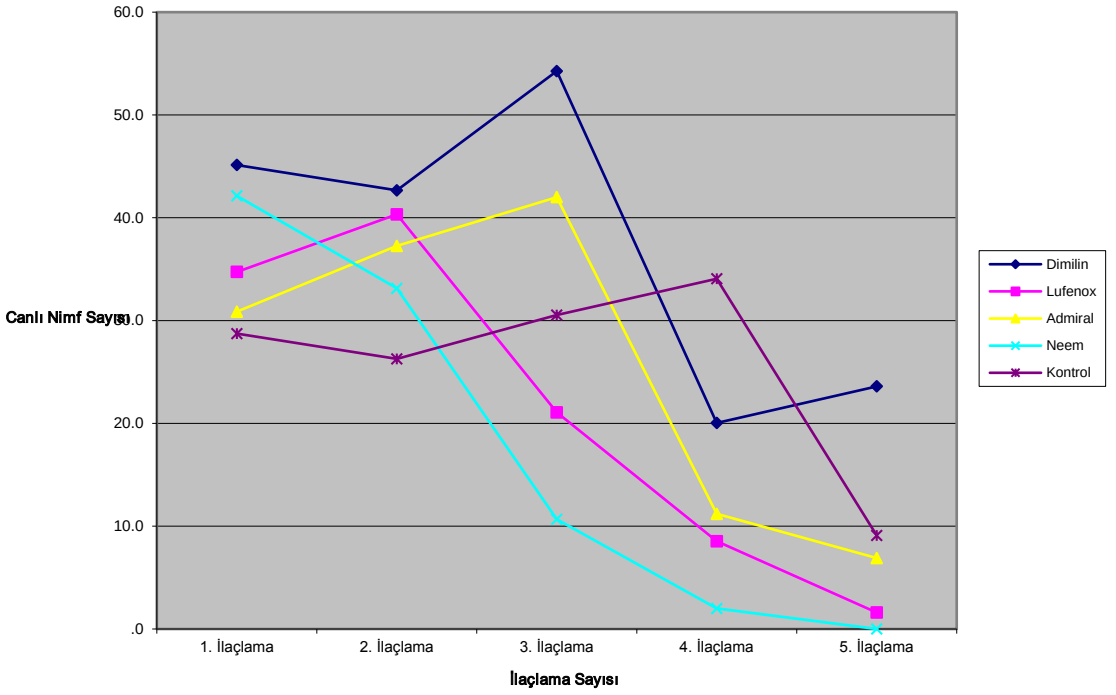

Şekil 1. 1. İlaç denemesi sonucunda gerçekleşen sera beyazsineği populasyon dalgalanması.

Çizelge 1. Denemede kullanılan insektisitler ve her iki denemede *Trialeurodes vaporariorum* nimflerinin ortalama canlı sayıları (± S.E.)

İlacın Adı	**1. Deneme**	**2.deneme**
Admiral	31.33 ± ab	26.40 ± a
Dimilin	43.07 ± b	36.87 ± ab
Lufenox	27.04 ± a	48.48 ± bc
Neem Azal-T/S	26.26 ± a	59.38 ± c
Kontrol	29.92 ± a	31.01 ± ab

Aynı sütunda aynı harfi taşıyan ortalamalar arasındaki fark istatistiksel olarak önemsizdir ($p<0.05$).

1. ilaç denemesinde sonuçlarından anlaşılacağı gibi, Lufenox ve NeemAzal-T/S uygulanan bitkilerde beyazsinek populasyonun kontrol grubu ile aynı, , Admiral ve Dimilin uygulanan bitkilerde ise zararlı populasyonunun kontrolden bile daha yüksek olduğu belirlenmiştir. Hatta Dimilin uygulanan saksılarda beyazsinek yoğunluğu en yüksek seviyede tesbit edilmiştir. Dolayısıyla 1. deneme itibariyla uygulanan ilaçların etkisi önemsiz bulunmuştur ($p> 0.05$, $F= 2.289$, $dF= 4.32$).

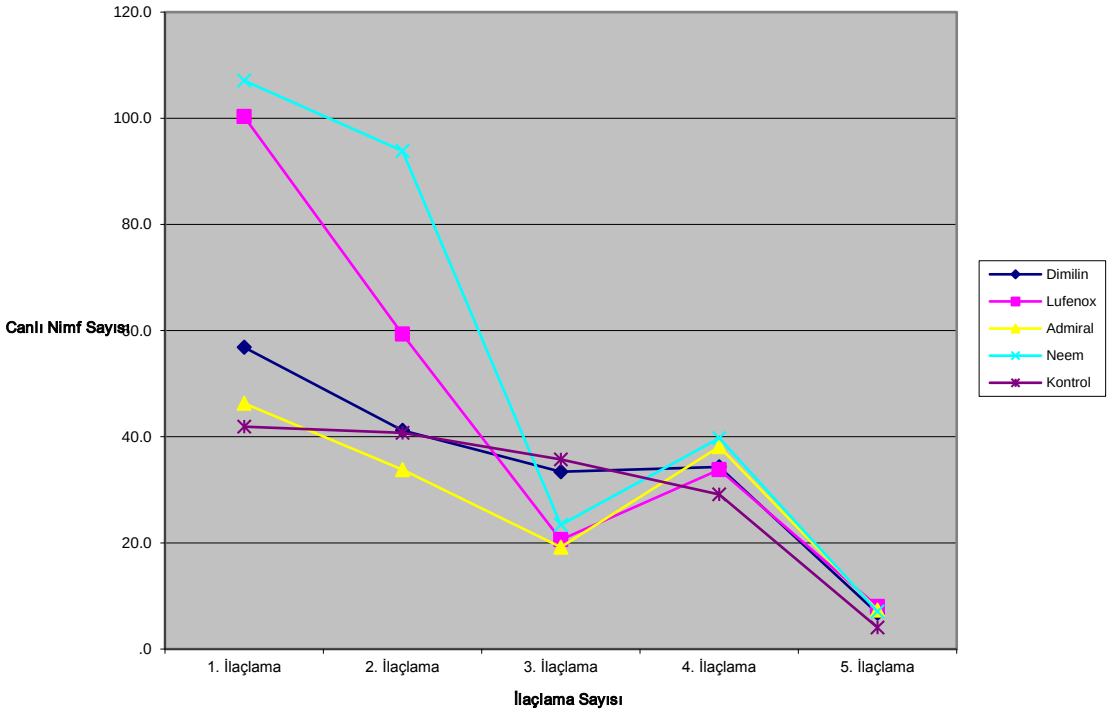

Şekil 2. 2. ilaçlama denemesi sonucunda gerçekleşen sera beyazsineği populasyonunun dalgalanma seyri.

2. ilaç denemesinde en düşük canlı nimf sayısı Admiral uygulanan saksılardan elde edilmiştir ve diğer uygulamalara göre aralarındaki fark önemli çıkmıştır ($p< 0.05$, $F=4.434$, $dF= 4.395$). Ancak bu önem kontrol grubuna yakındır. O nedenle kesin olarak etkili olduğunu söylemek anlamlı değildir. Buna karşılık en yüksek nimf yoğunluğu NeemAzal-T/S ve Lufenox uygulan bitkilerde tesbit edilmiştir.

Her iki ilaçlama sonucunda denemeye alınan ilaçların laboratuar koşullarında sera beyazsineği nimfleri üzerinde anlamlı bir etkiye sahip olmadıkları anlaşılmıştır. Sadece 2. uygulama denemesinde söz konusu zararlıya ruhsatlı olan Admiral isimli IGR ın düşük bir etkisi saptanabilmiştir.

Tartışma ve Sonuçlar

Sera beyazsineğinin gelişme süresi 31 gün olup ovipozisyon süresi 6 gündür. Dişi ömrü ise 5- 40 gündür. Buna göre bir dişi ömrü boyunca en az 1 olmak üzere 6- 7 kez yumurta bırakabilmektedir. Yumurta bırakma periyodunun kısa olması ve ergin öncesi dönemin 31 gün sürmesine bağlı olarak bir sera içerisinde bütün ergin öncesi dönemlerin bir arada olması, yani döllerin karışması söz konusudur (Chase, 2007). Gerçekleştirilen her 2 deneme sonucunda denemeye alınan doğal pestisitlrden beklenen sonuç alınamamasındaki temel nedeninin döllerin iç içe girmiş olmasından kaynaklandığı düşünülmektedir. Zira denemeye alınan ve alınmayan bitkilerde ergin beyazsinek populasyonu oldukça yüksek düzeyinde seyrettiği için bitkiler sürekli ve yoğun ergin saldırısına maruz kalmıştır. Uygulanan böcek gelişim düzenleyicisi etkisine sahip preparatların, böceklerde ergin öncesi dönemlerinde görülen kitin sentezini inhibe etmesi sebebiyle ergin üzerinde etkisi bulunmamaktadır. Dolayısıyla, yüksek zararlı ergin yoğunluğuna maruz kalan domates bitkilerinde denemeye alınan preparatların etkileri beklenilen düzeyde gerçekleşememiştir.

Elling et al. (2002), sera beyazsineği üzerinde NeemAzal-T/S ile yaptığı çalışmada Neem Azal-T/S' ın uygulama yapılmış yumurtalardan larva çıkışının %97' den daha fazla olduğunu ve dolayısıyla larva çıkışını etkilemediği ayrıca larva oluşumuna kadar geçen süreyi de etkilemediğini bulmuştur. Araştırıcılar, iyi bir takiple yumurtlamaların başladığı andan itibaren neem uygulamalarının da başlatılması gereğini

vurgulamaktadır., Ancak bu sayede yumurtalardan çıkan larvaların, Neem Azal-T/S uygulamaları sonucunda pupa olma oranlarında önemli ölçüde azalabildiğini belirtmişlerdir.

Yaşarakıncı ve Hıncal (1997), İzmir'de örtü altında yetiştirilen domates, hıyar, biber ve marulda bulunan zararlı ve yararlı türler ile bunların populasyon yoğunlukları üzerinde yapılan araştırmada seralarda sera beyazsineğine karşı üç günde bir ilaçlama yapılmasına karşın baskı altına alınamadığını belirtmişlerdir.

Zararlılar ile mücadelede çevreye zarar vermeyen doğal pestisitler kullanılmasına yönelik çalışmalarda özellikle son 10 yılda artış söz konusudur. Böcek büyüme düzenleyicileri, etki şekilleri ile diğer pestisitlerden ayrılmaktadır. Bunlar böcek gelişimini engellemekte ve faydalı böcekler gibi hedef olmayan organizmalara, diğer pestisitlere oranla çok daha az zararı olmaktadır. Bu özellikleri ile de entegre mücadele programlarında öncelikle yer almakta ve kullanılmaktadır (Öncüer, 2004). Seralarda beyazsineğe karşı mücadele programlarında biyolojik etkileri araştırılan böcek gelişim düzenleyicilere öncelikle yer verilmesi ve üreticilerin bu tür preparatların kullanımı konularında bilinçlendirilmesi ve yönlendirilmesi, zararlılarla yararlı türler arasındaki dengenin yeniden kurulmasına yardımcı olacaktır. Ancak zararlıların ergin öncesi dönemleri üzerinde etkili olan bu preparatların, başlangıç populasyonu ve üreme gücü çok yüksek olan zararlıların kontrolünde, ergin öldürücülük yeteneklerinin son derece kısıtlı olması nedeniyle zaman zaman sıkıntılar yaşanabilmektedir. Bu nedenle istenilen sonuçlar alınamayabilmektedir. Dolayısıyla sera beyazsineği gibi zararlılara karşı böcek gelişim düzenleyicileri kullanılacağı zaman, zararlının başlangıç populasyonu tespit edilmelidir. Eğer yüksekse, baskı altına alınabilme süreçlerini daha kısa ve ekonomik hale getirebilmek için etki süresi kısa, seçici bir sentetik insektisitin başlangıçta en düşük dozunda uygulanması ve sonraki uygulamalarda böcek gelişim düzenleyicilerin programa alınması son derece yararlı olacaktır.

Teşekkür

Çalışmamıza katkılarından dolayı sayın Doç. Dr. Hasan Sungur CİVELEK' e, beyazsinek tür teşhisini yapan sayın Prof. Dr. M. Rifat ULUSOY'a içtenlikle teşekkür ederiz.

Kaynaklar

Anonymous 2007. Tarımsal Araştırmalar Genel Müdürlüğü

http://www.tagem.gov.tr

Awad, T.I., Önder, F., Kısmalı, Ş. 1998. *Azadirachta indica* A.Juss (Meliaceae) Ağacından elde edilen doğal pestisitler üzerinde bir inceleme ,Türkiye Entomoloji Dergisi, Vol.22 No.3 ss225-237.

Chase,S. M., 2007. Unıversity of Connecticut Integrated Pest Management Program.

http://www.hort.uconn.edu

Condor A., F., 2007**.** Effect of neem (*Azadirachta indica* A. Juss) insecticides on parasitoids. Rev. peru. biol. 14(1): 069- 074

Copping, L. G. and J. J. Menn. 2000. Biopesticides: a review of their action, applications and efficacy. Pest Management Science, 56: 651–676.

Copping, L. G. 2001. The BioPesticide Manual. A World Compendium. 2nd ed British Crop Protection Council Publications, United Kingdom, 528 p.

Derinbay,V.,2008. Tarım Net http://www.volkanderinbay.net

Elling, K., Borgemeister, C., Setamou, M., Poehling, H.-M., 2002. The effect of NeemAzal- T/ S®, a commercial neem product, on different developmental stages of the common grenhouse whitefly *Trialeurodes vaporarium* Westwood (Hom., Aleyrodidae). J. Appl. Ent. 126, 40–45.

Lodos, N., 1986. Türkiye Entomolojisi 2 (Genel, Uygulamalı ve Faunistik). Ege Üniv. Ziraat Fak. Yayınları No.429, 580s.

Mart, C., Kişmir, A., Aktura, T., 2001**.** Pamukta Beyazsinek, *Bemisia tabaci* Genn. (Hom., Aleyrodidae) Mücadelesinde Böcek Gelişme Düzenleyicileri Buprofezin Ve Pyriproxyfen)' in Kullanım Olanakları, Fen Ve Mühendislik Dergisi, Cilt 4, Sayı 2

Miller, F. and S. Uetz. 1998**.** Evaluating biorational pesticides for controlling arthropod pests and their phytotoxic effects on greenhouse crops. HortTechnology, 8(2): 185–192.

Öncüer, C., Yoldaş, Z., Madanlar, N. Ve Gül, A. 1994. İzmir' de Sebze Seralarında Zararlılara Karşı Biyolojik Savaş Uygulamaları. Türkiye 3. Biyolojik Mücadele Kongresi(25–28 Ocak 1994) Bildirileri, İzmir, 395–407.

Öncüer, C. 2004**.** Tarımsal Zararlılarla Savaş Yöntemleri ve İlaçları. Adnan Menderes Üniveritesi Yayınları, Aydın, No:19 s: 56.

Schmutterer, H. 1990. Properties and potential of natural pesticides from the Neem tree, Azadirachta indica. Ann. Rev. Entomol., 35: 271-297.

Ulusoy, M., R., 2001. *Türkiye Beyazsinek Faunası*.Baki Kitabevi, Adana, 88,10- 11.

Ünal, G. Ve Gürkan,M. O., 2001. *İnsektisitler Kimyasal Yapıları, Toksikolojileri Ve Ekotoksikolojileri*, Ethemoğlu Ofset Matbaacılık, Ankara. 159,46-47

Yoldaş, Z. 1995**.** Hıyar seralarında zararlı *Bemisia tabacii* (Genn.) (Homoptera, Aleyrodidae)' ye karşı biyolojik savaşta *Encarsia formosa* (Gahan) (Hymenoptera, Aphelinidae)' nın etkinliği üzerinde bir araştırma. Türk. Entomol. Derg. 19(2). 95–99.

Zeki, C., Kedici, R., Çevik, T.Halıcı, S., Er, H. 1999. Bazı böcek büyüme düzenleyicileri ve yumurta parazitoiti *Trichogramma embryophagum* Hartig Hym.:Trichogrammatidae)'un elma içkurdu (*Cydia pomonella* L.) (Lep.: Tortricidae)'na karşı etkinlikleri üzerinde araştırmalar, Türkiye 4. Biyolojik Mücadele Kongresi Bildirileri ss.57-66.

Yaşarakıncı,N., Hıncal, P.1997. İzmir'de örtüaltında yetiştirilen domates, hıyar, biber ve marulda bulunan zararlı ve yararlı türler ile bunların popülasyon yoğunlukları üzerinde araştırmalar, Bitki Koruma Bülteni 37 (1-2) : 79-89.

International Conference on Science and Technology

ICONST 2018

5-9 September 2018 Prizren - KOSOVO

Nar Bahçelerinde Turunçgil Unlubiti (*Planococcus citri*, Risso (Hemiptera: Pseudococcidae)' nin Populasyon Dalgalanmaları ve Doğal Düşman Kompleksinin Saptanması / Population Density of *Planococcus citri*, Risso (Hemiptera: Pseudococcidae), Population Fluctuations and Determination of Natural Enemy Complex in Pomogranate Gardens

Mert Kosovaeri[1]*, Hasan Sungur Civelek [2]

Özet: Muğla' nın Ortaca ve Dalaman ilçelerinde, 2014 yılında 4 ay boyunca gerçekleştirilen bu çalışmada *Planococcus citri* Risso (Hem.:Pseudococcidae)' nin 5 farklı nar bahçesindeki (Geren, Eskiköy, Geren, Arıtma, Şerefler) lokasyonlarında % bulaşıklık oranları, zararlının popülasyon yoğunluğu, parazitoit tür kompleksi ve parazitoitlerin zararlıyı parazitleme oranları belirlenmiştir. % bulaşıklık oranları tüm bahçelerde genel olarak % 2-28 olarak kaydedilmiştir. Popülasyon yoğunluğu 2., 3. ve 4. bahçelerde Temmuz ayında, 1. ve 5. bahçelerde ise Eylül ayında yüksek seviyeye ulaşmıştır. Turunçgil unlubitinin popülasyon yoğunluğunun, tüm bahçelerde Eylül ayının ortasından itibaren hızla düşmekte olduğu anlaşılmıştır. 2014 yılı Temmuz-Eylül ayları boyunca, bahçelerde zararlıyı parazitleyen parazitoitlerin parazitoit kompleksini genel olarak Encyrtidae (Hymenoptera) familyasına ait 4 farklı tür oluşturmuştur. Bu türler: *Leptomastix dactylopii* Howard 1885, *Coccidoxenoides perminutus* Girault, 1915, *Anagyrus kamali* Moursi 1948, *Comperiella bifasciata* Howard, 1906 olarak belirlenmiştir. Söz konusu parazitoitlerden en yüksek % parazitleme oranı %33,33 ile *Leptomastix dactylopii* türünde saptanmıştır.

Anahtar Kelimeler: *Planococcus citri*, turunçgil unlubiti, nar, parazitoit, Encyrtidae

Abstract: In this study was carried out in 5 different pomogranate gardens in Ortaca and Dalaman in Muğla province in 2014. In this study was determined population fluctuations and, determination of natural enemy complex of *Planococcus citri* Risso (mealybug) (Hem.:Pseudococcidae) in 5 different pomogranate gardens (Geren, Eskiköy, Geren, Arıtma, Şerefler) Also, population densities of mealybug and % parasitisim rates of natural enemies on mealybag were determined. The % infetation rate of mealybug were generally recorded as % 2-28. The population density reached a high level in July, 2nd, 3rd and 4th gardens and September 1st and 5th gardens. It was determined that the population densities of was rapidly decreasing mealybug dramaticaly in all pomogranate gardes from the middle of september. The parasitoid complex of mealybug were determined 4 parasitod species which are *Leptomastix dactylopii* Howard 1885, *Coccidoxenoides perminutus* Girault, 1915, *Anagyrus kamali* Moursi 1948, *Comperiella bifasciata* Howard, 1906 belonging to Encyrtidae family (Hymenoptera). The highest percentage amoung the parasitoids was determined as *Leptomastix dactylopii* with 33.33%.

Keywords: *Planococcus citri*, mealybug, pomogranate, parasitoits, Encyrtidae.

[1] Muğla Sıtkı Koçman Üniversitesi, Fen Bilimleri Enstitüsü, Biyoloji Anabilim Dalı, TURKEY
*Correspondingauthor: mertkosovaeri88@gmail.com

Giriş

Nar, Lythraceae familyasının (Kınagiller), *Punica* cinsinden çok yıllık bir bitki olup ülkemizde yıllardır yetiştirilen geleneksel bir meyvedir (Yılmaz, 2007). Bununla beraber ticari değeri kadar kültürel hayatta da önemli yer işgal etmiş bu meyvenin, ticari türü olan *Punica granatum* L. Ortaçağ' da çekirdekli elma anlamına gelen "Pomuni granatum" dan adını almıştır (La Rue, 1980). Nar' ın endüstri ve insan sağlığındaki öneminin anlaşılmasıyla birlikte, dünyada ve ülkemizde nar üretim ve tüketiminde yıldan yıla artış kaydedilmektedir. TÜİK kaynaklarına göre (Anonim, 2015) Türkiye yaklaşık 304.548 da nar üretim alanı ve 397.335 ton üretimi ile dünya narcılığında dördüncü sırada yer almaktadır. Türkiye' deki nar üretiminin yaklaşık %53' ü Akdeniz Bölgesi' nden (211.087 ton), %31' i Ege Bölgesi' nden (124.473 ton) ve %12' si ise Güneydoğu Anadolu Bölgesi' nden (47.710 ton) sağlanmaktadır. Türkiye' deki nar üretimi konusunda ikinci bölgede yer alan Ege Bölgesi içerisinde ise 68.347 ton üretimi ile bölgedeki toplam üretimin yarısından fazlasını (% 54.90) sağlayan Muğla ili ilk sırada yer almaktadır.

Ülkemizde önemli bir yeri olan narın, yetiştiricilik sorunlarının yanında, üretiminde doğrudan etkili olan ve girdi artışı ortaya çıkaran, hastalık ve zararlılar önemli bir sorundur. Bu zararlıların başında, birçok ülke ve bölgede olduğu gibi narın ana zararlısı diyebileceğimiz turunçgil unlubiti, *Planococcus citri* Risso (Hemiptera: Pseudococcidae) gelmektedir.

Turunçgil unlubitleri çoğunlukla koloni halinde yaşamaktadırlar. Yumurta döneminin uzun olmasından dolayı, yumurta, nimf ve ergin bireyleri bir arada bulunmaktadır. Dişi bireyler üç nimf dönemi geçirerek ergin olmaktadırlar. Erkek bireyler kanatlı olup, iki larva, prepupa ve pupa dönemlerinde sonra ergin olmaktadırlar. Orantılı nemi yüksek, gölgeli ve sıcak yerler gelişmesi için en uygun alanlardır (Kaygısız, 2006). Yılda 3-5 döl vermekte ve kışı genellikle ergin dişi, yumurta ve çeşitli nimf dönemlerinde kabuk altı, gövde ve dallardaki çatlaklar ile kök boğazı civarında geçirmektedirler (Anonim 2008; Demirsoy, 2006; Kaygısız, 2006). Yaz başında kışlağı terk eden ergin dişi ve nimfler, beslenmek üzere narın yaprak ve sürgünlerine göç ederler. Yaz ortalarında ise, gelişmekte olan meyvelere geçerek meyve kaliksi veya meyvelerin birbirine değdiği yerlerde özsuyu emerek beslenirler (Anonim, 2008). Beslendikleri yerde salgıladıkları tatlımsı madde portakal güvesi (*Cryptoblabes gnidiella* Mill.) ve harnup güvesi (*Ectomyelois ceratoniae* Zell.)' nin ilk dönem larvalarının besin kaynağı olup dolaylı olarak bu zararlıların yüksek popülasyon oluşturmasına yol açmakta olup, ayrıca salgıladıkları bu tatlımsı madde bitki yüzeyini kaplar ve nemli, sıcak iklim koşullarında üzerinde saprofit mantarlar gelişerek fumajine neden olurlar. Ülkemizde "Karaballık" olarak da anılan, bitkinin yeterli fotosentez yapmasını engelleyen fumajin, bitki gelişmesini engellemekte, buna bağlı olarak da ürünün estetik ve pazar değeri düşmektedir (Düzgüneş, 1982; Lodos, 1982). Ayrıca *P. citri*' nin virüs vektörü olduğu konusunda birçok çalışma bulunmakta ve turunçgil unlubitinin bu özelliğinde dolayı düşük popülasyonların bile ekonomik öneme sahip olunduğu bilinmektedir (Cabaleiro ve Segura, 1997).

Materyal ve Yöntem

Arazi Lokasyonlarının Seçilmesi ve Seçilen Lokasyonlara Ait Özellikler

Ortaca ve Dalaman ilçeleri Türkiye' nin güneybatısında, Muğla il sınırlarının içerisinde bulunmaktadır. İlçelerde bulunan nar bahçelerinde gerçekleştirilen arazi çalışmalarına ait lokasyonlar seçilirken bilhassa nar üretiminin bol olarak yapıldığı lokasyonlar seçilmiştir. İlçeleri temsil edecek şekilde toplamda 5 farklı lokasyonda *Planococcus citri*' nin zarar belirtisinin gözlemlendiği, nar ağaçları bulunduran bahçeler seçilerek çalışmalara devam edilmiştir. Seçilen 5 lokasyonda arazi çalışmaları haftalık olarak düzenlenerek 2014 yılında Temmuz-Ekim ayları arasında yürütülmüştür. Seçilen bahçelerin koordinatları ve rakımlarına ait verilen Çizelge 1' de verilmiştir.

Çizelge 1. Beş farklı bahçeye ait koordinatlar ve rakım bilgileri

Bahçeler		Koordinatlar	Rakım (m)
1.	Geren Mevkii	36º48'38.71''K/28º38'39.37''D	0
2.	Eskiköy Mevkii	36º51'31.09''K/28º40'00.29''D	4
3.	Geren Mevkii	36º48'55.56''K/28º38'30.91''D	0
4.	Arıtma Mevkii	36º50'41.19''K/28º38'08.60''D	0
5.	Şerefler Mevkii	36º43'58.67''K/28º49'44.54''D	14

Bu çalışma 2014 yılında Türkiye' de, nar üretiminde önemli bölgeler arasında olan Muğla iline bağlı Ortaca ve Dalaman ilçelerinde yürütülmüştür. Çalışmanın ana materyalini turunçgil unlubiti (*Planococcus citri* Risso) ve turunçgil unlubiti ile bulaşık nar bahçeleri oluşturmuştur. Ortaca ilçesi' nde ilçeyi temsilen dört farklı nar bahçesi (1. bahçe: Sabri Akkır, Geren Mevkii, 2. bahçe: Erkan Yılmaz, Eskiköy Mevkii, 3. bahçe: Ahmet Manav, Geren Mevkii, 4. bahçe: Kubilay Keçeci, Arıtma Mevkii) ve Dalaman' da bir nar bahçesi (5. bahçe: Müdayir Erdoğan, Şerefler Mevkii) seçilerek toplamda 5 farklı nar üretimi yapan bahçeler kullanılarak çalışma yürütülmüştür. 2014 yılı Temmuz-Ekim ayları arasında haftalık olarak söz konusu bahçelere seyahatlar düzenlenmiştir. Burada ağaçların sayım yapılan tüm organlarında değil en sağlıklı popülasyonu içermeleri nedeniyle sadece meyvelerinden elde edilen veriler değerlendirilmiştir. Mart ve Altın (1992), Güneydoğu Anadolu Bölgesi nar alanlarında yaptıkları çalışmada, *P. citri*' nin narın meyve döneminde iken önemli zararlı olduklarını bildirmişlerdir. Turunçgil unlubiti ile bulaşık nar ağaçlarına ait meyveler, zararlının % bulaşıklık oranı ve popülasyon yoğunluğunun saptanması için her bahçeden rastgele 25 farklı ağaçtan 100 meyve bulaşık olup olmadığına göre ağaç üstünde kontrol edilmiş, kontrol edilen meyvelerde bir tek canlı birey (yumurta, nimf, ergin) dahi bulunsa meyve bulaşık olarak kabul edilmiştir. Ayrıca bu kontroller sırasında her bahçeden farklı ağaçlardan homojen olarak seçilen 5 meyve kesilip, poşetler içerisine konarak etiketlemeleri yapılmış ve Muğla Sıtkı Koçman Üniversitesi Fen Fakültesi Biyoloji Bölümü Entomoloji Laboratuvarı' na getirilmiştir.

Laboratuvar Çalışmaları

2014 yılı Temmuz-Ekim ayları arasında yapılan çalışma süresince laboratuvara getirilen turunçgil unlubiti ile bulaşık nar ağaçlarına ait meyvelerde bulunan bireylerin sayıları not edilerek *P. citri*' nin her bahçe için popülasyon dalgalanması ayrı ayrı hesaplanmıştır. Sayımı yapılan bulaşık meyveler, zararlının parazitoit kompleksinin ve zararlıyı parazitleme oranlarının belirlenmesi için 32x50x34 cm ebatlarındaki kültür kaplarına alınmıştır. Kültür kaplarındaki parazitoit çıkışları haftalık kontrol edilerek not edilmiştir. Çıkış yapan parazitoitler sayılarak tür teşhisi için % 70' lik alkol bulunan ependorf tüplerine alınmış ve etiketlenerek saklanmıştır. Böylece teşhis karakterlerinin zarar görmesi engellenmiştir. Tez çalışmaları çerçevesinde gerçekleştirilen arazilerden toplanan örneklerin, laboratuvar çalışmaları esnasında elde edilen *P. citri* ve parazitoitlerine ait fotoğrafları Leica EZ4D marka fotoğraf çekebilen stereo mikroskop altında 16X büyütmede çekilmiştir.

Veri Analizi

Popülasyon yoğunluğunu belirlemek için sayılan dişi unlubit bireylerine, IBM SPSS Statisitcs 20 programıyla tek yönlü varyans analizi ve duncan testi uygulanarak, 5 farklı nar bahçesindeki popülasyon değişimi istatistiksel olarak değerlendirilmiştir (p=0,05). Keçeci vd. (2008) formülü kullanılarak her bir parazitoit türü için parazitlenme oranları ve zararlının yüzde bulaşıklık oranları hesaplanmıştır. 2014 yılındaki arazi çalışmaları, Ekim ayının ilk haftasına kadar sürdürebilmiştir. Bulaşıklık ve parazitlenme oranları için kullanılan formüller aşağıda verilmiştir.

% Bulaşıklık= [(K)/(L)]X100
K: Bulaşık Meyve Sayısı
L: Toplam Meyve Sayısı

% Parazitleme= [(A)/(B+A)]X100
A: Parazitoit Ergin Sayısı
B: *P. citri* Ergin Sayısı

Bulgular

Popülasyon Dalgalanması ve % Bulaşıklık Oranlarına ait Sonuçlar

Popülasyon dalgalanmasının saptanabilmesi için 2014 yılında (Temmuz-Ekim ayları arasında) Ortaca' yı temsilen dört farklı bahçeden ve Dalaman' ı temsilen bir bahçeden toplanan ve laboratuvara getirilen *P. citri* ile bulaşık nar ağaçlarına ait meyvelerde bulunan birey sayıları not edilmiştir. Keçeci vd. (2008) formülüne göre hesaplanan bulaşıklık oranına ait veriler Çizelge 2' de meyve başına düşen *P. citri* birey ortalamalarıyla beraber aynı çizelgede verilmiştir.

Çizelge 2. 2014 yılı bahçelerdeki meyve başına olan birey ortalamaları ve % bulaşıklık oranları [Ort. ± Std.Hata (Minimum-Maksimum)]

Örnekleme Tarihi	1. Bahçe Dişi Birey	% Bulaşıklık	2. Bahçe Dişi Birey	% Bulaşıklık	3. Bahçe Dişi Birey	% Bulaşıklık	4. Bahçe Dişi Birey	% Bulaşıklık	5. Bahçe Dişi Birey	% Bulaşıklık
04.07.2014	4,80±0,48ab (3-6)	10,00	6,40±0,50bcd (5-8)	7,00	3,60±0,67bc (2-6)	3,00	3,20±0,37bc (2-4)	5,00	5,60±0,81abc (4-8)	10,00
11.07.2014	4,00±0,54ab (3-6)	8,00	5,60±0,87bcd (4-9)	6,00	4,40±0,92c (2-7)	4,00	4,00±0,83cd (1-6)	8,00	5,20±0,91abc (2-7)	12,00
18.07.2014	4,40±0,81ab (2-6)	6,00	4,80±1,06abcd (2-8)	6,00	4,00±0,44bc (3-5)	7,00	4,80±0,86d (2-7)	3,00	4,00±1,04a (2-8)	15,00
25.07.2014	4,80±1,11ab (1-7)	9,00	7,20±1,39cd (4-11)	10,00	3,60±1,02bc (2-7)	4,00	2,00±0,54ab (1-4)	9,00	6,00±0,83abc (3-8)	9,00
01.08.2014	5,60±0,81ab (3-8)	12,00	6,00±1,14bcd (3-9)	14,00	2,80±0,66abc (1-5)	2,00	1,20±0,20a (1-2)	5,00	4,40±1,28ab (2-9)	17,00
08.08.2014	5,20±0,58ab (4-7)	11,00	4,40±1,02abcd (2-7)	13,00	2,40±0,50abc (1-4)	4,00	1,60±0,50ab (0-3)	3,00	4,40±0,67ab (3-6)	21,00
15.08.2014	6,00±0,44ab (5-7)	15,00	4,00±1,37abc (1-9)	16,00	2,80±0,58abc (2-5)	4,00	2,40±0,50ab (1-4)	5,00	4,80±0,91ab (3-8)	25,00
22.08.2014	5,20±0,86ab (3-8)	12,00	7,60±0,74d (6-10)	21,00	2,80±1,11abc (1-6)	5,00	2,00±0,44ab (1-3)	6,00	4,00±0,83a (2-7)	28,00
29.08.2014	5,60±1,63ab (2-10)	12,00	6,40±1,02bcd (4-9)	19,00	2,80±0,37abc (2-4)	7,00	1,20±0,37a (0-2)	4,00	5,00±0,44ab (4-6)	24,00
05.09.2014	7,20±2,08b (1-12)	20,00	5,20±1,24bcd (3-10)	17,00	2,40±0,40abc (1-3)	6,00	1,40±0,50a (0-3)	4,00	6,80±1,24abc (4-10)	19,00
12.09.2014	10,40±0,74c (9-13)	25,00	5,60±0,97bcd (3-9)	18,00	2,00±0,83ab (0-4)	5,00	1,80±0,37ab (1-3)	5,00	8,00±1,76bc (2-12)	23,00
19.09.2014	6,80±1,93ab (3-14)	18,00	4,00±1,09abc (2-8)	11,00	2,00±0,77ab (1-5)	4,00	1,20±0,48a (0-3)	4,00	8,80±1,90c (3-15)	21,00
26.09.2014	6,40±0,67ab (5-8)	17,00	3,60±0,74ab (1-5)	9,00	1,20±0,37a (0-2)	5,00	0,80±0,37a (0-2)	2,00	5,60±1,43abc (2-10)	15,00
03.10.2014	3,20±0,58a (2-5)	8,00	1,60±0,40a (1-3)	4,00	0,80±0,48a (0-2)	2,00	1,00±0,54a (0-3)	3,00	4,00±0,31a (3-5)	13,00

*Aynı sütundaki ortalamaları takip eden farklı küçük harfler, ortalamaların istatistiksel olarak önemli derecede farklı olduğunu gösterir (Anova P<0,05, Duncan testi)

Çizelge 2' de görüldüğü gibi turunçgil unlubit bireylerinin sayım ortalamalarıyla bahçelerdeki % bulaşıklık oranları birbirlerini desteklemektedir. Bahçelerdeki meyvelerin *P. citri* ile yüzde bulaşıklık oranları aylık genel ortalamaları Geren Mevkii' nde ki 1. bahçe için Temmuz ayı %8,25, Ağustos ayı %12,40, Eylül ayı %20 ve Ekim ayı 8; Eskiköy Mevkii' nde ki 2. bahçe için Temmuz ayı %7,25, Ağustos ayı %16,60, Eylül ayı %13,75 ve Ekim ayı 4; Geren Mevkii' nde ki 3. bahçe için Temmuz ayı %4,50, Ağustos ayı 4,40, Eylül ayı 5 ve Ekim ayı 2; Arıtma Mevkii' nde ki 4. bahçe için Temmuz ayı %6,25, Ağustos ayı %4,60, Eylül ayı %3,75 ve Ekim ayı 3; Şerefler Mevkii' nde ki 5. bahçe için Temmuz ayı %11,50, Ağustos ayı %23, Eylül ayı %19,50 ve Ekim ayı %13 olarak hesaplanmıştır. ($F_{(1.\ bahçe)}$ (13,56): 2,555, p: 0,008, r: 0,61, $F_{(2.\ bahçe)}$ (13,56): 2,452, p: 0,010, r: 0,60, $F_{(3.\ bahçe)}$ (13,56): 2,087, p: 0,029, r: 0,57, $F_{(4.\ bahçe)}$ (13,56): 5,115, p: 0,000, r: 0,73, $F_{(5.\ bahçe)}$ (13,56): 1,780, p: 0,070, r: 0,54).

Parazitoitlerin, Parazitlenme Oranlarının ve Parazitoit Kompleksinin Belirlenmesine ait Sonuçlar

P. citri' nin parazitoitlerinin, parazitleme oranlarının ve parazitoit kompleksinin ortaya konulabilmesi için, 2014 yılında 4 ay boyunca (Temmuz-Ekim) her hafta düzenlenen arazi çalışmaları süresince, her bahçeden *P. citri* ile bulaşık 5 adet meyve toplanmıştır (5 bahçe X 5 adet meyve= 25 meyve). 5 farklı bahçeden toplanan, 25 meyveden her birinde bulunan canlı *P. citri* birey sayıları (nimf+ergin) ve parazitli nimf sayısı not edilerek laboratuvar ortamında kültüre alınmıştır. Kültüre alınan bu örneklerden en son aşama olarak çıkış yapan *P. citri*' nin parazitoitlerinin sayıları not edilmiştir. Her bir bahçe için elde edilen bulgular Çizelge 3' de verilmiştir. Aşağıdaki çizelgede yer alan parazitlenme oranları haftalık genel bir parazitlenme oranı vermesi için sadece parazitli nimf sayımları baz alınarak yapılmıştır. İleride ki bölümlerde her bahçe için parazitlenme oranı tür bazında ayrı ayrı verilecektir.

Çizelge 3. Toplanan Zararlının ve Doğal Düşmanlarına ait Sayıların Aylık Ortalamaları

Bahçe No	Ay	Canlı *P. citri* Sayısı	Parazitli Nimf Sayısı	*Parazitoit Ergin Sayısı	**Haftalık Parazitleme Oranı	% Bulaşıklık Oranı
1. Bahçe	**Temmuz**	22,50±0,95ab	2,00±0,40a	2,75±0,85ab	7,97±1,30ab	8,25±0,85bc
2. Bahçe		30,00±2,58c	2,00±0,57a	4,00±0,91b	6,23±1,70a	7,25±0,94ab
3. Bahçe		19,50±0,95ab	3,50±0,64a	4,00±0,40b	15,10±2,61bc	4,50±0,86a
4. Bahçe		17,50±2,98a	3,75±0,47a	4,25±0,85b	18,66±3,41c	6,25±1,37ab
5. Bahçe		26,00±2,16bc	2,50±0,64a	1,00±0,40a	9,03±2,77ab	11,50±1,32c
1. Bahçe	**Ağustos**	27,60±0,74d	2,40±0,24a	2,60±0,24a	8,01±0,83a	12,40±0,67b
2. Bahçe		28,40±3,31d	3,40±0,81a	5,20±1,39b	10,88±2,31a	16,60±1,50c
3. Bahçe		13,60±0,40b	3,60±0,40a	4,80±0,20ab	20,76±1,62b	4,40±0,81a
4. Bahçe		8,40±1,16a	3,80±0,58a	3,20±0,58ab	31,39±4,46c	4,60±0,50a
5. Bahçe		22,60±0,87c	2,20±0,48a	2,60±0,24a	8,78±1,82a	23,00±1,87d
1. Bahçe	**Eylül**	38,50±4,57c	1,25±0,25a	1,50±0,28a	3,29±0,79a	20,00±1,77c
2. Bahçe		23,00±2,38b	1,75±0,25ab	2,50±0,64a	7,14±1,08a	13,75±2,21b
3. Bahçe		9,50±1,25a	3,75±0,47c	3,50±0,28a	28,59±2,11b	5,00±0,40a
4. Bahçe		6,50±1,04a	3,25±0,47bc	2,75±0,47a	34,09±5,94b	3,75±0,62a
5. Bahçe		36,50±3,50c	2,75±0,85abc	2,00±1,41a	7,00±2,00a	19,50±1,70c

* Kültüre alındıktan sonra elde edilen parazitoit sayısı.

** Haftalık parazitlenme oranı, haftalık ortalama parazitlenme oranlarının bulunması amacıyla, parazitli nimf sayısı baz alınarak hesaplanmıştır.

*** Aynı sütundaki ortalamaları takip eden farklı küçük harfler, ortalamaların istatistiksel olarak önemli derecede farklı olduğunu gösterir (Anova P<0,05,Duncan testi).

Çizelge 3 incelendiğinde, *P. citri* sayısı Temmuz ayında, en fazla 2. bahçede en az 4. bahçede gözlemlenirken; 1. bahçe ile 3. bahçe istatistiksel olarak aynı grupta yer almıştır. *P. citri* sayısı Ağustos ayında, en fazla 2. bahçede, en az 4. bahçede gözlemlenirken 1. bahçe ile 2. bahçe istatistiksel olarak aynı grupta yer almıştır. Eylül ayına gelindiğinde ise *P. citri* sayısı en fazla 1. bahçede en az 4. bahçede gözlemlenmiş, 3. ve 4. bahçeler ile 1. ve 5. bahçeler istatistiksel olarak aynı grupta yer almıştır. Parazitli nimf sayıları Temmuz ayı içerisinde en az 1 ve 2 bahçede en fazla 4 bahçede gözlemlenmiştir. Aynı zamanda istatistiksel olarak bu ay içerisinde ki tüm bahçeler aynı grup içerisinde yer almıştır. Ağustos ayına geçtiğimizde parazitli nimfler en çok 4. bahçede en az 5. bahçede görülmüş olup istatistiksel olarak yine tüm bahçeler aynı grup içerisinde yer almıştır. Eylül ayında ise en fazla 3. bahçe, en az 1. bahçede parazitli nimf görülmüş olup, her bahçe istatistiksel olarak farklı gruplarda yer almıştır. Parazitoit ergin sayısı Temmuz ayında en fazla 4 bahçede en az 5 bahçede gözlemlenmiştir. İstatistiksel açıdan bakıldığında 2., 3., ve 4. bahçeler aynı grupta yer almıştır. Ağustos ayındaki parazitoit ergin sayısı en fazla 2. bahçede en az ise 1. ve 5. bahçede gözlemlenmiştir. İstatistiksel olarak açıdan 1. ve 5., 3. ve 4. Bahçeler aynı gruplar içerisinde yer almıştır. Eylül ayı içerisine girildiğinde en fazla 3. bahçede en az 1. bahçede parazitoit ergin sayısı belirlenmiş olup bu ay içerisinde tüm bahçeler istatistiksel olarak aynı grup içerisinde yer almıştır. Haftalık parazitleme oranları Temmuz ayı içerisinde en fazla 4. bahçede en az ise 2. bahçede görülmüş olup, istatistiksel olarak 1. ve 5. bahçeler aynı grup içerisinde yer almıştır. Ağustos ayında haftalık parazitleme oranı en fazla 4. en az 1. bahçede görülmüştür. İstatistiksel olarak 1., 2. ve 5. bahçeler aynı grup içerisinde yer almıştır. Eylül ayına gelindiğinde en fazla 4. en az 1. bahçede haftalık parazitleme oranları gözlemlenmiştir ve istatistiksel olarak 1., 2. ve 5 bahçeler, 3. ve 4. bahçeler aynı grup içerisinde yer almıştır. % Bulaşıklık oranı Temmuz ayı boyunca en az 3. bahçe, en fazla 5. bahçede görülmüş olup istatistiksel olarak 2. ve 4. bahçeler aynı grup içerisinde yer almıştır. Ağustos ayında % bulaşıklık oranı en fazla 5. bahçede en az 3. bahçede gözlemlenmiş olup, 3. ve 4. bahçeler aynı istatistiksel grup içerisinde yer almıştır. Son olarak % bulaşıklık oranı Eylül ayı içerisinde en fazla 1. bahçede en az 4. bahçede gözlemlenmiştir. İstatistiksel olarak ise 1. ve 5., 3. ve 4. bahçeler aynı grup içerisinde yer almıştır. Parazitoitlerin birey sayısı ve yüzde parazitlenme ortalamaları ile bulunma yüzdeleri Çizelge 4' te verilmiştir.

Çizelge 4. Parazitoitlerin birey sayısı ve % parazitleme ortalamaları ile bulunma yüzdeleri

Bahçe	Tür	Birey Sayısı	% Parazitleme	Toplam Birey Sayısı	Toplam % Parazitleme	Bulunma Yüzdesi
1. Bahçe	*L. dactylopii*	3,75±1,10b	4,38±1,02b	15	17,54	48,38
	C. perminutus	2,00±0,70ab	1,66±0,68a	8	6,64	25,80
	A. kamali	1,75±0,85ab	1,41±0,65a	7	5,64	22,58
	C. bifasciata	0,25±0,25a	0,18±0,18a	1	0,72	3,22
2. Bahçe	*L. dactylopii*	5,25±2,39a	3,96±1,55a	21	15,86	42,00
	C. perminutus	4,00±1,47a	3,21±1,08a	16	12,86	32,00
	A. kamali	2,25±1,10a	1,73±0,74a	9	6,92	18,00
	C. bifasciata	1,00±0,70a	0,72±0,48a	4	2,90	8,00
3. Bahçe	*L. dactylopii*	8,50±2,59b	19,58±4,68b	34	78,32	60,71
	C. perminutus	4,25±1,49ab	6,74±2,52a	17	26,99	30,35
	A. kamali	1,25±0,75a	2,30±1,34a	5	9,23	8,92
	C. bifasciata	0,00±0,00a	0,00±0,00a	0	0,00	0,00
4. Bahçe	*L. dactylopii*	5,75±1,93b	11,99±5,13b	23	48,07	51,11
	C. perminutus	3,50±1,19ab	10,42±2,11b	14	42,34	31,11
	A. kamali	1,50±0,86a	3,27±1,68ab	6	13,81	13,33
	C. bifasciata	0,50±0,50a	0,69±0,69a	2	2,78	4,44
5. Bahçe	*L. dactylopii*	1,50±0,86ab	1,15±0,67a	6	4,60	23,07
	C. perminutus	3,75±1,25b	4,01±0,77b	15	16,07	57,69
	A. kamali	0,75±0,47a	0,60±0,41a	3	2,42	11,53
	C. bifasciata	0,50±0,28a	0,45±0,26a	2	1,83	7,69

*Aynı sütundaki ortalamaları takip eden farklı küçük harfler, ortalamaların istatistiksel olarak önemli derecede farklı olduğunu gösterir (Anova P<0,05,Duncan testi).

Çizelge 4 incelenip 1. bahçe değerlendirildiğinde; parazitoitlerden birey sayısı ortalamasına en fazla *L. dactylopii,* en az *C. bifasciata* sahiptir. İstatistiksel olarak birey sayısı ortalamalarına bakıldığında *C. perminutus* ile *A. kamali* aynı grupta yer almıştır. Parazitleme yüzdelerine bakıldığında en fazla ortalamaya *L. dactylopii* sahipken en az ortalamaya *C. bifasciata* sahiptir. İstatistiksel olarak *C. perminutus, A. kamali* ve *C. bifasciata* aynı grupta yer alırken *L. dactylopii* farklı grupta yer almıştır. Bulunma yüzdesine en fazla *L. dactylopii* sahipken en az *C. bifasciata* sahiptir. 2. bahçe değerlendirildiğinde; parazitoitlerden birey sayısı ortalamasına en fazla *L. dactylopii,* en az *C. bifasciata* sahiptir. İstatistiksel olarak birey sayısı ortalamalarına bakıldığında hepsinin aynı grupta yer aldığı görülmektedir. Parazitleme yüzdelerine bakıldığında en fazla ortalamaya *L. dactylopii* sahipken en az ortalamaya *C. bifasciata* sahiptir. İstatistiksel olarak parazitoitlerin parazitleme oranları aynı grupta yer almıştır. Bulunma yüzdesine en fazla *L. dactylopii* sahipken en az *C. bifasciata* sahiptir. 3. bahçe değerlendirildiğinde; parazitoitlerden birey sayısı ortalamasına en fazla *L. dactylopii,* en az *A. kamali* sahipken *C. bifasciata*' ya bu bahçede hiç rastlanılmamıştır. İstatistiksel olarak birey sayısı ortalamalarına bakıldığında *A. kamali* ile *C. bifasciata* aynı grupta yer alırken *C. perminutus L. dactylopii*' ye yakın grupta yer almıştır. Parazitleme yüzdelerine bakıldığında en fazla ortalamaya *L. dactylopii* sahipken en az ortalamaya *A. kamali* sahiptir. İstatistiksel olarak *C. perminutus, A. kamali,* ve *C. bifasciata* aynı grupta yer alırken *L. dactylopii* farklı grupta yer almıştır. Bulunma yüzdesine en fazla *L. dactylopii* sahipken en az *C. bifasciata* sahiptir. 4. bahçe değerlendirildiğinde; parazitoitlerden birey ortalamasına en fazla *L. dactylopii,* en az *C. bifasciata* sahiptir. İstatistiksel olarak birey sayısı ortalamalarına bakıldığında *A. kamali* ile *C. bifasciata* aynı grupta *C. perminutus L. dactylopii*' ye yakın grupta yer almıştır. Parazitleme yüzdelerine bakıldığında en fazla ortalamaya *L. dactylopii* sahipken en az ortalamaya *C. bifasciata* sahiptir. İstatistiksel olarak *L. dactylopii* ve *C. perminutus* aynı grupta yer alırken *A. kamali* bunlara yakın grupta yer almıştır. Bulunma yüzdesine en fazla *L. dactyopii* sahipken en az *C. bifasciata* sahiptir. 5. bahçe değerlendirildiğinde; parazitoitlerden birey ortalamasına en fazla *C. perminutus,* en az *C. bifasciata* sahiptir. İstatistiksel olarak parazitoitlerin birey sayısı ortalamasına bakıldığında *A. kamali* ile *C. bifasciata* aynı grupta, *L. dactylopii C. perminutus*' yakın grupta yer almıştır. Parazitleme yüzdelerine bakıldığında en fazla ortalamaya *C. perminutus* sahipken en az ortalamaya *C. bifasciata* sahiptir. İstatistiksel olarak *L. dactylopii, A. kamali* ve *C. bifasciata* aynı grupta yer alırken *C. perminutus* farklı grupta yer almıştır. Bulunma yüzdesine en fazla *C. perminutus* sahipken en az *C. bifasciata* sahiptir.

Tartışma ve Sonuçlar

2014 yılı Temmuz-Ekim ayları arasında Muğla ili Ortaca ve Dalaman ilçelerindeki nar bahçelerinde *Planococcus citri* Risso (Hem.:Pseudococcidae)' nin popülasyon dalgalanması, bulaşıklık oranı, parazitoit tür kompleksi ve parazitleme oranlarının saptanması amacıyla yürütülen bu tez çalışmasında elde edilen değerler göz önünde bulundurularak *P. citri* ile yüzde bulaşıklık oranları için Geren Mevkii' ndeki 1. bahçe değerlendirildiğinde; aylık ortalaması sırasıyla %8,25, %12,40 ve %20,00 olarak seyretmiş olup örneklemeler boyunca en az %8,00, en fazla %25,00 olarak hesaplanmıştır. Eskiköy Mevkii' ndeki 2. bahçe değerlendirildiğinde; aylık ortalaması sırasıyla %7,25, %16,60 ve %13,75 olarak seyretmiş olup örneklemeler boyunca en az %4,00, en fazla %21,00 olarak hesaplanmıştır. Geren Mevkii' ndeki 3. bahçe değerlendirildiğinde; aylık ortalaması sırasıyla %4,50, %4,40 ve %5,00 olarak seyretmiş olup örneklemeler boyunca en az %2,00, en fazla %7,00 olarak hesaplanmıştır. Arıtma Mevkii' ndeki 4. bahçe değerlendirildiğinde; aylık ortalaması sırasıyla %6,25, %4,60 ve %3,75 olarak seyretmiş olup örneklemeler boyunca en az %2,00, en fazla %9,00 olarak hesaplanmıştır. Şerefler Mevkii' ndeki 5. Bahçe değerlendirildiğinde; aylık ortalaması sırasıyla %11,50, %23,00 ve %19,50 olarak seyretmiş olup örneklemeler boyunca en az %9,00, en fazla 28,00 olarak hesaplanmıştır. Özkan vd. (2001), 1995-1999 yıllarında turunçgil bahçelerinde yürüttükleri entegre mücadele çalışmasında, turunçgil unlubitinin ekonomik zarar eşiğini Nisan-Mayıs ayları arasında %5, meyve fındık iriliğinde iken %10, Temmuz ayından sonrası için %15-20 bulaşık meyve olarak bildirmişlerdir. Bu literatüre göre 3. ve 4. bahçelerinde ki turunçgil unlubit popülasyon seviyesinin EZE' nin aşağısında, diğer bahçelerdeki popülasyon seviyesinin ise EZE' nin yukarısında olduğu söylenebilir.

Turunçgil unlubitinin popülasyon dalgalanması için Geren Mevkii' ndeki 1. bahçe değerlendirildiğinde; aylık ortalaması sırasıyla 22,50, 27,60 ve 38,50 birey olarak seyretmiş olup örneklemeler boyunca en az 16 birey, en fazla 52 birey olarak sayılmıştır. Eskiköy Mevkii' ndeki 2. bahçe değerlendirildiğinde; aylık ortalaması

[1] Muğla Sıtkı Koçman Üniversitesi, Fen Bilimleri Enstitüsü, Biyoloji Anabilim Dalı, TURKEY
*Correspondingauthor: mertkosovaeri88@gmail.com

sırasıyla 30,00, 28,40 ve 23,00 birey olarak seyretmiş olup örneklemeler boyunca en az 8 birey, en fazla 38 birey olarak sayılmıştır. Geren Mevkii' ndeki 3. bahçe değerlendirildiğinde; aylık ortalaması sırasıyla 19,50, 13,60 ve 9,50 birey olarak seyretmiş olup örneklemeler boyunca en az 4 birey, en fazla 22 birey olarak sayılmıştır. Arıtma Mevkii' ndeki 4. bahçe değerlendirildiğinde; aylık ortalaması sırasıyla 17,50, 8,40 ve 6,50 birey olarak seyretmiş olup örneklemeler boyunca en az 4 birey, en fazla 24 birey olarak sayılmıştır. Şerefler Mevkii' ndeki 5. bahçe değerlendirildiğinde; aylık ortalaması sırasıyla 26,00, 22,60 ve 36,50 birey olarak seyretmiş olup örneklemeler boyunca en az 20 birey, en fazla 44 birey olarak sayılmıştır. Bahçelerde bulunan turunçgil unlubitinin popülasyon miktarları karşılaştırıldığında 2., 3. ve 4. bahçede bulunan unlubit popülasyonunun Ağustos ve Eylül aylarında düşüş gösterdiği, 1. bahçede bulunan popülasyonun Ağustos ve Eylül aylarında artış gösterdiği ve 5. bahçede bulunan popülasyonun ise Ağustos ayında azalış, Eylül ayında artış gösterdiği görülmektedir. Demirbaş ve Satar (2011b), Doğu Akdeniz Bölgesi' nde yaptıkları çalışmaya göre unlubit popülasyonunun Nisan ayında meyvelerde görülmeye başlandığı, en yüksek yoğunluğa Haziran ayı sonlarına doğru ulaştığı ve Temmuz ayından itibaren düşüşe geçerek Eylül-Nisan ayları arasında ise en düşük seviyede seyrettiğini bildirmişlerdir. Söz konusu literatür tez çalışmasında popülasyon miktarıyla alakalı bulunan sonuçların büyük bir kısmını destekler niteliktedir.

Turunçgil unlubitinin doğal düşmanlarına ait yapılan çalışmada Coccinellidae familyasına ait bir avcı tür, Encyrtidae familyasına ait 4 parazitoit tür elde edilmiştir. Elde edilen doğal düşmanların isimleri; *Leptomastix dactyopii* Howard 1885, *Coccidoxenoides perminutus* Girault 1915, *Anagyrus kamali* Moursi 1948, *Comperiella bifasciata* Howard, 1906 ve *Cryptolaemus montrozieri* Mulsant 1850' dir. Parazitoit tür kompleksini oluşturan türler için, 1. bahçe değerlendirildiğinde; örnekleme boyunca parazitoitlerin parazitleme oranlarının ortalaması *L. dactylopii*' nin %4,38, % *C. perminutus*' un %1,66, *A. kamali*' nin %1,41 ve *C. bifasciata*' nın %0,18 olarak hesaplanmıştır. 2. Bahçe değerlendirildiğinde; örnekleme boyunca parazitoitlerin parazitleme oranlarının ortalaması *L. dactylopii*' nin %3,96, *C. perminutus*' un %3,22, *A. kamali*' nin %1,73 ve *C. bifasciata*' nın %0,72 olarak hesaplanmıştır. 3. bahçe değerlendirildiğinde; örnekleme boyunca parazitoitlerin parazitleme oranlarının ortalaması *L. dactylopii*' nin %19,58, *C. perminutus*' un %6,75, *A. kamali*' nin %2,31 ve *C. bifasciata*' nın %0,00 olarak hesaplanmıştır. 4. bahçe değerlendirildiğinde; örnekleme boyunca parazitoitlerin parazitleme oranlarının ortalaması *L. dactlopii*' nin %12,02, *C. perminutus*' un %10,59, *A. kamali*' nin %3,45 ve *C. bifasciata*' nın %0,69 olarak hesaplanmıştır. 5. bahçe değerlendirildiğinde; örnekleme boyunca parazitoitlerin parazitleme oranlarının ortalaması *L. dactylopii*' nin %1,15, *C. perminutus*' un %4,02, *A. kamali*' nin %0,60 ve *C. bifasciata*' nın % 0,46 olarak hesaplanmıştır. Parazitoit tür kompleksini oluşturan türlerden *Leptomastix dactylopii'* nin örnekleme boyunca diğer elde edilen parazitoitlere oranla bariz bir üstünlüğü söz konusudur. 2014 yılında Temmuz-Ekim ayları arasında tespit edilen maksimum yüzde parazitlenme oranları, elde edildiği aylar ve bulunduğu bahçe ile birlikte büyükten küçüğe doğru sırasıyla; %33,33 *Leptomastix dactylopii* (Ekim, 3. bahçe), %23,53 *Leptomastix dactylopii* (Eylül, 4. bahçe), %7,19 *Leptomastix dactylopii* (Ağustos, 2. bahçe), %6,25 *Leptomastix dactylopii* (Temmuz, 1. bahçe), %5,83 *Coccidoxenoides perminutus* (Ağustos, 5. bahçe) olarak hesaplanmıştır. Avidov ve Harbaz (1969), İsrail' de yaptıkları bir çalışmada *Planococcus citri* nin genel predatörü olarak *Sypmherobius sanctus*, *Scymnus apetzi*, *Scymnus quadrimaculatus* ve *Scymnus suturalis*' i saptamışlardır. Mani ve Krishnamoorthy (2000), Hindistan' da nar bahçelerinde *P. citri*' nin biyolojik mücadelesinde *L. dactylopii* ve *C. peregrinus* parazitoitlerin etkili olduğunu bildirmişlerdir. Niyazov (1969), Türkmenistan ve Gürcistan' da *P. citri* popülasyonunda ki parazitizmin %20' sinin *Allotropa mecrida* tarafından gerçekleştirildiğini bildirmiştir. Mgocheki ve Addison (2009), Güney Afrika' da yaptıkları çalışmada, *C. perminutus*' un *Anagyrus* sp.' ne göre oldukça fazla miktarda unlubiti parazitlediğini bildirmişlerdir. Kaydan vd. (2006), 2001-2003 yılları arasında Ankara' da yapmış oldukları sörvey çalışmasında *Planococcus citri*' nin doğal düşmanlarından *A. pseudococci* elde etmişlerdir. Ceballo vd. (1998), Avustralya' da yaptıkları çalışmada, *Anagyrus* sp., *C. peregrinus*, *L. abnormis* ve *L. dactylopii*' nin *P. citri*' nin primer parazitoidi olduklarını belirtmişlerdir. Nalini ve Manickavasagam (2011), Hindistan' da *P. citri*' nin doğal düşmanları üzerine yaptıkları çalışmada, 29 parazitoit tür elde etmişler ve bunlardan birinin *A. kamali* olduğunu bildirmişlerdir.

Gerçekleştirmiş olduğumuz bu çalışmada *L. dactylopii* ve *C. perminutus* türleri baskın olarak belirlenirken diğer türler parazitleme oranları açısından *P. citri*' yi baskı altına almada diğerlerine göre düşük etkili olarak bulunmuştur. Sonuç itibariyle *L. dactylopii* türünün söz konusu zararlıyı baskı altına alma sürecinde son derece önemli bir tür olduğu anlaşılmaktadır. Yurdumuzda kışlayamayan ve insektaryumlarda yetiştirilen *L. dactylopii*, *P. citri* ile biyolojik mücadelede kullanılmaktadır. Yalnız ülkemizde *C. perminutus* türü *Anagyrus*

sp.' den daha fazla unlubit parazitlemesine ve kapsüllenmenin daha az olmasına rağmen yeteri kadar kullanılmadığı düşünülmektedir.

Bu çalışmanın sonuçları itibariyle mevcut literatüre de bu bağlamda katkısı olmuştur. Bu nedenle gelecekte yapılacak biyolojik mücadele çalışmalarında konu üzerinde daha ayrıntılı durulmasıyla daha iyi sonuçların elde edileceği düşünülmektedir. Zararlılarla mücadelede insan sağlığına zarar vermeyen biyolojik mücadele yöntemlerinden olan parazitoit türlerin tespiti ve parazitlenme oranları doğrultusunda etkin parazitoit türü/türlerinin belirlenmeye çalışıldığı günümüz bilimsel çalışmalarına paralel olarak gerçekleştirilen bu çalışma aynı zamanda bu anlamda kapsamlı bir çalışma olma özelliğine sahiptir. Söz konusu zararlının nar alanlarında kontrolünde biyolojik kontrol ajanlarının kullanılması çevre ve insan sağlığı, doğal denge açısından önemlidir. Bu amaçla *P. citri* üzerinde etkili hangi yararlı böcek türü/türleri olduğunun bilinmesi ve bu türün doğadaki yoğunluğunu korunması çalışmaları öncelikli olarak yapılması gereken çalışmalardır. Turunçgil unlubiti ile biyolojik mücadelenin yapılacağı alanlarda, zararlının baslangıç popülasyonun tespiti de oldukça önemlidir. Eğer başlangıç popülasyonu yüksekse, baskı altına alınabilme süreçlerini daha kısa ve ekonomik hale getirebilmek için etki süresi kısa, seçici bir sentetik insektisitin baslangıçta en düşük dozunda uygulanması, parazitleme faaliyeti en yüksek olan ve yöredeki iklim koşullarına adaptasyonu en yüksek olan parazitoitlerin erginlerinin kitle üretimlerinin yapılıp nar alanlarına salınması son derece yararlı olacaktır. Ayrıca zararlının popülasyonunun yoğun olduğu aylarda (Haziran-Ekim) ağaçlarda taze sürgün oluşumunun engellenmesi ve azotlu gübrelerin kullanım miktarı ve zamanlarının değiştirilmesiyle yaprakların olgunlaşması sağlanarak zararlının zarar şiddeti azaltılabilir. Son olarak ağaçların ana gövde ve yan dallarında ortaya çıkan ve piç dallar olarak adlandırılan yapraklar temizlenerek ve de zamanında meyvelerin teklemesinin yapılmasıyla zarar miktarı azaltılabilir.

Kaynaklar

Anonim, 2008. *Tarım ve Köyişleri Bakanlığı. Koruma ve Kontrol Genel Müdürlüğü. Nar Hastalık ve Zararlıları*, Ankara, 32s.

Anonim, 2015. Türkiye İstatistik Kurumu. Bitkisel Üretim İstatistikleri. Ankara (Son erişim: 19.05.2015).

AVIDOV, Z. and HARPAZ, I., 1969. *Plant Pests of Israel. Israel Unv. Pres*, Jerusalem, 549 p.

Cabaleiro, C. and Segura, A. 1997. Some characteristics of the transmission of grapevine leafroll associated virus 3 by Planococcus citri Risso. *European Journal of Plant Pathology* 103: 373–378.

Ceballo, F.A., Papacek, D. & Walter, G.H., 1998. Survey of mealybugs and their parasitoids in South-east Queensland citrus. *Australian Journal of Entomology*. 37, 275-280.

Demirbaş, H & Satar, S., 2011. Doğu Akdeniz Bölgesi Turunçgil Bshçelerindeki Karınca Türlerinin Saptanması ve Bazı Hemiptera Türleri İle İlişkilerinin Araştırılması. *Ç.Ü Fen ve Mühendislik Bilimleri Dergisi*. 26-3.

Demirsoy, A. 2006. *Yaşamın Temel Kuralları*, Ankara, 941/517.

Düzgünes, Z. 1982. *Türkiye'de bulunan Pseudococcidae (Hemiptera: Coccoidea) türleri üzerinde incelemeler*. Ankara Üniversitesi Ziraat Fakültesi Yayınları, 56s., Ankara

KAYDAN, M. B., ve KILINÇER. N., 2006 *Phenacoccus aceris* (Signoret) (Hem.: Pseudococcidae)'in doğal düşmanları ve bunların populasyon dalgalanmaları ile unlubit popülasyonuna etkilerinin belirlenmesi. Bitki *Koruma Bülteni*, 45 (1-4):79-97.

Kaygısız, 2006. *Bitkisel Üretimde Zararlı Böcekler*, İstanbul, 288/201.

Keçeci, M., Tepe, S., Tekşam, İ. 2008. Antalya İlinde Örtüaltı Domates ve Fasulye Yetiştiriciliğinde Zararlı Olan Yaprak Galerisineği [*Liriomyza trifolii* (Burgess)] İle Parazitoidlerinin Popülasyon Gelişmesi Üzerine Araştırmalar. *Batı Akdeniz Tarımsal Araştırma Enstitüsü Derim Dergisi*, 25, (2): 13-23.

LaRue, J. H. (1980). Growing Pomegranates in California, University of California, *California Agriculture and Natural Resources Leaflet*, No: 2459, s.8.

Lodos, N. 1982. *Türkiye Entomolojisi II*, Ege Üniversitesi Ziraat Fakültesi Yayınları, İzmir, 560s.

Mart, C., Altın N., 1992. Güneydoğu Anadolu Bölgesi Nar Alanlar ında Belirlenen Böcek ve Akar türleri, *Türkiye II Entomoloji Kongresi*, 28-31 Ocak 1992, s.725-731.

Mani, M. & A. Krishnamoorthy, 2000. Biological suppression of mealybugs Planococcus citri (Risso) and Planococcus lilacinus (Ckll.) on pomegranate in India, *Indian Journal of Plant Protection*, 28 (2): 187-189.

Mgocheki N and Addison P. 2009. Interference of ants with the biological control of the vine mealybug, *Biological Control* 49:180-185.

Nalini, T. & Manickavasagam S., 2011. Records of Encyrtidae (Hym.:Chalcidoidea) parasitoids on mealybugs (Hem.:Pseudococcidae) from Tamil Naui, India. *Check List and Authors*. 7:4, 510-515.

Niyazov, O. 1969. *Allotropa mecrida* (Walk.) (Hym.:Platygastridae) vine insect parasite in Turkmenia. Izv. Akad. Nauk Turkmensk. SSR Ser. Bio. Nauk (Ashkhabad) 1:78-81

Özkan, A., Gürol, M., Uysal, H., Çelik, G., Aktepe, Ş.A., Eray, N., Aytekin, H., Arslan, M., Kaplan, M., Dalka, Y., Akyel, E. & Tuncer, H., 2001. Antalya İli Turunçgil Bahçelerinde Entegre Mücadele Çalışmaları (1995-1999), *Bitki Koruma Bülteni*, 41(3-4): 135-166.

Yılmaz, C., 2007. *Nar*. Hasad Yayınları No: 276, Hasad Yayıncılık Ltd. Şti., P.K. 35, Ümraniye-İstanbul.

International Conference on Science and Technology

ICONST 2018

5-9 September 2018 Prizren - KOSOVO

The Beliefs of Physical Therapists' About Patients' Responses to Pain Related to Their Age and Gender / Fizyoterapistlerin Hastaların Yaş ve Cinsiyetine Göre Ağrıya Verdikleri Yanıtlara İlişkin İnanışları

Nadir Tayfun ÖZCAN[*1], Mesut ERGAN[1], Zeliha BAŞKURT[1], Ferdi BAŞKURT[1]

Özet: Ağrı, hastayı fizyoterapiste yönlendiren en yaygın şikayetlerden biridir. Beşinci yaşam bulgusu olarak da adlandırılan ağrı, fizyoterapistler tarafından dikkatli bir şekilde değerlendirilmelidir. Fizyoterapistlerin, hastaların ağrıya verdikleri yanıtlara dair inanışları, ağrı kontrolü ile ilgili alınan kararları etkileyebilir. Bu çalışma, fizyoterapistlerin hastaların yaş ve cinsiyetine göre ağrıya verdikleri yanıtlara ilişkin inanışlarını incelemek amacıyla yapılmıştır. Çalışmaya 192 fizyoterapist dahil edildi. Bu tanımlayıcı çalışmada sosyodemografik veri formu ve verilerin toplanmasında, daha önceki çalışmalardan yararlanılarak geliştirilen anket formu kullanılmıştır. Kullanılan anket altı başlık altında toplanmış (Ağrıya duyarlılık, Ağrı toleransı, Ağrıdan duyulan ızdırap, Ağrıyı ifade etme eğilimi, Ağrıyı abartma, Ağrının sözsüz ifadesi) 36 sorudan oluşmaktadır. İstatiksel analiz için SPSS 23.0 paket programı kullanıldı. Toplanan datalar yüzdelik olarak, ki-kare testi kullanılarak analiz edildi. Fizyoterapistlerin, hastaların ağrıya verdikleri yanıtlara dair inançları ile fizyoterapistlerin iş tecrübeleri karşılaştırıldığında, cinsiyet parametresine göre, ağrı toleransı başlığı ile fizyoterapistin iş tecrübesi arasında istatiksel olarak anlamlı bir ilişki olduğu saptanırken ($p< 0,05$) ağrıya duyarlılık, ağrıdan duyulan ızdırap, ağrıyı ifade etme eğilimi, ağrıyı abartma, ağrının sözsüz ifadesi başlıklarıyla arada istatiksel olarak anlamı bir ilişki saptanmadı. Hastaların yaşı parametresi incelendiğinde ise iş tecrübesi ve ağrıyla ilgili başlıklar arasında istatiksel olarak anlamlı bir ilişki saptanmadı ($p>0,05$)

Anahtar Kelimeler: Ağrı, Yaş, Cinsiyet, Fizyoterapist inançları

Abstract: Pain is one of the most common complaint for which patients seek the help of a physical therapist. Pain is called a fifth life-event that should be carefully assessed by physiotherapists. The physical therapist' beliefs about the patients' responses to pain may effects their decisions regarding pain control. The aim of this study was to investigate the effect of the patients' age and gender on physical therapist' beliefs about the patients' responses to pain. A total 192 physical therapists were attended the study. In this descriptive study, sociodemographic form was used and data were collected by a questionnaire that other researchers used earlier. The used questionnaire consisted of thirty-six question from six domain: sensitivity to pain, pain toleance, suffering from pain, a tendency to express pain, exaggerate pain and nonverbal expression of pain. Collected data were analyzed by percentage, chi square test in SPSS 23.0 packet programme. The beliefs about the response of the patient to pain were compared with the work experience of physiotherapists. According to patient's gender parameter, statistically significant relationship was found between the pain tolerance subscale and physiotherapist's work experience ($p<0,05$), but there was no significant difference sensitivity to pain, suffering from pain, a tendency to express pain, exaggerate pain and nonverbal expression of pain subscale ($p>0,05$). According to patient's age parameter, statistically significant relationship was no found between any subscale and physiotherapist's work experience.

Keywords: Pain, Age, Gender, Physical therapists' beliefs

Giriş

[1] Süleyman Demirel Üniversitesi, Sağlık Bilimleri Fakültesi, Fizyoterapi ve Rehabilitasyon Bölümü, 32260, Isparta, Türkiye
*Correspondingauthor: nadirozcan@sdu.edu.tr

Ağrı kelimesi İngiliz dilinde kökenini ceza, intikam, işkence anlamlarına gelen latince poena kelimesinden alır (Güler, 2006). Akyar ve arkadaşlarına (Akyar ve ark, 2008) göre, ‘’tanımı güç bir kavram olan ağrı; herhangi bir vücut kısmından köken alan, organizmayı tehdit eden fizyolojik ve ortamsal ya da olası tehlikeleri haber veren, dikkate alınması gereken, bireyde panik duygusuna ve ağrıyı durdurmayı amaçlayan tepkilere yol açan, kişinin önceki deneyimleri ile etkilenebilen, hoş olmayan, karmaşık bireysel bir algılama şeklidir’’. Ağrı bilişsel, duygusal, davranışsal, sosyal ve sembolik bileşenlerden oluşan öznel bir deneyimdir (Raffaeli ve ark, 2012). Nosiseptif ve nöropatik ağrı olmak üzere iki tip ağrı vardır. Nösiseptif ağrıda, ağrılı uyaran nösiseptör adı verilen serbest sinir uçları tarafından algılanır. Cilt, kas, eklem, iç organlar ve kemiklerdeki yerleşim gösteren nösiseptörler sıcaklığa, basınca ve kimyasal uyarana tepki gösterirler. Santral ve periferik sinir sistemi hasarı sonucu ortaya çıkan ağrı ise nöropatik ağrı olarak adlandırılır (Corey, 2016).

Subjektif ve objektif özellikler gösteren ağrı deneyimini tam olarak tanımlamak zordur. Ağrıyı algılama, tanımlama ve ağrıya karşı verilen reaksiyonlar kişiden kişiye değişiklik gösterir. Aynı derecede doku inflamasyonuna sahip olan hastalar farklı düzeyde ağrı deneyimi yaşayabilirler ve bireylerin ağrı deneyimindeki farklılıklar tanı ve tedavide ikilemlere yol açabilir. Ağrının değerlendirilmesinde fiziksel, psikososyal ve çevresel etkenler göz önünde bulundurulmalı ve bu etkenlerin birbirleriyle olan etkileşiminin ağrı algısını etkileyebileceği unutulmamalıdır (Akdemir ve ark, 2008; Çöçelli ve ark,2008). Kişisel bir deneyim olan ağrı değerlendirilirken hastanın verbal yanıtlarına bakılabileceği gibi ağlama, inleme, yüz ifadesi veya vücut dili gibi non-verbal yanıtlarında değerlendirilmesi gerektiği unutulmamalıdır (Werner ve ark, 2018)
Cavlak ve arkadaşlarına (Cavlak ve ark, 2015) göre, ‘’yapısı ve algılanması karmaşık olan ağrının inhibe edilmesi ve tedavi edilmesi de oldukça zordur. Ağrı duyusu birçok faktöre bağlı olarak, kişiden kişiye değişkenlik göstermektedir. Bu algılama farklılığına kişinin çevresi, cinsiyeti, kültürü, eğitimi gibi faktörler etki etmektedir’’. Kompleks biyopsikososyal bir fenomen olan ağrının yönetimi, dönemine göre farklılık gösterebilir. Akut ağrı yönetiminde amaç, ağrının nedenine odaklanmak iken, kronik ağrı yönetiminde ise ağrının etkilerine odaklanmalı ve hastanın fonksiyonelliği ve yaşam kalitesi maksimize edilmeye çalışılmalıdır (Mills ve ark, 2016).

Ağrı yönetimi fizyoterapi yaklaşımları içinde çok önemli bir yer tutar. Elektriksel ajanlar, yüzeyel ısı ajanları, manuel tedavi teknikler, egzersiz uygulamaları gibi fizyoterapi yaklaşımları ile fizyoterapistler, ağrı kontrolünün etkili bir şekilde yapılmasına katkı sağlarlar. Multidisipliner ekip yaklaşımıyla yürütülmesi gereken ağrı yönetiminde, ekip üyelerinin inançlarının, tercihlerinin ve beklentilerinin ağrı yönetimine olan etkileri de göz ardı edilmemelidir. Sağlık çalışanlarının inançları ağrının hem değerlendirilmesini hem tedavisini etkileyen önemli etkenlerdir (Main, 2010). Literatürde doktor, fizyoterapist veya romatolog gibi sağlık çalışanlarının inançları ile hastaya verilen tedavi önerileri arasındaki ilişkiyi gösteren çalışmalar bulunmaktadır (Simmonds ve ark, 2012; Coudeyre ve ark, 2006)

Materyal ve Yöntem

Çalışmamıza farklı illerde ve kurumlarda çalışan 192 fizyoterapist gönüllülük esasına göre dahil edilmiştir. Çalışma verilerinin toplanmasında fizyoterapistlerin demografik ve işle ilgili bilgileri için bilgi formu ve Güneş ve arkadaşlarının(Güneş ve ark, 2005) çalışmalarından yararlanılarak fizyoterapistlere uyarlanan anket formu kullanılmıştır. Bu ankette fizyoterapistlerin ağrılı hastanın yanıtlarına ilişkin inançları ile ilgili 36 madde bulunmaktadır. Katılımcılardan elde edilen tüm verilerin istatistiksel analizleri IBM SPSS Statistics versiyon 23.0 programı ile yapılmıştır. Çalışmanın bulguları sayısal ve yüzdelik verilerle özetlenmiştir. Verilerimizin analizinde ki-kare testi kullanılmıştır. Araştırmamızın yapıldığı kurumlardan ve fizyoterapistlerden sözlü onay alınmıştır.

Bulgular

Çalışmamıza katılan fizyoterapistlerin %38,0’ ı 24-29, %51,6’ sı 30-40 yaş, %10.4’ü ise ≥41 yaş grubunda yer almaktadır. Katılımcıların yaş ortalaması 32,04±5,81 yıl olarak saptandı. Fizyoterapistlerin %40.1’ i (77 kişi) erkek, %59.9’u(115kişi) kadınlardan oluşmaktadır. Fizyoterapistlerin %81.2’ si lisans, %14.6’ sı ise yüksek lisans mezunudur. Fizyoterapistlerin %41,7’ si 10 yıl ve daha uzun süredir çalışmaktadır. Çalışmamıza yoğunlukla (%63,5) kamu ve üniversite hastanelerinde çalışan fizyoterapistler katılmıştır. Katılımcıların %73,5’ i genel fizyoterapi alanında hizmet vermektedir (Tablo 1).

Tablo 1. Fizyoterapistlerin Demografik ve İşle İlgili Özelliklerinin Dağılımı

	N	%
Yaş		
24-29	73	38,0
30-40	99	51,6
≥41	20	10,4
Cinsiyet		
Erkek	77	40,1
Kadın	115	59,9
Eğitim Düzeyi		
Lisans	156	81,2
Yüksek Lisans	28	14,6
Doktora	8	4,2
İş Deneyimi		
0-9 yıl	112	58,3
≥10 yıl	80	41,7
Çalışılan Kurum		
Üniversite Hastanesi	67	34,9
Kamu Hastanesi	55	28,6
Özel hastane veya poliklinikler	56	29,2
Özel eğitim ve rehabilitasyon merkezi	14	7,3
Çalışılan Alan		
Ortopedi	20	10,4
Nöroloji	10	5,2
Pediatri	12	6,3
Kardiyopulmoner	4	2,1
Genel	141	73,5
Diğer	5	2,5
Toplam	192	100

Fizyoterapistlerin, hastaların yaşına göre ağrıya verdikleri yanıtlara ilişkin inanışlarına baktığımızda; ‘’Yaşlılar gençlerden daha fazla ağrı hisseder’’ (%79.2), ‘’Gençler yaşlılara göre daha şiddetli ağrıyı tolere eder’’ (%53.6), ‘yaşlılar gençlere göre ağrıdan daha fazla ızdırap duyar’ (%65,1), ‘’Gençler yaşlılara göre ağrıya daha çok katlanma ve ağrılarını daha az ifade etme eğilimindedir’’ (%53.6), ‘’Yaşlılar ağrılarını abartma eğilimindedir’’ (%49.5) ve ‘’Gençlerin ağrılarını sözel olmayan ifadelerle anlatma eğilimleri yaşlılardan fazladır’’ (%40,1) yanıtlarının daha çok verildiği görülmüştür (Tablo 2).

Fizyoterapistlerin, hastaların cinsiyetine göre ağrıya verdikleri yanıtlara ilişkin inanışlarına baktığımızda ise; ‘’Erkekler kadınlardan daha fazla ağrı hisseder’’ (%45.3), ‘’Erkekler kadınlara göre daha şiddetli ağrıyı tolere eder’’ (%74,5), ‘’Kadınlar erkeklere göre daha fazla ızdırap duyar’’ (%55.2), ‘erkekler kadınlara göre ağrıya daha çok katlanma ve ağrılarını daha az ifade etme eğilimindedir’ (%64,6) ve ‘kadınlar ağrılarını abartma eğilimindedir’ (%65,6) ve ‘’Erkeklerin ağrılarını sözel olmayan ifadelerle anlatma eğilimleri kadınlardan fazladır’’ (%44.8) yanıtlarının daha çok verildiği görülmüştür (Tablo 2).

Tablo 2. Hastaların Yaş ve Cinsiyetine Göre Fizyoterapistlerin Ağrıya Verdikleri Yanıtlara İlişkin İnanışları

Fizyoterapistlerin Hastaların Ağrıya Verdikleri Yanıtlara İlişkin İnanışları		N	%
Ağrıya Karşı Duyarlılık	Erkekler kadınlardan daha fazla ağrı hisseder	87	45,3
	Kadınlar erkeklerden daha fazla ağrı hisseder	52	27,1
	Kadın ve erkeklerin ağrıya karşı olan duyarlılıklarında fark yoktur	53	27,6
	Yaşlılar gençlerden daha fazla ağrı hisseder	152	79,2
	Gençler yaşlılardan daha fazla ağrı hisseder	28	14,6
	Yaşlıların ve gençlerin ağrıya karşı olan duyarlılıklarında fark yoktur	12	6,3
Ağrı Toleransı	Erkekler kadınlara göre daha şiddetli ağrıyı tolere eder	143	74,5
	Kadınlar erkeklere göre daha şiddetli ağrıyı tolere eder	33	17,2
	Kadın ve erkeklerin ağrı toleransları arasında fark yoktur	16	8,3
	Yaşlılar gençlere göre daha şiddetli ağrıyı tolere eder	78	40,6
	Gençler yaşlılara göre daha şiddetli ağrıyı tolere eder	103	53,6
	Yaşlıların ve gençlerin ağrı toleransları arasında fark yoktur	11	5,7
Ağrıdan Duyulan Izdırap	Erkekler ağrıdan kadınlara göre daha fazla ızdırap duyarlar	59	30,7
	Kadınlar erkeklere göre daha fazla ızdırap duyar	106	55,2
	Kadın ve erkeklerin ağrıdan duydukları ızdırap arasında fark yoktur	27	14,1
	Yaşlılar gençlere göre ağrıdan daha fazla ızdırap duyar	125	65,1
	Gençler yaşlılara göre ağrıdan daha fazla ızdırap duyar	57	29,7
	Yaşlıların ve gençlerin ağrıdan duydukları ızdırap arasında fark yoktur	10	5,2
Ağrıyı İfade Etme Eğilimi	Erkekler kadınlara göre ağrıya daha çok katlanma ve ağrılarını daha az ifade etme eğilimindedir	124	64,6
	Kadınlar erkeklere göre ağrıya daha çok katlanma ve ağrılarını daha az ifade etme eğilimindedir	61	31,8
	Kadın ve erkeklerin ağrıya katlanma ve ağrılarını ifade etme eğilimleri arasında fark yoktur	7	3,6
	Yaşlılar gençlere göre ağrıya daha çok katlanma ve ağrılarını daha az ifade etme eğilimindedir	48	25,0
	Gençler yaşlılara göre ağrıya daha çok katlanma ve ağrılarını daha az ifade etme eğilimindedir	103	53,6
	Yaşlıların ve gençlerin ağrıya katlanma ve ağrılarını ifade etme eğilimleri arasında fark yoktur	41	21,4
Ağrıyı Abartma	Erkekler ağrılarını abartma eğilimindedir	55	28,6
	Kadınlar ağrılarını abartma eğilimindedir	126	65,6
	Kadın ve erkeklerin ağrıyı abartma eğilimleri arasında fark yoktur	11	5,7
	Yaşlılar ağrılarını abartma eğilimindedir	95	49,5
	Gençler ağrılarını abartma eğilimindedirler	75	39,1
	Yaşlıların ve gençlerin ağrıyı abartma eğilimleri arasında fark yoktur	22	11,5
Ağrının Sözsüz İfadesi	Erkeklerin ağrılarını sözel olmayan ifadelerle anlatma eğilimleri kadınlardan fazladır	86	44,8
	Kadınların ağrılarını sözel olmayan ifadelerle anlatma eğilimleri erkeklerden fazladır	61	31,8
	Kadınların ve erkeklerin ağrılarını sözel olmayan ifadelerle anlatma eğilimleri arasında fark yoktur	45	23,4
	Yaşlıların ağrılarını sözel olmayan ifadelerle anlatma eğilimleri gençlerden fazladır	69	35,9
	Gençlerin ağrılarını sözel olmayan ifadelerle anlatma eğilimleri yaşlılardan fazladır	77	40,1
	Yaşlıların ve gençlerin ağrılarını sözel olmayan ifadelerle anlatma eğilimleri arasında fark yoktur	46	24,0

Erkek ve kadın fizyoterapistlerin hastaların ağrıya verdikleri yanıtlara ilişkin inanışlarında ise istatistiksel olarak anlamlı bir farklılık bulunmamıştır (Tablo 3).

Tablo 3. Erkek ve Kadın Fizyoterapistlerin Hastaların Ağrıya Verdikleri Yanıtlara İlişkin İnanışları

Fizyoterapistlerin Hastaların Ağrıya Verdikleri Yanıtlara İlişkin İnanışları		Erkek N	%	Kadın N	%	p
Ağrıya Karşı Duyarlılık	Erkekler kadınlardan daha fazla ağrı hisseder	31	40,3	56	48,7	0,401
	Kadınlar erkeklerden daha fazla ağrı hisseder	21	27,3	31	27,0	
	Kadın ve erkeklerin ağrıya karşı olan duyarlılıklarında fark yoktur	25	32,5	28	24,3	
	Yaşlılar gençlerden daha fazla ağrı hisseder	59	76,6	93	80,9	0,747
	Gençler yaşlılardan daha fazla ağrı hisseder	13	16,9	15	13,0	
	Yaşlıların ve gençlerin ağrıya karşı olan duyarlılıklarında fark yoktur	5	6,5	7	6,1	
Ağrı Toleransı	Erkekler kadınlara göre daha şiddetli ağrıyı tolere eder	62	80,5	81	70,4	0,291
	Kadınlar erkeklere göre daha şiddetli ağrıyı tolere eder	10	13,0	23	20,0	
	Kadın ve erkeklerin ağrı toleransları arasında fark yoktur	5	6,5	11	9,6	
	Yaşlılar gençlere göre daha şiddetli ağrıyı tolere eder	31	40,3	47	40,9	0,933
	Gençler yaşlılara göre daha şiddetli ağrıyı tolere eder	41	53,2	62	53,9	
	Yaşlıların ve gençlerin ağrı toleransları arasında fark yoktur	5	6,5	6	5,2	
Ağrıdan Duyulan Izdırap	Erkekler ağrıdan kadınlara göre daha fazla ızdırap duyarlar	20	26,0	39	33,9	0,398
	Kadınlar erkeklere göre daha fazla ızdırap duyar	47	61,0	59	51,3	
	Kadın ve erkeklerin ağrıdan duydukları ızdırap arasında fark yoktur	10	13,0	17	14,8	
	Yaşlılar gençlere göre ağrıdan daha fazla ızdırap duyar	50	64,9	75	65,2	0,794
	Gençler yaşlılara göre ağrıdan daha fazla ızdırap duyar	22	28,6	35	30,4	
	Yaşlıların ve gençlerin ağrıdan duydukları ızdırap arasında fark yoktur	5	6,5	5	4,3	
Ağrıyı İfade Etme Eğilimi	Erkekler kadınlara göre ağrıya daha çok katlanma ve ağrılarını daha az ifade etme eğilimindedir	57	74,0	67	58,3	0,061
	Kadınlar erkeklere göre ağrıya daha çok katlanma ve ağrılarını daha az ifade etme eğilimindedir	17	22,1	44	38,3	
	Kadın ve erkeklerin ağrıya katlanma ve ağrılarını ifade etme eğilimleri arasında fark yoktur	3	3,9	4	3,5	
	Yaşlılar gençlere göre ağrıya daha çok katlanma ve ağrılarını daha az ifade etme eğilimindedir	17	22,1	31	27,0	0,548
	Gençler yaşlılara göre ağrıya daha çok katlanma ve ağrılarını daha az ifade etme eğilimindedir	45	58,4	58	50,4	
	Yaşlıların ve gençlerin ağrıya katlanma ve ağrılarını ifade etme eğilimleri arasında fark yoktur	15	19,5	26	22,6	
Ağrıyı Abartma	Erkekler ağrılarını abartma eğilimindedir	17	22,1	38	33,0	0,224
	Kadınlar ağrılarını abartma eğilimindedir	56	72,7	70	60,9	
	Kadın ve erkeklerin ağrıyı abartma eğilimleri arasında fark yoktur	4	5,2	7	6,1	
	Yaşlılar ağrılarını abartma eğilimindedir	35	45,5	60	52,2	0,637
	Gençler ağrılarını abartma eğilimindedirler	33	42,9	42	36,5	
	Yaşlıların ve gençlerin ağrıyı abartma eğilimleri arasında fark yoktur	9	11,7	13	11,3	
Ağrının Sözsüz İfadesi	Erkeklerin ağrılarını sözel olmayan ifadelerle anlatma eğilimleri kadınlardan fazladır	37	48,1	49	42,6	0,212
	Kadınların ağrılarını sözel olmayan ifadelerle anlatma eğilimleri erkeklerden fazladır	27	35,1	34	29,6	
	Kadınların ve erkeklerin ağrılarını sözel olmayan ifadelerle anlatma eğilimleri arasında fark yoktur	13	16,9	32	27,8	
	Yaşlıların ağrılarını sözel olmayan ifadelerle anlatma eğilimleri gençlerden fazladır	32	41,6	37	32,2	0,325
	Gençlerin ağrılarını sözel olmayan ifadelerle anlatma eğilimleri yaşlılardan fazladır	30	39,0	47	40,9	
	Yaşlıların ve gençlerin ağrılarını sözel olmayan ifadelerle anlatma eğilimleri arasında fark yoktur	15	19,5	31	27,0	

Fizyoterapistlerin yaşının hastaların ağrıya verdikleri yanıtlara ilişkin inanışlarında da istatistiksel olarak anlamlı bir farklılık bulunmamıştır (Tablo 4).

Tablo 4. Fizyoterapistlerin Yaşının Hastaların Ağrıya Verdikleri Yanıtlara İlişkin İnanışlarına Etkisi

Fizyoterapistlerin Hastaların Ağrıya Verdikleri Yanıtlara İlişkin İnanışları		24-29 yaş N	%	30-40 yaş N	%	≥ 41 yaş N	%	p
Ağrıya Karşı Duyarlılık	Erkekler kadınlardan daha fazla ağrı hisseder	33	45,2	42	44,7	12	48,0	0,223
	Kadınlar erkeklerden daha fazla ağrı hisseder	21	28,8	21	22,3	10	40,0	
	Kadın ve erkeklerin ağrıya karşı olan duyarlılıklarında fark yoktur	19	26,0	31	33,0	3	12,0	
	Yaşlılar gençlerden daha fazla ağrı hisseder	61	83,6	70	74,5	21	84,0	0,483
	Gençler yaşlılardan daha fazla ağrı hisseder	7	9,6	18	19,1	3	12,0	
	Yaşlıların ve gençlerin ağrıya karşı olan duyarlılıklarında fark yoktur	5	6,8	6	6,4	1	4,0	
Ağrı Toleransı	Erkekler kadınlara göre daha şiddetli ağrıyı tolere eder	62	84,9	64	68,1	17	68,0	0,131
	Kadınlar erkeklere göre daha şiddetli ağrıyı tolere eder	7	9,6	20	21,3	6	24,0	
	Kadın ve erkeklerin ağrı toleransları arasında fark yoktur	4	5,5	10	10,6	2	8,0	
	Yaşlılar gençlere göre daha şiddetli ağrıyı tolere eder	29	39,7	38	40,4	11	44,0	0,777
	Gençler yaşlılara göre daha şiddetli ağrıyı tolere eder	39	53,4	50	53,2	14	56,0	
	Yaşlıların ve gençlerin ağrı toleransları arasında fark yoktur	5	6,8	6	6,4	0	0	
Ağrıdan Duyulan Izdırap	Erkekler ağrıdan kadınlara göre daha fazla ızdırap duyarlar	20	27,4	31	33,0	8	32,0	0,950
	Kadınlar erkeklere göre daha fazla ızdırap duyar	42	57,5	50	53,2	14	56,0	
	Kadın ve erkeklerin ağrıdan duydukları ızdırap arasında fark yoktur	11	15,1	13	13,8	3	12,0	
	Yaşlılar gençlere göre ağrıdan daha fazla ızdırap duyar	44	60,3	62	66,0	19	76,0	0,564
	Gençler yaşlılara göre ağrıdan daha fazla ızdırap duyar	24	32,9	27	28,7	6	24,0	
	Yaşlıların ve gençlerin ağrıdan duydukları ızdırap arasında fark yoktur	5	6,8	5	5,3	0	0	
Ağrıyı İfade Etme Eğilimi	Erkekler kadınlara göre ağrıya daha çok katlanma ve ağrılarını daha az ifade etme eğilimindedir	45	61,6	65	69,1	14	56,0	0,427
	Kadınlar erkeklere göre ağrıya daha çok katlanma ve ağrılarını daha az ifade etme eğilimindedir	25	34,2	25	26,6	11	44,0	
	Kadın ve erkeklerin ağrıya katlanma ve ağrılarını ifade etme eğilimleri arasında fark yoktur	3	4,1	4	4,3	0	0	

	Yaşlılar gençlere göre ağrıya daha çok katlanma ve ağrılarını daha az ifade etme eğilimindedir	14 19,2	26 27,7	8 32,0	
	Gençler yaşlılara göre ağrıya daha çok katlanma ve ağrılarını daha az ifade etme eğilimindedir	36 49,3	54 57,4	13 52,0	0,093
	Yaşlıların ve gençlerin ağrıya katlanma ve ağrılarını ifade etme eğilimleri arasında fark yoktur	23 31,5	14 14,9	4 16,0	
Ağrıyı Abartma	Erkekler ağrılarını abartma eğilimindedir	20 27,4	28 29,8	7 28,0	
	Kadınlar ağrılarını abartma eğilimindedir	48 65,8	62 66,0	16 64,0	0,933
	Kadın ve erkeklerin ağrıyı abartma eğilimleri arasında fark yoktur	5 6,8	4 4,3	2 8,0	
	Yaşlılar ağrılarını abartma eğilimindedir	34 46,6	47 50,0	14 56,0	
	Gençler ağrılarını abartma eğilimindedirler	33 45,2	34 36,2	8 32,0	0,608
	Yaşlıların ve gençlerin ağrıyı abartma eğilimleri arasında fark yoktur	6 8,2	13 13,8	3 12,0	
Ağrının Sözsüz İfadesi	Erkeklerin ağrılarını sözel olmayan ifadelerle anlatma eğilimleri kadınlardan fazladır	33 45,2	41 43,6	12 48,0	
	Kadınların ağrılarını sözel olmayan ifadelerle anlatma eğilimleri erkeklerden fazladır	20 27,4	37 39,4	4 16,0	0,091
	Kadınların ve erkeklerin ağrılarını sözel olmayan ifadelerle anlatma eğilimleri arasında fark yoktur	20 27,4	16 17,0	9 36,0	
	Yaşlıların ağrılarını sözel olmayan ifadelerle anlatma eğilimleri gençlerden fazladır	22 30,1	39 41,5	8 32,0	
	Gençlerin ağrılarını sözel olmayan ifadelerle anlatma eğilimleri yaşlılardan fazladır	29 39,7	38 40,4	10 40,0	0,368
	Yaşlıların ve gençlerin ağrılarını sözel olmayan ifadelerle anlatma eğilimleri arasında fark yoktur	22 30,1	17 18,1	7 28,0	

İş deneyimin, fizyoterapistlerin inanışlarına olan etkisine bakıldığında; ağrı toleransı alt boyutunun, 'erkekler kadınlara göre daha şiddetli ağrıyı tolere eder' yanıtı her iki grupta da daha çok tercih edilmiştir. Ancak 0-9 yıl arası deneyim sahibi fizyoterapistler, anlamlı şekilde bu yanıtı daha çok tercih etmiştir (p=0,000) (Tablo 5).

Tablo 5. İş Deneyiminin Fizyoterapistlerin Hastaların Ağrıya Verdikleri Yanıtlara İlişkin İnanışlarına Etkisi

Fizyoterapistlerin Hastaların Ağrıya Verdikleri Yanıtlara İlişkin İnanışları		**0-9 yıl deneyim** N %	**≥10 Yıl Deneyim** N %	**p**
Ağrıya Karşı Duyarlılık	Erkekler kadınlardan daha fazla ağrı hisseder	51 45,5	36 45,0	
	Kadınlar erkeklerden daha fazla ağrı hisseder	30 26,8	22 27,5	0,994
	Kadın ve erkeklerin ağrıya karşı olan duyarlılıklarında fark yoktur	31 27,7	22 27,5	
	Yaşlılar gençlerden daha fazla ağrı hisseder	92 82,1	60 75,0	
	Gençler yaşlılardan daha fazla ağrı hisseder	14 12,5	14 17,5	0,486
	Yaşlıların ve gençlerin ağrıya karşı olan duyarlılıklarında fark yoktur	6 5,4	6 7,5	
Ağrı Toleransı	Erkekler kadınlara göre daha şiddetli ağrıyı tolere eder	98 87,5	45 56,2	
	Kadınlar erkeklere göre daha şiddetli ağrıyı tolere eder	10 8,9	23 28,8	**0,000**
	Kadın ve erkeklerin ağrı toleransları arasında fark yoktur	4 3,6	12 15,0	
	Yaşlılar gençlere göre daha şiddetli ağrıyı tolere eder	48 42,9	30 37,5	
	Gençler yaşlılara göre daha şiddetli ağrıyı tolere eder	58 51,8	45 56,2	0,753
	Yaşlıların ve gençlerin ağrı toleransları arasında fark yoktur	6 5,4	5 6,2	
Ağrıdan Duyulan Izdırap	Erkekler ağrıdan kadınlara göre daha fazla ızdırap duyarlar	29 25,9	30 37,5	
	Kadınlar erkeklere göre daha fazla ızdırap duyar	67 59,8	39 48,8	0,213
	Kadın ve erkeklerin ağrıdan duydukları ızdırap arasında fark yoktur	16 14,3	11 13,8	
	Yaşlılar gençlere göre ağrıdan daha fazla ızdırap duyar	68 60,7	57 71,2	
	Gençler yaşlılara göre ağrıdan daha fazla ızdırap duyar	38 33,9	19 23,8	0,296
	Yaşlıların ve gençlerin ağrıdan duydukları ızdırap arasında fark yoktur	6 5,4	4 5,0	
Ağrıyı İfade Etme Eğilimi	Erkekler kadınlara göre ağrıya daha çok katlanma ve ağrılarını daha az ifade etme eğilimindedir	77 68,8	47 58,8	
	Kadınlar erkeklere göre ağrıya daha çok katlanma ve ağrılarını daha az ifade etme eğilimindedir	32 28,6	29 36,2	0,320
	Kadın ve erkeklerin ağrıya katlanma ve ağrılarını ifade etme eğilimleri arasında fark yoktur	3 2,7	4 5,0	
	Yaşlılar gençlere göre ağrıya daha çok katlanma ve ağrılarını daha az ifade etme eğilimindedir	23 20,5	25 31,2	
	Gençler yaşlılara göre ağrıya daha çok katlanma ve ağrılarını daha az ifade etme eğilimindedir	61 54,5	42 52,5	0,146
	Yaşlıların ve gençlerin ağrıya katlanma ve ağrılarını ifade etme eğilimleri arasında fark yoktur	28 25,0	13 16,2	
Ağrıyı Abartma	Erkekler ağrılarını abartma eğilimindedir	29 25,9	26 32,5	
	Kadınlar ağrılarını abartma eğilimindedir	78 69,6	48 60,0	0,346
	Kadın ve erkeklerin ağrıyı abartma eğilimleri arasında fark yoktur	5 4,5	6 7,5	
	Yaşlılar ağrılarını abartma eğilimindedir	55 49,1	40 50,0	
	Gençler ağrılarını abartma eğilimindedirler	49 43,8	26 32,5	0,053
	Yaşlıların ve gençlerin ağrıyı abartma eğilimleri arasında fark yoktur	8 7,1	14 17,5	
	Erkeklerin ağrılarını sözel olmayan ifadelerle anlatma eğilimleri kadınlardan fazladır	52 46,4	34 42,5	0,846

Ağrının Sözsüz İfadesi	Kadınların ağrılarını sözel olmayan ifadelerle anlatma eğilimleri erkeklerden fazladır	34 30,4	27 33,8	
	Kadınların ve erkeklerin ağrılarını sözel olmayan ifadelerle anlatma eğilimleri arasında fark yoktur	26 23,2	19 23,8	
	Yaşlıların ağrılarını sözel olmayan ifadelerle anlatma eğilimleri gençlerden fazladır	37 33,0	32 40,0	0,573
	Gençlerin ağrılarını sözel olmayan ifadelerle anlatma eğilimleri yaşlılardan fazladır	46 41,1	31 38,8	
	Yaşlıların ve gençlerin ağrılarını sözel olmayan ifadelerle anlatma eğilimleri arasında fark yoktur	29 25,9	17 21,2	

Tartışma ve Sonuçlar

Fizyoterapistlerin cinsiyet, yaş ve iş deneyimlerinin, hastaların ağrıya verdikleri yanıtlara ilişkin inanışlarına etkisinin incelendiği çalışmamızda, fizyoterapistlerin yaş ve cinsiyetlerinin, hastaların ağrıya verdikleri yanıtlara ilişkin inanışlarına etkisi olmadığı fakat 10 yıl altı deneyimi olan fizyoterapistlerin, istatistiksel olarak anlamlı şekilde erkeklerin kadınlara göre daha şiddetli ağrıyı tolere ettiğini düşündüğü görülmüştür.

Çalışmamızın sonucunda, fizyoterapistlerin %45.3' ü, ''Erkekler kadınlardan daha fazla ağrı hisseder'' ve %79.2'sinin ise, ''Yaşlılar gençlerden daha fazla ağrı hisseder'' görüşüne sahip olduğu saptanmıştır. Fizyoterapistlerin çoğunluğu hastanın cinsiyetinin ve yaşının ağrıya karşı duyarlılığını etkilediğine inanmaktadır. Literatür incelendiğinde bu konuyla ilgili farklı sonuçların elde edildiğini gördük. Riverst çalışmasında, kadınların ağrı duyarlılıklarını daha yüksek bulmuştur (Riverst, 2009). McCaffery ve Ferrell ise çalışmalarına dahil olan katılımcıların %63' ünün kadın ve erkeklerin ağrıya duyarlılıkları arasında fark olmadığı düşüncesine sahip olduğunu saptamışlardır (Güneş ve ark, 2005). Literatürdeki bu farklılığın, ağrı algısının oluşmasında hormonların ve genlerin dışında başka biyolojik, psikolojik, sosyokültürel ve çevresel faktörlerinde etkili olduğu (Bartley ve Palit, 2016) olgusuna bağlı olarak oluştuğunu düşünmekteyiz. Çalışmamızda yaşlıların, gençlere oranla ağrıya karşı daha hassas olduğu saptadık. Literatürde de bizim sonuçlarımızı destekleyecek birçok çalışma bulunmaktadır (Boccio, 2014; Boggero ve ark, 2015).
Çalışmamıza katılan fizyoterapistlerin %74.5'i ''Erkekler kadınlara göre daha şiddetli ağrıyı tolere eder'' %53.6' sı ise ''Gençler yaşlılara göre daha şiddetli ağrıyı tolere eder'' görüşündedir. Literatürde de erkeklerin ağrıyı daha iyi tolere ettiğini gösteren çalışmalar bulunmaktadır (Nayak ve ark, 2000; Robinson ve ark, 2003; Mitchell ve ark,2003; Jackson, 2007; Gupta ve ark, 2009). Katılımcı fizyoterapistlerin yarısından biraz fazlası ise gençlerin ağrı tolerasyonlarının daha yüksek olduğu görüşünü paylaşmıştır. Bu bulguların, gençlerin yaşlılara kıyasla anatomik, fizyolojik ve psikolojik olarak daha güçlü olması ve böylece ağrıyı daha iyi tolere edebileceği düşüncesinden kaynaklandığını düşünmekteyiz.

Katılımcıların %55.2' si '' Kadınlar erkeklere göre daha fazla ızdırap duyar'', %65.1' i ise ''Yaşlılar gençlere göre ağrıdan daha fazla ızdırap duyar'' görüşünü paylaşmıştır. Ağrı algısı acı ve ızdırap veren bir deneyimdir. Kadın ve erkek popülasyonun ağrı algılamasındaki farklılığın en önemli nedeni ağrının oluşum mekanizmasında önemli yer alan nöroaktif maddelerin seks ve hormon bağımlı olarak her iki cinste farklı üretilmesidir. Yaşlılarda ise, beyinde özellikle beyaz maddede oluşan atrofi, beyin hacmideki azalma, dendrit yapısı değişiklikleri, ağrı reseptördeki fonksiyon ve yoğunluk azalması sonucu ağrının algılanması da değişmektedir. Literatürde, ağrı algısı oluşturan minumum stimulus değeri olarak tanımlanan ağrı eşiğinin, kadınlarda ve yaşlılarda daha düşük olduğunu gösteren çalışmalar bulunmaktadır (Petersen ve ark, 1992; Lautenbacher ve ark,2005; Kirdemir ve Özorak, 2011). Çalışmamızda da fizyoterapistlerin büyük çoğunluğunun kadın ve yaşlıların ağrıdan daha fazla ızdırap duyduğu görüşünde olduğunu saptadık. Bu durumun kadınların ve yaşlıların ağrı eşiklerinin düşük olmasıyla ilişkili olabileceğini düşünmekteyiz.

Fizyoterapistlerin %64.6' sı ''Erkekler kadınlara göre ağrıya daha çok katlanma ve ağrılarını daha az ifade etme eğilimindedir, %53.6' sı ise, ''Gençler yaşlılara göre ağrıya daha çok katlanma ve ağrılarını daha az ifade etme eğilimindedir'' inancını taşımaktadır. Hastaların ağrıya daha çok katlanma ve ağrıyı daha az ifade etme eğilimi, hastaların ağrı toleransları ile paralellik göstermektedir. Çalışmamızda da, hastaların ağrıyı ifade etme eğilimi ile ilgili sonuçlarının, ağrı toleransı ile ilgili sonuçlarına benzer olduğu görülmektedir.

Ağrıyı felaketleştirme, ağrıyı aşırı biçimde abartma, ağrıyı olumsuz yorumlama gibi inançlar ağrı hastalarında, tedavideki prognozunun kötüleşmesine sebep olabilir (Babadağ ve ark, 2017). Çalışmamızda, katılımcıların %65.6' i, kadınların ağrılarını abartma eğiliminde olduğunu, %49.5' i ise yaşlıların ağrılarını abartma

eğiliminde olduğunu bildirmiştir. Ağrının başarılı bir şekilde tedavi edilememesinin nedenlerinden biri de, hastanın algıladığı ağrı ile tedavi eden kişinin ağrı algısı arasındaki farktır (Duignan ve Dunn, 2008). Çalışmamıza dahil olan fizyoterapistlerin çoğunluğu, kadın ve yaşlıların ağrılarını abartma eğilimde oldukları görüşündedir. Bu sonuçların, kadın ve yaşlıların etkili ağrı yönetiminin sağlanmasında yetersizliklere neden olabileceği düşüncesindeyiz. Ayrıca bu sonuçlardan yola çıkarak, fizyoterapistlerin bireysel özellikleri, ağrı inançları ve klinik deneyim gibi faktörlerin, hem ağrının değerlendirilme sürecini hem de tedaviyi etkileyebileceğini unutulmaması gerektiği önerilebilir.

Katılımcıların %44.8'i, ''Erkeklerin ağrılarını sözel olmayan ifadelerle anlatma eğilimleri kadınlardan fazladır'', %40.1' i ise, ''Gençlerin ağrılarını sözel olmayan ifadelerle anlatma eğilimleri yaşlılardan fazladır'' görüşündedir. Ağrı sadece duyusal ve emosyonel bir deneyim değil, aynı zamanda sosyal-iletişimsel bir olaydır (Walsh ve ark,2014). Sosyal, kültürel, emosyonel faktörlere, bilişsel yetilerdeki bozulmalara veya fonksiyonel kayıplara bağlı olarak hastalar ağrılarını sözel olarak ifade etmeyebilir. Yapılan bir çalışmada, hastaların aktivitelerinin mobilitelerinin, davranışlarının gözlemenin ve diğer etmenlerin hemşirelerin yarısından çoğunda ağrı değerlendirmesi ile ilgili kararları etkilediği saptamıştır (Güneş ve ark, 2005). Bu nedenle, fizyotepistlerin ağrının değerlendirilmesinde sözel olmayan ifadeleri de dikkate alması gerektiği önerilebilir.
Sonuç olarak; katılımcı fizyoterapistlerin büyük çoğunluğunun, hastaların yaş ve cinsiyetinin ağrıya olan yanıtlarını etkilediğine inandıkları saptanmıştır. Bu durum, fizyoterapistlerin ağrılı hasta ile iletişimlerini ve ağrı ile ilgili kararlarını etkileyebileceği için, lisans ve lisansüstü eğitimlerde öğrencilerin ağrı inançlarının değerlendirilerek eğitimlerin verilmesi ağrı tedavisinde daha başarılı sonuçların elde edilmesini sağlayacaktır.

Kaynaklar

Akdemir, N., Akyar, İ., & Görgülü, Ü. (2008). Hemşirelerin Fizik Tedavi ve Rehabilitasyon Kliniklerinde Yatan ya da Poliklinişe Başvuran Hastaların Aşrı Sorununa Yönelik Yaklaşımları. *Turkish Journal of Physical Medicine & Rehabilitation/Turkiye Fiziksel Tip ve Rehabilitasyon Dergisi, 54*(4).

Akyar, İ., Akdemir, N., & Görgülü, Ü. (2008). Hemşirelerin fizik tedavi ve rehabilitasyon kliniklerinde yatan ya da polikliniğe başvuran hastaların ağrı sorununa yönelik yaklaşımları. Türkiye Fiziksel Tıp ve Rehabilitasyon Dergisi, 54(4), pp. 157-163.

Babadağ, H. B., & Alparslan, G. B. (2017). Hemşirelik Öğrencilerinin Ağrı İnançları. Sürekli Tıp Eğitimi Dergis 26 (6), 244-250.

Bartley, E. J., & Palit, S. (2016). Gender and pain. Current Anesthesiology Reports, 6(4), 344-353.

Boccio, E. (2014). The relationship between patient age and pain management of acute long-bone fracture in the ED. American Journal of Emergency Medicine, 32(12), pp. 1516-1519.

Boggero, I. A., Geiger, P. J., Segerstrom, S. C., & Carlson, C. R. (2015). Pain Intensity Moderates the Relationship Between Age and Pain Interference in Chronic Orofacial Pain Patients. Experimental Aging Research, 41(4), pp. 463-474.

Cavlak U, Baş Aslan U, Yağcı N, Altuğ F. ile Yönetimi, F. R. (2015). Kronik Muskuloskeletal Ağrının Fizyoterapi-Rehabilitasyon ile Yönetimi. Turkiye Klinikleri J Physiother Rehabil-Special Topics, 1(1), 70-90.

Cleland, C. (2016). Pain. Biology: L-P, pp. 181-182.

Coudeyre, E., Rannou, F., Tubach, F., Baron, G., Coriat, F., Brin, S., ... & Poiraudeau, S. (2006). General practitioners' fear-avoidance beliefs influence their management of patients with low back pain. Pain, 124(3), 330-337.

Çöçelli, L. P., Bacaksız, B. D., & Ovayolu, N. (2008). Ağrı tedavisinde hemşirenin rolü. Gaziantep Tıp Dergisi, 14(2), 53-58.

Duignan, M., & Dunn, V. (2008). Congruence of pain assessment between nurses and emergency department patients: A replication. International Emergency Nursing, 16(1), pp. 23-28.

Gupta, D., Zailinawati, A. H., Lim, A. W., Chan, J., Yap, S., Hla, Y., ... & Teng, C. L. (2009). Are Indians and females less tolerant to pain? An observational study using a laboratory pain model. Medical Journal of Malaysia, 64, 111-113.

Güler D. Mastalji, yaşam kalitesi ve depresyon. T. C. Sağlık Bakanlığı Şişli Etfal Eğitim ve Araştırrma Hastanesi Aile Hekimliği Uzmanlık Tezi. İstanbul; 2006.

Güneş, Ü. Y., Eşer, İ., & Khorshid, L. (2005). Hekim ve hemşirelerin hastaların yaş ve cinsiyetine göre ağrıya verdikleri yanıtlara ilişkin inanışları. Ege Üniversitesi Hemşirelik Yüksekokulu Dergisi, 21(1), 145-156.

Kirdemir, P., & Özorak, Ö. (2011). Postoperatif Ağrı ve Analjezik İhtiyacı Preoperatif Dönemde Tahmin Edilebilir mi?. Turkiye Klinikleri Journal of Medical Sciences, 31(4), 951-959.

Lautenbacher, S., Kunz, M., Strate, P., Nielsen, J., & Arendt-Nielsen, L. (2005). Age effects on pain thresholds, temporal summation and spatial summation of heat and pressure pain. *Pain*, *115*(3), 410-418.

Main, C. J. (2010). How important are back pain beliefs and expectations for satisfactory recovery from back pain? Best Practice & Research: Clinical Rheumatology, 24(2), pp. 205-217.

McCaffery M, Ferrell BR (1991). Patient age: Does it effect your pain-control decisions. Nursing 91, 21(9):44-48.

Mills S, Torrance N, Smith BH. Identification and Management of Chronic Pain in Primary Care: a Review. Current Psychiatry Reports. 2016;18:22. doi:10.1007/s11920-015-0659-9.

Mitchell, S., Reading, I., Walter-Bone, K., Palmer, K., Cooper, C., & Coggon, D. (2003). Pain Tolerance in Upper Limb Disorders: Findings from a Community Survey. Occupational and Environmental Medicine, 60(3), pp. 217-221.

Nayak, S., Shiflett, S. C., Eshun, S., & Levine, F. M. (2000). Culture and gender effects in pain beliefs and the prediction of pain tolerance. Cross-cultural research, 34(2), 135-151.

Petersen, K. L., Brennum, J., & Olesen, J. (1992). Evaluation of pericranial myofascial nociception by pressure algometry. Reproducibility and factors of variation. Cephalalgia, 12(1), 33-37.

Raffaeli, W., Andruccioli, J., Florindi, S., Ferioli, I., Monterubbianesi, M. C., Sarti, D., . . . Giarelli, G. (2012). Qualitative Pain Classification in Hospice and Pain Therapy Unit. American Journal of Hospice and Palliative Medicine, 29(8), pp. 604-609.

Rivest, K. (2009). Relationships between pain thresholds, catastrophizing and gender in acute whiplash injury. Manual Therapy, 15(2), pp. 154-159.

Robinson, M. E., Gagnon, C. M., Riley, J. L., & Price, D. D. (2003). Altering gender role expectations: Effects on pain tolerance, pain threshold, and pain ratings. *Journal of Pain*, *4*(5), pp. 284-288.

Simmonds, M. J., Derghazarian, T., & Vlaeyen, J. W. (2012). Physiotherapists' knowledge, attitudes, and intolerance of uncertainty influence decision making in low back pain. The Clinical journal of pain, 28(6), 467-474.

Walsh, J., Eccleston, C., & Keogh, E. (2014). Pain communication through body posture: The development and validation of a stimulus set. Pain, 155(11), pp. 2282-2290.

Werner, P., Al-Hamadi, A., Limbrecht-Ecklundt, K., Walter, S., & Traue, H. C. (2018). Head movements and postures as pain behavior. PloS one, 13(2), e0192767.

International Conference on Science and Technology

ICONST 2018

5-9 September 2018 Prizren - KOSOVO

To Investigate The Effectiveness of Telerahabilition After Orthopedic Surgeries: A Systematic Review / Ortopedik Cerrahi Sonrası Telerehabilitasyonun Etkinliği: Sistematik Derleme

Nadir Tayfun ÖZCAN*[1], Tahir KESKİN[1], Zeliha BAŞKURT[1], Ferdi BAŞKURT[1]

Özet: Ortopedik rahasızlıklarda pre-op ve post-op dönemde uygulanan rehabilitasyon uygulamaları, hastaların fonksiyonel bağımsızlık düzeylerinin ve günlük yaşam aktivitelerine katılımının maksimize edilmesini sağlar. Rehabilitasyon uygulamaları, ortopedik cerrahiden sonra optimal fonksiyonel iyileşme için bir gerekliliktir. Telerehabilitasyon, bilgi ve iletişim teknolojilerini kullanarak uzaktan rehabilitasyon hizmetlerinin sağlanması olarak tanımlanmaktadır. Günümüzde telerehabilitasyon uygulamalarının kullanılmasıyla, hastalar ve rehabilitasyon ekibi, zaman, işgücü ve tedavi maliyetinden tasarruf etmektedir. Bu sistematik derleme, ortopedik cerrahi uygulamaları sonrası telerehabilitasyonun etkinliğini araştırmak ve telerehabilitasyonun konvansiyonel yöntemlerle karşılaştırılabilir olup olmadığını saptamak amacıyla yapıldı. Bu derlemede, farklı veri tabanları (Google Scholar, Pubmed, Cochrane, Science Direct, PEDro, CINAHL ve MEDLINE), '' Telerehabilitasyon, Ortopedik cerrahi sonrası telerehabilitasyon, Cerrahi sonrası telerehabilitasyon, teletıp ve mobil sağlık'' anahtar sozcukleri kullanılarak, 2008-2018 yılları arasını kapsayacak şekilde taranmıştır. Tarama sonucunda, 16 sonuç değerlendirmeye alinmiştir. Çalışmamıza dahil edilen makalelerin metodolojik kalitesinin ve kanıt gücünün değerlendirilmesinde PEDro ölçeği kullanılmıştır. Çalışmamız sonucunda, ortopedik cerrahi sonrası uygulanan telerehabilitasyon uygulamalarının, konvansiyonel tedavi yöntemleri kadar effektif bir tedavi yöntemi olduğuna dair güçlü kanıtlar bulundu. Ev içi telerehabilitasyon uygulamalarında hastaların yüksek memnuniyet derecesine sahip olduğuna dair ise orta dereceli kanıtlar bulundu. Telerehabilitasyonun standart fizik tedaviye tamamlayıcı bir tedavi olduğuna dair zayıf kanıtlar bulundu. Sonuç olarak, telerehabilitasyonun diz ve kalça cerrahisi sonrası etkili bir yöntem olduğu ve konvansiyonel tedavi uygulamaları gibi güvenilir bir şekilde kullanılabileceği saptanmıştır.

Anahtar Kelimeler: Telerehabilitasyon, ortopedik cerrahi, Sistematik derleme, Fizyoterapi

Abstract: Application of pre-op and post-op rehabilitation practices in orthopedic disease allow to maximize a patient's functional independence levels and their participation in activities of daily living in orthopedic disease. Rehabilitation is a requirement for optimal functional recovery after orthopedic surgery. Telerehabilitation is defined as the provision of rehabilitation services at a distance using information and communication. Nowadays, patients and rehabilitation team save time, labor and treatment costs, by using of telerehabilitation practices. The aim of this systematic review is to investigate the effectiveness telerehabilitation and to determine whether telerehabilitation is comparable with conventional methods after orthopedic surgeries. An online electronic search was performed from 2008 to 2018, using Google Scholar, Pubmed, Cochrane, Science Direct, PEDro, CINAHL and MEDLINE databases. The general keywords used were: telerehabilitation, telerehabilitation after orthopedic surgeries, post-surgery telerehabilitation, telemedicine, mobile health. 16 articles based on inclusion criteria consisted of the sample of the study. Pedro scale was used in order to assess the methodological quality of the included articles and to quantify the strength of evidence for each prognostic indicator, a grading tool was used. There were strong evidence supporting the idea that telerehabilitation is as an effective method as conventional therapy after orthopedic surgeries. There were also moderate evidence demonstrating that the satisfaction of the participants with in-home

[1]Süleyman Demirel Üniversitesi, Sağlık Bilimleri Fakültesi, Fizyoterapi ve Rehabilitasyon Bölümü, 32260,Isparta, Türkiye
*Correspondingauthor: nadirozcan@sdu.edu.tr

telerehabilitation were very high. There were weak evidence that telerehabilitation is a complementary treatment to standard physical therapy. As a result, Telerehabilitation is an effective method after knee and hip surgery and can be used reliably like conventional therapy.

Keywords: Telerehabilitation, Orthopedic surgeries, Systematic review, Physiotherapy

Giriş

Komünikasyon teknolojilerinde yaşanan gelişmeler ve düşük maliyetli internet kullanımın yaygınlaşması hem hastane ortamında hem de taburculuk sonrası sağlıkla ilgili teknoloji temelli çözümlerin yaygınlaşmasını sağlamıştır (Pastora-Bernal ve ark, 2017). Son yıllardaki demografik değişimler ve halk sağlığı harcamalardaki artış yeni rehabilitasyon uygulamalarını gerekli kılmıştır (Peretti ve ark, 2017). Hem kamu hem de özel sağlık sektöründe, rehabilitasyon alanına olan talep artmaktadır. Dünya Sağlık Örgütünün 2011 yılı verilerine göre Dünya çapında bir milyar insan rehabilitasyon hizmetlerine ihtiyaç duymaktadır. Özellikle gelişmiş ülkelerdeki refah seviyesindeki ve sağlık koşullarındaki artışa pararel olarak yaşlı nüfus artışı da, rehabilitasyon hizmetlerine olan ihtiyacı artırmaktadır (Ruiz-Fernandez ve ark. 2014)

Yaşlı popülasyonun ve obezite prevelansının artışı, genç nüfusun fiziksel fonksiyonelliğini iyileştirmek gibi faktörlere bağlı olarak, özellikle de eklem replasmanı gibi ortopedik cerrahi girişimlerin sayısında artış gözlemlenmektedir (Han ve ark, 2015). Ortopedik cerrahi girişimler sonrası, gecikmiş post-operatif toparlanma, cerrahi sonrası ana problemlerden biridir. Ayrıca gelişebilecek post-operatif komplikasyonlar hastanede kalış süresinin uzamasına, mortalitiye veya tedaviyle ilişkili maliyet artışlarına neden olabilir (Van Egmond ve ark, 2018). Cerrahi sonrası rehabilitasyon uygulamaları ise kas kuvvetinin, eklem hareket açıklığının, yürümenin, propriosepsiyonun toparlanmasını fasilite etmek ve hastanın günlük yaşam aktivitelerine katılımını artırmak ve optimal fonksiyonel kapasiteye ulaşması için bir gerekliliktir (Russell ve ark, 2011).

Hüzmeli ve arkadaşlarına (Hüzmeli ve ark, 2017) göre, ‘’rehabilitasyon hizmetlerinin farklı bir modelde sunumu olan telerehabilitasyon, rehabilitasyon hizmetlerine erişimin sağlanması ve hastaların bağımsızlık düzeylerinin geliştirilmesi amacıyla, rehabilitasyon hizmetlerinin bilgisayara dayalı teknolojiler ve iletişim araçları ile rehabilitasyon uzmanları tarafından verilmesidir. Gelişen teletıp uygulamalarında biri olan telerehabilitasyon, rehabilitasyon hizmetlerini uzaktan sağlamaya yardımcı bazı araç, protokol ve prosedürlerden oluşmaktadır (Rogante ve ark, 2015). Telerehabilitasyon uygulamaları nörolojik hastalıklar, yoğun bakım, kanser, felç, kronik obstrüktif akciğer hastalığı, muskuloskeletal hastalıklar gibi farklı alanlarda kullanılabilir (Pastora-Bernal ve ark, 2017).

İçerik olarak değerlendirme, eğitim, tedavi, gözlem ve egzersiz uygulamalarını kapsayan telerehabilitasyon yaklaşımı, son zamanlarda hızlı bir gelişim göstermekte ve taburculuk sonrası hastaların değerlendirilmesinde ve tedavisinde maliyet açısından daha uygun bir yöntem olarak karşımıza çıkmaktadır (Van Egmond ve ark, 2018). Özellikle post-op dönemde, telerehabilitasyon uygulamalarını koruyucu bakım yönetimi, esnek egzersiz saatleri, ulaşım masraflarının azaltılması, zaman tasarrufu, günlük yaşama adaptasyon gibi birçok alanda avantaj sağlamaktadır (Beaver ve ark, 2009). Hastalar herhangi bir sağlık kurumundan alabilecekleri hizmeti, daha yoğun olacak şekilde telerehabilitasyon yöntemi ile alabilirler. Ayrıca rehabilitasyon alanında bu tarz teknolojilerin kullanımının hasta ve sağlık çalışanlarının tatmini ve hastaların yaşam kalitesi üzerine olumlu katkı sağladığı da bilinmektedir (Head ve ark, 2011)

Material and Method

Bu sistematik derlemede; Google Akademik, Pubmed, Cochrane, Science Direct, PEDro, CINAHL ve MEDLINE veritabanlarında 2008-2018 yılları arasında yayınlanmış makaleler; ‘’telerehabilitasyon, ortopedik cerrahi sonrası telerehabilitasyon, cerrahi sonrası telerehabilitasyon, teletıp ve mobil sağlık anahtar sözcükleri kullanılarak taranmıştır. telerehabilitation,

Dâhil edilme- dışlanma kriterleri: Bu sistematik derleme; ortopedik cerrahi sonrası telerehabilitasyon ile ilgili yapılan kohort çalışmaları içermektedir. Çalışmaların son on yıl içinde yapılmış olması ve tam metinlerine

ulaşılabilmesi dâhil edilme kriterlerini oluşturmaktadır. Tam metnine ulaşılamayan çalışmalar, çalışma protokolleri, sözel veya poster bildiri olarak sunulmuş özet metinler çalışmanın dışında tutulmuştur. Ayrıca herhangi bir hastalığa sekonder olarak gelişen problemler sonrası yapılan ortopedik cerrahiler de çalışma dışında tutulmuştur.

Mevcut anahtar kelimelerle yapılan tarama sonucunda toplam 1718 çalışmaya ulaşılmıştır. 1600 çalışmanın başlığı telerehabilitasyonla ilgili olmadığı için elenmiştir. Kalan 118 çalışmanın özet metinleri okunmuş ve 20 çalışmanın iki arama motorunda eşleştiği, 74 çalışmanın konu ile direkt ilişkili olmadığı, 1 çalışmanın poster bildiri olduğu, 4 çalışmanın çalışma protokolü olduğu ve 3'ünün de dâhil edilme kriterlerine uymadığı tespit edilmiştir. Sonuç olarak 16 çalışma bu sistematik derlemenin örneklemini oluşturmuştur.

Metadolojik kalite ve kanıt düzeyi değerlendirmesi: Çalışmamız metadolojik kalite açısından pedro skalası ile değerlendirilmiştir. Pedro sklası 11 sorudan oluşmaktadır. Pedro skalasına göre 9'un üzerindeki puanlar mükemmel, 6-8 puan arası iyi, 4-5 puan kabul edilebilir ve 4'ün altındaki puanlar ise zayıf metadolojik kalitede çalışmaları göstermektedir.

Kanıt düzeyini belirlemek için Oxford Centre for Evidence Based Medicine tarafından geliştirilen derecelendirme aracı kullanılmıştır (Phillips ve ark, 2007). Kanıt düzeyi kategorileri ise güçlü, orta düzey, düşük, yetersiz ve çelişkili kanıt düzeyi şeklindedir (Tablo.1).

Tablo 1. Çalışmaları kanıt düzeyini belirlemek için kullanılan derecelendirme aracı

Güçlü kanıt değeri	**En az 2 kabul edilebilir kalitede kohort çalışmasında tutarlı kanıtlar bulunması**
Orta düzey kanıt değeri	Bir kabul edilebilir kalitede kohort çalışması ve bir düşük kaliteli kohort çalışmada tutarlı kanıtlar bulunması
Düşük kanıt değeri	Bir kabul edilebilir kalitede kohort çalışması veya 3 düşük kaliteli kohort çalışmasında tutarlı kanıtlar
Yetersiz kanıt değeri	Bir düşük kalitede kohort çalışması
Çelişkili kanıt değeri	Herhangi bir kohort çalışmasında birbiriyle çelişen kanıtlar

Bulgular

Ortopedik cerrahi sonrası telerehabilitasyonun etkinliğini araştırmak amacıyla yapmış olduğumuz bu sistematik derlemenin örneklemini oluşturan çalışmaların büyük çoğunluğu total diz protezi (9) ve total kalça protezi (5) üzerine yoğunlaşmıştır. Bir çalışma humerus kırıklarını, bir çalışma da karpal tünel sendromunu konu almıştır. Çalışmaların katılımcı sayıları 5 ile 274 arasında değişmektedir.

Çalışmalarda katılımcılara fonksiyonel mobilite değerlendirmeleri, ağrı, kas kuvveti, normal eklem hareketi ve denge değerlendirmeleri, yürüyüş analizleri, günlük yaşam aktivitesi değerlendirmeleri, fonksiyonel değerlendirmeler ve memnuniyet anketleri uygulanmıştır.

Sistematik derlememizde yer alan çalışmalardan 3'ünün Pedro skalasına göre puanı 9'dur. 4 çalışma 6 ve üzeri puan aralığında yer almaktadır. 2 çalışma 5 puan almış olup, 7 çalışma da 4 ve daha az puan almıştır.

Çalışmamızın sonuçlarına göre; ortopedik cerrahi sonrası telerehabilitasyonun konvansiyonel tedavi kadar etkili bir yöntem olduğunu destekleyen güçlü kanıtlar bulunmuştur. Evde yapılan telerehabilitasyon programlarından hasta memnuniyetinin yüksek olduğunu gösteren orta düzeyde kanıtlar, telerehabilitasyonun standart fizyoterapiye tamamlayıcı bir tedavi olduğuna dair zayıf kanıtlar bulunmuştur.

Çalışmanın sonuçları Tablo- 2'de özetlenmiştir.

Tablo-2. değerlendirmeye alınan çalışmaların özetleri

Yazar/ Yıl	Takip periyo-du	Katı-lımcı sayısı	Değerlendirme yöntemleri	Cerrahi uyg. bölge	Sonuç özetleri
Russel ve ark.(2)	6 Hafta	65	WOMAC, Patient-Specific Functional Scale, Timed up-and-go testi, diz fleksiyon, ekstensiyon normal eklem hareketleri, VAS, quadriseps kas kuvveti, yürüyüş analizi	Diz	6 haftalık telerehabilitasyon programı konvansiyonel tedavi kadar etkili bulunmuştur.
Tousignant ve ark. (3)	16 seans	5	Diz fleksiyon, ekstensiyon normal eklem hareketleri, denge, alt ekstremite kas kuvveti, locomotor performans, memnuniyet anketi.	Diz	Total diz artroplastisi sonrası telerehabilitasyon, rehabilitasyon servislerinin gerçek bir alternatifidir.
Cabana ve ark. (4)	-	15	TUG, kas kuvveti, tinetti, berg,	Diz	Klinik değişkenler, orta derecede güvenirlik seviyesinde yüz yüze rehabilitasyon ve telerehabilitasyonda benzerlik göstermektedir.
Moffet ve ark. (5)	4 ay	205	Health Care Satisfaction Questionnaire	Diz	Telerehabilitasyon, rehabilitason servislerine erişimi kolaylaştırmaktadır ve total diz artroplastisi sonrası hasta memnuniyeti üst düzeydedir.
Kalron ve ark. (6)	6 hafta	40	TUG, 2m yürüme testi, 10m yürüme testi, sit to stand test, yürüyüş hızı, ortalama adım uzunluğu	Kalça	Telerehabilitasyon standart fizyoterapiye tamamlayıcı bir tedavidir ve kalça cerrahisi sonrası mobilite üzerine olumlu etkileri bulunmaktadır.
Tousignant ve ark. (7)	8 hafta	17	McGill ağrı anketi, SF-MPQ, omuz fleksiyon, ekstansiyon, internal-external rotasyon, abdüksiyon normal eklem hareketleri, DASH, Health care satisfaction questionnaire	Kol	Telerehabilitasyon, rehabilitasyon servislerinin bir alternatifi olabilir.
Piqueras ve ark. (8)	3 ay	42	Normal eklem hareketleri, kas kuvveti, yürüyüş hızı, ağrı, WOMAC,	Diz	Telerehabilitasyon, rehabilitasyon servislerine ulaşımda güçlük çeken

					hastalar için konvansiyonel terapi kadar etkilidir.
Moffet ve ark. (9)	4 ay	205	WOMAC, KOOS, fonksiyon ve kuvvet testleri, functional and strength tests, diz normal eklem hareketleri	Diz	Telerehabilitasyon, rehabilitasyon servislerinin bir alternatifi olabilir.
Fusco ve ark. (10)	20 seans	-	Diz normal eklem hareketleri, cost-effective per QALY	Diz	Birincil bakım servislerine taşıma hizmetleri olmadığı zamanlarda telerehabilitasyon daha az maliyetlidir.
Nelson ve ark. (11)	-	75	Hastaların teknoloji kullanımı, teknolojiye erişimi ve teknoloji hakkındaki düşüncelerinin sorgulayan anket	Diz, kalça	Elektronik bir aygıttan video izleme teknoloji temelli ev egzersiz programı için tercih edilen bir metottur.
Bini ve ark.(12)	3 ay	51	Hasta memnuniyet anketi	Diz	Asenkron telererehabilitasyon kişisel bakım modeline klinik olarak eşdeğerdir.
Fung ve ark. (13)	2 hafta	40	2 dakika yürüme tsti, diz normal eklem hareketi, timed standing, Activity-specific Balance Confidence Scale, Lower Extremity Functional Scale, Numeric Pain Rating Scale	Diz	Total diz artroplastisi sonrası wee fi cihazı uygun oyunların seçimiyle denge ve postüral kontrolü sağlamak için kullanılabilir.
Li ve ark. (14)	6 ay	249	Harris scale, patient medical behavior questionnaire	Kalça	Telefonla uygulanan telerehabilitasyon hastanın doktor tavsiyesine uyumunu arttırmış ve rehabilitasyonu teşvik etmiştir.
Eiserman ve ark. (15)	6 ay	274	Harris Hip Score, Hospital for Special Surgery Score, FIM instrument, Hanover Functional Ability Questionnaire	Kalça	Bilgisayar destekli eğitim, rehabilitasyon programının sonuçları ile bağlantılı olarak geleneksel fizyoterapiye eşdeğer olarak kabul edilebilir.
Anton ve ark. (16)	19 seans	7	-	Kalça	KiReS ve benzeri telerehabilitasyon hizmeti sunan sistemlerin fizyoterapiye destek olarak kullanılabileceği belirtilmiştir.
Heuser ve ark. (17)	13 seans	5	Kas kuvveti, kavrama kuvveti değerlendirmesi	El bileği (karpal tünel cer.)	Rutgers Master II ile yapılan telerehabilitasyon sonrası kavrama kuvvetinde artış olmuştur.

Tartışma ve Sonuçlar

Bu sistematik derlemede; ortopedik cerrahi sonrası telerehabilitasyonun konvansiyonel tedavi kadar etkili bir yöntem olduğunu destekleyen güçlü kanıtlar bulunmuştur. Evde yapılan telerehabilitasyon programlarından hasta memnuniyetinin yüksek olduğunu gösteren orta düzeyde kanıtlar, telerehabilitasyonun standart fizyoterapiye tamamlayıcı bir tedavi olduğuna dair zayıf kanıtlar bulunmuştur.

Bu sistematik derlemenin örneklemini oluşturan klinik çalışmaların metadolojik kalitesi incelendiğinde; çalışmaların %50'sinden büyük kısmının zayıf metadolojik kalitede olduğu belirlenmiştir. Bu nedenle telerehabilitasyonu konu edinen daha yüksek kalitede çalışmalar yapılması gerektiği düşünülmektedir.

Telerehabilitasyon üzerine yapılan çalışmaların büyük bir kısmı alt ekstremite cerrahisini konu almaktadır. Kalça ve diz artroplastisi dışında sadece iki çalışma (Tousignant ve ark, 2014; Heuser ve ark, 2007) üst ekstremite cerrahisi ile ilgilidir. Günümüzde telerehabilitasyon hizmetlerinin çok geniş kapsamlı olduğu bilindiğinden üst ekstremite cerrahisi ve muskuloskeletal cerrahi sonrası telerehabilitasyonu konu edinen daha fazla çalışmaya ihtiyaç duyulduğu düşünülmektedir.

Bu sistematik derleme telerehabilitasyonun standart fizyoterapiye güçlü bir alternatif olduğunu göstermektedir. Telerahabilitasyon programlarında insan gücüne ve hastane ortamına çok fazla ihtiyaç duyulmadığından standart tedaviye göre maliyet çok daha düşüktür (Fusco ve ark, 2016). Bu nedenle telerehabilitasyon konusunda tedavi maliyetlerini araştıran daha çok çalışmaya ihtiyaç duyulduğu düşünülmektedir. Ayrıca fizyoterapist sayısı yeterli olmayan ülkelerde konu ile ilgili çalışmalara daha çok çalışma yapılması gerektiği düşünülmektedir.

Sonuç olarak; telerehabilitasyon standart fizyoterapinin güçlü bir alternatifi olabilir. Telerehabilitasyon programları ile ilgili yüksek metadolojik kalitede çalışmalar yapılması gereklidir. Telerehabilitasyon ile ilgili yapılacak çalışmaların üst ekstremite cerrahisi ve muskuloskeletal cerrahi sonrası telerehabilitasyonu konu edinmesinin faydalı olacağı düşünülmektedir. Ayrıca bu çalışmaların tedavi maliyetlerini de ele alması faydalı olacaktır.

Kaynaklar

Antón D, Nelson M, Russell T, Goñi A, Illarramendi A. Validation of a Kinect-based telerehabilitation system with total hip replacement patients. J Telemed Telecare 2016 Apr;22(3):192-197.

Beaver, K., Tysver-Robinson, D., Campbell, M., Twomey, M., Williamson, S., Hindley, A., ... & Luker, K. (2009). Comparing hospital and telephone follow-up after treatment for breast cancer: randomised equivalence trial. Bmj, 338

Bini SA, Mahajan J. (2017). Clinical outcomes of remote asynchronous telerehabilitation are equivalent to traditional therapy following total knee arthroplasty: A randomized control study. J Telemed Telecare. Feb;23(2):239-247.

Cabana F, Boissy P, Tousignant M, Moffet H, Corriveau H, Dumais R.(2010). Interrater Agreement Between Telerehabilitation and Face-to-Face Clinical Outcome Measurements for Total Knee Arthroplasty. Telemedıcıne and e-health, 16(3); 293-298

Eisermann U, Haase I, Kladny B. Computer-aided multimedia training in orthopedic rehabilitation. Am J Phys Med Rehabil2004 Sep;83(9):670-680.

Fung V, Ho A, Shaffer J, Chung E, Gomez M. Use of Nintendo Wii Fit™ in the rehabilitation of outpatients following total knee replacement: a preliminary randomised controlled trial. Physiotherapy 2012 Sep;98(3):183-188.

Fusco F, Turchetti G.(2016). Telerehabilitation after total knee replacement in Italy: cost-effectiveness and cost-utility analysis of a mixed telerehabilitation-standard rehabilitation programme compared with usual care. BMJ Open.;6: 1-10

Han, A. S., Nairn, L., Harmer, A. R., Crosbie, J., March, L., Parker, D., ... & Fransen, M. (2015). Early rehabilitation after total knee replacement surgery: a multicenter, noninferiority, randomized clinical trial comparing a home exercise program with usual outpatient care. Arthritis care & research, 67(2), 196-202.

Head, B. A., Keeney, C., Studts, J. L., Khayat, M., Bumpous, J., & Pfeifer, M. (2011). Feasibility and Acceptance of a Telehealth Intervention to Promote Symptom Management during Treatment for Head and Neck Cancer. The Journal of Supportive Oncology, 9(1)

Heuser A, Kourtev H, Winter S, Fensterheim D, Burdea G, Hentz V, et al. Telerehabilitation using the Rutgers Master II glove following carpal tunnel release surgery: proof-of-concept. IEEE Trans Neural Syst Rehabil Eng 2007 Mar;15(1):43-49.

Hüzmeli, E. D., Duman, T., & Yıldırım, H. (2017). Türkiye'de İnmeli Hastalarda Telerehabilitasyonun Etkinliği: Pilot Çalışma. *Turk J Neurol*, *23*, 21-25.

Kalrona A, Tawila H, Peleg-Shanic S, Vatineb JJ.(2018). Effect of telerehabilitation on mobility in people after hip surgery: a pilot feasibility study. Int J Rehabil Res. ;41(3):244-250

Li L, Gan Y, Zhang L, Wang Y, Zhang F, Qi J. The effect of post-discharge telephone intervention on rehabilitation following total hip replacement surgery. Int J Nurs Sci 2014 Jun;1(2):207-211.

Moffet H, Tousignant M, Nadeau S, M´erette C, Boissy P, Corriveau H et al.(2015). In-Home Telerehabilitation Compared with Face to Face Rehabilitation After Total Knee Arthroplasty. A Noninferiority Randomized Controlled Trial. J Bone Joint Surg Am.;97:1129-41

Moffet H, Tousignant M, Nadeau S, Mérette C, Boissy P, Corriveau H, et al. (2015). In-Home telerehabilitation compared with face-to-face rehabilitation after total knee arthroplasty: a noninferiority randomized controlled trial. J Bone Joint Surg Am, 15;97(14):1129-1141.

Nelson MJ, Crossley KM, Bourke MG, Russell GR.(2017). Telerehabilitation feasibility in total joint replacement. International Journal of Telerehabilitation, 9 (2); 31-38

Pastora-Bernal, J. M., Martín-Valero, R., Barón-López, F. J., & Estebanez-Pérez, M. J. (2017). Evidence of benefit of telerehabitation after orthopedic surgery: a systematic review. Journal of medical Internet research, 19(4).

Peretti, A., Amenta, F., Tayebati, S. K., Nittari, G., & Mahdi, S. S. (2017). Telerehabilitation: Review of the State-of-the-Art and Areas of Application. JMIR Rehabilitation and Assistive Technologies, 4(2).

Phillips B, Ball C, Sackett DL, Badenoch D, Straus S, Haynes B, DawesM(2007). Oxford Centre for Evidencebased Medicine Levels of Evidence. British Journal of Urology International 100: 975.

Piqueras M, Marco E, Coll M, Escalada F, Ballester A, Cinca C, et al.(2013). Effectiveness of an interactive virtual telerehabilitation system in patients after total knee arthoplasty: a randomized controlled trial. J Rehabil Med. Apr;45(4):392-396

Rogante, M., Kairy, D., Giacomozzi, C., & Grigioni, M. (2015). A quality assessment of systematic reviews on telerehabilitation: what does the evidence tell us?.

Ruiz-Fernandez, D., Marín-Alonso, O., Soriano-Paya, A., & García-Pérez, J. D. (2014). eFisioTrack: a telerehabilitation environment based on motion recognition using accelerometry. The Scientific World Journal, 2014.

Russell T, Buttrum P, Wootton R, Jull G. Internet-based outpatient telerehabilitation for patients following total knee arthroplasty: a randomized controlled trial. J Bone Joint Surg Am 2011 Jan 19;93(2):113-120.

Russell, T. G., Buttrum, P., Wootton, R., & Jull, G. A. (2011). Internet-based outpatient telerehabilitation for patients following total knee arthroplasty: a randomized controlled trial. JBJS, 93(2), 113-120.

Tousignant M, Boissy P, Corriveau H, Moffet H, Cabana F. (2009). In-Home Telerehabilitation for Post-Knee Arthroplasty: A Pilot Study. International Journal of Telerehabilitation, 1(1) :9-16

Tousignant M, Giguère A, Morin M, Pelletier J, Sheehy A, Cabana F.(2014). In-home telerehabilitation for proximal humerus fractures: a pilot study. Int J Telerehabil. ;6(2):31-37

Van Egmond, M., van der Schaaf, M., Vredeveld, T., Vollenbroek-Hutten, M., van Berge Henegouwen, M., Klinkenbijl, J., & Engelbert, R. (2018). Effectiveness of physiotherapy with telerehabilitation in surgical patients: A systematic review and meta-analysis. Physiotherapy, 104(3), pp. 277-298

International Conference on Science and Technology

ICONST 2018

5-9 September 2018 Prizren - KOSOVO

Investigation The Effectson Geometric Properties of Product and Wearing in Progressive Die /Ardışık Kalıplarda Kalıp Malzemesinin Kalıp Aşınması İle Ürün Geometrik Özellikleri Üzerindeki Etkilerinin Araştırılması

Ali ÖZCAN[1]*, Erkan ÖZTÜRK[2], İsmail OVALI[3]

Özet: Ardışık kalıplar otomotiv sektöründen tekstil sanayisine kadar geniş bir alanda kullanılmakta olup hem zaman hem de maliyet açısından önem arz etmektedir. Kalıp aşınmaları özellikle ürün boyutlarında farklılıklara sebep olmaktadır. Kullanılan kalıp malzemesi seçimi oluşacak aşınmaların belirli bir sürece yayılmasına olanak sağlar. Bu çalışma ile kalıp malzemesi olarak seçilen 2767, 2379 ve CPOH soğuk şekillendirme çelikleri kullanılarak belirli adetlerde yapılan üretim sürecinde ürün yüzey kalitesi ve kalıp aşınmaları incelenmiştir. Tasarlanan ürün kalıbı tüm çeliklere 0.01 mm hassasiyetinde uygulanmış ve 5000 adet ürün üretilerek bu ürünlerin birinci, bininci ve beş bininci örnekleri karşılaştırmalı olarak incelenmiştir. Bununla birlikte kalıp çeliklerindeki aşınmalarda değerlendirilmiştir. Bu değerlendirmeler sonucunda kalıp malzemesi olarak CPOH çeliğinin kullanılması ürün boyutlarını standartlaştırılması ve daha uzun üretim sürecine dayanabilmesi açısından avantajlı olduğu görülmüştür.

Anahtar Kelimeler: Ardışık kalıp, Geometrik özellikler, Aşınma, Yüzey kalitesi

Abstract: Progressive dies are used in a wide range from the automotive sector to the textile industry and are important in terms of both time and cost. Surface abrasions cause especially the differences in product dimensions. The sellection of die material make possible the spread over time of abrasions. In this study, product surface quality and die abrasion were investigated by using 2767, 2379 and CPOH cold forming steels selected as die materials in certain production processes. The form of chosen design has been moulded to all steels at a precision of 0.01 mm and 5.000 samples were produced and than the first, thousandth and fifth thousand product samples were examined comparatively. In addition, abrasion on dies has been evaluated. As a result of these evaluations, it has been found out that the use of CPOH steel is advantageous in terms of the standardization product dimensions and the longer lifetime.

Keywords: Progressive die, Geometric properties, Abrasion, Surface quality

Giriş

Endüstriyel alandaki teknolojik ilerlemeyle üretim miktarlarındaki artış, seri imalat yöntemlerine geçilerek daha kaliteli ve daha ucuz imalat yöntemlerine olan ihtiyacı rekabetin vazgeçilmez unsuru durumuna getirmiştir. Ardışık kalıplarla imalat sac metal üretim maliyetlerinin minimum seviyelere indirilmesini sağladığı gibi ürün kalitesinde de tekli kesme ve bükme kalıplarına göre avantajları oldukça yüksektir. Bir sac metal ürünü iki veya daha fazla kalıpla daha fazla sayıda pres tezgahı ve insan gücü kullanarak imalatını gerçekleştirmek yerine bu işlemi bir ardışık kalıpla yapmak daha yalın ve ekonomik olmaktadır. Bu şekilde hem pres hem insan gücü hem de zaman minimuma çekilmiş olmaktadır.

[1]Fatih Profil A.Ş. Denizli, 20330, TURKEY
[2]Pamukkale University, Faculty of Technology, Automotive Engineering Department, Denizli, TURKEY
[3]Pamukkale University, Faculty of Technology, Mechanical and Manufacturing Engineering Department, Denizli, TURKEY
*Corresponding author: tasarimmerkezi@fatih.com.tr

Ardışık kalıpların geliştirilmesi ve otomasyon sistemlerinin kalıpçılığa uygulanmasıyla sac metal kalıpçılığı endüstride önemli bir yer edinmiştir. Bu sayede daha az insan gücüyle daha çok sayıda ve kaliteli üretim yapılabilmektedir. Endüstride kalıpçılık sektörünün daha fazla kullanımı yaygın hale gelmektedir.
Sac metal şekillendirme ile ilgili yapılan çalışmalar nihai ürünün istenilen ölçü tamlığı ve geometrik düzgünlüğü üzerine yapılmaktadır. Sac ürün imalatı uzun ve maliyetli bir süreçtir. Ürün sayılarının fazla olması sebebiyle kalıplardaki değişiklikler maliyeti artırmaktadır. Bu süreçteki hata paylarının en az seviyede tutulmasının önemli sebeplerinden birisi de budur.

Sac metal üzerindeki geri esneme payları da dikkat edilmesi gereken önemli bir unsurdur. Bu konu ile ilgili bir çalışmada Gantar vd. (2002), sac metal kalıpçılığının uygulamaları arasında olan otomotiv endüstrisiyle ilgili bir çalışma ele almışlardır. En iyi ürün şekli, deformasyon ve geri esneme miktarlarını araştırmışlardır. Bilgisayar programlarıyla önceden tasarımı gerçekleştirilmiş olan modelleri simülasyonlarındaki hata paylarını gözlemleyerek üretim aşamasında bu hata paylarını en aza indirilebileceği belirtilmiştir.

Sac metal malzemelerdeki şekillendirme ile ilgili bir diğer çalışma Michel ve Picart (2002) tarafından yapılmıştır. Sac malzemenin fiziksel özelliklerinin boyut ve uzunluk üzerinde ilişkisi olmadığını ve bu nedenle metal şekillendirme süreçlerinde boyutsal etkilerin incelenmesinin uygun olmayacağı konusunda hem fikir olmuşlardır. Parçaların sac metal şekillendirmeleri için malzeme davranışları için teori geliştirmişler ve yapısal parametre uzunluğunu etkin plastik gerilim oranına ilişkilendirerek, bu oranı her bir birleşim noktasında kalınlık boyunca birleşim noktalarının koordinatlarında bağımlı olarak hesaplanmışlardır. Kalınlık boyunca etkin olan gerilme değişiminin, iteratif olarak çözümlenebileceğini belirtmişlerdir.

Sac metal kalıpçılığı ile ilgili üretimi yalın hale getirirken maliyeti azaltma ile ilgili uygulama çalışmaları yapılmaktadır. Bu çalışmalardan Hambli (2001) çalışmasında; sac metal şekillendirilmesindeki tasarımın ana amaçlarından birisi yeterli derecede kalıp tasarımını geliştirmek, kalıp ömrünü arttırmak, parça kalitesini arttırmak, daha sade hale getirmek ve üretim maliyetini azaltırken daha sistemli kalıp yerleşimi olduğunu belirtmiştir. Aynı zamanda sac metal kesme-delme işlemlerinde, sonlu elemanlar yöntemini kullanarak zımbanın aşınma durumunu önceden kestirmeyi amaçlamıştır. Bununla beraber yapılan uygulamalarda zımba ile ilgili verimli çalışmalar yapmışlardır.

Chan vd. (1998) yılında yaptıkları çalışma ile sac kesme kalıplarında kesme işlemi esnasındaki deforme olan yüzeyleri incelemek için kalıp seti tasarlayarak farklı malzemeler ile uygulamalar yapmışlardır. Bu uygulamalar sayesinde nihai ürün üzerindeki çapak oluşumunu ve kaplama yüzeylerini incelemişlerdir.

Literatürde ki araştırmalar incelendiğinde sac şekillendirmeyi etkileyen birçok etken bulunduğu ve her farklı malzeme için bu etkenlerin incelemek için daha birçok farklı araştırma yapılabileceği görülmektedir. Aynı zamanda sac malzeme üretiminde ürün kalitesi yönünden ardışık kalıp tasarımı, kalıplarda kullanılan çelikler ve kalıp kesme boşluğunun önemi oldukça büyüktür. Bu çalışmalar üzerine yapılan araştırmalar genelde teoride kalmış uygulamada yerini yeterince alamamıştır. Bu çalışma ile literatürde görülen çalışmalardan farklı olarak, ardışık kalıplarında soğuk iş çelik malzemelerin cinsine bağlı olarak kullanım ömrü değişimleri ile ürün kalitesi ve istenen yüzey kalitesinin elde edilmesinin yolu araştırılmıştır. Bu amaçla, ardışık bir kalıp tasarlanmış, farklı özellik ve maliyete sahip soğuk iş takım çeliklerinden en çok tercih edilen malzemeler kullanarak, sac ürün imalatı sürecinde çeliklerdeki aşınma ve kesim yüzey kalitesi deneysel olarak incelenmiştir. Ürünle ilgili işlem planlaması yapılarak üretimin iyileştirilmesi ve aynı kalıptan çıkan farklı malzemelere sahip ürünler karşılaştırılmıştır.

Materyal ve Yöntem

Elde edilen ürünlerin yüzeysel boyutları üç boyutlu lazer tarama yöntemi kullanılarak elde edilmiştir. Üç boyutlu lazer tarama sistemleri bir lazer ve bu lazer ışınının algıladığı alanı algılayan kamera teknolojisi ile üç boyutlu nokta bulutu elde etme prensibine dayalı olarak çalışır. Lazer tarama sistemleri lazer ışının parça üzerine yansıması ve bu ışının geri yansıması sonucu kameranın lazer ışınının üzerinde düşürdüğü noktaların koordinatlarının belirlenmesi ile boyutsal veriyi elde eder. Üç boyutlu lazer tarama sistemleri kamera ve lazer ışının birbirine göre yaptığı optimum açı ile maksimum veri ve maksimum hassasiyeti sağlamaktadır (PM

2018). Bu tarama sistemleri günümüzde yaygın olarak sac kalıbı ve imalatı, , kuyumculuk sektörü, otomotiv sanayisi ve bölgesel ölçüm teknolojisinin kullanıldığı sanayi alanlarında tercih edilmektedir. Kalite kontrol amaçlı yapılan tarama işlemi; 3D verisi mevcut olan ürün ve üretilen ürünün doğru üretilip üretilmediğinin (özellikle parçalı formlu geometriye sahipse) kontrolünü içerir. Üretimi yapılan parça lazer tarama cihazı ile taranır, tarama verisi (nokta bulutu) elde edilir, elde edilen tarama verisi, parçanın 3D verisi ile bilgisayar ortamında çakıştırılır, çakıştırma sonucunda üründeki form bozuklukları, kesim hattı hataları ve benzeri kalite hataları renk haritası yoluyla kontrol edilir. Renk haritasında görülen ölçü hataları istenilen tolerans dışındaysa gerekli önlemler alınır (OT 2018). Şekil 1'de lazer tarama ile kalite kontrol rapor örneği görülmektedir. Şekilde kırmızı bölgeler tam basma kısımlarını, mavi bölgeler ise aşınma kısımları ifade etmektedir. Ölçü kontrolü yapılan noktalarda, tolerans dışında kalan değerler zemini açık tonlu kırmızı rankle belirtilmiştir. Karşılaştırmalar ±0.5 µm tolerans aralığında gerçekleştirilmiştir.

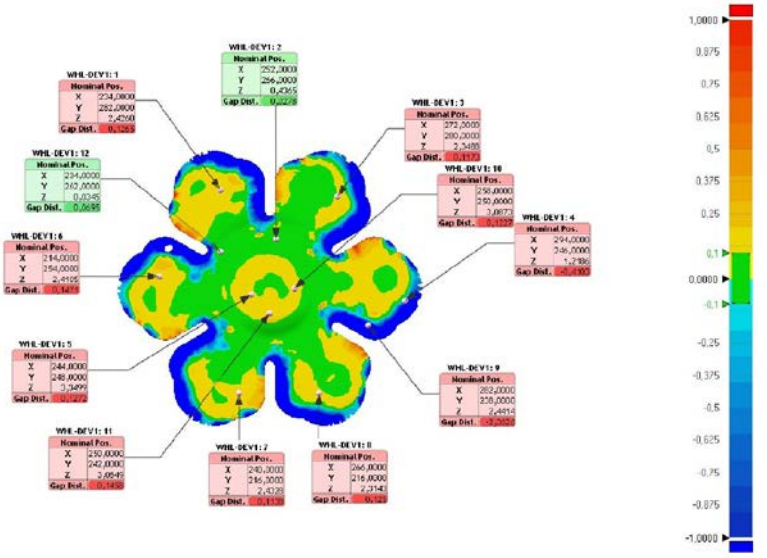

Şekil 1. 2767 malzemesinin üst kalıp lazer taraması

Bulgular

2767, CPOH ve 2379 soğuk iş çeliklerinin yüzeysel boyut ölçüm değerleri incelenmiş olup, elde edilen sonuçlar aşağıda irdelenmiştir. 2767 kalıp malzemesinden alınan birinci örneğin geometrik özellikleri Şekil 2'de görülmektedir. On altı noktadan alınan verilere göre, yedi farklı noktada sapmanın oldukça fazla olduğu gözlemlenmiş. Bu sapmaların ortalama değeri 1.365µm olarak belirlenmiştir. En büyük sapmanın 8 numaralı bölge üzerinde olduğu ve 2.076µm değerinde bir basmanın oluştuğu görülmüştür. Toleranslar arasında en düşük sapmanın ise 1 numaralı bölgede oluştuğu ve değerinin 0.7365µm düzeyinde olduğu bulunmuştur. Ürünün kesim bölgelerinde ise geometrik olarak fazlalıkların bulunduğu görülmektedir.

2767 kalıp malzemesinin beşbininci ürününde ise dokuz farklı noktasında geometrik farklılıklar gözlenmiştir. Ürün basım adetlerindeki artışa bağlı olarak aşınma noktalarında artış görülmektedir. Şekil 3'den görülebileceği gibi 12. ölçüm noktasında (WHL–DEV1:12) yaklaşık 0.16 µm düzeyinde bir aşınma gözlemlenmiştir. Yedi numaralı ölçüm noktasında 0.3563 µm'luk aşınma belirlenmiştir. On altı numaralı ölçüm noktasında ise 0.0656 µm'luk bir aşınma gözlemlenmiştir.

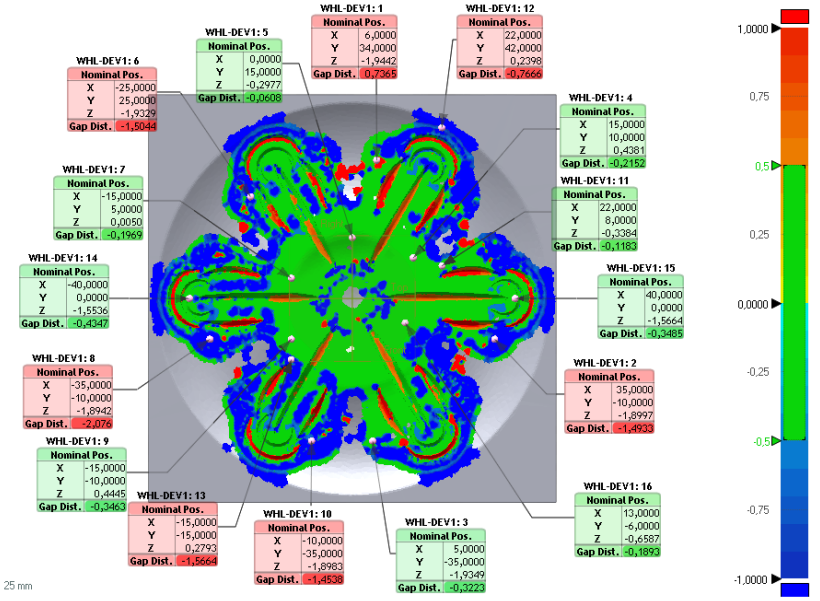

Şekil 2. 2767 birinci ürünün lazer tarama sonuçları

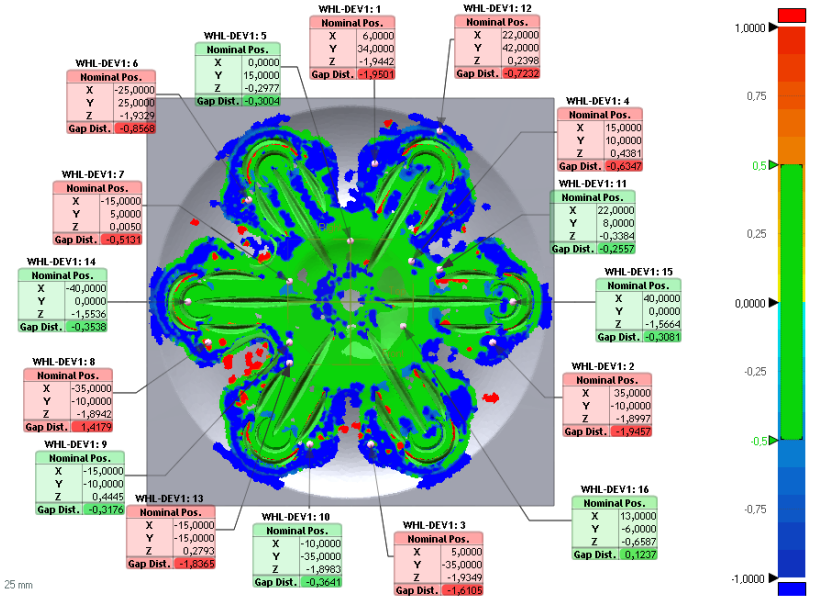

Şekil 3. 2767 beşbininci ürünün lazer tarama sonuçları

Şekil 4'deki 2379 kalıp malzemesinden alınan birinci ürününde dokuz noktada sapmanın fazla olduğu görülmektedir. 2379 malzemesinin diğer kalıp malzemesi olan 2767 malzemesinin birinci ürünü ile karşılaştırılması yapıldığında 8. noktada (WHL - DEV1:8) ortalama 0.808 µm sapma olduğu görülmektedir. Her iki malzemenin birinci ürünlerinde farklı bir nokta (WHL – DEV 1:2) alındığında değerinin 0.379 µm olduğu gözlemlenmiştir.

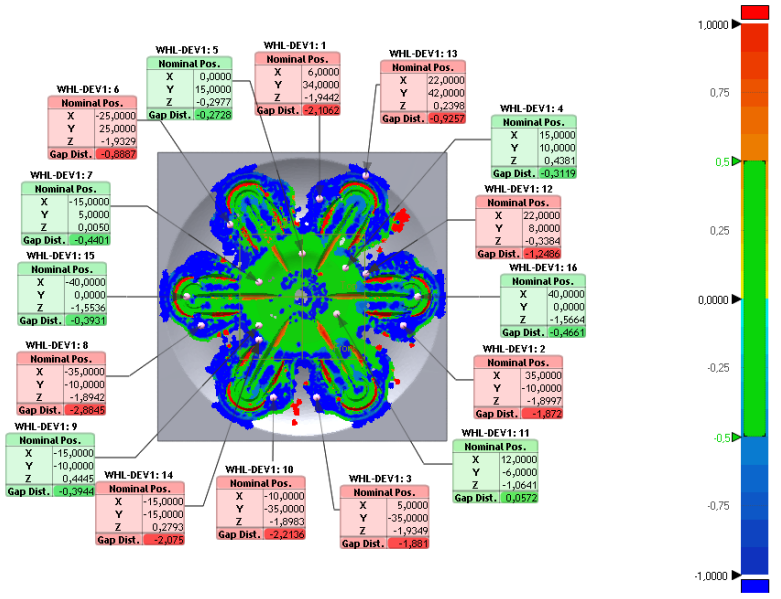

Şekil 4. 2379 birinci ürünün lazer taraması

Şekil 5.'de 2379 malzemesinin beş bininci basım ürününün lazer taraması görülmektedir. Beşbininci üründe de dokuz nokta kırmızı renkte görülmekte bununla beraber sapma miktarlarında basım adetleriyle birlikte artışlar belirlenmiştir. En fazla aşınma altı numaralı ölçüm noktasında 1.4352 µm olarak tespit edilmiş, 2 numaralı ölçüm noktasında ise 1.2091 µm ikinci en yüksek aşınma değeri belirlenmiştir. En az aşınma değeri 16. ölçüm noktasında 0.0019 µm olarak gözlemlenmiştir.

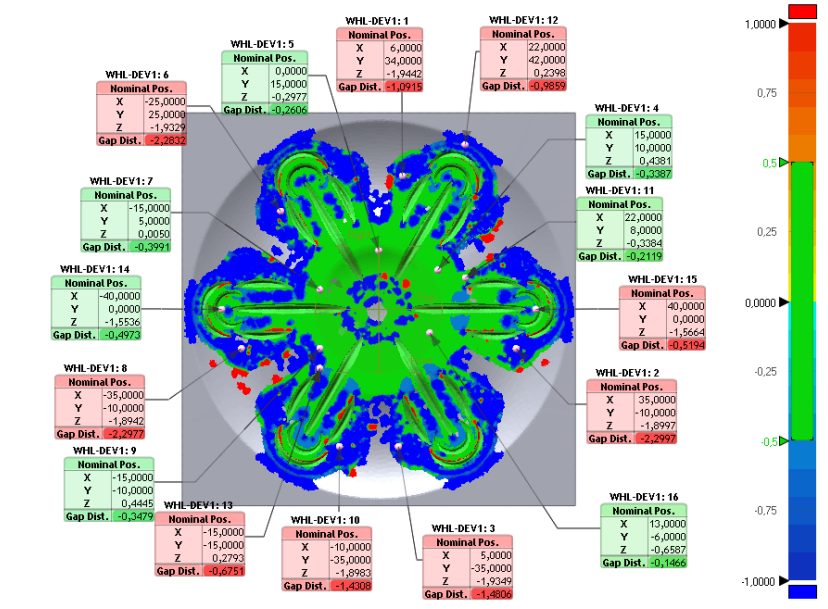

Şekil 5. 2379 beşbininci ürünün lazer tarama sonuçları

CPOH kalıp malzemesinin şekil 6'da görülen birinci üründe sekiz noktada sapma değerlerinin yüksek olduğu belirlenmiştir. En yüksek değer bir numaralı ölçüm noktasında 3.8661 µm olarak belirlenmiştir. En az aşınma değeri ise on beş numaralı ölçüm noktasında 0.0174 µm olarak gözlemlenmiştir.

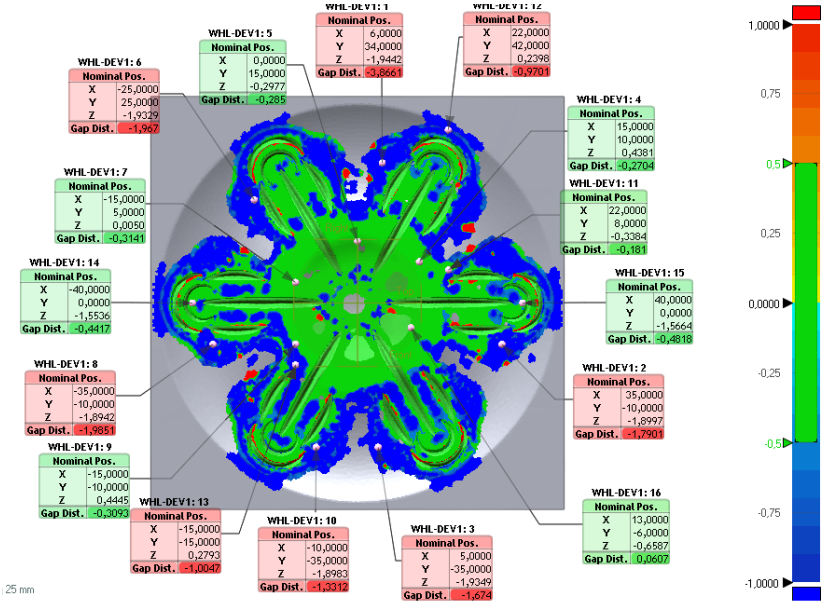

Şekil 6. CPOH birinci ürünün lazer taraması

CPOH kalıp malzemesinin Şekil 7'de görülen beşbininci üründe altı noktada sapma değerlerinin yüksek olduğu görülmektedir. Dokuz numaralı ölçüm noktasında 0.026 µm en az değer olarak gözlemlenmiştir. Beşbininci üründe ürün basım adedine bağlı olarak sapma değer noktalarının sayısında artış olması gerekirken bu durum gözlemlenememiştir. Sac basım esnasında esnemeden dolayı böyle bir durum olabileceği için onbininci ürünlerin basım işlemine ve bu ürünlerin lazer taramalarının incelenmesi yapılacaktır.

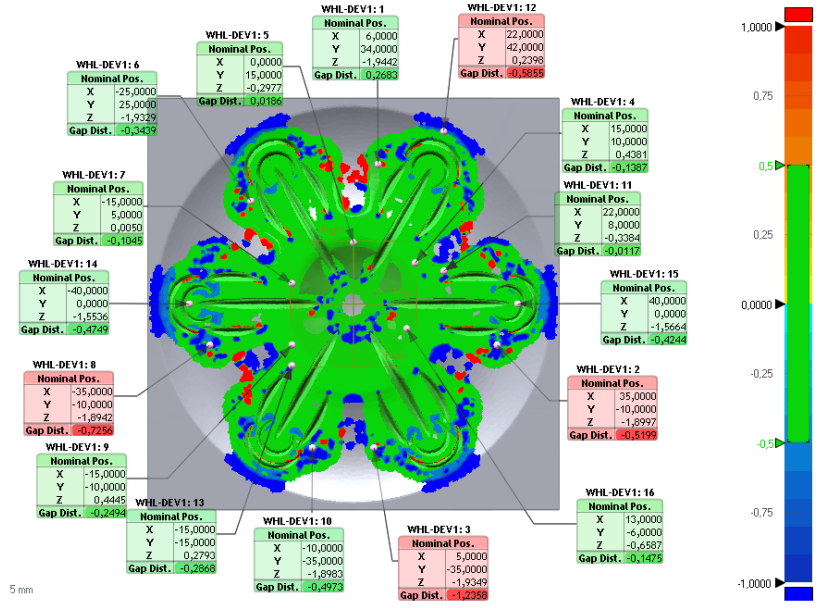

Şekil 7. CPOH beşbininci ürünün lazer tarama sonuçları

Tartışma ve Sonuçlar

Ardışık kalıplar ile üretimde, üretimde kalıp aşınmasına bağlı boyutsal değişimlerin üç boyutlu lazer tarama yöntemleri ile belirlendiği bu çalışma ile aşağıdaki sonuçlara ulaşılmıştır;

- CPOH soğuk iş çeliği ile yapılan kalıplar aşınmaya karşı daha dayanıklıdır.
- 2379 ve 2767 soğuk iş çelikleri ölçüm noktaları dikkate alındığında yakın sonuçlar vermektedir.
- 2379 soğuk iş çeliğinden imal edilen kalıp, ürünü diğer kalıplara göre daha çok basmaya maruz bırakmaktadır.
- CPOH soğuk iş çeliğinin ürün imalatı sürecinde en ideal sonucu verdiği belirlenmiştir.

Teşekkür

Bu çalışma Pamukkale Üniversitesinin 2017FEBE023 numaralı proje desteği ile gerçekleştirilmiştir. Yazarlar desteğinden dolayı Pamukkale Üniversitesine teşekkür ederler.

Kaynaklar

Gantar, G., Pepeljnak, T. and Kuzman, K., (2002) "Optimization of sheet metal forming processes by the use of numerical simulations", Journal of Materials Processing Technology, 130–131 , 54–59

Hambli, (2001) , Blanking Tool Wear Modeling Using the Finite Element Method

Michel and Picart, (2002) , Modelling the constitutive behaviour of thin metal sheet using strain gradient theory, Journal of Materials Processing Technology 125–126 (2002) 164–169

L.C. Chan, T.C. Lee, B.J. Wu ve W.M. Cheung, (1998) , "Experimental Study on the Shearing Behaviour of Fine-Blanking Versus Bar Cropping"

PM, (2018). Poligon Mühendislik. https://www.poligonmuhendislik.com/hizmetlerimiz/3-boyutlu-tarama/ (Erişim Tarihi:05.07.2018).

OT, (2018). Olympos Tasarım. http://olympostasarim.blogspot.com/2016/03/3.html (Erişim Tarihi:05.07.2018).

International Conference on Science and Technology

ICONST 2018

5-9 September 2018 Prizren - KOSOVO

Development of Novel Test Stand for Performance Evaluation of Elevator Motor Torque and Brake Torque

Semih Yüksel[1]*, Melih Küçükçalık[1], Zeki Alyanak[1], Barış Onur[1], Selim Hartomacıoğlu[2]

Abstract: Elevators, whether they are used for carrying cargo or people are governed by safety regulations "Elevator safety" means that a people or cargo equivalent to the nominal load of the elevator can safely be carried to a height, at a specified speed, during which adverse conditions may arrise. Hence, testing of electrical motors to its limits by using different types of tests conditions under controlled laboratory environment is required by the manufacturer to demonstrate the safety of the system and its durability against adverse situations. A test system that is cabapble of testing electric motor as well as the motor brake that secures and holds the elevator system are required to be tested for their full working range, thus one could monitor and record the conditions in real time and determine the operating conditions and the capacity of the loading of the motor and the brake. As this is governed by the safety regulations, the motor and the brake manufacturers, it is necessary to check the torque values of the motor and the brake system to make sure that they operate as specified and within the limits of their requirement. If these data are not checked, the following situations may arise. The torque of the elevator motor may not be suitable for the load and the motor may not be able to lift the elevatorThe torque of the motor brake may not be suitable to hold the elevator system which may slip and slide and the elevator cruising speed may exceed the safety limit. The brake torque may be low and could not actıvate and release the brake during operations In such cases, the failure of the elevator result of a malfunction of the control group. It may directly affect the safety of life or property, and may cause other mulfunctions as well. In order to prevent such situations, it is necessary to design a comprehensive motor and brake test system. Therefore, this article presents a universal test stand to carry out examination of elevator motor and brake applications. A complete load test stand was designed and manufactured for this purpose, with possibility of setting up and recording torque parameters for both the brake and the motor.

Keywords: Motor Test Stand; Motor Torque, Motor Brake; Braking Torque, Universal motor test stand

1. Introduction

Motor energy efficiency is important related to motor brake friction. Marko Šućurović is studied electromagnetic brake calibration [1].Mrs. Ertan is studied general view of the composotion and manufacturing parameters of polymer based brake pad materials.[2]. Mr.Oktem studied computer aided new type of brake pad friction tester produced for measure to natural dust reinforced brake pads.[3] So test devices are needed to develop brake pad study.Mr. Pakosta is studied design of the test stand for shafts with universal joints and constant velocity joints for testing equipment[4].

1Department of Research &Development-Arkel Elektrik ve Elektronik San. ve Tic. A.Ş. 34885,Istanbul, TURKEY
2Bilig Yenileşim San. Tic. Ltd. Şti.34906, Istanbul TURKEY
*Corresponding author: semihyuksel@yandex.com

With this test stand, the actual motor torques and braking torques is checked and compared to the design specification declared values. With this test stand, it will help to user gain knowledge and advance a new engine design and know-how. The schematic diagram of the test stand is shown Figure 1.

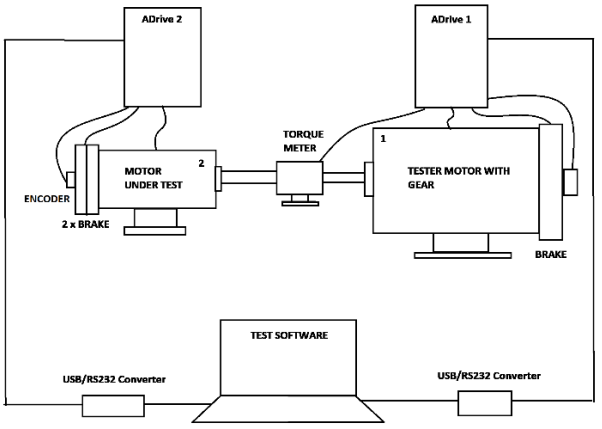

Figure 1: Schematic diagram of the test stand

We used one 7.5 kW Drive inverter device and one 15kW inverter device in this system. One of this devices 7.5 kW inverter is connected to the reducer load motor. The other one of the 15kW inverter connected to elevator motor. Both of these inverters have RS232 connections and have been connected to a PC for continious data monitör and storege. The DRVL-V-2000-W-0-K type torquemeter, (Max torque value 2000 Nm), was selected before connecting both motors. This torqometer has a 0.0 ± 10V analog signal output and the output is connected to a 7.5 kW drive inverter. Software has been developed to automatically drive motors by modifying the embedded software of the inverter drivers. Thanks to this software, all the information is transferred to the inverter device by means of the work order code on the motors automatically. With this information for the lift motor to be driven, it is possible to perform the auto tuning process by using the information contained in the inverter.

Figure 2: Test stand

The cardan shaft is installed between the elevator motor which will be driven by the torque meter. This loading torque operation is automatically initiated via the computer. With this interface design we have done when this test process is started, analogue signals called torque meter are converted to torque value. This torque value will load until to the nominal torque to be loaded and monitored on the graph. First of all, the brake switches are checked. We started to check respectively the holding capacity of the breaks individually, fisrt brake 1 by activating brake 2 and the doing the opposite. The elevator motor is driven and forced by the counter-reduction motor to simulate the load conditions. All of the readings are plotted to offer quick visual

Actual torque values; and thanks to this test stand it will lead us to do improvements and tune ups to the motor and brake design work.

2. Material and Method

Parameter settings of work of engine are programmed and controlled by using the our own software. The program allows previewing the set of parameters and observation of the changes directly on the test stand. The measurement results are displayed in binary and graphical mode, allowing observing proceedings of torque value of brake and motor. Archived results can be edited at any time and subjected to further treatment. System shows when the motor brake and motor torque does not have enough power. Additional hardware capabilities allow to control the working time and specify the time intervals between various stages of tests. This software is shown Figure 3.

The software of this test bench was developed in-house, using .NET Framework and C# language for the desktop graphical user interface and C language for motor drivers. Embedded software of ADrives were modified specially for our purpose, allowing real-time bi-directional communication with the desktop GUI.

The desktop software on the other hand, acts as the main program and consists of several parts;

- 2-axis line chart for displaying real-time torque and speed values on the screen,
- Communication system connected to both ADrives via RS232 serial ports,
- Tester commands the ADrives to stop, run etc. and compares their values with the desired values,
- Data entry part collecting the ID and special values of the motor with a barcode scanner and keyboard entries,
- And a database system that saves all the information, which will be used to identify the characteristics of each motor type.

Upon scanning the type barcode of the motor, nominal values of it are loaded and the software waits for further information, such as production number, inductance and resistance values of each winding and additional comments by the operator. Then, following button presses, tester part introduces the motor to ADrive and the selected test starts. These tests include;

- Auto-tune,
- Brake switch tests,
- Brake torque tests,
- Motor speed test,
- And motor torque test.

At each step of these tests, the tester checks if the values sent by ADrives are within the expected tolerances. If the test candidate passes all these tests, the tester deems it of high quality, then the motor is ready to be packed. Also after the test, whether it was successful or not, a report is generated and the values are saved into the database.

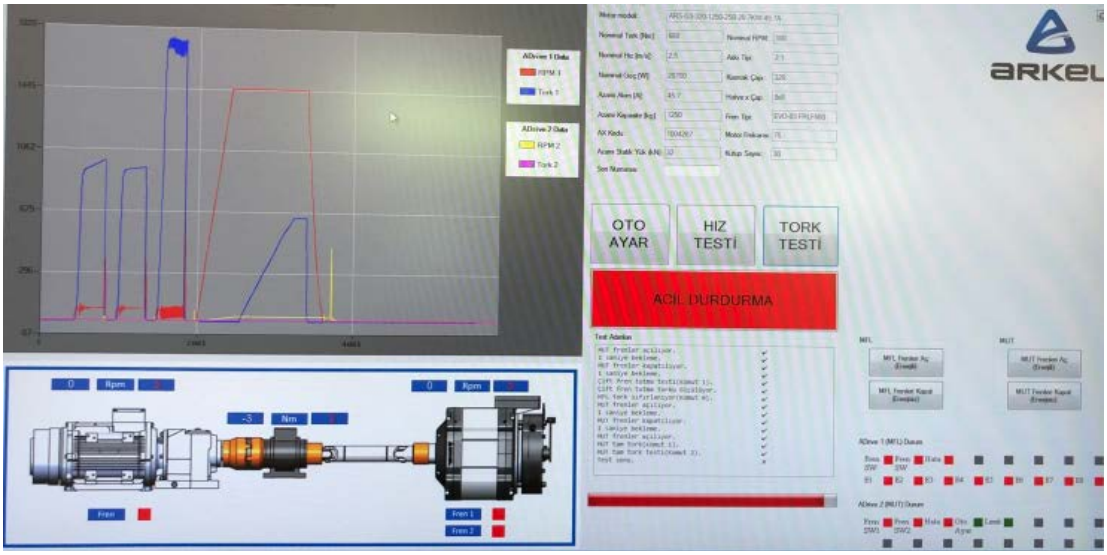

Figure 3: Test software

3. Results

With this test stand, it is checked that the engine torques and braking torques do not match the actual declared design values but slıghtly lower. This will help the designer to adjust the design and correct the parameters.

Figure 4: Motor Final Quality Test Stand

4. Discussion and Conclusion

This article presents a universal test stand to carry out examination of elevator motor application demonstrator. A complete load test stand was designed and manufactured for this purpose, with possibility of setting up and recording torque parameters. The Motor Final quality test Stand is shown at Figure 4.

Acknowledgements

Financial and manufacturing support during this study by Arkel Elektrik Elektronik San. Ve Tic. A.Ş. is gratefully acknowledged.

References

[1] M. Sucurovic, N. Mitrovic, and M. Bozic, “Calibration of the electromagnetic brake,” no. November, 2015.

[2] R. Ertan and N. Yavuz, “Polimer Matriksli Fren Balata Malzemelerinin Kompozisyon ve Üretim Parametreleri Açısından Değerlendirilmesi,” *Makina ve Mühendis*, vol. 47, no. 553, pp. 24–30, 2006.

[3] O. Sistemi, “Yeni bir tip fren balata test cihazının geliştirilmesi Development of a new type brake pad fr ct on tester,” vol. 22, no. 2, pp. 350–356, 2018.

[4] J. Pakosta and G. Achtenová, “Joint Shaft Test Stand,” *J. Middle Eur. Constr. Des. Cars*, vol. 15, no. 1, pp. 11–14, Jun. 2017.

International Conference on Science and Technology

ICONST 2018

5-9 September 2018 Prizren - KOSOVO

Chemical Properties and Therapeutic Effects of Thermal Waters in Zilan Valley and Their Relations with Geological Units (Erciş -Van, Turkey)

Hacer Düzen[1]

Abstract: In this study, therapetic effects of thermal waters were investigated in Zilan valley, eastern part of the Turkey. Purpose of this study is determination of chemical properties of thermal waters and investigation of therapautic effects of them in terms of human health. Also relations between chemical properties of thermal waters and geological units were investigated in Zilan Valley. Samples were collected from five sample points and anion / cation analyses were carried out for five thermal water samples (from three thermal wells and two thermal springs). First well was drilled in 1988 by MTA (Mining Research Center in Turkey) and sample was collected by MTA in 1988. Also other two thermal wells were drilled by MTA and samples were collected in 2000 by MTA. Analyses were carried out by MTA in 1988 and 2000. Two thermal spring waters were collected in 2014 in content of this study. Anion / cation analyses were carried out in content of this study in ACME Analytical Laborataries. Also, geological map of the Zilan Valley was prepared in content of this study.

As a result of the study, water types were detected as Na-Cl type for all thermal well waters (numbered ZG-1, ZG-2 and ZG-3 wells) and numbered 111 thermal spring. Water type was detected as Na-Cl-SO4 for numbered 112 thermal spring. Thermal waters with Na-Cl have a lot of therapeutic effects. Thermal waters with Na-Cl can be used in rheumatism, gynecologic diseases, neuritis, treatment of unconsolidated fractures and at the upper respiratory tract diseases. Geologically, all thermal waters are originated from marl (limestone with clay) units in Kızıldere Formation in the Zilan Valley. Cap rocks of the thermal system are Aladağ volcanics. Thermal waters in Zilan Valley are so important for human health and they should be use for treatments.

Keywords: Therapeutic, Chemical, Geological, Thermal, Zilan, Turkey.

Introduction

Hydrotherapy is one of the basic methods of treatment widely used in the system of the natural medicine, which is also called as water thetapy, aquatic therapy, pool therapy and balneotherapy.Use of water in various forms and in various temperatures can produce different effects on different system of the body. Many studies /reviews reported the effects of hydrotherapy only on very few systems and there is lack of studies/reviews in reporting the evidence-based effects of hydrotherapy on various systems (Mooventhan and Nivethitha, 2014). Chemical properties of the thermal water and relation with geological units is also important for hydrotherapy. Especially, salt water contains a unique combination of minerals and enzymes that help soften the skin. Salt water helps extract extra fluid from the skin, which helps with swollen joints and inflammation. People who suffer from arthritis can experience greater relief in a salt water. Dissolved mineral salts and sulfur compounds in the mud are used to treat skin inflammations such as eczema and psoriasis, as well as reduce stiffness and inflammation in joints due to osteoarthritis and rheumatoid arthritis (Bostwick, 2018).

[1]İstanbul University - Cerrahpaşa, Faculty of Engineering, Department of Geological Engineering, 34320, Avcılar, İstanbul, TURKEY
*Correspondingauthor: hcrduzen@gmail.com

In this study, chemical properties of thermal waters in Zilan valley and relations with geological units were investigated in the area. Also, therapeutic effects of thermal waters was examined in the area. Zilan valley is located in the eastern of the Turkey and it is shown in Figure 1.

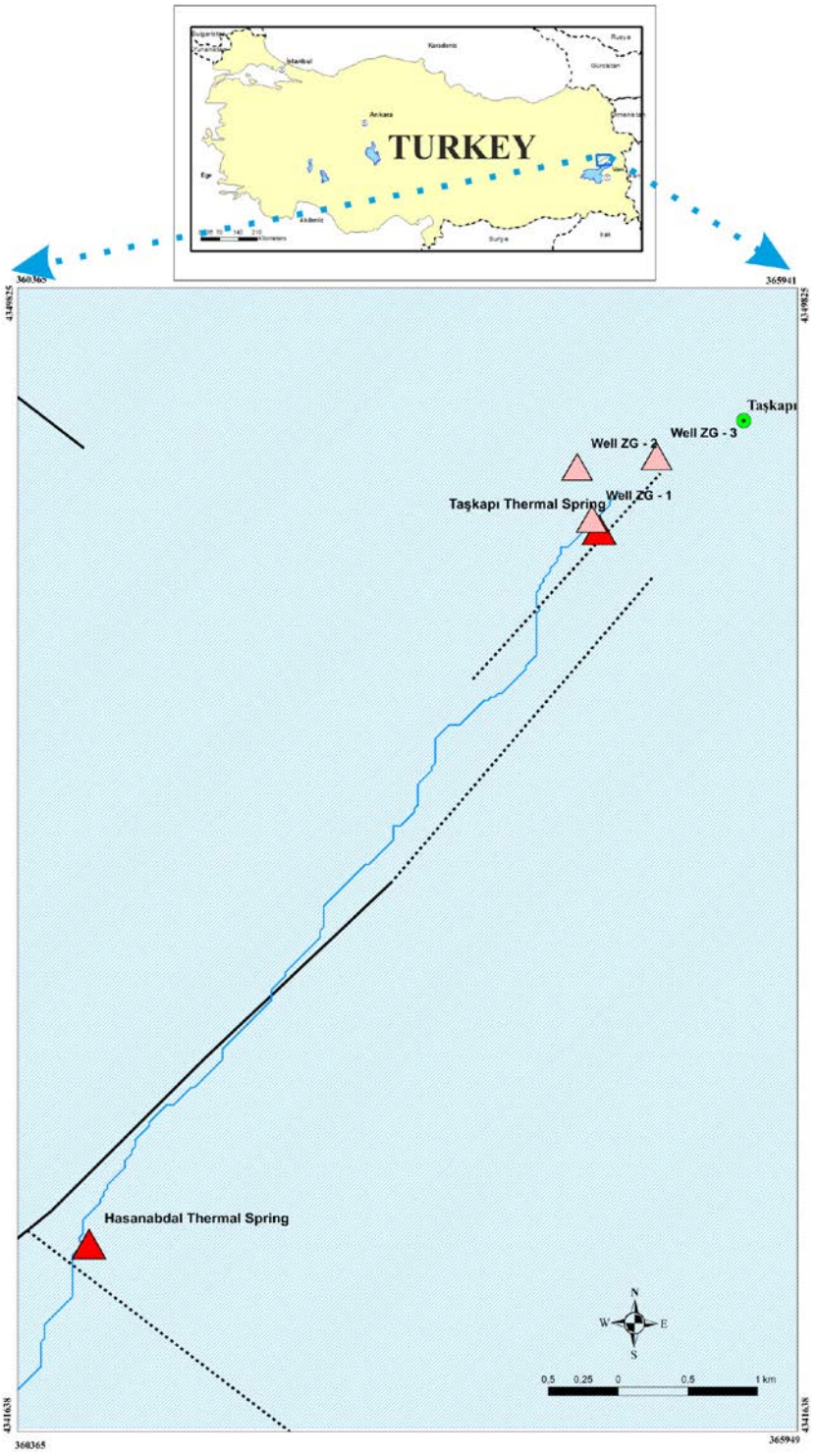

Figure 1. Location map of the study area.

Geological and Hydrogeological Setting

The basement of the stratigraphic column in the study area is consisted of Late Cretaceous Mehmetkaya Granitoid and other geological units follow from base to top including of Eocene clastics, Miocene units with clay and marl, Middle Miocene - Late Miocene Aladağ andesite, Late Miocene – Pliocene clastics, respectively. Quaternary alluviums cover all geological units (Figure 2 and Figure 3).

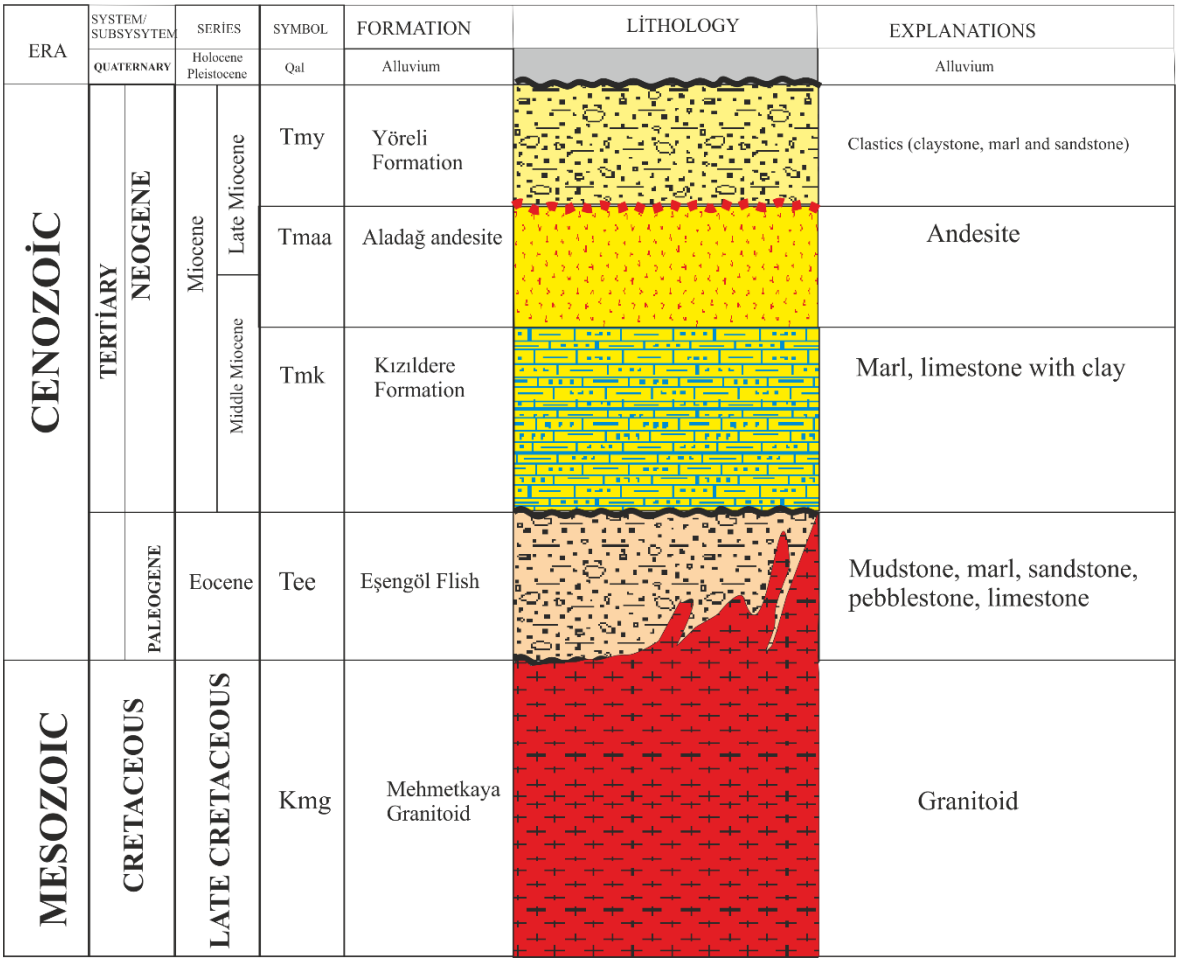

Figure 2. Stratigraphic column of the study area.

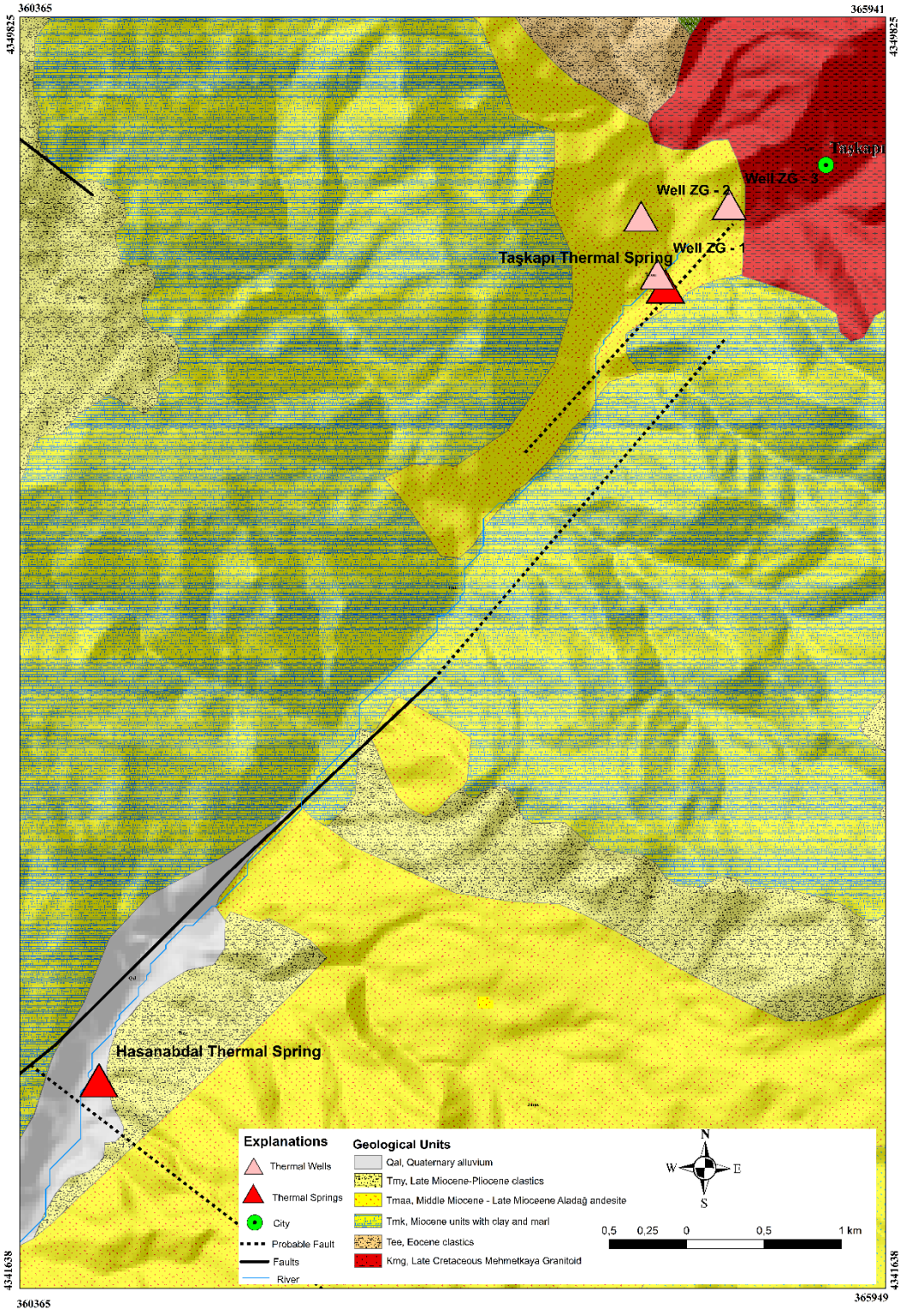

Figure 3. Geological map of the study area.

In the region, Neotectonic episode started in Middle Miocene. The compression regime has resulted in the regional uplifts (and subsidences) and the faults, trending E-W and inclined either to north or south have occurred along withfolds extending in E-W direction. In addition to these structures, dextral faults in NW-SE direction and sinistral faults extending along SW - NE have developed too. Most of the thermal waters discharge along the SW–NE trending faults in the Zilan valley. The circulation of thermal waters is closely related to major fault and fractured zones. Fractured Middle Miocene - Late Miocene Aladağ andesites are

assumed to be the cap rocks of the geothermal system and Miocene units with clay and marl are assumed to be the main reservoir rocks for the Zilan thermal waters.

Hydrogeologically, there are 3 rock types including permeable, semi-permeable and unpermeable in the Zilan valley. Unpermeable units which are magmatic rocks such as granitoid in Mehmetkaya Granitoid. Semi-permeable units are marl, limestone with clay in Kızıldere Formation, andesites in Aladağ andesites and clastics in Yöreli Formation and permeable units are alluviums. Numbered ZG-1, ZG-2 and ZG-3 wells and numbered 111 and 112 thermal springs are located at the permeable and semi-permeable units (Figure 4). Well numbered ZG-1 has 394.20 meters, ZG – 2 has 490 meters and ZG – 3 has 264.70 meters. Physical properties of wells were showed in Table 1.

Table 1. Wells in Zilan geothermal field (MTA, 2005).

Well Number	Date	Depth (m)	Tempererature (°C)	pH	TDS (mg/l)	EC (µohm/cm)	Discharge (l/s)
ZG - 1	1988	394.20	80	7.9	3330	3696.5	40
ZG - 2	2000	490	92	7.5	2793	3051.4	4
ZG - 3	2000	264.70	98	7.7	2843	3256.9	22

*TDS (Total dissolved solids), EC (Electrical Conductivity).

Table 2. Thermal Springs in Zilan geothermal field (Düzen, 2017).

Spring Number	Date	Tempererature (°C)	pH	TDS (mg/l)	EC (µohm/cm)
Hasanabdal Thermal Spring (Number 111)	2014	51	8.5	-	4620
Taşkapı Thermal Spring (Numbered 112)	2014	53	7.5	-	3800

*TDS (Total dissolved solids), EC (Electrical Conductivity).

Material and Method

Samples were collected from five sample points and anion / cation analyses were carried out for five thermal water samples (from three thermal wells and two thermal springs). First well was drilled in 1988 by MTA (Mining Research Center in Turkey) and sample was collected by MTA in 1988. Also other two thermal wells were drilled by MTA and samples were collected in 2000 by MTA. Analyses were carried out by MTA in 1988 and 2000. Two thermal spring waters were collected in 2014 in content of this study. Anion / cation analyses were carried out in content of this study in ACME Analytical Laborataries. Also, geological map of the Zilan Valley was prepared in content of this study.

Also, the analytical precision for the accurate measurements of ions was determined by calculating electrical neutrality (EN %) which is acceptable at ±5 % (Appelo and Postma, 1999). Samples which are ZG-1, 111 and 112 have EN % values within ±5 %. Other two samples (ZG-2 and ZG-3)which is made by MTA have not EN % values within ±5 %.

Electrical Neutrality = ((Σ Cation + Σ Anion) / (Σ Cation - Σ Anion)) x 100

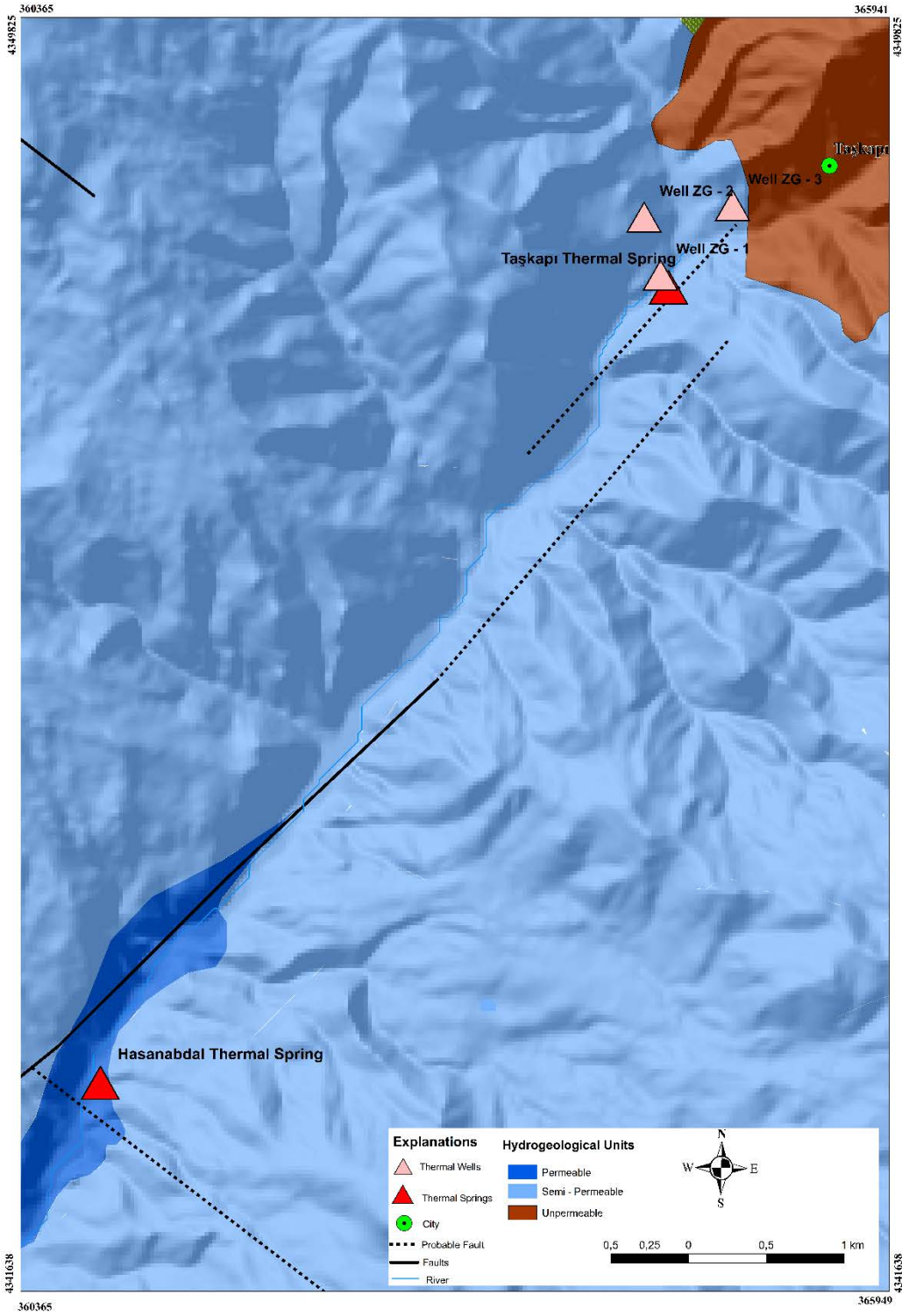

Figure 4. Hydrogeological map of the study area.

Results

1. Chemical Properties and Therapeutic Effects of Thermal Waters

Anion and cation analysis were carried out for Well ZG-1, ZG-2 and ZG-3 by MTA in Zilan Valley. Analyses of numbered 111 and 112 thermal springs were carried out by Düzen (2017). Water types were detected as Na-Cl type for all thermal well waters (numbered ZG-1, ZG-2 and ZG-3 wells) and numbered 111 thermal spring. Water type was detected as Na-Cl-SO4 for numbered 112 thermal spring (Table 3). Chemical analysis results are shown in Table 3 and in Figure 5.

Table 3. Chemical analysis of wells and thermal Springs in Zilan geothermal field (MTA, 2005; Düzen, 2017).

Cation/Anion	Unit	Well ZG-1	Well ZG - 2	Well ZG - 3	111	112
Calcium	mg/L	96	36,9	29,5	56,9	131,3
Magnesium	mg/L	56	54,6	47	24	52
Sodium	mg/L	830	773	858	1008	777
Potassium	mg/L	74	110	108	98	82
Bicarbonate	mg/L	994	897	779	220,00	214,00
Sulfate	mg/L	565	470	491	213	476
Chloride	mg/L	715	543	560	1440	1106
Water Type	-	Na-Cl	Na-Cl	Na-Cl	Na-Cl	Na-Cl-SO4

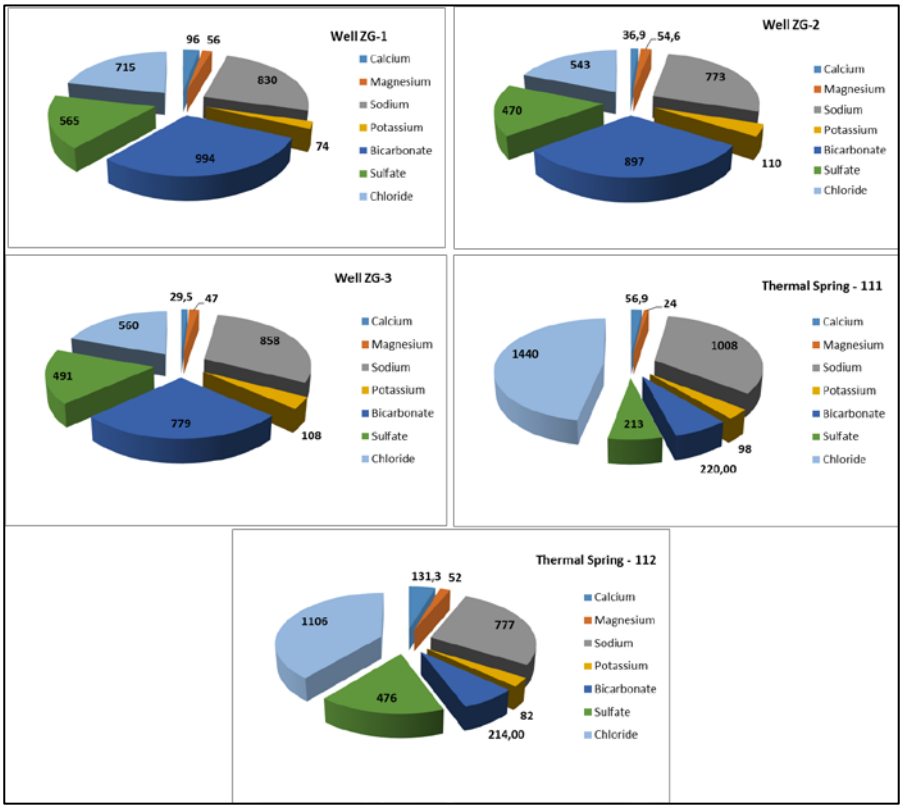

Figure 5. Pie charts of chemical analyses in the study area (mg/l).

Chemical properties of thermal waters in Zilan valley shows that salty waters for all thermal water samples. Water type of Well ZG-1, ZG-2 and ZG-3 and Hasanabdal thermal spring (numbered 111) is Na-Cl. Water type of Taşkapı thermal spring (numbered 112) is Na-Cl-SO4.

Thermal waters with Na-Cl have a lot of therapeutic effects. Thermal waters with Na-Cl can be used in rheumatism, gynecologic diseases, neuritis, treatment of unconsolidated fractures and at the upper respiratory tract diseases. Salt water helps extract extra fluid from the skin, which helps with swollen joints and inflammation. People who suffer from arthritis can experience greater relief in a salt water. Hasanabdal thermal spring is used as spa for rheumatism and treatment of unconsolidated fractures. Taşkapı thermal spring isn't used yet and it can be used therapeutically.

2. Relations Between Chemical Properties and Geological Units in Thermal Waters

Şahinci (1991) has suggested a theory about relations between ions in geological units (rocks) and waters which discharge from this geological unit. According to Şahinci (1991), waters which discharge from the acidic rocks (granite, granitoid etc…) are rich with alkaline elements such as sodium and potasium. Also amount of sodium is more than chlorid. Şahinci (1991) indicates that ion arrangement for waters discharge from acidic rocks is Na+K > Ca > Mg and HCO3 > SO4 > Cl or Cl > HCO3 > SO4. In additon to this, Şahinci (1991) indicates that ion arrangement for waters discharge from marl units is Na+K > Ca > Mg and Cl > SO4 > HCO3.

Table 4. Ion arrangement of thermal water samples in the study area.

Ions	**ZG -1**	**ZG -2**	**ZG -3**	**111**	**112**
Na (meq/l)	36,1	33,6	37,3	43,9	33,8
K (meq/l)	1,9	2,8	2,8	2,5	2,1
Na+K (meq/l)	38,0	36,4	40,1	46,4	35,9
Ca (meq/l)	4,8	36,9	29,5	2,8	6,6
Mg (meq/l)	4,6	54,6	3,9	2,0	4,3
HCO3 (meq/l)	16,3	14,7	12,8	3,6	3,5
Cl (meq/l)	20,2	15,3	15,8	40,6	31,2
SO4 (meq/l)	11,8	9,8	10,2	4,4	9,9
Na+K (%)	80,2	28,5	54,6	90,6	76,8
Ca (%)	10,1	28,8	40,2	5,5	14,0
Mg (%)	9,7	42,7	5,3	3,9	9,2
HCO3 (%)	33,8	36,9	32,9	7,4	7,9
Cl (%)	41,8	38,5	40,7	83,5	69,9
SO4 (%)	24,4	24,6	26,3	9,1	22,2
Σ Cation	47,392	127,933	73,45	51,2	46,7
Σ Anion	48,22	39,805	38,79	48,7	44,6
Ion Balance	0,9	52,5	30,9	2,5	2,3
Ion arrangement	Na+K > Ca > Mg - Cl > HCO3 > SO4	Mg > Ca > Na+K - Cl > HCO3 > SO4	Na+K > Ca > Mg - Cl > HCO3 > SO4	Na+K > Ca > Mg - Cl > SO4 > HCO3	Na+K > Ca > Mg - Cl > SO4 > HCO3

In this study, Wells numbered ZG-1, ZG-2 and ZG-3 are located in Taşkapı thermal field and they can be discharge from the Mehmetkaya Granitoid due to their ion arrangement. Numbered 112 thermal spring is located in Taşkapı thermal field too and it can be discharge from the marl units in Kızıldere Formation due to their ion arrangement. Numbered 111 thermal spring is located in Hasanabdal thermal field and it can be discharge from the marl units in Kızıldere Formation due to their ion arrangement. Ion balance was

controlled in content of this study for thermal water samples. Ion balance was detected suitable for Well ZG-1 which was analysed by MTA and 111 and 112 thermal springs which were analysed by Düzen (2017). Numbered ZG-2 and ZG-3 wells which were analysed by MTA are not suitable for ion balance but they are in same system with ZG-1. So, origin of ZG-2 and ZG-3 wells were accepted same with ZG-1. Ion arrangement table is shown in Table 4.

Discussion and Conclusions

In the study area, chemical properties of thermal waters in Zilan valley and relations with geological units were investigated and therapeutic effects were revealed. Water types were detected as Na-Cl type for all thermal well waters (numbered ZG-1, ZG-2 and ZG-3 wells) and numbered 111 thermal spring. Water type was detected as Na-Cl-SO4 for numbered 112 thermal spring. All thermal waters are rich with alkaline elements such as sodium and potasium. Chemical results show that Taşkapı thermal spring and Well ZG-1, ZG-2 and ZG-3 which discharge from the Mehmetkaya Granitoid and Hasanabdal thermal spring discharge from the marl units in Kızıldere Formation due to their ion arrangement. Ion balance was controlled in content of this study for thermal water samples. Ion balance was detected suitable for Well ZG-1 which was analysed by MTA and 111 and 112 thermal springs which were analysed by Düzen (2017). Numbered ZG-2 and ZG-3 wells which were analysed by MTA are not suitable for ion balance but they are in same system with ZG-1. So, origin of ZG-2 and ZG-3 wells were accepted same with ZG-1. Thermal waters with Na-Cl can be used in rheumatism, gynecologic diseases, neuritis, treatment of unconsolidated fractures and at the upper respiratory tract diseases. Salt water helps extract extra fluid from the skin, which helps with swollen joints and inflammation. People who suffer from arthritis can experience greater relief in a salt water. Hasanabdal thermal spring is used as spa for rheumatism and treatment of unconsolidated fractures. Taşkapı thermal spring isn't used yet and it should be used purpose of therapeutic.

Acknowledgements

This work was financially supported by Istanbul University Research Fund. The author acknowledges the support of Istanbul University Research Fund.

References

Appelo CAJ, Postma D. (1999) Geochemistry, groundwater and pollution, 4th edn. Balkema, Rotterdam 536.

Bostwick, H. (2018). Mineral Bath. http://www.bathsalt.net/Mineral_Bath.html (Access Date: 18.08.2018).

Düzen, H. (2017). Hydrogeological and Geothermal Studies of the Erciş-Çaldıran-Muradiye (Van) Region. Thesis (PhD). İstanbul University, Institute of Natural Science. İstanbul, Turkey.

Mooventhan, A., Nivethitha, L. (2014). Scientific evidence-based effects of hydrotherapy on various systems of the body. North American Journal of Medical Science, 6 (5), 199 – 209.

MTA, (2005). Geothermal Resources Inventory of Turkey. Ankara, Turkey.

Şahinci, A. (1991). Geochemistry of natural waters. Reform Press, İzmir, Turkey.

International Conference on Science and Technology

ICONST 2018

5-9 September 2018 Prizren - KOSOVO

Molecular Structural Analysis Of Cellulose Triacetate II And Influence With Aspergillus Niger Cellulase Enzyme

A. Demet Demirag[1] , Sefa Celik[2] , Aysen E. Ozel[1] , Sevim Akyüz[3]

Abstract: People have been forced to seek alternative sources because of the health problems created by the petrochemical products used in all areas of human life and the environmental problems they have caused because they remain unbroken for many years in the nature. The cellulose acetate, used in the making of varnishes, plastic materials, films and fibers, has rather low ignition and burning properties compared to cellulose nitrate. In addition, film strips made of cellulose acetate can remain without destruction for many years. In this study, molecular structure analysis of cellulose triacetate II (CTA II) molecule obtained from cellulosic and acetate, which is the most usable material in nature, has been performed. The determination of the structure of this molecule is very important in terms of structure-activity relationship. For this reason, the most stable molecular geometry of the cellulose triacetate II molecule was modeled by Density Function Theory using the Gaussian 05 program. Scaled vibration frequencies of this optimized geometry are calculated using the Molvib program. These obtained frequencies are transformed into the theoretical spectrum in the Lorentzian distribution. Aspergillus niger cellulase enzyme is an important enzyme that is active in cellulose digestion. In order to evaluate the interaction between the enzyme and CTA II, molecular docking studies were carried out. Using the molecular docking method based on key-lock theory, the region with the highest binding activity of the enzyme and the groups that interacted at the molecular level were identified as a result of the molecular interaction between Aspergillus niger cellulase enzyme-cellulose triacetate II (CTA II).

Keywords: Cellulose triacetate II, Molecular docking, Aspergillus niger cellulase enzyme, Density Function Theory

Introduction

It is known that CTA has two main types of crystal structures, called CTA I and CTA II, which correspond to cellulose I and II, respectively [1,2]. In experiments generally 92% of the hydroxyl groups of the cellulose acetate molecule are acetylated. For this reason, CTA II is more resistant to heat than cellulose acetate although they have the same chemical properties. CTA II is a cellulose triacetate polymorphism that reflects reversible and non-reversible crystal transformations. The transformation from Cellulose I to CTA II and from CTA I to CTA II is the case. These crystal structures have been investigated for many years, and several unit cell models were published. As for the structure of CTA II, the first structural approach was performed by Dulmage [2]. Later, Roche et al. determined the crystal structure of CTA II, using both X-ray and electron diffraction data [3]. They constructed a three-dimensional structure model of CTA II with 18 chains, and showed that it has the same basic shape with the experimentally obtained single crystal with micron-size. However, there was a short contact between the hydrogen atoms in the conformation at C6 acetyl residues in their CTA II crystal model. Zugenmaier revised this crystal structure of CTA II, given by Roche et al., to remove the close contact of the

[1] Istanbul University, Faculty of Science, Department of Physics, Vezneciler, 34134, Istanbul, Turkey
[2] Istanbul University-Cerrahpasa, Faculty of Engineering, Department of Electrical and Electronic Engineering, 34320 – Avcılar, İstanbul, Turkey
[4] Istanbul Kültür University, Faculty of Science and Letters , Department of Physics, 34156, Bakırköy-Istanbul,Turkey
*Correspondingauthor: dmtdemirag@gmail.com

hydrogen atoms in the structure [3]. They constructed a three-dimensional structure model of CTA II with 18 chains, and showed that it has the same basic shape with the experimentally obtained single crystal with micron-size. However, CTA is generally known to have poor solubility in most solvents. Although the dissolution properties of CTA are important for its industrial uses, the basic solubility and solution properties of CTA have not been fully understood therefore further investigation is required in this regard. Recently, there has been widespread use of CTA in new high-technology application fields such as chiral separation, medical membranes, and optical films with highly controlled optical properties [4,5].

Aspergillus niger is cultured for the industrial production of many substances. Various strains of A. niger are used in the industrial preparation of citric acid and gluconic acid and have been assessed as acceptable for daily intake by the World Health Organisation. A. niger fermentation is "generally recognized as safe" (GRAS) by the United States Food and Drug Administration under the Federal Food, Drug, and Cosmetic Act. Many useful enzymes are produced using industrial fermentation of A. niger. Another use for A. niger within the biotechnology industry is in the production of magnetic isotope-containing variants of biological macromolecules for NMR analysis [6,7].

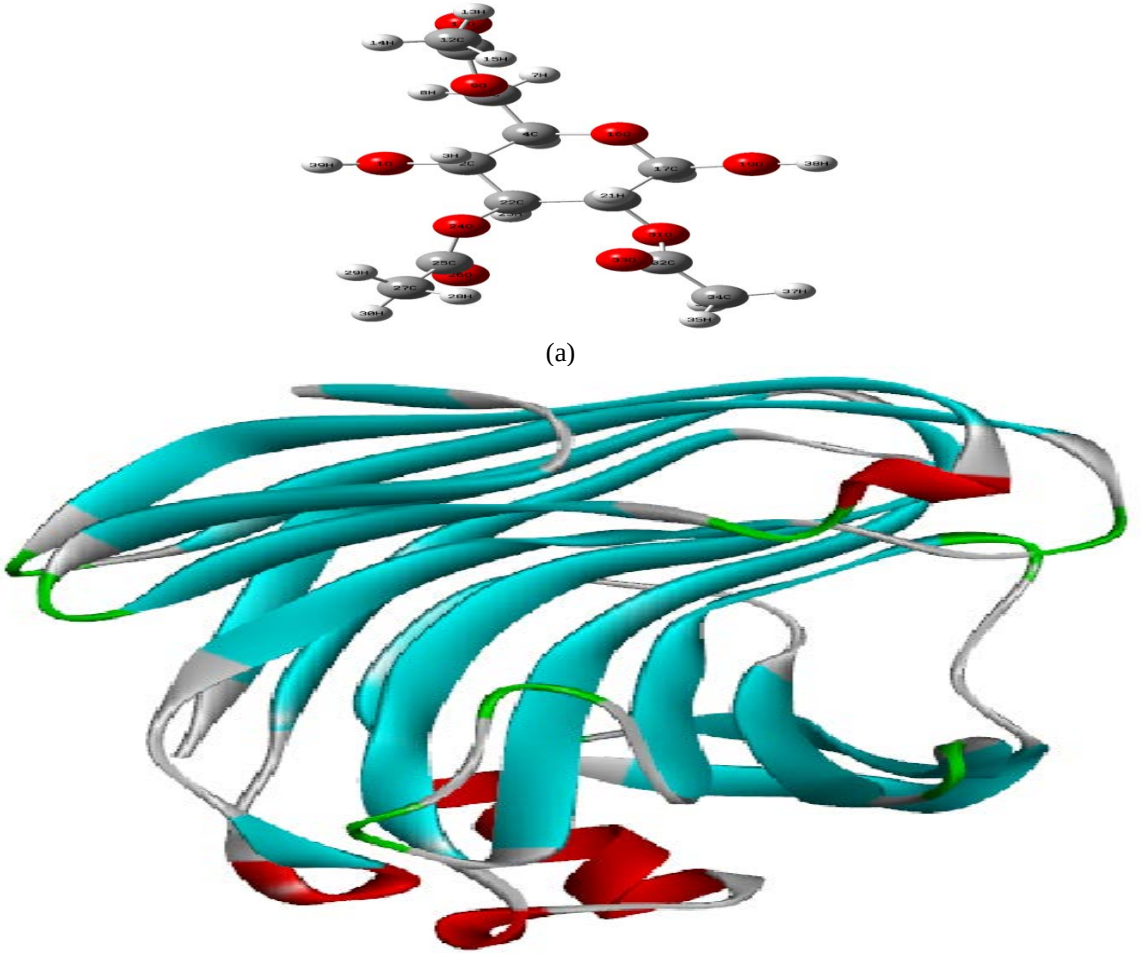

(a)

(b)

Figure 1. The receptor representation of (a) cellulose triacetate II (ligand) and (b) Aspergillus niger cellulase enzyme composed from 223 amino acid.

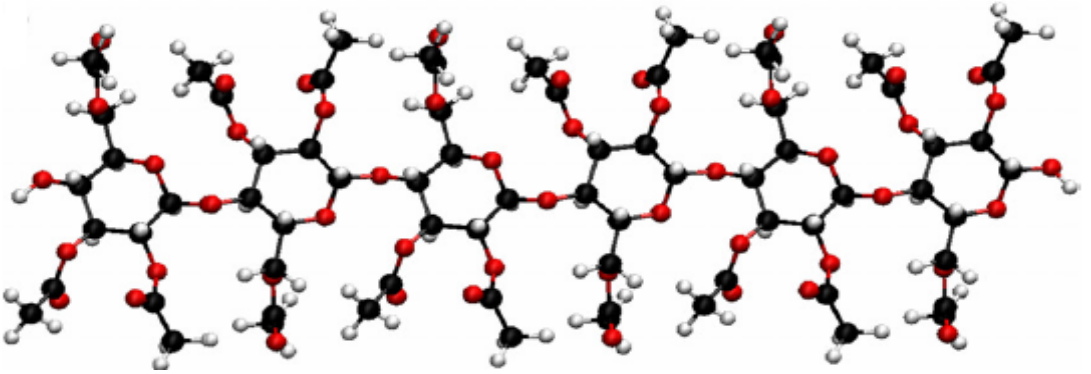

(a)

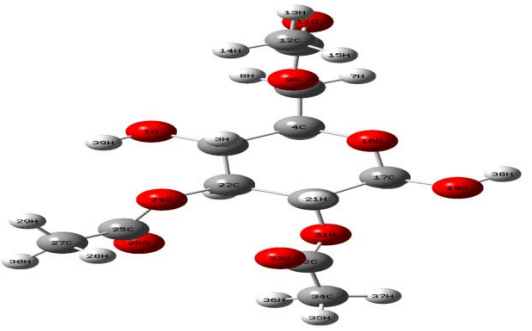

(b)

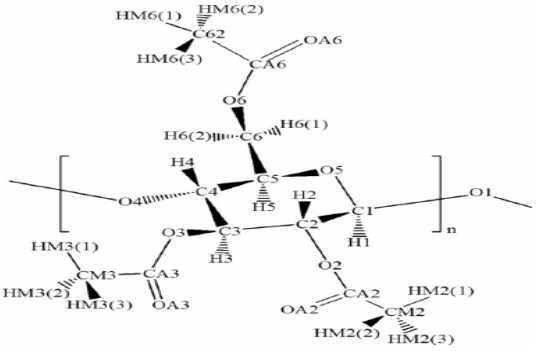

(c)

Figure 2. (a) Literature representation [8] (b) representation of optimized with DFT/ B3LYP/6-31G (d,p) basis set of the single ring of cellulose triacetate II and (c) the explicit representation of the single ring of cellulose triacetate II (CTA II) molecule [8].

Material and Methods

In this study, molecular structure analysis of cellulose triacetate II (CTA II) molecule obtained from cellulosic and acetate, which is the most usable material in nature, has been analyzed. The CTA II was optimized by Density Functional Theory (DFT), B3LYP function and 6-31G(d,p) basis set using Gaussian03 program [9,10]. The harmonic force field of the CTA II was evaluated by the scaled quantum mechanical force field procedure proposed by Pulay, Fogarasi, Pongor, Boggs, and Vargha (1983) [11].

IR intensities and potential energy distributions (PEDs) of vibrational modes were calculated using the MOLVIB program; force fields in Cartesian coordinates were transformed into natural internal coordinates

[12, 13]. In order to bring the calculation result of the CTA II molecule closer to the crystal result, the scale factors of the force constants for internal coordinates containing H atoms in the OH group were considered to be close to zero. In Table 2 frequencies below 50 cm^{-1} have not written to the table.

Scale factors used are:

Monomeric form:	
O-H stretch	almost 0
C-H stretch	0.91
N-H and C-H deformation	0.92
C=O stretch	0.86
all others	0.98

Result and discussion

1.Structure

The starting geometry of the cellulose triacetate II molecule was built from the PDB [14]. The most stable structure of the cellulose triacetate II molecule was obtained by optimization in the gas phase using DFT / B3LYP / 6-31G(d,p). The structural parameters of the optimized conformer of the cellulose triacetate II molecule are given in Table 1. The optimized molecular structure of the gas phase cellulose triacetate II molecule has been found to be similar to the structure of the crystalline cellulose triacetate II molecule obtained by Roche PDB et al [1].

The optimized molecular structure of the cellulose triacetate II molecule calculated by the gas phase DFT/B3LYP/6-3G(d,p) theory is shown in Figure 2.

Table 1. Structural parameters for single ring form of cellulose triacetate II (CTA II) obtained by DFT/B3LYP (6-31G(d,p)), in the gas phase.

Cellulose triacetate II (CTA II)									
Atoms	Mono[a]	Atoms	Mono[a]	Atoms	Mono[a]	Atoms	Mono[a]	Atoms	Mono[a]
R(1,2)	1.418	R(17,18)	1.1069	R(34,35)	1.0895	A(4,6,9)	108.5542	A(18,17,19)	111.9071
R(1,39)	0.9667	R(17,19)	1.3872	R(34,36)	1.0948	A(7,6,8)	108.8327	A(18,17,20)	109.196
R(2,3)	1.0982	R(17,20)	1.5338	R(34,37)	1.0923	A(7,6,9)	109.5852	A(19,17,20)	107.8594
R(2,4)	1.5331	R(19,38)	0.9672	A(2,1,39)	107.0253	A(8,6,9)	109.759	A(17,19,38)	107.6846
R(2,22)	1.5315	R(20,21)	1.0927	A(1,2,3)	111.316	A(6,9,10)	115.6519	A(17,20,21)	109.3234
R(4,5)	1.104	R(20,22)	1.5329	A(1,2,4)	107.9697	A(9,10,11)	123.3937	A(17,20,22)	110.2922
R(4,6)	1.5169	R(20,31)	1.4371	A(1,2,22)	110.9224	A(9,10,12)	110.7527	A(17,20,31)	106.1601
R(4,16)	1.4252	R(22,23)	1.0943	A(3,2,4)	107.7839	A(11,10,12)	125.8535	A(21,20,22)	110.6263
R(6,7)	1.0931	R(22,24)	1.4465	A(3,2,22)	108.8264	A(10,12,13)	109.3915	A(21,20,31)	109.8906
R(6,8)	1.0928	R(24,25)	1.3639	A(4,2,22)	109.9663	A(10,12,14)	110.0512	A(22,20,31)	110.4467
R(6,9)	1.4388	R(25,26)	1.2098	A(2,4,5)	108.5718	A(10,12,15)	110.0343	A(2,22,20)	112.0297
R(9,10)	1.3553	R(25,27)	1.5062	A(2,4,6)	113.6515	A(13,12,14)	109.9228	A(2,22,23)	109.9966
R(10,11)	1.2107	R(27,28)	1.0951	A(2,4,16)	108.7601	A(13,12,15)	110.0639	A(2,22,24)	105.491
R(10,12)	1.5094	R(27,29)	1.0921	A(5,4,6)	106.94	A(14,12,15)	107.3554	A(20,22,23)	109.7092
R(12,13)	1.0893	R(27,30)	1.0897	A(5,4,16)	110.4418	A(4,16,17)	113.4303	A(20,22,24)	110.8198
R(12,14)	1.0939	R(31,32)	1.3582	A(6,4,16)	108.4631	A(16,17,18)	108.858	A(23,22,24)	108.6772
R(12,15)	1.0938	R(32,33)	1.2114	A(4,6,7)	110.1991	A(16,17,19)	108.401	A(22,24,25)	108.5253
R(16,17)	1.4212	R(32,34)	1.5064	A(4,6,8)	109.9012	A(16,17,20)	110.6216	A(24,25,26)	123.93

[a] R and A stand for bond(Å), angle (deg) respectively.

[1] Istanbul University, Faculty of Science, Department of Physics, Vezneciler, 34134, Istanbul, Turkey
[2] Istanbul University-Cerrahpasa, Faculty of Engineering, Department of Electrical and Electronic Engineering, 34320 – Avcılar, İstanbul, Turkey
[4] Istanbul Kültür University, Faculty of Science and Letters , Department of Physics, 34156, Bakırköy-Istanbul,Turkey
*Correspondingauthor: dmtdemirag@gmail.com

2. Molecular electrostatic potential

The molecular electrostatic potential (MEP) provides a visual method for understanding the relative polarity of a molecule. It is very useful in understanding the electrophilic and nucleophilic reaction regions for the biological recognition process and hydrogen bonding interactions research. In order to predict the reactive positions for the electrophilic and nucleophilic attack for the examined molecule, MEP was calculated in the optimized geometry (blue as positive, blue as positive) obtained in the theory of B3LYP/6-31G(d,p) using the DFT method.

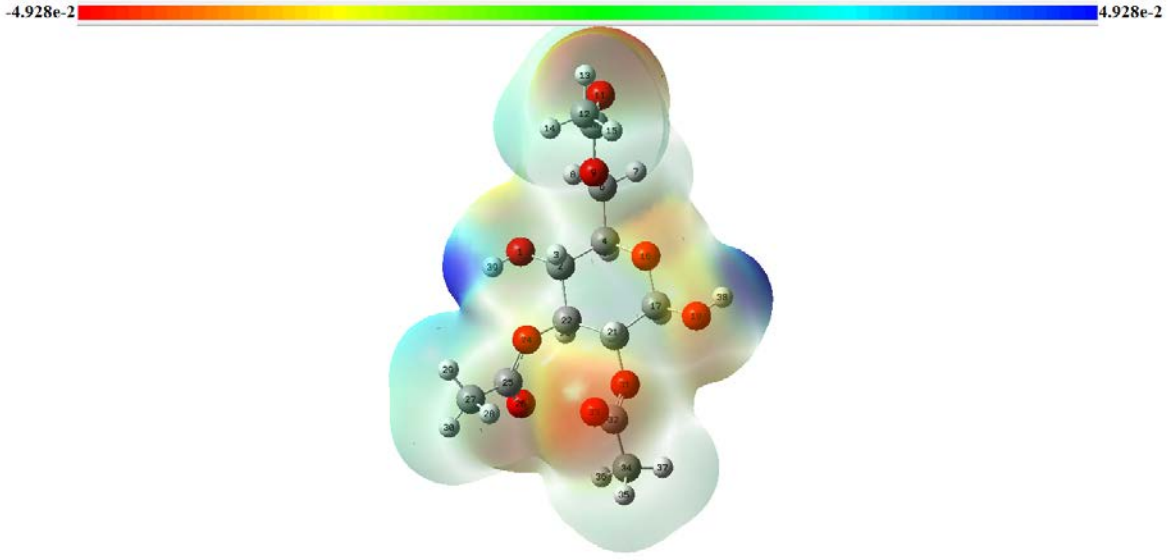

Figure 3. Molecular electrostatic potential (MEP) of cellulose triacetate II (CTA II) of the single ring obtained by DFT/ B3LYP/6-31G(d,p) basis set using GaussView.

The molecular electrostatic potential surface of cellulose triacetate II is shown in Figure 3. Different colors represent the magnitude of the electrostatic potential. Red and blue colors represent regions where the electrostatic potential is most electronegative and most electropositive respectively. In addition, the electrostatic potential increases in order red <orange <yellow <green <blue <. The color code of the cellulosetriacetate map ranges from -1.34 V (dark red) to +1.34 V (dark blue). According to these calculated results, the MEP map shows that the negative potential areas are on the oxygen atom and that the positive potential areas are also around the hydrogen atoms.

3. Vibrational analysis

The C-H stretching modes of cellulose triacetate were observed around 3020-2895 cm^{-1} (IR) and 3025-2850 cm^{-1} (Ra) [14]. In this study, PED contributions of the C-H stretching modes, which are 3036, 3035, 3034, 2995, 2995, 2994, 2990, 2978, 2953 , 2943, 2927, 2926, 2926, 2904, 2840, 2802 cm-1, have been calculated %100, %95, %96, %95, %96, %100, %100, %95, %94, %100, %98, %100, %98, %97, %98, %99, respectively using DFT / B3LYP / 6-31G(d,p) at the theory level.

The C = O stretching vibration gives a strong band in the region of 1730-1660 cm^{-1} [15,16,17]. This modes of cellulose triacetate II were observed as 1750 cm^{-1} (IR) and 1745 cm^{-1} (Ra) [14]. In this study, the theoretical vibration frequencies of C = O tensile modes were calculated at 1716, 1715, 1706 cm-1 with %80,% 74 and 79% PED contributions , respectively.

[1] Istanbul University, Faculty of Science, Department of Physics, Vezneciler, 34134, Istanbul, Turkey
[2] Istanbul University-Cerrahpasa, Faculty of Engineering, Department of Electrical and Electronic Engineering, 34320 – Avcılar, İstanbul, Turkey
[4] Istanbul Kültür University, Faculty of Science and Letters , Department of Physics, 34156, Bakırköy-Istanbul,Turkey
*Correspondingauthor: dmtdemirag@gmail.com

The HCH in-plane bending vibrations DFT / B3LYP / 6-31G (d, p) at the theory level with % 29, 67, 72,69,70, 62 and 69 PED additives are 1467, 1444, 1444, 1443, 1439, 1438 and 1437 cm-1 [18].

According to a report on 1-ethyl-3-methyl immidazolium, the HCH bending modes were observed around 1447-1422 cm^{-1}. HCH in-plane bending modes of cellulose triacetate were observed as 1440 and 1380 cm^{-1} (Ra) [14].

Table 2. Calculated and experimental wavenumbers (cm^{-1}) and PED of the vibrational modes of the cellulose triacetate of single ring (CTA II).

Assignment	**FTIR [14]**	**Raman [14]**	**PED% (≥ 5 %) Cellulose triacetate 6- 31G(d,p)**		
			$\nu_{cal(S)}$	IR	
ν_{CH}			3036	8	$\nu_{CH}(100)$
ν_{CH}			3035	7	$\nu_{CH}(95)$
ν_{CH}	3020	3025	3034	7	$\nu_{CH}(96)$
ν_{CH}			2995	0	$\nu_{CH}(95)$
ν_{CH}			2995	9	$\nu_{CH}(96)$
ν_{CH}			2994	10	$\nu_{CH}(100)$
ν_{CH}			2990	5	$\nu_{CH}(100)$
ν_{CH}			2978	7	$\nu_{CH}(95)$
ν_{CH}	2962		2953	11	$\nu_{CH}(94)$
ν_{CH}	2947	2942	2943	14	$\nu_{CH}(100)$
ν_{CH}			2927	1	$\nu_{CH}(98)$
ν_{CH}			2926	2	$\nu_{CH}(100)$
ν_{CH}			2926	1	$\nu_{CH}(98)$
ν_{CH}	2895	2895	2904	21	$\nu_{CH}(97)$
ν_{CH}		2850	2840	33	$\nu_{CH}(98)$
ν_{CH}			2802	53	$\nu_{CH}(99)$
ν_{C0}	1750	1745	1716	316	$\nu_{CO}(80) + \nu_{CC}(5)$
ν_{C0}			1715	233	$\nu_{CO}(74) + \nu_{CC}(6)$
ν_{C0}			1706	104	$\nu_{CO}(79) + \nu_{CC}(5)$
δ_{HCH}			1467	12	$\delta_{HCH}(29)+ \delta_{HCO}(21)+ \Gamma_{OCCH}(13)+ \Gamma_{CCCH}(6)$
δ_{HCH}			1444	1	$\delta_{HCH}(67)$
δ_{HCH}			1444	8	$\delta_{HCH}(72)+ \Gamma_{OCCH}(14)$
δ_{HCH}			1443	13	$\delta_{HCH}(69)$
δ_{HCH}			1439	1	$\delta_{HCH}(70)$
δ_{HCH}	1430	1440	1438	29	$\delta_{HCH}(62)$
δ_{HCH}			1437	9	$\delta_{HCH}(69) + \delta_{CCH}(6)$
ν_{CO}			1405	45	$\nu_{CO}(19) + \delta_{HCO}(12) + \nu_{CC}(9) + \Gamma_{HCCO}(8)+ \Gamma_{COCH}(6) + \Gamma_{HCCC}(6)$
ν_{OC}			1390	2	$\nu_{OC}(12) + \nu_{CC}(8) + \delta_{OCH}(8) + \Gamma_{HCCO}(6) + \Gamma_{HCCH}(5)$
ν_{CC}			1385	19	$\nu_{CC}(10) + \delta_{CCH}(7) + \Gamma_{CCCH}(6) + \Gamma_{OCCH}(6)$
ν_{CC}		1380	1379	27	$\nu_{CC}(25) + \delta_{CCH}(18) + \nu_{OC}(7)$
ν_{CC}	1368		1365	44	$\nu_{CC}(21) + \delta_{CCH}(14)$
ν_{CC}			1356	33	$\nu_{CC}(19) + \delta_{HCC}(8) + \Gamma_{HCOC}(5)$
δ_{CCH}			1351	109	$\nu_{CC}(13) + \delta_{CCH}(26)$
δ_{CCH}			1348	93	$\delta_{CCH}(31) + \nu_{CC}(8) + \delta_{HCH}(12)$

δ_{HCO}			1338	6	$\delta_{HCO}(5)$
Γ_{HCCH}	1320	1320	1324	19	$\Gamma_{HCCH}(16)+ \delta_{HCO}(9) + \delta_{CCH}(7) + \Gamma_{HCCO}(7) + \nu_{CC}(7)$
ν_{CC} , Γ_{HCCH}			1277	70	$\nu_{CC}(10) +\Gamma_{HCCH}(10) + \delta_{CCH}(8) + \nu_{CO}(6)$
ν_{OC}		1270	1266	216	$\nu_{OC}(46)$
ν_{OC}			1258	184	$\nu_{OC}(21) + \nu_{CC}(5) + \delta_{CCH}(5)$
ν_{OC}	1232		1252	673	$\nu_{OC}(43) + \nu_{CC}(6)$
δ_{HCO}			1241	9	$\delta_{HCO}(40) + \delta_{CCH}(18)+\Gamma_{HCCH}(15)$
ν_{OC}	1215	1222	1225	188	$\nu_{OC}(45) + \nu_{CC}(10)+ \delta_{CCH}(7) + \delta_{OCC}(5) + \delta_{OCO}(5)$
ν_{CO}	1165	1165	1174	46	$\nu_{CO}(72)$
ν_{CO}			1139	47	$\nu_{CC}(31) + \nu_{CO}(37)$
ν_{OC}			1132	19	$\nu_{OC}(48) + \nu_{CC}(17)$
ν_{OC}	1122	1125	1121	96	$\nu_{OC}(69) + \nu_{CC}(6)$
ν_{CC}			1110	3	$\nu_{CC}(41) + \nu_{CO}(7)$
ν_{OC}			1095	104	$\nu_{OC}(35) + \nu_{CC}(29)$
ν_{CO}		1080	1083	129	$\nu_{CC}(29) + \nu_{CO}(37)$
ν_{CO}	1070		1068	7	$\nu_{CO}(22) + \nu_{CC}(36)$
ν_{CO}		1055	1061	102	$\nu_{CO}(54)$
ν_{CO}	1048		1052	156	$\nu_{CO}(50)$
δ_{CCH}			1039	1	$\delta_{CCH}(69) + \Gamma_{OCCH}(7)$
δ_{CCH}			1038	6	$\delta_{CCH}(64) + \Gamma_{OCCH}(6)$
δ_{CCH}			1037	6	$\delta_{CCH}(61) + \Gamma_{OCCH}(9)$
ν_{CO}			1025	76	$\nu_{CO}(40) + \delta_{CCH}(18)$
ν_{CO}			1021	21	$\nu_{CO}(19) + \delta_{CCH}(13) + \nu_{CC}(6)$
δ_{HCC}	990		987	46	$\delta_{HCC}(15) + \delta_{OCH}(9) + \Gamma_{COCH}(7) +\Gamma_{HCOH}(6) + \nu_{CC}(5) + \nu_{OH}(5)$
δ_{CCH}		980	982	9	$\delta_{CCH}(34) + \nu_{CO}(9) + \nu_{CC}(6)$
ν_{CC}			966	18	$\nu_{CC}(27) + \delta_{CCH}(12) + \nu_{CO}(14)$
ν_{CO}			962	1	$\nu_{CO}(20) + \nu_{CC}(19) + \delta_{CCH}(6)$
ν_{CO}	952		943	20	$\nu_{CC}(24) + \nu_{CO}(26)$
ν_{CO}	920	920	909	6	$\nu_{CO}(27) + \nu_{CC}(8) + \delta_{CCH}(7)$
ν_{CO}	901		900	14	$\nu_{CO}(42) + \delta_{COC}(6)$
ν_{CO}	874	885	886	11	$\nu_{CO}(19) + \nu_{CC}(14) + \delta_{CCH}(6)$
ν_{CO}	837	840	861	7	$\nu_{CO}(30) + \nu_{CC}(22)$
ν_{CO}	720	720	681	4	$\nu_{CO}(17) + \nu_{CC}(15)+ \delta_{CCO}(7)$
ν_{CC}	693		664	20	$\nu_{CC}(13) + \nu_{CO}(12)+ \delta_{COC}(6)$
ν_{CC}	660	660	648	5	$\nu_{CC}(28) + \delta_{OCO}(21) + \delta_{COC}(14)$
ν_{CC}	642	640	640	10	$\nu_{CC}(36) + \delta_{OCO}(17) + \delta_{COC}(6)$
δ_{OCO}	603	605	611	37	$\delta_{OCO}(16) + \nu_{CC}(12)$
δ_{CCH}			592	1	$\Gamma_{COCO}(16) + \delta_{CCH}(22)$
δ_{CCH}			589	5	$\delta_{CCH}(22) + \Gamma_{COCO}(13)$
δ_{CCH}			585	4	$\delta_{CCH}(19) + \Gamma_{COCO}(12) + \Gamma_{OCCH}(6)$
δ_{OCO}	558	560	552	3	$\delta_{OCO}(5)$
δ_{OCC}		520	527	21	$\delta_{OCC}(14) + \Gamma_{COCC}(5)$
δ_{OCC}	490	490	508	0	$\delta_{OCC}(35)$
δ_{OCC}	477		475	16	$\delta_{OCC}(18) + \delta_{COC}(7)$
δ_{OCC}	450		447	5	$\delta_{OCC}(15)$
δ_{OCC} , δ_{COC}	430	430	414	14	$\delta_{OCC}(12) + \delta_{COC}(12) + \nu_{CH}(5)$
δ_{OCC}	392	390	398	6	$\delta_{OCC}(45) + \delta_{CCH}(5)$
δ_{OCC}			368	19	$\delta_{OCC}(22) + \nu_{CC}(7)$

δ_{OCC}	337	11	$\delta_{OCC}(16)$
Γ_{OCCO}	313	3	$\Gamma_{OCCO}(7)$
δ_{COC}	278	1	$\delta_{COC}(6)$
Γ_{OCCH}, Γ_{CCCH}	269	12	$\Gamma_{OCCH}(14) + \Gamma_{CCCH}(14) + \Gamma_{CCCO}(5) + \Gamma_{OCCO}(5)$
δ_{OCC}, ν_{CC}	263	9	$\delta_{OCC}(7) + \nu_{CC}(7)$
Γ_{COCO}	226	1	$\Gamma_{COCO}(7)$
δ_{COC}	202	2	$\delta_{COC}(14) + \Gamma_{COCO}(6)$
δ_{COC}	191	4	$\delta_{COC}(27) + \Gamma_{CCOC}(8) + \Gamma_{COCO}(5)$
δ_{COC}	181	1	$\delta_{COC}(28)$
Γ_{COCC}	159	1	$\Gamma_{COCC}(21) + \Gamma_{COCO}(11) + \Gamma_{HCOC}(19)$
Γ_{OCCH}	135	2	$\delta_{COC}(15) + \Gamma_{OCCH}(21)$
Γ_{OCCH}	127	0	$\Gamma_{OCCH}(98)$
Γ_{OCCH}	118	0	$\Gamma_{OCCH}(98)$
Γ_{HOCC}	101	10	$\Gamma_{HOCC}(11) + \Gamma_{COCO}(6)$
Γ_{OCCH}	78	1	$\Gamma_{OCCH}(45) + \Gamma_{CCOC}(9)$
Γ_{OCCH}	77	0	$\Gamma_{OCCH}(98)$
Γ_{CCOC}	71	9	$\Gamma_{COCC}(11) + \Gamma_{C0CO}(9)$
Γ_{CCOC}	68	2	$\Gamma_{CCOC}(25) + \Gamma_{HCOC}(7) + \Gamma_{OCCH}(15)$
Γ_{OCCH}	60	1	$\Gamma_{OCCH}(61)$
Γ_{OCCH}	52	2	$\Gamma_{OCCH}(38)$

4. Molecular docking studies

The three-dimensional crystal structure of Aspergillus niger cellulase enzyme was obtained from Protein Data Bank (PDB ID: 1KS5) [19]. Aspergillus niger cellulase enzyme in the removal of water molecules and the addition of polar hydrogen was added to the clamping. Kollman's Aspergillus niger cellulase enzyme charges were also detected. The gas phase CTA II molecule was optimized and adapted for insertion. Partial loads of the CTA II molecule were calculated using the Geistenger method. The active region of the protein was defined within the 40 × 40 × 40 Å grid size. During the docking calculation 9 possible stable poses were obtained (Table 3 and Figure 4(a)). One of the 9 most stable poses having a binding affinity of -6.6 kcal / mol, which is well connected to the active site was selected and shown in Figure 4(b). As shown in Figure 4(b), CTA II binds with the active site H-binding interactions of the Aspergillus niger cellulase enzyme.
Enzyme–ligand interaction shows that there are three H-bonds between CO group of CTA II and amino groups of ASN18, ASN20 and ASN63 (2.66 Å, 2.82 Å and 2.07 Å). Other H-bond interaction is also observed between OH group of SER16 and CO group of CTA II as 1.99 Å in Figure 5.

Table 3. The affinity values of the 9 most possible orientations as a result of ligand-receptor interaction.

Mode	Affinity (kcal/mol)	Dist. from best mode	
		RMSD l.b.	RMSD u.b.
1	-6.6	0.000	0.000
2	-6.4	5.338	7.396
3	-6.3	1.144	3.423
4	-6.2	2.350	6.552
5	-6.2	5.944	10.351
6	-6.2	1.653	3.493
7	-6.1	3.598	6.464
8	-5.9	10.677	14.301
9	-5.9	4.724	7.726

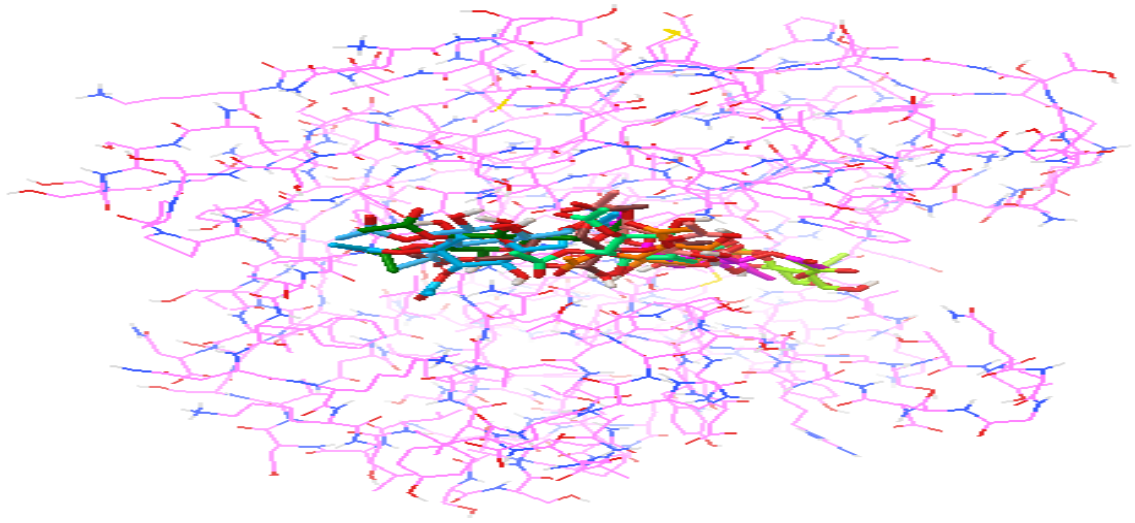

(a)

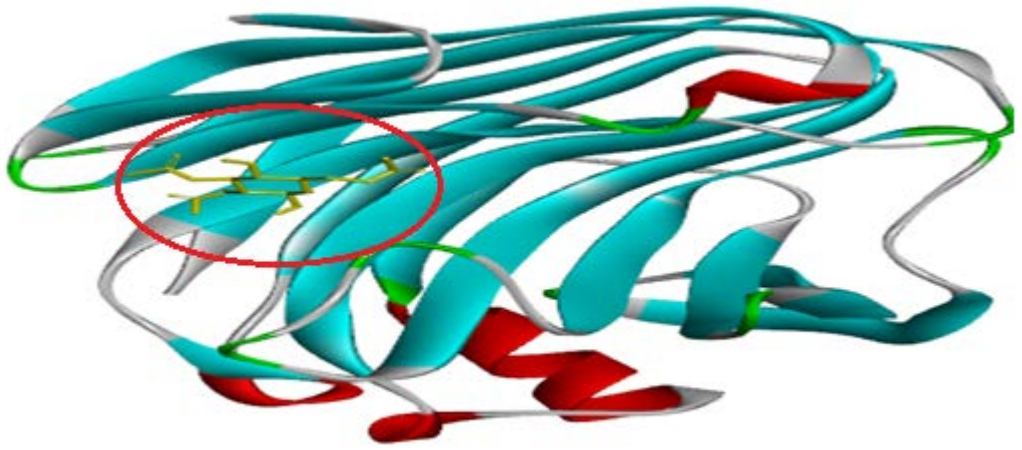

(b)

Figure 4. (a) Orientation of nine conformation of cellulose triacetate II (CTA II) molecule and Aspergillus niger cellulose enzyme (receptor-ligand interaction) and (b) the most stable orientation.

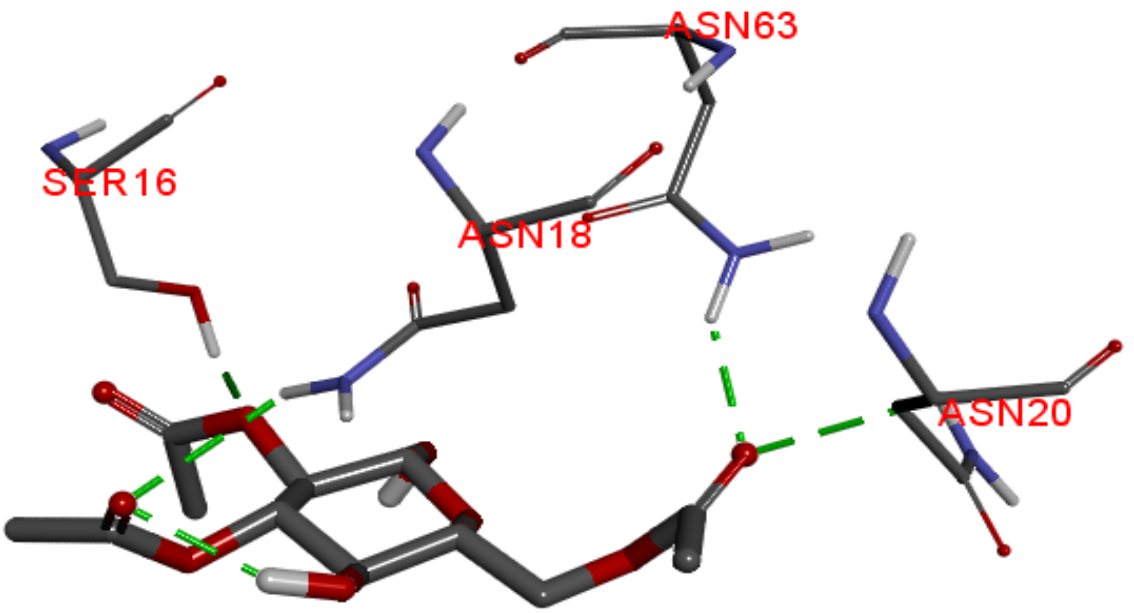

Figure 5. Representation of amino acids bound by cellulose triacetate II molecule as a result of receptor-ligand interaction.

Discussion and Conclusions

Cellulose is an abundant and renewable biological source on the earth. Today, with the decline of organic food, these innovative studies will makes cellulose an important raw material for food, energy, fuel, drug design and industry in the future.

References

1. Roche, E.; Chanzy, H.; Boudeulle, M.; Marchessault, R. H.; Sundararajan, P. Macromolecules 1978, 11, 86–94.

2. Sikorski, P.; Wada, M.; Heux, L.; Shintani, H.; Stokke, B. T. Macromolecules 2004, 37, 4547–4553.

3. Dulmage, W. J. J. Polym. Sci. 1957, 26, 277–288.

4. Francotte, E. J. Chromatogr. A 1994, 666, 565–601.

5. Sata, H.; Murayama, M.; Shimamoto, S. Macromol. Symp. 2004, 208, 323–333.

6. Brooks, B. R.; Bruccoleri, R. E.; Olafson, B. D.; Swaminathan, S.; Karplus, M. J. Comput. Chem. 1983, 4, 187–217.

7. https://www.ncbi.nlm.nih.gov/pubmed.

8. Daichi Hayakawa, Kazuyoshi Ueda, Chihiro Yamane, Hitomi Miyamoto, Fumitaka Horii (2011) Molecular dynamics simulation of the dissolution process of a cellulose triacetate-II nano-sized crystal in DMSO. Carbohydrate Research, 346, 2940–2947.

9. Becke, A.D., 1993, J. Chem. Phys., 98, 5648.

10. Frisch, M.J., Trucks, G.W., Schlegel, H.B., et al., 2004, Gaussian 03, Gaussian, Inc., Wallingford, CT.

11. Pulay, P., Fogarasi, G., Pongor, G., Boggs, J.E. and Vargha, A. (1983) Combination of Theoretical Ab Initio and Experimental Information to Obtain Reliable Harmonic Force Constants. Scaled Quantum

Mechanical (SQM) Force Fields for Glyoxal, Acrolein, Butadiene, Formaldehyde, and Ethylene. Journal of the American Chemical Society, 105, 7037-7047.

12. T. Sundius and Kj. Rasmussen, J. Mol. Struct., 65 (1980) 215-218.

13. T. Sundius (1990). MOLVIB: A program for harmonic force field calculations, QCPE program no. 604. Journal of Molecular Structure, 218, 321-326.

14. Firsov, S. P., & Zhbankov, R. G. (1982). Raman spectra and physical structure of cellulose triacetate. Journal of Applied Spectroscopy, 37(2), 940-947.

15. Mary, Y. S., Ushakumari, L., Harikumar, B., Varghese, H. T., & Panicker, C. Y. (2009). FT-IR, FT-Raman and SERS spectra of L-proline. Journal of the Iranian Chemical Society, 6, 138–144.

16. Padmaja, L., Ravikumar, C., James, C., Jayakumar, V. S., & Joe, I. H. (2008). Analysis of vibrational spectra of lalanylglycine based on density functional theory calculations. Spectrochimica Acta Part A: Molecular and Biomolecular Spectroscopy, 71, 252–262.

17. Roeges, N. P. (1994). A guide to the complete interpretation of infrared spectra of organic structures. New York, NY: Wiley.

18. Mao, J. X., Lee, A. S., Kitchin, J. R., Nulwala, H. B., Luebke, D. R., & Damodaran, K. (2013). Interactions in 1-ethyl-3-methyl imidazolium tetracyanoborate ion pair: Spectroscopic and density functional study. J. Mol. Struct., 1038, 12-18.

19. Khademi, S., Zhang, D., Swanson, S. M., Wartenberg, A., Witte, K., & Meyer, E. F. (2002). Determination of the structure of an endoglucanase from Aspergillus niger and its mode of inhibition by palladium chloride. Acta Crystallographica Section D: Biological Crystallography, 58(4), 660-667.

International Conference on Science and Technology

ICONST 2018

5-9 September 2018 Prizren - KOSOVO

Scaling Effect on Detecting Streamflow Data Trend: A Case Study of Filyos River

Nermin ŞARLAK[1]*, Ruqaya Mahmood JASIM[2]

Abstract: Scaling effect on detecting trend from different segments or different extends from the same time series is a well-known problem. A highly significant increasing trend may be found in a given segment, while a statistically non-significant trend may be found in a different segment. The reconstructed series obtaining from tree ring data which extended from 1657 to 1997 for a length of 341 years was considered as well as observed data from 1964 to 1997 to discuss this effect. Mann-Kendall trend analysis was used on both data series. The main objective of this study was to illustrate the effect of scaling on detecting trend. The present study clearly reveals that both observed and reconstructed data nearly throughout exhibit persistence behaviors. Similar decreasing trend patterns were observed at the different time scales although the trend result for observed time series was not statistically significant. As a result, we should be aware of the changing trend results under the effect of scaling. It will affect the making stationarity and climate change interpretations which are very important to time series model.

Keywords: Trend, scaling effect, reconstructed data, tree ring, Mann Kendall, nonstationarity

Introduction

The assumption, which is called stationarity that implies time-invariant statistical characteristics of the time series, is in question at all. This assumption is under discussion with climate change effect. A huge number of studies have been applied in the scopes of hydro-climatology and hydro-meteorology to show and quantify the existence of trends. Some of the most common variables included in these studies are temperature (Piŝoft et al., 2004; Prokoph and Patterson, 2004; Mohsin and Gough, 2010; Mahmmod Agha and Sarlak, 2016), streamflow (Zhang et al., 2001; Burn and Elnur, 2002; Anctil and Coulibaly, 2004; Zume and Tarhule, 2006, Partal, 2010), precipitation (Kim and Jain, 2011; Mishra and Singh, 2010; Mahmmod Agha and Sarlak, 2016), and snowpack (Hamlet et al., 2005). Koutsoyiannis (2003) discussed the nonstationarity versus scaling in hydrology. He mentioned that nonstationarity approach is contradictory in its logical and even in the terms it uses. Milly et al., (2008) discussed the stationarity approach under climate change issue. The main objectives as for this study are: 1) discuss the scaling effect using the reconstructed series obtaining from tree ring data which extended from 1657 to 1997 for a length of 341 years as well as observed data from 1964 to 1997. 2) study the trend results obtained from both time series whether the results are statistically significant or not and the effects of these results on stationarity and climate change interpretations which is very important to time series model. Mann-Kendall (MK) trend test is prefered in this study, since it is well-known trend analysis test.

Material and Method

The Filyos gagging station (EIE 1335) was selected (can be seen in Figure 1), since Sarlak (2014) reconstructed this streamflow data during 1657-1997 by utilizing NPP-LOCFIT method (Sarlak, 2014).

[1]Karamanoğlu Mehmetbey University, Faculty of Engineering, 70200, Karaman, TURKEY
[2]University of Gaziantep, Faculty of Engineering, 27310, Gaziantep, TURKEY
*Correspondingauthor: nsarlak@kmu.edu.tr

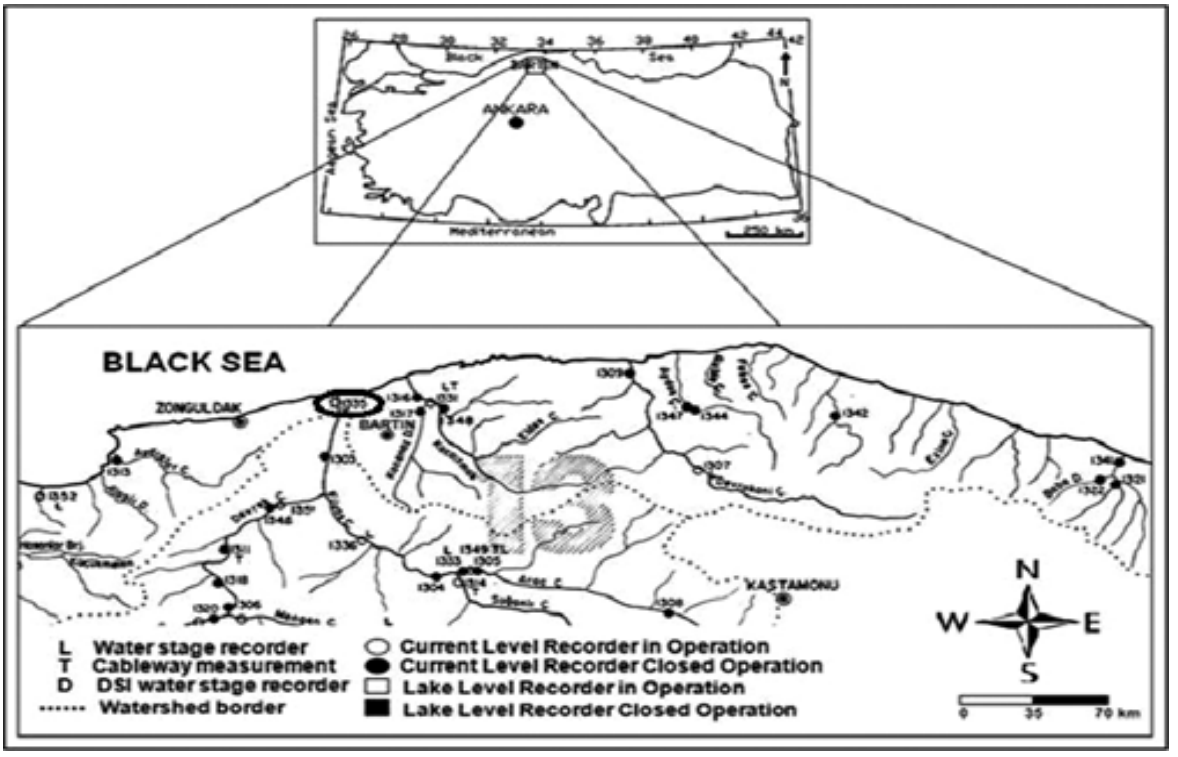

Figure 1. Stream Gagging Station on the Map

Mann- Kendall (MK) test is widely used statistical test in the trend analysis, since it is distribution free (non-parametric). Second advantage of this test is to be characterized with low sensitivity to abrupt change as a result of the inhomogeneous time series. In accordance with this test, the null hypothesis, H_0 presumes that there is no trend. It means that the data is independent and random. The p-value test is prefered to evaluate H_0. If the p-value $\leq \alpha$, it implies that there is a trend in the time series.

The serial correlation at the data of time series, if it exists, has been removed before applying this test. It may cause detecting pseudo significant trend (Kulkarni and Van Storch, 1995).

Results

MK test on Mean Spring-Summer Data

In this section, we were utilized the mean spring-summer data for 34 years from 1964 to 1997. The reason of this is that Sarlak (2014) reconstructed mean spring-summer data. She emphasized that the statistically significant relationship was obtained between the mean spring-summer data and tree ring chronologies. The autocorrelation and partial autocorrelation values were found to be not significant at 95% level. The MK test results were shown in Table 1. H_0 could not be rejected since the calculated p-value was greater than the significance level. We should note that the results obtained from mean spring-summer data were same with obtained from the result's of observed annual data exactly.

Table 1. The results for mean spring-summer data

Statistic S	Kendall's Tau	Var (S)	Mean	p	Alpha	Outcome
-64	-0.114	4549.333	76.54706	0.35028	0.05	Accept H_0

Mann-Kendall Test on Reconstruction Data

Trend analysis of reconstructed data obtained from NPP-LOCFIT method was done in this study with using 341 years of reconstruction data from 1657 to 1997. The serial correlation effect in the reconstructed time series was statistically significant. To eliminate this effect the pre-whitened time series were calculated. After removing the lag-1 serial correlation effect on the time series, the serial correlation effect was managed to eliminate at 95% level. Then the test was utilized for pre-whitened reconstructed data series. The results were presented in Table 2. The calculated p value was less than the significance level α (= 0.05). In this case the null hypothesis, H_0 which there is no trend should be rejected. We found statistically significant decreasing trend from reconstructed data.

Table 2. The results for reconstruction data

Statistic S	Kendall's Tau	Var (S)	Mean	p	Alpha	Outcome
-5412	-0.0939	4386284	141.7105	0.0097769	0.05	Reject H_0

Discussion and Conclusions

The smaller the number of available time periods that means became the sample size is smaller, the higher the potential of error. The longest the time period and more information is to accurately determine the patterns of change. The aim of the following study was to emphasize the effect of data size or scaling on detecting trend. For this aim, different segments from the observed data series were considered. The test results for the period between 1964 and 1967 were given in the Table 3. It could not be detected statistically significant decreasing trend. Since this period was not enough to confirm the results, the longer period from 1964 to 1990 was utilized. The test results for period from 1964 to 1990 were represented in the Table 3 also.

The last segment considered was from 1964 to 1994. Kahya and Kalayci (2004) found statistically significant decreasing trend from monthly data for same station spanning from 1964 to 1994. Whether there is also significant decreasing trend for annual data or not, the same duration was utilized. The test results were summarized in Table 3. Although they concluded that there was significant decreasing trend on monthly data, our results showed that this decision did not valid for annual data. The same result was obtained from the last segment from 1964 to 1997.

Table 3. Comparsion results from different segments

The period (data size)	Mann-Kendall Statistic S	p	Alpha	Outcome	Detecting Trend
1964 - 1967	-4	0.30818	0.05	Accept H_0	No Trend
1964 – 1990	-34	0.49139	0.05	Accept H_0	No Trend
1964 – 1994	-56	0.34982	0.05	Accept H_0	No Trend
1964 - 1997	-64	0.35082	0.05	Accept H_0	No Trend

The current study clearly shows that both observed and reconstructed data almost over exhibit persistence behaviors. Similar decreasing trend patterns were observed at the different time scales, although the trend result for observed time series was not statistically significant. As a result, the scaling effects influence the interpretation of results to detect trend. It certainly affects making stationary and climate change decisions which are very important for time-series model. Although the best way is to utilize more than one different segments from the reconstructed data series to discuss the scaling effect, the results show that the comparing the limited observed data series is also very useful to emphasize the scaling effect.

Acknowledgements

The first author wishes to thank to Karamanoğlu Mehmetbey University Scientific Research Projects Coordinatorship (Project No: 09-AG-18) for providing financial support.

References/Kaynaklar

Anctil, F., Coulibaly, P. (2004). Wavelet analysis of the interannual variability in Southern Quebe streamflow. American Meteorological Society, 163-173.

Hamlet, A.F., Mote, P.W., Clark, M.P., Lettenmaier, D.P. (2005). Effects of temperature and precipitation variability on snowpack trends in the western United States. Journal of Climate, 18, 4546-4561.

Kahya, E., Kalaycı, S. (2004). Trend analysis of streamflow in Turkey. Journal of Hydrology, 289(1–4), 128-144.

Kim, J-S., Jain, S. (2011). Precipitation trends over the Korean peninsula: typhoon-induced changes and a typology for characterizing climate-related risk. Environmental Research Letters, 6, 034033.

Koutsoyiannis, D. (2003). Climatic change, the hurst phenomenon and hydrological statistics. Hydrological Science Journal, 48 (1), 3–24.

Kulkarni, A., Von Storch, H. (1995). Monte carlo experiments on the effect of serial correlation on the Mann-Kendall test of trend. Meteorologische Zeitschrift, 4(2), 82-85.

Mahmood Agha, O., Sarlak, N. (2016). Spatial and temporal patterns of climate variables in Iraq. Arabian Journal of Geosiences, 9, 302.

Mishra, A.K., Singh, P. (2010). Changes in extreme precipitation in Texas. Journal of Geophysical Research, 115, D14106.

Milly, P.C.D., Betancourt, J., Falkenmark, M., Hirsch, R.M., Kundzewicz, Z.W., Lettenmaier, D.P., Stouffer, R.J. (2008). Stationarity Is Dead: Whither Water Management? Science, 319, 573-574.

Mohsin, T., Gough, W. (2010). Trend analysis of long-term temperature time series in the Greater Toronto Area (GTA). Theoretical and Applied Climatology, 101(3), 311-327.

Partal, T. (2010). Wavelet transform-based analysis of periodicities and trends of Sakarya Basin (Turkey) streamflow data. River Research and Applications, 26, 695-711.

Pišoft, P., Kalvova, J., Brazdil, R. (2004). Cycles and trends in the Czech temperature series using wavelet transforms. International Journal of Climatology, 24,1661-1670.

Prokoph, A., Patterson, R. T. (2004). Application of wavelet and regression analysis in assessing temporal and geographic climate variability: Eastern Ontario, Canada as a case study. Atmosphere Ocean, 43(2), 201-212.

Sarlak, N. (2014). Filyos River Streamflow Reconstruction from Tree-Ring Chronologies with Nonparametric Approaches. Journal of the American Water Resources Association, JAWRA 50 (5), 1102-1110.

Zhang, X., Harvey, K.D., Hogg, W.D., Yuzyk, T.R. (2001). Trends in Canadian streamflow. Water Resources Research, 37(4), 987-998.

Zume, J., Tarhule, A. (2006). Precipitation and streamflow variability in Northwestern Oklahoma, 1894-2003. Physical Geography, 27(3), 189-205.

International Conference on Science and Technology

ICONST 2018

5-9 September 2018 Prizren - KOSOVO

The Effects of Landscape Designs Applied in Housing and Site Areas on Housing Sales 'Case of Kastamonu City Center '

Sevgi Öztürk[1], Merve Kalaycı[1*]

Abstract: Housing is a whole perceived with its environment. Housing design principles show integrity and parallelism with the housing environment. Reflection of changes in production processes depends on not a plan, depends on planning principles. While the formation of the plan depends on the social culture; elements used in the implementation of the plan and the external environment influencing the designer in the planning process, it depends on the economic and social inputs. A building gains aesthetic value with contrasts created with plants and spaces, shapes and color rhythms. When the building is perceived, the surrounding open and green areas have great effect. It only adapts to the environment in this way. In the cities that are changing rapidly and growing without plans, concretion, disfiguration and due to come to an unhealthy state the quality of housing and living environments has also affected negatively. In the study, at the Kastamonu city center scale, the effect of landscape design on housing prices in residential surroundings was discussed. Two sites in Kuzeykent and Olukbaşı of Kastamonu city center were selected as sample. In the first stage, a literature search of the subject was made. In the second stage, field observations were carried out, in the third stage; by analyzing the questionnaires made with residents, the results confirming the hypothesis were obtained. As a result of the study in general; it cannot be ignored that the importance given to the urban green areas in the sample area scale and housing prices are on the way of boosting the effect on it.
The results of this study showed that urban green areas, which increase the level of environmental prosperity, have impacts on the housing market. The most important result obtained from the research is that urban green areas are measurable values.

Keywords: Landscape, Design, Housing, Kastamonu, Economy

Introduction

The decline in the amount of green fields has increased the longing of people for the nature. Especially in big cities, increasing land values in parallel with the population have resulted in conversion of existing open spaces not to green fields, but to housings. This caused a decrease in green fields, thus an increased demand for such areas. It is observed in Turkey that, in a parallel with the industrialization starting in the 1950's, the concept of urbanization has become highly intensified due to socio-economic and cultural developments. While approximately 18.3% of the country population lived in cities during the World War II, this rate has today increased to 60% and up to 70% (Gül and Küçük, 2001).
The tendency towards rapid, irregular and unplanned urbanization in Turkey, with planning and applications not based on ecological foundations, bring along many problems and seriously affect the human life and living quality negatively. Cities with such structures stray people away from natural environments, render them monotonous, and result in physically and mentally negative consequences. General characteristic of a city is determined by architectural structures, open-green areas as well as their relationship and integrity (Öztürk and Bozdoğan, 2014). Open-green areas play an important role in balancing the disrupted relationship between humans and nature and improving city life conditions. Therefore, qualities and

[1]Kastamonu University, Faculty of Engineering and Architecture, 37200, Kastamonu, TURKEY
*Corresponding author: mkalayci@kastamonu.edu.tr

quantities of open-green areas in developed countries are considered as an indicator of civilization and life quality. Within this scope, many developed countries work towards planning and creating the most convenient city space and ecology for human life, taking into consideration the mental and physical needs of people. Environmental concerns as well as economic and social concerns must be taken into consideration in shaping the surroundings of housing areas. The relationship between socio-economic and ecological factors is an undeniable fact. And the indicator of the effect of landscaping on economy is that houses in a good environment with a better view are more valuable than others. However, environmental factors of such effect and significance are not attached due importance in political priorities and urban-rural planning (Luttik, 2000). Green areas are functional areas that create benefits in urban spaces in terms of physical and social environment based on their spatial structures and functional features. Direct assessment the economic values of such benefits is not possible. However, there are methods available for assessing the economic values of the such benefits (Alaca, 2010).

The purpose of this study is to determine whether there is a relationship between urban green area spaces and housing purchases and prices. It will be demonstrated with this study whether the urban environmental quality and visual landscaping values result in a change in housing prices and whether users tolerate the costs of benefits to be gained from a quality-environment.

Material and Method

The study has been conducted in Kastamonu province, which is located in Western Black Sea Region between 41°30'0" Northern latitudes and 33°41'0" Eastern longitudes. The surface area of the city is 13,108,1 kilometer squares and its 76.6% consists of mountains and forestry, 21.6% of plateau and 3.8% consists of lowlands (İbret and Aydınözü, 2009). Population of the city center is 110,908 (TUİK, 2015). There are two different climate types in Kastamonu province. While Black Sea climate is dominant in the Northern part of the province, continental effects of the Central Anatolia climate are seen in the South. One of the most significant factors shaping the climate of the city is the land forms. Küre Mountains in the Northern part of Kastamonu province, located parallelly to the sea, creates a barricade between the coastal region and the inner parts of the city. Therefore, the effects of the Black Sea climate decreases towards the inner parts, substituted with harsh and continental characteristics of the Central Anatolia climate. Throughout the city, the economy is built on education, agriculture, husbandry, and tourism. The first settlements in the city have been on the eastern and western sides of the Karaçomak Stream which trails through the middle of the city (İbret and Aydınözü, 2009; Şen et al., 2018). However, new settlements have been created in the northern and southern parts of the city due to the increase in the central population. In the study, the Akademi site (Figure 1), which is located in Kuzeykent Neighborhood located in the northern part and where the Kastamonu University campus is located, and Silüet site (Figure 2), which is located in the Olukbaşı settlement located on the Kastamonu-Ankara highway have been analyzed. Kuzeykent settlement is at 6.18 km distance and Olukbaşı settlement is at 2.14 km distance to the city center (Öztürk and Özdemir, 2013). Kuzeykent settlement is the largest and most densely populated (24,012 people) neighborhood. The population of the Olukbaşı settlement (Saraçlar Neighborhood) is 10,394 (TÜİK, 2015).

Figure 1. Images of the Akademi site

Figure 2. Images of the Silüet site

The study has been conducted in 3 stages.
1. Literature research
2. Field study
3. Analysis

Literature Research: In the literature research on the subject of the study, many written theses and articles have been examined regarding the concept of open and green areas, the significance of housing concept, its functions as well as factors affecting the housing supply-demand status. Case studies have been utilized for survey questions. Furthermore, an effort has been made to attain the available data on the sample area.

Conducting the Field Study: Initially, the aim has been to determine the parking areas, playgrounds, parking lot vegetation areas in the two selected samples through on-site observation and available maps. The structures and arrangements of the dwellings as well as their interactions with the surrounding green fields have also been inspected.

Photographs of the research areas have been taken and transferred to digital media. Afterwards, a questionnaire study has been conducted with the residents of Siluet and Akademi sites in order to determine their socio-economic states, opinions on the area, likings and, most importantly, levels of willingness to pay.

The questionnaire used in the research consisted of five chapters and a total of 56 questions. Questions on household and socio-economic state have been asked in the first chapter, and general features of dwellings in the site in the second chapter; perceived physical environment in the third chapter; general features of the site in the fourth chapter, and the level of willingness to pay for landscaping design works in the fifth chapter

have been questioned. The questionnaires have been conducted through face-to-face meeting method with 67 randomly selected subjects. The last three chapters of the questionnaire have been assessed within the 5-point Likert scale (1: strongly disagree, 2: disagree, 3: undecided, 4: agree, 5: strongly agree).
Analysis: As a result of the attained literature data, observations and questionnaires, an effort has been made to determine the effects of landscaping designs on housing prices and the residents' awareness of the relationship between landscaping designs and housing prices.

Results

A questionnaire has been conducted with a total of 67 households, namely 26 from Kuzeykent Akademi site and 41 from Siluet site. Household and socio-economic state have been demonstrated in the first chapter of the questionnaire. Generally, in the Kuzeykent Akademi Settlement; spouses work and they have two children. Most of the subjects work as public or private office holders. Their monthly salaries vary between TRY 3,500 and 8,000. Current sales price of a housing is between TRY240,000 to TRY250,000.
In the families resident in Olukbaşı Siluet settlement, mostly both spouses work and they have one child. They work in senior management in public or private sector, or are self-employed experts (doctor, architect, lawyer). Their monthly salaries vary between TRY5,000 and TRY10,000. Current sales price of a housing is TRY300,000-450,000. Kuzeykent akademi site consists of block-apartments and is 4 years old. There are 150 parking lots. In general, there are two or three rooms facing green areas. Olukbaşı Silüet site is a block-apartment site and 2 years old. There are 300 parking lots. There are generally four rooms facing green areas. 10 questions in the second chapter are about the physical environment perceived by the participants. The questions in the third chapter have been analyzed collectively for both sites.
In the perceived physical environment chapter of the questionnaire, 27 of 67 participants responded "agree" to the question that the traffic density is high. And 30 of them responded "agree" to the question that there are adequate green areas (Table 1).

Table 1. Perceived Physical Environment

	Strongly Agree	Agree	Undecided	Disagree	Strongly Disagree
Traffic intensity is high in your environment.	14.9%	40.3%	4.5%	31.3%	9%
Structural intensity is high in your environment.	25.3%	31.4%	11.9%	26.9%	4.5%
Air pollution exists in your environment.	9%	14.9%	6%	49.2%	20.9%
Green areas in your environment are adequate.	18.7%	52.1%	7.5%	18.7%	3%
Noise pollution exists in your environment.	6%	20.9%	6%	52.2%	14.9%

In positional characteristics chapter of the questionnaire, 62.7% of 67 participants have strongly agreed to the proposition that proximity to means of public transportation is significant. And 51% of participants have agreed to the proposition that proximity to green areas is significant.
Participants have mostly preferred the "strongly agree" answer for propositions regarding proximity to market places, means of public transportation, healthcare, and education facilities while preferring the "agree" answer for propositions regarding proximity to cultural facilities, green areas, recreational areas, and playgrounds (Table 2).

Table 2. Positional characteristics of sites

	Strongly Agree	Agree	Undecided	Disagree	Strongly Disagree
Proximity to market place is significant.	43%	39%	1.5%	14.9%	1.5%
Proximity to means of public transportation is significant.	68.7%	29.8%	-	1.5%	-
Proximity to education facilities is significant.	39%	39%	3%	16%	3%
Proximity to healthcare facilities is significant.	52.2%	37.3%	1.5%	9%	-
Proximity to cultural facilities is significant.	25.3%	37.3%	32.9%	1.5%	3%
Proximity to green areas is significant.	35.8%	53.7%	3%	7.5%	-
Proximity to parking areas is significant.	23.9%	52.2%	4.5%	11.9%	7.5%
Proximity to affirmative conditions such as sea, recreational areas is significant.	11.9%	39%	7.5%	25.3%	16.3%
Proximity to playgrounds is significant.	35.8%	47.8%	1.5%	11.9%	3%

In the question querying the willingness of participants to pay additional prices for houses for various landscaping works, the factors that positively affect the answers to the propositions and in which highest agree-strongly agree answers have been received are as follows (Table 3):

- proximity to areas with resting functions,
- availability of areas convenient for exercising,
- desire to live in an environment with children's park,
- view of the housing,
- proximity to socio-cultural areas,
- availability of activity areas for different age groups,
- abundance of not only visual but also useable green areas.

Participants have replied negatively to the proposition for converting green areas for different uses and have not supported this idea. Furthermore, they stated that they will move to places with more open-green areas when under economically more convenient conditions (Table 3).

Table 3. Level of Willingness to Pay for Landscaping Design Project

	Strongly Agree	Agree	Undecided	Disagree	Strongly Disagree
I am influenced by proximity to areas with resting functions (resting sites, tea gardens, restaurants, scenery terraces, etc.) when choosing a housing location.	39%	37.2%	6%	16.3%	1.5%
I am influenced by proximity to areas with cultural functions (open show areas, open exhibition and sales areas, etc.) when choosing a housing location.	26.9%	31.4%	16.3%	20.9%	4.5%
I am influenced by proximity to areas with recreational functions (playgrounds for age groups, adventure play areas, chess areas, waterworks parks, lightworks, skating parks, etc.) when choosing a housing location.	14.9%	40.3%	7.5%	31.3%	6%

I am influenced by proximity to areas with exercising functions (water sports, football, basketball, volleyball, tennis, etc.) when choosing a housing location.	35.8%	40.3%	6%	14.9%	3%
I am influenced by proximity to areas with natural functions (vegetation, greenhouse, water elements, etc.) when choosing a housing location.	19.4%	43.4%	16.3%	16.4%	4.5%
I am influenced by the view when choosing a housing location.	71.4%	28.6%	-	-	-
I am willing to pay more taxes to live in an environment with resting, exercising, and playground areas.	36.8%	32.8%	10%	12.9%	7.5%
I am willing to live farther away from my workplace to live in an environment with resting, exercising, and playground areas.	23.9%	37.3%	14.9%	19.4%	4.5%
I am willing to live farther away from shopping and cultural centers to live in an environment with resting, exercising, and playground areas.	29.8%	28.4%	11.9%	23.9%	6%
I am willing to pay more for my housing to live in an environment with solely visually valuable green area.	18%	35.8%	16.3%	23.9%	6%
I am willing to pay more taxes for my housing to live in an environment with solely visually valuable green areas.	16.4%	26.9%	14.9%	29.9%	11.9%
I want to live in an environment with more green areas when my level of income increases.	31.4%	52.2%	11.9%	3%	1.5%
Abundance of green areas in the environment increase the sales or rental value of my housing.	32,8%	41.9%	11.9%	11.9%	1.5%
I approve converting green areas for housing, commerce, etc. purposes.	1.5%	3%	6%	37.3%	52.2%
Sales or rental value of my housing would be much higher if green areas in the environment were used for housing, commerce, etc. purposes.	9%	24%	16.3%	35.8%	14.9%
I will allow for conversion of green areas for housing, commerce, etc. purposes if I will achieve higher profit.	-	14.9%	10.5%	38.8%	35.8%
If green areas in the environment are converted for other purposes, I will move to a place with more green areas.	32.8%	44.8%	14.9%	6%	1.5%

Discussion and Conclusions

Today, importance of green areas in terms of both environment and psychological and physical health of humans are known to everyone. When all urban models from past to present are analyzed, it is understood that green areas play an important role as much as other urban functional areas. The complicated aspect in this situation is assessing the real values of green areas and the components establishing such areas (vegetation, water bodies, etc.).

Önder and Akbulut (2011) has mentioned the difficulty of assessing the landscaping values of wood-like and herbaceous plants (planted or natural), which have many benefits such as carbon retention, soil conservation, climate conditioning, protecting biological diversity as shelters to other creatures, embellishing the view, etc., included in the city landscaping. As according to Kaya (2009), such plants have effects such as clearing the air, releasing oxygen, preventing erosion, and arousing delightfulness, which do not have a market and therefore, cannot be monetarily expressed and are regarded as environmental (natural) positive externalities in terms of economics (Özgüç Erdönmez, 2009; Bekiroğlu, 2008).

Challenges faced in determining the importance and values of green areas, when regarded as a kind of environmental externality, have been the main starting point of the study. Within this scope, an effort has been made to determine the economic values of green areas which are difficult to assess, based on their roles in housing prices.

The purpose of the study has been to analyze the changes of housing prices caused by urban environmental quality and visual landscaping value, and whether users will tolerate the cost of benefits to be gained from a qualified environment within the scope of Kuzeykent-Olukbaşı settlement sample.

In the study, initially theoretical data has been analyzed, and then environmental analyses have been conducted on the research area and reflected on the questionnaire, the results of which have been used. As a result of all findings, it can be safely said that the importance attached within the sample area to urban green

areas is undeniable and increases the housing prices. It has been shown with the study that green areas, tending to increase the level of environmental welfare, are also influential in the housing market. The most important finding attained in the study is that urban green areas have an assessable effect. However, urban green areas with different characteristics have different levels of effectiveness on the prices of surrounding housings. This indicates that people now take into consideration not only structural properties, but also location and environmental characteristics of the housing when purchasing a house. Therefore, two housings with the same interior features but different environmental factors hold different values. In this case, it can be said that prices of housings with environmental design, social facilities, locations close to urban green areas positively increase. In other words, this supports the hypothesis that "Green areas have an increasing effect on housing prices", which constitutes the essential subject of this study.

Acknowledgements

We thank Aleyna Yılmaz, of the 2016-2017 Academic Year graduates of Kastamonu University Department of Landscape Architecture, for the support in the field work.

References

Alaca, T. (2010). Kentsel yeşil alanların konut değerine etkisi üzerine bir araştırma: İstanbul Bahçeşehir toplukonut yerleşkesi örneği. İ.Ü. Institute of Science Master's Thesis. İstanbul.

Gül, A., Küçük, V. (2001). Kentsel açık-yeşil alanlar ve Isparta kenti örneğinde irdelenmesi. Orman Fakültesi Dergisi, 2(3), 6-9.

İbret, B. Ü., Aydınözü, D. (2009). A sample for the effect of the wrong settlement choıce ın urbanızatıon on aır pollutıon: the center of Kastamonu. İ.Ü. Faculty of Literature Department of Geography Coğrafya Dergisi, 18, 71-88.
Erdönmez İ.M.(2009). Doğal ve kültürel kaynakların peyzaj planlama açısından değerlendirilmesinde bir yöntem yaklaşımı: Fatih ormanı (İstanbul) örneği. Bartın University Orman Fakültesi Dergisi, cilt.1.

Kaya, L. G. (2009). Assessing forests and lands with carbon storage and sequestration amount by trees in the State of Delaware, USA. Scientific research and essays 4(10):1100-1108.

Luttik, J. (2000). The value of trees, water and open space as reflected by house prices in netherlands, Alterra, green world research. Landscape and Urban Planning, 48, 161-167.

Önder, S., Akbulut, Ç D. (2011). Kentsel açık-yeşil alanlarda kullanılan bitki materyalinin değerlendirilmesi: Aksaray kenti örneği. Selçuk University Selçuk Tarım ve Gıda Bilimleri Dergisi 25 (2): 93-100 ISSN:1309-0550.

Özgüç Erdönmez, İ. M., Bekiroğlu, S. (2008). Kartal Belediyesi sınırları içinde izinsiz kesilen ağaçların görsel değerlerinin hesaplanması hakkında rapor. İ. Ü. Orman Fakültesi. İstanbul.

Öztürk, S., Özdemir, Z. (2013). Kentsel açık ve yeşil alanların yaşam kalitesine etkisi: Kastamonu örneği. Kastamonu University Orman Fakültesi Dergisi 13 (1): 109-116.

Öztürk, S., Bozdoğan, E. (2014). Determination of the perceived quality of urban life in new and traditional housing textures, Fresenius Environmental Bulletin, Vol. 23 – No 10, 2415-2421.

Şen, G., Güngör, E., Şevik, H. (2018). Defining the effects of urban expansion on land use/cover change: a case study in Kastamonu, Turkey. Environmental Monitoring and Assessment 190 (454), DOI:10.1007/s10661-018-6831-z

TÜİK. (2015). Türkiye İstatistik Kurumu. http://www.tuik.gov.tr/Start.do (Erişim Tarihi: 10.08.2017).

International Conference on ScienceandTechnology

ICONST 2018

5-9 September 2018 Prizren - KOSOVO

Casein Based Green Multifunctional Composite Cotton Fabric

Mevlüde Bilgiç[1]*, Şule Sultan Uğur[2]

Abstract: The objectives of this research are as follows: to develop new green nano finishing treatment with casein for cotton fabrics. The effect of different casein add-ons (namely 1, 5, 10 wt. %) has been thoroughly investigated. The finishing treatment should have high tensile strength, flame resistance, environmentally-friend, low add-on levels and cost effectiveness. Tensile tests, flame retardancy and air permeability were used to investigate the effects of the treatment. The fabric surfaces were also observed by Scanning Electron Microscopy (SEM) and Fourier Transform Infrared Spectroscopy (FTIR). According to the all test results, it can be concluded that casein is a green excellent agent for improving the tensile strength and flame retardancy properties of cotton fabrics.

Keywords: Caseins, Nanocomposite cotton, Ecofriendly, Flame retardancy, Tensile Strength

Introduction

Nowadays, significant scientific efforts focus on nanotechnology and green material. Caseins which contain phosphorus elements have presented a great potentiality as flame retardant systems for cellulosic substrates like cotton fabrics (Alongi et al., 2013). Casein is the major protein component of milk, which is composed of C (52.96%), H (7.13%), O (22.47%), N (15.60%), P (0.86%) and S (0.78%) (Macej et al., 2002). Also despite of the other flame retardants caseins have acceptable costs, meeting the current health, safety and environmental issues. Multilayer films created by electrostatic self-assembly (ESA) or layer by layer (LBL) deposition are currently used to modify the surface properties of materials used in various fields of science. In this study we have been investigated the possibility of caseins film deposition on cotton fabrics via LBL deposition.

Material and Method

The fabric was supplied by the Çalık Denim, Turkey. The characteristic of the cotton fabric was as follows: woven, 294 g/m², warp and weft yarns density 27 and 21 threads per cm, respectively. Casein was purchased from Fluka. Poly(sodium 4-styrene sulfonate) (PSS, Mw=70.000) and poly(diallyldimethylammonium chloride) (PDDA, Mw=100,000-200,000) were purchased from Sigma-Aldrich.The fabric samples were washed by nonionic washing agents with laboratory type washing machine at 30 °C for 1 hour and then dried in air. For cationic surface charge, cotton fabric was pretreated with 2,3-epoxypropyltrimethylammonuium chloride (EP3MAC) by pad-batch method. The caseins powder (1, 5, 10 wt %) was dispersed in distilled water under mechanical stirring (300 rpm) and heated at 60 °C and pH was adjusted to 10 by using HCl. The receipts that used were shown in Table 1. For the Casein/PDDA multilayer film deposition process, the positively charged cotton fabrics were applied in the following solutions alternately for 5 min periods: the anionic casein solution, the deionized water, the cationic PDDA solution and the deionized water. 40 layer of Casein/PDDA

[1]Suleyman Demirel University, Faculty of Engineering, 32260, Isparta, TURKEY
[2]Suleyman Demirel University, Faculty of Engineering, 32260, Isparta, TURKEY
*Correspondingauthor: mevludeakkaya@gmail.com

multilayer films were deposited on the cotton fabrics by dip coating method. For the (PSS/PDDA) + Casein multilayer film deposition process, the positively charged cotton fabrics were applied in the following solutions alternately for 5 min periods: the anionic PSS solution, the deionized water, the cationic PDDA solution and the deionized water. After 40 PSS/PDDA multilayer films were deposited on the cotton fabrics by dip coating method, cotton fabrics were dipped in the casein suspension (1, 5, 10 wt %) for 5 min. After process fabrics were at 100 °C for 6 minutes and cured at 130 °C for 5 minutes. A QUANTA 400F scanning electron microscope (SEM) was used to examine the surfaces of fabrics at an acceleration voltage of 5kV to investigate the chemical structure of samples. The spectroscopic analyses of the samples were performed on KBr disks by using an FTIR instrument (Perkin Elmer Spectrum BX model). The same amount of fabric was cut into small pieces and mixed in KBr to prepare the KBr disks. The number of scans was 16 and the resolution was 4 cm^{-1} during the analysis. Flame retardant properties of the fabrics were determined according to ASTM D1230-94 ("Standard Test Method for Flammability of Apparel Textiles", reapproved in 2001) by using a 45° flammability tester BV AFC Auto test instrument. Untreated and treated fabric samples mounted in a spicemen holder were brushed, dried at 105 °C for 30 min, cooled down in a desicator containing a drying agent for 90 min and then moved to the 45° flammability tester with the spicemen positioning at an angle of 45°. The spicemen was exposed to a standard butane flame for 3 s to cause ignition and combustion, then the burning time and burning characteristics were recorded. The arithmetic mean burning time of 5 specimens and the burning characteristics were used as the basis to determine the flammability classifications. The mechanical tests were performed on a Lloyd LR5K Plus electronic tensile strength machine according to TS EN ISO 13934-1 (Textiles- Tensile properties of fabrics- Part 1: Determination of maximum force and elongation at maximum force using the strip method) Standard. Fabrics were kept for 24 h at ambient conditions (20 ºC and 65 % RH) before the mechanical test. Textest FX 3300 Air Permeability Tester was used to measure air permeability of fabrics according to TS EN ISO 9237 (1995) test method. Ten tests were done on each fabric at the same air pressure (100 Pa) and the average value was calculated.

Table1. Receipt contents of finishing solutions (%w/w)

ID	Receipt	Concentration	Temperature and Layer number
1	$(PSS+PDDA)_{40}$+Casein	5 g/l PSS, 5 g/l PDDA, 1 g/l C	60 ºC, 40 layer
2	$PSS+PDDA)_{40}$+Casein	5 g/l PSS, 5 g/l PDDA, 5 g/l C	60 ºC, 40 layer
3	$PSS+PDDA)_{40}$+Casein	5 g/l PSS, 5 g/l PDDA, 10 g/l C	60 ºC, 40 layer
4	$(Casein /PDDA)_{40}$	1 g/l C, 5 g/l PDDA	60 ºC, 40 layer
5	$(Casein /PDDA)_{40}$	5 g/l C, 5 g/l PDDA	60 ºC, 40 layer
6	$(Casein /PDDA)_{40}$	10 g/l C, 5 g/l PDDA	60 ºC, 40 layer

Results

Untreated and treated fabric tensile strength and flame retardancy tests were performed. The tensile strength test and flame retardancy test results clearly demonstrate that casein with the increase in high amounts leads to high values. The presence of casein in the fabric after treatment is verified with SEM analysis. SEM

investigates the changes in the surface the presence of casein on fabrics after finishing treatment is verified with SEM analysis. Figure 1 illustrates the SEM images of raw cotton fabric, receipt 1, 2, 3, 4, 5, 6. Well-defined contour lines of scale edge can be seen on the surface of the untreated cotton fibers clearly for the both fabric. SEM investigates the changes in the surface of the treated fabrics compared with untreated ones. It is clearly seen that the casein deposited on the surface of the fabrics. The surface of the treated cotton fibers was coated with a film layer and scales of cotton fibers were covered, blunt obviously.

Untreated cotton fabric

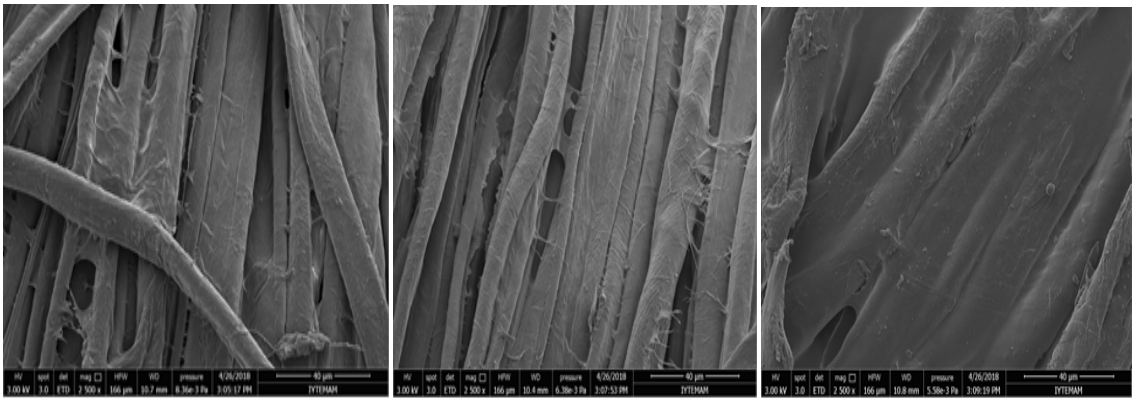

1 2 3

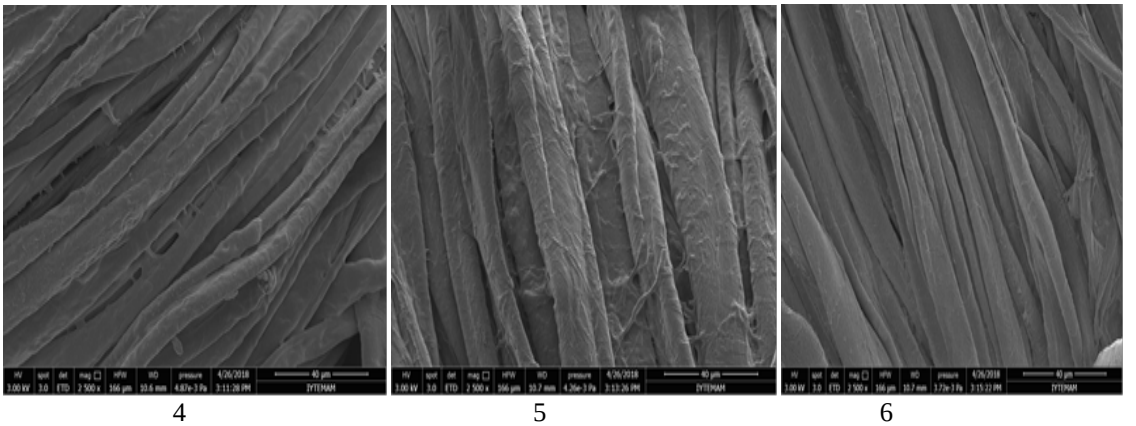

4 5 6

Figure 1. SEM images of fabric

The FTIR spectra of untreated cotton fabric and cotton fabric treated with receipt 4, 12, 17 and 25 are shown in Figure 2. For all samples a broad band between 3100-3700 cm^{-1} centered around 3360 cm^{-1} illustrated

characteristics of OH functional groups in cellulose. A strong adsorption band with a maximum at 1030 cm^{-1} is a result of the overlapping bands attributed to the functional groups of cellulose, namely the C-C, C-O and C-O-C stretching vibrations (Uğur et al., 2010). As shown in Figure 2, caseins band occur in the 1635 and 1510 cm^{-1} to amide I and amide II vibrational modes, typical of proteins (Socrates 2004, Carosio et al., 2014).

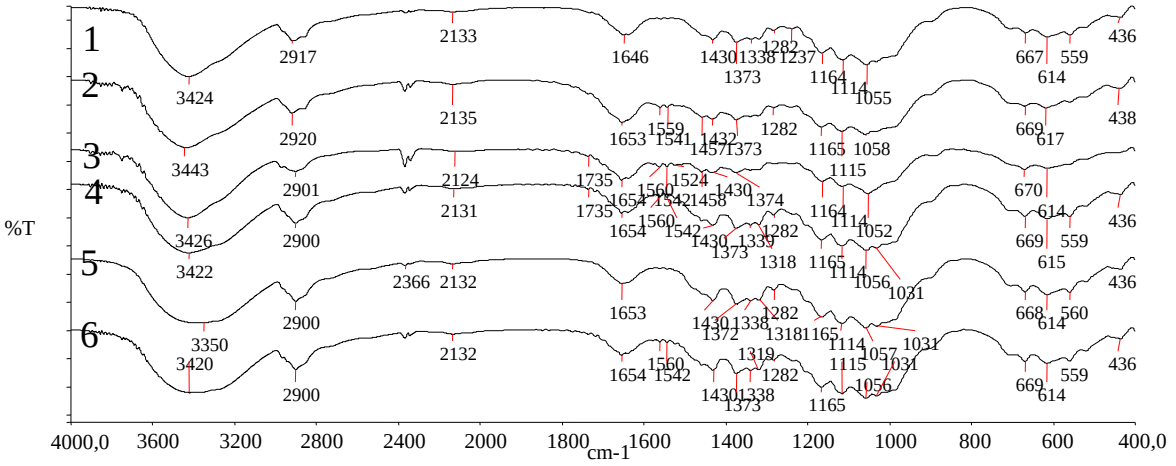

Figure 2. FTIR spectra of fabrics

To determine flame retardant properties of samples, the flame is applied to the fabrics for 8 seconds for raw fabric and cationized fabric and 15 seconds for treated samples. We record that untreated % 100 cotton fabric was burned in 56.3 seconds and cationized cotton fabric was burned 58.6 seconds. It is seen that after LBL treatment with casein, the average burning time has nearly doubled in some cases.

Table 2. Flame retardant test results of fabrics after LBL process

	Concentration	**Temp. and layer nmb**	**Avarage time to ignition (s)**	**Avarage burning time (s)**	**% change**
Raw fabric	**-**	**-**	8	56.3	**-**
Cationized fabric	**-**	**-**	8	58.6	**-**
$(PSS+PDDA)_{40}$+Casein	5 g/lt,5 g/lt,1 g/lt	60 ºC, 40 layer	15	63.45	12,7
$(PSS+PDDA)_{40}$+Casein	5 g/lt,5 g/lt,5 g/lt	60 ºC, 40 layer	15	62.9	11,7
$(PSS+PDDA)_{40}$+Casein	5 g/lt,5 g/lt,10 g/lt	60 ºC, 40 layer	15	72	27,9
$(Casein /PDDA)_{40}$	1 g/l, 5 g/l	60 ºC, 40 layer	15	66	17,2
$(Casein /PDDA)_{40}$	5 g/l, 5 g/l	60 ºC, 40 layer	15	88.7	57,5
$(Casein /PDDA)_{40}$	10 g/l, 5 g/l	60 ºC, 40 layer	20	102.3	81,7

Fabrics were kept for 24 h at ambient conditions (20 °C and 65 % RH) before the tensile test. Tensile strengths of fabric samples are shown in Table 3. It is observed that if casein amount is increased, tensile strength both warp and weft direction will increase.

Table 3. Tensile strength results

Receipt	Tensile strength (weft direction)		Tensile strength (warp direction)	
	N	% change	N	% change
Raw fabric	806,5	-	966,25	-
Cationized fabric	807,4	0,11	970,21	0,4
1	808,8	0,29	969,37	2,4
2	810,7	0,52	1001,76	3,7
3	810,9	0,55	1007,7	4,3
4	806,8	0,04	1031,84	6,8
5	808,4	0,24	1039,4	7,6
6	811,6	0,63	1056,24	9,3

Air permeability is a test of how well fabric allows air passage through the fabric. As it is seen in Table 4, untreated fabrics have higher air permeability, compared to the fabrics treated with casein. As known, LBL deposition process reduce the air permeability of the fabric by filling the space between warp and weft yarn of the fabrics.

Table 4. Air permeability values of the fabrics

Receipt	Air permeability values	
	(l/m²/s)	% change
Raw fabric	35.68	
Cationized fabric	31.08	-12,9
1	25.48	-28,6
2	24.78	-30,5
3	23.46	-34,2
4	22.64	-36,5
5	21.27	-40,4
6	19.25	-46

Discussion and Conclusions

During this investigation, caseins from bovine milk have been deposited on cotton fabric by layer by layer deposition process. SEM analyses were displayed to examine the nanocomposite multilayer films on cotton fibers. Mechanical tests showed that there is a linear relationship between the deposited of casein amount and layers. Using casein in finishing solutions, flammability properties and tensile strength values were increased. The experimental results showed that casein may have efficient green material for textile finishing applications.

Acknowledgements

This research work has been supported by research grants from SüleymanDemirel University Scientific Research Project 3669-D2-13.

References

Alongi, J., Carletto, R. A., Bosco, F., Carosio, F., Di Blasio, A., Antonucci, V., et al. (2013), Caseins and hydrophobins as novel green flame retardants for cotton fabrics.

Alongi, J., Carletto, R. A., Di Blasio, A., Cuttica, F., Carosio, F., Bosco, F., and Malucelli, G. (2013), Intrinsic intumescent-like flame retardant properties of DNA-treated cotton fabrics, Carbohydrate Polymers, 296-304.

Carosio, F., Di Blasio, A., Cuttica, F., Alongi, J., Malucelli, G. (2014) Flame Retardancy of Polyester and polyester-cotton blens treated with caseins, Industrial & Engineering Chemistry Research, 3917-3923.

Macej, O. D., Jovanovıc, S. T., Denindjurdjevic, J. D. (2002). The influence of high temperatures on milk proteins, 123-130.

Socrates, G. (2004) Infrared and raman characteristic group frequencies: Tables and Charts, Oxford, U.K.

Uğur Ş.S., Sarıışık M., Aktaş A.H., Uçar M.Ç., Erden E. (2010). Modifying of cotton fabric surface with nano-ZnO multilayer films by Layer-by-Layer deposition method, Nanoscale Research Letters, 1204–1210.

International Conference on Science and Technology

ICONST 2018

5-9 September 2018 Prizren - KOSOVO

Evaluating The Work Environment in Turkish Furniture Industry From The Point Of Occupational Health And Safety[3]

Devrim Karademir[1]*, Küçük Hüseyin KOÇ[2]

Abstract: Preparing a healthy and safe working environment for the employee is an important issue for enterprises. Especially for SMEs, This issue is an important obstacle in our country. Small businesses often ignore this problem because of not having sufficient knowledge of the subject or, financial inadequacies. Legal sanctions and audits cannot be fully implemented due to the lack of physical and financial structures despite the legal infrastructure. The work environments of SMEs in the furniture sector were examined in this study. Thermal comfort (temperature, humidity, and air flow velocity), noise and ambient lighting parameters were investigated in 255 enterprises. In addition, wood dust parameter was studied in 40 enterprises. When the data obtained are examined; It is seen that about 60% of the enterprises were below the ideal temperature, 30% were airless and 40% were so draughty. From the point of wood dust parameter, wood dust exposure of the work environment is above the limit value of 5 mg/m3 at 90% of enterprises. It is observed that the limit value of 5 mg/m3 is doubled at the 35% of these enterprises, tripled at the 40% of them and quadrupled at the 15% of them. The results obtained in this study have been examined in detail and suggestions have been tried to develop for the sector enterprises, chambers, and governments.

Keywords: Work environment, Occupational health and safety, Turkey Furniture Industry, Occupational accident and occupational diseases, EU Legislation.

Introduction

One of the most important problems faced by enterprises is that employees do not have a safety and healthy work environment. This subject, is a major problem, especially in small and medium-sized enterprises (SMEs), which is not adequately emphasized, ignored with concern bringing the financial burden, or arising from the ignorance of employers and employees. This problem can be a serious problem on an enterprise basis as well as on sectoral basis or also on a country basis. Enterprises in conjunction with governments, unions, trade associations and bodies, are required to carry out comprehensive and planned work for employees' occupational health and safety.

The Law on Occupational Health and Safety No. 6331, which regulates the working life in our country, was adopted in 2012 and the enforcement of the laws, especially those related to SMEs, entered into force in 2014. According to the risks they bear, the law is divided enterprises into three groups: low hazardous, hazardous and high hazardous. Therefore, All enterprises have to perform a risk assessment and determine which group they are involved in. It is stated in the "Occupational Health and Safety Risk Assessment Directive" how to conduct a risk assessment of the enterprises. The problem at this point, it should be needed how to, what to or when enterprises to make these assessments, should not be adequately informed about the content and cost of risk assessments and what to expect if not done.

[1]Ordu University, Social Sciences Vocational School, 52200, Ordu, TURKEY
[2]Istanbul University-Cerrahpasa, Faculty of Forestry, Department of Forest Industry Engineering, 34473, Istanbul, TURKEY
*Corresponding author: dkarademir@yandex.com
[3] This study has been prepared using data obtained from a part of the doctoral thesis which called "European Union Harmonisation With Small And Medium-Sized Enterprises Of The Turkish Furniture Industry" prepared by Devrim Karademir.

The enterprises in the furniture sector are in the dangerous and very dangerous categories. Processes such as chipping, drilling, cutting, assembly are evaluated in the hazardous class, while painting and varnishing processes are considered as high hazardous.

When the statistics of SSI's occupational accidents and occupational diseases are examined; 1360 employees lost their lives due to 191389 work accidents and 371 occupational diseases in 2013, 1626 employees lost their lives due to 221366 work accident and 494 occupational diseases in 2014, 1252 employees lost their lives due to 241547 work accidents and 510 occupational diseases in 2015 and 1405 employees lost their lives due to 286068 work accidents and 597 occupational diseases in 2016 (SSI:2013, 2014, 2015, 2016). When the data for the next 4 years after the implementation of the law were examined, it was observed that the number of work accidents and occupational diseases increased 1.5 times and there was no decreasing tendency in the number of the death.

According to TURKSTAT 2016 data, a total of 2,677,316 enterprises are operating in our country and 2,672,458 of them are defined as SMEs. Within the total number of enterprises, the rate of SMEs was 99.8% whereas the employment rate they created was 73.5%. As the classification of SMEs in TURKSTAT data is different, the ratio of micro, small and medium-sized enterprises aren't shown separately. The ratio of micro-scale in SMEs was determined as 97.5% (TurkStat, 2016a)

According to TURKSTAT 2016 data in furniture sector, the number of enterprises is 33.859 and the number of employees is 187.189 (TurkStat, 2016b). The number of employees in the furniture sector is thought to be over 300,000 with employees in the retail sector and other subsidiary sectors. When evaluated from the point of employment, the furniture sector has a share of approximately 10% of the manufacturing industry and 2% of the total employment (Karademir ve Koç, 2016).

Works done in the furniture sector are described as standing and heavy works. The machines and tools used during these works such as cutters, trimmers, thinners, saws and knives are risky, and so they are needed to be used carefully. Therefore, it is needed that workers in the furniture sector cannot lose their attention while using these machines and tools. Workers may also be exposed to wood dust, during the process as cutting, forming, chipping, sanding. A potential loss of attention can cause to fatal or injured accidents, or exposure to persistent wood dust can lead to a variety of occupational diseases.

This study was carried out in order to examine the working environments of the SMEs in the furniture sector, especially at small-scale enterprises, to reveal the situation and to assess the current situation in terms of occupational health and safety.

Material and Methods

In this study, thermal comfort (temperature, humidity, air flow rate), noise, ambient lighting and wood dust parameters are taken into account while the work environment is handled in the enterprises. "Extech EN300 Noise, Light, Temperature, Humidity and Air Velocity Meter" was used to measure these parameters. 255 enterprises were visited separately for parameter measurements, and in order to guarantee the homogeneity and reliability of the measurements, it was studied for 10 minutes standard time with Extech EN300 device for each parameter. "Side Pak Personal Aerosol Monitor Model AM510" device was used for the wood dust parameter. It was made the measurement at 40 enterprises, and the minimum, maximum and average values were recorded with an hour measurement for each enterprise. In the measurements, 500 different data were collected periodically in each enterprise.

In order to determine the research population, the table developed by Yazıcıoğlu and Erdoğan (2004) was used, and a sampling population of 25,000 was used as the basis for a sampling error of 0.05. Due to the difficulty in measuring wood dust exposure, the study was limited to 40 enterprises in the Ankara region.

89% of the enterprises visited for the implementation are micro-scale enterprises with 1-9 employees and 11% of them are small-scale enterprises with 10-49 employees.

Microsoft Office Excel and SPSS programs were used to evaluate the obtained data. Application development and editing in the Excel program, relationship analysis and reliability tests in the SPSS program were made. The results obtained were passed through the significance analysis, and then the providing sufficient consistency results were evaluated.

Results

Ambient Air Conditions at Workplaces

When the works done in the furniture sector are examined, it is seen that there are heavy works which are generally standing. It is seen for these works that in Table 1, the ambient temperature should be 17 °C, the humidity 50% and the air flow rate should be 0.2-0.4 m/s.

Table 1. Weather conditions required to provide at workplaces (Hayta, 2007).

Work Type	Temperature (°C)			Humidity (%Rh)			Air Flow (m/s)
	Least	**Optimal**	**Most**	**Least**	**Optimal**	**Most**	
Office works	18	21	24	30	50	70	0,1
Sedentary works	18	20	24	30	50	70	0,1
Standing works	17	18	22	30	50	70	0,2
Heavy works	15	17	21	30	50	70	0,4

Measurements at workplaces visited for implementation were conducted between November to February. In Figure 1, Figure 2 and Figure 3, the red line shows the minimum and maximum weather conditions and the green line shows ideal weather conditions. In Figure 1, It is shown that the lowest ambient temperature at workplaces is 7.2 ° C and the highest ambient temperature is 21.4 ° C. It was observed that about 60% of the workplaces were below the ideal temperature value and 40% were below the acceptable values.

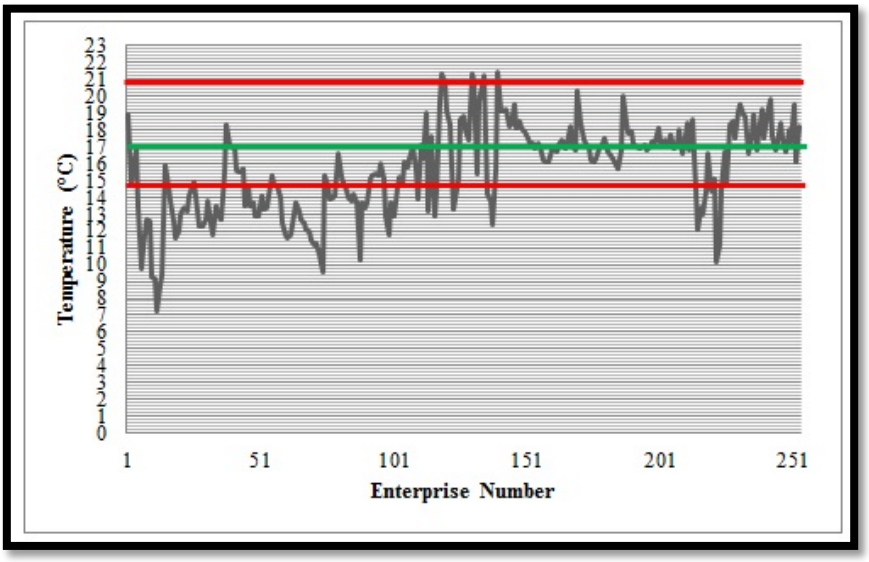

Figure 1. Ambient Temperature (Karademir, 2014)

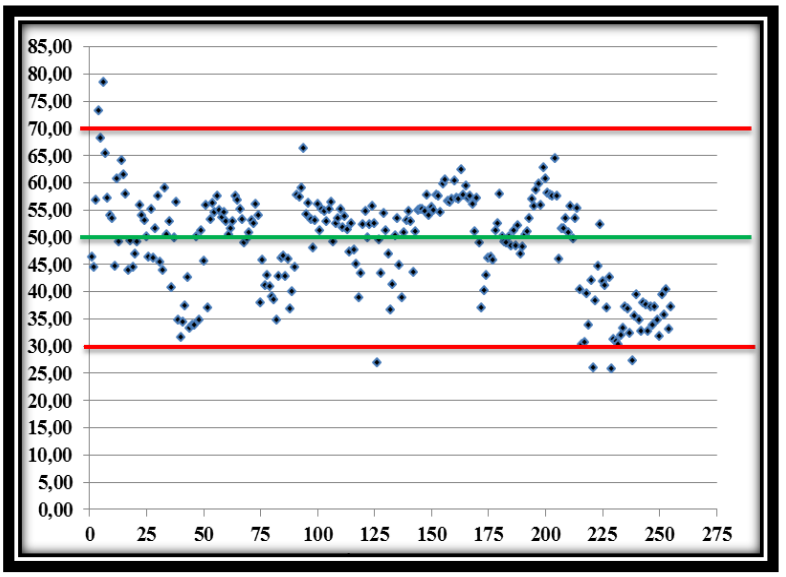

Figure 2. Ambient Humidity (Karademir, 2014)

Ambient humidity values in workplaces are shown in Figure 2. It is seen that the values in ambient humidity range between 25.8% and 78.4%. It is observed that ambient humidity is below 50% in 50% of the workplaces and 98% is in acceptable values.

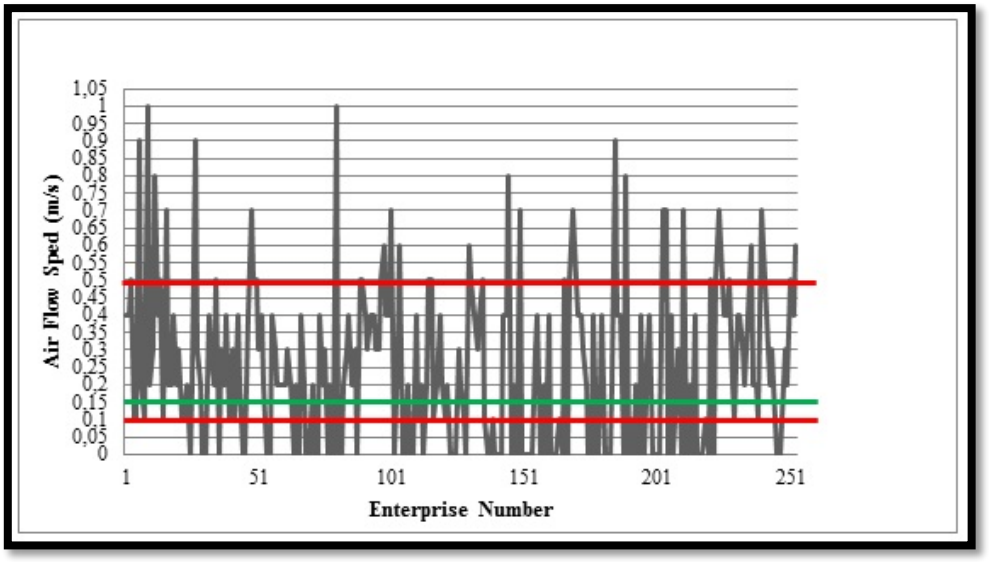

Figure 3. Ambient Air Flow Speed (Karademir, 2014)

Figure 3 shows the change in air flow velocities in workplaces. From the figure, It is observed that the average air flow rates in the workplaces vary between 0 m/s and 1 m/s. It is seen that the air circulation rate is close to the ideal values in 25% of the enterprises.

When the data obtained from the research is examined; in an approximately 60% of the enterprises the ambient temperature is seen to be below the ideal temperature. The working environment is airless at 30% of enterprises and is so draughty at 40% of enterprises. It was seen to be among the proposed limits of only humidity findings in the study.

Ambient Lighting Conditions at Workplaces

The change of an amount of ambient lighting in the workplaces is shown in Figure 4. It is seen in the figure that approximately 70% of the ambient lighting of enterprises have less than 200 lux and 95% have less than 400 lux (Karademir, 2014). According to the relevant regulation, it is needed that 100 lux is required for coarse assembly, 200 lux for normal assembly, 300 lux for the works where detail is in the foreground and 500 lux for the delicate works requiring continuous attention (O.J., 2013).

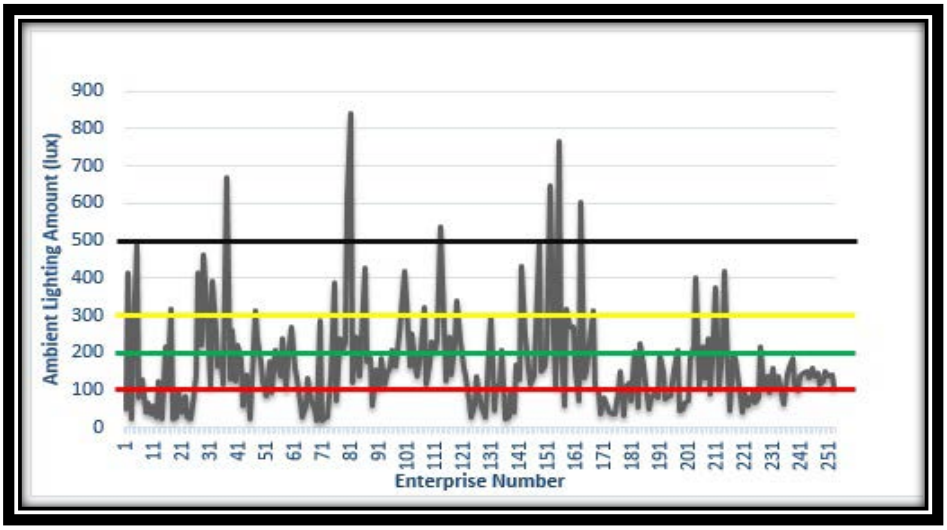

Figure 4. Ambient Lighting Amount (Karademir, 2014)

Lighting is also important in increasing the efficiency of the furniture industry and the amount of light required in the production varies between 100-500 lux. For example, it is required that 400 luxury in the coating of large surfaces and the construction process, 500 luxury in the process of a polishing, varnishing and varnish sanding,400 luxury in the assembly process or 500 luxury lighting in quality control operations is required (Kurtoglu and Dilik, 2013). Ambient lighting is under 300 lux at approximately 80% of the enterprises and is also under 500 lux at 95% of the enterprises.

Ambient Noise Conditions at Workplaces

According to the related articles of the regulation, the daily noise exposure limit values were determined as 85 dB for the 8-hour studies and 87 dB for the weekly noise exposure level (O.J., 2013b). Figure 5 shows that the average noise exposure values at workplaces are 85 dB and less in only a few enterprises. The red thick line in the figure is shown the desired maximum noise exposure value indicated.

Table 2 is shown the hearing loss depending on the noise level. It is determined in research conducted that no loss of hearing is observed in the exposure values of 80 dB or less, and a 55% hearing loss is observed at the end of 10 years in an exposure value of 110 dB (Hayta, 2007).

Table 2. Hearing Loss Percentages Depending on Noise Level (Hayta, 2007)

Noise Level (dB)	Hearing Loss Percentages (%)		
	5 Year	10 Year	20 Year
80	0	0	0
90	4	10	16
100	12	29	42
110	26	55	78

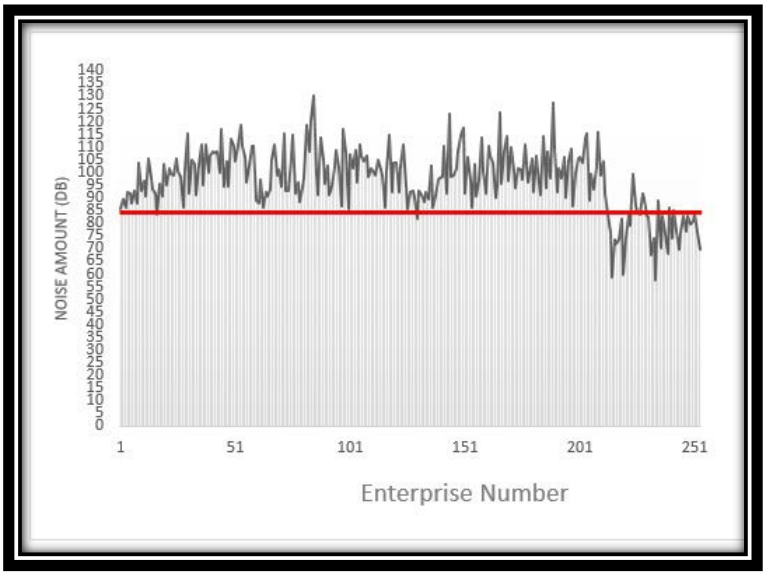

Figure 5. Ambient Noise Amount (Karademir, 2014)

"According to research by WHO and ILO, the effects of various levels of noise are:

- No disturbance between 0-30 dB
- 30-60 dB psychological,
- 60-80 dB psychological and physiological,
- 85-125 dB psychological, physiological and otological disorders are classified as noise levels." (Ekiz, 2009).

It is seen that only about 15% of the enterprises have 85 dB level, about 50% have over 100 dB, and about 25% have over 110 dB. The maximum noise exposure is over 85 dB at almost entire enterprises.

Conditions for Wood Dust Exposure at Workplaces

The most important factors of occupational diseases are dust, gas and toxic substances. Dust and gas are the most important factors for also the furniture sector. Wood dust can cause respiratory diseases, allergic effects, cancer, and many lung diseases. It is exposed to dust more intensively in the furniture sector, especially in the jobs where machines such as sanding, thickness, planing, sawdust, drawing, milling, dust collecting units are used (Karademir and Koç, 2016).

According to the Dust Occupational Exposure Limit Values Table attached to the relevant regulation, the amount of respirable wood powder is given as 5 mg / m^3 in 8 hour periods (O. J., 2013c). It is seen in Figure 6 that the maximum values measured in the one hour periods in the analyzed enterprises exceed the limit of 5 mg / m3 which is in the regulation and based on the EU directive.

From the point of wood dust parameter, wood dust exposure of the work environment is above the limit value of 5 mg/m^3 at 90% of enterprises. The limit value of 5 mg/m^3 is doubled at the 35% of these enterprises, tripled at the 40% of them and quadrupled at the 15% of them.

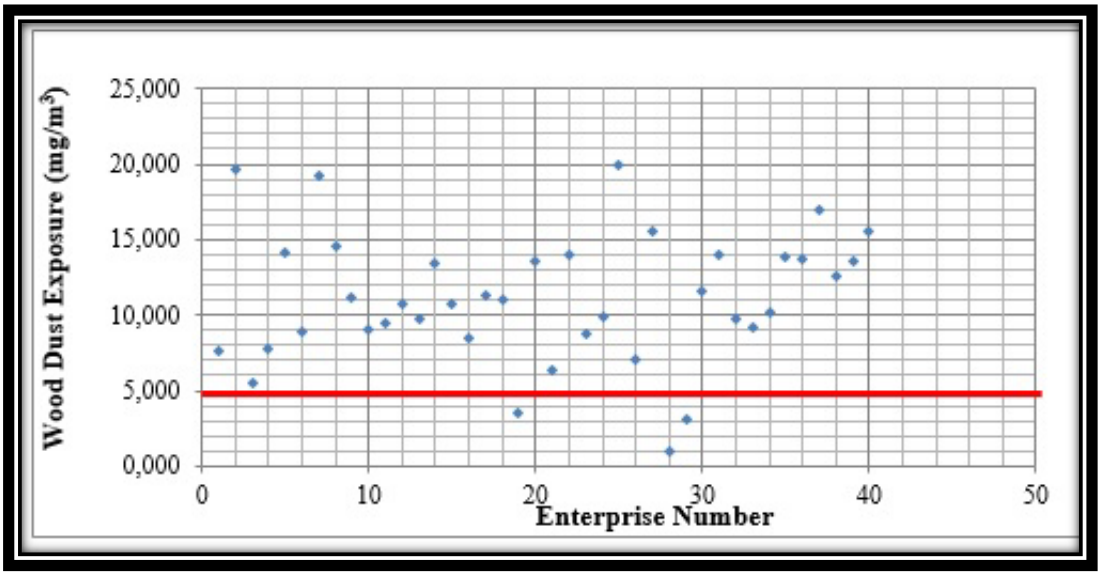

Figure 6. Ambient Wood Dust Level (Karademir, 2014)

Discussion and Conclusion

Approximately 60% of enterprises have an ambient temperature below the ideal temperature. It was determined that only moisture findings are within the recommended limit values. The working environment is airless in 30% of the enterprises and is so draughty in excess of 40%. Ambient lighting; approximately 95% of the enterprises are below 500 lux. The maximum noise exposure near the end of the enterprises is over 85 dB. Wood dust exposure at workplaces is above the limit value of 5 mg / m^3 in 90% of enterprises.

It is seen that the enterprises in the furniture sector - especially SMEs - cannot comply with the Technical Regulations and EU directives in terms of many parameters. Many structural improvements are needed in terms of national and international competitiveness of sector enterprises. The relevant legal regulations have been completed to a large extent. The main problem is in the stage of implementation and supervision of these improvements. At this point, the state and professional organizations should be role models and the enterprises should be encouraged, supported and audited in terms of technical adaptation. Preparing and implementing compliance projects at various scales will accelerate compliance with EU technical legislation.

When the research results were analyzed, the work environment of SMEs in Turkey Furniture sector, especially the small-scale enterprises, have been seen to threaten the health of employees. Air quality and lighting are very insufficient in the enterprises' work environment. The environment is excessively loud or dusty. Insufficiently lightning or poor quality air can affect the health of employees and can also cause loss of their attention. Due to these attention losses, injuries or deaths may occur. Furthermore, an extremely loud or dusty environment can cause a variety of illnesses for employees. Especially wood dust is known to be carcinogenic.

Therefore, it is necessary that primarily the governments will be rapidly complete the infrastructure works, move the enterprises to the prepared areas and provide financial support for enterprises to improve the work environment. It should be ensured that the enterprises that make production between the local neighborhoods should be moved quickly to small and organized industrial zones. When choosing a location in small and organized industrial zones, attention should be paid to the climate and terrain characteristics and harmony of the region. Later, the governments in conjunction with professional bodies have to inform enterprises about the occupational health and safety and arrange training in the enterprises. After these studies are completed, enterprises should be checked permanently according to the relevant legislation.

Acknowledgement: For this study, I would like to thank Istanbul University Institute of Science.

References

Ekiz, N., (2009). OHS Conditions in the furniture sector in Turkey, Problems and Proposed Solutions (ISGUM Adana-Kayseri, Izmir, Kocaeli Laboratories Study Results), Kayseri.

Hayta, A.B., (2007). Effect of Working Environment Conditions on Operational Efficiency. Journal of the Faculty of Commerce and Tourism Education 2007/1.

Karademir, D. (2014). European Union Harmonisation with Small and Medium-Sized Enterprises of the Turkish Furniture Industry. Unpublished Ph.D. Thesis, I. U. Institute of Science and Technology, Istanbul.

Karademir, D. and Koç, K.H. (2016). The Expected Physical Environmental Problems of The Turkey's Furniture Enterprises in the EU Process, Selcuk University Technical Online Journal, Special Issue-2 (NFC-2015),1205-1218, ISSN: 1302-6178.

Kurtoğlu, A., Dilik, T., (2013). Furniture Industry Unpublished Course Notes. I.U. Faculty of Forestry, Forest Industry Engineering Department, Istanbul.

O. J. (2013a). Regulation on Health and Safety Measures to be Taken in Workplace Buildings and Additions. Turkish Republic Prime Ministry Legislation Development and Publication General Directorate, Official Journal, dated 17.07.2013 and numbered 28710, www.resmigazete.gov.tr/eskiler/2013/07/20130717.pdf, [Access Date: 15.06.2018].

O. J., (2013b). Regulation on Protection of Employees from Noise-Related Risks, Republic of Turkey Prime Ministry Legislation Development and Publication, Official Journal dated 28.07.2013 and numbered 28721, www.resmigazete.gov.tr/eskiler/2013/07/20130728.pdf, [Access Date: 15.06.2018].

O. J., (2013c). Dust Control Regulation. Republic of Turkey Prime Ministry General Directorate of Legislation Development and Publication, Official Journal dated 5.11.2013 and numbered 28812, www.resmigazete.gov.tr/eskiler/2013/11/20131105.pdf [Access Date: 15.06.2018].

SSI, (2013). Social Security Institution Statistical Annuals. http://www.sgk.gov.tr/wps/portal/sgk/tr/kurumsal/istatistik/sgk_istatistik_yilliklari (Access Date:15.06.2018).

SSI, (2014). Social Security Institution Statistical Annuals. http://www.sgk.gov.tr/wps/portal/sgk/tr/kurumsal/istatistik/sgk_istatistik_yilliklari (Access Date:15.06.2018).

SSI, (2015). Social Security Institution Statistical Annuals. http://www.sgk.gov.tr/wps/portal/sgk/tr/kurumsal/istatistik/sgk_istatistik_yilliklari (Access Date:15.06.2018).

SSI, (2016). Social Security Institution Statistical Annuals. http://www.sgk.gov.tr/wps/portal/sgk/tr/kurumsal/istatistik/sgk_istatistik_yilliklari (Access Date:15.06.2018).

TURKSTAT, (2016a). Small and Medium Sized Enterprise Statistics, TURKSTAT, Ankara.

TURKSTAT, (2016b). Annual Industry and Service Statistics, 2014, TURKSTAT, Ankara.

Yazıcıoğlu, Y. and Erdoğan, S., (2004). SPSS Applied Scientific Research Methods. Detay Publishing, Ankara.

International Conference on Science and Technology

ICONST 2018

5-9 September 2018 Prizren - KOSOVO

Determination of Efficiency of an Electric Current Activated Sintering System

Tuba Yener[1], Şuayb Çağrı Yener[2]*, Reşat Mutlu[3]

Abstract: Energy sources such as oil and coil are being depleted in today's world and energy sources are becoming costlier, and power and efficiency of electrical devices becoming more important than ever. Electric current activated/assisted sintering(ECAS) systems is a method to produce metallic and nonmetallic samples in a cheap way and in a short time compared to traditional methods. Some ECAS systems use DC current and have thyristor-based rectifiers to control the output power. In this paper, efficiency of an electric current activated/assisted sintering system with a controlled-rectifier is examined during sample production. The efficiencies of the power electronics section and the ECAS container section is examined separately. A power analyzer device is used to measure and record the input power and another to record the dc bar input power and the ECAS container power. The ECAS container resistance is temperature dependent and, therefore, the efficiency of the ECAS system varies during sample manufacturing process. The conduction loss to the ECAS container is very low. The system efficiency is mainly defined by the power unit. Also the temperature dependency of the losses during the sample production process and time-dependency of the efficiencies are demonstrated. Process Energy Efficiency is also calculated. The information given here can be used to design ECAS systems with better efficiencies.

Keywords: electric current activated sintering, power and energy efficiency analysis, controlled-rectifiers.

Introduction

Electric current assisted sintering technique (ECAS) is an energy-friendly system based on sintering of materials from very different material groups such as metal, ceramics, intermetallic in a very short time (Firmansyah, Sukarto, Hermanto, Asta, & Nugraha, 2016; Grasso, Sakka, & Maizza, 2009; Orrù, Licheri, Locci, Cincotti, & Cao, 2009; S. C. Yener, Yener, & Mutlu, 2018; Ş. Ç. Yener, Yener, & Mutlu, 2017; T. Yener & Zeytin, 2014; T Yener, Okumus, & Zeytin, 2015; T Yener & Zeytin, 2017; Tuba Yener, 2016).Contrary to ECAS system, in conventional hot pressing techniques, the powder container is typically heated by radiation from the enclosing furnace through external heating elements and convection of inert gases if applicable (Orrù et al., 2009; Weintraub & Rush, 1913; Tuba Yener & Zeytin, 2014). Hence, the sample is heated as a result of the heat transfer occurring by conduction from the external surface of the container to the powders. In this method heating rate is then slow and the process can last hours. Furthermore, so much heat is being wasted as the entire volume of the area is heated and the sample indirectly receives heat from the hot media. Apparently than the conventional methods, ECAS processes can be characterized by the efficient use of the heat input, especially when a vacuum environment is used and the electric current is applied for extremely short duration (Orrù et al., 2009; Tuba Yener, 2016).

A three phase electric arc furnace is a commonly used metallurgical method to produce metals (Arnold, 1934). In literature, the efficiency of electrical arc furnaces is well studied. The efficiency improvement of an electrical

[1]Sakarya University, Engineering Faculty, Metallurgy and Materials Engineering Department 54187, Sakarya, TURKEY
[2]Sakarya University, Engineering Faculty, Electrical and Electronics Engineering Department 54187, Sakarya, TURKEY
[3]Namık Kemal University, Çorlu Engineering Faculty, Electronics and Communication Engineering Department, Çorlu, Tekirdağ, TURKEY
*Corresponding author: syener@sakarya.edu.tr

arc furnaces is studied using SVC and STATCOM in (Kashani, Babaei, & Bhattacharya, 2013). Its efficiency improvement is studied by Optimal Setting of the Series Reactor and Transformer Taps Using a Nonlinear Model in (Samet, Ghanbari, & Ghaisari, 2015). Its Energy efficiency increment of an Electric Arc Furnace with SVM-RFE is studied in (Amado, Crispin, Martinez Haydee, Rafael, & Malaquias, 2015). Improving efficiency of ultra-high power arc furnaces with thyristor control voltage of furnace transformer is done in (Yakimov & Gorokhov, 2016). Increasing the output and the energy efficiency of electric arc furnaces with shaft heating of metal scrap is shown in (Tuluevskii & Zinurov, 2014). A high efficiency environment-friendly electric arc furnace with energy recovery is reported in (Nagai et al., 2015). Analysis of electric arc furnaces efficiency via frequency spectrum-based arc coverage detection is examined (Torres-Rentería, Damián-Cuallo, Mayo-Maldonado, & Micheloud-Vernackt, 2017). Electromagnetism and the arc efficiency of electric arc steel melting furnaces is examined and results of analytically studied effect of electromagnetic blowing and the slag height on the arc efficiency are stated in (Makarov, Rybakova, & Galicheva, 2014).

Although ECAS system is also an old method like arc furnaces, a quick literature search shows that the ECAS process efficiency is not well-examined as done for arc furnaces. A review on ECAS processes and systems can be found in (Orrù et al., 2009). Simulation of thermal and electric field evolution during spark plasma sintering is done in without considering circuit efficiency (Tiwari, Basu, & Biswas, 2009). Modelling of Micro/Macro Densification Phenomena of CuPowder during Capacitor Discharge Sintering is given but its efficiency is not considered in (Maizza & Tassinari, 2009). The main mechanisms involved during electric field densification and the interplay between the applied electrical current and densifying materials during field assisted sintering (electrical discharge, constriction resistance, current uniformity, heating rate and the pressure effects) is addressed without considering circuit efficiency in (Groza & Zavaliangos, 2003). Ultra-fast and energy-efficient sintering of ceramics by electric current concentration is examined in (Zapata-Solvas, Gómez-García, Domínguez-Rodríguez, & Todd, 2015). Energy efficiency during a conventional and a novel sintering processes is examined in (Musa et al., 2009). The literature research shows that ECAS process efficiency is rarely examined while as electrical arc furnace process and/or system efficiencies have been examined in detail. In addition to that, the overall ECAS system efficiency is not examined in literature yet. To take full advantage of the method, its efficiency must be examined as done for arc furnaces. In this study, a thyristor-controlled ECAS system efficiency is examined experimentally for the first time in literature.

The paper is arranged as follows. In the second section, the mechanic structure and the electrical power circuit of the ECAS system are briefly explained and also ECAS power calculations from an experiment in which an intermetallic sample is produced are done. In the third section, efficiency analysis of the ECAS system using the experimental results are presented. The paper is concluded with the last section.

Electric Current Activated Sintering System and Power Calculations

Block view of the ECAS system used in this study is shown in Figure 1. The DC bar and the ECAS container connection to them area lso shown in the figure. The system has a delta/star connected three-phase transformer rated at 60 kVA and has an AC chopper placed at the input to adjust the rms voltage value of the phase voltages of its delta connected primary windings. The secondary side has two center-tapped rectifier. Each winding only provides current for just an alternance to prevent the very high currents from damaging or overheating of the transformer windings. The rectifier is an uncontrolled rectifier. However, the AC chopper at primary side results in overall system behaving as a controlled rectifier. The system user is able to set the desired DC current manually flowing through the ECAS container in which the sampleis placed. The system measures a (the DC shunt) resistor current placed in series with the sample for that purpose and trigger the thyristors accordingly. The ECAS system container can reach temperatures as high as 900 ^{0}C.

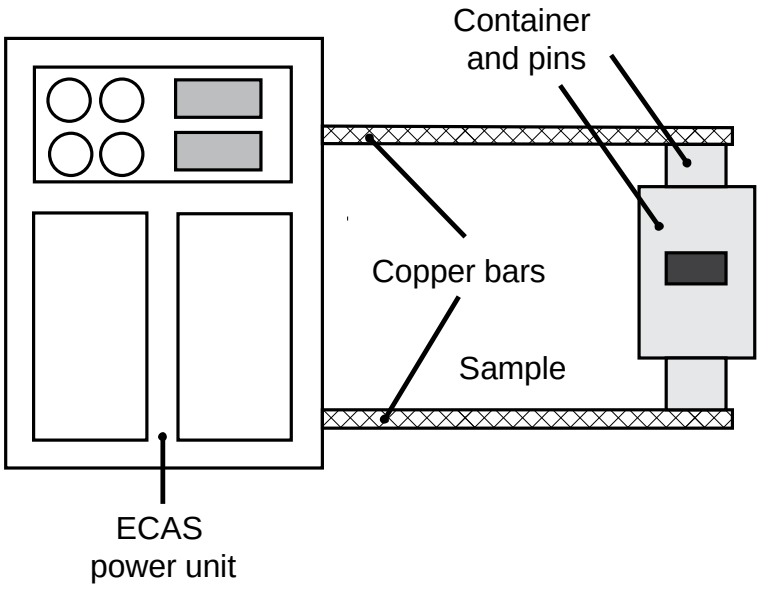

Figure 1. Block diagram of ECAS with DC Bars and the container

The power flow diagram of the ECAS system is shown in Figure 3. The losses can be separated into parts and explained in the following. The input power of the ECAS system is the electrical power drawn from utility. Cooling fan is used to cool down the power electronic components such as thyristors of the AC chopper and power diodes of the rectifier and run during all the time sample is produced. The electronic control circuit power is negligible (in the order of several watts) compared to the powers (in the order of hundreds of watts) dissipated within the other parts. Three phase rectifier diode currents can be as high as 3000 Amps in the ECAS system. Therefore, the diode conduction powers can be around 5000 kilowatts. If the diode turn-on and turn-off losses are included, the rectifier losses can be a lot higher. Unfortunately, it has not been measured yet. It can be guessed that AC chopper losses are not that high since the chopper phase currents are low compared to the ECAS container current. DC bar (connection) losses is low compared to the ECAS container. We guess that's why the power loss of the shunt resistor which is used to measure the DC bus current is also very low. We don't expect the transformer losses to be very high however the losses due the harmonics should be higher than the case in which it is fed by pure sinusoidal voltages. The shock coil losses can be higher due to the high discontinuous mode operation of the rectifier and high DC bus current.

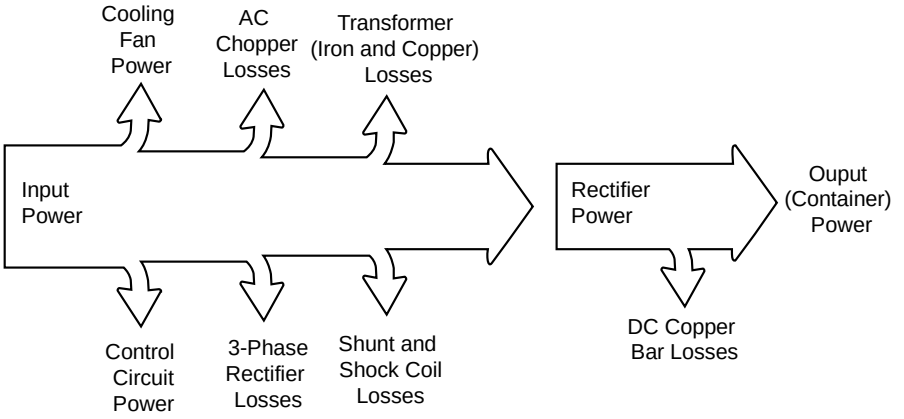

Figure 2. Power flow diagram of an ECAS system

The input active power of the three-phase (AC chopper+transformer+rectifier) system is

$$P = 3V_0 I_0 + 3\sum_{k=1}^{\infty} V_k I_k \cos(\varphi_{Vk} - \varphi_{Ik}) \quad \textbf{(1)}$$

Where I_k, V_k, I_0 and V_0 are the Fourier series coefficients of the phase current and voltages.
The input active power of the three-phase system is measured for the intermetallic sample production process with a power analyzer. The electrical or the input power is shown in Figure 3.

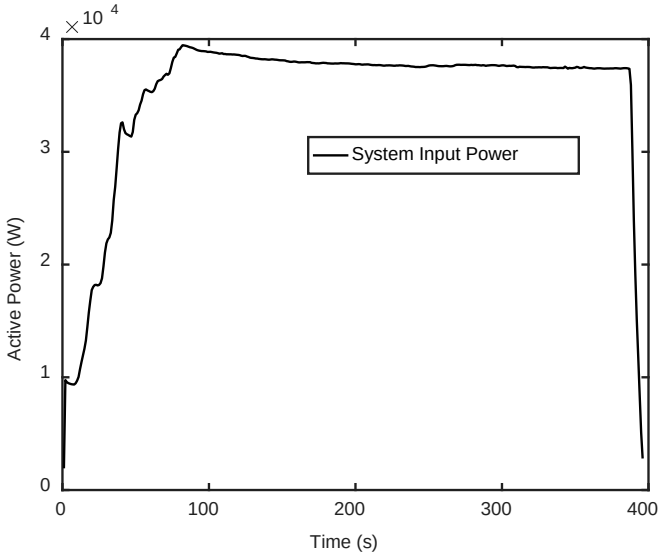

Figure 3. Input active power

The connection to the ECAS container from the output of the rectifier system is made with copper bars. Copper is a better electrical conductor than steel and also the copper bars has a larger cross-section compared to the steel container. The rectifier output power is equal to the DC bar input power and can be expressed as

$$p_{\mathrm{Re}ctifier}(t) = \left(R_{bar} + R_{Container}(T)\right).i^2(t) \quad \textbf{(2)}$$

The voltage drop across copper bars defines the connection power loss which can be expressed as

$$p_{Connection}(t) = R_{bar}.i^2(t) \quad \textbf{(3)}$$

The ECAS container power is

$$p_{Container}(t) = R_{Container}(T).i^2(t) \quad \textbf{(4)}$$

The ECAS container temperature varies during the intermetallic sample production process and shown in Figure 4.

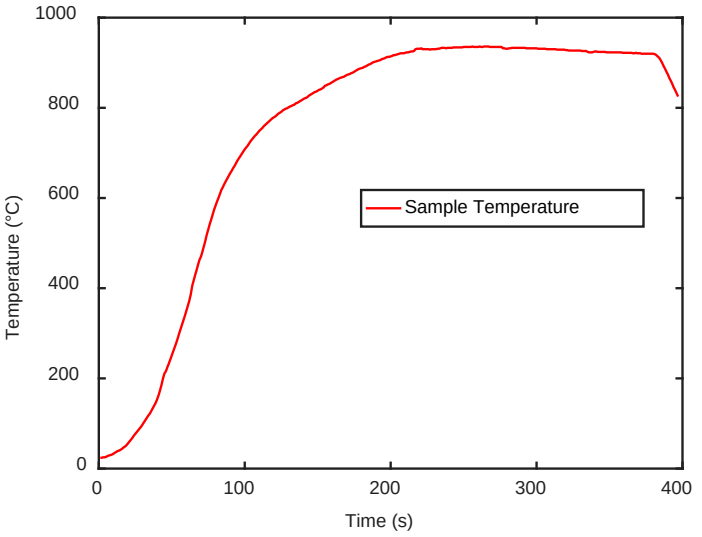

Figure 4. The container temperature vs. time for the sample

The ECAS container power and the rectifier output power are measured experimentally and shown in Figure 5. The system input energy, the rectifier output energy and the ECAS container energy is shown in Figure 6.

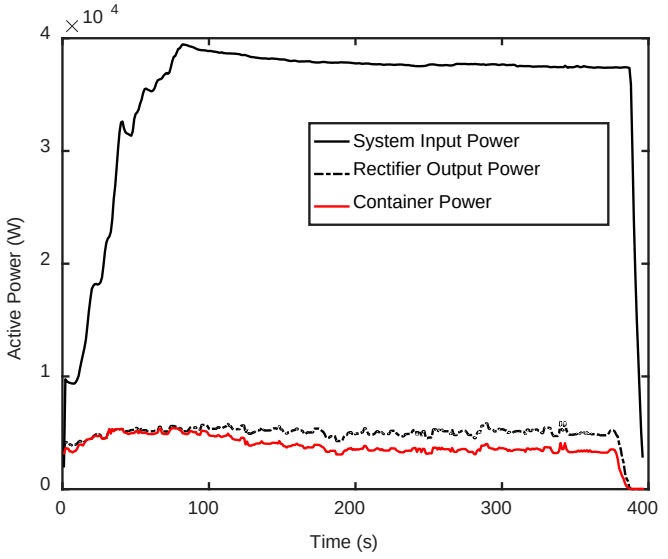

Figure 5. The input, the rectifier and the ECAS container power vs. time

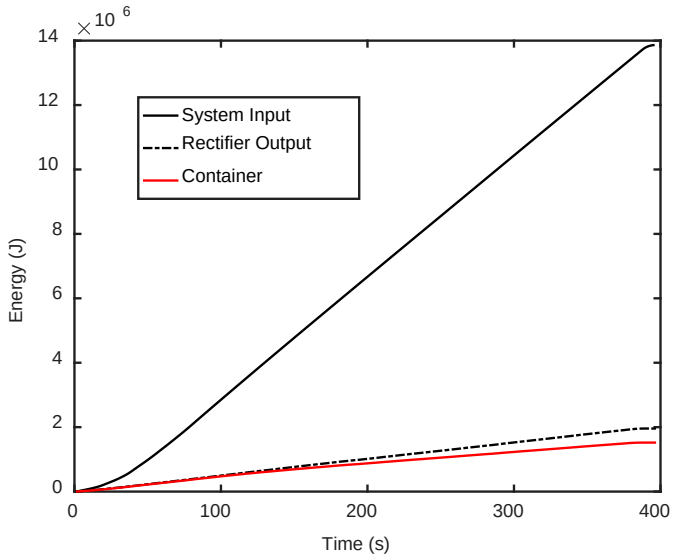

Figure 6. The system input energy, the rectifier output energy and the ECAS container energy vs time

EfficiencyAnalysisof Electric Current Activated SinteringSystem

The power electronics and transformer system efficiency can be given as

$$\eta_1 = \frac{P_{dcbar}}{P_{electrical}} \tag{5}$$

The connection efficiency is calculated as

$$\eta_2 = \frac{P_{Container}}{P_{dcbar}} \tag{6}$$

Total efficiency of the system:

$$\eta = \eta_1 \eta_2 = \frac{P_{Container}}{P_{Electrical}} = \frac{R_{Container}(T)}{R_{bar} + R_{Container}(T)} \tag{7}$$

The efficiencies are plotted in Figure 7 for the intermetallic sample production process.

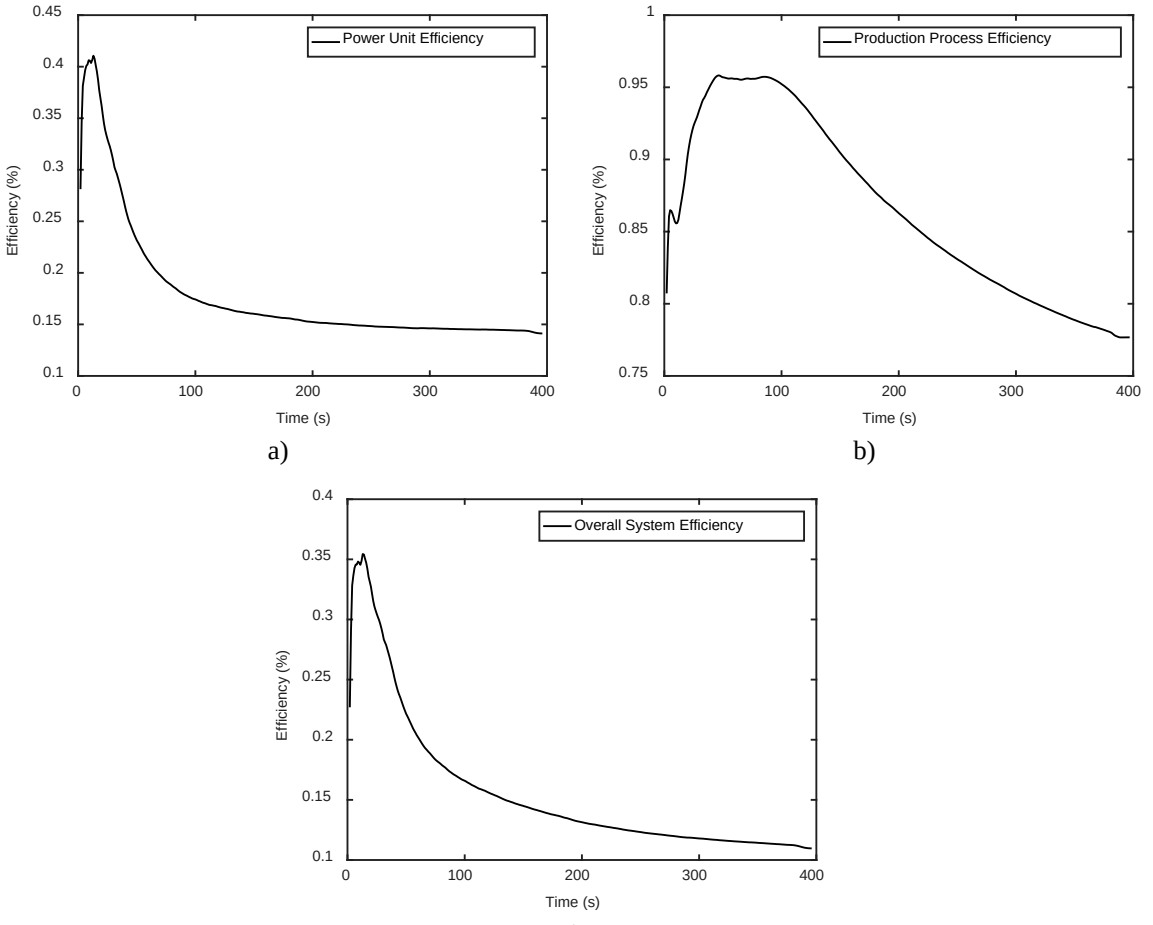

Figure 7. a) Transformer and Power Electronics System Efficiency, b) ECAS Container Efficiency, c) Overall System Efficiency

As shown in Figure 8, the ECAS container or the production system efficiency is actually very high: most of the rectifier power is turned into heat within the container whileas only a small fraction of its is dissipated on the conductor bars (dc bar). Most of the power loss occurs within the ECAS power electronics systems and three phase transformer. All efficiencies are low at the beginning, starts increasing, then reaches to maximum and falls down after the peak while time increases.

In this paper, we define the Process Energy Efficiency as

$$\eta_{PE} = \frac{\int_0^{\tau} P_{Container}\, dt}{\int_0^{\tau} P_{Electrical}\, dt} \qquad \textbf{(8)}$$

The Process Energy Efficiency is found to be 10.97% with ECAS system and its container consuming 3.85kWh and 0.42kWh respectively. If the same process is made with a sintering oven, it is around 12kWh and takes 4 hours to complete. This also shows the superiority of the energy efficiency and the speed of the ECAS system compared to the other method. The ECAS system consumes 32% of the energy consumed by the sintering oven. However, the ECAS system can consume less power if especially the losses in the power unit should be

decreased sufficiently. The solution is using low loss power electronics and magnetic components. It might also be possible that an electronic feedback control can be used for a better efficiency.

Conclusion

The electric activated sintering is an important sample production method which produces samples quickly. In this paper, the power flow of an ECAS system is described and efficiencies of subsections of a manually-controlled ECAS system are examined experimentally. The system input power, the rectifier output power and the container power are measured. The efficiencies are calculated from the measurements. It has been found that the power unit (the power electronics and the three phase transformer) has higher losses than the copper conductors. The conduction loss to the ECAS container is very low. The overall ECAS system has a low efficiency. The system efficiency is mainly defined by the power unit. Also the temperature dependency of the losses during the sample production process and time-dependency of the efficiencies are demonstrated. Process Energy Efficiency is also calculated. Although the system efficiency is as low as 16%, less energy is wasted to produce the sample in the ECAS system than to produce it in a metallurgical oven (Almost at the 1/3rd of it). For a better efficiency, especially the losses in the power unit should be decreased sufficiently. These can be done using low loss power electronics and magnetic components. It might also be possible that an electronic feedback control can be used for that purpose. Some of the methods used to improve the electrical arc furnace efficiencies can also be used to improve the ECAS system efficiency. The information given in this paper can be used as a starting point to design ECAS systems with better efficiencies.

References

Amado, S., Crispin, H., Martinez Haydee, P., Rafael, O., & Malaquias, Q. P. (2015). Energy efficiency of an Electric Arc Furnace with SVM-RFE. In *2015 International Conference on Electronics, Communications and Computers (CONIELECOMP)* (pp. 161–167). IEEE. https://doi.org/10.1109/CONIELECOMP.2015.7086944

Arnold, S. (1934). The 3-phase electric arc furnace. *Electrical Engineering*, *53*(3), 452–452. https://doi.org/10.1109/EE.1934.6538874

Firmansyah, I., Sukarto, W. A., Hermanto, B., Asta, J. M., & Nugraha, H. (2016). Wi-Fi based temperature monitoring system for thermal analysis with Kalman Filter implementation. In *2016 International Conference on Computer, Control, Informatics and its Applications (IC3INA)* (pp. 1–5). IEEE. https://doi.org/10.1109/IC3INA.2016.7863013

Grasso, S., Sakka, Y., & Maizza, G. (2009). Electric current activated/assisted sintering (ECAS): a review of patents 1906–2008. *Science and Technology of Advanced Materials*, *10*(5), 53001. https://doi.org/10.1088/1468-6996/10/5/053001

Groza, J. R., & Zavaliangos, A. (2003). Nanostructured bulk solids by field activated sintering. *Reviews on Advanced Materials Science*, *5*(1), 24–33.

Kashani, M. G., Babaei, S., & Bhattacharya, S. (2013). SVC and STATCOM application in Electric Arc Furnace efficiency improvement. In *2013 4th IEEE International Symposium on Power Electronics for Distributed Generation Systems (PEDG)* (pp. 1–7). IEEE. https://doi.org/10.1109/PEDG.2013.6785641

Maizza, G., & Tassinari, a. (2009). Modelling of Micro/Macro Densification Phenomena of Cu Powder during Capacitor Discharge Sintering. *COMSOL Conference 2009*. Retrieved from http://www.uk.comsol.com/papers/7263/

Makarov, A. N., Rybakova, V. V., & Galicheva, M. K. (2014). Electromagnetism and the Arc Efficiency of Electric Arc Steel Melting Furnaces. *Journal of Electromagnetic Analysis and Applications*, (June), 184–192.

Musa, C., Licheri, R., Locci, A. M., Orrù, R., Cao, G., Rodriguez, M. A., & Jaworska, L. (2009). Energy efficiency during conventional and novel sintering processes: the case of Ti-Al2O3-TiC composites. *Journal of Cleaner Production*, *17*(9), 877–882. https://doi.org/10.1016/j.jclepro.2009.01.012

Nagai, T., Sato, Y., Kato, H., Fujimoto, M., Sugasawa, T., Steel, J. P., & Co, P. (2015). The most advanced power saving technology in EAF Introduction to ECOARC ™ Contact data Summary 1 . Introduction High

efficiency process, (June), 15–19.

Orrù, R., Licheri, R., Locci, A. M., Cincotti, A., & Cao, G. (2009). Consolidation/synthesis of materials by electric current activated/assisted sintering. *Materials Science and Engineering: R: Reports*, *63*(4–6), 127–287. https://doi.org/10.1016/j.mser.2008.09.003

Samet, H., Ghanbari, T., & Ghaisari, J. (2015). Maximum Performance of Electric Arc Furnace by Optimal Setting of the Series Reactor and Transformer Taps Using a Nonlinear Model. *IEEE Transactions on Power Delivery*, *30*(2), 764–772. https://doi.org/10.1109/TPWRD.2014.2336693

Tiwari, D., Basu, B., & Biswas, K. (2009). Simulation of thermal and electric field evolution during spark plasma sintering. *Ceramics International*, *35*(2), 699–708. https://doi.org/10.1016/j.ceramint.2008.02.013

Torres-Rentería, A., Damián-Cuallo, M., Mayo-Maldonado, J., & Micheloud-Vernackt, O. (2017). Analysis of electric arc furnaces efficiency via frequency spectrum-based arc coverage detection. *Ironmaking and Steelmaking*, *44*(4), 255–261. https://doi.org/10.1080/03019233.2016.1210361

Tuluevskii, Y. N., & Zinurov, I. Y. (2014). Increasing the output and the energy efficiency of electric arc furnaces with shaft heating of metal scrap. *Russian Metallurgy (Metally)*, *2014*(6), 460–465. https://doi.org/10.1134/S0036029514060159

Weintraub, G., & Rush, H. (1913). Process and apparatus for sintering refractory materials. *Google Patents*. US Patent.

Yakimov, I. A., & Gorokhov, V. L. (2016). Improving efficiency of ultra-high power arc furnaces with thyristor control voltage of furnace transformer. In *2016 2nd International Conference on Industrial Engineering, Applications and Manufacturing (ICIEAM)* (pp. 1–5). IEEE. https://doi.org/10.1109/ICIEAM.2016.7910894

Yener, S. C., Yener, T., & Mutlu, R. (2018). A process control method for the electric current-activated/assisted sintering system based on the container-consumed power and temperature estimation. *Journal of Thermal Analysis and Calorimetry*, 1–10. https://doi.org/10.1007/s10973-018-7453-y

Yener, Ş. Ç., Yener, T., & Mutlu, R. (2017). Electrically-assisted Sintering System Container Temperature Versus Time During Cooling. In *ICCESEN 2017 4rd International Conference on Computational and Experimental Science and Engineering October 4-8, 2017, Kemer, Antalya, Turkey* (p. 434).

Yener, T. (2016). *ECAS Yöntemiyle Üretilmiş Ti-Al Esaslı İntermetalik Kompozit Malzemelerin Geliştirilmesi*. *Sakarya Üniersitesi, Fen Bilimleri Enstitüsü*. Fen Bilimleri Enstitüsü.

Yener, T., Okumus, S. C., & Zeytin, S. (2015). In Situ Formation of Ti-TiAl 3 Metallic-Intermetallic Composite by Electric Current Activated Sintering Method. *Acta Physica Polonica A.*, *127*(4), 917–920. https://doi.org/10.12693/APhysPolA.127.917

Yener, T., & Zeytin, S. (2014). Synthesis and characterization of metallic-intermetallic Ti-TiAl3, Nb-Ti-TiAl3 composites produced with Electric-Current-Activated Sintering (ECAS). *Materiali in Tehnologije*, *48*(6).

Yener, T., & Zeytin, S. (2014). Synthesis and characterization of metallic-intermetallic Ti-TiAl3, Nb-Ti-TiAl3 composites produced with Electric-Current-Activated Sintering (ECAS). *Materiali in Tehnologije*, *48*(6), 847–850.

Yener, T., & Zeytin, S. (2017). Production and Characterization of Niobium Toughened Ti-TiAl 3 Metallic-Intermetallic Composite. *Acta Physica Polonica A.*, *132*(3–II), 941–943. https://doi.org/10.12693/APhysPolA.132.941

Zapata-Solvas, E., Gómez-García, D., Domínguez-Rodríguez, A., & Todd, R. I. (2015). Ultra-fast and energy-efficient sintering of ceramics by electric current concentration. *Scientific Reports*, *5*, 1–7. https://doi.org/10.1038/srep08513

International Conference on Science and Technology

ICONST 2018

5-9 September 2018 Prizren - KOSOVO

Design of a Microcontroller-Based Chaotic Circuit of Lorenz Equations

Şuayb Çağrı Yener[1]*, Cihan Barbaros[2], Reşat Mutlu[2], Ertuğrul Karakulak[3]

Abstract: The Lorenz system is a system of ordinary differential equations which are a simplified mathematical model for atmospheric convection first studied by Edward Lorenz in 1963. They have chaotic solutions for certain parameter values and initial conditions and commonly used for chaos studies. In particular, the Lorenz attractor is a set of chaotic solutions of the Lorenz system which, when plotted, resemble a butterfly or figure eight. The Lorenz equations also emerge in simplified models for lasers, dynamos, thermosyphons, brushless DC motors, electric circuits, chemical reactions and forward osmosis. In literature, Lorenz equations have chaotic solutions for certain parameter values and initial conditions. Implementation of a circuit which mimics Lorenz equations is important for the practical real-world circuit design. System dynamics can be emulated using analog multipliers. Alternatively, the circuit can be made cheap and easy-to-build off-the shelves components. In this work, a new microcontroller-based Chaotic Circuit to simulate Lorenz equations is presented. To do this, first Simulink is used to solve the Lorenz equations and gain some experience about them. Then, the microcontroller-based chaotic circuit is programmed and simulated in Proteus. This circuit employs an Arduino Mega 2560 R3 microcontroller which solves The Lorenz equations numerically with Runge-Kutta method and obtains the chaotic signals using digital-analog-converters. x, y and z waveforms obtained from the Proteus simulation. The waveform matches well the one obtained from the Simulink waveform. Results show that the microcontroller-based circuit performs well. It can be used in chaos studies and educational purposes.

Keywords: Lorenz Equations, chaotic circuit, microcontroller based circuit design, Runge-kutta method

Introduction

The Lorenz system is a system of ordinary differential equations which are a simplified mathematical model for atmospheric convection first studied by Edward Lorenz in 1963 (Lorenz & Lorenz, 1963). They have chaotic solutions for certain parameter values and initial conditions and commonly used for chaos studies. In particular, the Lorenz attractor is a set of chaotic solutions of the Lorenz system which, when plotted, resemble a butterfly or figure eight. The Lorenz equations also emerge in simplified models for lasers, dynamos, brushless DC motors, electric circuits, chemical reactions and forward osmosis (Haken, 1975; Hemati, 1994; Knobloch, 1981; Poland, 1993; Tzenov, 2014).

Analog circuit implementations of Lorenz system are commonly used for chaos studies (Blakely, Eskridge, & Corron, 2007; Cuomo & Oppenheim, 1993; Gonzales, Han, de Gyvez, & Sanchez-Sinencio, 2000; Radwan, Soliman, & El-Sedeek, 2004). It may be possible that such chaotic Lorenz system circuits can be used in

[1]Sakarya University, Engineering Faculty, Electrical and Electronics Engineering Department 54187, Sakarya, TURKEY
[2]Namık Kemal University, Çorlu Engineering Faculty, Electronics and Communication Engineering Department, Çorlu, Tekirdağ, TURKEY
[3] Namık Kemal University, Electronics Department, Vocational school of Technical Sciences, Tekirdag, TURKEY
*Corresponding author: syener@sakarya.edu.tr

communication circuits (Blakely et al., 2007; Cuomo & Oppenheim, 1993). Such as systems can also be used in cryptosystems (Gonzales et al., 2000). MOS Realization of the Modified Lorenz Chaotic Systems can be found in (Radwan et al., 2004). A reconfigurable hardware platform is used to obtain memristor-based chaotic systems in (Arık & Kılıç, 2014; Tahir, Ali, & Fortuna, 2014). A memristive chaotic circuit is studied in (Ş. Ç. Yener & Kuntman, 2014) and examined using a microcontroller-based circuit in (S. C. Yener, Barbaros, Mutlu, & Karakulak, 2017). Such a method can also be easily used to simulate a Lorenz system. In this study, a microcontroller-based circuit is used to solve the Lorenz system differential equations and send the solved state-variables out as binary numbers and then using Digital analog converters, obtaining their time-dependent waveforms. Such a circuit can be built easily with cheap microcontroller such a PIC or Arduino. In this study, a cheap, rugged, easy-to-use microcontroller Arduino Mega 2560 R3 microcontroller is used.

To do this, first Simulink™ is used to solve the Lorenz equations and gain some experience about them. Then, the microcontroller-based chaotic circuit is programmed and simulated in Proteus™. Finally, the experimental circuit is assembled and the chaotic waveforms are obtained experimentally.

The paper is arranged as the follows. In the second section, the Lorenz equations are introduced, and its simulation results obtained from Simulink™ is given. In the third section, the microcontroller-based chaotic circuit is introduced. In the fourth section, Microcontroller-based Memristive Chaotic Circuit schematic and its Proteous™ simulation are given. In the fourth section, the experimental results of the circuit are given. The paper is finished with the conclusion section.

Lorenz Equations and its Simulation in MATLAB

The following set of equations describes the Lorenz equations/system:

$$\begin{aligned} \frac{dx}{dt} &= a(y-x) \\ \frac{dy}{dt} &= x(b-z)-y \\ \frac{dz}{dt} &= xy-cz \end{aligned} \qquad \textbf{(1)}$$

where x, y and z are the state variables, t is time. a, b, c are the system parameters and they are normally positive. The Lorenz equations for these values, a=10, b=28 and c=8/3, and nearby values exhibits chaotic behavior. The values are also to be used in this study. The Lorenz system is simulated in Simulink™ toolbox of MATLAB ™ using Runge-Kutta method in time domain and the results are shown in F'gure 1 and two-dimensional phase portraits of the system is shown in Figure 2.

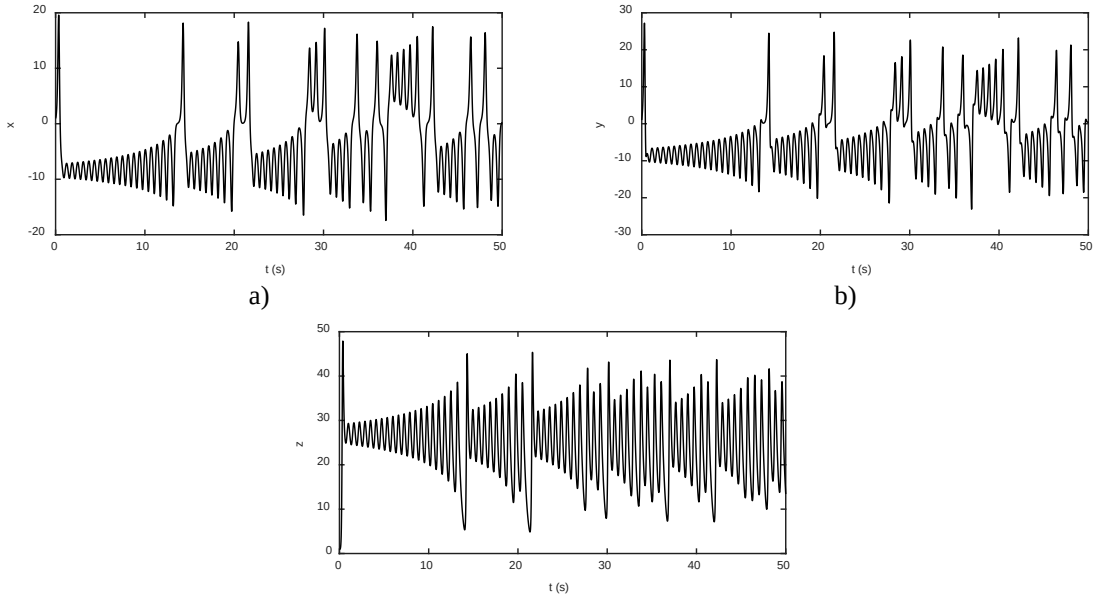

Figure 1. Time domain waveforms from MATLAB simulations for a=10, b=28 and c=8/3 a) x(t), b) y(t) c) z(t)

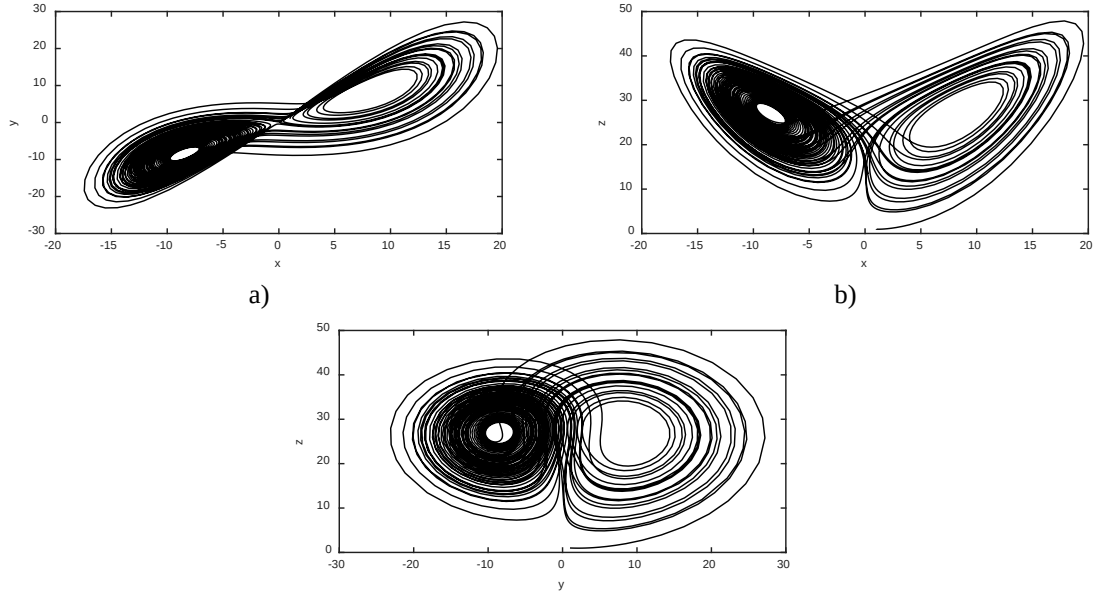

Figure 2. Two-dimensional phase portraits obtained by Simulink simulation of the chaotic circuit equations for a=10, b=28 and c=8/3: a) y versus x, b) z versus x, c) z versus y

Microcontroller-based Chaotic Circuit

Proteous schematic of the microcontroller-based circuit of Lorenz System is shown in Figure 3. It consists of the Ardunio Mega microcontroller, two DACs and two Op-amp-based inverting amplifiers. The microcontroller solves the desired state variables of the Lorenz equations x, y, and z using Runge-Kutta method and sends them to the output using the DACs and operational amplifiers as shown in the Figure 3.

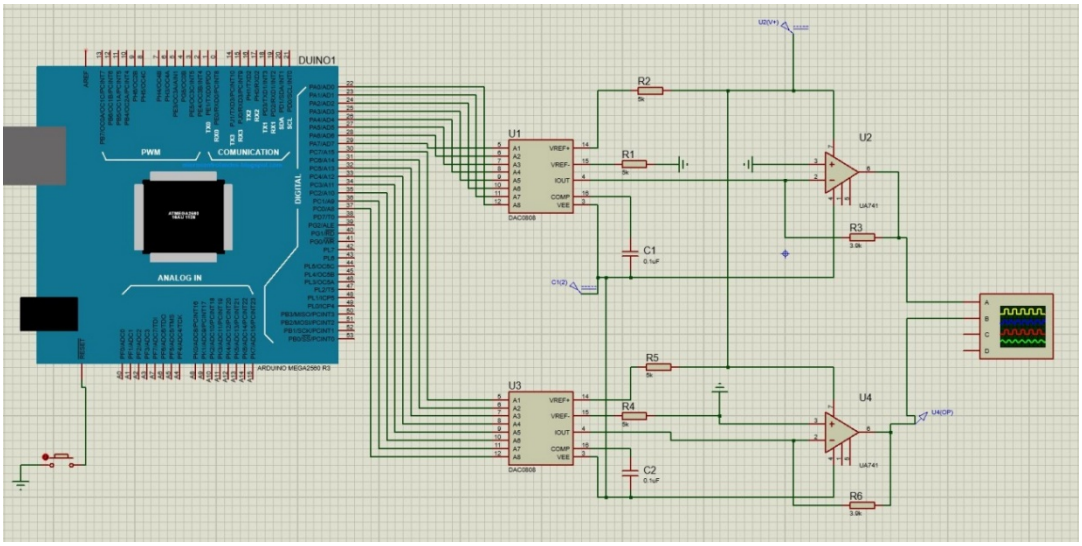

Figure 3. Circuit schematic drawn in Proteus

The circuit is also simulated in Proteus™. x, y and z waveforms obtained from the Proteus simulation is shown in Figure 4. The waveform matches well the one obtained from the Simulink waveform. Due to space consideration, phase-portait waveforms are not given.

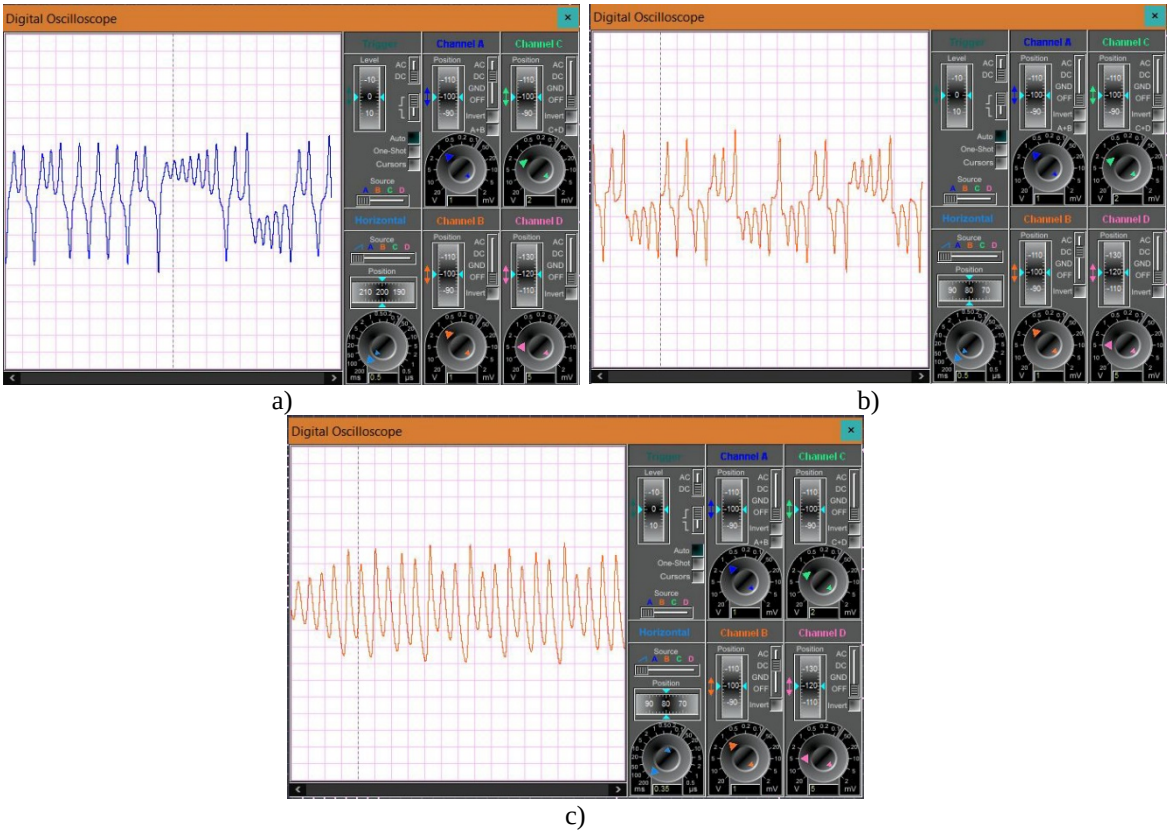

a) b)

c)

Figure 4. Time domain waveforms of the microcontroller-based Chaotic circuit in time domain obtained from the Proteus simulations a) x(t), b) y(t) c) z(t)

Conclusions

In this study, a microcontroller-based chaos circuit of Lorenz system is designed. With its DACs, it is able to produce chaotic output signals of Lorenz equations. With proper modifications of its program and with a real implementation it can allow examination of bifurcation of the Lorenz system or the effect of the parameters on it easily. Since the chaos waveforms are produced in a hybrid way not in an analog way, the effect of using different numerical methods such as Euler method and different Runge-Kutta methods on the bifurcation of the Lorenz system can be examined easily. Such a circuit can also be used in circuit laboratories for educational purposes.

References

Arık, S., & Kılıç, R. (2014). RECONFIGURABLE HARDWARE PLATFORM FOR EXPERIMENTAL TESTING AND VERIFYING OF MEMRISTOR-BASED CHAOTIC SYSTEMS. *Journal of Circuits, Systems and Computers*, *23*(10), 1450145. https://doi.org/10.1142/S021812661450145X

Blakely, J. N., Eskridge, M. B., & Corron, N. J. (2007). A simple Lorenz circuit and its radio frequency implementation. *Chaos: An Interdisciplinary Journal of Nonlinear Science*, *17*(2), 023112. https://doi.org/10.1063/1.2723641

Cuomo, K. M., & Oppenheim, A. V. (1993). Circuit implementation of synchronized chaos with applications to communications. *Physical Review Letters*, *71*(1), 65–68. https://doi.org/10.1103/PhysRevLett.71.65

Gonzales, O. A., Han, G., de Gyvez, J. P., & Sanchez-Sinencio, E. (2000). Lorenz-based chaotic cryptosystem: a monolithic implementation. *IEEE Transactions on Circuits and Systems I: Fundamental Theory and Applications*, *47*(8), 1243–1247. https://doi.org/10.1109/81.873879

Haken, H. (1975). Analogy between higher instabilities in fluids and lasers. *Physics Letters A*, *53*(1), 77–78. https://doi.org/10.1016/0375-9601(75)90353-9

Hemati, N. (1994). Strange attractors in brushless DC motors. *IEEE Transactions on Circuits and Systems I: Fundamental Theory and Applications*, *41*(1), 40–45. https://doi.org/10.1109/81.260218

Knobloch, E. (1981). CHAOS IN THE SEGMENTED DISC DYNAMO. *Physics Letters*, *82A*(9), 439–440. Retrieved from http://tardis.berkeley.edu/reprints/papers/Kn_PLA82_1982.pdf

Lorenz, E. N., & Lorenz, E. N. (1963). Deterministic Nonperiodic Flow. *Journal of the Atmospheric Sciences*, *20*(2), 130–141. https://doi.org/10.1175/1520-0469(1963)020<0130:DNF>2.0.CO;2

Poland, D. (1993). Cooperative catalysis and chemical chaos: a chemical model for the Lorenz equations. *Physica D: Nonlinear Phenomena*, *65*(1–2), 86–99. https://doi.org/10.1016/0167-2789(93)90006-M

Radwan, A. G., Soliman, A. M., & El-Sedeek, A. (2004). MOS realization of the modified Lorenz chaotic system. *Chaos, Solitons & Fractals*, *21*(3), 553–561. https://doi.org/10.1016/S0960-0779(03)00077-8

Tahir, F. R., Ali, R., & Fortuna, L. (2014). ANALOG PROGRAMMABLE ELECTRONIC CIRCUIT-BASED CHAOTIC LORENZ SYSTEM. *Basrah Journal for Engineering Sciences*, *14*(1).

Tzenov, S. I. (2014). Strange Attractors Characterizing the Osmotic Instability. Retrieved from http://arxiv.org/abs/1406.0979

Yener, S. C., Barbaros, C., Mutlu, R., & Karakulak, E. (2017). Implementation of Microcontroller-Based Memristive Chaotic Circuit. *Acta Physica Polonica A*, *132*(3–II), 1058–1061. https://doi.org/10.12693/APhysPolA.132.1058

Yener, Ş. Ç., & Kuntman, H. H. (2014). Fully CMOS memristor based chaotic circuit. *Radioengineering*, *23*(4).

International Conference on Science and Technology

ICONST 2018

5-9 September 2018 Prizren - KOSOVO

MOSFET-Only Current-Mode LP/BP Filter With Very Small Layout Area

Emre Arslan[1]*, Şafak Murat Kızılırmak[1]

Abstract: In this work a MOSFET-only implementation of an analog, continuous time BP/LP filter is proposed. The core circuit of the proposed filter circuit contains only a few MOS transistors. The transconductances (g_m) and also the gate-to-source capacitances (C_{GS}) are used instead of physical circuit elements like resistors and capacitors. By doing so, it is possible to implement the filter circuit with a very small layout area, reduced power consumption and also very high operating frequency. AMS 0.35µm model parameters are used for HSPICE simulations and it is shown that the theoretical results harmonise with the simulated ones.

Keywords: MOSFET, Analog Filter, Transconductance, Gate-to-Source Capacitance

Introduction

In this study MOS-only filters which do not employ any external passive circuit elements like resistors and capacitors are studied [Ismail vd. 1991; Metin vd.2011; Thanachayanon, 2002]. The transconductances (g_m) and gate-to-source capacitances (C_{GS}) of MOS transistors are used instead of physical resistors and capacitors, respectively. The MOSFET-only filters occupy very small numbers of transistors to provide the transfer functions of filters, inductance simulators and oscillators. It is clear that they have many significant advantages when compared to circuits that include active circuits like current conveyors, current differencing buffered amplifiers, current feedback amplifiers, operational amplifiers, etc. : they have very small layout area and simple circuit structures, it is easy to operate the filter circuits at higher operaing frequencies, they have lower power consumptions and it is also easy to tune the filter parameters electronically.

In this paper, simple filter topologies that can be used to implement second-order MOS-only filters are proposed. When compared to classical filter circuits employing passive circuit elements [Chang vd., 2007; Gupta vd., 2003; Jiang vd., 2009; Karsılayan vd., 2000; Zhao vd., 2010], the proposed filter circuits have very simple circuit topologies, they employ very low number of transistors (lower than 5 transistors in the core circuits) and very low power consumption. HSpice simulations are performed to verify the theoretical results.

The paper is structured as follows: The proposed filter circuit is given in detail in the following section. The next section includes the simulation results. Finally, the last section concludes the paper.

The Proposed Circuits

The core structures of the proposed single-input multi-output (SIMO) current mode filters employing only MOS transistors are given in Fig. 1. All the transistors operate in the saturation region. It is important to note that external resistors and capacitors have not been used in the proposed filter circuits. The bulk terminals of

[1]Marmara University, Faculty of Engineering, Electrical and Electronics Engineering Dept., 34722, İstanbul, TURKEY
*Corresponding author: emre.arslan@marmara.edu.tr

the NMOS transistors are connected to ground and the bulk terminals of the PMOS transistors are connected to the positive power supply rail.

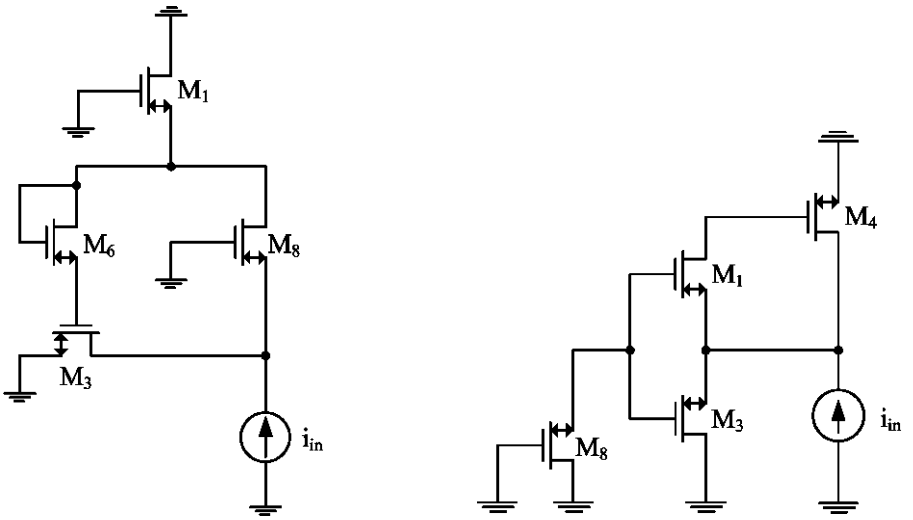

a- The first SIMO filter topology b- The first SIMO filter topology

Figure 1. The core circuits of current-mode MOS-Only SIMO filter circuits

The symbols used for the transistors mean that the relevant transistor can be an NMOS or a PMOS with appropriate terminal connections. The arrow headed terminal always refer to a source terminal, the other terminal forms the drain and the control terminal is the gate. Fig. 1 shows only the ac equivalents of the core filter circuits.

Considering the AC small signal equivalent circuits and neglecting the output transconductance values, g_{ds}, Low-Pass (LP) and Band-Pass (BP) current transfer functions for the filter circuit in Fig. 1.a can be obtained as follows:

For the circuit in a:

$$i_{LP} = \frac{g_{m3}g_{m6}}{g_{m3}g_{m6}+g_{m1}g_{m6}+s(g_{m1}C_3+g_{m6}C_1+g_{m6}C_3)+s^2C_1C_3} \quad (1)$$

$$i_{BP} = \frac{sg_{m6}C_3}{g_{m3}g_{m6}+g_{m1}g_{m6}+s(g_{m1}C_3+g_{m6}C_1+g_{m6}C_3)+s^2C_1C_3} \quad (2)$$

The LP transfer function is obtained from the drain current of M3, whereas the BP transfer function is obtained using the drain current of M6. The center frequency and the quality factor of the filter circuits can be given as follows:

$$\omega_0 = \sqrt{\frac{(g_{m1}+g_{m3})g_{m6}}{C_1C_3}} \quad (3)$$

$$Q = \sqrt{\frac{C_1C_3(g_{m1}+g_{m3})g_{m6}}{[C_1g_{m6}+C_3(g_{m1}+g_{m6})]^2}} \quad (4)$$

Similarly, the LP and BP filter transfer functions for the filter circuit in Fig. 1.b can be obtained as:

$$i_{LP} = \frac{g_{m1}g_{m4}}{g_{m1}g_{m4}+s(g_{m3}C_4+g_{m1}C_4)+s^2C_4(C_1+C_3)} \quad (5)$$

$$i_{BP} = \frac{sg_{m3}C_4}{g_{m1}g_{m4}+s(g_{m3}C_4+g_{m1}C_4)+s^2C_4(C_1+C_3)} \quad (6)$$

The LP transfer function is obtained from the drain current of M4, whereas the BP transfer function is obtained using the drain current of M3. The center frequency and the quality factor can be calculated as:

$$\omega_0 = \sqrt{\frac{g_{m1}g_{m4}}{C_4(C_1+C_3)}} \quad (7)$$

$$Q = \sqrt{\frac{(C_1+C_3)g_{m1}g_{m4}}{C_4(g_{m1}+g_{m3})^2}} \quad (8)$$

Material and Method

The core circuit of the filter circuit is obtained by the help of Mathematica and Matlab tools. The simulations are performed in HSPICE using AMS 0.35µm model parameters. As a first step, only the core filter circuit is simulated and ideal simulation results are obtained with no load. Then, the core circuit is biased using transistors, voltage and current sources and it is simulated under different loads. It is shown that the simulation results are in good aggreement with the theoretical ones.

Results

In order to demonstrate the performance of the proposed MOS only filter circuits, HSpice simulations are performed using AMS 0.35µm CMOS parameters. The supply voltage is selected as 1.5V. All the aspect ratios are selected as 5µm/0.35µm for NMOS transistors and 15µm/0.35µm for PMOS transistors.

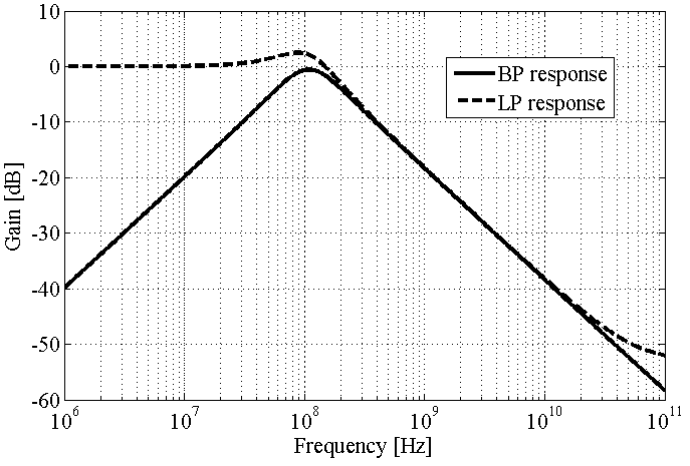

Figure 2. Frequency response of the filter circuit in Fig. 1.b

Fig. 2 depicts the frequency response of the proposed filter given in Fig. 1.b. Center frequency and quality factor of the proposed filter structure are obtained as 108 MHz and 0.8 respectively. The power consumption of the filter circuit is only 250µW.

Discussion and Conclusions

When compared to classical filter circuits that employs physical resistors and capacitors, the proposed filter operates in higher frequencies and it has very small layout area. The problem that needs to be solved is about the parasitic capacitances of the MOS transistors. As stated in the paper, instead of parasitic capacitances like C_{GS}, some other stable capacitances should be preferred.

References

Chang, C. M., Soliman, A. M., Swamy, M. N. S. (2007). Analytical synthesis of low-sensitivity high-order voltage-mode DDCC and FDCCII-grounded R and C all-pass filter structures. IEEE Trans Circuits Syst I: Regular Papers,54(7), 430–1443.

Chang, C. M., Tu, S. H. (1998). Universal current-mode filters employing CFCCIIs. Int J Electron, 85(6), 749–54.

Ferri, G, Guerrini N. C. (2003). Low-voltage low-power CMOS current conveyors. Kluwer Academic Publishers. AH Dordrecht, Netherlands.

Gupta, S. S., Senani, R. (2003). Realisation of current-mode SRCOs using all grounded passive elements. Frequenz, 57(1-2), 26–37.

Ismail, M., Wassenaar, R., Morrison, W. (1991). A high speed continuous-time bandpass VHF filter in MOS technology. Proc. IEEE Int . Symp. on Circuits and Systems, 3, 1761-1764.

Jiang, J., He, Y. (2009). Tunable frequency versatile filters implementation using minimum number of passive elements. Analog Integr Circuits Signal Process, 59, 53–64.

Karsilayan, A. Schaumann, R. (2000). A high-frequency high Q CMOS active inductor with DC bias control. Proc. IEEE Midwest Symp. Circ. Syst.,486-489.

Manetakis, K., Park, S., Payne, A., Setty, S., Thanachayanont, A., Toumazou, C. (1996). Wideband CMOS analog cells for video and wireless communications. Proc. Int. Conf. Electron., Circ.Syst., 227-230.

Metin, B., Arslan, E., Herencsar, N., Cicekoglu, O. (2011). Voltage-mode MOS-only all-pass filter. Proc. Int. Conf. on Tel. Signal Proc., 317-318.

Ngowand, S., Thanachayanont, A. (2003). A low-voltage wide dynamic range CMOS floating active inductor. Proc. Conf. Convergent Tech. for Asia-Pacific Reg., 4, 1640- 1643.

Uyanik, H. Tarim, N. (2007). Compact low voltage high-Q CMOS active inductor suitable for RF applications. Analog Int. Circ. Signal Process., 51 191-194.

Thanachayanont, A., Payne, A. (1996). VHF CMOS integrated active inductor. IEE Electron. Lett., 32, 999-1000.

Thanachayanont, A. (2002). CMOS transistor-only active inductor or IF/RF applications. Proc. IEEE Int. Industrial Tech. Conf., 2, 1209-1212.

Zhao, J., Jiang, J. G., Liu, J. N. (2010). Design of tunable biquadratic filters employing CCCIIs: state variable block diagram approach. Analog Integr Circuits Signal Process, 62, 397–406.

International Conference on Science and Technology

ICONST 2018

5-9 September 2018 Prizren - KOSOVO

The Evaluation of Leader and Leader Candidate Seafarers' Leadership Motivation, Leadership Fear, Regulatory Focus and Role Model

Leyla Tavacıoğlu[1]*, Özge Eski[1], Neslihan Gökmen[1], Burak Uzun[1], Ufukcan Tizgil[1]

Abstract: The aim of this research was to evaluate the relations among selective information processing about role models (SIP), motivation to lead (MTL), fear of leadership (FOL), role model evaluation and regulatory focus. It is obvious that the appropriate leadership are essential for safety at sea. In literature review, innotivation in academic and health domains by positive and negative role models depending on regulatory focus was investigated. This research study targets leader and leader candidate seafarers and uses randomsampling methods. Data were collected from 200 students of ITU Maritime Faculty and 40 master (leader) seafarers working in the Shipping companies. Data were gathered online through Qualtrics. 6 different types of questionnaires were applied. SIP, a hypothetical role model text describing the event of the leading seafarer was presented. Role model evaluation, participants were asked to rate how happy-unhappy, successful-unsuccessful they thought the leader was and how positive-negative the leadership experience of the role model was and how much they aspired to be like this role model. MTL has three subscales: affective, noncalculative, social-normative. Regulatory focus is composed of two subscales assessing prevention and promotion focus. FOL has 16 items that comprised of a list of possible negative consequences of leadership. Finally, 7 demographic questions were asked. Bivariate correlation analysis was used to determine relations between scales and Structural Equation Model (SEM) is developed to test relationships between SIP, MTL, FOL, role model evaluation and regulatory focus. Bivariate correlations with Pearson coefficients between all variables are utilized. Correlation analysis led to SEM. As a result of SEM analysis, relations between scales have statistically significant path coefficients. Theoretical and practical implications of the findings are discussed.

Keywords: Leadership, Motivation, Role Model, Seafarer

Introduction

An example is given to explain the role model evaluation: Person B is the master of Person A, the master on the Sismik ship. A wants to become a master in the future by observing B's successes. However, person C, who works on the same ship under B at the same time as A, decides that there should not be a master in the future after observing B's problem in family life. What could be the underlying reason for the different decisions that A and B made about becoming masters, assuming they knew B's life at an equally well? The main reason why they are involved in different aspects of the role model is the difference in evaluating the role model. This difference can be a result of the individual difference in their regulatory focus. The purpose of this study is to investigate the relationship between regulatory focus, fear of leadership, role model evaluation, selective information processing on role models and motivation to lead.

[1]İstanbul Techinical University, Faculty of Maritime, 34940, İstanbul, TURKEY
*Corresponding author: tavaciog@itu.edu.tr

Previous studies have investigated motivation in healthcare field and academic domain with positive and negative role models depending on the regulatory focus. Nevertheless, a single role model has both positive and negative experiments, instead of having totally positive or negative experiments. On such an occasion, what is positive or negative to evaluate the role model is part of the role model's experiment of people's participation. We recommend that the role model be evaluated differently by people with different regulatory focus by selectively processing information about role models. People who have promotion focus are more likely to evaluate the role model positively owing to the selective processing of positive experiments of a role model and people who have prevention focus are more likely to evaluate the role model negatively owing to the selective processing of negative experiences of a role model.

Higgins (1997) expressed that there are two subscales in regulatory focus theory: prevention focus and promotion focus. Prevention focus are responsive to presence and absence of negative outcomes and oppositely, promotion focus are responsive to presence and absence of positive outcomes. Brockner and Higgins (2001) suggested that leadership behaviors can be perceived as part of promotion-focus assumptions, and then encourage creative behaviors by revealing employees' promotion focus. We expected, Regulatory focus will predict motivation to lead and fear of leadership. Luria and Berson (2013) expressed that motivation to lead was associated with both formal and informal leadership emergence. Participants with low MTL were selected as leaders by less group members and less inclined to assume leadership roles in comparison to participants with high MTL. We expected, role model evaluation will predict MTL. In the this study, we investigated whether regulatory focus, selective information processing, role model predicts motivation to lead and fear of leadership. It is obvious that the leadership are essential for maritime sector, because of the fact that hierarchy is more predominant in the management of maritime sector compared to most inland based businesses (Tavacıoğlu, 2014). In this direction, we have three hypotheses:

Hypothesis 1: Motivation to lead (MTL) will be predicted by regulatory focus, Selective Information Processing (SIP) and role model. People with promotion focus will positively evaluate the motivation to lead.

Hypothesis 2: Fear of leadership (FOL) will be predicted by regulatory focus and SIP. People with prevention focus will positively evaluate the fear of leadership.

Hypothesis 3: Prevention focus and promotion focus will covariates with each other oppositely.

Material and Method

Data were collected from 200 maritime students and 40 masters (leaders) in maritime company. Data were gathered online and anonymously through Qualtrics. Sample was recruited by sharing the Qualtrics link with our network and through e-mails. The response rate is 64% (118 students, 35 masters). The leadership text consisting of 4 paragraphs on maritime was given in the first part. We offered three questions to check that the participants actually read the paragraph. Those who responded wrongly to at least one fell down. 5 positive and 5 negative sentences existing in the text are selected and these sentences are marked in a box after the participants read the text (SIP). For the role model evaluation, participants were asked to rate how happy-unhappy, successful-unsuccessful they thought the leader was and how positive-negative the leadership experience of the role model was and how much they aspired to be like this role model (rated 0 to 100). The Questionnaires were asked into that order: MTL, Regulatory Focus, FOL. Finally, Participants were asked to report their gender, educational level, whether they are currently employed or not.

Descriptive statistics were calculated for continous variables (mean, standard deviation (SD), minimum, maximum, median) and categorical variables (N, %) showed in Table 1.

Table 1. Demographic characteristics of the participants (N=153)

		Mean±SD	Median (Min-Max)
Age		27,5±9,3	24 (19-70)
How many years of work experience do you have?		7,1±9,8	2,7 (0,08-43,0)
		N	**%**
Gender	**Female**	22	14.9
	Male	126	85.1
Education	**High School**	58	39.2
	Bachelor's Degree	7	4.7
	Master's Degree	62	41.9
Occupation	**Employee**	35	22.8
	Student	118	77.1
Position	**Administrative**	11	7.2
	Not Administrative	24	15.7

Selective Information Processing About Role Model (SIP)

A hypothetical role model text was presented about maritime. On the top of the text, they saw a page in which it is written that they should carefully read the following text, since there will be questions about the text and they had 5 minutes to read it. The text had the same amount of sentences presenting positive and negative experiences of the role model. Three questions were presented to check whether the participants really read the paragraph and who responded wrongly to at least one dropped out. After answering check questions, they selected the sentences that they thought are indicated in the text. 5 positive and 5 negative sentences existing in the text are selected and for measuring SIP about role model number of the positive sentences in the box were subtracted from number of negative sentences in the box. The mean number of negative sentences selected was 2.76 (SD=1.58). The mean number of positive sentences selected was 2.95 (SD=1.61). The mean of calculated SIP was -0.2 (SD=1.4). It showes that positive sentences picked more than negatives.

Role Model Evaluation

For the role model evaluation, semantic differentials were used. That is, participants were asked to rate how happy-unhappy, successful-unsuccessful they thought the leader was and how positive-negative the leadership experience of the role model was and how much they aspired to be like this role model (Sandal, 2014).

Motivation to Lead Scale

The original MTL scale was composed of 27 items developed by Chan and Drasgow (2001). The scale has three subscales: affective, noncalculative, social-normative. For purposes of this study, we only used 18 items that are related to affective and social-normative subscales. Items are scored on a 5-point Likert scale (1= totally disagree to 5= totally agree). Cronbach's alpha was .78 for the current study and it shows that the scale was consistent. The mean of MTL was 3.3 (SD=0.5)

Regulatory Focus Scale

The 18 items questionnaire developed by Lockwood et al. (2002) was used to measure regulatory focus of participants. The questionnaire has two subscales: prevention and promotion goals. Items are scored on a 5-point Likert scale (1= totally disagree to 5= totally agree). Turkish version of the questionnaire was obtained from Canacik (2006) and used in this study. Cronbach's Alpha was .70 for prevention focus subscale and .76 for promotion focus subscale, indicating that both subscales are consistent. The mean of prevention focus was 2.9 (SD=0.8) and promotion focus was 3.7 (SD=0.7). The mean of promotion focus was found higher than prevention focus.

Fear of Leadership Scale (FOL)

The 16-item scale was developed by Aycan et al. (2014). They rated items on a 5-point Likert scale ranging from “very low levels of anxiety” to “very high levels of anxiety. The items comprised of a list of possible negative consequences of leadership. The reliability for the current study was .87. The mean of FOL was 3.3 (SD=0.6)

Procudure

In order to evaluate bivariate relationships between scales, Pearson correlation analysis was used. All parametric assumptions are satisfied for each variables of conceptual model. So, Structural Equation Model (SEM) with Maximum Likelihood (ML) method is used to test conceptual model (Awang, 2015). Figure 1 shows the conceptual model structure. It is aimed to examine regression and path coefficients between latent factors and observed variables in accordance with established conceptual model. Chi-square to df ratio ($\chi 2$/df), RMSEA, CMIN/DF, SRMR model fit indices are used to evaluate model fit of established SEM (Gökçek, 2018).

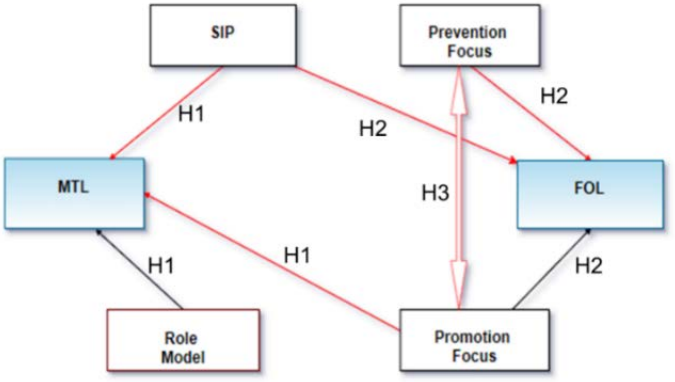

Figure 1. Conceptual Model

Results

In established SEM, MTL ve FOL is assigned as latent exogenous variable; Role model, Prevention and Promotion focus are assigned as latent endogenous variable; SIP is assigned as observed endogenous variable.

Residual error terms are included for each endogenous variable to treat disturbance as latent variables. MTL latent variable predicted by SIP, Promotion focus and Role model. FOL latent variable predicted by SIP, Promotion focus and Prevention focus. Prevention and promotion focus with eachother. Before testing of conceptual model, bivariate correlations with Pearson correlation coefficients between all variables are utilized. Results of correlation are presented in Table 2.

Table 2. Correlation between all variables

r; p	1	2	3	4	5	6
SIP[1]	1.000					
Role model[2]	0.141	1.000				
	0.093					
MTL[3]	**0.167**	0.108	1.000			
	0.045	0.199				
Prevention focus[4]	-0.036	-0.150	**0.195**	1.000		
	0.670	0.074	**0.019**			
Promotion focus[5]	**0.178**	**0.172**	**0.437**	**0.218**	1.000	
	0.033	**0.040**	**<0.001**	**0.008**		
FOL[6]	0.139	0.055	0.134	**0.418**	**0.212**	1.000
	0.099	0.520	0.110	**<0.001**	**0.011**	

There are statistically significant correlations between MTL and Role model; Prevention focus and MTL; Promotion focus and SIP, Role model, MTL, Prevention focus; FOL and Prevention focus, Promotion focus. All correlations are positive direction. There is a moderate correlation between promotion focus and MTL (.437), FOL and Prevention focus (0.418) and there is weak correlation with other pairs.

Those results provide support to established conceptual model of research. After correlation analysis, SEM is conducted with ML estimation method. Path coefficients and regression loads related to tested conceptual model is presented in Figure 2 and p values of variables are given in Table 3.

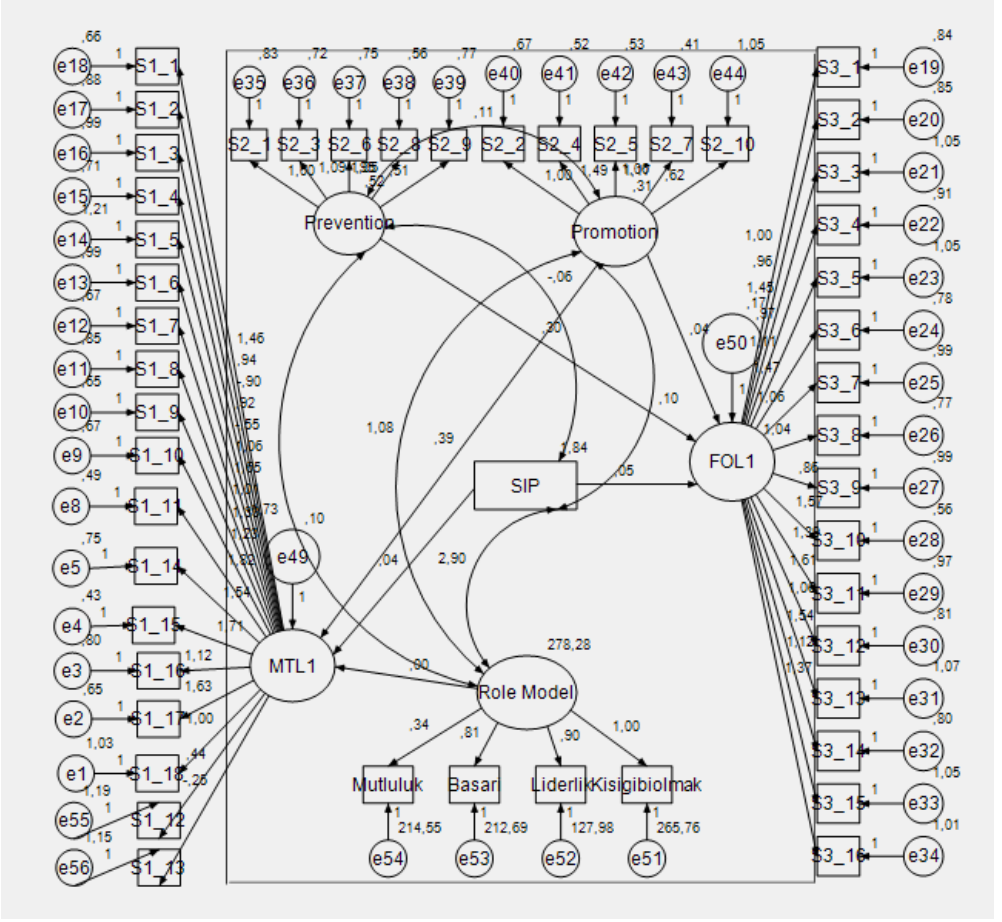

Figure 2. Path Coefficients of Conceptual Model

According to results of SEM analysis, relation between Role Model and MTL, Promotion focus and FOL have no statistically significant critical ratio value ($p>0.05$). The p values above 0.10 were accepted by 90% confidence. Paths which has insignificant p values should be excluded from SEM. Therefore, paths between Role Model and MTL, Promotion focus and FOL are removed. S1_12 and S1_13 are found to be not significant relation with MTL, these items are removed, and SEM is re-established. Critical ratios for all other regression weights are acceptable at the 0.05 level (Hoyle, 1995). Path coefficients and regression loads related to re-established conceptual model is presented in Figure 3 and coefficients and p values of variables are given in Table 4.

Table 3. Regression weights and their critical ratios of SEM

			Estimate	S.E.	C.R.	p
FOL1	<---	Prevention	.299	.088	3.395	**<.001**
MTL1	<---	Promotion	.386	.118	3.255	**.001**
MTL1	<---	SIP	.040	.024	1.669	**.095**
FOL1	<---	SIP	.053	.030	1.792	**.073**
MTL1	<---	Role Model	.001	.006	.180	.858
FOL1	<---	Promotion	.037	.083	.444	.657
S1_18	<---	MTL1	1.000			
S1_17	<---	MTL1	1.632	.418	3.905	**<.001**
S1_16	<---	MTL1	1.123	.328	3.423	**<.001**
S1_15	<---	MTL1	1.712	.422	4.057	**<.001**
S1_14	<---	MTL1	1.538	.405	3.794	**<.001**
S1_13	<---	MTL1	-.245	.248	-.989	.323
S1_12	<---	MTL1	.436	.266	1.640	.101
S1_11	<---	MTL1	1.824	.449	4.058	**<.001**
S1_10	<---	MTL1	1.225	.338	3.626	**<.001**
S1_9	<---	MTL1	1.327	.356	3.723	**<.001**
S1_8	<---	MTL1	1.012	.313	3.234	**.001**
S1_7	<---	MTL1	1.651	.423	3.902	**<.001**
S1_6	<---	MTL1	1.065	.333	3.198	**.001**
S1_5	<---	MTL1	-.550	.279	-1.972	**.049**
S1_4	<---	MTL1	.921	.285	3.234	**.001**
S1_3	<---	MTL1	-.903	.307	-2.946	**.003**
S1_2	<---	MTL1	.936	.303	3.094	**.002**
S1_1	<---	MTL1	1.456	.382	3.808	**<.001**
S3_1	<---	FOL1	1.000			**<.001**
S3_2	<---	FOL1	.963	.238	4.046	**<.001**
S3_3	<---	FOL1	1.451	.313	4.639	**<.001**
S3_4	<---	FOL1	.967	.242	3.991	**<.001**
S3_5	<---	FOL1	1.109	.269	4.126	**<.001**
S3_6	<---	FOL1	1.465	.300	4.885	**<.001**
S3_7	<---	FOL1	1.056	.259	4.084	**<.001**
S3_8	<---	FOL1	1.035	.241	4.303	**<.001**
S3_9	<---	FOL1	.857	.236	3.635	**<.001**
S3_10	<---	FOL1	1.573	.304	5.178	**<.001**
S3_11	<---	FOL1	1.393	.300	4.636	**<.001**
S3_12	<---	FOL1	1.610	.323	4.988	**<.001**
S3_13	<---	FOL1	1.062	.264	4.019	**<.001**
S3_14	<---	FOL1	1.542	.312	4.943	**<.001**
S3_15	<---	FOL1	1.121	.270	4.151	**<.001**
S3_16	<---	FOL1	1.367	.299	4.569	**<.001**
S2_1	<---	Prevention	1.000			**<.001**
S2_3	<---	Prevention	1.095	.178	6.138	**<.001**
S2_6	<---	Prevention	.951	.164	5.785	**<.001**
S2_8	<---	Prevention	1.051	.167	6.280	**<.001**
S2_9	<---	Prevention	.511	.129	3.957	**<.001**
S2_2	<---	Promotion	1.000			**<.001**
S2_4	<---	Promotion	1.488	.245	6.069	**<.001**
S2_5	<---	Promotion	1.058	.192	5.512	**<.001**
S2_7	<---	Promotion	1.167	.197	5.925	**<.001**
S2_10	<---	Promotion	.625	.190	3.291	**.001**
Mutluluk	<---	Role Model	1.000			
Basari	<---	Role Model	2.409	.628	3.836	**<.001**
Liderlik	<---	Role Model	2.680	.684	3.920	**<.001**
Kisi gibi olmak	<---	Role Model	2.962	.764	3.875	**<.001**
Prevention	<->	Promotion	.111	.046	2.396	**.017**

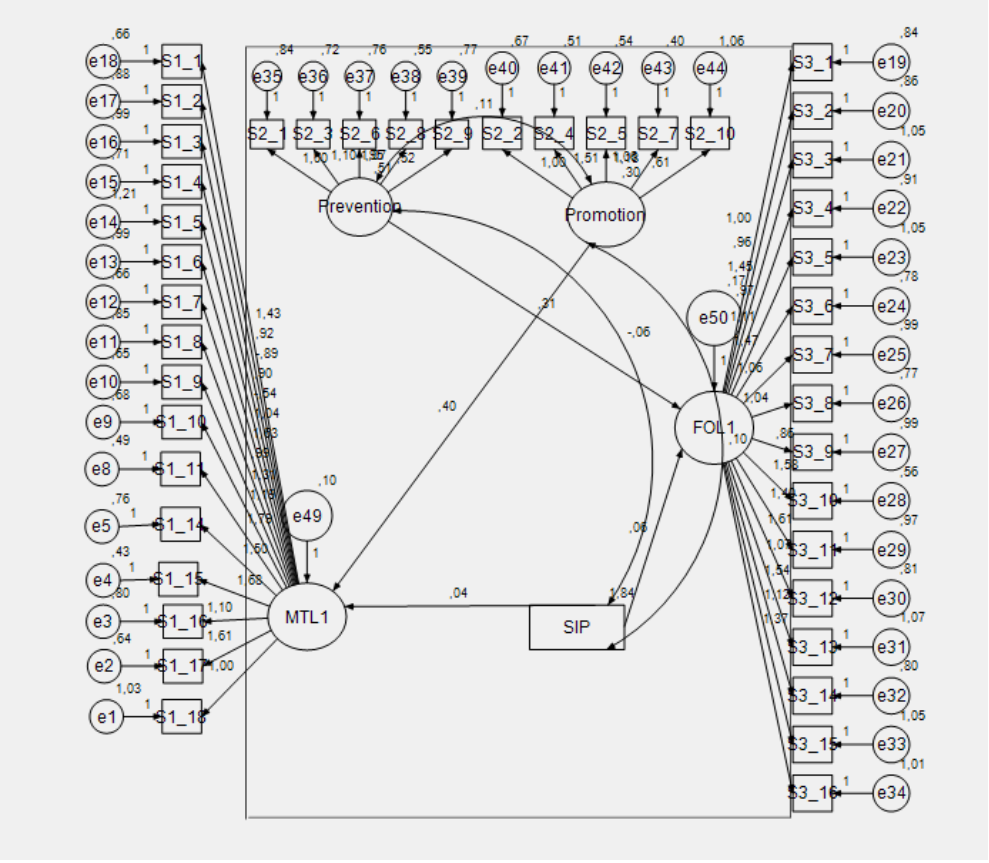

Figure 3. Re-Established Path Coefficients of Conceptual Model

Results of re-established SEM analysis is showed that critical ratios for all other regression weights are acceptable at the 0.010 (90% confidence) level (Table 5). This model is tested with model fit indices. $\chi 2/df$ value for SEM is found as 1.934 ($\chi 2=265.818$, df=162) and it refers to perfect model (Tabachnick, 2013). Besides, absolute fit indices (RMSEA, SRMR) values suggest a good model fit. AIC are given to compare initial conceptual model with final model. Results of indices are shown in Table 4. According to path coefficients and p values, H1, H2, H3 are found acceptable at the level of 0.010 (Table 5). All acceptable hypothesizes of whole conceptual model are shown in Figure 4.

Table 4. Descriptive items of model fit indices of SEM

	Good Fit	**Sample Statistics**		**Rationale**
		Initial Model	**Re-Established Model**	
CMIN/DF	$0 \leq \chi 2/df \leq 5$	1.863	1.934	Wheaton, Muthen, Alwin, and Summers (1977)
RMSEA	$0 \leq RMSEA \leq .08$	0.075	0.078	Steiger (2007)
SRMR	$SRMR \leq .10$	0.1030	0.1029	Çokluk, Şekercioğlu, Büyüköztürk (2016)
AIC	Min. value	2296.634	1835.420	Wagenmakers and Farrel (2002)

Table 5. Regression weights and their critical ratios of re-established SEM

			Estimate	S.E.	C.R.	p
FOL1	<---	Prevention	.312	.088	3.566	**<.001**
MTL1	<---	Promotion	.398	.121	3.299	**<.001**
MTL1	<---	SIP	.041	.024	1.708	**.088**
FOL1	<---	SIP	.056	.029	1.898	**.058**
S1_18	<---	MTL1	1.000			
S1_17	<---	MTL1	1.611	.406	3.971	**<.001**
S1_16	<---	MTL1	1.100	.318	3.457	**<.001**
S1_15	<---	MTL1	1.682	.408	4.125	**<.001**
S1_14	<---	MTL1	1.498	.390	3.838	**<.001**
S1_11	<---	MTL1	1.790	.434	4.124	**<.001**
S1_10	<---	MTL1	1.195	.326	3.662	**<.001**
S1_9	<---	MTL1	1.309	.346	3.780	**<.001**
S1_8	<---	MTL1	.989	.303	3.258	**.001**
S1_7	<---	MTL1	1.632	.411	3.968	**<.001**
S1_6	<---	MTL1	1.042	.323	3.223	**.001**
S1_5	<---	MTL1	-.542	.273	-1.983	**.047**
S1_4	<---	MTL1	.901	.276	3.258	**.001**
S1_3	<---	MTL1	-.890	.299	-2.976	**.003**
S1_2	<---	MTL1	.917	.294	3.116	**.002**
S1_1	<---	MTL1	1.429	.370	3.862	**<.001**
S3_1	<---	FOL1	1.000			
S3_2	<---	FOL1	.964	.239	4.037	**<.001**
S3_3	<---	FOL1	1.454	.314	4.628	**<.001**
S3_4	<---	FOL1	.969	.243	3.985	**<.001**
S3_5	<---	FOL1	1.115	.270	4.127	**<.001**
S3_6	<---	FOL1	1.470	.301	4.878	**<.001**
S3_7	<---	FOL1	1.058	.259	4.077	**<.001**
S3_8	<---	FOL1	1.039	.242	4.299	**<.001**
S3_9	<---	FOL1	.859	.237	3.629	**<.001**
S3_10	<---	FOL1	1.576	.305	5.165	**<.001**
S3_11	<---	FOL1	1.396	.302	4.627	**<.001**
S3_12	<---	FOL1	1.614	.324	4.977	**<.001**
S3_13	<---	FOL1	1.066	.265	4.017	**<.001**
S3_14	<---	FOL1	1.545	.313	4.931	**<.001**
S3_15	<---	FOL1	1.123	.271	4.145	**<.001**
S3_16	<---	FOL1	1.372	.301	4.563	**<.001**
S2_1	<---	Prevention	1.000			
S2_3	<---	Prevention	1.104	.181	6.094	**<.001**
S2_6	<---	Prevention	.947	.166	5.698	**<.001**
S2_8	<---	Prevention	1.069	.171	6.257	**<.001**
S2_9	<---	Prevention	.523	.131	3.994	**<.001**
S2_2	<---	Promotion	1.000			
S2_4	<---	Promotion	1.508	.249	6.051	**<.001**
S2_5	<---	Promotion	1.060	.194	5.471	**<.001**
S2_7	<---	Promotion	1.180	.200	5.908	**<.001**
S2_10	<---	Promotion	.613	.191	3.216	**.001**
Prevention	<->	Promotion	.112	.046	2.457	**<.001**

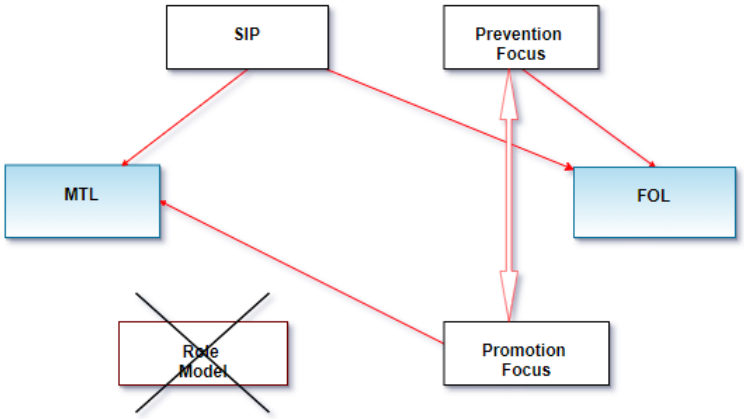

Figure 4. Acceptable Hypotheses of Conceptual Model.

Discussion and Conclusions

The main purpose of the study was to examine the role of regulatory focus, role models and FOL in MTL. We expected that the relation between promotion focus and selective information processing (SIP) found in consumer research will reveal itself also when people evaluating the role model in terms of role model's success, happiness and positivity of leadership experience and aspiration to be like the role model.

Motivation to lead (MTL) was defined as "an individual differences construct that affects a leader's or leader-to-be's decisions to assume leadership training, roles, and responsibilities and that affect his or her intensity of effort at leading and persistence as a leader" (Chan & Drasgow, 2001, p.487). Participants with high MTL were both selected as leaders by more group members and tended to assume leadership roles when compared to participants with low MTL (Sandal, 2014). We expected that role model evaluation will predict MTL. Promotion focus and SIP were found to have a significant effect on MTL. According to SEM results, promotion focus was 40% effective on MTL and SIP 4% effective on MTL. In the first hypothesis, the role model effect thought was not significant.

Drawing upon the conceptualization of FOL, we suggested that if people have high levels of FOL, prevention focus is increased. Thus, we predicted that FOL and prevention focus have relationship. SEM results showsPrevention focus and SIP were found to have a significant effect on FOL. Prevention focus was 31% effective on FOL and SIP was 6% effective on MTL. Prevention and promotion focus covariates and 11% effective with eachother.

The first limitation of the present study was sample characteristics in terms of gender. Our sample consisted mostly of men. Therefore, we cannot generalize our findings to women. This is acceptable because maritime is mostly preferred by men. The second limitation of the present study was that our data was based on self-report.

The insignificant results regarding role model might be attributed to the use of self report in process of information. Future studies might use brain activities or attention measures to determine the role model. In addition, future studies might look for other possible predictors which predicts MTL and FOL. Despite those limitations, the findings are expected to contribute human resources policies. The present study shows the relation between regulatory focus and MTL, FOL.

References

Hoyle, R.H., (1995). Structural Equation Modeling: Concepts, Issues, and Applications: Sage.

Chan, K. Y., & Drasgow, F. (2001). Toward a theory of individual differences and leadership: Understanding the motivation to lead. Journal of Applied Psychology, 86, 481–498.

Brockner, J., Higgins, E.T., (2001). Regulatory focus theory: implications for the study of emotions at work. Organizational Behavior & Human Decision Processes 86 (1), 35–66.

Wagenmakers E., Farrel S. (2002). AIC model selection using Akaike weights. Psychonomic Bulletin & Review, 11, 192-196.

Lockwood, P., Jordan, C., & Kunda, Z. (2002). Motivation by positive or negative role models: Regulatory focus determines who will best inspire us. Journal of Personality and Social Psychology, 83, 854–864.

Lockwood, P., Sadler, P., Fyman, K., & Tuck, S. (2004). To do or not to do: Using positive and negative role models to harness motivation. Social Cognition, 22, 422-450.

Lee, A., & Aaker, J. (2004). Bringing the frame into focus: The influence of regulatory fit on processing fluency and persuasion. Journal of Personality and Social Psychology, 86, 205–18.

Lockwood, P., Chasteen, A. L., & Wong, C. (2005). Age and regulatory focus determine preferences for health-related role models. Psychology and Aging, 20, 376-389.

Canacik, B. (2006). Environmental scanning and interpretation of institutionalism by middle sized family enterprises in the Marmara Region, Turkey. Master's Thesis, Koc University, Istanbul, Turkey.

Higgins, E. T. (2012). Regulatory focus theory. In P. Van Lange, A. Kruglanski, & E. Higgins (Eds.), Handbook of theories of social psychology. 1, 483-505, London: SAGE Publications Ltd.

Tabachnick, B.G., and Fidell, L.S., (2013). Using Multivariate Statistics (Sixth ed.). Boston: Pearson.

Luria, G., & Berson, Y. (2013). How do leadership motives affect informal and formal leadership emergence?. Journal of Organizational Behavior, 34, 995-1015.

Tavacioglu, L., Cap, H., Bolat, P., Zorluoglu. G. "Investigation of The Management and Leadership Concepts in Maritime Sector: A Sample Study Amongst Turkish Seafarers", 06/2014, s. 110-117, 6th International conference on Maritime Transport, Barcelona, 25.06.2014 - 27.06.2014.

Aycan, Z., Baskurt, A. B., Bicaker, E. et.al. (2014). Conceptualization and measurement of fear of leadership (FOL). Presented at International Congress of Applied Psychology. Paris, July.

Sandal, C. (2014). Motivation to Lead: The Role of Regulatory Focus, Role Models and Fear of Leadership. Yüksek Lisans Tezi. Koç Üniversitesi, Türkiye: İstanbul.

Awang, Z., Afthanorhan, W.M.A.W., and Asri, M., (2015). Parametric and NonParametric Approach in Structural Equation Modeling (SEM): The Application of Bootstrapping. Modern Applied Science, 9(9), 58.

Çokluk, Ö. Şekercioğlu, G. Büyüköztürk, Ş. (2016). Sosyal Bilimler İçin Çok Değişkenli İstatistik: SPSS ve LISREL Uygulamaları. Pegem Akademi Yayıncılık. 4.Baskı. Ankara.

Gökçek, V., Tavacıoğlu, L. (2018). A Quantitative Analysis on Leisure Particibation of Turkish Seafarers by Structural Ecuation Modeling, Engineering Science, 2/13, 137-155.

International Conference on Science and Technology

ICONST 2018

5-9 September 2018 Prizren - KOSOVO

A Research As Mobbing Examination in Maritime Sector

Leyla Tavacıoğlu[1]*, Neslihan Gökmen[1], Özge Eski[1], Vedat Sarı[1], A.Ceren Yılmaz[1]

Abstract: In the maritime industry, a person of lower class or rank is exposed to mobbing, which can easily be observed. In Turkey, instead of expressing mobbing in a specific word as "bullying in the workplace", replaced it as "emotional harassment", "psychological violence at work", "intimidation". The aim of the study is to determine the factors that affect the mobbing. Survey participants are 178 volunteers, almost all of the maritime university faculties and several private companies participated the survey. Data were collected in May 2018 in Turkey. Mobbing Scale (Leymann's LIPT-The Leymann Ivertory of Psychological For Social Sciences) was used. Mobbing scale has 5 factors: relationship, threat and harassment, business and career-related obstacles, private life, commitment to work. According to demographics, relationships between factors were assessed by correlation analysis. Multiple linear regression analysis was used to determine the factors affected the mobbing. 5 regression models were set up for each 5 factors. Bivariate correlations with Spearman's rho coefficients between all factors are utilized. According to regression results, it is seen that variables affected mobbing significantly. Demographics are effective in determining mobbing. Theoretical and practical implications of the findings are discussed.

Keywords: Mobbing, LIPT, Mobbing Scale.

Introduction

From hospitals to universities, employees encounter various problems in work environment. Mobbing is one of the most serious of these problems. Mobbing is psychological harassment or violence that is continuously or systematically applied by employees or employers for psychological or social reasons (Leymann 1990; Zapf, 1999; Einersen et al., 2003; Lewis, 2003; Tınaz, 2006). Mobbing is a term used to describe psychological terror, emotional lynching, abuse, bullying and terrorization in the workplace. There are many studies related to mobbing in the literature. In 1960, the definition of mobbing was first used to analyze animal behavior by Konrad Lorenz. Brodsky (1976) defines mobbing as repressive, frightening, scary and uncomfortable behaviors that are repeatedly and intentionally displayed by one repeatedly and persistently to intimidate and annihilate another. Thylefors (1987) defines mobbing as repetitive negative behaviors against one or more people by one or more people. Matthiesen, Raknes ve Rrökkum (1989) defines mobbing as repetitive negative behaviors that one or more people carry out against one or more persons in the working environment. Leyman (1990) defines mobbing as hostile and unethical behaviors carried out by one or more people systematically. Kile (1990) defines mobbing as a derogatory action that a superior is performing openly or secretly. Wilson (1991) defines mobbing as continuous and intentional maltreatment towards an employer. Adams (1992) defines mobbing as behaviors aimed at giving spiritual suffering to those who are unable to defend themselves. Vartia (1993) defines mobbing as regularly humiliating behavior against one person by one or more people. Björkqvist, Österman ve Hjelt-Back (1994) defines mobbing as a superior authority to use subordinates in humiliating, arbitrary punishment (Einarsen, 2000). Zapf, Knorz ve Kulla (1996) describe mobbing as any negative behavior that affects both the psychology and the physical well-being of the victim. Davenport, Schwartz, and Elliott define mobbing as a collection of evil movements, ideals and actions that are intended to force a person or group of a worker to resign (2003).

[1] Istanbul Technical University, Faculty of Maritime, 34940, Istanbul, TURKEY
*Correspondingauthor: : tavaciog@itu.edu.tr

Mobbing is an universal problem and can be observed in any industry. Regardless of their demographic characteristics, every employee can be exposed to mobbing. Mobbing has different negative effects on employees' work life and private life; such as insomnia, anxiety, depression, irritability (Einarsen, 1999; Leymann, 1990), lack of concentration (Namie, 2008), loneliness (Huse and Cummings, 1985), alienation from work/organization (Tolan, 1981), desensitization to organizational values, goals and ethical rules (Tutar, 2004). Mobbing is a process that can be end up with the resignation of the employee (Paparella et al., 2004).

There are several studies on mobbing-personal and organizational reasons, mobbing-organizational culture and organizational climate. These studies indicate that mobbing has negative effect on performance and productivity of the employee and the organization (Vartia, 2003). The maritime sector is one of the sectors where mobbing is often encountered. Yıldırım and Tavacıoğlu (2017), determined the relationship between the job performance and job stress of the seafarers and carried out that mobbing increases working stress and decreases personal performance. But, there is a big gap in this issue in the literature. The aim of this study is to examine the mobbing perceptions of seafarers in terms of general variables such as age, gender, education level, experience on board, and position at work.

Material and Method

Data were collected from 220 seafarers, but, in total, 178 seafarers participated in the survey (Response rate: 81%). Data were gathered online and anonymously through SurveyMonkey. Sample was recruited by sharing the SurveyMonkey link with our network and through e-mails. To understand and measure mobbing, the Leymann Inventory for Psychological Terrorisation (LIPT) scale was used. Questionnaire form was derived from LIPT. The questionnaire consists of two parts. First part includes demographic characteristics of the participants. The second part of the questionnaire includes mobbing questions. 7-point Likert scale ranging from "strongly disagree" through to "strongly agree'' was used. Descriptive statistics were calculated for continous variables (mean, standard deviation (SD), minimum, maximum, median), categorical variables (N, %) and distribution of scales showed in Table 1. Pearson correlation analysis was used to determine two normally distributed variables and Spearman's rho correlation analysis was used to determine two non-normally distributed variables. It is shown in Table 2 and Figure 1. Comparison of two independent and normally distributed variables Student's t test was used, to compare two independent and non-normally distributed variables Mann Whitney U test was used. Comparison of more than two independent and normally distributed variables One Way ANOVA test was used, to compare more than two independent and non-normally distributed variables Kruskal Wallis test was used. It is shown in Table 3. Multiple linear regression modeling was used to examine the effect of independent variables on the continuous dependent variable, and the Backward variable selection method was used. It is shown in Table 4. Statistical significance level was determined as 0.05. The analysis was conducted by utilising SPSS 24.0 (Statistical Package for the Social Sciences).

According to Table 1, 22 women (12,4%) and 156 men (87,6) participated in this study. 83 of 178 participants (46,6%) are between 18-25 years. The educational status of 128 of 178 participants (71,9%) is bachelor degree. 55 of 178 participants (31,1%) have worked on board for 3-6 months. 80 of 178 participants (45,2%) are deck/engine cadets.

Table 1. Demographic characteristics of the participants (N=178) and distributions of scales

		N	%
Age (years)	18-25	83	46.6
	25-30	51	28.7
	30-45	33	18.5
	45-60	9	5.1
	60 and older	2	1.1
Gender	Female	22	12.4
	Male	156	87.6
Education	High School	7	3.9
	Associate Degree	8	4.5
	Bachelor Degree	128	71.9
	Graduate Level	35	19.7
Department	Deck	128	71.9
	Engine	50	28.1
Experience (on board)	3-6 months	55	31.1
	6-12 months	45	25.4
	1-3 years	28	15.8
	3 years and over	49	27.7
Position	Deck/Engine Cadet	80	45.2
	3.Officer /4. Engineer	18	10.2
	2.Officer /3. Engineer	27	15.3
	Chief Officer /2. Engineer	24	13.6
	Master/Chief Engineer	17	9.6
	Other	11	6.2
	N	**Mean±SD**	**Median (Min.-Max.)**
Relationship with Colleagues	178	2.45±1.18	2.18 (1-7)
Threat and Harassment	178	1.64±0.84	1.43 (1-7)
Barriers Related to Job and Career	178	2.92±1.5	2.44 (1-7)
Interference in Private Life	178	2.05±1.22	1.88 (1-7)
Commitment to Work	178	2.56±1.63	2.00 (1-7)

Results

According to correlation analysis, there is no significant relationship between relationship with colleagues and other scales (Spearman's rho p>0.05). There are positive moderate statistically significant correlations between threat and harassment and barriers related to job and career; interference in private life and commitment to work. There is a positive weak correlation between barriers related to job and career and interference in private life. There is a positive moderate statistically significant correlations between barriers related to job and carrier and interference in private life (Table 2) (Zou et al., 2003; Rumsey, 2007). Figure 1 supports the correlation results.

Table 2. Correlation analysis between scales

r **p**	**Relationship with Colleagues**	**Threat and Harassment**	**Barriers Related to Job and Career**	**Interference in Private Life**	**Commitment to Work**
Relationship with Colleagues	1.000				
Threat and Harassment	-0.056	1.000			
	0.461				
Barriers Related to Job and Career	-0.002	**0.471**	1.000		
	0.984	**<0.001**			
Interference in Private Life	-0.143	**0.609**	**0.379**	1.000	
	0.057	**<0.001**	**<0.001**		
Commitment to Work	-0.023	**0.544**	**0.705**	**0.481**	1.000
	0.762	**<0.00**	**<0.001**	**<0.001**	

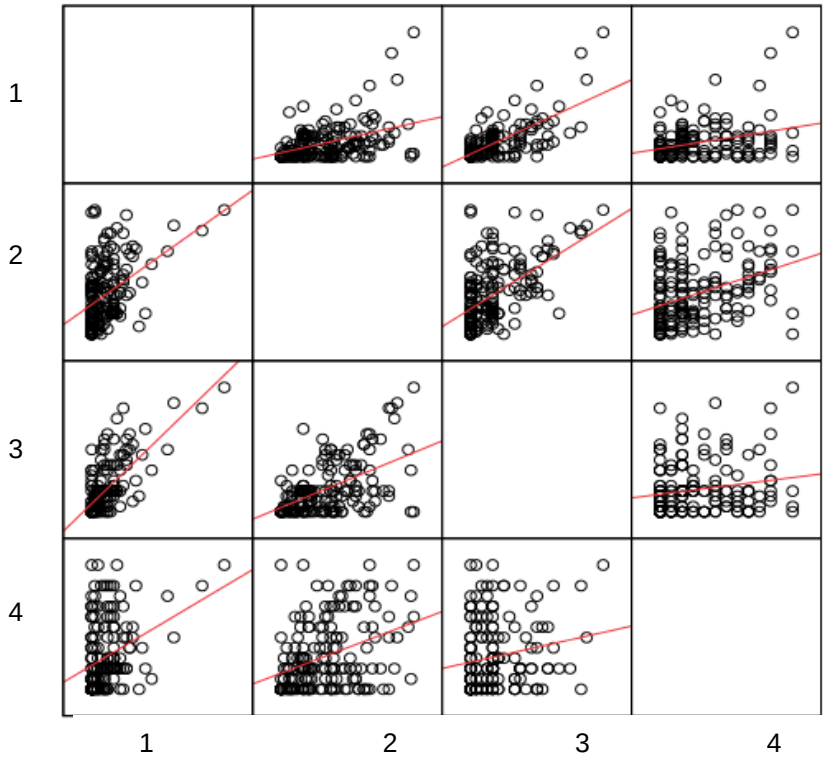

Figure 1. Scatter plots of correlations

1. Threat and Harassment 2. Barriers Related to Job and Career 3. Interference in Private Life 4. Commitment to Work

Table 3. Comparison of Scales According to Demographics

Mean±SD Median (Min.-Max.)		Relationship with Colleagues	Threat and Harassment	Barriers Related to Job and Career	Interference in Private Life	Commitment to Work
Age	**18-25**	2.6±1.2 2.3 (1-7)	1.7±0.9 1.6 (1-7)	3.1±1.5 3 (1-7)	2.2±1.3 2 (1-7)	2.7±1.7 2 (1-7)
	25-30	2.4±1.4 2 (1-6.4)	1.5±0.9 1.1 (1-6)	3.1±1.7 2.7 (1-7)	1.9±1.3 1.5 (1-6.2)	2.8±1.7 2.5 (1-7)
	30-45	2.2±0.6 2.3 (1.2-3.7)	1.5±0.5 1.4 (1-2.4)	2.5±1.06 2.1 (1-5.2)	1.8±0.9 1.7 (1-4.5)	2.1±1.2 2 (1-5)
	45 and older	2.1±0.8 2.1 (1.2-4.1)	1.8±0.9 1.7 (1-3.4)	1.7±0.7 1.7 (1-3.4)	1.9±1.1 2 (1-5)	2.1±0.7 2 (1-3.5)
	p*	0.199	0.165	**0.006**	0.576	0.285
Gender	**Female**	2.7±1.1 2.3 (1.3-5.3)	1.9±0.9 1.6 (1-4.4)	2.9±1.2 2.7 (1-5.1)	2.4±1.3 2 (1-5)	2.6±1.6 2 (1-6)
	Male	2.4±1.2 2.2 (1-7)	1.6±0.8 1.3 (1-7)	2.9±1.5 2.4 (1-7)	2±1.2 1.7 (1-7)	2.5±1.6 2 (1-7)
	p	0.221	0.068	0.456	0.191	0.658
Education	**High School**	3.3±1 3.6 (1.9-4.6)	2.3±0.9 2 (1-3.7)	3.1±1.2 3 (1.9-5)	2.6±1.3 2 (1-5)	2.7±1.5 2.5 (1-5)
	Associate Degree	2.4±0.9 2.1 (1.3-4.5)	1.5±0.7 1.2 (1-3.1)	3.5±2.6 2.1 (1.2-7)	1.6±0.7 1.5 (1-3)	3.2±1.4 3.2 (1-5.5)
	Bachelor's Degree	2.5±1.3 2.1 (1-7)	1.7±0.9 1.4 (1-7)	2.9±1.6 2.7 (1-7)	2.1±1.3 1.9 (1-7)	2.6±1.7 2 (1-7)
	Graduate Level	2.1±0.7 2.2 (1-4.7)	1.5±0.5 1.3 (1-2.7)	2.5±0.9 2.2 (1-4.9)	1.8±1 1.5 (1-4.7)	2.1±1.2 2 (1-7)
	p*	0.177	0.221	0.532	0.261	0.263
Department	**Deck**	2.4±1.1 2.1 (1-7)	1.6±0.8 1.4 (1-7)	2.9±1.5 2.4 (1-7)	2±1.2 2 (1-7)	2.6±1.6 2 (1-7)
	Engine	2.5±1.2 2.2 (1-6)	1.7±0.9 1.4 (1-6)	2.9±1.6 2.4 (1-6.7)	2.1±1.3 1.6 (1-6)	2.5±1.6 2 (1-6)
	p	0.937	0.569	0.826	0.938	0.726
Experience (on board)	**3-6 months**	2.6±1.1 2.3 (1-5.1)	1.7±0.6 1.7 (1-3.7)	3.2±1.7 3 (1-7)	2.1±1.1 2 (1-5.5)	2.5±1.6 2 (1-7)
	6-12 months	2.5±1.4 2.2 (1.1-6.4)	1.5±0.7 1.3 (1-4.4)	3.2±1.6 3.2 (1-6.9)	2.1±1.2 1.7 (1-6)	2.8±1.9 2 (1-6)
	1-3 years	2.7±1.4 2.3 (1-7)	1.9±1.5 1.5 (1-7)	2.9±1.4 2.4 (1.2-7)	2.3±1.7 2 (1-7)	2.9±1.7 2.5 (1-7)
	3 years and more	2.1±0.7 2 (1-4.7)	1.4±0.6 1 (1-3.4)	2.2±1.1 2 (1-5.2)	1.8±0.9 1.7 (1-5)	2.2±1.3 2 (1-7)
	p*	0.163	**0.028**	**0.005**	0.444	0.194
Position	**Deck/Engine Cadet**	2.6±1.3 2.3 (1-7)	1.7±0.8 1.5 (1-7)	3.4±1.6 3.3 (1-7)	2.1±1.3 2 (1-7)	2.8±1.8 2 (1-7)
	3.Officer /4.Engineer	3±1.4 2.4 (1.41-6.24)	1.7±0.9 1.2 (1-4.71)	3.0±1.7 2.3 (1.25-6.75)	2.2±1.5 1.8 (1-6.25)	2.2±1.3 1.7 (1-5)
	2.Officer /3.Engineer	2.1±0.9 2.1 (1-6)	1.6±0.9 1.4 (1-6)	2.5±1.1 2.2 (1-6)	2.0±1.2 1.7 (1-6)	2.4±1.5 2 (1-7)
	Chief Officer /2. Engineer	2.1±0.6 2.1 (1-4.29)	1.4±0.6 1 (1-3.14)	2.2±1.0 2 (1-4.75)	1.7±0.8 1.5 (1-4.25)	2.1±1.5 1.2 (1-7)
	Master/Chief Engineer	1.9±0.6 1.9 (1.18-3.65)	1.4±0.4 1.1 (1-2.43)	2.2±1.3 2 (1-5.25)	1.6±0.7 1.2 (1-3.75)	2.2±1.2 2 (1-5)
	Other	2.5±0.9 2.3 (1.35-4.18)	2.0±0.7 2 (1-3.43)	2.6±1.1 2.2 (1.25-5.13)	2.4±1.2 2 (1-5)	2.5±1.2 2.5 (1-6)
	p*	0.064	0.066	**0.004**	0.454	0.218

There is a statistically significant difference in terms of threat and harassment distribution relative to the length of time they have been working on board (Kruskal Wallis $p<0.05$). Threats and harassment averages were found to be higher among those who worked 1-3 years (Mann-Whitney U $p<0.008$ Bonferroni correction). There is a statistically significant difference in terms of barriers related to job and career relative to the length of time they have been working on board, age and position (Kruskal Wallis $p<0.05$). Participants with age group 45 and above had a lower average of barriers related to job and career than the other age groups. Employees on board for 3 years and more were found to have lower average barriers to job and career (Mann-Whitney U $p<0.008$ Bonferroni correction). Deck / Engine Cadets' average of barriers related to job and career were statistically significantly higher than those of Chief Officers/ 2. Engineers(Mann-Whitney U $p<0.005$ Bonferroni correction).

.

After the comparison of the demographics, the regression model given in Table 4 was formed. Barriers to job and career is dependent variable; age, position and experience on board were modeled as independent variables and Backward variable selection method was used. There is no multicollinearity (VIF<10) and autocorrelation (Durbin-Watson$\leq$2). So, model can be interpreted and was found statistically significant ($p<0.001$). Age group of 25 to 30 were reduced the barriers related to job and career by 1.25 (1/0.794) times according to the age group of 18 to 25 and were reduced that scale by 1.15 (1/0.871) times according to the age group of 30 to 45. 2.Officer/3.Engineer were reduced the barriers related to job and career by 1.49 times according to the Deck/Engine Cadet and Chief Officer/2.Engineer were reduced that scale by 1.84 times according to the Deck/Engine Cadet. Master/Chief Engineer were reduced the barriers related to job and career by 1.50 times according to the Deck/Engine Cadet and Other position were reduced that scale by 1.11 times according to the Deck/Engine Cadet.

Table 4. Regression analysis

	Unstandardized β	**Standard Deviation**	**Standardized** β	**t**	**p**	**VIF**
Constant	3.287	0.165		19.936	<0.001	
Age 25-30	0.794	0.286	0.240	2.775	**0.006**	1.486
Age 30-45	0.871	0.394	0.226	2.210	**0.028**	2.082
Position 3.Officer /4.Engineer	-0.656	0.382	-0.132	-1.721	0.087	1.176
Position 2.Officer /3.Engineer	-1.491	0.371	-0.357	-4.020	**<0.001**	1.573
Position Chief Officer /2. Engineer	-1.836	0.427	-0.419	-4.296	**<0.001**	1.892
Position Master/Chief Engineer	-1.501	0.426	-0.295	-3.523	**0.001**	1.393
Position Other	-1.114	0.467	-0.179	-2.385	**0.018**	1.124
R^2	0.390					
F/p	4.318/**<0.001**					

Discussion and Conclusions

In this study, it is aimed to examine seafarers' mobbing perceptions depending on the general variables, such as age, gender, education level, experience on board, and position at work. It is found that gender and education level didn't make any difference on mobbing perceptions of the seafarers. Maritime sector is a men-oriented sector. According to the Fourth European Working Conditions Survey (2007), women are more exposed to mobbing than men. Ness et al. (2000) indicated that men are more exposed to mobbing than women. In the study conducted by Mikkelsen and Einarsen (2002), there was no significant difference according to gender. Regardless of educational level of seafarers, they can be exposed to mobbing on board.

Age, experience on board and position at work made difference on mobbing perceptions of the seafarers. With the increase of the age and the experience on board, seafarers are less exposed to mobbing. This result is parallel with the findings of Acar and Dündar (2008) and Özyer and Orhan (2012). The height of the deck/engine cadets' mobbing average can be explained in this way.

Working on board is a though and complex situation, there are lots of stressor factors such as being far away from home and loved ones, fatigue, long working hours, limited space, insufficient sleep and multinationality (Amy, 2015). Effects of mobbing on seafarers can be decrased by improving work environment on board.

The first limitation of the study was sample characteristics in terms of gender. Our participants consist mostly of men. Therefore, we cannot generalize our findings to women. The second limitation of the study was that all participants were from Turkey. The study can be expandable by choosing multinational seafarers coming from different countries.

References

Acar, A.B., Dündar, G. (2008). İş yerinde psikolojik yıldırmaya (mobbing) maruz kalma sıklığı ile demografik özellikler arasındaki ilişkinin incelenmesi. İstanbul Üniversitesi İşletme Fakültesi Dergisi, 37(2), 111-120.

Amy, S.I. (2015). The rationale of the workplace issues of a stress management event; an approach to address this issue in organisations and on -board vessels. International Journal of Business and General Management, 4, 1–8.

Davenport, N., Schwartz, R. D., Elliott, G. P. (2003). Mobbing işyerinde duygusal taciz (O. C. Önertoy Çev.). Sistem Yayıncılık, İstanbul.

Einarsen, S. (1999). The nature and causes of bullying at work. International Journal of Manpower, 20(1-2), 16-28.

Einarsen, S. (2000). Harassment and bullying at work: A revıew of the Scandinavian approach. Aggression and Violent Behavior, 5(4), 379–401.

Einersen, S., Hoel, H., Zapf, D., Cooper, C. L. (2003). Bullying and emotional abuse in the workplace: international perspectives in research and practice. Taylor & Francis Books, London.

Fourth European Working Conditions Survey (2007). Preventing violence and harassment in the workplace. European Foundation for the Improvement of Living and Working Conditions.

Huse, E. F., Cummings, T. G. (1985). Organization development and change. West Publishing Company, USA.

Lewis, D. (2003). Voices in the social construction of bullying at work: exploring multiple realities in further and higher education. International Journal Management and Decision Making, 4(1), 65-81.

Leymann, H. (1990). Mobbing and psychological terror at workplaces, Violence and Victims, 5(2), 119-126.

Mikkelsen, E.G., Einarsen, S. (2002). Relationships between exposure to bullying at work and psychological and psychosomatic health complaints: the role of state negative affectivity and generalized self-efficacy. Scandinavian Journal of Psychology, 43, 397-405.

Namie, G. (2008). The Workplace Bullying & Trauma Institute. www.workplacebullying.org/.../N-N-2000.pdf (Erişim Tarihi: 01.08.2018).

Ness, G.J., House, A., Ness, A.R. (2000). Aggression and violent behaviour in general practice: population based survey in the north of England. BMJ, 320, 1447-1148.

Ozyer, K., Orhan, U. (2012). Akademisyenlere uygulanan psikolojik tacize yönelik ampirik bir araştırma. Ege Academic Review, 12(4), 511-518.

Paparella, D., Rinolfi, V., Cecchini, F. (2004).
Eurofound. https://www.eurofound.europa.eu/publications/article/2004/increasing-focus-on-workplace-mobbing (Erişim Tarihi: 01.08.2018)

Rumsey, D. (2007). Intermediate statistics for dummies. Wiley. Hoboken, NJ.

Tınaz, P. (2006). İşyerinde psikolojik taciz (mobbing). Beta Basım Yayım, İstanbul.

Tolan, B. (1981). Çağdaş toplumun bunalımı: Anomi ve yabancılaşma. İktisadi ve Ticari İlimler Akademisi Yayınları, Ankara.

Tutar, H. (2004). İşyerlerinde psikolojik şiddet. Platin Yayıncılık, Ankara.

Vartia, M. (1996). The sources of bullying-psychological work environment and organizational climate. European Journal of Work and Organizational Psychology, 2, 203-214.

Yıldırım, H., Tavacıoğlu, L. (2017). Behavioral dimensions of seafarers and self-confidence analysis. Eurasian Academy of Sciences Eurasian Business & Economics Journal, 9, 33-44.

Zapf, D. (1999). Organisational, work group related and personal causes of mobbing/bullying at work. International Journal of Manpower, 20(1/2), 70-85.

Zapf, D., Knorz, C., Kulla, M. (1996). On the relationship between mobbing factors, and job content, the social work environment and health outcomes. Europe Journal of Work Organizational Psychology, 5(2), 215-237.

Zou, K.H., Tuncali, K., Silverman, S.G. (2003). Correlation and simple linear regression. Radiology, 227, 617-628.

International Conference on Science and Technology

ICONST 2018

5-9 September 2018 Prizren - KOSOVO

Investigation of The Effect of Marble Dust on The Mechanical Properties of Cement Mortar İcle / Mermer Tozunun Çimento Harcının Mekanık Özellkilerine Etkisinin Araştırılması

İsmail Demir[1]*, Cüneyt Doğan[1], M. Serhat Başpınar[2], Erhan Kahraman[1]

Özet: Mermer tozu (MT) inşaat teknolojisi üzerinde miktar ve kalite açısından önemli bir etkiye sahiptir. Farklı endüstriyel atıkların MT ile birlikte kullanılması ile, farklı amaçlarla kullanılabilen harçlar üretilebilmektedir. Bu çalışmada, MT katkısının harcın mekanik özelliklerine etkisi araştırılmış ve yürütülen deneysel çalışmanın sonuçları sunulmuştur. Çalışmada CEM I 42.5 R tipi çimento kullanılarak toplam 15 harç karışımı üretilmiştir. Su/çimento oranı 0,58 olarak seçilmiş, ince kum (FS) serisine % 0, % 5, % 10, % 20, % 30, % 40, % 50, % 70 oranlarında, kaba kum (CS) serisinde ise % 0, % 10, % 20, % 30, % 40, % 50, % 70 oranlarında MT ikamesi ile harç örnekleri üretilmiştir. Prizma kalıplarda üretilen deney örnekleri 24 saat açık hava ve 27 gün boyunca suda kür edilmiştir. Deney sonuçları, MT katkısının taze harcın kıvamını azalttığını göstermiştir. Bununla birlikte, sertleşmiş harcın eğilme mukavemeti, FS ve CS serilerinde % 38'e kadar önemli ölçüde artmıştır. Aynı şekilde, basınç mukavemeti % 40'a kadar artmıştır. Ayrıca, su emme oranı, MT artış oranı ile artmaktadır. MT ikameli harçların mukavemet özelliklerini olumlu yönde geliştirdiği sonucuna varılmıştır.

Anahtar Kelimeler: Beton, Mermer tozu, İnce kum, Kaba kum, Fiziksel ve Mekanik özellikler.

Abstract: Marble powder (MP)has a significant impact on construction technology in terms of quantity and quality. Usage of different industrial wastes together with marble powder results in the production of mortars that serve different purposes. This study investigates the usage of marble powder on mortars and presents the results of an experimental study to determine the effects of marble powder on mechanical properties of mortar. A total of 15 mortar mixes produced which were CEM I 42.5 R type cement used. Mortar samples were produced with 0%, 5%, 10%, 20%, 30%, 40%, 50%, 70% ratios of fine sand (FS) series and 0% 10%, 20%, 30%, 40%, 50%, 70% ratios of coarse sand (CS) series and was choosen water/cement ratio of 0,58. Mixes moulded three gang moulds wherein open air for 24 hours and in curing tank for 27 days. The experimental results showed that usage of marble powder in mortars reduces the consistency of fresh mortar. However, bending strength of hardened mortar significantly increased in fine and coarse sand series up to 38%. Likely, compression strength increased up to 40%. Also, absorption increases by the increase rate of marble powder. It has been determined that the strength properties of MP substituted mortars have been developed positively.

Key Words: Concrete, Marble powder, Fine sand, Coarse sand, Phsical and Mechanical properties.

[1]Afyon Kocatepe University, Faculty of Engineering, 03200, Afyonkarahisar, TURKEY
[2] Afyon Kocatepe University, Faculty of Technology, 03200, Afyonkarahisar, TURKEY
*Correspondingauthor: idemir@aku.edu.tr

Giriş

Yılda milyonlarca ton dekoratif doğal taş üretilir ve bu da milyonlarca ton MT atığı ile çevre kirliliğine neden olur. MT'nun harçlarda kullanılması, harçların mekanik özelliklerini iyileştirmek, doğal kaynakları korumak ve çevreyi korumak gibi birçok faydaya sahiptir. Ayrıca, MT atıklarının boşaltılması ve depolanması ekonomik dezavantaja sahiptir.

Türkiye'de yılda 7.000.000 ton mermer üretilir ve bu tesislerin atık malzemelerinin milyonlarca tona ulaştığı görülebilir (Ulubeyli ve Artir, 2015). Bu atık malzemelerin stoklanmasında son derece zorluklar vardır (Alyamaç ve İnce 2009). Sayısız faydalar nedeniyle, inşaat teknolojisinde MT'nin geri dönüşümü, devam etmekte olan birçok araştırma için odak noktasıdır. Mermerlerin ocaktan çıkarılması, blok mermerin fabrikada işlenmesi esnasında ortaya çıkan ve mamul mermer üretiminden geriye kalan bütün mermer parça ve tozları mermer atığı olarak kabul edilmektedir (Demir, 2009).

Ammary, MT çamurunun test edilen en düşük orandaki (% 10) standart silis kumu yerine kullanılmasının harç küplerinin mukavemetine çok zarar verdiğini bulmuştur. MT çamurunun oranı arttıkça, beton örneklerin mukavemeti azalmıştır. Deneyde % 100 çamur kullanıldığında, ortalama küp mukavemeti MT çamuru ikameli olmayan küplerin mukavemetinin sadece %20'si kadardır (Ammary, 2007).

Atık mermer granüllerini arttırmanın, betonun basınç dayanım değerlerinin her bir kürlenme zamanında artma eğiliminde olduğunu göstermiştir. Ayrıca, mermer granülleriyle beton karışımlarının ortalama mukavemeti referans betonlardan % 5-10 daha yüksektir. Atık mermer karışım betonunun eğilme dayanımı, atık mermer oranının artmasıyla artış göstermiştir (Ulubeyli ve Artir, 2015).

Al-Zboon ve Al-Zou'by, beton ve çimento harcı karışımlarında MT çamur atıklarının kullanımı, beton ve harç karakteristiklerini geliştirmiş ve MT oranı arttıkça beton işlenebilirliği azalmıştır (Al-Zboon ve Al-Zou'by, 2014).

Singh vd, MT içeriğinin harç karışımında arttırılması, kuruma büzülmesini 56 gün sonunda azaltmaktadır. Bu, MT'nun mikro dolgu etkisine atfedilebilir. MT'nun ince taneleri, beton matrisindeki gözenek boşluklarını işgal eder ve böylece fazla suyun buharlaşmasıyla betonun büzülmesini kısıtlar. MT'nun, kuruma büzülmesini azaltmak için sağladığı bu özellik, diğer faydalarına ek olarak, çevresel etkilerden beton bozulmalarının önlenmesine katkı sağlanabilmektedir (Singh vd., 2017).

Mermer tozu yüksek Blain inceliğine sahip olup (1,5 m2/g), %90'ı 50 μm elek geçmektedir (Corinaldesi et al. 2005). Mermer tozu katkılı betonların performansı üzerinde çok sayıda teorik çalışmalar yürütülmüştür (Wu et al 2001, Binici et al 2007; Corinaldesi et al 2010). Mermer tozu betona filler malzeme olarak katıldığında fiziksel ve mekanik özelliklerini geliştirmektedir. (Monica and Dhoka, 2013; Malpani et al. 2014). İnce tane boyutu sayesinde agrega ile kolayca karışarak mükemmel bağ oluşturur. Mermer tozu betonun mevcut boşlukları doldurarak ve normal betona göre basınç dayanımını artırmaktadır (Corinaldesi et al 2010, Andrej et al 2014). Kireç içeriği nedeniyle reaktiviteyi artırdığı için mermer tozunun betonda, çimento ile ikame edilerek potansiyel kullanımı ideal bir seçenektir.

Materyal ve Yöntem

1. Karışımlar

İdeal karışım oranını elde etmek için, her biri 7 farklı elek ve otomatik elek sarsıcı kullanılarak FS, CS ve MT malzemeleri elenmiştir. CS sonuçları % 35.9'luk kaba tane, % 48.4'ü orta tane ve % 15.7'lik ince taneden oluşmaktadır. FS sonuçları% 0,2 kaba, % 29,6 orta, % 70,2 ince ve MT değerleri % 0 kaba, % 0,36 orta ve % 99,64 ince taneli yapıya sahiptir. Agrega üçgeni kullanılarak karışım oranını belirlemek için bu yüzdeler kullanılmıştır (Tablo 1).

Tablo 1. Elek Analizi Sonuçları

Tane büyüklüğü	Kaba Kum (%)	İnce Kum (%)	Mermer Tozu (%)
Kaba	35.90	0.20	0.00
Orta	48.40	29.60	0.36
İnce	15.70	70.20	99.64

FS serisi karışım oranı 1800g ince kum, 600g 42.5R sınıfı çimento ve 350 g su 1/3 olarak seçilmiştir. MT, % 0 (referans harcı), % 5, % 10, % 20, % 30, % 40, % 50 ve % 70 sırasıyla 0, 90 g, 180 g, 360 g, 540 g, 720 g, 900 g ve 1260 g olmak üzere 8 numuneye ikame edildi (Tablo2).

Tablo 2. FS Serisi Karışım Oranları

Numune No	İnce Kum (g)	Mermer Tozu (g)	Mermer Tozu (%)	Çimento (g)	Su (g)	Akışkanlaştırıcı (g)
1Fs	1800	0	0	600	350	-
2Fs	1710	90	5	600	350	-
3Fs	1620	180	10	600	350	-
4Fs	1440	360	20	600	350	-
5Fs	1260	540	30	600	350	-
6Fs	1080	720	40	600	350	4,7
7Fs	900	900	50	600	350	4,2
8Fs	540	1260	70	600	350	3,32

CS serisi karışım oranı 1800g kaba kum, 600g 42.5R sınıfı çimento ve 350g su 1/3 olarak seçilmiştir. MT, % 0 (referans harcı), % 10, % 20, % 30, % 40, % 50 ve % 70 sırasıyla 0, 180 g, 360 g, 540 g, 720 g, 900 g ve 1260 g olmak üzere 7 numuneye ikame edildi (Tablo 3).

Tablo 3. CS serisi karışım oranları

Numune No	Kaba Kum (g)	Mermer Tozu (g)	Mermer Tozu (%)	Çimento (g)	Su (g)	Akışkanlaştırıcı (g)
1CS	1800	0	0	600	350	-
3CS	1620	180	10	600	350	-
4CS	1440	360	20	600	350	-
5CS	1260	540	30	600	350	-
6CS	1080	720	40	600	350	-
7CS	900	900	50	600	350	-
8CS	540	1260	70	600	350	2,57

2. Harcın Hazırlanması

FS serisinde hassas terazi üzerinde ince kum, MT, çimento ve su tartıldı, daha sonra otomatik harç karıştıcısında plastikleşene kadar karıştırıldı. Plastisite eksikliği nedeniyle 6FS, 7FS ve 8FS numunelerinde sırasıyla 4.7g, 4.2g ve 3.32g Sika Viscocrete -20 HE akışkanlaştırıcı kullanılmıştır. Numuneler 24 saat prizma kalıplar içinde sertleştikten sonra 27 gün boyunca kür tankında bekletilmiştir (Şekil 1).

Şekil 1. Numune Kalıp İşlemi

CS serisinde iri kum, MT, çimento ve su hassas terazi üzerinde tartıldı (Şekil 2), daha sonra otomatik harç karıştıcısında plastikleşene kadar karıştırıldı. Plastisite eksikliği nedeniyle 8CS örneğinde 2.57g Sika Viscocrete-20 HE akışkanlaştırıcı kullanılmıştır. Numuneler 24 saat prizma kalıplar içinde sertleştikten sonra 27 gün boyunca kür tankında bekletildi.

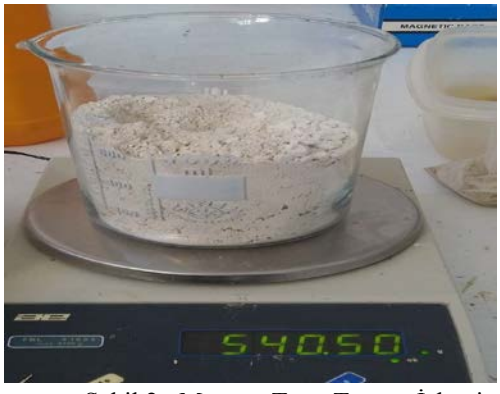

Şekil 2. Mermer Tozu Tartma İşlemi

Şekil 3. Kıvam Testi

Tartışma ve Sonuçlar

1. **Kıvam Testi**

Harcın kıvamını belirlemek için tüm harç serileri için yayılma tablası kullanılmıştır (Şekil 3). Yayılma tablasının ortasındaki kalıp, 2 kat taze harçla doldurulduu ve her tabaka, tokmak ile on kez sıkıştırıldı.

FS serisinde, kıvam testi sonuçları harçlarda MT kullanılmasının harcın kıvamını önemli ölçüde azalttığını göstermektedir. 720 g MT, % 58 kıvam kaybına neden olmuştur. Plastisite eksikliğinden dolayı, 6FS, 7FS ve 8FS numunelerinde kullanılan akışkanlaştırıcı kabul edilebilir kıvam değerleri sağlamıştır.

FS serilerinde olduğu gibi, CS serisinde de kıvam test sonuçları harçlarda MT kullanılmasının önemli ölçüde harcın kıvamını azalttığını göstermektedir.

2. **Eğilme Mukavemeti Testi**

Eğilme mukavemeti testi için form-test marka test makinesi kullanıldı. Aralarında 100 mm bulunan iki mesnet üzerinde duran numunenin tam ortasından dik yönde düşey yük uygulanmıştır. Yükün hızı darbesiz

10 N/s sabit ivmeli olarak seçilmiştir. Harçlarda kullanılan MT'nin FS ve CS serilerinde eğilme mukavemetine yarar sağladığı gözlemlenmiştir.

FS serisinde kullanılan 180g MT (% 10) ikame maksimum eğilme mukavemeti sağlamıştır. 3Fs (% 10 ikame) sonrasında eğilme mukavemeti azalmıştır, ancak 7FS (%50) ikame ile artış göstermiştir. Maksimum eğilme dayanımı referans harçtan % 38 daha fazladır (3Fs - 7.75MPa). Tüm MT ikameli numuneler referans harca göre daha fazla eğilme mukavemetine sahiptir. Eğilme mukavemeti sırasıyla % 11, % 38, % 36, % 15, % 17, % 31, % 32 artmıştır (Şekil 4).

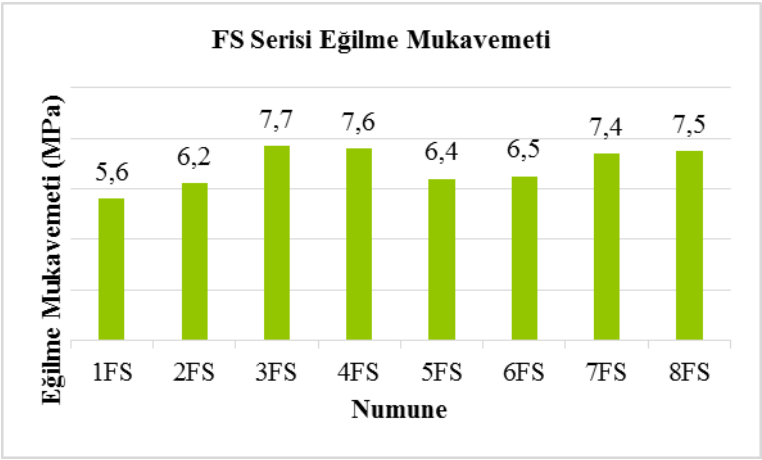

Şekil 4. FS Serisi Eğilme Mukavemeti

CS serisinde, eğilme mukavemeti 360g MT (% 20) değerine kadar artmış, ancak sonrasında azalma göstermiştir. Eğilme mukavemeti 540 g MT (% 30) ikame ile referans harçtan daha az mukavemete sahiptir. Maksimum eğilme mukavemeti 7.492 MPa (4CS - 360g -% 20) ve minimum eğilme mukavemeti 6.242 MPa'dır (8CS - 1260g -% 70) (Şekil 5).

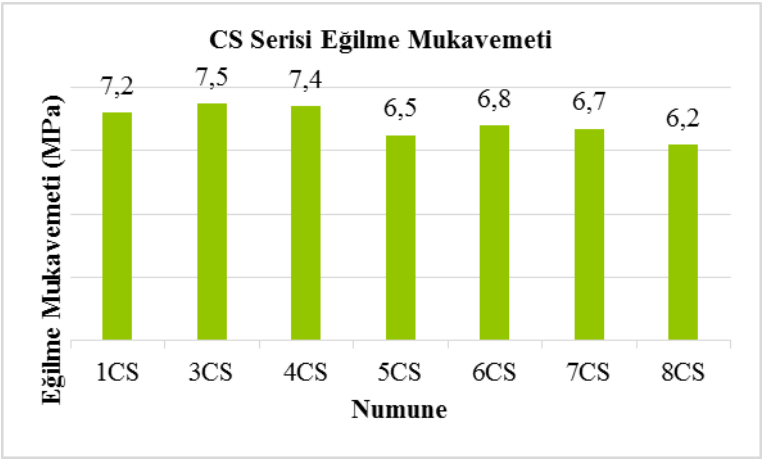

Şekil 5. CS Serisi Eğilme Mukavemeti

3. Basınç Mukavemeti Testi

Basınç testi için, yükü BS EN 01015-11-1999'da belirtilen standartlarda uygulayabilen standart test makinesi kullanılmıştır (Şekil 6). Yük darbesiz olarak saniyede 10 N olarak seçilmiştir.

Şekil 6. Basınç Mukavemeti Testi

Tüm MT ikameli FS numuneleri referans harçtan daha yüksek basınç mukavemetine sahiptir. 720g (% 40) ikame, maksimum basınç mukavemeti sağlar. Basınç mukavemeti 6FS'ye (% 40 ikame) kadar artış göstermiş ve sonrasında azalmıltır. Maksimum basınç mukavemeti (6FS - 46.19MPa) referans harçtan % 40 daha yüksek elde edilmiştir. Basınç mukavemeti sırasıyla; % 18, % 14, % 28, % 22, % 40, % 25, % 22 artmıştır (Şekil 7).

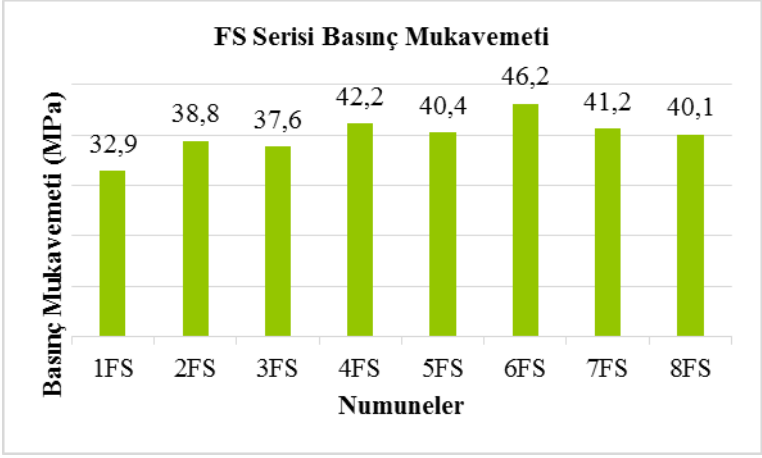

Şekil 7. FS Serisi Basınç Mukavemeti

CS serisinde ise, basınç mukavemeti 4CS'ye (360 g, % 20) kadar artıp sonraki serilerde düşüş eğilimi göstermiştir. Maksimum basınç mukavemeti 360 g MT (% 20) ikameli 4CS serisinde 47,7 MPa olarak elde edilmiştir. 8CS (% 70 ikameli), 34,9 MPa olan minimum basınç mukavemetine sahiptir. 8CS hariç, tüm numuneler referans harçtan daha yüksek basınç mukavemetine sahiptir. Basınç mukavemeti sırasıyla, % 10, % 25, % 5, % 10, % 7 artış göstermiş olup yalnızca 8CS serisinde % 8 oranında düşüş görülmüştür. (Şekil 8).

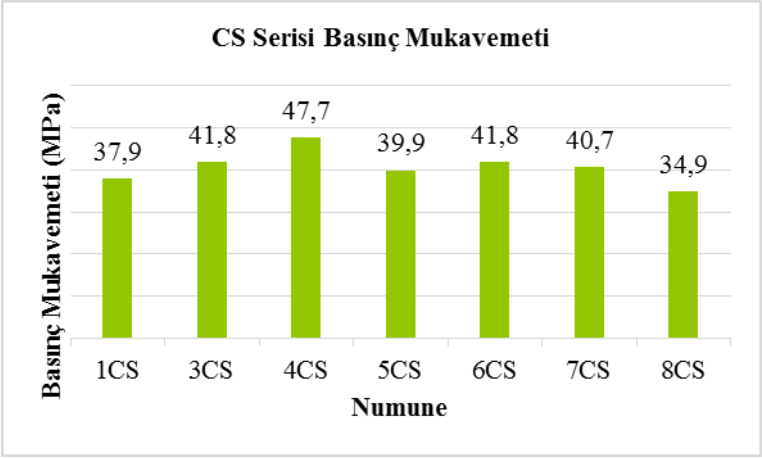

Şekil 8. CS Serisi Basınç Mukavemeti

Öneri ve Tartışmalar

MT'nun harçlarda geri dönüşümünün birçok yararı vardır. MT'nun çevre ve kaynakları koruma amaçlı olarak harçlarda kullanımı, harçlara dayanım ve dayanıklılık özelliklerini geliştirebilmektedir.

MT'nun FS ile ikame edilmesi, harcın tüm mekanik özelliklerini iyileştirir. MT ikameli harçlar taşıyıcı yapı elemanlarında kullanılabilir. Daha yüksek miktarlarda MT ilavesi harçlarda akışkanlaştırıcı kullanımın gerektirmektedir. Aksi takdirde yetersiz kıvam nedeni ilee mekanik özellikler olumsuz etkilenecektir. MT ikameli harçlarda su ihtiyacını artıran en önemli etken, MT'nin ince taneleri sayesinde oluşan yüksek yüzey alanıdır. Maksimum eğilme mukavemeti % 10'luk ikame ile elde edilirken, maksimum basınç mukavemeti % 40'lık ikame ile sağlanmıştır.

MT'nun CS ile ikame edilmesi, harçların eğilme ve basınç mukavemetini artırıcı etki yapmıştır. Maksimum eğilme ve basınç mukavemeti için ideal yüzde % 20'lik ikamedir ve % 30'u aşan ikame, referans harçtan daha düşük eğilme mukavemetine neden olmuştur. % 20'lik ikame, agregga üçgeni kullanılarak ideal karışım oranı için uygundur. MT (% 100 ince), FS (% 70 ince,% 29 orta) ve CS (% 15 ince,% 48 orta ve% 35 kaba) maksimum mukavemet sağlar.

Mermer tozunun betonda katkı olarak kullanımı doğal kaynakların ve çevrenin korunması, geri dönüşüm uygulamalrı sebebi ile değer taşımaktadır. Ayrıca harçların fiziksel ve mekanik özelliklerini geliştirmesi ile kitlesel kullanımı teşvik edilmesi gereken bir uygulama olabilmektedir.

Kaynaklar

Andrej I., Roman G., Toma V., Ven Weslav K., Jadran M., Anton M., (2011),Carboaluminate Phases Formation During the Hydration of Calcite-Containing Portland Cement. J. Am. Ceram. Soc., 94 [4] 1238–1242.

Alyamaç, K.E., İnce, R. (2009), A preliminary concrete mix design for SCC with Marble Powders, Construction and Building Materials, 23, 1201–1210.

Al-Zboon, K., Al-Zou'by J. (2014). Recycling of stone cutting slurry in concrete mixes, Journal Mater Cycles Waste Management, 17:324–335

Ammary, B.Y. (2007). Clean production in stone cutting industries, Environment And Waste Management, Vol. 1, Nos. 2/3.

Binici H., Kaplan H. and Yilmaz S., (007), Influence of marble and limestone dusts as additives on some mechanical properties of concrete", Scientific Research and Essay, 2(9), pp 372379.

Corinaldesi V., Giacomo Moriconi and Tarun R. Naik.(2005), Characterization of marble powder for its use in mortar and concrete. NMET/ACE International Symposium on Sustainable Development of Cement and Concrete, October 5-7, Toronto, Canada.

Corinaldesi V., Moriconi G, Naik TR, (2010), ―Characterization of marble powder for its use in mortar and concrete‖, Const. Build. Mat., 24, pp 113-117.

Demir, İ., (2009), Mermer Tozu Ve Atıklarının Kullanım Alanları", Mermer Sektörü ve Bilişim Çalıştayı", Afyonkarahisar.

Ms. Monica C. Dhoka (2013), Green Concrete: Using Industrial Waste of Marble Powder, Quarry Dust and Paper Pulp, International Journal of Engineering Science Invention, Volume 2 Issue 10, , 67-70.

Ronak Malpani, Sachith Kumar Jegarkal, Rashmi Shepur, Ravi Kiran H. N, Veena Kumara Adi (2014), Effect of Marble Sludge Powder and Quarry Rock Dust as Partial Replacement for Fine Aggregates on Properties of Concrete, International Journal of Innovative Technology and Exploring Engineering (IJITEE),Volume-4, Issue-1, 39-42.

Singh, M., Srivastava, A., Bhunia, D. (2017), An investigation on effect of partial replacement of cement by waste marble slurry, Construction and Building Materials 134, 471–488.

Ulubeyli, G.C., Artir, R. (2015), Properties of Hardened Concrete Produced by Waste Marble Powder, Social and Behavioral Sciences 195, 2181 – 2190.

Teşekkür: Bu çalışma Afyon Kocatepe Üniversitesi BAPK tarafından desteklenmiştir.(BAPK 18.Kariyer 99.)

International Conference on Science and Technology

ICONST 2018

5-9 September 2018 Prizren - KOSOVO

A Simple Transition Method to Reduce Conducted Emission for Automotive Seat Heater Low Side PWM Power Switch

Ahmet Küçükkömürler[1*], Kubilay Taşdelen[2]

Abstract: In this paper a simple circuit design technique has been studied to lower the conducted emission to acceptable level for most of the Automotive End Manufacturers (OEM) agrees on. In order to achieve allowable level of conducted emission on battery power lines a simple low pass filter inserted to the gate of the power switch before microcontroller PWM (µC-PWM) driver. Conducted emission results are given before and after simple circuit insertion. A simple low pass filter achieves almost equal to the ambient level of conducted emission without any circuit performance degradation.

Keywords: Automotive EMC, Conducted Emission, Low Side Power Switch, PWM driver

Introductıon

The term Conducted Emissions (CE) in automotive refers to the mechanism that enables electromagnetic energy to be created in an electronic device and coupled to its battery line. The allowable conducted emissions from electronic devices are controlled by OEMs.

The primary reason that conducted emissions are regulated is that electromagnetic energy that is coupled to a battery power line can find its way to the entire power distribution network that the product is connected to and use the larger network to radiate more efficiently than the product could by itself. Other electronic devices can then receive the electromagnetic interference through a radiated path (or, much less frequently, a direct electrical connection).

Conducted emissions are regulated by the Federal Communications Commission (FCC), and the Comité International Spécial des Perturbations Radioélectriques (CISPR). When testing a device for compliance with the FCC and CISPR regulatory limits [1], a Line Impedance Stabilization Network (LISN) must be inserted [2] between the power and ground wires of the Device Under Test (DUT) and the battery B+ and B -.

Test Setup

Procedure: The power and ground wires of the DUT harness were cut to a length of 220mm and connected to the B+ the Line Impedance Stabilization Network (LISN) and B- LISN output ports respectively. The remainder of the harness was left at a length of 1.5 meters. The one side of the harness is then connected to the control module and the other side is connected to the LED power indicator, load network, and the power connector. The measuring coaxial cable is then connected to the measuring port of the B+ LISN network and readings were taken by the computer according to OEM specifications. Once the test on the B+ LISN is completed the measuring coaxial cable is then connected to the B- LISN measuring port. Both B+ LISN and B- LISN measurements were taken for both modules as described above.

[1]Calsonic Kansei Inc., 2700 Hills Tech Court Farmington Hills, MI 48331-5725 United States of America
[2]Isparta Uygulamalı Bilimler Universitesi, Faculty of Technology, 32260, Isparta, TURKEY
*Corresponding author: mailto:ahmet_kucukkomurler@ck-mail.com

Ambient conditions of the test lab: Temperature: 22°C, Relative Humidity: 32%
Images of test set up: DUT and test set up inside the EMC chamber is shown below Figure 1.

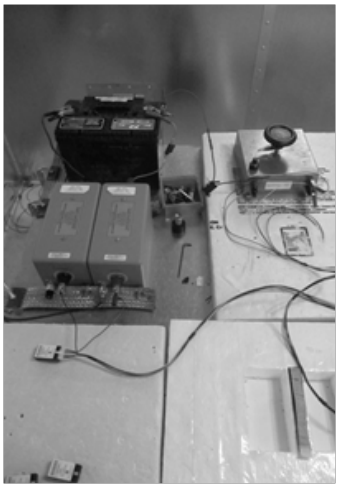

Figure 1. Control module (DUT) test set up inside the EMC chamber

Test Results: 42dBuV is the threshold (red line) for most of the OEMs agrees on. It is shown that on Figure 2a CE levels (green) are above high for the frequency spectrum which needs to be suppressed. Blue line is the ambient CE values. A simple Low side power switch and µC-PWM driver is shown Figure 2b. µC-PWM driver frequency and level are 5Hz and %50 respectively. However after the Low Pass Filter (LPF) insertion (Figure 3b) between the µC-PWM driver and the low side power switch CE levels are decreased dramatically for all frequency spectrums, and follows almost equal to ambient CE values, depicted on Figure 3a.

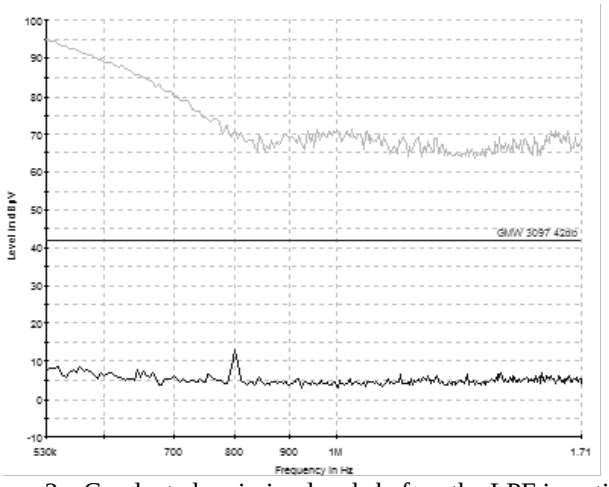

Figure 2a. Conducted emission levels before the LPF insertion

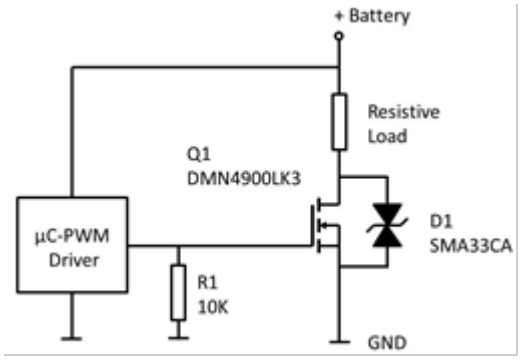

Figure 2b. Circuit Schematic

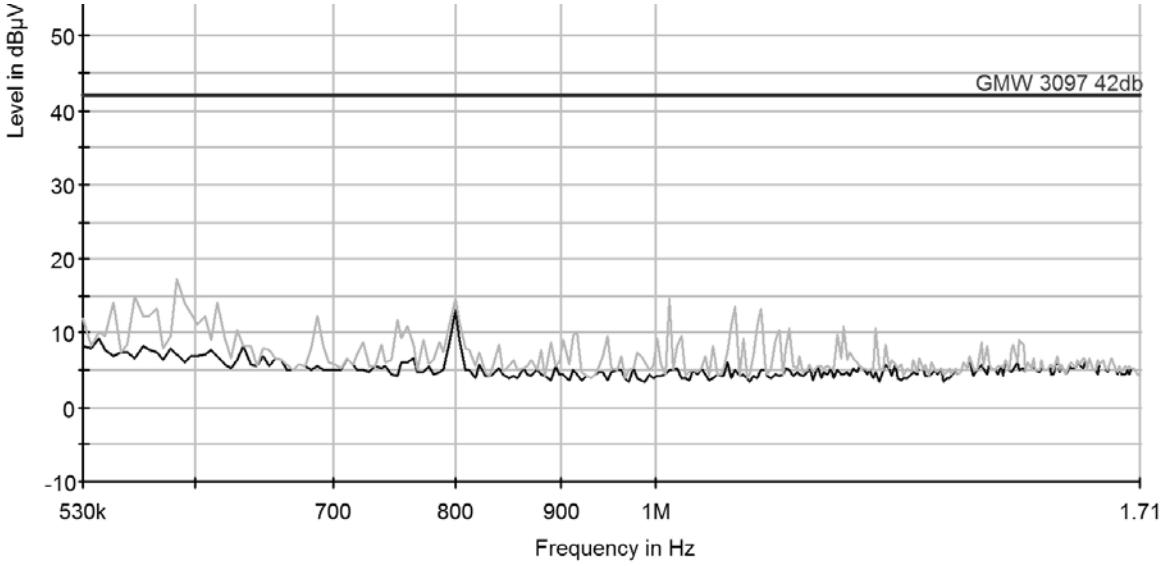

Figure 3a. Conducted emission levels after the LPF insertion

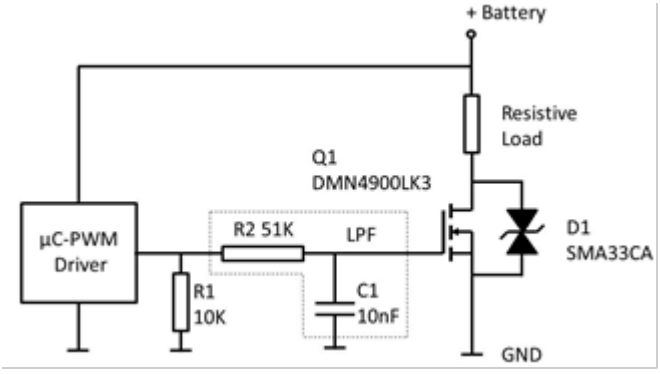

Figure 3b. Circuit Schematic with LPF

Both circuit schematics employed R1 resistor in case µC-PWM driver fail, R1will protect seat surface from uncontrolled heat. This is requirement to safe fail by OEMs; in addition to that this is also good design practice not to leave float the gate of the power MOSFET. LPF (R2-C1) insertion is simple called edge shaping [3] to reduce electromagnetic emission which can be seen below gate drive signal waveforms. On the other hand LPF insertion is not only slowing the falling and rising edge but also suppressed the high frequency component of the gate drive signals which can be seen easily before and after LPF insertion Fig 4a and 4b respectively.

Actual Gate Drive: Both circuits power MOSFET gate signal waveform, rise and fall time are given below Figure 4a and 4b respectively.

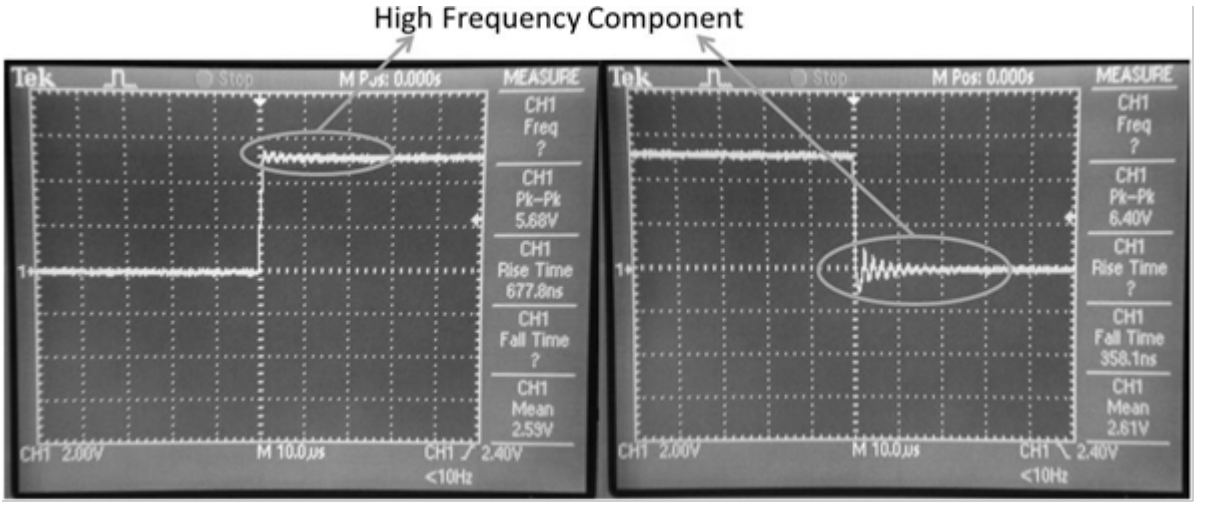

Figure 4a. Rising and falling waveform at the gate of the DMN4900LK3, before LPF insertion

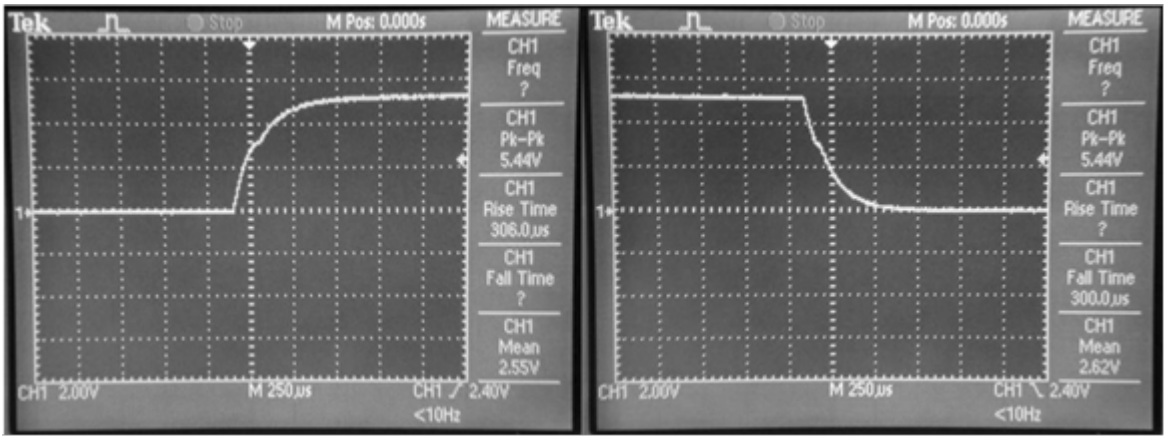

Figure 4b. Rising and falling waveform at the gate of the DMN4900LK3, after LPF insertion

As it seen from waveforms, before LPF insertion rise and fall time are ~677ns, ~358ns respectively and after the insertion of LFP rise and fall times are ~300µs. Rise and fall time needs to be scale down from ns level to µs in order to achieve acceptable level of CE for the frequency spectrum.

Conclusıon

As it seen from the CE levels and the actual gate drive waveforms slowing down the gate of the power switch using LPF is enough to achieve acceptable level for CE. Slowing the gate will increase the conducted power dissipation however the low side power switch can handle power dissipation easily (DMN4009LK3 is 40V/18A drain source on resistance at 14A/10V is 8.5mΩ) [4]. Thus solution to the CE is a simple low pass filter insertion works fine and does not require too many components and it will make layout design engineer life easier.

References

[1] Paul, C. Introduction to Electromagnetic Compatibility, John Wiley & Sons, 1992

[2] B. Deutschmann, R. Illing, B. Auer, “Edge Shaping to Reduce the Electromagnetic Emissions”, Proc. of the 10th Int. Symposium on Electromagnetic Compatibility (EMC Europe 2011), York, UK, September 26-30, 2011

[3] P. J. Doriol, et. al., “EMC-aware Design on a Microcontroller for Automotive Applications”, Design, Automation & Test in Europe Conference & Exhibition, 2009. DATE '09.

[4] http://www.diodes.com/datasheets/DMN4009LK3.pdf

International Conference on Science and Technology

ICONST 2018

5-9 September 2018 Prizren - KOSOVO

An Assessment of the Geo-Spatial Proximity and Evaluation of Magnetic Pollution from 132kV and 330kV Power Transmission Lines to Infrastructures: A Case Study of Osogbo, Nigeria

Rahmon Ariyo Badru [1,*], Oluwatosin Iyanu Akinwale [2], Ayodeji Olalekan Salau [3], Kayode Olorunyomi [4], Joshua Alwadood [5], and Abimbola Atijosan [6]

Abstract: Urbanization and development within cities has made people to build houses, workshops, religious centres, schools and farms close to or under transmission power lines. Meanwhile, transmission power lines produce electromagnetic fields which are harmful to humans. This study practically examines the magnetic field component of electromagnetic field generated around a transmission line using Osogbo as case study. Measurements were taken with a gaussmeter at a vertical distance of 1.04 meters at the center, right and left side of a selected number of power transmission lines respectively. The results were evaluated with the standard limit of exposure established by International Commission on Non-Ionizing Radiation Committee (ICNIRP). This paper also carried out a survey research with the use of GIS analysis, using the satellite image of osogbo in ARCGIS environment in order to map out the power lines and infrastructures close to the transmission power line in osogbo. A buffer of 500 m interval was created along the power lines, this was used to measure the distance from the power lines from the nearest infrastructure. The Power Holding Company of Nigeria (PHCN) regulations, Lagos State Urban and Regional Planning (LSURP) regulations and Occupational Health and Safety Code (OHSC) regulations were used to assess the infrastructure close to the power lines to determine the infrastructures violating the regulation and those which could expose inhabitants to health hazards which result from exposure to electromagnetic radiation.

Keywords: Magnetic flux pollution, Power transmission lines, Remote sensing, ICNIRP, Occupational and general public exposure.

1. Introduction

High population growth coupled with a corresponding increase in infrastructural development around or under power transmission lines (PTL) has caused numerous adverse effects to humans resulting from electromagnetic radiation emitted from transmission lines. These effects include damage to the human body tissues, cardiovascular disorders, low sperm counts and many other effects on live-line workers who regularly service the lines [1]. Also, proximity of these PTL cause destruction of lives and property in the advent of the tranmission lines falling on close-by infrastructure. This is because eletric and magnetic fields are generated around an electric power transmission line. Although, the amount of power transmitted during the transmission and distribution reduces with increase in the distance. Thus reducing the electromagnetic radiation being received by the object as it moves further away from the transmission lines.

Futhermore, because of the need for electric power to be distributed to distant locations, there is a need to increase the overhead power transmission thus leading to a high voltage overhead so as to satisfy the electric consumers at far distance. The high voltage technology ensures that the line voltage is held relatively constant over time while currents are permitted to rise and fall with power demand. Magnetic fields are generated due to the moving current in the PTL. From previous research carried out, magnetic fields have

[1, 5, 6] Cooperative Information Network (COPINE), National Space Research and Development Agency, Obafemi Awolowo University, Ile-Ife, Nigeria.
[3] Department of Electrical/Electronic Engineering, Afe Babalola University, College of Engineering, Ado-Ekiti, Nigeria.
[2, 4] African Regional Centre for Space Science Education in English (ARCSSTEE), Obafemi Awolowo University, Ile-Ife, Nigeria.
* Corresponding author: olasunkonmi@yahoo.com

been stated to be capable of penetrating into inner organs of human body because they are made up of conducting particles [2]. Magnetic field intensity reduces with distance, therefore at large distances away from the transmission lines, the magnetic field intensity might be zero.

Although, the magnetic fields produced by high voltage power transmission lines are in the extremely low frequency (ELF) range of the electromagnetic spectrum, they still can cause serious health effects if concentrated on the human body for a long period of time.Several problems arising from exposure of humans to electromagnetic radiation from PTL makes humans easily vulnerable to the health hazards. Numerous epidemiological research works have been carried out on the magnetic field created around the wire by the flowing current. These works have shown that it has adverse biological effects on humans like neurological, cardiovascular disorders and low sperm count in live-line workers [2, 3].

The remainder of this paper is organized as follows. The related works is presented in Section 2. Section 3 explains our proposed method. Section 4 presents and discusses the results, and the paper is finally concluded in section 5.

2. Related Works

Several studies have been carried out on the effects of magnetic and electric field pollution from transmission power lines on lives and property. This section provides an overview of related works in this area. More recently, authors in [4] have presented an evaluation of electric field pollution from 132 kV power transmission lines (PTLs) in Ibadan using the PHCN, LSURP, OHSC and the ICNIRP standard to determine the safest distance of proximity of infrastructures to power transmission lines. From their findings, they obtained that 12.5% of the infrastructures assessable complied with the PHCN regulation, 56.85% complied with the LSURP regulation and 78.12% compiled with the OHSC regulation. Authors in [5], presented an evaluation of the magnetic field produced by a 132kV and a 330kV high voltage transmission line (HVTL) at mid-span with horizontal and vertical configuration in Akure, South Western Nigeria using analytical methods from electromagnetic field theory. They obtained that power lines are being violated as buildings exist less than 15m and 25m away from the 132kV and 330kV transmission lines respectively. The 132kV power line and 330kV transmission line are both maintained by the Transmission Company of Nigeria (TCN). Similarly, authors in [6] carried out an analysis of smart grids using 132/33kV sub-transmission lines for power transmission in rural areas in Bangladesh. In their work, an assessment of the geo-spatial proximity and magnetic pollution from 132kV power transmission lines (PTLs) in Osogbo was carried out. Authors in [7], presented a study of the overvoltages due to the energisation of a 132 kV underground cable was analyzed using simulation software such as MATLAB. MATLAB simulations were carried out to obtain the overvoltage values at the sending and receiving end. These values are seen to vary approximately between 1.8 p.u. to 2.1 p.u. Furthermore, [8] presented an exposure assessment of live-line workers exposed to electric and magnetic fields from power transmission line for the Saudi Electricity Company (SEC). They obtained that the levels of safety workers exposures to extremely low frequency (ELF) electromagnetic field fall well below the recommended international standards limits.

This paper presents an assessment of the geo-spatial proximity and an evalution of magnetic pollution from 132kV and 330kV power transmission lines to infrastructures in Osogbo, Nigeria.

2.1. Power Transmission Lines

Power transmission lines (PTL) are used for distribution of electricity from where it is generated at power stations by electromechanical generators to electrical substation and distribution centres. High-voltage direct-current (HVDC) technology is used for efficient transmission of electric power over very long distances like hundreds of miles away. Electricity is transmitted at high voltages to reduce the energy loss which usually occurs in long-distance transmission. Therefore, overhead power lines are commonly used to transmit power. The Voltage varies from 11kV to 765kV and radiates powerful electromagnetic fields (EMFs). However, high voltage power transmission lines supply electrical energy to our cities and the strongest magnetic fields are usually emitted from high voltage transmission lines [9]. These transmission lines are major sources of electromagnetic field which pollutes the immediate environment with extremely low frequency [10]. There

are various researches that identified the dangers of this pollution to life in our environment. Some epidemiologic residential and occupational studies have suggested a weak relation with a few types of cancer in humans, particularly leukaemia in children as well as brain and breast cancer in adults, while others reported no consistent evidence of relations between magnetic field exposure and any type of cancer [11]. International Commission on Non-Ionizing Radiation Protection (ICNIRP) gives recommendations on limiting exposure of radiation; it develops and publishes guidelines, statement and reviews used by regional, national and international radiation protection bodies such as World Health Organisation [12].

2.2. Power Line Configuration

The geometric configuration of a power transmission line (PTL) is shown in Figure 3 and a picture of the PTL is shown in Figure 1. The phase conductors are represented with A, B and C, and the vertical distance between them is represented with *av*, while *ah* is the separation between the phase conductors of the horizontal geometry and *Ht* is the distance of the lowest conductor from the ground at the tower. It is important that the towers of the two lines are not co-located in order to reduce/eliminate the combined magnetic field strength underneath the lines. Although for this work, we assumed their mid-span are in the same region for worst case scenario.

2.3. Interaction of Human Body with Electric and Magnetic Fields of Power Lines

Electric and magnetic fields generated by electric power transmission lines are harmeful to the human body. Expose to these field cause damages to the body tissues. For the electric field generated, Ohm's Law relates the current density (J) and electric field (E) [13] as shown in (1):

$$J = \sigma E \tag{1}$$

A study of the effect of electric field exposure on human beings was presented in [14]. They observed that at certain distances human are mostly likely to experience these health treats: the ground (0 m), exposure of the heart (1, 5m) and brain exposure (1.8m). The reference level of the allowed magnetic field exposure is shown in Table 1.

Table 1. Reference levels of magnetic field exposure [15].

Exposure characteristic	Frequency range	Magnetic field (μH)	Magnetic field at 50Hz (mG)
Occupational exposure	0.025 – 0.82kHz	25/ f	5000
General public exposure	0.025 – 0.82kHz	5/ f	1000

2.4. Regulatory Agencies

The responsible regulatory agencies have layed down guidelines and technical specification to determine the permissible exposure limit of human beings to magnetic and electrical fields [16]. Most regulatory agencies have contributed to this standard. The agencies include, the International Commission on Non-Ionizing Radiation Protection [13], the Council for European Union [15], World Health Organisation [12], Lagos State Urban and Regional Planning (LSURP), PHCN [18] and Institute of Electronic and Electrical Engineers [17], have recommended permissible limits to exposure of electric and magnetic fields.

3. Materials and Method

Primary and secondary data were collected for this work. The global positioning system (GPS) coordinates (Longitude, Latitude and Height) of the spatial locations were obtained using a GPS receiver with following specification; model GPSMAP 78 Series and error margin of 3metres. GPS values of strategic points were taken, such as the infrastructure closest to the left and right side of the power line tower and GPS points under the power line tower. The mid-span magnetic field distribution in the vertical plane with minimum

ground clearance was considered, in case there are regions where the two power lines are close to each other in Osogbo.

Secondary data were collected and were used to identify infrastructures that were located around the power lines in the study area and also to extract the road network. ARCGIS environment was used to map out Osun State from the map of Nigeria. Thereafter, Osogbo which is the study area of this research work was mapped out as shown in Figure 2. The GPS sample points of the transmission towers were plotted on the satellite image of Osogbo in ARCGIS environment in other to map out the power lines. A buffer of 500 m interval was created along the power lines as shown in Figure 4. This was used to measure the distance from the power lines from the nearest infrastructure. After the distances were recorded, a waveform of the spatial location's distance (metres) to nearest infrastructure from the 330 kV transmission lines was plotted and another waveform showing the spatial location's distance (metres) of nearest infrastructure from the 132 kV transmission lines was plotted. Afterwards, a table was created to show the types of infrastructure located under and near the power lines. The tables comprises of the list infrastructure found at the left and right side of the power line, the frequency of the structures and the total number of infrastructures observed. A graph showing the frequency and percentage of different Infrastructure located close to power lines was plotted. Questionnaires were used to obtain other required information from residents and users of the pathway. All measurements were taken at one metre (1.04m) from the ground surface. The magnetic flux density was obtained using Field Test Meter with following characteristics: model 3120-EN-00 and measuring Capacity from 0.01μT to 19.99 μT. Magnetic field strength of strategic points was taken at the infrastructure closest to the left and right side of the power line tower and under the power line tower itself. All measurements were taken at one metre (1.04m) from the ground surface. The measurements were recorded into a spread sheet on Microsoft Office Excel. Afterwards, waveforms were generated from the results on the table using Microsoft Excel tools. The comparative analysis of the results of Magnetic Flux Density at nearest infrastructure to Right, Left and Under the Tower were recorded into a spread sheet on Microsoft Office Excel. Afterwards, the waveforms were generated from the results on the table using Microsoft Excel tools. There are different regulatory standards on limits of human exposure to magnetic field resulting in the guidelines of minimum distance which an infrastructure can be located close to power lines. The results of the magnetic field measured were compared with these standards. The regulatory agencies include, the Power Holding Company of Nigeria (PHCN), Institute of Electronic and Electrical Engineers (IEEE), Lagos State Urban and Regional Planning (LSURP), Occupational Health and Safety Code (OHSC) and International Commission on Non-Ionizing Radiation Protection guidelines (ICNIRP). Waveforms were plotted to show the comparative analysis of all the measurements of magnetic field recorded around the power lines based on the guidelines of PHCN, LSURP, OHSC and ICNIRP.

Figure 1. Automobile mechanical workshop under 330/220 kV power transmission line in Osogbo.

Figure 2. Map of the study area (Osogbo).

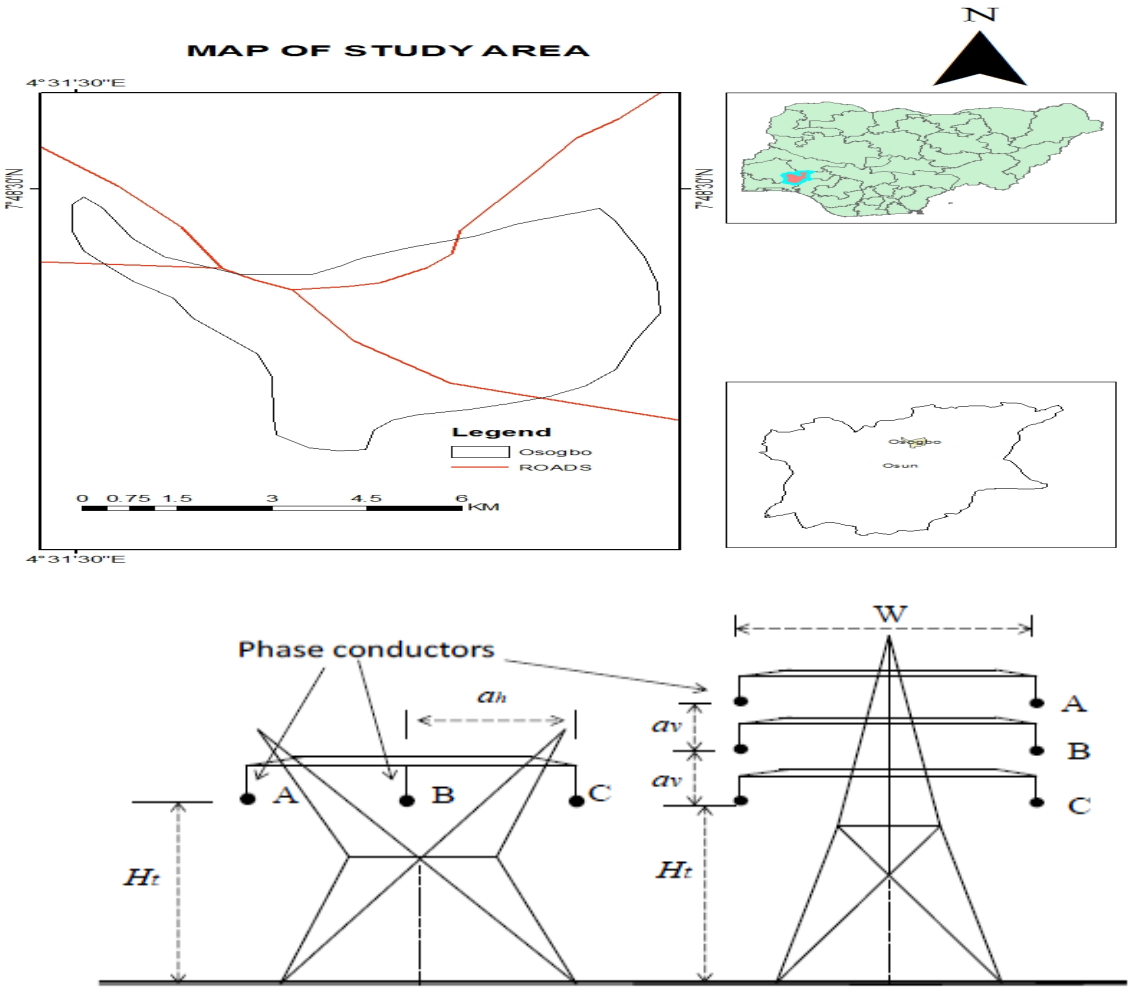

Figure 3. Schematic diagram of the configuration of a power line.

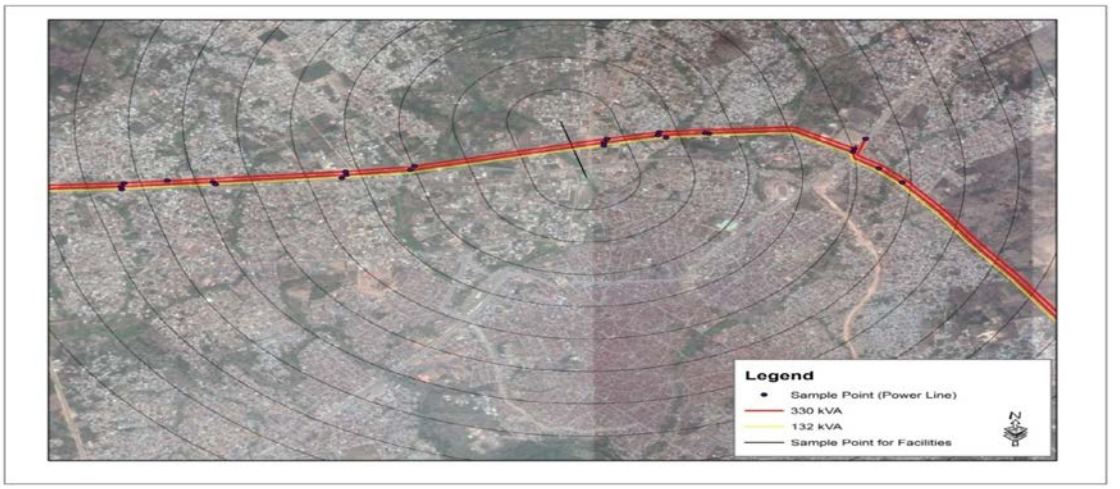

Figure 4. Buffering of 500 m along power lines along Osogbo.

4. Results and Discussion

From the waveform plotted for the magnetic field values recorded under the tower, at the left and right side of the tower as shown in Figure 5, Figure 6 and Figure 7 respectively, and the obtained values are shown in Tables 4, 5 and 6 respectively. It was observed that the magnetic field is dense at the side lines of the transmission tower (TT) with high values obtained for point 23 (right side of the TT), point 3 (under the TT) and point 20 (left side of the TT) as shown in Figure 8, although less than the guide line of ICNIRP (about 100μT). This implies that infrastructures on both sides of the tower are exposed to the higher range of magnetic field. The Infrastructures found at the power line are workshop, shop, church, farm lands, residential houses, block industries and schools. Workshops and shops such as mechanic workshops, furniture workshop, are more frequently located near power lines. Block industries were also found frequently located, especially under the towers as shown in Table 2. Residential houses were located near the power lines. Meanwhile, most schools compiled to the guidelines set by International Commission for Non-Ionizing Radiation Protection on the exposure limit of human being to magnetic field, the results in Table 4, Table 5 and Table 6 clearly show that the values are still very low and in a safe limit of exposure which is 100μT as shown in Figure 10.

However, the standard of the regulatory agencies along the power lines are being violated as buildings exist less than 15m and 25m away from the 132kV and 330kV lines respectively as shown in Figure 13 from the spatial distance between the nearest infrastructure and the transmission lines using Satellite. Work places for various occupations and makeshift structures exist directly below the power lines. The spatial distance of infrastructure is shown in Figure 9 and there related frequency is shown in Figure 10. The results as shown in Figure 10, clearly show that only schools and churches partially meet the requirement for spatial proximity of infrastructure to PTL. The encroachment of the proximity is higher using PHCN standard (about 42%) as shown in Figure 12. Block industries and workshops are more pronounced under the power line within Osogbo metropolis. Lastly, it was observed that many infrastructures violate the minimum distance that buildings should be away from power lines. From the field work, within the power line area covered, 57.89% infrastructure complied with the PHCN regulation and 78.95% complied with Lagos State Urban and Regional planning, while 89.47% complied with the OHSC regulation as shown in Table 3 and shown in the waveform in Figure 11. With the results obtained, there is need for regulatory/law enforcement agents to further ensure that the standards/regulations along the power lines are observed by the general public as a result of the thermal effects of prolonged electromagnetic pollution on human health.

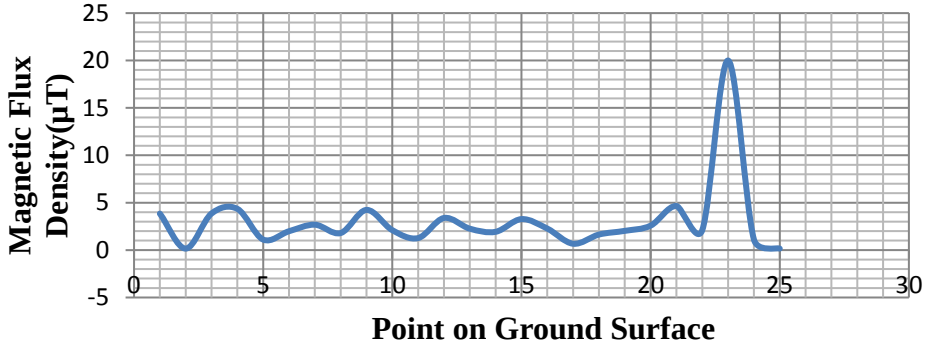

Figure 5. Waveform of the Magnetic field under the transmission Tower @ 1.04 m to ground surface.

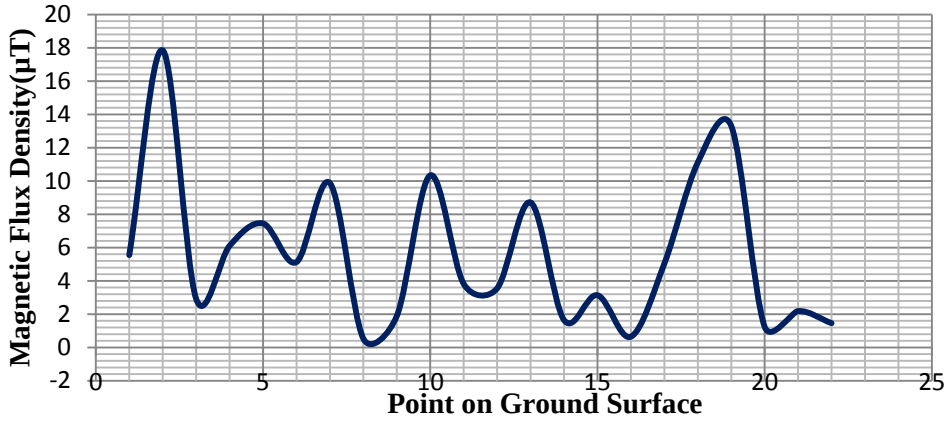

Figure 6. Waveform of the Magnetic field Left side of transmission Tower @ 1.04 m to ground surface.

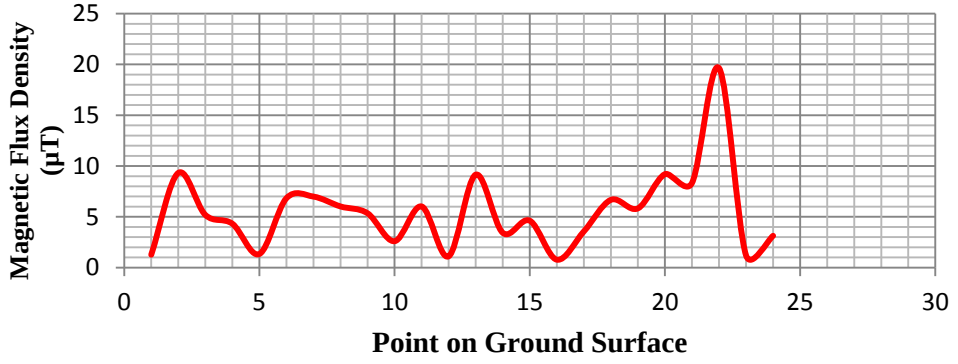

Figure 7. Waveform of the Magnetic field @ Right side of transmission Tower @ 1.04 m to ground surface.

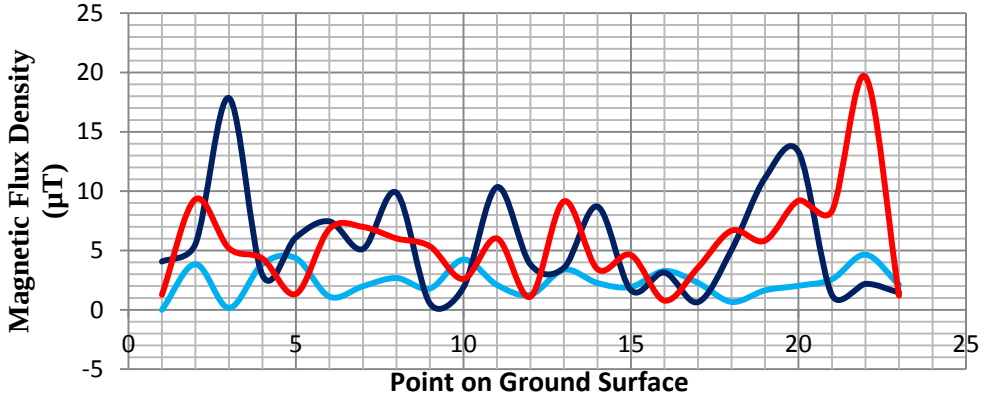

Figure 8. comparative analysis of values of the Magnetic field strength.

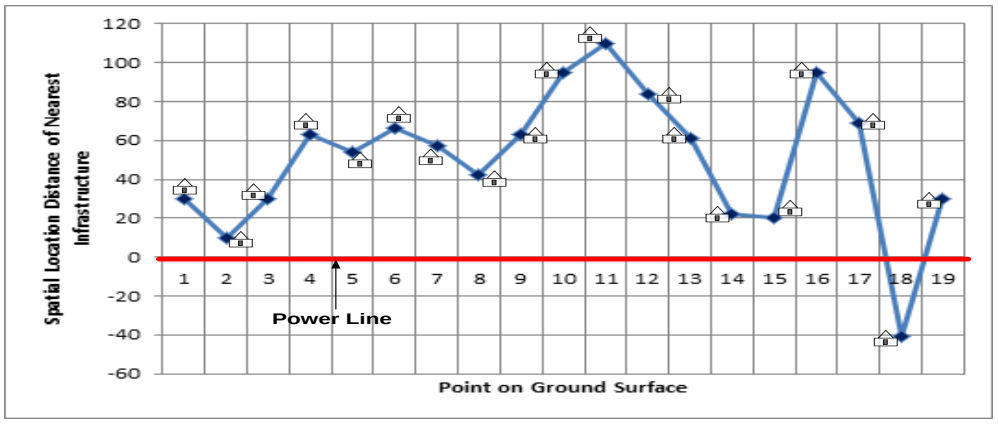

Figure 9. Spatial location's distance (m) to nearest infrastructure from the 330 kV transmission line.

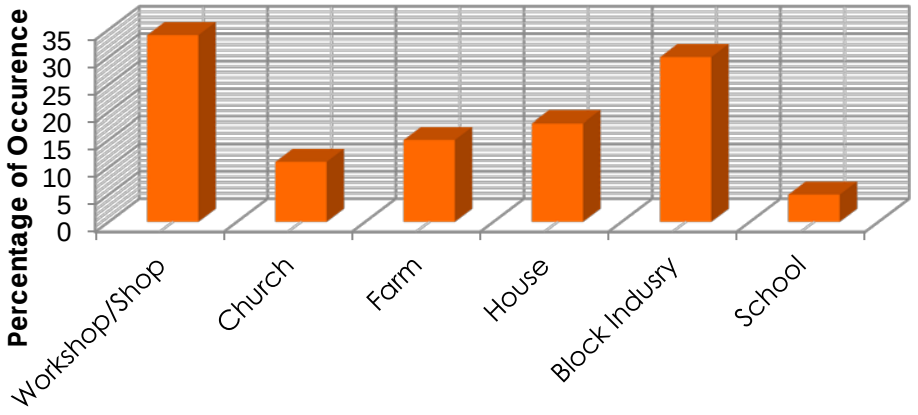

Figure 10. Percentage of the frequency of different infrastructure located close to power lines.

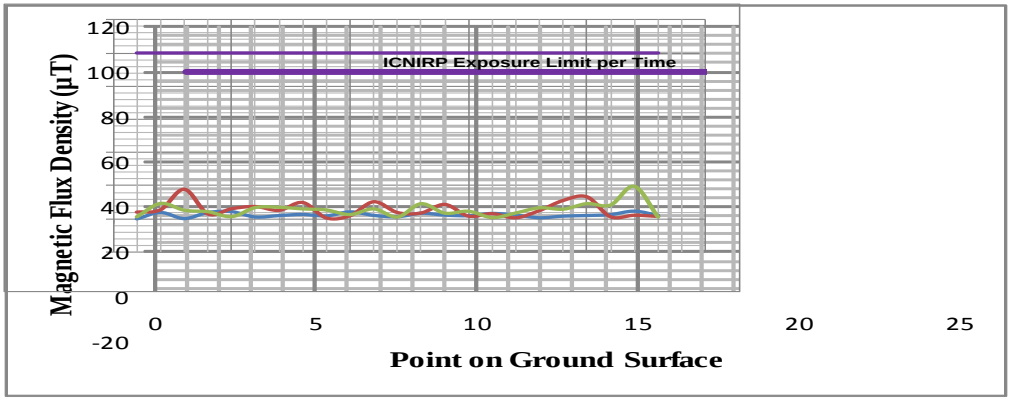

Figure 11. Comparative analysis of all the measurement of Magnetic field recorded around the power line based on ICNIRP.

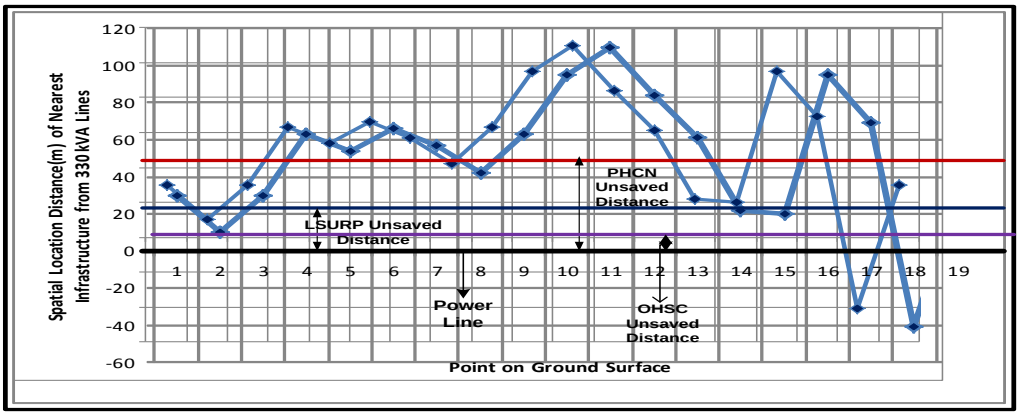

Figure 12. Comparative analysis of all the measurement of Magnetic field recorded around the power line based on power standard and regulations.

Table 2. Infrastructures under and close to the power lines.

S/N	Infrasructure	Under Lines	Left to Lines	Right to Lines	Frequency	Percentage
1	Workshop/Shop	5	3	5	13	34
2	Church	0	2	2	4	11
3	Crop Farm	0	1	1	2	5
4	House	2	2	3	7	18
5	Block Indusry	1	4	7	12	30
6	School	1	0	0	1	5
					39	100%

Table 3. Percentage of Compliance to Regulations and Standards.

S/N	Organisation	Power Transmission Rating	Regulation and Standards	Compliance
1.	PHCN	330kV	50 m pathway proximity	57.89%
2.	LSURP	330kV	22.5m pathway proximity	78.95%
3.	OHSC	230kV, 500kV	5 – 7 m pathway proximity	89.47%

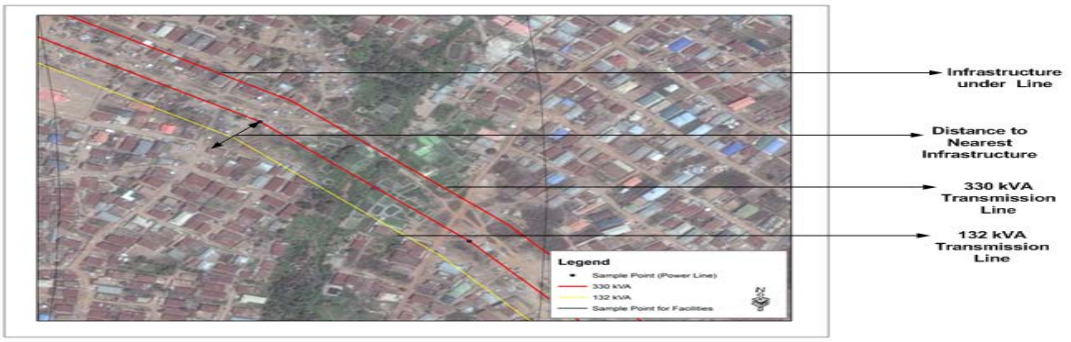

Figure 13. Results on spatial distance between the nearest infrastructure and the transmission lines using Satellite based system.

Table 4. Results of magnetic flux density under transmission Tower @ 1.0 m to ground surface.

Point on Ground Surface (P)	Magnetic Field @ Infrastructure B_T (μT)	GPS Values @ Towers X_{UT} (N)	Y_{UT}(E)	Z_{UT}(m)	Range (m) R_{UT}(m)
1	3.68	674256	862165	344	0(Ref. Pt)
2	3.85	674471	861944	330	308.65
3	0.16	674133	862620	356	351.49
4	3.86	674029	862464	357	375.63
5	4.35	674018	862414	353	384.57
6	1.11	672685	862697	335	1658.67
7	1.99	672649	862706	333	1675.16
8	2.68	669960	862196	319	1689.27
9	1.8	669324	862111	334	1696.81
10	4.24	669332	862063	331	1773.35
11	2.1	669289	862012	333	2087.05
12	1.27	672225	862719	326	2249.06
13	3.39	672213	862670	332	1409.20
14	2.26	672287	862637	325	2983.19
15	1.93	671742	862618	339	2998.63
16	3.27	671715	862563	340	2096.30
17	2.27	671711	862515	336	1862.16
18	0.67	669921	862134	315	1515.11
19	1.64	668121	861911	321	4368.75
20	2.03	668096	861953	321	4413.11
21	2.58	667275	861933	335	4535.54
22	4.65	667245	861880	332	4640.50
23	2.11	667254	861835	330	4759.26
24	20	665450	861718	329	1535.00
25	1.12	667676	861970	323	1577.07
26	0.16	665452	861662	329	1788.61

Table 5. Results of magnetic flux density at nearest infrastructure to Left side of Tower.

Point on Ground Surface (P)	Magnetic Field B_{LT} (μT)	GPS Values @ Towers X_{LT} (N)	Y_{LT} (E)	Z_{LT} (m)	Range (m) R_{LT} (m)
1	4.07	674631	861861	347	0(Ref.Pt)
2	5.55	674339	862232	338	472.21
3	17.85	673334	862701	345	1545.25
4	2.92	674028	862467	342	854.90
5	6.11	674029	862406	352	812.07
6	7.45	669940	862171	317	4701.32
7	5.13	669322	862093	333	5314.08
8	9.87	669334	862047	331	4701.32
9	0.53	669286	861997	335	5314.08
10	1.89	672228	862709	329	5300.29
11	10.34	672224	862654	332	5346.74
12	3.82	672274	862646	327	2548.30
13	3.55	671744	862604	339	2534.31
14	8.71	671724	862544	338	2484.36
15	1.65	671728	862506	338	2887.01
16	3.14	669917	862151	316	2973.80
17	0.65	668113	861892	318	4723.01
18	5.04	668084	861968	321	6547.93
19	11.11	667272	861951	336	7359.55
20	13.31	667251	861864	335	7380.0
21	1.24	667262	861826	331	7369.1
22	2.19	667682	861946	320	6949.57
23	1.46	665454	861676	331	9178.88

Table 6. Results of magnetic flux density at nearest infrastructure to Right side of Tower.

Point on Ground Surface (P)	Magnetic Field B_{RT} (μT)	GPS Values @ Towers X_{RT} (N)	Y_{RT}(E)	Z_{RT}(m)	Range (m) R_{RT}(m)
1	1.27	674317	862223	340	0 (Ref. Pt)
2	9.32	673570	862713	340	893
3	5.19	674033	862451	353	364.43
4	4.32	674025	862430	355	358.24
5	1.34	672650	862630	331	1715.99
6	6.83	669948	862208	319	4369.08

7	6.99	669331	862137	334	4986.75
8	6.02	669322	862085	336	4996.90
9	5.35	669283	862023	334	5037.97
10	2.6	672232	862728	331	2145.30
11	6.02	672222	862686	333	2145.56
12	1.11	672295	862621	327	2060.83
13	9.15	671727	862638	334	2623.04
14	3.43	671722	862591	340	2620.96
15	4.62	671725	862534	340	2610.59
16	0.78	669915	862129	317	4403.06
17	3.56	668132	861892	318	6193.89
18	6.67	668116	861931	321	6207.90
19	5.83	667274	861914	336	7049.77
20	9.2	667271	861965	334	7050.72
21	8.33	667255	861834	333	7072.71
22	19.64	665455	861706	331	8877.07
23	1.2	667692	862007	328	6628.53
24	3.13	665455	861659	330	8879.93

5. Conclusion

In this paper, we present an assessment of the geo-spatial proximity and evaluation of the magnetic pollution from 132 kV and 330 kV power transmission lines in Osogbo, Nigeria. The results from the tests carried out showed that 57.89% of the infrastructure complied with the PHCN regulations, 78.95% compiled with the Lagos State Urban and Regional Planning (LSURP) regulation and 89.47% compiled with the Occupational Health and Safety Code (OHSC) regulation. Furthermore, to support the analysis, these results were compared with the ICNIRP standard and the allowable occupational exposure level was found to be in a safe limit of exposure.

References

[1] Aliyu, O.I., Ali, H. (2011). Analysis of magnetic field pollution due to 330kVA and 132kVAtransmission lines. Abubakar Tafawa Balewa University Bauchi, Nigeria. Journal of Technology and Educational Research, 4(20), 87-93.

[2] Nafar, M., Solookinnejad, G., Jabbari, M. (2013). Magnetic field calculation of 63kv transmission lines. International Journal of Recent Research and Applied Studies, 17(2), 218-224.

[3] Siaka, M. (2010). Highlighting the dangers of living under high tension cables. Business day Newspaper.

[4] Badru, R.A., Olorunyomi, K.P., Salau, A.O., Akinwale, O.I., Alwadood, J., Atijosan, A.O. (2017). Evaluation of electric field pollution from 132 kVA power transmission lines to proximity of

ınfrastructures in Ibadan, Nigeria. Bilge International Journal of Science and Technology Research, 1(2), 46-58.

[5] Akinlolu, P., Kazeem, A. (2015). Assessment of human exposure to magnetic field from overhead high voltage transmission lines in a city in south western Nigeria. American Journal of Engineering Research, 4(5), 154-162.

[6] Hasan, A.S.M., Habibullah M.D. (2013). Analysis of smart grid with 132/33 kV sub-transmission line in rural power system of Bangladesh. American Journal of Electrical Power and Energy Systems, 2(4), 106-110. Doi: 10.11648/j.epes.20130204.12

[7] Daud, M.Z., Ciufo, P., Perera, S. (2009). Statistical analysis of overvoltages due to the energisation of a 132 kV underground cable. In: 6th International Conference on Electrical Engineering/Electronics, Computer, Telecommunications and Information Technology (ECTI-CON), 54-57.

[8] Habiballah, I.O., Abdel-Galil, T.K., Dawoud, M.M., Belhadj, C.A., Arif Abdul-Majeed, M., Al-Betairi, T.A. (2006). ELF electric and magnetic fields exposure assessment of live-line workers for 132 kV transmission line of SEC. IEEE PES Transmission and Distribution Conference and Exposition, Latin America, Venezuela, 1-6.

[9] Neuert, M.R. (2012). Possible safety distances to consider for emf sources. Neuert Electromagnetic Services. [Online]: http:www.emfinfo.org.

[10] Ozovehe, A., Ibrahim, M., Hamdallah, A. (2011). Analysis of magnetic field pollution due to 330kv and 132kv transmission lines. Journal of Trainee Teacher Educational Research, 4(2), 87-93.

[11] Forseen, U.M., Feychting, M., Rutqvist, L.E., Floderus, B., Ahlbom, A. (2000). Occupational and residential magnetic field exposure and breast cancer in females. Epidemiology, 11(1), 24 – 29.

[12] World Health Organization, (1998). Electromagnetic fields and public health; physical properties and effects in biological systems. Fact sheet number, 182.

[13] ICNIRP, (1998). Guidelines for limiting exposure to time-varying electric, magnetic, and electromagnetic fields, quantities and units. Health Physics, 74, 494–522.

[14] Rachedi, B.A., Babouri, A., Berrouk, F. (2014). A study of electromagnetic field generated by high voltage lines using COMSOL multıphysıcs. In: International Conference on Electrical Sciences and Technologies in Maghreb, Tunis 2014, 1-5.

[15] European Commission: Report on the implementation of the council recommendation on the limitation of exposure of the general public to electromagnetic fields (0 Hz – 300 GHz), (2008). 1-110. [Online]: https://ec.europa.eu/health//sites/health/files/electromagnetic_fields/docs/bipro_staffpaper_en.pdf

[16] Yu, H., Baodang, B., Dexin, X. (2002). The electromagnetic field distribution in the human body under the ultra-high voltage transmission line. IEEE, 2243-2246.

[17] Institute of Electrical and Electronics Engineers, (2002). Safety levels with respect to human exposure to electromagnetic fields, 0–3 kHz. IEEE New York 2002.

[18] Taboola, P. (2012). PHCN warns against building structures under Power lines. Vanguard 2012. [Online]: http://www.vanguardngr.com/2012/07/phcn-warns-against-building-structures-under-power-lines/

International Conference on Science and Technology

ICONST 2018

5-9 September 2018 Prizren - KOSOVO

Determining of a Voice Note Value by Using of Matlab

Hayati Mamur[1]*, Ayberk Aktaş[1], Sergen Kuzey[1]

Abstract: Sounds obtained from musical instruments refer to specific notes. Which of these notes are known to those who have a good music ear or have been trained. It is very difficult to know by any of them. If these notes are known and can be transferred to the computer environment, comparisons with other played instruments would be possible. In addition, the construction of new music tracks could be performed by means of a computer. For this purpose, in this study, it is aimed to record these sounds that is played a music tool from a musical instrument on a computer and then determine which note was played by using the Matlab program. First, these sounds from the musical instrument were recorded in Matlab software. Secondly, in Matlab software, these sound data were processed and its frequencies were determined and it was deduced which note belongs. Finally, Matlab Graphical User Interface (GUI) screen, the musical notation of the note that was visualized and presented to the user. The correctness of the implemented software has also been verified via a music note recognizing software.

Keywords: Matlab, GUI, Fourier transform, determination of sounds

Özet: Müzik aletlerinden çıkan sesler belirli notaları ifade eder. Bu notaların hangilerinin olduğu iyi bir müzik kulağına sahip olan veya bu eğitimi almış kişiler tarafından bilinebilir. Bunların herhangi biri tarafından bilinmesi çok zordur. Eğer bu notalar bilinir ve bilgisayar ortamına aktarılırsa diğer çalınan aletlerle ilgili kıyaslamalar yapılabilecektir. Ayrıca yeni müzik parçalarının yapılması bilgisayar aracılığı ile gerçekleştirilebilecektir. Bu amaçla, bu çalışmada, bir müzik aletinden reel olarak çalınan veya müzik aletinden çıkan sesin bilgisayara kaydedip sonrasında Matlab programı kullanarak hangi notanın çalındığının belirlenmesi amaçlanmıştır. İlk olarak, müzik aletinden çıkan sesin Matlab ortamına kaydedilmesi gerçekleştirilmiştir. İkinci olarak, Matlab programında ses verileri işlenerek frekansları belirlenmiş ve hangi notaya ait olduğu çıkarılmıştır. Son olarak da Matlab Grafik Kullanıcı Arayüzü (GUI - Graphical User Interface) ekranında müzik aletinden çıkan notanın hangi nota olduğu görselleştirilerek kullanıcılara sunulmuştur. Gerçekleştirilen yazılımların doğruluğu müzik notası tanıyıcı bir yazılımla da doğrulanmıştır.

Anahtar Kelimeler: Matlab, GUI, Fourier dönüşümü, ses belirlenmesi

Giriş

Sinyal işleme analog ve dijital sinyaller üzerinde analizler yapmaktır ve ayrıca bunlarda meydana gelen zamansal ve mekansal değişiklikleri belirleyip çeşitli yollarla sistemlere işlenmiş veri olarak göndermektir. [1-3]. Elde edilen bu veriler kontrol sistemlerinde, haberleşme cihazlarında ve görüntü aletlerinde yaygınlıkla kullanılmaktadır. Analog ve dijital sinyal işlemenin farklı yolları vardır. Genel olarak dört sınıfta toplanılabilir. Bunlar: (a) Analog sinyal işleme [4], (b) Ayrık zamanlı sinyal işleme [5], (c) Dijital sinyal işleme [3] ve (d) Lineer olmayan sinyal işlemedir [6].

[1]Manisa Celal Bayar University, Faculty of Engineering, 45140, Manisa, TURKEY
*Corresponding author: hayati.mamur@cbu.edu.tr

Sinyal işlemenin amaçları arasında sinyal kazancının arttırılması, kalitesinin yükseltilmesi ve özelliklerinin belirlenmesi gibi hususlar vardır. Sinyal kazancının arttırılması ve işlenerek yeniden yapılandırılması bu sinyalleri depolamaya ve istediğimiz amaçlar doğrultusunda kullanmaya yaramaktadır. Sinyal kalitesinin arttırılması, sinyalde bulunan görüntü kalitesinin yükseltilmesi ve gürültünün en aza indirilmesini sağlar. Bunların yanı sıra ses, görüntü ve video gibi sıkıştırma işlemleri ile depolama alanlarının daha efektif olarak kullanılmasına yardımcı olur.

Sinyaller işlenirken bize yardımcı olacak en önemli araçlardan biri hızlı Fourier (FFT - Fast Fourier Transform) dönüşümüdür. Sinyaller ifade edilirken ilk olarak zaman gösterilir. FFT ile bir sinyalin zaman domeninden frekans domenine geçişi sağlanır. FFT bir sinyalin içerdiği frekansı ifade eder ama zaman aralıklarındaki bulunan frekansların hangilerinin olduğunu açıklayamaz [7]. Eğer zamana göre değişmeyen sistemlerin FFT'leri çıkarılmak istenirse bunların analizlerinde çok başarılı bir teknik FFT'dir. Geçici durum analizleri gibi zamanla değişen sistemler için FFT çok başarılı değildir [8]. Bundan dolayıdır ki kısa zaman FFT çevrimlerine başvurulur. Fakat burada da frekans değerleri için problemler çıkmaktadır.

Sinyal işlemenin ses ve görüntü konusunda yapılmış çalışmalara literatürde çoklukla rastlamak mümkündür. Dikici [9] işaret işleme teknikleri ile nota analizlerini Matlab'ta yapmıştır. Bu çalışmada, görüntü işleme teknikleri kullanılarak nota belgelerinin basit ve anlaşılır bir şeklide hesaplayan bir yöntem geliştirilmiştir. Bülbül ve Karacı [10] bilgisayar ortamında sesli komutları tanıma ile ilgili araştırmaları vardır. Bu çalışmada örüntü yöntemi kullanılarak ses tanıyan bir bilgisayar yazılımı hazırlanmış ve ses tanımayla ilgili temel ilkeler sistematik bir içerikle anlatılmıştır. Sonuç olarak geliştirdikleri yazılımda ses tanımayla ilgili ön işlemler kullanıcı kontrolünde tek tek uygulanarak her uygulamanın sonucunda çıkan ses sinyalinin grafiği şekil olarak görüntülenmiştir. Bray ve Tzanetakis [11] sesin algılanmasını güçleştiren gürültülerle ilgili bir çalışma yapmışlardır. Algılama sırasında ortaya çıkan sesin belirlenmesini güçleştiren gürültülerin nasıl yok sayılması gerektiği hakkında bilgiler verilmişlerdir. Dede ve Sazlı [12] Matlab yardımıyla ses tanıma modülü simülasyonu ile ilgili çalışmalar yürütmüşlerdir. Onlar çalışmalarında, biyometrik sisteme ait ses tanıma modülünün simülasyonu amacıyla bir yazılım geliştirmişlerdir. Daha sonra, sistem genelinde on kişiden alınan yirmişer yetki talebi ile yapılan toplam 200 denemede yalnızca iki tane yanlış sonuç alınmış, diğer 198 denemede ise başarılı olunmuştur. Bu denemelerin sonucunda ise sistemin başarısı %99 olarak ölçülmüştür.

Gerçekleştirilen bu çalışma bir müzik aletinden çıkan notların bir bilgisayara kaydedilerek nota değerlerinin belirlemesini amaçlamıştır. Bu nota değerlerinin belirlenmesi ancak iyi bir müzik eğitimi almış ve müzik kulağı iyi olan kişiler tarafından bilinebilmektedir. Bu yazılım Matlab Grafik Kullanıcı Arayüzü (GUI - Graphical User Interface) ile notalar rahatlıkla belirlenebilmiştir. Çalışmanın ilk bölümünde konunun genel bir tanıtımı yapıldıktan sonra, diğer bölümde materyal ve metotlar sunulmuştur. Araştırma bulguları ve tartışma bölümünde de yapılan çalışmadan elde edilen neticeler verilmiş ve bunlar değerlendirilmiştir. Son olarak da sonuç ve öneriler sunulmuştur.

Materyal ve Metotlar

Matlab GUI ekranı hazırlanırken, ilk olarak, gerçekleştirilecek bir algoritma belirlenmiştir. Bu algoritma grafiksel düzenin belirlenmesi, program çıktılarının alınması ve çıktıların GUI aktarımı şeklinde üç ana parçadan oluşturulmuştur. Grafiksel düzenleme bölümünde önce analiz ve veri çıktıları için 'Analysis' adında bir panel oluşturulmuştur. Manisa Celal Bayar Üniversitesi logosu için yeni bir axes grafiği eklenmiş ve 'imshow' komutu ile logonun ekranda görüntülenmesi sağlanmıştır. Program çıktılarını belirleme kısmında yapılması amaçlanan programın vermesi gereken bilgiler ve grafikler düşünülerek bu verilerin GUI ekranına aktarımını yapacak olan program kümelerinin algoritmaları yazılmıştır. Öncelikli olarak sesin dış ortamdan alınması veya bilgisayar dizin sisteminde kayıtlı olan sesin okunması gerekmektedir. Sesin dış ortamdan aktarımını sağlamak amacıyla alt bir program daha geliştirilmiştir. Oluşturulan buton ile global değişkenler yani programın tamamında geçerli olacak değişken terimler tanımlanmıştır. Bu şekilde alınan ses verilerinin dış ortamdan kayıt ortamına alınması sorunsuz ve gürültüsüz bir şekilde gerçekleştirilmiştir. Çıktıların GUI aktarımı için bir adet axes grafik bölümü ve üç adet static text bölümü oluşturulmuştur. Elde edilen ve sonuçların çıktı olarak sunulduğu GUI arayüzü Şekil 1'de verilmiştir. Program yapısı üç tane küçük program parçasından oluşturulmuştur. Bunlar; kayıtlı ses dosyasının frekansının belirlenmesi için kullanılan 'frekansbul.m', bulunan frekansların notaya dönüştürülmesi için 'nota.m' ve elde edilen sonuç çıktılarının

gösterilmesi için ‘gui.m’. Oluşturulan programın akış basamakları Şekil 2’de verilmiştir.

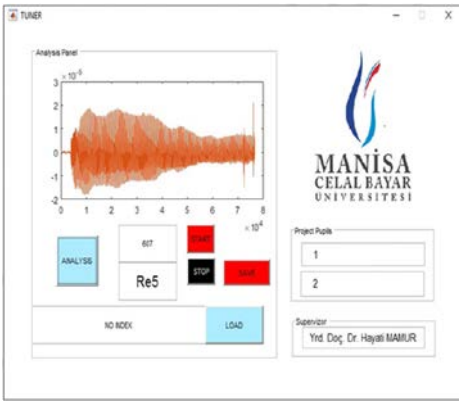

Şekil 1. Oluşturulan GUI.

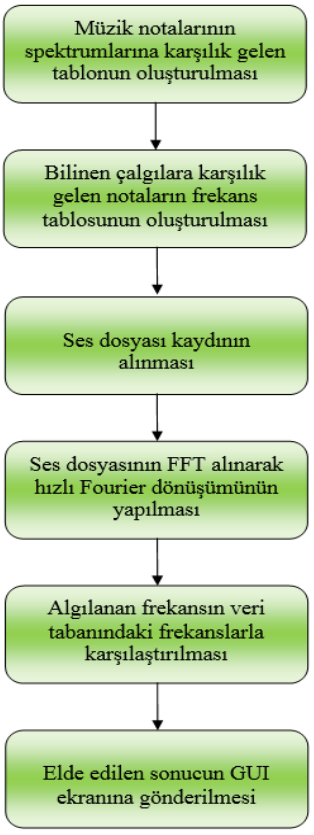

Şekil 2. Oluşturulan programın akış basamakları.

Araştırma Bulguları ve Tartışma

Gerçekleştirilen çalışmanın doğruluk testi için Android ve IOS platformları için tasarlanmış olan, müzik dünyasında aletlerin akort ayarları için en yaygın olarak kullanılan 'gStrings' adlı programı referans olarak alınmıştır. Burada yapılan karşılaştırma işlemi yazılan programın GUI ekranında verilen frekans değeri ve bu frekans değerinin hangi notaya karşılık geldiğidir. Program yazıldıktan sonra yapılan karşılaştırmalarda kullandığımız Android programı olan gStrings ile aynı sonuçları verdiği gözlemlenmiştir. Testler sonucunda programın eksiksiz çalıştığı görülmüştür. Yazılan programda GUI çıktısı olarak verilen nota değeri ile

referans program olarak kullanılan program verileri tam olarak uyuşmuştur. Karşılaştırma olarak kullanılan program ve yazılan programın çıktıları Şekil 3'de verilmiştir. İsteğe bağlı olarak kayıt altına alınan seslerin dizin kontrolleri yapılmış ve doğru yerlere doğru şekilde ses sinyallerinin yazıldığı ispatlanmıştır.

Matlab GUI ortamında tasarlanan çalışmanın benzetim testlerinde elde edilen sonuçlar çerçevesinde problemler de saptanmıştır. Bu problemlerden en belirgin ve giderilmesi gerekeni dış ortamdan alınan dip ses ve gürültülerin ayıklanması işlemi olmuştur. Çünkü dış ortamdan alınan saf sesin içine karışan gürültüler referans alınması gereken frekans değerinin değişikliğe uğramasına sebep olmaktadır. Bu sebeple başlatılan araştırmalar sonucu Cepstrum Dönüşümüne ulaşılmıştır. FFT uygulanmış ses sinyali doğrusal olmayan bir sinyal dizisi elde edilmesini sağlamıştır. Bu doğrusal olmayan sinyalin Cepstrum Dönüşümü ile üzerinde bulunan en baskın frekansı elde edilmiştir.

Ses sinyali bir temel frekans ve onun üzerinde oluşan harmoniklerden meydana geldiği gelmektedir. Bu sayede kulağa güzel gelen nota sesleri ortaya çıkmaktadır. Bu temel frekans değerini bulmak için ise öncelikli olarak FFT ve sonrasında Cepstrum dönüşümü kullanılmıştır. Bu nedenle ortaya çıkan temel frekans ise kabul edilen frekans değerlerinden oluşturulan database üzerinden karşılaştırma yapılarak ses sinyalinin nota değerine ulaşılmıştır.

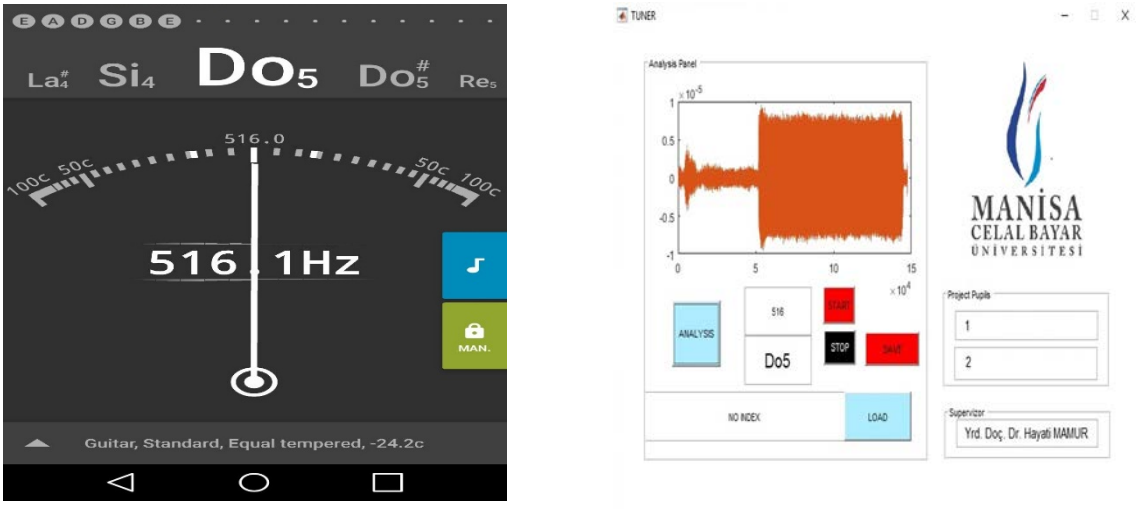

Şekil 3. Android programı ile yazılan programın sonuçlarının karşılaştırılması.

Sonuç ve Öneriler

Gerçekleştirilen bu çalışmada, Matlab ortamında sesin analizi ile nota değerinin belirlenmesi başarılı bir şekilde gerçekleştirilmiştir. Ses analizlerinin nasıl yapılacağı detayları ile sunulmuştur. Bir ses parçası içerisindeki en baskın frekans değeri o sesin notasyonunu vermektedir. Analizi yapılacak müzik aletinin çıkarmış olduğu ses sinyali içerisinde baskın olarak bulunan frekans değeri belirlenmiştir. Algoritması yazılan program ile ister sesin gerçek zamanlı olarak aktarımı isterse kayıtlı olan sesin analizi ile ses sinyalinin spektrumu ve frekans değeri belirlenmiştir. Bu frekans değeri de kabul edilmiş olan nota frekans değerleriyle karşılaştırıp yapılan yazılımın doğruluğu ispatlanmıştır. GUI aktarımını sağlamak için de gerekli program parçacıkları yazılmıştır. Tüm bunların sonucunda, ses sinyallerinin GUI gerçek zaman analizi, kayıtlı ses analizi ve ses kaydının yapılması, ortaya çıkan frekans, nota ve spektrum bilgilerini aktarma işlemleri başarılı bir şekilde uygulanmıştır.

Bu çalışmanın sonraki bölümlerinde, elektrik-elektronik cihazların çalışma seslerinin sisteme öğretilmesi ve bunlarda meydana gelen ses değişiklerinin algılanıp kullanıcılara iletilmesi hedeflenmektedir. Böylelikle ses değişikliği ile arızalanan veya arızalanma ihtimali olan cihazların tespit edilmesi sağlanacaktır.

Teşekkür

Bu çalışma, Manisa Celal Bayar Üniversitesi Bilimsel Araştırma Koordinasyon Birimi (No: 2018-137) tarafından desteklenmiştir.

Referanslar

1. Basseville, M. (1989). Distance measures for signal processing and pattern recognition. Signal processing, 18(4), 349-369.
2. Rabiner, L. R., & Gold, B. (1975). Theory and application of digital signal processing. Englewood Cliffs, NJ, Prentice-Hall, Inc., 1975. 777 p.
3. Antoniou, A. (2016). Digital signal processing. McGraw-Hill.
4. Athreyas, N., Gupta, D., & Gupta, J. (2017). Analog signal processing solution for machine vision applications. Journal of Real-Time Image Processing, 1-22.
5. Oppenheim, A. V., & Schafer, R. W. (2014). Discrete-time signal processing. Pearson Education.
6. Bilgehan, B. (2015). Efficient approximation for linear and non-linear signal representation. IET Signal Processing, 9(3), 260-266.
7. Katoh, K., Misawa, K., Kuma, K. I., & Miyata, T. (2002). MAFFT: a novel method for rapid multiple sequence alignment based on fast Fourier transform. Nucleic acids research, 30(14), 3059-3066.
8. Brigham, E. O., & Brigham, E. O. (1988). The fast Fourier transform and its applications (Vol. 448). Englewood Cliffs, NJ: prentice Hall.
9. Dikici, E. (2006). İşaret İşleme Teknikleri İle Nota Analizi.
10. Bülbül, H. İ., & Karacı, A. (2007). Bilgisayar Ortaminda Sesli Komutlari Tanima: Örüntü Tanima Yöntemi. Kastamonu Eğitim Dergisi, 15(1), 45-62.
11. Bray, S., & Tzanetakis, G. (2005, September). Distributed Audio Feature Extraction for Music. In Ismir (pp. 434-437).
12. Dede, G., & Sazlı, M. H. (2010). Biyometrik Sistemlerin Örüntü Tanıma Perspektifinden İncelenmesi ve Ses Tanıma Modülü Simülasyonu. EEBM Ulusal Kongresi.

International Conference on Science and Technology

ICONST 2018

5-9 September 2018 Prizren - KOSOVO

Hybrid Renewable Energy System Feasibility for a Public Building

Hayati Mamur[1]*, Mert Can Yakar[1], Atakan Zerafet[1]

Abstract: Today, it is a hot working area to meet the electricity needs of a building with hybrid renewable energy sources. For this reason, in this study, an analysis was carried out to meet the electricity needs of Kozlu Vocational and Technical Anatolian Highschool, an education building, with solar and wind hybrid renewable energy sources. Firstly, annual electric energy expenditures of the selected public buildings were examined. Based on these invoice values, the maximum and minimum monthly electricity energy expenditures are determined. Annual average energy expenditure is calculated. Analyses were conducted to establish a hybrid renewable energy source system with wind and solar hybrid network. Once the analysis is carried out with normal calculations, the Homer Pro program is utilized for the detailed calculations. As a result of the analysis, it has been determined that a 36 kW wind turbine and 23 kW solar panel combination with grid connection could meet the electric energy requirement of Kozlu Vocational and Technical Anatolian Highscool. In this case, it was determined that while some of the electric energy in December was purchased from the grid, it could give electricity to the network in the following months. As a result of these, it was determined that the established system could amortise itself after 7.8 years.

Keywords: Renewable energy resource, wind energy, solar panel, hybrid system

Özet: Günümüzde bir binanın elektrik enerjisi ihtiyacının yenilenebilir enerji kaynakları ile karşılanması sıcak bir çalışma alanıdır. Bu nedenle, bu çalışmada, bir kamu binası olan Kozlu Mesleki ve Teknik Anadolu Lisesinin güneş ve rüzgâr yenilenebilir hibrit enerji kaynakları ile elektrik ihtiyacının karşılanması için bir analiz gerçekleştirilmiştir. İlk olarak seçilen kamu binasının yıllık elektrik enerjisi giderleri incelenmiştir. Bu fatura değerlerine bağlı olarak maksimum ve minimum elektrik enerjisi harcanan aylar belirlenmiştir. Yıllık ortalama enerji harcaması hesaplanmıştır. Rüzgâr ve güneş hibrit şebeke bağlantılı yenilenebilir enerji kaynağı sisteminin kurulması için analizler yapılmıştır. Analizler normal hesaplamalar ile yapıldıktan sonra detaylı hesaplamalar için Homer Pro programı kullanılmıştır. Yapılan analizler sonucunda, 36 kW rüzgâr türbini ve 23 kW güneş panelli şebeke bağlantılı hibrit yenilenebilir enerji sisteminin Kozlu Mesleki ve Teknik Anadolu Lisesinin elektrik enerjisi ihtiyacını karşılayabileceği belirlenmiştir. Bu durumda Aralık aynında elektrik enerjisinin bir kısmı şebekeden satın alınırken, diğer aylarda şebekeye elektrik enerjisi verebileceği belirlenmiştir. Bunların sonucunda da kurulan sistemin 7,8 yıl sonra kendini amorti edebileceği belirlenmiştir.

Anahtar Kelimeler: Yenilenebilir enerji kaynağı, rüzgar enerjisi, güneş enerjisi, hibrit sistem

Giriş

Enerjiye olan ihtiyacın hızla artmasıyla birlikte enerji kaynaklarının ileri bir zamanda tükenmesi kaçınılmazdır. Fosil yakıtlı geleneksel enerji kaynaklarının sürekli kullanılması zararlı sera gazı

[1]Manisa Celal Bayar University, Faculty of Engineering, 45140, Manisa, TURKEY
*Corresponding author: hayati.mamur@cbu.edu.tr

salınımlarının artmasına neden olmaktadır. Bu fosil yakıtlı enerji kaynakları ile birlikte yenilenebilir enerji kaynaklarının kullanımının arttırılması sürdürülebilir bir çevre ve enerji politikaları için gereklidir. Ayrıca bu durum enerji çeşitliliğini de arttıracaktır [1-2].

Rüzgâr ve güneş enerji sistemleri şebekeye bağlı veya bağlantısız olarak elektrik enerji üretimi yapabilirler. Şebekeden bağımsız çalışan güneş enerji sistemleri çıkış gerilimlerinin doğru akım olmasından dolayı DC yükleri direkt olarak besleyebilirler. Eviriciler yardımıyla da AC yüklere enerji sağlarlar. Rüzgâr enerjisi sistemleri ise genellikle AC çıkış gerilimine sahiptirler ancak yine dönüştürücüler yardımıyla DC'ye daha sonra da AC'ye çevrilerek cihazları beslerler [3-5]. Bir binanın veya konutun elektrik ihtiyacını karşılamak için yenilenebilir enerji kaynakları özendirilmektedir. Bu konuda yönetmelikler çıkarılmaktadır. Yenilenebilir enerji kaynağı olarak da rüzgar ve solar enerji kaynaklarının birlikte kullanımı oldukça yaygınlaşmaktadır. Çünkü eğer yalnız solar enerji kaynağı kullanılsa geceleri elektrik enerjisi üretimi yapılamayacak ve sistemde bulunan akü grubunun enerjisi harcanacaktır. Rüzgar enerji çevrim sistemlerinin kullanımı ile birlikte elektrik enerjisi üretiminin sürekliliği sağlanmaktadır. Rüzgar olduğunda geceleri ve gündüzleri de rüzgar türbinlerinden faydalanılmaktadır [6-9].

Hibrit yenilenebilir enerji kaynakları ile konutların veya belirli bir gölgedeki yerleşim alanının elektrik enerjisinin sağlanması için fizibilite çalışmaları gerçekleştirilmiştir. Bu bağlamda, Özcan [4] yük olarak belirlediği Gebze'de bulunan bir fabrikanın elektrik enerjisi ihtiyacını karşılayacak şebeke bağlantılı örnek bir hibrit enerji sisteminin modellenmesini ve analizini gerçekleştirmiştir. Uysal [10] Selçuk Üniversitesi Kampüs alanı içerisinde, rüzgâr ve güneş enerjisinden üretilen elektrik enerjisinin analizi yapmıştır. Dolaşır ve Ceylan [11] kampüslerinde bulunan KYK binasının elektrik enerjisi ihtiyacının hibrit enerji sistemi tarafından karşılanabilmesi için gerekli hesaplamaları ve analizleri yapmışlardır. 1 MW rüzgâr türbininin 70 m kule yüksekliğine kurulması durumunda yapılan hesaplama ve analizlerden, ortalama rüzgâr hızının 6,8 m/s ve yıllık elektrik enerjisi üretiminin 3.015,216 kWh olacağını hesaplamışlardır.

Bu çalışmanın amacı, yük olarak belirlenen Kozlu Mesleki ve Teknik Anadolu Lisesi`nin elektrik enerji ihtiyacının yenilenebilir enerji kaynakları olan güneş ve rüzgar ile karşılanması için bir fizibilite çalışması yapmaktır. Bunun için de Homer (Hybrid optimization model for electric renewables) programından yararlanılmıştır. Bu program vasıtasıyla şebeke bağlantılı örnek bir hibrit enerji sisteminin modellenmesi, benzetimi ve optimizasyonu gerçekleştirilmiştir.

Materyal ve Metotlar

Öncelikle, Zonguldak Kozlu Mesleki ve Teknik Anadolu Lisesi`nin fiziki özellikleri araştırılarak yapı planları incelenmiştir. Bu sayede okul binasının enerji verimliliği etüdü çalışmasına altyapı hazırlanmıştır. Son bir yılın elektrik enerjisi tüketimleri incelendiğinde Kasım-Mart ayları arasındaki dönemde yoğunluğun arttığı gözlemlenmiştir. Okula ait bir yıllık elektrik tüketim değerleri Tablo 1'de verilmiştir. Güneş enerjisi potansiyelini belirlemek için önemli faktörlerden biri güneşlenme süreleridir. Zonguldak ilinin ortalama güneş radyasyon değeri 3,67 kWh/m^2-gün iken ortalama güneşlenme süresi ise 6,51 saat'tir. Zonguldak iline ait aylık ortalama sıcaklık değerleri de Meteoroloji Genel Müdürlüğünün internet sitesinden alınmıştır. NASA Surface verilerine göre Zonguldak iline ait 50 m yükseklikteki rüzgâr verileri belirlenmiştir. Bu sonuçlara göre 50 m yükseklikteki ortalama rüzgâr hızı 5,91 m/s'dir. Kozlu ilçesi ortalama rüzgâr hızı, rüzgâr haritası dikkate alındığında yaklaşık 5-6 m/s aralığında olduğu görülmüştür. Ekonomik bir rüzgâr enerji santral yatırımı için 7 m/s üzerinde rüzgâr hızı gerekmektedir [12]. Kozlu ilçesine tek başına kurulacak bir rüzgar enerji santrali ekonomik olmadığından hibrit bir sistem üzerinde çalışma yapılmıştır. Kozlu Mesleki ve Teknik Anadolu Lisesi 2016-2017 yılındaki elektrik enerjisi tüketimleri incelendiğinde en fazla enerji tüketiminin Aralık ayında olduğu gözükmektedir. Aralık ayı ve düşük tüketimli yaz ayları ortalama elektrik enerjisi hesabının dışında tutulduğunda ortalama tüketimin 4512 kWh olduğu bulunmuştur. Bu ortalama değerin üstünde kalan aylardaki enerji ihtiyacının karşılanabilmesi için şebeke bağlantısı yapılması gerektiği öngörülmüştür. Bu hesaplama sonucunda ve gerçekleştirilen fizibiliteler sonucunda; 23 kW fotovoltaik güç sistemi ile 36 kW gücünde bir rüzgar türbini kurulmasının uygun olacağı ortaya çıkmıştır. Ayrıca Kozlu Mesleki ve Teknik Anadolu Lisesi çatı uygulamalı olarak 23 kWh gücünde bir fotovoltaik güç sistemi kurulması planlanmıştır. Tasarlanan sistemin şematik yapısı Şekil 1'de verilmiştir.

Tablo 1. Kozlu Mesleki ve Teknik Anadolu Lisesi elektrik enerjisi tüketim tablosu

Elektrik enerjisi tüketim tablosu 03.2016–02.2017			
Fatura tarihi	**Abone unvanı**	**Elektrik Tüketimi (kWh)**	**Fatura Tutarı (TL)**
Ocak	Kozlu EML	5791	2432,22
Şubat	Kozlu EML	6198	2603,16
Mart	Kozlu EML	5404	2269,68
Nisan	Kozlu EML	3259	1368,78
Mayıs	Kozlu EML	2694	1131,48
Haziran	Kozlu EML	1662	698,04
Temmuz	Kozlu EML	480	201,6
Ağustos	Kozlu EML	520	218,4
Eylül	Kozlu EML	567	238,14
Ekim	Kozlu EML	2526	1060,92
Kasım	Kozlu EML	5714	2399,88
Aralık	Kozlu EML	9638	4047,96
Toplam Tutar		**44453**	**18670,26**

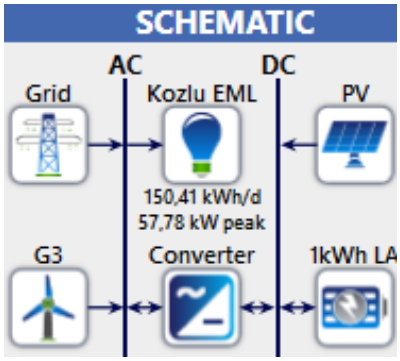

Şekil 1. Tasarlanan sistem.

Araştırma Bulguları ve Tartışma

Kozlu Mesleki ve Teknik Anadolu Lisesi`nden alınan son on iki aylık elektrik enerjisi tüketim değerleri üzerinde analiz yapılarak hafta içi ve hafta sonu olmak üzere saatlik yük değerlerine ulaşılmıştır. Bu analiz çalışmasında öğrenci ve personelin okulda olduğu 08.00–20.00 saatleri için aylık toplam elektrik tüketiminin %82'sinin harcandığı öngörülmüştür. Gece 20.00–08.00 için ise bu oranın %10 olabileceği düşünülmüştür. Hafta sonu için belirlenen oran ise %8'dir. Yük profili girildikten sonra hibrit kurulum için rüzgar türbini ve güneş paneli seçilmiştir. Homer programı ile optimizasyon sonuçları kısmında 600 tane farklı konfigürasyon modellenmiştir. En ekonomik olanı burada seçilmiştir. Kış ayları tüketiminin ortalama elektrik enerjisi tüketiminden fazla olmasından dolayı sistemi şebekeye bağlama ihtiyacı doğmuştur. Şebeke bağlantısı olmadan hibrit enerji kurulumu tercih edilseydi, kurulum için gereken maliyet daha da fazla olacaktır. Yıllık net şebekeye satılan enerji yani şebekenin sisteme dahil edilmesiyle elde edilen kazanç değeri yıllık 861,61 TL olmuştur. Kurulumda kullanılan 15 kW değerlikli konvertör için analizler incelendiğinde kapasite faktörünün %21,9 olduğu görülmüştür. Solar paneller için analizlerde ortalama çıkış gücünün 3,58 kW, ortalama günlük çıkış gücü 85,9 kWh/gün belirlenmiştir. Kapasite faktörü %15,6 olup 1 yıllık toplam enerji üretimi ise 31,367 kWh/yıl'dır. Rüzgâr türbininin duyarlılık sonuçlarındaki analiz değerlendirmelerine göre de ortalama güç çıkışı 5,12 kW, kapasite faktörü %14,2 ve yıllık toplam üretim 44.880 kWh/yıl değerinde belirlenmiştir.

Sonuçlar

Bu çalışmada, güneş-rüzgâr hibrit güç sistemindeki enerji ihtiyacının karşılanacağı Kozlu Mesleki ve Teknik Anadolu Lisesi için aylık enerji tüketim bilgileri alınmıştır. Okulun yaz aylarında çok fazla enerjiye gereksinimi olmadığından üretilecek enerjinin şebekeye satılabilmesi adına tasarlanan sistem şebeke bağlantılı kurulmuştur. Elektrik tüketimi açısından diğer aylarla büyük fark bulunan Aralık ayı içinse aynı şebekeden enerji satın alınabileceği öngörülmüştür. Fizibilite çalışmasında ise yaz ayları ve Aralık ayı hesabın dışında tutularak, diğer ayların ortalama elektrik enerjisi tüketim değerleri göz önüne alınmıştır. Bunların sonucunda rüzgâr türbini ve güneş paneli kapasitesi 36 ve 23 kW seçilmiştir. Güneş panelinin daha üst kapasite değerlerde seçildiği durumlarda maliyette gereksiz bir artış ve Aralık ayında bile şebekeye satabilecek kadar enerji üretimi oluşmuştur. Sistemin kurulumuyla birlikte son bir yılın toplam elektrik fatura değeri yani 18.670,26 TL kadar kar sağlanmış olacaktır. Aynı zamanda sistem şebekeye sattığı enerji sayesinde her yıl 861,61 TL kar elde edilebilecektir. Bu iki değerin toplamının sistem kurulumu için gerekli maliyete bölünmesiyle sistemin kendisini 7,82 yılda karşılayacağı sonucuna ulaşılmıştır.

Teşekkür

Bu çalışma, Manisa Celal Bayar Üniversitesi Bilimsel Araştırma Koordinasyon Birimi (No: 2018-137) tarafından desteklenmiştir. Ayrıca verilerin sağlanmasında katkı sağlayan Ali Özdemir'e teşekkür ederiz.

Referanslar

1. Balamurugan, P., Ashok, S., & Jose, T. L. (2009). Optimal operation of biomass/wind/PV hybrid energy system for rural areas. International Journal of Green Energy, 6(1), 104-116.
2. Bauwens, T. (2016). Explaining the diversity of motivations behind community renewable energy. Energy Policy, 93, 278-290.
3. Wagh, S., & Walke, P. V. (2017). Review on wind-solar hybrid power system. International Journal of Research In Science & Engineering, 3.
4. Özcan, H. (2009). Bir hibrid enerji sisteminin modellenmesi ve analizi. İstanbul Teknik Üniversitesi Fen Bilimleri Enstitüsü. Yüksek Lisans Tezi. İstanbul, Turkey.
5. Güven, A. F. (2016). Bahçelievler Belediye Başkanlık Binasının enerji ihtiyacının güneş ve rüzgar sistemi ile karşılanması, optimizasyonu ve maliyet analizi. Sinop Üniversitesi Fen Bilimleri Dergisi, 2(1), 24-36.
6. Sinha, S., & Chandel, S. S. (2015). Review of recent trends in optimization techniques for solar photovoltaic–wind based hybrid energy systems. Renewable and Sustainable Energy Reviews, 50, 755-769.
7. Fathima, A. H., & Palanisamy, K. (2015). Optimization in microgrids with hybrid energy systems–A review. Renewable and Sustainable Energy Reviews, 45, 431-446.
8. Kannan, N., & Vakeesan, D. (2016). Solar energy for future world:-A review. Renewable and Sustainable Energy Reviews, 62, 1092-1105.
9. Harish, V. S. K. V., & Kumar, A. (2016). A review on modeling and simulation of building energy systems. Renewable and Sustainable Energy Reviews, 56, 1272-1292.
10. Uysal, N. (2011). Konya ili için rüzgâr ve güneş enerjisinden elektrik üretimi ve kullanımının araştırılması, Selçuk Üniversitesi, Yüksek Lisans Tezi, Konya, Turkey.
11. Ata, R. Dolaşır, E., & Ceylan, C. (2015). Celal Bayar Üniversitesi Muradiye KYK Kız Yurdu için hibrid enerji sistemi fizibilite çalışması, EMO Dergisi.
12. Li, H., & Chen, Z. (2008). Overview of different wind generator systems and their comparisons. IET Renewable Power Generation, 2(2), 123-138.

International Conference on Science and Technology

ICONST 2018

5-9 September 2018 Prizren - KOSOVO

Design of Efficiency Controlled Cleaning System for Solar Panel

Abdullah Özdemir[1], Burak Aladağ[1], Kubilay Taşdelen[1], Ahmet Ali Süzen[2*]

Özet: Bu çalışmada güneş panellerinin yüzeylerinindeki toz oranı ile verim kontrolü yaparak panelleri otomatik temizleyen bir sistem tasarımı gerçekleştirilmiştir. Tasarlanan sistem ile güneş panellerinden elde edilen verimi maksimum düzeyde tutmak amaçlanmaktadır. Güneş panellerine bağlı olan verim cihazı ile panellerin verimi anlık olarak ölçülmektedir. Sistemin çalışması, güneş panellerinden alınan verimin belli bir değer altına düşmesi ile başlamaktadır. Ayrıca temizleme işleminin başlaması ile beraber panellerden alınan verimde artış olmaz ise sorumlu kişilere bildirim gitmektedir. Güneş panellerinin temizlenmesi için sisteme bağlı su tankından saf suyu çekilmektedir. Çekilen saf su güneş enerjisi panelinin üzerinde bulunan kollara aktarılmaktadır. Aktarılan su, kol içinde dâhil olan temizleyici plastik cam silme bandına akarılmaktadır. Güneş paneli temizleme sisteminde, paneldeki verimlilik üzerindeki toz oranı ile belirlenmektedir. Bu tespit için toz sensörü kullanılmaktadır. Panellerden alınan veriler Arduino geliştirme kartı ile işlenmektedir. Sonuç olarak geliştirilen sistem ile panellerden elde edilen verimin maksimum düzeyde tutulması hedeflenmektedir.

Anahtar Kelimeler: Arduino, Güneş Paneli, Fotovoltaik, Otomatik Temizleme, Toz Algılama, Verimlilik.

Abstract: In this study, a system design was carried out by the dust ratio on the surfaces of solar panels and cleaning the panels with efficiency control. The system is designed to keep the maximum level of data obtained from solar panels. The efficiency of the panels is measured instantaneous with the efficiency device connected to solar panels. The operation of the system starts with the data from the solar panels falling below a certain value. In addition, with the start of the cleaning process does not increase the efficiency of the panels are notified to the responsible people. Pure water is drawn from the water tank attached to the system for cleaning the solar panels. The pure water taken is transferred to the arms located on the solar panel. The transmitted water is transferred to the cleaner plastic glass wiping tape, which is included in the arm. The solar panel cleaning system is determined by the powder rate on the efficiency of the panel. The dust sensor is used for this detection. The data from the panels is processed by the Arduino development card. As a result, it is aimed to keep the data obtained from the panels at maximum level with the developed system.

Keywords: Arduino, Automatic Cleaning, Dust Detection, Efficiency, Fotovoltaik, Solar Panel.

Giriş

Enerji ihtiyacının karşılanması için kullanılan güneş panelleri güneşten gelen ışık enerjisini elektrik enerjisine çevirmektedir (Batman, 2001). Bu donanım teknik olarak fotovoltik yarı iletken silikon ve levhadan oluşmaktadır. Güneş panellerinin üzerinde gelen ışınları soğurmaya sağlayan güneş hücresi bulunmaktadır. Güneşten gelen ışık enerjisi belirli bir verimlilikte kullanılmaktadır. Güneş panellerinden elde edilen elektrik enerjisi doğru akımda depolanabilmektedir. Depolanan doğru akım kaynağı istenilirse dönüştürücüler ile alternatif akıma dönüştürülmektedir (Çelebi, 2002).

Güneş panellerinde dönüşüm verimliliği panel yapısına göre %21 ile % 35 arasında değişmektedir (Hee vd., 2012). Panellerden maksimum verimlilik optik yoğunlaştırıcılar kullanıldığında sağlanmaktadır. Elde edilen verimlilik oranları panel üzerinde toz, kir, polen ve çeşitli partiküllerinde birikmesi ile ortalama %4 oranında verim azalmaktadır (Park vd., 2011). Güneş panellerinin 20 derecenin üzerinde bir açı ile yerleştirilirse

[1] Applied Sciences University of Isparta, Electrical And Electronic Engineering, 32260, Isparta, TURKEY
[2] Applied Sciences University of Isparta, Computer Technologies 32260, Isparta, TURKEY
*Corresponding author: ahmetsuzen@isparta.edu.tr

yağmur suyu sayesinde temizlenebilmektedir (Demirtaş, 2006). Bunun harici durumlarda verimliliğin düşmemesi için belirli aralıklar ile panellerin temizlenmesi gerekmektedir. Panel temizleyicileri, panellerde oluşan kirlerin temizlenmesiyle birlikte gerekli olan verimi panelden alınmasını sağlayan donanımlardır. Bu temizleyici donanımların kullanılmadığı durumlarda panelin performans oranı zamanla düşmektedir. GEP (Güneş Paneli) tozlanma, yağmur damlası, kar vb. doğal etkenlerle kirlenmesinden dolayı yüzeyinin temizlenmesi gerekmektedir (Turhan ve Çetiner, 2012). Temizleme işlemi, temizleme robotları veya insan gücü ile belli zamanlarda manuel veya otomatik olarak yapılmaktadır. Bu temizleme işlemlerini yaparken kullanılan deterjanlar ve kimyasal temizleyiciler panellere zarar vermektedir (Özyalçin vd.,2015).

Bu çalışmada güneş panellerin kirlenmesinden dolayı düşen verimliliğin geri kazanılması için panel temizleme sistemi tasarlanmıştır. Sistemin test edilmesi için 5W güneş panelini temizlemeyi sağlayan düzenek kurulmuştur. Panel yüzeyi üzerindeki toz miktarı artığında ve panelden üretilen akım değeri düştüğünde sistem çalışmaktadır. Sonuç olarak panel üzerinden tozdan kaynaklık verimlilik kayıplarının en aza indirilmesi amaçlanmaktadır.

Materyal ve Yöntem

Arduino Uno Geliştirme Kartı

Arduino, nesnelerin interneti ve kontrol sistemleri çalışmalarında kullanılan açık kaynak kod ve donanımlı mikrokontrolcü platformudur. Arduino esnek yazılım ve donanım mimarisine sahiptir. Bundan dolayı kullanım alanları ve giriş-çıkış pin sayılarına göre farklı modelleri bulunmaktadır. Maliyet, giriş-çıkış pin sayısı ve kullanılan mikrodenetleyiciye göre en çok kullanılan Arduino Uno modelidir. Arduino Uno modelinde ATmega328 mikrodenetleyici, 14 dijital 6 analog giriş çıkış pini, 32KB hafıza ve 1KB EEPROM bulunmaktadır (Juang ve Lurrr, 2013).

Optik Toz Sensörü

Optik toz sensörleri yüzeyde veya havadaki çok ince partiküllü toz tanelerine kadar tespit edilmesinde kullanılan bir sensör çeşidir. Sensör üzerinde yer alan kızıl ötesi verici ve fototransistör sayesinde yayılan kızılötesi ışının toz partiküllerinden yansımasını ölçerek çalışmaktadır. Gerçekleştirilen çalışmada panel üzerindeki tozun tespit edilmesi için Sharp GP2Y10 Optik Toz Sensörü kullanılmıştır (Araújo vd., 2015).

Su Motoru (900L/H)

Su motoru su veya sıvıları aktarmak için kullanılan 12V DC motorlu bir mekanizmadır. Su pompaları düşük basınç – yüksek basınç prensibine göre çalışır. Mekanizma 1.75MPa ‘a kadar su basıncını desteklemektedir. Sensör dakika yaklaşık 2 litre suyu taşıyabilmektedir.

Verimlilik Kontrollü Temizleme Sistemi Tasarımı

Temizleme sisteminde, panel üzerinde toz algılandığı ve panel akım değeri %10’nun altına indiği zaman sistem çalışmaktadır. Panel üstüne monte edilen hareketli kızak sistemi DC motorların hareketi ile temizleme işlemini yapmaktadır. Toz sensöründen gelen verinin sonlanması ve panel akım değerinin artması ile temizleme sonlandırılmaktadır. Temizleme sisteminin test işlemlerinde kullanılan güneş paneline ait teknik özellikler Tablo 1’de verilmiştir.

Tablo 1. Güneş panelinin özellikleri

Özellik	Değer
Güç	5W
Voltaj	18V
Akım	0.28A

Kontrol Kartı Tasarımı

Panel temizleme sisteminin mekanik tasarımının çalışması için Arduino Uno ile kontrol kartı geliştirilmiştir. Kart anlık olarak toz miktarının elektriksel değerini ve panelden gelen akımı ölçmektedir. Panel temizleme anında su motoru ile mekanizmalarını hareketlendirmek için servo motorlar çalıştırmaktadır. Tasarlanan kontrol kartının devre şeması Şekil 1'de gösterilmektedir. Panel üzerindeki tozun algılanmasını sağlayacak toz sensörü Şekil 2'deki gibi kontrol kartına bağlanmıştır.

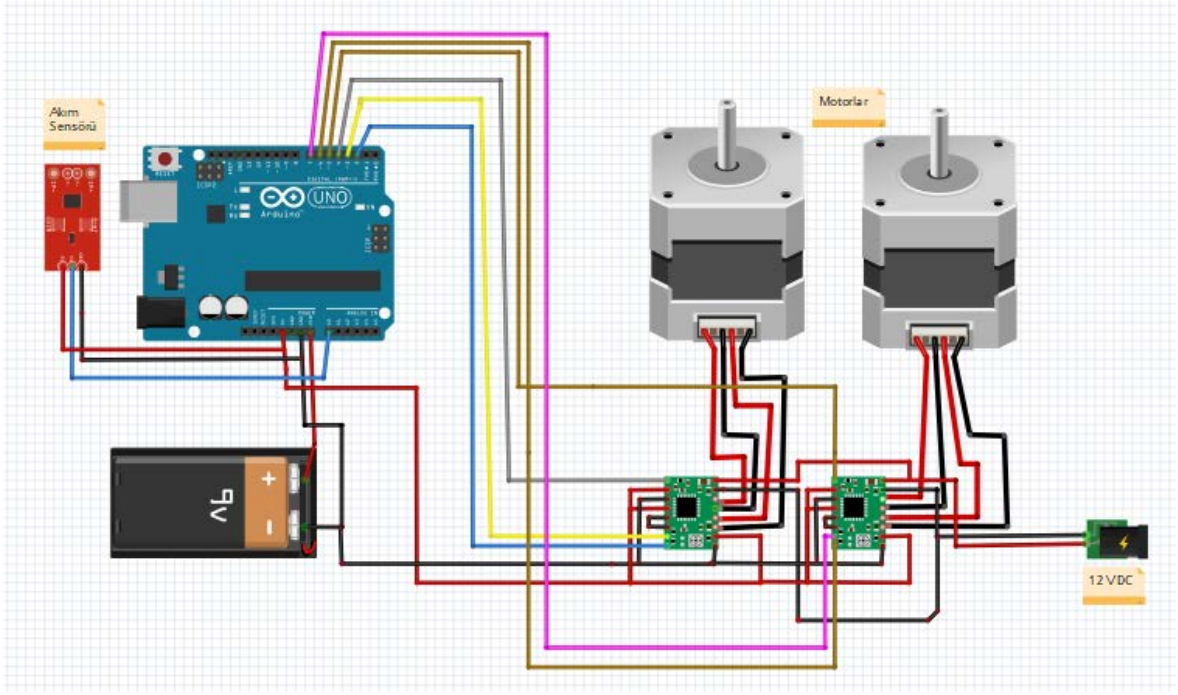

Şekil 1. Kontrol kartı devre şeması

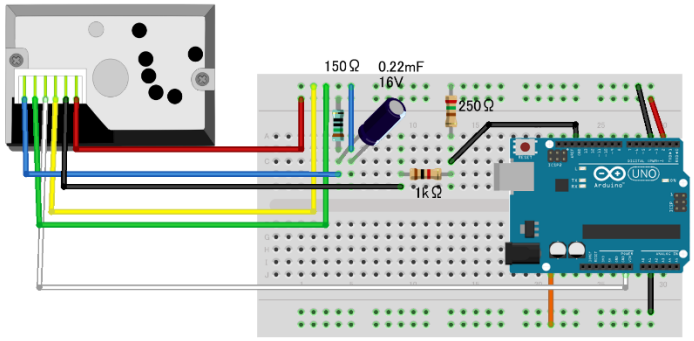

Şekil 2. Toz sensörünün bağlantı şeması

Kontrol kartı tasarımı ve devre bağlantıları kurulduktan sonra sistemin çalışmasını sağlayacak yazılım geliştirilmiştir. Arduino Uno üzerinde çalışacak yazılım Arduino IDE yazılımı üzerinde yazılmıştır. İlk olarak devre elemanlarının giriş çıkış pinlerinin yazılıma tanıtılması yapılmıştır. Her giriş ve çıkış pininin değişken adı ve pin modu tanımlanmıştır. Su motoru, servo motorun çalışması için *digitalWrite(kontropini, HIGH)* fonksiyonu kullanılır. Toz ve Akım sensöründen gelen veriler *analogRead(pin)* fonksiyonu ile alınmaktadır.

Sistemin Mekanik Tasarımı

Tasarlanan temizleme sistemin mekanik bölümünde temizliği yapılması için panel üzerine kızaklı ve vidalı ray sistemi tasarlanmıştır. Bu ray sistemi servo motorlar yardımı ile hareket ettirilmektedir. Temizleme işlemi için panel yanına su tankı yerleştirilmiştir. Sistem çalışırken ihtiyaç anında su tankındaki su, motorlar sayesinde panel üstündeki hortumlara iletilmektedir. Böylece temizleme işlemi gerçekleştirilmektedir.

Temizleme sistemi için geliştirilen protatip tasarım Şekil 3'de gösterilmiştir. Ayrıca tasarlanan sistemin şeması Şekil 4'de verilmiştir.

Şekil 3. Temizleme Sisteminin protatipi

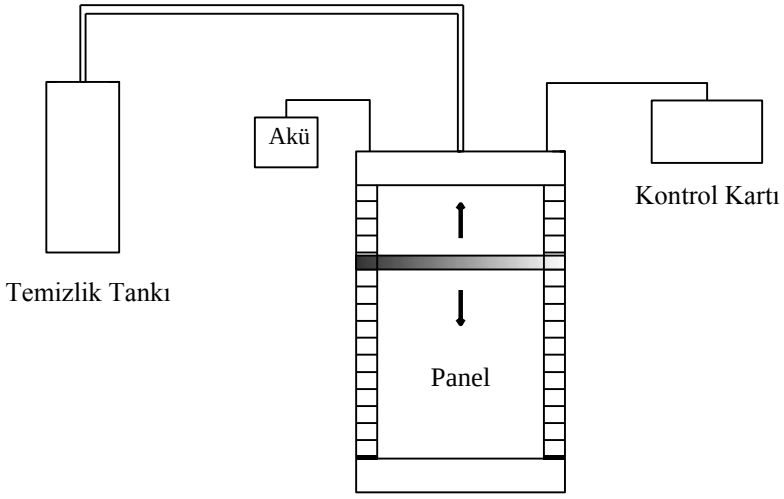

Şekil 4. Panel temizleme sisteminin şeması

Sonuçlar

Güneş panelleri, güneş enerjisi potansiyeli oldukça yüksek olan ülkemizde öncelikle elektrik enerjisi olmayan bölgelerde veya alternatif enerji kaynağı olarak birçok alanda kullanılmaktadır (Sayin ve İlhan, 2011). Güneş panelleri sürekli dış ortamlarda kaldıklarından dolayı zamanla ortam koşullarına göre kirlenmektedir. Belirli bir süre sonra panellerin kirlenmesi veriimliliği düşürmektedir (Özyalçin vd., 2015).

Bu çalışmada güneş panellerinde kullanılmak üzere toz ve panel verimlilik değerine göre temizleme işlemi yapan bir sistem tasarlanmıştır. Önerilen sistem panel üzerinde anlık olarak toz kontrolü yapmaktadır. Ayrıca panelin ürettiği akım sürekli olarak ölçülmektedir. Toz kontrolünün yapılması ile hava değişikliklerinden dolayı meydana gelen akım azalmalarından dolayı temizlik işleminin başlamasını önlemektedir. Ayrıca şebeke suyu ve taşıma su ile yapılan yanlış temizlik neticesinde oluşan kireç izleride panele zarar vermekte ve uzun vadede verimliliği düşürmektedir. Bu yüzden sistemde bulunan su tankında iyonize saf su kullanılmıştır.

Kaynaklar

Araújo, A., Portugal, D., Couceiro, M. S., & Rocha, R. P. (2015). Integrating Arduino-based educational mobile robots in ROS. *Journal of Intelligent & Robotic Systems*, *77*(2), 281-298.

Batman, M. A. (2001). Elektrik Üretimi İçin Güneş Pillerinin Kullanımında Verimi Arttırıcı Yeni Bir Yöntem, Doctoral dissertation, Fen Bilimleri Enstitüsü.

Çelebi, G. (2002). Bina Düşey Kabuğunda Fotovoltaik Panellerin Kullanim Ilkeleri. Gazi Üniversitesi Mühendislik-Mimarlık Fakültesi Dergisi, 17(3).

Demirtaş, M. (2006). Bilgisayar Kontrollü Güneş Takip Sisteminin Tasarımı ve Uygulaması. Politeknik Dergisi, 9(4).

Hee, J. Y., Kumar, L. V., Danner, A. J., Yang, H., & Bhatia, C. S. (2012). The effect of dust on transmission and self-cleaning property of solar panels. Energy Procedia, 15, 421-427.

Juang, H. S., & Lurrr, K. Y. (2013, June). Design and control of a two-wheel self-balancing robot using the arduino microcontroller board. In *Control and Automation (ICCA), 2013 10th IEEE International Conference on* (pp. 634-639). IEEE.

Özyalçin, I., Çakir, M., Çelik, A., & Tekeş, V. (2015), Mikrodenetleyicili temizlik robotu tasarimi, 4th International Vocational Schools Symposium.

Park, Y. B., Im, H., Im, M., & Choi, Y. K. (2011). Self-cleaning effect of highly water-repellent microshell structures for solar cell applications. *Journal of Materials Chemistry*, *21*(3), 633-636.

Sayin, S., & İlhan, K. O. Ç. (2011). Güneş Enerjisinden Aktif Olarak Yararlanmada Kullanilan Fotovoltaik (Pv) Sistemler Ve Yapilarda Kullanim Biçimleri. Selçuk Üniversitesi Mühendislik, Bilim ve Teknoloji Dergisi, 26(3), 89-106.

Turhan, S., Çetiner, İ. (2012). Fotovoltaik sistemlerde performans değerlendirmesi. 6. Ulusal Çatı & Cephe Sempozyumu, Bursa.

International Conference on Science and Technology

ICONST 2018

5-9 September 2018 Prizren - KOSOVO

Design of RFID Controlled Wireless Charging System for Electric Vehicles

Halil Türkmenoğlu[1], Nazar Mammedov[1], Kubilay Taşdelen[1], Ahmet Ali Süzen[2*]

Özet: Otomotiv teknolojisinin gelişmesi ve ihtiyaçları doğrultusunda elektrikli araçlar tasarlanmıştır. Elektrikli araçların ortaya çıkmasıyla daha temiz bir çevre oluşturulması amaçlanmaktadır. Aynı zamanda petrol savaşlarınında azalması hedeflenmektedir. Elektrikli araçlar kablolu ve kablosuz olarak şarj edilmektedir. Araçların şarj olmasında, pratik ve kullanım kolaylığı sağladığı için kablosuz sistemler daha çok tercih edilmektedir. Elektrikli araçların şarj edilmesinde, hayatı daha da kolaylaştırmak ve araçların kullanımını arttırmak gibi bazı kriterler göz önünde bulundurularak yeni teknolojik çalışmalar sürdürülmektedir. Bu çalışmada elektrikli araçların RFID etiket kontrollü, kablosuz ve kolay şarj edilmesini sağlayan bir sistem tasarlanmıştır. Tasarlanan araç tanıma ve şarj sistemi, aracın tüm verilerine ulaşarak araca ait güce göre şarj edilmesini sağlamaktadır. Aracın kablosuz olarak şarj edilmesi için alıcı kontrol kutusu ve güç aktarımı için verici kontrol kutusu geliştirilmiştir. Kontrol kutularında Arduino mikrodenetleyici kartı kullanılmıştır. Sistemin çalışması için araç bilgilerinin daha önceden RFID alıcı kartı yüklenmesi gerekmektedir. Araç şarj istasyonunda kablosuz aktarım yapılacak bölgeye ulaştırılır. Verici devre araçta bulunan RFID üzerinden plaka ve akü güç bilgisi alınarak şarj süresi belirlenir. Veri aktarımı bittikten sonra aracın aküleri kablosuz olarak şarj edilir. Sonuç olarak çalışmanın uygulanabilirliği ile düşük maliyetli, kullanımı kolay ve pratik bir sistem hedeflenmektedir.

Anahtar Kelimeler: Arduino, Elektrikli Araçlar, Kablosuz Şarj, RFID, Şarj İstasyonu.

Abstract: Electric vehicles are designed because of the development and necessity of automotive technology. The emergence of electric vehicles is aimed at a cleaner environment. It is also aimed to decrease the oil wars. Electric vehicles are charged wired and wireless. Wireless systems are more preferred because they provide practical and ease of use in charging vehicles. New technological studies are being carried out in consideration of some criteria, such as the charging of electric vehicles, making life easier and increasing the use of vehicles. In this study, the system is designed to provide RFID tag controlled, wireless and easy charging of electric vehicles. The vehicle recognition and charging system is designed to ensure that the vehicle's data is charged according to its power. The Transmitter control box is developed for the receiver control box and power transmission for wireless charging of the vehicle. The Arduino microcontroller card is used in the control boxes. In order to operate the system, the vehicle information must be installed before the RFID receiver card. The vehicle is delivered to the area where the wireless transfer will be transferred at the charging station. The transmitter circuit, the vehicle on the RFID plate and battery power information is determined by reading the charging time. After the data transfer is finished, the vehicle's batteries are charged wirelessly. As a result, the applicability of the study is aimed at a low-cost, useful and practical system.

Keywords: Arduino, Charging Station, Electric Vehicle, RFID, Wireless Charger.

[1] Applied Sciences University of Isparta, Electrical And Electronic Engineering, 32260, Isparta, TURKEY
[2] Applied Sciences University of Isparta, Computer Technologies 32260, Isparta, TURKEY
*Corresponding author: ahmetsuzen@isparta.edu.tr

Giriş

Kablolu olarak yapılan enerji iletimlerinde verimin yüksek olması, bir avantaj olmasına rağmen en büyük kayıp zaman olmaktadır. Ayrıca kablolu olması şehir içi ve şehir dışı şarj istasyonlarında zaman ve kullanım zorluğuna neden olmaktadır. Araba şarj edilirken belirlenen şarj istasyonlarına gidilmesi gerekir. Bununla beraber bu şarj istasyonlarında yetkilendirilen görevli gözetiminde şarj işlemleri yapılmaktadır. Bu işlemlerin gerçekleştirilmesi ciddi bir zaman sarfiyatı ile olmaktadır. Tüm bunların yanı sıra kablolu enerji aktarımlarında yüksek güç çekilmesinden dolayı güvenlik çok önemlidir. Kabolarda oluşabilecek izole bozulmalarında enerjiyi araçın metal aksamına verebilir. Bunun sonucunda can ve mal kayıplarına neden olunabilmektedir (Bal, 2012).

Kablosuz olarak gerçekleştirilen enerji transferinde enerji manyetik alan kullanılarak iletilmektedir. Kablosuz enerji iletimde verim düşük olması bir dezavantajdır. Bakır ve nüve kayıplarının yanı sıra, saçak etkisinden dolayı oluşan kayıplar vardır. Ama yüksek güvenilirlikte olması otoparkları, yol kenarları, ev garajları, şehir içi yol kenarı otoparklar gibi farklı yerlere kurulabilme imkânı sunmaktadır. Böylelikle zamandan tasarruf edilebilmektedir. Kapalı otopark ve yol kenarı otoparkları bu sayede verimli bir şekilde kullanılmış olacaktır. Oluşabilecek manyetik alan kayıpları farklı yöntemler ile azaltılır ve verim arttırılabilir (Agbinya, 2012).

Materyal ve Yöntem

Enerji İletimi

Elektrik enerjisinin üretildiği santraller çoğu zaman tüketim bölgelerinden uzakta kurulur. Bu bakımdan elektrik enerjisinin üretildiği yerlerden tüketim bölgelerine taşınması gerekmektedir. Günlük hayatta pek çok kullanma alanı bulunan elektrik enerjisinin iletim ve dağıtımının ekonomik bir şekilde yapılabilmesi, enerji alanında en önemli konulardan biridir. Enerji iletimi kablolu ve kablosuz olarak gerçekleştirilir (Gürbüz, 2012).

Kablolu Enerji İletimi

Enerjiyi biryerden başka biryere iletmek için kablolar kullanılmalıdır. Kablolarda elektron hareketleri ile elektrik iletilmektedir. Kablolu elektrik iletimi daha az kayıplarla iletim sağlanmaktadır. Düşük güçlerde kısa mesafelere yapılan iletimlerde kayıplar yok denilecek kadar azdır. Bu oran %1 ile %3 arasında değişmektedir (Gürbüz, 2012). Bununla birlikte dezavantajları bulunmaktadır. Bunlar kablo karmaşıklığı, iletim hatlarının maliyeti, daha yüksek güçlerde kablo kesitinin artmasına, kabloların günlük kullanım alanlarında izole edilmesidir (Agbinya, 2012).

Kablosuz Enerji İletimi

Kablosuz enerji iletimi manyetik alan ile gerçekleştirilmektedir. Kablosuz enerji ya da kablosuz enerji transferi, insan yapımı iletken olmadan güç kaynağından elektriksel alana elektrik transferidir. Kablosuz transfer kabloların bağlantısının uygunsuz, tehlikeli ve imkânsız olduğu durumlarda kullanışlıdır. Kablosuz enerji transferindeki problem kablosuz telekomünikasyondan sistemlerinden farklıdır. İkinci olarak, alınan enerjinin yayılması sadece sinyal çok az olduğunda kritik olmaktadır. Kablosuz enerji için yeterlilik çok önemli bir parametredir. En yaygın kablosuz elektrik transfer şekli manyetik resonator tarafından direk indüksiyon olarak kullanılmasıdır (Agbinya, 2012).

Arduino

Arduino temel olarak açık kaynaklı donanıma dayalı bir fiziksel programlama platformudur. Bu sayede gömülü sistemlerden biri olarak takip edilen mikroişlemciler programlanabilir. Piyasada en çok kullanılan PIC, ARM gibi gömülü sistem yazılımlarına alternatif olarak doğmuş, onlara göre çok daha kolay bir şekilde programlanabilme ve sahip olduğu geniş kütüphanesi sayesinde çok kısa kodlar ile karmaşık işlerin yapılmasına imkân sağlamaktadır (Ferdoush ve Li, 2014).

Arduino tek başına çalışan interaktif nesneler geliştirmek için kullanılabileceği gibi bilgisayar üzerinden çalışan yazılımlarada bağlanabilir. Hazır üretilmiş kartlar olarak bilinsede kensileri üretmek isteyenler için donanım tasarımı ile ilgili bilgiler mevcuttur. Arduino kartlarında 5V regüle devresi ve 16KHz kristal osülatör bulunur. ATmega8, ATmega168, ATmega328 işlemcilerini kullanır (Arduino, 2018).

RFID

Radyo Frekanslı Tanımla canlıları ya da nesneleri radyo dalgaları ile tanımlamak için kullanılan teknolojilere verilen genel isimdir. RF-ID temel olarak bir etiket ve okuyucudan meydana gelir. RF-ID etiketleri Elektronik ürün kodu (EPC) gibi nesne bilgilerini almak, saklamak ve göndermek için programlanabilirler. Ürün üzerine yerleştirilen etiketlerin okuyucu tarafından okunmasıyla bilgiler otomatik olarak kaydedilebilir veya değiştirilebilir (Igoe, 2012).

RF-ID etiketleri pasif, yarı pasif veya aktif olmak üzere üç çeşittir. En ucuz etiket çeşidi olan pasif etiketlerin kendi güç kaynakları bulunmaz ve okuyucunun gücüyle çalışırlar. Buna karşılık yarı pasif etiketlere ise, gelen sinyalden güç almaya gerek bırakmayacak küçük bir pil eklenmiştir. Daha geniş okunma alanına sahip bu etiketler daha güvenilir oldukları gibi, okuyucuya daha çabuk cevap verebilirler (Finkenzeller, 1999).

RDIF Kontrollü Kablosuz Şarz İstasyonu Tasarımı

Kontrol Kartı Tasarımı

Gerçekleştirilen çalışmada Arduino kontrol kartı sistemin çalışması için önemlidir. Tüm kontroller ve iletişim bu kart üzerinden yapılmaktadır. Kontrol kartında Arduino Uno geliştirme kartı kullanılmıştır. Sistemde RFID ile verilerin alıması RC522 okuyucu modülü ile gerçekleştirilmektedir. RFID okuyucudan gelen bilgi okunduktan sonra kontrol kartı, rölenin tetiklenip tetiklenmeyecegine karar verir ve verici manyetik alan sargısı kontrol edilir.

Şekil 1'de sistemin akış diyagramı görülmektedir. Bu akış diyagramı istasyonun çalışma adımları verilmiştir. Araç geldiginde RFID etiketin kendine ait bilgileri okur. Daha sonra araç bilgileri kontrol edilir. Eğer bilgiler doğru ise enerji iletimimine başlanır. Bu işlem aracın şarjı dolana kadar devam eder ve daha sonra işlem sonlardırır.

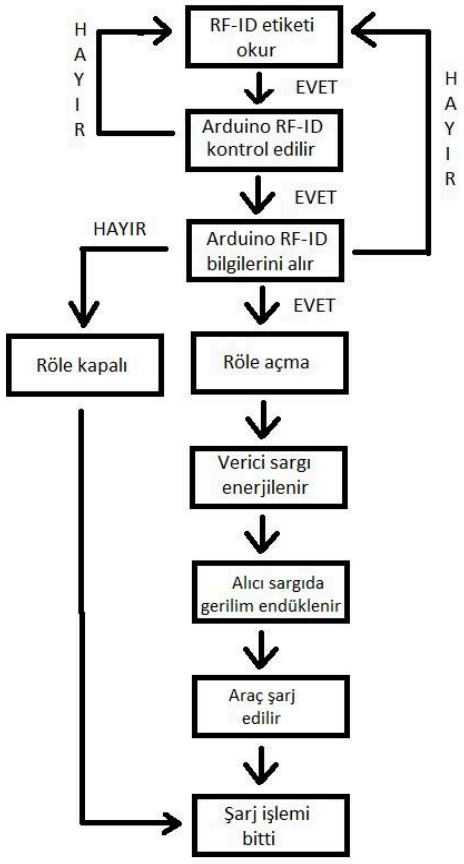

Şekil 1. Kontrol kartı yazılımının çalışma şeması

Manyetik Alan Sargıları

Manyetik alan sargıları ile manyetik alan oluşturularak enerji iletimi yapılmaktadır. Sistemde alıcı ve verici olmak üzere 2 adet manyetik alan sargısı bulunmaktadır. Şebekeden çekilen 220V gerilim degeri trafo yardımı ile 12V degerine düşürülerek verici sargısına uygulanır. Her iki sargı da E şeklindeki silisli saçlardan oluşturulmuş Şekil 2'de görüldüğü gibi ferromanyetik nüve üzerine sarılmıştır. Verici devresinde ısınmasını önlemek için kalın bobin teli kullanılır. Alıcı devresinde ise ince ama daha fazla sarım kullanılır.

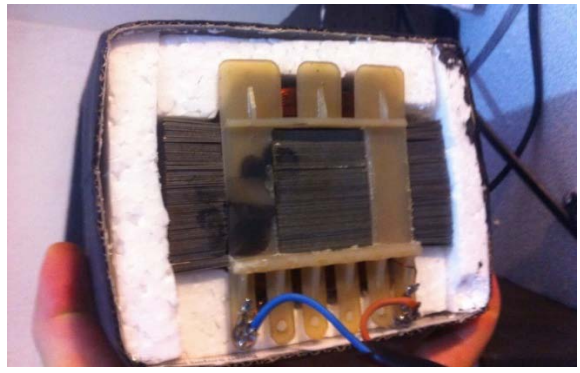

Şekil 2. İzole edilmiş manyetik alan sargısı

Bu devre trafo mantığı ile çalışmaktadır. Fark olarak sadece sargılar ferromanyetik nüve üzerinde bulunur. İki sargı arsındaki hava boşlugunuda geçirgenligi çok zayıf olsa dahi havaninda bir geçirgenlik katsayısı vardır.

Sistemin Test Edilmesi

RFID kontrol kartı arabaya yerleştirilmiş olan etiketi okumaktadır. Bu etiket sisteme tanımlanmış veya tanımlanmamış olabilir. Tanımlanmış bir etiket ise Arduino röleyi tetikler ve verici manyetik alan sargısını enerjilendirir. Böylelikle enerji iletimi başlamış olacaktır. Etiket tanımlanmamış ise kırmızı ışık yanacak ve uyarı verecektir. Tanımlanmış bir etiket gelmesi halinde bile bilgi okunur okunmaz enerji iletime başlamayacaktır. Çünkü bu araba sistemin üstünden geçip gitme ihtimali olduğundan, sistemimiz etiket bilgisi okunduktan sonra 5 sn sonra aynı etiket bilgisi okunması durumunda iletime başlayacak şekilde tasarlanmıştır.
Sistemin çalışmasına ait seri port görüntüsü Şekil 3'de verilmiştir.

Şekil 3. Seri port görüntüsü

Sistem çalışırken istasyon girişinde beyaz ışık yanar ve bunun yanında kırmızı ve yeşil ışıkta bulunur. İstasyon dolu ise kırmızı, şarj için müsait ise yeşil yanar. Şarj işlemi bittikten sonra araba istasyondan ayrılma süresi olarak 5 sn tanımlanmıştır. Bu zaman diliminde yine istasyon girişindeki kırmızı ısık yanacak, kart okunsa dahi enerji iletimi yapılmayacaktır.

Şekil 4'de çalışma diyagramı verilen sistemde RFID kartı Kontrol ünitesi tarafından okunarak röleyi tetiklemektedir. Röle açılması ile aracın konumu şarj konumunda olacağından verici sargıları enerji iletimine başlayacaktır. Alıcı sargılar ise manyetik enerjiyi alacak ve bataryanın şarj işlemine uygun şekilde elektronik dogrultma koruma gerilim bölücüler ile düzenleyerek aracın şarj işlemi başlayacaktır. Arac şarj işlemi doldugunda ise röle kendini kapatacaktır ve verici sargıları enerji kesilecek alıcı sargılar enerjisiz kalacaktır. Şekil 4' de alıcı devresi olarak gösterilen kısım içinde hem alıcı manyetik alan sargısını hem dogrultma devresini içinde bulundurmaktadır.

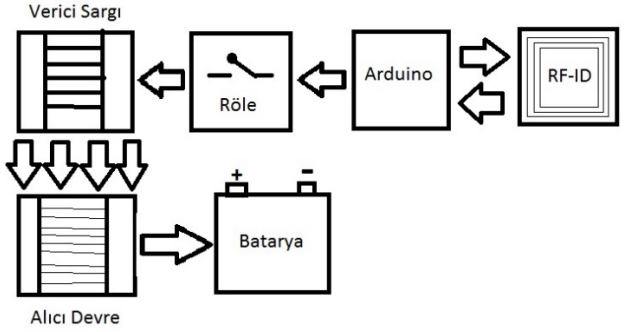

Şekil 4. Sistem Çalışma Diyagramı

Verici manyetik alan sargısına elektrik, röle devresi üzerinden geçerek besleme yapmaktadır. Açma kapama işlemlerini röle yapar. Bu röle 10A akıma kadar kullanılabilir. Alıcı manyetik alan sargısında AC gerilim endüklenir. Akü ve bataryaların DC gerilim olmasından dolayı alıcı manyetik alan sargı çıkışında doğrultma yapılır ve şarj için bataryaya bağlanır.

Şekil 5 ve Şekil 6'da geliştirilen sistem için tasarlanan örnek şarj istasyonu görülmektedir. Bu sistemde düşürücü trafo ile 220-12V AC ye dönüştürmektedir. 12 V ile beslenen verici ile alıcı transformatör arasında kablosuz enerji iletimi sağlanmıştır.

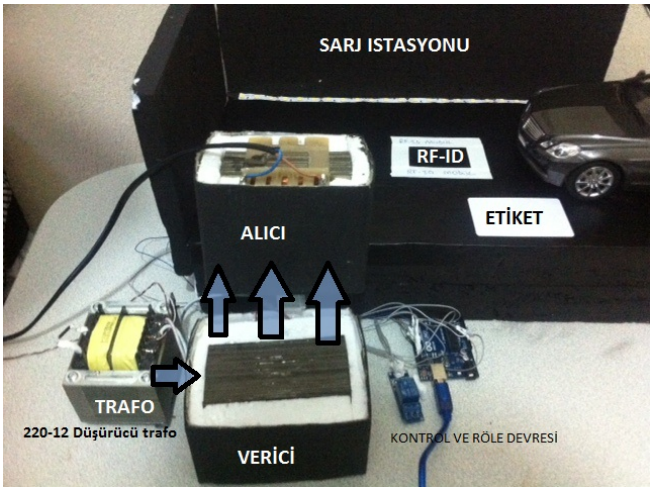

Şekil 5. Geliştirilen tasarımın görüntüsü


Şekil 6. Şarj istasyonunda araç şarj edilmesi

Sonuçlar

Yapılan çalışmanın test işlemlerinde elektrik ve elektronik yapılarında olumlu sonuçlar alınmıştır. Kullanılacak olan nüve yapısı sabit olduğundan verimi arttırmak için 2 yöntem kullanılabilir.

- Verici devresine uygulanan akım değeri artırmak.
- Sarım sayısı artırmak.

Bunun yanı sıra aradaki mesafeyi azaltılarak daha fazla akım ve gerilim iletimi yapılabilmektedir. Yapılan deneyler sonucunda manyetik alan sargılarıyla yapılan iletim verimi bobin sargılarından daha verimli olduğu görülmüştür.

Tesla bobini iletim tekniklerinde ise yüksek güçlere çıkartarak iletimi sağlaması ve akıyı tek yön değilde alana yayarak iletmesidir. Buda enerji kaybını artırmaktadır. Bu şekilde iletimlerde oluşabilecek sorunlar manyetik alanın elektronik eşyaları bozabilecegi gibi kullanılacak sistemde metal aksamlarda mıknatılanma oluşmasına sebep olacaktır. Bu mıknatıslanma ise istenmeyen durumdur ve metal aksamın topraklanmasını gerektirmektedir. Projenin Tesla bobininden farkı bir yönde akı oluşumunun sağlaması ve daha az enerji harcayarak daha düşük güçlerde çalışabilme özelligidir. Projede iletim tek yönde iletim sagladıgı için etrafa daha az miktarda manyetik akı gönderdigi için topraklanmaya daha az ihtiyaç duyulacaktır ve yapılacak olan izole sistemi ile tamamen mıknatıslanmayı ortadan kaldıracaktır. Projede bir yöne elektrik iletimi gerçekleştirildigi için enerji kaybı sadece nüve kaybı (Trafo Yapısı) ve hava aralıgına baglı olarak artacaktır.

Verim mesafe ile ters orantılıdır bu yüksek araçlarda sorun arz edebileceginden her bir araba için ayrı bir alıcı sargı oluşturularak verici sargıları sabit tutulabilir ve sisteme ek olarak mesafe sensörü kullanılır. Hareket için servo veya step motor kullanılabilir. Verici devresini üzerinde bulunduran motor, sensör kontrollü olarak alıcı devresine yaklaştırılarak verimi artırılabilir.

Gerçekleştirilen çalışma hem gerçek hayatta uygulamaya hem geliştirilmeye açık bir projedir. Çalışmanın amaçlarından biride gelişmekte olan elektrikli araçları şarj ederken hem zamandan tasarruf etmek hem güvenilir bir sistem oluşturmaktır. Yapılmış olan bu prototip gerçek hayatta kullanılmak amaçlanarak tasarlanmıştır.

Kaynaklar

Andre K.,, Aristeidis K.,, Robert ., J. D. Joannopoulos, Peter F.,, Marin S., (2007). Wireless Power Transfer via Strongly Coupled Magnetic Resonances. http://www.sciencemag.org/cgi/content/full/1143254/DC1 (Erişim Tarihi: 21.11.2014).

Agbinya, J., (2012). Wireless Power Transfer. River publishing, p397. Danimark

Arduino, (2018). http://www.arduino.cc (Erişim Tarihi: 17.04.2018).

Bal, G., (2012). Transformatorlar. Seçkin Yayıncılık, 166s. Ankara.

Fitzgerald E., Charles K., Jr., Stephen D. U.,, 1992. Electrical Machinary. McGraw Hill Publishing Company.

Ferdoush, S., & Li, X. (2014). Wireless sensor network system design using Raspberry Pi and Arduino for environmental monitoring applications. Procedia Computer Science, 34, 103-110.

Finkenzeller K., (1999). RFID Handbook: Radio-frequency identification fundamentals and applications. New York: Wiley.

Gürbüz, Ö., (2012). Hücresel Sistemlere Kıyasla Orta Gerilim Enerji Merkezleri ve İletim Hatlarındaki Elektromanyetik Alan Değerlerinin İncelenmesi ve Olumsuz Etkilerini Öneriler. Bilgi Teknolojileri ve İletişim Kurumu, Teknik Uzmanlık Tezi, 100s, Diyarbakır.

Harold Timmes, (2011). Pracrical Arduino Engineering. 196p. New York.

Igoe,T., (2012). Getting Started with RFID. O'Reilly Media,Inc., 29p. United States of America.

Leander W. Matsch, J. Derald M., (1987). Electromagnetic and Electromechanical Machines. John Wiley and Sons, New York.

Massimo Benzi, (2011). Getting Started with Arduino. O'Reilly Media, Inc., 118p. United States of America.

Nikola Tesla, (1898). The Sun, 21. Kasım 1898. New York.

Stephan B. M.,, Sanjay E. S.,, John R. W.,, (2008). RFID Technology and Applications. Cambridge University Press, 218p. Cambridge.

Qualcomm Technologies. Inc., (2011). https://www.qualcomm.com/products/halo (Erişim tarihi: 07.01.2018).

International Conference on Science and Technology

ICONST 2018

5-9 September 2018 Prizren - KOSOVO

Oxidation of Manganese with Active Use of Potassium Permanganate in the Water Treatment plants in the Town of Gjilan, Republic of Kosovo

Valdrin M. Beluli*[1]

Abstract: Gjilan (42°27'48''N 21°28'09.7''E) is one of the seven biggest cities in the Republic of Kosovo. Water supply for this city is enough for reasons of functioning of two plants of water processing in the city of Gjilan. One of the biggest plants for water is in Perlepnica village and another plant with smaller dimension to supply drink water is in Velekica village. The main issue focuses on the water treatment plant in the Velekica village because the presence of manganese (Mn^{+2}) as metal is always present in six underground springs. Quantity of Mn mg/L in groundwaters is out of norms allowed under WHO. The presence of this metal forces the water industry to use $KMnO_4$ continuously. In the water the present of this metal is from (0.05-0.0015) mg dm^{-3} during 2017 and January 2018 and after the manganese processing process is reduced to (0.11- 0.31) mg dm^{-3}. While in the water treatment plant in Përlepnica village, there is no problem with heavy metals and the process of processing continues today without any problems.

Keywords: Water industry, Groundwaters, Manganese, Chemical reactor, Oxidation

Introduction

As a town Gjilan there are two state water treatment plants, one built in the former Yugoslavia in the village of Përlepnica but renovated again by the state of Switzerland and another plant was built by the Swiss state in the village Velekica on the outskirts of the city. The surface water treatment plant in Përlepnica has large processing of capacity when in one dam there are approximately 5 million m^3 where the whole water is collected from the atmospheric precipitation, while the water processing plant at Velekica has a small processing of capacity because water is taken underground water as in the Figure 1 and exactly this plant has serious problem with one ion, which is dangerous for healthy and this is manganese Mn^{+2}, as a consequence of this potassium permanganate is active all the time to reduce the value of this metal by providing water as suitable for drinking, so without water there is life and includes one of the basic and necessary conditions for the existence of life and every industry.

Economic enterprises and all industries supply with water from natural. Of the used water are by sweet surface water including rivers, lakes but during geological research work until now significant groundwater reserves have been discovered, which are of particular importance to the development of the industry, especially in poor regions with other water sources (Agolli, 1983). Manganese (Mn^{+2}) is present mostly at the end of collecting water reservoirs because the elements fall down due to gravity retraction. Mn (II) is also used as a low catalyst acid-base in some enzymes. Spectroscopic detectors change depending on the oxidation state. Mn^{+2} is not considered a highly dispersed element (Atkins et al, 2014). In order to provide a normal performance of industrial processes, a set of measurements with working parameter values should be performed. The system that operates or intervenes to achieve this goal, regardless of the disorders that may arise during the development of the process, are related to the automatic control system (Pinguli et la, 2017). The manganese oxidation reaction is fast and efficient enough using potassium parabens, but potassium permanganate often also contains chlorine, but its products do not pose any problems, see at the reactions below:

[1]Department of Technology, Faculty of Food Technology, University of Mitrovica "Isa Boletini", Industrial park Trepça 40000, Kosovo
Correspondent author: valdrin_beluli@hotmail.com

$$2Mn^{+2} + O_2 + 2H_2O \rightarrow 2MnO_2 + 4H^+$$

$$3Mn^{+2} + 2KMnO_4 + 2H_2O \rightarrow 5MnO_2 + 2K^+ + 4H^+$$

$$Mn^{+2} + Cl_2 + H_2O \rightarrow MnO_2 + Cl^- + H_3O^+$$

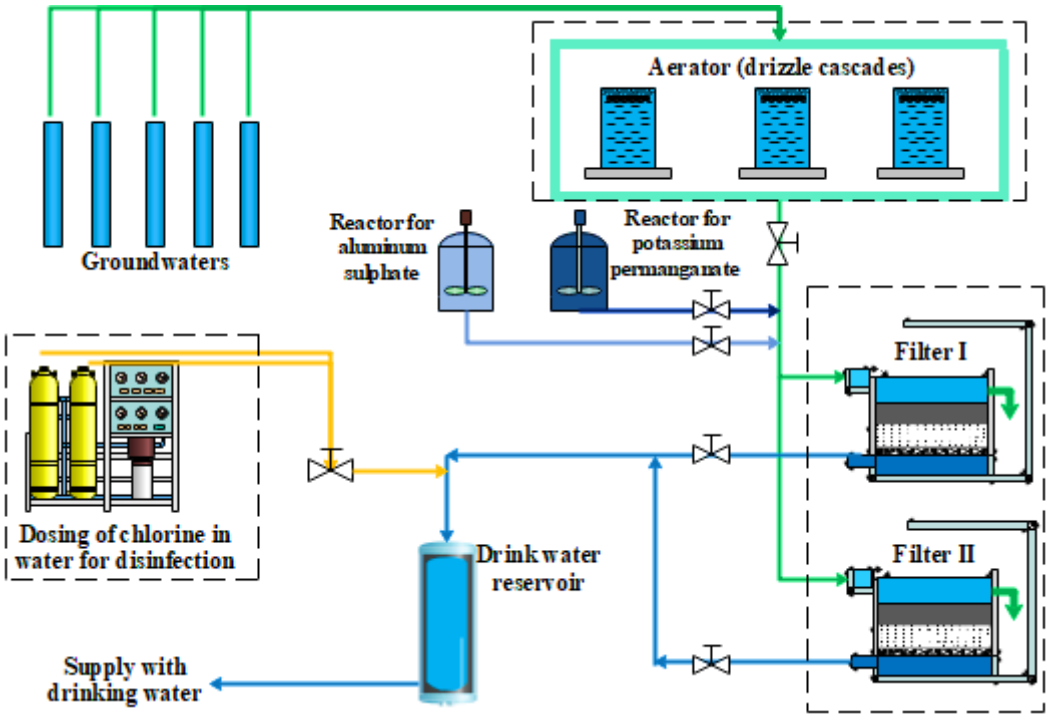

Figure 1. Industrial process of groundwaters treatment in Velekinca plant in municipality of Gjilan

Materials and Methods

Preparation of potassium permanganate aqueous solution ($KMnO_4$) for manganese oxidation (Mn)

The ideal mix reactor represents an uninterrupted device where the concentration of each component is the same at each point of the volume of the apparatus. In this way, the concertation of each component in effluent in this reactor will be equal with his concertation inside the reactor (Malollari et al, 2017). The chemical reactor is in continuous operation that manganese as heavy metal is oxidized as fast as possible by potassium permanganate ($KMnO_4$). Permanganate potassium in water flow as required, if Mn grows as metal in the nitrogenous water the concentration of $KMnO_4$ increases. Generally, the $KMnO_4$ solution is prepared from (700-1500) gr in the chemical reactor with a capacity of 750 dm^3. Schematic, the ideal mix reactor is shown in Figure 2.

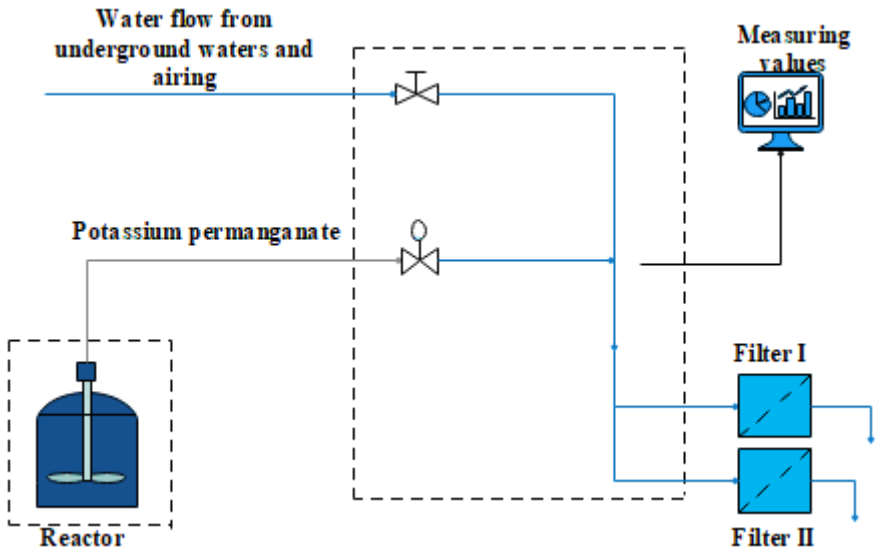

Figure 2. Water solution dosage with $KMnO_4$ for Mn oxidation before water filtration

Chemical properties of potassium permanganate ($KMnO_4$)

Potassium permanganate is a purplish colored crystalline solid. Non-combustible but accelerates the burning of combustible material. If the combustible material is finely divided the mixture may be explosive. Contact with liquid combustible materials may result in spontaneous ignition. Contact with sulfuric acid may cause fire or explosion. Used to make other chemicals and as a disinfectant (PubChem, 2018). Potassium permanganate, or $KMnO_4$, is a common inorganic chemical used to treat drinking water for iron, manganese and sulphur. It can be used as a disinfectant as well, keeping drinking water free of harmful bacteria. Drinking water facilities commonly use potassium permanganate in the early part of the disinfecting process to reduce the amount of later disinfectants, like chlorinated compounds, that must be used (Becca Bartleson, 2017).

The method of defining manganese (Mn) and potassium permanganate ($KMnO_4$)

Determining $KMnO_4$ is often complicated during titration because it needs high precision. Before titration into an erlenmeyer, put 100 ml of sample water and add approximately 5 ml of H_2SO_4 1/3, then place erlenmeyer in an electric heater. After a short heat we add 15 ml $KMnO_4$ and stand in the electric heater for approximately 10 minutes. After 10 minutes with pipette, add oxalic acid ($H_2C_2O_4$) with a volume of 15 ml with a concentration of 0.05 mol / dm^3 and the solution will boil until staining, then titrate with $KMnO_4$ to a purple colour and read the volume in the burette (Korça, 2013). The formula for $KMnO_4$ calculation uses the equation below:

$$KMnO4\frac{mg}{L} = \frac{[(15 + V_{KMnO4}) * C_{KMnO4} - 2 * 15 * 0.05/5] * 158.04 * 1000}{V_{mostrës}}$$

Manganese determination method with spectrophotometer

Absorption spectrometry in the ultraviolet and visible region is based on the electromagnetic radiation absorption of molecules in the UV spectra of 160–400 nm and VIS 400–780 nm range. UV-VIS radiation absorption causes the excitation of the electrons of chemical bonds by passing the molecules to higher energy levels (Vasjari et al, 2013). The absorption of UV-VIS radiation from complex molecules and inorganic salts of transitional metals, as well as of lanthanides and actinides, causes the molecule to move from its basal to its excited state (Lazo et al, 2017). The Hach Model DR/2010 Spectrophotometer is a microprocessor-controlled single-beam instrument for colorimetric testing in the laboratory or in the field. The instrument is precalibrated for over 120 different colorimetric measurements and allows convenient calibrations for user-entered and future Hach methods (DR/2010 Spectrophotometer instrument manual, 1999). With the instrumental method of using spectrophotometer DR / 2010 for determining Mn, in which this measurement is much faster than through the analytical method. Before the spectrophotometer is worked, blank test should be performed and then the analysis will begin with the 279.5 nm value length program for determining Mn. The sample cell is filled with water to the mark and put the powder reagent, but the reaction time after the program is 5 minutes and should be waved after this time interval, set the reading stone and get the result obtained on the monitor.

Discussion of results

During February 2017 the amount of Mn was very high to 0.33 mg dm^{-3} and was reduced after oxidation up to 0.02 mg dm^{-3}, as seen in Figure 3. In March, the amount of Mn reached 0.27 mg dm^{-3}, but during the oxidation of Mn, its amount is reduced to 0.02 mg dm^{-3}. The World Health Organization (WHO) has a special criterion for heavy metals especially for Mn. According to WHO, the value of Mn in water is only allowed at 0.05 mg dm^{-3}. During May, Mn was 0.28 mg dm^{-3} in groundwaters, but when using potassium parchment, the value of Mn was reduced to a very high level at 0.01 mg dm^{-3}. During the month of June, the atmospheric precipitation is not so present that even Mn as metal in these groundwater decreases its quantity. In this month the amount of Mn is 0.28 mg dm^{-3}, while the lowest is 0.13 mg dm^{-3}. During oxidation of this heavy metal its quantity is 0.01 mg dm^{-3}. In July, the value of Mn is not higher than 0.28 mg dm^{-3}, while during oxidation the amount of Mn is reduced to 0.01 mg dm^{-3}. In the month of August, the amount of Mn was no more than 0.28 mg dm^{-3} and the reduction of Mn after the process was reduced to 0.01 mg dm^{-3}, as seen in Figure 3. So, in July with the month of August, the quantity of Mn as heavy metal was the same and there was no change, while in September the amount of Mn was up to 0.24 mg dm^{-3} and during oxidation of this metal the amount of Mn was in 0.04 mg dm^{-3}, the reduction of Mn in this month has almost been a bit more difficult compared to the other month. In October, the amount of Mn was not higher than 0.24 mg dm^{-3}, while during oxidation it was reduced to 0.01 mg dm^{-3}, see Figure. During November, the amount of Mn included this value of 0.22 mg dm^{-3} and this value was not very high during this month, in some way did not change the amount of Mn. During oxidation of this metal the amount is reduced to 0.02 mg dm^{-3}. The amount of Mn in the groundwaters of this industry was higher in October than in November. In December the snow precipitation was very high so that the amount of Mn as heavy metal reached 0.25 mg dm^{-3}, while during the oxidation of Mn the value has been reduced by oxidation at 0.01 mg dm^{-3}. In January 2018, the value of Mn was raised to 0.26 mg dm^{-3}, much more compared to other months. Manganese during oxidation has reached this month to be reduced to 0.05 mg dm^{-3}. This value is very close to disagreement with WHO rules. Mn as heavy metal is in accordance at 0.05 mg dm^{-3} and this value is acceptable. As a conclusion to these discussions of these results is that during Mn oxidation has done a very good job by greatly reducing Mn and all values obtained after processing are in accord with the WHO regulation, see in Figure 3.

The potassium permanganate in our case as a user of Mn oxidation is greatly reduced. Reduction of $KMnO_4$ after the process is a very important process during processing because it gives evidence that the higher the $KMnO_4$ reduces, the faster the Mn is oxidized. The quantity of $KMnO_4$ is greatly reduced as seen in the Figure 4 during the process of processing these underground waters due to the high quantity of Mn.

In the surface water industry in the village of Përlepnica, Gjilan municipality, there is no evidence of a problem with heavy metal such as Mn. Usually in this water processing industry Mn as heavy metal can be present when the dam level drops too low. Usually during the summer season, the atmospheric precipitation is not very high, so the water collection is not very large. In July, when the dam level dropped, the amount of Mn was very high and so $KMnO_4$ was used as an oxidant of Mn. The amount of Mn in this month July was 0.28 mg dm^{-3}. While throughout the year the quantity of Mn is very low as value and does not express any major concern in comparison with the Velekica underground water treatment plant, see Figure 5.

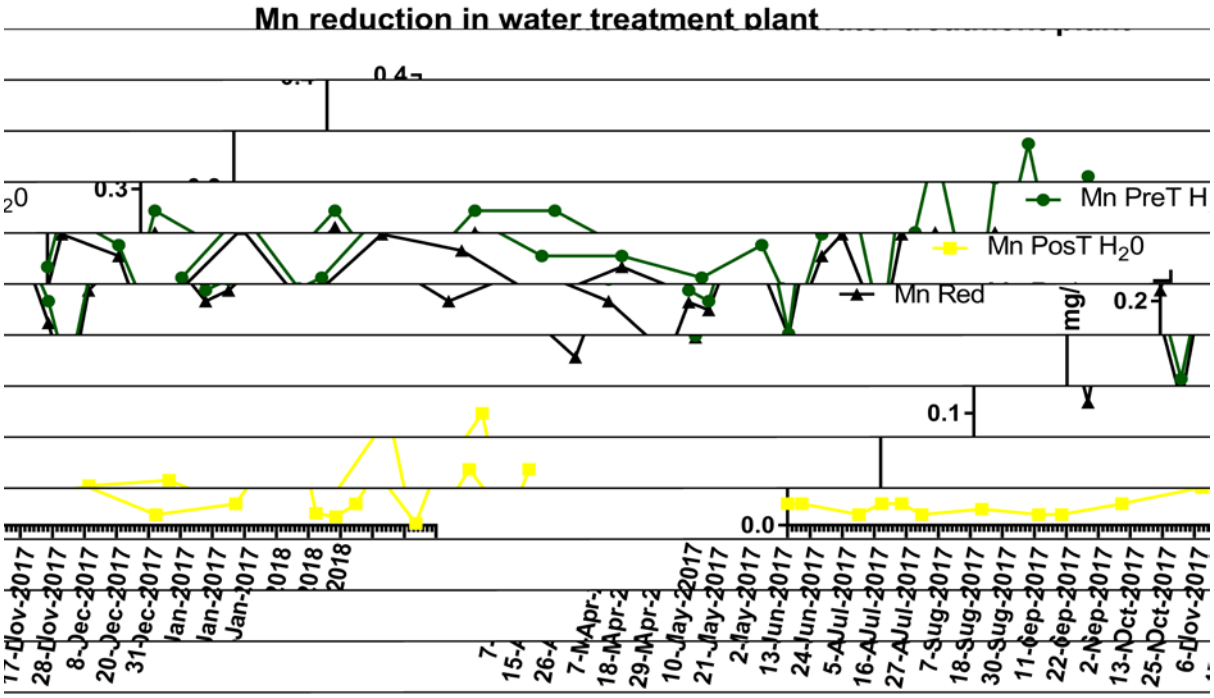

Figure 3. Manganese data (Mn) at the water processing plant in Velekica village

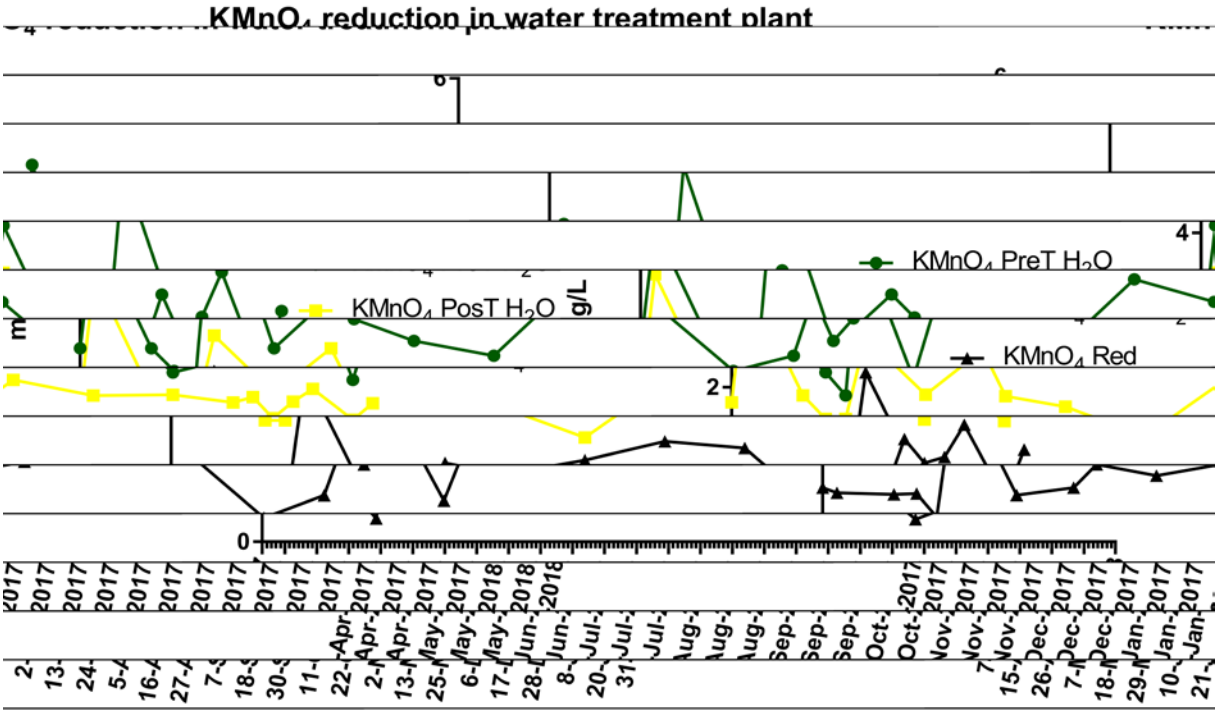

Figure 4. Potassium permanganate data ($KMnO_4$) at the water processing plant in Velekica

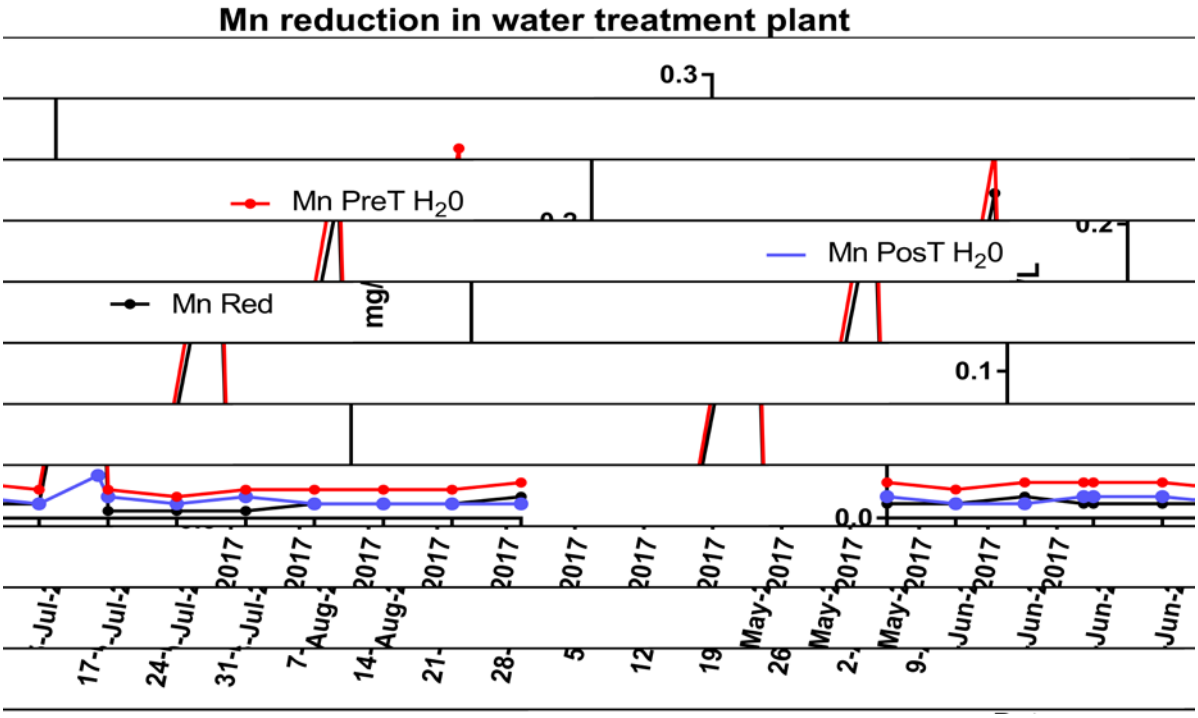

Figure. 5. Manganese data (Mn) at the water treatment plant in the village of Përlepnica

Conclusion

The site of the water treatment plant in the Velekica village of Gjilan municipality has a major problem with the connection to a heavy metal such as manganese (Mn). This industrial plant is supplied with underground water with a depth of 40 m diameter 70 cm. The analyses involved almost in 2017 send us to the conclusion that the manganese (Mn) before processing its value as metal is very high, but during the processing of these underground springs, the water plant operators have been given special care by reduce the amount of Mn to the permissible levels of WHO and EU for heavy metals and this is a good achievement that is offered to a good quality water service and special care for the health of human health. Regarding the surface water treatment plant in the village of Përlepnica there is a great certainty about the development of the processing process and this is seen in the analyses that we have realized. The world today is increasingly struggling for health security to enjoy ever better health. In the end, these heavy metals in the Velekica industrial plant are very high in Mn and it is also impossible to remove potassium parchment ($KMnO_4$) as heavy metal oxide, such as Mn. $KMnO_4$ is active at all times to oxidize Mn and we have achieved to actually oxidize it and walk with a high work safety in the processing of these groundwaters.

Reference

Agolli, F. (1983). Teknologjia Kimike Inorganike; Mitrovicë, Kosovë, pp 47

Atkins, P. Overton, T. Rourke, J. Weller, M. Aemstrong, F. (2014). Kimia Inorganike; Oxford, UK, pp 765

Pinguli, L.; Malollari, I.; Manaj, H. (2017). Kontrolli dhe Rregullimi i Proceseve të Industrisë Kimike, Tiranë, Shqipëri, pp 11-12.

Malollari, I. Pinguli, L. Inxhinieria e Reaksioneve Kimike, Tiranë, Shqipëri, viti; pp 49.

https://pubchem.ncbi.nlm.nih.gov/compound/potassium_permanganate#section=Top (12.02.2018)

https://sciencing.com/potassium-permanganate-water-treatment-5179576.html (12.02.2018)

Korça, B. (2013). Analiza Kimike e Ujit, Prishtinë, Kosovë, pp 79.

Vasjari. M, Shehu. A, Baraj. B, Çullaj. A. (2013). Metodat instrumentale të analizës, Tiranë, p. 52

Lazo. P, Çullaj. A. (2017). Metoda të analizës instrumentale, Tiranë, p. 59

DR/2010 Spectrophotometer instrument manual, general description, USA, 1999, p. 15

International Conference on Science and Technology

ICONST 2018

5-9 September 2018 Prizren - KOSOVO

Estimation of Solar Radiation Using Artificial Neural Network with Meteorological Data of Marmara University Goztepe Campus / Marmara Üniversitesi Göztepe Kampüsü Meteorolojik Verilerini Kullanarak Yapay Sinir Ağı Yardımıyla Güneş Radyasyonu Tahmini

Şafak Sağlam[1]*, Onur Akar[2], Bülent Oral[1]

Özet: Fotovoltaik paneller güneş enerjisini, elektrik enerjisine dönüştürmek için çok yaygın olarak kullanılanılmaktadırlar. Bununla beraber güneş enerjisinin doğası itibarı ile fotovolatik paneller her zaman aynı elektriksel verim karakteristiğinde çalışmazlar. Özellikle atmosferik koşullardaki değişiklikler panellerin üretecekleri enerji üzerinde büyük etkiye sahiptirler. Bu çalışmada meteorolojik koşullar ile yer seviyesindeki güneş radyasyonu arasındaki ilişki incelenmiştir. Sıcaklık, nem, açık hava basıncı, rüzgar hızı ve güneş radyasyonu değerleri Marmara Üniversitesi Göztepe kampüsünde bulunan Teknoloji fakültesinin çatısına yerleştirilen bir meteoroloji istasyonu ile ölçülerek kaydedilmişlerdir. Yapay sinir ağları modelinde Sıcaklık, nem, açık hava basıncı ve rüzgar hızı verileri girdi olarak kullanılarak 100 gizli katman aracılığı ile güneş radyasyonu çıktısı tahmin edilmiştir. Yapay sinir ağları modelinin ölçülmüş veriler kullanılarak eğitilmesinden sonra % 87,927 doğruluk oranı ile tahminlerin yapıldığı görülmüştür. Bu çalışmanın sonuçlarına göre bir bölgenin güneş radyasyonu potansiyelinin o bölgeye ait meteorolojik tahmin sonuçları kullanılarak önceden hesaplanabileceği görülmüştür. Buda aynı zamanda bölgedeki fotovoltaik panellerin üretebileceği elektrik enerjisinin büyük bir doğrulukla tahmin edilebileceğini göstermektedir.

Anahtar Kelimeler: PV Panel, Güneş Radyasyonu, Sinir Ağları, Elektrik Enerjisi, Tahmin

Abstract: Photovoltaic panels (PV) are one of the most widely used devices for converting solar energy to electricity. However, because the nature of solar energy, PV's can not always show the same electricity efficiency characteristics. Especially the changes that atmospheric conditions show have a great influence on the energy that the PV's will generate. In this study, the relationship between meteorological conditions and ground-level solar radiation is investigated. Temperature, humidity, air pressure, wind speed and solar radiation data are measured and recorded with the meteorology station located on the roof of the technology faculty located at Marmara University Göztepe campus. In the artificial neural network model, only one output (total global sunshine radiation) was estimated by using 100 hidden layers as input, 4 meteorological parameters as temperature, humidity, wind speed and air pressure. After training of artificial neural networks with measured data, it was observed that 87,927% of the radiation values which are estimated by the model fit the measured values during the tests. According to the results of this study, it is seen that the potential of solar radiation to be realized in that region could be estimated using meteorological estimations in a region. This demonstrates that the electric energy that can be produced by the PV panels in the region can be estimated with great accuracy.

Keywords: PV Panel, Solar radiation, Neural Networks, Electricity energy, Estimation

[1]Marmara University, Technology Faculty, 34722, Istanbul, TURKEY
[2]Istanbul Gedik University, Vocational School, 34700, Istanbul, TURKEY
*Corresponding author: ssaglam@marmara.edu.tr

Giriş

Genel olarak meteorolojinin çoğunlukla insan hayatını doğrudan etkileyen hava sıcaklığı, nem, basınç gibi değerler ile ilgili olduğu düşünülmekte iken son zamanlarda Yenilenebilir Enerji Üretimi (YEÜ) sektöründe de çok önemli olduğu kanaatine varılmıştır. Meteorolojik veriler çok sayıda değişkene bağlı olmaları ve her yerde yüksek doğrulukla ölçülememeleri sebebiyle, çeşitli yöntemler ile modellenmeye ve bu modeller yardımıyla tahmin edilmeye çalışılmaktadır (Behrang vd., 2010; Işık vd., 2017; Atik vd., 2007). Türkiye'de Enerji sektörünün sürdürülebilirliği açısından Yenilenebilir Enerji Genel Müdürlüğü (YEGM) kurulmuştur. YEGM tarafından yapılan çalışmaya göre, Türkiye'nin ortalama günlük güneşlenme süresi toplam 7,2 saat ve ortalama günlük toplam ışınım şiddeti 3,6 kWh/m² dir. Türkiye güneş kuşağı olarak adlandırılan bölgede bulunmakta olup güneş enerjisi açısından zengin bir ülkedir ve güneş enerjisi potansiyeli 380 milyar kWh/yıl olarak hesaplanmıştır. Yeryüzünde belirli bir bölgeye gelen güneş enerjisi potansiyelinin belirlenmesi çok önemlidir. Belirli bir bölgedeki güneş enerjisi potansiyelini belirlemek amacıyla yapılan meteorolojik gözlemler, nitelikli insan gücü ve önemli ekonomik yatırımlar gerektirmektedir (Sahan vd., 2016).

Ölçme ve kayıt altına alma sistemelerinde yaşanan zorluklar, güneş enerjisi potansiyelini belirlemek için güneş radyasyonu tahmin modellemesi çalışmalarını gündeme getirmiştir. Yatay düzleme gelen küresel güneş enerjisi miktarını tahmin etmek amacıyla deneysel veya teorik pek çok model geliştirilmiştir. Literatürde güneş radyasyonu tahmin etmek için bağıl nem, bulutluluk, buhar basıncı, güneşlenme süresi, toprak sıcaklığı gibi çeşitli iklim parametreleri kullanarak oluşturulan YSA modellerinin diğer deneysel regresyon modellerinden daha üstün olduğu görülmüştür (Mubiru vd., 2008; Fadare vd., 2010; Alama vd., 2006; Krishnaiah vd., 2007).

Bilgisayar ortamında, beynin yaptığı işlemleri yapabilen, karar veren, sonuç çıkaran, yetersiz veri durumunda var olan mevcut bilgiden yola çıkarak sonuca ulaşan, sürekli veri girişini kabul eden, öğrenen, hatırlayan algoritma "Yapay Sinir Ağları" kısaca "YSA" olarak adlandırılır. Yapay sinir ağları, insan beyni esas alınarak modellenmiş bir sistemdir. Klasik yöntemlerle çözülemeyen problemleri insan beyninin çalışma sistemine benzer yöntemlerle çözmeye çalışırlar. YSA'lar 1950'li yıllarda ortaya çıkmalarına rağmen, ancak 1980'li yılların ortalarında genel amaçlı kullanım için yeterli seviyeye gelebilmişlerdir (Kalogirou, 2001; Uğur, 2007).

Güneş enerjisinden doğrudan elektrik enerjisi üreten sistemlere Fotovoltaik(PV) sistemler denir. PV sistemler maliyetleri gelişen teknoloji ile azalmakta ve bunun sonucu olarak bu tür sistemlerin kullanımları giderek yaygınlaşmaktadır. Ancak çeşitli atmosferik olaylar nedeniyle PV sistemlerden herhangi bir zamanda ne kadar elektrik üretilebileceği kesin olarak hesaplanamamaktadır. Bu nedenle yeryüzüne düşen güneş radyasyonunun doğru tahmin edilmesi gerekmektedir (Kalogriou, 2000). Bu çalışmamızda daha önce ölçülmüş meteorolojik verileri kullanarak YSA yardımıyla ölçümlerin alındığı yer seviyesine düşen güneş radyasyonunu tahminini gerçekleştirmektir.

Materyal ve Yöntem

Bu çalışmada, İstanbul Marmara Üniversitesi Göztepe Yerleşkesine kurulan meteorolojik veri istasyonundan 2014 yılı Haziran ayı boyunca 5 dakikada bir alınan; sıcaklık, nem, basınç, rüzgar hızı ve güneş radyasyonu olmak üzere toplam beş farklı parametreden oluşan 5371 x 5 veri kullanılmıştır.

YSA insan beyninin çalışma ilkesinden esinlenilerek beyindeki sinir hücrelerinin yapay olarak taklit edilmesi ve karmaşık problemleri çözmek amacıyla bilgisayar sistemlerine uygulanması sonucu ortaya çıkmış bir veri işleme tekniğidir. YSA kendisine verilen örnekleri kullanarak öğrenmekte, veriler ve genel olarak veriler arasındaki ilişkilerin çok karmaşık ve doğrusal olmadığı durumlarda kullanılmaktadır (Graupe, 2007; Krishnaiah, 2009; Sahan vd., 2016).

YSA, kontrolden robotik uygulamalarına, örüntü tanımadan tahmin uygulamalarına, güç sistemlerinden optimizasyona kadar çok geniş bir kullanım alanına sahiptir. Bu sistemler özellikle sistem modelleme uygulamalarında çok faydalıdır. Yapay sinir ağları, lineer olmayan kompleks problemlerin çözümünde özellikle son yıllarda kullanılmaya başlanan alternatif bir çözüm metodudur. Bu metot, eksik verilerin

tamamlanması ve güneş enerjili sistemlerinin modellenmesi konularında da oldukça geniş bir uygulama alanına sahiptir (Kalogirou, 2001; Kalogriou, 2000; Karaarslan vd., 2012).

YSA'nın temel yapı birimini oluşturan yapay sinir hücrelerinin (nöronların) genel yapısı; Şekil 1'de görüldüğü gibi, girdiler (xi), ağırlıklar (wi), toplam fonksiyonu (birleştirme fonksiyonu), aktivasyon (transfer) fonksiyonu ve çıktı olmak üzere beş ana kısımdan oluşmaktadır. Girdilerin her biri ağırlık ile çarpılarak elde edilen ürünler basitçe eşik değeri (bias) ile toplanır ve sonucu oluşturmak için aktivasyon fonksiyonu ile işlem yapılır ve çıkışı alınır. Bir yapay sinir hücresinin öğrenme yeteneği, seçilen öğrenme algoritması içerisinde ağırlıkların uygun bir şekilde ayarlanmasına bağlıdır (Graupe, 2007; Okur, 2016; Karaarslan, vd., 2012; Elmas, 2016).

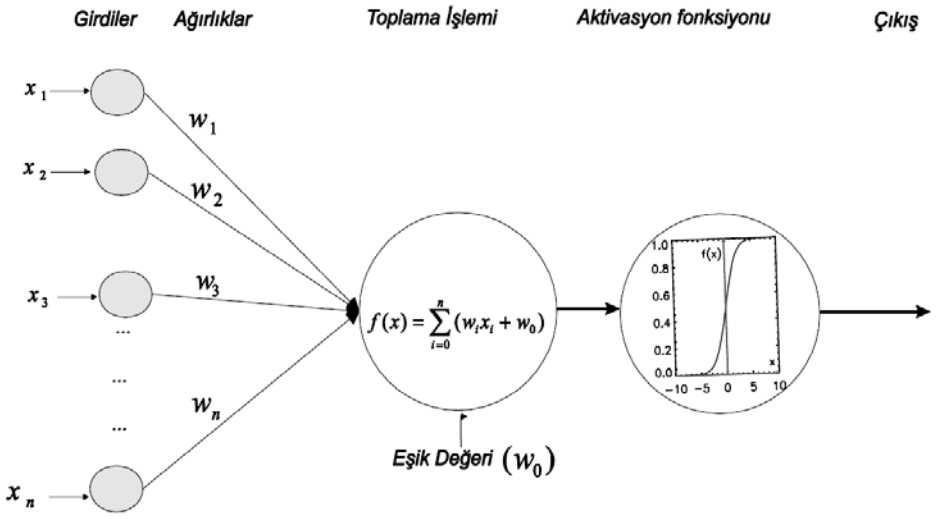

Şekil 1. Yapay sinir hücresinin genel giriş-çıkış yapısı (matematiksel mimarisi) (Graupe, 2007)

Yapay sinir ağlarında çok miktarda ağ yapısı modelleri vardır. Bunların içinden en çok kullanılan ağ yapılarından birisi çok katmanlı perseptrondur. Çok katmanlı perseptronda bilgi akısı ileri yönlüdür. Öğrenme ve eğitme algoritması olarak genelde türeve dayalı geriye yayılım (back propagation) algoritmaları kullanılır. MATLAB' da kullanabileceğimiz pek çok eğitim algoritması bulunmaktadır. En temel algoritma geriye yayılım tabanlı toplu gradyent azaltım algoritmasıdır. Fakat MATLAB' da varsayılan eğitim algoritması olarak Levenberg- Marquardt (trainlm) seçilmiştir. Günümüzde en yaygın olarak kullanılan çok katmanlı algılayıcı modelinde genel olarak aktivasyon fonksiyonu olarak sigmoid fonksiyonu kullanılmaktadır. Sigmoid fonksiyonunu Şekil 2'de görüldüğü gibidir. Sigmoid, doğrusal olmayan logaritmik bir fonksiyondur. Giriş değerleri hangi aralıkta olursa olsun, çıkış 0 ile 1 arasında olmaktadır. Türevlenebilir olduğu için geriye yayılım logaritmaları ile de kullanılabilir. Tercihen doğrusal olmayan problemlerin çözümünde kullanılmaktadır (Uğur, 2007; Şahin, 2010). Matematiksel olarak ifade edecek olursak Eşitlik 1 de belirtilmiştir;

$$f(x)=1/(1+e^{(-net)}) \qquad (1)$$

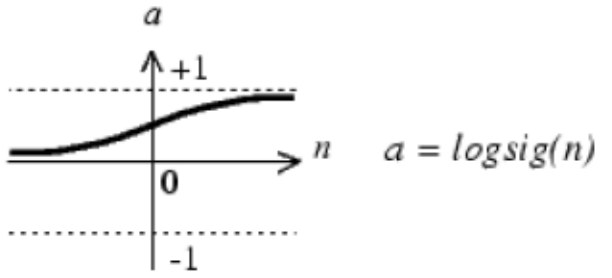

Şekil 2. Sigmoid Transfer Fonksiyonu (Şahin, 2010)

Sinir ağları, eğitilebilir yani özel bir giriş, özel bir hedef çıktısına götürür. Bu durum aşağıdaki Şekil 3'de verilmiştir. Ağın çıkısı istenilen hedefe ulaşıncaya kadar çıkış ile hedef karşılaştırılarak ağın eğitimi (ağırlık değerlerinin ayarlanması) gerçekleştirilir.

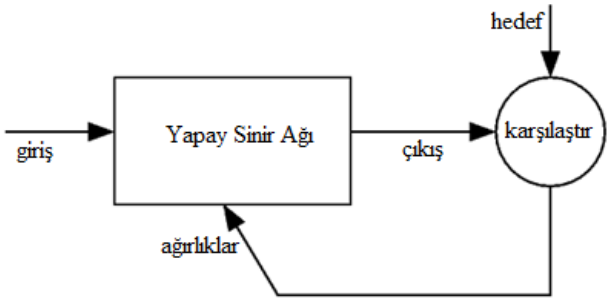

Şekil 3. YSA'nın eğitilmesi

YSA modelleri yapılarına, katmanlarına ve öğrenme algoritmalarına göre sınıflandırılmaktadır. Ağın yapısını ağı meydana getiren nöronlar arasındaki bağlantıların yapısı belirler (Bahadır, 2008). En basit hali ile çok katmanlı ileri beslemeli bir YSA'nın mimari yapısı Şekil 4'te verilmiştir. Çok katmanlı ileri beslemeli bir YSA'nın mimari yapısı girdi (input), gizli (hidden) ve çıktı (output) olmak üzere üç katmandan ve her bir katman nöron ya da işlem elemanı olarak adlandırılan bir ya da daha fazla sayıda basit yapay sinir hücresinden oluşmaktadır.

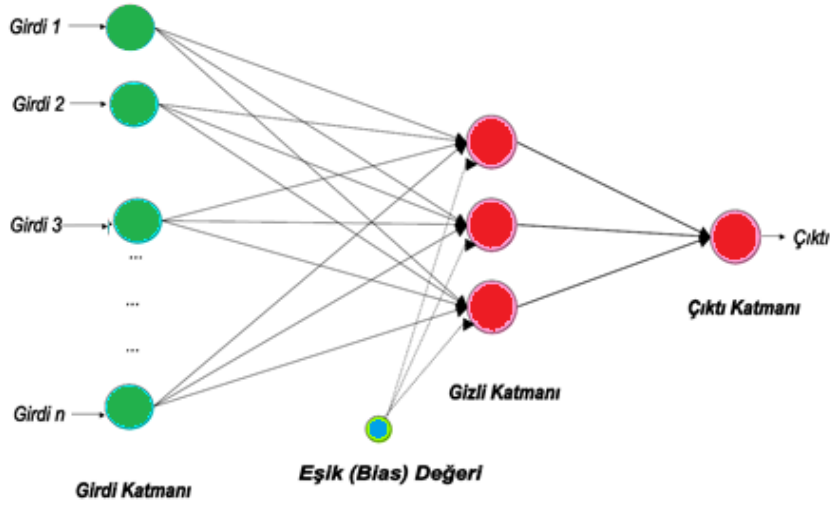

Şekil 4. İleri beslemeli bir YSA mimarisinin genel yapısı (Okur, 2016)

YSA kullanılarak herhangi bir problemin modellenmesindeki en önemli nokta, çözümlenmesi istenilen probleme en iyi çözümü verecek en uygun YSA mimarisini, yani YSA'daki gizli katman sayısını ve gizli katman/katmanlardaki işlem elemanı sayısının/sayılarının belirlenmesidir (Hawley vd., 1990). Mühendislikte ve pek çok alanda en çok kullanılan öğrenme algoritması, geriye yayılma algoritmasıdır. Bunun en büyük nedeni, öğrenme kapasitesinin yüksek ve algoritmasının basit olmasıdır (Kaya vd., 2005; Deniz vd., 2007). Kullanılacak veri grubunun büyüklüğü her probleme göre değişik olabilir, bu nedenle yapay sinir ağlarının başarıya ulaşması için gereken iterasyon (döngü) sayısı problemden probleme değişebilir. Öğrenmenin üzerinde etkin rol oynayan bir başka faktör, o yapay sinir ağı üzerinde kullanılan katman sayısıdır. Modelden modele katman sayısı değişiklik gösterse de; 3 basamaktan oluşan bir yapay sinir ağı modelinin en karmaşık problemlere dahi yeterli olduğu kabul edilmektedir (Şahin, 2010). İstenilen hedefe ulaşmak için bağlantıların

nasıl değiştirileceği öğrenme algoritması tarafından belirlenir. Kullanılan bir öğrenme kuralına göre, hatayı sıfıra indirecek şekilde, ağın ağırlıkları değiştirilir.

Meteorolojik Verilere YSA Uygulaması

Burada güneş radyasyonu tahmin edilen değerlerinin performansını değerlendirmek amacıyla istatistiksel test yöntemi olarak literatürde YSA belirlemede en çok kabul gören model performans kriterleri Eşitlik 2'de verildiği gibi sırasıyla Korelasyon Katsayısı (R^2), Hata Kareleri Ortalaması (MSE) dır (Kalogriou, 2010; Okur, 2016).

$$R = \frac{\sum_{i-1}^{n}(x_i - \bar{x}_i)(y_i - \bar{y}_i)}{\sqrt{\sum_{i-1}^{n}(x_i - \bar{x}_i)}\sqrt{\sum_{i-1}^{n}(_i - \bar{y}_i)}}, \qquad MSE = \frac{1}{n}\sum_{i-1}^{n}(x_i - y_i)^2 \tag{2}$$

Bu çalışmada, MATLAB programı içinde bulunan, Neural Network Toolbox (nntool) kullanılarak MATLAB ortamında çalışan bir bilgisayar programı geliştirilmiştir. 2014 yılı Haziran ayı boyunca 5 dakikada bir alınan; sıcaklık, nem, basınç, rüzgar hızı ve güneş radyasyonu olmak üzere toplam beş farklı parametreden oluşan 5371 x 5 veri kullanılmıştır.

YSA modelinde girdi olarak, sıcaklık, nem, Rüzgar hızı ve açık hava basıncı olarak 4 adet meteorolojik parametre, 100 gizli katman kullanılarak sadece bir çıktısı (toplam global güneşlenme radyasyonu) tahmin edilmiştir. YSA'nın mimari yapısı Şekil 5'te verilmiştir.

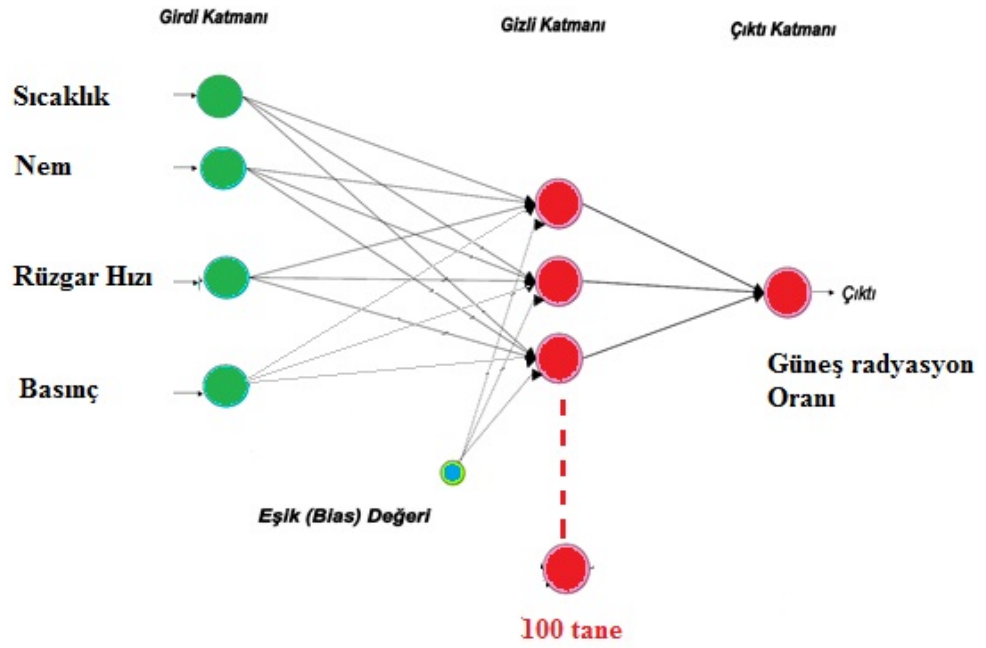

Şekil 5. Dört girişli, yüz gizli katmanlı ve bir çıkışlı ileri beslemeli YSA mimarisinin genel yapısı.

Aylık ortalama toplam güneş radyasyon verilerini tahmin etmek için ileri beslemeli çok katmanlı YSA modeli kullanılmıştır. Şekil 6'da görüldüğü gibi başlangıçta, verilerin ortalama % 70'i ağı eğitmek amacıyla ağda girdi "input" olarak, kalan %20'si doğrulamak ve %10 ise test etmek amacıyla değerlendirme ve test

tekniği kullanılmıştır. Meteorolojik sıcaklık, nem, basınç, rüzgar hızı ve güneş radyasyonu olmak üzere toplam beş farklı parametreden oluşan 5371 x 5 veri işlenmiştir.

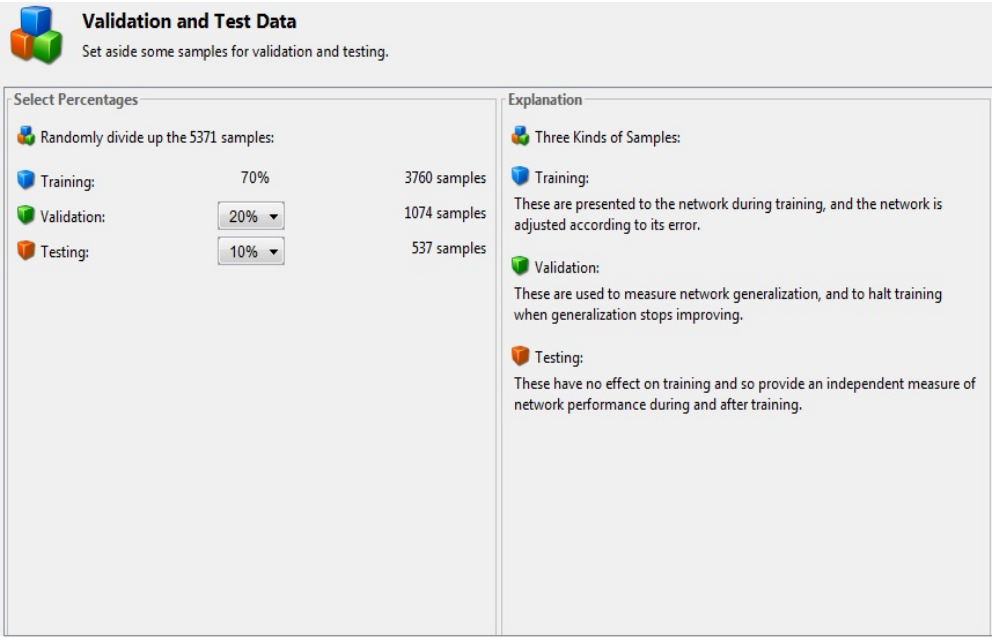

Şekil 6. Değerlendirme ve test bilgileri

Şekil 7'de YSA' nın, giriş, gizli, çıkış katmanları ve eşik(bayes)' i gösteren blok diyagramı yer almaktadır. Ayrıca blok içi diğer katmanlar, ağırlık ve aktivasyon fonksiyonunun blok diyagramı yer almaktadır.

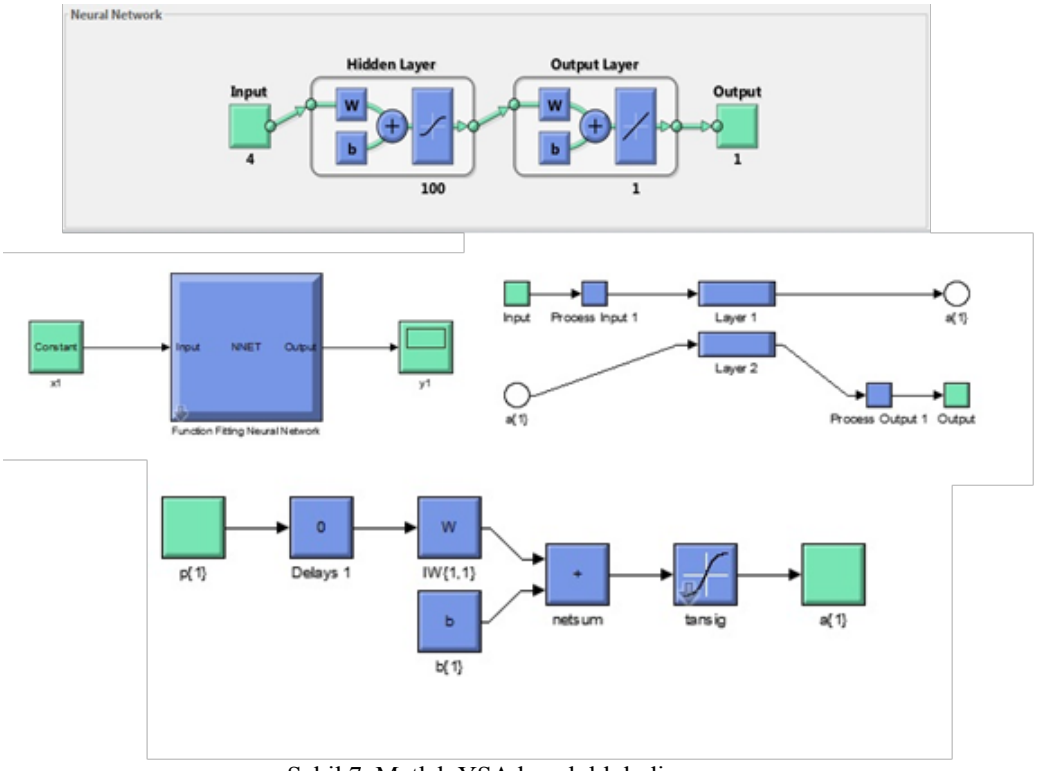

Şekil 7. Matlab YSA kapalı blok diyagramı

Şekil 8'de YSA'nın MATLAB ortamında oluşturulan 4 giriş, 100 gizli ve 1 çıkış katmanından oluşan şeklinin PC ekranında % 7 küçültülmüş ve %100 görüntüsü verilmiştir. Ayrıca şekil üzerinde açık bir şekilde ağırlıklar ve sinir bağlantı uçları gözükmektedir.

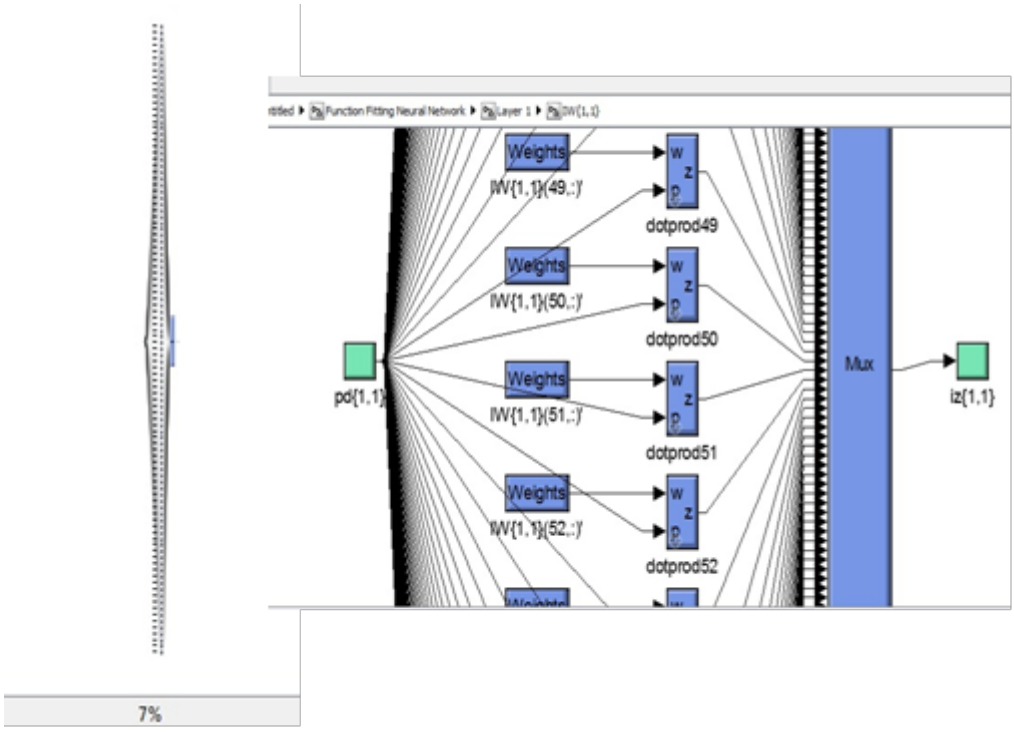

Şekil 8. Matlab YSA ağırlık blok diyagramı

Şekil 9'da görüldüğü gibi veri akışı rastgele alınmış eğitim algoritması Levenberg-Marquardt kullanılmıştır. İstatistiksel işlem olarak Hata Kareleri Ortalaması (MSE), program hesaplama olarak Matlab Executable (MEX) kullanılmıştır. Eğitim esnasında 85 kere ağırlık hesaplaması ve eğitim işlemi gerçekleştirilmiştir. Bu eğitim işlemi 18 dakika 22 saniye sürmüştür.

Şekil 9. Matlab YSA algoritması

Matlab YSA eğitim sonuç grafiği (Şekil 10) incelendiğinde grafikler üzerindeki renkli düz çizgiler ile kesik çizgilerin üst üste gelmesi YSA eğitiminin tam anlamıyla yüzde yüz örtüşmesi demektir. Grafikler üzerindeki noktacıklar ise verilerimizi ifade etmektedir. Eğitimde korelasyon olarak % 87,927 dağılım gerçekleşmiştir. Bu değerde yaklaşık olarak % 90 kabul edilebilir.

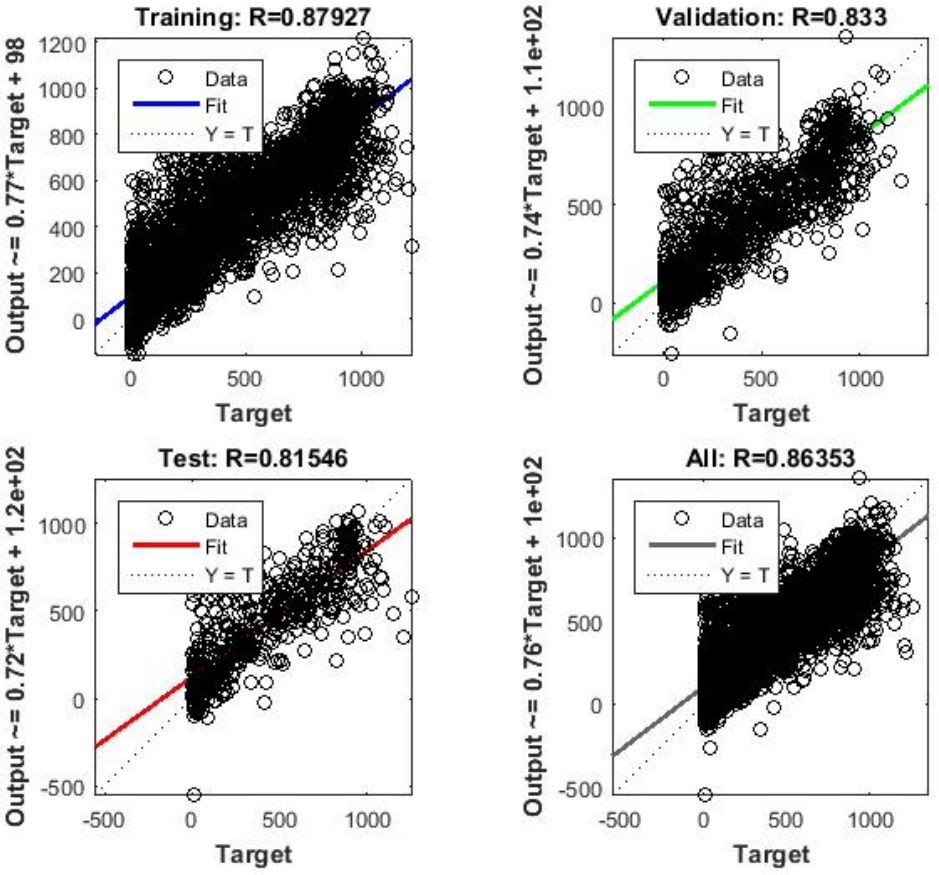

Şekil 10. Matlab YSA eğitim sonuç grafiği

Ölçülen Değerler ve YSA da tahmin edilen değerlerin örtüştürülmesi Şekil 14 deki grafikte gözükmektedir. Burada x ekseni güneş radyasyon değerini y ekseni 5371 x 2 örneklem sayısını göstermektedir. Hemen hemen ölçülen güneş radyasyon değeri ile YSA' da tahmin edilen güneş radyasyon değerlerinin yaklaşık % 90' nın uyuştuğu görülmektedir.

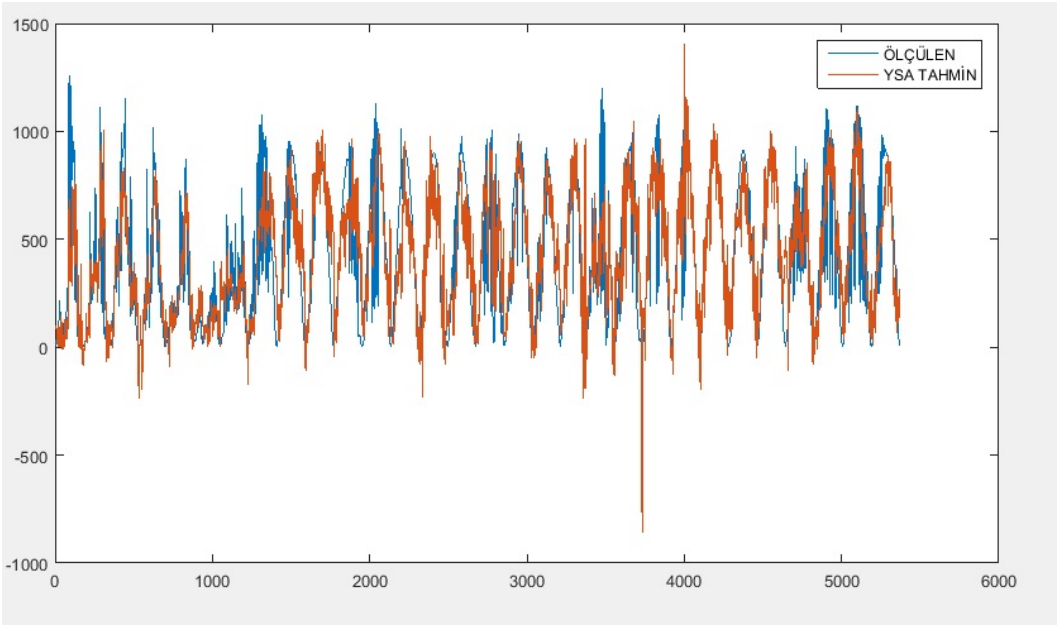

Şekil 14. Ölçülen Değerler ve YSA da tahmin edilen güneş radyasyon değerlerin örtüştürülmesi

Sonuç ve Değerlendirme

Bu çalışmada YSA kullanılarak yer seviyesindeki güneş radyasyonu değerinin tahmini gerçekleştirilmiştir. İstanbul Marmara Üniversitesi Göztepe Kampüsü meteoroloji istasyonundan kayıt altına alınan 2014 Haziran ayının verileri kullanılmıştır. Ölçülmüş veriler YSA'da eğitilerek tahmini güneş radyasyon değeri elde edilmiştir. Ölçülen ve tahmin edilen değerlerin % 87,927 uyuştuğu sonucuna varılmıştır.

Ölçüm sonuçlarının doğruluğunun yüksek olması yer seviyesindeki güneş enerjsini elektrik enerjisine dönüştüren fotovoltaik panellerin üreteceği enerji miktarının aynı doğrulukta tahmin edilebileceği anlamına gelir. Buda bize bir bölge için üretlen sayısal meteorolojik tahmin verilerini kullanarak bu model yardımı ile aynı bölgede tahmin süreci boyunca üretilebilecek elektrik enerjisini belirlemede yardımcı olacaktır. Ancak unutulmamalıdır ki sayısal meteorolojik tahmin modeli sonuçlarının tutarlılıkları ne kadar yüksek ise enerji üretimi tahmini tutarlılığıda o ölçüde tutarlı olur.

Bu doğrultuda güneş radyasyonu ile PV panellerden elektrik üreten santrallerde meteorolojik veriler yardımıyla belirli bir zaman aralığı içerisinde santrallerde ortalama ne kadar elektrik enerjisi üretilebileceği tahmin edilip bu doğrultuda elektrik enerjisi üretimi planlaması yapılabilir. Bu çalışmada YSA ile herhangi bir bölge için toplam güneş radyasyon değeri tahmin edilebileceği kanaatine varılmıştır.

Kaynaklar

Alama, S., Kaushikb, S.C., Garg, S.N., (2006). Computation of beam solar radiation at normal incidence using artificial neural network. Science Direct Renewable Energy, 31, 1483-1491.

Atik, K., Deniz, E., Yıldız, E. (2007). Meteorolojik Verilerin Yapay Sinir Ağları ile Modellenmesi. KSÜ Fen ve Mühendislik Dergisi, 10(1), 114-121.

Bahadır, İ. (2008). Bayes teoremi ve yapay sinir ağları modelleriyle borsa gelecek değer tahmini uygulaması. Yüksek Lisans Tezi, TOBB Ekonomi ve Teknoloji Üniversitesi, Fen Bilimleri Enstitüsü, Ankara.

Behrang, M. A., Assareh, E., Ghanbarzadeh, A., Noghrehabadi, A. R. (2010). The Potential of Different Artificial Neural Network (ANN) Techniques in Daily Global Solar Radiation Modeling Based on Meteorological Data. Solar Energy, 84, 1468–1480.

Deniz, E., Atik, K., (2007). Güneş Işınım Şiddeti Tahminlerinde Yapay Sinir Ağları ve Regresyon Analiz Yöntemleri Kullanımının İncelenmesi. Isı Bilimi ve Tekniği Dergisi, 27, 2, 15-20.

Elmas, Ç. (2016). Yapay Zeka Uygulamaları. ISBN 978 975 02 36 86 0, Seçkin Yayıncılık, 3. Baskı, Ankara.

Fadare, D.A., Irimisose, I., Oni, A.O., Falana, A. (2010). Modeling of solar energy potential in Africa using an artificial neural network. American Journal ofScientific and Industrial Research, 1, 144-157.

Graupe, D., (2007). Principles of artificial neural networks, (2nd Edition), advanced series on circuits and systems, 6, World Scientific Publishing Co. Pte. Ltd.

Hawley, D.D., Johson, J.D., Raina, D., (1990). Artificial neural systems: A New tool for financial decision making. Financial Analysts Journal, 46, 63-72.

Işık, E., İnanlı, M.(2017). İklim Sistemlerinin Projelendirilmesini Etkileyen Meteorolojik Verilerin Akıllı Sistemlerle Tahmini Ve Örnek Uygulama.
http://www1.mmo.org.tr/resimler/dosya_ekler/8fa466cc53578f7_ek.pdf Erişim Tarihi: 15.05.2018)

Kalogirou, S. A. (2001). Artificial neural networks in renewable energy systems applications: a review. Renewable and Sustainable Energy Reviews, Volume 5, Issue 4, 373–401.

Kalogriou, S.A. (2000). Applications of artificial neural-networks for energy systems. Applied Energy, 67, 17-35.

Karaarslan, E., Orhun, M., Hocaoğlu, F.M., Çınar, S.M., (2012). Output Power Modeling of PV Modules Produced by Different Technologies. ELECO '2012 Elektrik - Elektronik ve Bilgisayar Mühendisliği Sempozyumu, Bursa.

Kaya, İ., Oktay, S., Engin, O. (2005). Kalite kontrol problemlerinin çözümünde yapay sinir ağlarının kullanımı, Erciyes Üniversitesi, Fen Bilimleri Enstitüsü Dergisi, 21 (1-2), 92-107.

Krishnaiah, T., SrinivasaRao, S., Madhumurthy, K., Reddy, K.S. (2007). Neural network approach for modeling global solar radiation. Journal of Applied Sciences Research, 3, 1105-1111.

Krishnaiah, T., SrinivasaRao, S., Madhumurthy, K., Reddy, K.S. (2009). Neural network approach for modelling global solar radiation. Journal of Applied Sciences Research, 3, 1105-1111.

Mubiru, J., Banda E.J.K.B. (2008). Estimation of monthly average daily global solar irradiation using artificial neural networks. Science Direct Solar Energy, 82, 181-187.

Okur, Y., (2016). Akdeniz bölgesine ait meteorolojik veriler kullanılarak yapay sinir ağları yardımıyla güneş enerjisinin tahmini. Yüksek Lisans Tezi, Fen Bilimleri Enstitüsü, Osmaniye Korkut Ata Üniversitesi, Osmaniye.

Sahan, M., Okur, Y. (2016). Akdeniz Bölgesine Ait Meteorolojik Veriler Kullanılarak Yapay Sinir Ağları Yardımıyla Güneş Enerjisinin Tahmini. SDU Journal of Science (E-Journal), 11, 61-71.

Şahin, M. (2010). Yapay Sinir Ağları ile Dahili Ortamlardaki Aydınlık Düzeyinin Analizi. Yüksek Lisans Tezi, Marmara Üniversitesi Fen Bilimleri Enstitüsü, İstanbul.

Uğur, L.O. (2007). Yapı Maliyetinin Yapay Sinir Ağı İle Analizi. Doktora Tezi, Gazi Üniversitesi Fen Bilimleri Enstitüsü, Ankara.

International Conference on Science and Technology

ICONST 2018

5-9 September 2018 Prizren - KOSOVO

Study on Efficiency of In-Wheel BLDC Motors used in Light Electric Vehicle for Different Magnet Materials and Magnet Embrace Ratio

Ali Sinan Çabuk[1], Şafak Sağlam[2]*, Özgür Üstün[3]

Abstract: Type and placement of permanent magnets of In-Wheel Brushless Direct Current (BLDC) motor have an effect on motor performance, loss and efficiency. This paper relates and identifies the motor design parameters that influence the efficiency of in-wheel BLDC motor. Permanent magnets are the most important material for produce high torque of electric motor, but if the designer select unstable magnet for the electric motor, the cogging torque can be higher, rated torque can be change and the efficiency is lower. Besides magnet embrace ratio of in-wheel BLDC motor is defined incorrect position, the same effects can be seen as cogging torque and efficiency. In this study, different types of magnets and magnet embrace ratio, which is used in propulsion system of Light Electric Vehicle (LEV), are investigated an in-wheel BLDC motor design. The in-wheel BLDC motor used in this study has 2.5 kW output power, 150 V terminal voltage and 900 rpm shaft speed, which is widely used in traction system of LEV.

Keywords: In-Wheel BLDC Motor, Efficiency, Permanent Magnet, Magnet Embrace Ratio, Light Electric Vehicle.

Introduction

The important environmental problems have arisen increasing use of fossil fuels as transportation and industrial area. This negative condition of environmental impact has led technology developments to more environmentalist approaches. Therefore, electric vehicle (EV) technology is one of the most important approach among and which have been taken drive much more daily life as increasingly rapid. There are a lot of electric cars, electric bicycles and light electric vehicles (LEV) on the roads. These trends bring significant improvements in technologies for electric vehicles. Today, most automotive manufacturers have concentrated their research and development activities in the field of electric vehicles (Ustun et al. 2009; Lee et al. 2016; Bouscayrol et al. 2016; Zarko et al. 2007)

One of the remarkable concepts in EV technology is energy planning. Therefore, energy efficient electric motors have highest importance. Minimizing losses and increasing efficiency of electric motor have become first target for all electric motor designers. Hence a lot of researchers and manufacturers go towards brushless direct current (BLDC) motors. There are two advantages of using this kind of electric motor: decreasing the energy consumption per kilometer and increasing the driving distance. It can be enforced that research and develop activities of EV and LEV manufacturers focus on these beneficial topics (Cabuk et al. 2016)

[1,3] Istanbul Technical University, Faculty of Electrical and Electronics Engineering, 34469, Maslak, İstanbul / TURKEY
[2]Marmara University, Technology Faculty, 34722, Istanbul, TURKEY
*Corresponding author: ssaglam@marmara.edu.tr

It is known that one of the parameters of BLDC motor efficiency is permanent magnet material. Other important parameter as related to magnet is magnet embrace ratio. Investigations targeted at working the problem would come up with results that showing the importance of high efficiency motors and low energy consumption per kilometer (Cabuk et al. 2017; Cabuk et al. 2016)

It is apparent that the propulsion requirements of light electric vehicles lead the designers to research different electric motor topologies and structures. An in-wheel type electric bicycle motor is a prominent example of those efforts. As a LEV, electric bicycles require slim, high torque – low speed. Most of studies are mainly on the different magnet combinations and different shape of magnet. The design progresses based on recent studies have brought easily manufactured motor topologies, modular designs, more magnet utilization, low cogging motor designs etc.

The aim of this study is to find out the effect of different permanent magnet variations and magnet embrace ratio on losses, efficiency and cogging torque of LEV in-wheel BLDC motor. A finite element based computational software is conducted in the simulation study to obtain the needed data, a prototype of the designed motor is manufactured and the test results are compared to calculated values. ANSYS Electronics Desktop software was used as finite element method. Prototype was made with results of simulation and perform test was done on test setup.

Preliminary Design Study

The steps taken in this phase of study are shown in Figure 1. A pre-design study is performed by an electrical motor design configurator, i.e. ANSYS Electronics Desktop (ANSYS RmXprt and Maxwell). The high quality designs are investigated by the detailed electromagnetic Finite Element Analysis (FEA) to get more certain results. The design is developed by using an algorithm loop, which is providing a strong convergence to the aimed design values (Cabuk et al. 2016; Cabuk et al. 2017; Cabuk et al. 2016)

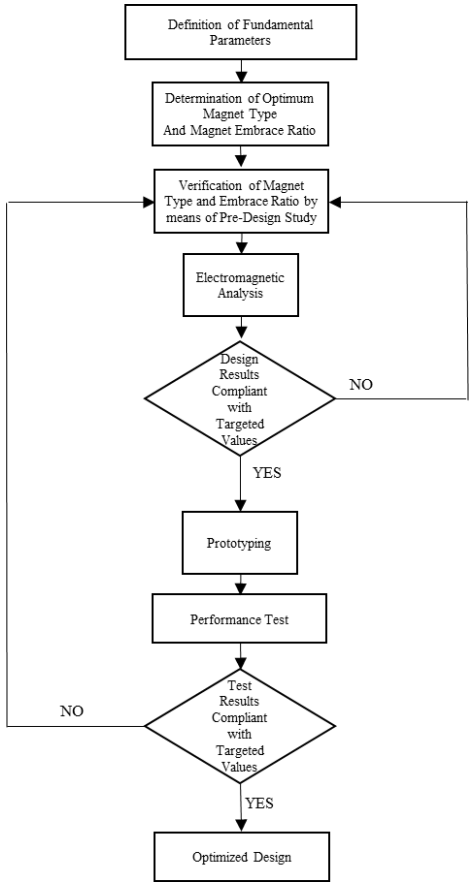

Figure 1. Design flow chart of in-wheel BLDC motor

The prime constraint of this study is the output power, rated Voltage and Max Vehicle Speed, i.e. 2.5 kW., 150 V and 100 km/h. All design parameters in Table I are considered by means of their impacts on the motor performance. Other constraints are; slot fill factor in the range of 60-70%, current density of 6 A/mm^2, 90 °C steady state operation winding temperature and air gap length of 1 mm. In the light of these parameters, the different magnets of Neodymium Iron Boron (NdFeB), Samarium-Cobalt (SmCo) and Aluminum-Nickel-Cobalt (AlNiCo) as commercially available that are used for in-wheel BLDC motor structure are investigated by means of FEA study (Cabuk et al. 2017)

Table 1. Initial design values of in-wheel BLDC motor

Parameters	**Value**
Output Power [W]	2500
Rated Voltage [V]	150
Max Vehicle Speed [km/h]	100
Min Vehicle Weighty [kg]	250
Diameter of Wheel [mm]	320
Outer Diameter of Stator [mm]	239.8
Outer Diameter of Rotor [mm]	273
Length of Motor [mm]	30

One of the most important parameters of efficiency for electric motors is; (MTPA - Maximum Torque Per Ampere) and is the concept of producing the maximum torque with the lowest possible current. These higher values indicate minimum copper losses and lower heating of electric motor.

The magnet specific values and the ferromagnetic material quality must be high for increase MTPA value. Hence the highest quality materials impact a high-efficiency and high-performance.

In this study, firstly magnetic material types were carried out to provide high efficiency and high torque production. Therefore, all the materials in the catalogs of the companies producing permanent magnets were compared under some conditions as given below;

- BH curve
- Demagnetization values
- Curie temperature
- Volume-weight ratio
- Core loss
- Material of cost

Different Permanent Magnet Types

Applicable stator and rotor material of brushless direct current motor (BLDC) is the most important parameter for manufacture. If incompatible material is used as steel and permanent magnet in BLDC motor, it can obtain non-productive and poor performer motor. In this study, effects of stator, rotor and permanent magnet being manufactured of different materials were evaluated on the loss and efficiency. Accordingly the data of Table 1 was used for pre-design. Also half coil concentric winding was chosen the design, which is frequently used winding structure for do not require high power application as LEV. Solid-Steel 1010 was selected as back iron steel, which is known that it gives good results than other steel material. Different types of magnets as an available on the magnetic material manufacturer are compared each other an in-wheel BLDC motor design. The investigation of different magnet material with steel material is given in Table 2.

It is seen here that M19_26G and M27_26G as the stator material (the steel materials), NdFeB_N32, NdFeB_N38, NdFeB_N45, NdFeB_N50, SmCo_R26 and SmCo_R30 as the magnet types gave better results.

Table 2. Magnet Material versus Stator Steel

Type of Magnet	Stator Steel								
	M19_26G	M22_24G	M22_26G	M27_24G	M27_26G	M36_24G	M36_26G	M43_24G	M43_26G
NdFeB_N32	91.7208	90.5957	91.4319	90.128	90.9035	89.5613	90.3991	88.7825	89.852
NdFeB_N34	91.6018	90.437	91.3001	89.9509	90.7516	89.3604	90.2258	88.5646	89.6676
NdFeB35	91.4394	90.223	91.1218	89.6963	90.5325	89.0705	89.9748	88.2516	89.4018
NdFeB_N36	91.546	90.3646	91.2399	89.8684	90.6807	89.2664	90.1444	88.4626	89.5811
NdFeB_N38	91.3811	91.3358	91.5112	90.9024	91.6222	90.3731	91.1521	89.6523	90.6468
NdFeB_N39	91.4848	90.2815	91.1705	89.7705	90.5964	89.1569	90.0496	88.3429	89.4794
NdFeB_N40	91.4987	90.2998	91.1859	89.7926	90.6155	89.1801	90.0698	88.369	89.5017
NdFeB_N42	91.0843	91.0786	91.5275	90.6567	91.3526	90.1676	90.9175	89.4439	90.4067
NdFeB_N44	91.6768	90.534	91.3814	90.0584	90.8445	89.4784	90.3282	88.6961	89.7796
NdFeB_N45	91.1532	91.1703	91.6014	90.7594	91.4388	90.2855	91.0172	89.5747	90.5153
NdFeB_N48	91.079	91.0718	91.522	90.6488	91.346	90.1576	90.909	89.4338	90.3984
NdFeB_N50	91.5224	91.4939	91.3097	91.3506	91.5231	90.9541	91.5711	90.349	91.1445
SmCo_24	91.728	90.6048	91.4396	90.1378	90.9121	89.5718	90.4083	88.7945	89.8623
SmCo_R26	91.7268	90.6038	91.4388	90.1357	90.9104	89.5686	90.4056	88.7918	89.8602
SmCo_28	91.6189	90.4596	91.3189	89.9762	90.7734	89.3885	90.2501	88.595	89.6934
SmCo_R29	91.6533	90.5049	91.3568	90.027	90.8172	89.4448	90.2989	88.6566	89.7459
SmCo_R30	91.0423	91.0213	91.4812	90.5933	91.2992	90.0954	90.8563	89.3626	90.3391
SmCo_R32	90.6166	90.4545	91.3152	89.9696	90.7681	89.3789	90.2421	88.5873	89.6873
SmCo_R33	91.5477	90.367	91.242	89.8701	90.6823	89.2675	90.1455	88.4646	89.5829
Alnico 5	87.2896	87.2896	87.2897	87.3619	87.3620	87.3620	87.5461	87.5461	87.5461

These results are a guide to us, with no definitive judgment, because the analysis of this structure, which is made with the understanding that the effects such as flux distributions and motor heating are important. However, when the above mentioned structures are re-simulated, when the cogging torque effect, the armature current density, the output power and the torque value are also examined, in addition to this, when the material is added to the market in terms of availability and cost; Steel 1010 as a rotor material, NdFeB_N38 as a magnet has reached to knowledge that will have a much better result. Also M27_26G steel is chosen for laminate steel, magnetic properties, cost and easy availability are the best material for in-wheel BLDC motor. The steel material was used the same previous studies for LEV application, which make a great contribution as motor performance.

Magnet Embrace Ratio Design Study

Magnet embrace ratio of in-wheel BLDC motor affects cogging torque and efficiency. If the ratio is defined as incorrect position, motor performance can change. After the permanent magnets are identified as NdFeB_N38H, and the design was analyzed with different magnet embrace ratio.

Change of the magnet embrace ratio was investigated to understand the effect on efficiency and cogging torque. The investigation of different magnet embrace ratio is given in Table 3.

As can be seen in Table 3, when the magnet embrace ratio increases and the radial lengths of the magnets increase, accordingly the distances of magnets to each other decrease. Also Table 3 is shown magnet embrace ratio of in-wheel BLDC motor affect an efficiency. Vibration of the motors is the one of significant parameters as the point to be emphasized. Cogging torque change with magnet embrace ratio can be seen in Table 3.

Table 3. Magnet Embrace Ratio

Magnet Embrace Ratio [%]	Slot/Pole Structure	Rated Speed [rpm]	Cogging Torque [Nm]	Armature Current Density [A/mm^2]	Rated Torque [Nm]	Input Current [A]	Efficiency [%]
95%	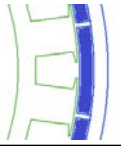	819.321	1.33294	4.08918	29.1362	18.0888	92.1371
90%		841.486	1.17072	4.10085	28.3701	18.0711	92.2278
85%		840.411	0.432195	4.11644	28.4067	18.05	92.3362
80%		836.847	0.609565	4.12204	28.5285	18.022	92.4824
75%		830.82	1.1235	4.1224	28.7355	17.987	92.6624
70%		825.019	0.738807	4.13259	28.9364	17.9487	92.8565

In Figures 2,3 and 4, the simulated values of cogging torque versus magnet embrace ratio, efficiency versus magnet embrace ratio and rated speed versus magnet embrace ratio are presented, consecutively.

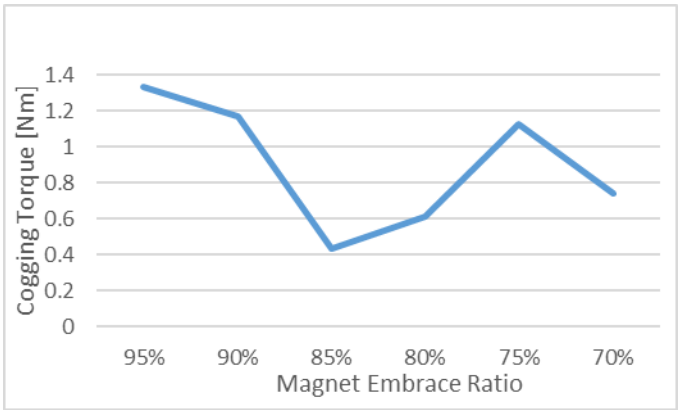

Figure 2. Cogging Torque versus Magnet Embrace Ratio

Cogging torque produces vibration of the motor. Vibration affects mechanical parts of the motor. This effect should be minimized. It can seen change of cogging torque in Figure 2, which magnet embrace ratio should be chosen between 85% and 80%.

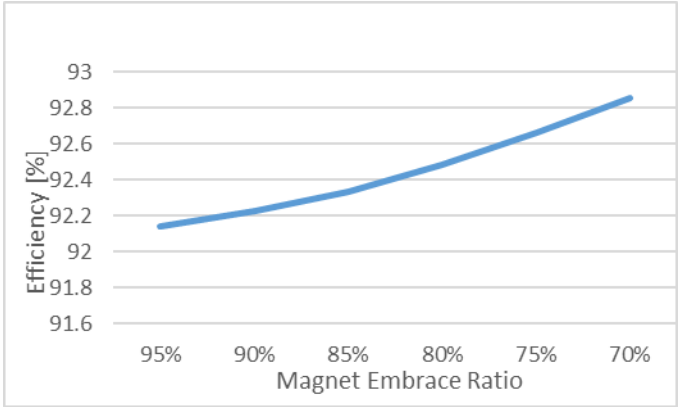

Figure 3. Efficiency versus Magnet Embrace Ratio

The efficiency and the related total loss values variation with magnet embrace ratio is shown in Figure 3. It has been found that the efficiency exhibited a maximum for lower than 85% ratio configuration.

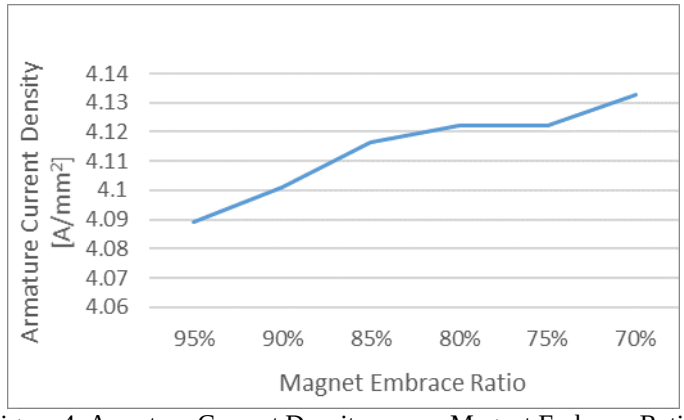

Figure 4. Armature Current Density versus Magnet Embrace Ratio

Induced armature current density variation, which is one of the most significant parameters in motors that decides whether the motor should be cooled by natural or forced convection is given in Figure 4. All magnet embrace ratio values are permissible limits.

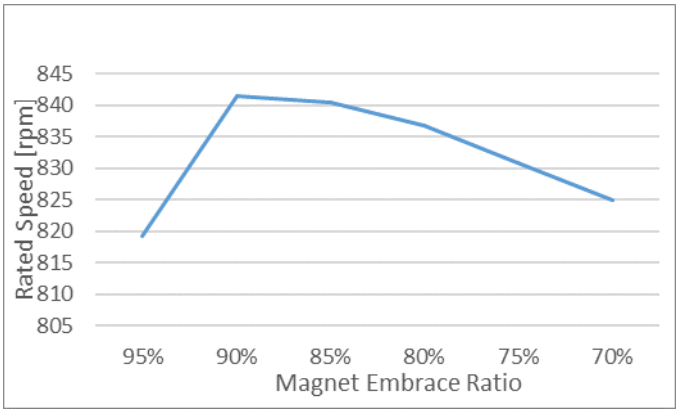

Figure 5. Rated Speed versus Magnet Embrace Ratio

Rated speed variation with magnet embrace ratio is shown in Figure 5. Desired speed value of the motor between 90% and 80% ratio configuration.

The results of Table 2 are optimized to figure out optimum efficiency and cogging torque. Magnet embrace ratio is found adequate 80% for lower cogging torque and high efficiency.

Performance Test

The determined electrical steel material (M27-26G) is used for the stator manufacture by the help of simulated results. The stator laminate is provided by laser cutting technic to remove any edge impurity. Total number of 56 laminations are stacked and fixed properly. After produce of stator, winding fabrication is completed.

The conductors installed in stator slots are selected with the cross sectional area of 2.2 mm^2. The slot fill factor is defined as 65% which is an enough value for manufacture fabrication. The overhangs of stator windings are kept up to a adequate limit which is providing in-wheel motor structure.

A test bench is consisted by using a loading mechanism which is forming of an adjustable eddy current braking and a BLDC motor controller and voltage-current measurement devices. Eddy current brake as braking device is connected to the in-wheel BLDC motor via a torque transducer. In the eddy current brake, the loading power is exterminated on aluminum brake disc. The principal schema of test bench with the braking device is given in Figure 6. Also in Figure 7 The picture of test bench with brake loading mechanism is shown.

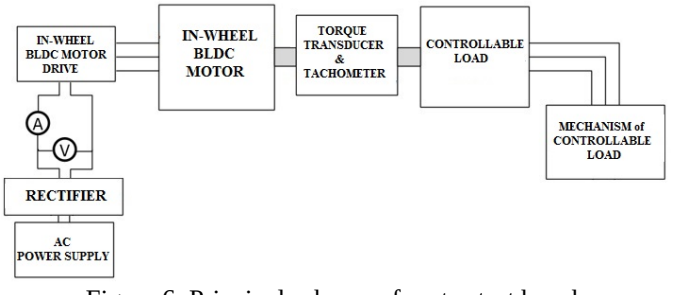

Figure 6. Principal schema of motor test bench

Due to the accurate sensibility and high frequency response measurement requirements, entire parts of the test bench are set, pick up and calibrated precisely. 2.5 kW, 150 V in-wheel BLDC motor is supplied via a BLDC motor driver which is designed especially for testing purposes. The in-wheel BLDC motor performance is tested for different loadings and the overloading tests are conducted. The no-load speed and no-load current of the tested in-wheel BLDC motor are measured as 1016 rpm and 2.1 A respectively.

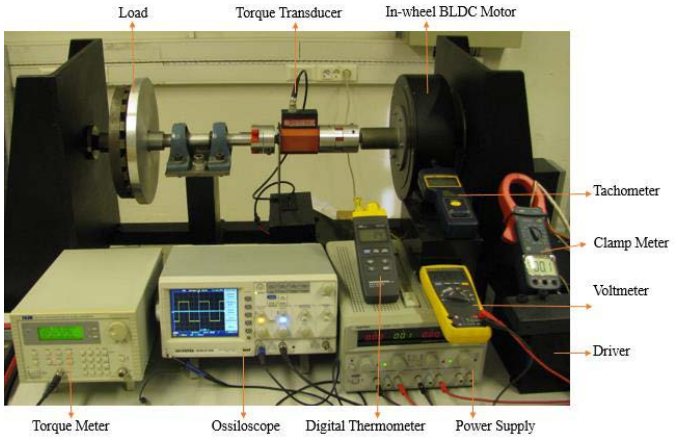

Figure 7. Motor test bench during motor testing

Load current, phase voltages, input currents and speed are measured by measurement devices, also input power of the motor is measured by a power analyzer that is giving the reliable values of input power measurement. In Figures 8 and 9, the simulated and measured values of efficiency versus shaft speed and shaft torque versus input current are presented, consecutively.

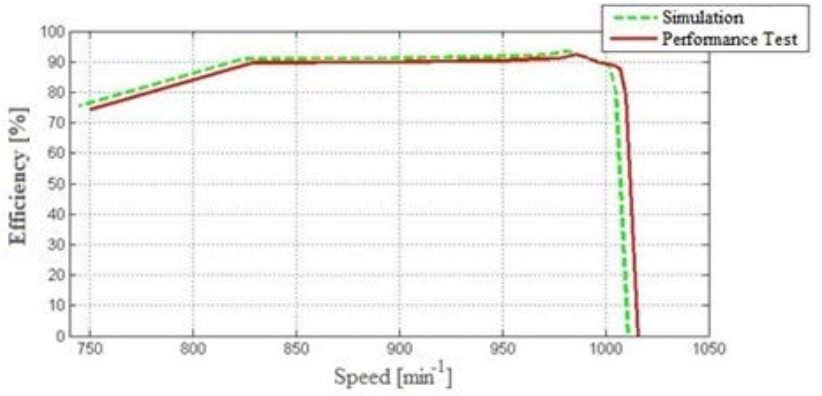

Fig.8. Efficiency versus shaft speed

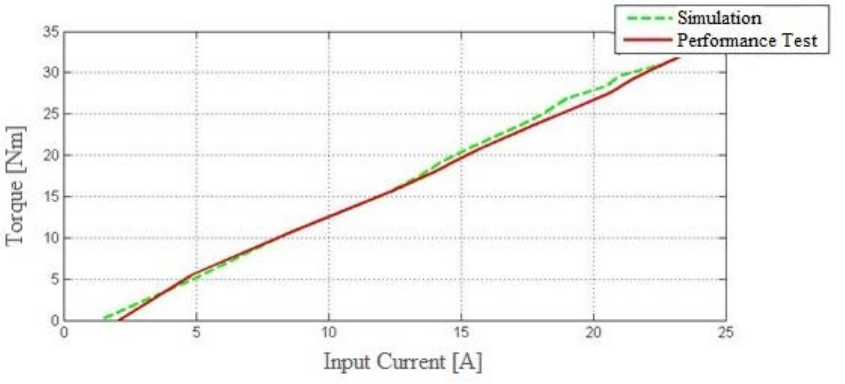

Fig.9. Shaft torque versus input current

In analysis of the test results, an agreement is shown between the calculated and the tested values of in-wheel BLDC motor performance. Thus, the comparison of the simulated and tested results match the validation the design study.

Conclusion

The in-wheel BLDC motor structure is designed for a direct driven LEVs. For proper propulsion of LEVs, the in-wheel BLDC motor has some certain performance requirements including efficiency. Type of permanent magnets and magnet embrace ratio of in-wheel BLDC motor affect especially efficiency and cogging torque. Consequently both permanent magnet and magnet embrace ratio are focused on parameters for in-wheel BLDC motor. If the designer select unstable magnet for the motor, the cogging torque can be higher, rated torque can be change and the efficiency is lower. Besides magnet embrace ratio of in-wheel BLDC motor is defined incorrect position, the same effects can be seen as cogging torque and efficiency.

The design study is based on permanent magnets variations with magnet embrace ratio and their effect on preferential performance parameters such as efficiency, cogging torque and rated torque. NdFeB_N38H magnets are more useful for LEV as 2.5 kW and 150 V in-wheel BLDC motor. Magnet embrace ratio can be chosen 80% for lower cogging torque, high rated torque and high efficiency. The test and simulation results are compared with each other to investigate the optimization approach.

References

Bouscayrol, A., Boulon, L., Hofman, T., and Chan, C.C. (2016). Special Section on Advanced Powertrains for More Electric Vehicles, IEEE Transactions on Vehicular Technology, vol. 65, no. 3, 995 – 997.

Cabuk, A.S., Saglam, S., Tosun, G. and Ustun, O. (2016) Investigation of Different Slot-Pole Combinations of An In-Wheel BLDC Motor for Light Electric Vehicle Propulsion, National Conference on Electrical, Electronics and Biomedical Engineering (ELECO 2016), Bursa-Turkey, 298–302.

Cabuk, A.S., Saglam, S., and Ustun, O. (2017) Impact of Various Slot-Pole Combinations on an In-Wheel BLDC Motor Performance, I.U. - Journal of Electrical & Electronics Engineering, 17 (2), 3369-3375.

Cabuk A.S. (2016). A Novel Approach to Optimized Design of In-Wheel BLDC Motors, (In Turkish) Ph.D. thesis, Institute for Graduate Studies in Pure and Applied Sciences, Marmara University, Istanbul, Turkey,

Lee, J.H., Kim, D., Song, J., Jung, S., and Kim, Y. (2016). Design of 100kW propulsion motor for electric conversion vehicle based on vehicle driving performance simulation, IEEE Transportation Electrification Conference and Expo, Busan, Korea(South), 412-416.

Ustun, O., Yilmaz, M., Gokce, C., Karakaya, U., and Tuncay, R. N. (2009). Energy Management Method for Solar Race Car Design and Application, IEEE International Electric Machines and Drives Conference, Miami, USA, 804-811.

Zarko, D., Ban, D. and Lipo, T.A. (2007) Analytical Solution for Cogging Torque in Surface Permanent-Magnet Motors Using Conformal Mapping," IEEE Transactions on Magnetics, vol. 44, no. 1, 52-64.

International Conference on Science and Technology

ICONST 2018

5-9 September 2018 Prizren - KOSOVO

Effects of Different Silicon Levels on Plant Growth and Fe Nutrition of Strawberry Cultivar "Camarosa"

Şeyma Arikan[1], Muzaffer İpek[1], Lütfi Pirlak[1*], Ahmet Eşitken[1], Murat Şahin[2]

The Fe deficiency is so important for plant nutrition especially strawberry plants in horticultural species. The high calcareous cause higher soil pH and Fe is not uptake sufficiently by plants. This causes low plant development, productivity and fruit quality. The aim of this research was to determine silicon treatment effects on plant growth and Fe uptake of the strawberry plant.

The present study was conducted in greenhouse condition at the University of Selçuk, Faculty of Agriculture and Horticulture Department. The effects of five silicon levels (1, 2, 3, 4, and 5 mM) on plant growth and Fe uptake were investigated. The Camarosa strawberry cultivar was used as a plant material. The runner plant number, stem diameter, fresh plant and root weight, root length, leaf area, leaf relative chlorophyll content, stomatal conductance, membrane permeability and Fe nutrient content was determined.

The Fe and silicon (5 mM) treatment both alone and mixed were found more effective than other treatment on plant growth and Fe uptake in strawberry plants. The runner plant number reached the highest number in silicon treatment (5 mM) and Fe treatment with 2.31 and 2.25 runner plant per mother plant, respectively. The lowest runner plant number was obtained from the control group with 1.48 runner plant per mother plant. The highest Fe content was determined in silicon (5 mM) treatment with 163.39 mg kg^{-1}.

The result of plant growth parameters and Fe uptake showed that silicon application promoted plant growth and Fe uptake in strawberry plants.

Keywords: Iron, Plant Growth, Silicon, Strawberry

Introduction

The strawberry is an important fruit that is grown in Turkey and the World. Turkey is the fourth biggest country in strawberry production with 372.498 tons (Anonymous, 2018). Generally, strawberry growing was done at the near seaside but nowadays it has been started to grow at a higher altitude. Strawberry fruits are susceptible for the transport from growing field to market, so it should be grown in field close markets. Because of the soil properties and climatic conditions, strawberry growing could not be in everywhere economically. The Turkey soil features show calcareous characteristic and higher calcerous limits strawberry growing because strawberry is susceptible fruit in horticultural species. The higher calcerous soil inhibits to taking iron (Fe) by plants from the soil. Fe is a crucial element for plants and takes part in a number of proteins and enzymes activity. Although Fe is the fourth most abundant elements in the earth crust, Fe-induced chlorosis is shown in a calcareous soil and Fe deficiency is a major limiting factor for plant growth and yield in all over the world (Vose, 1982).

The silicon is the most abundant mineral in the world but it is not accepted as an essential element for plants. It is known that silicon effectively alleviates environmental stress such as salinity, water deficiency, heavy metal toxicity, waterlogging, pathogens and, pets. In addition, some researchers reported that silicon promotes Fe uptake and reduce the effect of the Fe deficiency in plants (Bityutskii et al., 2014; Gonzalo et al., 2013).

In this study, it was aimed to determine different silicon levels effect on plant growth and Fe nutrition in strawberry plants

[1]Selçuk University, Faculty of Agriculture, 42075, Konya, TURKEY
[2]Siirt University, Faculty of Agriculture, 56100, Isparta, TURKEY
*Corresponding author: pirlak@selcuk.edu.tr

Material and Method

This study was carried out in greenhouse condition at the University of Selçuk, Faculty of Agriculture and Horticulture Department. The effects of five silicon levels (1, 2, 3, 4, and 5 mM) on plant growth and Fe uptake were investigated. The Camarosa strawberry cultivar was used as a plant material. Fe was applied as Fe EDDHA form with 36mg kg^{-1}. Hoagland solution without Fe was used plant nutrition and was applied biweekly. Soil composition were pH 7.49, Calcium Carbonate (CaCO3) 29.55%, Sodium (Na) 0.95, Potassium (K) 8.62, Magnesium (Mg)2.46, Calcium (Ca) 14.75 me $(100\ g)^{-1}$; Phosphorus (P) 28, Fe 0.80, Manganese (Mn)14.69, Zinc (Zn) 1.73, Cupric (Cu) 0.68, Boron (B) 0.31 mg kg^{-1}; organic matter 2.12%.

Measurement of the morphological parameters

As morphological parameters, runner plant number, stem diameter, fresh plant and root weight, root length, leaf area were determined. At the end of the growing season, plants were removed from pods and were cleaned with distilled water. The runner plant was counted and, stem diameter was measured with digital precision caliper compass after cleaning. The green biomass and root were divided into as two parts to weigh with a digital scale with 0.01 sensitively. The divided roots were measured by digital precision caliper compass. The leaf area was measured by Winfolia leaf area meter (Ipek et al., 2014).

Measurement of the physiological parameters

Leaf relative Chlorophyll content (LRCC) of leaves was determined using portable chlorophyll reader SPAD-502 (Konica Minolta), measuring absorbance at 650 nm, as a nondestructive method. Three readings were made on each leaf. The results were expressed in SPAD units.

Stomatal conductance (mmol $m^{-2}\ s^{-1}$) was measured with a leaf porometer once a month during the growth season (fifteen leaves in per treatment, measured in two sides in a leaf between 11:00 and 13:00 local time).

Leaves of five plants per treatment were harvested and were cut 1 cm^2 leaf disks. Leaf disks were washed with three changes of double distilled water to remove surface-adhered electrolytes. Leaf disks were placed in culture tubes containing 10 ml of double distilled water and incubated at 25 °C on a rotary shaker. The electrical conductivity of the bathing solution (EC_1) was determined by EC-meter after 24 h. Samples were then autoclaved at 121 °C for 15 min. and a last electrical conductivity reading (EC_2) was obtained upon equilibration at 25 °C. The electrolyte leakage was calculated as EC_1/ EC_2 and expressed as percent (Lutts et al., 1996).

Determination of iron content of the leaf

Leaves in 1 cm of shoot tips were used in the analysis. Fe contents of plants were analyzed after wet digestion of dried and ground sub-samples with a HNO_3-H_2O_2 acid mixture (2:3 v/v) at three steps (first step: 145 ºC, 75% RF, 5 min; second step: 180 ºC, 90% RF, 10 min and third step: 100 ºC, 40% RF, 10 min) in a microwave oven (Berghof Speedwave Microwave Digestion Equipment MWS-2) (Mertens, 2005a). Fe was determined using an Inductively Couple Plasma spectrometer (Perkin-Elmer, Optima 2100 DV, ICP/OES, Shelton, CT 06484-4794, USA) (Mertens, 2005b).

Data analyzes

The experiment was a completely randomized design model with three replicates and 10 plants per a replicate. Totally 210 strawberry plants were used. The data were analyzed using one-way ANOVA followed by Duncan's multiple range test. Duncan's multiple range test at the 0.05 significance level was conducted, and data were presented by average.

Results

Table-1 shows that 5 mM of silicon treatment and Fe treatment increased runner plant number at 2.31 and 2.25 runners per mother plant, respectively. The plant stem diameter was measured in 5 mM Si (44.96 mm), Fe (44.75 mm), 4 mM Si (44.46 mm) and, 3 mM Si (43.11 mm), higher than other treatments. The plant fresh weight was found higher in 5 mM Si (76.61 g), 4 mM Si (75.63 g) and, 3 mM Si (75.60 g). The treatment of 5 mM Si, 4 mM Si and, 3 mM Si had the higher fresh root weight with 60.33 g, 59.39 g and, 58.31 g, respectively. These three treatments were determined to increase both fresh plant weight and fresh root weight. In terms of the root length, the treatment of Fe obtained the highest root length with 31.74 cm in all treatments. As a result of the root length,

the Fe treatment was found to increase leaf area at 22.77 cm^2. The smallest leaf was obtained from Fe (-) + silicon (-) (19.29 cm^2) and Si (1 mM) (19.69 cm^2) treatments (Table-1).

The leaf relative chlorophyll content was measured higher in Fe (30.37 SPAD Units) and, Si (5 mM) (30.01 SPAD Units) treatments. The lowest leaf relative chlorophyll content was in Fe (-) + silicon (-) (23.31 SPAD Units). The stomatal conductance was measured higher in Si (5mM) with 259.46 mmol m^{-2} s^{-1} and Si (4 mM) with 257.08 mmol m^{-2} s^{-1} than other silicon and Fe treatments. The lowest stomatal conductance was determined in Fe (-) + silicon (-) with 175.65 mmol m^{-2} s^{-1}. The highest membrane permeability was calculated in Fe (-) + silicon (-) at 24.73% while the lowest membrane permeability was Si (5 mM) at 11.60% (Table-1).

The leaf Fe content was significantly increased by Si (5 mM) (163.40 mg kg^{-1}), Si (4 mM) (162.81 mg kg^{-1}) and, Fe (160.71 mg kg^{-1}). The lowest leaf Fe content was obtained from treatment of Fe (-) + Si (-) with 126.90 mg kg^{-1} (Table-1).

Discussions and Conclusion

The effects of silicon on plant metabolism have not fully understood, yet but there are some studies about Si increases plant tolerance to abiotic stress condition such as drought, salinity, high and low temperature and, heavy metal (Gong et al., 2005; Romero-Aranda et al., 2006). Also, it has been reported that Si contributed plants to take up minerals such as Manganese, Aluminum, Cadmium (Epstein, 1999; Hattori et al., 2005; Liang et al., 2007; Liang et al., 2005; Ma, 2004; Shi et al., 2005; Zsoldos et al., 2003). The plants having sufficient silicon content are more tolerant to water loss, diseases, pests and, the toxicity of manganese and iron excess (Ma et al., 2001). There are limited studies about silicon treatment on Fe uptake in plants. The silicon treatments increased plant growth and development such as a number of runner plant, stem diameter, fresh plant weight, fresh root weight, root length and leaf area. These results are supported by Gonzalo et al (2013) study on soybean and cucumber and Muneer and Jeong (2015) study on soybean. Gonzalo et al. (2013) reported that when silicon is treated alone to plants, the iron content, chlorophyll content decreased in soybean and cucumber. However, they found that when silicon together with iron is applied to soybean and cucumber, iron and chlorophyll content in plants was found increasing. On the other hand, Muneer and Jeong (2015) found that when silicon together with iron is applied to soybean, fresh leaf and root weight, dry leaf and root weight, Fe content of shoot and root and leaf relative chlorophyll content were increased. Also, researchers reported that silicon treatment increases stomatal conductance and photosynthetic activity. Our study shows that silicon treatment to strawberry under nutrient stress condition (higher calcareous soil) decreased membrane permeability and it increased stomatal conductance, chlorophyll content and iron content.

As a result, Si is an essential mineral and until now, the effects of Si on heavy metal have been focused on in researches. However, it should be focused on the effects of silicon on plant growth and development and, mineral uptake especially iron.

Acknowledgment

Table-1. Result of the morphological, physiological properties and Fe content

Treatments	Runner Plant Number	Stem Diameter (mm)	Fresh Plant Weight (g)	Fresh Root Weight (g)	Root Length (cm)	Leaf Area (cm^2)	Fe Content ($mg\ kg^{-1}$)	LRCC (SPAD Unit)	Stomatal Conductance ($mmol\ m^{-2}\ s^{-1}$)	Membrane Permeability (%)
Fe (-) + Si (-)	1.48^{E}	34.17^{D}	60.83^{D}	45.09^{C}	20.26^{E}	19.29^{D}	126.90^{D}	23.31^{F}	175.65^{F}	24.73^{A}
Fe	2.25^{AB}	44.75^{A}	72.08^{C}	54.85^{B}	31.74^{A}	22.77^{A}	160.71^{AB}	30.37^{A}	250.11^{BC}	19.87^{B}
Si (1 mM)	1.77^{D}	37.21^{C}	61.45^{D}	47.55^{C}	20.82^{DE}	19.69^{D}	137.44^{CD}	27.37^{E}	236.81^{D}	15.72^{C}
Si (2 mM)	1.96^{CD}	42.00^{B}	72.71^{BC}	54.27^{B}	22.06^{CD}	20.66^{C}	139.75^{C}	27.60^{E}	246.05^{C}	15.26^{C}
Si (3 mM)	1.97^{CD}	43.11^{AB}	75.60^{AB}	58.31^{A}	22.62^{BC}	21.05^{BC}	149.40^{BC}	28.40^{D}	252.88^{B}	14.07^{C}
Si (4 mM)	2.08^{BC}	44.46^{A}	75.63^{AB}	59.39^{A}	22.72^{BC}	21.27^{B}	162.81^{A}	29.18^{B}	257.08^{A}	13.65^{CD}
Si (5 mM)	2.31^{A}	44.96^{A}	76.61^{A}	60.33^{A}	24.15^{B}	21.42^{B}	163.40^{A}	30.01^{A}	259.46^{A}	11.60^{D}

[1]Selçuk University, Faculty of Agriculture, 42075, Konya, TURKEY
[2]Siirt University, Faculty of Agriculture, 56100, Isparta, TURKEY
*Corresponding author: pirlak@selcuk.edu.tr

References

Anonymous (2018). www.fao.org (Access Date: 01.08.2018).

Bityutskii, N., Pavlovic J., Yakkonen K., Maksimović V., Nikolic M. (2014). Contrasting effect of silicon on iron, zinc and manganese status and accumulation of metal-mobilizing compounds in micronutrient-deficient cucumber. Plant physiology and biochemistry. 74:205-211.

Epstein, E. (1999). Annual Review of Plant Physiollogy and Plant Molecular Biology. Silicon. 50.

Gong, H., Zhu X., Chen K., Wang S., Zhang C. (2005). Silicon alleviates oxidative damage of wheat plants in pots under drought. Plant Science. 169:313-321.

Gonzalo, M. J., Lucena J. J., Hernández-Apaolaza L. (2013). Effect of silicon addition on soybean (Glycine max) and cucumber (Cucumis sativus) plants grown under iron deficiency. Plant physiology and biochemistry. 70:455-461.

Hattori, T., Inanaga S., Araki H., An P., Morita S., Luxová M., Lux A. (2005). Application of silicon enhanced drought tolerance in Sorghum bicolor. Physiologia Plantarum. 123:459-466.

Ipek, M., Pirlak L., Esitken A., Figen Dönmez M., Turan M., Sahin F. (2014). Plant growth-promoting rhizobacteria (PGPR) increase yield, growth and nutrition of strawberry under high-calcareous soil conditions. Journal of plant nutrition. 37:990-1001.

Liang, Y., Sun W., Zhu Y.-G., Christie P. (2007). Mechanisms of silicon-mediated alleviation of abiotic stresses in higher plants: a review. Environmental pollution. 147:422-428.

Liang, Y., Zhang W., Chen Q., Ding R. (2005). Effects of silicon on H+-ATPase and H+-PPase activity, fatty acid composition and fluidity of tonoplast vesicles from roots of salt-stressed barley (Hordeum vulgare L.). Environmental and Experimental Botany. 53:29-37.

Lutts, S., Kinet J., Bouharmont J. (1996). NaCl-induced senescence in leaves of rice (Oryza sativa L.) cultivars differing in salinity resistance. Annals of botany. 78:389-398.

Ma, J., Miyake Y., Takahashi E. (2001) Silicon as a beneficial element for crop plants. In: Studies in plant Science, vol 8. Elsevier, pp 17-39.

Ma, J. F. (2004). Role of silicon in enhancing the resistance of plants to biotic and abiotic stresses. Soil Science and Plant Nutrition. 50:11-18.

Mertens, D. (2005a). AOAC official method 922.02. Plants Preparation of Laboratuary Sample Official Methods of Analysis, 18th edn Horwitz, W, and GW Latimer,(Eds):20877-22417.

Mertens, D. (2005b). AOAC official method 975.03. Metal in Plants and Pet Foods Official Methods of Analysis, 18th edn Horwitz, W, and GW Latimer,(Eds):3-4.

Muneer, S., Jeong B. R. (2015). Silicon decreases Fe deficiency responses by improving photosynthesis and maintaining composition of thylakoid multiprotein complex proteins in soybean plants (Glycine max L.). Journal of plant growth regulation. 34:485-498.

Romero-Aranda, M. R., Jurado O., Cuartero J. (2006). Silicon alleviates the deleterious salt effect on tomato plant growth by improving plant water status. Journal of plant physiology. 163:847-855.

Shi, X., Zhang C., Wang H., Zhang F. (2005). Effect of Si on the distribution of Cd in rice seedlings. Plant and Soil. 272:53-60.

Vose, P. (1982). Iron nutrition in plants: a world overview. Journal of Plant Nutrition. 5:233-249.

Zsoldos, F., Vashegyi A., Pecsvaradi A., Bona L. (2003). Influence of silicon on aluminium toxicity in common and durum wheats. Agronomie. 23:349-354.

[1]Selçuk University, Faculty of Agriculture, 42075, Konya, TURKEY
[2]Siirt University, Faculty of Agriculture, 56100, Isparta, TURKEY
*Corresponding author: pirlak@selcuk.edu.tr

International Conference on ScienceandTechnology

ICONST 2018

5-9 September 2018 Prizren - KOSOVO

The Effect of Plant-Based Oils and Cellulose Fillers on The Rheologicaland Physico-Mechanical Properties of Tire Tread

Anıl Alkan[1], Alev Akpinar Borazan[1]*

Abstract: In this study, commercial tire tread which should be as an economical and more environmentally friendly was aimed to be modified by using cellulosic fiber and/or plant-based oil.The ratio of cellulose fiber (from the waste chestnut shell, the waste pistachio shell and pinecone) to carbon black in the manufacture of tire's tread was used as 0.33:1. Three plant-based oil (canola, corn and sunflower oil) used as 20.8 phr instead of the aromatic oil in the mixture of the tire's tread. The tire treads were prepared by using 10 different mixture, one of them was control and others testing mixture. Rheological tests before vulcanization and physico-mechanical tests (tensile strength, elongation at break, tear strength, 300% modulus, hardness, abrasion, density) after vulcanization were applied to these prepared mixtures. Vulcanization characteristics were obtained by using a moving die rheometer (190°C,3min); minimum torque, maximum torque, cure rate, the scorch and cure time of the prepared rubber mixture. All tests were carried out in accordance with the relevant ASTM D standard test procedure.According to the test results, the rheological, physical and mechanical properties showed significant changes depending on the natural fillers. The values of the curing time and scorch time were increased while the maximum and minimum torque values were reduced for rubber samples produced using plant-based oil and/or cellulose fiber.Plant-based oil had higher cure extent values than the cellulose fiber this represents a higher cross-linking degree during cure reaction. The measured values of the abrasion and tensile strength were reduced negatively with all types of cellulose fillers. Test results of all of the different types of Plant-based oil were proper in standard values except tear strength.

Keywords: Cellulose fiber, Plant-basedoil, Physico-mechanical, Rheologicalproperties, Tire tread

Introduction

Today, rubber materials are located in many areas of our lives.The rubber industry in the world can be constantly made innovations because of the properties of rubber; easily processability, availability in different application areas, and usability as a semi-processed product. These are all the preferred properties for any manufacturing material in this market (Öter et al. 2011; Namazi 2017).

In the world, the waste of rubber materials especially in the form of used tires caused to the serious environmental problem due to their very complex structure and composition, this increases year by year. Many countries have changed in their policy or legislated to prevent this situation and to protect the environment (ETRMA 2013; Garciaet al.2017; Sienkiewicz et al. 2017). Rubber material essentially is consisting of the rubber, the reinforcing fillers, the process oils, and additives. The mechanical and rheological performance of rubber materials are changeable with the filler loading, the dispersing quality of fillers and the other additives (Sobhy et al. 2003; Öter et al. 2011).Since January 2010, highly aromatic oils

[1]Bilecik Seyh Edebali University, Faculty of Engineering, 11210, Bilecik, TURKEY
*Correspondingauthor: alev.akpinar@bilecik.edu.tr

including PAH were banned according to a European Directive, to avoid contaminating the environment (ETRMA 2013).Some researchers and manufacturers have turned to plant-based oils and other natural tire ingredients to reduce cost, and increase the sustainability of the tire (Öter et al. 2011; Saxena 2011; Chokan and Sombat et al. 2014; Zanchet et al. 2016).

The subject covered in this study is the determination of the physicomechanical and rheological behavior of rubber blends for the tire tread affected by cellulosic fibers and/or plant-based oils.

The original aim is to reduce the cost of rubber blends and improve the tire properties, but the main advantage of selected fillers is that it allows them to focus on forwarding sustainability.

Material and Method

The cellulose fibers were obtained from the waste chestnut shell, the waste pistachio shell and pinecone with the end of some processing. The ratio of cellulose fiber to carbon black in the manufacture of tire's tread was used as 0.33:1. Three plant-based oils (canola, corn and sunflower oil) were provided from local suppliers in Turkey. They were used as 20.8 phr instead of the aromatic oil in the mixture of the tire's tread. The tire treads were prepared by using 10 different mixture, one of them was control (RC) and others testing mixture. The chemical compositions and quantities of all additives used in the production of commercial tire tread (RC) given in the Table 1. is subject to the confidentiality agreement with the company.

Table 1. Alternative formulation of tire treads

Codes of the Tire tread / Function/ Compounds	RC	R1	R2	R3	R4	R5	R6	R7	R8	R9
	Amount (phr)									
Matrix										
Rubber Blend (Natural &Butadien Rubber Mix)	100	100	100	100	100	100	100	100	100	100
Filler										
Carbon Black (N330)	66.67	50	50	50	66.67	66.67	66.67	66.67	50	50
Alternative; Cellulose fiber filler										
pinecone	----	16.67	----	----	----	----	----	----	16.67	----
chestnut shell	----	----	16.67	----	----	----	----	----	----	16.67
Pistachio shell	----	----	----	16.67	----	----	----	----	----	----
Chemicals										
Activator	4.41	4.41	4.41	4.41	4.41	4.41	4.41	4.41	4.41	4.41
Homogenizer	1.81	1.81	1.81	1.81	1.81	1.81	1.81	1.81	1.81	1.81
Antiozonant/Antioxidant	3.94	3.94	3.94	3.94	3.94	3.94	3.94	3.94	3.94	3.94
Process oil										
Distillate Aromatic Extract (DAE)	20.83	20.83	20.83	20.83	----	----	----	10.42	10.42	10.42
Alternative; Plant based oils										
Canola oil	----	----	----	----	20.83	----	----	----	----	----
Corn oil	----	----	----	----	----	20.83	----	----	----	----
Sunflower oil	----	----	----	----	----	----	20.83	10.42	10.42	10.42
Vulcanization agents										

Curing/vulcanizing agent	1.67	1.67	1.67	1.67	1.67	1.67	1.67	1.67	1.67	1.67
Activator/ Accelerator	1.77	1.77	1.77	1.77	1.77	1.77	1.77	1.77	1.77	1.77

Firstly, polymer mixtures were prepared as a master batch in an internal mixer by a laboratory two-roll mill (HMO Mak San Tic.Ltd.) with 2.5kg capacity and friction factor 1.1. The temperature of the mill did not exceed 95 °C and rotor speed was 5 rpm while working. Mixing procedure is given in Table 2.

Table 2.Mixing procedure of tire tread' compounds

Master batch	**Time(min.)**
Charge Rubbers	20-32
Filler & process oil &chemicals	10-15
Discharge mill	9-14
Final batch	
Master batch	10-15
Vulcanization agents	12-23
Discharge mill	10-19

The rheological properties of polymer samples were obtained by using a moving die rheometer (MDR, Gotech M2000A) at 190°C according to ASTM D 1646 standard. The values of t_{s2}, t_{90}, M_L, M_H were measured; cure extent and cure rate index (CRI) were calculated from the values according to Equation 1 and Equation 2, respectively.

$$\text{Cure extent} = M_H - M_L \quad (1)$$

$$CRI = 100 / (t_{90} - ts_2) \quad (2)$$

The vulcanization of polymer samples were carried out with a DEVOTRANS DVT NP Y sample preparation press at 170 °C under 15 MPa pressure for specified times which correspond to their t_{90}. From compression molded sheets (Figure 1.) specimens were prepared in required dimensions by standard to study the physico-mechanical properties of vulcanizates.

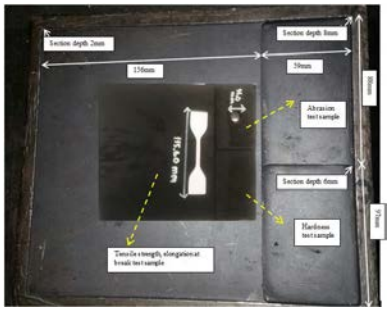

Figure 1. Scaling of the mold to standard blades (Akpinar Borazan, 2017)

Tensile strength, elongation at break, tensile modulus (300%) and tear strength were determined by using Tensile Testing Machine (DEVOTRANS-Dvt BE), according to ASTM D412. Both tensile and tear properties used a testing speed of 500 mm/min. The density of the vulcanized rubber samples were determined according to Archimedes Principle based on the ASTM D 297. DEVOTANS DVT DA 6 were used for measuring abrasion of the rubber vulcanizates, according to ASTM D 5963 Hardness of the vulcanized samples was determined according to ASTM D2240 by using a Shore A durometre.

After physico-mechanical tests, the surface morphology of some vulcanized rubber samples were examined under the scanning electron microscope (SEM., Zeiss Supra 40VP, Germany) at an acceleration voltage of 10kV.

Results

In this study, the effects and usability of plant based-oil and /or cellulose fiber on different tire tread compounds were evaluated.

For cure system crosslinking isotherms were given in Figure 2a.which was taken at 190°C for 3 minutes. The resulting scorch time, cure time, minimum rheometer torque and maximum rheometer torque were given in Figure 2b. for comparison cure system of polymer samples.

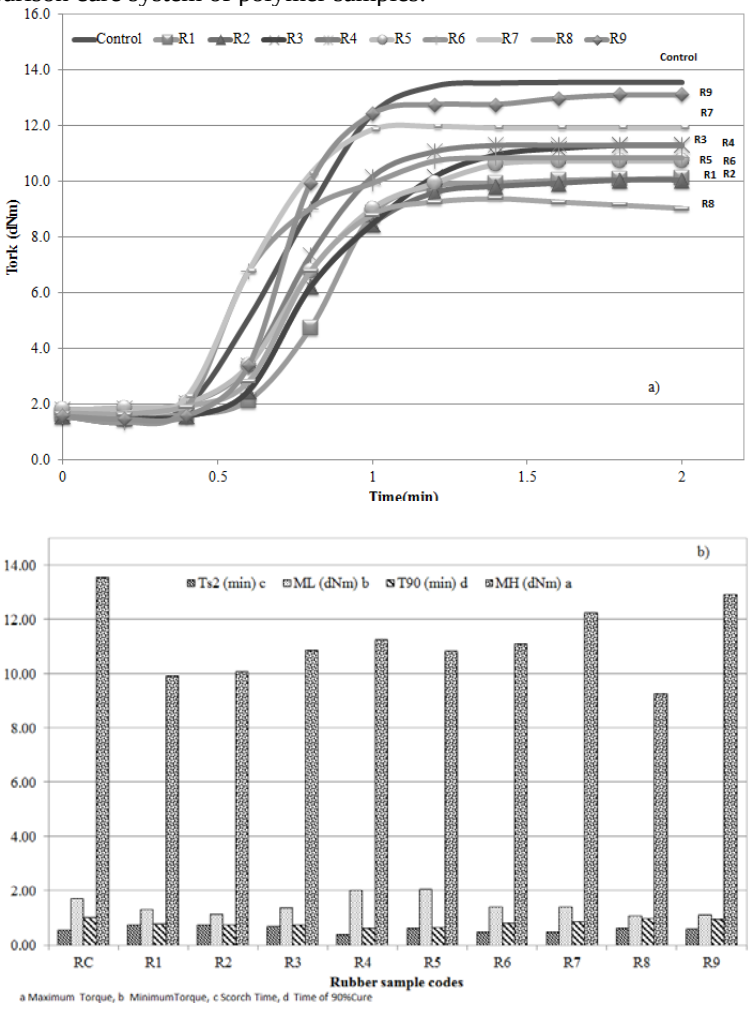

Figure 2. For all different rubber samples **a)** Crosslinking isotherms, **b)**Rheological properties

The values of the curing time(t_{90}) and scorch time(t_{s2}) were increased while the maximum (M_H) and minimum (M_L) torque values were reduced for rubber samples producedusing plant-based oil and/or cellulose fiber. Plant-based oil had higher cure extent values than the cellulose fiber this represents a higher cross-linking degree during cure reaction (Table 3.).Maximum rheometer torque, M_H, which is related to the stiffness of cured compound, is minimum for R8 with made of pinecone and sunflower oil.

Table 3. Cure characteristics

	RC	R1	R2	R3	R4	R5	R6	R7	R8	R9
Cure extent (dNm)	11.83	8.61	8.92	9.48	9.24	8.78	9.71	10.83	8.16	11.82
CRI (min-1)	8.45	11.61	11.22	10.55	10.82	11.39	10.30	9.24	12.26	8.46

When mechanical properties of the plant-based oil and cellulose fiber were compared eachother, plant-based oil, especially sunflower oil and the combination of sunflower oil with aromatic oil have shown similar test results with control samples (Figure 3.).

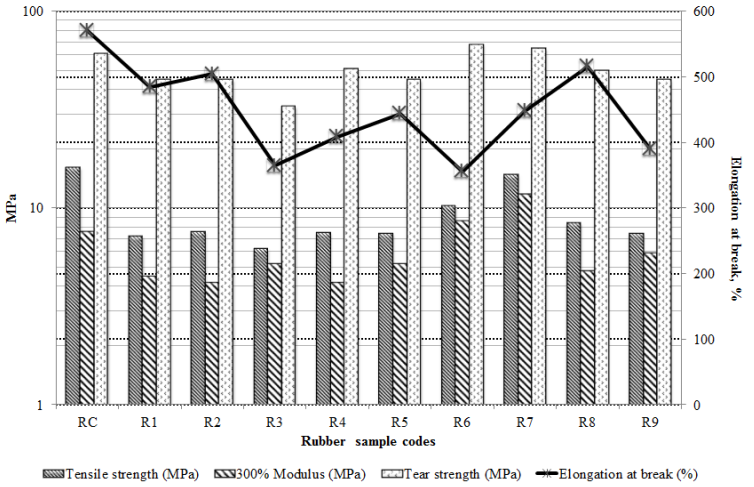

Figure 3. Effect of the cellulose fiber and/or plant-based oil fillers on some mechanical properties of tire treads

In vulcanizates containing sunflower oil (R6, R7) have been enhanced tensile strength, tear strength and modulus 300% values. On the other hand, it has been found that these properties were decreased when cellulose blend filler was added to the blends. Sunflower and pinecone fillers (R8) have better interaction than the sunflower and chestnut shell fillers (R9) were determined according to the test results of the mechanical properties of the tire tread.

Hardness valuesof the rubber samples were varying between 63 and 68.Plant-based oils were reduced hardness values in vulcanized rubber samples.

Figure 4.shows that the abrasion rate of vulcanized rubber samples (R1, R2 and R3) increases sharply with cellulose fiber filler. Abrasion resistance is usually affected by hardness, filler dispersion, and chemical structure of rubber.It has been determined that R7 has the highest abrasion resistance to the lowest abrasion in all vulcanized rubber samples.

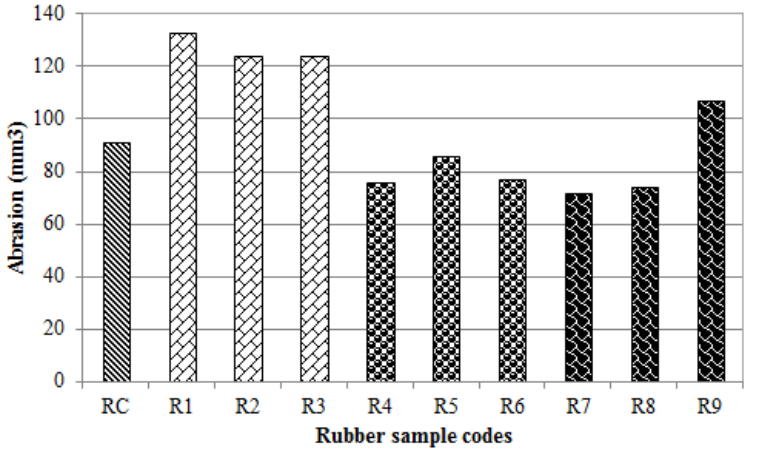

Figure 4. Effect of the cellulose fiber and/or plant-based oil fillers on abrasion of tire treads

SEM images of some vulcanized rubber samples are shown in Figure5. The dark backgrounds represent the rubber matrix and the bright parts are the fragments of additives which could not be dispersed homogenously.

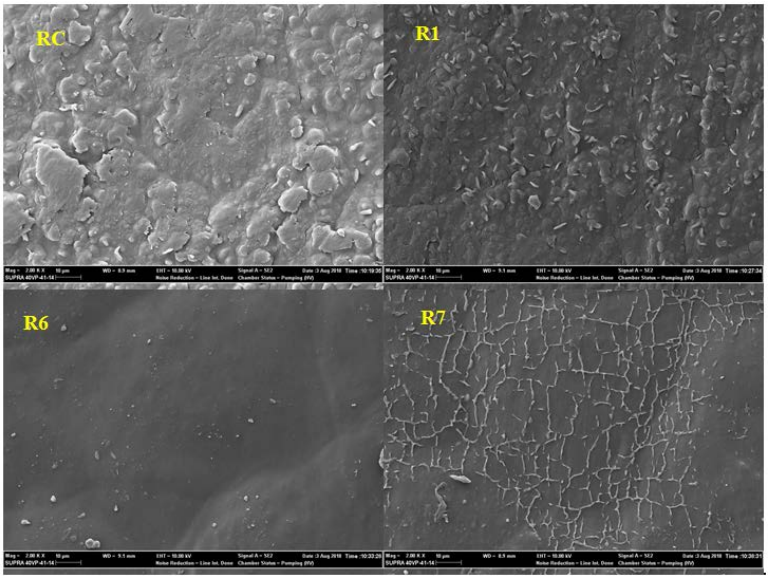

Figure 5. SEM image of thesurfacefromtherubbersamples at 2KX magnification.

A surfacemorphology of the pinecone fibers (R1) is shown (Figure 5.) where it can be observed that they are tubular with a circular section. The use of natural oils, as sun flower (R6 and R7) improves the dispersion and distribution of fillers in rubber samples.

The quality of the fiber–matrix interface is important when using natural fibers as reinforcement in the rubber matrix. Some physical and chemical methods are suggested to improve this interface. Physical treatment is the first step when used to natural fibers.This changes the structural and surface properties of the fibers but does not change the chemical compositions of them. At the later stage of this work, chemical treatment must be applied to the natural fibers before adding to the tire mixture.

Discussion and Conclusions

The experimental results showed that rheological properties of the tire tread after the substitution of aromatic oils with sunflower oil and substitution of carbon black with chestnut shell have not been deteriorated significantly.

Physical and mechanical properties of the vulcanizates were changed with natural filler.As a result of the experimental tests, cellulose fibres and plant based-oils are as alternative fillers for carbon black, aromatic oil that provides valuable data for manufacturers by small formulation adjustments.The further studies, especially plant-based oils can be compared with aromatic oil to make some required modifications in properties of physico-mechanical and rheological.

Acknowledgements

The authors would like to acknowledge the BİLLAS Tire and Rubber Industry Trade Co. for kindly supplying the equipment with all mixture ingredients for this research.

References

Akpinar Borazan, A. (2017). Preparation and characterization of ethylene propylene diene monomer (EPDM) rubber mixture for a heat resistant conveyor belt cover, Anadolu University Journal of Science and Technology A- Applied Sciences and Engineering, 18(2), 507 – 520.

ASTM, Standard Test Method for Rubber Property—Abrasion Resistance (Rotary Drum Abrader), In ASTM Annual Book of Ame.Soc. for Testing and Materials Standards, Easton, MD, USA, D5963 - 15.

ASTM, Standard Test Method for Rubber Property—Durometer Hardness, In ASTM Annual Book of American Society for Testing and Materials Standards, Easton, MD, USA, D2240 - 15.

ASTM, Standard Test Methods for Rubber Products—Chemical Analysis, , In ASTM Annual Book of American Society for Testing and Materials Standards, Easton, MD, USA, D297- 15.

ASTM, Standard Test Methods for Rubber—Viscosity, Stress Relaxation, and Pre-Vulcanization Characteristics (Mooney Viscometer, In ASTM Annual Book of American Society for Testing and Materials Standards, Easton, MD, USA, D1646-15.

ASTM, Standard Test Methods for Vulcanized Rubber and Thermoplastic Elastomers_Tension, In ASTM Annual Book of American Society for Testing and Materials Standards, Easton, MD, USA, D412-15.

Chokanandsombat, Y., Sirisinha, C. (2014). Influence of Aromatic Content in Rubber Processing Oils on Viscoelastic Behaviour and Mechanical Properties of Styrene-butadiene-rubber For Tyre Tread Applications. Polymers & Polymer Composites, 22(7), 599- 606.

ETRMA -EuropeanTyreRubberManufacturesAssociation, (2013). EuropeanTyreandRubberIndustry e Statistics. http://www.etrma.org/uploads/Modules/Documentsmanager/20131015---statistics-booklet-2013-final2.pdf (Accessed:18/07/ 2017).

Garcia, R., Vendrell, L., Mesas, M., Stan, F., Gheorghe, A., Ghenea, A., Spatzierer, L., Schweiger,S., Mattenberger, H. (2017) State of the art of waste preventıon and management strategıes ın “urban-wins” countrıes and munıcıpalıtıes, https://www.urbanwins.eu/wp-content/uploads/2017/06/UrbanWINS-D1.1.-State-of-the-art-of-waste-prevention-and-management.pdf(Accessed:18/07/ 2016).

Namazi, H.(2017). Polymers in ourdaily life. BioImpacts, 7(2), 73-74.

Öter, M., Karaağaç, B., Deniz, V. (2011). Substitution of aromatic processing oils in rubber compounds. http://akademikpersonel.kocaeli.edu.tr/bkaraagac/sci/bkaraagac05.08.2011_14.57.35sci.pdf (Accessed: 05/06/2018).

Saxena, M., Pappu, A., Sharma, A., Haque, R., Wankhede, S.(2011) Composite Materials from Natural Resources: Recent Trends and Future Potentials, Chp 6, pp.121-162. Advances in Composite Materials -Analysis of Natural and Man-Made Materials, Dr. PavlaTesinova (Ed.), ISBN: 978-953-307-449-8, InTech, https://www.intechopen.com/books/advances-in-composite-materials-analysis-of-natural-and-man-made-materials/composite-materials-from-natural-resources-recent-trends-and-future-potentials
(Accessed: 25/04/2017).

Sienkiewicz, M., Janik, H., Borzedowska-Labuda, K., Kucinska-Lipka, J. (2017). Environmentally friendly polymer-rubber composites obtained from waste tyres: A review. Journal of Cleaner Production, 1(2017), 560-571.

Sobhy, M.S., El-Nashar, D.E., Maziad, N.A. (2003). Cure Characteristics and Physicomechanical Properties of Calcium Carbonate Reinforcement Rubber Composites. Egyptian Journal of Solids, 26(2), 241-257.

Zanchet, A., Garcia, P.S., Nunes, R.C.R., Crespo, J.S., Scuracchio, C.H. (2016). Sustainable Natural Rubber Compounds: Naphthenic Oil Exchange for another Alternative from Renewable Source. International Refereed Journal of Engineering and Science, 5(12), 10-19.

International Conference on Science and Technology

ICONST 2018

5-9 September 2018 Prizren - KOSOVO

Assesment of Antioxidant Actvity of *Enteromoprha intestinalis* (Linnaeus) Nees and *Ceramium rubrum* C. Agardh

Gülen Türker[1], İlknur Ak[2]*

Abstract: In this study, the green alga *Enteromorpha intestinalis* and the red alga *Ceramium rubrum* were screened for potential antioxidant activity. The algae collected from Çanakkale Strait, Turkey in February 2018. The antioxidant activity, total phenolic, flavonoid, carotenoid and condensed tannin contents were quantified in ethanol extracts. The IC50 values of *E. intestinalis* and *C. rubrum* were determined as 3.81±0.06 µg/g Ext. and 3.56±0.04 µg/g Ext., respectively. *C. rubrum* exhibited highest phenolic content at 497.69± µg/g Ext. The maximum total flavonoid (2604.00±89.27 µg/g Ext.) and total carotenoid (4.21±0.21 µg/g Ext.) content were measured in *E. intestinalis*. The condensed tannins values changed 1474.92±64.97 µg/g Ext. (*E. intestinalis*) to 122.37±7.61 µg/g Ext. (*C. rubrum*). According to our results, *E. intestinalis* and *C. rubrum* from Çanakkale, Turkey could be use source for future applications in medicine, dietary supplements, functional foods, cosmetics and agriculture.

Keywords: *Enteromorpha intestinalis, Ceramium rubrum, Antioxidant activity, Condensed tannin, Marine biotechnology*

Introduction

Green and red macro algae contains bioactive compounds which have antioxidant and antimicrobial activities such as phenolics, flavonoids carotenoids and tannins as well as macro and micro nutrients (Matsukawa et al., 1997; Cornish and Garbary, 2010; Farasat el al., 2014). In recent years, studies focused on antioxidant activity of macro algae or their extracts (Dykens et al., 1992; Matsukawa et al., 1997; Matanjun et al., 2008; Akköz et al., 2009; Cornish and Gabary, 2010, Kelman et al., 2012) and these studies shows that macro algae are a new promising source of novel bioactive compounds that can be used for drug development (Zerrifi et al., 2018).

Antioxidant compounds act as free radical scavengers and protect organisms from production of reactive oxygen species (ROS) Halliwel et al., 1995). Many macro algae species have natural antioxidant capacity that can protect the human body from free radicals and other strong oxidizing agent (Dykens et al., 1992; Matanjun et al., 2008; Meenakshi et al., 2009; Collins et al., 2016). Among natural antioxidants, phenolic and flavonoid compounds are commonly found in photosynthetic organisms (Duan et al., 2006). They act by chelating metal ions and improve the antioxidant endogenous system under stress environmental conditions (Rodrigo and Bosco, 2006). Similar attitude was reported for carotenoid pigments of macro algae, especially β carotene (Plazaet al., 2010). Condensed tannins or proanthocyanidins are widely distributed in plants from seaweeds to high plants (Mueller-Harvey, 2006; Zubek et al., 2012). They absorb UV radiation and act as photo protective for cell (Zubek et al., 2012).

[1] Çanakkale Onsekiz Mart University, Çanakkale School of Applied Sciences, Department of Food Technology 17100, Çanakkale/Turkey
[2] Canakkale Onsekiz Mart University, Faculty of Marine Sciences and Technology, Department of Aquaculture, 17100, Çanakkale/Turkey
*Corresponding author: ilknurak@gmail.com

The aim of the study is to investigate antioxidant activities of the green alga *Enteromorpha intestinalis* and the red alga *Ceramium rubrum* from Çanakkale, Turkey for future applications in medicine, dietary supplements, functional foods, cosmetics and agriculture.

Material and Methods

Macro algae

Green alga *Enteromorpha intestinalis* and red alga *Ceramium rubrum* were collected from Çanakkale (40° 6' 43¨ N, 26° 24' 15¨ E). The harvested seaweed samples were cleaned from their epiphytes, dried at 30 °C and milled into powder before extraction.

DPPH free radical-scavenging activity assay

DPPH (2,2-diphenyl-1-picrylhydrasyl) radical scavenging activity was measured according to the Brand-Williams et al. (1995). Each sample was diluted in methanol prior to the analysis (1 mg/ml). The DPPH solution was added to the diluted sample, thoroughly mixed, then left for 30 min for the reaction to occur. The absorbance of the sample as measured a 515 nm using a UV–Vis spectrophotometer (Thermo Aquamate). The absorbance of DPPH solution in methanol, without any antioxidant (control), was also measured. The percentage of DPPH radical scavenging activity was calculated by using the following equation:

$$\text{DPPH scavenging (\%)} = [(A_{control} - A_{sample})/A_{control}] \times 100$$

where A sample is the absorbance of the sample after the time necessary to reach the plateau (30 min) and A control is the absorbance of DPPH. Extract concentrations providing IC50 inhibition values were calculated from graph plotting using nonlinear regression. Butylated hydroxytoluene (BHT), α tocopherol and Vitamin C were used as positive controls.

Determination of phenolic contents

Total content of phenolic contents of algae were determined spectrophotometrically using Folin-Ciocalteu reagent according to the method described in Djeridane et al. (2006) it was expressed as microgram per gram extract.

Determination of flavonoid contents

The total flavonoid content was determined according to Quettier- Deleu et al. (2000) and it was expressed as microgram per gram extract.

Determination of total carotenoid contents

The carotenoid content of two macro algae was determined spectrophotometrically (480 nm) according to Lichtenthaler and Buschmann (2001). The concentration of the carotenoids is expressed as microgram per gram extract.

Determination of condensed tannin contents

Condensed tannin content was evaluated according to Price et al., (1978).

Results and Discussion

The scavenging effects of *E. intestinalis* and *C. rubrum* on DPPH free radical are summarized in Table 1. *C. rubrum* showed the highest antioxidant potential with a low IC50 (3.56±0.04 mg/g Ext.) and significantly lower than three commercial antioxidants tested, BHT (1.33±0.01 mg/g Ext.) α-tocopherol (1.48±0.02 mg/g

Ext.) and Vitamin C (1.35±0.02 mg/g Ext.) in agreement with the studies of Zubia et al. (2007) and Farasat el al. (2014).

Table 1. The DPPH radical scavenging activities of *E. intestinalis* and *C. rubrum*

Species	IC50 inhibition values (mg/g Ext.)	% Inhibition
E. intestinalis	3.81±0.06	41.23±0.48
C. rubrum	3.56±0.04	39.45±0.14
Butylated hydroxytoluene	1.33±0.01	99.00±0.11
α-tocopherol	1.48±0.02	96.00±0.15
Vitamin C	1.35±0.02	98.00±0.10

The phenolic content of the algae varied form 273.73±3.19 µg/g Ext. to 497.69±6.18 µg/g Ext (Table 2). Several studies have shown a highly significant correlation between the phenolic content and the antioxidant activity in seaweed extracts (Oki et al., 2002; Zubia et al., 2007). The red alga *C. rubrum* showed significantly higher phenolic content than the green alga *E. intestinalis* (Table 2). Phenolic compounds are secondary plant metabolites that are found naturally in all primer producers and these compounds can be used to enhance the properties of foods, for both nutritional purposes and for preservation (Rice-Evans et al., 1997; Huyut et al., 2017). The macro algae extracts were rich for total flavonoids (Table 2). The highest total flavonoid content was detected in *E. intestinalis* (4.21±0.21 µg/g Ext.). According to results, *E. intestinalis* could be a good candidate for flavonoid sources. Total carotenoid content of two macro algae was shown Table 2. The highest total carotenoid content was found in *E. intestinalis* (4.21±0.21 µg/g Ext.) and lowest in *C. rubrum* (2.14±0.66 µg/g Ext.). According to Plaza et al., (2010) pigments help in cell communications and human health maintenance. Also, algal carotenoids have an antioxidant activity against human diseases related to ROS (Collins et al., 2016). The total condensed tannin contents of *E. intestinalis* and *C. rubrum* were shown in Table 2. The condensed tannin content of *E. intestinalis* (1474.92±64.97 µg/g Ext.) is 12 time higher than *C. rubrum* (122.37±7.61 µg/g Ext.). According to Machu et al. (2015) condensed tannins found in green algae an in lower amounts in some red algae. Our results show similarity with this study. The phenolic, flavonoid and carotenoid contents in this study were significantly correlated to IC50 inhibition values (Figure 1). Also, condensed tannin contents were highly positively correlated with IC50 inhibition values (Figure 1). The same correlation of antioxidant activity was reported Chakraborty et al., (2013) and Ismail (2016) with some edible brown, green and red seaweeds of rich phenolic content

.

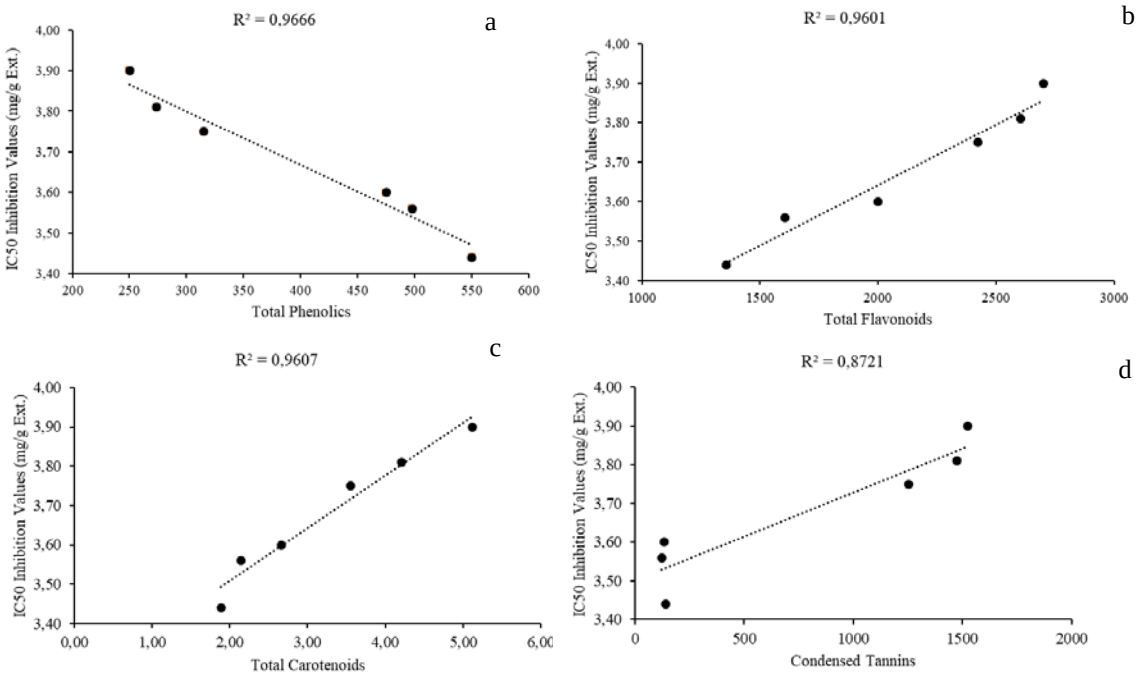

Figure 1. Correlation between IC50 inhibition values ((mg/g Ext.) and (a) Total Phenolics (mg GAE/g Ext.), (b) Total Flavonoids (mg/g Ext.), (c) Total Carotenoids (µg/g Ext.) and (d) Condensed Tannins (µg/g Ext.)).

Table 2. The total phenolics, flavonoids, carotenoids and condensed tannins of *E. intestinalis* and *C. rubrum*.

Species	Total Phenolics (µg/g Ext.)	Total Flavonoids (µg/g Ext.)	Total Carotenoids (µg/g Ext.)	Condensed Tannins (µg/g Ext.)
E. intestinalis	273.73±3.19	2604.00±89.27	4.21±0.21	1474.92±64.97
C. rubrum	497.69±6.18	1605.96±75.28	2.14±0.66	122.37±7.61

Conclusion

Marine algae have good sources of bioactive compounds such as phenols, flavonoid, carotenoids and condensed tannins. In the present research, antioxidant activity of *E. intestinalis* and *C. rubrum* from Çanakkale were evaluated. The results clearly showed that tested macroalgae have antioxidant activity. *E. intestinalis* exhibited high total flavonoid, carotenoid and condensed tannin contents. Also, both macro algae have high antioxidant activity with low IC50 inhibition values. But, the highest total phenolic content was found in *C. rubrum*. We conclude that the main contributors of antioxidant activity these two seaweeds according to significant correlation between IC50 inhibition values and total phenolic, flavonoids and carotenoids. It is apparent from the findings of this study that further investigations are required to assess effects of light intensities, salinity, nutrient levels, and reproductive stage on observed antioxidant activity. Thus, the antioxidant activity of macro algae distributed in Çanakkale could become a source for future applications in medicine, dietary supplements, functional foods, cosmetics and agriculture.

References

Akköz C., Arslan D., Ünver A., Özcan M.M., Yılmaz B. (2009). Chemical Composition, Total Phenolic and Mineral Contents of *Enteromorpha intestinalis* (L.) Kütz. And *Cladophora glomerata* (L.) Kütz. Seaweeds. Journal of Food Biochemistry, 35, 513 – 523.

Brand-Williams W., Cuvelier M.E., Berset C. (1995). Use of a free radical method to evaluate antioxidant activity. LWT - Food Sci. Technol., 28; 25-30.

Chakraborty K., Praveen N., Vijayan K.K., Rao G.S. (2013). Evaluation of phenolic contents and antioxidant activities of brown seaweeds belonging to *Turbinaria* spp. (Phaeophyta, Sargassaceae) collected from Gulf of Mannar. Asian Pacific Journal of Tropical Biomedicine, 3(1), 8-16.

Collins K.G., Fitzgerald G.F., Stanton C., Ross R.P. (2016). Looking beyond the terrestrial: the potential of seaweed derived bioactives to treat non-communicable diseases. Marine Drugs, 14(60), 1-31.

Cornish M.L., Garbary D.J. (2010). Antioxidants from Macro algae: Potential Applications in Human Health and Nutrition. Algae, 25, 155–171.

Djeridane A., Yousfi M., Nadjemi B., Boutassouna D., Stocher Vidal N. (2006). Antioxidant activity of some Algerian medicinal plants extracts containing phenolic compounds. Food Chem., 97, 654–660.

Dykens J. A., Shick J. M., Benoit C., Buettner G.R., Winston G.W. (1992). Oxygen radical production in the sea anemone *Anthopleura elegantissima* and its endosymbiotic algae. Journal of Experimental Biology, 168, 219–241.

Farasat, M., Khavari – Nejad R.A., Nabavi S.M.B., Namjooyan F. (2014). Antioxidant Activity, Total Phenolics and Flavonoid Contents of some Edible Green Seaweeds from Northern Coasts of the Persian Gulf. Iranian Journal of Pharmaceutical Research, 13(1), 163 – 170.

Halliwell B., Aeschbach R., Löliger J., Aruoma O.I. (1995). The characterization of antioxidants. Food Chem Toxicol., 33, 601–617.

Huyut Z., Beydemir Ş., Gülçin İ. (2017). Antioxidant and antiradical properties of selected flavonoids and phenolic compounds. Hindawi biochemistry reseach international, 2017, 1-10.

Ismail G.A., 2016. Biochemical composition of some Egyptian seaweeds with potent nutritive and antioxidant properties. Food Science and Technology, 37(2), 294 – 302.

Kelman D., Posner E.K., McDermid K.J., Tabandera N.K., Wright P.R., Wright, A.D. (2012). Antioxidant Activity of Hawaiian Marine Algae. Marine Drugs, 10(2),403-416.

Kulevanova S., Stefova M., Stefkov G., Stafilov T. (2001). Identification, isolation and determination of flavones in *Origanum vulgare* from Macedonian flora. Journal of Liquid chromatography and related technologies, 24(4), 589–600.

Lichtenthaler H.K., Buschmann C. (2001). Current Protocols in Food Analytical Chemistry. John Wiley and Sons, Inc., New York F4.3.1- F.4.3.8

Machu, L., Misurcova L., Ambrozova J.V., Orsavova J., Mlcek J., Sochor J., Jurikova T. (2015). Phenolic content and antioxidant capacity algal food productions. Molecules, 20, 1118 – 1133.

Matanjun P, Suhaila M., Mohamed M.N., Kharidah M., Hwee M.C. (2008). Antioxidant activities and phenolics content of eight species of seaweeds from north Borneo. Journal of Applied Phycology, 367(20),1573-5176.

Matsukawa R., Dubinsky Z., Kishimoto E., Masaki K., Masuda Y., Takeuchi T., Chihara M., Yamamoto Y., Niki E., Karube I. (1997). A Comparison of Screening Methods for Antioxidant Activity in Seaweeds. J. Appl. Phycol., 9, 29-35.

Meenakshi S., Gnanambigai D.M., Mozhi S.T., Arumugan M., Balasubramanian T. (2009). Total Flavanoid and in vitro antioxidant activity of two seaweeds of Rameshwaram coast. Global Journal of Pharmacology, 3(2), 59 – 62.

Mueller-Harvey I., (2006). Unravelling the conundrum of tannins in animal nutrition and health. J. Sci. Food Agric., 86, 2010–2037.

Plaza M., Santoyo S., Jaime L., García-Blairsy Reinac G., Herrero M., Señoráns F.J., Ibánez E. (2010). Screening for bioactive compounds from algae. Journal of Pharmaceutical and Biomedical Analysis, 51(2), 450-455.

Price M.L., Vanscoyoc S., Butler L.G. (1978). Critical evaluation of Vanillin reaction as an assay for tannin in sorghum grain. J. Agric. Food Chem., 26,1214-1218.

Rodrigo R., Bosco C. (2006). Oxidative stress and protective effects of polyphenols: comparative studies in human and rodent kidney: a review Comp. Biochem. Physiol., 142, 317-327

Rice-Evans C., Miller N.J., Paganga G. (1997). Antioxidant properties of phenolic compounds. Trends in plant Science, 2(4), 152 – 159.

Quettier-Deleu C., Gressier B., Vasseur J., Dine T., Brunet J., Luyck M., Cazin M., Cazin J.C., Bailleul F., Trotin F. (2000). Phenolic compounds and antioxidant activities of buckwheat (Fagopyrum esculentum Moench) hulls and flour. J. Ethnopharmacol., 72, 35-40.

Zerrifi S.A., Khalloufi F., Oudra B., Vasconcelos V. (2018). Seaweed Bioactive Compounds against Pathogens and Microalgae: Potential Uses on Pharmacology and Harmful Algae Bloom Control. Marine Drugs, 16,55.

Zubek S., Mielcarek S., Turnau K. (2012). Hypericin and pseudohypericin concentrations of a valuable medicinal plant *Hypericum perforatum* L. are enhanced by arbuscular mycorrhizal fungi. Mycorrhiza, 22(2): 149-156.

Zubia M., Robledo D., Frelie-Pelegrin Y. (2007). Antioxidant activities in tropical marine macroalgae from the Yucatan Peninsula, Mexico. J Appl Phycol, 19, 449 – 458.

International Conference on Science and Technology

ICONST 2018

5-9 September 2018 Prizren - KOSOVO

Determination of Phenological and Pomological Characteristics of Some Asian Pear Cultivars

Mahmut Yavuz[1] , Lütfi Pirlak[2*]

Abstract: This study was carried out on the four asian pear varieties grown in Ereğli district of Konya province between the 2017-2018. Within the scope of this work, some phenological and pomological characteristics of Hosiu, Kosiu, Hakko and Shinseiki cultivars were examined. 122,00 -206,00 g fruit weight, 58,97-72,78 mm fruit width, 47,85-70,01 mm fruit size, 2.80-5,48 Ib fruit firmness, 11,83-16,90 % total soluble solids and 1.02-5.66 % titratable acidity ratio were found as research results. As a result of this work on Asian Pear cultivars, in 2017, swollen bud term was carried out as 02-04 April, beginning of flowering 18-19 April, full bloom 23-25 April, harvest date 05-09 August and the period from blooming to harvest date is determined between 133-137 days. For 2018, swollen bud term was observed on 05-07 March, beginning of flowering was on 23-27 March, full bloom was on 26-29 March, harvest date 14-16 August and the period from blooming to harvest date is determined between 141-143 days. As a result of this study, four Asian Pear cultivars's phenological and pomological caracteristics were determined in Ereğli district. The obtained result are thought to be important for regional-based and country-based for fruit growing.

Keywords: Ereğli-Konya, Asian Pear, phenological properties , pomological properties

Introduction

The pear is one of the fruit species that are grown and consumed in many countries in the hot climate zone. It is known that pear production has a long history. At the beginning of the earliest places where pear production is made, Anatolia, ancient Greece and Rome are coming. It is known that the pear production as well as the western world has a long history in China (Akçay ve Yücer, 2008a).

Most of the cultivars that are subject to world trade on the five continents (Africa, America, Asia, Europe and Oceania) have come from the *Pyrus communis* (European pears) and *Pyrus pyrifolia* (Asian pears). The vast majority of other species are used as rootstocks in the cultivation of cultivars of these two species. Despite the fact that there is a group of Asian Pears with a high share in world production, most of the pear varieties subject to world trade are in the European group (Akçay ve Yücer, 2008b).

According to the FAO data for 2016, China received the first rank with 19.499,487 tons in pear production, while Argentina received the second rank with 905,605 tons in production. United States 738.770 tonnes, 701.928 tonnes Italy, Turkey 472.250 tonnes and South Africa 433.105 tonnes of pears realized production. Our country is in the 5th place in world production with 472.250 tons of pears produced in 2016 (FAO, 2016).

Pear production in Turkey's pome fruits is second ranks after apples. The reason for the fact that production is considerably low compared to apple is that there are few varieties resistant to fire blind disease (Şehirali ve Özgen, 1987).

[1]Agriculture and Forest Ministry, Ereğli District Directorate, Ereğli, Konya, TURKEY
[2]Selçuk University, Faculty of Agriculture, 42075, Konya, TURKEY
*Corresponding author: pirlak@selcuk.edu.tr

The production of Asian pears in our country is increasing in recent years. One of the important production places of Asian pears is Ereğli district of the Konya province, and new orchards are established every year in the district. The phenological development and pomological characteristics of the new varieties should be determined in order to determine suitable varieties in Ereğli district of Konya province which is one of the important pear growing areas in our country.

Material and Method

This research was carried out in the Asian Pear garden consisting of 4 year old trees cultivated commercially in the Ereğli district of Konya province in 2017-2018. The phenological and pomological characteristics of Hosiu, Kosiu, Hakko and Shinseiki varieties were investigated. Phenological characteristics (swollen bud, beginning of flowering, full bloom and harvest date) and pomological characteristics (fruit weight, fruit diameter, fruit height, stem length, shell color, fruit meat color, elasticity, fruit meat hardness, soluble solids content, pH and acidity). The measurements were made on 10 fruits. Fruit width, length and stem lengths were determined with 0.05 mm precision calipers, fruit meat hardness penetrometer, soluble solids content with hand refractometer and titratable acidity with titration.

Ereğli, which is located in the south-east of Konya Province, is hot, cold and snowy in winters and hot and dry in summers. The average annual temperature is 11.2°C, with an average annual rainfall of 332 mm. The highest temperature encountered is 40°C, while the lowest is -28.2°C. On average 10 days a year, the temperature is lower than -10°C. The number of days of frost is 90-100 days. Frost events can be seen between early Autumn (early September) and late Spring (May 15-20) (Anonymous, 2018).

In the research conducted in the garden in the first week of April, 2018, about 90% of the flowers suffered frost damage. Due to this damage, the fruitness of the Asian Pear varieties in the research in 2018 was very low.

Results and Discussion

Phenological Characteristics

Beginning of flowering started at Hosiu, Shinseiki and Hakko at the earliest on April 18, followed by Kosiu on April 19th. Full bloom was detected in Hosiu, Shinseiki and Hakko on April 23, Kosiu on April 25. On the 5th of September, Shinseiki reached the earliest harvest in the cultivars examined, and it was followed by Hakko and Hosiu on September 6th. The latest harvest was discovered on 9 September at the Kosiu variety. The period between full bloom and harvesting in 2017 was 134 days in Hosiu and Hakko, 137 days in Kosiu and 133 days in Shinseiki (Table 1).

Table 1. Phenological Observation Date in Asian Pear Varieties (2017)

VARIETIES	PHENOLOGICAL CHARACTERISTICS				
	Swollen Bud	Beginning of Flowering	Full Bloom	Harvest Date	From Full Bloom to Harvest (Day)
Hakko	02.04	18.04	23.04	06.09	134
Hosiu	02.04	18.04	23.04	06.09	134
Kosiu	04.04	19.04	25.04	09.04	137
Shinseiki	02.04	18.04	23.04	05.09	133

Due to the warm winter in 2018, early wake-ups were observed in varieties compared to 2017. In the cultivars examined, the swollen bud was found in the Hosiu variety on March 5, the Kosiu and Hakko on March 6, and the Shinseiki variety on March 7. Beginning of flowering was determined on March 23 in the Hosiu and Hakko

varieties, and March 27 in Kosiu and Shinseiki varieties. Full bloom was determined in Hosiu and Hakko on March 26, Kosiu and Shinseiki on March 29. Harvest occurred in Hakko on August 14, Hosiu and Shinseiki on August 15, Kosiu on August 16. The period between full bloom and harvest in 2018 was 141 days in Hakko, 142 days in Hosiu, 143 days in Kosiu and 142 days in Shinseiki (Table 2).

Table 2. Phenological Observation Date in Asian Pear Varieties (2018)

VARIETIES	PHENOLOGICAL CHARACTERISTICS				
	Swollen Bud	**Beginning of Flowering**	**Full Bloom**	**Harvest Date**	**From Full Bloom to Harvest (Day)**
Hakko	06.03	23.03	26.03	14.08	141
Hosiu	05.03	23.03	26.03	15.08	142
Kosiu	06.03	27.03	29.03	16.08	143
Shinseiki	07.03	27.03	29.03	15.08	142

Pomological Characteristics

The highest fruit weight was determined in Hosiu with 154.42 g in 2017 for the pear varieties examined. Shinseiki is 150.83 g and Kosiu followed this with 136.71 g. The lowest fruit weight was found in Hakko with 122.00 g.

In 2018, the highest fruit weight was determined in Shinseiki with 206.00 g. This was followed by Hosiu with 201.00 g and Hakko with 193.00 g. The lowest fruit weight was found in Kosiu with 186.60 g.

In 2017, the highest fruit size was determined in Kosiu with 62,00 mm, followed by Shinseiki with 60,95 mm and Hakko with 52,81 mm. The lowest fruit size was determined in the Shinseiki variety with 47.85 mm.

In 2018, the highest fruit size in varieties was determined in Shinseiki with 70,01 mm, followed by Hakko with 68,62 mm and Kosiu with 65,69 mm. The lowest fruit size was determined in Hosiu variety with 65,62 mm. For the year 2017, Hosiu with the largest fruit diameter of 72.00 mm, followed by Shinseiki (68,15 mm), Kosiu (60,14 mm) and Hakko (58,97 mm) respectively.

In 2018, the largest fruit diameter was observed in the Hosiu variety with a 72.78 mm, followed by Shinseiki (72,31 mm), Kosiu (70,21 mm) and Hakko (69,66 mm) respectively.

The stem length of the fruit was found at the longest Kosiu range of 3,30 cm in 2017. Followed by Shinseiki varieties with 3.20 cm and Hakko and 3.00 cm respectively. The shortest fruit stem was found in Hosiu variety with 2.80 cm.

In 2018, the longest fruit stem was found in Kosiu with 2.89 cm, followed by 2.86 cm with Hakko and 2.47 cm with Shinseiki variety. The shortest fruit stem was found in the Hosiu range with 1.86 cm.

Flesh firmness is observed in Kosiu (3.01 Ib) in 2017, followed by Shinseiki (2.96 Ib), Hakko (2.91 Ib) and Hosiu (2.80 Ib).

In 2018, flesh firmness of Shinseiki is 5.48 Ib, followed by Kosiu (3.71 Ib), Hakko (3.53 Ib) and Hosiu (3.50 Ib).

The hardness of the crustaceans was found to be 5.96 Ib in Kosiu, 5.48 Ib in Shinseiki, 5.41 Ib in Hosiu and 4.81 Ib in Hakko in 2017.
In 2018, Shinseiki is 8,06 Ib, 7,36 Ib in Kosiu, 6,18 Ib in Hakko and 4,73 Ib in Hosiu.
The fruit flesh color was found to be 104.20 in Hosiu in 2017, 103.79 in Hakko, 101.48 in Kosiu and 101.81 in Shinseiki.

In 2018, it was 105,54 in Hosiu, 101,35 in Kosiu, 99,34 in Shinseiki and 99,29 in Hakko.
The fruit shell color h * value was determined in Hakko variety with highest 94,72 in 2017 followed by Hosiu 90,27, Shinseiki 87,67 and Kosiu 84,07 respectively.
In 2018, the highest value of fruit crust h * value was found in Hakko 106,65, followed by Shinseiki 88,67, Kosiu, 85,11 and Hosiu 84,86.

The highest amount of soluble solids content was found in Hosiu variety with 14.49%, followed by Hakko with 14.41%, Hosiu with 12.43% and Shinseiki with 12.40%.
In 2018, the highest soluble solids content was 16,90%, followed by Hosiu with 15,53%, Shinseiki with 14,83% and Hakko with 11,83%.
The amount of titratable acidity of varieties was determined in Hakko with the highest rate of 5.66% in 2017, followed by Kosiu with 3.93%, Hosiu with 2.00% and Shinseiki with 1.74%.
The highest rate was determined in Kosiu by 3.74% in 2018, followed by Hakko with 2.64%, Shinseiki with 1.70% and Hosiu with 1.02%.
The fruit juice pH value was determined in the Hosiu range with the highest 5.04 in 2017. Kosiu (4,62), Shinseiki (4,58) and Hakko (4,06) were followed, respectively.
In 2018, the highest pH value was determined in the Hosiu range with 4.92. The pH values of other varieties were 4.87 in Shinseiki, 4.62 in Kosiu and 4.62 in Hakko.
Vitamin C value in fruit juice was observed in Hakko variety with the highest 0,45 mg in 2017. This was followed by Kosiu (0.43 mg), Hosiu (0.33 mg) and Shinseiki (0.30 mg), respectively.
In 2018, the highest value was found in Hosiu with 0,77 mg followed by Hakko (0,76 mg), Kosiu (0,57 mg) and Shinseiki (0,55 mg)

Table 3. Pomological Characteristics of Asian Pear Varieties

	Hosiu		**Hakko**		**Kosiu**		**Shinseiki**	
	2017	**2018**	**2017**	**2018**	**2017**	**2018**	**2017**	**2018**
Fruit Weight (g)	154,42	201,00	122,00	193,00	136,71	186,60	150,83	206,00
Fruit Diameter (mm)	72,00	72,78	58,97	69,66	60,14	70,21	68,15	72,31
Fruit Length(mm)	62,00	65,62	52,81	68,62	47,85	65,69	60,95	70,01
Fruit Flesh Color	104,20	105,54	103,79	99,29	101,47	101,35	101,80	99,34
Fruit Shell Color H	90,27	84,86	94,72	106,65	84,07	85,11	87,67	88,67
Fruit Stem Length (cm)	2,80	1,86	3,20	2,86	3,30	2,89	3,00	2,47
Hardness of the Fruit Flesh(lb)	2,80	3,50	2,91	3,53	3,02	3,71	3,16	5,48
Hardness of the Crustaceans (lb)	5,41	4,73	4,81	6,18	5,96	7,36	5,48	8,06
pH	5,04	4,92	4,06	4,62	4,62	4,62	4,58	4,87
Soluble Solids content (%)	14,93	15,53	14,41	11,83	12,43	16,90	12,40	14,83
Acidity (%)	2.00	1,02	5,66	2,64	3,93	3,74	1,74	1,70
Vitamin C (mg)	0,33	0,77	0,45	0,76	0,43	0,57	0,30	0,06

In our country, there are many studies about this kind of subjects in different regions. Different results have been obtained due to the variety of species used and the different ecological conditions used in these studies. Yarılgaç ve Yıldız (2001), as a result of their studies with local pear varieties in the Adilcevaz district, fruit weights of 89.73-368.02 g, soluble solid content is 9.80-18.00%; Edizer and Günes (1997), in Tokat province

also found that their fruit weight 54.05-197.94 g, soluble solid content 10.88% -15.44%; Ünal et al. (1997), 21.30-337.00 g fruit weight and 5.50-17.00% soluble solid content in the study conducted in the Aegean region Karadeniz and Sen (1990) reported fruit weights of 50.00-175.00 g in the study conducted with local pear varieties grown in and around Tirebolu (Karlıdağ and Eşitken, 2006). In a survey conducted in the Erciş district of Van province, the Mellaki Pear's swollen bud was determined between April 15-27. The time between full bloom and harvest date is determined between 136-145 days (Aşkın and Oğuz, 1995). In a survey of 11 local and standard pear varieties in Yalova Atatürk Horticultural Research Institute, the fruit diameter was found between 3.5 cm and 6.2 cm (Özdemir ve ark., 2016). In a survey of 22 local pear cultivars grown in the Camili region of Artvin, soluble solid content varied between 9.0-15.1% (Serdar et al., 2007). In a study conducted at pear garden in Uşak / Ulubey, titratable acidity values of the four aged Atago, Chojuro, Hosui and Kosui Asian pear varieties were determined between 0.10 g / 100 ml and 0.26 g / 100 ml between 2013 and 2014 (Ekici and Yıldırım, 2017). The fruit juice pH varied from 3.80 to 6.25 in a study of some local pear varieties with high fruit quality and high market value in Ordu province (Özkaplan, 2010).

Late spring frosts can be seen in the Ereğli District until the last week of April. The blooms in Hakko, Hosiu, Kosiu and Shinseiki varieties which are studied on the beginning of flowering started the 3rd week of April in 2017. The winter which is relatively warm in 2018 and the bloom due to the breeze were seen in the 3rd and 4th weeks of March. On the 4th and 5th day of April, the style and ovaries are frozen in 90% of the flowers with the night temperature dropping -5 0C. In this respect, there is a risk of catching up late in the first spring after warm winter months.

The harvest in 2017 was carried out on the first and second weeks of September for all four varieties. In 2018, the harvest was realized on the 2nd week of August. Hence, the harvest was one month earlier than the previous year. The first Autumn frosts in Ereğli province are generally observed in the last week of September. In this respect, it can be said that the varieties studied are very unlikely to be damaged by early autumn frosts.
As a result of the study, the phenological and pomological characteristics of Hosiu, Kosiu, Hakko and Shinseiki Asian Pears cultivated commercially in Ereğli district have been determined.
Knowing the phenological and pomological characteristics of the cultivars to be used in fruit growing and having he region to be cultivated in accordance with the climatic conditions has a vital priority in fruit growing in our country. Similar studies should be done not only on pear but also on other species.
The characteristics of Hosiu, Kosiu, Hakko and Shinseiki have been found valuable because of some properties such as early harvest, excellent taste in harvest, aroma and crispy fruit flesh. In addition that the four varieties have got more resistance to *Erwinia amylovora* and *Cacopsylla pyri* than other pear cultivars.
The varieties studied have their flowering beginnings and fruit harvest dates close to one another. All 4 types can be adversely affected by spring late frost. Eregli's climate can meet the chilling requirement of all four cultivars. warming and warming of the fruits of the Ereğli District meet the desires.
In terms of market, the stains found on Hosiu and Kosiu fruits can be misinterpreted by consumers as rust stains. For this reason, problems can be seen in marketing these two types. Hakko and Shinseiki are preferred by the consumer because they have no stain on the fruit and the fruit has a nice yellow color on the harvest. Within this scope, Hakko and Shinseiki types seem to be more fortunate in terms of marketing.

References

Akçay, M. E. ve Yücer, M. M., 2008, Armut, *İstanbul*, Hasad Yayıncılık, p.

Anonymous, 2018, https://www.mgm.gov.tr/?il=Konya&ilce=Eregli (erişim tarihi :15.07.2018),

Aşkın, M. ve Oğuz, H., 1995, Erciş'te yetiştirilen ümitvar mellaki armut tiplerinde bazı meyve ve ağaç özelliklerinin tesbiti üzerinde araştırmalar. II, *Ulusal Bahçe Bitkileri Kongresi*, 1, 84-88.

Ekici, İ. ve Yıldırım, A., 2017, Asya armut (Pyrus pyrifolia) çeşitlerinin Uşak koşullarında morfolojik, fenolojik, pomolojik ve bazı biyokimyasal özelliklerinin belirlenmesi, *Süleyman Demirel Üniversitesi Fen Bilimleri Enstitüsü Dergisi*, 21 (1), 118-124.

FAO, 2016, http://www.fao.org/faostat/en/#data/QC

Karlıdağ, H. ve Eşitken, A., 2006, Yukarı Çoruh vadisinde yetiştirilen elma ve armut çeşitlerinin bazı pomolojik özelliklerinin belirlenmesi, *Yüzüncü Yıl Üniversitesi Tarım Bilimleri Dergisi*, 16 (2), 93-96.

Özdemir, Y., Akcay, M. E., Ercisli, S., Ozkan, M. ve Ozyurt, U., 2016, Physical, chemical, sensorial and bioactive characteristics of local and standard pear cultivars in Turkey, *Acta Sci. Pol. Hortorum Cultus*, 15 (3), 127-139.

Serdar, Ü., Ersoy, B., Öztürk, A. ve Demirsoy, H., 2007, Saklı Cennet Camili'de Yetiştirilen Yerel Elma Çeşitleri, *Türkiye V. Ulusal Bahçe Bitkileri Kongresi*, 1, 575-579.

Şehirali, S. ve Özgen, M., 1987, Bitki genetik kaynakları, *Ankara Üniv. Ziraat Fak. Yayınları* (1020).

International Conference on Science and Technology

ICONST 2018

5-9 September 2018 Prizren - KOSOVO

Bryophytes and Heavy Metals

Özlem Tonguç Yayıntaş[1]*

Abstract: Environmental pollution is increasing day by day, posing a very serious problem for the flora and fauna. A large number of pollutants including heavy metals are adversely affecting our environment. Heavy metals are emitted from solid fuel combustion, vehicular emissions and in industrial processes. Bryophytes are widely used as bio-indicators for their unique and very specific responses. Some bryophyte species are extremely sensitive to pollutants and exhibit visible injury symptoms even in the presence of very minute quantities of pollutants.

Keywords: Bryophytes, heavy metals, pollution, environment.

Introduction

Since the last fifty years, countries have become more interested in pollution problems. Environmental contamination by toxic metals is a serious problem due to their incremental accumulation in the food chain and continued persistence in the ecosystem.

There are many pollutants in the air such as sulfur oxides (SOx), nitrogen oxides (NOx), carbon monoxide (CO), ozone (O3), different types of particles, heavy metals and various types of volatile organic compounds. Heavy metals are discharged in small quantities into environment through numerous industrial activities. Such as chromium, copper, lead, nickel in wastewater are hazardous to the environment and health. The primary source of air pollution is the consumption of fossil fuels to produce energy, various industrial operations and transportation activities.

The first studies on the use of mosses to measure atmospheric accumulation date back to the late 1960s. In the studies conducted by Rühling and Tyler, *Hypnum cupressiforme* samples obtained from the south of Sweden were found to have significantly higher concentrations of metals than those obtained from the north west of the same country. Ruhling and Tyler explained this difference with the presence of large industrial areas in Europe (Ruhling and Tyler, 1968) and since then, mosses are simple, inexpensive, and are widely used in biosensing studies because of the advantage that most species of mosses can be used for this purpose.

In recent years, many European countries have been monitoring their heavy metal accumulation at regular intervals using monitoring techniques with their mosses (Stamenov et al., 2002). In addition, these pollution studies are carried out not only in the densely populated urban areas and industrial zones, but also in the transport of these pollutants passing through the national borders (Herpin et al., 1996) In our country, the mosses are used for the determination of the accumulation of heavy metals of atmospheric origin and especially for the detection of heavy metals pollution in industrially oriented regions and on busy roadside.

It is possible for the mosses to live and reproduce in a high rate and in a short time, their ability to accumulate metals, in city centers and industrial areas. They can also be cultured under controlled conditions (Manning et al., 1986). Due to these properties, they can be used regularly in the monitoring of metal accumulation in large

[1]Canakkale Onsekiz Mart University, Canakkale School of Applied Science,
Fisheries Technology, 17100, Canakkale, TURKEY
*Correspondingauthor: ozlemyayintas@hotmail.com

areas. By analyzing certain elements from these plants, the level of contamination can be revealed and new zoning areas are opened in cities according to these biological maps.

Literature Knowledge

Bryophytes also help cover the forest floor and tree trunks and protect moisture. Many mosses provide a perfect seed bed environment for the diversification of tree species. Therefore, bryophytes play an important role in the renewal and protection of forests. The minerals supplied from rain water are filtered and kept by bryophytes covering the surface. Routine monitoring of certain mosses in polluted areas indicates that they are resistant to air pollution. The frequencies of these types of mosses in these places are regularly investigated and calculated by IAP (Atmospheric Cleaning Index). In addition, mosses can be stored for chemical analysis without deteriorating for years (Saxena, 2004; Glime, 2007). As a result of the rapid and efficient nutrient uptake of bryophytes, they usually contain metal and metal-like elements, such as those required only in trace amounts (eg, Cu, Fe, Mn, Zn), which do not require elements such as (Cd, Cr, Hg). They often accumulate elements such as, Ni, Pb, Se, Ti, V… and so on. Some of these elements they accumulate in their bodies are taken from the environment in which they are found, and others are taken from the particles transported to the environment by the wind and rain.

Air pollution greatly affects mineral concentration in mosses. Absorption efficiency of mosses for heavy metals; It is affected by the ratio of free cation exchange regions, the form of accumulation of heavy metals, solid and liquid state, ion exchange reactions (Poikolainen, 2004). In addition, minerals and heavy metals and other cations compete for the same cation exchange regions. In addition to storage and common ion exchange processes, the concentration of minerals in the mosses, the processes in the cycle of natural elements, climatic conditions, mineral composition and water of the soil, height, types of mosses, biomass of mosses are also influenced by factors such as (Ross, 1990; Ford et al., 1995; Steinnes, 1995; Reimann, 2001). The mosses have more functions than the rainforest in the atmospheric carbon cycle. It is estimated that the amount of carbon they catch throughout the year is almost equal to the amount of atmospheric carbon (Clymo, 1998).

In the literature, there are several studies on the determination of heavy metals that are collected from mosses. Galsomies et al. (2003) analyzed the *Hypnum cupressiforme*, *Pleurozium schreberi* and *Scleropodium purum* species in France for 36 elements using neutron activation analysis (INAA) and induction-matched plasma ve mass spectrometry (ICP-MS). The concentrations of Al, Co, Cs, Fe, K, Mg, Na, Rb and Ti as determined in *Scleropodium purum* were found to be 1.6-3.3 times higher than those determined in *Hypnum cupressiforme*. However, the highest concentrations were determined in *Hypnum cupressiforme* for chlorine and nickel. Research in northern European countries is carried out every 5 years to determine the temporal or spatial changes of atmospheric accumulation, and these studies extend to other parts of Europe. *Hylocomium splendens* is a type of moss routinely used in Scandinavia (Poikolainen, 2004). This is preferred because of the fact that the growth rate of the species of moss is easily recognized and widespread in Scandinavia. In the study using the species of *Fabriona ciliaris* and *Leskea angustata* moss in Mexico, the sequence of metal concentrations was Zn> Pb> Cr> Cd.

In a study aimed to determine the heavy metal accumulation in some mosses in the vicinity of thermal power plants in Muğla region, 12 types of mosses collected from the vicinity of Yatağan, Yeniköy and Kemerköy thermal power plants were analyzed for Cd, Pb, Cu, Ni and Zn in autumn and spring periods and and it showed a significant change compared to the seasons (Tonguc, 1998). Accordingly, pollution values in mosses are not only dependent on species selection. Many other conditions, such as the sampling period or sampling method, vary the propensity of the mosses to accumulate. According to the results obtained from *Hypnum cupressiforme* samples in Karabuk region in three months' period, it was seen that when the order of pollutant elements was made in order of magnitude, the relation was Fe> Al> Mn> Pb> Zn> As> Cu> Ni> Cr> Co> Cd. As a result of the study, it was found that the most important source of heavy metal contamination in the region was KARDEMİR. In addition, the wet and dry deposition rates for each metal were evaluated and it was observed that the accumulation of the elements other than Mn and Zn in wet samples was more than the accumulation in dry samples (Uğuz, 2007).

Another study was carried out in an annual period between October 2008 and October 2009 with the aim of investigating the levels of heavy metal accumulation formed in the vicinity of the Sakarya province industrial zone and in the city center through a biomonitor moss (*Hypnum cupressiforme* Hedw.) and soil samples. The method of wet burning method was applied for the moss and superficial soil samples and the atmospheric heavy metal accumulation values in the working time were measured by ICP-OES or ICP-MS. According to the results of the analysis, the amount of the pollution-causing elements in the soil Al> Fe> Mn> Cr> V> Ni> Zn> Cu> Pb> Co> As> Sn> Mo> Cd, the amount of moss on the accumulation of the elements of the amount of moss It was found that Al> Fe> Mn> Zn> Cu> Pb> V> Ni> Cr> Co> As> Sn> Mo> Cd. When these two sequences were compared, it was found that the lowest accumulation values of Al, Fe and Mn were found to belong to Co, As, Sn, Mo and Cd, respectively, in terms of the elements that showed the highest accumulation in both surface soil and moss (Yücel, 2010).

Results

Mosses have several advantages as a bio-indicator of heavy metal pollution:

Mosses species have a wide distribution; they grow in urban, industrial and unpolluted areas (Figure 1); they uptake nutrients from precipitation; accumulate nutrients and pollutants by passive transport and metal concentrations in the mosses tissues reflects the atmospheric deposition.

Figure 1. https://archaeologynewsnetwork.blogspot.com

Some bryophyte species are extremely sensitive to pollutants and exhibit visible injury symptoms even in the presence of very minute quantities of pollutants. Such species serve as good bio-indicators and act as a **"warning giver"** regarding the effect on the solubility of the environment (Figure 2 and 3).

Figure 2. https://tr.pinterest.com

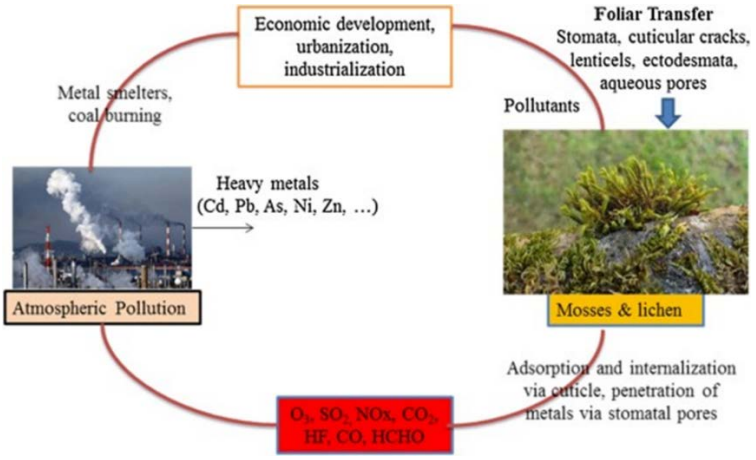

Figure 3. Foliar heavy metal uptake by mosses and lichen (Shahid et al.,2016).

Bryophytes are known as efficient accumulator of heavy metals because of their following properties:

- They lack true root system and depend largely on atmospheric deposition for their requirements of mineral elements (Figure 4).
- They usually lack continuous cuticle layer and thus their tissues are easily permeable to water and minerals, including the gaseous pollutants in the atmosphere and the metal ions.

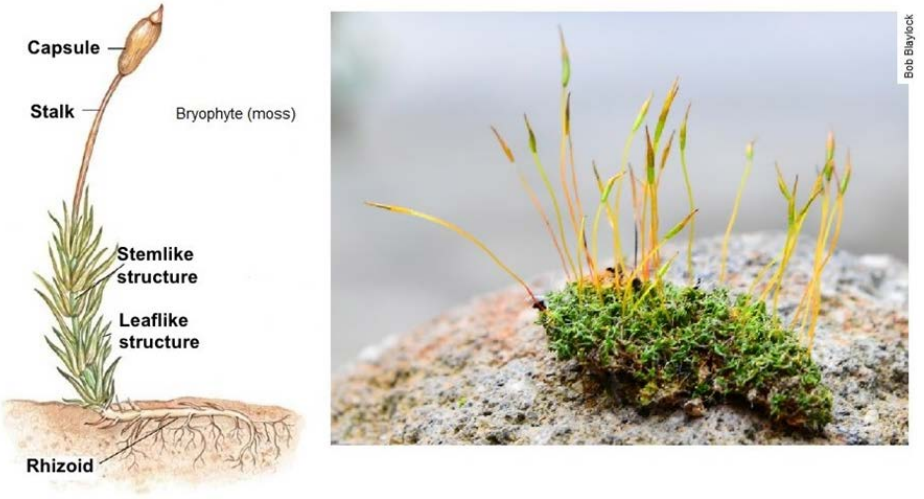

Figure 4. Mosses

- Their tissues have numerous negatively charged groups and act as an efficient cation exchanger. Their cell walls possess high exchange capacity and even their dead tissues have capacity to bind ions.
- They generally obtain mineral nutrition from wet and dry deposition of particles and soluble salts. However, in certain bryophytes, uptake of metals from substrate occurs, mainly with rising capillary water. Such bryophyte species are less suitable for the monitoring of heavy metals (Figure 5).

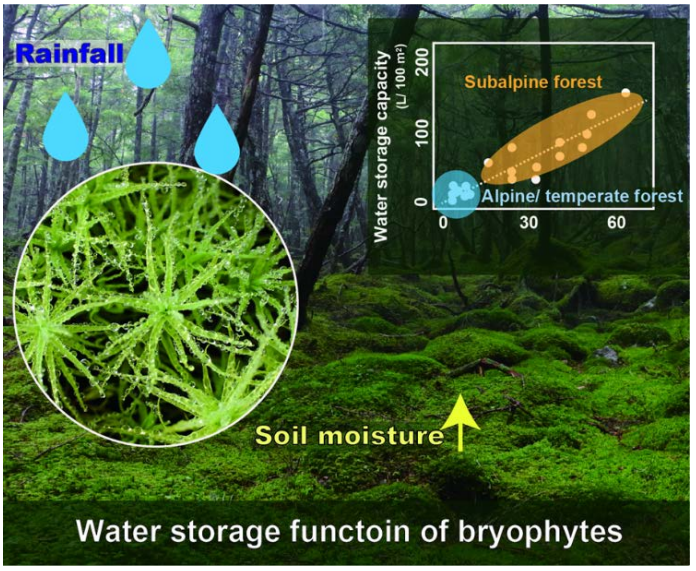

Figure 5. Water storage (Oishi, 2018).

Heavy metals are known to interfere with chlorophyll synthesis either through the direct inhibition of an enzymatic step or through the induced deficiency of an essential nutrient. Chlorophyll degradation can occur when heavy metals enter the photobiont cells (Figure 6a, b). The decline in total chlorophyll content in all the investigated bryophytes under heavy metal stress could be a result of the heavy metal interference with chlorophyll synthesis either through the direct inhibition of an enzymatic step or by inducing the deficiency of an essential nutrient (Zengin and Munzuroglu 2005). The differences in the reduction of chlorophyll content under various heavy metals could be explained by the different uptake and action mechanisms for these metals (Bruns et al. 2001; Shakya et al; Stanković, 2018).

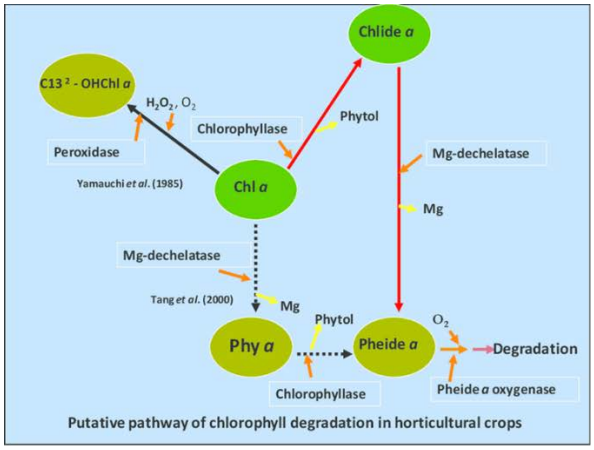

Figure 6a. Prasajith Kapila Dissanayake, 2012.

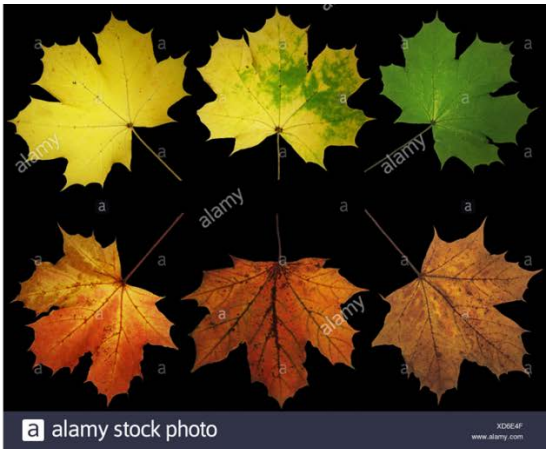

Figure 6b. https://www.alamy.com

Tolerance of bryophytes to pollution

Some bryophytes are metal tolerant and are able to withstand levels of heavy metals that are toxic to other species. *Marchantia polymorpha*, *Solenostoma crenulata*, *Ceratodon purpureus* and *Funaria hygrometrica* are some of the metal tolerant populations (Figure 7a, b, c).

Figure 7a, Marchantia polymorpha

Figure 7b. Funaria hygrometrica

Figure 7c. Ceratodon purpureus

Bryophytes have been used as a **bryometer** to assess the air quality. Thus, bryophytes are being used for air quality monitoring in various countries (Figure 8).

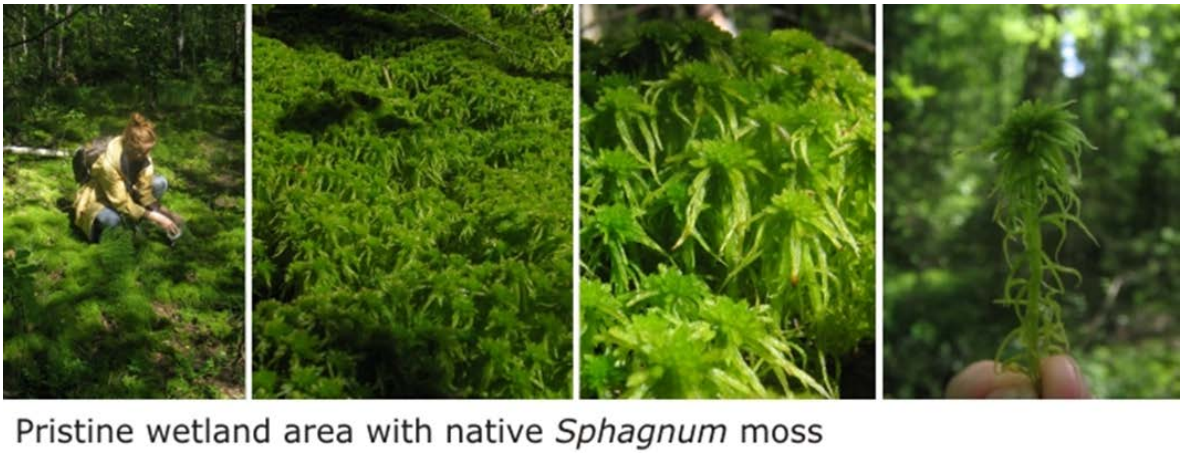

Figure 8. *Sphagnum sp*.moss

Although, heavy metals are predominantly bound extracellularly to cation-exchange sites on the cell wall. Monitoring of heavy metals through bryophytes is not only cost-effective, but it also provides efficient way to assess the qualitative and quantitative differences in metal concentrations at distinct locations and on local and landscape scales (Figure 9).

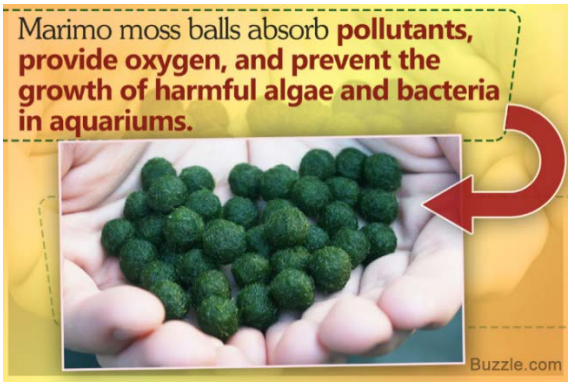

Figure 9. https://www.lelong.com.my/marimo-moss-ball-m-aquarium-aquascape-plant-paludarium-aquacult

References

Bruns, I., Sutter, K., Menge, S., Neumann, D., Krauss, G. J. (2001). Cadmium lets increase the glutathione pool in bryophytes. Journal of Plant Physiology 158, 79-89.

Clymo, S, Turunen, J., Tolonen, K. (1998) Carbon Accumulation in Peatland R. Oikos Vol. 81:2, 368-388.

Ford, J., E. Crecelius, B. Lasorsa, S. Allen-Gil, J. Martinson, and D. Landers (1995). Inorganic contaminants in Arctic Alaskan ecosystems: long range atmospheric transport or local point sources? Sci. Tot. Environ. 160/161: 323-335.

Galsomies, L., Ayrault, S., Carrot, F., Deschamps, C., Letrouit Galinou, M.A. (2003). Interspecies Calibration in Mosses at Regional Scale-Heavy Metal and Trace Elements Results from Ilede-France, Atmospheric Environment, 37, 241-251.

Glime M.J. (2007) Bryophyte Ecology. Sponsored by MTU, BSA and IAB. Published online at. http://www.bryoecol.mtu.edu/.

Herpin, U., Berlekamp, J., Markert, B., Wolterbeek, B., Grodzinska, K., Siewers, U., Lieth, H. and Weckert, V. (1996). The distribution of heavy metals in a transect of the three states the Netherlands, Germany and Poland, determined with the aid of moss monitoring, The Science of the Total Environment, Vol. 187, pp. 185198.

Macedo Miranda G, Avila Pérez, P., Gil Vargas P., Zarazúa G., Sánchez Meza, J.C, Zepeda Gómez, C.and. Tejeda, S. (2016). Accumulation of heavy metals in mosses: a biomonitoring study, SpringerPlus 5:715, DOI 10.1186/s40064-016-2524-7.

Manning, W.J. and Feder, W.A. (1980). Biomonitoring air pollutants with plants, Applied Science Publishers Ltd., Ripple Road, Barking, Essex, England, ISNB: 085334-916-9.

Muhammad Shahid, Camille Dumat, Sana Khalid, Eva Schreck, Tiantian Xiong, et al. (2016). Foliar heavy metal uptake, toxicity and detoxification in plants: A comparison of foliar and root metal uptake. Journal of Hazardous Materials, Elsevier, Vol. 325, 36-58.

Oishi, Y. (2018). Evaluation of the Water-Storage Capacity of Bryophytes along an Altitudinal Gradient from Temperate Forests to the Alpine Zone. Forests, 9, 433.

Poikolainen, J., Kubin, E., Piispanen, J. and Karhu, J. (2004) Atmospheric heavy metal deposition in Finland during 1985–2000 using mosses as bioindicators. The Science of the Total Environment, Vol. 318, 171–185.

Reimann C, Niskavaara H, Kashulina G, Filzmoser P, Boyd R, Volden T, Tomilina O and Bogatyrev I (2001) Critical remarks on the use of terrestrial moss (Hylocomium splendens and Pleurozium schreberi) for monitoring of airborne pollution, Environ. Pollut., 113: 41-57.

Ross, H.B. (1990). On the use of mosses (Hylocomium splendens and Pleurozium schreberi) for estimating atmospheric trace metal deposition. Water, Air, Soil Poll., 50: 63-76.

Rühling, Å., Tyler, G. (1968). An ecological approach to the lead problem. Botaniska Notiser, Vol. 122, 248-342.

Saxena, D.K. (2004). Harinder Uses of bryophytes. Resonance, 9:56–65.

Shakya, K., Chettri, M. K., Sawidis, T. (2008). Impact of heavy metals (copper, zinc, and lead) on the chlorophyll content of some mosses. Archives of Environmental Contamination and Toxicology 54, 412-421.

Stamenov, J., Iobchev, M., Vachev, B., Gueleva, E., Frontasyeva, M.V., Pavlov, S.S., Strelkova, L.P., Yurukova, L., Ganeva, A., Mıtrıkov, M., Antonov, A., Varbanov, Z., Batov, I., Damov, K. and Marınova, E. Investigation of Air Pollution in Bulgaria by Moss Biomonıtoring Technique Employing Neutron Activatıon Analysis (Moss Survey 2000-2002).

Stanković J. D., Sabovljević A. D., Sabovljević M. S. (2018). Bryophytes and heavy metals: a review. Acta Bot Croat, DOI: 10.2478/botcro--0014

Steinnes, E. 1995. A critical evaluation of the use of naturally growing moss to monitor the deposition of atmospheric metals, The Science of the Total Environment 160/161, 243-249.

Tonguç, Ö. (1998). Determination of Heavy Metal Levels in Some Moss Species Around Thermic Power Stations'', Turkish Journal of Biology, 22, 171-180 (1998).

Uğuz, U. (2007). Karabük Demir-Çelik İşletmeleri (Kardemir)' in Çevrede Oluşturduğu Ağır Metal Birikiminin Biyomonitör olan Karayosunları (Mosses) Üzerinden Araştırılması. Zonguldak Karaelmas Üniversitesi Fen Bilimleri Enstitüsü Biyoloji Anabilim Dalı, Yüksek Lisans Tezi, Zonguldak.

Yücel, D. (2010). Sakarya İli sanayi bölgesinin yakın çevresinde ve şehir merkezinde oluşturduğu atmosferik ağır metal birikim seviyelerinin bir biyomonitör karayosunu (Hypnum cupressiforme Hedw.) ve toprak örnekleri üzerinden araştırılması. Zonguldak Karaelmas Üniversitesi Fen Bilimleri Enstitüsü Biyoloji Anabilim Dalı, Yüksek Lisans Tezi, Zonguldak.

Zengin, F. K., Munzuroglu, O. (2005). Effects of some heavy metals on content of chlorophyll, proline and some antioxidant chemicals in bean (Phaseolus vulgaris L.) seedlings. Acta Biologica Cracoviensia Series Botanica 47, 157-164

International Conference on Science and Technology

ICONST 2018

5-9 September 2018 Prizren - KOSOVO

Volatile Components of *Sideritis congesta* P.H. Davis & Hub. - Mor. Grown in Kütahya Gediz Province (Turkey)

Hüseyin Fakir[1]*, Sabri Erbaş[2]

Abstract: The Sideritis genus has more than 150 species which are distributed in tropical and mild regions of the Northern Hemisphere. The genus Sideritis (Lamiaceae) is represented by 46 species and altogether 55 taxa, of 41 are endemic to Turkey. Sideritis species are used as antiinflammatory, antimicrobial, antioxidant, antirheumatic, antispasmodics, antiulcer sedative, antitussive, stomach, cytotoxic and analgesic, in the treatment of coughs due to colds and for curing gastrointestinal disorders in different countries including Turkey. Sideritis species are widely known as "mountain tea" in Anatolia and consumed as herbal tea. Sideritis congesta P.H. Davis & Hub.-Mor. is called "başak çayı" by local people. In this study, it was aimed to determination to volatile components of S. congesta which are endemic species from in Turkey. Plant material of S. congesta was collected from Kütahya Gediz in Turkey. In this study that was conducted in 2018 vegetation period, the volatile components of the leaves and flowers in the flowering period for S. congesta, were determined by gas chromatography mass spectroscopy (GC-MS) by using headspace solid phase microextraction (HS-SPME) with carboxen/polydimethylsiloxane (CAR/PDMS) fiber. 39 different volatile components were identified in S. congesta. The major volatile components of was α-pinene as 33.41 %. The other important volatile components were identified such as β-pinene 21.87%, trans-caryophyllene 12.15% and limonene 9.25%.

Keywords: *Sideritis congesta*, Lamiaceae, Volatile components, α-pinene, β-pinene, Kütahya, Turkey.

Introduction

The genus Sideritis species which are an important species of Lamiaceae family, are represented by approximately 150 taxon species and 54 species and sub-species, 41 of which are endemic grown in the Mediterranean region (Davis, 1975, Aytaç and Aksoy, 2000, Barber et al., 2002). Sideritis species are annual or perennial aromatic herbs. The mountain tea species (Sideritis spp.) are not cultivated in our country. Sideritis congesta et Huber-Morath is endemic to Turkey and located in natural flora of our country. Most types of the endemic mountain tea species, especially the S. congesta, collected from Turkey's natural flora as a result of uncontrolled, intensive, continuous and unconscious and its populations is decreasing (Bilginoğlu and Kan, 2017). S. congesta is known as "başak çayı" with local names in Turkey and it is used as an antispasmodic, anti-inflammatory, analgesic, anti-depressants, digestive, antiulcer, diuretic, antioxidant, stomach pain, throat inflammation, neural appeaser and cold (Öztürk et al., 1996, Baytop, 1999, Küpeli et al., 2007, Charami et al., 2008, Fakir, 2009, Erkan et al., 2011). Plant material of S. congesta was collected from Kütahya Gediz in Turkey. In this study the floral scent compositions of the leaves and flowers in the flowering period for S. congesta, were determined by head space solid phase microextraction gas chromatography mass spectroscopy (HS-SPME-GC-MS).

[1]Isparta University of Applied Sciences, Faculty of Forestry, Department of Forest Engineering, 32260, Isparta/Turkey
[2]Isparta University of Applied Sciences, Faculty of Agriculture Sciences and Technology, 32260 Isparta/Turkey
*Corresponding author: huseyinfakir@isparta.edu.tr

Material and Methods

HS-SPME-GC-MS analysis

Plant material of S. congesta was collected from Kütahya Gediz in Turkey. In this study that was conducted in 2018 vegetation period. The leaves and flowers S. congesta were subjected to solid phase microextraction (SPME, Supelco, Germany) with a fibre precoated with a 75 µm-thick layer of Carboxen/Polydimethylsiloxane (CAR/PDMS). 2.5 g of plant samples was put into a 10 mL vial, which was then immediately sealed with a silicone septum and a crimp cap. After incubation for 30 min at 60ºC, SPME fibre was pushed through the headspace of a sample vial to adsorbed the volatiles, and then inserted directly into the injection port of the GC-MS (Shimadzu 2010 Plus GC-MS with the capillary column, Restek Rxi®-5Sil MS 30 m x 0.25 mm, 0.25 µm) at a temperature of 250°C for desorption (5 min) of the adsorbed volatile compounds for analysis. Identification of constituents was carried out with the help of retention times of standard substances by composition of mass spectra with the data given in the Wiley, NIST Tutor, FFNSC library. LRIs (Linear Retention Indices) were calculated by using a series of the standards of C7-C30 saturated n-alkanes (Sigma-Aldrich Chemical Co., USA) for reference in the same column and conditions as described above for GC-MS analysis.

Results and Discussion

By analysis, 39 volatile component of S. congesta were determined and all results were given in Table 1. The major volatile components of was α-pinene as 33.41 %. The other important volatile components were identified such as β-pinene 21.87%, trans-caryophyllene 12.15% and limonene 9.25%. The most abundant compounds in the volatile component were Aromatic alcohols (3.13%), monoterpene hydrocarbons (77.00%), oxygenated monoterpenes (4.73%), benzenoid compounds (0.14%), sesquiterpenes hydrocarbons (14.29%), bicyclic monoterpenes (0.22%), respectively.

Table 1. The results of HS-SPME-GC-MS in leaves and flower of *S. congesta*

RT (min)	Compounds	Formula	Class	Ratio (%)
2.230	3-Methylbutanal	$C_5H_{10}O$	AA	0.46
2.319	2-Methylbutanal	$C_5H_{10}O$	AA	0.30
2.513	1-Pentene-3-ol	$C_5H_{10}O$	AA	0.44
2.679	Pentanal	$C_5H_{10}O$	AA	1.07
4.601	Hexanal	$C_6H_{12}O$	AA	0.67
6.095	2-Hexenal	$C_6H_{12}O$	AA	0.19
8.503	α-Thujene	$C_{10}H_{16}$	MH	2.57
8.772	α-Pinene	$C_{10}H_{16}$	MH	33.41
9.320	Camphene	$C_{10}H_{16}$	MH	0.33
9.479	Verbenene	$C_{10}H_{14}$	MH	0.21
10.224	Sabinene	$C_{10}H_{16}$	MH	2.86
10.389	β-Pinene	$C_{10}H_{16}$	MH	21.87
10.910	β-Myrcene	$C_{10}H_{16}$	MH	2.09
11.494	α-Phellandrene	$C_{10}H_{16}$	MH	0.58
11.589	δ-3-Carene	$C_{10}H_{16}$	MH	0.95
11.921	α-Terpinene	$C_{10}H_{16}$	MH	0.18
12.212	p-Cymene	$C_{10}H_{14}$	MH	1.45
12.400	Limonene	$C_{10}H_{16}$	MH	9.25
12.500	Eucalyptol	$C_{10}H_{18}O$	OM	1.23
12.713	*cis*-Ocimene	$C_{10}H_{16}$	MH	0.88
13.120	β-OCIMENE	$C_{10}H_{16}$	MH	0.12
13.540	γ-Terpineol	$C_{10}H_{18}O$	OM	0.30
14.019	3,5-Octadien-2-one	$C_8H_{12}O$	BC	0.14
14.603	α-Terpinolene	$C_{10}H_{16}$	MH	0.25
15.217	Linalool	$C_{10}H_{18}O$	OM	0.39

16.189	α-Campholene aldehyde	$C_{10}H_{16}O$	OM	0.28
17.544	Pinocarvone	$C_5H_{10}O$	OH	0.33
18.813	Myrtenal	$C_{10}H_{14}O$	OM	0.27
19.281	Berbenone	$C_{10}H_{14}O$	OM	0.26
20.900	Linalyl acetate	$C_{12}H_{20}O$	OM	1.46
22.127	Bornyl acetate	$C_{12}H_{20}O$	OM	0.21
25.344	α-Copaene	$C_{15}H_{24}$	SH	0.36
25.620	β-Bourbonene	$C_{15}H_{24}$	SH	0.21
25.800	Nepetalactone	$C_{10}H_{14}O_2$	BM	0.22
26.845	*trans*-Caryophyllene	$C_{15}H_{24}$	SH	12.15
27.935	β-Farnesene	$C_{15}H_{24}$	SH	0.20
28.007	α-Humulene	$C_{15}H_{24}$	SH	0.23
28.849	Germacrene-D	$C_{15}H_{24}$	SH	0.65
29.328	β-Cyclo germacrene	$C_{15}H_{24}$	SH	0.49
Total				**99.51**

Aromatic alcohols (AA): 3.13%
Monoterpene hydrocarbons (MH): 77.00%
Oxygenated monoterpenes (OM): 4.73%
Benzenoid compounds (BC): 0.14%
Sesquiterpenes hydrocarbons (SH): 14.29%
Bicyclic monoterpenes (BM): 0.22%

In the literature, there were reports on the components of S. congesta (Kırımer et al., 2001, Kırımer et al., 2004, Bilginoğlu ve Kan, 2017). The essential oil of S. congesta was analyzed, and β-Pinene (34.6 %), α-Pinene (24.6 %) and epi-cubebol (7.1 %) were identified as the major components of the sample from Antalya: Alanya, Sapadere, Beldibi-Başköy (Kırımer et al., 2001). β-Pinene (23-36 %), α-Pinene (12-30 %) and epi-cubebol (4-7 %) were reported as the main constituents in the volatile oil (0.4 -0.85%, v/w) of S. congesta (Kırımer et al., 2004). In another study, β-Pinene (48.3 %), α-Pinene (33.7 %) and linalool (3.72 %) were found as most abundant compounds in the essential oil (0.26 %, v/w) of S. congesta from Turkey (Bilginoğlu ve Kan, 2017). Results were compared with the other studies which were put forwarded by same species in other regions of Turkey. There are small differences between chemical components of essential oils of S. congesta collected from mediterranean and middle Anatolian regions in Turkey which may be due to differences in geographical locations, climatic conditions and kind of soils.

References

Aytaç, Z., & Aksoy, A. 2000. A new Sideritis species (Labiatae) from Turkey. Flora Medit, 10:181-184.

Barber, J.C., Francisco-Ortega, J., Santos-Guerra, A., Turner, K.G., & Jansen, R.K. 2002. Origin of Macaronesian Sideritis L. (Lamioideae: Lamiaceae) inferred from nuclear and chloroplast sequence datasets. Molecular Phylogenetics and Evolution, 23(3):293-306.

Baytop, T. 1999. Therapy with medicinal plants in Turkey (Past and Present). Nobel Tıp Kitapevi, Istanbul, p. 193.

Bilginoğlu, E. & Kan, Y. 2017. The Investigation on Drug Yield and Some Quality Characteristics of Mountain Tea (Sideritis congesta) Cultivated in Turkey, Int. J. Sec. Metabolite, 4(3):264-269.

Davis, P.H. 1975. Flora of Turkey and The East Aegean Islands, Vol. 10, Univ. Press, Edinburgh.

Fakir, H., Korkmaz, M. & Güller, B. 2009. Medicinal Plant Diversity of Western Mediterrenean Region in Turkey, Journal of Applied Biological Sciences, 3(2):30-40.

Kırımer, N., Tabanca, N., Baser, K.H.C. & Tümen, G. 2001. Composition of the Essential Oil of Sideritis congesta P.H.Davis et Hub.-Mor., Journal of Essential Oil Research, 13(2):132-133.

Kırımer, N., Baser, K.H.C., Demirci, B. & Duman, H. 2004. Essential Oils of Sideritis Species of Turkey, Belonging to the Section Empedoclia, Chemistry of Natural Compounds, 40(1):19-23.

Kupeli, E., Sahin, P.F., Calış, I., Yeşilada, E., & Ezer, N. 2007. Phenolic compounds of Sideritis ozturkii and their in vivo anti-inflammatory and anticiceptive activites, J. Ethnopharmacol. 112:356-360.

M. Charami, Lazari, D., Karioti, Skaltsa, H., Hadjipavlou-Litina, C. & Souleles, C. 2008. Antioxidant and anti-inflammatory activities of Sideritis perfoliata subsp. perfoliata (Lamiaceae), Phytother. Res. 22:450-454.

Erkan, N., Cetin, H. & Ayranci, A. 2011. Antioxidant activities of Sideritis congesta Davis et Huber-Morath and Sideritis arguta Boiss et Heldr: Identification of free flavonoids and cinnamic acid derivatives, Food Res. Int., 44:297-303.

Öztürk, Y., Aydin, S., Öztürk, N., & Başer, K.H.C. 1996. Effects of extracts from certain Sideritis species on swimming performance in mice. Phytotherapy Research, 10(1):70-73.

International Conference on Science and Technology

ICONST 2018

5-9 September 2018 Prizren - KOSOVO

Muscling Traits Affecting Meat Quality in Extensively Reared Sheep in Turkey

Sinan Ogun [1]*, Onur Yilmaz[2]

Abstract: The present study aimed to identify muscle characteristics affecting meat quality in Akkaraman and Dorper sheep breeds reared in extensive production systems in Turkey. Animal material for the study consisted of 68 male lambs Akkaraman (32) and Dorper (36) in three and six month age groups raised solely on pasture after weaning. Muscle area in 3 and 6 month old lambs were 13.55 and 15.88 cm^2, respectively, while muscle depth for the same ages were 3.81 and 4.10 cm, respectively. Akkaraman lambs showed slight superiority in terms of muscle area, muscle depth and muscle width in *Musculus longissimus dorsi* (MLD) samples in 3 month age groups. However growth over a 6 month period was significantly more productive for the Dorper lambs. MLD values obtained in the present study were lower than those of earlier studies mainly due to the sole pasture based extensive production system of this study. However when compared to other supplementary fed semi-intensive systems the results showed a significantly productivity increase for the present study's grazing groups. The study indicated that in the extensive production system used whilst it was profitable to maintain the Dorper breed for the 6 months and less so for the Akkaraman. In terms of backfat thickness (BFT) values, the Dorper breed has a much leaner carcass than the Akkaraman breed. The effects of breeds and muscle types on cooking loss and slice shear force were significant ($P < 0.01$). The cooking loss values obtained were within the expected limits. The highest shear force value in the studied muscle regions was obtained in *Musculus semitendinosus* (MST), indicating that MLD was more tender than MST, yet both findings were well within the consumer preference norms for lamb meat in Turkey. Results from the present work provided insight into the variation of muscling traits affecting meat quality and productivity in feding periods in two potential lamb meat breeds in Turkey. The positive findings can be used to develop strategies to increase lamb meat consumption and improve profitability.

Keywords: Meat quality, FCR, MLD, MST, Dorper, Akkaraman

Introduction

Meeting the food needs of a rapidly growing world population sustainably is a major problem for the globes farmers. Red meat from small ruminants are a main contributor to the protein needs of a healthy human diet. Turkey's sheep production, which also has an important historical background, is generally based on extensive conditions. Meat production is the most important source of income for the sheep industry throughout Turkey as it is in the world (De Rancourt et al., 2006; Montossi et al., 2013; Gürsoy, 2006). There are various factors affecting quality and quantity of lamb meat production, which plays an important role in supplying animal protein needs (Karaca et al. 1999; Sanudo et al., 1998; Priola et al. 2001; Zygoyiannis, 2006). These factors can be classified as genetic and/or environmental, such as; breed, sex, climate, slaughter procedure and hygiene (Sanudo et al., 1998; Priola et al. 2001, Chestnutt, 1994). Meat structure, biochemical changes in muscle occurring before and after slaughtering, technological and organoleptic properties of meat are influenced by these factors (Hopkins and Fogarty, 1998; Beriain et al. 2000). Lamb meat is the preferred red meat option in most parts of Turkey, and is also the main source of income rather

[1]Rural Revival Research Ltd. - Istanbul, TURKEY
[2]Adnan Menderes University, Faculty of Agriculture, Department of Animal Science, Biometry & Genetics Unit. Aydin, TURKEY
*Corresponding author: sinansotheremail@gmail.com

than wool or milk for the country's sheep industry. Therefore, there is a need to obtain further data to identify and improve the meat production ability of sheep breeds in both qualitative and quantitative terms. *Musculus longissimus dorsi* (MLD) and *Musculus semitendinosus* (MST) are important indicator muscles for determining the valuable meat content of the lamb carcass (Dransfield and Jones, 1981; Wood, 1995; Biatek et al., 2018). One of the breeds was Akkaraman, the most commonly used breed in Turkey for lamb production, with a population of around 16,000,000 it makes up more than 50% of the national sheep herd (TUIK, 2018). The other breed used for the study was Dorper, a recently introduced exotic breed to improve the productivity of the country's lamb industry (Ocak et al., 2016; Yilmaz et al, 2016). With this comparison the study wanted to also ascertain whether poor genetics were a factor in the industrys decline over the recent decades. The study hoped that the information obtained from these muscle characteristics at different age groups of the lambs would provide significant contributions to breeders in terms of economic fattening time. The results showed important characteristics of MLD and MST in the Akkaraman and Dorper male lambs in both the three and six month age groups raised solely on pasture. Some additional economic parameters associated with fattening periods were also tested and provided significant findings related to productivity.

Material and Method

Animal material for the study consisted of 68 male lambs in three and six month age groups raised in extensive condition belonging to Akkaraman and Dorper sheep breeds (Table 1).

Table 1. Animal material

Breeds	3 months of age	6 months of age	Total
Akkaraman	16	16	32
Dorper	18	18	36
Total	34	34	68

Animals were all weaned at 30 days after being gradually introduced to pasture. Post weaning 16 of each breed were slaughtered at 90 days and 18 of each breed was slaughtered at 180 days of age. Lambs were transported to the abbattoir one day prior to slaughter and rested in a paddock to avoid transport stress affecting carcass quality. Prior to slaughter lambs were placed on a 12 h fast with free access to water after which they were weighed, recorded and humanely slaughtered under veterinary supervision. M. longissimus dorsi (MLD) and M. semitendinosus (MST) samples were taken from the left side of each carcass (Figure 1).

Figure 1. Sampling location of Musculus longissimus dorsi (MLD) and Musculus semitendinosus (MST) muscle

Section taken from the 12th and 13th rib area of the *M. longissimus dorsi* (MLD) was drawn on parchment paper and back fat thickness (BF), muscle depth (MD), muscle width (MW), muscle area (MA) were measured with planimeter (USHIKATA X-PLAN 380 DIII, Japan) (Figure 2).

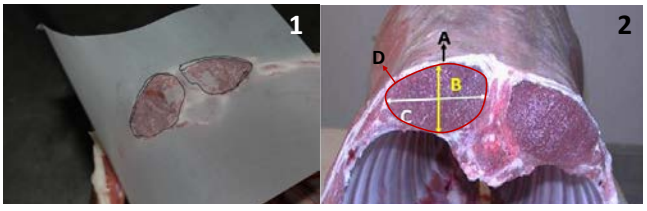

Figure 2. Drawings of MLD muscle (1) and measurement points (2)

(**A:** Backfat thickness, **B:** muscle depth, **C:** muscle width, **D:** muscle area)

Instrumental meat quality characteristics investigated in the study were; cooking loss (%) and Warner Bratzler shear force (kg/cm^2). Other parameters measured were; hot carcass weight and slaughter weight. Cost comparisons were made with ADG of the same age between the breeds to evaluate economical net margins which the authors termed Feed Expense Efficiency (FEE). This was calculated by initially estimating the average daily feed cost (FE_{pd}) then multiplied by 1000/ADG (g).
Formula for feed expense efficiency

$$FEE = FE_{pd} x \frac{1000\ (g/LW)}{ADG\ (g)}$$

Where

FEE	=	Feed Expense Efficiency	FE_{pd}	=	Feed Expense per day
LW	=	Live weight	ADG	=	Average daily gain

The UNIVARIATE procedure of SAS (1999) statistical package program was used to check normality of the data. The result of this analysis showed that the data for all the measured characteristics were normally distributed. Afterwards, all characteristics investigated were analysed using the Generalized Linear Models (GLM) procedure of SAS (1999) software. The mathematical model used for the least-squares analysis was as follows,
Model for muscle properties of animals,

$$\mathcal{Y}_{ijk} = \mu + \alpha_i + b_j + \beta_1\left(X_{ij} - \bar{X}\right) + e_{ijk}$$

Model for hot carcass weight of animals,

$$\mathcal{Y}_{ijk} = \mu + \alpha_i + b_j + \beta_2\left(A_{ij} - \bar{A}\right) + e_{ijk}$$

Y_{ijk}	=	Observations for muscle traits	a_i	=	Fixed effect of breeds (*i*=Akkaraman and Dorper)
μ	=	Overall mean of the trait	b_j	=	Fixed effect of birth type (j= Singleton, twin)
X_{ij}	=	Hot carcass weight of animals	β_1	=	Regression coefficient of hot carcass weight
$\bar{X}$	=	Mean hot carcass weight of animals	β_2	=	Regression coefficient of salughter weight
A_{ij}	=	Slaughter weight of animals	$\bar{A}$	=	Mean slaughter weight of animals
e_{ijk}	=	Random errors with the assumption of N (0, σ^2)			

The phenotypic correlations between variables were also obtained using the PROC CORR procedures in SAS (1999).

Results

The least squares mean and standard errors for MLD properties in two different age groups are given in Table 2.

Table 2. Least square means and standard errors belong to MLD properties in two different age groups

Factors	3-Months Age						6-Months Age					
	N	MA (cm^2)	MD (cm)	MW (cm)	BFT (mm)	HCW	N	MA (cm^2)	MD (cm)	MW (cm)	BFT (mm)	HCW
Breeds		P=0.342	P=0.917	P=0.879	P=0.000	P=0.000		P=0.031	P=0.817	P=0.165	P=0.000	P=0.000
Akkaraman	16	13.83±0.376	3.82±0.177	4.77±0.134	2.24±0.117	9.79±0.142	16	17.63±0.955	4.04±0.316	5.78±0.353	2.50±0.182	19.81±0.171
Dorper	18	13.27±0.290	3.80±0.137	4.74±0.104	0.59±0.09	11.67±0.119	18	14.14±0.823	4.16±0.273	4.97±0.304	0.83±0.157	22.44±0.16
Birth type		P=0.716	P=0.318	P=0.483	P=0.639	P=0.183		P=0.335	P=0.314	P=0.942	P=0.037	P=0.326
Singleton	24	13.62±0.184	3.90±0.087	4.81±0.066	1.38±0.057	10.86±0.095	27	16.33±0.396	4.25±0.131	5.39±0.147	1.86±0.076	21±0.108
Twin	10	13.48±0.315	3.72±0.149	4.71±0.112	1.44±0.098	10.60±0.157	7	15.43±0.814	3.94±0.270	5.36±0.301	1.47±0.155	21.26±0.228
Reg Linear		P=0.000	P=0.007	P=0.002	P=0.001			P=0.000	P=0.175	P=0.021	P=0.002	
HCW		1.320±0.153	0.208±0.072	0.186±0.055	0.168±0.048			1.773±0.379	0.174±0.126	0.342±0.14	0.241±0.072	
						P=0.000						P=0.000
SW						0.436±0.038						0.486±0.059
Overall	34	13.55±0.173	3.81±0.082	4.76±0.062	1.41±0.054	10.73±0.088	34	15.88±0.446	4.10±0.148	5.38±0.165	1.66±0.085	21.13±0.121

MA: Muscle area, MD: Muscle depth. MW: Muscle width. BFT: Back fat thickness, HCW: Hot carcass weight, SW: Slaughter weight

Muscle area in 3 and 6 months of ages were 13.55 and 15.88 respectively, while muscle depth for the same ages were 3.81 and 4.10, respectively. Results of the analysis carried out on MLD did not show a significant difference between breeds for the 3 month age group, however showed significance for the for MA in the 6 months of age. There were highly significant differences (P<0.001) in BFT and HCW (P<0.01) between the breeds in both age groups. The coefficients of regression of hot carcass weight on all the muscle characteristics were also seen to be significant in both age groups, except musle depth determined only in 6 months of age. Akkaraman lambs showed slight superiority in terms of muscle area, muscle depth and muscle width in MLD samples in both 3 and 6-month age groups. Birth type was not statistically significant on the muscle characteristics studied in both age groups (P>0.05). The least squares mean and standart errors for shear force and cooking loss according to age groups are given in Table 3.

Table 3. Least squares mean and standard errors for cooking loss and shear force, according to different age groups

Factors	3-Months Age				6-Months Age			
	N	CL (%)	N	SSF (kg)	N	CL (%)	N	SSF (kg)
Breed		P=0.021		P=0.000		P=0.000	N	P=0.017
Akkaraman	31	41.91±0.264	29	4.40±0.291	32	43.32±0.315	32	5.08±0.381
Dorper	37	41.06±0.242	36	5.94±0.261	35	40.95±0.302	33	6.39±0.375
Muscle Type		P=0.000		P=0.000		P=0.000		P=0.000
MLD	33	39.69±0.257	33	3.66±0.273	33	40.85±0.311	33	4.37±0.375
MST	35	43.28±0.249	32	6.68±0.279	34	43.43±0.307	32	7.11±0.381
Overall	68	41.48±0.179	65	5.17±0.195	67	42.14±0.218	65	5.74±0.267

CL: Cooking loss, SSF: Slice shear force

The effect of breed and muscle type on cooking loss and slice shear force were significant (P <0.01). The cooking loss values obtained were within the expected limits. The highest shear force value in the studied muscle regions was obtained in Musculus Semitendinosus. The phenotypic correlation coefficients between slaughter weight, hot carcass weight and muscle characteristics are given in Table 4.

Table 4. Phenotypic correlation coefficients between slaughter weight, hot carcass weight and *Musculus longissimus dorsi* properties

Breed	Age		SW	HCW	MA	MD	MW
Akkaraman	3 Months	HCW	0.937^{***}				
		MA	0.923^{***}	0.890^{***}			
		MD	0.609^{*}	0.641^{**}	0.554^{*}		
		MW	0.621^{**}	0.648^{**}	0.729^{**}	0.517^{*}	
		BFT	0.714^{**}	0.670^{**}	0.713^{**}	0.330^{ns}	0.545^{*}
	6 Months	HCW	0.839^{***}				
		MA	0.787^{***}	0.551^{*}			
		MD	0.251^{ns}	0.097^{ns}	0.367^{ns}		
		MW	0.549^{*}	0.441^{ns}	0.571^{*}	-0.191^{ns}	
		BFT	0.681^{**}	0.434^{ns}	0.677^{**}	0.171^{ns}	0.583^{*}
Dorper	3	HCW	0.920^{***}				
		MA	0.946^{***}	0.877^{***}			
		MD	0.553^{*}	0.542^{*}	0.554^{*}		
		MW	0.585^{*}	0.604^{**}	0.646^{**}	0.285^{ns}	
		BFT	0.647^{**}	0.510^{*}	0.569^{*}	0.493^{*}	0.355^{ns}
	6	HCW	0.854^{***}				
		MA	0.919^{***}	0.825^{***}			
		MD	0.544^{*}	0.404^{ns}	0.675^{**}		
		MW	0.525^{*}	0.443^{ns}	0.507^{*}	-0.175^{ns}	
		BFT	0.617^{**}	0.695^{**}	0.552^{*}	0.452^{ns}	0.156^{ns}

MA: Muscle area. MD: Muscle depth. MW: Muscle width. BFT: Back fat thickness. Hot carcass weight. SW: Slaughter weight. *:P<0.05. **: P<0.01. ***:P<0.001, ns: non-significant

Correlation between SW, HCW and MLD properties showed expected significance for the 3 month age groups but for Akkaraman this diminished at the 6 month age while Dorper maintained a good correlation between the properties into the latter growth and development stage. In other words the results showed that while there was significantly productive growth and development in the Dorper breed between 3 to 6 months, the difference in the rate of growth and development for Akkaraman didin't really justify basis for aging the Akkaraman an additional 3 month from a profitability standpoint when Tables 5 and 6 are taken into account. Comparison between the 2 breeds for slaughter weight (SW) and average daily gain (ADG) according to age groups are given in Table 5.

Table 5. Breed and age comparison for slaughter weight and average daily gain

Breeds	Variable	Age	N	$\bar{X} \pm S_{\bar{X}}$	CV(%)	Min	Max
Akkaraman	SW	3-Months Age	16	19.89±1.86	9.34	16.62	22.49
		6-Months Age	16	39.19±1.53	3.90	36.49	41.47
	ADG	3-Months Age	16	186.73±18.78	10.06	157.88	215.76
		6-Months Age	16	198.25±7.72	3.90	180.82	207.83
Dorper	SW	3-Months Age	18	23.01±2.71	11.78	19.05	27.15
		6-Months Age	18	41.54±1.96	4.72	38.75	46.25
	ADG	3-Months Age	18	221.58±24.91	11.24	183.52	256.18
		6-Months Age	18	210.06±7.56	3.60	198.89	225.95

SW: slaughter weight, ADG: average daily gain, CV: variation coefficient

The lambs were slaughtered at 90 and 180 days of age. Whilst the initial Birth Weights (BW) of all lambs were similar (mean 3.65 kg.), Dorper lambs had the heaviest Slaughter Weights (SW) for both 30 days and 60 days - mean 23.1 kg. and 41.5 kg respectively, Akkaraman mean SW's for the two age groups were 19.9 kg. and 39.2 kg. Average Daily Gain (ADG) for 3 and 6 month age Dorper lambs were 221.6 g. and 210 g. while Akkaraman displayed gains of 186.7 g. and 198.3 g, respectively.

To show efficiency and productivity of weight gain as related to feed, the authors applied their devised formula to feed conversion ratio which they termed Feed Expense Efficiency (FEE). The animals daily weight gain is calculated according to the cost of producing that feed. Theis cost was calculated by estimating the establishment and maintenance cost of the 6ha. of irrigated pasture and the 12 ha. of non irrigated native pasture paddocks used for the study, including cost of labour (shepherd, farmer etc.), watering, fertilising, fencing and all ancillarries. The feed expence efficiency for both breeds and their respective ages are given in Table 5

Table 6. Feed Expense Efficiency

Factors	Akkaraman		Dorper		Factors	3-Months Age		6-Months Age	
	N	FEE ($/kg)	N	FEE ($/kg)	Breeds	N	FEE ($/kg)	N	FEE ($/kg)
Ages	P=0.023		P=0.130			P=0.000		P=0.000	
3-Months Age	16	0.49±0.009	18	0.41±0.008	Akkraman	16	0.49±0.012	16	0.46±0.004
6-Months Age	16	0.45±0.009	18	0.43±0.008	Dorper	18	0.41±0.011	18	0.43±0.004
Mean	32	0.47±0.007	36	0.42±0.006	Mean	34	0.45±0.008	34	0.44±0.003

FEE: feed expense efficiency

Discussion and Conclusion

Results indicated that MLD was more tender than MST in the two breeds yet both findings were well within the consumer preference norms for lamb meat in Turkey. Whilst MLD analysis for tenderness showed that the Akkaraman breed had more tender meat, the Dorper breed maintained leaner meat characteristics. In terms of BFT values, the Dorper had a much leaner carcass than the Akkaraman breed. The thin layer of backfat in Dorper lambs made this breed superior in terms of carcass quality. This suggested that the recently introduced Dorper into the Turkish national sheep herd had significant potential for lean lamb production which is becoming a growing consumer preference in Turkey. MLD values obtained in the present study

were lower than those of earlier studies. However those studies had included supplementary feed into the lambs diet. When comparared with the present study, which only utilised pasture as feed, the differentiation in weight gain were significantly productive for the grazing groups, this was in keeping with results of Ocak et al., 2016. This was particularly seen for Dorper breed where efficiencies of feed conversion in relation to cost were significantly higher than those of Akkaraman. The highest phenotypic correlation coefficients were obtained between slaughter weight, fat thickness and muscle area. With regards to muscle development per age and breed, the MLD values obtained in the present study were lower than those of earlier studies, due more than likely to the sole pasture based diet. The phenotypic correlation results also showed that while there was significant productive growth and development for the additional 3 month of feeding for the Dorper, the Akkaraman didin't really show a significant benefit from a profitability factor. This was apparent both for slaughter and hot carcass weight as well as muscle development.

As lambs are often slaughtered between 3-6 months in Turkey the productivity and cost efficiency of growth and development during this period whilst maintaining meat quality are important factors for the estute producer. Taking into account these factors together with the leaner carcass the results of this study has shown the Dorper breed as a more efficient feed convertor and more profitable breed for the suggested rearing periods.

Acknowledgements

Authors would like to express their gratitude to Red Rock Agricultural for the use of their facilities and the animal material and Agricultural Biotechnology and Food Safety Application and Research Centre (ADÜ-TARBİYOMER) of Adnan Menderes University for providing laboratory facilities to carry out meat quality analysis.

References

Beriain, M.J., Purroy, A., Treacher, T., Bas, P. (2000). Effect of animal and nutritional factors and nutrition on lamb meat quality. In Sheep and goat nutrition: Intake, digestion, quality of products and rangelands (ed Ledin I and Morand-Fehr P), pp. 75-86. Zaragoza, Spain.

Biatek, M., Czauderna, M., Biatek, A. (2018). Partial replacement of rapeseed oil with fish oil, and dietary antioxidants supplementation affects concentrations of biohydrogenation products and conjugated fatty acids in rumen and selected lamb tissues. Animal Feed Science and Technology, 241, 63-74.

Chestnutt, D.M.B., 1994. Effect of lamb growth rate and growth pattern on carcass fat levels. . Animal Production 58, 77-85.

De Rancourt, M., Fois, N., Lavín, M. P., Tchakérian, E., Vallerand, F. (2006). Mediterranean sheep and goats production: An uncertain future. Small Ruminant Research, 62(3), 167-179.

Dransfield, E., Jones, R.C. (1981). Relationship between tenderness of three beef muscles. Journal of the Science of Food and Agriculture, 32(3), 300-304.

Gürsoy, O. (2006). Economics and profitability of sheep and goat production in Turkey under new support regimes and market conditions. Small Ruminant Research, 62(3), 181-191.

Hopkins, D.L., Fogarty, N.M. (1998). Diverse lamb genotypes—2. Meat pH, colour and tenderness. Meat Science, 49(4), 477-488.

Karaca, O., Yıkılmaz, H., Cemal, İ., Atay, O. (1999). Çine Tipi ve Menemen x Çine Tipi (F1) melezi kuzuların kimi gelişme özellikleri. Uluslararası Hayvancılık'99 Kongresi, 21-24 Eylül 1999, Ege Üniversitesi Ziraat Fakültesi, Bornova, İzmir, Turkey, 776-770.

Montossi, F., Fonti Furnols, M., del Campo, M., San Julián, R., Brito, G., Sañudo, C. (2013). Sustainable sheep production and consumer preference trends: Compatibilities, contradictions, and unresolved dilemmas. Meat Science, 95, 772–789.

Ocak, S., Ogun, S., Yilmaz, O. (2016). Dorper sheep utilizing feed resources efficiently: a Mediterranean case study. Revista Brasileira de Zootecnia, 45(8), 489-498

Priolo, A., Micol, D., Agabriel, J. (2001). Effects of grass feeding systems on ruminant meat colour and flavour. A review. Animal Research, 50(3), 185-200.

Sanudo, C., Campo, M. M., Sierra, I., María, G. A., Olleta, J. L., Santolaria, P. (1997). Breed effect on carcase and meat quality of suckling lambs. Meat Science, 46(4), 357-365.

SAS, 1999. The SAS System. Version 8. Copyright (c) 1999 by SAS Institute Inc., Cary, NC, USA.

TUİK (2018) Türkiye İstatistik Kurumu Hayvancılık istatistikleri http://tuikapp.tuik.gov.tr. (Access date: 06.08.2018).

Wood, J.D. (1995). The influence of carcass composition on meat quality. Quality and grading of carcasses of meat animals, 131-155.

Yılmaz, O., Ocak, S., Ogun, S. (2016). Ultrasonic carcass assessment of Dorper and Dorper x Merino lambs using MLD and body measurements. Turkish Journal of Agriculture- Food Science and Technology, 4(5),395-400.

Zygoyiannis, D. (2006). Sheep production in the world and in Greece. Small Ruminant Research, 62(1-2), 143-147.

International Conference on Science and Technology

ICONST 2018

5-9 September 2018 Prizren - KOSOVO

Photoelectric Effect and Solar Cells Technology

Vehebi Sofiu[1]

Abstract: The sun is an inexhaustible source of renewable energy which has enough potential for fulfillment of all humanity needs using modern technology in compliance with contemporary standards for the economic environment, the social and social to nature. In the photoelectric effect, electrons are emitted from solids, liquids or gases when they absorb light energy. Photoelectric effect requires photons with energy of 1eV up to the higher elements 1 MeV in the periodic system. During normal conditions, on the surface can be achieved the radiation intensity of 1.0 kW/m², and the true value of intensity depends on location where the system is installed, on geographic location, season of the year, sunny weather, whether it is cloudy or rainy. Photovoltaic Solar Panel with great absorbing force, during all radiation times with the type of solar panels of 320W, provides the highest efficiency performance seemingly exploiting 96 feedback contacts of solar cells. The highest amount of energy that the absorber of collector receives from the Sun is when the collector is at right angle to the sun's rays. It is important to note that the angle of collector compared with the horizontal plane cannot be less than 20° because there is a possibility that the collector due to the small slope to be covered with filth and rain water cannot purify it.

Keywords: cells technology, structure of photons, density of radiation, fusion of solar energy.

Introduction

Due to the constant climate changes and the taking of preventive measures against CO_2 emissions, the global demand for sustainable development has been launched. Photovoltaic renewable energy requirements from solar energy - have become one of the most popular phenomena in contemporary technology. Nowadays, the solar technology has been found to be applicable in all industries, including households and residential economies, by meeting one of the standards under the European Directive 20 + 20 + 20. Solar cells are mainly made from silica of crystals. Sunlight in the cell has effects on the p-n passageway conductivity when exposed to light at a frequency of about 10^{15} Hz creating a intersection in the flow process between the silicon cell lines of the modules installed on the solar panels. The word "Spectrum" means that we have many frequencies of light ranging from blue to ultraviolet and in the other direction from red to infrared. However, the group flow of light rays into an improvised glass surface shows that the blue color has evident reflexes with radiant lines fracture, while the red light has a breakdown of the leakage stream group. The highest amount of energy transferred from electricity to a single cell (single node intersection) is 33%. The efficiency of solar radiation is being made possible by the impurity of materials and the persistence of technologies for eliminating of these absorbent barriers in order to generate the generation security in the system. The absorbent material of light is a semiconductor material, the main part of the solar cell, which is used to absorb solar light. And as mentioned earlier - the most common material for solar cells is silicon, mainly because it is one of the most abundant minerals on Earth. The absorbed light results in the creation of charged

[1]University for Business adn Technology, Prishtinë, Kosovo
Email: Vehebi.sofiu@ubt-uni.net

carriers, which are moved to contacts later, in order to achieve the efficiency with the high effectiveness of transforming solar energy into electricity. Solar light drainage layers have a purpose to reduce light reflections from the front of the cell or, in other words, to increase the transmission through the solar cell surface and to reduce the light output from the cell within the system. Special layers called – Coating against reflection (the most common is silicon nitride (SiN), which causes the solar cells to appear bluish). The load division (p-n intersection) has an integrated voltage that is a force for the electrons transferred by the solar light in order to be transferred to contacts. There are several variations of the contact structure used in photovoltaic. Most of the silicon solar cells have a contact structure that can be called the standard used for the same operating system conditions, so due to this reason, the device optimization should also be carried out. Tile covers are not recommended to be metal because they have low radiation and absorb all light, so that the lumps do not work in optimal mode*(metsolar.eu/, 2018).*

1. Photoelectric Effect

Photo (light) + electric
If a photon hits an atom of a certain material, it may be absorbed by an electron of that material. However, if the photon has enough energy, the electron is ejected, or emitted, from the atom. In this way, light energy changes into electrical energy figure 1. Why is the photoelectric effect so important?
It helped explain the particle nature of light.
It is the basis of the quantum theory.
It is used in photocells e.g. in solar calculators, alarms, automatic garage door openers, flash of a camera*(okorder solar, 2018).*

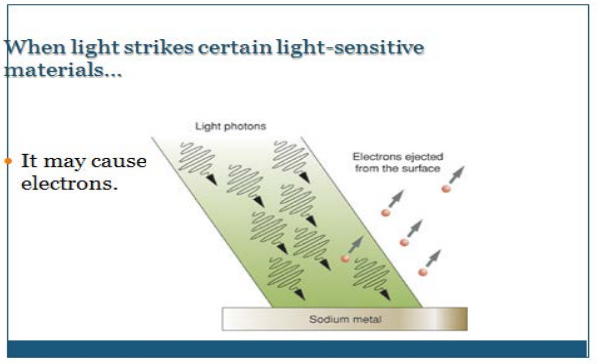

Figure 1: Sunlight materials convert to the energy

2. Solar cells technology

Solar cells are totally simply semiconductors with the halved capacity for absorbing the rays of light in order to convert at a fraction of its energy, photons that are absorbed in the transformed electrical current converted in semi-conductors diode with electrons in the form of holes preferentially in a certain direction, so that solar cells are simply a semi-conductors diode that absorb sunlight and the same directly in efficient electric energy from the sun.

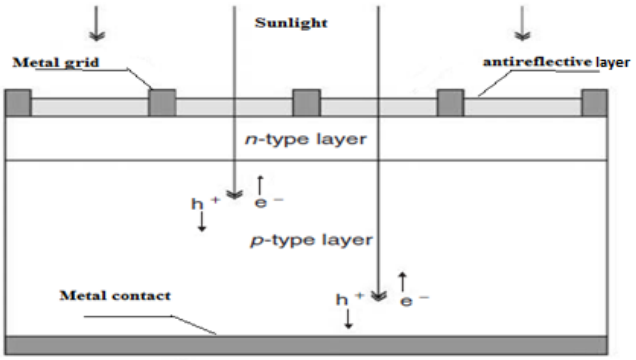

Figure 2: The rays of the sun radiation electron-hole.
Source: Boer. K, 1990

A simple structure of conventional solar cell is presented in Figure 1, e^- and h^+ e described in the front of the solar cell.

In a conventional solar cell, the doping of the front side emitter is a trade-off between series resistance and efficiency: a lighter doped front side emitter would improve the quantum fficiency and reduce the emitter saturation current density, but it would increase the series resistance of the cell *(Markvart. T & Gastaner. L, 2003).*

Radioactive isotopes are used as fuel in nuclear power plants that are formed in profusion electrons. All electromagnetic rays, including sunlight, can carry special amount of energy particles called photons whose wavelength is shown by their source wave-wave λ, being associated with photon energy E where,

$E=hc/\lambda = h\nu$

$\Delta E = E_2 - E_1 = h\gamma$ (1) $\Gamma = {}^1/T$

h - is constant basis
c - is the speed of light and
ν – frequency,

Einstein's formula relates to the maximum kinetic energy (K max) of photo electrons to the absorbed photon frequency (f) and the frequency threshold (fo) to the surface of photo emissions, as shown in Figure 3. However approximate formulas are necessary for Compton Effect *(Orhana. N, 1986).*

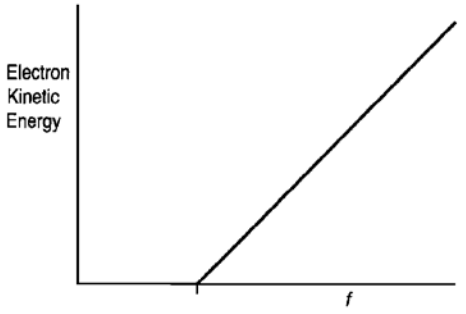

Figure 3: The kinetic energy of electrons with light intensity.
Source: Orhana.N, 1986

The minimum energy required to release the photoelectron from the panel surface is called the work function, Kmax, of the solar panel.

$$Kmax = h (f - f_o) \quad (2)$$

Or if we prefer the absorbed energy of photons on the surface of solar panels (E) and the work function(φ) then appear:

$$Kmax = E - \varphi \quad (3)$$

E- is the energy of the absorbed photons,
λ- is the wavelength,
f- is the length of rays,

$$E = hf = hc \quad (4)$$

Maximum kinetic energy (Kmax) of photo electrons can be determined by stopping potential (V_O).
$Vo = W = Kmax$, so $Kmax = eV_O$ (5)

Eq = Energy will be calculated in Joule . When the basic load, energy is will be calculated in electron volts (eV).
Degree (n/t) in which are presented photo electrons are emitted from a picture surface of photo emission that can be determined by placing the photoelectric effect (I).

$$I = q = n = NE \quad (6)$$

so that the Planck't constatnt is:
$h = 6{,}625 \times 10^{-34}$ Js = $4{,}14 \times 10^{-15}$ eV s (7)
$HC = 1{,}99 \times 10^{-25}$ J m = 1.240 nm eV.

3. Photosynthesis and photovoltaic solar energy

Much of the chemical energy produced by life forms, such as cases of burning fossils is derived from the use of solar energy through photosynthesis. Solar energy is produced by thermonuclear fusion process in the core of the Sun. Radioactive isotopes used as fuel in nuclear power plants. Food supernova is a type of fuel for which humans and animals need. Solar Energy supports almost all life organisms on earth through the photosynthesis process since the first appearance of the organisms when people use solar energy for lighting, warmth, and growth of crops and the conversion of the radiation of the sun into electricity.

Heat produced by sunlight determines climate and changing of seasons on earth. Solar cells are semiconductor materials that convert sunlight directly into electricity *(Energy and Climate Change, Professional Development Workshop Materials, 2006–2007).*

4. Measuring the radiation of the sun based on corners of sun-earth

Passing the rays of the sun in empty space does not change the density of the spread radiant spectrum in relation to the square of the distance from the source of the solar radiation by the formula:

$$E_o = (R_S^2/D^2) E_S \quad (8)$$

Where:

E_S - is the energy density on the surface of the Sun, which is set to black body radiation according to Stefan-Boltzmann's law (6.3×10^6 W/m^2),

R_S - is the radius of the Sun (6, 96 ·10^8 m), and
D - is the distance where is the estimated density of radiation from the Sun. For different planets now we can calculate the density of the radiation system according to Table 1 *(H. Dieter Zeh, 2007).*

Table 1: Constant solar radiation by planets

Planet	Distance(x109m)	Solar constant(W/m^2)
Mercury	57	9228
Venus	108	2586
Mars	150	1367
Jupiter	227	586
Saturn	778	50
Uron	1426	15
Neptun	2868	4
Pluton	4497	2

Extraterrestrial radiation is a radiation shown in the upper surface of the soil in the limits of the atmosphere. The distance of the Earth from the Sun varies over the years and extraterrestrial radiation varies from a minimum value of 1321 W/m^2 to 1412 W/m^2 greater, while the standardized constants of sun radiation is I_0 = 1367 W/m^2 *(Dan Chiras & Robert Aram & Kurt Nelson, 2009).*

The perpendicular solar radiation of the extraterrestrial surface calculated for a day of the year is determined by expression:

$$I_{0j}(j) = \varepsilon(j) \cdot I_0 = \left(1 + 0{,}03344\ cos\left(\frac{2\pi j}{3\cos 65{,}25} - 0{,}048869\right)\right) I_0 \qquad (9)$$

I_0 – is the sun constant,
ε (j) irregular rotation in the orbit of the Earth,
j- ordinal number of days (j= 1,2,3,4,5,.....365*) (The Sun As A Source of Energy, 2011").*

Solar radiation in the horizontal plane can be calculated from the extraterrestial surface of the perpendicular sun radiation towards the direction of the earth:

$$I_{oh} = I_0 \varepsilon\ cos\zeta_s \left[\frac{W^2}{m}\right] \qquad (10)$$

A general case for a time interval from ω_1 to ω_2:

$$G_{0(12)} = I_0 \varepsilon \frac{T}{2\pi}\left[\sin\emptyset\ sin\delta(\omega_2 - \omega_1) + \ cos\emptyset\ cos\delta(sin\omega_2 - sin\omega_1)[J/m^2]\right] \qquad (11)$$

-The values in each hour, | ω_2 - ω_1 | = π / 2 me ζS> 0 during the hours:

$$G_{0h} = I_0 \varepsilon \frac{T}{2\pi}[\sin\emptyset \sin\delta \frac{\pi}{2} + cos\emptyset cos\delta(sin\omega_2 - sin\omega_1)][J/m^2] \qquad (12)$$

-Daily value, $\omega_1 = \omega S$, $\omega_2 = \omega S$:

$$G_{0h} = I_0 \varepsilon \frac{T}{2\pi} cos\emptyset cos\delta(sin\omega_{s\_} - \omega_s sin\omega_s)[J/m^2] \qquad (13)$$

Parameter T equation (13) is the duration of the Earth's rotation around its own axis, T = 86400 s (24 h). When irradiation values are used the symbol $\dot{G}_{o(12)}$ replaces G_{0h} to indicate average values *(Irradiation Calculations, Sections; Solar Photovoltaics, 2012).*

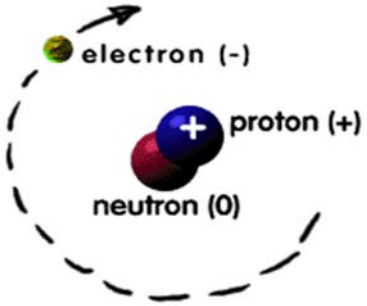

Figure 4: Fusion of structure of the atom in the form of nucleons
Source: J. Guitton, 1991

Our understanding of electrical current must begin with the nature of matter. All molecules are made up of atoms, which are themselves made up of electrons, protons, and neutrons (Basic Electrisity, 2014).

The main components of atoms are protons, neutrons and electrons. The atom is the basic unit of construction of the case, and is the smallest unit of matter that has characteristics typical of chemical elements. There are three main components of atoms: protons, neutrons and electrons. Protons are positively charged particles located in the nucleus with neutrons that are the same size as protons. The thing that makes each of those elements different is the number of electrons, protons, and neutrons (Andrew. R, 2014).

Distribution of the sun radiation is studied in Germany in 1890 by Wilhelm Wien, the idea of the study was that every ray of the sunlight that enters in a small hole is scattered in a wavelength intervals of time with maximum shifts when the temperature is increased in wavelengths by February, as shown in Diagram 1

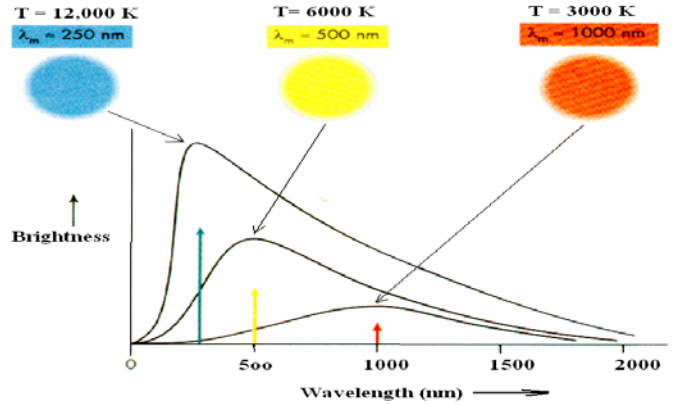

Diagram 1: Wavelength of the sun's radiation in time intervals.
Source: Author, 2012 + Institute of the USA, 2012

Wien's law for high frequencies says that when the temperature is raised to maximum by sunlight it is expressed in quantitative form of normal observations of displaced objects.
Such objects emit infrared rays with T = 950 K with a slight sheen which is not noticed and the color of lighting is orange when the temperature is raised. Bulbs with thin wire is T = 2500 K that emits bright light but the culmination of the spectrum is colored infrared according to Wien's law. Point shifts of yellow colours are more visible when is T = 6000 K on the sun's surface, and all these features are synthesized by physicist Max Planck that otherwise is called the Planck's curves. Electrically charged particles in

proportion, according to the force load (electrostatic) which was appointed by French physicist Charles Augustin (1736 - 1806.), who first discovered that the force is proportional to their size and inversely proportional to the square of the distance among them:

$$F = k\frac{Q_1 \cdot Q_2}{r^2} \qquad (14)$$

where (Q1 and Q2 are proportion, r distance, k is a constant in a vacuum, which is one). According to the unit of Coulomb (C) and electrically charged loads, where C is defined as the amount of charge that passes through the section cut to a second current constant of one ampere (C = A s). Load power is a major force in describing the interaction between the proton and the electron. Each electron has a negative charge e- = 1,6 10 protons and the electrons are drawn by a force load (Teacher's Reference Handbook, 2014).

5. Sunlight energy in the form of fusion

In reality, the sun is in the form of nuclear energy that is formed through the fusion of hydrogen atoms, so in this case the fused energy after this process is passing into helium.
The material used for solar collectors is often dangerous for personnel who work with them because they contain arsenic and cadmium. The sun is very hot indeed, but all kinds of heating, even light coming from the sun as a result of a fusion of the sun occurs in the depth of core of the sun. The core of the sun extends outward toward the centre about 0.2 solar radiuses as shown in Figure 6. Solar energy is a form of energy which is formed through nuclear fusion of hydrogen atoms, and the energy which goes during that process in helium with 600 million tons of hydrogen are converted into helium. This fusion reaction releases a large amount of heat energy which is largely free and unexploited.

The mass of a body is a measure for its energy content, therefore, the total energy content of a particle at rest with mass m is:

$$E = mc2 \qquad (15)$$

E – Energy,
m – Mass,
c – Speed of light in a vacuum (3 108 m/s).

Solar energy is inexhaustible source of energy production. Today is mostly used for heating the water because it is more efficient and cheaper. Based on the Earth's surface (510.1 106 km2) we can conclude that we are dealing with large amounts of solar energy (about 109 TWh/year) *(Brandt. S, 2008).*

Conclusions

The conversion of the sun's rays is mainly performed through two systems that are used as:
- the passive system being used as a medium for air circulation or warm fluids,
- the active system being used by collector technology connected to the pumping system or photovoltaic cells as a sunlight energy converter.

The base condition for solar collectors is the effective and efficient absorption of sun's rays through high suction collectors (black collectors) or concentric collectors with the help of mirrors or lenses that increase the radiant power.
Convergence mirrors are also a kind of concentric collectors that allow the increase of the efficiency of the radiant power including the types of colors in order to collect the temperatures even in those places where the temperatures are low.
The concentrating efficiency of the collector depends on the absorption temperature of the work and the building up of the needs of installation collectors.
The parabolic collector technology allows rational utilization of the absorption of the sun's rays, and any line of sun rays locks the angles in the form of mirrors of 60°.

Solar energy is clean, does not emit pollution, the only pollution produced as a result of solar energy is the production of solar energy at the factory, freight transport and installation.
One of the major benefits of solar energy is the ability to use electricity in remote locations that are not connected to the national grid.
Global radiation in Kosovo is about 1400 kWh/m^2, Kosovo possesses the geographical latitude: from 41° 52 up to 43° 16 (N) and 19° 59 up to 21° 16 (E).
Data on solar radiation in three cities of Kosovo, Pristina, Peja and Prizren are data of average radiation whose values are optimal for the conversion of sunlight into energy.
The panel collector should be placed in the south-east direction as the optimally orientation position in the direction of the sun's rays, while for Kosovo the optimal slope is from 33° to 36° with radiant power from 1530 kWh/m² to 1680 kWh/m²*(Sharkawi. E & Mohamed A. "Electrical).*

Refernce

1. https://metsolar.eu/blog/introduction-photovoltaics-solar-cells/
2. https://www.okorder.com/solar-cells/pl4972.html?gclid=EAIaIQobChMIkKi-kKzT3QIVFed3Ch1hnwCNEAAYASAAEgKmjfD_BwE
3. [(Nexhat Ohrana, Bazat e Elektroteknikes I, 1986, Prishtine)].
4. [(AP® Environmental Science, Energy and Climate Change, Professional Development Workshop Materials, 2006–2007.
http://apcentral.collegeboard.com/apc/public/repository/06_Environmental_Science_Special_Focus.pdf].

5. [Dick Swanson, Sunpowercorp technology in Germany, 2010].
http://www1.eere.energy.gov/solar/pdfs/sssummit2012_plenary_swanson.pdf].
6. [(Antonio Luque & Steven Hegedus, Handbook of Photovoltaic Science and Engineering, 2003, United Kingdom)].
7. [(Kasthurirangan Gopalakrishnan & Siddhartha Kumar Khaitan & Soteris Kalogirou, 2010, Soft Computing in Green and Renewable Energy Systems, 201, Berlin Hidelberg)].
8. [Shur. M, Physics of Semiconductor Devices, Prentice Hall, Englewood Cliffs, NJ, 1990].
9. [(John A. McNeill, "Renewable Energy Applications", Worcester Polytechnic Institute in Electrical and Computer Engineering, Aprill 2012, pp3)].
10. [Bruno Motik, „ Zelena energija", Zagreb, 2005, pp69-70].
11. [Bloc solar Avago Technology, 2012].
http://investors.avagotech.com/phoenix.zhtml?c=203541&p=quarterlyEarnings].
12. [(P.Solar.Hr, National Solar Jobs Census, 2013, p23)].
13. [Lof, G. "Active Solar Systems," Cambridge, 1993].
14. [(Harry Wirth, Fraunhofer ISE, Photovoltaic Module Systems and Reliability, Freiburg, Germany, April 10, 2014, pp31),
http://www.ise.fraunhofer.de/en/publications/veroeffentlichungen-pdf-dateien-en/studien-und-konzeptpapiere/recent-facts-about-photovoltaics-in-germany.pdf].
15. [Sharkawi. E & Mohamed A. " Electrical energy", 2005, pp102]

International Conference on Science and Technology

ICONST 2018

5-9 September 2018 Prizren - KOSOVO

The Topological Optimization of Corrugated Core Sandwich Structure Subjected to Planar Impact

Erman Zurnacı[1]*, Hasan Gökkaya[2]

Abstract: Sandwich structures with low weight, high strength and effective impact resistance performance are increasingly used in engineering applications. Reducing the weight of sandwich structures used as a structural component is an important for defence, aviation, space and transportation industries. Because low weight requires less fuel consumption. The majority of the weight of the sandwich structure is the weight of the sandwich structure core. The objective of this study is to reduce the weight of the corrugated strip core sandwich panel by topology optimization applied to the core form. The core unit cell is redesigned according to the cell optimization results. The new unit cell design model and the existing design model are analysed under planar impact load using the finite element method and the results are compared. The proposed design optimization significantly increased the impact resistance performance while reducing the sandwich panel weight.

Keywords: Sandwich Structure, Weight Reduction, Topological Optimization, Finite Element Method, Planar Impact.

Introduction

Lightweight sandwich structures which consist of low density cores and stiff face sheet frequently preferred in engineering applications. Sandwich structures as an engineering material are widely used in defence, aviation, space and transportation industries due to its low weight as well as its many advantages (Rejab and Cantwell, 2013). The academic studies on the design and optimization of sandwich structures has been increasing in recent years. The investigation of the mechanical properties of sandwich structures and the production of sandwich panels suitable for different needs are important. The core and face sheet materials of the sandwich structures are selected from different materials such as metal, polymer, fibre reinforced polymer and balsa (Mohmmed et al., 2014). The core of sandwich structure are produced in different forms such as honeycomb, foam, corrugated and lattice truss. Face sheet materials show resistance to in-plane and lateral loads, while core of sandwich structure increases strength and contributes to important structural properties such as durability (Vinson, 1999). There are different constraints that need to be taken into account when designing a sandwich (Steeves and Fleck, 2004) and these constraints have different significance ratings according to the use area of the sandwich structure.

The sandwich structure design needs to be optimized in order to achieve sandwich structure lightness at the top of one's most important advantages (Li et al., 2012). The majority of the sandwich structure weight is the core and the mechanical performance of the sandwich panel is largely influenced by the core structure (Hou et al., 2013). The sandwich panel core undergoes plastic deformation during the impact, absorbing most of the impact energy (Zhu et al., 2010). While the weight of the sandwich structure design is reduced in the optimization, the impact resistance should not be reduced. Studies in the literature are usually focused on the reduction of the weight with the optimization of the sandwich panel core design.

[1]Duzce University, Dr. Engin PAK Cumayeri Vocational School, Electronic and Automation Department, Cumayeri 81700, Düzce, Turkey
[2]Karabuk University, Engineering Faculty, Mechanical Engineering Department, Balıklarkayası 78050 Karabük, Turkey
*Corresponding Author: ermanzurnaci@duzce.edu.tr

Liang et al. (2001) investigated optimum weight designs of metallic corrugated sandwich structures subjected to blast load in transverse and longitudinal directions. The Feasible Direction Method (FDM) combined with the Backtrack Program Method (BPM) is used for optimization. The results show that the core length, groove angle and core thickness are the most important components for the surface layer and the core pitch length thickness is the most important parameter for face sheet layer. Tapp et al. (2004); have developed an intuitive approach to reducing the weight of sandwich panels. The developed approach calculates damage failure mechanisms for different load cases using the structural analysis with finite element method. According to the calculation results, materials are added to the zones subjected to high stress and materials are removed from the regions subjected to low stress. The validity and success of the developed methodology and in weight reduction are demonstrated with the implemented examples. Steeves and Fleck (2004); analytically investigated the flexural strength of sandwich panels having composite face sheets (woven glass–epoxy) and polymer foam cores of three different mechanical properties. They have optimized the sandwich panel design to reduce peak force, reduce failure failures and reduce weight. Failure mechanism maps are created and minimum weight designs are obtained. The authors have found that composite face sheet materials are more advantageous than metallic surface plates to decreasing weight. Meidell (2009); the sandwich panel with honeycomb core has achieved minimum weight optimization in the specified strength conditions. An algorithm has been developed that determines the design parameter values to provide the minimum weight requirement for the specified strength value. The developed algorithm also considers the dimensional constraints that may be necessary for the manufacturing process. Li et al. (2012); have developed an optimization method in order to reduce the weight of sandwich structures subjected to torsional loading. This method takes into account the criteria for torsional rigidity and structural stiffness. The proposed method has been tested with numerical and experimental tests performed. Two different face sheet materials, isotropic (aluminium) and orthotropic (GFRP) composite, were used to determine the impact of material selection on impact resistance performance. The results show that in the optimum design the core weight constitutes 66.7% of the whole sandwich panel. Wu (2016); aimed at designing a sandwich panel to replace heavy and large sandwich panels for the control of the cab noise and the saving of fuel in the air transport industry. Topology optimization has been used to achieve the design required to reduce the weight. The optimization computes the bandwidth that will reduce noise and reduce panel weight.

The aim of this study is to reduce the weight of the corrugated strip core sandwich panel by design optimization applied to the core form. For this purpose, a two-stage approach, including conceptual design and detailed design has been developed. In the first stage of the study; topology optimization has been applied to the core unit cell and material regions that can be subtracted from the design area have been determined to provide the maximum stiffness criteria. In the second stage of the study; a detailed design of the core unit cell model suitable for the optimization results was carried out and the new design was analysed using the finite element method under the dynamic planar impact load. Finally the weights of proposed new unit cell design and existing unit cell design designs are compared and the impact resistance performance is examined.

Material and Methods

Unit Cell of Sandwich Structure Core

Frequently preferred corrugated core form in sandwich panel design provides effective impact energy absorbing performance while at the same time it is light (Fleck, 2004). The corrugated core form is produced in different geometries, such as square, triangular, round and trapezoidal by means of sheet metal forming method. The core form of corrugated sandwich structure consists of repeatedly linked unit cells. Repeating linked unit cells move as a whole like a network structure (Lin et al., 2010). For this reason, the mechanical performance of the unit cell represents the overall mechanical performance of the sandwich panel.

For this study, a sandwich panel with corrugated strip core was selected and the trapezoidal geometry was specified as the corrugated profile. Three-dimensional sandwich panel models were created with Solidworks 2018 software. The sandwich panel structure (Fig. 1a) and the unit cell of the corrugated strip core to be optimized (Fig. 1b) were given in Figure 1.

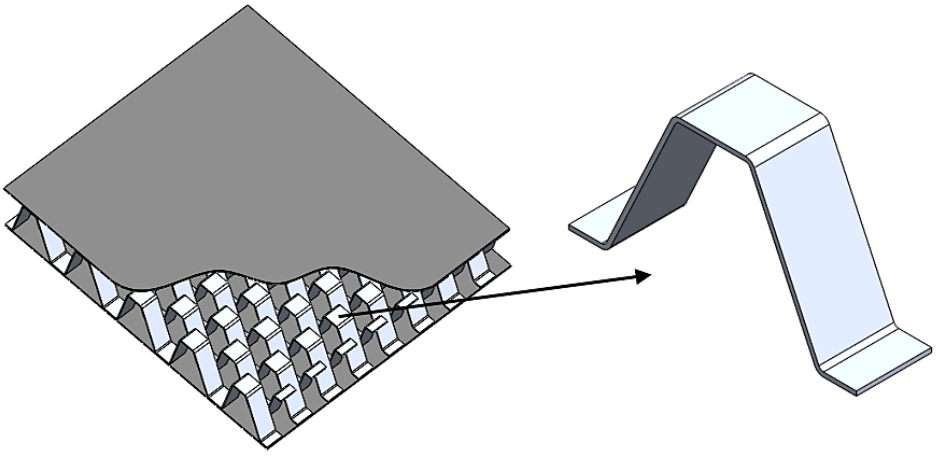

a) b)

Figure 1. Three-dimensional sandwich panel model (a) and unit cell (b).

Design and optimization studies were carried out using unit cells. The unit cell thickness used in the study was 0.2 mm and the width was 5 mm and the geometric parameters were given in Figure 2. Aluminium 2024 material was selected as the core material and Al 2024's density 2780 kg/m3, elastic modulus 70.6 GPa and Poisson's ratio 0.3 were defined on the software.

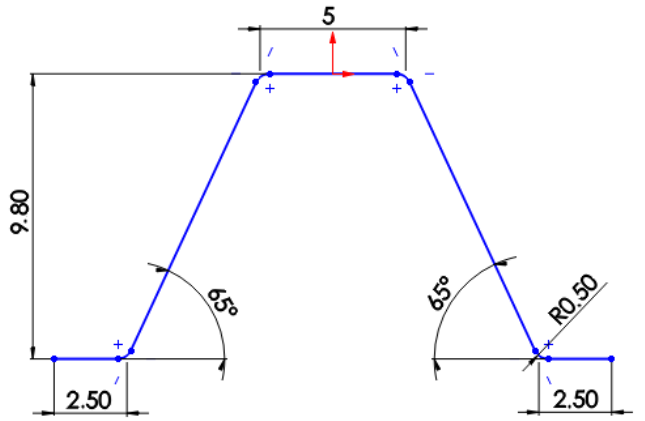

Figure 2. Geometric parameters of the unit cell

The Topological Optimization of Unit Cell

Topology Optimization aims to find the most appropriate material distribution in a defined design area (Bendsøe and Sigmund, 2003). The material that makes up the design is defined as the design variables in topology optimization (Park, 2007). The weight is reduced by distributing it to the minimum material design area that provides the specified design constraints. Optimization is applied during the conceptual design phase and leads to detailed design (Lee and Park, 2012). In this study; Solidworks 2018 Topological Optimization tool was used to optimize the design of the sandwich panel core unit cell. The unit cell finite element model consists of 28746 four nodes tetrahedral elements with a dimension of 0.25 mm. The existing unit cell design model (Design_1) was analysed under a planar static load of 5N (Figure 3).

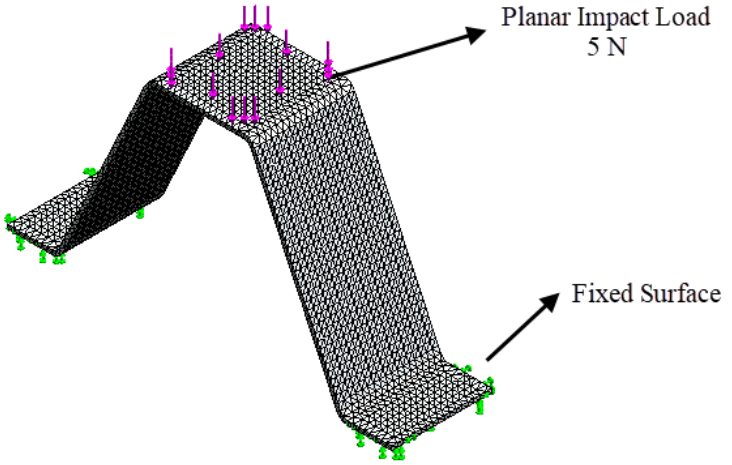

Figure 3. Analysis model of topology optimization.

As a result of the optimization, areas of material that can be removed from the design area have been determined. Best stiffness to weight ratio is chosen as the optimization criterion. The values of the stress on the unit cell model are taken into account when the material areas to be removed from the design are determined. Figure 4a shows the stress values formed on the unit cell. The blue regions shown in Figure 4b shows regions that are suitable for removal of material, while regions that are yellow indicate regions that should remain in the design.

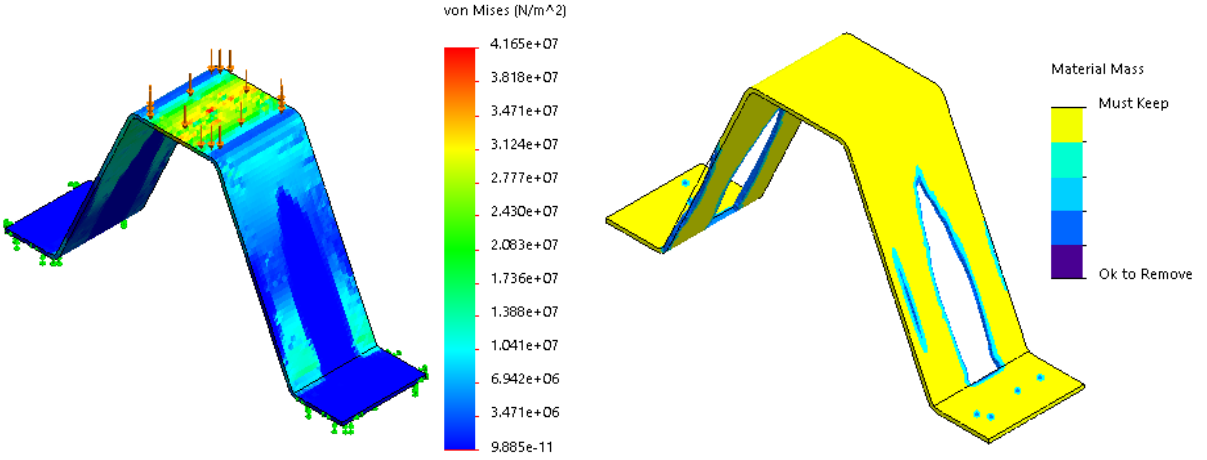

a) b)

Figure 4. Stress values on the unit cell (a) and result of topology optimization (b).

Detailed design of the new unit cell model has been realized using topology optimization results. The generated new unit cell design (*Design_2*) was given in Figure 5. Unit cell weight was reduced by approximately 22% with the new design. Table 1 shows the change in volume and weight in the unit cell structure.

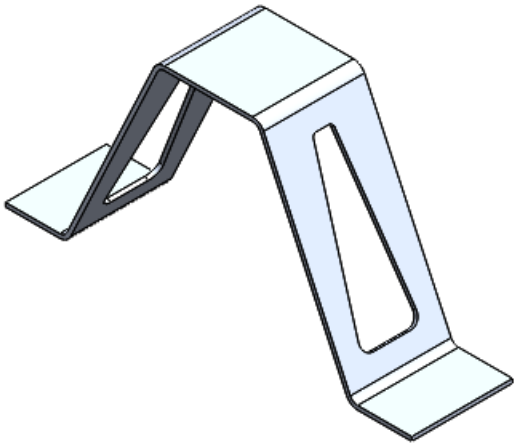

Figure 5. New unit cell design.

Table 1. Volume and weight change of the unit cell structure as a result of optimization.

	Design_1	*Design_2*	Percent of change
Volume (mm^3)	31.35	24.82	%20.8
Weight (gram)	0.09	0.07	%22.2

Dynamic Analysis of New Unit Cell Subjected to Planar Impact

Sandwich panels are subjected to dynamic loads during their product lifetime (Tilbrook et al., 2007). Dynamic impact loads cause different failure modes in the sandwich panel core. For this reason, the behaviour of the new unit cell model under dynamic load must be analysed. The new unit cell model was analysed under dynamic planar load using Abaqus 6.13 finite element software. It is aimed to determine the impact resistance performance of the *Design_1* and *Design_2* designs with the analyses were performed. The unit cell model was fixed between the rigid two plates by adhesive surfaces and a mass of 0.5 kg was assigned to the upper rigid plate. The upper rigid plate was allowed to move only in the vertical direction and the movement of the lower rigid plate in all directions was restricted (Figure 6).

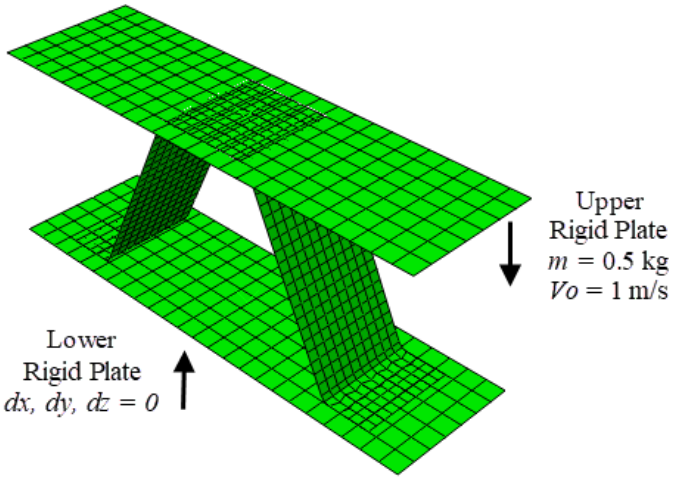

Figure 6. Analysis scenario of planar dynamic impact analysis.

The adhesion between the rigid surfaces and the unit cell was assumed to be perfect. New unit cell were modelled with 4 nodes having 5 integration points. Finite element dimensions for face sheets and core were

specified as 1 mm and 0.5 mm respectively. Subsequently, the upper rigid plate was subjected to the unit cell at a speed of 1 m/sec in the vertical direction. The analysis results show the impact resistance performance of two different designs.

Results

Design_1 and *Design_2* were displaced in different amounts after the planar impact load. The amount of displacement represents the amount of deformation occurring in the unit cell structure and is directly proportional to the amount of absorbed energy. Deformation and force-displacement graphs in the *Design_1* and *Design_2* designs were given in Figures 7a and 7b, respectively.

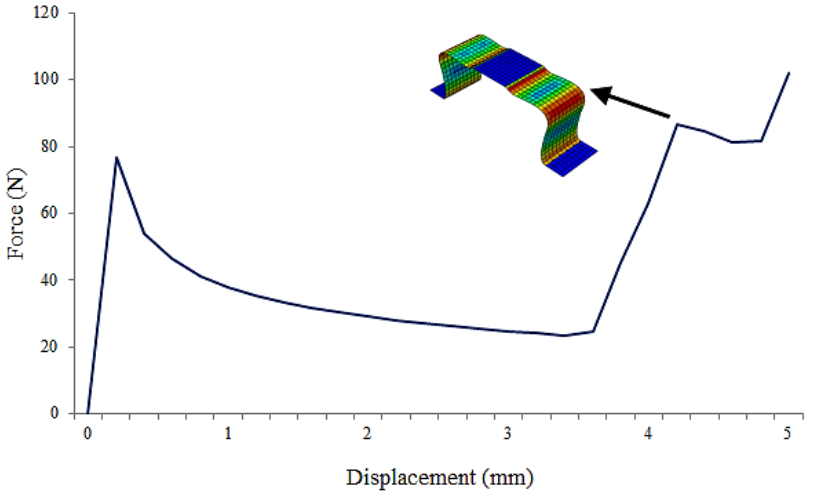

a)

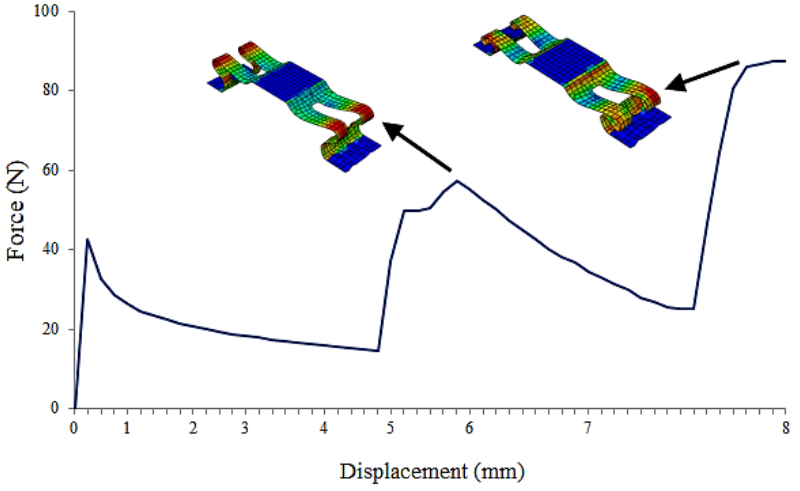

b)

Figure 7. Deformations and force-displacement graphics.

When the graphs in Fig. 6 are examined, it is seen that *Design_1* was deformed by 4.84 mm and *Design_2* was deformed by 7.96 mm. The *Design_2* unit cell model which is reduced in weight was absorbed about 20% more energy. In addition, *Design_2* was reduced the maximum impact force by about 14% while reducing the average crushing force by about 17% (Table 2).

Table 2. Results of planar dynamic impact analysis

	Design_1	*Design_2*	Percent of change
Maximum Force (N)	101.961	87.540	%14.143
Average Crushing Force (N)	44.825	37.010	%17.434
Absorbed Energy (mJ)	190	239	%20.502

Discussion

The proposed optimization method was reduced the weight of the sandwich panel and significantly was increased the impact resistance performance of the sandwich structure. Results shows that design optimization using topology optimization was provided controlled deformation of the unit cell structure. The material removed from the design zone in order to reduce weight was increased the deformation of the structure and reduced the severity of impact energy. By reducing the maximum impact force, it is possible to reduce the severity of sudden quakes that can occur in sandwich construction.

Acknowledgement

This work is supported by Project Directorate of Scientific Researches Project of Karabük University within the scope of the project named as KBÜBAP-17-DR-458.

References

ABAQUS Version 6.13 (2013). Analysis User's manual. Providence, RI: Dassault Systemes Simulia Corp.

Bendsøe, M.P. and Sigmund, O. (2003). Topology Optimization: Theory, Methods, and Applications, Springer, Berlin.

Fleck, N.A. and Deshpande, V.S. (2004). The resistance of clamped sandwich beams to shock loading. Journal of Applied Mechanics, 71(3), 386-401.

Hou, S., Zhao, S., Ren, L., Han, X. and Li, Q. (2013). Crashworthiness optimization of corrugated sandwich panels. Materials and Design 51, 1071-1084.

Lee, H.A. and Park, G.J. (2012). Topology Optimization for Structures With Nonlinear Behavior Using the Equivalent Static Loads Method. Journal of Mechanical Design 134(3), 031004-031017.

Li, X., Li, G., Wang, C.H. and You, M. (2012). Minimum-Weight Sandwich Structure Optimum Design Subjected to Torsional Loading. , Applied Composite Materials, 19(2), 117–126.

Liang, C.C., Yang, M.F., Wu, P.W. (2001). Optimum design of metallic corrugated core sandwich panels subjected to blast loads. Ocean Engineering, 28(7), 825-861.

Lin, J., Luo, Z. and Tong, L. (2010). Design of Adaptive Cores of Sandwich Structures Using a Compliant Unit Cell Approach and Topology Optimization. Journal of Mechanical Design 132(8), 0810121-0810128.

Meidell, A. (2009). Minimum weight design of sandwich beams with honeycomb core of arbitrary density. Composites Part B: Engineering, 40(4), 284–291.

Mohmmed, R., Ahmed, A., Mohamed, A.E. and Ali, H. (2014). Low Velocity Impact Properties of Foam Sandwich Composites: A Brief Review. International Journal of Engineering Science and Innovative Technology, 3(2), 579-591.

Park, G.J. (2007). Analytic Methods for Design Practice, Springer, Germany.

Rejab, M.R.M. and Cantwell, W.J. (2013). The mechanical behaviour of corrugated-core sandwich panels. Composites Part B: Engineering, 47, 267-277.

Solidworks (2018), User Manual, Dassault Systemes SolidWorks Corp., Concord, Massachusetts.

Steeves, C.A. and Fleck, N.A. (2004). Collapse mechanisms of sandwich beams with composite faces and a foam core, loaded in three-point bending. Part I: analytical models and minimum weight design. International Journal of Mechanical Sciences, 46(4), 561–583.

Tapp, C., Hansel, W., Mittelstedt, C. and Becker, W. (2004). Weight-Minimization of Sandwich Structures by a Heuristic Topology Optimization Algorithm. Computer Modeling in Engineering and Sciences 5(6), 563-573.

Tilbrook, M.T., Radford, D.D., Deshpande, V.S. and Fleck, N.A., (2007). Dynamic crushing o sandwich panels with prismatic lattice cores. International Journal of Solids and Structures 44, 6101-6123.

Vinson, J.R., (1999). The Behavior of Sandwich Structures of Isotropic and Composite Materials. Thechnomic Publishing Co. Inc., Lancaster, PA, USA.

Wu, J. (2016). Topology Optimization Studies for Light Weight Acoustic Panels. Master of Applied Science Graduate Department of Aerospace Science and Engineering, University of Toronto.

Zhu, F., Lu, G., Ruan, D. and Wang, Z. (2010). Plastic Deformation, Failure and Energy Absorption of Sandwich Structures with Metallic Cellular Cores. International Journal of Protective Structures, 1(4), 507-541.

International Conference on Science and Technology

ICONST 2018

5-9 September 2018 Prizren - KOSOVO

Ewe Live Weight at Birth and Lamb Birth Weight in Karya Sheep

Orhan Karaca[1], Nezih Ata[1], İbrahim Cemal[1], Onur Yilmaz[1*]

Özet: Sunulan çalışmanın amacı Karya ırkı koyunlarda kuzuların gelişme özellikleri ve yaşama güçleri üzerine oldukça önemli etkisi olan koyunda doğum canlı ağırlığı ve kuzu doğum ağırlıklarının tanımlanmasıdır. Çalışmanın hayvan materyalini Karya ırkından 10 335 baş koyun ve 106 146 kuzu oluşturmuştur. Veriler 2011 ve 2016 yılları arasında yetiştirici koşullarında toplanmıştır. Doğumda koyun canlı ağırlığı ve kuzu doğum ağırlığı ortalamaları sırası ile 56.11 kg (n=10 335) ve 3.73 kg (n=106 146) olmuştur. Koyununun doğumdaki ağırlığı üzerine tabakalar dışında, il, yıl, koyun yaşı ve doğum ayı gibi sabit etkilerin etkisi istatistik olarak önemli bulunmuştur. Değerlendirmeye alınan tüm çevre faktörlerinin (il, tabaka, koyun yaşı, doğum ayı, doğum tipi ve cinsiyet) kuzu doğum ağırlığı üzerine etkisi de istatistik olarak önemli olmuştur ($P<0.01$). Ara elit sürülerde yer alan kuzuların doğum ağırlıklarının taban işletmelerdekinden daha yüksek olduğu söylenebilir. Doğumda koyun ağırlığı ve kuzu doğum ağırlığının ilerleyen koyun yaşı ile birlikte bir artış gösterdiği gözlemlenmiştir. Özellikle 6 ve ≥7 yaş grubundaki koyunlardan doğan kuzuların doğum ağırlıklarının sırasıyla 3.80 ve 3.78 kg gibi yüksek olarak gerçekleşmesi dikkate değer bir bulgudur.

Anahtar Kelimeler: Karya, koyun, doğum ağırlığı

Abstract: The aim of the present study was to determine lamb birth weight and ewe live weight at birth which have significant effect on the growth characteristics and survival rate of lambs in Karya sheep. The animal material of the study consisted of 10 335 ewe and 106 146 lambs from Karya breed. Data were recorded in farmers' conditions years between 2011 and 2016. The overal mean of the ewe live weight at birth and lamb birth weight were 56.11 kg (n=10 335) and 3.73 kg (n=106 146), respectively. The effects of fixed factors such as province, year, age of ewe and month of birth except tiers on the ewe live weight at birth were found to be statictically significant. All the environmental factors (province, tiers, year, age of ewe, month of birth, birth type and gender) were found to be statistically significant effect on the lamb birth weight ($P<0.01$). It can be said that the lambs in the multiplier flocks have a better performance than the lambs in the based flocks in terms of birth weight. It has been observed that the ewe live weight at birth and lamb birth weight are increased with the advancing of ewe age. It is an interesting finding that especially ewes with 6 and ≥7 age groups have high values of lamb birth weights as 3.80 and 3.78 kg, respectively.

Keywords: Karya, sheep, birth weight

[1] Adnan Menderes University, Faculty of Agriculture, Department Of Animal Science, Aydin, TURKEY
*Corresponding author: oyilmaz@adu.edu.tr

Giriş

Döl verimi ve kuzu gelişme özellikleri bakımından ön plana çıkan ve Batı Anadolu'da oldukça geniş bir bölgede yetiştiriciliği yapılan Karya koyunu, son 30-40 yıllık dönemde yetiştiriciler tarafından bölgedeki koyun ırklarının Sakız, Kıvırcık veya Sakız x Kıvırcık melezi koçlarla sistemsiz geriye melezlenmesi sonucu oluşmuştur. Genotipe, geçmişte bölgede hüküm süren Karya uygarlığının isminin verilmesi uygun görülmüştür. Döl verimi ve gelişme özellikleri üzerine yetiştirici koşullarında gerçekleştirilen ıslah çalışmaları sayesinde Karya koyunu 2013 yılında milli ırk olarak tescil edilmiştir (Cemal vd., 2009; Karaca vd., 2009a; Karaca vd., 2009b; Yilmaz vd., 2009; Yılmaz vd., 2011; Yılmaz ve Karaca, 2012; Karaca vd., 2013; Yılmaz vd., 2013a; Yılmaz vd., 2013b).

Kuzu doğum ağırlığı ve doğumda koyun ağırlığı kuzularda büyümeyi karakterize eden önemli özelliklerdendir. Bir canlının doğum ağırlığı ile çeşitli dönemlerindeki canlı ağırlıkları genotip ve çevresel faktörlerin etkisi ile şekillenir. Koyunlardan daha fazla kuzu üretimi, koyun başına döllü yumurta sayısının arttırılması yanında döllenmiş yumurtaların döl yatağında normal gelişip büyümesine ve bunun sonucu olarak doğum ağırlığı yüksek, sağlıklı kuzulara sahip olmasına bağlıdır (Sezenler vd., 2008; Karaca vd., 2009a; Yılmaz vd., 2011).

Kuzu doğum ağırlığı 1.5- 6 kg arasında değişebilir. Bu değişimler ana yaşı, beslenme, ikizlik gibi plasental beslemeyi etkileyen faktörlerle ilgilidir. Kuzu doğum ağırlığında meydana gelen değişimler ölüm oranında artış, gelişme özelliklerinde düşüş ve karkasta yağlanma gibi olumsuzluklara neden olabilmektedir. Doğum ağırlığı kuzuların yaşama gücünü büyük çapta etkiler. Doğum ağırlığının düşmesiyle ölümler de artar. Doğum ağırlığı 1.7 kg'ın altında olan kuzularda ölümün % 94 dolayında olduğu bildirilmektedir (Yılmaz vd., 2011; Hinch ve Brien, 2014; Juengel vd., 2018,). Doğum ağırlığını yükseltmekle yaşama gücü belli bir sınıra kadar iyileştirilebilir.

Doğumda koyun ağırlığı ise doğacak kuzuların doğum ağırlıklarının önemli bir göstergesi olarak karşımıza çıkmaktadır. Koyunların beslenmesinde en kritik dönemler aşım, gebelik ve laktasyon devresi olarak sıralanabilir. Özellikle gebeliğin son dönemindeki besleme, anaların doğum sırasındaki kondisyonunu ve erken laktasyonda süt veriminin artışı yanında, kuzuların doğum ağırlığını ve büyüme dönemindeki ağırlık artısı ile yaşama güçlerini yükselttiği bildirilmektedir (Juengel vd., 2018; Hinch and Brien, 2014; Dwyer vd., 2016). Doğum ağırlığı üzerine genotip ile birlikte cinsiyet, doğum tipi, ana yaşı, doğum mevsimi ve ananın beslenme durumunun etkili olduğu bildirilmiştir (Yılmaz vd., 2009; Hinch ve Brien, 2014; Dwyer vd., 2016). Sunulan çalışmada Batı Anadolu'da oldukça yaygın bir şekilde yetiştirilen Karya ırkı koyunlarda kuzuların gelişme özellikleri ve yaşama güçleri üzerine oldukça önemli etkisi olan koyunda doğum canlı ağırlığı ve kuzu doğum ağırlıklarının tanımlanması amaçlanmıştır.,

Materyal ve Metod

Proje Kapsamında yer alan ara elit ve taban işletmelerdeki doğuran 10 335 baş koyun ve bunlardan doğan 106 146 baş kuzu çalışmanın hayvan materyalini oluşturmuştur. Doğumda koyun ağırlığı ve kuzu doğum ağırlığı elektronik kantar yardımıyla tespit edilmiştir. Tüm sürülerde doğan kuzuların ağırlıkları ve doğumda koyun canlı ağırlıkları doğumu izleyen ilk 24 saat içerisinde elektronik kantarlar yardımıyla tespit edilerek kayıt altına alınmıştır.

Verilerin normal dağılışa uygunluğu SAS (1999) paket programındaki UNIVARIATE prosedürü kullanılarak test edilmiştir. Normal dağıldığı tespit edilen veriler yine aynı istatistik paket programında bulunan Generalized Linear Models (GLM) prosedürü kullanılarak analiz edilmiştir. Analizlerde kullanılan kesikli faktörler Çizelge 1'de verilmiştir.

[1] Adnan Menderes University, Faculty of Agriculture, Department Of Animal Science, Aydin, TURKEY
*Corresponding author: oyilmaz@adu.edu.tr

Çizelge 1. Ele alınan özelliklerin analizlerinde kullanılan kesikli ve sürekli etmenler

	Doğumda Koyun Ağırlığı	Kuzu Doğum Ağırlığı
Kesikli Etmenler	İl	İl
	Tabaka	Tabaka
	Yıl	Yıl
	Koyun Yaşı	Koyun Yaşı
	Doğum ayı	Doğum ayı
		Doğum tipi
		Cinsiyet

Bulgular

Karya ırkı koyunların doğumda koyun ağırlıkları ve kuzu doğum ağırlığına ilişkin en küçük kareler ortalamaları ve standart hatalarını gösteren bulgular Çizelge 2'de verilmiştir**.**

Çizelge 2. Karya ırkında doğumda koyun ağırlıkları ve kuzu doğum ağırlığına ilişkin en küçük kareler ortalama ve standart hataları

Faktörler	N	Doğumda Koyun Ağırlığı	N	Kuzu Doğum Ağırlığı
İl		P=0.009		P=0.000
Aydın	275	48.86±2.928	26685	3.54±0.014
Denizli	10060	63.36±2.712	79461	3.93±0.013
Tabaka		P=0.611		P=0.000
Taban	278	57.52±2.728	90339	3.68±0.013
Ara Elit	10057	54.70±2.888	15807	3.79±0.014
Yıl		P=0.000		P=0.000
2011	1177	58.77±0.567	10676	3.81±0.015
2012	1212	58.30±0.535	16435	3.77±0.014
2013	1942	55.13±0.523	18424	3.74±0.014
2014	2055	54.08±0.521	21015	3.76±0.014
2015	2118	54.90±0.522	20795	3.71±0.014
2016	1831	55.49±0.524	18801	3.63±0.014
Ana Yaşı		P=0.000		P=0.000
1	663	53.79±0.608	6598	3.66±0.016
2	1129	53.95±0.542	15359	3.70±0.014
3	1955	54.95±0.517	19137	3.70±0.014
4	1783	56.91±0.533	19948	3.75±0.014
5	1608	58.40±0.537	18940	3.76±0.014
6	1518	57.65±0.539	14530	3.80±0.014
≥7	1679	57.12±0.541	11634	3.78±0.015
Doğum Ayı		P=0.000		P=0.000
Ocak	1318	54.95±0.392	11314	3.74±0.008
Şubat	1317	53.48±0.381	11340	3.75±0.009
Mart	813	51.75±0.431	8921	3.66±0.009
Nisan	333	51.67±0.589	5400	3.74±0.012
Mayıs	98	54.64±0.977	1705	3.80±0.019
Haziran	6	64.58±3.920	214	3.65±0.054
Temmuz	-	-	41	3.45±0.122
Ağustos	69	58.23±1.177	341	3.75±0.043
Eylül	421	60.38±0.549	3292	3.82±0.014
Ekim	798	55.58±0.431	7774	3.86±0.010
Kasım	3233	55.90±0.330	21353	3.83±0.007
Aralık	1929	56.05±0.346	34451	3.79±0.007
Doğum Tipi				P=0.000
1			54798	4.36±0.013

[1] Adnan Menderes University, Faculty of Agriculture, Department Of Animal Science, Aydin, TURKEY
*Corresponding author: oyilmaz@adu.edu.tr

2			46512	3.74±0.013
≥3			4836	3.10±0.016
Cinsiyet				P=0.000
Erkek			53345	3.79±0.013
Dişi			52801	3.68±0.013
Genel	10335	56.11±0.47	106146	3.73±0.013

Genel ortalaması 56.11 kg olan doğumda koyun canlı ağırlıkları bakımından tabaka bazlı değerlendirme yapıldığında ara elit ve taban işletmeler için ortalamalar sırasıyla 54.70 ve 57.52 kg bulunmakla birlikte tabakalar arası fark istatistiki olarak önemli bulunmamaıştır. Tabakalar dışında kalan tüm kesikli etmenlerin doğumda koyun canlı ağırlığı üzerine etkisi istatistiki olarak önemlidir (P<0.01). Doğumda koyun ağırlığı değeri bakımından Denizli ilindeki koyunların Aydın ilindekilere oranla yaklaşık 15 kg daha ağır oldukları gözlenmiştir. Koyun canlı ağırlıklarının ilerleyen yaşla birlikte yükselme eğilimi gösterdiği dikkati çekmektedir. Kuzu doğum ağırlığı bulgularına paralel olarak en yüksek koyun canlı ağırlığı değeri 2011 yılı için (58.77 kg) elde edilmiştir.

Genel doğum ağırlığı ortalaması 3.73 kg bulunmuştur. Koyun canlı ağırlığında olduğu gibi kuzu canlı ağırlığı bakımından da Denizli ilindeki işletmelerdeki kuzuların ortalaması Aydın ilindekilerden daha yüksektir (sırasıyla 3.93 ve 3.54 kg). Tabakalar bakımından ele alındığında ise ortalamalar ara elit sürü için 3.79 kg, taban sürüler için ise 3.68 kg olmuştur. Yıllar bakımından en yüksek kuzu doğum ağırlığı değeri ise 3.81 kg ortalama ile 2011 yılında ortaya çıkmıştır. Kuzu doğum ağırlıkları için ara elit ve taban işletmelerde ele alınan tüm kesikli etmenlerin etkisi istatistik olarak çok önemli bulunmuştur (P<0.01). Ortaya çıkan farklılıklarda işletmelerdeki bakım ve yönetim farklılıklarının belirleyici olarak öne çıktığı kabul edilebilir. Anayaşı artıkça kuzu doğum ağırlıklarının da oransal olarak yükseldiği söylenebilir. Özellikle 6 ve ≥7 grubunda sırasıyla elde edilen 3.80 ve 3.78 kg gibi yüksek kuzu doğum ağırlığı değerleri ilginç bir gözlem olarak ortaya çıkmaktadır. Kuzu doğum ağırlığı sonuçları bakımından cinsiyet ayrımı erkekler lehine ve istatistiki olarak çok önemlidir. Doğum tipi bakımından üç farklı grup ayrımı yapılmıştır (Tekiz, ikiz, üçüz ve üstü). Gerçekleştirilen analizlerde her iki işletme tipi içinde tekiz doğanların diğerlerine göre üstünlük sağlaması beklenen bir bulgudur.

Tartışma ve Sonuç

Özellikle her iki özellik için de yıllar bazında meydana gelen dalgalanmalar ani iklim değişimleri ve yetiştiricilerin farklı bakım besleme uygulamaları sonucu olarak karşımıza çıkmaktadır. İlerleyen yaşla birlikte düşme eğilimine girmesi beklenen kuzu doğum ağırlıklarında yükselme görülmesinin mevcut materyalin bakım yönetim özgünlüğünden kaynaklandığı söylenebilir. Daha önceden yapılan araştırmalarda da (Sönmez ve Kızılay, 1972; Esen ve Yıldız, 2000) benzeri gözlemler elde edilmiştir. Bu durum yüksek verimli hayvanların çok ileri yaşlara kadar elde tutulma eğiliminin somut bir kanıtı olarak kabul edilebilir. Koyunlarda canlı ağırlığın yaş gruplarına göre dağılımı giderek artan sonra azalan bir eğilim göstermektedir. Bu değişim genel bilgilerle uygunluk içindedir. Tabaklar bakımından ara elit sürülerde doğumda koyun ağırlığı için elde edilen düşük değerler özellikle ara elit sürülerdeki Karya ırkı koyunlarda çoğuz doğumların fazlalığı ile açıklanabilir.

Doğumda koyun ağırlığı ve kuzu doğum ağırlıkları için elde edilen değerler yerli ırklarda gerçekleştirilen bazı çalışmalarda elde edilen değerlerden (Ceyhan vd., 2007; Şireli vd., 2015) bazılarından ise yüksek (Karaca vd., 2011; Sezenler vd., 2014; Şirin vd., 2018) düşük bulunmuştur. Doğum tipi bakımından elde edilen sonuçlar değerlendirildiğinde çoğuz doğumlarla birlikte doğum ağırlıklarının düşmesi doğal bir gözlem sürecidir. Anılan ayrımlar istatistiki anlamda çok önemlidir. Erkek kuzuların dişilere, tek doğanların ise çoğuz doğanlara karşı üstün olduğu görülmektedir. Bu durum konuyla ilgili literatür ile uyum içerisindedir (Ceyhan vd., 2007; Yılmaz vd., 2009; Karaca vd., 2011; Yılmaz vd., 2011; Sezenler vd., 2014; Şirin vd., 2018).

İşletmelerin özgün bakım yönetim koşullarından kaynaklı doğum ağırlığı ve doğumda koyun ağırlığında ortaya çıkan varyasyon ayrı bir değerlendirme konusudur. Ancak klasik sistematik çevre etmenleri olarak

[1] Adnan Menderes University, Faculty of Agriculture, Department Of Animal Science, Aydin, TURKEY
*Corresponding author: oyilmaz@adu.edu.tr

değerlendirebileceğimiz yıl, ana yaşı, cinsiyet, doğum tipi ve ana canlı ağırlığının ortaya koyduğu varyasyonun konuyla ilgili bir literatürle (Karaca ve Okut, 1991) uyum içinde olduğu söylenebilir.

Sonuç olarak, yetiştirici koşullarında oldukça büyük bir veri seti kullanılarak gerçekleştirilen bu çalışmadan elde edilen bulgular incelendiğinde Karya koyunlarda yürütülen ıslah programında gerçekleştirilen tabaka ayrımlarının oldukça isabetli olduğu net bir şekilde görülmektedir. Diğer yandan konuyla ilgili literatür değerlendirildiğinde ekstansif koşulları oldukça iyi değerlendiren, üstün bir döl verimi ve gelişme özelliğine sahip olan Karya ırkı hayvanların yerli ve yabancı ırklarla kıyaslandığında hiçte küçümsenmeyecek bir potansiyele sahip olduğu söylenebilir. Elde edilen bilgi birikimi Karya ırkı yanında diğer yerli koyun populasyonlarımızda şekillendirilecek ıslah progamları için de oldukça aydınlatıcı olacaktır.

Teşekkür

Hayvan materyalini sağlayan Tarımsal Araştırmalar ve Politikalar Genel Müdürlüğü'ne (TAGEM) ve sürülerinde tanımlama ve ıslah çalışmalarının yapılmasına izin vererek destek sağlayan Karya koyunu yetiştiricilerine teşekkürlerimizi sunarız.

Kaynaklar

Cemal, İ., Karaca, O., Yılmaz, O., Yılmaz, M. (2009). Karya kuzularda pazarlama dönemi canlı ağırlığı ile göz kası özelliklerine ait ultrason ölçüm parametreleri. 6. Ulusal Zootekni Bilim Kongresi, 24-26 Haziran, Erzurum, 63-69.

Ceyhan, A., Erdoğan, İ., Sezenler, T. (2007). Gen Kaynağı Olarak Korunan Kıvırcık, Gökçeada ve Sakız Koyun Irklarının Bazı Verim Özellikleri. Tekirdağ Ziraat Fakültesi Dergisi, 4(2), 211-218.

Dwyer, C.M., Conington, J., Corbiere, F., Holmoy, I. H., Muri, K., Nowak, R., Rooke, J., Vipond, J., Gautier, J.M. (2016). Invited review: improving neonatal survival in small ruminants: science into practice. Animal, 10(3), 449-459.

Esen, F., Yıldız, N. (2000). Akkaraman. Sakız x Akkaraman melez (F1) kuzularda verim özellikleri. I. Büyüme, yaşama gücü, vücut ölçüleri. Turkish Journal of Veterinary and Animal Sciences, 24, 223–231.

Hinch, G.N., Brien, F. (2014). Lamb survival in Australian flocks: a review. Animal Production Science, 54(6), 656-666.

Juengel, J.L., Davis, G.H., Wheeler, R., Dodds, K. G., Johnstone, P.D. (2018). Factors affecting differences between birth weight of littermates (BWTD) and the effects of BWTD on lamb performance. Animal Reproduction Science, 191, 34-43.

Karaca, O., Okut, H. (1991). Kuzuların gelişme özelliklerinde kimi çevre etmenleri. Yüzüncü Yıl Üniversitesi Ziraat Fakültesi Dergisi, 1(2), 138-147.

Karaca, O., Cemal, İ., Altın, T., Yılmaz, O. (2009a). Karya koyunlarda yumurtlama sayısı ve batın genişliği temel parametreleri. 6. Ulusal Zootekni Bilim Kongresi, 24-26 Haziran, Erzurum, 346-354.

Karaca, O., Cemal, İ., Yılmaz, O., Yılmaz, M. (2009b). Karya koyunu. Türkiye Ulusal Koyunculuk Kongresi, 12-13 Şubat, İzmir, 225-234.

Karaca, O., Yılmaz, O., Cemal, İ. (2011). Karya kuzularda büyüme özellikleri. 7. Ulusal Zootekni Bilim Kongresi, 14-16 Eylül, Adana, 250.

Karaca O., Yılmaz O., Cemal İ. (2013). Cervical insemination in Karya sheep. Scientific Papers Series D. Animal Science, 56, 152-156.

SAS (1999). The SAS System. Version 8. Copyright (c) 1999 by SAS Institute Inc., Cary, NC, USA.

Sezenler, T., Köycü, E., ve Özder, M. (2008). Karacabey Merinosu koyunlarda doğum kondüsyon puanının kuzuların gelişimi üzerine etkileri. Tekirdağ Ziraat Fakültesi Dergisi, 5(1), 45-53.

[1] Adnan Menderes University, Faculty of Agriculture, Department Of Animal Science, Aydin, TURKEY
*Corresponding author: oyilmaz@adu.edu.tr

Sezenler, T., Köycü, E., Yaman, Y., Ceyhan, A., Küçükkebapçı, M., Yüksel, M.A. (2014). Reproductive and growth characteristics during the first age of Kıvırcık, Sakız and Gökçeada indigenous sheep breeds. Turkish Journal of Agriculture-Food Science and Technology, 2(3), 106-111.

Sönmez, R., Kızılay, E. (1972). Ege Üniversitesi Ziraat Fakültesi Menemen uygulama çiftliğinde yetiştirilen İvesi, Kıvırcık, Sakız ve Ödemiş koyunlarının verimle ilgili özellikleri üzerinde mukayeseli bir araştırma. Ege Üniversitesi Ziraat Fakültesi Dergisi, 9 (1), 3-51.

Şirin, E., Uçan, Ü., Şen, U., Soydan, E. (2017). Effect on birth and other weights of the lambs of add feeding at late gestation in Akkaraman sheep. Turkish Journal of Agriculture-Food Science and Technology, 5(11), 1353-1359.

Şireli, H.D., Vural, M.E., Karataş, A., Akca, N., Koncagül, S., Tekel, N. (2015). Birth and weaning weights of Awassi lambs raised in the GAP International Agricultural Research and Training Center. Ankara Universitesi Veteriner Fakültesi Dergisi, 62, 139-145.

Yılmaz, O., Karaca, O., Altın, T., Cemal, İ. (2009). Karya kuzularda pazarlama dönemi gelişme özellikleri ve yaşama gücü. 6. Ulusal Zootekni Bilim Kongresi, 24-26 Haziran, Erzurum, 165-173.

Yılmaz, O., Yılmaz, M., Cemal, İ., Karaca, O., Ata, N. (2011). Karya kuzularda sütten kesime kadar yaşama gücü. 7. Ulusal Zootekni Bilim Kongresi, 14-16 Eylül, Adana, 251.

Yilmaz, O., Karaca, O. (2012). Paternity analysis with microsatellite markers in Karya sheep. Kafkas Üniversitesi Veteriner Fakültesi Dergisi, 18(5), 807-813.

Yılmaz, O., Cemal, İ., Karaca, O., Ata, N. (2013a). Genetic diversity of Karya and Çine Çaparı sheep. Scientific Papers Series D. Animal Science, 56, 31-35.

Yilmaz, O., Cemal, İ., Karaca, O. (2013b). Estimation of mature live weight using some body measurements in Karya sheep. Tropical Animal Health and Production, 45(2), 397-403.

[1] Adnan Menderes University, Faculty of Agriculture, Department Of Animal Science, Aydin, TURKEY
*Corresponding author: oyilmaz@adu.edu.tr

International Conference on Science and Technology

ICONST 2018

5-9 September 2018 Prizren - KOSOVO

Genetic Diversity and Bottleneck Analysis of Three Different Sheep Breeds in Turkey

Onur Yılmaz[1*], İbrahim Cemal[1], Nezih Ata[1], Orhan Karaca[1]

Abstract: The present study was performed to reveal genetic variability, population structure and potential genetic bottleneck in Chios (CH), Gökçeada (GA), and Çine Çaparı (CC) sheep breeds raised in different regions of Turkey using genotypes for thirteen microsatellite markers. The animal material of the study consisted of 121 animals from CH (n=61), GA (n=30), and CC (n=30) sheep breeds. A total 310 alleles observed for thirteen microsatellites used in this study. The highest number of alleles (36) and effective number of alleles (18.64) were monitored at OarJMP29 locus. It can be said that all microsatellites were highly informative when the PIC values that ranging from 0.89 (OarFCB20) to 0.97 (OarJMP29) were examined. The overall mean of F_{IS}, F_{IT} and F_{ST} values, which are important parameters in describing population characteristics, were found as 0.125, 0.231 and 0.121, respectively. The mean of observed and expected heterozygosity were 0.66 and 0.87, respectively. All the microsatellites studied deviated from the Hardy-Weinberg equilibrium ($P<0.05$). The value obtained for the global coefficient of gene differentiation showed that the majority of the total genetic variation is due to individual differences (89.00%). The genetic polymorphism statistics obtained from the present study indicated that the total analyzed population is characterized by noticeable genetic variability. The expected numbers of loci with heterozygosity excess in CH, GA and CC sheep breeds were found to be 7.71 ($P>0.05$), 7.76 ($P<0.05$) and 7.61 ($P<0.05$) in Two Phase Model of Mutation (TPM) in the Wilcoxon rank test. TPM values in Wilcoxon rank test and Mode shift graph indicated absence of bottleneck in sheep populations studied.

Keywords: Microsatellites, population structure, genetic diversity, bottleneck

Introduction

Turkey, located in Fertile Crescent, which is regarded as the first domestication center of the sheep by archaeozoological evidence, has a considerable diversity of sheep breeds (Koban, 2004; Meadows et al., 2006; Zeder, 2008). Although there are many different sheep breeds and their crossbred varieties in Turkey, only twenty sheep breeds have been officially registered by the Republic of Turkey Ministry of Food Agriculture and Livestock General Directorate of Agricultural Research and Policy (GDAR, 2011). Indigenous animal breeds that are very well adapted to the ecological and economic conditions of different geographies all over the world, is one of the most important milestones of animal breeding (Abdelkader et al., 2018; Cemal et al., 2013; Yilmaz et al., 2013). The identification of genetic diversity and the genetic characterization of breeds are quite vital for animal breeding and genetic resource conservation programs. Chios (known and called as Sakız in Turkey), Gökçeada and Çine Çaparı sheep breeds, which has unique characteristics such as high fertility, ability to adapt to poor conditions, high survival rate and high milk production, are important native sheep breeds raised along the coastline of the Aegean region (Cemal et al., 2013; Yilmaz et al., 2014; Yilmaz et al., 2015).

In recent years, there have been incredible developments in the science of molecular biology and statistics. This situation has enabled us to have an important knowledge accumulation in the field of animal science

[1]Aydın Adnan Menderes University, Faculty of Agriculture, 09010, Aydın, TURKEY
*Correspondingauthor: oyilmaz@adu.edu.tr

(Montaldo and Meza-Herrera, 1998; Dekkers and Hospital 2002). Especially, molecular genetic technologies has made possible the identification of animal genetic diversity and to discover new genes related to animal production. In developed countries, these methods began to be widely used to assist animal breeding studies. In particular, microsatellites markers specific to DNA regions are valuable molecular genetic marker due to their dense distribution in the genome, great variation, codominant inheritance and easy genotyping. Microsatellites identifying genetic diversity at the DNA level, have been extensively used in parentage testing, linkage analysis, population genetics, bottleneck tests and other genetic studies (Bruford et al., 1996; Montaldo and Meza-Herrera, 1998; Beuzen et al., 2000; Gündüz et al., 2016).

The aims of the present study was to determine the genetic variability, structure of population and potential genetic bottleneck in Chios, Gökçeada, and Çine Çaparı sheep breeds raised in different regions of Turkey using genotypes for thirteen microsatellite markers.

Material and Methods

Animal material and DNA extraction

All experimental procedures were achieved according to the Animal Care and Ethics rules in presented article. The animal material of the study consisted of 121 animals from Chios (CH), Gökçeada (GA), and Çine Çaparı (CC) sheep breeds (Table 1). Blood samples collected from jugular vein into tubes containing K3EDTA as coagulant were stored at -20 °C until DNA extraction. Genomic DNA was isolated from blood samples using the isolation kit (Applied Biological Materials Inc., Canada) according to the manufacturer's instructions. Subsequently, the quality and quantity of the DNA sample were checked using NanoDrop 2000 (Thermo Scientific, Waltham, MA).

Table 1. Origin and size of samples from sheep breeds

Breeds	Abbreviations	Sample Size	Location
Chios (Sakız)	CH	61	Aydın
Gökçeada	GA	30	Bandırma
Çine Çaparı	CC	30	Aydın

Polymerase chain reaction and fragment analysis

Polymerase chain reaction (PCR) were implemented in a total of 20 µl volume including 0.10 µM for each forward and reverse primers, 0.20 mM dNTPs, 2.0 mM $MgCl_2$, 1X PCR buffer, 1 U of Taq DNA polymerase (Applied Biological Materials Inc.) and ~50 ng of genomic DNA.

Thirteen microsatellite markers, recommended by FAO (2011), used to reveal genetic diversity, population structure and bottleneck test. Microsatellites combined in 2 multiplex groups and amplified with Touchdown PCR reported by Hecker and Roux (1996) (Table 2).

Table 2. Amplification conditions for touchdown PCR protocol

Multiplex Group	Loci	I. Denaturation	Denaturation	Annealing	Extension	Cycles	Final Extension
M1	OarFCB193 OarFCB304 INRA0023 OarFCB20 OarAE0129 OarCP34 INRA0132 BM1818 D5S2	95 °C (5 min)	95 °C (40 s)	60-50 °C (40 s)	72 °C (60 s)	30	72 °C (10 min)
M2	BM8125 MCM0527	95 °C (5 min)	95 °C (40 s)	60-50 °C (40 s)	72 °C (60 s)	30	72 °C (10 min)

OarFCB128	
OarJMP29	

Beckman Coulter GeXP genetic analyzer (Beckman Coulter, Inc., USA) was used for the separation and sizing of the PCR fragments. GenomeLab™ DNA Size Standard Kit 400 was used for determination of fragment size.

Statistical Analysis

The polymorphism statistics such as number of alleles per locus (Na), mean number of alleles (MNa), effective number of alleles (Ne), observed heterozygosity (Ho), expected heterozygosity (He) and Hardy–Weinberg equilibrium were calculated using GenAlEx (Peakall and Smouse, 2012) and POPGENE (Yeh et al., 1997). Polymorphic information content (PIC) and null allele frequencies were calculated using CERVUS 3.0.3 (Marshall et al., 1998; Kalinowski et al., 2007), while Wright's F-statistics (F_{IT}, F_{IS}, F_{ST}) (Weir and Cockerham, 1984; Wright, 1990) were obtained with POPGENE 1.32 (Yeh et al., 1997). Population 1.2.32 (Langella, 1999) and FigTree 1.4.2. (Rambout, 2006) software were used to generate phylogenetic tree between breeds according to Nei's Da distance matrix (Nei et al., 1983). Robustness of the dendrogram topology was tested by bootstrap resampling (n=1000). FSTAT version 2.9.3 software (Goudet, 2001) was used to obtain values belong to genetic diversity statistics such as Nei's diversity between breeds (D_{ST}) and coefficient of gene differentiation (G_{ST}).

Bottleneck events were tested with Sign, Standardized differences and Wilcoxon sign–rank tests under the different mutation models such as Infinite Allele Model (IAM), Stepwise Mutation Model (SMM), and Two Phase Model of Mutation (TPM) model in Bottleneck software version 1.2.02 (1 000 simulation) (Piry et al., 1999).

Results

A total 310 alleles observed for thirteen microsatellites used in this study. Genetic diversity statistics were given in Table 3.

Table 3. Genetic diversity parameters of the thirteen investigated loci in all sheep breeds studied

Loci	Na	Ne	Ho	He	PIC	D_{ST}	G_{ST}	$F_{IS}^{\#}$	$F_{IT}^{\#}$	$F_{ST}^{\#}$	F(Null)	HWE
OarFCB304	31	16.06	0.65	0.94	0.95	0.099	0.106	0.364	0.439	0.119	0.0124	***
OarFCB193	28	6.42	0.83	0.84	0.93	0.089	0.102	-0.094	0.030	0.113	0.0013	***
INRA0023	26	12.69	0.66	0.92	0.94	0.096	0.105	0.435	0.502	0.119	0.0147	***
OarFCB20	20	4.59	0.63	0.78	0.89	0.210	0.267	-0.037	0.246	0.273	-0.0212	***
OarAE129	15	3.86	0.54	0.74	0.90	0.016	0.022	0.212	0.238	0.033	0.1678	***
BM1818	19	4.95	0.38	0.80	0.92	0.233	0.305	0.315	0.532	0.316	0.0876	***
INRA0132	27	16.45	0.74	0.94	0.95	0.062	0.066	0.128	0.195	0.077	0.0867	***
OarCP34	17	10.85	0.88	0.91	0.94	0.085	0.094	-0.114	-0.002	0.101	0.0052	***
D5S2	17	6.43	0.58	0.84	0.92	0.118	0.137	0.159	0.283	0.148	0.1806	***
MCM0527	21	6.70	0.74	0.85	0.93	0.043	0.049	0.058	0.114	0.060	0.0309	***
BM8125	25	7.68	0.75	0.87	0.92	0.045	0.052	0.037	0.097	0.062	-0.0029	***
OarFCB128	28	9.56	0.63	0.90	0.93	0.064	0.074	0.182	0.251	0.084	0.0197	***
OarJMP29	36	18.64	0.84	0.95	0.97	0.080	0.084	-0.009	0.085	0.093	0.0086	***
Overall	23.85	9.61	0.66	0.87	0.93	0.095	0.110	0.125	0.231	0.121		

Na: number of alleles, Ne: effective number of alleles, Ho: observed heterozygosity, He: expected heterozygosity, PIC: polymorphic information content, D_{ST}: the diversity between breeds, G_{ST}: coefficient of gene differentiation $^{\#}$ Wright's F-statistics (Weir and Cockerham, 1984), F(Null): null allele frequency, HWE: Hardy-Weinberg Equilibrium, *** P<0.001

The highest number of alleles (36) and effective number of alleles (18.64) were monitored at OarJMP29 locus. It was determined that all microsatellites were highly informative when the PIC values that ranging

from 0.89 (OarFCB20) to 0.97 (OarJMP29) were examined. D_{ST} revealing the diversity between breeds and G_{ST} described as the coefficient of gene differentiation values were found as 0.095 and 0.110, respectively. The overall mean of F_{IS}, F_{IT} and F_{ST} values, which are important parameters in describing population characteristics, were found as 0.125, 0.231 and 0.121, respectively. The thirteen microsatellite loci used in the study were tested using the χ^2 test in terms of compliance with Hardy-Weinberg equilibrium (HWE). The χ^2 test findings demonstrated that the allele distributions of all microsatellite markers deviated from the Hardy-Weinberg equilibrium ($P<0.05$). The null allele frequency values obtained from the studied microsatellite loci were below 20%.

Genetic polymorphism parameters belong to three autochthonous Turkish sheep breeds raised in different regions were given in Table 4.

Table 4. Genetic diversity parameters per breed across 13 microsatellites studied

Breeds	MNa	$\hat{H}$		F_{IS}	HWE
		Ho	He		
GA	8.08	0.65	0.74	0.135	8
CH	19.08	0.62	0.84	0.265	13
CC	8.85	0.72	0.70	-0.015	2

GA: Gökçeada, CH: Chios (Sakız), CC: Çine Çaparı, MNa: Mean number of alleles, $\hat{H}$: Average heterozygosity, Ho: mean observed heterozygosity, He: mean expected heterozygosity, F_{IS}: within-breed heterozygote deficiency, HWE: number of loci not in the Hardy-Weinberg equilibrium ($P < 0.05$)

The lowest and highest number of alleles were observed in CH (19.08) and GA (8.08) breeds, respectively, while the highest observed heterozygosity value (0.72) was calculated in CC breed. F_{IS} which is also known as the inbreeding coefficient and measures the reduction in heterozygosity, varied between -0.015 (CC) and 0.265 (CH). The dendrogram revealed two clusters (Figure 1). The first cluster was consisted by Gökçeada and Chios sheep breeds and the second cluster was formed by Çine Çaparı sheep breed conserved as a genetic resource.

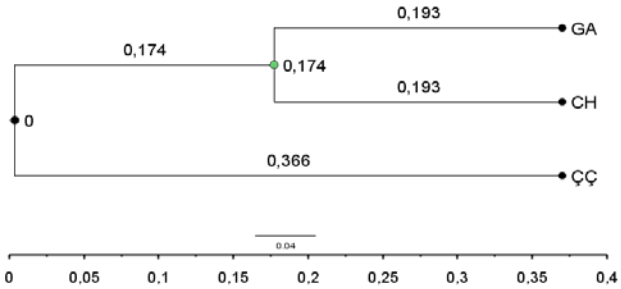

Figure 1. Dendrogram based on Nei's Da (Nei 1983) distance matrix among three native sheep breeds (bootstrap resampling methodology, 1000 replicates)

Genetic bottleneck analysis was performed to investigate whether there was a bottleneck in Chios, Gökçeada and Çine Çapari sheep breeds. The data set obtained was tested according to three different mutation models known as Infinite Allele Model (IAM), Stepwise Mutation Model (SMM), and Two Phase Model of Mutation (TPM) model reported by Cornuet and Luikart (1996), Luikart and Cornuet (1998) and Piry et al., (1999). (Table 5).

Table 5. Test for null hypothesis under three microsatellite evolution models for bottleneck analysis

Breeds	Mutation Models	Sign test			Standardized differences test		Wilcoxon rank test (one tail for H excess)
		Hee	He	P	T2	P	P
GA	IAM	7.71	10	0.156	1.95	0.026	0.0199
	TPM	7.75	10	0.161	-0.16	0.438	0.2487
	SMM	7.73	5	0.105	-3.91	0.000	0.9761

	IAM	7.87	8	0.591	-0.220	0.413	0.4197
SZ	TPM	7.76	3	0.008	-5.784	0.000	0.9980
	SMM	7.78	1	0.000	-13.02	0.000	0.9998
	IAM	7.71	7	0.446	0.53	0.297	0.3178
CC	TPM	7.61	5	0.118	-2.08	0.019	0.9161
	SMM	7.57	3	0.011	-6.27	0.000	0.9985

GA: Gökçeada, SZ: Sakız, CC: Çine Çaparı, IAM: The infinite allele model, TPM: Two-phase mutation model, SMM: The stepwise mutation model, Hee: Expected number of loci with heterozygosity excess, He: heterozygosity excess

The expected numbers of loci with heterozygosity excess in Gökçeada, Chios and Çine Çapari were found to be 7.75 (P>0.05), 7.76 (P<0.05) and 7.61 (P<0.05) in TPM in the Wilcoxon rank test. As it can be seen from mode-shift graph, a L-shaped chart consistent with the distribution ranges of the normal frequency class was obtained in the bottleneck test performed for the studied populations.

A mode-shift graph was obtained using allele frequency classes of 13 microsatellite to identify potential bottlenecks in the studied populations as a second method (Figure 2). As it can be seen from mode-shift graph, a L-shaped chart consistent with the distribution ranges of the normal frequency class was obtained in the bottleneck test performed.

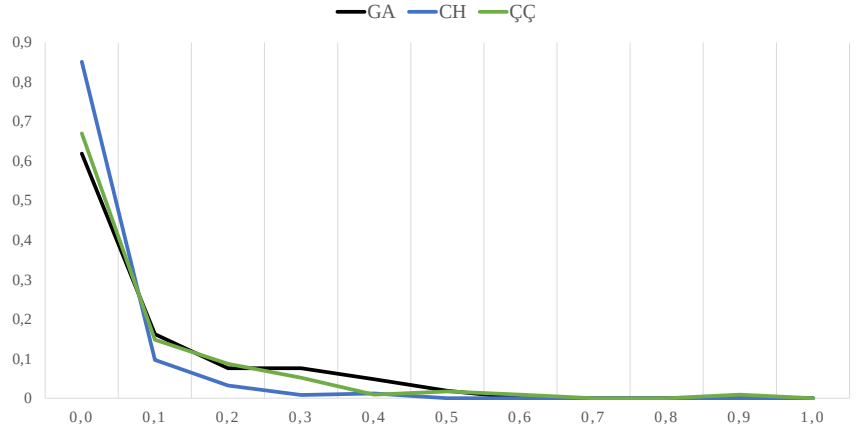

Figure 2. Mode-shift graph for bottleneck in the Gökçeada (GA), Chios (CH) and Çine Çaparı (ÇÇ) sheep breeds

Discussion and Conclusions

The mean allele numbers and PIC values indicate that the breeds studied have high genetic diversity. It can be regarded as an important indicator of the success of the microsatellites used to reveal genetic diversity. The molecular genetic parameters such as number of allele, effective allele number, polymorphic information content, Ho and He were higher than values reported in the previous studies (Cemal et al., 2013; Yilmaz et al., 2014; Yilmaz et al., 2015; Kavitha et al., 2015; Salamon et al., 2015; Arora et al., 2016; Guang-Xin et al., 2016). Similar findings for Ho and He values have been expressed in the previous literature conducted in Turkish native and foreign sheep breeds (Grigaliunaite et al., 2013; Yilmaz et al., 2014;) while these values lower than the values reported by Abdelkader et al., (2018). These differences with the literature is thought to be due to the difference in the number of microsatellites and sampling methodology used in this study.

F_{IS} values, which is a measure of the deviation of genotypic frequencies from panmixia in populations in terms of heterozygous deficiency or excess, showed that loss of heterozygosity at four microsatellite loci (OarFCB193, OarFCB20, OarCP34 and OarJMP29) studied. Similar findings have been expressed in the previous literature conducted in different goat breeds (Salamon et al., 2015; Loukovitis et al., 2016; Othman et al., 2016).

The global F_{ST} value (0.121) was lower than the values stated in the earlier studies (Mukesh et al., 2006; Arora et al., 2011), but higher than that reported in other literature (Santos-Silva et al., 2008; Cemal et al., 2013; Ocampo et al., 2016; Sassi-Zaidy et al., 2016). This finding can be interpreted as a sign that the genetic diversity among populations is relatively low. The global G_{ST} value showed that 89.00% of the total genetic variation can be explained by genetic differences among individuals. It can be accepted that the overall genetic diversity value (D_{ST}) obtained from the present study was an indication that the inter-population variability is not high. The χ^2 test results showed that allele distributions of thirteen microsatellite markers studied were not in the Hardy-Weinberg equilibrium. It is expected results that the studied loci will deviate from the Hardy-Weinberg equilibrium because of the selection and conservation studies which are carried out in the populations studied. Observed null allele frequencies for the all microsatellites below the critical value (20%) reported by Dakin and Avise (2004) indicated that these markers studied can be used confidently to identify genetic diversity in these native sheep breeds.

In the present study, the calculated MNa value belonging to Chios sheep breed was found to be higher than the values stated in some studies on the same breeds (Yilmaz et al. 2014; Yilmaz et al. 2015) while the values obtained from CC and GA sheep breed was lower than the values reported in the earlier studies (Cemal et al., 2013; Yilmaz et al., 2015). Expected heterozygosity (He) values for GA, CH and ÇÇ sheep breeds were lower than the values obtained from Algerian (Abdelkader et al. 2018) and Greek (Loukovitis et al., 2016) native sheep breeds. This is thought to be due to the difference in the number of microsatellites and sampling methodology used in this study. F_{IS} value, defined as inbreeding coefficient, indicated that there is no loss of heterozygosity in populations except CC sheep breed. The χ^2 test results revealed that the 8, 13 and 2 microsatellite loci deviated from the Hardy-Weinberg equilibrium in the Gökçeada, Chios and Çine Çaparı sheep populations, respectively. Deviations from the Hardy-Weinberg equilibrium should be regarded as a natural consequence of the animal breeding and genetic conservation activities that have been practiced in the populations for many years.

It is known that the infinite allele model (IAM) and the stepwise mutation models (SMM) cause inconsistent results in studies using microsatellites. Therefore, it is reported that the two-phase mutation model (TPM) is the most useful model to test the heterozygosity excess in the bottleneck tests performed with microsatellites (Dirienzo et al., 1994; Luikart et al., 1998; Piry et al., 1999). On the other hand, it has been reported that the Wilcoxon test, which has high statistical confidence even in bottleneck analysis studies using a limited number of loci (<20), can be used with high confidence in bottleneck studies (Piry et al., 1999).
The population studied was found to be bottlenecked by the Wilcoxon test according to the infinite allele model (IAM). But it should not be forgotten that the most suitable model for microsatellites in the Wilcoxon test is the TPM model. In this context, it can be said that serious demographic bottlenecks have not been experienced in the sheep populations studied given that considering the TPM model of Wilcoxon test results. The mode shift graph method, which is a qualitative graphical representation of the allele frequency distribution, was first proposed by Luikart et al. (1998). The "L-shaped distribution" of the allele frequency distribution graph is used as a criterion for the bottleneck. If the graph shows the normal distribution (L-shaped), then the mutation-migration balance is concerned. Obtained L-shaped distribution suggests that there is not a genetic bottleneck in the studied populations that is large enough to be considered recently (last 40-80 generations).

In conclusion, the present study has revealed an important knowledge about the genetic diversity and the relationship between three sheep breeds raised in diferent region in Turkey. Consequently, the present study results indicated that genetic diversity was significantly high in the gene pool belonging to sheep breeds studied. It can be said that microsatellites used in the study have a high potency for the determination of genetic diversity and bottleneck in the studied breeds. Obtained results will help to interpret the genetic structure of native sheep and will be of benefit to the efforts for animal breeding and genetic conservation studies. The strong inference that the sheep breeds studied have not undergone major bottlenecks is also important for sheep breeders and animal breeding program or conservation programs implemented.

Acknowledgements

Authors would like to express their gratitude to the Agricultural Biotechnology and Food Safety Application and Research Centre (ADÜ-TARBİYOMER) of Adnan Menderes University for providing laboratory facilities to carry out molecular genetic analyses.

References

Ameur, A., Ata, N., Benyoucef, M.T., Djouat, A., Azzi, N., Yilmaz, O., Cemal, İ., Gaouar, S.B.S. (2018). New genetic identification and characterization of twelve Algerian sheep breeds by microsatellite markers. Italian Journal of Animal Science, 17(1), 38-48.

Arora, R., Kulkarni, V. S., Jain, A., Yadav, D. K. (2016). Yalaga sheep-A microsatellite based genetic profile. The Indian Journal of Animal Sciences, 86(10).

Arora, R. J., Bhatia, S., Mishra, B. P., Jain, A., Prakash, B. (2011). Diversity analysis of sheep breeds from Southern peninsular and Eastern regions of India. Tropical Animal Health and Production, 43(2), 401-408.

Cemal, İ., Yilmaz, O., Karaca, O., Binbaş, P., Ata, N. (2013). Analysis of genetic diversity in indigenous Çine Çaparı sheep under conservation by microsatellite markers. Kafkas Üniversitesi Veteriner Fakültesi Dergisi, 19(3), 383-390.

Cornuet, J.M., Luikart, G., (1996). Description and power analysis of two tests for detecting recent population bottlenecks from allele frequency data. Genetics, 144(4), 2001-2014.

Dakin, E.E., Avise, J.C. (2004). Microsatellite null alleles in parentage analysis. Heredity, 93, 504-509.

Dekkers, J.C., Hospital, F. (2002). Multifactorial genetics: The use of molecular genetics in the improvement of agricultural populations. Nature Reviews Genetics, 3(1), 22-32.

Dirienzo, A., Peterson, A.C., Garza, J.C., Valdes, A.M., Slatkin, M., Freimer, N.B. (1994). Mutational processes of simple-sequence repeat loci in human-populations. Proceedings of the National Academy of Sciences, 91(8), 3166-3170.

FAO (2011). Molecular genetic characterization of animal genetic resources, FAO, Rome.

GDAR (2011). Domestic animal genetic resources in Turkey. Republic of Turkey Ministry of Food Agriculture and Livestock General Directorate of Agricultural Research and Policy. http://www.tagem.gov.tr (Access date: 10.05.2012)

Grigaliunaite, I., Tapio, M., Viinalass, H., Grislis, Z., Kantanen, J., Miceikienė, I. (2003). Microsatellite variation in the Baltic sheep breeds. Veterinarija ir zootechnika, 21, 43.

Goudet, J. (2001). FSTAT, a program to estimate and test gene diversities and fixation indices (version 2.9. 3). Available via http://www.unil.ch/popgen/softwares/fstat.htm (Access date: 02.03.2005).

Guang-Xin, E., Zhong, T., Ma, Y.H., Gao, H.-J., He, J.N., Liu, N., Zhao, Y.J., Zhang, J.H., Huang, Y.F. (2016). Conservation genetics in Chinese sheep: diversity of fourteen indigenous sheep (Ovis aries) using microsatellite markers. Ecology and Evolution, 6, 810–817.

Gündüz, Z., Yılmaz, O., Cemal, İ., Biçer, O., 2016. A comparison of old and modern type DNA marker technologies and their impact on animal breeding programs. Iğdır Üni. Fen Bilimleri Enst. Der. 6(2): 175-180.

Hecker, K.H., Roux, K.H. (1996). High and low annealing temperatures increase both specifity and yield in touchdown and stepdown PCR. Biotechniques, 20, 478-485.

Kalinowski, S.T., Taper, M.L., Marshall, T.C. (2007). Revising how the computer program CERVUS accommodates genotyping error increases success in paternity assignment. Molecular Ecology ,16, 1099-1106.

Kavitha, S. T., Subramanian, A., Sivaselvam, S. N., Thiagarajan, R., Balasubramanian, S. (2015). Genetic characterisation of Tiruchy Black sheep of Tamil Nadu using microsatellite markers. Indian Journal of Animal Research, 49(3), 320-324.

Koban, E. (2004). Genetic diversity of native and crossbreed sheep breeds in Anatolia. PhD. Thesis, Department of Biology, Middle East Technical University, pp.125.

Langella, O. (1999). Populations 1.2.32 http://bioinformatics.org/tryphon/populations/ (Acces date: 09.07.2015).

Luikart, G., Allendorf, F.W., Cornuet, J.M., Sherwin, W.B. (1998). Distortion of allele frequency distributions provides a test for recent population bottlenecks. Jorunal of Heredity, 89(3), 238-247.

Luikart, G., Cornuet, J.M. (1998). Empirical evaluation of a test for identifying recently bottlenecked populations from allele frequency data. Conservation Biology, 12(1), 228-237.

Loukovitis, D., Siasiou, A., Mitsopoulos, I., Lymberopoulos, A. G., Laga, V., Chatziplis, D. (2016). Genetic diversity of Greek sheep breeds and transhumant populations utilizing microsatellite markers. Small Ruminant Research, 136, 238-242.

Marshall, T.C., Slate, J., Kruuk, L.E.B., Pemberton, J.M. (1998). Statistical confidence for likelihood-based paternity inference in natural populations. Molecular Ecology, 7, 639-655

Meadows, J.R., Cemal, I., Karaca, O., Gootwine, E., Kijas, J. (2006). Five ovine mitochondrial lineages identified from sheep breeds of the near East. Genetics, 175(3), 1371-1379.

Montaldo, H.H., Meza-Herrera, C.A. (1998). Use of molecular markers and major genes in the genetic imrovement of livestock. Electronic Journal of Biotechnology, 1, 83-89.

Mukesh, M., Sodhi, M., Bhatia, S. (2006). Microsatellite -based diversity analysis and relationships of three Indian sheep breeds. Journal of Animal Breeding and Genetics, 123(4), 258-264.

Nei, M., Tajima, F., Tateno, Y. (1983). Accuracy of Estimated Phylogenetic Trees from Molecular-Data .2. Gene-Frequency Data. Journal of Molecular Evolution, 19, 153-170.

Ocampo, R., Cardona, H., Martínez, R. (2016). Genetic diversity of Colombian sheep by microsatellite markers. Chilean Journal of Agricultural Research, 76(1), 40-47.

Othman, O.E.M., Payet-Duprat, N., Harkat, S., Laoun, A., Maftah, A., Lafri, M., Da Silva, A. (2016). Sheep diversity of five Egyptian breeds: Genetic proximity revealed between desert breeds: Local sheep breeds diversity in Egypt. Small Ruminant Research, 144, 346-352.

Peakall, R., Smouse, P.E. (2012). GenAlEx 6.5: genetic analysis in Excel. Population genetic software for teaching and research – an update. Bioinformatics, 28, 2537-2539.

Piry, S., Luikart, G., Cornuet, J.M. (1999). BOTTLENECK: A computer program for detecting recent reductions in the effective population size using allele frequency data. Journal of Heredity 90(4), 502-503.

Rambout, A. (2006). FigTree 1.4.2 http://tree.bio.ed.ac.uk/ (Acces date: 09.07.2015).

Salamon, D., Gutierrez-Gil, B., Simcic, M., Kompan, D., Dzidic, A. (2015). Microsatellite based genetic structure of regional transboundary Istrian sheep breed populations in Croatia and Slovenia. Mljekarstvo/Dairy, 65(1), 39-47.

Santos-Silva, F., Ivo, R.S., Sousa, M.C.O., Carolino, M.I., Ginja, C., Gama, L.T. (2008). Assessing genetic diversity and differentiation in Portuguese coarse-wool sheep breeds with microsatellite markers. Small Ruminant Research, 78(1), 32-40.

Sassi-Zaidy, Y.B., Maretto, F., Charfi-Cheikhrouha, F., Mohamed-Brahmi, A., Cassandro, M. (2016). Contribution of microsatellites markers in the clarification of the origin, genetic risk factors, and implications for conservation of Tunisian native sheep breeds. Genetics and Molecular Research, 15(1).

Yeh, F.C., Yang, R. Boyle, T.(1997). POPGENE Version 1.32. Agriculture for Molecular Biology and Biotechnology Centre, University of Alberta and Center for International Forestry Research, Canada

Yılmaz, O., Sezenler, T., Sevim, S., Cemal, İ., Karaca, O., Yaman, Y., Karadağ, O. (2015). Genetic relationships among four Turkish sheep breeds using microsatellites. Turkish Journal of Veterinary and Animal Sciences, 1411(46), 576-582.

Yilmaz, O., Cemal, İ., Karaca, O. (2014). Genetic diversity in nine native Turkish sheep breeds based on microsatellite analysis. Animal Genetics, 45(4), 604–608.

Yılmaz, O., Cemal, İ., Karaca, O., Ata, N. (2013). Genetic diversity of Karya and Çine Çaparı sheep. Scientific Papers Series D. Animal Science, 56, 31-35.

Weir, B.S., Cockerham, C.C. (1984). Estimating F-statistics for the analysis of population-structure. Evolution, 38(6), 1358-1370.

Wright, S. (1990). Evolution in Mendelian Populations (Reprinted from Genetics, Vol 16, Pg 97-159, 1931). Bulletin of Mathematical Biology, 52, 241-295.

Zeder, M.A. (2008). Domestication and early agriculture in the Mediterranean Basin: Origins, diffusion, and impact. Proceedings of the National Academy of Sciences, 105(33), 11597-11604

International Conference on Science and Technology

ICONST 2018

5-9 September 2018 Prizren - KOSOVO

Solving Electromagnetic Scattering Integral Equations Using Monte Carlo Integration Technique

Fadil Kuyucuoglu[1]*

Abstract: In this study, electromagnetic scattering integral equations are solved using Monte Carlo Integration technique. Scattering from a planar, infinitely long, perfectly conducting, strip geometry is considered. E-polarized plane wave incidence is taken as a source. Unknown current coefficients are obtained using Monte Carlo Integration technique and matrix inversion process. First, integral equations are converted to discrete domain using Method of Moments (MoM). In Method of Moments calculations, singularity problems arise. Calculation of these integrals requires some other techniques. In our problem, firstly geometry is discretized into small regions in one dimension. Integral equation is transformed to matrix equation using MoM. Subdomain basis functions are utilized due to small electrical size of the scatterer. Integrals are evaluated using Monte Carlo Integration. Matrix equations are obtained. Unknown current distribution on the scatterer is evaluated using matrix inversion. MoM solution with numerical integral calculation and proposed method calculations are compared. Singularity problems are removed using the proposed method. Current distribution pattern is calculated very fast. More complex geometries could be solved very efficiently with this method. Monte Carlo integration nature gives to evaluate multidimensional integral equations very rapidly. Also singularity problems are avoided. During integration calculations, high performance is observed. Large electrical dimensions can be analysed very fast.

Keywords: Scattering, Monte Carlo Integration, Method of Moments, Current distribution

Introduction

Electromagnetic scattering is one of the major topics in electromagnetics. Various geometries such as strip, cylindirical, spherical conducting material scattering are studied in the literature (Arnold, 2006; Ruppin, 2006a; Ruppin, 2006b) . Some techniques are employed for the solution of the scattering problems. Method of Moments (MoM) is a widely used technique which involves expanding the unknown current density on the scattering object. Geometry is discretized and subdomain or entire domain known basis functions are utilized. In electrically small problems, subdomain basis functions are used. During evaluation of integrals for each matrix elements, singularity problems may arise. Some analytical or semi-analytical techniques play important role for the singularity treatments. Monte Carlo Integration (MCI) is a calculation tool in numerical integration using statistics. In MCI, points on the scatterer are randomly generated. Integrals are basic sum of functional values averages. MCI exhibits very fast and efficient solutions. Singular points are avoided by excluding sample point in the singularity region.

[1]Manisa Celal Bayar University, Faculty of Engineering, Electrical-Electronics Eng. Dept., Yunus Emre, 45140, Manisa, TURKEY
*Corresponding author: fadilkuyu@gmail.com

Material and Method

Firstly, electric field integral equation (EFIE) is written in equation (1) (Mishra et al., 2008)

$$E^s = 1/(j\omega\varepsilon_0\mu_0)[\nabla(\nabla\cdot\vec{A}) + k^2\vec{A}] \quad (1)$$

where E^s is the scattered electric field, A is vector potential given as

$$\vec{A}(\vec{r}) = \mu\int \vec{J}(r')G(r,r')dr' \quad (2)$$

G(r,r') is defined as Green function (Cay, 2005) . In two dimensional problems, Green function is Hankel function. Unknown current density (J) can be expanded to known functions with unknown coefficients to be determined. Since strip is located in x direction, J is in the same direction. Strip width is selected as w and length of the strip is infinite in the z direction.

$$J(x') = \sum_{n=1}^{M} a_n f_n(x') \quad (3)$$

Using boundary conditions and inner product operations, equation (1) is transformed into a matrix equation given in equation (4).

$$Z_{MxM}\, a_{Mx1} = B_{Mx1} \quad (4)$$

In MoM calculations, every element in Z matrix is evaluated numerically using MCI technique. In MCI, uniform sampling integration is evaluated sum of functional values of sampled points as in equation (5) (Mishra et al., 2008).

$$\int_C f(x)dx = \frac{C}{N}\sum_{i=1}^{N} f(x_i) \quad (5)$$

Geometry of the problem is given in Fig.1. Strips are defined as perfectly conducting material with zero thickness and infinitely long in the z axis. Width of the strip is chosen as w. This width is normalized with wavelength of the incident wave.

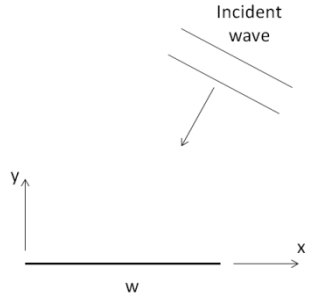

Figure 1. Problem Geometry

Results

When E-polarized plane wave is incident on the strip with incidence angle θ, surface currents induce on the object. Evaluating these currents on the scatterer strip is the key problem of this study.

Surface current distibution on scatterer is plotted in Figure 2 both for MoM and MCI methods. In MoM, integrals are evaluated numerically. In MCI, MoM formulation used but instead of numerical integration, MCI method is utilized. It is seen that both method results are very close. In Fig.2, number of segments are chosen as 20, width of the strip w=1λ, incidence angle is 45°. Number of random points is chosen as 200 for each segment in MCI.

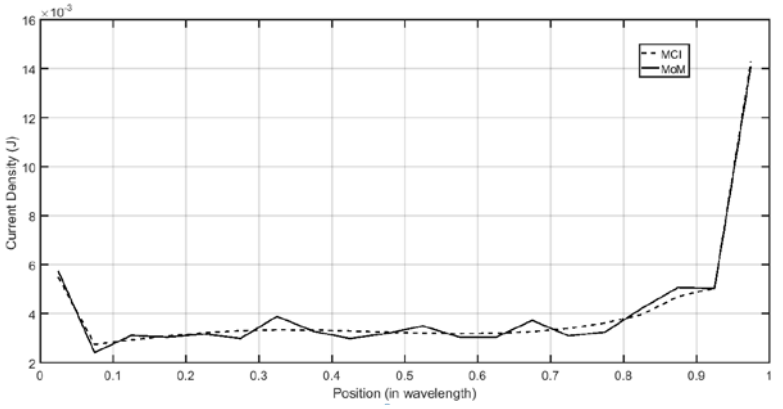

Figure 2. Surface current density distribution on the scatterer for MoM and MCI methods.

Increasing number of segments gives better results for MoM. More random points in each segments in MCI integration presents more accurate results.

Discussion and Conclusions

In this study, infinitely long, perfectly conducting, finite width strip scattering is analysed. MoM solutions are evaluated with numerically and MCI methods respectively. MoM with numerical integration takes more computation time. MCI technique gives rapid calculation time without singular points. Electrically big problems can be solved with the proposed technique without any difficulties.

Acknowledgements

No acknowledgements.

References

Arnold, M. D. (2006). An efficient solution for scattering by a perfectly conducting strip grating. JEMWA, 20(7), 891‑900.

CAY, Zarife (2005). Uzayda ve çok katmanlı düzlemsel ortamlarda iki boyutlu mükemmel iletken şeritlerden elektromanyetik saçınımın moment metot çözümleri, MSc Thesis.

Mishra, M., Gupta, N. (2008). Singularity treatment for integral equations in electromagnetic scattering using Monte Carlo integration technique, Microwave and Optical Technology Letters, 50(6), 1619-1623.

Ruppin, R., (2006a). Scattering of electromagnetic radiation by a perfect electromagnetic conductor sphere. JEMWA, 20(12), 1569‑1576.

Ruppin, R., (2006b). Scattering of electromagnetic radiation by a perfect electromagnetic conductor cylinder.JEMWA, 20(13), 1853‑1860.

International Conference on Science and Technology

ICONST 2018

5-9 September 2018 Prizren - KOSOVO

Numerical Solution of Laplace Equation For Two Dimensional Geometries

Fadil Kuyucuoglu[1]*

Abstract: In this study, two dimensional electromagnetics Laplace equation numerical solution is presented. Partial differential equations are used to model various engineering problems such as fluid mechanics, heat problems and electromagnetics. Laplace equation is a partial differential equation and its solution is one of the key points in electromagnetics. In our problem, geometry is comprised of 4 conducting walls with known electric potential values. The wall lying along y axis is at some potential and others are at 0 potential. Unknown field variable resides interior region of the walls. Firstly, Laplace equation is written in partial differential equation form with x and y variables. Neumann and Dirichlet boundary conditions are explained. Region is meshed in x-y plane. For each node, difference equation is written and linear equation set is obtained. Gauss-Siedel method is utilized for the solution of node voltages. Since Gauss-Siedel method is an iterative tool, iteration number is chosen a reasonable value. After that, exact solution given as an infinite series sum is used for comparison. Surface and contour plots of two solutions are given as separate figures. Correctness of the method is evaluated and presented in matrix form as the relative error of numerical values of each node voltages and series sum solution values.

Keywords: Laplace equation, Finite difference method, Potential distribution, Numerical calculation

Introduction

Partial differential equations (PDE) are used to model many enginering problems in the literature. Fluid dynamics, heat problems, wave equations contain PDEs. Laplace equation in electrodynamics is a PDE and its solution plays an important role for understanding physical phenemonas. It can be used to analyse problems in electromagnetics, fluid mechanics, heat problems (Patil et al., 2013). Unknown variable may be electrical potential, heat, stress and so on. In this study, unknown potential distribution is solved numerically. Neumann and Dirichlet boundary conditions are given conditions for the solution of the unknown variable.

In 2 dimensions, Laplace equation is given as;

$$\frac{\partial^2 U}{\partial x^2}+\frac{\partial^2 U}{\partial y^2}=0 \qquad (1)$$

where U is the unknown electric potential distribution. Potential values on the boundaries are given as

[1]Manisa Celal Bayar University, Faculty of Engineering, Electrical-Electronics Eng. Dept., Yunus Emre, 45140, Manisa, TURKEY
*Corresponding author: fadilkuyu@gmail.com

$$U = a\,(Dirichlet)$$
$$\frac{\partial U}{\partial n} = b\,(Neumann) \qquad (2)$$

Dirichlet and Neumann boundary conditions. Boundary normal is designated as 'n'.

Material and Method

In order to solve partial differential equation, firstly geometry is meshed in x and y directions. Differential equation is transformed into discrete domain using central finite difference method (Patil et al. 2013).

$$U_{i,j} = \frac{U_{i-1,j} + U_{i+1,j} + U_{i,j-1} + U_{i,j+1}}{4} \qquad (3)$$

For each node in the geometry, equation (3) is written with known and unknown potential values. Finally, a set of linear equations are obtained. Afterthat, solving these linear equations gives the unknown potentials in the geometry. Problem geometry is given in Fig.1. Walls of the structure are conductor with the potentials 0 and 100 Volts. Inside region is free space

.

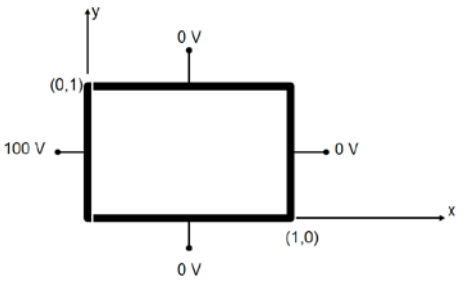

Figure 1. Problem Geometry

Firstly, geometry is meshed with x and y axis with 0.1 interval. Dimension of the region is 1x1 so there will be 9x9 points in the interior region.

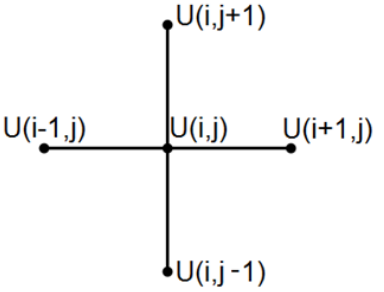

Figure 2. Mesh points in the problem geometry

After writing difference equations for each node using eq(3), linear algebraic equations have to solved using several methods. Gauss-Siedel is chosen to determine node voltages (Ubaidullah et al., 2016). This method uses iterations with initial conditions. After several iterations, node voltages converge. In this paper, 200 iterations applied for the solution.

In order to guarantee correctness of the solution of Gauss- Siedel Metod, potential distribution should be compared with the exact solution. This problem has a solution as a sum of infinite series given in literature (Cheng, 1989).

$$U(x,y)=\frac{4V_0}{\pi}\sum_{n=odd}^{\infty}\frac{\sinh(n\pi(a-x)/b)}{n\sinh(n\pi a/b)}\sin(\frac{n\pi y}{b}) \quad (4)$$

where a=b=1 and V_0=100 V.

Meshing can be done as shown in Fig.3.

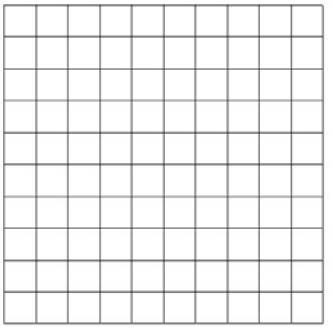

Figure 3. Meshing the problem in two dimensions

Results

After applying Gauss-Siedel Method, one can find the potential values in each node after 200 iterations. Surface plot of the potential distribution is given in Figure 4.

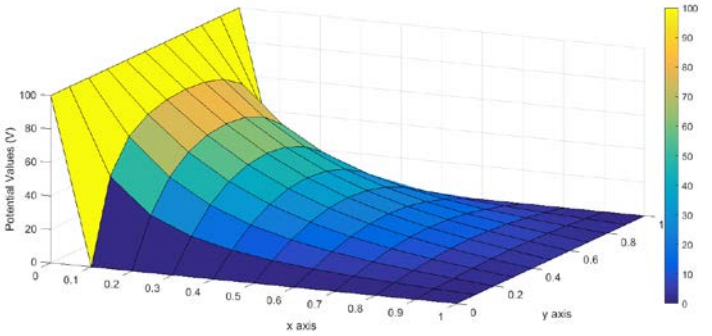

Figure 4. Surface plot of potential distribution

These potential values can be plotted in 2 dimensions. Contour plot of the distribution is presented in Figure 5.

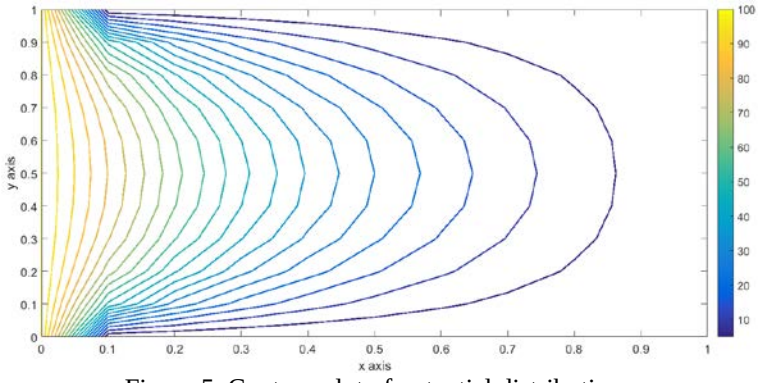

Figure 5. Contour plot of potential distribution

In order to prove the correctness of the method, infinite sum solution results are needed. Using equation (3), surface and contour plots of the potential distributions are given in Figure 6 and 7 respectively. It is seen that both solutions are very close to each other.

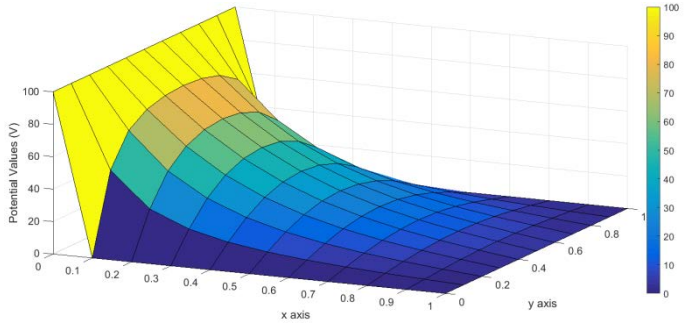

Figure 6. Surface plot of potential distribution using infinite sum solution

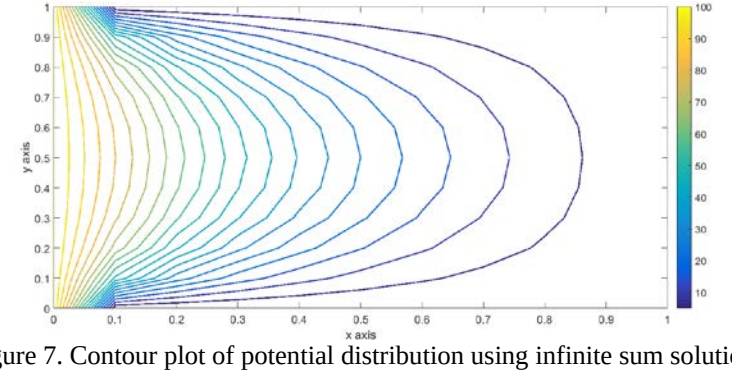

Figure 7. Contour plot of potential distribution using infinite sum solution

Relative error of each node can be obtained using $|U_1-U_2|/U_1$ and is given in Table 1. U_1 is the potential value result of infinite sum solution; U_2 is the result of the finite difference method solution. Very small relative error values are obtained.

Table 1. Relative error of potential values

	j=2	j=3	j=4	j=5	j=6	j=7	j=8	j=9	j=10
i=2	0.000275	0.024775	0.024133	0.019331	0.015664	0.01356	0.012569	0.012216	0.012146
i=3	0.011073	0.00102	0.006028	0.008627	0.009405	0.009768	0.010142	0.010536	0.01084
i=4	0.00671	0.005675	0.001834	0.001584	0.004126	0.006043	0.007527	0.008626	0.009313
i=5	0.004276	0.005724	0.004405	0.001814	0.001001	0.003553	0.005645	0.00719	0.008138
i=6	0.003592	0.005499	0.004954	0.002778	2.58E-09	0.002699	0.004973	0.006664	0.007701
i=7	0.004276	0.005724	0.004405	0.001814	0.001001	0.003553	0.005645	0.00719	0.008138
i=8	0.00671	0.005675	0.001834	0.001584	0.004126	0.006043	0.007527	0.008626	0.009313
i=9	0.011073	0.00102	0.006028	0.008627	0.009405	0.009768	0.010142	0.010536	0.01084
i=10	0.000275	0.024775	0.024133	0.019331	0.015664	0.01356	0.012569	0.012216	0.012146

Discussion and Conclusions

Finite difference solution of the Laplace equation is calculated and compared with exact solution in infinite sum form. Both methods plots are plotted and it is seen that very close results are obtained. Relative error of each mesh point also shows that finite difference approximates solution very well. Bigger and complex geometries can be solved using the proposed method easily and effectively.

Acknowledgements

No acknowledgements.

References

Cheng, D.K., Field and Wave Electromagnetics, Addison-Wesley, Second Edition, 1989.

Patil, P.V., Prasad, J.S.V.R.K. (2013). Numerical Solution for Two Dimensional Laplace Equation with Dirichlet Boundary Conditions. IOSR Journal of Mathematics (IOSR-JM), 6(4), 66-75.

Ubaidullah, Chandio, M.S. (2016). Finite Difference Method with Dirichlet Problems of 2D Laplace's Equation in Elliptic Domain. Pakistan Journal of Engineering, Technology & Science, 6 (2), 136-144.

International Conference on Science and Technology

ICONST 2018

5-9 September 2018 Prizren - KOSOVO

Power Comparison of a Photovoltaic System with and without a Solar Tracker

İsmail Sepetyapan[1], Serkan Şahin[1], Yusuf Erkan Görgülü[1]*, Kubilay Taşdelen[1]

Abstract: In recent years there is a fast-growing amount of research being made in the area of renewable energy sources. Rapid depletion of current energy sources, price rise in raw energy sources, their negative effects on the environment and human health, hardships in their usage have accelerated the studies on renewable energy sources. Since the rays of the sun does not hit earth continuously with right angle there exists solar tracker systems to track sun rays. These tracking systems comes with some cost compared to trackerless ones. On a monthly or daily basis these systems become more advantageous to one another. South Europe and most parts of Turkiye is considered efficient for photovoltaic systems. Radiation distribution from south to north decreases naturally in sun map of Turkiye, radiation intensity differs based on climate and surface shapes. In this study a comparison system is developed to select one of the systems with a tracker or without it. Thus the most efficient system with minimal cost can be built.

Keywords: Arduino UNO, Solar Tracking, C#, Solar Map, Photovoltaic

Introduction

It is of utmost importance to benefit from sun's energy. In order to harvest maximum efficiency from photovoltaic (PV) systems, rays of sun should fall orthogonal on to the PV cell's surface. Otherwise the efficiency of the system may decrease. It is obvious that sun's path differs according to seasons and the duration of the day. Thus, a tracking system may promise orthogonality using tracking algorithms. A feasibility research should be conducted before building tracker systems.

(Çıtıroğlu, 2009) have conducted research on a PV-hydrogen hybrid energy source in their research on lighting. (Kelly et.al. 2009) raised efficiency of their PV panels under cloudy weathers. Also (Kelly et.al. 2011) have further developed their research to adapt environmental changes and seasons to increase energy throughput. In Spain, (Cruz-Peragón et.al. 2011) have evaluated advantages of energy production of solar tracker systems. (Chong et. al. 2009) tried to improve the tracking accuracy of their proposed solar tracker collector. (Abdallah et.al. 2008) studied how much the usage of solar tracker systems affect efficiency compared to the trackerless systems.

(Abdallah et.al. 2004) designed a programmable logic controller (PLC) based two-axis solar tracker system. They calculated the location of the sun four times per day and also based on this calculations they predicted the speed of the sun in the sky. Using the calculated speed they adapted the designed system to turn accordingly. The energy output of the system have generated 41% more energy compared to another 32° tilt angled fixed trackerless system but the tracking system demanded 3% more of what they gained from tracking system.

[3]Isparta Uygulamalı Bilimler Üniversitesi, Faculty of Technology, 32260, Isparta, TURKEY
*Corresponding author: yergeur@gmail.com

(Huang et.al. 2007) developed a one-axis three-position solar tracking system. They used a low concentration ratio reflector which led a %23 raise in the power output of the system. (Bakos, 2006) designed a two-axis sun tracking system for parabolic trough collector.

(Abu-Khader et.al. 2008) developed a PLC controlled two-axis solar tracker system. This system is turned four times per day depending on the location of the sun. Compared to fixed system the proposed system produced 30% to 45% more energy. Also the energy consumption of the designed system is detected to fell below 3% of the energy produced.

Since the cost of solar tracker systems are high (Lynch et.al. 1990) proposed a two-axis electronically controlled low-cost solar tracker system. System is composed of two electro-optic sensors, a low-cost control circuit, high torque direct current(DC) motor and other auxiliary materials. The tracker circuit has a tracking resolution of 0.1°. Electro-optic sensors restricts the movements of the system under cloudy weather conditions. Thus solar tracker system's energy consumption minimizes.

Another research focuses on low-cost systems is proposed by (Zogbi et.al. 1984). They used four electro-optic sensors, motion motors and electronic control circuit. (Rumala, 1986) proposed a shadow method and used servo motors, photo-resistors and a signal processing circuit to implement this system. (Sefa et.al. 2009) designed a one-axis microcontroller based solar tracker system. They chose RS-485 serial communication interface. Since the mechanism is easy to use, they proposed that setup and maintenance costs may have reduced.

(Demirtaş, 2009) manufactured a computer controlled two-axis solar tracker system. Horizontal and vertical movements of the system is maintained by step motors. A microcontroller based interface was used to control the system and also transfer data. Proposed system generated 18.5 Volts when sun rays are orthogonal to the PV panel, otherwise produced 12 Volts. On the other hand when tracker was unable to follow the sun or the weather was cloudy, designed system produced 10 Volts. Compared to the fixed system, they justified the tracking system have produced 35% more energy.

(Saavedra, 1963) developed an electro-mechanic system to track sun and manufactured. Platform was moved by two small DC motors. Sun rays are measured using a pyrheliometer directly. Since, under cloudy weather the measurement system fails. Thus, they conveyed a computer software to compensate this gap until sun arises. They justified that the system is efficient and other than using PV panels, collector systems can be used for other purposes.

(Abu-Malouh et.al. 2011) manufactured a spherical solar cooker with automatic sun tracker system. They focused sun rays to the center of the sphere and maintained 93°C of heat which is enough to cook a meal. In the same manner (Al-Soud et.al. 2010) manufactured a parabolic two-axis solar tracking system to gather rays of sun. The center point of the parabolic solar cooker reached 90°C of heat. (Sungur, 2009) in his research calculated the azimuthal and altitude angles of the sun and controlled the tracking system using a PLC according to the sun's movement. In his research he pointed out that compared to a fixed system, proposed system produced 42.6% more energy. (Eke et.al. 2012) compared energy generation of a two-axis solar tracker system to a fixed system with the same latitude angle. As a result of this comparison through April 2010 to March 2011, the measurements on one year basis has shown that solar tracker system produced 30.79% more energy than the fixed system.

In this study, a system to track the sun rays is developed using light dependent resistors (LDR), a DC servo motor, Arduino Uno and Nano, C# for serial communications. Both tracker and trackerless systems' current and voltage readings from sensors are measured and transferred to Arduino microcontroller. Arduino microcontroller then prints corresponding information on both LCD panels and on PC screen. results are obtained on a daily basis. A one-day data is used to evaluate the performance of the two systems. The observations are made between 10:00 am and 16:30 pm. The results are measured as a multiplication of two observations current and voltage. As the results indicates the tracker system generates %29 more power than the trackerless one.

Material and Method

In this research, a fixed and a solar tracker system has been developed. Fixed panel is located with a 45 degrees angle. The solar tracker is designed as a two-axis system. Thus the solar panel can be turned right or left and up and down. Maximum and minimum angles of solar tracker system is 0°-180° in horizontal axis, and 15° to 80° in vertical axis. Figure 1 shows these two systems.

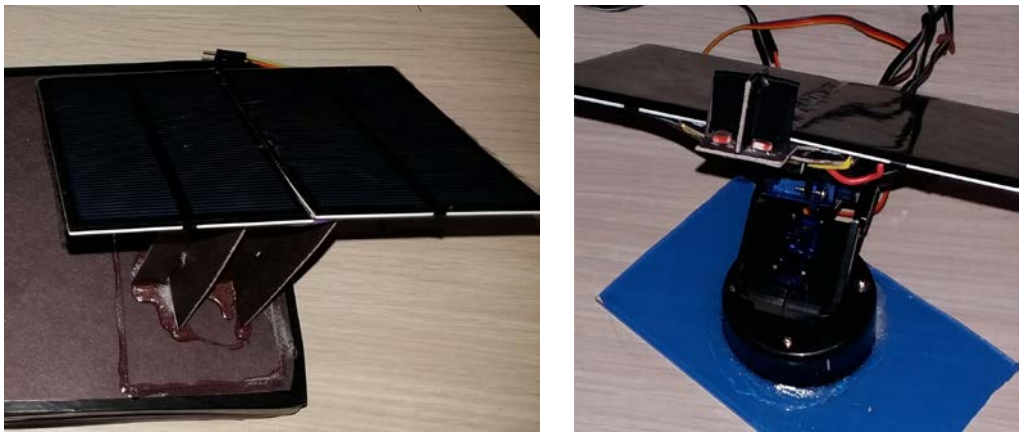

Figure 1. Fixed system(a), tracker system(b)

Fixed system is located at the optimum angle to benefit from rays of the sun. On the other hand, solar tracker uses a serial protocol to move servo motors via Arduino microcontroller. Servo motors are controlled by a light dependent resistor(LDR) system. LDRs are located at four poles and detect light accordingly. The software developed in C# controls the movements of solar tracker panel and transfers and prints both systems' data to PC and LCD screen on Arduino. Graphical interface also shows the measurements from sensors. In Figure 2 a block diagram summarizes the systems workflow.

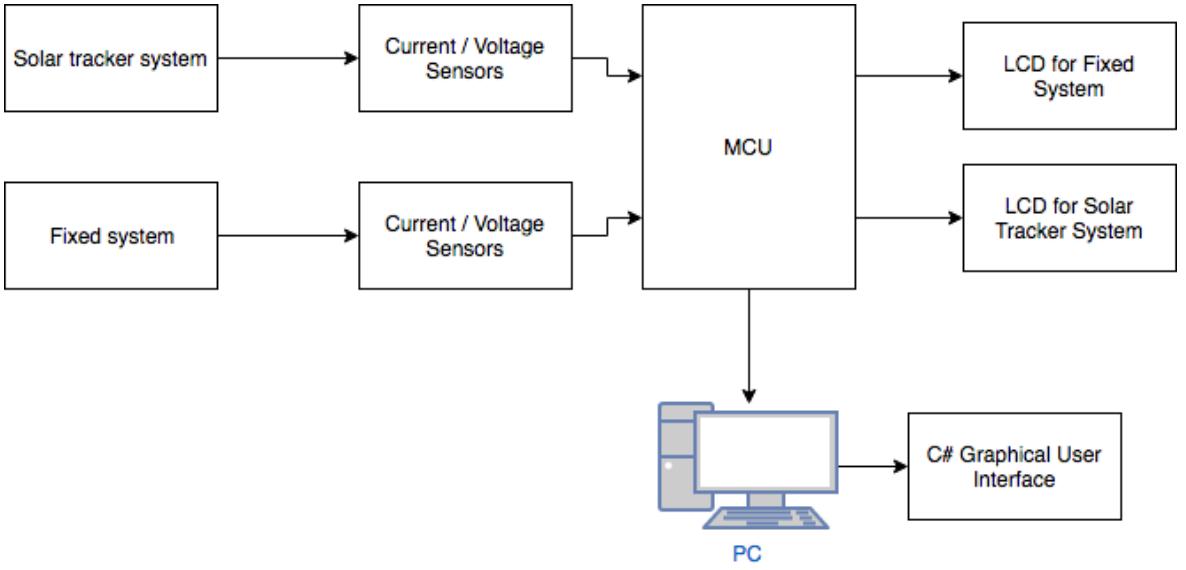

Figure 2. Block diagram of whole system

Designed solar tracker system consists of LDRs located in North,South, East and west directions to measure light intensity. LDR sensors are located at the top-middle of the panel. This circuitry acts like a voltage

divider. Also a low pass filter and a zener diode is added to filter out high frequency components and to avoid high voltage fluctuations. Figure 3 shows the LDR circuit.

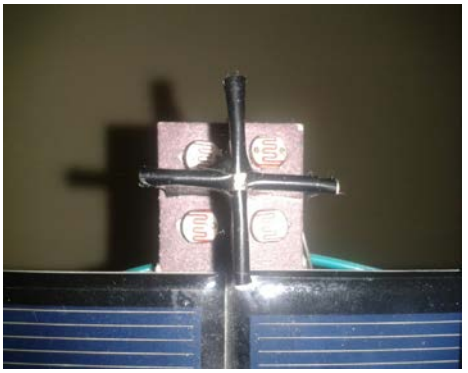

Figure 3. LDR circuit

Arduino microcontroller software controls the servo motors, measures the voltage and current values of solar panels. Depending on LDR circuit microcontroller unit controls the servos. Another Arduino microcontroller reads the measurements of panels and prints them on two LCDs and also sends datas to PC using serial communication protocol. C# graphical user interface (GUI) receives the information and prints current and voltage values on a table.

Results

A one day measurements from both systems are evaluated for comparison. Given in Table 1 are the readings of this measurement. It is obvious in Table 1 that between 10:00 am and 16:30 pm values are nearly the same for both systems. Power is calculated as the multiplication of current and voltage values.

As the results indicate ratio of tracker sistem to fixed one is calculated as 1.287. In other words solar tracker system produces 29% percent more power than the fixed system. If you focus on before 10:00 am and after 16:30 pm the solar tracker outperforms the fixed system.

Discussion and Conclusions

Although tracking system produces nearly %30 percent more energy, it has also disadvantages. Area demand of tracker system is more than the other system. Energy requirement of motors to drive tracking system and maintenance costs of tracking equipment can be counted as disadvantages of the tracker system.

It can be concluded from Table 1 solar tracker system generates more power compared to the fixed one. On a partly cloudy day this difference may show itself strongly. Depending on motors used to drive panels it may or may not exceed the fixed system. Also the setup cost of the tracker system is high. In order to outcome disadvantages of solar tracking system high-efficient panels may be used.

Table 1. Power outputs of both tracker and fixed systems on one day

Systems	Solar Tracker	Fixed
Time(Hour)	Power Generated(W)	Power Generated(W)
6:00 – 6:30	0,21	0
6:30 – 7:00	0,96	0
7:00 – 7:30	1,85	0,24
7:30 – 8:00	1,95	0,96
8:00 – 8:30	2,00	1,10
8:30 – 9:00	2,00	1,22
9:00 – 9:30	2,04	1,46
9:30 – 10:00	2,08	1,96
10:00 – 10:30	2,12	2,00
10:30 – 11:00	2,12	2,02
11:00 – 11:30	2,18	2,08
11:30 – 12:00	2,32	2,24
12:00 – 12:30	2,42	2,42
12:30 – 13:00	2,42	2,40
13:00 – 13:30	2,38	2,36
13:30 – 14:00	2,30	2,26
14:00 – 14:30	2,28	2,24
14:30 – 15:00	2,28	2,20
15:00 – 15:30	2,26	2,14
15:30 – 16:00	2,24	2,04
16:00 – 16:30	2,02	1,96
16:30 – 17:00	2,12	1,22
17:00 – 17:30	1,84	0,92
17:30 – 18:00	1,68	0,24
18:00 – 18:30	1,04	0
18:30 – 19:00	0,40	0
19:00 – 19:30	0	0
19:30 – 20:00	0	0

References

Abdallah, S., Badran, O.O. (2008). Sun tracking system for productivity Enhancement of solar still. Desalination, 220, 669-676

Abdallah, S., Nijmeh, S. (2004). Two axes sun tracking system with PLC control. Fuel and Energy Abstracts, 45(6), 410. doi:10.1016/s0140-6701(04)80711-2

Abu-Khader, M.M., Badran O.O. and Abdallah S. (2008). Evaluating multi-axes sun-racking system at different modes of operation in Jordan. Renewable and Sustainable Energy Reviews, 12, 864-873.

Abu-Malouh, R., Abdallah, S., Muslih, I. M. (2011). Design, construction and operation of spherical solar cooker with automatic sun tracking system. Energy Conversion and Management,52(1), 615-620. doi:10.1016/j.enconman.2010.07.037

Al-Soud, M. S., Abdallah, E., Akayleh, A., Abdallah, S., Hrayshat, E. S. (2010). A parabolic solar cooker with automatic two axes sun tracking system. Applied Energy, 87(2), 463-470. doi:10.1016/j.apenergy.2009.08.035

Bakos, G. C. (2006). Design and construction of a two-axis Sun tracking system for parabolic trough collector (PTC) efficiency improvement. Renewable Energy, 31(15), 2411-2421. doi:10.1016/j.renene.2005.11.008

Çelik, A.N., Açıkgöz, N. (2003). 240 W Gücünde Akü Depolu Bağımsız Bir Fotovoltaik Enerji Sistem Tasarımı ve Uygulaması, Güneş Enerjisi Sistemleri Sempozyumu ve Sergisi, 20-21 Haziran 2003, Mersin, Bildiriler Kitabı, E/2003/321, 23-32.

Chong, K., Wong, C. (2009). General formula for on-axis sun-tracking system and its application in improving tracking accuracy of solar collector. Solar Energy, 83(3), 298-305. doi:10.1016/j.solener.2008.08.003

Çıtıroğlu, A. (2000). Güneş enerjisinden yararlanarak elektrik üretimi. Mühendis ve Makina, 485(41), 32-33.

Cruz-Peragón, F., Casanova-Peláez, P. J., Díaz, F. A., López-García, R., & Palomar, J. M. (2011). An approach to evaluate the energy advantage of two axes solar tracking systems in Spain. Applied Energy, 88(12), 5131-5142. doi:10.1016/j.apenergy.2011.07.018

Demirtaş, M. (2009). Design and Implementation of PLC Controlled Solar Tracking System. Technological Applied Sciences, 4(3), 315-329

Eke, R., & Senturk, A. (2012). Performance comparison of a double-axis sun tracking versus fixed PV system. Solar Energy, 86(9), 2665-2672. doi:10.1016/j.solener.2012.06.006

Fıratoğlu, Z.A.,Yeşilata, B. (2003). Maksimum Güç Noktası İzleyicili Fotovoltaik Sistemlerin Optimum Dizayn ve Çalışma Koşullarının Araştırılması. DEÜ Mühendislik Fakültesi Fen ve Mühendislik Dergisi, 1, 147-158.

Huang, B., Sun, F. (2007). Feasibility study of one axis three positions tracking solar PV with low concentration ratio reflector. Energy Conversion and Management, 48(4), 1273-1280. doi:10.1016/j.enconman.2006.09.020

Kelly, A.N. and Gibson, T.L. (2011). Increasing the solar photovoltaic energy capture on sunny and cloudy days. Solar Energy, 85, 111-125.

Kelly, A.N. and Gibson, T.L. (2009). Improved photovoltaic energy output for cloudy conditions with a solar tracking system. Solar Energy, 83, 2092-2101.

Lynch, W. A., Salameh, Z. M. (1990). Simple electro-optically controlled dual-axis sun tracker. Solar Energy, 45(2), 65-69. doi:10.1016/0038-092x(90)90029-c

Rumala, S.N. (1986) A Shadow Method for Automatic Tracking. Solar Energy, 37, 245-247. http://dx.doi.org/10.1016/0038-092X(86)90081-2

Saavedra, A. S. (1963). Diseño de un servomecanismo seguidor solar para un instrumento registrador de la irradiación solar directa. Memoria, Universidad Técnica Federico Santa Maria, Valparaiso, Chile.

Sefa, İ., Demirtas, M., Çolak, İ. (2009). Application Of One-Axis Sun Tracking System. Energy Conversion and Management, 50, 2709-2718.

Sungur C. (2009), Multi-axes sun tracking system with PLC control for photovoltaic panels in Turkey. Renewable Energy, 34(4), 25-1119.

Zogbi, R., Laplaze, D. (1984) Design and Construction of a Sun Tracker. Solar Energy, 33, 369-372. http://dx.doi.org/10.1016/0038-092x(84)90168-3

International Conference on Science and Technology

ICONST 2018

5-9 September 2018 Prizren - KOSOVO

Remote Control of Television using Voice Commands

Emre Palaz[1], Ercan Bıçakçı[2], Yusuf Erkan Görgülü[3]*, Kubilay Taşdelen[4]

Abstract: In this study, remote control of televisions (TV) using voice commands is provided. First, the voice commands are created then a comparison between the application is being made. As a result of these comparison convenient outputs are gathered. EasyVR voice module make it possible to recognize voice commands. The voice commands are created using EasyVR Commander software. EasyVR module and the compatible Arduino UNO platform's hardware and software settings are done by using EasyVR Commander software. Required infrared (IR) modulation schemes are used to remote control of TVs. Comparison results have been used to send IR modulation signals via predetermined Arduino platform's digital outputs. Finally, voice commands are able to control TVs remotely.

Keywords: Arduino UNO, EasyVR Commander, IR, Remote Control

Introduction

There have been numerous researches conducted related with this study using different methods. One of which is published by (Barış et. al. 2002). In this study a PIC microcontroller was able to control a designed system via short messages transmitted by a mobile phone. Thus, it was possible to control the system without being bound to place and time constraints. In another research (Edizkan et.al. 2007), a mobile vehicle has been controlled using voice commands. In this study common vector approach (CVA) method was used. CVA has demonstrated comparable results against hidden markov models(HMM) in isolated word recognition systems. The mobile vehicle can be controlled with five commands: "forward", "backward", "turn right", "turn left" and "stop". CVA demonstrated high voice recognition rates in field studies.

Yet in another study (Barış et.al. 2002), a system using artificial neural networks (ANN) to identify speakers' identity was developed. Since people have different voice characteristics by the help of feature extraction techniques which depends heavily on mathematical computations, it is now frequently being used in daily life. In this study, samples gathered from 7 people have been gone through a series of feature extraction systems and 260 cepstral coefficient were calculated and stored in a dataset. A designed ANN architecture in MATLAB was trained using this dataset and also evaluated. The ANN identified %90 of the speakers' identities successfully.

Another research (Subaşıoğlu, 2000) was conducted on the Internet access of disabled people. Researches in disabled peoples' Internet and computer technologies have led this research possible. Especially with the help of adapted technologies, blind or deaf people are able to communicate over telephone and many disabled people can read through a PC screen using voice synthesis or read automatically generated Braille images. Physically disabled people can use their computers by sip and puff switches and even by voice commands.
In (Çubukçu et. al. 2015) paper, a home automation system was designed using a ZigBee wireless module and Arduino microcontroller. This study is designed in a two layered scheme. First a speech recognition

[3]Isparta Uygulamalı Bilimler Üniversitesi, Faculty of Technology, 32260, Isparta, TURKEY
[4]Isparta Uygulamalı Bilimler Üniversitesi, Faculty of Technology, 32260, Isparta, TURKEY
*Corresponding author: yergeur@gmail.com

system designed in MATLAB using Mel Frequency Cepstrum Coefficients and dynamic time warping techniques are used to extract features and matching. When command is recognised Arduino microcontrollers related pin is changed via USB. Zigbee wireless module monitors related pin and if recognizes any change, the device on this pin is controlled. Finally, (Baygin et. al. 2012) have published a paper on smart home automation using real-time voice recognition. This study involves creating a dataset gathered from 5 people and extracting features from them. Afterwards, extracted features are used in training and test stages of the given methods respectively; Euclidean distance method, ANN and dynamic time warping algorithm. In recognition step the accuracy of the system has been verified by implementation of given commands.

In our study we develop a system using EasyVR card, Arduino microcontroller and infrared led. There are fifteen commands in total to control TV. First, these fifteen commands are gathered using EasyVR Commander software. In the implementation, a command is said like “mute”, then EasyVR captures and processes the voice to make a comparison in the given dataset. After a match occurs Arduino sends the related hexadecimal code using IR modulation signal to TV. There are some drawbacks in this study such as background noise, lack of sample voices (only 2 different people) in the dataset, noise generated from the same person (sickness etc.). The implemented system is cheap in cost and does not depend on a auxiliary computing source (like PC).

Material and Method

Initially voice recordings of user are gathered. Afterwards, user says the appropriate command inside the room. EasyVR recognizes the command and preprocesses it according to the inner procedure. Command is then compared with the pre-recorded command set. If comparison result is unidentified, then system does nothing. On the other hand, if the command is recognized then corresponding hexadecimal data is transferred via IR led to the TV. Figure 1 shows the flowchart of the implemented system.

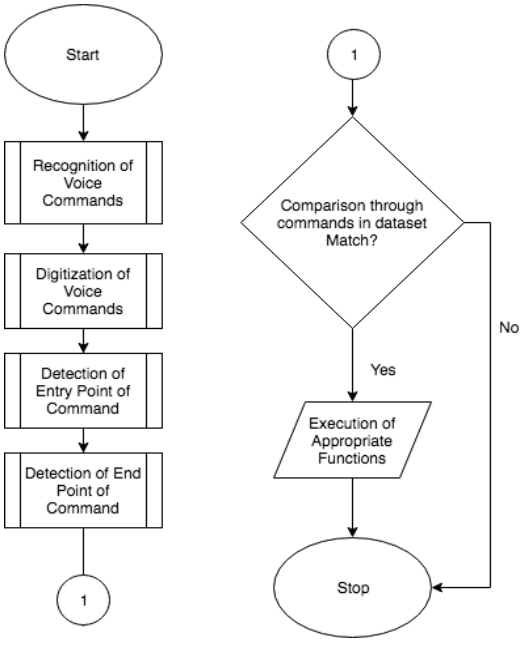

Figure 1. Flowchart of the system

A regular TV is used to see the results of the proposed system. Since the diffraction of IR signals, TV is located 3 meters away from the module. Microphone and designed module is located near the person to command the TV. Thus, recognition errors are thought to be minimized. Figure 2 shows the implemented circuitry of the module.

Since there exist two users in this study two recordings are gathered per command. As recordings channel numbers from “one to nine” and “mute”, “voice up”, “shut down” are proposed in Turkish language. Figure 3 shows the Turkish command dataset. Continuous monitoring of EasyVR is avoided using the trigger function. “TV” word is selected to trigger EasyVR card. Unless TV word is captured, system does nothing since these words can be used in daily life for other purposes. After recognising “TV” word system starts to implement the required commands. After this step the system goes to standby mode.

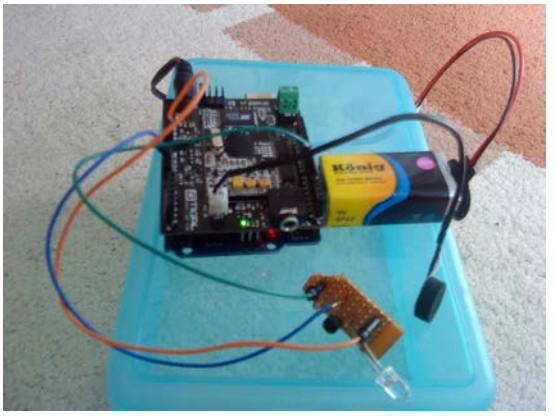

Figure 2. Arduino EasyVR shield and the implemented circuitry

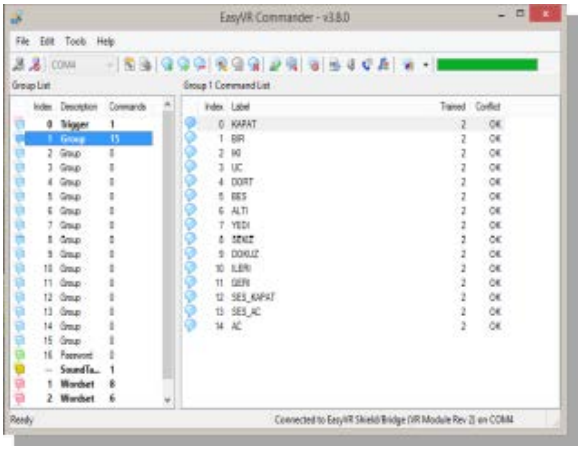

Figure 3. EasyVR Commander screen for Turkish voice commands

Discussion and Conclusions

According to the experiments made during this study, efficiency of this system varies. As a major issue, at each repetition of command, words may differ time to time. This results in nonrecognition of commands by EasyVR system. As another issue, existing background noise can reduce recognition rate. Even the same user may experience difficulties when they become sick. As our system does not depend on a personal computer, it is a minimalist and cheap system. The designed system can be further improved by implementing more microphones. This study may further developed to control other devices like wheelchairs or PCs.

References

Barış, İ., Erdamar, M., Sümer, E., & Erdem, H. (2002). Ses İşaretlerinin Yapay Sinir Ağları ile Tanınması ve Kontrol İşlemleri için Kullanılması. URSI. http://www.ursi.org.tr/2002-1.Ulusal%20Kongre/ursicd1/C16.pdf (Erişim Tarihi: 10.08.2018).

Baygin, M., Karakose, M. (2012). Real time voice recognition based smart home application. 2012 20th Signal Processing and Communications Applications Conference (SIU). doi:10.1109/siu.2012.6204694

Çayırlıoğlu, İ., Görgünoğlu, S. (2010). Mobil Telefon ve Pic Mikrodenetleyici Kullanarak Uzaktan Esnek Kontrol Sağlanması. International Journal of Engineering Research and Development, 2 (1), 23-27. Retrieved from http://dergipark.gov.tr/umagd/issue/31719/345708

Çubukcu, A., Kuncan, M., Kaplan, K., Ertunc, H. M. (2015). Development of a voice-controlled home automation using Zigbee module. 2015 23nd Signal Processing and Communications Applications Conference (SIU). doi:10.1109/siu.2015.7130204

Edizkan, R., Tiryaki, B., Büyükcan, T., & Uzun, İ. (2007). Ses Komut Tanıma ile Gezgin Araç Kontrolü. IX. Akademik Bilişim Konferansı Bildirileri, Dumlupınar Üniversitesi, Kütahya, 31.

Subaşıoğlu, F. (2000). Engellilerin Internet'e Erişimi Üzerine. Türk Kütüphaneciliği, vol. 14, n. 2, pp. 188-204.

International Conference on Science and Technology

ICONST 2018

5-9 September 2018 Prizren - KOSOVO

The Thrust of Rockets

Mukadder İĞDİ ŞEN [1]*

Abstract: The rockets are launched giving direction as mechanical and driven by the propulsion given to it by the fuel; they are used to transport the cargo to its destination according to ballistic balances; they are structurally different from missiles. The missiles has various systems such as image sensor, thermal sensor, inertial sensor, radar, GPS according to usage purposes; equipped with a warhead that explodes before crashing or at the time of a crash with the help of special mechanisms their carried; carry radio-controlled or guided weapons. In our work, we provide information about rockets and missiles, and the methods of increasing the thrust in rockets is explained with calculation. Several examples of today's rocket and missile systems are given.

Keywords: rocket, missile, guided weapons, thrust

Introduction

Rockets

A rocket is a cylindrical projectile that can be propelled to a great height or distance by the combustion of its contents (CD, 2014). A vehicle powered by a rocket engine is called a “rocket”. Rocket parts include engines, payload, control system, propellant tanks, and propellants. A rocket engine is a type of engine that uses stored propellant or other means to create a high velocity gas jet. It may carry an oxidizer or use oxygen in the atmosphere. Rockets work on Newton's third law: every action has an equal and opposite reaction. Modern rockets were developed in the late 19th century and early 20th century. In the Second World War, the rocket was used as a weapon in the second stages of the war. Currently two classes of rockets are used; These are chemically reinforced rockets and electrically powered rockets. It is the old and more dominant form, which is chemically strengthened, and used in both atmospheric and space missions. Chemically working rockets use solid fuel or liquid fuel. Also, a rocket is a type of engine designed to provide thrust with a high-speed exhaust from a nozzle. In its simplest form, the rocket is a chamber surrounding a gas under pressure. A small opening at one end of the chamber allows the gas to escape and thus provides a thrust that moves the rocket in the opposite direction (Agrawal, 2010). A good example of this is a balloon. The air in the balloon is compressed by the walls of balloon. The air is pushed back so that the forces on each side are balanced. When the nozzle is released, the air escapes and the balloon advances in the opposite direction. With space rockets, gas is produced by the combustion of propellants which may be in solid or liquid form, or by a combination of both (M1, 1996). The rocket can be mechanically, chemically or electrically propelled. Currently, chemical propellants are the most dominant forms (RA, 2015). Some examples of rockets are shown in Figure 1 and Figure 2. Modern rockets were developed in the late 19th and early 20th centuries (RM1, 2013). A rocket lunch can be seen in Figure 3.

[1]Trakya University, Edirne Vocational College of Technical Sciences, 22020, Edirne, TURKEY
*Corresponding author: mukaddersen@trakya.edu.tr

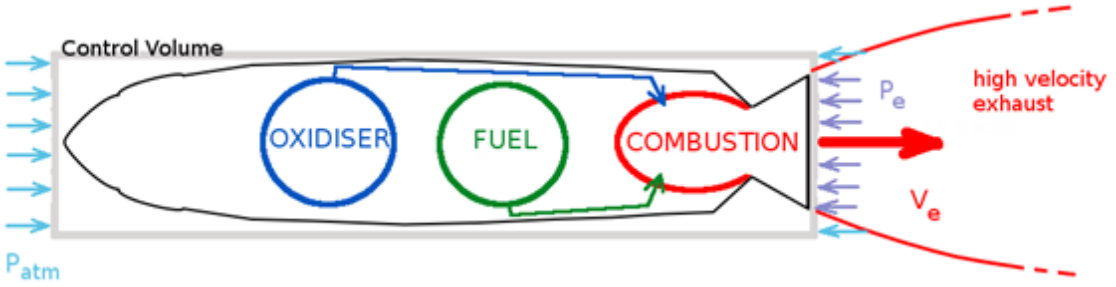

Figure 1. A simple scheme for a rocket (RA, 2015).

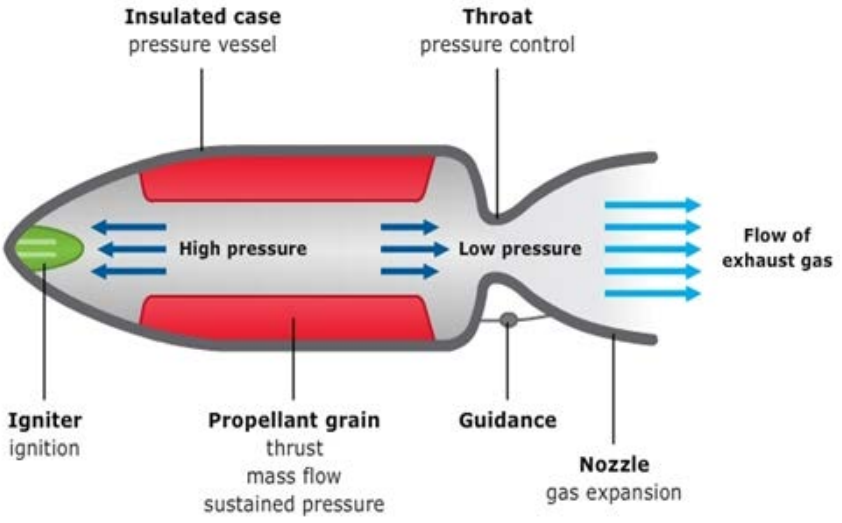

Figure 2. An example of a rocket (F1, 2017)

Figure 3. A rocket lunch (SS, 2015).

Missiles

The missile is a rocket-guided weapon designed to offer an explosive warhead with great precision at high speed. The missiles are different from small tactical weapons that are as effective as strategic weapons of more than a few hundred meters with a range of a few thousand kilometers. An example of the structure of a missile is shown in Figure 4. A propeller-based underwater missile is called as “torpedo”. A guided missile (ballistic) powered along a low, level flight path by an air-breathing jet engine is called as “cruise missile”.

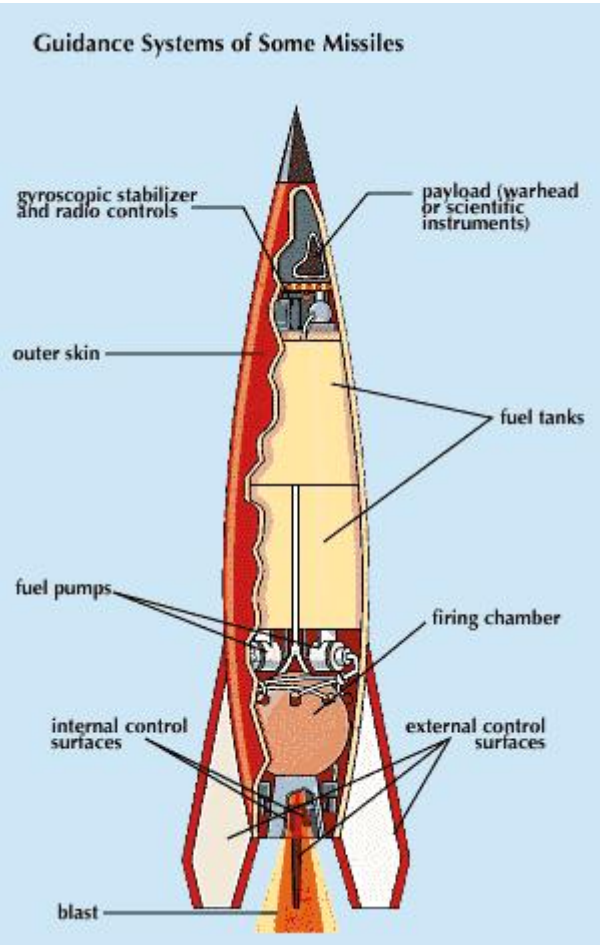

Figure 4. The structure of a missile (EEB2, 2010).

A vehicle powered by rockets (self-propelled) to carry a warhead is known as “missile”. Missiles are categorized by the launch platform, intended target, and the navigation and guidance. The categories are surface-to-surface, air-to-surface, surface-to-air, and anti-satellite missiles. Depending on the guidance system, missiles are categorized into ballistic, cruise, and other types. They also can be classified using the intended target: anti-ship, anti-tank, and anti-aircraft are examples for those categories. Individually, these categories may contain numerous missiles with hybrid capabilities; therefore, an explicit classification cannot be provided. Any missile consists of four fundamental subsystems; guidance/navigation/targeting systems, flight systems, rocket engine and warhead (RM1, 2013). Missile is an object which is propelled by either hand or from a mechanical weapon (ELU, 2014). Military weapons are aimed towards some target, and are essentially considered as a type of powered munitions. When it goes through the air, it is dubbed a missile. The missiles during World War II was controlled by a basic radio control system which was run by the operator (TD, 2018). An example of a missile is given in Figure 5.

Figure 5. RIM-162 Evolved Sea Sparrow missile (TD, 2018).

The Differences Between Rockets and Missiles

The differences between rocket and missile are shown in Table 1.

Table 1. Briefly, the differences between rocket and missile (RM1, 2013).

Rocket	Missile
A rocket is a missile or spacecraft that acquires high speeds from a rocket engine.	A missile is a self-driven munitions system that is powered by a rocket.
Rocket needs guidance.	Missile has own guided system.
A rocket is a powerful spacecraft that holds the capacity to produce remarkable acceleration and to achieve extremely high speeds.	A missile is a rocket defense application, such as a precision-based munition system, four basic subsystems: Guidance systems, Rocket engine, Battle Capture and Flight Systems.

Method

In our study the following equations were used. The value of every element in the equations was regularly changed and evaluations were made. A computer program was written to calculate all values.

The Forces on a Rockets

A rocket in the air has four forces as you have seen in Figure 6: Lift, weight, drag and thrust forces. Lift Force: It moves perpendicular to the direction of movement. Lifting is used to balance and control of the flight direction. In an aircraft, lift is used to exceed of the weight force; In a rocket, thrust is used to exceed of the weight. In a rocket, lift is produced by the nose cone, the rocket body and fins. Drag Force: It opposes the direction of movement. It is caused by the interaction of the rocket body with air and the rocket shape. Weight: Created by the gravitational attraction of an object. Weight force is directed towards the center of the Earth. Weight = mass x gravitational acceleration. On Earth: Weight = mass x 9.8 m / s^2. The magnitude of this force depends on the mass of all parts of the rocket, plus the amount of fuel and payload. The weight is distributed throughout the rocket, but we can think of it from a single point called the center of gravity. It is the average position of the weight of an object. It is distributed to the mass and weight throughout the object (Hampton, 2014). Thrust: Thrust is a reaction force that moves the rocket in the air and in space.

When describing the action of forces, the magnitude and the direction must be consider. The direction of the thrust is generally along the longitudinal axis of the rocket through the gravity center of rocket. But on some

rockets, the exhaust nozzle and the thrust direction can be rotated, or gimbaled. Later, the rocket can be maneuvered by using the torque about the gravity center (Benson, 2014a).

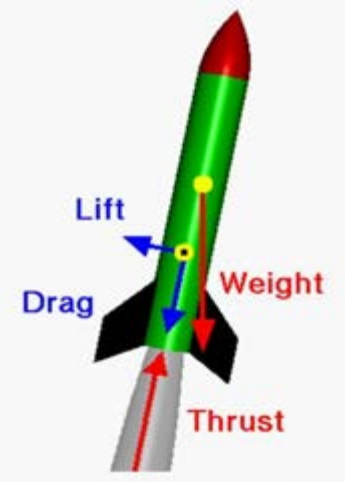

Figure 6. Four forces for a rocket in the air (Benson, 2014a).

Three basic Newton Laws are being used in a rocket. Newton's first law can be expressed as: A resting object tends to remain at rest, and a moving object tends to remain in motion unless it moves with unstable force. If an object such as a rocket is stationary, the forces on it are balanced. An additional power is required to balance forces and move the object. If the object is already moving, it gets an unbalanced power, to stop it, change its direction from a straight line path, or change its speed. A rocket is balanced on the launch pad. The pad's surface pushes the rocket up while trying to pull down gravity. When the engines are ignited, the thrust from the rocket becomes unstable and the rocket moves upwards. Then, when the rocket is running out of fuel, it slows down, stops at the highest point of the plane, and then falls back to Earth. Newton's Second Law of Motion is actually a mathematical equation. Three parts of the equation are mass (m), acceleration (a) and force (F), the equation can be written as follows:

$$F = ma \quad (1)$$

When applied this principle to a rocket, the controlled explosion inside of the rocket engine is created the pressure called as thrust force which moves in direction of its. It continues during this controlled explosion that is, as long as the fuel is burned. Rocket needs this combustion for moving in asked route. Combustion continues until fuel is exhausted. Over time, fuel is reduced. To equalize both sides of the equation (1) since mass decreased, acceleration of the rocket increased. Thus a rocket begins to move slowly and moves faster and faster as you climb into space.

According to Newton's second law of motion: If the greater fuel burned, the rocket produced the faster gas thus the rocket has greater upward thrust. Newton's Third Law can be stated as: Every action has an equal and opposite reaction (M1, 1996). The thrust force, is measured using the International System of Units (SI) in Newton's (symbol: N), and represents the amount needed to accelerate 1 kilogram of mass at the rate of 1 meter per second per second. A Pratt & Whitney F100 jet engine is being tested in Figure 7 (WK1, 2015).

For three Laws: an unbalanced force must be applied for a rocket to change speed or direction (first law). The amount of thrust (force) will be determined by the mass of rocket fuel (second law). The reaction of the rocket is equal and in the opposite direction of the action (third law) (M1, 1996). Thrust is generated using the rocket engine by the reaction of accelerating a mass of gas. (Hampton**,** 2014**;** Benson, 2014b).

Rockets depend on a lot of things such as auxiliary reaction engines, momentum, gimballed thrust, propellant flow, exhaust stream deflection, gravity, momentum wheels, spin and airfoils to aid direct flight (TD, 2018).

Figure 7: A Pratt & Whitney F100 jet engine is being tested (WK1, 2015).

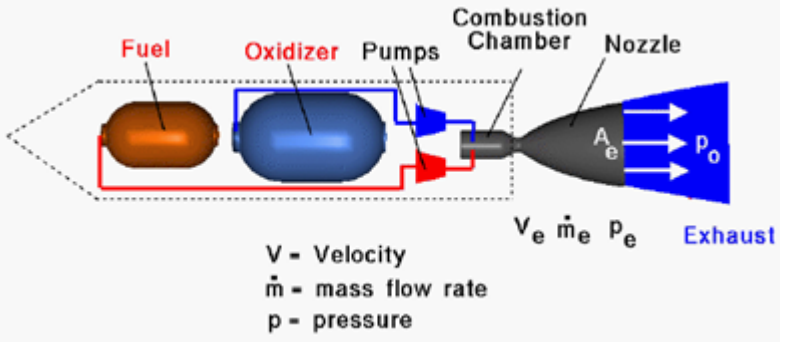

Figure 8. An example of a rocket system.

The magnitude of thrust in Figure 8 can be calculated, when dealing with a gas, by the basic thrust equation (2): From Newton's second law of motion, we can define a force to be the change in momentum of an object with change in time. Momentum is the object's mass times the velocity.

$$F = \dot{m}_e V_e - \dot{m}_0 V_0 + (p_e - p_0)A_e \tag{2}$$

where p_e is the pressure in the exhaust acting on an exhaust area, A_e, and p_0 is the pressure of the surrounding atmosphere. Thrust F is equal to the exit mass flow rate $\dot{m}_e$ times the exit velocity V_e minus the free stream mass flow rate $\dot{m}_0$ times the free stream velocity V_0 plus the pressure difference across the engine p_e - p_0 times the engine area A_e. If the rocket is operating within an atmosphere then there will be additional force components due to a pressure imbalance. The propellants, fuel and oxidizer for liquid or solid rocket engines are carried on board. There is no free stream air brought into the propulsion system, so **the thrust equation** simplifies to:

$$\boldsymbol{Thrust = \ F = \dot{m}_e V_e + (p_e - p_0)A_e} \tag{3}$$

where we have dropped the exit designation on the mass flow rate. This thrust equation works for both liquid and solid rocket engines. The mass flow rate through the propulsion system is determined by the nozzle design. When we divided with $\dot{m}$:

$$\frac{F}{\dot{m}} = V_e + (p_e - p_0)A_e / \dot{m} \tag{4}$$

$$V_{eq} = V_e + (p_e - p_0)A_e / \dot{m} \quad (5)$$

The equivalent exhaust velocity is V_{eq}, there is no free stream mass times free stream velocity term in the thrust equation because no external air is brought on board. Since the oxidizer is carried on board the rocket, rockets can generate thrust in a vacuum where there is no other source of oxygen.

$$F = \dot{m}\, V_{eq} \quad (6)$$

The total impulse (I) of a rocket is defined as the average thrust times the total time of firing. the total time is "Δt".

$$I = F\, \Delta t \quad (7)$$

Since the thrust may change with time, we can also define an integral equation for the total impulse.

$$I = \int F\, dt \quad (8)$$

$$I = \int (\dot{m}\, V_{eq}) dt \quad (9)$$

Remember that $\dot{m}$ is the mass flow rate; it is the amount of exhaust mass per time that comes out of the rocket. Assuming the equivalent velocity remains constant with time, Then we can calculate the equation:

$$I = m\, V_{eq} \quad (10)$$

where m is the total mass of the propellant. We can divide this equation by the weight of the propellants to define the specific impulse which characterize the efficiency of the propulsion system ("specific" is "divided by weight"). The specific impulse I_{sp} in a vacuum is:

$$I_{sp} = Total\ impulse/Weight = I/(\dot{m}\, g_0) = V_{eq}/g_0 \quad (11)$$

where g_0 is the gravitational acceleration constant (32.2 ft/sec^2 in English units, 9.8 m/sec^2 in metric units). Now, if we substitute for the equivalent velocity in terms of the thrust:

$$I_{sp} = F / (\dot{m}\, g_0) \quad (12)$$

the I_{sp} is a ratio of the thrust produced to the weight flow of the propellants. A quick check of the units for I_{sp} shows that: I_{sp} = m/sec / m/sec^2 = sec

We can use the specific impulse to determine the thrust of a rocket, if we know the weight flow rate through the nozzle. Therefore, it is an indication of the engine efficiency. If the specific impulse is higher than the other, it produces more thrust for the same amount of propellant. The result of the thermodynamic analysis is a certain value of specific impulse. The rocket weight will define the required value of thrust. Dividing the thrust required by the specific impulse will give us how much weight flow of propellants from the engine must produce. This information determines the physical size of the engine (Benson, 2014b).

The thrust equation was shown above works for both liquid rocket and solid rocket engines. There is also an efficiency parameter called the specific impulse which works for both liquid rocket and solid rocket engines and greatly simplifies the performance analysis for rockets (Benson, 2014c).

The design of the nozzle determines the exit velocity for a given pressure and temperature. Therefore, the nozzle design determines the thrust of the propulsion system. An example of rocket body and nozzle is shown in Figure 9. The equations are (Benson, 2014d):

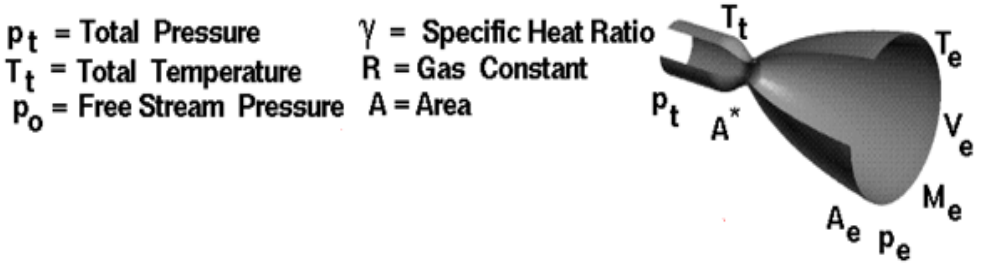

Figure 9. An example of a rocket body and its nozzle (Benson, 2014d).

Mass Flow Rate : $$\dot{m} = \frac{A^* p_t}{\sqrt{T_t}} \sqrt{\frac{\gamma}{R}} \left(\frac{\gamma+1}{2}\right)^{-\frac{\gamma+1}{2(\gamma-1)}} \quad (13)$$

Exit Mach : $$\frac{A_e}{A^*} = \left(\frac{\gamma+1}{2}\right)^{-\frac{\gamma+1}{2(\gamma-1)}} \frac{\left(1+\left(\frac{\gamma-1}{2}\right)M_e^2\right)^{\frac{\gamma+1}{2(\gamma-1)}}}{M_e} \quad (14)$$

Exit Temperature : $$\frac{T_e}{T_t} = \left(1+\left(\frac{\gamma-1}{2}\right)M_e^2\right)^{-1} \quad (15)$$

Exit Pressure : $$\frac{p_e}{p_t} = \left(1+\left(\frac{\gamma-1}{2}\right)M_e^2\right)^{-\frac{\gamma}{\gamma-1}} \quad (16)$$

Exit Velocity : $$V_e = M_e \sqrt{\gamma R T_e} \quad (17)$$

Then the thrust equation in Eq.(3) can be written for calculations.

The Shape of Nozzle

The hot gas produced in the combustion chamber is permitted to escape through an opening (the "throat"), and then through a diverging expansion section. When sufficient pressure is provided to the nozzle (about 2.5-3 times ambient pressure), the nozzle chokes and a supersonic jet is formed, and accelerating the gas, converting most of the thermal energy into kinetic energy. Exhaust speeds vary depending on the expansion ratio of the nozzle, but exhaust speeds as high as ten times the speed of sound in air at sea level are not uncommon. About half of the rocket engine's thrust comes from the unbalanced pressures inside the combustion chamber, and the rest comes from the pressures acting against the inside of the nozzle (see Figure 10).

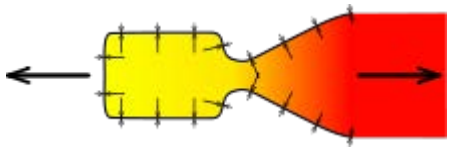

Figure 10. General structure of a rocket (WK2, 2017).

The expansion regimes of a de Laval nozzle can be under-expanded, perfectly expanded, over-expanded and grossly over-expanded. The most commonly used nozzle, the Laval nozzle, is a fixed geometry nozzle with a high expansion ratio. The wide bell or cone-shaped nozzle extension beyond the throat gives the rocket

engine in a characteristic shape. The output static pressure of the exhaust jet depends on the chamber pressure and the rate at which the nozzle moves to the throat area.

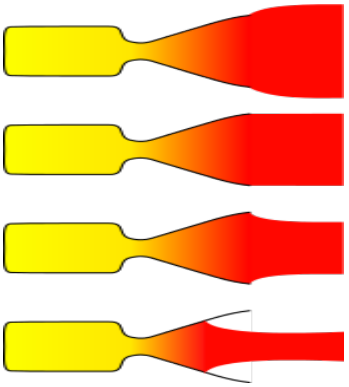

Figure 11. Nozzle examples (WK2, 2017).

Another Thrust Control Mechanisms

There are four major components to any full scale rocket; structural system or frame, the payload system, the guidance system, and the propulsion system. The guidance system of a rocket includes very sophisticated sensors, on-board computers, radars, and communication equipment. The guidance system has two main roles during the launch of a rocket; to provide stability for the rocket, and to control the rocket during maneuvers. A lot of different methods have been developed to control rockets in flight.

The movement of any object in flight is a combination of rotation of the gravity center and rotation of the object about the gravity center, also called the center of mass. All control methods produce a torque about the gravity center of the rocket, which causes rotating of the rocket in the flight center. By understanding the forces acting on the rocket and the resulting movement, the rocket guidance system can be programmed to stop targets or fly into orbit. Early rockets and available air-to-air missiles usually use moving fins at the back of the rocket. The moving fins adjusts the amount of aerodynamic force on the rocket. The aerodynamic force normally moves through the pressure center which is not in the center of the gravity center. The difference in the ground produces the torque of the center of gravity or center of mass. In Figure 12, the trailing edge of the fin facing us was magenta and diverted to the right. The resulting aerodynamic force moved the nose of the rocket to the right. Most modern rockets rotate the nozzle to produce the control torque. In an gimbaled thrust system, the rocket's exhaust nozzle can be turned from side to side. When the nozzle is moved, the thrust direction varies with the gravity center of the rocket. In Figure 12, the rocket nozzle is magenta and rotated to the right. The resulting thrust would move the rocket's nose to the right. Some ancient rockets, like the Atlas missile, used small additional rocket engines to create the control torque at the bottom of the main rocket. Small control rockets were called “vernier rockets”. In the figure, the right Vernier rocket engine is magenta colored and fired to cause the larger rocket's nose to move to the right. Due to the additional weight for fuel and plumbing, vernier rockets are no longer used. In some early rockets, such as V2 and Redstone rockets, a small thrust fin was placed in the exhaust flow of the main rocket to divert the thrust force and create a control torque. In the figure, a thrust vane is deflected to the right in the magenta color. This causes the exhaust flow to change the direction and the nose of rocket moves to the right. (Benson, 2014e).

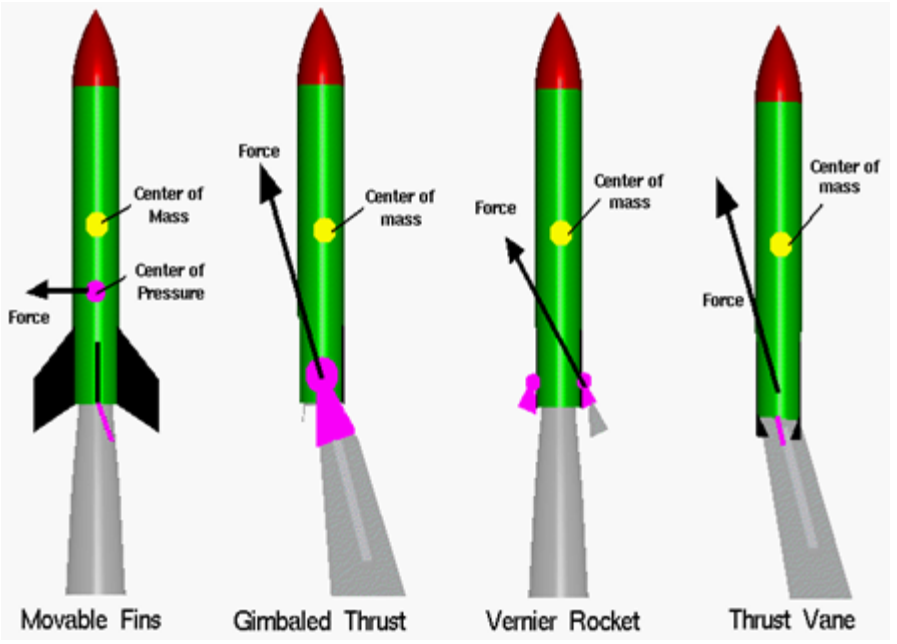

Figure 12. Control examples (Benson, 2014e).

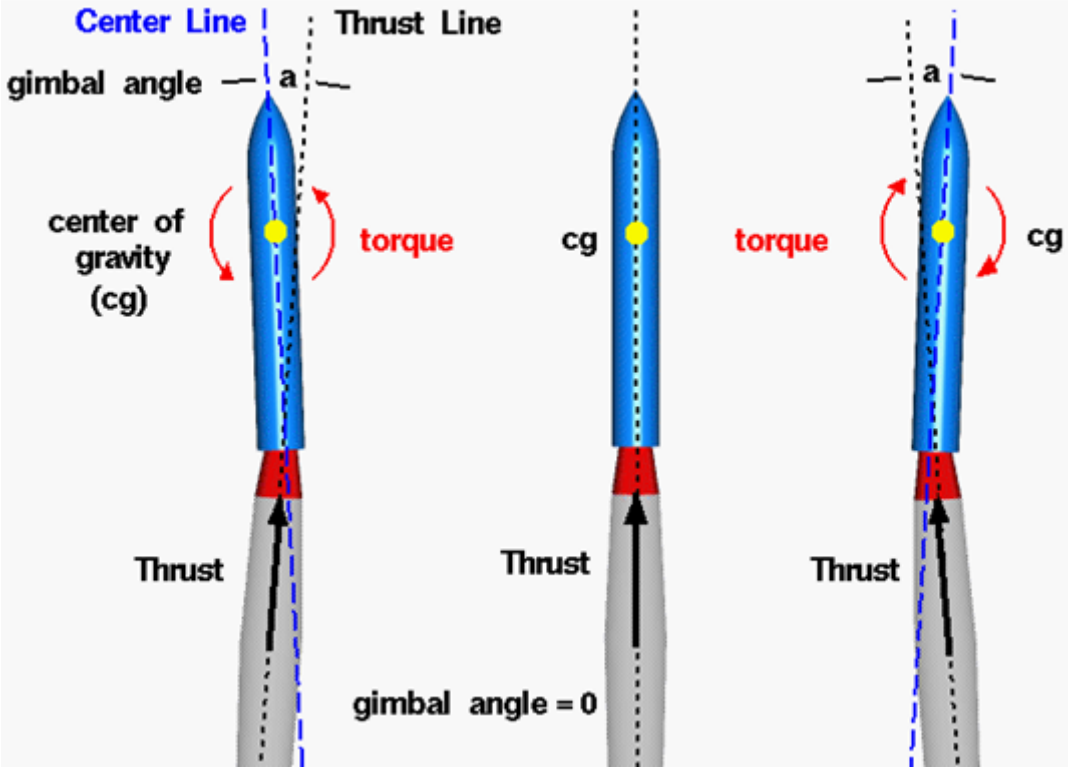

Figure 13. Gimbaled thrust (Benson, 2014f).

Several different systems can be used to maneuver the rocket during flight. Early rockets and some air-to-air missiles use moving aerodynamic surfaces such as elevators on an airplane. Of course, this system only works on rockets which remain in the atmosphere. The subsequent rockets, which were designed to leave the atmosphere, used small vanes in the nozzle exhaust to make the thrust vector. The most modern rockets, like

the Space Shuttle and Saturn V moon rockets, are using a system called gimbaled thrust. In a gimbaled thrust system, the rocket's exhaust nozzle can be turned from side to side. When the nozzle is moved, the thrust direction varies with the gravity center of the rocket. Figure 13 shows the these three cases. The middle rocket shows the "normal" flight configuration along the centerline of the rocket and along the gravity center of the rocket. In the left rocket, the nozzle is diverted to the left, and the push line is inclined to an angle of rotation (called the gimbal angle). Since the overthrust no longer runs through the center of gravity, a torque is created around the center of gravity and the nose of the rocket turns to the left. If the nozzle is returned along the centerline, the rocket moves to the left. On the right rocket, the nozzle was diverted to the right and the nose was moved to the right (Benson, 2014f).

Also the methods to increase the thrust are the location of fins, the shape of rockets (thickness etc.): depending on the volume of the load it carries, rocket weight, loads weight, their volume and weight and strength of the rocket motors.

Mass of the Rockets

For a rocket to leave the ground, the engine must produce a thrust that is greater than the total mass of the vehicle. For an typical rocket, in the total mass of the vehicle, 90% is the propellants; 6% is the structure (tanks, engines, fins, etc.); and 4% can be the payload. In determining the effectiveness of a rocket design, to calculate the terms of mass fraction (MF), the mass of the propellants of the rocket divided by the total mass of the rocket gives mass fraction:

$$MF = (\text{Mass of Propellants})/(\text{Total Mass}) \quad (18)$$

MF for a typical rocket is 0.80 which is a good balance between payload-carrying capability and range. If MF is equal to 1 we can say that the entire rocket would be nothing more than a lump of propellants. The larger MF can carry the less payload. The Space Shuttle has to MF of ~0.82. The MF varies between the different orbiters in the Space Shuttle fleet and with the different payload weights of each mission (M1, 1996).

Rocket Engines and Their Propellants

Most rocket today works with solid or liquid propellants. The word propellant does not only mean fuel, which means fuel and oxidizer. Fuel is a chemical rocket burn, but an oxidizer (oxygen) must be present for combustion. Jet engines draw oxygen from the air around them. Rockets must carry oxygen with them into space, where there is no air. The fuel of liquid fueled rocket's is usually kerosene or liquid hydrogen; The oxidizer is usually liquid oxygen. They are combined in a space called as a combustion chamber where the propellants burn and accumulate high temperatures and pressures, and the expanding gas escapes through the nozzle at lower end. To get the most power from the propellants, it should be mixed as completely as possible. Hybrid rockets combine elements from both rocket types. In a hybrid rocket, a gas or liquid oxidizer is stored in a tank separate from a solid fuel particle. The most important benefit of robust rockets on hybrid rockets (and liquid systems) is their simplicity. Hybrid systems has better performance than liquid systems (M1, 1996).

A new type of rocket engine is an electric motor, also called as ion motor. The working fluid for an electrical motor consists of very small charged particles called ions. The acceleration of the working fluid is produced by electrostatic forces, not by combustion. Ion motors produce very small amounts of thrust, but mass flow rates are very small, they can produce a thrust for a long time. Ion engines have very high specific impulses compared to chemical rockets. Another new type of rocket engine is a nuclear thermal engine where the nuclear reactor provides a continuous source of heat used to accelerate the working fluid. The working liquid may be any gas heated or passed through the reactor and heated when it is passed through the nozzle. The temperature of the exhaust and the resulting output speed may be much higher than the typical chemical rocket. The temperature of the exhaust, and the resulting exit velocity, can be much higher than for the typical chemical rocket (Benson, 2014a).

Results

Momentum is very important to increase the thrust in Eq. (2). According to Figure 2, p_e must be very high than p_0. The engine area (A_e) also can be large which depends on the specific heat ratio (γ) in Eq. (14). As the γ grow, the A_e value will also increase. When looked to Eq. (13), the mass flow rate also depends on to γ. High total pressure will also increase the mass flow rate and exit pressure (See Eq. 13 and 16). T_e will increase as the total temperature increases. Also the raise of V_e depends on T_e and high ((γ)) as well as M_e (in Eq. (17)). According to Eq. (3), how small p_0 (the pressure of the surrounding atmosphere) will be bigger the second part of the equation.

The inside pressure of the combustion chamber increases in bigger thrust. The place of fins, the shape of rockets (thickness etc.), the volume of the loads, rocket weight, loads weight, rocket volume and its weight, strength of the rocket motors also important for thrust. The terms of mass fraction (MF) can be near to 0.80 for a good result. Despite Ion motors produce very small amounts of thrust and the mass flow rates are very small, they can produce a good thrust for a long time.

References

Agrawal, J. P., 2010. High Energy Materials: Propellants, Explosives and Pyrotechnics, WILEY-VCH Verlag GmbH & Co. KgaA, ISBN: 978-3-527-32610-5 P:209-233

Benson, T., 2014a. Rocket Thrust, https://www.grc.nasa.gov/www/k-12/rocket/rktth1.html, [visiting date: 12th August 2018].

Benson, T., 2014b. Specific Impulse, https://www.grc.nasa.gov/www/k-12/rocket/specimp.html, [visiting date: 12th August 2018].

Benson, T., 2014c. Rocket Thrust Summary, https://spaceflightsystems.grc.nasa.gov/education/rocket/rktthsum.html, [visiting date: 12th August 2018].

Benson, T., 2014d. General Thrust Equation, https://www.grc.nasa.gov/www/k-12/rocket/thrsteq.html, [visiting date: 12th August 2018].

Benson, T., 2014e. Examples of Controls, http://www.grc.nasa.gov/ www/k-12/rocket/rktcontrl.html, [visiting date: 12th August 2018].

Benson, T., 2014f. Gimbaled Thrust, https://www.grc.nasa.gov/www/k-12/rocket/gimbaled.html, [visiting date: 12th August 2018].

CD (Concise Dictionary English-English),2014. V&S Publishers. ISBN: 978-93-505713-8-5. P:575

EEB1 (The Editors of Encyclopaedia Britannica), 2010. Missile, https://www.britannica.com/technology/missile, [visiting date: 12th August 2018].

EEB2 (The Editors of Encyclopaedia Britannica), 2010. https://www.britannica.com/technology/missile/media/385396/53401, [visiting date: 12th August 2018].

ELU (English Language & Usage), 2014. What is the difference between a 'rocket' and a 'missile', https://english.stackexchange.com/questions/185955/what-is-the-difference-between-a-rocket-and-a-missile, [visiting date: 12th August 2018].

F1, 2017, Rockets Work in a Vacuum. https://www.theflatearthsociety.org/forum/index.php?topic=67626.930, [visiting date: 12th August 2018].

Hampton, A., 2014. Four Forces of Flight, https://www.slideserve.com/adena-hampton/four-forces-of-flight, [visiting date: 12th August 2018].

M1, 1996, The Rockets, MIT Department of Aeronautics and Astronautics, http://web.mit.edu/16.00/www/aec/rocket.html, [visiting date: 15th August 2018].

RA, 2015. Simple Rocket Analysis, http://www.aerodynamics4students.com/propulsion/simple-rocket-analysis.php, [visiting date: 10th August 2018].

RM1, 2013. Difference Between Rocket and Missile, https://www.differencebetween.com/difference-between-rocket-and-vs-missile/), [visiting date: 15th August 2018].

SS (Sensing Systems), 2015. High Capacity Load Cells: One Million Pounds and Higher, http://www.sensing-systems.com/blog/high-capacity-load-cells-one-million-pounds, [visiting date: 12th August 2018].

TD, 2018. Difference between Rocket and Missile, https://theydiffer.com/difference-between-rocket-and-missile/, [visiting date: 15th August 2018].

WK1, 2015, The Thrust, https://en.wikipedia.org/wiki/Thrust, [visiting date: 12th August 2018].

WK2, 2017, Rocket propellant, https://en.wikipedia.org/wiki/Rocket_propellant, [visiting date: 12th August 2018].

International Conference on Science and Technology

ICONST 2018

5-9 September 2018 Prizren - KOSOVO

Determination of Properties of Apple Processing Waste and Investigation of Appropriate Disposal Methods

Kemal Sülük[1,2*], İsmail Tosun[1], Kamil Ekinci[3]

Özet: Türkiye elma ve elma işleme ürünleri, meyve üretim alanı ve üretim miktarları bakımından ilk on ülke arasında yer almaktadır. Dünyadaki elma üretimi çoğunlukla Çin, ABD ve Türkiye'de gerçekleştirilmektedir. Türkiye'de üretilen elmaların % 76.3'ü on ilde gerçekleştirilmektedir. Bu iller arasında ilk sırada yer alan Isparta'yı Niğde, Karaman ve Antalya takip etmektedir. Elma işleme endüstrisinin ön eleme-temizleme işlemlerinden kaynaklanan atıklar, işleme için uygun olmayan yapraklar, dallar ve meyvelerden oluşmaktadır. Elma işleme atığının yaklaşık % 20'si hayvan yemine katkı maddesi olarak kullanılmakta ve geri kalan % 80'i düzenli / düzensiz depolama ve yakma işlemleri ile bertaraf edilmektedir. Bu çalışmada, elmanın ön işlemlerinden kaynaklanan atıkların fiziksel ve kimyasal özellikleri belirlenmiş ve bu atıkların bertarafı için stratejilerin geliştirilmesi amaçlanmıştır. Bu çalışmada kullanılan katı ve atık su örnekleri, Isparta'da faaliyet gösteren Elmataş Göller Bölgesi Meyve ve Sebze Değerlendirme Şirketi'nden alınmıştır. Elde edilen örnekler su muhtevası, birim hacim ağırlığı (BHA), serbest boşluk oranı (FAS), organik madde (OM) içeriği, pH ve elektriksel iletkenlik (EC) değerleri, C/N oranı, amonyum ve nitrat değişimleri açısından analiz edilmiş ve elde edilen sonuçlar değerlendirilmiştir. Elma işleme işleminden önce ve işlem sırasında aşırı su kullanılmaktadır. Elma işleme endüstrisinde ön eleme-temizleme atıklarında yapılan deneylerde su içeriği % 82.5, BHA 0,78 kg/l, FAS % 30.46, OM içeriği % 94.62, pH 4.12, EC 1.05 dS/m ve C/N oranı 30 olarak bulunmuştur. Elma işleme endüstrisi ön eleme-temizleme atıklarının organik madde içeriği yüksek olduğundan biyolojik arıtma için uygundur. Su içeriği yüksek olduğu için, su içeriği farklı atıklarla karıştırılarak ve anaerobik arıtma için uygun hale getirildikten sonra aerobik kompostlama ile değerlendirmek de mümkündür.

Anahtar Kelimeler: Elma işleme atıkları, kompostlama, yakma, bertaraf stratejileri, Isparta

Abstract: Turkey is among the top ten countries in terms of apple and apple processing products, fruit production area and production quantities in the world. Most of the apple production in the world are realized in China, the US and Turkey. 76.3% of the apples produced in Turkey are performed in ten provinces. Isparta is ranked the first follwed by Niğde, Karaman and Antalya. The wastes from pre-screening-cleaning processes in the apple processing industry are composed of leaves, branches, and fruit that are not suitable for processing. Approximately 20% of the apple processing waste is used as an additive to animal feed, and the remaining 80% is disposed of by regular / irregular disposal and burning operations. In this study, the physical and chemical properties of wastes from pre-processing of apples were determined and the strategies for disposal of these wastes were aimed to be developed. Solid and wastewater samples used in this study were obtained from Elmataş Göller Region Fruit and Vegetable Processing Company operating in Isparta. The obtained samples were analyzed for water content, weight per unit volume (BHA), free air space (FAS), organic matter (OM) content, pH and electrical conductivity (EC) values, C/N ratio, phosphorus, ammonium and nitrate changes and the results obtained were evaluated. Excess water was used before the apple processing process and during the process. THe results obtained from the wastes from pre-screening-cleaning processes in the apple processing industry showed that water content, BHA, FAS, OM, pH, EC, and C/N ratio were 82.5%, 0.78 kg/l, 30.46%, 94.62%, 4.12, 1.05 dS/m, and 30, respectively. The apple processing

[1]Suleyman Demirel University, Faculty of Engineering, 32260, Isparta, TURKEY
[2]Mus Alparslan University, Faculty of Engineering, 49250, Muş, TURKEY
[3]University of Applied Sciences, Isparta, Faculty of Agricultural Sciences and Technologies, 32260, Isparta, TURKEY

*Corresponding author: kemalsuluk@sdu.edu.tr

industry pre-screening-cleaning wastes are suitable for biological treatment since their organic matter content was high. It is also possible to evaluate by aerobic composting once the water content is reduced by mixing with different wastes as well as being suitable for anaerobic treatment since the water content is high.

Keywords: Apple processing wastes, composting, incineration, disposal strategies, Isparta.

1. Giriş

Elma ılıman iklim meyve türleri grubu içinde yer alan ve dünyada üretimi çok olan meyvelerden biridir. Yetiştiriciliği çok geniş alanlara yayılmış olan ve kültürü milattan öncesi dönemlere dayanan elma; sofralık olarak tüketilmekle birlikte püre, cips, sirke, çay, reçel, marmelat, tıbbi bitki ve meyve suyu olarak da kullanılmaktadır. Dünya'da ve Türkiye'de elma üretimi sırasıyla 80 milyon (FAO, 2013) ve 3 milyon tondur (TUİK, 2017). Dünya elma üretiminde önde gelen ülkeler arasında Çin, Amerika Birleşik Devletleri (ABD) ve Türkiye yer almaktadır. 39 milyon tonluk elma üretimi ile üretim yapan Çin'i, 4 milyon ton ile ABD, 3.1 milyon ton ile Türkiye izlemektedir. Ülkelere göre elma üretim miktarları Tablo 1' de gösterilmiştir (FAO,2013).

Dünyada elma üretim miktarı yaklaşık %37'lık sürekli artış göstermesine rağmen elma üretim alanları 1990'lı yılların ortaları itibariyle azalma eğilimi göstermiş ve bu eğilim 2009 yılı itibariyle artışa geçmiştir. İlk yıllarda elma üretim alanlarında azalmasının olmasına rağmen elma üretiminde artışlar gözlenmiştir. Elma ıslah çalışmalarının her geçen gün artması ve tarımsal teknolojilerinin gelişmesi verimliliği artırmış ve üretime olumlu yansıdığı görülmüştür (Aras, 2015). Ülkelerin yıllara göre elma üretimindeki gelişimi Şekil 1'de gösterilmiştir.

Tablo 1. Ülkelerin Dünya elma üretimindeki yeri

Ülkeler	Elma Üretimi (ton)	Oran (%)
Çin	39.682.618	49.10
ABD	4.081.608	5.05
Türkiye	3.128.450	3.87
Polonya	3.085.074	3.82
İtalya	2.216.963	2.74
Hindistan	1.915.000	2.37
Fransa	1.737.482	2.15
Şile	1.709.582	2.12
İran	1.693.370	2.10
Rusya	1.572.000	1.95
Arjantin	1.245.018	1.54
Brezilya	1.231.472	1.52
Ukranya	1.211.400	1.50
Özbekistan	937.000	1.16
Meksika	858.608	1.06
Diğer ülkeler top.	14.516.876	17.95
Dünya	**80.822.521**	**100**

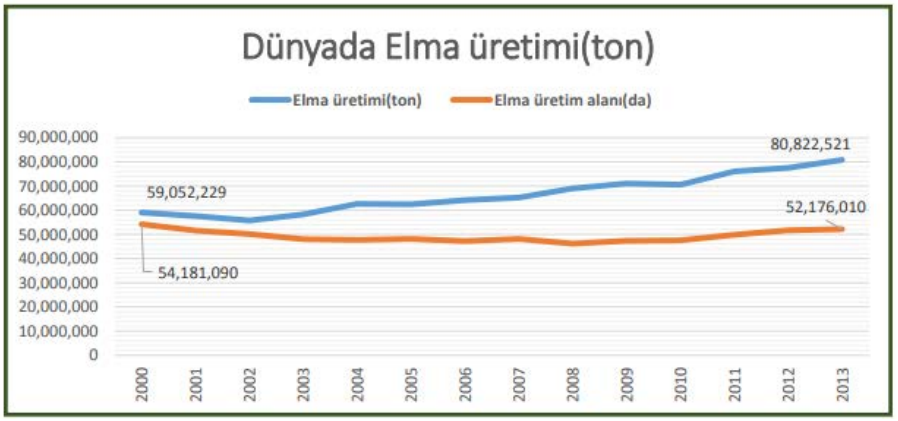

Şekil 1. Yıllara göre ülkelerin elma üretim miktarları ve elma üretim alanları

1.1. Türkiye'de elma üretimi

Elma uzun yıllardır Türkiye'de en çok üretimi yapılan meyve türüdür ve tarihsel süreçte ekonomik anlamda da Türkiye'nin en favori meyve türü olmuştur (Ercişli 2004). Ülkemizin coğrafi yapısı ve iklim koşullarına en uygun meyve olması hemen her bölgede yetiştirilmesine olanak sağlamaktadır. Ülkemizde tarıma elverişli alanların yaklaşık %15'inde meyve yetiştiriciliği yapılmakta, toplam meyve alanlarının %5,3'ünü elma oluşturmakta ve 2014 yılında yaklaşık 1,8 milyon dönümlük alanda 2,5 milyon ton elma üretilmiştir. (Anonim, 2014). TÜİK verilerine göre Türkiye'de yıllara göre üretilen meyve çeşitleri ve üretim miktarları Tablo 2'de gösterilmiştir.

Ülkemizde elma üretimi iller düzeyinde incelendiğinde tüm illerimizde elma yetiştiriciliğinin yapıldığı ancak ticari düzeyde üretimin en çok başlıca 10 ilde gerçekleştiği ve üretimin % 75.5'i kısmını oluşturduğu görülmektedir. Sırasıyla Isparta (%20,4), Karaman (%13,6), Niğde (%12,9), Antalya, Denizli, Çanakkale, Mersin, Kayseri, Kahramanmaraş ve Konya elma üretiminin en fazla yapıldığı illerdir (TÜİK, 2017).

Isparta ilinin genelinde açık ve kapalı elma bahçe sayısının fazla olması, ülke elma üretimi içindeki payını artırmaktadır. Bölgede elma yetiştiriciliği 1960'lı yıllarda başlamış ve günümüze 646.266 ton üretime kadar yükselmiştir. Elma üretiminde Eğirdir, Gelendost, Yalvaç, Senirkent, Isparta Merkez ve diğer ilçeler takip etmektedir (İşçi, 2014). Isparta ili ve ilçelerinde yetiştirilen elma üretim miktarları Tablo 3'te gösterilmiştir (TUİK 2017). Ispartada faaliyet gösteren meyve suyu fabrikaları Asya Meyve Suyu Fabrikası ve Elmasu Fabrikası, Elmataş Fabrikası ve Anadolu Etap Meyve Suyu fabrikasıdır.

Tablo 2. Türkiye'de yıllara göre meyve üretimi (ton)

Yıllar	Üzüm	Elma	Portakal	Kayısı	Şeftali
2001	3 250 000	2 450 000	1 250 000	517 000	460 000
2002	3 500 000	2 200 000	1 250 000	352 000	455 000
2003	3 600 000	2 600 000	1 250 000	499 000	470 000
2004	3 500 000	2 100 000	1 300 000	350 000	372 000
2005	3 850 000	2 570 000	1 445 000	894 000	510 000
2006	4 000 063	2 002 033	1 535 806	483 459	552 775
2007	3 612 781	2 457 845	1 426 965	589 732	539 435
2008	3 918 442	2 504 494	1 427 156	750 574	551 906
2009	4 264 720	2 782 365	1 689 921	660 894	547 219
2010	4 255 000	2 600 000	1 710 500	476 132	539 403
2011	4 296 351	2 680 075	1 730 146	676 138	545 902
2012	4 234 305	2 888 985	1 661 111	795 483	611 165

2013	4 011 409	3 128 450	1 781 258	811 609	637 543
2014	4 175 356	2 480 444	1 779 675	278 210	608 513
2015	3 650 000	2 569 759	1 816 798	696 100	642 727

Tablo 3. Isparta ili ve ilçelerinde yetiştirilen elma üretim miktarları (TÜİK, 2017)

	2010	2011	2012	2013	2014	2015	2016	2017
Aksu	17876	18434	19910	15067	15309	12310	14642	15524
Atabey	15535	10840	9836	11526	8166	3097	9575	10514
Eğirdir	154084	217889	230994	235901	247318	259898	249110	287492
Gelendost	193243	186427	196994	196932	195242	77835	183654	183047
Gönen	15761	16260	17662	17170	19941	5984	5416	5293
Keçiborlu	8256	5596	5596	4921	4920	4520	3287	3261
Merkez	17241	16742	16896	14149	9973	6653	9380	7233
Senirkent	35613	53746	56614	56107	60578	18148	70472	52466
Sütçüler	3040	3040	3040	3022	3177	1741	1576	1512
Uluborlu	27710	19143	18778	18226	18431	1960	9233	9904
Yalvaç	43938	40461	34407	36249	35961	13371	17032	17114
Yenişarbademli	2420	2720	2720	4621	5348	5067	2569	2524
Şarkikaraağaç	14654	18631	21348	20971	21902	25354	20557	21491
Toplam	549.371	609.929	634.795	634.862	646.266	435.938	596.503	617.375

1.2. Elma suyu üretim teknolojisi

Meyve suyu; sağlam, olgun, taze veya soğukta muhafaza edilmiş meyvelerden, tek meyveden veya daha fazla meyvenin karışımından elde edilen, elde edildiği meyve ve meyvelerin karakteristik renk, aroma ve tadına sahip, fermente olmamış ancak fermente olabilen ürün olarak tanımlanmaktadır (Resmi gazete, 2006).

Ana hatlarıyla elma suyu endüstriyel üretim prosesi iş akış şeması Şekil 2 ve 3'te gösterilmiştir. Elmalar, stok alanından, meyve boşaltma havuzlarına alınarak dik helezon yardımı ile, meyve yıkama havuzlarına aktarılmaktadır. Yıkama havuzlarında, elma ile taşınan toprak, taş, yaprak vb. maddelerin uzaklaştırılması için, ham su ile yıkama işlemi uygulanmaktadır. 2. Kademe yıkamada ters osmoz suyu ile yıkanıp, son duşlama (durulama) yapılmaktadır. Yıkama işlemi tamamlanan meyveler, konveyör bant aracılığı ile, meyve parçalama bölümüne iletilmeden önce, seçme işlemine tabi tutulmaktadır. Seçme bölümünde, hammaddeki ham, çürük, ezik, vb. kusurlu meyvelerin ve sap, yaprak gibi yabancı maddelerin seçilme işlemi gerçekleştirilmektedir. Yıkanarak temizlenmiş meyveler, çekirdek çıkarma işleminin ardından, değirmende parçalanarak elekten geçirilip, meyve eti değirmenine aktarılmaktadır. Parçalanmış meyve eti (mayşe), konsantre renk kaybını önlemek amacıyla, ısıtma işlemine tabi tutulmaktadır. Uygulama sıcaklığı 50-70 ℃ arasında değişmektedir. Isıtma işlemine tabi tutulan mayşenin, mayşe tanklarında renk veya mayşe enzim ilavesi yapılabilmektedir. Mayşe enzimasyonunda, en önemli etken bekleme süresi ve sıcaklıktır. Böylelikle, yardımcı enzim ilaveleri ile, elmadan maksimum verim alınması sağlanmaktadır. Enzimasyon işleminin ardından presleme bölümüne aktarım yapılmaktadır. Presleme ile, mayşedeki sıvı fazın, meyve suyu olarak ayrılması gerçekleşmektedir. Presleme işleminin ardından ön evaporasyon ve pastörizasyon işlemine tabi tutulan elma meyvesi, bu işleminin ardından, enzimasyon ve durultma işlemine tabi tutulmaktadır. Devamında pastörizasyon, ultra filtrasyon ve evaporasyon işlemi ile, sterileze edilmiş, konsantre edilmiş, kimyasal değişmeye karşı stabilize edilmiş ve hacim azalışı sağlanmış olan elma suyu üretilmektedir. İş akım şemasında da görüldüğü gibi proses esnasında bazı katı ve sıvı yan ürünler-atıklar oluşmaktadır. Katı atıklar; elma posası ile ön eleme temizleme atıklarından, atıksu ise 1. ve 2. Yıkama işleminden meydana gelmektedir.

1.3. Elma işleme atıklarının bileşimi

Elma işleme atıkları ön eleme-temizleme atıklarından ve posadan meydana gelmektedir. Meyve suyu üretim tesisin işleyişine bağlı olarak bu atıklar ayrı ayrı depolanmakla birlikte karışık bir şekilde de depolanabilmektedir. Ön eleme-temizleme atıkları; elma posası ile birlikte ham, çürük, ezik, kusurlu meyvelerin ve sap, yaprakları, yabancı maddelerden meydana gelmektedir. Elma posası, elma suyu üretimi esnasında oluşan yan ürün olup, meyve suyu sanayi atıklarının %25-35'ini oluşturmaktadır (Djilas vd. 2009, Vendruscolo vd., 2008). Elma posası ve kabuğu, sellüloz, mineral ve fenolik bileşiklerce zengin bir yapıya sahiptir. Benzer şekilde Türkiye'de faaliyet gösteren meyve suyu fabrikalarından önemli miktarlarda elma posalarının artık olarak kaldığı bilinmektedir. Özellikle bölgemizde (Isparta ve çevresi) büyük miktarda elma posaları ve işlem atıkları meydana gelmektedir. Elma posası, kabuk, çekirdek, tohum, çanak yaprak, saptan ve yumuşak dokudan oluşmaktadır (Grigelmo vd.,1999). Yüksek su içeriğine sahip olmakla birlikte basit şekerler, az miktarlarda mineraller, proteinler ve vitaminler, elma posasının bileşiminde bulunmaktadır (Jin vd., 2002). Elma posasının bileşimi, proseste kullanılan elmanın çeşidine ve işleme aşamasında kullanılan preslemenin niteliğine ve tekrarına bağlı olarak değişiklik göstermektedir (Paganini ve ark. 2005). Tablo 4'te elma posasında fiziksel ve kimyasal bileşimlerine ait bazı değerler verilmiştir (Bhushan ve ark. 2008).

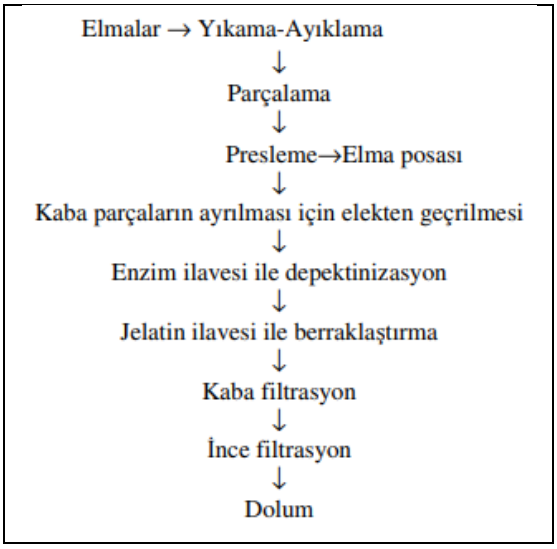

Şekil 2. Elma suyu üretimi iş akış şeması (Cemeroğlu,2009)

Tablo 4. Elma posasının fiziksel ve kimyasal bileşenleri

Bileşen	**Miktar (kuru madde)**	**Bileşen**	**Miktar (kuru madde)**
Nem (%)	3.90–10.80	**Karbonhidratların alkolde eriyebilir fraksiyonu**	
Protein (%)	2.94–5.67	Sakaroz (%)	3.80–5.80
Toplam Karbonhidrat (%)	48.0–62.0	Fruktoz (%)	19.50–19.70
Lif (%)	4.70–51.10	Glikoz (%)	48.30
Suda çözünebilir Lif (%)	36.50	Ksiloz, mannoz, galaktoz (%)	1.20–4.40
Suda çözünemez Lif (%)	14.60	L-malik asit (%)	2.60–3.20
Yağ (%)	1.20–3.90	Arabinoz ve ramnoz (%)	7.90–6.0
Pektin (%)	3.50–14.32	Glikooligosakkaritler (%)	3.40–3.80
Kül (%)	0.50–6.10	Ksilooligosakkaritler (%)	3.0–3.70
Mineraller		Arabinooligasakkaritler (%)	0.20–0.40
Fosfor (%)	0.07–0.076	Üronik asit (%)	2.70–3.40
Potasyum (%)	0.43–0.95	**Karbonhidratların alkolde çözünemez fraksiyonu**	
Kalsiyum (%)	0.06–0.10	Glukan (%)	41.90–42.90
Sodyum (%)	0.20	Nişasta (%)	14.40–17.10
Magnezyum (%)	0.02–0.36	Selüloz (%)	7.20–43.60

Bakır (%)	1.10	Ksiloz polisakkarit, mannoz-galaktoz (%)	13.0–13.90
Çinko (%)	15.00	Arabinoz ve ramnoz polisakakrit (%)	8.10–9.0
Manganez (%)	3.96–9.00	Asit deterjan lignin (%)	15.20–20.40
Demir (mg/kg)	31.80–38.30	Üronik asit (%)	15.3

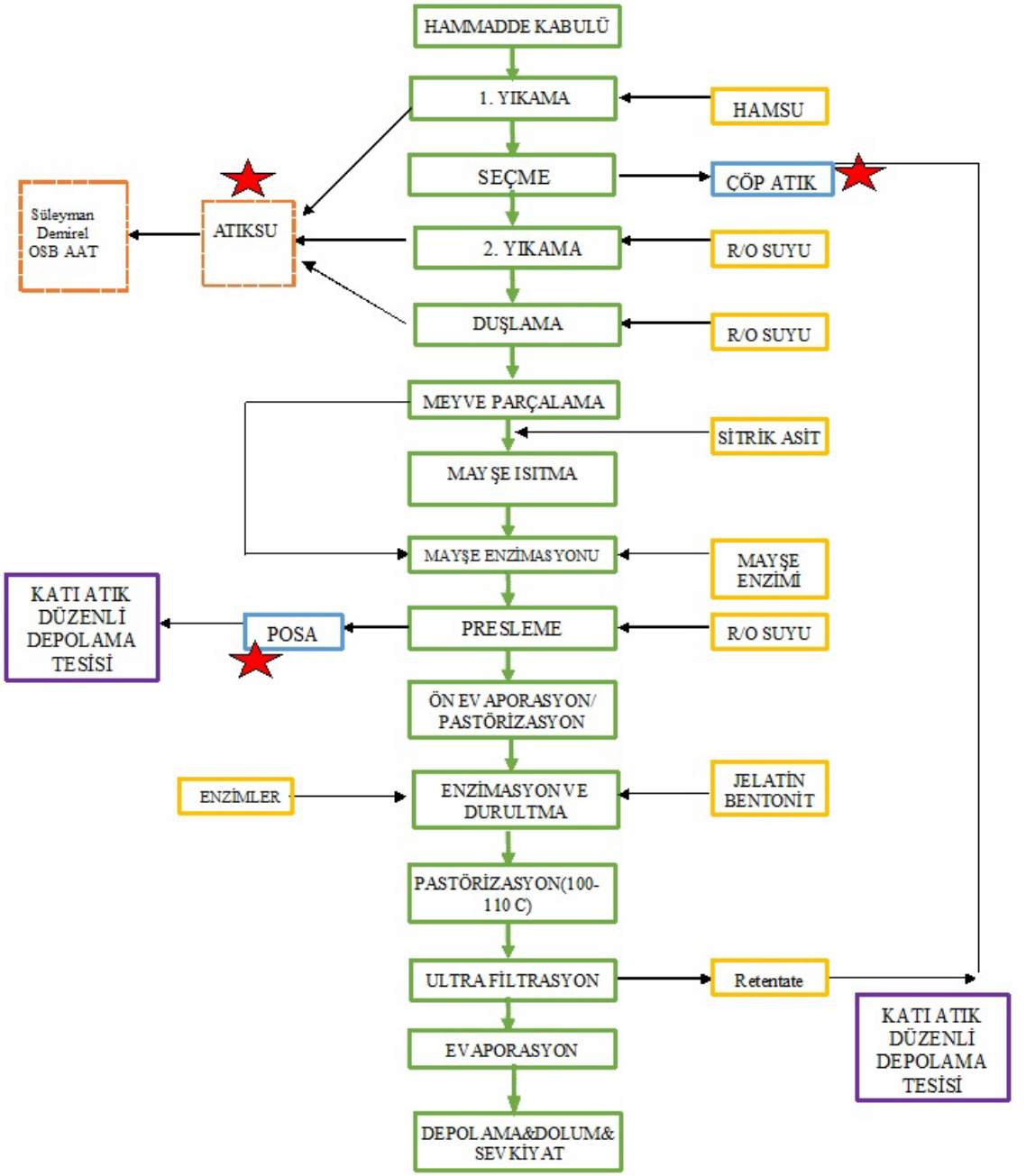

Şekil 3. Endüstriyel elma suyu üretimi iş akış şeması (Isparta)

1.4. Elma işleme atıklarının kullanım alanları

Elma suyu üretim prosesi ön eleme-temizleme esnasında çıkan atıklar çöp olarak nitelendirilmekte ve hiçbir işleme tabi tutulmadan düzenli/düzensiz depolama sahalarında biriktirilmektedir. Ayrıca tesiste uzun zamandır biriken bu atıklar doğal yollarla kurumuş ise doğrudan yakılarak bertaraf edilmektedir. Elma suyu üretim prosesinin diğer yan ürünü olan elma posasından faydalanmanın mümkün olan stratejileri son yıllarda incelenmeye başlanmıştır. İdeal kullanım alanı hakkında tam belirlenmemiş olup elma posasından pektin üretiminin hem ekonomik hem de ekolojik açıdan en uygun kullanım alanı olduğunu kabul edilmektedir. Elma suyu üretiminde kullanılan çeşitli enzimlerden dolayı, posada biriken enzimlerden kaynaklı enzimatik esmerleşmenin sebep olduğu koyu renkten dolayı açık renkli yiyeceklerde kullanımı sınırlı olabilmektedir (Schieber vd., 2001). Elma posasından farklı bileşenlerin üretimi ve geri kazanımı konusunda da çok sayıda çalışmalar bulunmaktadır.

Posanın içerdiği bileşenlerin besin değerlerinin yüksek olması ve geri kazanımlarının mümkün olabilmesi, posa atıkların gıda katkısı ve tamamlayıcısı olarak kullanım imkanını doğurmuş ve atıklara olan ilgiyi artırmıştır. Ancak bu işlemler endüstriyel boyutta ileri teknoloji maliyetlere ihtiyaç duyduğu için zaman zaman sadece bilimsel araştırmadan öteye geçemeyen çalışmalar bulunmaktadır. Enzim üretimi (Joshi ve ark. 2006, Schemin ve ark. 2005), organik asitlerin üretimi (Shojaosadati ve Babaeipour 2002), etanol (Hang vd., 1981), aroma bileşenleri (Medeiros vd., 2000), doğal antioksidanlar (Lu ve Foo, 2000) ve yenilebilir liflerin üretimi (Masoodi vd., 2002) ile ilgili çalışmalar yapılmıştır.

1.5. Elma suyu işleme atıklarının çevresel etkileri

Meyve işleme sanayi yan ürünleri doğal ve insan yaşamı üzerinde olumsuz etkileri bulunan atıklar oluşturmaktadır:

a) ***Atıksu:*** Meyve işleme endüstrisi atıksuları yüksek oranda biyolojik olarak parçalanabilir organik madde muhtevasına sahiptir. Bu organik maddeler, doğrudan toksik veya zararlı olmamakla birlikte çoğunlukla şeker türevi içeren bileşiklerden meydana gelmektedir. Ancak bu atıksuların kanalizasyona veya su kaynaklarına deşarj edilmesi durumunda oksijen tüketiminin artmasına sebep olmaktadırlar. Meyve suyu üreten fabrikalar, atıksularını alıcı ortama veya kanala deşarj etmeden önce bu atıksularını arıtmaları gerekir ancak arıtma maliyeti yüksek olması durumunda alıcı ortama kaçak deşarjlar yapabilmektedirler. Yüksek miktarda organik asit içermesi (düşük pH), azot ve fosfor eksikliğinden kaynaklanan besin miktarının az olması, üretim prosesine bağlı olarak atıksuyun miktar ve bileşimindeki dalgalanmalardan dolayı ham atıksuyun arıtılması zor ve maliyeti yüksektir. Fakat alıcı ortama deşarj yapılması düşünüldüğü taktirde bazı arıtım seçenekleri zorunlu hale gelmektedir: Deşarj eğer bir su ortamına yapılacaksa tam arıtım yapılarak; kanalizasyona deşarj yapılacaksa ön arıtma yapılmak zorundadır (Elmaslar,2002).

b) ***Katı atıklar:*** Meyve işleme sanayinin katı atıkları kabuklar, tohumlar, dal ve yapraklar, çürümüş, ezik meyveler ve elma posası içeren bitkisel atıklardır. Meyve suyu üretimin her geçen gün artması ile birlikte mikrobiyal bozunmaya eğilimli organik madde içeriği bulunan bu atıkların da miktarı artmakta giderek büyüyen bir sorun haline gelmektedir. Bu atıkların depolanması, kurutulması ve taşınması da maliyet gerektiren işlemlerdir. Meyve işleme endüstrisine ait bitkisel kaynaklı katı atıklar oluşumundan sonra mikrobiyolojik olarak bozulmaya başlarlar. Bu da görüntü ve koku kirliliğine sebep olmaktadır. Bu problemlerin oluşmaması için kurutulması alternatifi ön plana çıkmakta ancak maliyeti yüksek olduğundan dolayı bu işlem de birçok üretici tarafından göz ardı edilmektedir.

2. Materyal ve Yöntem

Çalışmaya konu olan elma işleme (ön eleme-ayırma) katı atıkları Isparta'da faaliyet gösteren Elmataş Göller Bölgesi Meyve ve Sebze Değerlendirme Şirketi'nden temin edilmiştir (Şekil 4). Atıklar arazide bir süre kurutulduktan sonra parçalayıcı yardımıyla öğütülmüş ve analizleri gerçekleştirilmiştir. Yapılan analizlere ilişkin analiz metotları Tablo 5'de verilmiştir.

Şekil 4. Elma işleme ön eleme-temizleme atıkları

Tablo 5. Elma işleme atıklarında yapılan analizler ve metotları

Parametre	**Birimi**	**Analiz Yöntemi**	**Analiz Metodu**
SM	%	65 °C'de 3 gün	TMECC method
BHA	kg/L	Birim hacimdeki ağırlığın belirlenmesi	TMECC method
FAS	%	hava boşluk oranının belirlenmesi	TMECC method
OM	%	550 °C'de 4 saat	TMECC method 03.02-A
pH		1:10 (dw:v)	TMECC method 04.11-A1:5
EC	dS/m	1:10 (dw:v)	TMECC method 04.10-A 1:5.
C/N		Vario MACRO CN analizörü yüksek sıcaklıkta yakma ve gravimetrik olarak belirleme	
Fosfor	mg/kg	Spektrofotometrik, SnCl2metodu	APHA (1995)
Amonyum	mg/kg	Nessler yöntemiyle tayin	SSSA, 1996
Nitrat	mg/kg	Nessler yöntemiyle tayin	SSSA, 1996

3. Bulgular

Meyve suyuna işlenen toplam meyve miktarları 2000 yılında 433 000 ton iken 2007 yılında 737 000 ton, 2008 yılında ise 771 000 tondur. Meyve suyuna işlenen elma ise yıllar içerisinde 244 bin ton ile 409 bin ton arasında değişiklik göstermekte ve işlenen meyveler içinde her yıl en yüksek oranda kalmıştır. 2000 ile 2008 yılları arasında meyve suyuna sanayisinin işlediği meyve ve sebze miktarları (Tablo 6) göz önüne alındığında Türkiye'de yıllara göre meyve üretimine göre her yıl yaklaşık ortalama üretilen elmanın %13,5'i meyve suyu olarak işlenmektedir (MEYED, 2008). Ülkemizde hammadde olarak elmanın payı yıldan yıla azalmakla beraber %43,3 ile ilk sırada yer almaktadır (Tablo 7). Diğer meyvelere oranla en fazla oranda işlenen ve her yıl giderek üretimi artan elmanın (Tablo 2) meyve suyuna işlenmesi sonucunda ortaya çıkan atıkları da artmaktadır. Elma işleme atıkları (posa dahil), elma suyu üretim atıklarının %25-35'ini oluşturmaktadır. Yani 2016 yılı üretim verilerine göre ülkemizde 133.125 ton elma işleme atığı oluşmuş olup bu atıkların büyük çoğunluğu herhangi bir işleme tabi tutulmadan düzenli/düzensiz depolama tesislerine gönderilmiştir. Dünya genelinde ise bu rakam yaklaşık 4.2 milyon tonlara kadar ulaşmakta ve çevre için ciddi bir problem teşkil etmektedir (Vendruscolo ve ark. 2008).

Tablo 6. Meyve suyuna işlenen meyve miktarları (bin ton)

Meyve	2000	2001	2002	2003	2004	2005	2006	2007	2008
Vişne	20.4	28.2	9.9	54.7	35.7	37.1	52.2	72.6	54.6
Kayısı	26.7	37.2	13.9	34.8	24.8	30.8	36.1	38.2	74.9
Şeftali	44.8	31.5	26.2	51.5	30.2	75.9	65.3	90.1	118.8
Elma	**311.5**	**272.9**	**244.5**	**341.5**	**338.0**	**409.2**	**282.9**	**356.8**	**333.8**
Portakal	22.9	12.6	31.7	28.3	46.2	33.1	37.8	53.3	63.9
Nar	-	-	-	-	-	17.6	46.6	57.5	49.5
Havuç	-	-	-	-	-	-	-	30.6	30.7
Üzüm	-	-	-	-	-	10.9	8.4	18.3	16.9
Çilek	-	-	-	-	-	-	-	4.1	7.7

Tablo 7. İşlenen meyvelerin türlere göre dağılımı (%)

Meyve	2000	2001	2002	2003	2004	2005	2006	2007	2008
Vişne	4.7	7.3	2.9	10.5	7.0	5.9	8.9	9.8	7.1
Kayısı	6.2	9.6	4.0	6.7	4.9	5.0	6.2	5.2	9.7
Şeftali	10.3	8.1	7.6	9.9	5.9	11.9	11.2	12.2	15.4
Elma	**71.9**	**70.3**	**70.7**	**65.5**	**66.2**	**65.1**	**48.6**	**48.4**	**43.3**
Portakal	5.3	3.2	9.2	5.4	9.1	5.3	6.5	7.2	8.3
Nar	-	-	-	-	-	2.7	8.0	7.8	6.4
Havuç	-	-	-	-	-	-	-	4.2	3.9
Üzüm	-	-	-	-	-	1.7	1.4	2.5	2.2
Çilek	-	-	-	-	-	-	-	0.6	1.0

Çalışmada kullanılan elma işleme ön eleme-temizleme atıklarının bazı fiziksel ve kimyasal analizleri yapılmış olup Tablo 8'de verilmiştir. Analiz sonuçlarına bakıldığında organik madde muhtevasının çok yüksek olduğu görülmüş olup literatür çalışmaları ile de benzerlik göstermektedir (Tablo 4). Ayrıca pH değeri çok düşük olmamakla birlikte elektriksel iletkenlik değeri de (1.05 ds/m) düşüktür. Nitrat değerlerine bakıldığında yüksek olduğu görülmekte, bunun sebebinin de elma üretimi esnasında verilen kimyasal azot kaynaklı ilaçların atıklara kadar taşınmasından kaynaklandığı düşünülmektedir. Ayrıca atığın çok yüksek su muhtevasına sahip olması (%82.5), ele alınması gereken en önemli parametrelerden biri olduğunu göstermektedir.

Tablo 8. Elma işleme ön eleme-temizleme atığının fiziksel ve kimyasal özelikleri

Parametre	Elma İşleme ön eleme-temizleme atığı
MC (%)	82.5
OM (%)	94.62
pH	4.12
EC (dS/m)	1.05
TC (%)	44,28
TN (%)	1,48
C/N	30
BHA (kg/lt)	0.78
FAS (%)	30.46
NH_4^+-N (mg/kg)	34
NO_3-N (mg/kg)	537

4. Tartışma ve Sonuçlar

Isparta'da son 10 yılda elma üretimi ortalama olarak 590 000 ton/yıl olmuştur. Türkiye'deki üretimi en çok Isparta'da gerçekleştirlmekte olup (%20,4), bunu Karaman (%13,6), Niğde (%12,9) ve Antalya izlemektedir. Proses sonrası açığa çıkan atık miktarı, prosese giren elmanın %25-35'i kadardır. Elma işleme prosesinde yıkama ve durulama esnasında yıllık ortalama 100.000 tonluk hammaddenin yıkanması için, günlük 2.500 m^3 yıkama suyuna ihtiyaç duyulmaktadır. Bu nedenle, elmaların yıkanması sonucu günde 2.500 m^3 atıksu oluşmaktadır. Oluşan atıksu ya paket arıtma (fiziksel, kimyasal ve biyolojik arıtma) ile arıtılarak kanalizasyona deşarj edilmekte ya da ön çökeltim havuzunda bekletilerek alıcı ortama deşarj edilmektedir.

Elma işleme prosesi sonucunda oluşan katı atıklar ön eleme-temizleme atıkları ve posa olmak üzere 2 grupta ayrılmaktadır. Ön eleme-temizleme atıkları dal-budak atıkları, bitki kökü, sapı ve gövdesi, yapraklar, ezik-çürük meyveler ve diğer atıklardan oluşmaktadır. İkinci grup ise işleme sonrası ayrılan ve presten geçen tohum, pulp, posa ve kabuklardır. Birinci grupta ayrılan atıklar genelde biyogaz, kompost, hayvan yemi ve gübrelemede kullanılmaktadır. Sadece yaklaşık % 20 sinin hayvan yemi olarak kullanılması, bu atıklar için daha efektif bertaraf stratejisi olan kompostlamayı ön plana çıkarmaktadır. Her iki atık türünün organik madde açısından zengin olması (%94.62), bu atıkların kompostlaştırma ile değerlendirilebileceğini bertaraf alternatifini daha güçlü hale getirmektedir. Ancak posa ve ön eleme-temizleme atıklarının su muhtevasının yüksek olması (82.5), bu atıkların suyunu azalttıktan sonra aerobik kompostlaştırma yoluyla değerlendirmenin daha elverişli olacağını göstermektedir. Elma işleme ön eleme-temizleme atıklarından elde edilecek kompost ürünü elma bahçelerinde, diğer meyve-sebze bahçelerinde ve yeşil peyzaj alanlarında kullanılabilir.

Sonuç olarak, meyve işleme prosesi esnasında ortaya çıkan katı atıkların etkili bir şekilde değerlendirilmesi, yalnız çevre kirliliğinin önlenmesi açısından değil, katma değerinin olması ve ürün çeşitliliği açısından da önemlidir. Artan nüfus ile birlikte meyve işleyen fabrikaların sayısının da gün geçtikçe artması göz önüne alınarak, atık miktarlarının artması ve buna paralel olarak yeni atık problemlerinin ortaya çıkmasını kaçınılmaz hale getirmektedir. Bu nedenle atıkların kompostlaştırılarak katma değeri yüksek bir ürün eldesi ve yeni meyve ürünlerinin üretilmesinde kullanılması insan sağlığı, çevre kirliliği ve ülke ekonomisi açısından önem arz etmektedir.

5. Kaynaklar

Akdağ, E., Budaklıoğlu E., (2009). MEYED - Türkiye Meyve Suyu Endüstrisi İstatistiki Değerlendirme Raporu 2000-2008.

Anonim, T.C. Isparta Valiliği, http://www.isparta.gov.tr/isparta-elmasi (erişim tarihi: 11.07.2018).

Aras, İ. (2015) Elma Sektörü Raporu-Karaman, Mevlana Kalkınma Ajansı, Konya.

Bhushan S., Kalia K., Sharma M., Singh B., Ahuja P.S. (2008). Processing of Apple Pomace for Bioactive Molecules. Critical Reviews in Biotechnology, 28:285–296.

Cemeroğlu B. (2009). Bazı Meyvelerin Meyve Suyuna Đşlenmeleri. Meyve ve Sebze Đşleme Teknolojisi, Cemeroğlu B, Gıda Teknolojisi Derneği, Ankara, 615-616.

Djılas S., Čanadanovıć J., Ćetkovıć B.G. (2009). By-products of fruıts processıng As a source of phytochemıcals. Chemical Industry & Chemical Engineering Quarterly, 15(4): 191- 202.

Elmaslar, E. (2002). "Meyve suyu endüstrisi atık sularının ardışık kesikli reaktör sistemi ile arıtılabilirliği" İstanbul Üniversitesi, Fen Bilimleri Enstitüsü, Çevre Mühendisliği Anabilim Dalı, Yükseklisans Tezi.

Ercişli, S. (2004). A Short Review of the Fruit Germplasm Resources of Turkey. Genetic Resources and Crop Evolution 51: 419 – 435

FAO. (2016). FAOSTAT production data [online]. Available at http://faostat3.fao.org/faostatgateway/go/to/download/Q/QV/E (Acces data: 21.01.2016)

Grigelmo-Miguel N., Gorinstein S., Martín-Bellosso O. (1999). Characterisation of peach dietary fibre concentrate as a food ingredient. Food Chemistry, 65: 175-181.

Hang Y.D, Lee C.Y., Woodams E.E., Cooley H.J. (1981). Production of Alcohol from Apple Pomace. Applied and Environmental Microbiology, 42: 1128-1129.

İşçi, M. (2014). “Isparta ilinde elma bahçelerinde zararlı olan elma içkurdu [Cydia pomonella (L.) Lep.: Tortrıcıdae]’NUN yaygın olarak kullanılan bazı insektisitlere karşı duyarlılık düzeylerinin belirlenmesi” SDÜ Fen Bilimleri Enstitüsü Bitki Koruma Anabilim Dalı, Doktora Tezi.

Jin H., Kima H.S, Kim S.K., Shin M.K., Kim J.H., Lee J.W. (2002). Production of heteropolysaccharide-7 by Beijerinckia indica from agro-industrial by products. Enzyme and Microbial Technology, 30: 822–827.

Leccese, A., Bartolini, S., Viti, R. (2009). Antioxidant properties of peel and flesh in ‘GoldRush’ and Fiorina’ scab-resistant apple (Malus domestica) cultivars. New Zealand Journal of Crop and Horticultural Science 37: 71–78.

Lu Y., Foo L.Y. (2000). Antioxidant and radical scavenging activities of polyphenols from apple pomace. Food Chemistry, 68: 81-85.

Masoodi F.A., Sharma B., Chauhan G.S. (2002). Use of apple pomace as a source of dietary fibre in cakes. Plant Foods Human Nutrn., 57: 121–128.

Medeiros A.B.P, Pandey A., Freitas R.J.S, Christen P., Soccol C.R. (2000). Optimization of the production of aroma compounds by Kluyveromyces marxianus in solid state fermentation using factorial design and response surface methodology, Biochem. Eng. 6: 33–39.

Paganini C., Nogueira A., Silva N.C., Wosiacki G. (2005). Utilization of apple pomace for ethanol production and food fiber obtainment. Ciênc. Agrotec. 29: 1231-1238.

Rupasinghe, H.P.V., Kean, C. (2008). Polyphenol concentrations in apple processing by-products determined using electrospray ionization mass spectrometry. Canadian J Plant Sci. 88: 759-762.

Schieber A., Stintzing F.C., Carle R. (2001). By-products of plant food processing as a source of functional compounds recent developments. Trends in Food Science & Technology, 12: 401–413.

Sekhon-Loodu, S. Warnakulasuriya, S.N., Rupasinghe, H.P.V., Shahidi, F. (2013). Antioxidant ability of fractionated apple peel phenolics to inhibit fish oil oxidation. Food Chem. 140: 189–196.

Shojaosadati SA, Babaeipour V. (2002). Citric acid production from apple pomace in multilayer packed bed solid-state bioreactor. Process Biochemistry, 37: 909–914.

T.C. Resmi Gazete (2016), Türk gıda kodeksi meyve suyu ve benzeri ürünler tebliği (Tebliğ No: 2006/56). Sayı : 26392, Tarih: 30.12.2016.

TÜİK 2017. Türkiye İstatistik Kurumu. http://www. tuik.gov.tr) Erişim Tarihi: (22.01.2018).

Vendruscolo F., Albuquerque P.M., Streit F. (2008). Apple Pomace: A Versatile Substrate for Biotechnological Applications. Critical Reviews in Biotechnology, 28: 1–12.

International Conference on Science and Technology

ICONST 2018

5-9 September 2018 Prizren - KOSOVO

Biofiltration of Ammonia Produced in Sewage Sludge Composting / Arıtma Çamuru Kompostlaştırılmasında Oluşan Amonyağın Biyofiltrasyonu

Fevzi Şevik[1]*, İsmail Tosun[1], Kamil Ekinci[2]

Özet: Kompostlaştırma işlemi organik atıkların tarımda kullanılabilirliği için alternatif bir yöntemdir. Kompostlaştırma işleminde en büyük problemlerden birisi kokudur. İnorganik ve organik kökenli çok sayıda bileşik koku rahatsızlığına neden olmaktadır. Koku gerek insanlarda oluşturduğu rahatsızlık ve gerekse içerdiği kirleticilerin yol açtığı çevresel etkileri nedeniyle günümüzde önem kazanmaktadır. Kompostlaştırma sürecinde oluşan kokular biyofiltrasyon işlemi ile giderilebilmektedir. Laboratuvar ölçekli yapılan kompostlaştırma işleminde materyal olarak evsel atıksu arıtma çamuru, sığır gübresi ve domates sapları kullanılmıştır. Kompostlaştırma işlemi otomasyon kontrollü paslanmaz çelikten imal edilen 100 litrelik 6 adet reaktörde gerçekleştirilmiştir. Kompost karışımları iki gruptan oluşmaktadır. Birinci grup karışımlar C/N oranı 15, FAS 27-32-37%, ikinci grup karışımlar ise C/N oranı 20, FAS 27-32-37% olarak ayarlanmıştır. Biyofiltre malzemesi olarak iki faz pirina kompostu kullanılmıştır. Kompost reaktörlerinden çıkan amonyak gazları biyofiltre reaktörü içerisinden geçirilerek biyofiltrenin amonyak tutma verimliliği belirlenmiştir. Biyofiltrasyon işleminin başlangıcında ve sonunda biyofiltre malzemesinin su muhtevası, organik madde muhtevası, pH ve elektriksel iletkenlik değerleri, C/N oranı, fosfor, amonyum ve nitrat değişimleri incelenmiş ve elde edilen sonuçlar değerlendirilmiştir. Kompostlaştırma prosesinde kompost karışımlarının FAS oranına bağlı olarak amonyak oluşumu da artış göstermiştir. Biyofiltrasyon sonrasında yapılan analizler incelendiğinde su muhtevası, organik madde, pH, elektriksel iletkenlik değerleri arasında belirgin bir değişim olmadığı görülmüştür. C/N oranları kompost reaktörlerinin başlangıç C/N oranlarına bağlı olarak değişim göstermiştir. Amonyum değerlerinde bariz bir değişim olmazken, nitrat değerlerinde ise belirgin bir artış görülmüştür. Biyofiltrasyon çalışmalarında yüksek oranda amonyak tutma verimi gerçekleşmiştir. Kompostlaştırma sürecinde oluşan kokunun giderilmesi için biyofiltrasyon işleminin etkili bir yöntem olduğu belirlenmiştir.

Anahtar Kelimeler: Amonyak kaybı, arıtma çamuru, kompostlaştırma, biyofiltre

Abstract: Composting is an alternative method for the use of organic wastes in agriculture. One of the most important problems in composting is odor. Numerous compounds of inorganic and organic origin cause odor problems. The odor problem is gaining importance nowadays due to the discomfort that people have and the environmental effects caused by the pollutants they contain. The odor formed in the composting process can be eliminated by the biofiltering process. Sewage sludge, dairy manure and tomato stalks were used in the laboratory scale composting process. Automatically controlled composting process was carried out in six 100 liter reactors manufactured from stainless steel. Compost mixtures consist of two groups. The first group mixtures were set to C/N ratio 15, free air spaces (FAS) 27, 32, and 37%, the second group mixtures C/N ratio 20, FAS 27, 32, and 37%. Compost obtained from a two phase olive mill processing waste was used as the biofilter material. Ammonia gases from the compost reactors were passed through the biofilter reactor to

[1]Süleyman Demirel University, Faculty of Engineering, 32260, Isparta, TURKEY
[2]University of Applied Sciences, Isparta, Faculty of Agricultural Sciences and Technologies, 32260, Isparta, TURKEY
* Corresponding author: sevikfevzi@hotmail.com

determine the ammonia removal efficiency of the biofiltration. At the beginning and end of the biofiltering process, the water content, organic matter content, pH and electrical conductivity, C/N ratio, phosphorus, ammonium and nitrate changes of the biofilter material were analyzed and the results obtained were evaluated. In composting process, ammonia formation also increased due to the increase of FAS ratio of compost mixtures. When the analysis was examined after biofiltration process, it was seen that there was no significant change between water content, organic matter, pH and electrical conductivity values. The final C/N ratios varied depending on the initial C/N ratios of the compost reactors. While there was no significant change in the ammonium values, a significant increase in the nitrate values was observed. In the biofiltering studies, a high rate of ammonia removal was achieved. It has been determined that the biofiltration process is an effective method for removing odor from the composting process.

Keywords: Ammonia loss, Biofiltration, Composting, Sewage sludge

Giriş

Kompostlaştırma işlemi, düşük maliyetli, kolay uygulanabilirliği ve düşük kirlilik nedeniyle arıtma çamurunun bertaraf edilmesinde en çok kullanılan yöntemlerden birisidir (Wang vd., 2011). Kompostlaştırma işleminde en büyük problemlerden birisi kokudur. Koku parametresi gerek insanlarda oluşturduğu rahatsızlık ve gerekse içerdiği kirleticilerin yol açtığı çevresel etkileri nedeniyle günümüzde önem kazanmaktadır. İnorganik ve organik kökenli çok sayıda bileşik koku rahatsızlığına neden olmaktadır. Kokulu bileşiklerin emisyonu, endüstriyel üretim prosesleri yanında tarım ve hayvan yetiştiriciliği sektöründe ve atıkların bertaraf edildikleri tesislerde (kompost, atık su arıtma, katı atık depolama) belirgin bir şekilde oluşmaktadır.

Tarımsal faaliyetlerden, endüstriyel tesislere ve atık bertarafına kadar geniş bir kaynak grubu için koku yasal düzenlemelerle kontrol edilmesi gereken bir kirleticidir. Koku emisyonlarının kontrolü amacıyla fizikokimyasal (yoğunlaştırma, adsorpsiyon, absorpsiyon, oksidasyon, yakma vb.) ve biyolojik (biyofiltreler) prosesler yaygın bir şekilde kullanılmaktadır (Uyar, 2007).

Azot amonyak formunda uçucu olarak kolayca kaybolmakta, gübreleme miktarını azaltmakta ve çevresel koku kirliliği sorunlarına neden olmaktadır (Ogunwande vd., 2008). Kompostlaştırma süresince amonyak emisyonları, agronomik üretim değerlerinin azalmasına neden olur ve ayrıca havayı kirletebilir (Li vd., 2013).

Biyofiltre malzemesinin seçiminde ve işletmeciliğinde bakterilerin büyümesi için çevresel (sıcaklık, nem) ve besi ihtiyaçları birinci önceliğe sahip olup kolay temin edilebilmesi ve maliyetlerinin düşük olması, nem tutma kapasitesi, basınç düşmesi ve uzun kullanım ömrü gibi özellikler de diğer öncelikler arasındadır (Uyar, 2007). Biyolojik koku gideriminde dolgu malzemesi olarak kullanılan malzemelerden bir tanesi komposttur (Yılmaz, 2016).

Bu çalışmada Şevik vd., 2018 tarafından arıtma çamuru, sığır gübresi ve domates saplarının kompostlaştırılması esnasında oluşan amonyak gazının biyofiltrasyonu araştırılmıştır. Kompostlaştırma esnasında oluşan amonyak gazı biyofiltreden geçirilerek amonyak tutma verimi ve biyofiltre malzemesine katkıları araştırılmıştır.

Materyal ve Yöntem

Kompostlaştırmada kullanılan materyaller

Süleyman Demirel Üniversite Kompost Laboratuvarında yapılan kompostlaştırma işleminde materyal olarak evsel atıksu arıtma çamuru (AÇ), sığır gübresi (SG) ve domates sapları (DS) kullanılmıştır. Arıtma çamuru Isparta Atıksu Arıtma Tesisinden temin edilmiştir. Sığır gübresi ve domates sapları Isparta şehrinde tarımsal işletmelerden temin edilmiştir. Çalışmada kullanılan materyallerin özellikleri Tablo 1'de verilmiştir (Şevik vd., 2018).

Tablo 1. Kompostlaştırma işleminde kullanılan materyallerin fiziksel ve kimyasal özellikleri

Parametre	AÇ	SG	DS
Su muhtevası (%)	75.89	82.28	20.77
Organik madde (%)	74.20	86.58	77.86
pH	6.05	8.55	7.92
Elektriksel iletkenlik (dS/m)	5.62	5.64	7.43
Toplam karbon (TC) (%)	43.89	42.05	35.04
Toplam azot (TN) (%)	4.04	1.57	2.23
C/N	10.86	26.78	15.71
Serbest hava boşluğu (FAS) (%)	6.50	17.50	60.00
Birim hacim ağırlığı (BHA) (kg/L)	0.23	0.14	0.25
Toplam fosfor (mg/kg)	5890	4948	1142
$\mathbf{NH_4^+ - N}$ (mg/kg)	202	46	65
$\mathbf{NO_3^- - N}$ (mg/kg)	1364	1916	1577

Karışımların C/N oranları 15 ve 20, FAS oranları ise 27%, 32% ve 37% olarak hazırlanmıştır. Kompost karışımlarının kuru madde bazında yüzdeleri ve başlangıç C/N ve FAS oranları Tablo 2'de verilmiştir (Şevik vd., 2018).

Tablo 2. Kompost karışımları (kuru bazda) ve karışımların C/N ve FAS oranları

	K1	K2	K3	K4	K5	K6
AÇ (%)	42.51	38.24	33.57	14.35	10.09	5.47
SG (%)	36.31	31.72	26.71	66.07	60.37	54.17
DS (%)	21.18	30.05	39.73	19.58	29.54	40.37
C/N	15	15	15	20	20	20
FAS (%)	27	32	37	27	32	37

Biyofiltrasyon deney düzeneği

Kompostlaştırma işleminde K1-K6 karışımlarından oluşan 6 kompost reaktörünün çıkış egzoz gazları biyofiltre sisteminden geçirilmiştir. Biyofiltre için 60 L'lik polietilen reaktörler kullanılmıştır. Ayrıca ortamdan kaynaklı amonyak girişiminin olup olmadığını kontrol etmek için ayrı bir kontrol reaktörü hazırlanmıştır (BF-Kontrol). Kompostlaştırma ve biyofiltrasyon sisteminin genel görünümü ve biyofiltrasyon sisteminin akım şeması Şekil 1 ve 2'de gösterilmiştir. Biyofiltrre reaktörlerinin taban kısmında olası sızıntı suyunun toplanması ve gazın biyofiltre kütlesine homojen dağılımı için 3 L'lik hacim bırakılmış olup, bu kısmın üzerine ızgara, agrega tabakası ve biyofiltre materyali (etkin hacim 50 L) yerleştirilmiştir. Reaktörün üst kısmında ise gaz boşluğu için 7 L'lik hacim bırakılmıştır.

Biyofiltre materyali olarak tüm reaktörlerde, Sülük vd., 2017 tarafından iki faz pirina, tavuk gübresi ve domates hasat atıklarının kompostlaştırılmasından elde edilen kompost kullanılmıştır. Her bir reaktöre aynı biyofiltre malzemesinden 12 kg (kuru madde) yerleştirilmiştir. Biyofiltre malzemesi olarak kullanılan kompostun fiziksel ve kimyasal özellikleri Tablo 3'te verilmiştir.

Tablo 3. Biyofiltrede kullanılan kompostun fiziksel ve kimyasal özellikleri

SM (%)	OM (%)	pH	EC (dS/m)	C (%)	N (%)	C/N	BHA (kg/L)	FAS (%)
48.75	81.73	9.17	3.58	41.27	2.01	20.53	0.47	55.50

Kompost reaktörlerinden çıkan egzoz gazının bir kısmının biyofiltrelerden geçirilmesi vakum pompası yardımıyla sağlanmıştır. Ayrıca sistemden zamanlayıcı yardımıyla kesikli hava çekilmiştir.

Şekil 1. Kompostlaştırma ve biyofiltrasyon sistemi görünümü

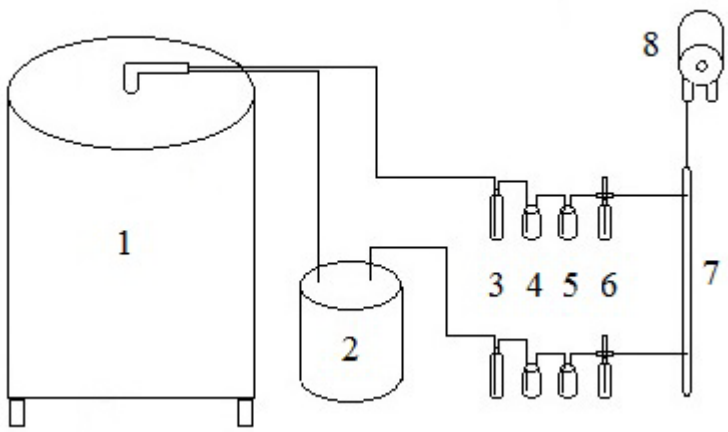

1. Reaktör, 2. Biyofiltre, 3. Gaz sıyırıcı, 4. Nem yoğuşturma, 5. Nem tutucu, 6. Akış metre, 7. Gaz toplama hattı, 8. Vakum pompası

Şekil 2. Biyofiltrasyon sistemi akım şeması

Biyofiltre sisteminden geçen egzoz gazının debisi akış düzenleyici yardımıyla 2,9 L/dk olarak ayarlanmıştır. Her bir kompost reaktörü çıkışından 6 mm çaplı iki hortumla gaz çekilmiş olup, bir tanesi biyofiltre reaktörüne ve devamında amonyak tutuculara, diğeri ise doğrudan amonyak tutuculara verilmiştir. Kontrol reaktörüne ise ortamdan çekilen hava verilmiştir. Amonyak tutma sistemi sırasıyla gaz sıyırıcı, nem yoğuşturucu, nem tutucu, akış metre, gaz toplama hattı ve vakum pompasından oluşmaktadır. Gaz sıyırıcı sonrasında yoğuşturucu ve nem tutucu ($CaS0_4$) yerleştirilmiştir. Gaz sıyırıcı şişelerde borik asit (H_3BO_3) çözeltisi içerisinde tutulan amonyak H_2SO_4 ile titrasyon yapılarak belirlenmiştir.

Bulgular

Kompostlaştırma işleminde reaktörlerden çıkan egzoz gazları biyofiltre içerisinden geçirilerek biyofiltrenin amonyak tutma verimliliği belirlenmiştir. Çalışmada kullanılan biyofiltre materyalinin boyut dağılımı analizi yapılmış ve Şekil 3'te gösterilmiştir. Şekilden görüldüğü gibi biyofiltrenin %70.4'ünün boyutu 4.76 mm'nin altındadır. Biyofiltre malzemesinin çok boşluklu bir malzeme olması durumunda kompostlaştırma esnasında çıkan gazın biyofiltre ile çok temas etmeden sistemi terketmesi sonucu amonyak tutma verimi düşmesi beklenmektedir. Aynı zamanda koku problemi de artış göstermesi öngörülmüştür. Biyofiltre malzemesinin boşluk oranının çok az olması durumunda da amonyak gazının biyofiltreden geçişi çok yavaş olarak gerçekleşmesi düşünülmüştür. Biyofiltre malzemesinin boyut dağılımı amonyak tutma işlemi için önemlidir.

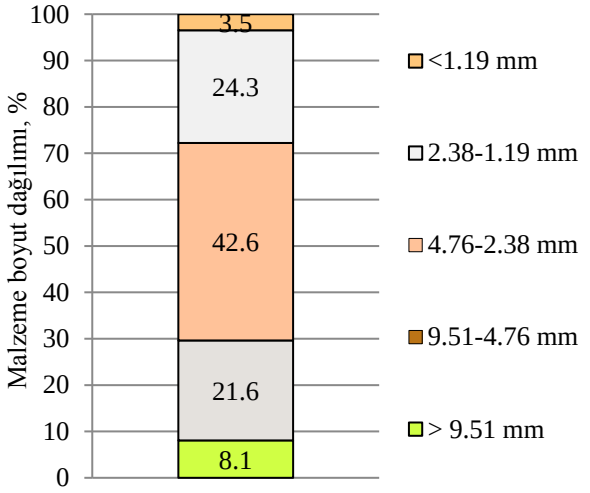

Şekil 3. Biyofiltre malzemesinin boyut dağılımı

Kompostlaştırma sürecinin başlangıcında ve bitiminde biyofiltrede SM, OM, pH, EC, C/N, fosfor, amonyum ve nitrat analizleri yapılmış ve elde edilen sonuçlar Tablo 4'te verilmiştir. Çizelge incelendiğinde başlangıç ve bitiş SM, OM, pH ve EC değerleri arasında belirgin bir değişim olmadığı görülmüştür. Biyofiltre reaktörlerinin bitiş C/N oranları kompost reaktörlerinin başlangıç C/N oranlarına bağlı olarak değişim göstermiştir. Toplam fosfor konsantrasyonları başlangıç değerlerine göre hem kontrol reaktöründe hem de diğer biyofiltre reaktörlerinde artış göstermiştir. Amonyum değerlerinde fazla bir değişim olmazken, nitrat değerlerinde ise belirgin bir artış görülmüştür.

Tablo 4. Biyofiltre reaktörlerinin başlangıç ve bitiş analiz sonuçları

Biyofiltre No	SM (%)	OM (%)	pH	EC (dS/m)	C/N	T. Fosfor (mg/kg)	NH_4 mg/kg	NO_3 mg/kg
BF-Başlangıç	48.75	81.73	9.17	3.58	20.53	1740	346	1077
BF-Kontrol	47.70	84.11	9.42	3.85	20.29	4397	329	1235
BF-1	47.73	82.91	9.37	3.23	18.96	5282	352	10710
BF-2	50.24	83.29	9.52	3.86	18.43	4460	321	4585
BF-3	48.95	83.47	9.38	3.53	17.70	4479	401	7342
BF-4	48.55	84.00	9.33	3.37	17.48	4628	332	5177
BF-5	48.77	82.47	9.39	3.64	17.12	3005	300	2671
BF-6	49.92	84.75	9.31	3.63	16.96	3931	291	2183

Kompost karışımlarından oluşan amonyak gazı konsantrasyonlarının belirlenmesi için biyofiltre (BF) giriş ve çıkış değerleri belirlenmiş ve Şekil 4'te gösterilmiştir. Kompost karışımlarında FAS oranı 27, 32 ve 37% olarak artış gösterirken, amonyak oluşumu da artış göstermiştir. Biyofiltre çıkışı amonyak değerleri 1 mg/kg KM'nin altında gerçekleşmiştir. Ayrıca tüm biyofiltrelerin amonyak tutma verimi %99 olarak belirlenmiştir.

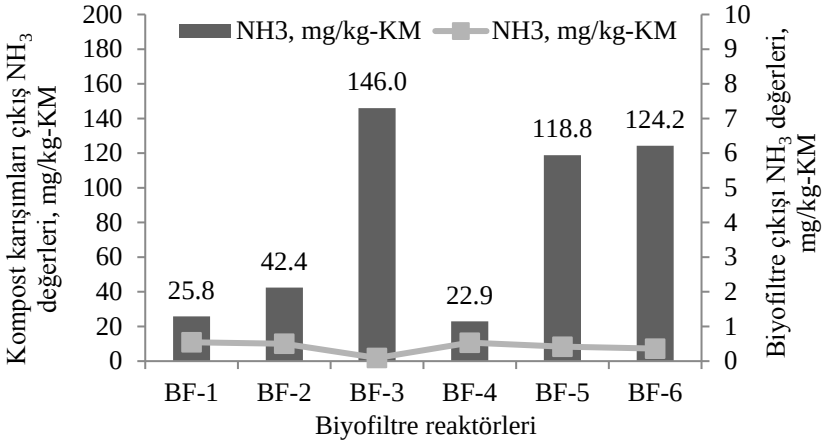

Şekil 4. Biyofiltre ve reaktör çıkış amonyak değerleri

Tartışma ve Sonuçlar

Biyofiltre materyalinde yapılan su muhtevası, organik madde, pH, ve elektriksel iletkenlik analizlerinde bitiş değerlerinde başlangıca göre belirgin bir değişimin olmadığı görülmüştür. Fosfor değerlerinde başlangıca göre bir artış gözlenmiştir. Amonyum değerlerinde bir değişim olmazken, nitrat değerlerinde belirgin bir artış olduğu belirlenmiştir. Kompost karışımlarından çıkan gazların biyofiltreden geçirilmesiyle biyofiltre çıkışı amonyak değerlerinin 1 mg/kg kuru maddenin altına düştüğü ve tüm biyofiltre reaktörlerinde amonyak tutma veriminin %99 seviyesinde olduğu belirlenmiştir. Biyofiltrasyon çalışmalarında yüksek oranda amonyak tutma verimi gerçekleşmiştir. Kompostlaştırma sürecinde oluşan kokunun giderilmesi için biyofiltrasyon işleminin etkili bir yöntem olduğu belirlenmiştir.

Teşekkür

Bu çalışma Süleyman Demirel Üniversitesi Bilimsel Araştırma Projeleri Koordinasyon Birimince Desteklenmiştir. Proje Numarası: 3815-YL1-13.

Kaynaklar

Uyar, Ö. (2007). Biyofiltrelerle Amonyak Emisyonları Kontrolü, Yüksek Lisans Tezi, Fen Bilimleri Enstitüsü, İstanbul Teknik Üniversitesi, İstanbul.

Şevik, F., Tosun, İ., Ekinci, K. (2018). The effect of FAS and C/N ratios on co-composting of sewage sludge, dairy manure and tomato stalks. Waste Management, https://doi.org/10.1016/j.wasman.2018.07.051.

Sülük, K., Tosun, İ., Ekinci, K. (2017). Co-composting of two-phase olive-mill pomace and poultry manure with tomato harvest stalks. Environmental technology, 38(8), 923-932.

Ogunwande, G.A., Osunade, J.A., Adekalu, K.O., Ogunjimi, L.A.O. (2008). Nitrogen loss in chicken litter compost as affected by carbon to nitrogen ratio and turning frequency. Bioresource Technology 99, 7495-7503.

Wang, K., Li, W., Guo, J. (2011). Spatial distribution of dynamics characteristic in the intermittent aeration static composting of sewage sludge. Bioresource Technology 102, 5528-5532.

Li Y., Li W., Liu B., Wang K., Su C., Wu C. (2013). Ammonia emissions and biodegradation of organic carbon during sewage sludge composting with different extra carbon sources. International Biodeterioration&Biodegradation, 85, 624-630.

Yılmaz, M. (2016). Gıda Fermantasyon Sektöründen Kaynaklanan Koku Emisyonlarının Biyofiltre Sistemi Kullanılarak Giderilmesi, Yüksek Lisans Tezi, Fen Bilimleri Enstitüsü, İstanbul Teknik Üniversitesi, İstanbul.

International Conference on Science and Technology

ICONST 2018

5-9 September 2018 Prizren - KOSOVO

Preparation and Performance of Electroless Nickel on HVOF (High-Velocity Oxygen Fuel) Sprayed Inconel 625 Nickel Coating for Corrosion Protection Applications

Ramazan Haldun Topcu[1], Harun Mındıvan[2*]

Abstract: High Velocity Oxy-Fuel (HVOF) spraying is one of the preferred surface engineering technologies that can offer advantages such as user-friendliness and cost-efficiency in mass production of coatings for various applications. While the main applications of the HVOF process are related to wear, corrosion resistance can be one of the important desired features of the surface engineering process. However, the porosity of HVOF sprayed coatings is usually a problem when coatings are used in corrosion applications. Low carbon steel substrates were High-Velocity Oxygen Fuel (HVOF) sprayed with Inconel 625 and then coated with a thin film of electroless nickel (electroless nickel plating). Reference sample without electroless nickel was sprayed at the same time. Characterization of the coatings was made by X-Ray diffraction analyses, microstructural surveys, cross-section and corrosion tests. Results showed that sequential application of HVOF spraying and electroless coating processes provided the multi-layered coating consisting of an inner inconel 625 based layer and an outer Ni-P layer. Electroless Ni-P also caused the remarkable increasing in the corrossion resistance as compared to the as-HVOF sprayed state.

Keywords: Corrosion, HVOF Spraying, Inconel 625, Electroless Nickel.

1. Introduction

The use of thermal sprayed corrosion-resistant coatings to protect an underlying steel substrate has received much interest over the past few years [Johnson et al., 2011]. The advantage of this method is the substantial weight and cost reduction compared to using bulk alloys [Hjornhede and Nylund, 2004]. A number of thermal spraying methods are available including flame spraying, plasma spraying, arc thermal spraying, and high velocity oxy-fuel (HVOF) spraying [Sidhu et al., 2005]. In particular, HVOF is the most extended method to process Inconel 625 coatings [Johnson et al., 2011]. However, deposited Inconel 625 coating designed for use in harsh service environments can be damaged because some residual oxides and porosity remain at splat boundaries [Rakhes et al., 2011; Poza et al., 2014]. To protect the HVOF sprayed Inconel 625 coating from the above aspects, extensive research is going on in the field of laser cladding onto the Inconel 625 coating by HVOF process [Nemecek et al., 2014]. Nevertheless, it was found that the laser coating demonstrated poor corrosion performance because cracking due to rapid melt pool solidification acted as sites for crevice and pitting corrosion [Abioye et al., 2015]. Therefore, we additionally carried electroless deposition process to improve the corrosion performance onto the HVOF sprayed Inconel 625 coating to reduce corrosion attack at the coating surface to any open porosity or splat boundaries. According to the available literature, there is no such report on the HVOF sprayed Inconel 625 coating deposited with electroless Ni-P. In the present study,

[1]Suleyman Demirel University, Faculty of Forestry, 32260, Isparta, TURKEY
[2]Suleyman Demirel University, Faculty of Engineering, 32260, Isparta, TURKEY
*Correspondingauthor: mevludeakkaya@gmail.com

the HVOF-sprayed Inconel 625 coating has been subjected to Ni-P coating and then its structural characterization and corrosion properties have been evaluated.

2. Material and Method

Commercially available spheroidal, gas atomized powder (Diamalloy-1005) manufactured by Sulzermetco company with a nominal particle size range of –45 to +11 μm was used for this study. These particles are similar to Inconel 625 properties and composition (Table 1). It is used in corrosive and erosive applications like seawater environments. Inconel 625 was deposited onto rectangular low carbon steel specimens with dimensions of 100 mm x 50 mm x 4 mm (length x width x thickness). The substrates were sandblasted to remove the oxide film which could be formed onto the surface and cleaned with acetone to eliminate any residue.

Table 1. Chemical Composition of Diamalloy-1005 Powder.

Powder Material	Chemical Composition				
	Ni	Cr	Mo	Fe	Co
Inconel 625	66.5	21.5	8.5	3	0.5

Before electroless Ni-P coating, the surfaces of the HVOF sprayed Inconel 625 coating were ground using 1200 grit SiC paper and mechanically polished with a fine grade Al_2O_3 paste to achieve a certain surface uniformity. Finally, the surfaces were thoroughly degreased with acetone, ultrasonically cleaned and etched in a 30 vol. % HCl solution for 1 min. The commercial Ni–P electroless solution (Durni-Coat DNC 520-9) containing 5 g/L nickel, 40 g/L NaH_2PO_2 and suitable amounts of additive and stabilizer were used. The stirring rate of plating bath was about 250 r/min, using a magnetic stirrer and a polytetrafluoroethylene (PTFE) coated magnet with 2 cm length and 5 mm in diameter. The deposition was carried out in a 250 ml thermostated double wall beaker at 90 °C and pH 4.6 for 1 h to achieve a thickness of 11.5 μm.

Characteristics of the HVOF sprayed Inconel 625 and Ni-P treated coating were investigated by microscopic examinations, X-ray diffraction (XRD) analyses, microhardness measurements and corrosion tests. The cross-sectional microstructure of the coatings was inspected with an Optical Microscopy (OM) and a Scanning Electron Microscope (SEM) equipped with an Energy Dispersive Spectroscopy (EDS). The cross-sectional microhardness measurements were carried out using a Vickers microhardness tester (Shimadzu) with a load 50 g and a dwell time of 10 s.

The electrochemical corrosion tests of the coatings were performed utilizing a typical three electrode potentiodynamic polarization test unit in the corroding media of aerated solution of 3.5 wt. % NaCl at room temperature. Before potentiodynamic polarization measurements, an initial delay of 30 min. was employed in order to measure the open circuit potential between working and reference electrodes. Potentiodynamic polarization curves were generated by sweeping the potential from cathodic to anodic direction at a scan rate of 1 mVs^{-1}, starting from – 0.8 up to - 0.2 V. The corrosion potential (E_{corr}) and corrosion current density (i_{corr}) were determined using the Tafel extrapolation method. Finally, the surface images of the corroded coatings were examined using an OM in order to determine the morphology of the developed corrosion.

3. Results and Discussion

Figure 1 shows OM images of the cross section of the HVOF sprayed Inconel 625 coating on low carbon steel substrate. The characteristic structure of an as-sprayed Inconel 625 coating with thickness of approximately 350 μm, formed by incremental deposition of powder particles which deform on impact is shown in Fig. 1 (a). Three discernable levels of contrast, white, black, and gray, were seen in the microstructure. The black regions mostly located along the interface of the splats were identified as pores (Fig. 1 b, as shown by the white arrows). EDS characterization was conducted to determine the composition of the white and gray areas. According to the EDS results, white regions represented the base material (Inconel 625) and the gray region represented oxide.

Figure 2 depicts surface morphology and cross-sectional micrograph of the Ni–P deposit. Because of the low amount of nodules on the Ni–P deposit (Fig. 2 a), it seems that the Ni-P coated surface had a low roughness value Ra = 0.16 ± 0.01 μm. Using the EDS analysis, it was determined that the Ni–P deposit contains 13 wt. % phosphorous and 87 wt. % nickel. The coating with thickness of approximately 11.5 μm was rather compact without macro-defects such as porosity and showed a relatively good adherence to the HVOF sprayed Inconel 625 coating (Fig. 2 b). After electroless Ni-P coating, a 1.16 fold increase in hardness (415 $HV_{0.05}$) was achieved compared to the HVOF sprayed Inconel 625 coating not subjected to electroless deposition (355 $HV_{0.05}$).

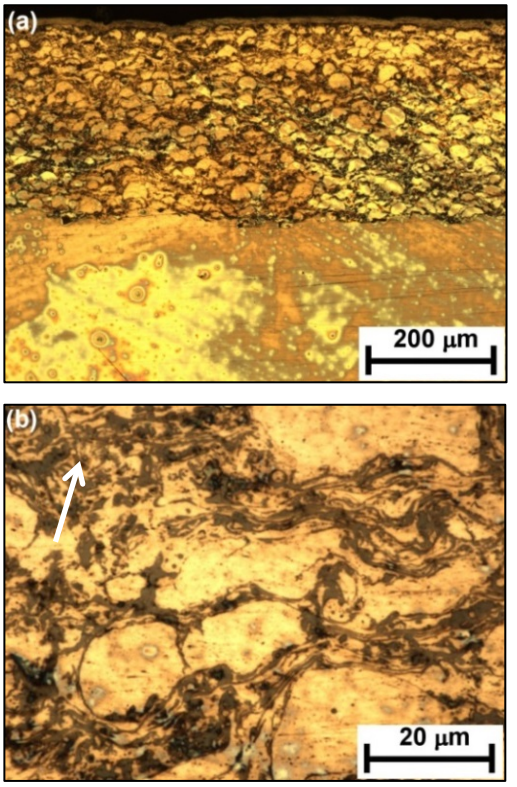

Figure 1. Cross sectional observations of HVOF sprayed Inconel 625 coating (a) low-magnification and (b) high-magnification.

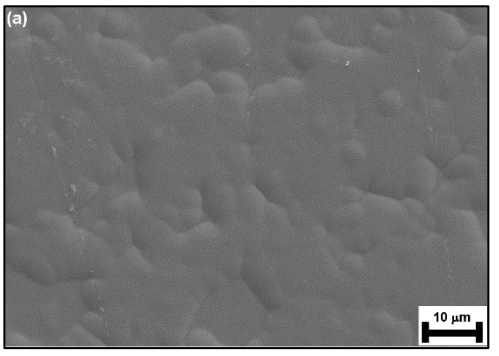

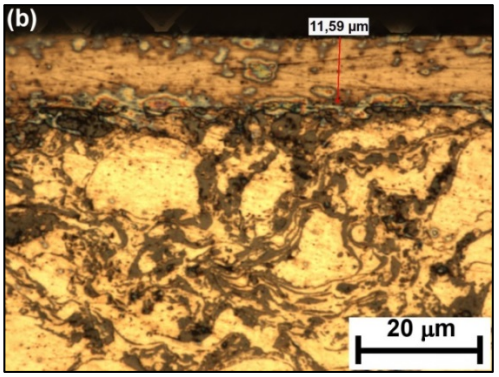

Figure 2. (a) Surface morphology and (b) cross-section image of the Ni–P deposit.

The XRD patterns of the examined coatings are presented in Figure 3. The HVOF sprayed Inconel 625 coating presented FeNi, Ni, Fe_2O_3 and NiO phases. After electroless plating on the HVOF sprayed Inconel 625 coating, Ni-P fully coated on the surface as shown in XRD pattern of the Ni-P deposit. XRD pattern of the Ni–P deposit exhibited a single broad peak indicative of the amorphous nature of the coating along with the presence of a small crystallite in the coating microstructure (Fig. 3).

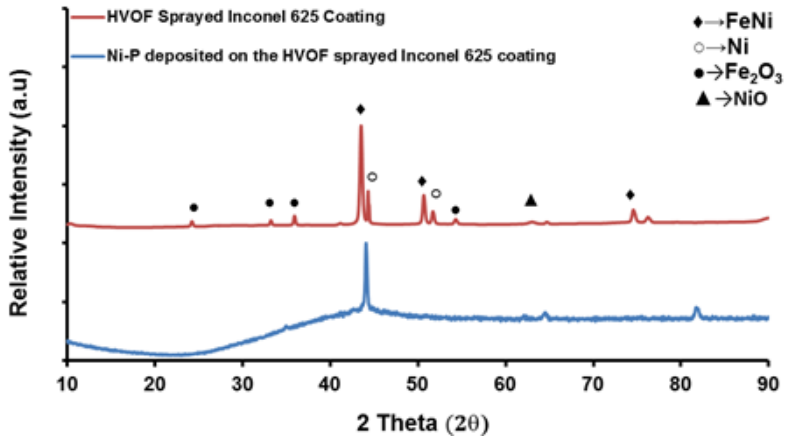

Figure 3. XRD patterns of the examined coatings.

Representative potentiodynamic polarization curves obtained for all the coatings are displayed in Fig. 4. The corresponding electrochemical corrosion parameters are shown in Table 2. As can be seen from Fig. 4, the equilibrium corrosion potential (E_{corr}) of the HVOF sprayed Inconel 625 coating was -575 mV, and the corrosion current density (I_{corr}) was 3.38 x 10^{-6} Acm^{-2}. The corrosion potential and corrosion current density of the Ni-P deposit were changed. The Ni-P deposit's E_{corr} was -487 mV, which was positively shifted 88 mV. Besides, the I_{corr} was 2.04 x 10^{-6} Acm^{-2} which was reduced 1.34 x 10^{-6} Acm^{-2}. E_{corr} indicates the tendency of the sample to corrode. The more negative the value is, the more likely it is that electrochemical corrosion will occur. I_{corr} indicates how quickly the sample corrodes once it has been corroded. Therefore, from the analysis results shown in Fig. 4 and Table 2, the improved corrosion resistance for Ni-P deposit in comparison with the HVOF sprayed Inconel 625 coating is ascribed to dense and porosity free coating as revealed from microhardness evaluation. The results suggest that the Ni-P deposit is more protective in nature than HVOF sprayed Inconel 625 coating. In agreement with these results, this significant enhancement in the corrosion resistance of amorphous electroless Ni-P (with high P content) coating is due to the absence of grain boundaries and the possible formation of a protective layer of nickel oxide and phosphorus compound [Yan et al., 2015].

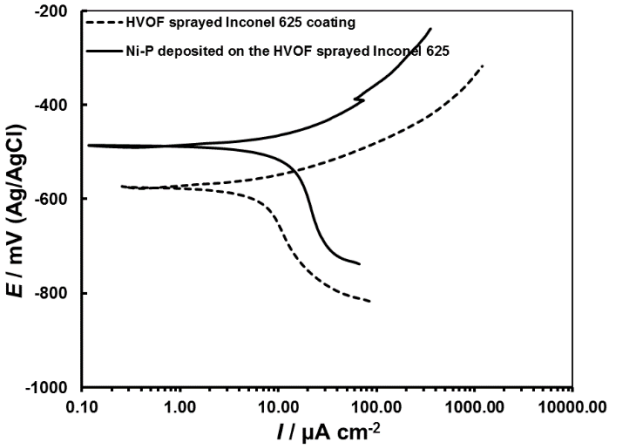

Figure 4. Potentiodynamic polarisation curves for the examined coatings in a 3.5 wt.% NaCl solution.

Table 2. Corrosion potential and corrosion current density values obtained from the polarization curves.

Type of coating	**E_{corr}, (mV)**	**Icorr, Acm^{-2}, ($x10^{-6}$)**
HVOF sprayed Inconel 625 coating	-575	3.38
Ni-P deposited on the HVOF sprayed Inconel 625 coating.	-487	2.04

Figure 5 shows the corroded surfaces of the coatings. After polarization testing in 3.5 wt. % NaCl solution, the HVOF sprayed Inconel 625 coating showed an isolated corrosion pits on the surface. However, a lower Inconel 625 layer obtained by HVOF thermal spray process with an upper electroless Ni-P deposit was quite smooth and did not show sign of corrosion.

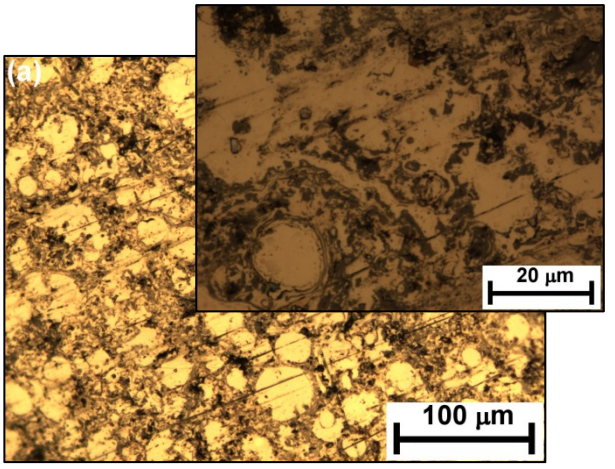

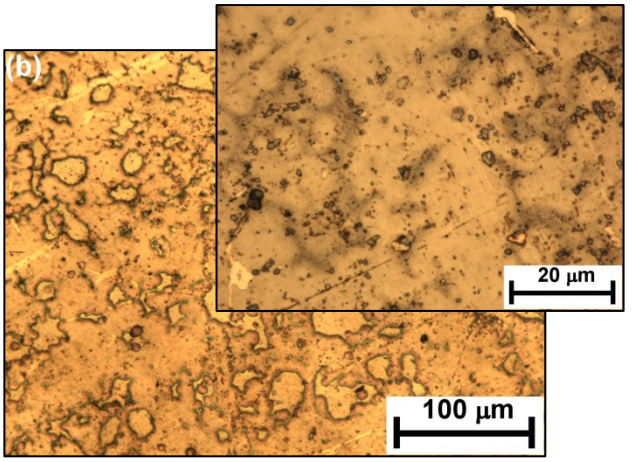

Figure 5. OM images of the (a) HVOF sprayed Inconel 625 coating and (b) Ni-P deposited on the HVOF sprayed Inconel 625 coating after polarization test.

4. Conclusions

HVOF thermal spray layer (Inconel 625) was coated with electroless Ni-P. The coatings were characterised by microstructure analysis, microhardness measurements and corrosion tests, and the most relevant conclusions can be summarised as follows:

HVOF sprayed Inconel 625 coating followed by electroless Ni-P showed higher hardness and denser structure without porosity when compared to the coating without Ni-P deposit. The corrosion resistance of Inconel 625 coating obtained by HVOF thermal spray technology has been enhanced by adding an upper layer of a Ni-P deposit.

References

Abioye, T.E., McCartney, D.G., Clare, A.T. (2015). Laser cladding of Inconel 625 wire for corrosion protection. Journal of Materials Processing Technology, 217, 232-240.

Hjornhede, A., Nylund, A. (2004). Adhesion testing of thermally sprayed and laser deposited coatings. Surface and Coatings Technology 184, 208–218.

Johnson, L., Niaz, A., Boatwright, A., Voisey, K.T., Walsh, D.A. (2011). Scanning electrochemical microscopy at thermal sprayed anti-corrosion coatings: Effect of thermal spraying on heterogeneous electron transfer kinetics. Journal of Electroanalytical Chemistry, 657, 46–53.

Nemecek, S., Fidler, L., Fišerova, P. (2014). Corrosion resistance of laser clads of Inconel 625 and Metco 41C. Physics Procedia, 56, 294 – 300.

Poza, P., Múnez, C.J., Garrido-Maneiro, M.A., Vezzù, S., Rech, S., Trentin, A. (2014). Mechanical properties of Inconel 625 cold-sprayed coatings after laser remelting. Depth sensing indentation analysis. Surface & Coatings Technology, 243, 51–57.

Rakhes, M., Koroleva, E., and Liu, Z. (2011). Improvement of corrosion performance of HVOF MMC coatings by laser surface treatment. Surface Engineering, 27 (10), 729-733.

Sidhu, T. S., Prakash, S., and Agrawal, R. D. (2005). Studies on the properties of high-velocity oxy–fuel thermal spray coatings for higher temperature applications. Materials Science, 41(6), 805-823.

Yan, D., G. Yu, B. Hu, J. Zhang, Z. Song, X. Zhang. (2015). An innovative procedure of electroless nickel plating in fluoride-free bath used for AZ91D magnesium alloy. Journal of Alloys and Compounds 653, 271-278.

International Conference on Science and Technology

ICONST 2018

5-9 September 2018 Prizren - KOSOVO

Some Metals and Anti-browning Agents Effects on Polyphenol Oxidase from Princess Tree Leaves

Gulnur Arabaci[1]* , Cengiz Cesko[2], Ayse Usluoglu[3]

Abstract: The polyphenol oxidase (PPO) enzyme is an important enzyme that causes browning reactions in fruit and vegetables due to oxidation during handling and storage processes. Enzymatic browning reaction is the one of the biggest problem in the food processing industries during processing and storge of vegetables and fruits. Polyphenol oxidase (PPO) enzyme is a metalloenzyme containing a copper and catalyzes the conversion of phenolic compounds to quinones and assists the polymerization of their products. Lately, researchers are very interested in developing new PPO inhibitors to slow the enzymatic browning. Natural anti-brown compounds commonly used for the PPO enzyme are honey, aliphatic alcohols, ascorbic acid and cysteine. In addition to these substances, some metals can affect enzyme activities positively or negatively. For example iron, copper and zinc are essential metals for plant life, but some heavy metals such as mercury, lead, etc. can adversely affect enzymes in the plant defense system. In this work, the effects of some metals, anti-browning compounds and their complexes were examined on the PPO enzyme from princess tree (Paulownia tomentosa) leaf. The results demonstrated that glutathione (GSH) was more powerful anti-browning compound than the others. Ni(II) and Mn(II) rised princess tree PPO activity. But, Pb(II) was the efficient PPO inhibitor. Na(I), Cu(II) and Fe(II) had no considerable effect on PPO enzyme activity. Additionally, metal and anti-browning compound mixtures' effects on the PPO enzyme were examined. Our results showed that metal-L-Cys, metal-Ascorbic acid and metal-GSH complexes had inhibitory effects but metal- EDTA complexes showed no considerable effect on princess tree PPO enzyme.

Keywords: Polyphenol oxidase (PPO), princess tree, anti-browning, metal, inhibition

Introduction

The browning event, which affects the taste and color of food, is an enzymatic reaction and one of the most important reactions observed in all fruits and vegetables. This reaction is carried out by an enzyme called polyphenol oxidase (PPO) in an oxygenated environment. This enzyme has the ability to catalyze two different reactions. It primarily catalyzes monofenols to o-diphenols thus it has monophenolase activity and then catalyzes the o-diphenols to o-quinones thus it has diphenolase activity [1, 2]. Then, the obtained quinones become polymerized and form black or brown color onto surface of fruits and vegetables. This brown color causes nutritional changes in foodstuffs and reduces the quality of food. The enzymatic browning rection has been a main trouble for the food production. Thus, the control and inhibition of enzymatic browning has a great importance for the food industry. Nowadays, there are many important studies based on the control and inhibition of enzymatic browning by many different natural and unnatural compounds such as ascorbic acid [3, 4] and thiol containing subtances like glutathione (GSH) and L- cysteine [1].

*Corresponding Author: Assoc. Prof. Gulnur Arabaci, Sakarya University, Chemistry Department, Sakarya, 54187, Turkey Phone:90 264 2956048, e-mail: garabaci@sakarya.edu.tr.
[1]First Author Assoc. Prof. Gulnur Arabaci, ,Sakarya, Turkey, e-mail: garabaci@sakarya.edu.tr.
[1]Third Author Cengiz Cesko, Sakarya, Turkey, e-mail: cengizchesko@hotmail.com.

In recent years, polyphenol oxidase enzymes have been widely charactherized and purified from various plant sources [5] such as mulberry [6], artichoke [7], iceberg lettuce [8], cleomegynandra [9], broccoli [10], butter lettuce [11] and peppermint [12]. In addition to these studies, there are many inhibitor studies on this enzyme because it causes a major problem in the food industry. Natural substances such as ascorbic acid, honey, natural aliphatic alcohols and L-cysteine can be used as anti-browning agents since they act as inhibitors for polyphenol oxidase enzyme.

Previous studies have shown that L-cysteine forms a stable complex with the copper atom at the reaction center of PPO enzymes and as a result of that the enzymatic browning can be delayed [13]. Ascorbic acid is a well known inhibitor of polyphenol oxidase enzymes and has been commonly used for slowing down the enzymatic browning in food industiries. Because it behaves like an oxygen molecule scavenger to remove the oxygen atom in the browning reaction catalyzed by the enzyme polyphenol oxidase [1]. Some studies of polyphenol oxidase from peach suggested that EDTA (ethylenediaminetetraacetic acid) was not a very effective inhibitor [14]. It can only been used to prevent browning rection in food processes with other chemicals. All the aboved mentioned compounds are used as anti-browning agents and they all inhibit polyphenol oxidase enzyme by slowing the browning reaction in the food industries.

Lately, some studies show that heavy metal pollution in the soil hinders polyphenol oxidase enzyme activity and even prevents growth and proliferation of plants by killing this enzyme [15, 16]. Some metals such as copper (Cu), nickel (Ni) and zinc (Zn) may be micronutrients for plants if they are present in trace quantities, but if tehy are present in excess amounts, all metals can be harmful to plants, animals and humans. Non-essential metals such as Pb, Sn and Hg are harmful to all organisms in their all amounts [3, 17]. There are several studies about the effects of some metals on to various plants and the enzymes in plants to assess their biochemical behaviours [18, 19]. These studies are getting great attention regarding the relationship among metals, chemicals, and different biochemical properties of the enzymes in plants [16]. However, no reports have been found on investigation of metal and anti-browning effects on polyphenol oxidase enzyme from princess tree leaf (Paulownia tomentosa). Therefore, we aim to study the isolation and biochemical characterization of thepolyphenol oxidase enzyme from the princess tree leaf (Paulownia tomentosa). Additionally, the effects of some metals, anti-browning compounds and their complexes on the enzyme activity were investigated.

Experimental

Chemicals

Princess tree leaf (Paulownia tomentosa) was supplied from Sakarya region to use in this work and kept at –20°C. Ammonium sulphate ((NH4)2SO4) polyviniylpolypyrolidone (PVP), Sephadex G-100, and other chemicals were provided from Sigma Chemical Co., St. Louis, MO.

Extraction of Polyphenol oxidase enzyme

15 g of Princess tree leaves (Paulownia tomentosa). were mixed to 10 ml 50mM sodium phosphate buffer (pH; 7.0) with 0.3 g polyvinylpolypyrolidone (PVPP), to prepare the PPO enzyme extraction. The mixture was homogenized and filtrated. The filtrate was then centrifuged at 14.000xg for 30 min and the supernatant was collected. The extraction was separated to different tubes and solid (NH4)2SO4, was added to the supernatant until having 80% saturation The mixture was centrifuged and the precipitate was dissolved in phosphate buffer solution in small quantities and dialyzed at 4 ° C for 24 hours in the same buffer, changing the buffer three times. Then, the dialyzed enzyme sample was centrifuged and loaded onto Sephadex G-100 column already equilibrated with extraction tampon, and washed with the tampon to eleminate unbound enzymes. The samples were collected as the enzyme sample for the rest of the tests. The quantity of the PPO enzyme was determined like Bradford method and bovine serum albumin was used as a standard for the experiment [20].

Polyphenol oxidase activity assay

The polyphenol oxidase activity was evaluated by reading the rate of initial kinon generation, as shown by an rise in absorbance at 420 nm. The PPO enzyme activity was determined using L-Tyrosine, 4-methyl catechol, catechol, L-Dopa and pyrogallol as the known PPO substrates. Kinetic properties for the substrates were determined from the graph formed with the activity versus the substrate concentrations. The Km of Michaelis-Menten constant and Vmax (the maximum velocity) values were calculated was determined using Lineweaver-Burk graph [21].

Effects of pH and temperature

The polyphenol oxidase activity was evaluated at 4.5-5.5 pHs at 50 mM acetate tampon, 6.5-7.5 pHs at 50 mM phosphate tampon and 8.0-9.0 pHs at 50 mM. Tris-HCl and Tris-Base tampon to determine the optimal pH of the PPO enzyme. The determined optimum pH values of this experiment were applied the rest of the applications. The temperature effect of princess tree leaf PPO enzyme activity was also determined at various temperature ranges from 4 to 60 ° C. The optimum temperature of the enzyme was evaluated from the above temperature range.

Effect of metals on the enzyme activity

Cu(II) (CuSO4) , Fe(III) (FeCl3), Na(I) (NaCl), Pb (II) (PbCl2), Mn(II) (MnCl2), Ni (II) (NiCl2), were preferred to identify their effects on princess tree leaf PPO enzyme activity. They were used at their different concentrations as in 1 and 10 mM.

Effect of anti-browning compounds on the enzyme activity

Ethylenediamine-tetraacetic acid (EDTA), L-ascorbic acid, L-cysteine and glutathione (GSH) were known as anti-browning compounds for PPOS. They were selected to evaluate their effects on the princess tree leaf PPO activity at their different concentrations for 1 and 10 mM.

Effect of metals and anti-browning compound complexes on the enzyme activity

A metal and an anti-browning compound were pre-incubated for 30 minutes at room temperature to give the metal- anti-browning compound complex. Subsequently, the effects of complexes on princess tree leaf PPO enzyme activity were examined by kinetic methods using catechol as the substrate at pH 7.0. The remaining PPO enzyme activity was determined for the metals, anti-browning compounds and metal-anti-browning complexes.

Results and Discussion

Extraction and substrate specificity of Polyphenol oxidase enzyme

Polyphneol ozidase enzyme was extracted from princess tree leaves (Paulownia tomentosa) with appropriate pH 7.0 buffer system explained in materials and method section. Then this crude extract was precipitated with (NH4)2SO4 from 10% to 80% salt saturation and thn dialized with pH 7.0 buffers. The enzyme solution then was applied to gel filtration column and PPO enzyme was eluted and the fractions with enzyme were collected. Then the enzyme activity and substrate specificity were determined with 5 different known substrates of polyphenol oxidase. The enzyme did not show any activity towards monophenol, L-Tyrosine, substrate But Four different substrates, (L-Dopa, pyrogallol, catechol and 4-methyl catechol) are extensively catalayzed by the enzyme, demonstrating Michaelis–Menten kinetics. The values of Michaelis–Menten constants (Km and Vmax) of princess tree leaf PPO were determined from the linear regression analysis of Lineweaver–Burk plot and the Km and Vmax values are presented in Table 1. But Calculated Km values with the lowest Km value that define good affinity to the enzyme substrate are as follows. 4-methylcatechol, catechol, pyrogallol and L-Dopa. It can be suggested that the substrate-interacting region of princess tree leaf PPO enzyme has a good attraction for small o-diphenols, such as 4-methylcatechol and catechol however it has a lesser amount of attraction to the bigger o-diphenols like L-Dopa, and pyrogallol (triphenol) according to their Km values. Our results gave parallel results with the earlier works on plant PPOs [22].

pH and temperature effects on the enzyme activity

The profiles of pH and temperature on princess tree leaf polyphenol oxidase enzyme were seperatly determined with different substrates as presented in Table 1. The optimum pH of the princess tree leaf PPO enzyme was determined 7.0 with 4-methyl catechol, 7.5 with catechol and pyrogallol and 8.0 with L-Dopa. The optimal pH value for the enzyme that oxidizes the catechol substrate is 7.5 as seen in figure 1. The optimum pH value of princess tree leaf PPO enzyme is pH 7.5 as is the case in previous studies in which most PPOs exhibited optimum activity [4, 10, 23]. The enzyme activity at acidic and basic pH ranges is very low which is due to the instability of the enzyme at these pHs. (Fig. 1).

The princess tree leaf PPO activity was also determined at various temperatures to estimate its optimum temperature (Table 1). The optimum temperature of the enzyme was determined at 25°C with catechol substrat as seen in Figure 2. The other optimum temperatures were also determined as followed at 25°C with 4-methyl catechol, at 35°C with pyrogallol and 20°C with L-Dopa. These values were parallel to those of medlar [24] and peppermint PPO [12]. But they were different from Barbados cherry PPO [22].

Effect of some metals and anti-browning compounds on the enzyme activity

Effects of some metals and anti-browning compounds on princess tree leaf PPO enzyme were determined with catechol substrate (Table 2). According to the results, glutathione (GSH) compound was the most effective anti-browning compound for princess tree leaf PPO enzyme. The other compounds were identified as anti-browning compounds by behaving like GSH. These are, respectively, ordered by L-ascorbic acid, L-cysteine and EDTA at 10 mM concentrations (Table 2). According to the studies in the literature, among the anti browning compounds, L-cysteine was identified as the most effective anti browning compound for the apple PPO enzyme [13]. Ascorbic acid has been found to be an effective reversible inhibitor for different PPOs [3, 6, 8] and is widely used as an additive in many food fields. These two naturally occurring and non-toxic substances also acted as good inhibitors for princess tree leaf PPO enzyme and may be useful for preventing the enzymatic browning of princess tree leaves in future studies. Previous studies have shown that the active thiol molecules L-cysteine (L-Cys) and reduced glutathione (GSH) play an excellent role in preventing enzymatic browning of plants by inhibiting the enzyme PPO enzyme. [1, 23, 25]. Our results also support these studies in the literature. The other known anti browning compound is EDTA which is widely used as a chemical preservative in food processes. EDTA displayed minimum inhibitory effect on princess tree leaf polyphenol oxidase activity by having similar results in cherry plypehnol oxidase activity [22].

The effects of Cu(II), Fe(III), Na(I), Pb(II), Mn (II) and Ni (II) as metals with different concentrations (1-10 mM) were determined on princess tree leaf PPO enzyme activity (Table 2). The results indicated that Cu (II) and Fe (II) metals increased the princess tree leaf PPO enzyme activity in 1 mM concentration, whereas decreasing the enzyme activity in10 mM concentrations Aydemir reported that Cu (II) and Fe (II) metals at the same concentrations and the same effect on the polyphenol oxidase enzyme activity obtained from the artichoke heads [7], as in our study. Pb (II) heavy metal showed the highest inhibitory effect on the PPO enzyme activity at 10 mM concentration. Although heavy metals are harmful to whole plant and human health, Na(I), Mn(II) and Ni(II) had no considerable influence on princess tree leaf PPO enzyme activity, whereas the same metals showed strong inhibitory effect on other plant PPO activities in the previous studies mentioned [9].

Metal with anti-browning compound complex effect on the enzyme activity

The effect of metal and anti-browning compound complex on the PPO enzyme from princess tree leaf was measured using catechol substrate. The results are presented in Fig. 3. According to the results, there was no significant effect on the enzyme activity of the metal-EDTA complex. Metal-L-ascorbic acid, Metal-L-Cys and metal-GSH complexes had high inhibitory effect on princess tree leaf PPO enzyme activity. It can be concluded that the metal-anti-browning compound complexes can enhance the inhibitory effect of anti-browning compounds on the enzymatic browning in plants and proctect the plant PPO enzymes from the toxic effects of metals in the soil.

Conclusion

A polyphenol oxidase enzyme was successfully extracted and characterized from princess tree leaf (Paulownia tomentosa) as a new plant enzyme source. The enzyme showed good substrate specificity di and three phenols but not monophenols. The effects of metals, anti-browning compounds and their complexes on the new plant polyhenol oxidase activity were also examined. The results showed that they all had mostly anti-browning and inhibitor effects on princess tree PPO. Therefore, this study can provide useful information that the use of complexes of metal-anti-browning compounds may increase the effect of antifungal agents used in enzymatic browning, as well as reduce the effects of toxic metals on plant PPO enzyme activities in the soil. Enzymatic browning in plants is recognized as a severe problem in food processes. We can conclude that future studies may help to realize the relation between the browning reaction and PPO activity of fruits and vegetables during storage and processing in food industries.

Acknowledgments

This work has been financed by the Scientific Research Unit of Sakarya University. Project Number: FBDTEZ-2016-50-02-001.

Table 1. The substrate specificities and optimum pH and temprature valuesof princess tree leaf PPO enzyme

PPO Substrates	Km (mM)	Optimum pH	Optimum temperature (°C)
Catechol	4.55	7.5	25
4-Methyl Catechol	2.17	7.0	25
Pyrogallol	4.77	7.5	35
L-Dopa	6.6	8.0	20

Table 2. The percent remaining activity of princess tree leaf PPO enzyme with Metals and Metal-Anti-browning compounds

	Remaining Activity (%)	
Metals	**(1 mM)**	**(10 mM)**
$CuSO_4$	117	15
$FeCl_3$	120	16
NaCl	97	84
$PbCl_2$	89.3	0
$MnCl_2$	102	66.7
$NiCl_2$	105	108
Anti-Browning Compounds		
L- Ascorbic Acid	55	2
EDTA	96	91
L-Cysteine	63	43
Glutathione (GSH)	12	0

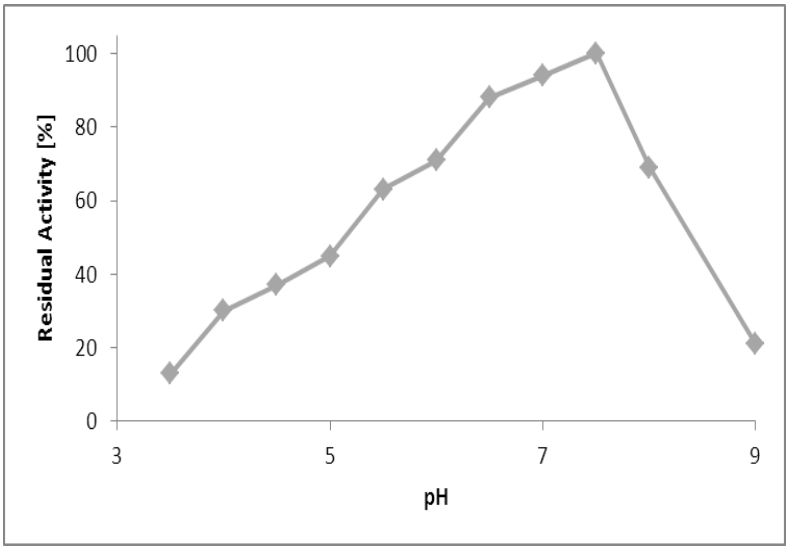

Fig. 1: pH effect on princess tree leaf PPO enzyme activity with catechol

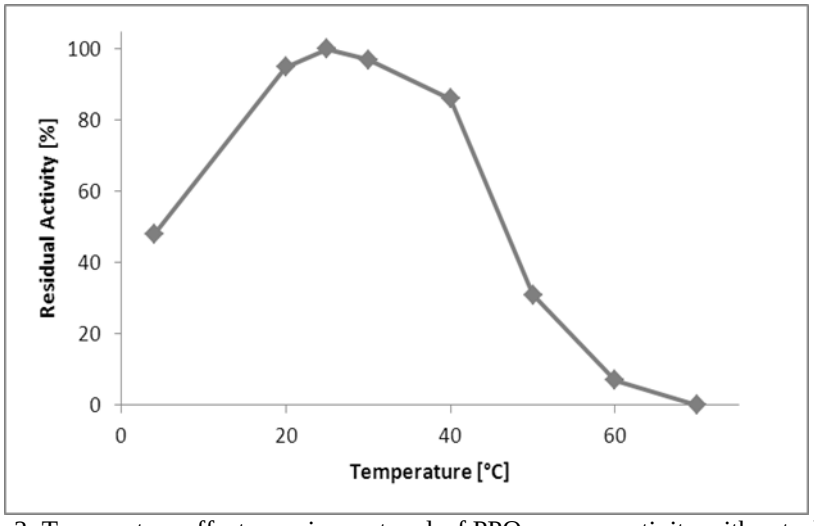

Fig. 2: Temperature effect on princess tree leaf PPO enzyme activity with catechol

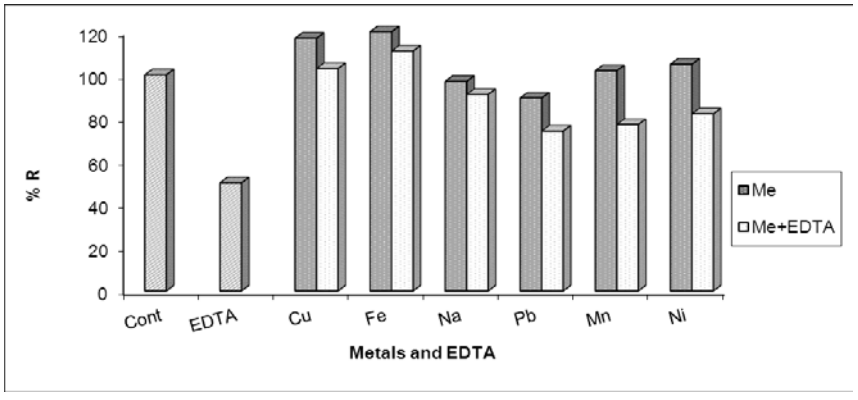

a

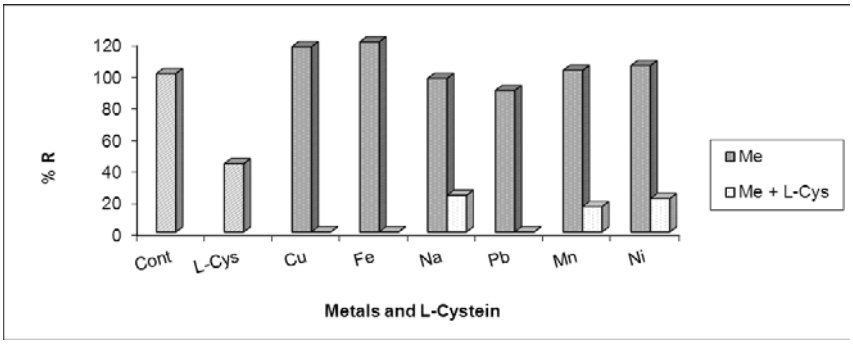

b

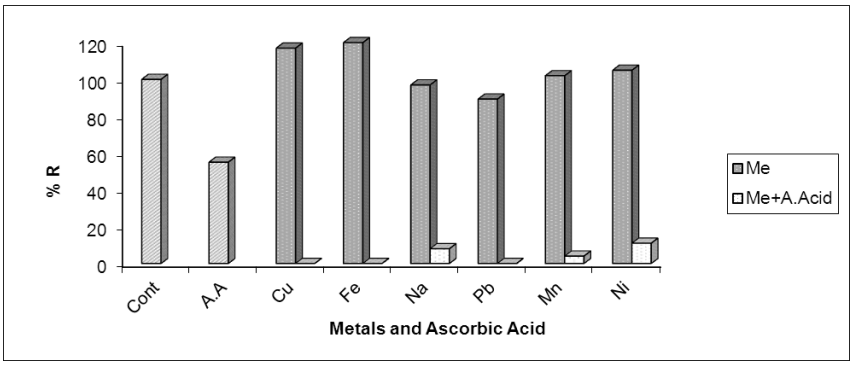

c

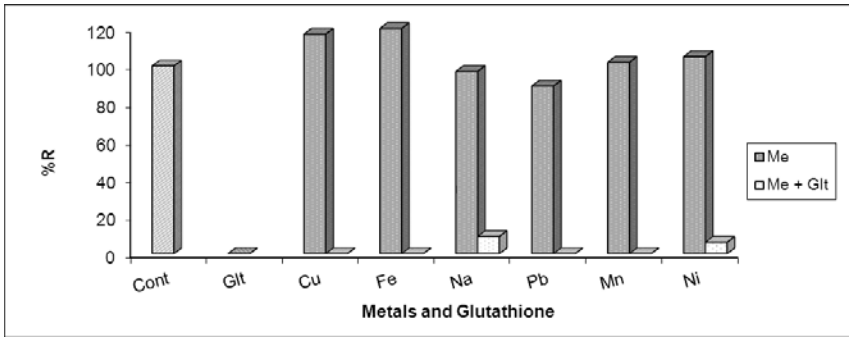

d

Fig. 3: %R relative activities of princess tree leaf PPO enzyme with metals and metal-anti-browning compound complexes. (a) Metals and Metal+ EDTA, (b) Metal and Metal+ L-Cystein, (c) Metal and Metal+ Ascorbic Acid, (d) Metal and Metal+ GSH.

References

1. M. Friedman, Food Browning and its Prevention: An Overview, J. Agric. Food Chem.,44, 631 (1996).
2. D. F. Holderbaum, T. Kon and M. P. Guerra, Enzymatic Browning, Polyphenol Oxidase Activity, and Polyphenols in Four Apple Cultivars: Dynamics during Fruit Development, Hortiscience, 45(8),1150 (2010).
3. M. Beaulieu, M. Be'liveau, G. D'Aprano and M. Lacroix, Dose Rate Effect of Irradiation on Phenolic Compounds, Polyphenol Oxidase, and Browning of Mushrooms (Agaricusbisporus), J. Agric. Food Chem., 47, 2537 (1999).
4. K. M. Mdluli, Partialpurification and characterisation of polyphenoloxidase and peroxidase from marula fruit (Sclerocaryabirreasubsp. Caffra), Food Chem., 92, 311 (2005).

5. O. Arslan and S. Doğan, Inhibition of Polyphenol Oxidase Obtained from Various Sources by 2,3-Diaminopropionic Acid, J. Sci. Food Agric, 85, 1499 (2005).
6. O. Arslan, M. Erzengin, S. Sinan and O. Ozensoy, Purification of Mulberry (Morusalba L.) Polyphenol Oxidase by Affinity Chromatography and İnvestigation of ıts Kinetic and Electrophoretic Properties, Food Chem., 88, 479 (2004).
7. T. Aydemir, Partial purification and characterization of polyphenol oxidase from artichoke (Cynarascolymus L.) heads. Food Chem., 87, 59 (2004).
8. S. Chazarra, F. Garcia-Carmona and J. Cabanes, Evidence for a Tetrameric form of IcebergLettuce (Lactucasativa L.) PolyphenolOxidase: Purification and Characterisation, J. Agric. and Food Chem., 49, 4870 (2001).
9. Z. J. Gao, J. B. Liu and X. G. Xiao, Purification and Characterisation of Polyphenol Oxidase from Leaves of Cleomegynandra L., Food Chem.,129, 1012 (2011).
10. U. Gawlik-Dziki, U. Szymanowska and B. Baraniak, Characterization of Polyphenol Oxidase from Broccoli (Brassicaoleracea var. botrytisitalica) Florets, Food Chem., 105, 1047 (2007).
11. U. Gawlik-Dziki, Z. Złotek, and M. S´wieca, Characterisation of Polyphenol Oxidase from Butter Lettuce (Lactucasativa var. capitata L.), Food Chem., 107, 129 (2008).
12. D. Kavrayan and T. Aydemir, Partial Purification and Characterization of Polyphenol Oxidase from Peppermint (Menthapiperita), Food Chem., 74, 147 (2001).
13. H. Ozoglu, and A. Bayindirli, Inhibition of Enzymic Browning in Cloudy Apple Juice with Selected Anti-browning Agents, Food Control, 13(4), 213 (2002).
14. K. D. Sanjeev and K. M. Sarad, Purification and Biochemical Characterization of Ionically Unbound Polyphenol Oxidase from Musa paradisiaca Leaf, Prep. Biochem. Biotechnol., 41,187 (2011).
15. A. M. Balsberg-Pahlsson, Toxicity of HeavyMetals (Zn, Cu, Cd, Pb) to Vascular Plants, Water Air Soil Pollut.,47, 287 (1989).
16. S. C. Barman, R. K. Sahu, S. K. Bhargava and C. Chatterjee, Distribution of Heavy Metals in Wheat, Mustard, and Weed Grown in Fields İrrigated with İndustrial Effluents, Bull. Environ. Contam. Toxicol., 64, 489 (2000).
17. M. Dazy, J. F. Masfaraud and J. F. Férard, Induction of Oxidative Stress Biomarkers Associated with Heavy Metal Stress in Fontinalis Antipyretica Hedw., Chemosphere, 75, 297 (2009).
18. R. Chandra, R. N. Bhargava, S. Yadav and D. Mohan, Accumulationand Distribution of Toxic Metals in Wheat (Triticumaestivum L.)and Indian Mustard (Brassicacampestris L.) İrrigated with Distilleryand Tannery Effluents, J. Hazard. Mater., 162, 1514 (2009).
19. S. Gupta, S. Satpati, S. Nayek and D. Gorai, Effect of Wastewater İrrigation on Vegetables in Relation of Heavy Metals and Biochemical Changes, Environ. Monit. Assess., 165, 169 (2010).
20. M. A. Bradford, A rapid and Sensitive Method for the Quantitation of Microgram Quantities of Protein Utilizing the Principle of Protein-dye Binding, Anal. Biochem., 72, 248 (1976).
21. H. Lineweaver and D. Burk, The Determination of Enzyme Dissociation Constants, J. Am. Chem. Soc., 56, 658 (1934).
22. V. B. A. Kumar, T. C. Kishor Mohan and K. Murugan, Purification and Kinetic Characterization of Polyphenol Oxidase from Barbados Cherry (Malpighiaglabra L.), Food Chem., 110, 328 (2008).
23. Y. Z. Dogru, M. Erat and A. Demirkol, Investigation of some kinetic properties of polyphenol oxidase from parsley (Petroselinumcrispum, Apiaceae), Food. Res. Int., 49, 411 (2012).
24. B. Dincer, A. Colak, N. Aydin, A. Kadioglu and S. Guner, Characterization of Polyphenol Oxidase from Medlar Fruits (Mespilusgermanica L., Rosaceae), Food Chem., 77, 1 (2002).
25. F. C. Richard-Forget, P. M. Goupy and J. J. Nicolas, Cysteine as an Inhibitor of Enzymatic Browning Kinetic Studies, J. Agric. Food Chem., 40(11), 2108 (1992).

International Conference on Science and Technology

ICONST 2018

5-9 September 2018 Prizren - KOSOVO

A Case Study for Pozzolanic Activity of Rice Wastes: Rice Straw Ash and Rice Husk Ash

Serhat Oğuzhan Kıvrak [1*], Celalettin Başyiğit [2]

Abstract: In this study, the potential use of rice wastes as pozzolan in concrete production was investigated. For this purpose, rice straw and rice husk wastes were burned for 90 min at 600 ^{o}C degrees and rice straw ashes (RSA) and rice husk ashes (RHA) were produced. Their chemical structures were determined by X-Ray diffraction analysis and pozzolanic activities were determined by pozzolanic activity tests. Concrete specimens were prepared by replacing 5% of cement additionally to the control mix. Concretes were casted into 12 pieces of 15x15x55 cm prismatic and 15x15x15cm cube molds. Specimens demolded after 1 day of casting and cured in water for 7, 28, 56 and 90 days. The flexural and compressive strengths of concretes were determined at 7, 28, 56 and 90 days by three point flexural tests and uniaxial compressive tests, respectively. XRD test results showed that RHA has amorphous phase. Crystalline phases were observed in the XRD analysis of RSA besides the amorhous phase. RHA also exhibited higher pozzolanic activity than the RSA by considering the results of pozzolanic activity tests under compression. When compressive test results were taken into consideration, RHA performed higher pozzolanic activity than the RSA specimens at all curing ages. At 7 days of curing, the compressive strengths of RHA and RSA incorporated concretes were lower than the control concrete as expected. However, when the curing age increased, the use of RHA and RSA enhanced the compressive strengths (after the 28 and 90 days for RHA and RSA respectively). In conclusion, pozzolanic activity can be obtained by burning not only the rice husks but also the rice straws under controlled burning condiditons. Early age compressive strengths were decreased by use of RSA and RHA however final compressive strengths of concrete can be succesfully enhanced.

Keywords: Rice straw ash, rice husk ash, pozzolanic activity, flexural, compressive.

Introduction / Giriş

Pozzolan is a siliceous or siliceous and aluminous material which in itself possess little or no cementitious value but when it finely divided form and in the presence of moisture chemically reacts with calcium hydroxide and form compounds that possessing hydraulic cement properties (S.T. Erdoğan and T.Y. Erdoğan, 2014). In general pozzolans can be considered as natural and artificial pozzolans. Artificial products are usually obtained from the industrial wastes. Today various types of artificial pozzolans (fly ash, granulated blast furnace slag, silica fume etc.) are commonly used in the production of cement and concrete in order to ensure economic, mechanical and durability aspects (S.T. Erdoğan and T.Y. Erdoğan, 2014).

The rice straws and husks, which are agricultural waste, cause a serious stock problem in the regions where rice production is made. The rice husk is rich in silica-carbon content (92 - 93% siliceous). By burning rice husks at a certain temperature and time, the high amount of silica in the rice husk ash (RHA) became amorphous and can be used as pozzolan in concrete production (Mehta, 1977). On the other hand, the straw

[1]Hitit University, Vocational School of Technical Sciences, 19169, Çorum, TURKEY
[2]Suleyman Demirel University, Faculty of Engineering, Departmant of Civil Engineering, 32200, Isparta, TURKEY
*Correspondingauthor: oguzhankivrak@hitit.edu.tr

is left as it is harvested in the field, and burned to be disposed of for agricultural purposes. As a result of this uncontrolled incineration the earth are negatively affected and serious environmental problems arise.

Sensale (2006) showed that the use of RHA as pozzolan in concrete can enhance the compressive strengths at 91 days when compared to conventional concrete. Yıldız et al. (2007) produced the RHA by burning rice husks at 600ºC and produced concrete specimens by replacing this ash with cement in various ratios. As a result, the compressive and flexural strengths of the concrete specimens prepared by 10% RHA replacement were greater than the control concrete. In the production of high strength concrete, it was stated that the optimum substitution rate of RHA is found as 5-10% for maximum compressive strength (Mahmud et al., 2009).

Recently, there is a growing interest in producing pozzolan by burning rice straw at controlled burning conditions. Munshi et al. (2013) burned rice straws, prepared concrete samples by replacing RSA 5-10-15% by weigth of cement and concluded that the use of RSA by 10% of cement increased the compressive strength up to 12.5%. Roselló et al. (2017) resulted that cementing CSH gel is formed after 7 and 28 days at room temperature from the pastes prepared by mixing RSA and calcium hydroxide. They also prepared mortar specimens by using ordinary Portland cement (OPC) and RSA, and concluded that mortars with 10% RSA replacement ratio reached 98.4% of the strength found for OPC control mortar after 7 days, and 107.1% after 28 days.

In this study, the potential use of rice wastes as pozzolan in concrete production was investigated. The efficiency of RSA as pozzolan was compared with the RHA. Pozzolanic activities of RSA and RHA were explored by X-Ray diffraction analysis and mechanical tests. Also, the effect of RSA and RHA addition to the compressive and flexural strengths of concrete was investigated at 7, 28, 56 and 90 days durations.

Material and Method

In order to obtain the RSA and RHA, the rice husk obtained from the paddy processing factories located in the Osmancık region of Çorum and rice straws remaining in the fields after the harvest were used. The rice husk and straws were subjected to pre-burning process for preventing the smoke and gas release that would be generated during controlled burning. After pre-burning stage, ashes were burned under controlled incineration process at 600 ºC for 90 min by using a laboratory type high tempretature oven (Figure 1).

Figure 1. Controlled incineration process of ashes.

After the preparation of RSA and RHA, their pozzolanic activities were explored by using X-Ray diffraction (XRD) analysis and mechanical tests in accordance with the TS 25. From the XRD results, XRD patterns of both RSA and RHA was obtained and their chemical structures (amorphous and cyrsitaline phases) were commented. XRD analysis on RSA and RHA samples was performed with Shimadzu XRD-6000 model device. The device had a Copper (Cu) X-Ray tube and CuKα X-ray with a wavelength of 1.544 Å was used.

In addition to XRD analysis, pozzolanic activity of RSA and RHA were determined by compression tests in accordance with the TS 25 and ASTM C349. Material used for the specimen preparation and mixture properties were presented in Table 1. The mortars were placed in 40x40x160 mm molds and then kept in a room temperature of 23+2 ° C for 24 hours. In order to prevent evaporation on the molds glass plate in 210x185 mm dimensions and 6 mm thickness was plasced on the molds. After 24 hours, the molds were left in an oven at 55+2 °C for 6 more days without removing the molds. The samples were then removed from the oven, cooled to room temperature and demolded. Their compressive strengths were determined under compression according to ASTM C349.

Table 1. Material used for the specimen preparation and mixture properties.

Materials and Mixture properties	
Standard sand	1350 gr
$Ca(OH)_2$	150 gr
RSA or RHA (P)	2 x 150 (δ_p/δ_k)
Water	0,5 x (150+P)

* δ_p: Density of Pozzolan, δ_k: Density of $Ca(OH)_2$.

After determination of pozzolanic properties of RSA and RHA, a control concrete and ash incorporating concrete specimens were prepared by replacing 5% of cement by ashes. In concrete production, CEM II/A-LL 42.5 N type cement and crushed limestone aggregates with the largest grain size of 25 mm were used. Sikament NP superplasticizer (SP) (Type F according to ASTM C494) was also used for achieving a proper workability in the fresh state. Concrete mix proportions were given in Table 2.

Table 2. Concrete mix proportions (kg/m^3)

Specimen	Cement	Water	Aggregate				SP	RSA	RHA
			0-4 mm	4-12 mm	12-16 mm	16-25 mm			
Control	335.00	175	790	400	300	480	4	0	0
RSA	318.25							16.75	0
RHA	318.25							0	16.75

Ingredients were mixed in a pan type labratory mixer (56 lt of active mixing capacity). Fresh state concretes were casted into 12 pieces of 15x15x55 cm prismatic and 15x15x15cm cube molds. Specimens demolded after 1 day of casting and cured in water for 7, 28, 56 and 90 days. The flexural and compressive strengths of concretes were determined in accordance with the TS EN 12390-3 and TS EN 12390-5 standards at 7, 28, 56 and 90 days by three point flexural tests and uniaxial compressive tests, respectively.

Results and Discussion

X-Ray Diffraction Analysis

XRD patterns of RSA and RHA were shown in Figure 2. From the XRD results, RHA has more amorhous structure when compared to RSA. Crystalline phases were observed in the XRD analysis of RSA besides the amorhous phase while RHA shows remarkable high amounts of amorphous phase. As a result, it can be stated that RHA has much pozzolanic activity than the RSA.

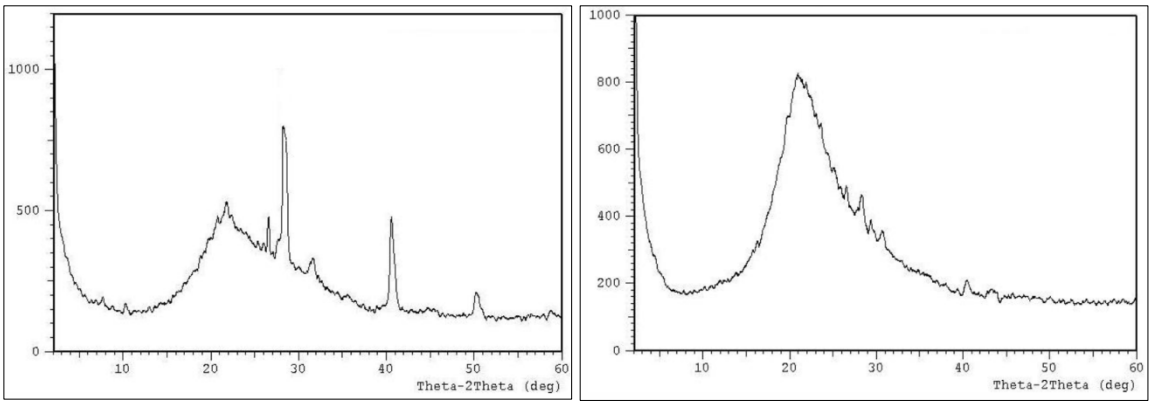

(a) (b)

Figure 2. XRD patterns of a) RSA, b) RHA.

Determination of Pozzolanic Activity under Compression

Pozzolanic activity of RSA and RHA were determined mechanically by using compressive strengths obtained from the compression tests in accordance with the TS 25 and ASTM C349. Results were given in Figure 3. According to TS 25, minimum compressive strength of specimens should be over 4 MPa. RSA specimens exhibited a compressive strength of 9.4 MPa while the RHA specimens exhibited 10.2 MPa which are 135% and 155% higher than the standard value. In addition to the XRD analysis, compressive tests results showed that both RSA and RHA has pozzolanic activity.

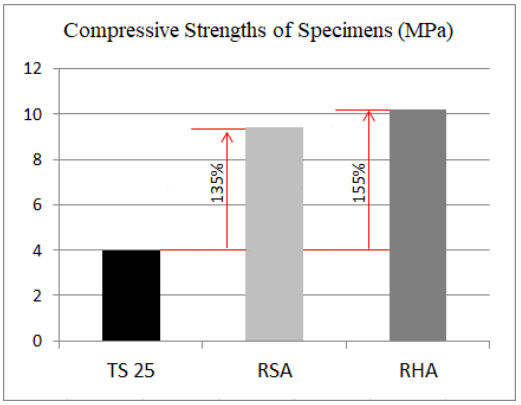

Figure 3. Compressive strengths of specimens

Determination of RSA and RHA addition to the Mechanical Performance of Concrete

Flexural Test Results

Flexural strengths of concrete specimens were given in Figure 4 by considering both RSA-RHA addition and curing times into consideration.

In general the addition of RSA and RHA by 5% of cement weigth decreased the flexural strengths. At early ages (7 days of curing), the flexural strength of concrete were decreased with the addition of RSA by 17% and RHA by 12%. However, in all specimens after 28 days of curing, flexural strengths had a stable increase and the amount of reduction in flexural strengths was slightly decreased and ranged between 0-4%.

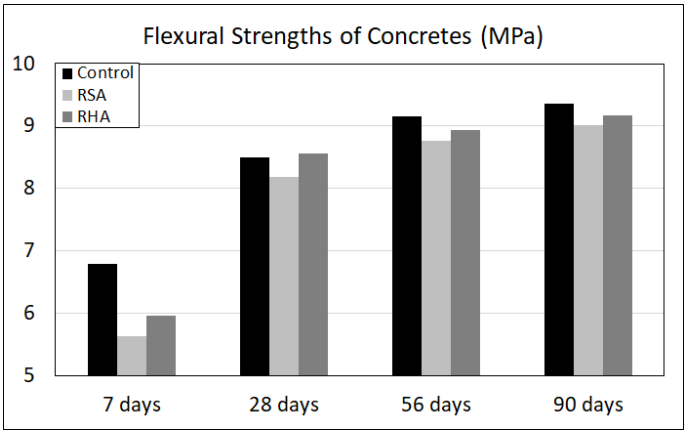

Figure 4. Flexural strengths of concrete specimens

Compressive Test Results

Compressive strengths of concrete specimens were presented in Figure 5 by considering both RSA-RHA addition and curing times into consideration.

At 7 days of curing, compressive strengths were also decreased as being seen in the flexural strengths. At 28 days of curing, the compressive strength of RHA was slightly higher than the control concrete while the compressive strength of RSA was slightly lower. At 56 days of curing, the highest compressive strength value was obtained from the RHA reached approximately to the same compressive strength value with the control concrete. Further increasing the curing age to the 90 days, both RSA and RHA exhibited higher compressive strengths from the control concrete and the highest compressive strengths were still obtained from the RHA specimens.

By considering the results generally, it can be concluded that the contrubiton of RSA and RHA to the compressive strength is increased by curing age and both RSA an RHA has increased the final compressive strengths. This situation can be explained with by the general aspects of pozzolan-Calcium Hydroxide ($Ca(OH)_2$) reaction. As the curing time progresses, cement hydration took place and more $Ca(OH)_2$ had been released. Then RSA and RHA chemically reacted with the $Ca(OH)_2$ and secondary calcium-silicate-hydrate gel were produced which possibly resulted a dense transition zone and reduction in concrete pores. Therefore, the compressive strengths were affected positively with the RSA and RHA addition. In addition to that, RHA showed higher binding properties than the RSA as a result of its high amount of amorphous phase and high pozzolanic activity. This caused early and higher compressive strength gain (at 28 days) when compared to RSA.

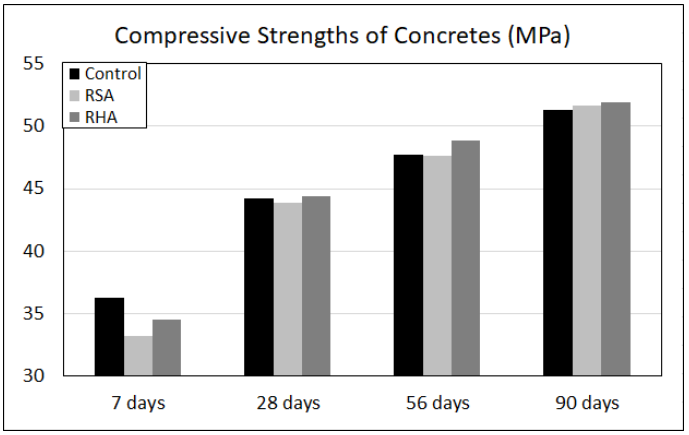

Figure 5. Compressive strengths of concrete specimens

Conclusions

In this study, the potential use of rice wastes as pozzolan in concrete production was investigated and the efficiency of RSA as pozzolan was compared with the RHA. Based on the experimental results of this study, the following conclusions can be drawn:

- Pozzolans compatible to use in concrete production was successfully prepared by using rice husk and rice straws under controlled burning conditions (600 ^{o}C for 90 min).

- The pozzolanic activity of RSA and RHA was verified with XRD and compressive strengths tests. XRD test results showed that RHA had significantly high amount of amorphous phase while some crystalline phases were observed in the XRD analysis of RSA besides the amorhous phase which foresee the both RSA and RHA had pozzolanic activity. The results of XRD analysis were supported with the pozzolanic activities which obtained from the compressive tests results.

- The effect of RSA and RHA to the mechanical properties of concrete was also investigated. Test result showed that the use of RSA and RHA slightly decreased the flexural strengths. The amount of reduction in flexural strengths was decreased as curing time increased and ranged between 0-4% which can be considered as mechanically acceptable.

- The contrubiton of RSA and RHA to the compressive strength was increased by curing age and both RSA an RHA increased the final compressive strengths. As the curing time progressed, cement hydration took place and more $Ca(OH)_2$ had been released. Then RSA and RHA chemically reacted with the $Ca(OH)_2$ and secondary calcium-silicate-hydrate gel were produced which possibly resulted a dense transition zone and reduction in concrete pores, therefore, the compressive strengths were affected positively with the RSA and RHA addition.

- RHA showed higher binding properties than the RSA as a result of its high amount of amorphous phase and high pozzolanic activity. This caused higher early and final compressive strength gain (at 28 days) when compared to RSA.

- In general, RSA can be stated as a promising pozzolan and an alternate to RHA.

Acknowledgements

Financial support was provided by Süleyman Demirel University Scientific Research Projects Management Deparment under the Grant No. 2203-D-10.

References

ASTM C349. (2014). Standard Test Method for Compressive Strength of Hydraulic-Cement Mortars (Using Portions of Prisms Broken in Flexure), ASTM International, West Conshohocken, PA, 2014, www.astm.org

ASTM C494. (2017). Standard Specification for Chemical Admixtures for Concrete, ASTM International, West Conshohocken, PA, 2017, www.astm.org

Erdoğan, Sinan T., Erdoğan, Turhan Y. (2014). Basic materials of construction, METU Press Publishing Company, Ankara, Turkey.

Mahmud, H. B., Malik, M. F. A., Kahar, R. A., Zain, M. F. M., & Raman, S. N. (2009). Mechanical properties and durability of normal and water reduced high strength grade 60 concrete containing rice husk ash. Journal of advanced concrete technology, 7(1), 21-30.

Mehta, P. K. (1977). Properties of blended cements made from rice husk ash. In Journal Proceedings, 74(9), 440-442.

Munshi, S., Dey, G., & Sharma, R. P. (2013). Use of rice straw ash as pozzolanic material in cement mortar. pan, 25(100), 00.

Roselló, J., Soriano, L., Santamarina, M. P., Akasaki, J. L., Monzó, J., & Payá, J. (2017). Rice straw ash: A potential pozzolanic supplementary material for cementing systems. Industrial crops and products, 103, 39-50.

Sensale, G. R. (2006). Strength development of concrete with rice-husk ash, Cement & Concrete Composites, 28 (2), 158-160.

TS 25. (2008). Natural pozzolan (Trass) for use in cement and concrete - Definitions, requirements and conformity criteria. Turkish Standardization Institute (in Turkish).

TS EN 12390-3. (2010). Testing hardened concrete - Part 3: Compressive strength of test specimens. Turkish Standardization Institute (in Turkish).

TS EN 12390-5. (2010). Testing hardened concrete - Part 5: Flexural strength of test specimens. Turkish Standardization Institute (in Turkish).

Yıldız, S., Balaydın, İ., & Ulucan, Z. Ç. (2007). Pirinç Kabuğu Külünün Beton Dayanımına Etkisi. Science and Engineering Journal of Fırat University, 19(1), 85-91.

International Conference on Science and Technology

ICONST 2018

5-9 September 2018 Prizren - KOSOVO

Surface Stainability of Cad/Cam and Nanocomposite Resin Materials

Merve Erken[1], Zeynep Başağaoğlu Demirekin[1], Banu Esencan Türkaslan[2]
Serhat Süha Türkaslan[1]

Abstract: The surface stainability of recently introduced computer-assisted design/computer-assisted manufactured (CAD/CAM) hybrid ceramic and resin nanocomposite is unknown. The purpose of this in vitro study was to compare the effect of surface treatment with coffee and cola, on the color of 3 different CAD/CAM restorative materials and a nanocomposite resin. Hybrid dental ceramic (VITA Enamic) and a nanocomposite resin (Filtek Supreme Ultra Universal) specimens were evaluated for color change when dipped into coffee (n=5) and cola (n=5). Specimens 0.5 and 1 mm in thickness were dipped in coffee and cola for different time intervals. CIEDE2000 color differences (ΔE00) due to coffee and cola were calculated using spectrophotometer. Significant differences at different time intervals were analyzed with the Tukey-Kramer test. For color difference due to staining, thickness was not significant. Regarding the analysis of color differences, there was significantly difference between the tested materials and control groups (P<.001). Also significantly difference is recorded among the groups with different dipping media. It may be concluded that both coffee and cola have significant effect on the color change of dental restorative materials.

Keywords: Resin-composites, CAD/CAM materials, Staining, Colour stability.

Introduction

Modern dentistry has increased the demand for highly aesthetic restorations by color comparison as an important criterion. Permanent color stability of dental restorative materials is a challenging factor because it distinguishes between the success and failure of restorations. In this context, the properties and production techniques of the materials play an important role in determining the behavior of the material upon different conditions, that provides the restoration success (2,8,18).

Dental porcelain, which combines wear resistance, strength, toughness and excellent aesthetics, is considered as a reference material for prosthetic rehabilitation. Composite resins have been widely used since their introduction because of their ease of use in evaluation and luting procedures.

The latest innovations in composite resin technology are the application of nanocomposite theories to restorative materials. Modern nanocomposite materials combine scientific principles for increased longevity to enhance aesthetic and durability (15,19,20).

Dental CAD/CAM technology has been on the market for many years and has been becoming increasingly popular for esthetic restorations. This technology has been developed to solve some challenges, such as working with high-strength materials in one session and performing restorations that are closest to the natural appearance, combining the dental clinic and dental laboratory in a single center.

[1]Suleyman Demirel Univercity.Faculty of Dentistry,32200,Isparta,TURKEY
[2]Suleyman Demirel Univercity.Faculty of Engineering,32200, Isparta,TURKEY
Correspondingauthor:dtmerverken@gmail.com

CAD / CAM blocks increase the internal strength of the restorations compared to laboratory restorations when they are produced under optimal conditions. Ensuring the best natural appearance can be handled using all ceramic materials. However, all ceramic materials may exhibit some disadvantages. The fragile nature of traditional ceramic materials potentially leads to catastrophic fractures. This phenomenon directly affects the life of the restoration. Glass ceramics introduced to the market were reinforced for fracture resistance. These materials, after exhaustion, still do not show satisfactory mechanical properties under the load. Recently, resin ceramic hybrid materials were developed for CAD / CAM systems instead of machinable ceramics, and they aimed to eliminate the fragile behavior of all the ceramics under load (7,12).

During the functional life of the restoration, color stability is as important as the mechanical properties of the material. Over time, discoloration may limit the life and quality of restorations. When exposed to oral environment, discoloration may occur due to external and internal factors. Extrinsic factors, exogenous sources (eg. As a result of incoming pollution, food colorants contain adsorption or absorption of colorants. The degree of discoloration varies according to oral hygiene, eating / drinking and smoking habits of patients. On the other hand, intrinsic stains may also be due to a change in the material itself (for example, oxidation of monomer now). In this context, resin matrix composition, hydrophilic / hydrophobicity, fill load, particle size and nature, amount of photo-initiator or inhibitor and the degree of conversion of composite resin have a strong effect on the smudge density (2,16).

Advances in nanocomposite technology affect not only mechanical and physical properties of composite materials, but also color characteristics and optical properties. Since more dentists work independently of a technician, it is essential to better understand the optical properties of new materials in order to obtain closer match between natural tooth - composite resins with natural tooth - CAD / CAM as an alternative to ceramic materials. Vita ENAMIC CAD / CAM is a hybrid tooth ceramic (HC) and a resin nanoceramic (filtek ultimate) CAD / glass processing material that can be commercially available. A new ceramic-polymer hybrid restorative material class, which can be manufactured in a single grinding step without heat treatment, has been introduced. The materials in this class include a ceramic (Enamic; VITA, bad Säckingen, Germany) and nano ceramic reinforced polymer (filtek) that has been infused with the polymer (5,9).

Nanoceramics and resin composites have the same microstructure but are different proportions. They fill about 80% of the weight of a polymeric matrix and ceramic nanoparticles. In addition, filler materials have sizes smaller than 100 nm. These fillers may consist of a combination of traditional ceramics, polycrystalline ceramics (zirconia) or both (10).

The new Vita enamic material (Vita Zahnfabrik; bad Sackingen, Germany) combines the properties of ceramics and polymers. The dual-network consists of a hybrid structure called a hybrid, with two interconnected ceramic and polymer networks. Thanks to the fine structure of the nets formed between Feldspat ceramic and acrylate polymer, ENAMIC exhibits abrasion, bending strength and flexibility similar to dentine. The evaluation of Vickers hardness of the material produced the values between dentine and enamel. While wear can be compared to common dental ceramics, wear of the antagonistic teeth is low. (6)
However, each material must be evaluated separately according to its mechanical and aesthetic characteristics. The literature contains limited data on the color stability and transparency of newly introduced CAD / CAM milling blocks. Therefore, the aim of this study was to determine the effects of stain solutions and surface finishing on the color stability and translucency of hybrid materials. The null hypothesis of this study was that both dyeing solutions and surface finishing did not correlate with the stainability and half transparency of hybrid ceramics (HC) and resin nanosemics (RNC).

Material and Methods

Two different materials Hybrid dental ceramic (VITA Enamic) and a nanocomposite resin (Filtek Supreme Ultra Universal) specimens were prepared (n=5 per group) to test their color stainability against coffee and cola media. CAD / CAM blocks were sliced with a slow-speed Diamond blade (Buehler wafting blades, series 15 LC Diamond; microstructural analysis) and a cutting machine (vari / cut VC-50; Leco Corp) in 0,5 and 1 mm rectangular plate slices. For each sample, the final thickness was measured using a digital micrometer (Digital Indicator 0001-2; Mitutoyo). Nano composite resin is packed into a

polytetrafluoroethylene mold on a glass sheet. After the composite resin was packed, the Mylar film was laid on top of the sample. To achieve a single Disc Thickness, a glass plate is pressed onto the Mylar film to prevent gaps and surface irregularities. The glass sheet was removed and samples were slightly polymerized using a light polymerization unit (TC-01; Spring health) from a thin Mylar film with an effective output density of 800 mW / cm2. Teleportation from the upper surface. For 40 seconds. After the specimen was removed from the mold, 40 seconds lighter polymerization was repeated from both surfaces to ensure that polymerization was completed. Composite resin samples are polished with silicon carbide abrasive paper (600, 800, 1200 grit) after polymerization. The final thickness is measured with a digital micrometer, as in other examples.

In this study, two of the most popular CAD / CAM ceramics were selected. The white Vita Enamic stains Kit (Vita Zahnfabrik, Germany) following the manufacturer's instructions. 2m2 Color Vita 3D-master shade Guide for enamic samples (Vita Zahnfabrik, Germany) has been selected. The 2M2 colour for Enamic specimens was chosen according to the Vita 3D-Master shade guide (Vita Zahnfabrik, Germany) which corresponds with the Filtek (filtek Ultimate specimens A2 colour according to the Vitapan Classical shade guide (Vita Zahnfabrik, Germany).

Spectrophotometric measurements were performed using a white background as in other studies. Before each sample measurement, the spectrophotometer was calibrated using a given calibration standards according to the manufacturer's recommendations. The color measurements were performed according to the same procedure for 1 week (T1), 2 weeks (T2), 3 weeks (T3) and one month (T4). The stain solutions were kept at 37 ° C and were renewed every 2 days to prevent bacteria or yeast contamination. According to the CIEE2000 formula published by the ciede 2000 in 2001, the color differences between baseline (T0) and T1 – T4 measurements for each resin-based composite material (COMPOSITE) and stain solution (staining) were calculated using the SpectroShade software. The CIE L * A * B * system was chosen to measure the color of samples because it is very suitable for the determination of small color differences and is widely used in previous studies. Statistical analysis was carried out with software (statistical analysis software SAS 9.3; SAS Institute). Covariance analysis of color differences due to colorization (ANOVA) used, categorical factor material and linear thickness is the actual thickness. Differences in mean thickness were analyzed by Tukey-Kramer test (a = .05).

Results

For color difference due to staining, thickness was not a significant covariate (P<.001). Regarding the analysis of color differences, every pair of the tested materials was significantly different (P<.001).

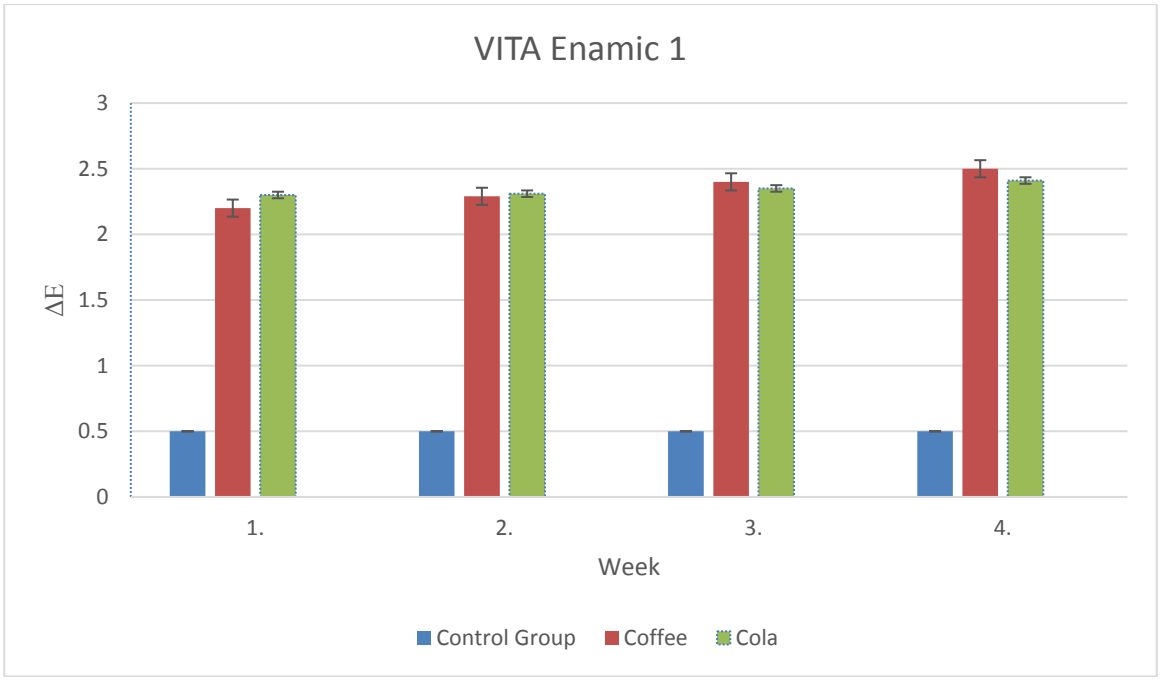

Orange Line(ΔE average)ΔE_{00}:2,34

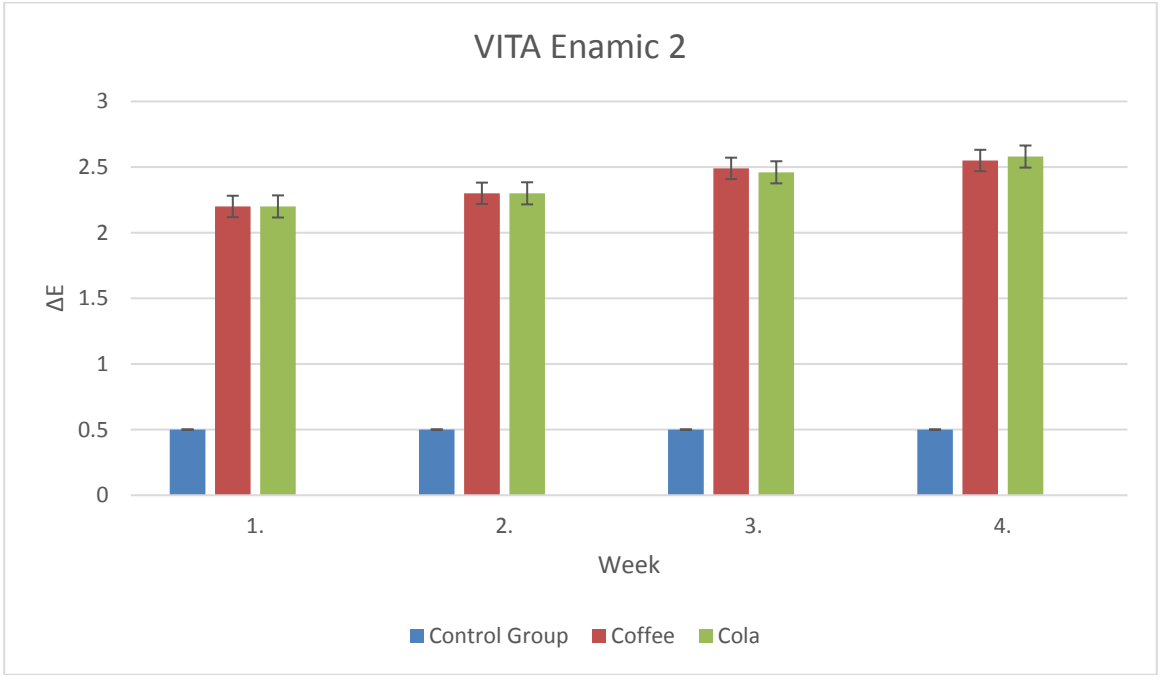

Orange Line(ΔE average) ΔE_{00}: 2,36

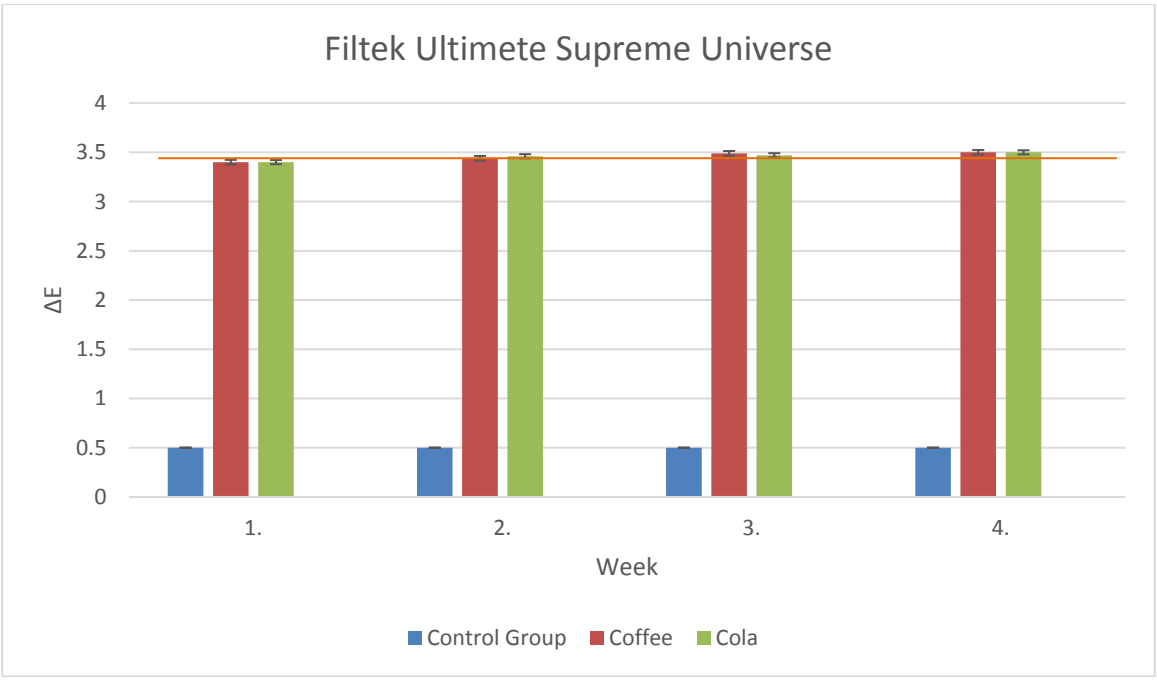

Orange Line(ΔE average) ΔE00: 3,46

Discussion

One of the problems with the failure of aesthetic restorations is the unpredictability and stability of the color stain. There are variable factors that cause discoloration in restorations: plaque accumulation, pigmentation effect of dyeing solutions, dehydration, water absorption, surface hardness and chemical degradation.

In this study, a spectrophotometric device was used to make an objective evaluation of the lens and a quantitative color assessment was allowed. In this study, color stainability was evaluated using beverages consumed frequently in our daily diet, for example coffee and smells are known to have the potential to paint restorative materials. In this study, there was an increase in ΔE * values in Cola and coffee groups for both HC and RNC samples. The decision of using the CIEDE 2000 as a reference model has been made, as this is the newest and more performing formula proposed by the CIE (Commission Internationale del'Eclairage)

One limitation of this study is that it is a In vitro study that allows stains on both sides of the material. In a clinical case, the material is bonded to a dental structure and only one side is exposed to solutions and light. In addition, the color of the samples is a combination of the gray background and the color of the sample, and the color coordinate values may change when different backgrounds are used. The results of this study should be supported by clinical studies.

More clinical and in vitro studies are required to assess the sensitivity of hybrid tooth ceramics and resin nano composite materials to other beverages and foodstuffs discoloration.(4,11,13,14,18)
In this study, discoloration was evaluated using coffee and cola, a commonly consumed beverage. The limitation of this work is that in vitro work permits stains on both sides of the material. In addition, the color of the samples is a combination of the gray background and the color of the sample, and the color coordinate values may change when different backgrounds are used. The results of this study should be supported by clinical studies.(1)

Previous studies have reported the low hydrophilicity, low viscosity and solubility of this monomer, which contributes to less water absorption and therefore more color retention. The sensitivity of resin-based composite materials is directly related to the degree of water absorption affected by the hydrophilic / hydrophobic nature of the resin matrix.(17)

According to Gawriołek et al, ceramic materials exhibit better color stability than composite resins, and the results of this study are acceptable.(3)

Arocha and colleagues compared the color stainability of CAD / CAM composite resins and composite resins processed in the laboratory and reported high stainability of CAD / CAM composite resins, including one of the materials tested in this study. This result is consistent with clinically unacceptable discoloration observed with Filtek ultimate samples in this study. The stainability of the assessed materials may be related to monomer hydrophobicity and water absorption.(14)

In a recent study, Acar et al. he evaluated the optical properties of nanocomposite resins and ceramics in various thicknesses of coffee. For lava Ultimate and Filtek Supreme plus, they reported that Coffee thermoplasmosis causes a clinically unacceptable color change and that Enamic color changes can be detected but can be clinically acceptable. In addition, considering the discoloration of coffee, Enamic concluded that lithium distillate produced by minimal invasive techniques could be an alternative to ceramic restorations. Unlike this study, a spectro-radiometer was used to measure spectral radiation of samples. A limitation of this study was the lack of thermal Cycling for coffee stains. However, like this study, Lava Ultimate, acar et all, showed more colouring in the study than Enamic.(1)

Similarly, in a recent study awad et al. reported that Lava Ultimate was more transparent than Enamic in two different sample thicknesses (1 mm and 2 mm). CAD / CAM ceramics in 3 Surface conditions, polished surfaces and grinding surfaces with 1200 grrit and 500 gr SIC grinding plates. In addition, they concluded that enamic had reached the lowest TP values since it was a high amount of Al2O3 (approximately 23%). In addition, material composition has strongly influenced translusense. Lava Ultimate is an RNC containing 80% silica and zirconia nanoparticles and nanoclusters by weight attached to the resin matrix. Ceramic particles consist of three different ceramic fillings that strengthen a highly cross-linked polymeric matrix consisting of 20 Nm silica and 4-11 Nm zirconia particles. A previous study found that Lava frame was the most transparent material between different transfer methods and light flow and different zirconia materials.(5)

Conclusion

It may be concluded that both coffee and cola have significant effect on the color change of dental restorative materials. Ceramic material are less sensitive to colored bevarages than nano composite resins.

References

1. Acar O, Yılmaz B, Altıntas SH, Chandrasekaran I, Johnston WM. Color stainability of CAD/CAM and nanocomposite resin materials. J Prosthet Dent. 2016;115:71–75.
2. Alharbi A., Arsu S.,Bortolotto T., Krejci I.Stain susceptibility of composite and ceramic CAD/CAM blocks versus direct resin composites with different resinous matrices. Odontology.2016
3. Ardu S, Feilzer AJ, Devigus A, Krejci I. Quantitative clinical evaluation of esthetic properties of incisors. Dental Materials 2008;3:333–40
4. Arocha A.M.,, Basilio J, Llopis J, Bella E., Roig M, Ardu S, Mayoral J.R. Colour stainability of indirect CAD–CAM processed composites vs. conventionally laboratory processed composites after immersion in staining solutions . J Dent. 2014 Jul;42(7):831-8
5. Awad D, Stawarczyk B, Liebermann A, Ilie N. Translucency of esthetic dental restorative CAD/CAM materials and composite resins with respect to thickness and surface roughness. J Prosthet Dent. 2015;113:534–540.
6. Clinical Performance of a New Biomimetic Double-Network Material Inclusive Magazine:Volume 6, Issue 2
7. Davidowitz G, Kotick PG. The use of CAD/CAM in dentistry. Dent Clin North Am 2011;55:559-70. Oh SH, Kim SG. Effect of abutment shade, ceramic thickness, and coping type on the final shade of zirconia all-ceramic restorations: in vitro study of color masking ability. J Adv Prosthodont 2015;7:368-74.
8. Fontes ST, Fernandez MR, De Moura CM, Meireles SS. Color stability of a nanofill composite: effect of different immersion media. J App Oral Sci. 2009;17:388–91.

9. Güth JF, Kauling AEC, Ueda K, Florian B, Stimmelmayr M. Transmission of light in the visible spectrum (400-700 nm) and blue spectrum (360-540 nm) through CAD/CAM polymers. Clin Oral Investig. 2016;20:2501–2506.
10. Lambert H., Durand J.D., Jacquot B. , Fages M. Dental biomaterials for chairside CAD/CAM: State of the art. J Adv Prosthodont. 2017 Dec; 9(6): 486–495.
11. Lee YK. Comparison of CIELAB DeltaE(*) and CIEDE2000 color-differences after polymerization and thermocycling of resin composites. Dental Materials 2005;21:678–82.
12. Lee WS, Kim SY, Kim JH, Kim WC, Kim HY. The effect of powder A2/powder A3 mixing ratio on color and translucency parameters of dental porcelain. J Adv Prosthodont 2015;7: 400-5
13. Nakazawa M. Color stability of indirect composite materials polymerized with different polymerization systems. Journal of Oral Science 2009;51:267–73.
14. Nasim I, Neelakantan P, Sujeer R, Subbarao CV. Color stability of microfilled, microhybrid and nanocomposite resins—an in vitro study. Journal of Dentistry 2010;38: e137–42.
15. O'Brien WJ. Dental materials and their selection. 4th ed. Chicago: Quintessence Publishing; 2008. p. 114-34.
16. Sagsoz O*, Demirci T, Demirci G, Sagsoz N.P., Yildiz M.The effects of different polishing techniques on the staining resistance of CAD/CAM resin-ceramics. J Adv Prosthodont. 2016 Dec; 8(6): 417–422.
17. Samra APB, Pereira SK, Delgado LC, Borges CP. Color stability evaluation of aesthetic restorative materials. Braz Oral Res. 2008;22:205–210.
18. Sharma G, Wu W, Dalal E. The CIEDE2000 color-difference formula: Implementation notes, supplementary test data, and mathematical observations. Color Research and Application 2005;30:21–30
19. Vichi A, Louca C, Corciolani G, Ferrari M. Color related to ceramic and zirconia restorations: a review. Dent Mater 2011;27:97-108.
20. Terry DA. Direct applications of a nanocomposite resin system: Part 1-The evolution of contemporary composite materials. Pract Proced Aesthet Dent 2004;16:417-22

International Conference on Science and Technology

ICONST 2018

5-9 September 2018 Prizren - KOSOVO

Green Synthesis of Graphene Oxide

Banu Esencan Türkaslan[1]*, Mihrace Filiz[2]

Abstract: In recent years carbon-based nanomaterials have been preferred in many fields due to their unique chemical, electrical and mechanical properties. Especially graphene and its derivatives, can be seen as a very good alternative to other materials with its outstanding features such as easy functioning of the surfaces to provide various properties, high mechanical strength and maximum surface / volume ratio. Graphene oxide (GO) is the most popular modification of the graphene which synthesized using various oxidizers. Graphene oxide has various functional groups (carboxyl, hydroxyl, epoxy) containing oxygen. These oxygenated groups allow the graphene oxide to function with different molecules. In this study, Improved Hummer method was modified to synthesize GO from graphite without using sodium nitrate (NaNO3) which causes toxic gas formation. In the literature according to other methods Improved Hummers method is simpler and less costly in terms of processing steps. It is also a more safe and environmentally friendly method than the Hummers method.

Keywords: Graphene Oxide, Green Synthesis, Improved Hummer

Introduction

Carbon materials are known to be more environmentally and biologically friendly than inorganic materials, since the carbon is one of the most common elements in our ecosystem. In particular, graphite is a naturally occurring material that has been used in our daily lives for hundreds of years without critical toxicity issues (Tran ve Mulchandani, 2016).

Graphene is an allotrope of carbon which is made up of single layer 2-dimensional structure nanomaterial with unique physicochemical properties (Kumar vd., 2017). The oxidized form of graphene named as “Graphene oxide” (GO) are produced by oxidation of graphite in a mixture of acid and oxidizing agent, is a water-dispersiblegraphene derivative (Marcano vd., 2010; Singh vd., 2016).

Graphene oxide (GO), has many extraordinary properties and has great potential among nanomaterials. Since its discovery, it has been studied by many researchers for a variety of novel applications due to its excellent chemical and physical properties, including low density, exceptional mechanical properties, large surface area, me¬chanical strength, and excellent electrical conductivity (Singh vd., 2016; Wang vd., 2011; Shil vd., 2016).

Graphene oxide have a mixed structure of oxygen-containing various functional groups like epoxy (> O), hydroxyl (-OH), carbonyl (C=O) and carboxylic (-COOH) groups as shown in Fig. 1. These functional groups attached to GO hold great promise for potential applications in many technological aspects as photo

[1]Suleyman Demirel University, Faculty of Engineering, 32260, Isparta, TURKEY
*Correspondingauthor: banuturkaslan@sdu.edu.tr

catalyst (Li vd., 2016; Small, 2013). electronics (Fu vd., 2010; Xu vd., 2016) , composites (Vianna vd., 2016; Kumar vd., 2012), electron field emission (Kumar vd., 2017a,b) and energy storage devices (Kumar vd., 2014; Kumar vd., 2015).

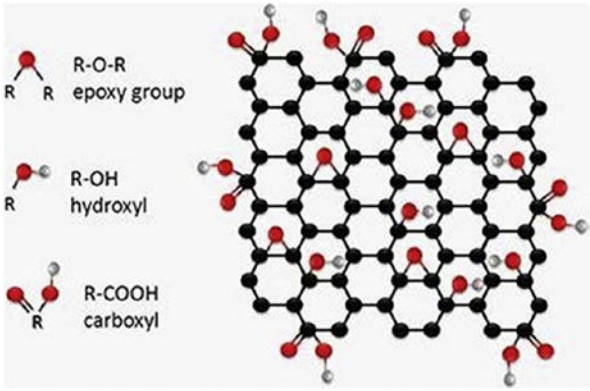

Figure 1. GO structure containing various functional groups on surfaces and at edges (Chiu vd., 2013).

GO is commonly produced by using the Brodie, Staudenmaier, and Hummers methods or these methods with minör modifications (Botas vd., 2013) .In this study we demonstrate that GO can be produced using an improved Hummers method without using NaNO3. This method decreases the cost and environmental duty of GO production. This modification, eliminating the evolution of NO2/N2O4 toxic gasses.

Material and Method

Graphite powder (1 g) was mixed with 50 ml H2SO4 in an ice bath. KMnO4 (4 g) was slowly added to the mixture. The solution was heated at 40°C for 30 min, and then diluted with 100 ml of water. In one hour, the solution was further diluted by adding an additional 200 ml of water, followed by the slow addition of 4 ml of H2O2 (30% v/v). After these steps the black graphite suspension was converted into a bright yellow graphite oxide solution (Figure 2).

Figure 2. Digital photograph of graphite suspension and graphite oxide solution

The aqueous graphite oxide solution was stirred for 3 h and centrifuged at 7000 rpm/min for 10 minutes to remove the unexfoliated graphite. Then washed with 5% HCl (v/v) and 3-4 times with distilled water to remove the remnant Mn ions and later dried.

Results

X-ray diffraction analysis

The strongest peak in the XRD pattern of GO shows a characteristic peak at 2θ = 11.5◦ (Figure 3), corresponding to interlayer spacing of 0.75 nm, indicating the presence of oxygen-containing functional groups formed during oxidation. Pristine graphite exhibits a basal reflection (002) peak at 2θ = 26.6o (d spacing = 0.33 nm). Compared with pristine graphite, the increase in d-spacing is due to the intercalation of water molecules and the formation of oxygen-containing functional groups between the layers of the graphite (Gurunathan vd.,2013).

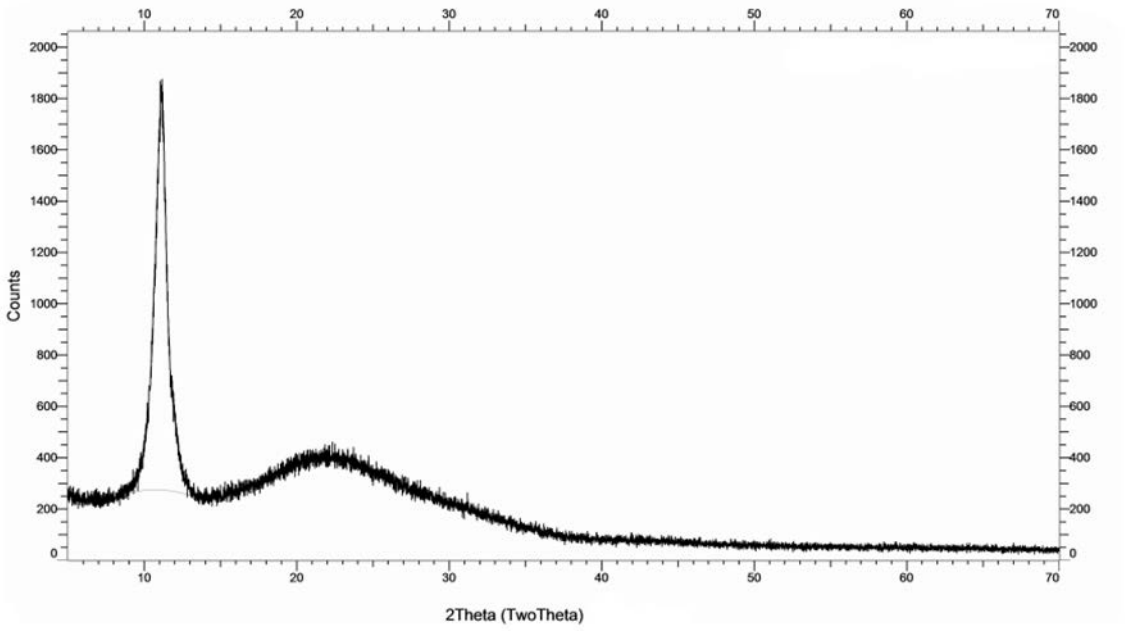

Figure 3. XRD Patterns of graphene oxide

FT-IR analysis

The FT-IR analysis of GO in Fig. 4 shows the existence of H-bonded OH stretch at 3434 cm−1, C-H stretch at 2930 cm−1, C=O in carboxylic acid group at 1734 cm−1, C= C in conjugated ketones at 1635 cm−1, phenol C-O stretch at 1239 cm−1, and primary alcohol C-O stretch at 1074cm−1.

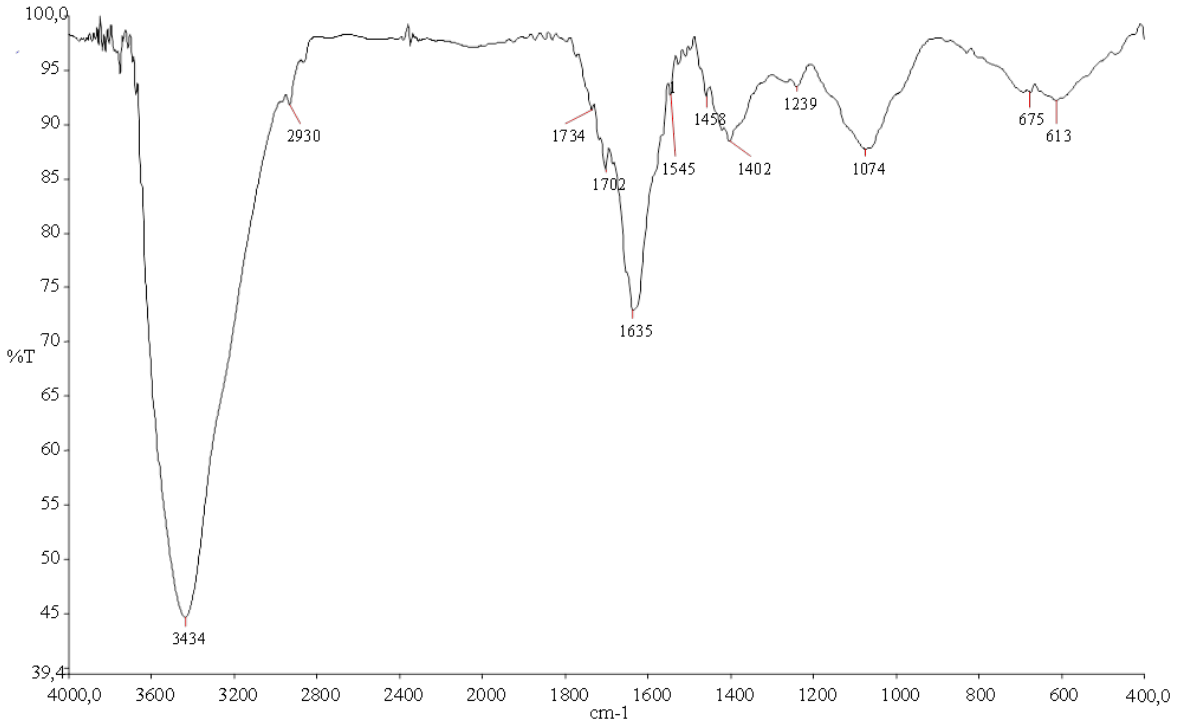

Figure 4. Fourier transform infrared (FTIR) of GO

Discussion and Conclusions

The graphene oxide was succesfully synthesized by using improved Hummers method without using NaNO3. GO products prepared by both the improved and conventional Hummers methods are nearly the same the exclusion of NaNO3 does not affect the yield of the reaction. This improved method eliminates the generation of toxic gasses. The improved Hummers method described here can be used to prepare GO and its composites through environmentally friendly approaches.

References

Bai, S., Shen, X.(2012). Graphene-inorganic nanocomposites, RSC Adv. 2. 64–98.

Botas, C., Alvarez, P., Blanco, P., Granda, M., Blanco, C., Santamaría, R., Romasanta, L.J., Verdejo, R., Lopez-Manchado, M.A., Menendez, R. (2013). Graphene materials with different structures prepared from the same graphite by the Hummers and Brodiemethods, Carbon 65. 156–164.

Chiu, N.-F., Huang, T.-Y., Lai, H.-C. (2013). Graphene oxide based surface plasmon resonance biosensors, in: M. Aliofkhazraei (Ed.), Advances in Graphene Science, InTech, Rijeka, p. Ch. 08.

Dong, X., Huang, W., Chen, P.(2010). In situ synthesis of reduced graphene oxide and gold nanocomposites for nanoelectronics and biosensing, Nanoscale Res. Lett. 6. 60.

Fu, W., Liu, L., Wang, W., Wu, M., Xu, Z., Bai, X., Wang, E.(2010). Carbon nanotube transistors with graphene oxide films as gate dielectrics, Sci. China Phys. Mech. Astron. 53. 828–833.

Gui, D., Liu, C., Chen, F., Liu, J. (2014). Preparation of polyaniline/graphene oxide nanocomposite for the application of supercapacitor, Appl. Surf. Sci. 307. 172–177.

Guo,Y., -a.Di, C., Liu, H., Zheng, J., Zhang, L., Yu, G., Liu, Y.(2010). General route toward patterning of graphene oxide by a combination of wettability modulation and spin-coating, ACS Nano 4. 5749–5754.

Gurunathan,Sangiliyandi., Woong Han, Jae., Kim, Jin-Hoi., Gurunathan, S., Han, J.W., Kim, J. (2013). Green chemistry approach for the synthesis of biocompatible graphene 31 July 2013:8 (1) Pages 2719-2732 International Journal of Nanomedicine.

Konwar, A., Kalita, S., Kotoky, J., Chowdhury, D.(2016). Chitosan–iron oxide coated graphene oxide nanocomposite hydrogel: a robust and soft antimicrobial biofilm, ACS Appl. Mater. Interfaces 8. 20625–20634.

Kumar, R., Joanni, E., Singh, R.K., Silva da, E.T.S.G., Savu ,R., Kubota, L.T., Moshkalev, S.A., (2017). Direct laser writing of micro-supercapacitors on thick graphite oxide films and their electrochemical properties in different liquid inorganic electrolytes, J. Colloid Interface Sci. 507. 271–278.

Kumar, R., Kim, H.-J., Park, S., Srivastava, A., Oh, I.-K. (2014). Graphene-wrapped and cobalt oxide-intercalated hybrid for extremely durable super-capacitor with ultrahigh energy and power densities, Carbon 79. 192–202.

Kumar, R., Oh, J.-H., Kim, H.-J., Jung, J.-H., Jung ,C.-H., Hong,W.G., Kim, H.-J., Park, J.-Y., Oh, I.-K. (2015). Nanohole-structured and palladium-embedded 3D porous graphene for ultrahigh hydrogen storage and CO oxidation multifunctionalities, ACS Nano 9. 7343–7351.

Kumar, R., Savu, R., Joanni, E., Vaz, A.R., Canesqui, M.A., Singh, R.K., Timm, R.A., Kubota, L.T., Moshkalev, S.A. (2016). Fabrication of interdigitated micro-supercapacitor devices by direct laser writing onto ultra-thin, flexible and free-standing graphite oxide films, RSC Adv. 6. 84769–84776.

Kumar, R., Savu, R., Singh, R.K., Joanni, E., Singh, D.P., Tiwari, V.S., Vaz, A.R., Silva da, E.T.S.G., Maluta, J.R., Kubota, L.T., Moshkalev, S.A. (2017). Controlled density of defects assisted perforated structure in reduced graphene oxide nanosheets-palladium hybrids for enhanced ethanol electro-oxidation, Carbon 117. 137–146.

Kumar, R., Singh, R.K., Dubey, P.K., Singh, D.P., Yadav, R.M. (2015). Self-assembled hierarchical formation of conjugated 3D cobalt oxide nanobead–CNT–graphene nanostructure using microwaves for high-performance supercapacitor electrode, ACS Appl. Mater. Interfaces 7. 15042–15051.

Kumar, R., Singh, R.K., Dubey, P.K., Singh, D.P., Yadav, R.M., Tiwari, R.S. (2015). Freestanding 3D graphene–nickel encapsulated nitrogen-rich aligned bamboo like carbon nanotubes for high-performance supercapacitors with robust cycle stability, Adv. Mater. Interfaces 2. 1500191.

Kumar R., Singh, R.K., Kumar Dubey, P., Singh, D.P., Yadav, R.M., Tiwari, R.S.(2015). Hydrothermal synthesis of a uniformly dispersed hybrid graphene-TiO_2 nanostructure for optical and enhanced electrochemical applications, RSC Adv. 5. 7112–7120.

Kumar, R., Singh, R.K., Savu, R., Dubey, P.K., Kumar, P., Moshkalev ,S.A. (2016). Microwaveassisted synthesis of void-induced graphene-wrapped nickel oxide hybrids for supercapacitor applications, RSC Adv. 6. 26612–26620.

Kumar, R., Singh, R.K., Singh, A.K., Vaz, A.R., Rout, C.S., Moshkalev, S.A. (2017). Facile and single step synthesis of three dimensional reduced graphene oxide-$NiCoO_2$ composite using microwave for enhanced electron field emission properties, Appl. Surf. Sci. 416. 259–265.

Kumar, R., Singh, R.K., Singh, D.P., Joanni, E., Yadav, R.M., Moshkalev, S.A. (2017). Laserassisted synthesis, reduction and micro-patterning of graphene: recent progress and applications, Coord. Chem. Rev. 342 34–79.

Kumar, R., Singh, R.K., Singh, D.P., Vaz, A.R., Yadav, R.R., Rout, C.S., Moshkalev, S.A. (2017). Synthesis of self-assembled and hierarchical palladium-CNTs-reduced graphene oxide composites for enhanced field emission properties, Mater. Des. 122. 110–117.

Kumar, R., Singh, R.K., Singh, J., Tiwari, R.S., Srivastava, O.N. (2012). Synthesis, characterization and optical properties of graphene sheets-ZnO multipod nanocomposites, J. Alloys Compd. 526. 129–134.

Kumar, R., Singh, R.K., Vaz, A.R., Moshkalev, S.A. (2015). Microwave-assisted synthesis and deposition of a thin ZnO layer on microwave-exfoliated graphene: optical and electrochemical evaluations, RSC Adv. 5. 67988–67995.

Kumar, R., Singh, R.K., Vaz, A.R., Savu, R., Moshkalev, S.A. (2017). Self-assembled and one step synthesis of interconnected 3D network of Fe3O4/reduced graphene oxide nanosheets hybrid for high-performance supercapacitor electrode, ACS Appl. Mater. Interfaces 9. 8880–8890.

Kumar, R., Singh, R.K., Vaz, A.R., Yadav, R.M., Rout, C.S., Moshkalev, S.A. (2017). Synthesis of reduced graphene oxide nanosheet-supported agglomerated cobalt oxide nanoparticles and their enhanced electron field emission properties, New J. Chem. 41. 8431–8436.

Li, X., Yu, J., Wageh, S., Al-Ghamdi, A.A., Xie, J.(2016). Graphene in photocatalysis: a review, Small 12 6640–6696.

Marcano, D.C., Kosynkin, D.V., Berlin, J.M., Sinitskii, A., Sun, Z., Slesarev, A., Alemany, L.B., Lu,W., Tour, J.M. (2010). Improved synthesis of graphene oxide, ACS Nano 4. 4806–4814.

Nanocomposites with tunable band structure and enhanced visible light photocatalytic activity, Small 9. (2013). 3336–3344.

Shao, D., Gao, J., Xin, G., Wang, Y., Li, L., Shi, J., Lian, J., Koratkar, N., Sawyer, S. (2015). Cldoped ZnO nanowire arrays on 3D graphene foam with highly efficient field emission and photocatalytic properties, Small 11 4785–4792.

Shil,Y.Y., Lil, M., Liul, Q., Jial, Z.J., Xul, X.C., Chengl,Y., Zhengl,Y.F.(2016). J Mater Sci: Mater Med. Electrophoretic deposition of graphene oxide reinforced chitosan–hydroxyapatite nanocomposite coatings on Ti substrate 27: 48.

Singh, R.K., Kumar, R., Singh, D.P. (2016). Graphene oxide: strategies for synthesis, reduction and frontier applications, RSC Adv. 6 64993–65011.

Tang, Y.-J., Wang,Y., Wang, X.-L., Li, S.-L., Huang,W., Dong, L.-Z., Liu, C.-H., Li, Y.-F., Lan,Y.-Q. (2016). Molybdenum disulfide/nitrogen-doped reduced graphene oxide nanocomposite with enlarged interlayer spacing for electrocatalytic hydrogen evolution, Adv. Energy Mater. 6 (1600116-n/a).

Tran, T.T. & Mulchandani, A. (2016). Carbon nanotubes and graphene nano field-effect transistor-based biosensors. *Trends in Analytical Chemistry* 79: 222-232. doi:10.1016/ j.trac.2015.12.002.

Vianna, P.G., Grasseschi, D., Costa, G.K.B., Carvalho, I.C.S., Domingues, S.H., Fontana, J., Matos de, C.J.S.(2016). Graphene oxide/gold nanorod nanocomposite for stable surface-enhanced Raman spectroscopy, ACS Photon. 3. 1027–1035.

Yadav, S.K., Kumar, R., Sundramoorthy, A.K., Singh, R.K., Koo, C.M. (2016). Simultaneous reduction and covalent grafting of polythiophene on graphene oxide sheets for excellent capacitance retention, RSC Adv. 6. 52945–52949.

Zhang, H., Hines, D., Akins, D.L. (2014). Synthesis of a nanocomposite composed of reduced graphene oxide and gold nanoparticles, Dalton Trans. 43. 2670–2675.

Zhu,Y.F., Jiang, Q.(2016). Edge or interface effect on bandgap openings in graphene nanostructures: a thermodynamic approach, Coord. Chem. Rev. 326. 1–33.

Zhu, J., Yang, D., Yin, Z., Yan, Q., Zhang, H.(2014). Graphene and graphene-based materials for energy storage applications, Small 10. 3480–3498.

Zubir, N.A., Yacou, C., Motuzas, J., Zhang, X., Diniz da Costa, J.C.(2014). Structural and Functional Investigation of Graphene Oxide–Fe_3O_4 Nanocomposites for the Heterogeneous Fenton-like Reaction, 4, p. 4594.

Xu, Y., Liu, J.(2016). Graphene as transparent electrodes: fabrication and new emerging applications, Small 12. 1400–1419.

Wang,Y., Li, Z., Wang, J., et al. (2011). Graphene and graphene oxide: biofunctionalization and applications in biotechnology. Trends Biotechnol. 29: 205–12.

Wang, Z., Zhao, C., Gui, R., Jin, H., Xia, J., Zhang, F., Xia, Y. (2016). Synthetic methods and potential applications of transition metal dichalcogenide/graphene nanocomposites, Coord. Chem. Rev. 326. 86–110.

Wan, C., Chen, B. (2012). Reinforcement and interphase of polymer/graphene oxide nanocomposites, J. Mater. Chem. 22. 3637–3646.

International Conference on Science and Technology

ICONST 2018

5-9 September 2018 Prizren - KOSOVO

Generalization of the Energy based entropy for Ecological Communities in the frame of Tsallis Statistic

Kürşad Özkan[1]*

Abstract: The equation, nH = (T+n) ln(T+n)-T ln T -n ln n, is the core of ecological quantum analysis called as energy based entropy or Plank entropy. The generalized form of nH in the frame of Tsallis (q) entropy is $nH_q = -\{n(\ln_q(n) \overset{q}{\ominus} \ln_q(T+n)) + T(\ln_q(T) \overset{q}{\ominus} \ln_q(T+n))\}$. In the present study, ecological quantum parameter (nH) was computed from $q = 0.0001$ to $q = 1.99999$ using a hypothetical five community data. Principle component analysis (PCA) was applied using all the computed generalized entropic values. The results suggest that the generalization of energy based entropy gives a wide range of opportunity to better estimate potential energy footprint of the ecological communities.

Keywords: complex system, entropic index, generalization, scale, quantum ecology

Introduction

The study done by Santos et al. (2003) is based on derivation a proof of the quantum *H*-theorem by including the effects of Kanaidakis statistics on the quantum entropy (S^Q). As was shown in that study, the quantum entropy (S^Q) is defined by the following equation (Santos et al., 2003).

$$S^Q = -\sum[n_\alpha \ln_\alpha(n_\alpha) \mp (g_\alpha \pm n_\alpha) ln(g_\alpha \pm n_\alpha) \pm g_\alpha \ln_\alpha(g_\alpha)] \quad (1)$$

Where g_α is the number of states, n_α the number of the particles.

If S^Q is written by the following equation then it is equal to $S_N = k \ln R = k\{(N+P) \ln(N+P) - N \ln N - P \ln P\}$ (Planck, 1901).

$$S^Q = (g_\alpha + n_\alpha) ln(g_\alpha + n_\alpha) - n_\alpha \ln_\alpha(n_\alpha) - g_\alpha \ln_\alpha(g_\alpha) \quad (2)$$

In quantum ecology, $S_N = nH$, energy based entropy (Orlóci, 2013; Özkan, 2017) is defined as:

$$nH = (T+n) \ln(T+n) - T \ln T - n \ln n \quad (3)$$

where T denotes energy units and n resonators. In this case, $T = n_\alpha$ and $n = g_\alpha$.

In the context of given information above, a study was done by Orlóci and Özkan (2018) for generalizing the energy based entropy (nH) by κ (Kaniadakis) framework. However Kaniadakis statistic is one of the options for generating energy based entropy among various extended logarithmic forms. Among those forms, the first and the most popular function is Tsallis (q) statistic.

[1]Isparta University of Applied Science, Faculty of Forestry, 32260, Isparta, TURKEY
*Correspondingauthor: kursadozkan@sdu.edu.tr

The aim of the paper is to present the generalization of the energy based entropy (nH) by q (Tsallis) framework using the same hypothetical data used by Orlóci and Özkan (2018) for generalization of nH by κ (Kanadiankis) framework.

Generalization of the energy based entropy (nH)

From the mathematical viewpoints, the κ-framework is based on κ-exponential and κ-logaritmic functions. Among them, κ-logaritmic function is defined as:

$$\ln_{\mathcal{K}}(f) = \frac{f^{\kappa} - f^{-\kappa}}{2\kappa} \tag{4}$$

The κ-parameter less in the interval $0 \leq \kappa < 1$ and, the real index $\kappa \to 0$, the above expression reproduces the usual logarithmic properties, so that $\ln_{\kappa}(f)$ constitutes direct generalizations of the usual logarithmic functions $\forall_{\mathcal{K}} \neq 0$ (Santos et al., 2003).

S_{κ}^{Q} is the generalized entropic measure given by Santos et al. (2003):

$$\begin{aligned} S_{\kappa}^{Q} &= -\sum\{n_{\alpha}\left(\ln_{\kappa}(n_{\alpha}) \overset{\kappa}{\ominus} \ln_{\kappa}(g_{\alpha} \pm n_{\alpha})\right) \pm g_{\alpha}\left(\ln_{\kappa}(g_{\alpha}) \overset{\kappa}{\ominus} \ln_{\kappa}(g_{\alpha} \pm n_{\alpha})\right)\} \\ &= -\sum\left\{n_{\alpha}\ln_{\kappa}\left(\frac{n_{\alpha}}{g_{\alpha} \pm n_{\alpha}}\right) \pm g_{\alpha}\ln_{\kappa}\left(\frac{g_{\alpha}}{g_{\alpha} \pm n_{\alpha}}\right)\right\} \end{aligned} \tag{5}$$

which is summarized as:

$$\begin{aligned} S_{\kappa}^{Q} &= -\{n_{\alpha}\left(\ln_{\kappa}(n_{\alpha}) \overset{\kappa}{\ominus} \ln_{\kappa}(g_{\alpha} + n_{\alpha})\right) + g_{\alpha}\left(\ln_{\kappa}(g_{\alpha}) \overset{\kappa}{\ominus} \ln_{\kappa}(g_{\alpha} + n_{\alpha})\right)\} \\ &= -\left(n_{\alpha}\ln_{\kappa}\left(\frac{n_{\alpha}}{g_{\alpha}+n_{\alpha}}\right) + g_{\alpha}\ln_{\kappa}\left(\frac{g_{\alpha}}{g_{\alpha}+n_{\alpha}}\right)\right) \end{aligned} \tag{6}$$

S_{κ}^{Q} can be expressed using the terms of quantum ecology as:

$$\begin{aligned} \mathrm{nH}_{\kappa} &= -\{\mathrm{T}\left(\ln_{\kappa}(\mathrm{T}) \overset{\kappa}{\ominus} \ln_{\kappa}(\mathrm{T} + \mathrm{n})\right) + \mathrm{n}\left(\ln_{\kappa}(\mathrm{n}) \overset{\kappa}{\ominus} \ln_{\kappa}(\mathrm{T} + \mathrm{n})\right)\} \\ &= -\left(\mathrm{T}\ln_{\kappa}\left(\frac{\mathrm{T}}{\mathrm{T}+\mathrm{n}}\right) + \mathrm{n}\ln_{\kappa}\left(\frac{\mathrm{n}}{\mathrm{T}+\mathrm{n}}\right)\right) \end{aligned} \tag{7}$$

S_{κ}^{Q} is also rewritten as:

$$\begin{aligned} S_{\kappa}^{Q} &= -\sum_{\alpha} n_{\alpha}\left[\ln_{\kappa}(n_{\alpha})\sqrt{1 + \kappa^2[\ln_{\kappa}(g_{\alpha} \pm n_{\alpha})]^2} - \ln_{\kappa}(g_{\alpha} \pm n_{\alpha})\sqrt{1 + \kappa^2[\ln_{\kappa}(n_{\alpha})]^2}\right] \\ &\pm \sum_{\alpha} g_{\alpha}\left[\ln_{\kappa}(g_{\alpha})\sqrt{1 + \kappa^2[\ln_{\kappa}(g_{\alpha} \pm n_{\alpha})]^2} - \ln_{\kappa}(g_{\alpha} \pm n_{\alpha})\sqrt{1 + \kappa^2[\ln_{\kappa}(g_{\alpha})]^2}\right] \end{aligned} \tag{8}$$

which is summarized as follows:

$$\begin{aligned} S_{\kappa}^{Q} &= -n_{\alpha}\left[\ln_{\kappa}(n_{\alpha})\sqrt{1 + \kappa^2[\ln_{\kappa}(g_{\alpha} + n_{\alpha})]^2} - \ln_{\kappa}(g_{\alpha} + n_{\alpha})\sqrt{1 + \kappa^2[\ln_{\kappa}(n_{\alpha})]^2}\right] \\ &+ g_{\alpha}\left[\ln_{\kappa}(g_{\alpha})\sqrt{1 + \kappa^2[\ln_{\kappa}(g_{\alpha} + n_{\alpha})]^2} - \ln_{\kappa}(g_{\alpha} + n_{\alpha})\sqrt{1 + \kappa^2[\ln_{\kappa}(g_{\alpha})]^2}\right] \end{aligned} \tag{9}$$

The equation (9) can be re-expressed by the terms of quantum ecology as follows (Orlóci and Özkan, 2018):

$$\begin{aligned} \mathrm{nH}_{\kappa} &= -\mathrm{T}\left[\ln_{\kappa}(\mathrm{T})\sqrt{1 + \kappa^2[\ln_{\kappa}(\mathrm{T} + \mathrm{n})]^2} - \ln_{\kappa}(\mathrm{T} + \mathrm{n})\sqrt{1 + \kappa^2[\ln_{\kappa}(\mathrm{T})]^2}\right] \\ &+ \mathrm{n}\left[\ln_{\kappa}(\mathrm{n})\sqrt{1 + \kappa^2[\ln_{\kappa}(\mathrm{T} + \mathrm{n})]^2} - \ln_{\kappa}(\mathrm{T} + \mathrm{n})\sqrt{1 + \kappa^2[\ln_{\kappa}(\mathrm{n})]^2}\right] \end{aligned} \tag{10}$$

where n is the number of resonators (the number of species) and T the number of energy units (the number of individuals).

Plank entropy can be also generalized by Tsallis entropy $\left(H_q\right)$. On this context, the scale value, q, is used due to the fact that Tsallis entropy is converted to Kaniadakis entropy. In this sense Kaniadakis entropy $\left(H_{\mathcal{K}}\right)$ can be computed using Tsallis entropy $\left(H_q\right)$ by the following equation.

$$H_{\mathcal{K}} = \frac{H_{q=(1+\mathcal{K})} + H_{q=(1-\mathcal{K})}}{2} \tag{11}$$

By means of the above equation, $nH_{\mathcal{K}}$ is computed as follows:

$$nH_{\mathcal{K}} = \frac{nH_{q=(1+\mathcal{K})} + nH_{q=(1-\mathcal{K})}}{2} \tag{12}$$

The generalized energy based entropy in the q-framework $\left(\mathrm{nH}_q\right)$ is defined by the following equation.

$$\mathrm{nH}_q = -\left\{\mathrm{n}\left(\ln_q(\mathrm{n}) \overset{q}{\ominus} \ln_q(\mathrm{T}+\mathrm{n})\right) + \mathrm{T}\left(\ln_q(\mathrm{T}) \overset{q}{\ominus} \ln_q(\mathrm{T}+\mathrm{n})\right)\right\} = -\left(\mathrm{n}\ln_q\left(\frac{\mathrm{n}}{\mathrm{T}+\mathrm{n}}\right) + \mathrm{T}\ln_q\left(\frac{\mathrm{T}}{\mathrm{T}+\mathrm{n}}\right)\right)$$
$$= -\mathrm{n}\left[\ln_q(\mathrm{n})\sqrt{1+q^2\left[\ln_q(\mathrm{T}+\mathrm{n})\right]^2} - \ln_q(\mathrm{T}+\mathrm{n})\sqrt{1+q^2\left[\ln_q(\mathrm{n})\right]^2}\right]$$
$$+\mathrm{T}\left[\ln_q(\mathrm{T})\sqrt{1+q^2\left[\ln_q(\mathrm{T}+\mathrm{n})\right]^2} - \ln_q(\mathrm{T}+\mathrm{n})\sqrt{1+q^2\left[\ln_q(\mathrm{T})\right]^2}\right] \tag{13}$$

In the equation 13, q-deformed logarithm ($\ln_q \mathrm{x}$) is defined as:

$$\ln_q \mathrm{x} = \frac{\mathrm{x}^{1-q}-1}{1-q} \tag{14}$$

Note that energy based entropy (nH) is identified as a species case of the generalized energy based entropy in the q-framework $\left(\mathrm{nH}_q\right)$ at order 1, i.e. when q is approaching 1.

A hypothetic data example

Assume that A, B, C, D and E are the ecological communities. The number of the resonators (n) and the energy units (T) of the communities are n_A=10, T_A=180; n_B=11, T_B=182; n_C=10, T_C=280; n_D=34, T_D=220 and n_E=11, T_E=172 respectively (Orlóci and Özkan. 2018).

The generalized nH results of all the communities are given in Table 1 and illustrated in Figure 1. As can be seen in Figure 1a A, B and E communities have the similar trends from $q = 0.0001$ to $q = 1.99999$. That is an expected result due to fact that n and T values of A, B and E communities are very close each other. However, the trends of those communities are not parallel each other with increasing of q values. For instance, entropic value of E ($\mathrm{nH_E} = 20.67$) is bigger than that of A ($\mathrm{nH_A} = 18.94$) at the value of $q = 0.0001$. However, the profiles of $\mathrm{nH_A}$ and $\mathrm{nH_E}$ cross about at $q = 1.7$ and beyond of this point, all the values of $\mathrm{nH_E}$ are lower than those of $\mathrm{nH_A}$. At the end of the profiles i.e. $q \to 2$, the values of $\mathrm{nH_E}$ and $\mathrm{nH_A}$ correspond to 182.99 and 189.99 respectively (Table 1 and Figure 1).

Table 1: The computed nH values of the communities from $q = 0.0001$ to $q = 1.99999$

q	nH_A	nH_B	nH_C	nH_D	nH_E
0.00001	18.94	20.74	19.31	58.89	20.67
0.1	19.82	21.69	20.24	61.25	21.61
0.2	20.83	22.79	21.34	63.86	22.70
0.3	22.01	24.06	22.63	66.76	23.95
0.4	23.39	25.54	24.17	70.00	25.40
0.5	25.01	27.27	26.02	73.62	27.10
0.6	26.92	29.31	28.25	77.69	29.10
0.7	29.20	31.72	30.96	82.28	31.45
0.8	31.93	34.60	34.29	87.46	34.25
0.9	35.21	38.04	38.39	93.32	37.58
0.99999	39.17	42.19	43.49	99.98	41.58
1.1	43.99	47.20	49.87	107.57	46.40
1.2	49.88	53.28	57.91	116.24	52.23
1.3	57.10	60.70	68.08	126.16	59.32
1.4	66.01	69.80	81.03	137.54	67.97
1.5	77.04	80.99	97.61	150.63	78.56
1.6	90.74	94.80	118.94	165.73	91.58
1.7	107.84	111.92	146.52	183.17	107.65
1.8	129.24	133.21	182.31	203.36	127.54
1.9	156.12	159.77	228.97	226.78	152.24
1.99999	189.99	192.99	289.99	253.99	182.99

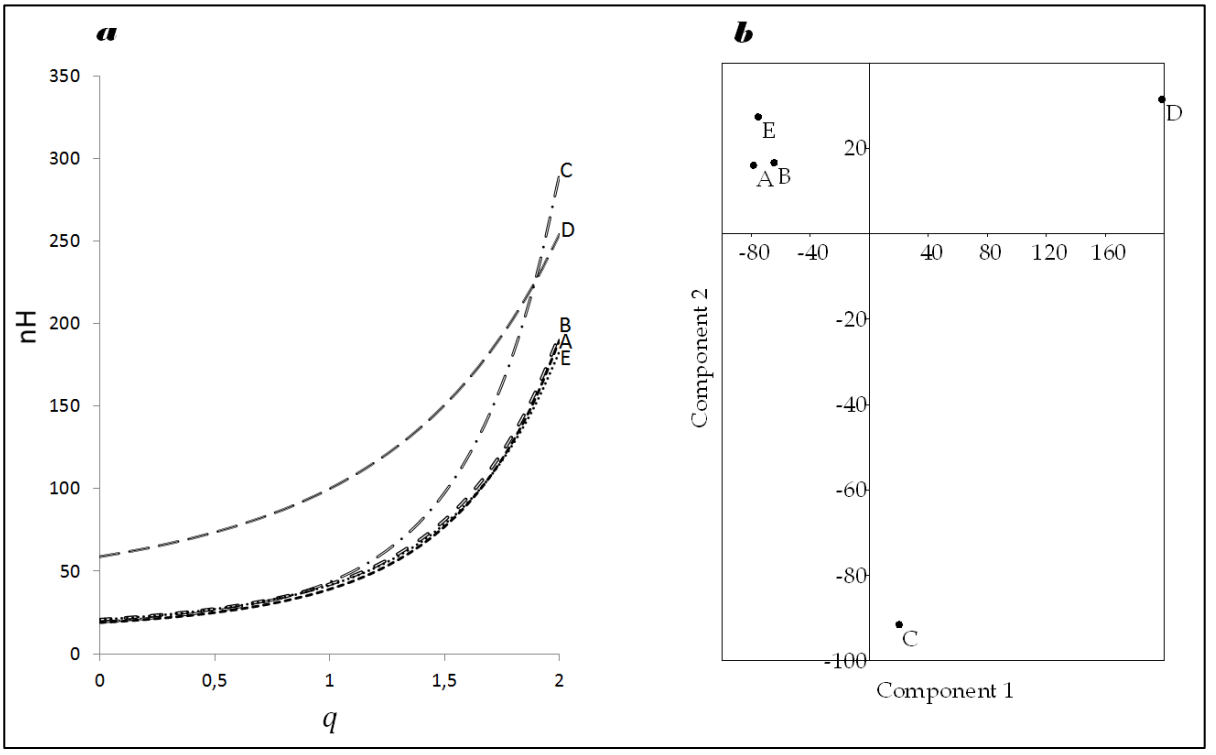

Figure 1: The generalized nH results of the communities ($0 < q < 2$) (*a*) and the PCA results applied to the matrix composed of the generalized nH values (*b*)

A and C communities have the same n values but there is a considerable difference between their T values i.e. the value of T_C is more than 1.55 times of that of T_A. Even though such difference is important from ecological point of view (when considering the genetically differences among the individuals of a given species), their entropic values are very close each other ($nH_C = 43.49$ and $nH_A = 39.17$) at $q \to 1$ which corresponding the same nH values found by the original energy based entropy ($nH = (T+n)\ln(T+n) - T\ln T - n\ln n$). The highest difference between nH values of both of two communities is observed at $q = 1.99999$ ($nH_C = 289.99$ and $nH_A = 189.99$) where the value of nH_D is 253.99 which is close to nH_C. This result is also unreasonable. Because n is the most important contributor to nH and, the value of n_D is more than 3 times than that of n_C. The most clear differences among A, C and D seems to be between $1.4 < q < 1.6$. Also this interval is available in comparison with B and E communities to A, C and D communities. As a result for this hypothetical community data, we can prefer to define nH values at any q value between 1.4 and 1.6. However such a selection way for q scale value is based on intuitive approach.

The fact that there is not a rule which q scale value is the best option for a comparison of the potential energy footprint values of the communities allows us to employ a holistic approach to obtain a summary result as a product of a whole. Hence, principle component analysis (PCA) was applied to the data including all nH values of the communities from $q = 0.0001$ to $q = 1.99999$. As a result of the applied PCA, the eigenvalues of the first axis to the last one were found 13935.5 (83.94%). 2664.37 (16.05%), 0.0091 (0.00055%), 0.00036 (2.14E-06%) respectively. It is clear that most of the percentage of the total variance (83.94%) is explained by the first axis. According to the first axis, as can be seen in Figure 1b, A, B and E communities are located in the left site opposite to the location of Community D. Community C is located between Community D and the group composed of community A, B and E along the first axis. The location of Community C is available because C is located in a considerable distance from A, B and E communities and furthest to community D along the first axis. As a conclusion, the result of the applied PCA seems to be reasonable from ecological point of view**.**

Discussion

Shannon entropy is the most popular entropic measure derived from information theory (Shannon, 1948). Generalized form of Shannon entropy was first introduced by Renyi (1961). Later various generalized entropic measures such as Tsallis entropy (Tsallis, 1988), Abe entropy (Abe, 2000) and Kaniadakis entropy (Kaniadakis, 2001) have been developed and used in computer science, cryptography, physics, neuroscience, linguistics, bioinformatics, ecology and the other fields. All of those entropies are disorder based and disorder is the progenitor of diversity (Orlóci ,2014; Orlóci ,2015). Therefore, those measures are generally called as diversity based entropies (DBE).

Plank (energy based) entropy (Plank. 1901) was first employed by Orlóci (2013) in the field of ecology. This quantity is different from the diversity based entropies (DBE) due to the fact that all DBE quantities use the proportional values of the species whereas EBE quantity uses their non-negative integer values.

Even though the concepts, definitions and quantities based on Orlóci's doctrine in ecological quantum analysis (Orlóci, 2013; Orlóci, 2014; Orlóci, 2015.) have well-explained, the matter of the generalization of EBE has been recently paid attention and merely focused on Kaniadakis statistic (Orlóci and Özkan, 2018)

In the present study, generalization of the energy based entropy was employed in the q frawework.

The order scaler q takes the values from within $0 < q < 2$ whereas the value interval is between 0 and 1 when κ-algebra is used (Orlóci and Özkan, 2018). This condition is amply satisfied in the example of the present study by the range $0.00001 \leq q \leq 1.99999$.

The example data was composed of five hypothetic community data which were previously used by Orloci and Özkan (2018) for generalization of nH in the frame of κ statistic. According to the results of that study, Kanaidakis' κ-based generalization of entropy has much utility in ecology. Likewise, in the present study, the generalized nH and PCA results in the frame of q statistic emphasize the requirement of the

generalization of energy based entropy from ecological viewpoint. In other words, the generalized energy based entropy approach in the q framework seems to be promising for ecological community analysis. Surely further studies should be generated to better understand the advantages aiming at generalization of ecological quantum parameters using real ecological data.

Conclusions

The ecosystems are the complex system. Thus, when the object is an ecosystem, holistic approach is essential (Özkan, 2017). There is no any universal rule or a sort of recipe in a holistic study. This allows us to choose a flexible approach and search for alternative solutions. Indeed, it must be accepted that there can be various solutions to the same problem, or more than one answer to the same question. All of them will be dependent on scale, theme and frame (Orloci and Özkan 2018). In the present study, the focal matter is scale. Since scale means generalization, it can be defined by κ algorithm as done by Orlóci and Özkan (2018) or q statistic as was shown in the present study.

References/Kaynaklar

Abe, S. and Rajagopal, A., 2001. Nonadditive conditional entropy and its significance for local realism. _/ Phys. Lett. A 289: 157-164.

Kaniadakis, G., 2001. Non-linear kinetics underlying generalized statistics, Physica A 296(3-4):405-425. DOI: 10.1016/s0378-4371(01)00184-4.

Orlóci, L., 2013. Quantum Ecology. The energy structure and its analysis. SCADA. Publishing, Canada, Online Edition: https://createspace.com/4406077.

Orlóci, L., 2014. The vegetation process. A holistic study of long-term community energetics in East Beringia. SCADA Publishing, Canada, Online Edition: https://createspace.com/4760258.

Orlóci, L., 2015. Energy based vegetation mapping. A case study in statistical quantum analysis. 2nd enlarged edition. SCADA Publishing, Canada Online Edition: https://createspace.com/5750582.

Orlóci, L., Özkan, K., 2018. Energy based entropy and its generalization. Part 1. Concept and ecological significance. Ol10.13140/RG.2.2.29595.57121.

Özkan, K., 2017. Doğanın Kuantum Analizi. Süleyman Demirel Üniversitesi, Orman Fakültesi Yayın No: 102, ISBN: 978-605-9454-08-7, Isparta, 148 s.

Planck, M., 1901. On the Law of Distibution of Energy in the Normal Spectum, Ann. Phys, Vol. 4, P. 553.

Rényi, A., 1961. On measures of entropy and information. In: J. Neyman (ed.), Proceedings of the 4th Berkeley Symposium on Matmematical Statistics and Probability, pp. 547-561. University of California Pres, Berkeley.

Santos, A.P., Silva, R., Alcaniz, J.S., Anselmo, D.H.A.L., 2011. Kaniadakis statistics and the quantum *H*-theorem, Physics Letters A 375, 352-355.

Shannon, C. E., 1948. A mathematical theory of communication. Bell Syst. Tech. J. 27: 379-423, pp. 623-656.

Tsallis, C., 1988. Possible generalization of Boltzmann-Gibbs statistics. J. Stat. Phys., 52, 479-487.

International Conference on Science and Technology

ICONST 2018

5-9 September 2018 Prizren - KOSOVO

Examination of The Effectiveness of Sarah (Strengthening and Stretching for Rheumatoid Arthritis of The Hand) Exercise Protocol on Hand Functions in Rheumatoıd Arthrıtıs Patıents / Romatoid Artrit Hastalarında SARAH (Strengthening and Stretching for Rheumatoid Arthritis of the Hand) Egzersiz Protokolunün El Fonksiyonları Üzerine Etkinliğinin İncelenmesi

Elif Gür Kabul[1], Bilge Başakcı Çalık[1], Murat Taşçı[2], Nadir Tayfun Özcan[3]*

Özet: El egzersizleri, 50 yıldır Romatoid Artritin (RA) tedavisinde kullanılmasına rağmen, aktif ve özellikle dirençli egzersizlerin yararı halen tartışılmaktadır. SARAH (Strengthening and Stretching for Rheumatoid Arthritis of the Hand) egzersiz protokolü, RA' lı hastalarda kuvvetlendirme ve germe egzersizlerinden oluşan bir protokoldür ve İngiltere'de geliştirilmiştir. Bu çalışma, SARAH egzersiz protokolünün RA hastalarının el fonksiyonları üzerine etkisini araştırmak amacıyla planlandı. Çalışmaya yaş ortalaması 46.63±10.60 yıl olan, Amerikan Romatoloji Derneği (ACR) 2010 kriterlerine göre Romatoid Artrit (RA) tanısı almış toplam 11 kadın çalışmaya dahil edildi. Tedavi öncesi ve tedavi sonrası katılımcıların dominant ve nondominant elde kavrama kuvveti Jamar dinamometresi ile, el fonksiyonları Dokuz Delikli Peg Testi (DDPT) ile, fiziksel özürleri ise Health Assesment Questionnaire (HAQ) ile değerlendirildi. SARAH el egzersiz protokolü, günde bir defa 12 hafta süresince haftada 3 gün yüz yüze, diğer günler ise ev programı olarak uygulandı. Verilerin analizi sonrası; katılımcıların tedavi öncesi ve tedavi sonrası DDPT sonuçları karşılaştırıldığında, fark istatiksel olarak anlamlı bulundu (p=0.010); tedavi öncesi ve tedavi sonrası kavrama kuvveti (p=0.424) ve HAQ (p=0.123) sonuçları karşılaştırıldığında ise aradaki farkın istatiksel olarak anlamlı olmadığı saptandı. Çalışmamız sonucunda RA' lı hastalarda SARAH egzersiz protokolünün el fonksiyonlarını geliştirdiği saptanmıştır. SARAH egzersiz protokolü, standardize bir eklem yaklaşımı olarak RA' lı hastalar için önerilmektedir.

Anahtar Kelimeler: Romatoid artrit, El, Egzersiz, SARAH egzersiz protokolü

Abstract: Although hand exercises have been used in the treatment of Rheumatoid arthritis (RA) for 50 years, active and particularly resistant exercises are still under debate. The SARAH (Strengthening and Stretching for Rheumatoid Arthritis of the Hand) exercise protocol is a protocol of strengthening and stretching exercises in patients with RA and developed in the UK. This study was planned to investigate the effect of SARAH exercise protocol on hand functions of RA patients. A total of 11 women diagnosed with rheumatoid arthritis (RA) according to the American College of Rheumatology (ACR) 2010 criteria, whose mean age was 46.63 ± 10.60 years, were included. At before and after treatment, participants' dominant and nondominant hand grip strength was measured by using Jamar dynamometer, hand functions was assessed by Nine-Hole Peg Test (DDPT), and Physical Disability was measured by Health Assesment Questionnaire (HAQ). when compared to pre-treatment and post-treatment results, a statically significant difference was found in DDPT results (p = 0.010) but there was not any significant difference in the grip strength result (p = 0.424) and HAQ result (p = 0.123). Our results have shown that SARAH exercise protocol improves hand

[1] Pamukkale Üniversitesi, Fizik Tedavi ve Rehabilitasyon Yüksekokulu, 20070, Denizli, Türkiye
[2] Pamukkale üniversitesi, Tıp Fakültesi, Dahili Tıp Bilimleri ABD, Romatoloji BD, 20070, Denizli, Türkiye
[3] Süleyman Demirel Üniversitesi, Sağlık Bilimleri Fakültesi, Fizyoterapi ve Rehabilitasyon Bölümü, 32260, Isparta, Türkiye
*Correspondingauthor: nadirozcan@sdu.edu.tr

function in RA patients. The SARAH exercise protocol is recommended for patients with RA as a standardized joint approach.

Keywords: Rheumatoid artritis, Hand, Exercise, SARAH exercise protocol

Giriş

Romatoid Artrit (RA), genellikle el ve ayakların küçük eklemlerinde simetrik tutulumun görüldüğü otoimmün bir hastalıktır. Etiyolojisi tam olarak bilinmeyen ve kronik bir rahatsızlık olan RA eklem sertliklerine, kronik ağrıya, progresif eklem yıkımlarına ve ciddi özürlülüğe neden olabilecek deformitelere neden olabilmektedir (Gamal ve ark. 2016). Eksaserbasyon ve remisyonlar ile sayreden RA eklem yıkımlarına, deformitelere, iş gücü kayıplarına ve ciddi özürlülüğe yol açabilmektedir. RA tedavisinin amacı, hastalığın remisyon süresini uzatmak, semptomları hafifletmek, hastalığın yol açabileceği özürlülüğü engellemek ve hastanın yaşam kalitesini artırmak olarak özetlenebilir (Nogas ve ark, 2017). Hastanın karşılacağı sorunlara cevap verecek bütünleştirilmiş, interdisipliner bakım planı; erken ve doğru tanı, farmakolojik tedavi, eğitim, egzersiz ve eklem koruma, sosyal, mesleki ve uğraşı desteğini içerir. Rehabilitasyon uygulamaları gibi nonfarmakolojik yöntemler yalnızca medikal tedavinin başarısız olduğu veya deformiteler gibi yapısal bozuklukların ve fonksiyonel yetersizliklerin geliştiğinde düşünülecek yaklaşımlar olarak görülse de, holistik yaklaşım gereği rehabilitasyon uygulamaları tedavinin ilk aşamasından itibaren medikal tedaviyle birlikte uygulanması gerekir (Bodur, 2009).

RA hastalarında, tedavinin başarısı açısından büyük önem taşımakta nonfarmakolojik yöntemlerden biri olan rehabilitasyon uygulamaları kapsamlı bir tedavinin ayrılmaz parçasıdır. Holistik yaklaşımın değerlerinden biri olan rehabilitasyon uygulamaları ile kinezyoterapi, fizyoterapi, elektroterapi, kriyoterapi, manuel terapi, yumuşak doku terapisi gibi yöntemler hastalara uygulanarak hastalık aktivitesinin, ağrı yoğunluğunun azaltılıp, hastaların lokomotor fonksiyonlarında artış amaçlanır (Ksiezopolska-Orłowska ve ark, 2016; Nogas ve ark, 2017).

Rehabilitasyon modalitelerinden biri olan egzersiz uygulamaları, eklem yıkımında ve hastalık aktivitesinde artışa neden olmadığından, romatizmal hastalıklarda güvenle kullanılabilirler. Son yıllarda yapılan çalışmalar da egzersiz uygulamalarının, RA' lı hastaların rehabilitasyonunda kilit rol oynadıklarını göstermiştir. Egzersizler, kas kitle kaybını (romatoid kaşeksi) engelleyerek fonksiyonel kaybı engeller ve hem özürlülük hem de kardiyovasküler komorbidite görülme riskini azaltır. Hastalığın ileri evrelerinde eklem çevresi yapılardaki yapısal değişiklikler, kontraktil yapılarda, cilt ve konnektif dokuda görülen kısalıklar ve sertlikler eklem hareket açıklığında kayıplara neden olarak kontraktürlerin oluşmasına zemin hazırlar. RA' lı hastalarda oluşabilecek eklem hareket açıklığı kayıpları ile kontraktürlerin rehabilitasyonunda da germe egzersizleri önerilmektedir(Kennedy, 2006; Henchoz ve ark, 2013; Patel ve ark, 2018).

Sinovyal enflamasyonla karakterize RA' da %90 oranında el ekleminin tutulumu görülmektedir. Tedavi edilmediği takdirde, el ve el bileği tutulumuna bağlı olarak oluşan kavrama, tutma ve pinç aktivitelerindeki azalma, hastaların günlük aktivitelerini yapmasını zorlaştırabilir. Ayrıca bu hastalarda ağrı, sabah tutukluğu, parestezi, eklemdeki yapısal değişiklikler ve deformiteler nedeniyle estetik yakınmalar ile de karşılaşılmaktadır. El ve el bileğinde görülen bu semptomların tedavisinde splintleme, hasta eğitimi, masaj uygulaması, enjeksiyon uygulamaları, cerrahi yöntemler gibi tedavi seçeneklerinin yanında egzersiz uygulamaları da tedavi sürecine katkı sağlar. RA hastalarında, İngiltere' de geliştirilen ve bireysel-progresif germe ve kuvvetlendirme egzersizlerinden oluşan SARAH egzersiz protokolü el fonksiyonunu artırmak adına düşük maliyetli bir yöntem olarak tercih edilebilir. (Horsten ve ark, 2010; Taskiran, 2011; Henry ve ark, 2013; Williamson ve ark, 2017).

Materyal ve Yöntem

Çalışmaya yaş ortalaması 46.63±10.60 yıl olan Amerikan Romatoloji Derneği 2010 kriterlerine (RA tanısı için, klasifikasyon kriterlerine ait puanlamanın 6/10 ve üzeri olması gerekir) göre RA tanısı almış toplam 11 kadın dahil edildi. Değerlendirme öncesinde katılımcıların yaşı, boyu, vücut ağırlığı, dominant üst ekstremite bilgisi sorgulandı ve kaydedildi. Tedavi öncesi ve sonrasında katılımcıların dominant ve nondominant elde kavrama kuvveti Jamar dinamometresi ile, el fonksiyonları DDPT ile, fiziksel özürleri ise HAQ ile değerlendirildi. Katılımcıların kavrama gücü katılımcı oturur pozisyonda, omuz nötralde ve dirsek 90 derece fleksiyonunda iken Jamar dinamometresi ile ölçüldü. Ölçüm üç kez tekrar edilip ortalaması alındı. El fonksiyonlarının değerlendirilmesinde kullanılan DDPT kısa, standardize, nicel bir üst ekstremite fonksiyon testidir. Hastalardan mümkün olan en kısa sürede platform üzerindeki dokuz ahşap çiviyi toplaması ve yerleştirmesi istenir (Tarakçı ve Uyanık, 2012). Her katılımcıdan testi üç defa yapması istenildi ve elde edilen değerlerin ortalaması alındı. Katılımcıların fiziksel özürlerinin değerlendirildiği HAQ ise giyinme, doğrulma, yemek yeme, yürüme, hijyen, uzanma, kavrama ve günlük işler adı altında 8 aktivitenin sorgulandığı toplam 20 sorudan oluşan bir ankettir. Toplam puan 0-3 arasında değişmektedir ve puan arttıkça fonksiyonel bağımlılık düzeyi artmaktadır. Türkçe geçerlik ve güvenilirlik çalışması yapılmıştır (Küçükdeveci ve ark. 2004). SARAH el egzersiz protokolü, günde bir defa 12 hafta süresince haftada 3 gün yüz yüze diğer günler ev programı olarak uygulandı. İstatistiksel analiz SPSS 23.0 paket programı kullanılarak yapıldı. Belirlenen ortalama değerler ± standart sapmaları ile ifade edildi. Verilerin analizinde Wilcoxon testi kullanıldı ve $p<0.05$ değerleri istatistiksel olarak anlamlı kabul edildi.

Bulgular

Tüm katılımcıların bayan olduğu çalışmamızda, katılımcıların yaş ortalaması 46,63±10,60 yıl, BMI ortalamaları 28,32±4,67 kg/cm^2 ve ortalama tanı süreleri 14,13±12,02 yıl olarak saptandı (Tablo 1.).

Tablo 1. Hastaların Demografik Özellikleri

Değişken	(Min-Max)	X±SD
Yaş (n=11)	30-65	46,63±10,60
BMI (n=11)	18,87-37,33	28,32±4,67
Tanı Süresi (n=11)	0,5-35	14,13±12,02

Katılımcıların el kavrama kuvveti, egzersiz sonrası artış gösterse de, egzersiz sonrası oluşan fark istatiksel olarak anlamlı değildi (p=0,424) . Katılımcıların egzersiz sonrası DDPT tamamlama süreleri incelendiğinde ise istatiksel olarak anlamlı azalmalar saptandı (p=0,010). HAQ' den alınan değerler incelendiğinde de egzersiz sonrası, katılımcıların fiziksel özürlerinde azalma olduğu fakat oluşan farkın istatiksel olarak anlamlı olmadığı saptandı (p=0,123).

Tablo 2. Hastaların Tedavi Öncesi ve Sonrası Kavrama Kuvveti, DDPT ve HAQ Değerlerinin İstatiksel Olarak Karşılaştırılması

Değişken	Tedavi Öncesi	Tedavi Sonrası	p*
Kavrama Kuvveti	13,64±5,05	15,81±3,97	0,424
DDPT	20,37±2,50	18,83±1,80	0,010
HAQ	0,97±0,49	0,78±0,44	0,123

Tartışma ve Sonuçlar

Çalışmamız sonucunda, 12 hafta uygulanan SARAH el egzersiz protokolünün romatoid artrit tanılı katılımcılarda, kavrama kuvvetini artırdığı, fonksiyonel iyileşme sağladığı ve fiziksel özürlülüğü azalttığı saptandı. Katılımcıların egzersiz öncesi ve sonrası değerleri istatiksel olarak incelendiğinde ise sadece DDPT sonuçlarında saptanan farkın istatiksel olarak anlamlı bir fark olduğu saptandı.

Literatürde çalışma sonuçlarımızı destekleyecek çalışmalar bulunmaktadır. El ağrısı veya disfonksiyonu tanımlayan 490 romatoid artritli hastanın dahil olduğu bir çalışmada, katılımcılara uygulanan klasik tedavi

yöntemleri ile bireysel kuvvetlendirme ve germe egzersiz programları karşılaştırıldığında, egzersiz uygulamasının el fonksiyonlarını iyileştirmede daha effektif bir yöntem olduğu saptanmıştır (Lamb, 2015). RA tanılı hastalarda yapılan randomize kontrollü başka bir çalışmada da, kuvvetlendirme ve mobilizasyon egzersizlerinin, germe egzersizi ve hasta eğitimine kıyasla fonksiyonel iyileşme üzerinde daha etkili olduğu saptanmıştır (O'Brien ve ark, 2006). Doğu ve ark, 2013, yaptıkları çalışmanın sonucunda izometrik ve izotonik egzersizlerin, el fonksiyonlarında anlamlı iyileşme sağladığını saptamışlardır. Bizim çalışmamızdan farklı olarak bu çalışma sonucunda, izometrik egzersizlerin dominant elde kavrama kuvvetini artırdığı, izotonik egzersizlerin ise non-dominant elde kavrama kuvvetini artırdığı saptanmıştır. Bu farkın oluşmasında, bizim çalışmamıza dahil olan katılımcıların hastalık durasyonunun daha fazla olmasıyla ilişkili olabileceğini düşünmekteyiz.

Yaptığımız literatür çalışması ve kendi çalışmamızdan elde ettiğimiz veriler doğrultusunda, RA tanılı hastalarda el egzersizlerinin hastalık aktivitesini ve ağrıyı artırmadan fonksiyonellik, kavrama kuvveti, özürlülük üzerine pozitif bir etkisi olduğu görüldü. Fakat egzersizlerin türü, yoğunluğu ve durasyonu konusunda tam netliğe ulaşılmadığından, bu konuyla ilgili daha ileri çalışmalara ihtiyaç olduğu ve bu konuyla ilgili veriler artıkça daha kesin sonuçlar elde edileceği düşüncesini taşımaktayız.

Kaynaklar

Gamal, R. M., Mahran, S. A., Abo El Fetoh, N., & Janbi, F. (2016). Quality of life assessment in Egyptian rheumatoid arthritis patients: Relation to clinical features and disease activity. The Egyptian Rheumatologist, 38(2), pp. 65-70.

Nogas, A., Grygus, I., & Prymachok, L. (2017). Application physiotherapy in rehabilitation rheumatoid arthritis. Journal of Education, 6(11), pp. 184-194.

Bodur, H. (2009). Romatoid Artritte Fizik Tedavi ve Rehabilitasyon. Turkiye Klinikleri Journal of Rheumatology Special Topics, 2(1), 97-106.

Księzopolska-Orłowska, K., Pacholec, A., Jędryka-Góral, A., Bugajska, J., Sadura-Sieklucka, T., Kowalik, K., . . . Łastowiecka-Moras, E. (2016). Complex rehabilitation and the clinical condition of working rheumatoid arthritis patients: Does cryotherapy always overtop traditional rehabilitation? Disability and Rehabilitation, 38(11), pp. 1034-1040.

Henchoz, Y., Zufferey, P., & So, A. (2013). Stages of change, barriers, benefits, and preferences for exercise in rheumatoid arthritis patients: A cross-sectional study. SCANDINAVIAN JOURNAL OF RHEUMATOLOGY, 42(2), pp. 136-145.

Kennedy, N. (2006). Exercise therapy for patients with rheumatoid arthritis: Safety of intensive programmes and effects upon bone mineral density and disease activity: a literature review. Physical Therapy Reviews, 11(4), pp. 263-268.

Patel, M. V., Patel, K. B., Patel, M. M., & Gupta, S. (2018). Effect of Nadi svedana with simultaneous passive stretching on correction of sandhijadya. Journal of Ayurveda and Integrative Medicine, 9(1), pp. 61-63.

Henry, J., Roulot, E., & Gaujoux-Viala, C. (2013). The rheumatoid hand. PRESSE MEDICALE, 42(12), pp. 1607-1615.

Taskiran, O. O. (2011). Rheumatoid hand/Romatoid el. Turkish Journal of Physical Medicine and Rehabilitation, 57(3), p. S19.

Horsten, N., Ursum, J., Roorda, L., Schaardenburg, v., D, Dekker, J., & Hoeksma, A. (2010). Prevalence of Hand Symptoms, Impairments and Activity Limitations in Rheumatoid Arthritis in Relation to Disease Duration. Journal of Rehabilitation Medicine, 42(10), pp. 916-921.

Williamson, E., McConkey, C., Heine, P., Dosanjh, S., Williams, M., & Lamb, S. E. (2017). Hand exercises for patients with rheumatoid arthritis: An extended follow-up of the SARAH randomised controlled trial. BMJ Open, 7(4)
Tarakci, E., & Uyanik, M. (2012). Multipl Sklerozun Farklı Tiplerinde Ergoterapinin Etkinliğinin Karşılaştırılması. Turkiye Klinikleri Journal of Medical Sciences, 32(2), 316-323.

Küçükdeveci, A. A., Sahin, H., Ataman, S., Griffiths, B., & Tennant, A. (2004). Issues in cross-cultural validity: Example from the adaptation, reliability, and validity testing of a Turkish version of the Stanford Health Assessment Questionnaire. Arthritis Care & Research, 51(1), 14-19.

Lamb, S. E. (2015). Exercises to improve function of the rheumatoid hand (SARAH): A randomised controlled trial. Lancet, The, 385(9966), pp. 421-429.

Dogu, B., Sirzai, H., Yilmaz, F., Polat, B., & Kuran, B. (2013). Effects of isotonic and isometric hand exercises on pain, hand functions, dexterity and quality of life in women with rheumatoid arthritis. Rheumatology International, 33(10), pp. 2625-2630.

O'Brien, A., Jones, P., Mullis, R., Mulherin, D., & Dziedzic, K. (2006). Conservative hand therapy treatments in rheumatoid arthritis - A randomized controlled trial. Rheumatology, 45(5), pp. 577-583.

Rheumatoid artritis, Hand, Exercise, SARAH exercise protocol

International Conference on Science and Technology

ICONST 2018

5-9 September 2018 Prizren - KOSOVO

Development of Cyclodextrin Particle Reinforced Composites Containing Tea Tree Oil for The Treatment of Horse Nail Fractures

Kamila Sobkowiak[1], Ayşe Kocabıyık[2], Mustafa Karaboyacı[3*]

Abstract: This study focuses on the evaluation of properties of differently composed composite materials based on polyurethane reinforced with tea tree oil (TTO)/ β-cyclodextrin (β -CD) inclusion complex. Tea tree oil encapsulated cyclodextrin was used as a reinforcing element in the preparation of particulate reinforced composite. Five different contents of reinforcement where used in the study: 0%, 1%, 3% 5% and %10 to find out the most favourable properties. Mechanical tests of the composites were performed according to ASTM composite standards. Notched impact strengths were performed according to ASTM D 256, the compression test were performed ASTM D6641 and tensile tests were performed , according to ASTM D3039. Properties of sample containing 1% of tea tree oil/cyclodextrin inclusion complex were the most satisfying and were assumed to suit the role of the hoof crack filler.

Keywords: poly urethae, β cyclodextrine, horse nail, composite filler

Introduction

Hoof-wall defects are very common for all horses. Horses with reduced activity are particularly vulnerable to injuries. Many causes of quarter cracks have been described, such as trauma to the coronet, pre-existing damage to the dermis from infection, abnormal hoof conformation, short shoes, inappropriate farrier practices, or an abnormal landing pattern when the foot strikes the ground (O'Grady, 2010).

On the other hand, the season has also affects the condition of the hoof. In winter hooves grow more slowly, so if any crack appears, it takes more time to heal. Generally, most of hoof cracks are not dangerous. If crack is small enough, it doesn't deepen, there is nothing to worry about. Although it is very difficult to realize that the crack is not superficial enough to neglect the problem. Very often people realize that there is a problem when it is already too late and vet's involvement is necessary. This is why it is significant to react at the very beginning. It is crucial to stabilize the hoof wall to decrease the dysfunctional motion of the hoof capsule and prevent further spreading of the cracks. Many actions can be taken: appropriate boots, pads, clamps, wires, stitches but there is one more solution that will not hurt the healthy part of the hoof – filling cracks with synthetic material. "Briefly, the equine hoof is designed to transfer the vertical and transverse forces from the distal phalanx to the ground surface. It also has to be strong enough to provide grip, resist wear and allow growth to replace the ground contacting surface."(Wilson, 1998). These are reasons why composite material seems to be a good solution to cracking problem. Healthy and cracked horse nails are seen in figure 1 and 2.

[1]Lodz University of Technology, Faculty of Chemistry, Institute of Polymer and Dye Technology, POLAND
[2]Applied Sciences University Of Isparta Şarkikaraağaç Vocational School, TURKEY
[3]Suleyman Demirel University, Faculty of Engineering, Chemical Engineering Dept. 32260, Isparta, TURKEY
*Correspondingauthor: mustafakaraboyaci@sfu.edu.tr

	
Figure 1. Example of the healthy horse hoof (www.equinescience.co.uk)	**Fiigure 2**. Example of the crack which goes through the horse hoof wall

The key is the polymer-based hoof filler whose domain is to reinforce the hoof wall. As far as chance for infections is high when filling hooves with polymers or similar substances, using correct ingredients is principal. The matrix is a polyurethane. The reinforcement is made of tea tree oil/cyclodextrin inclusion complex.

Polyurethane is a polymer formed by reacting a polyol with polymeric isocyanate. This thermoplastic copolymer is biocompatible so it is successfully used as a biomaterial. These elastomers have high strength; extremely good abrasion resistance; good resistance to gas, greases, oils, and hydrocarbons; and excellent resistance to oxygen and ozone (Ebewele, 2000).

A true quarter crack usually leads to instability, inflammation, and infection (O'grady, 2001). That is why we decided to add an ingredient that will contribute to treatment. The essential oil of Melaleuca alternifolia, which comes from Australia or New Zealand, is also known as tea tree oil (TTO) and seemed to be the most adequate substance to fulfil the assumed task. Like many essential oils, tea tree oil is commonly used with success in many aspects of our life, especially both in medicine and veterinary, owing to its various properties. TTO can be used as antifungal, antibacterial, antiseptic, anti-inflammatory, anti-cancer, insect repellent and insecticide (Callander, 2012). These all activities are owed to the presence of terpineol. TTO consists of terpene hydrocarbons, predominantly monoterpenes, sesquiterpenes, and their associated alcohols. TTO has a relative density of 0.885 to 0.906 (89) (Carson, 2006). It is sensitive to heat, humidity, oxygen and light. It has low surface tension as well as poor capability of being mixed with products based on water due to its lipophilic properties. A sufficient and appropriate barrier to increased solubility in water and volatilization is needed. The tea tree oil encapsulation is a way to attain these aims.

In order to protect materials or their mixtures (guests) from heat degradation and/or oxidation, they are coated or entrapped into other materials (hosts). This technique is called ‘encapsulation’. Moreover, under specific conditions, the release rate of ‘guests’ can be controlled and handling of active ingredients is more convenient. Encapsulation can be accomplished using a great variety of techniques, including spray drying, spray cooling and chilling, extrusion, fluidised bed coating, coacervation, co-crystallization, emulsification and molecular inclusion (Fang, 2012). Among the techniques for encapsulation of essential oils, molecular inclusion in β-CD is the most successful (Bhandari, 1998).

Cyclodextrins (CD) are cyclic oligosaccharides composed of six or more α-1,4-linked D-glucopyranose units. They are one of the most commonly used drug-carriers. CD is a biodegradable compound produced during enzymatic degradation of starch. The supramolecular structure of CD possess a hydrophobic cavity and an hydrophilic external surface. Owing to their structure, cyclodextrins are used to dissolve non-polar compounds in polar environments. Inclusion complexes can be formed from CDs (cyclodextrin inclusion complex – CD-IC). These complexes are divided into two parts: hosts and guests. The cyclodextrin acts as

the host, while a wide variety of organic molecules might be the guest. Stabilization and protection to the guest molecules in CD-IC from evaporation, degradation and oxidation is provided by the cyclodextrin cavity. Hence, the CD-IC can control and/or delay the release of the guest molecules. There are three mostly used cyclodextrins: α-CD, β-CD, and γ-CD containing 6, 7, and 8 glucopyranose units in the cyclic structure. Beta-cyclodextrin (b-CD) is the most suitable compound for encapsulation of essential oil, due to adequate cavity size of b-CD molecules (0.6–0.8 nm) for inclusion of essential oil compounds (80–250 molecular mass), and the ease of production and low cost (Kurkov, 2013).

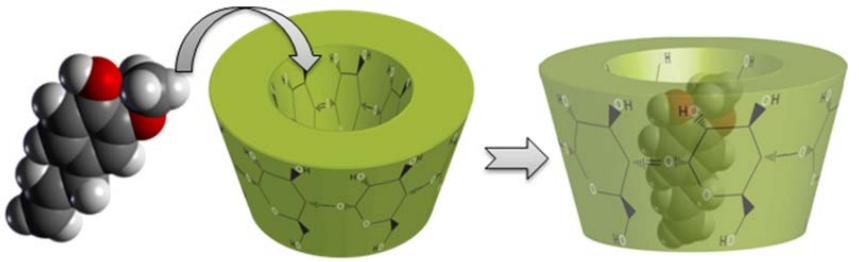

Figure 3. Cyclodextrin encapsulation process (http://unam.bilkent.edu.tr/)

The aim of this work was to evaluate properties of differently composed composite materials based on polyurethane reinforced with tea tree oil (TTO)/ β-cyclodextrin (β -CD) inclusion complex, compare them and choose the most suitable composition for the horse crack filler. The solubility and stability against light, pH, storage and thermal treatment of the formed complexes were evaluated.

Material and Method

B-cyclodextrin was obtained from Ashland, “Cavamax W7 Pharma”.Tea tree oil was purchased from Botalife %100 containd TTO. Polyol and isocyanate were obtained from Poliser “Creapol RW” All solvents used in the studies were analytical grade.

Preparation of tea tree oil/cyclodextrin inclusion complex

The inclusion complex was received by following the ‘Paste method’ recipe described in Shrestha, M., Ho, T. M., & Bhandari, B. R. (2017 The amount of ingredients were changed. At the beginning 90,5 g of cyclodextrin and 70 ml of distillation water were mixed for around 10 minutes to form a paste. Afterwards 9,5 g of tea tree oil was added and mixed gently by a mixer (WiseStir, HS-30D, Korea) for around 20 minutes until the paste became dense enough. The paste was disposed in the vacuum (Nüve, FN 400 Sterillizer, Turkey) to dry (70˚C for 17h). Subsequently, the dried solid complex was ground to a powder using a mortar and pestle and passed through a sieve (210 Mic.) to obtain as fine powder as possible. The product was being kept in the refrigerator.

Preparation of the composite material

The composite materials were obtained by mixing gently the tea tree oil/cyclodextrin inclusion complex powder with the polyol. Then the isocyanate was added, mixed together rapidly and placed quickly in aluminium forms. Four types of composite products were obtained, for which only the amount of tea tree oil/cyclodextrin inclusion complex was variable:

1.	0% of TTO/β -CD	50% polyol, 50% isocyanate
2.	1% of TTO/β -CD	49% polyol, 49% isocyanate
3.	3% of TTO/β -CD	48,5% polyol, 48,5% isocyanate
4.	5% of TTO/β -CD	47,5% polyol, 47,5% isocyanate

Impact resistance

The resulting composite product will be applied to cracks in horse hoof and so will be continuously impacted during use. For this reason the material has been tested for impact resistance. Impact resistance test was performed according to ASTM D 256 standard test method for determining the Izod Pendulum impact resistance of plastics. For this reason, 5 test specimens were prepared with lengths of 64 x 12.7 x 3.2 mm. Impact strength (J/m) was calculated by dividing the recorded absorbed impact energy by the thickness of the specimen in meters.

Tensile strengths

The tensile strengths of the materials were compared to determine the extent of pores and the degree of composite strength. Tensile testing was performed according to ASTM D3039 that measures tensile properties data generation for reinforced composites materials including tensile strength. For this reason, 5 test specimens were prepared with lengths of 250 x 25 x 5 mm.

Compression test

The compression test was conducted following the procedure specified in ASTM D6641. The test was performed in MTS Landmark servo-hydraulic machine testing machine. Specimen sizes are 12 x 12 x 140 mm.

Total Oil Extraction

For determination of total oil content of the cyclodextrin tea tree oil inclusion complexes, 2 grams of encapsulated cyclodextrin with constant weighing was boiled in hexsane (powder hexane ratio is 1to 20) for 30 minutes. After 30 minutes 100 mL destilled water was added to the solution and filtered. Filtrate was rinsed with hexane again and this proses was repeated for 3 times. The last filtrate was analyses with GCMS to be sure about there are no oil in the filtrate. Obtaioned residue was dried in an oven at 70 C over a night. The amount of mass lost from inclusion complex was calculated as the oil ratio of the complex.

Total Moisture Content

The total moisture contetn of tea tree oil filled cyclodextrin powder complexes was determined by AOAC 925.45 method (AOAC, 1996). 2 g of samples was weighed into aluminum weighing container and dried in a at 70 C. After drying, the conteiner was covered and cooled to 25 C in a desiccator with silica gel for about 20 min before weighing. This process was repeated every hour until the mass change was less than 2 mg.

Results

Table 1 shows the impact resistance values of the composites. The rigid structure of the cyclodextrin particle reinforced composites structure was deteriorated and porous due to the boiling of the tea tree oil in the composite content at the reaction temperature.

Table 1. Impact resistance values of the composites

Raw	612.9 j/m
%1 cyclodextrin	551.6 j/m
%3 cyclodextrin	490.3 j/m
%5 cyclodextrin	459.7 j/m

The rigid structure of the cyclodextrin particle reinforced composites structure was deteriorated and porous due to the boiling of the tea tree oil in the composite content at the reaction temperature.

Table 2 shows the tensile strength (MPa) of the composites. As it is expected from the impact resistance tests, tensile strength is decreasing by increasing amount of cyclodextrin particles. Because of getting porous structure of composite structure naturally loses its strength.

Table 2. Tensile strength of the composites

Raw	10,407 MPa
%1 cyclodextrin	9,309 MPa
%3 cyclodextrin	2,127 MPa
%5 cyclodextrin	1,438 MPa

Table 3. Compressive strength of the composites

Raw	22.82 MPa
%1 cyclodextrin	18.54 MPa
%3 cyclodextrin	3.708 MPa
%5 cyclodextrin	2.48 MPa

Table 3 shows the compressive strength (MPa) of the composites. As expected, there is also a marked decrease in the compressive strength with the increasing amount of cyclodextrin.

As a result of the total oil extraction analysis, it was determined that the cyclodextrin inclusion complex contains 8.1% Tea tree oil.

The moisture content of the β-cyclodextrin inclusion complex was calculated 10% by the vacuum-drying method (AOAC, 1990).

Discussion and Conclusions

Mechanical tests of the obtained composite material shows that, rainforcement of polyurethane polymer not increase the mechanical properties. Normaly particle rainforcemet needs to increase mechanical properties of the composite. Tea tree oil is very sensitive to heat and it boils at the curing temperature of the polymer. With the casue of the boiling, bubbles occurs inside the composite and these bubble are cause of the decreasing resistance.

The strength of composites containing 1% cyclodextrin was slightly reduced compared to raw polymer. Therefore, 1% cyclodextrin containing composite material will be applied to the horse nail and the results will be reported in the medical section of the study.

References

AOAC. In Official Methods of Analysis of the Association of Official Analytical Chemists, 5th ed.; Helrich, K., Ed.; AOAC International: Arlington, VA, 1990; p 1010.

Bhandari, B. R., D'Arc, B. R., & Thi Bich, L. L. (1998). Lemon oil to β-cyclodextrin ratio effect on the inclusion efficiency of β-cyclodextrin and the retention of oil volatiles in the complex. Journal of Agricultural and Food Chemistry, 46(4), 1494-1499.

Callander, J. T., & James, P. J. (2012). Insecticidal and repellent effects of tea tree (Melaleuca alternifolia) oil against Lucilia cuprina. Veterinary Parasitology, 184(2-4), 271-278.

Carson, C. F., Hammer, K. A., & Riley, T. V. (2006). Melaleuca alternifolia (tea tree) oil: a review of antimicrobial and other medicinal properties. Clinical microbiology reviews, 19(1), 50-62.

Ebewele, R. O. Polymer science and technology. 2000, 458-459.

Fang, Z., & Bhandari, B. (2012). Encapsulation techniques for food ingredient systems. Food materials science and engineering, 320-348.

Figure. 1. https://www.equinescience.co.uk/a-healthy-hoof-makes-for-a-happy-and-healthy-horse/

Kurkov, S. V., & Loftsson, T. (2013). Cyclodextrins. International journal of pharmaceutics, 453(1), 167-180.

O'grady, S. E. (2001). Quarter crack repair: an overview. Equine Veterinary Education, 13(4), 216-219

O'Grady, S. E. (2010). How to Manage a Quarter Crack. In Annual Convention of the AAEP (pp. 141-147)

Wilson, A. M., & Pardoe, C. H. (1998). Equine hoof cracks: mechanical considerations and repair techniques. Equine Veterinary Education, 10(S4), 52-56.

International Conference on Science and Technology

ICONST 2018

5-9 September 2018 Prizren - KOSOVO

Investigation of the Usability of Planar Air Solar Collectorized Storage System in District Heating / Düzlemsel Havalı Güneş Kolektörlü Depolama Sisteminin Mahal Isıtmada Kullanılabilirliğinin Araştırılması

Gamze Soytürk[1]*, Ahmet Kabul[2]

Özet: Bu çalışmada, Isparta ilinde bulunan ortalama 100 m^2'lik bir konutun güneş enerjisi kaynaklı depolama sistemi vasıtasıyla ısıtılarak, kesintili bir enerji kaynağı olan güneş enerjisinin sürekli hale getirilmesi hedeflenmektedir. Bu amaçla çevre sıcaklığı, rüzgâr hızı, ışınım şiddeti gibi parametreler dikkate alınarak ısınma ihtiyacının en fazla olduğu Ocak ayına göre kolektör tasarımı yapılmıştır. Dizayn edilen sistem için kullanılacak faz değiştiren madde (FDM) seçiminde FDM'ye ait fiziksel ve kimyasal özellikler, ulaşılabilirlik, maliyet gibi özellikler göz önüne alınarak sodyum asetat trihidrat kullanılmasına karar verilmiştir. Yapılan hesaplamalar sonucunda ısıtma ihtiyacının karşılanabilmesi için 64 adet düzlemsel havalı güneş kolektörüne ve 1171 kg sodyum asetat trihidrata ihtiyaç duyulmuştur. Tasarlanan sistem ısıtma ihtiyacının en fazla olduğu Ocak ayını karşılayacak şekilde dizayn edildiği için diğer aylardaki ısıtma ihtiyacının tamamını karşılamaktadır.

Anahtar Kelimeler: Güneş enerjisi, enerji depolama, düzlemsel havalı güneş kolektörleri, faz değiştiren madde, sodyum asetat trihidrat.

Abstract: In this study, it is aimed to make solar energy, which is an intermittent energy source, continuous by heating the average 100 m^2 house in Isparta province through solar energy source storage system. For this purpose, the collectors were designed according to the month of January, where the warming requirement is the greatest considering the parameters such as ambient temperature, wind speed, radiation intensity. It has been decided to use sodium acetate trihydrate in consideration of the physical and chemical properties of phase change material (PCM), availability, cost, etc., in selecting PCM to be used for the designed system. As a result of the calculations made, 64 planar air solar collectors and 1171 kg of sodium acetate trihydrate were needed to meet the heating needs. The designed system meets the full heating needs of the other months as it is designed to meet the January requirement, where the heating needs are greatest.

Keywords: Solar energy, energy storage, planar solar air collectors, phase change material, sodium acetate trihydrate.

Giriş

Dünya üzerinde çoğalan nüfus, zamanla enerji tüketiminin artmasına neden olmakta ve buna bağlı olarak ülkeler enerji üretimini artırmaya çalışmaktadır. Artan enerji üretim miktarı, ülkelerin ekonomik ve kültürel

[1]Suleyman Demirel University, Faculty of Technology, 32260, Isparta, TURKEY
[2]Suleyman Demirel University, Faculty of Technology, 32260, Isparta, TURKEY
*Correspondingauthor: gamzeyildirim@sdu.edu.tr

seviyeleri hakkında yorum yapabilmeyi de mümkün kılmaktadır. Günümüzün enerji kaynakları yenilenemeyen (konvansiyonel) ve yenilenebilen enerji kaynakları olarak sınıflandırılmaktadır (Çakır, 2008).

Kömür, petrol, doğalgaz gibi enerji kaynakları tükendikten sonra tekrar oluşmamalarından yada uzun süreçler sonucunda oluşmalarından dolayı konvansiyonel olarak adlandırılırken, güneş, rüzgar ve jeotermal gibi enerji kaynakları tükendikten sonra kendiliğinden ve kısa sürede oluştukları için yenilenebilir enerji kaynakları olarak adlandırılır (Arı, 2007).

Yenilenebilir enerji kaynakları potansiyeli açısından oldukça zengin olan Türkiye, coğrafi konumu sayesinde de sahip olduğu güneş enerjisi potansiyeli açısından birçok ülkeye kıyasla oldukça avantajlı durumdadır. Güneş enerjisi yaşam boyu var olan, çevre dostu, güvenilir, tükenmeyen, karbon, kükürt ve gaz salınımı yapmayan, sera gazı etkisi olmayan enerji kaynağıdır. Güneş enerjisi bol, yenilenebilir ve bedava enerji kaynağıdır. Bunun yanı sıra güneş enerjisi dalgalı ve kesintili güç karakteristiğine sahiptir. Yeryüzüne ulaşan güneş enerjisi, mevsimler arasında ve gün boyunca aynı derecede değildir. Güneş enerjisinin sürekli olmaması ancak enerji ihtiyacının devam etmesi depolama çalışmaları üzerine yoğunlaşmayı gerektirmektedir. Ayrıca güneş enerjisinden faydalanma oranının yükseltilmesi amacıyla enerji depolama uygulamaları gündeme gelmektedir. Güneş enerjisi temel olarak iki amaç için kullanılabilmektedir. Bu amaçlar, güneş enerjisini kullanarak ısı eldesi ve güneş enerjisini kullanarak elektrik eldesidir. Bu iki amaç için farklı teknolojiler kullanılmakta ve günden güne bu teknolojilerin verimlilikleri artmaktadır. Güneş enerjisinin ısı enerjisine dönüştürülmesi kolektörler ile gerçekleştirilir.

Güneş kolektörleri güneş enerjisini ısı enerjisine dönüştüren en basit düzeneklerdir. Güneş kolektörleri dolaştırılan akışkanın cinsine göre sıvı ve hava ısıtmalı güneş kolektörleri olmak üzere iki gruba ayrılırlar. Hava ısıtmalı güneş kolektörlerinde, basit olarak yutucu yüzeye gelen güneş ışınlarının büyük bir bölümü yutulur ve taşınımla sistemde dolaşan havaya aktarılırken, çevreye de yutucu yüzey sıcaklığına ve dış ortam şartlarına bağlı olarak ısı kaybı olur. Ayrıca gelen enerjinin bir kısmı kolektörün ısı kapasitesi için harcanır.

Herhangi bir maddenin faz değişimi esnasındaki gizli ısısından yararlanarak güneş enerjisinin depolanmasında kullanılan malzemelere Faz Değiştiren Madde (FDM) denir. Faz değiştiren maddeler, faz değişimi esnasında yüksek miktarda enerji depolama veya depoladığı enerjiyi çevreye verme özelliğine sahip maddelerdir.

Kabeel vd. (2016), Mısır'ın Tanta şehrinde yaptıkları çalışmalarında, faz değiştiren madde olarak parafin mumu kullanmış, düz ve V oluklu plakalı hava ısıtıcılarının deneysel incelemesini yapmışlardır. Çalışmalarında düz ve V oluklu plakalı güneş hava ısıtıcılarının termal performansını etkileyen parametreleri FDM'li ve FDM'siz olarak incelemişlerdir. Guarino vd. (2017), yaptıkları çalışmada, soğuk iklim koşullarında solaryumun enerji performansını artırmak için binaya entegre edilmiş termal bir depolama sisteminin performansını incelemişlerdir. Termal depo olarak, duvara gömülü faz değiştirme malzemeleri içeren güney yöne bakan bir duvar kullanmışlardır. Deneysel ve simülasyon çalışmalarının sonucunda düşünülen sistemin özellikle solaryum uygulamalarında yapılan yenilemeler için uygun olduğu sonucuna varmışlardır. Khadraoui vd. (2017) FDM kullanarak dolaylı tip zorlanmış taşınımlı güneş kurutucusu tasarlamış ve deneysel olarak incelemişlerdir. Yaptıkları çalışmada güneş kurutucusunu FDM'li ve FDM'siz olarak test etmişlerdir. Çalışmalarında FDM'li havalı güneş kolektörü kullanarak gündüz saatlerinde güneş enerjisini depolayıp gece boyunca kullanmayı hedeflenmişlerdir. Sarhaddi vd. (2017), tarafından yapılan çalışmada güneşli ve yarı bulutlu günlerde FDM depolamalı ve FDM depolaması olmaksızın iki adet weir tipi kaskadlı güneş enerjisi sisteminin performasını incelemişler ve bu sistemlerin enerji ve ekserji analizini yapmışlardır.

Bu çalışmada, Isparta ilinde bulunan ortalama 100 m^2'lik bir evin faz değiştiren maddeli depolama sistemi ile ısıtma ihtiyacının karşılanması hedeflenmektedir. Bu amaçla, düzlemsel havalı güneş kolektörlü depolama sistemi tasarlanmıştır. Tasarlanan sistem ile güneş enerjisinden yararlanılarak FDM üzerinde enerjinin depolanıp kesikli olan güneş enerjisinin sürekli hale gelmesi amaçlanmaktadır. FDM üzerinde depolanan enerji daha sonra ortam ısıtılması amacıyla kullanılmaktadır. Böylece depolanan enerjinin diğer zamanlarda kullanılması sağlanarak güneş enerjisinden yararlanma süresinin artırılması hedeflenmektedir. Güneş

enerjisinin depolanıp ısıtma amacıyla kullanılması sayesinde enerjiden tasarruf sağlanacaktır. Böylece ülke ekonomisine katkı sağlanmış olacaktır.

Materyal ve Yöntem

Güneş enerjisi sistemlerinde üretilen enerji süreç açısından kesikli ve yoğunluk açısından değişkenlik gösterdiğinden bu enerjinin depolanmasına ihtiyaç duyulmaktadır. Yapılan bu çalışma kapsamında, Isparta ilindeki bir konutun güneş enerjisi kaynaklı depolama sistemi vasıtasıyla ısıtılarak, kesintili bir enerji kaynağı olan güneş enerjisinin sürekli hale getirilmesi hedeflenmektedir. Bu amaçla Isparta şartlarında 100 m^2'lik bir evin Ocak ayı günlük ısıtma enerjisi ihtiyacını karşılamak için düzlemsel havalı güneş kolektörlü depolama sistemi tasarlanmıştır. Tasarlanan sistem için kullanılacak FDM seçiminde FDM'ye ait fiziksel ve kimyasal özellikler, ulaşılabilirlik, maliyet gibi özellikler göz önüne alınmıştır. Bu parametreler dikkate alındığında FDM olarak sodyum asetat trihidrat seçilmesine karar verilmiştir. Düzlemsel havalı güneş kolektörlü depolama sistemi hava sirkülasyonunun sağlanması için kolektör ve ısıtma fanı, havalı güneş kolektörü ve FDM deposundan oluşmaktadır. Sistemin genel akış şeması Şekil 1'de görülmektedir. Şekil 1'de görülen düzlemsel havalı kolektörlü depolama sistemi; FDM'nin şarjı ve deşarjı olmak üzere iki kısımdan oluşmaktadır. FDM'nin şarj bölümünde; düzlemsel havalı kolektörler ile ısıtılan hava FDM deposuna gönderilerek depo içinde bulunan sodyum asetat trihidrata ısısını verir ve FDM'nin sıvılaşması sağlanır. Deşarj kısmında ise; bir kısmı içerden, bir kısmı da taze hava olarak alınan hava ısıtma fanı ile faz değiştiren madde deposuna gönderilir. Burada depolanan ısı faz değiştiren maddenin katılaşmasıyla birlikte havaya aktarılır ve ısıtılan hava iç ortama verilir. Böyle bir sistemle gündüz saatlerinde ısıtılan hava ile hem hedeflenen ortam ısıtılacak hem de faz değiştiren maddenin sıvılaşması sağlanarak termal enerji depolanacaktır.

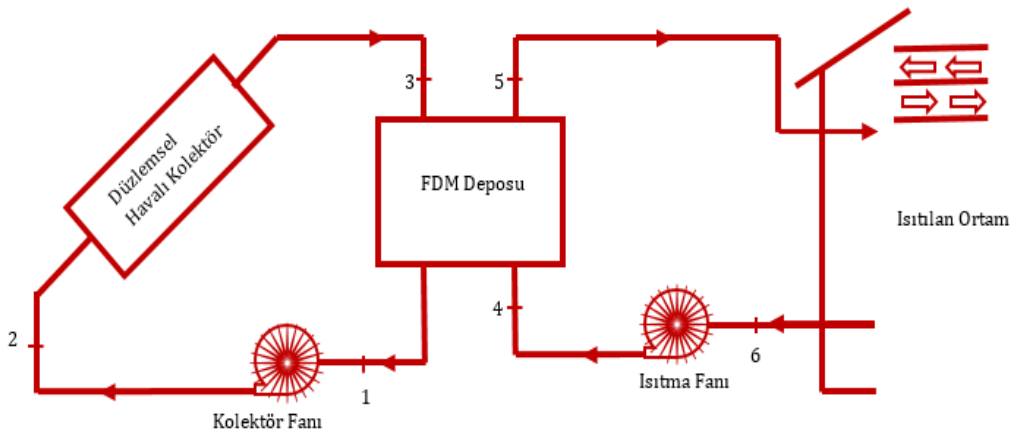

Şekil 1. Düzlemsel havalı güneş kolektörlü depolama sistemi tesisat şeması

Düzlemsel havalı güneş kolektörünün ısıl analizleri yapılırken Tablo 1'de verilen parametreler kullanılmıştır.

Tablo 1. Düzlemsel kolektör dizayn parametreleri

AÇIKLAMA	SEMBOL	DEĞER-BİRİM
Kolektör boyu	L	2 m
Kolektör genişliği	w	1 m
Kolektör derinliği	s	0.2 m
Havanın ısı iletim katsayısı	k	0.029 W/mK
Stephan-Boltzman sabiti	σ	$5.67x10^{-8}$
Havanın giriş sıcaklığı	T_i	1.8°C
Havanın çıkış sıcaklığı	T_0	74.55°C
Havanın kütlesel debisi	ṁ	0.09445 kg/s
Emici plaka sıcaklığı	T_p	67°C
Arka yüzey sıcaklığı	T_b	61°C
Eğim açısı	ɵ	37.4
Güneşin sıcaklığı	$T_{güneş}$	5739 K
Isı transfer akışkanının özgül ısısı	C_p	2 kj/kgK
Yalıtım kalınlığı	z	0.05 m
Yalıtımın ısıl iletkenliği	k_b	0.0036 W/mK
Emici plaka yüzey yayınım katsayısı	ε_p	0.92
Arka plaka yüzey yayınım katsayısı	ε_b	0.92

Isparta İli Güneş Verileri

GEPA'dan alınan verilere göre Isparta ili için güneş enerjisi potansiyeli Şekil 2'de verilmiştir. Şekilde görüldüğü gibi Isparta, güneş enerjisi uygulamalarına imkân sağlayan yüksek radyasyon miktarına sahiptir.

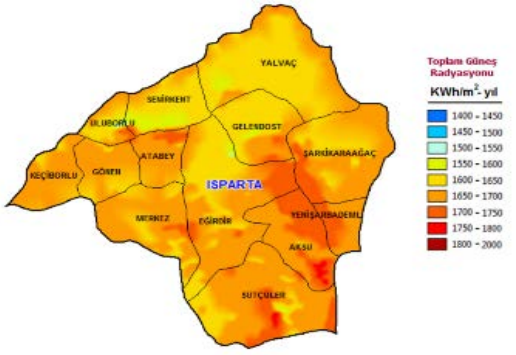

Şekil 2. Isparta ili için güneş enerjisi potansiyel atlası (GEPA, 2017)

Isparta iline ait aylık ortalama güneşlenme süresi GEPA'dan alınan verilere göre Şekil 3'de verilmiştir.

Şekil 3. Aylık ortalama güneşlenme süresi (GEPA, 2017)

Tasarlanan sistem için parametrelerin belirlenmesinde Isparta ili çevre şartları önem taşımakta olup Isparta ili için aylara göre ortalama çevre sıcaklıkları ve ortalama rüzgâr hızları Meteoroloji Genel Müdürlüğü (MGM)'nden alınan değerlere göre Şekil 4 ve Şekil 5'de verilmiştir.

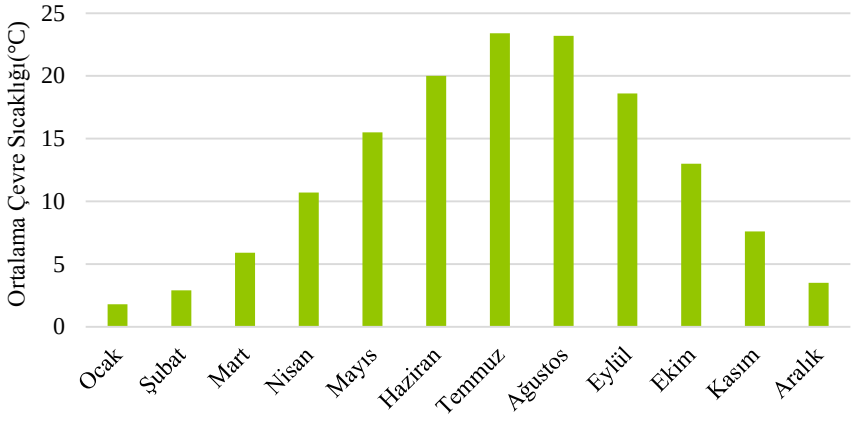

Şekil 4. Aylık ortalama çevre sıcaklıkları (MGM, 2017)

Şekil 5. Aylık ortalama rüzgâr hızları (MGM, 2017)

Düzlemsel havalı güneş kolektörlerinde eğik yüzeylere gelen toplam güneş ışınımının hesaplanmasında, yatay düzleme gelen radyasyonlardan yararlanılır. Düzlemsel kolektörlerin eğim açısı enlem derecesi ile aynı kabul edildiği için eğik düzleme gelen güneş ışınımları hesaplanmıştır. Eğik düzleme gelen ışınım şiddeti hesaplanırken GEPA verilerine göre, enlem derecesi 37.4° olan Isparta iline ait yatay düzleme gelen toplam ışınım şiddeti hesaplanarak Şekil 6'da gösterilmiştir.

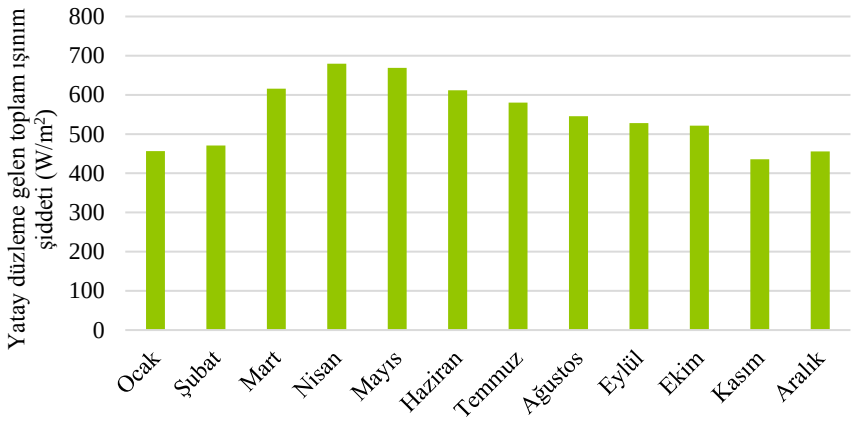

Şekil 6. Isparta ili yatay düzleme gelen aylık toplam ışınım şiddeti

Açı faktörü eğik bir yüzey üzerine gelen güneş radyasyonunun, yatay düzleme gelen güneş radyasyonuna oranını ifade etmektedir. Direkt radyasyon açı faktörü (DİRAF) tüm aylar için ortalama 1.38 kabul edilmiştir. Eğik düzleme gelen toplam ışınım şiddeti, yatay düzleme gelen toplam ışınım şiddeti ile DİRAF 'ın çarpılması sonucu elde edilerek Şekil 7'de gösterilmiştir.

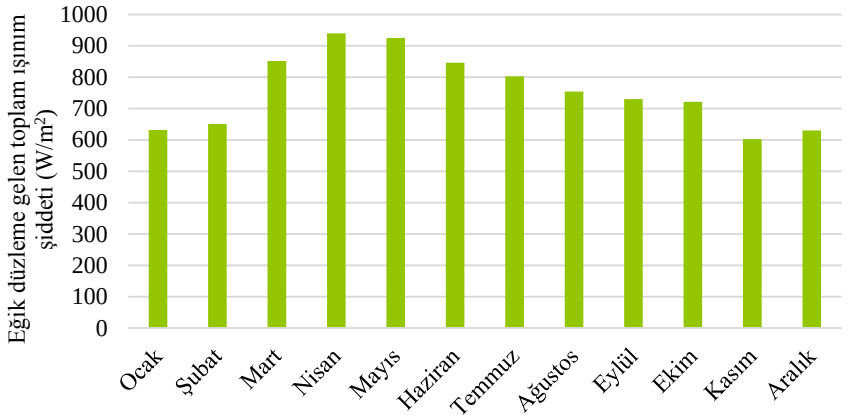

Şekil 7. Isparta ili eğik düzleme gelen aylık toplam ışınım şiddeti

Düzlemsel Havalı Güneş Kolektörünün Isıl Analizi

Havalı bir güneş kolektörünün anlık verimi (η), yararlı ısının kolektör üzerine gelen güneş ışınımına oranı olarak tanımlanır (Kalogirou, 2009).

$$\eta = \frac{Q_u}{A_c G} \quad (1)$$

Burada; Q_u(W) güneş kolektörü tarafından emilen faydalı enerjiyi, A_c(m^2) kolektör alanını, G(W/m^2) kolektör üzerine düşen güneş ışınım miktarını belirtmektedir.

Kolektör tarafından emilen yararlı enerji (Q_u), aşağıdaki eşitlik ile hesaplanabilir (Kalogirou, 2009).

$$Q_u = A_c F_R [S - U_L(T_i - T_a)] \quad (2)$$

Burada; F_R kolektör ısı kazanç faktörünü, S (W/m^2) kolektör yüzeyi tarafından yutulan güneş ışınımı miktarını, U_L (W/m^2K) toplam ısı kayıp katsayısını, T_i (K) havanın kolektöre giriş sıcaklığını ve T_a (K) ortam sıcaklığını ifade etmektedir.

Kolektör ısı kazanç faktörü (F_R), kolektör tarafından toplanan yararlı enerjinin, emici yüzeyin her yerinin havanın giriş sıcaklığında olması durumundaki toplayacağı enerjiye oranı olarak tanımlanır (Kalogirou, 2009).

$$F_R = \frac{\dot{m}c_p}{A_c U_L}\{1 - \exp[-\left(U_L F' \frac{A_c}{\dot{m}c_p}\right)]\} \quad (3)$$

Burada $\dot{m}$(kg/s) kolektöre giren toplam hava debisini, c_p (J/kgK) havanın özgül ısısını, F' kolektör verim faktörünü ifade etmektedir.

Gerekli hava debisi ($\dot{m}$) aşağıdaki eşitlik ile hesaplanabilir.

$$\dot{m} = \rho V A_ç \quad (4)$$

Burada; ρ (kg/m^3) havanın yoğunluğunu, V havanın hızını, $A_ç$ (m^2) kolektör kesit alanını ifade etmektedir.

Toplam ısı kayıp katsayısı (U_L) aşağıdaki eşitlik ile hesaplanabilir (Kalogirou, 2009).

$$U_L = U_t + U_b \quad (5)$$

Burada; U_t (W/m^2K) camın üzerindeki yüzey için toplam ısı taşınım katsayısı, U_b (W/m^2K) arka yüzey için ısı taşınım katsayısını ifade etmektedir.

Camın üzerindeki yüzey için toplam ısı taşınım katsayısı (U_t) aşağıdaki eşitlik ile hesaplanabilir (Kalogirou, 2009).

$$U_t = \left(\frac{1}{h_{c_{p-c}} + h_{r_{p-c}}} + \frac{1}{h_{r_{c-a}} + h_w}\right)^{-1} \quad (6)$$

Burada; $h_{c_{pc}}$(W/m^2K) paralel tabakalar arasından cam örtüye olan taşınım katsayısını, $h_{r_{pc}}$ (W/m^2K) paralel tabakalar arasından cam örtüye olan ışınım katsayısını, $h_{r_{ca}}$ (W/m^2K) koruyucu cam dış yüzeyinden ortam havasına olan ışınım katsayısını, h_w ise rüzgâr ısı transfer katsayısını ifade etmektedir.

$h_{c_{p-c}}$ aşağıdaki eşitlik ile hesaplanabilir (Kalogirou, 2009).

$$h_{c_{p-c}} = Nu\frac{k}{L} \quad (7)$$

Burada; Nu Nusselt sayısını, k (W/mK) ısı transfer katsayısını, L (m) iç cam kapak ile emici arasındaki boşluğu ifade etmektedir.

Hollands (1976) hava için yaptığı deneysel çalışmaların sonucunda 0°-75° arasındaki eğim açıları için Rayleigh sayısı ile Nusselt sayısı arasında bir bağıntı önermiştir. Nu cam örtü ve yutucu levha ile oluşturulan kanal içindeki taşınım için Nusselt sayısıdır ve aşağıdaki eşitlik ile bulunur.

$$\mathrm{Nu} = \frac{h_{c_{p-c}} L}{k} = \left[1 + 1.446\left[1 - \frac{1708}{\mathrm{Ra}\cos(\theta)}\right]^{+}\left\{1 - \frac{1708[\sin(1.8\theta)^{1.6}}{\mathrm{Ra}\cos(\theta)}\right\} + \left\{\left[\frac{\mathrm{Ra}\cos(\theta)}{5830}\right]^{0.333} - 1\right\}^{+}\right] \quad (8)$$

Burada; Ra Rayleigh sayısını, θ (°) kolektör eğimini ifade etmektedir. Parantez üzerindeki (+) işareti, parantez içerisindeki değerin pozitif olması durumda hesaplamaya alınacağını negatif olması durumunda ise parantez değeri yerine sıfır yazılarak hesaplamalara devam edilmesi gerektiğini gösterir bir semboldür.

$$\mathrm{Ra} = \frac{g\beta' \mathrm{Pr}}{\nu^2}(T_p - T_{c)} L^3 \quad (9)$$

Burada; g (m/s^2) yer çekimi ivmesini, β' (K^{-1}) ısıl genleşme katsayısını, Pr Prandtl sayısını, ν (m^2/s) kinematik viskoziteyi, T_p (K) emici plaka sıcaklığını, T_c (K) koruyucu cam sıcaklığını ifade etmektedir.

$h_{r_{p-c}}$ aşağıdaki eşitlik ile hesaplanabilir (Kalogirou, 2009).

$$h_{r_{p-c}} = \frac{\alpha\left(T_p + T_c\right)\left(T_p{}^2 + T_c{}^2\right)}{\left(\frac{1}{\varepsilon_p}\right) + \left(\frac{1}{\varepsilon_c}\right) - 1} \quad (10)$$

Burada; ε_p emici plakanın yayma katsayısını, ε_c koruyucu camın yayma katsayısını ifade etmektedir.

$h_{r_{c-a}}$ aşağıdaki eşitlik ile hesaplanabilir (Kalogirou, 2009).

$$h_{r_{c-a}} = \frac{\varepsilon_c \sigma\left(T_c{}^4 + T_{sky}{}^4\right)}{T_c - T_a} \quad (11)$$

Burada; σ(W/m^2 K^4) Stefan-Boltzman sabitini ifade etmektedir.

$$h_w = 5.7 + 3.8V \quad (12)$$

$h_{c_{c-a}}$ aşağıdaki eşitlik ile hesaplanabilir (Kalogirou, 2009).

$$h_{c_{c-a}} = \frac{8.6V^{0.6}}{L^{0.4}} \quad (13)$$

Burada; $T_{gök}$ (K) gökyüzü sıcaklığını ifade etmektedir.

$$T_{gök} = 0.0552T_a^{1.5} \quad (14)$$

Arka yüzey için ısı taşınım katsayısı (U_b) aşağıdaki eşitlik ile hesaplanabilir (Kalogirou, 2009).

$$U_b = \frac{1}{\frac{t_b}{k_b} + \frac{1}{h_{c_{b-a}}}} \quad (15)$$

Burada; t_b (m) arka yüzeydeki yalıtım kalınlığını, k_b (W/mK) arka yüzeydeki yalıtımın ısı iletkenlik katsayısını, $h_{c_{b-a}}$ (W/m^{2}K) arka yüzeyden ortama taşınımla olan ısı transfer katsayısı ifade etmektedir. $h_{c_{b-a}}$(W/m^{2}K) değeri genellikle 0.3-0.6 (W/m^{2}K) arasında alınmaktadır (Kalogirou, 2009).

Akışkanın kolektörden çıkış sıcaklığı (T_0), aşağıda verilen eşitlik ile hesaplanabilir (Kalogirou, 2009).

$$T_0 = T_i + \left(\frac{1}{U_L}\right)[S - U_L(T_i - T_a)][1 - \exp[-\left(U_L F' \frac{A_c}{\dot{m}c_p}\right)] \quad (16)$$

Kolektör yüzeyi tarafından yutulan güneş ışınım miktarı (S) aşağıdaki eşitlik ile hesaplanabilir (Kalogirou, 2009).

$$S = G(\tau\alpha) \quad (17)$$

Burada; $(\tau\alpha)$ etkinlik katsayısını ifade etmektedir.

Havalı güneş kolektörleri için verim faktörü (F') aşağıdaki eşitlik ile hesaplanabilir (Kalogirou, 2009).

$$F' = \frac{h}{h + U_L} \quad (18)$$

Burada; h(W/m^{2}K) taşınım ile olan ısı transfer katsayısını ifade etmektedir.

Taşınım ile olan ısı transfer katsayısı (h) aşağıdaki eşitlik ile hesaplanır (Kalogirou, 2009).

$$h = h_{c_{p-a}} + \frac{1}{\left(\frac{1}{h_{c_{b-a}}}\right) + \left(\frac{1}{h_{r_{p-b}}}\right)} \quad (19)$$

$$h_{c_{p-a}} = h_{c_{b-a}} \quad (20)$$

$$h_{r_{p-c}} = h_{r_{p-b}} \quad (21)$$

Burada; $h_{c_{p-a}}$ (W/m^{2}K) paralel tabakalar arasından ortam havasına ışınımla olan ısı transfer katsayısını, $h_{c_{b-a}}$(W/m^{2}K) arka yüzeyden ortam havasına taşınımla olan ısı transfer katsayısı, $h_{r_{p-c}}$ (W/m^{2}K) paralel tabakalar arasından cam örtüye taşınımla olan ısı transfer katsayısını, $h_{r_{p-b}}$(W/m^{2}K) ise paralel tabakalar arasından arka yüzeye olan ışınım katsayısını ifade etmektedir.

Taşınımla olan ısı transfer katsayısı $h_{c_{p-a}}$ aşağıdaki eşitlik ile hesaplanabilir (Kalogirou, 2009).

$$h_{c_{p-a}} = \left(\frac{k}{D}\right) 0.0158(Re^{0.8}) \quad (22)$$

Burada; D (m) hidrolik çapı, Re Reynolds sayısını ifade etmektedir.

$$Re = \frac{\dot{m}D}{A\mu} \quad (23)$$

Burada; μ (kg/ms) dinamik viskoziteyi ifade etmektedir. A_c (m^2) ve D (m) aşağıdaki eşitlik ile hesaplanabilir (Kalogirou, 2009).

$$A_c = Ws \tag{24}$$

$$D = 2s \tag{25}$$

Burada; s (m) hava kanalı derinliğini, W (m) kolektör genişliğini ifade etmektedir.

Emici plakadan arka plakaya ışınımla olan ısı transfer katsayısı ($h_{r_{p-b}}$) aşağıdaki eşitlik ile hesaplanabilir (Kalogirou, 2009).

$$h_{r_{p-b}} = \alpha\left(T_p + T_b\right)\frac{\left(T_p^2+T_b^2\right)}{\left(\frac{1}{\varepsilon_p}\right)+\left(\frac{1}{\varepsilon_b}\right)-1} \tag{26}$$

Burada; α (W/m^2K^4) kolektör yüzeyinin güneş ışınımını yutma katsayısını, T_b (K) arka yüzey sıcaklığını ifade etmektedir. ε_p emici plakanın yayma katsayısını, ε_b arka plakanın yayma katsayısını ifade etmektedir.

Enerji Analizi

Sürekli akışlı açık sistem üzerinde enerji analizi yapılırken kütle ve enerji temel denge denklemleri kullanılmıştır. Kararlı bir kontol hacmindeki sistem için kütle dengesi aşağıdaki şekilde ifade edilmektedir (Çengel ve Boles, 2007).

$$\sum \dot{m}_g = \sum \dot{m}_ç \tag{27}$$

Burada ṁ kütlesel akış debisini ifade etmektedir.

Termodinamiğin I. Yasa analizi enerjinin korunumunu belirtmektedir. Sistem üzerinde enerjinin korunumu denklemi aşağıdaki şekilde verilmiştir.

$$\dot{Q} + \sum(\dot{m}h)_g = \dot{W} + \sum(\dot{m}h)_ç \tag{28}$$

Burada; $\dot{Q}$ ısının enerjisini, $\dot{W}$ işin enerjisini göstermekte ṁh ise kütle akışı ile birlikte giren ve çıkan enerjinin hesaplamasıdır.

Yukarıda denklemler, incelenen düzlemsel güneş kolektörlü depolama sistemine uygulanmış ve her bir sistem elemanı için kütle ve enerji denge denklemleri çıkartılmıştır (Tablo 2).

Tablo 2. Düzlemsel havalı güneş kolektörlü enerji depolama sistemi denge denklemleri

Sistem Elemanları	Kütle Korunumu	Enerji Korunumu
Düzlemsel Kolektör	$\dot{m}_3 - \dot{m}_2 = 0$	$\dot{E}_1 + \dot{W} = \dot{E}_2$
Kolektör Fanı	$\dot{m}_2 - \dot{m}_1 = 0$	$\dot{E}_1 + \dot{W} = \dot{E}_2$
FDM Deposu (Şarj)	$\dot{m}_3 - \dot{m}_1 = 0$	$\dot{E}_3 = \dot{E}_1 + \dot{E}_{FDM_{şarj}}$
FDM Deposu (Deşarj)	$\dot{m}_5 - \dot{m}_4 = 0$	$\dot{E}_4 + \dot{E}_{FDM_{deşarj}} = \dot{E}_5$
Isıtma Fanı	$\dot{m}_6 = \dot{m}_4$	$\dot{E}_6 + \dot{W} = \dot{E}_4$

Bulgular

Bu çalışmada, Isparta şartlarında 100 m^2'lik bir evin günlük ortalama ısıtma ihtiyacının; düzlemsel havalı güneş kolektörleri ile FDM'ler üzerinde depolanarak karşılanabilirliği araştırılmıştır. Bu amaçla ısıtma ihtiyacının en fazla olduğu Ocak ayı değerleri referans alınmıştır. Buna göre Ocak ayı için ışınım şiddeti 631.65 W/m^2, güneşlenme süresi 4.38 saat, çevre sıcaklığı 1.8 °C ve rüzgar hızı 2.87 m/s olarak dikkate alınarak bir günlük ısıtma ihtiyacı 87.12 kWh olarak hesaplanmıştır. Bu ihtiyacı karşılayabilmek için düzlemsel havalı güneş kolektörlü depolama sistemi tasarlanarak güneşlenme süresi boyunca ısıtma ihtiyacını karşılayacak kolektör kapasitesi belirlenmiştir. Ayrıca kolektörden gelen faydalı ısı hesaplanarak gereken kolektör sayısı belirlenmiştir.

Kabul edilen çalışma şartları altında elde edilen değerler kullanılarak, sistemin her noktası için termodinamiksel değerler Tablo 3'de verilmiştir.

Tablo 3. Sistemin noktasal termodinamiksel değerleri

	P(kPa)	T(℃)	ṁ(kg/s)	h(kj/kg)	E(kj/kg)
1	101.3	27	0.09445	300.2	0.006724
2	101.3	29	0.09445	302.2	0.02678
3	101.3	74.5	0.09445	347.7	3.764
4	101.3	29	0.09445	302.2	0.02678
5	101.3	37	0.09445	310	0.2369
6	101.3	27	0.9445	300.2	0.006724

Güneş yılın her döneminde farklı açı ve ışınım şiddeti ile yeryüzüne gelmekte olup dönemlere göre güneşlenme süresi değişkenlik göstermektedir. Bilindiği üzere yaz aylarında güneşlenme süreleri artarken kış aylarında azalmaktadır. Hesaplamalar yapılırken, aylara göre ısıtma ihtiyacı Soytürk'ün 2018 yılında yaptığı tez çalışmasındaki değerler kabul edilmiştir. Yılın her ayı için ortalama ışınım şiddeti, çevre sıcaklığı, rüzgâr hızı ve güneşlenme süresi dikkate alındığında, aylık ısıtma ihtiyacı ve sistemde üretilen ısıtma kapasitesi ve ihtiyacı Tablo 4' de verilmiştir.

Tablo 4. Aylara göre ısıtma kapasitesi ve ısıtma ihtiyacı

Aylar	Işınım Şiddeti (W/m^2)	Çevre Sıcaklığı (°C)	Rüzgâr Hızı (m/s)	Güneşlenme Süresi (h/gün)	Isıtma Kapasitesi (kW)	Isıtma Enerjisi (kWh)	Isıtma İhtiyacı (kWh)
Ocak	631.65	1.8	2.87	4.38	20.15	88.25	87.12
Şubat	651.12	2.9	2.72	5.46	20.31	110.89	78.96
Mart	851.90	5.9	3.15	6.82	28.14	191.91	59.28
Nisan	940.02	10.7	2.80	7.77	29.52	229.37	29.04
Mayıs	925.15	15.5	2.75	9.42	28.74	270.73	6.72
Haziran	846.20	20	2.49	11.10	25.14	279.05	0
Temmuz	802.80	23.4	2.48	11.70	23.74	277.75	0
Ağustos	754.43	23.2	2.58	11.13	22.69	252.53	0
Eylül	730.41	18.6	2.45	9.64	21.57	207.93	0
Ekim	721.57	13	2.45	7.17	21.4	153.43	17.28
Kasım	602.66	7.6	2.58	5.44	18.33	99.71	46.8
Aralık	630.37	3.5	2.56	3.95	19.16	75.68	73.92

Sistemin üretebileceği ısıtma kapasitesi (kW) Şekil 8'de aylara göre gösterilmiştir. Şekil 9'da ise güneşlenme süreleri de hesaba katılarak sistemin bir gün içerisinde üretebileceği toplam ısıtma enerjisi (kWh) gösterilmektedir.

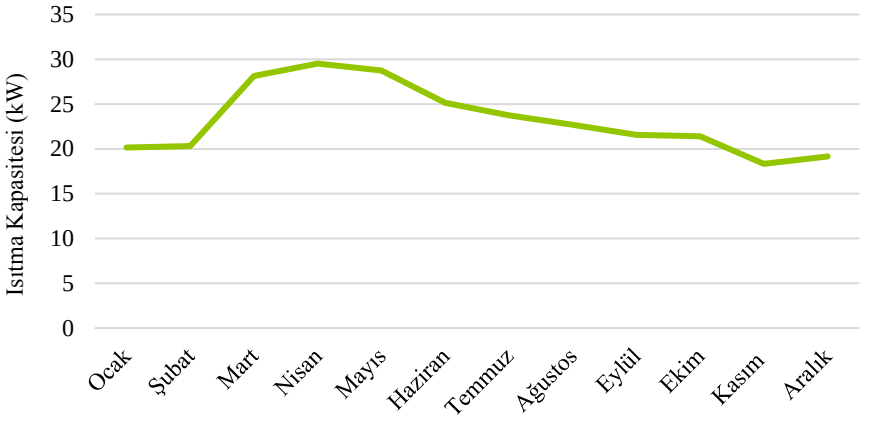

Şekil 8. Aylara göre ısıtma kapasitesi

Şekil 9'da görüldüğü gibi yaz aylarında ışınım şiddeti, güneşlenme süresi, çevre sıcaklığı gibi parametrelerin etkisiyle toplam ısıtma enerjisi artmıştır.

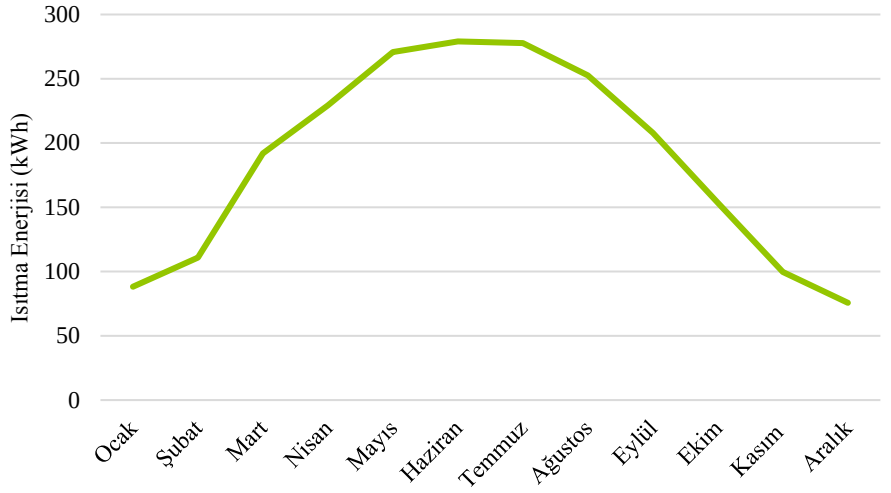

Şekil 9. Aylara göre toplam ısıtma enerjisi

Aylara göre günlük ortalama ısıtma ihtiyacı ve bu ihtiyacın tasarlanan sistem ile karşılanma oranları Şekil 10'da gösterilmektedir. Buna göre sistem tüm aylarda ısıtma ihtiyacının tamamını karşılamaktadır.

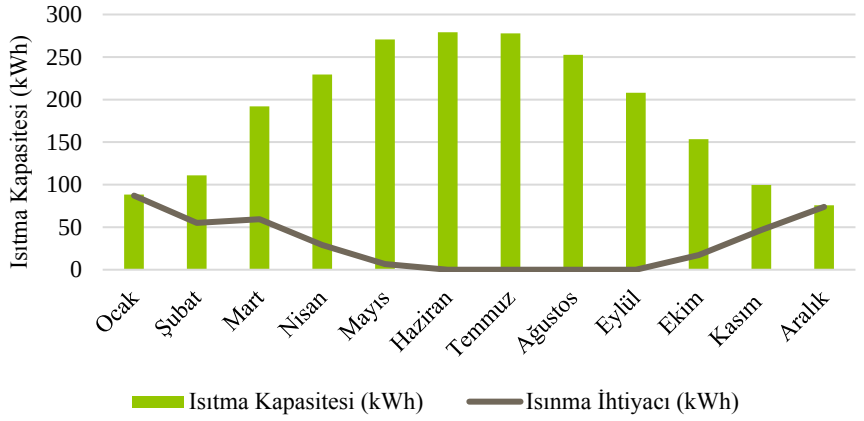

Şekil 10. Sistemin aylara göre ısıtma ihtiyacını karşılama oranı

Tartışma ve Sonuçlar

Bu çalışmada, Isparta ilinde bulunan bir evin düzlemsel havalı güneş kolektörlü depolama sistemi ile ısıtma ihtiyacının karşılanabilmesi hedeflenmektedir. Bu amaçla Ocak ayına ait ışınım şiddeti, çevre sıcaklığı, rüzgâr hızı ve güneşlenme süresi gibi parametreler dikkate alınarak kolektör tasarlanmış ve kolektörlerden gelen faydalı enerji hesaplanmıştır. Istma ihtiyacının karşılanabilmesi için kolektörlerden gelen enerji ve güneşlenme süresi dikkate alınarak kaç tane kolektöre ihtiyaç olduğu hesaplanmıştır. Hesaplamalara göre Ocak ayı şartlarında ısıtma ihtiyacını karşılayabilmek için 64 adet (2m x 1m) düzlemsel havalı güneş kolektörüne ihtiyaç duyulmuştur. Düzlemsel havalı güneş kolektörlü depolama sisteminde gerekli olan sodyum asetat trihidrat miktarı Ocak ayı için bir günde 1171 kg hesaplanmıştır. 268 kj/kg faz değişim ısısında 1171kg sodyum asetat trihidratın toplam enerjisi 313828 kj'dür. Bu enerji 4.38 saat olan güneşlenme süresinde karşılandığı için FDM kapasitesi 19.90 kW olarak hesaplanmıştır. Sistem, ısıtma ihtiyacının en fazla olduğu Ocak ayını karşılayacak şekilde dizayn edildiği için diğer aylardaki ısıtma ihtiyacının tamamını karşılamaktadır.

Teşekkür

Bu araştırma için beni yönlendiren, karşılaştığım zorlukları bilgi ve tecrübesi ile aşmamda yardımcı olan değerli Danışman Hocam Sayın Prof. Dr. Ahmet KABUL'e teşekkürlerimi sunarım. Her anlamda yardımlarını ve desteğini esirgemeyen değerli arkadaşım Arş. Gör. Serpil ÇELİK'e teşekkür ederim.

Tezimin hiçbir aşamasında beni yalnız bırakmayan, her zorlukta yanımda olan biricik kızım Reyyan Esma SOYTÜRK' e ve eşim Mustafa SOYTÜRK'e sonsuz sevgilerimi sunarım.

Kaynaklar

Arı, V. (2007). Türkiye enerji kaynakları, Enerji Planlaması ve Enerji Stratejileri. Çukurova Üniversitesi, Fen Bilimleri Enstitüsü, Yüksek Lisans Tezi, 170s, Adana.

Çakır, A.T. (2008). Türkiye'nin enerji potansiyeli, dağılımı, izlenilen enerji politikaları ile bu potansiyelin kullanılması ve Türkiye'de enerjinin geleceği. Eskişehir Osmangazi Üniversitesi, Fen Bilimleri Enstitüsü, Yüksek Lisans Tezi, 221s, Eskişehir.

Çengel, Y.A., Boles, M.A. (2007). Mühendislik Yaklaşımıyla Termodinamik, Güven Bilimsel Yayınevi (Beşinci Baskı), 946s, İzmir.

GEPA, (2017). Yenilenebilir Enerji Genel Müdürlüğü. http://www.eie.gov.tr (Erişim Tarihi: 20.04.2017).

Guarino, F., Athienitis, A., Cellura, M., Bastien, D. (2017). PCM thermal storage design in buildings: experimental studies and applications to solaria in cold climates. Applied Energy, 185, 95-106.

Kabeel, A.E., Khalil, A., Shalaby, S.M., Zayed, M.E. (2016). Experimental investigation of thermal performance of flat and v-corrugated plate solar air heaters with and without PCM as thermal energy storage. Energy Conversion and Management, 113, 264-272.

Kalogirou, S.A. (2009). Solar energy engineering: Processes and systems. Academic Press, Oxford, UK.

Khadraoui, E.A., Bouadila, S., Kooli S., Farhat, A., Gıizani, A. (2017). Thermal behavior of indirect solar dryer: Nocturnal usage of solar air collector with PCM.

MGM, (2018). İllere Ait Mevsim Normalleri. https://www.mgm.gov.tr/veridegerlendirme/il-ve-ilceler-istatistik.aspx?m=ISPARTA (Erişim Tarihi: 19.04.2018).

Soytürk, Y.G. (2018). Faz Değiştiren Madde İle Güneş Enerjisinin Depolanmasının ve Isıtma Uygulamalarında Kullanımının İncelenmesi. Süleyman Demirel Üniversitesi, Fen Bilimleri Enstitüsü, Yüksek Lisans Tezi, 87s, Isparta.

Sarhaddia, F., Tabrizi, F.F., Zoori, H.A., Hossein, S.A., Mousavi, S. (2017). Energy Conversion and Management, 133, 97-109.

International Conference on Science and Technology

ICONST 2018

5-9 September 2018 Prizren - KOSOVO

Investigation of the Feasibility of Electricity and Heating Requirement for a House in Isparta Conditions with a Parabolic Solar Collector System / Parabolik Güneş Kolektörlü Bir Sistem ile Isparta Şartlarındaki Bir Evin Elektrik ve Isıtma İhtiyacının Karşılanabilirliğinin Araştırılması

Serpil Çelik[1]*, Ahmet Kabul[2], Reşat Selbaş[3]

Özet: Bu çalışmanın amacı güneş enerji kaynaklı kojenerasyon sistemi ile Isparta şartlarında yer alan bir evin elektrik ve ısıtma ihtiyacının karşılanabilirliğinin araştırılmasıdır. Güneş enerjisi, parabolik güneş kolektörleri yardımıyla toplanarak Organik Rankine Çevriminde(ORC) güç üretimi yapılır. ORC'nin kondenser kısmından atılan ısı çevreye atılmak yerine, kışın evin ısıtma ihtiyacını karşılamak üzere ısıtma sistemine gönderilir. Bu kojenerasyon sistem ile nisan ile eylül ayları arasında elektrik ihtiyacının tamamımı, ocak, şubat, mart, ekim, kasım ve aralık aylarında ise sırasıyla % 26, % 41, % 81, % 78, % 40 ve % 24'ü oranında karşılanabileceği görülmüştür. Isıtma ihtiyacı ocak ayında % 45, aralık ayında ise % 48 oranında karşılanırken diğer tüm aylarda % 100 oranında karşılanabileceği hesaplanmıştır.

Anahtar Kelimeler: Parabolik Güneş Kolektörü, ORC, Isıtma

Abstract: The aim of this study is to investigate the affordability of the electricity and heating needs of a house located in Isparta conditions with the solar energy cogeneration system. The solar energy is collected by means of parabolic solar collectors to produce power in the Organic Rankine Cycle (ORC). The heat from the condenser side of the ORC is sent to the heating system to meet the winter heating needs of the home, instead of being thrown into the environment. With this cogeneration system, it can be seen that the electricity needs between April and September can be covered by 26%, 41%, 81%, 78%, 40% and 24% respectively in January, February, March, October, November and December. It is estimated that the heating requirement can be met 100% in all other months while 45% in January and 48% in December.

Keywords: Parabolic Solar Collector, ORC, Heating

Giriş

Enerji, ülkelerin refah düzeyini gösteren birincil etken olarak kabul edilir ve ekonomik gelişimin göstergesidir. Teknolojinin gelişmesi, nüfus artışı, sanayileşme ve insanların yaşam konforu gibi birçok nedenlerden dolayı enerji ihtiyacı gün geçtikçe artmaktadır. Günümüzde artan enerji ihtiyacının büyük bir

[1]Suleyman Demirel University, Faculty of Technology 32260, Isparta, TURKEY
[2]Suleyman Demirel University, Faculty of Technology 32260, Isparta, TURKEY
*Correspondingauthor: serpilcelik@sdu.edu.tr

kısmı birincil enerji kaynaklarından karşılanmaktadır. Fosil yakıtlı kaynakların tükenmesi, nüfus artışı ve iklim değişikliği gibi çeşitli sorunlar yenilenebilir enerji kaynaklarından biri olan güneş enerjisinin kullanımını önemli hale getirmiştir (Francesconi ve Antonelli, 2018).

Güneş enerjisi üzerindeki ilk çalışmalar, ısıtma, kurutma, sıcak su elde etme ve pişirme üzerine olmuştur. Teknolojinin gelişmesiyle birlikte buhar ve elektrik üretimi güneş enerjisinin uygulama alanları haline gelmiştir. Özellikle güneş enerjisinden elektrik üretilmesi konusunda çalışmalar yoğunlaşmış ve güneş enerjisinden yüksek sıcaklıklarda buhar elde edilerek elektrik üretimi yaygınlaşmaya başlamıştır (Öztürk, 2009).

ORC, güneş enerjisinden yararlanarak enerji üretimi yapan sistemlerde yaygın olarak kullanılmaya başlanmıştır. Isıdan elektrik üretiminde kullanılan geleneksel teknoloji buhar türbinidir, ancak uygun işletim için yüksek sıcaklık ve basınç gerektirmektedir. Düşük sıcaklıklarda (<150 °C) tercih edilen güç üretim teknolojisi ORC'dir. Su ve yüksek basınçlı buhar yerine, düşük kaynama noktasına sahip ve yüksek moleküler ağırlıklı organik akışkanlar kullanılmaktadır (Özden ve Paul, 2011).

Kent ve Kaptan (2009), yaptıkları çalışmada, güneş enerjisi destekli ısıtma ve absorbsiyonlu soğutma uygulamasıyla, Antalya ilindeki elli yataklı bir otelin yaz ve kış şartlarında iklimlendirilmesini ve sıcak su ihtiyacının karşılanabilirliğini incelemişlerdir. İlk olarak Antalya ili için güneş ışınımı ve meteorolojik veriler ile otelin ısıtma, soğutma ve sıcak su ısıl yük değerlerini hesaplamışlardır. Güneş enerji tesisatının geri ödeme süresini yaklaşık 4 yıl olarak hesaplamışlardır. Al-Sulaiman vd. (2011), yaptıkları çalışmada katı oksit yakıt hücreli trijenerasyon sisteminin, biyomas kaynaklı trijenerasyon sisteminin ve parabolik güneş kolektörlü trijenerasyon sisteminin performanslarını karşılaştırmışlardır. Çalışmalarında enerji verimi, net elektrik gücü, ısıtma-soğutma elektrik oranı ve sera gazı emisyonları gibi farklı çıkış parametrelerini hesaplamışlardır. En yüksek elektriksel verime katı oksit yakıt hücreli trijenerasyon sisteminde ulaşmışlardır. En yüksek verim, parabolik güneş kolektörlü trijenerasyon sisteminde hesaplanmıştır. Ayrıca bir birim elektrik enerjisi için çevreye atılan CO_2 miktarının en fazla biyomas ve katı oksit yakıt hücreli trijenerasyon sisteminde ortaya çıktığını belirtmişlerdir. Al-Suluiman (2014), parabolik güneş enerjili ısı güç sistemlerini incelediği çalışmasında, güneş kolektörlü buhar rankine çevrimini ve buhar rankine çevriminine entegre edilmiş ORC sisteminin ekserji analizini hesaplamıştır. ORC'de R134a, R152a, R134a, R152a, R290, R407c, R600, R600a ve amonyak gibi yedi farklı soğutucu akışkanı kullanmıştır. Çalışmasının sonucunda ekserji veriminin en yüksek değerini R134a akışkanının kullanıldığı durumda, en düşük verimini ise R600a akışkanının kullanıldığı durumda hesaplamıştır. U.Caldino-Herrera vd. (2017), yaptıkları çalışmada, parabolik güneş kolektörlü ORC sistemini modellemişlerdir ve sistemin performans analizini incelemişlerdir. Bellos ve Tzivanidis (2018), parabolik güneş kaynaklı trijenerasyon sistemini incelemişlerdir. Çalışmalarının sonucunda elektrik üretimini 7.16 kW, ısıtma üretimini 9.35 kW ve soğutma üretimini ise 8.55 kW olarak hesaplamışlardır. Eisavi vd (2018), çalışmalarında güneş enerjisi ile çalışan kombine soğutma, ısıtma ve güç sistemini incelemişlerdir.

Bu çalışmada Isparta şartlarında yer alan bir evin elektrik ve ısıtma ihtiyacının parabolik güneş kolektörlü ORC sistemi ile karşılanabilirliği araştırılmıştır. Kojenerasyon sisteminden elde edilen elektrik ve ısıtma kapasiteleri her ay için ayrı ayrı hesaplanarak evin elektrik ve ısıtma ihtiyacını karşılama oranları hesaplanmıştır. Ayrıca sistemde yer alan her bir noktanın basınç, sıcaklık, entalpi gibi termodinamiksel değerleri bulunmuştur.

Materyal ve Yöntem

Bu çalışmanın amacı, Isparta şartlarında yer alan bir evin elektrik ve ısıtma ihtiyacınının parabolik güneş kolektörlü kojenerasyon sistemi ile karşılanabilirliğini incelemektir. Bir evin ortalama elektrik enerjisi ihtiyacı 10 kWh olarak kabul edilmiştir (Yiğit, 2014). Nisan ayında evin bir günlük elektrik ihtiyacının tamamını karşılayabilecek güneş enerjisi kaynaklı kojenerasyon sistemi dizayn edilmiştir. Dizayn edilen kojenerasyon sisteminden elde edilen elektrik ve ısıtma enerjisi her ay için ayrı ayrı hesaplanmıştır. Elde edilen hesaplamalara göre, evin elektrik ve ısıtma ihtiyacının tasarlanan kojenerasyon sistem ile karşılanabilirliği araştırılmıştır. Parabolik güneş kolektörlerinden toplanan faydalı ısıdan ORC'de güç üretimi

yapılarak evin elektrik ihtiyacı karşılanır. Sistemin kondenser kısmından atılan ısı ise kışın evin ısıtılmasında kullanılmak üzere ısıtma sistemine gönderilir.

Parabolik güneş kolektörlü kojenerasyon sisteminin şematik gösterimi Şekil 1'de verilmiştir. Parabolik güneş kolektörleri, güneşten parabolik yüzeye gelen ışınları, sistemin odağında yer alan ve eksen boyunca uzanan emici boruya yoğunlaştırma yapan sistemlerdir (Öztürk vd., 2009). Parabolik güneş kolektörleri yardımıyla toplanan ısı, parabolik güneş kolektörü sisteminde kullanılan therminol-66 akışkanına aktarılır. Therminol-66 akışkanın ısısı, bir ısı değiştiricide ORC sisteminde kullanılan R245fa akışkanına aktarılır. ORC'de güç üretimi yapıldıktan sonra sistemin kondenser kısmından atılan ısı, kışın evin ısıtılmasında kullanılmak üzere ısıtma sistemine gönderilir.

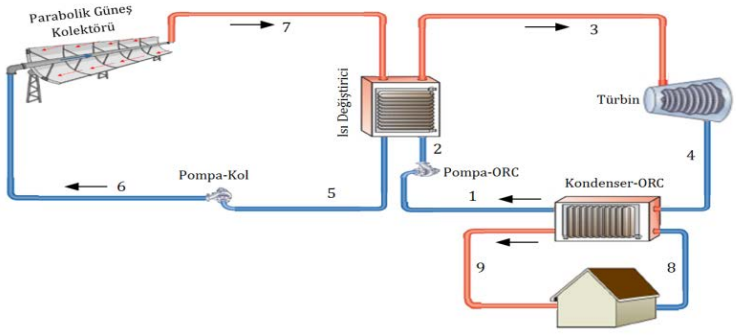

Şekil 1. Güneş enerjisi kaynaklı kojenerasyon sisteminin şematik gösterimi

Kojenerasyon sisteminde kullanılan parabolik güneş kolektörü için dizayn çalışma parametreleri Tablo 1'de verilmiştir.

Tablo 1. Parabolik kolektör dizayn parametreleri

AÇIKLAMA	**DEĞER - BİRİM**
Borunun iç çapı	0.042 m
Borunun dış çapı	0.044 m
Camın çapı	0.102 m
Kolektör boyu	4.29 m
Kolektör genişliği	2.5 m
Camın yayıcılık katsayısı	0.96
Borunun yayıcılık katsayısı	0.96
Borunun ısı iletim katsayısı	15 W/mK
Akışkanın kütlesel debisi	0.25 kg/s
Stephan-Boltzman sabiti	$5.67\ 10^{-8}$
Havanın ısıl iletkenliği	0.027
Camın tahmini sıcaklığı	60 °C
Borunun sıcaklığı	175 °C
Akışkanın giriş sıcaklığı	155 °C
Güneşin sıcaklığı	5739 K
Boru içerisindeki ısı taşınım katsayısı	330 W/m^2K
Isı transfer akışkanının özgül ısısı	2032 j/kgK

Kabul edilen parametreler doğrultusunda nisan ayında elektrik ihtiyacının tamamının karşılanabilmesi için 5 adet parabolik güneş kolektörü kullanılması gerektiği hesaplanmıştır.

Güneş İle İlgili Veriler

Isparta, Türkiye'nin en fazla güneş ışınımı alan illeri arasında bulunmaktadır (Külcü, 2015). Isparta ilinde kurulan kojenerasyon sisteminde, parabolik güneş kolektöründen elde edilen faydalı ısı, her ay için hesaplanmıştır. Eğik yüzeye gelen güneş radyasyonunun hesaplanabilmesi için bölgenin enlem derecesi, kolektör eğim açısı, aylık atmosfer öncesi ortalama radyasyon değerleri, aylık yeryüzü ortalama radyasyon değerleri, direkt, difüz ve yansıtılmış radyasyon açı faktörlerinin bilinmesi gerekir (Uyarel, 1987). Fiziksel olarak ortalama atmosferik radyasyon geçirgenliğinin göstergesi olan berraklık indeksi (BUF), yeryüzü radyasyon değerinin (YYRA) atmosfer öncesi radyasyon değerine (AÖRA) oranı kullanılarak hesap edilmiştir ve Tablo 2'de gösterilmiştir.

Tablo 2. Isparta ili için berraklık indeksi

Aylar	Ocak	Şubat	Mart	Nisan	Mayıs	Haziran	Temmuz	Ağustos	Eylül	Ekim	Kasım	Aralık
BUF	0.410	0.454	0.491	0.510	0.567	0.598	0.633	0.623	0.614	0.530	0.483	0.415

Meteoroloji istasyonlarının toplam radyasyon ölçüm değerleri yılın her ayı için ortalama olarak hazırlanmaktadır. Hazırlanan radyasyon ölçüm değerleri direkt ve difüz radyasyonun toplamıdır (Uyarel, 1987). Parabolik çizgisel odaklamalı güneş kolektörlerinde sadece direkt radyasyon miktarı kullanıldığından toplam yeryüzü radyasyon miktarının, ne kadarının direkt radyasyon (DİR) olduğu belirlenmiştir. Difüz radyasyonun bulunması amacıyla Uyarel'in kullandığı "$\text{DİF} = (1 - 1.097 \text{ x BUF}) \text{ x YYRA}$" formülü kullanılmış ve toplam YYRA'dan DİF radyasyon miktarının çıkarılması ile DİR radyasyon miktarı bulunmuştur. Her ay için yeryüzü radyasyon değerinin ne kadarının direkt radyasyon olduğunu gösteren yüzdelik oran Tablo 3'de verilmiştir.

Tablo 3. Isparta ili için YYRA'nın ne kadarının DİR olduğunu gösteren yüzdelik oran

Aylar	Ocak	Şubat	Mart	Nisan	Mayıs	Haziran	Temmuz	Ağustos	Eylül	Ekim	Kasım	Aralık
Oran	0.45	0.50	0.54	0.56	0.62	0.66	0.69	0.68	0.67	0.58	0.53	0.46

Parabolik güneş kolektörünün eğim açısı enlem derecesi kabul edildiği için eğik düzleme gelen güneş ışınımları hesaplanmıştır. Eğik düzleme gelen ışınım şiddeti hesaplanırken GEPA verilerine göre, enlem derecesi 37.4° olan Isparta iline yatay düzleme gelen DİR hesaplanmıştır ve Şekil 2'de gösterilmiştir. Açı faktörü eğik bir yüzey üzerine gelen güneş radyasyonunun, yatay düzleme gelen güneş radyasyonuna oranını ifade etmektedir. Direkt radyasyon açı faktörü (DİRAF) tüm aylar için ortalama 1.38 kabul edilmiştir. Eğik düzleme gelen direkt ışınım şiddeti, yatay düzleme gelen direkt ışınım şiddeti ile DİRAF'ın çarpılması sonucu elde edilerek Şekil 3'de gösterilmiştir.

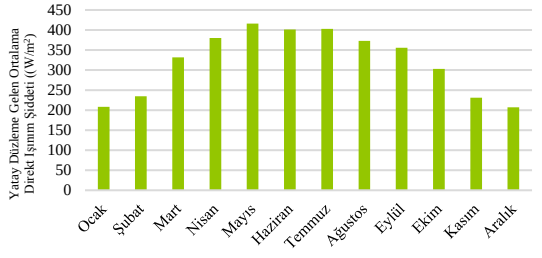

Şekil 2. Isparta ili yatay düzleme gelen aylık ortalama direkt ışınım şiddeti

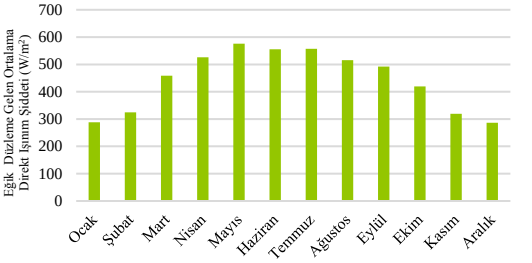

Şekil 3. Isparta ili eğik düzleme gelen aylık ortalama direkt ışınım şiddeti

Hesaplamalar için ışınım şiddetinin yanı sıra ortalama çevre sıcaklığı, rüzgâr hızı, güneşlenme süresi de önemlidir. GEPA'dan alınan verilere göre Isparta iline ait aylık ortalama güneşlenme süresi Şekil 4'de verilmiştir.

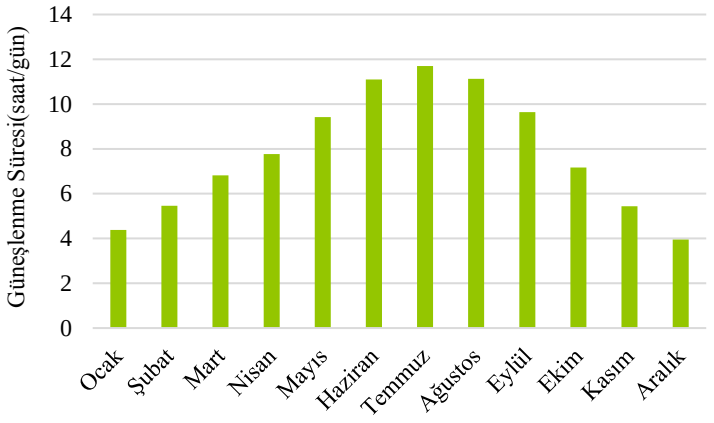

Şekil 4. Aylık güneşlenme süresi (GEPA, 2017)

Meteoroloji Genel Müdürlüğü'nden (MGM) alınan verilere göre Isparta ili için aylara göre ortalama çevre sıcaklıkları ve rüzgâr hızları sırasıyla Şekil 5'de ve Şekil 6'da verilmiştir.

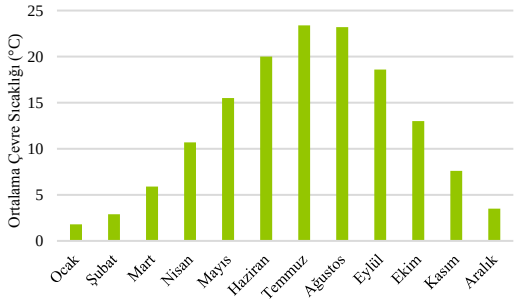

Şekil 5. Isparta ili aylık ortalama çevre sıcaklığı (MGM, 2017)

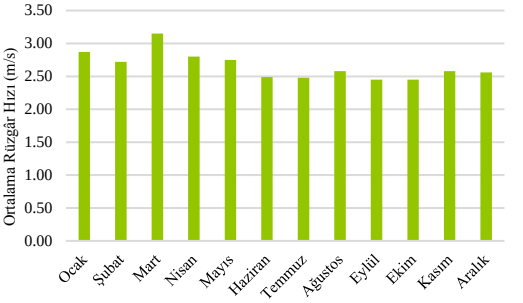

Şekil 6. Isparta ili ortalama rüzgâr hızı (MGM, 2017)

Sistemin Teorik Analizi

Parabolik güneş kolektöründen toplanan faydalı enerji denklem (1) ile bulunur (Kalogirou, 2009).

$$Q_u = F_R\left[G\,A_{aç} - A_r U_L\left(T_{giren,kol} - T_a\right)\right] \quad (1)$$

Burada, F_R ısı taşıma faktörü, G ışınım şiddeti, $A_{aç}$ açıklık yüzey alanı, A_r boru yüzey alanı, U_L kolektörden çevreye olan toplam ısı kayıp katsayısı, T_a hava sıcaklığı ve $T_{giren,kol}$ kolektöre giren akışkan sıcaklığıdır. Parabolik güneş kolektöründen elde edilen faydalı enerji, kolektöre giren ve çıkan akışkanın özeliklerine göre aşağıdaki gibi hesaplanır (Kalogirou, 2009).

$$Q_u = \dot{m}_{kol} c_{p,kol}\left(T_{giren,kol} - T_{çıkan,kol}\right) \quad (2)$$

Burada, $\dot{m}_{kol}$ kolektördeki akışkanın kütlesel debisini, $c_{p,kol}$ akışkanın özgül ısısını ve $T_{çıkan,kol}$ kolektörden çıkan akışkanın çıkış sıcaklığını temsil etmektedir.

Isı taşıma faktörü olan aşağıdaki formül ile hesaplanır (Kalogirou, 2009).

$$F_R = \frac{\dot{m}_{kol} c_{p,kol}}{A_r U_L}\left[1 - \exp\left(-\frac{U_L F' A_r}{\dot{m}_{kol} c_{p,kol}}\right)\right] \quad (3)$$

Burada, F' kolektör etkinlik faktörüdür ve şu şekilde bulunur:

$$F' = {U_0}/{U_L} \tag{4}$$

Burada, U_0 toplam ısı transfer katsayısıdır ve aşağıdaki denklem ile hesaplanır.

$$U_0 = \left[\frac{1}{U_L} + \frac{D_0}{h_{fi} D_i} + \left(\frac{D_0 \ln\left({D_0}/{D_i}\right)}{2k}\right)\right]^{-1} \tag{5}$$

Burada, D_0 boru dış çapı, D_i boru iç çapı, k_r alıcı boru ısı iletim katsayısı ve h_{fi} ise boru içindeki akışkanın ısı transfer katsayısıdır.

Kolektörden çevreye olan toplam ısı kayıp katsayısı şu şekilde bulunur.

$$U_L = \left[\frac{A_r}{\left(h_{t,c-a} + h_{r,c-a}\right)A_c} + \frac{1}{h_{r,r-c}}\right]^{-1} \tag{6}$$

Burada, A_c cam yüzey alanı, $h_{t,c-a}$ hava ile cam arasındaki taşınımla olan ısı transfer katsayısı, $h_{r,c-a}$ hava ile cam arasındaki ışınımla olan ısı transfer katsayısı, $h_{r,r-c}$ cam ile boru arasındaki ışınımla olan ısı transfer katsayısıdır. Bu üç ısı transfer katsayısı aşağıdaki denklemler ile hesaplanır.

$$h_{t,c-a} = \frac{Nu_a\, k_a}{D_c} \qquad \begin{matrix} 0.1 < Re < 1000 & Nu_a = 0.4 + 0.54\, Re^{0.52} \\ 1000 < Re < 50000 & Nu_a = 0.3\, Re^{0.6} \end{matrix} \tag{7}$$

Burada, k_a havanın ısıl iletkenliğini, D_c camın çapını, Nu_a Nusselt sayısını, Re ise Reynolds sayısını ifade etmektedir.

$$h_{r,c-a} = \varepsilon_{y,c}\sigma(T_c - T_a)\left(T_c{}^2 + T_a{}^2\right) \tag{8}$$

Burada, σ=5.670x10-8 W/m^2.K^4 değeri Stefan-Boltzmann sabiti, $\varepsilon_{y,c}$ camın yayıcılık katsayısı, T_c ise cam sıcaklığıdır.

$$h_{r,r-c} = \frac{\sigma(T_r^2 + T_c^2)(T_r + T_c)}{\frac{1}{\varepsilon_{y,r}} + \frac{A_r}{A_c}\left(\frac{1}{\varepsilon_{y,c}} - 1\right)} \tag{9}$$

Burada, $\varepsilon_{y,r}$ alıcı boru yayıcılık katsayısını ifade etmektedir.

Kararlı ve sürekli akışlı sistemler için kütlenin korunumu ifadesi aşağıdaki eşitliklikle verilir.

$$\sum \dot{m}_g = \sum \dot{m}_ç \tag{10}$$

Burada g ve ç alt indisleri sırasıyla girişi ve çıkışı ifade etmektedir. Kinetik ve potansiyel enerjiler ihmal edildiğinde enerji denkliği aşağıdaki şekilde tanımlanabilir (Çengel ve Boles, 2007).

$$\dot{Q} + \sum \dot{m}_g h_g = \dot{W} + \sum \dot{m}_ç\, h_ç \tag{11}$$

Burada, $\dot{Q}$ ısı transferini $\dot{W}$ sistemdeki iş etkileşimini, h ise entalpiyi ifade etmektedir.

Birinci yasa verimi elde edilmek istenen değerin harcanan değere oranıdır.

$$\eta_I = \frac{\text{Elde edilmek istenen değer}}{\text{Harcanan Değer}} \tag{12}$$

Sistemde yer alan herbir eleman için kütle ve enerji denge denklemleri Tablo 4'de verilmiştir.

Tablo 4. Sistem elemanlarının termodinamiksel denge denklemleri

Sistem Elemanları	Kütlenin Korunumu	Enerjinin Korunumu
Pompa-ORC	$\dot{m}_1 = \dot{m}_2$	$\dot{m}_1 h_1 + \dot{W}_{Pompa-ORC} = \dot{m}_2 h_2$
Isı Değiştirici	$\dot{m}_2 = \dot{m}_3$ $\dot{m}_5 = \dot{m}_7$	$\dot{m}_2 h_2 + \dot{m}_7 h_7 = \dot{m}_3 h_3 + \dot{m}_5 h_5$
Türbin	$\dot{m}_3 = \dot{m}_4$	$\dot{m}_3 h_3 = \dot{m}_4 h_4 + \dot{W}_{Tür}$
Kondenser-ORC	$\dot{m}_4 = \dot{m}_1$	$\dot{m}_4 h_4 + \dot{m}_8 h_8 = \dot{m}_1 h_1 + \dot{m}_9 h_9$
Pompa-Kol	$\dot{m}_5 = \dot{m}_6$	$\dot{m}_5 h_5 + \dot{W}_{Pompa-Kol} = \dot{m}_6 h_6$
Parabolik Kolektör	$\dot{m}_6 = \dot{m}_7$	$\dot{m}_6 h_6 + \dot{Q}_{Güneş.} = \dot{m}_7 h_7$

Bulgular

Isparta ilinde yer alan bir evin elektrik ve ısıtma ihtiyacının, dizay edilen güneş enerjili kojenerasyon sistemi ile karşılanabilirliği araştırılmıştır. Dizayn edilen kojenerasyon sisteminin çalışma şartları belirlenirken nisan ayına ait ışınım şiddeti, güneşlenme süresi, çevre sıcaklığı ve rüzgâr hızı referans alınmıştır.

Kojenerasyon sisteminin her bir noktası için hesaplanan termodinamiksel değerler Tablo 5'de verilmiştir.

Tablo 5. Sistemin herbir noktası için termodinamiksel değer

	Akışkan Türü	P (kPA)	T (°C)	ṁ (kg/s)	h (kj/kg)	e (kj/kg)	Ex (kW)
1	R245fa	343.2	50.00	0.0762	26.73	3.539	0.250
2	R245fa	790.8	50.26	0.0762	266.7	3.903	0.297
3	R245fa	790.8	166.1	0.0762	560.0	68.25	5.200
4	R245fa	343.2	146.3	0.0762	542.1	48.21	3.673
5	Therminol-66	101.3	154.6	0.2500	282.5	50.96	12.74
6	Therminol-66	101.3	155.0	0.2500	283.3	51.23	12.81
7	Therminol-66	101.3	197.0	0.2500	371.9	83.68	20.92
8	Su	202.7	30.00	0.0719	125.9	2.727	0.196
9	Su	202.7	99.76	0.0719	418.2	48.74	3.504

Isparta ilinin ışınım şiddeti, güneşlenme süresi, rüzgâr hızı ve çevre sıcaklığı aylara göre farklılıklar göstermektedir. Yılın her ayı için ışınım şiddeti, rüzgâr hızı, çevre sıcaklığı ve güneşlenme süresi dikkate alındığında kojenerasyon sisteminde üretilen elektrik enerjisi ve ısıtma kapasitesi Tablo 6'da verilmiştir. Yıllık elektrik ihtiyacının karşılanabilirliğini görebilmek için her ay türbinden elde edilen güç, güneşlenme süresi ile çarpılarak toplanır. Elde edilen toplam elektrik enerjisinin yıllık ortalaması alındığında, yıllık elektrik ihtiyacının karşılandığı görülmüştür.

Sistemin üretebileceği elektrik ve ısıtma kapasiteleri Şekil 7'de aylara göre gösterilmiştir.

Tablo 6. Aylara göre elektrik üretimi ve ısıtma kapasiteleri

Aylar	Işınım Şiddeti (W/m^2)	Çevre Sıcaklığ (°C)	Güneşlenme Süresi (h/gün)	Kolektör Kapasitesi (kW)	Türbin Kapasitesi (kW)	Isıtma Kapasitesi (kW)
Ocak	288.21	1.8	4.38	9.44	0.611	9.067
Şubat	324.38	2.9	5.46	11.37	0.751	10.85
Mart	458.98	5.9	6.82	18.41	1.190	17.46
Nisan	525.93	10.7	7.77	22.14	1.363	21.02
Mayıs	575.61	15.5	9.42	24.93	1.482	23.69
Haziran	555.13	20	11.10	24.04	1.445	-
Temmuz	557.19	23.4	11.70	24.26	1.454	-
Ağustos	515.57	23.2	11.13	22.04	1.359	-
Eylül	492.28	18.6	9.64	20.68	1.298	-
Ekim	419.22	13	7.17	16.67	1.100	15.81
Kasım	319.37	7.6	5.44	11.28	0.745	10.77
Aralık	286.66	3.5	3.95	9.46	0.613	9.085

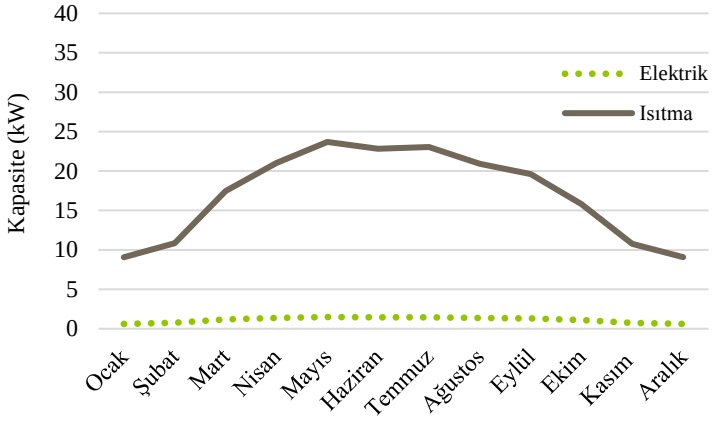

Şekil 7. Aylara göre elektrik ve ısıtma kapasitesi

Aylara göre sistemden üretilen günlük elektrik miktarının, günlük elektrik ihtiyacı 10 kWh olarak kabul edilen bir evin elektrik ihtiyacını karşılama durumu Şekil 8'de görülmektedir. Sistemde üretilen elektrik enerjisi, ocak ayında ihtiyacın % 26'sını, şubat ayında % 41'ini, mart ayında % 81'ini, ekim ayında % 78'ini, kasım ayında % 40'ını, aralık ayında ise % 24'ünü, diğer aylarda ise elektrik ihtiyacının tamamından daha fazlasını karşılamaktadır.

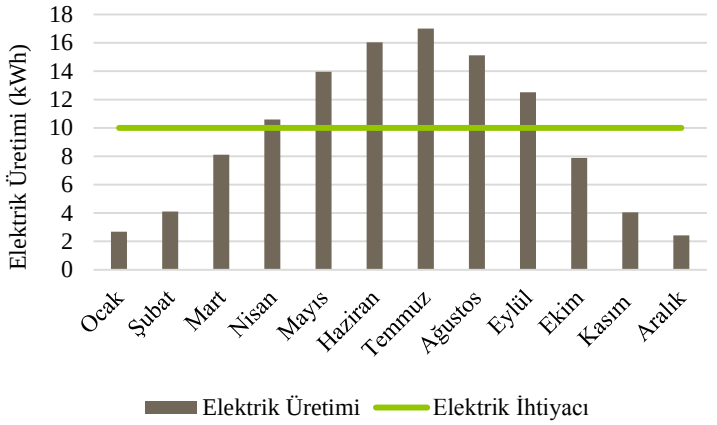

Şekil 8. Sistemin aylara göre günlük elektrik ihtiyacını karşılama oranı

Isparta şartlarındaki bir evin aylara göre ısıtma ihtiyacı, Özdemir'in 2018 yılında yaptığı tez çalışmasındaki değerler kabul edilmiştir ve aylara göre ısıtma ihtiyacı Tablo 7'de verilmiştir. Aylara göre bir evin günlük ortalama ısıtma ihtiyacının, kojenerasyon sisteminden günlük üretilen ısıtma ihtiyacından karşılama oranı Şekil 9'da verilmiştir. Şekil 9'da görüldüğü gibi tasarlanan kojenerasyon sistemi, evin ısıtma ihtiyacını ocak ayında % 45, aralık ayında % 48 oranında karşılarken diğer tüm aylarda % 100 oranında karşılamıştır.

Tablo 7. Isparta ili aylara göre ısıtma ihtiyacı(kW)

Aylar	Ocak	Şubat	Mart	Nisan	Mayıs	Haziran	Temmuz	Ağustos	Eylül	Ekim	Kasım	Aralık
Isıtma İhtiyacı	3.63	2.29	2.47	1.21	0.28	0	0	0	0	0.72	1.95	3.08

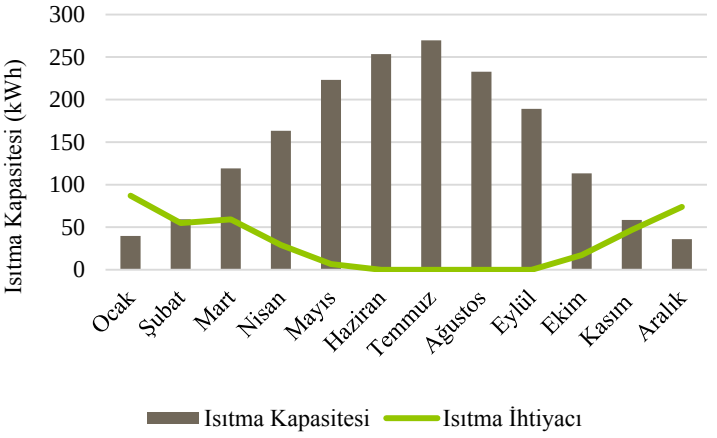

Şekil 9. Sistemin aylara göre günlük ısıtma ihtiyacını karşılama oranı

Farklı ışınım şiddetine göre sistem elemanlarının kapasitelerindeki değişim Şekil 10'da verilmiştir. Grafikten de görüldüğü gibi ışınım şiddeti arttıkça elemanların kapasitelerinin arttığı görülmüştür.

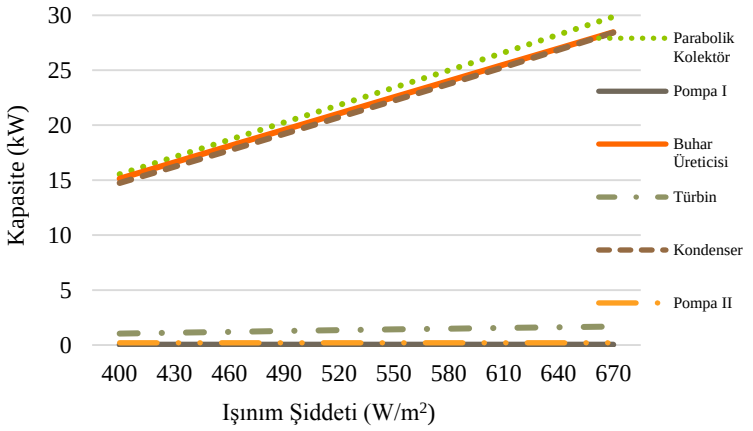

Şekil 10. Işınım şiddetine göre sistemdeki elemanların kapasitesindeki değişim

Tartışma ve Sonuçlar

Bu çalışmada, Isparta şartlarında bulunan bir evin elektrik ve ısıtma ihtiyacının güneş enerjisi kaynaklı kojenerasyon sistemi ile karşılanabilirliliği araştırılmıştır. Isparta ilinin nisan ayına ait ışınım şiddeti, güneşlenme süresi, çevre sıcaklığı ve rüzgâr hızı dikkate alınarak, günlük elektrik ihtiyacı 10 kWh olan bir evin elektrik ihtiyacını karşılamak için parabolik güneş kolektörlü kojenerasyon sistemi dizayn edilmiştir. İncelenen sistemde, değişen ışınım şiddetine göre kolektör verimi, ORC ısıl verimi ve sistemde kullanılan elemanların kapasitelerindeki değişim incelenmiştir.

Tasarlanan parabolik güneş kolektörlü kojenerasyon sisteminin yılın tüm aylarında evin elektrik ve ısıtma ihtiyacını karşılama oranları hesaplanmıştır. Elde edilen hesaplamalara göre dizayn edilen kojenerasyon sistemle, evin elektrik ihtiyacı ocak ayında % 26, şubat ayında % 41, mart ayında % 81, ekim ayında % 78, kasım ayında % 40, aralık ayında %24 oranında karşılanabilirken; geri kalan tüm aylarda ise tamamının karşılanabilir olduğu tespit edilmiştir. Sistemden üretilen elektrik enerjisi, yılın 6 ayı konutun elektrik ihtiyacını karşılayamayacağı tespit edilmiştir. Sistemden üretilen 3435 kWh yıllık elektrik miktarı, bir konutun 3650 kWh olan yıllık enerji ihtiyacını hemen hemen karşılamıştır. Kojenerasyon sistemi, ışınım şiddeti, güneşlenme süresi ve rüzgâr hızının düşük olduğu ocak ayı referans alınarak hesaplansaydı, sistemin yatırım maliyeti nisan ayına göre çok yüksek olacağı dikkate alınmalıdır.

Dizayn edilen güneş enerjili kojenerasyon sistem ile konutun ısıtma ihtiyacının ocak ayında % 45'i, aralık ayında % 48'i karşılanırken diğer tüm aylarda ise tamamının karşılandığı hesaplanmıştır.

Bu çalışmada, yenilenebilir enerji kaynaklarından biri olan güneş enerjisili mikro kojenerasyon sisteminin modellemesine ve uygulanabilirliğine yer verilmiştir. Ayrıca sistemde tek bir enerji kaynağı kullanılarak evin elektrik ve ısıtma ihtiyacı karşılanmıştır. Kojenerasyon sisteminde güneş enerjisi kullanılarak fosil yakıt tüketimi ve emisyonlar azalacak, kullanım sonrası fazla kalan elektrik enerjisi şebekeye geri satılabilecek ve yerel üretimden dolayı sistem kayıpları önlenebilecektir.

Teşekkür

Bu araştırma için beni yönlendiren, karşılaştığım zorlukları bilgi ve tecrübesi ile aşmamda yardımcı olan değerli Danışman Hocam Prof. Dr. Ahmet KABUL'e teşekkürlerimi sunarım. Bu çalışmada her konuda desteklerini ve yardımlarını gördüğüm değerli arkadaşım Arş. Gör. Gamze SOYTÜRK'e teşekkür ederim.

Kaynaklar

Al-Sulaiman, F.A., Dincer, İ., Hamdullahpur, F. (2011). Exergy modeling of a new solar driven trigeneration system. Solar Energy, 85, 2228-2243.

Al-Sulaiman, F.A. (2014). Exergy analysis of parabolic trough solar collectors integrated with combined steam and organic rankine cycles. Energy Conversion and Management, 77, 441-449.

Bellos, E., Tzivanidis, C. (2018). Energetic and exergetic evaluation of a novel trigeneration system driven by parabolic trough solar collectors. Thermal Science and Engineering Progress, 6, 41-47.

Çengel Y.A., Boles M.A. (2007). Mühendislik Yaklaşımıyla Termodinamik. Güven Bilimsel Yayınevi, İzmir, Türkiye.

Eisavi, B., Khalilarya, S., Chitsaz, A., A. Rosen, M. (2018). Thermodynamic analysis of a novel combined cooling, heating and power system driven by solar energy. Applied Thermal Engineering, 129, 1219-1229.

Francesconi, M., Antonelli M. (2018). A CFD analysis to investigate thermal losses in a panel composed of several CPC concentrators, Therm. Sci. Eng. Progress. 5, 278–288.

GEPA, (2017). Erişim Tarihi: 20.04.2017. http://www.eie.gov.tr/

Herrera, U.C., Castro, L., Jaramillo, O.A., Garcia, J.C., Urquiza, G., Flores, F. (2017). Small organıc rankine cycle coupled to parabolic trough solar concentrator. Energy Procedia, 129, 700-707.

Kalogirou, S.A. (2009). Solar thermal collectors and applications. Progress in Energy and Combustion Science, 30(3), 231-295.

Kent, E.F., Kaptan, İ.N. (2009). Güneş enerji destekli isıtma ve absorbsiyonlu soğutma uygulaması.

Külcü, R. (2015). Isparta ili için yeryüzüne ulaşan güneş işınımının modellenmesi. SDÜ Ziraat Fakültesi Dergisi, 10, 19-25.

MGM, (2017). İllere Ait Mevsim Normalleri. Erişim Tarihi: 03.04.2017. https://www.mgm.gov.tr/veridegerlendirme/il-ve-ilceler-istatistik.aspx?m=ISPARTA

Özdemir, B. (2018). Güneş enerjisi kaynaklı ev tipi trijenerasyon sisteminin termodinamik analizi. Süleyman Demirel Üniversitesi, Fen Bilimleri Enstitüsü, Yüksek Lisans Tezi, 88s, Isparta.

Özden, H., Paul, D. (2011). Organik rankine çevrim teknolojisiyle düşük sıcaklıktaki kaynaktan faydalanılarak elektrik üretimi örnek çalışma: sarayköy jeotermal santrali. 10. Ulusal tesisat mühendisliği kongresi, İzmir.

Öztürk, H.K., Şanlı, G., Yılancı, A. (2009). Parabolik oluk tipi güneş kolektörlerinin performans analizi. Cilt 51, Sayı 609.

Uyarel, A.Y., Öz, E.S. (1987). Güneş enerjisi ve uygulamaları. Birsen Yayınevi, 244s, İstanbul.

Yiğit, F., Kabul, A. (2014). Isparta yöresinde bir evin elektrik ihtiyacının rüzgâr enerjisi ile karşılanmasının ekonomik analizi. Teknolojik Araştırmalar, Makine Teknolojileri Elektronik Dergisi, 11(2), 1-9.

International Conference on Science and Technology

ICONST 2018

5-9 September 2018 Prizren - KOSOVO

Graft Polymerization of Waste PAN Fibers onto Sunflower Stalk

Mustafa Karaboyacı[1]*, Mustafa Cengiz[2]

Abstract: In thıs study, it was investigated that grafting of waste PAN fibers onto sunflower stalk with graft polymerization method. Because graft copolymerization of acrylic monomers onto natural polymers is an efficient approach to achieve biopolymer-based superabsorbing hydrogels. In this study waste PAN was directly grafted onto lignocellulosic material. Optimum grafting time also invesitigated. Grafting performance was anaylsed with FTIR spectrum.

Keywords: graft polymerization, PAN, sunflower stalk

Introduction

Environmental pollution is one of the most important problems for humanity after the industrial revolution. The desire of human beings to dominate nature and the consumption craze has advanced this problem well. Nature of waste treatment capacity and endurance limit are known to be very high in their functions, but human factors cause or exceed the limit of resistance of this capacity. The human being aware of this has resorted to artificial waste treatment methods in order to help nature. Adsorption is a preferred treatment method because of its low cost in waste treatment and its environmental friendliness. Any substance that may be present in water is harmful to health on a certain concentration. Substances with toxic effects can cause health and even death by damaging human health even if they are present in low concentrations. Among the substances that are inconvenient even in trace amounts, the most important group is the so-called heavy metals, Sb, Ag, Pb, As, Be, Cd, Cr, Mn, Hg, Ni, Se, T, Zn.

Shibi and Anirudhan (2005) studied about, removal of cobalt(II) ion from nuclear power plant waste water with carboxyl functionalized banana stalk. A novel adsorbent was synthesized by grafting of the acrylamide onto the banana stalk and the banana stalk (BS) (MusaParadisiaca) containing the carboxylate functional group at the end of the ring using the iron ammonium sulfate and H_2O_2 redox initiator system (PGBS-COOH). The ability of this adsorbent to remove Co (II) from the water was investigated using batch adsorption technique. The adsorbent exhibited very high adsorption potential for Co^{2+}.

In this study waste poly acrylonitrile (PAN) fibes was obtained from İPLİKSAN AŞ. Company produces hand kintting yarn by using PAN fibers. Around 10% waste acrylic fiber is formed during the yarn production process.

The annual amount of plantial and agricultural residues in the world is approximately 2.273.080.000 tons. In Turkey, every year, 36.94 million tons of agriculture is now being obtained that 18 million tons of wheat stalks, 8 million tons of barley straw, 2.5 million tons of corn stalks, 3 million tons of cotton stalk, 2.5 million tons of sunflower stalks, 200 thousand tons Rice stalk, 240 thousand tons of rye stalk, 300 thousand tons of tobacco stalk, 2 million tons of self-portrait, 200 thousand tons of lake cane constitutes (Republic of Turkey

Prime Ministry State Institute of Statistics Publications, Agricultural Structure and Production, Ankara, 1995).

Therefore, as a lignocellulosic source, sunflower stalk with a large waste potential was chosen in the study. The PAN-grafted cellulosic structure to be obtained will be used as intermediate product in the production of superabsorbents.

Material and Method

Reaction mechanism for obtaining new polymers by graft polymerization onto lignocellulosides is designed with that hypothesis. Target grafting molecule is hydroxil groups, (OH) that is main fonctional group of cellulose. and cellulose is the main componenet of lignocellulosiccs. Also lignin have phenolic OH groups.

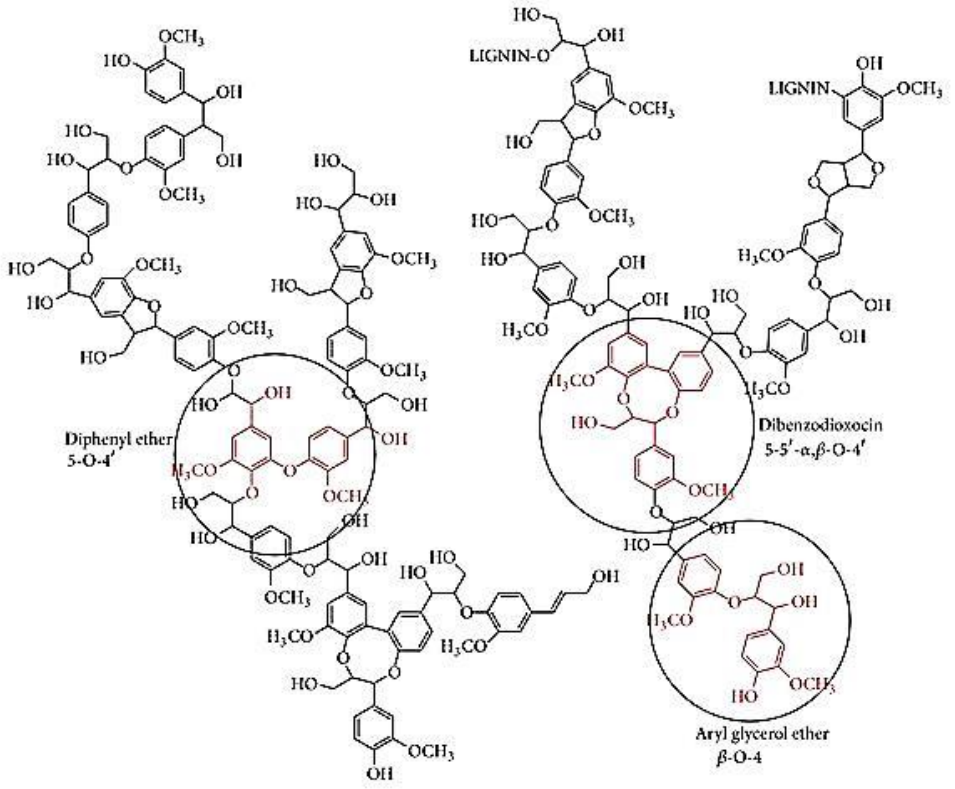

Figure 1. Common chemical structure of lignin (Wang, et al. 2013)

The dried sunflower stalk were milled in the mill and sieved through the No. 100 sieve (pore diameter 150 μm). Sifted sunflower was washed with distilled water to remove dust and similar impurities inside the milled stalk and then dried by filtration.

1 g of acrylic fiber was dissolved in 250 ml of DMF and then 10 g of sunflower stalk was added. Following this, 25 ml of ferrous sulfate solution was added to the reaktion mixture. After stirring for 1 minute, 1 gram of potassium persulfate was added as an initiator. $FeSO_4$ solution was prepared by dissolving 0.01 g of ferrous sulphate in 100 ml of water and adding 2 ml of concentrated H_2SO_4.

The experiments were repeated for 3, 6 and 12 hours for t obtain optimum grafting time. The resultant solution was washed with 5 ml of DMF for 2 times and then with 5 ml of distilled water for 2 times. And then obtained material was dried.

Results

Figure 2 shows the FTIR spectrum of the raw sunflower stem. 3000-3600 cm^{-1} and 1640 cm^{-1} shows characteristic OH bands. Also at 2940 and 1040 cm^{-1}, characteristic tensile bands of cellulose ring is seen. Figure 3 shows the FTIR spectrum of the raw PAN. At 2240 cm^{-1}, Characteristic C≡N stretching bands are seen. The FTIR spectrum of the three-hours experiment result is shown in figure 4, the FTIR spectrum in the six-hour experiment is shown in figure 5 and the FTIR spectrum obtained in the twelve-hour experiment is shown in figure 6.

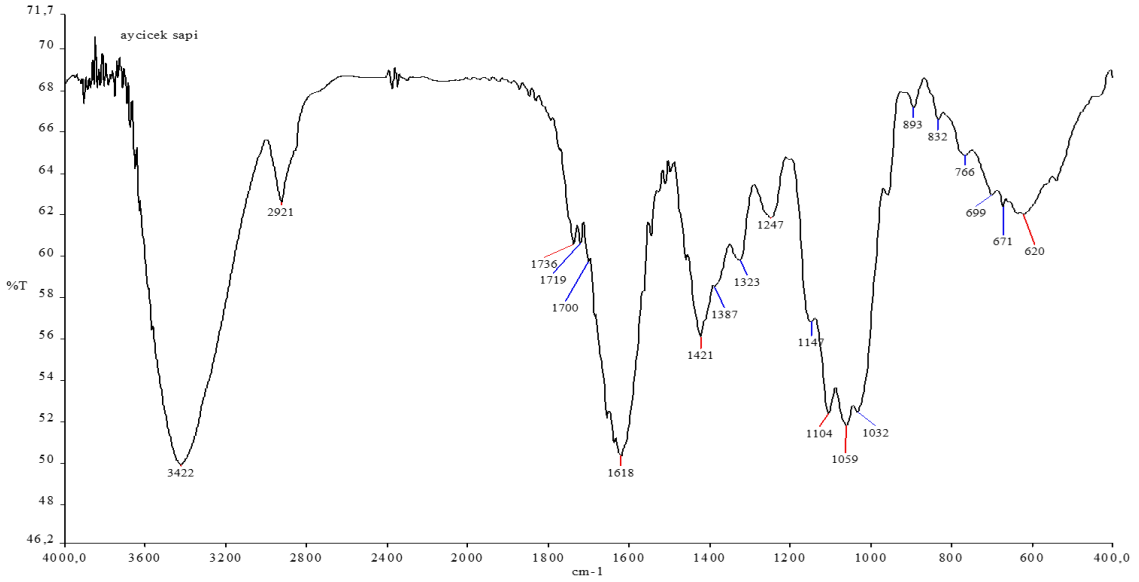

Figure 2: FTIR spectrum of raw sunflower stalk

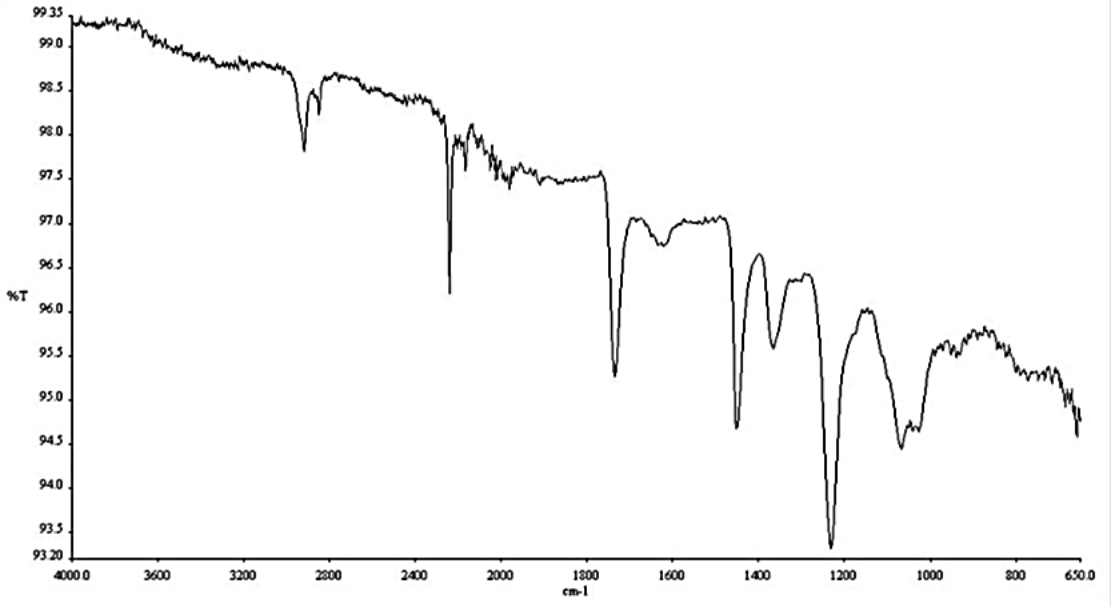

Figure 3: FTIR spectrum of raw PAN fiber

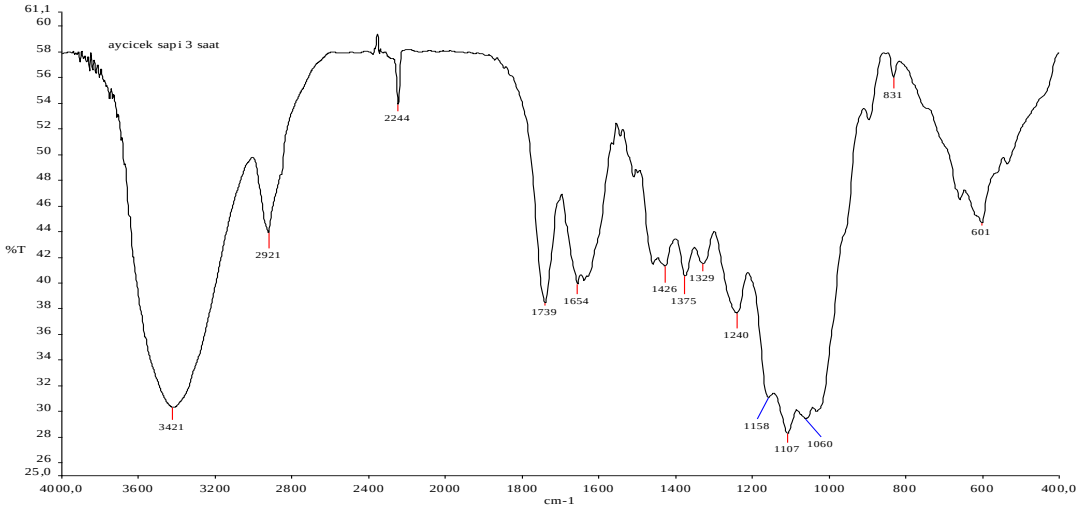

Figure 4: FTIR spectrum 3 hours grafting experiment

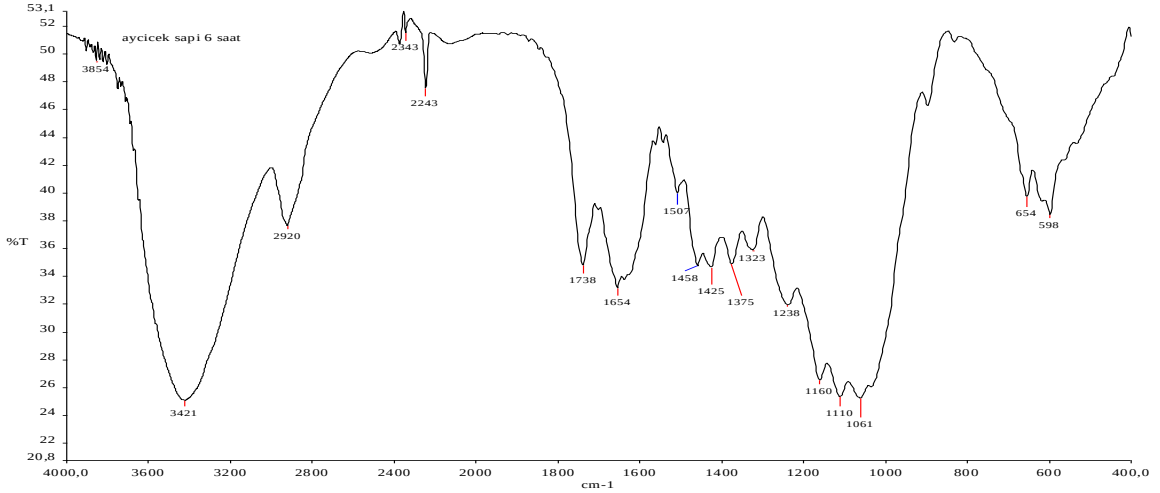

Figure 5: FTIR spectrum 6 hours grafting experiment

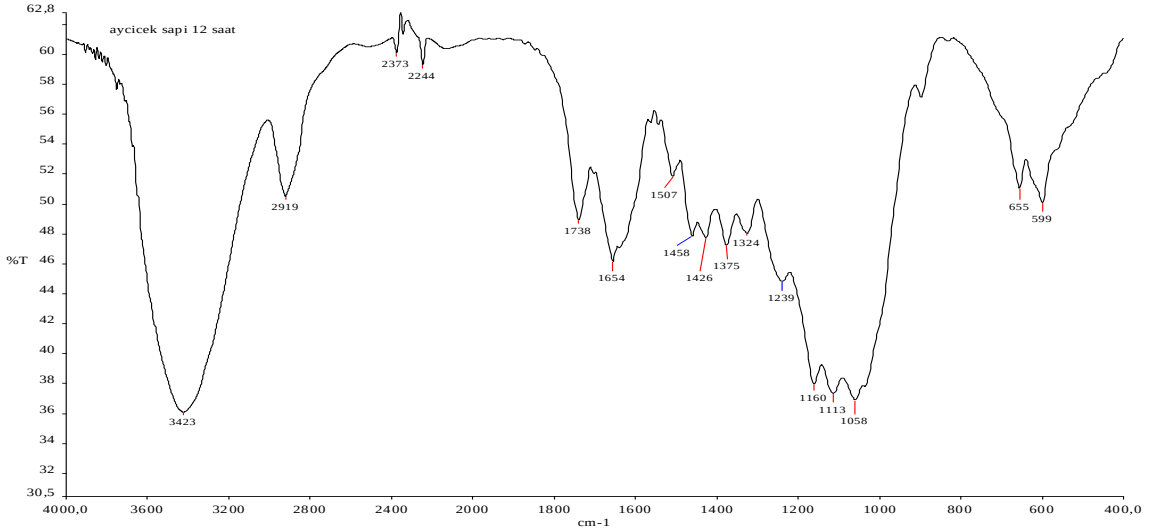

Figure 6: FTIR spectrum 12 hours grafting experiment

When we compara raw sunflower stalk and PAN grafted sunflower stalk. there is a new band at 2240 cm-1 in the grafted stalk FTIR spectrum. This band is belongs to the CN group of acrylonitrile. At 667 cm-1 CH = CH off-plane bending also comes from the acrylic structure. These are proof of the grafted PAN molecules onto lignocellulosic material.

Discussion and Conclusions

When the 3 experiments were examined, the grafting experiment, which was maintained for six hours, was chosen as the most suitable time. Although the grafting was performed in all three trials, the sharpest and deepest band was obtained in 6 hours experiments. This indicates that most acrylics are bonded during this period**.**

Khullar et al (2008) was grafted acyronitrile onto bamboo. . Their optimum reaction conditions obtained for grafting of acrylonitrile onto cellulosic material were duration of dipping cellulosic material in CAN solution 1 hr, CAN concentration 0.02 M, acrylonitrile concentration 24.6 mol/AGU, temperature of reaction 40°C and polymerization time 4 hrs.

Singha et al (2009) studied about graft copolymerization of acrylonitrile (AN) onto Saccharum cilliare fiber in air in the presence of ferrous ammonium sulfate - potassium persulphate (FAS - KPS) as redox initiator. They studiedvarious parameters such as solvent, time, temperature, pH and concentration of monomer and initiator. Their maximum grafting yield was 69%. This method is smilr to our method but we use PAN.
Main target of this study is reassessmentof waste polymer and agricultural products. Results shows that our graftimg method is successful.

References

Khullar, R., Varshney, V. K., Naithani, S., & Soni, P. L. (2008). Grafting of acrylonitrile onto cellulosic material derived from bamboo (Dendrocalamus strictus). Express Polymer Letters, 2(1), 12-18.

Singha, A. S., Shama, A., & Thakur, V. K. (2009). Graft copolymerization of acrylonitrile onto Saccharum cilliari fiber. e-Polymers, 9(1).

Shibi, Indira G., and Thayyath S. Anirudhan. "Polymer- grafted banana (Musa paradisiaca) stalk as an adsorbent for the removal of lead (II) and cadmium (II) ions from aqueous solutions: kinetic and equilibrium studies." Journal of Chemical Technology & Biotechnology: International Research in Process, Environmental & Clean Technology 81.3 (2006): 433-444.

T.C. Başbakanlik Devlet İstatistik Enstitüsü Yayinlari, Tarımsal Yapı ve Üretimi, Ankara, 1995

Wang, H., Tucker, M., & Ji, Y. (2013). Recent development in chemical depolymerization of lignin: a review. Journal of Applied Chemistry, 2013.

International Conference on Science and Technology

ICONST 2018

5-9 September 2018 Prizren - KOSOVO

MPMG Metodu ile Üretilen YBCO(358) Süperiletkeninin Tuzakladığı Manyetik Alan / Trapped Magnetic Field of YBCO(358) Superconductors Produced by MPMG Method

Mehmet Başoğlu [1,2,*] , Şeyda Duman[2,3], Bakiye Çakır[3], Alev Aydıner[2]

Özet: Son 10 yılda keşfedilen YBCO(358) süperiletkeni MPMG metodu kullanılarak üretildi. Maksimum sinterleme sıcaklığı 1030°C, 1040°C ve 1050°C olmak üzere üç farklı örnek üretildi. Üretilen örneklerin XRD ölçümleri ve tuzakladığı manyetik alan değerleri ölçüldü. Ölçüm sonuçlarına göre bütün örneklerde süperiletken fazın oluştuğu gözlendi. 1050°C üretilen örneğin tuzakladığı manyetik alan değeri daha yüksek olmasına ragmen, 1030°C ve 1040°C'de üretilen örneklerin tuzaklanan manyetik alan dağılımı tek kristale benzemektedir.

Anahtar Kelimeler: Yüksek sıcaklık süperiletkenleri, Y358 süperiletkenleri, tuzaklanan manyetik alan, Eritme-Toz-Eritme-Büyütme (MPMG)

Abstract: The YBCO (358) discovered in the last decade has been produced using the superconducting MPMG method. Three different samples were produced with maximum sintering temperatures of 1030°C, 1040°C and 1050°C. The XRD measurements and trapped magnetic field of the samples were measured. As a result of the measurement, superconducting phase was observed in all samples. Although the trapped magnetic field value of the sample produced at 1050°C is higher than the other samples, trapped magnetic field distribution of the samples produced at 1040°C and 1030°C is uniform like single crystal.

Keywords: High-temperature superconductors, Y358 superconductors, trapped magnetic field, Melt-Powder-Melt-Growth (MPMG).

Giriş

1911 yılında Kamerling H. Onnes tarafından sıvı helyum sıcaklığında (4,2 K) civanın direncinin aniden sıfıra düşüşün gözlenmesi ile süperiletkenlik keşfedildi (Rose-Innes ve Rhoderick,1980). Direncin sıfıra gittiği bu sıcaklık değerinin altında maddenin süperiletken, üzerinde ise normal halde olması bunun bir faz geçişi olarak değerlendirilmesine neden olmuştur. Hal değişiminin olduğu bu sıcaklık değeri kritik sıcaklık (T_c) olarak bilinmektedir. Süperiletkenler geçiş sıcaklığının altındaki sıfır direnç özelliklerinden dolayı büyük öneme sahiptirler. Bu nedenle birçok metalik maddelerde ve alaşımlarda kritik sıcaklığı artırma çalışmaları yapılmış ve bu çalışmaların uzun süre almasına rağmen en yüksek kritik sıcaklık 1973 yılında Nb_3Ge alaşımında 23,2 K değerine kadar çıkartılabilmiştir ki, bu hala süperiletkenliğin gözlenmesinde sıvı helyuma bağımlılığı gerektirmektedir. Sıvı azot sıcaklığının (77 K) üzerinde ve oda sıcaklığına yakın kritik sıcaklığa sahip süperiletken hazırlama çalışmaları metallerde ve metal alaşımlarında bir sonuca ulaşmamıştır. Ancak metaller haricindeki malzemelerde başlangıçta çok düşük olan kritik sıcaklıkta 1986'da IBM Laboratuarında G. Bednorz ve A. Muller tarafından hazırlanan $La_{2-x}Ba_xCuO_4$ seramiğinde 30 K'de süperiletkenliğin

[1] Gümüşhane Üniversitesi, Mühendislik ve Doğa Bilimleri Fakültesi, Enerji Sistemleri Mühendisliği, 29100, Gümüşhane, TÜRKİYE
[2] Karadeniz Teknik Üniversitesi, Fen Fakültesi, Fizik Bölümü, 61080 Trabzon, TÜRKİYE
[3] Artvin Çoruh Üniversitesi, Sağlık Hizmetleri Meslek Yüksek Okulu, 08000 Artvin, TÜRKİYE
* Corresponding author: mehmetbasoglu@gumushane.edu.tr

gözlenmesiyle yeni bir çığır açılmıştır. Bu çalışmanın ardından "bakır oksit seramikleri" veya "yüksek kritik sıcaklık süperiletkenleri (YSS)" adı verilen bu grupta önce Ba yerine Sr ve Ca katkılayarak $La_{2-x}Sr_xCaCuO_4$ ile 60 K'e ulaşılmıştır. Daha sonraki çalışmalarda $YBa_2Cu_3O_7$ (Y123) ile 92 K (Wu vd., 1987), $Bi_2Sr_2Ca_2Cu_3O_{10}$ (BSCCO) ile 110 K (Maeda vd., 1988), $Tl_2Ba_2Ca_2Cu_3O_{10}$ (TBCCO) ile 125 K (Sheng ve Hermann, 1988), $HgBa_2Ca_2Cu_3O_{8+x}$ ile 132 K (Schilling ve Cantoni, 1993) kritik sıcaklık değerlerine ulaşılmıştır. Bu çalışmalara ek olarak 2009 yılında YBCO süperiletken ailesinden olan yeni bir süperiletkenlik fazı ($Y_3Ba_5Cu_8O_{18}$ (Y358)) keşfedilmiştir (Aliabadi vd., 2009). Bu fazın yapısal özelliği YBCO ailesinin diğer fazları gibi perovskit yapıda olup, yapısındaki oksijen miktarına göre tetragonal veya orthorombiktir. Birim hücresinin a ve b örgü parametreleri Y123 süperiletkeninkine yakın c parametresi ise yaklaşık üç katıdır ve bulunan en yüksek kritik geçiş sıcaklığı ise 102 K'dir (Aliabadi vd., 2009).

Süperiletkenlerin külçe özellikleri teknolojik uygulamalar için önem taşımaktadır. Külçe süperiletkenlerin endüstriyel uygulamaları için iki malzeme özelliği vardır. (Hull, 2000). Bunlardan biri, külçe süperiletkenlerin taşıyabildiği ağırlığı belirleyen kaldırma kuvveti ve diğeri de külçe süperiletkenlerin üretebildiği maksimum alanı belirleyen tuzaklanan alandır. Külçe süperiletkenlerin mühendislik uygulamalarında kullanılabilmeleri için akım taşıma kapasitelerinin (J_c) ve alan tuzaklama özelliklerinin arttırılması gereklidir. Bu nedenle tane boyutunda meydana gelebilecek bir genişleme ve dolayısıyla büyük taneli külçe süperiletken üretiminde kullanılan yöntem ve üretim şartları temelde çok önemlidir. Külçe süperiletken üretiminde "Katıhal Tepkime Yöntemi" ve "Eritme Yöntemleri" kullanılmaktadır. Eritme yöntemlerinin süperiletken üretiminde daha başarılı sonuçlar verdiği bilinmektedir (Murakami, 1992). Bu çalışmada, Y358 süperiletkeni Eritme-Toz-Eritme-Büyütme [Melt-Powder-Melt-Growth (MPMG)] yöntemi kullanılarak üretildi. Üretilen örneklerin XRD ölçümleri ile tuzakladığı manyetik alan ölçümleri yapılarak karekterize edildi.

Materyal ve Yöntem

Süperiletken örnekler Eritme-Toz-Eritme-Büyütme [Melt-Powder-Melt-Growth (MPMG)] yöntemi kullanılarak üretildi. $Y_3Ba_5Cu_8O_{18}$ (Y358) bileşiğini elde etmek için Y_2O_3, $BaCO_3$ ve CuO oksitleri kullanıldı. Başlangıç tozlarının miktarları aşağıdaki kimyasal tepkime kullanılarak belirlendi.

$$1{,}5(Y_2O_3) + 5(BaCO_3) + 8(CuO) \rightarrow Y_3Ba_5Cu_8O_{18+x} + 5(CO_2)$$

Stokiyometrik oranda tartılan başlangıç tozları agad öğütme kabına konularak el ile 15 dak. karıştırıldı ve elde edilen toz karışım homojen bir karışım elde etmek için öğütme aletine konularak 1 saat öğütüldü. Öğütülen toz Al_2O_3 pota içine konularak kare fırında yaklaşık 880°C'de 24 saat kalsinasyon işlemi yapıldı. Kalsinasyon işlemi sırasında 880°C'de toz fırından çıkarılarak bir ara öğütme yapıldı ve tekrar fırına yerleştirilerek ısıl işleme devam edildi.

Kalsinasyon sonrasında tozlar platin pota içerisinde kare fırına konularak 1450 °C'ye ısıtıldı, bu sıcaklıkta 5 dak. bekletildikten sonra pota fırından alınarak hızlı soğutma ve yönlendirme için bakır bir levha üzerine döküldü ve yine bakır bir levha ile üzerine vurularak hızlı soğuması sağlandı. (Şekil 1).

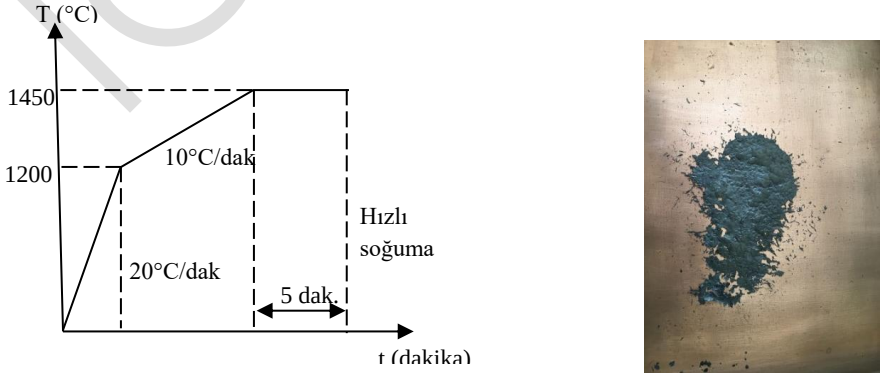

Şekil 1. Y358 toz karışımının eritme ısıl işlem şeması ve hızlı bir şekilde soğutulan toz

Eritme işlemi sonrasında elde edilen tozlar önce elde daha sonra öğütme aletine konularak 1 sa. öğütüldü. Daha sonra bu tozlardan tartılan yaklaşık 15 g toz 20 mm çapında kalıba konuldu ve 5 ton kuvvet uygulanarak silindir şeklinde tabletler elde edildi. Tabletler alümina pota üzerine konularak yüksek sıcaklık silindir fırın içine yerleştirilerek kristal büyütme işlemi yapıldı. Kristal büyütme için kullanılan ısıl işlem şeması şekil 2'de verildi. Şekilde verilen $T_{maks.}$ 1030°C, 1040°C ve 1050°C alınarak 3 farklı örnek üretildi. Üretilen örneklerin 20-60 derece aralığında XRD ölçümü alındı. Sonra yüzey manyetik alan değeri 500 mT olan 20 mm çapında NdFeB sürekli mıknatısı ile örneklerin üzerine konularak sıvı azot sıcaklığına soğutuldu. Örnek sıvı azot sıcaklığında tutularak mıknatıs uzaklaştırıldı ve örneğin tuzakladığı alan 0,25 mm hassasiyetinde yer değiştirme 1 mT hassasiyetindeki manyetik alan ölçer ile 1 mm yukarıdan ölçüldü.

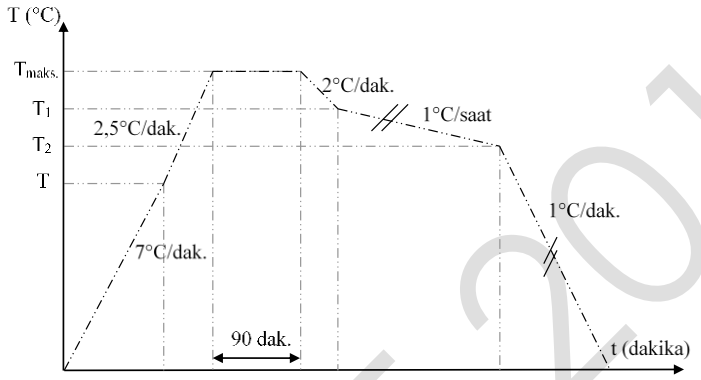

Şekil 2. MPMG yöntemi ile kristal büyütmek için kullanılan ısıl şema.

Bulgular ve Tartışma

Örneklerin x-ışını kırınım desenleri Şekil 3'te görülmektedir. Kırınım desenlerinde başlangıç tozlarının ikili veya üçlü fazlarının (Y_2BaCuO_5 (211), $BaCuO_2$, Y_2O_3, CuO) varlığını görülmemesi ve karakteristik piklerin gözlenmesi süperiletken yapının oluştuğu gösterir. 1030°C de üretilen örneğin çok sayıda pik içerdiği görümektedir. Bu durum örneğin farklı yönelimlere sahip taneler içerdiğini gösterir. Sıcaklık artmasıyla küçük piklerin yok olduğu bununla birlikte yaklaşık 33°'de oluşan piklerin yüksekliğinin arttığı gözlendi. Bu durum 1040°C ve 1050°C de üretilen örneklerde baskın bir süperiletken yapının olduğunu ifade eder. Bu nedenle 1040-1050°C sıcaklık aralığın büyük taneli Y358 üretimi için uygun olduğu söylenebilir.

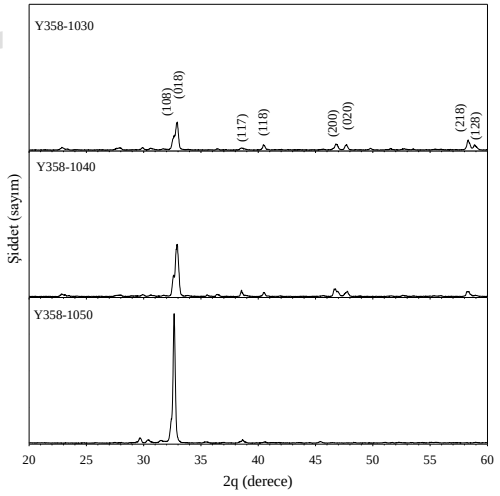

Şekil 3. Örneklerin X-ışınları kırınım desenleri.

Şekil 4'te örneklerin tuzakladığı manyetik alanın örnek yüzeyinde probun bulunduğu yere göre grafiği verilmektedir. Örneklerin üretildiği maksimum sıcaklık arttıkça örneklerin tuzaklanan manyetik alan değerlerinin de artığı gözlendi. Tuzaklanan manyetik alan değerinin yüksek olması için örneklerin akım taşıma kapasitelerinin yüksek olması ve manyetik akıların örneğin içerisinde etkin bir şekilde çivilenmesi gerekir. Süperiletken olmayan fazların ve yapısal kusurların (dislokasyonlar, tane sınırları vb.) süperiletken örneklerde etkin çivileme merkezleri olarak kullanıldığı bilinmektedir [Jun vd., 2011].

Ayrıca tuzaklanan alan değeri örneğin tekmi yoksa polikristalmi olduğu hakkında bilgi de vermektedir. 1030°C ve 1040°C'de üretilen örneklerin tuzakladığı manyetik alan deseni incelendiğinde manyetik olarak tek domain olduğu ve 1050°C örnekte ise kabaca 2 manyetik bölge olduğu gözlendi. X-ışını kırınım desenlerinden 1030°C örneğinde daha fazla pik gözlendiğinden diğer örneklere göre daha taneli bir yapıda olduğu düşünülmesine rağmen tuzaklanan manyetik alan desenleri incelendiğinde tek bir domain olduğu gözlendi bu durumun örneğin tane sınrlarının temiz olması dolayısıyla tane bağlantılarının iyi olmasından kaynaklandığı düşünülmektedir. Diğer yandan, 1050°C örneğinin en yüksek tuzaklanan manyetik alan değerine sahip olmasının yanında manyetik bölge sayısının diğer örneklere göre fazla olmasından dolayı bu örneğin tane bağlatılarının zayıf olabileceği düşünülmektedir.

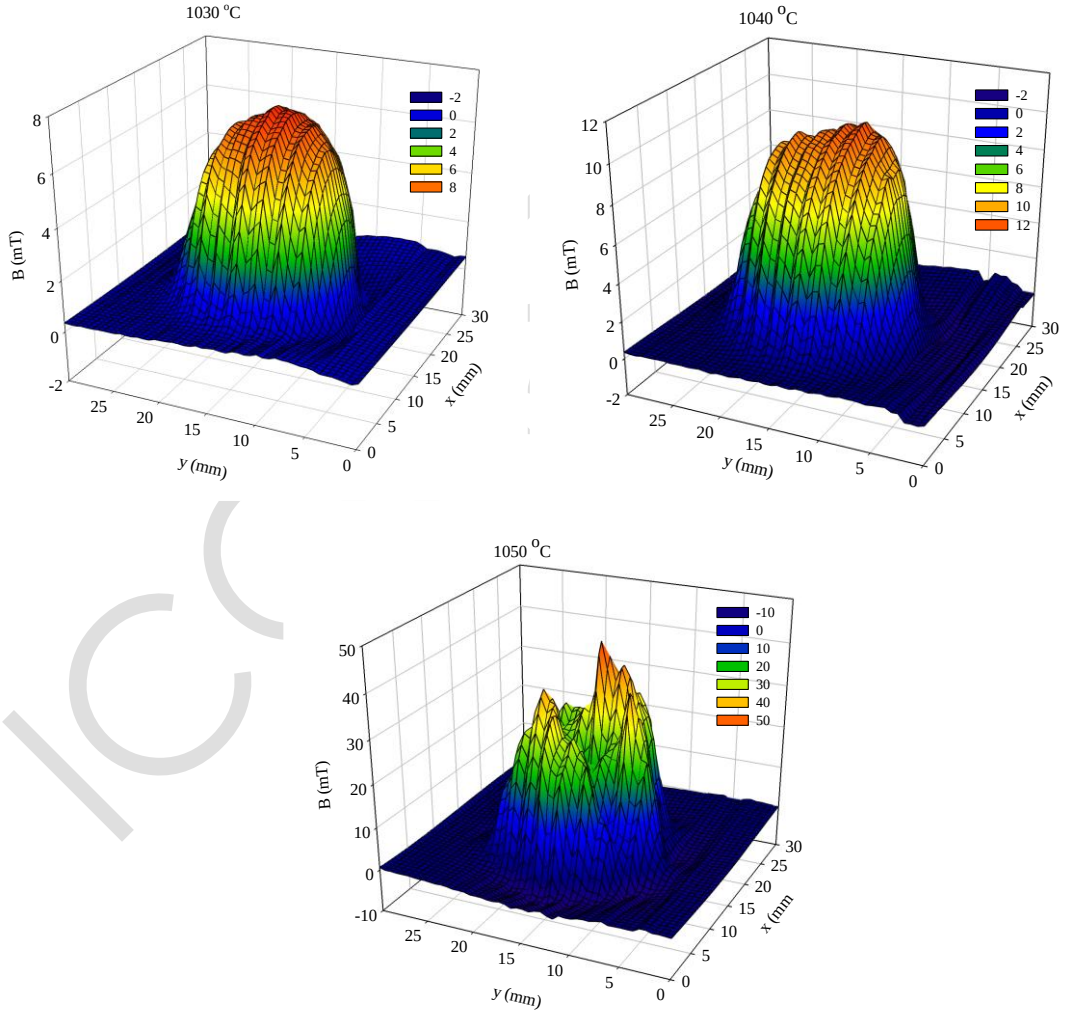

Şekil 4. Örneklerin tuzakladığı manyetik alan değerlerinin yüzey yerdeğiştirmesine karşı grafiği.

Sonuçlar

MPMG yöntemi kullanılarak farklı büyütme sıcaklıklarında üç örnek üretildi ve örneklerin üretiminde Y2O3 tozu kullanıldı. Örneklerin X-ışını kırınım desenlerinden tüm örneklerde Y358 süperiletken yapısının oluştuğu ve örneklerin taneli bir yapıda olduğu gözlendi. 1040-1050°C de üretilen örneklerin 1030 örneğie göre daha fazla taneli olduğu dolayısıyla 1040-1050°C sıcaklık aralığının büyük taneli Y358 üretimi için en uygun sıcaklık aralığı olduğu görüldü.

1040 ve 1050°C üretilen örneklerin tuzaklanan manyetik alan değerlerin daha yüksek olduğu fakat 1050°C'de üretilen örneğin diğer örneklere göre fazla manyetik domaine sahip olmasından tane bağlantılarının zayıf olduğu söylenebilir.

Teşekkür

Bu çalışma TÜBİTAK tarafından desteklenmiştir (Proje no: TBAG-117F484)

Kaynaklar

Aliabadi, A., Farshchi, Y.A., Akhavan, M. 2009. "A new Y-based HTSC with Tc above 100 K", Physica C, 469, 2012-2014.

Bednorz, J. G. ve Müler, K. A. 1986. "Possible High Tc Superconductivity in the La-Ba-Cu-O System", Z. Phys. B-Condensed Matter, 64, 189-193.

Hull, J.R. 2000. "Superconducting Bearings", Supercond. Sci. Technol., 13, R1-R15.

Jun B.H., Jung S.H., Park S.D., Park B.J. Han Y.H. ve Kim C.J. 2011. "Effects of Y_2O_3 additions on the oxygen diffusion in top-seeded melt growth processed $YBa_2Cu_3O_{7-y}$ superconductors" Physica C. 471, 876-879.

Maeda, H., Tanaka, Y., Fukutami, M. ve Asano, T. 1988. "A New High-Tc Oxide Superconductor without a Rare Earth Element", Jpn. J Appl. Phys. Lett., 27, L209-L210.

Murakami, M. 1992. "Processing of Bulk YBaCuO", Supercond. Sci. Technol. 5, 185-203.

Rose-Innes, A.C. ve Rhoderick, E.H. 1980. "Introduction to Superconductivity (Second Edition)", England: Pergamon Press Ltd.

Schilling, A. ve Cantoni, M. 1993. "Superconductivity above 130 K in the Hg–Ba–Ca–Cu–O system", Nature, 363, 56-58.

Sheng, Z. Z. ve Hermann, A. M. 1988. "Superconductivity in the rare-earth-free Tl–Ba–Cu–O system above liquid-nitrogen temperature", Nature, 332, 55-59.

Wu, M. K., Ashburn, J. R., Torng, C. J., Hor, P. H., Meng, R. L., Gao, L., Huang, Z. J., Wang, Y. Q., Chu, C.W. 1987. "Superconductivity at 93 K in a new mixed-phase Y-Ba-Cu-O compound system at ambient pressure", Phys. Rev. Lett. 58, 908-910.

International Conference on Science and Technology

ICONST 2018

5-9 September 2018 Prizren - KOSOVO

Assessment of Energy Saving Potential for Mehmet Akif Ersoy University Campus With Using a Co-Generation System

Sertaç GÖRGÜLÜ[1*], Arif Emre ÖZGÜR[2]

Özet: Kojenerasyon uygulamaları enerji ekonomisi açısından önemli olduğu gibi çevre açısından olumlu bir uygulamadır. Özellikle elektrik enerjisinin fosil kaynaklı yakıtlardan elde edildiği uygulamalar daha büyük önem arz etmektedir. 2014 yılında, yakıt yakılarak elde edilen yerel elektrik üretim verimi, Avrupa Birliğinde ortalama % 47,6 iken ülkemizin ve AB üyesi olmayan diğer iki ülke (İzlanda ve Norveç) ortalaması ise % 41,8 olarak gerçekleşmiştir.

Bu çalışmada, bir üniversite kampüsünün, kojenerasyon uygulaması ile toplam enerji tasarrufuna ait bir değerlendirme sunulmuştur. Tüm veriler Mehmet Akif Ersoy Üniversitesinin İstiklal yerleşkesi için alınmıştır. Hem ısıtma hem de elektrik enerjisi gereksinimlerini karşılamak üzere bir sistem modellenmiştir. Kampüs coğrafyasının zorluğu ve kampüs binaları arasındaki mesafeler nedeniyle, sistem kapasitesi sınırlandırılmıştır. Bu durumda, bazı kampüs binalarının ısıtma enerjisi ihtiyacı kojenerasyon sistemi ile karşılanırken, yerleşkenin elektrik ihtiyacının tamamı kojenarasyon sistemi ile elde edilebilmektedir. Ekonomik ve enerji performansı değerlendirmeleri, bu strateji için yapılmıştır. Sonuçlar, tablolar halinde sunulmuştur.

Anahtar Kelimeler: Kojenerasyon, kampüs, enerji değerlendirmesi, Mehmet Akif Ersoy Üniversitesi.

Abstract: Cogeneration technologies are a positive application in terms of environment as well as important in terms of energy economy. Especially when electricity energy is derived from fossil fuels, these matters are much more important. In 2014, average electricity generation efficiency from fossil fuels was 47.6% in the European Union. However, this rate was 41.8% for our country and the other two non-EU countries (Iceland and Norway). These values indicate the importance of cogeneration applications.

In this study, an assessment of total energy saving potential for a University Campus is presented with using co-generation application. All data has been obtained from İstiklal Campus of Mehmet Akif University. A system is modelled for heating and electricity requirements. Because of the campus geography difficulties and distances from the faculty buildings suggested system capacity is limited. So heating energy requirement of some faculty buildings can be produced by the system. However, the total electricity requirement can be obtained with the system. Economical and energetic evaluations are made for this strategy. Results are presented with tables.

Keywords: Co-generation, campus, energy assessment, Mehmet Akif Ersoy University.

Introduction

Cogeneration technologies are positive applications in terms of environment as well as important in terms of energy economy. Especially when electricity energy is derived from fossil fuels, these matters are much more important (Şenol and Musayev, 2017). In 2014, average electricity generation efficiency from fossil fuels was

[1] Mehmet Akif Ersoy University, Engineering and Architecture Faculty, 15030, Burdur, TURKEY
[2] Isparta Applied Science University,Technology Faculty, 32260, Isparta, TURKEY
*Corresponding author: sgorgulu@mehmetakif.edu.tr

47.6% in the European Union. However, this rate was 41.8% for our country and the other two non-EU countries (Iceland and Norway). (EEA, 2015). These values indicate the importance of cogeneration applications. Taking into consideration that both the electricity and the heat energy are needed for a large part of the enclosed spaces, the simultaneous supply of this need from the same source means a decrease in the energy costs. Simultaneous electricity and heat production can lead to successful results, especially in buildings where there is intense activity throughout the day, such as university buildings. For example, Macquarie University is told to save a total of 20 million dollars in energy costs for 23 years with a $ 6.3 million investments to purchase two natural gas generators (2x760 kW). With this investment, it is stated that the university. In addition, emissions of carbon dioxide are indicated to be reduced by 5,400 tons per year (NSW, 2013). According to a research conducted in the USA in 2016, it is stated that a total of 272 universities and colleges developed solutions with simultaneous heat and electricity production (Control Engineering, 2017). Another study by Üçgül and Elibüyük, 2015 underlines that a university tri-generation application is essential in terms of sustainability and the system has a payback period of 25 months (Üçgül and Elibüyük, 2015).

Material and Method

This study was carried out in Mehmet Akif Ersoy University, which is located in the province of Burdur in the Mediterranean region. The largest campus of the university, İstiklal Campus, is located 6 km southeast of the city center, at the 10th kilometer of the Burdur-Antalya highway. As of the end of 2016, University has 10 Faculties, 4 Institutes, 5 Schools, 13 Vocational Schools and Turkish Music State Conservatory. Various numerical data related to the university for the years 2015 and 2016 are presented in Table 1. (Mehmet Akif Ersoy University Internal Evaluation Report, 2016).

Table 1. Information about the University

	2015	**2016**
Number of Campus	11	12
Total open space (m^2)	9,990,040.86	9,990,040.70
Total indoor space (m^2)	232,589	290,542
Number of students	25,047	29,482
Indoor space of Istiklal Campus (m^2)	167,052	219,399

According to the data between 1931 and 2016, Burdur province has an annual average temperature of 13.2 ºC, an annual average maximum temperature of 19.3 ºC and an annual average minimum temperature of 7.5 ºC. The highest temperature measured between the same years is 41 ºC, the lowest temperature is -16.7 ºC (MGM, 2017).

Electricity and natural gas consumption of the İstiklal Campus for the year 2016 are given in Table 2. It is observed that most of the natural gas boilers used on the campus are three-pass gas-fired hot water boilers. The average thermal efficiency can be 94% for this system (Erensan, 2007). By the end of 2016, the calculated thermal power capacity of the campus is approximately 18,250 kW. This data was calculated considering the sum of the label values existing natural gas boilers on campus. Reserve boilers are not included in this calculation. In addition, the peak energy usage of the campus for 2016 was 690,600 kWh / month in December. It is accepted that approximately 15% of this value is related to secondary education activities on campus.

Table 2. Monthly Electricity and Natural Gas Usage of MAKÜ Istiklal Campus in 2016.

Months	Electricity (kWh)	Natural gas (kWh)
January	634.633,70	4.044.615,97
February	553.656,27	2.696.490,26
March	600.529,50	2.304.844,21
April	484.793,80	894.231,38
May	467.847,45	263.804,11
June	466.268,80	72.359,29
July	409.553,50	47.622,14
August	535.685,40	68.824,75
September	429.465,00	73.324,47
October	493.006,70	149.480,98
November	589.409,20	1.952.733,40
December	**690.600,00**	**4.163.703,38**
TOTAL	***6.355.449,32***	***16.732.034,34***

Figure 1a shows the whole campus area. Figure 1b shows the working campus area.

Figure 1. University's whole campus area and working campus area

1	Rectorates	6	Scientific and Technology Research and Application Center
2	Faculty of Economics and Administrative Sciences	7	Avşar Han
3	Veterinary Clinic Building	8	Faculty of Education
4	Faculty of Veterinary Medicine	9	Faculty of Art and Science
5	Faculty of Health Sciences	10	Library (under construction)

A study by Kıncay and Yumurtacı, 2006 investigates Yildiz Technical University's cogeneration system of electrical energy usage. In 2006, for Yıldız Technical University Davutpaşa Campus, the study was carried out an economic analysis of suitable cogeneration systems according to the annual consumption of electricity and heat (Kıncay and Yumurtacı, 2006). In this study, a power account was made for the use of energy, taking into consideration the duration of electricity use for 26 days a month and 15 hours a day. According to this approach, it is understood that a 1.77 MW electrical power system may be sufficient in order to meet peak usage values for the campus area. Considering 22 days a month and 10 hours a day, it is calculated that, 3.14 MW electric power systems will be required in order to meet peak usage. Considering under construction buildings in the campus and 220 operating hours per month, 4 MW electrical power system will be required. It has been evaluated that the cogeneration system with this electric power can meet the heat energy needs of buildings, which are expressed in Table 3 in dark. In this evaluation, the electrical power generation efficiency and thermal efficiency of the cogeneration system are taken as 45.7% and 45% respectively (2G Kojenerasyon, 2018). So the total efficiency of co-generation unit is assumed that 90.7%.

Table 3. Boiler Capacity of Campus Buildings

Faculty Name	Boiler Capacity (kW)
Faculty of Veterinary Medicine	***3,198***
Faculty of Health Sciences	***698***
Faculty of Economics and Administrative Sciences	1,810
Veterinary Clinic Building	1,454
Faculty of Art and Science	5,200
Faculty of Education	*2,326*
Faculty of Divinity	*582*
Rectorates	1,950
Scientific and Technology Research and Application Center	600
MAKÜ Sports Area	2,152
Avşar Han	932
Library (under construction)	608
TOTAL	***21,510***

Total natural gas volume to produce electricity capacity of selected co-generation system can be calculated with following equation.

$$\dot{V}_{gas,cogen} = \frac{\dot{W}_{electricity}}{h_{l,gas} \cdot \eta_{electricity,cogen}}$$

Simultaneoulsy produced heat by co-generation system with same natural gas volume can be calculated with;

$$\dot{Q}_{heat} = \dot{V}_{gas,cogen} \cdot \eta_{gas,cogen} \cdot h_{l,gas}$$

equation. If same electricity and heat capacity produced with co-generation unit is obtained with conventional methods, the required natural gas volume will increase. At this time, the required electricity capacity is obtained from national electricity distribution network and the required heat is produced with conventional gas boilers. This increased natural gas volume is obtained from;

$$\dot{V}_{gas,conventional} = \frac{\dot{W}_{electricity}}{h_{l,gas} \cdot \eta_{electricity,ned}} + \frac{\dot{Q}_{heat}}{h_{l,gas} \cdot \eta_{gas,boiler}}$$

The difference between these two natural gas volume is indicator for energy saving potential with using co-generation unit. This difference has been calculated and presented in the next. The lower heating value of

natural gas is assumed as 32.56488 MJ/m^3. The used efficiency values in the analysis is summarized with table 4.

Table 4. The used efficiency values in the analysis.

Efficiency	Value
$\eta_{electricity,cogen}$	0.457
$\eta_{gas,cogen}$	0.45
$\eta_{electricity,ned}$	0.418
$\eta_{gas,boiler}$	0.94

Results

The difference between required natural gas volume rate for investigated two scenarios (cogeneration system and conventional usage) are presented with figure 2.

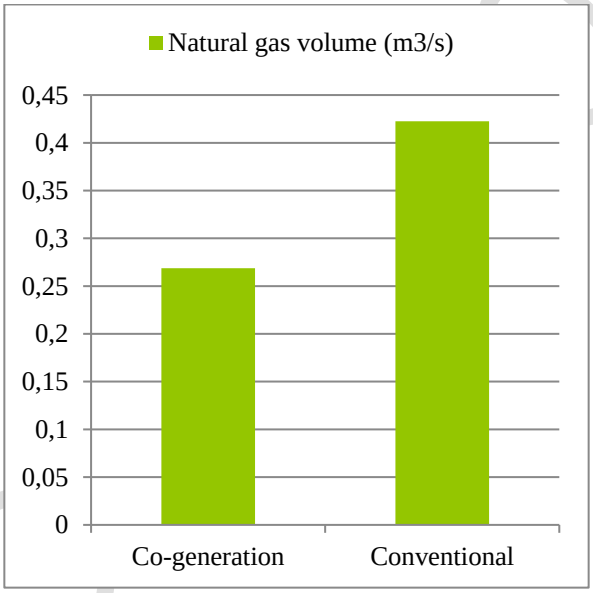

Figure 2. The difference between required natural gas volume rate for investigated two scenarios.

One can be concluded that from this table, total energy saving rate is 36.4% (for 220 operation hour per a mounth). The natural gas price for Burdur is 0.9689 TL/m^3 at August 2018 (http://www.torosgaz.com.tr/isparta/faturaparametreleri.html). At this time total cost saving is 825,000 TL for 7 months operation period. If heating capacity will used for swimmimng pool water heating in summer session, this cost saving can be reached 1,400,000 TL. The cogeneration system installation cost can be assumed 30.000.000 TL (4.000.000 €) for 4 MW electricity capacity. The actual electricity price per kwh is 0,229814 TL for August 2018. At this time the invest payback time 14.8 year with no increase rate for electricity price per kwh. So one can be concluded that, the cogernation system payback time can be lower than 14.8 year for the university campus. If increase rates of natural gas and electricity prices are assumed 3% and 5% for a year, respectively, the payback time can be obtained about 10 years.

Discussion and Conclusions

In this study, a co-generation unit is exaimed in point of view energy saving potential for a university campus. System elecrticty capacity is sufficient for campus usage. However, heating capacity obtained with the system is sufficient for only two building of the campus. It is observed that the co-genertion system payback time can

be low as 10 years. Energy saving potential is obtained 36.4% for the campus. This results have important for environmental and national economics.

References

2G Kojenerasyon ürün kataloğu, (2018). https://www.2-g.com/module/dateidownload/erdgas_b.37_tr_2.1.pdf (Erişim Tarihi: 01/08/2018).

Control Engineering, (2017). https://www.controleng.com/single-article/chp-makes-sense-for-universities/e0b0c4ca70d83a5a443b5e65eaa64d26.html (Erişim Tarihi: 17/12/2017).

EEA, (2015). European Environment Agency. https://www.eea.europa.eu/data-and-maps/indicators/efficiency-of-conventional-thermal electricity-generation-4/assessment-1 (Erişim Tarihi: 18/03/2018).

Erensan, (2007). http://www.erensan.com.tr/tr/urun_trp.asp (Erişim Tarihi: 01/04/2018).

Kıncay, O., Yumurtacı Z. (2006). Bir Üniversite Kampüsü için Uygun Enerji Sisteminin Seçimi. Tesisat Mühendisliği Dergisi 95, 5 – 12.

Mehmet Akif Ersoy University Internal Evaluation Report, (2016). https://sgdb.mehmetakif.edu.tr/files/2016-yili-Kurum-ic-Degerlendirme-Raporu.pdf (Erişim Tarihi: 14/09/2017).

MGM, (2017). Tarım ve Orman Banalığı, Meteoroloji Genel Müdürlüğü Resmi İstatistikleri https://mgm.gov.tr/veridegerlendirme/il-ve-ilceler-istatistik.aspx?k=A&m=BURDUR (Erişim Tarihi: 17/10/2017).

NSW, (2013). https://www.energy.nsw.gov.au/energy-consumers/sustainable-energy/cogeneration (Erişim Tarihi: 17/05/2018).

Şenol, Ü., Musayev Z. (2017). Rüzgar Enerjisinden Elektrik Üretiminin Yapay Sinir Ağları İle Tahmini, Bilge International Journal of Science and Technology Research 1(1), 23 – 31.

Torosgaz, (2018). http://www.torosgaz.com.tr/isparta/faturaparametreleri.html (Erişim Tarihi: 29/08/2018).

Üçgül, İ., Elibüyük, U. (2015). Üniversite Yerleşkeleri İçin Doğalgazlı Trijenerasyon Sisteminin Değerlendirilmesi. Süleyman Demirel Üniversitesi Mühendislik Bilimleri ve Tasarım Dergisi 3(2), 105-109.

International Conference on Science and Technology

ICONST 2018

5-9 September 2018 Prizren - KOSOVO

Determination of Waste Heat Potential of A Cement Production Facility

Mehmet ALTINKAYNAK[1]*, Ali Kemal YAKUT[1], Arif Emre ÖZGÜR[1]

Abstract: Cement is at the top of the building materials in the world. Therefore, there are high-level production facilities and capacities. Looking at the side of energy input, the cement sector, which takes place in the first place in terms of energy demand of the industry, is also in the top rank according to the amount of fuel used. Cement factories, mainly limestone, marble and clay mixture is milled in a mill to produce coal, natural gas, etc. from the raw material called farina type fuels to produce clinker. Fuel energy released during this clinker is used to preheat cyclones before entering the farina rotary kiln. It is possible to recover the waste heat in this preheating and in the chimney. There are a total of 52 cement factories in Turkey as of 2018. In this study, the potential of the energy of the burned gas circulating in the preheating process, namely cyclones and chimneys, will be presented in a point-by-point manner, taking into account the actual cement factory data. By placing steam exchangers in these potential points, it will be expressed that power generation can be done by Rankine cycle.

Keywords: Cement, Heat Recovery, Energy, Klinker, Farine.

Introduction

Cement is derived form " caementum " Word and it means that, a piece of stone. It has been used 1300 years at France. The last name is " cement " at England and that means " connective ". (http://www.betonvecimento.com/cimento/cimento-2).

The first cement factory was established at 1848 in England. The biggest cement production in our world at China. At 2015, cement production reached 4.6 billion tons. While cement production make in 149 countries, but it is never produced in 17 countries. Cement production quantities is given in Figure 1. The largest production is in China with 2350 million tons.

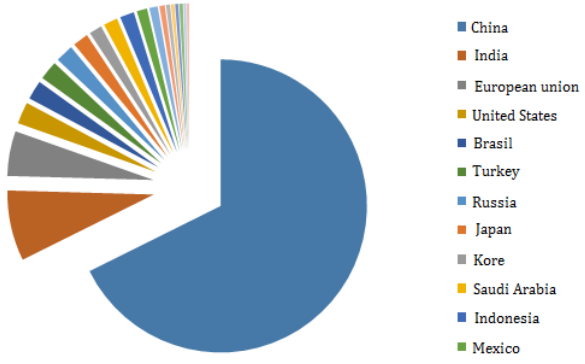

Fig 1. Distribution of Word cement production in 2015 (Cembureau,2015).

[1]Isparta University of Applied Sciences, Technolgy Faculty, 32260, Isparta, TURKEY
*Correspondingauthor: mehmetaltinkaynak@gmail.com

The first cement factory was established at 1911 in Turkey in İstanbul of Darıca religion. It has 20000 tons. At 2016, in Turkey's cement factories' capacity; Marmara Region has 29.3 million tons, Mediterranean Region has 35.5 million tons, Central Anatolia has 18.9 million tons, Black sea Region has 14.7 million tons, Southeastern Anatolia has 10.3 million tons, Aegean sea Region has 10.7 million tons and the last one Eastern Anatolia Region has 13.2 million tons. Turkey regional cement production quantities is given in Figure 2.

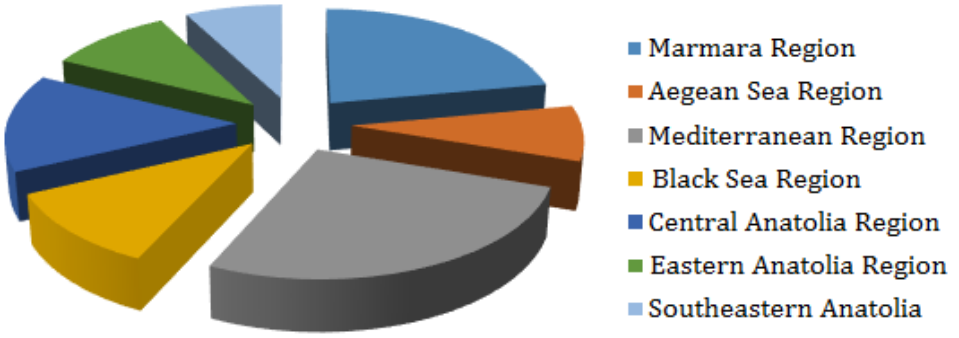

Fig 2. Turkey regional cement production quantities (TCMB, 2017a)

2. Cement Production Stages

The cement production is given in Figure 3. 1-3 stages is seen, raw material preparation, 3-4 stages is seen, farine preparation, 4-6 stages is seen, clinker formation, 6-7 stages is seen, cement grinding and packaging indicate.

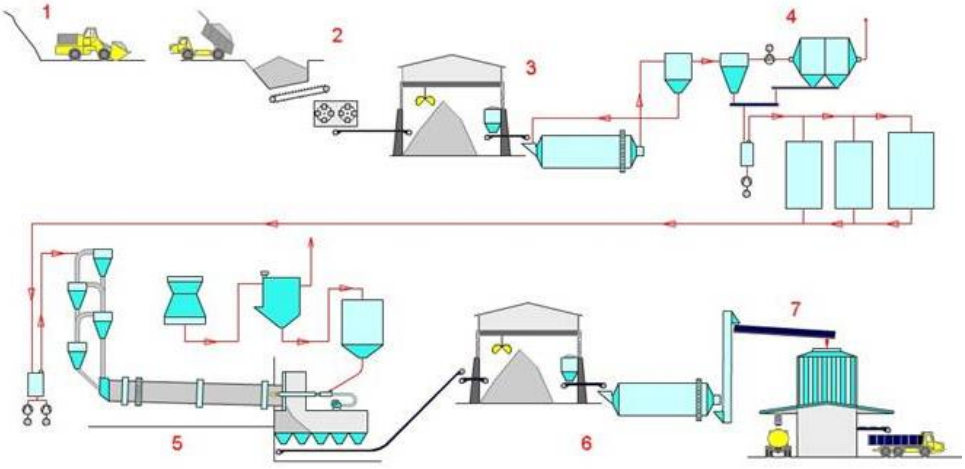

Fig 3. Cement production line general schema (TCMB, 2017b)

3 . Thermodynamic Analysis

In this study, a cement factory with two production lines (system 1 and system 2) has been examined. The Rankine Cycle was applied to these two lines and is named system 3. Schematic drawing of the system 3 is given at Figure 4.

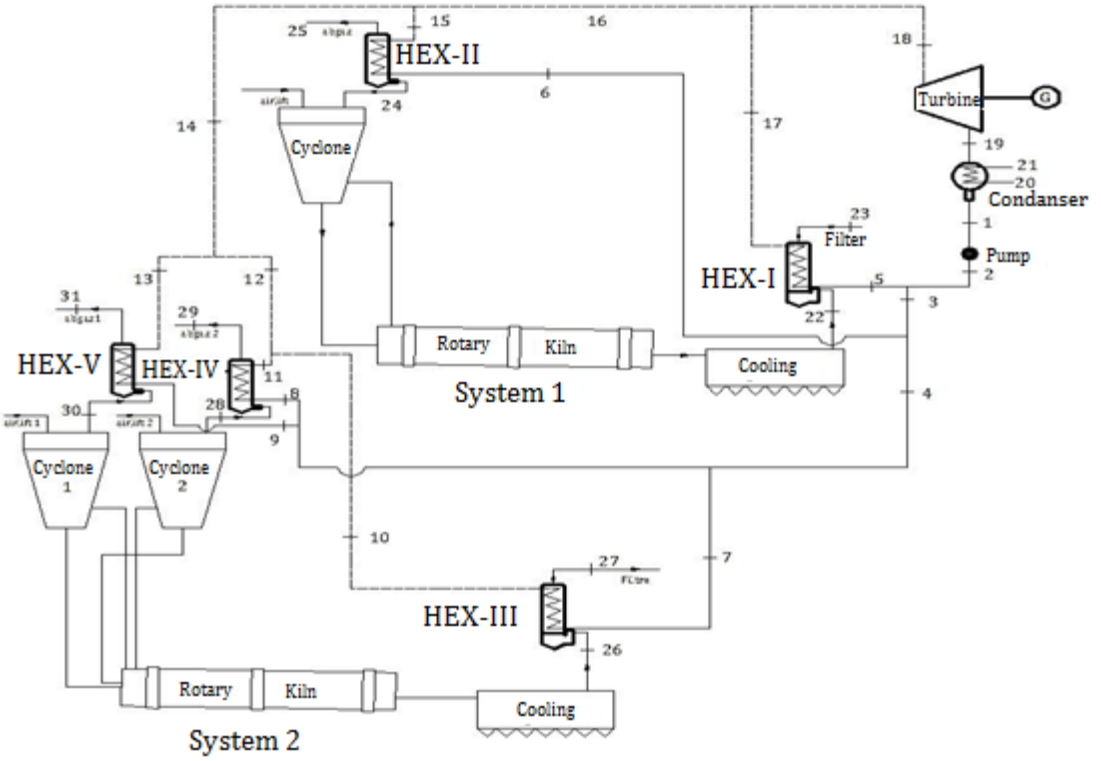

Fig 4. Schematic drawing of the system 3

First and second law analysis of the system components are summarized in table 1.

Table 1. First and second law analysis of the system components (Dincer,2011;Dincer, 2013;)

Component	*Schematic Figure*	*Mass, Energy, Exergy Balance*
Pump	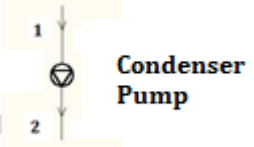	$\dot{m}_1 = \dot{m}_2$ $\dot{m}_1 h_1 + \dot{W}_{pump} = \dot{m}_2 h_2$ $\dot{m}_1 ex_1 + \dot{W}_{pump} = \dot{m}_2 ex_2 + \dot{E}x_{d,pump}$
Heat Exchanger I	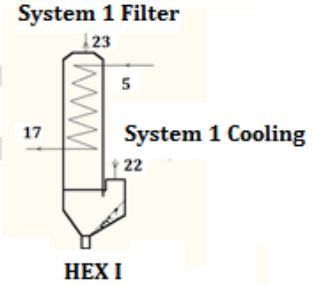	$\dot{m}_5 + \dot{m}_{22} = \dot{m}_{17} + \dot{m}_{23}$ $\dot{m}_5 h_5 + \dot{m}_{22} h_{22} = \dot{m}_{17} h_{17} + \dot{m}_{23} h_{23}$ $\dot{m}_5 ex_5 + \dot{m}_{22} ex_{22} = \dot{m}_{17} ex_{17} + \dot{m}_{23} ex_{23} + \dot{E}x_{d,HEX\ I}$

Heat Exchanger II	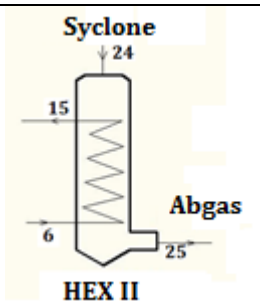	$\dot{m}_6 + \dot{m}_{24} = \dot{m}_{15} + \dot{m}_{25}$ $\dot{m}_6 h_6 + \dot{m}_{24} h_{24} = \dot{m}_{15} h_{15} + \dot{m}_{25} h_{25}$ $\dot{m}_6 ex_6 + \dot{m}_{24} ex_{24} = \dot{m}_{15} ex_{15} + \dot{m}_{25} ex_{25} + \dot{E}x_{d,HEX\ II}$
Heat Exchanger III	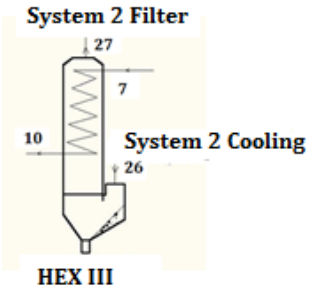	$\dot{m}_7 + \dot{m}_{26} = \dot{m}_{10} + \dot{m}_{27}$ $\dot{m}_7 h_7 + \dot{m}_{26} h_{26} = \dot{m}_{10} h_{10} + \dot{m}_{27} h_{27}$ $\dot{m}_7 ex_7 + \dot{m}_{26} ex_{26} = \dot{m}_{10} ex_{10} + \dot{m}_{27} ex_{27} + \dot{E}x_{d,HEX\ III}$
Heat Exchanger IV	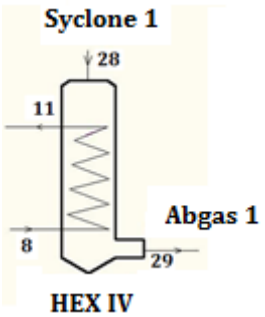	$\dot{m}_8 + \dot{m}_{28} = \dot{m}_{11} + \dot{m}_{29}$ $\dot{m}_8 h_8 + \dot{m}_{28} h_{28} = \dot{m}_{11} h_{11} + \dot{m}_{29} h_{29}$ $\dot{m}_8 ex_8 + \dot{m}_{28} ex_{28} = \dot{m}_{11} ex_{11} + \dot{m}_{29} ex_{29} + \dot{E}x_{d,HEX\ IV}$
Heat Exchanger V	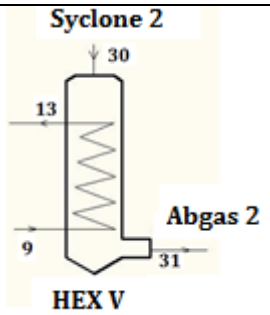	$\dot{m}_9 + \dot{m}_{30} = \dot{m}_{13} + \dot{m}_{31}$ $\dot{m}_9 h_9 + \dot{m}_{30} h_{30} = \dot{m}_{13} h_{13} + \dot{m}_{31} h_{31}$ $\dot{m}_9 ex_9 + \dot{m}_{30} ex_{30} = \dot{m}_{13} ex_{13} + \dot{m}_{31} ex_{31} + \dot{E}x_{d,HEX\ V}$
Turbine	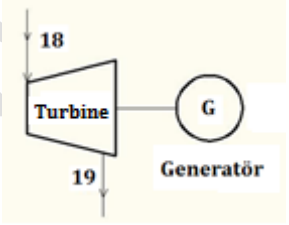	$\dot{m}_{18} = \dot{m}_{19}$ $\dot{m}_{18} h_{18} = \dot{m}_{19} h_{19} + \dot{W}_{türbin}$ $\dot{m}_{18} ex_{18} = \dot{m}_{19} ex_{19} + \dot{W}_{türbin} + \dot{E}x_{d,turbine}$

Condenser	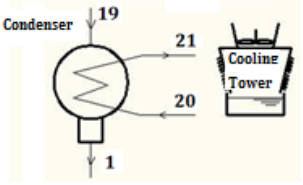	$\dot{m}_{19} + \dot{m}_{20} = \dot{m}_1 + \dot{m}_{21}$ $\dot{m}_{19}h_{19} + \dot{m}_{20}h_{20} = \dot{m}_1 h_1 + \dot{m}_{21}h_{21}$ $\dot{m}_{19}ex_{19} + \dot{m}_{20}ex_{20} = \dot{m}_1 ex_1 + \dot{m}_{21}ex_{21} + \dot{E}x_{d,Condanse}$

4. Results And Discussion

As a result of the thermodynamic analyzes applied to System 1 and System 2, in System 3, the potential points to which the Rankine cycle is applied are determined.
These points;

- The first one, between cooling unit and filter of System 1, HEX-I.
- Secondly, System 1 has preheater cyclone inlet HEX-II.
- Thirdly, between cooling unit and filter of System 2, HEX-III.
- The other one, System 2 has first preheater cyclone inlet HEX-IV.
- The last one is, System 2 has second preheater cyclone inlet HEX-IV.

As it seen in Figure 4, these heat exchangers will be established. Total steam produced in heat exchangers has 320-380 °C temperatures, it is used for Rankine Cycle in power generation.
According to turbine inlet temperature, power generation and System efficiency is given Figure 5.

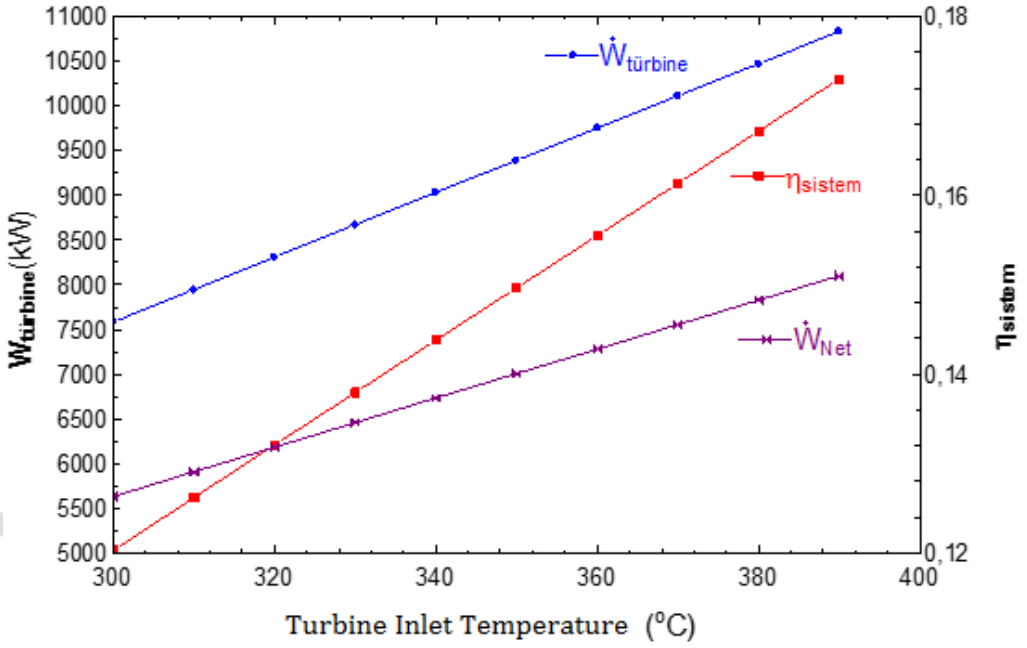

Fig 5. Turbine inlet temperature, power generation and System efficiency

According to turbine inlet temperature, exergy efficiency, exergy destroyed and turbine power is given Figure 6.

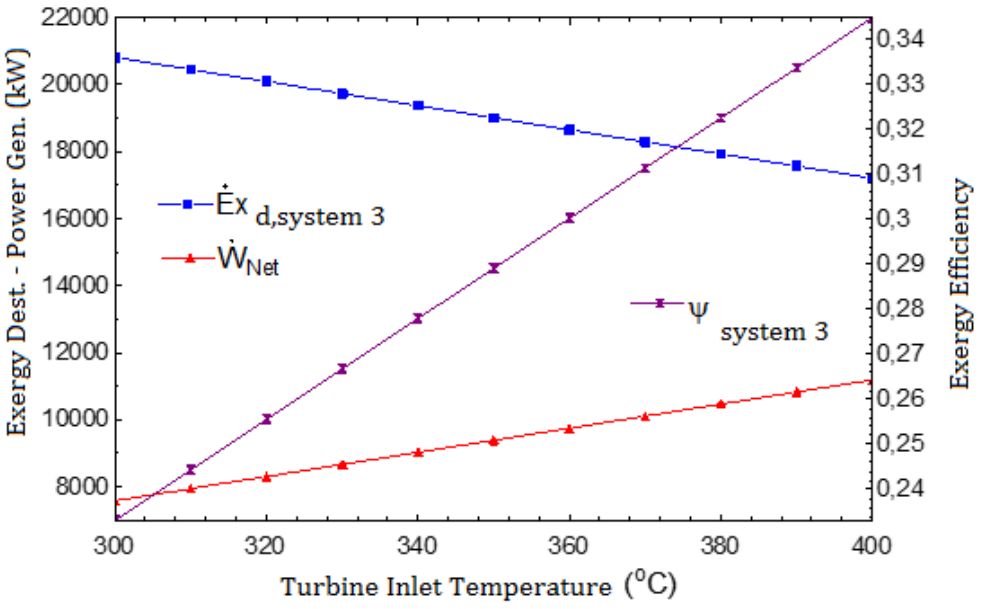

Fig 6. Exergy eficiency and exergy destroyed of the system 3

5. References

Cembureau, 2015. http://cembureau.eu/media/1503/2015activityreport_cembureau.pdf (Erişim Tarihi: 10.03.2017.)

Dincer, C. Zamfirescu, Sustainable energy systems and applications, New York, NY: Springer, 2011.

Dincer, I., Rosen, M. A. Exergy: Energy, Environment and Sustainable Development, Elsevier, 225 Wyman Street, Waltham, MA 02451, USA, Second edition 2013.

TCMB, 2017a. Türkiye Çimento Mühtahsilleri Birliği. http://www.tcma.org.tr/index.php?page=icerikgoster&cntID=29(Erişim Tarihi : 10.03.2017.)

TCMB, 2017b. Türkiye Çimento Mühtahsilleri Birliği. http://www.tcma.org.tr/images/file/ocak%202017%20cimento%20harita.jpg (Erişim Tarihi : 10.03.2017)

International Conference on Science and Technology

ICONST 2018

5-9 September 2018 Prizren - KOSOVO

Efficiency Analysis of A Single Stage Subcritical R744 Heat Pump

Arif Emre ÖZGÜR[1*], Hilmi Cenk BAYRAKÇI[2], Ahmet ELBİR[3], Özdemir DENİZ[3], Mehmet ALTINKAYNAK[2]

Abstract: CO2 has excellent thermophsical properties. However, CO2 has unity global warming potential and zero ozone depletion potential. So, CO2 is a unique alternative cycle fluid for heat pumps cycles. An experimental set up has been produced for analysis study. The system has different capilar tubes. It has been planned that experimental measurements will be presented. In this study, the effectiveness of a single – stage CO2 transcritical heat pump cycle was presented. Thermodynamic analysis of a transcritical CO2 heat pump has been presented. Thermodynamic properties of CO2 have been made using software (Engineering Equation Solver – EES).

Keywords: CO2, transcritical, heat pump cycle, analysis.

Introduction

Increased global warming and environmental damage will be much smarter to use environmentally friendly refrigerants in industrial cooling systems. In recent years, synthetic refrigerants have been seen much more damage to the environment in cooling technology, and the use of CO2 (R744), which is a natural refrigerant, has increased. The CO2 gas is a refrigerant with ODP = 1 and GWP = 0 properties. Transcritical CO2 has come into use effectively in heating and cooling systems. The costs of transcritical systems are considerably higher than those of traditional HFC- based systems. However, operating costs are less. There are more than four million installed transcritical CO2 household heat pumps throughout the world.

R-744 is not flammable and also not explosive. It is also nontoxic. The evaporation latent heat of R-744 is high. Therefore, the amount of fluid to be loaded into the cooling system is relatively low. The biggest problem with the systems in which the R-744 is used is the presence of higher operating pressures than conventional systems. Since R-744 has a low critical temperature, it is necessary to use transcritical cycles.

Yang and etc. (2010) have focused on the modeling and simulation of transcritical CO2 heat pump systems in their study. In this study, a heat pump model was established and the conditions required to obtain maximum Coefficient of Heating Performance (COP) were tried to be established. Experimental results also show that increasing the flow of coolant and decreasing the gas cooler inlet temperature have improved the system performance and reduced the optimum heat release rate. In the experimental system, a compressor, a gas cooler, an evaporator and an expansion valve were used. In addition to these four basic elements, a high-pressure accumulator is installed to store residual refrigerant at the gas cooler outlet and provide simple working pressures. In addition, the evaporator keeps liquid at the outlet and the compressor is also placed in the low pressure receiver for steam input only. Two water tanks are installed to adjust the inlet temperatures

[1]Isparta Applied Sciences University, Technology Faculty, Energy Syst. Eng. Dept., 32260, Isparta, TURKEY
[2]Isparta Applied Sciences University, Technology Faculty, Mechatronics Eng. Dept., 32260, Isparta, TURKEY
[3]Isparta Applied Sciences University, Graduate Institute, 32260, Isparta, TURKEY
*Corresponding author: emreozgur@sdu.edu.tr

of the gas cooler and evaporator. There are also 2 water pumps to control the flow of cooling and chilling water. As a result, the compressor discharge pressure was changed between 7.5 MPa and 11.5 MPa, and the results were obtained. It was observed that, decreasing the inlet temperature, increasing the flow rate of the fluid, increased the system performance.

Lin and etc. (2013) have studied the modeling and simulation of transcritical carbon dioxide heat pump systems in their study. In the installed CO2 system, dry thermometer temperature, relative humidity, inlet water temperature, compressor speed, capillary tube length are taken into consideration. The dry bulb temperature and the evaporator's input relative humidity increased with COP. The cooling flow rate increased with the input water temperature, which COP is dependent on. Although increasing the compressor speed gives a high heating capacity, it does not have a lower COP value. The established experimental system is the most basic cycle, with a gas cooler, an evaporator, a compressor and an expansion device. Water is used to extract heat from CO2. The gas cooler is a simple twin tube heat exchanger. The expansion part is provided with a capillary tube. The sensors used are the heat and pressure sensors placed in each pipe to which the elements used in the system are connected to each other. There is also a flowmeter (flowmeter) between the capillary tube and the gas cooler. Mixed configurations of the heat exchangers, geometric variations of the gas cooler and the evaporator are also evaluated to increase the realism of the work. When the results of the study were evaluated, the system COP value and heating capacity increased with the increase of the dry thermometer temperature in the evaporator. The effect on relative system performance in the evaporator is similar to that of dry thermometer temperature. The system rises with COP value, heating capacity and discharge pressure relative humidity. The inlet water temperature of the gas cooler has a great impact on system performance. CO2 mass flow increases with input water temperature. Increasing compressor speed reduces COP. It does not depend much on the capillary tube length of the COP value because there is very little enthalpy exchange.

The main purpose of this study is the thermodynamic analysis of a transcritical CO2 heat pump. Analysis study has been made with various gas cooler pressures. However, the temperature of CO2 has been selected as a variable parameter. Some assumptions have been defined to introduce analysis equations. Parametric analysis has been made using software (Engineering Equation Solver – EES).

Material and Method

A standart heat pump system has been set up for experimental data. The setup is consisting of a compressor, an evaporator and a gas cooler, different types of capillary tubes, two water tanks and two water circulation pumps. The following values are measured from the system:

- ✓ Evaporator inlet coolant temperature
- ✓ Evaporator outlet coolant temperature
- ✓ Gas cooler inlet coolant temperature
- ✓ Gas cooler outlet coolant temperature
- ✓ Evaporator inlet water temperature
- ✓ Evaporator outlet water temperature
- ✓ Gas cooler inlet water temperature
- ✓ Gas cooler outlet water temperature
- ✓ Evaporator inlet coolant pressure
- ✓ Evaporator outlet coolant pressure
- ✓ Gas cooler inlet coolant pressure
- ✓ Gas cooler outlet coolant pressure
- ✓ Coolant flow rate
- ✓ Water flow rate
- ✓ Power consumption of the whole system

A schematic representation of the system in theoretical can be seen in figure 1.

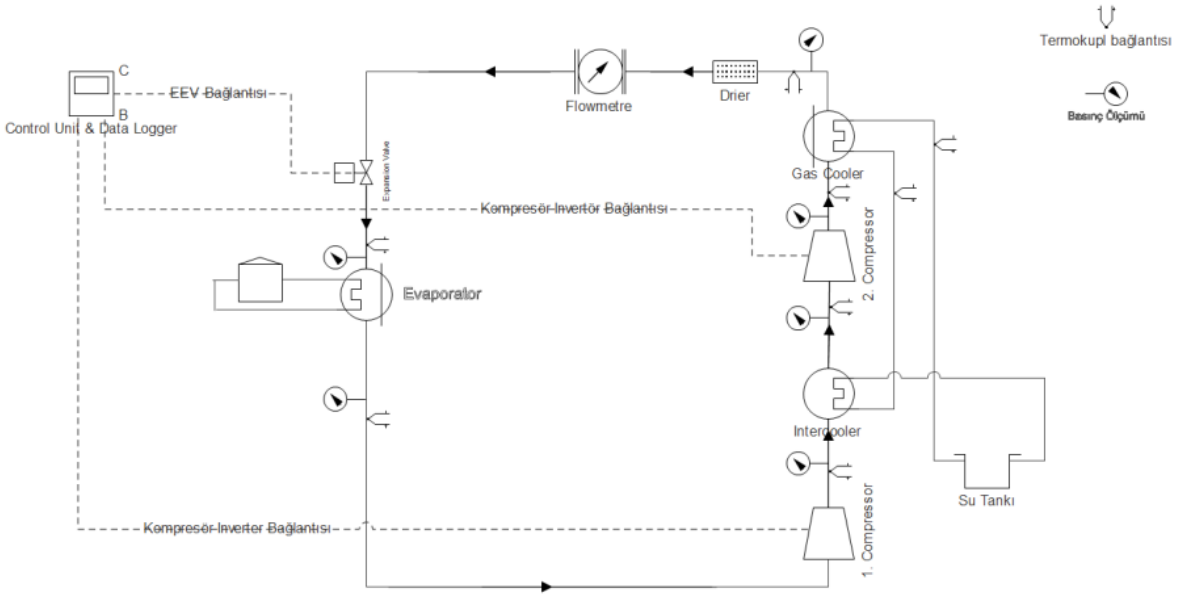

Figure 1. Experimental setup schematic drawing.

In experimental study the high pressure compressor of the system and the intercooler is bypassed. Data measurements are made with single compressor and different capillary tubes. Experimental system can be seen in figure 2.

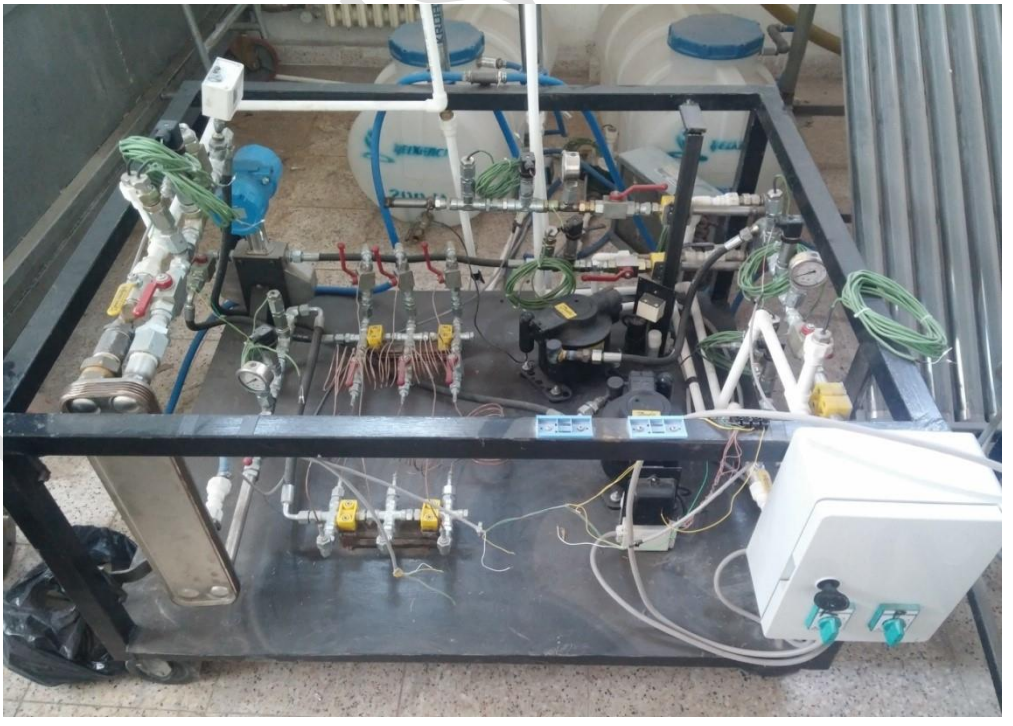

Figure 2. Experimental system

K type thermocouples are used for measuring temperature, piezo pressure transmitters are used for measuring pressures. Coriolis effect flowmeter is used for measuring the amount of the coolant. Water flowmeters measures the amount of the water circulating in the evaporator and the gas cooler. A wattmeter is placed on the power line of the system which feeds the compressor and the two water pumps.

System has been designed as a water to water heat pump. So plate heat exchangers were used as evaporator and gas cooler. System has a one CO2 compressor to increase refrigerant pressure.

Coefficient of heating performance is main metric to evaluate a heat pump. This metric can be calculated with following equation.

$$COP_h = \frac{\dot{Q}_{heating}}{\dot{W}_{system}}$$

In this equation $\dot{Q}_{heating}$ is the heat obtained from system gas cooler. This heating capacity can be obtained from with neglecting heat losses from the gas cooler;

$$\dot{Q}_{heating} = \dot{m}_{water} \cdot c_{water} \cdot (T_{water\ out} - T_{water\ in}) = \dot{m}_{CO2} \cdot (h_{CO2\ in} - h_{CO2\ out})$$

$\dot{W}_{system}$ is the total energy consumption of system. This parameter was measured. At the same time, energy consumptions of system compressor and water circulating pumps were measured with wattmeter.

Results

Experimental measurements has been made and presented with table 1.

Parameter	Value
Evaporator inlet CO2 temperature (ºC)	1.4
Evaporator outlet CO2 temperature (ºC)	27.3
Gas cooler inlet CO2 temperature (ºC)	94.4
Gas cooler outlet CO2 temperature (ºC)	30.9
Evaporator inlet water temperature (ºC)	27.4
Evaporator outlet water temperature (ºC)	21.6
Gas cooler inlet water temperature (ºC)	27.4
Gas cooler outlet water temperature (ºC)	33.6
Evaporator pressure (bar)	29.5
Gas cooler pressure (bar)	67
Coolant flow rate (kg/min)	0.408
Water flow rate (kg/min)	2.38
Power consumption of the system (Watt)	654

System COP was obtained as 1.573 with these measruments. The crtitical pressure is CO2 is 73.8 bar. So, experimental system pressure has not been increased above this pressure. Therefore system can not been reached optimum gas cooler pressure. System has been performed as a subcritical cycle.

Discussion and Conclusions

Alternative refrigerants have been widely choosen due to their environmental properties. CO2 or R744 has a great alternative refrigerant for heat pump and refrigeration systems. In this study, a single stage CO2 heat pump system has been produced. System COP was experimentally obtained. System COP is obtained as 1.573 for specific working conditions. Higher values can be obtained with obtaining optimum working conditions. System gas cooler pressure can be increased to higher values than the critical pressure. So system

can be perfomed as a transcritical heat pump. Futhermore, two stage compression and intercooling cycle can be performed to obtain higher COP values.

Acknowledgements

The authors gratefully acknowledge The Scientific and Technological Research Council of Turkey (TUBİTAK) for supplying laboratory devices.

References/Kaynaklar

FAQ, (2016). R744.com. http://www.r744.com/knowledge/faq (Erişim Tarihi: 29.08.2018)

Heat Pumps (2008). The Engineering Toolbox. https://www.engineeringtoolbox.com/heat-pump-efficiency-ratings-d_1117.html (Erişim Tarihi: 29.08.2018)

Lin, K.H., Cheng, S.H., Wang, C.C., vd. (2013). Modeling and simulation of the transcritical CO2 heat pump system. International Journal of Refrigeration. 36. 2048-2064.

NYTIMES, (2016). The New York Times. https://www.nytimes.com/2016/08/10/science/air-conditioner-global-warming.html (Erişim Tarihi: 29.08.2018)

Yang, J.L., Li. M.X., Ma., Y.T., vd. (2010). Modeling and simulating the transcritical CO2 heat pump system. Fuel and Energy Abstracts, 35(12), 4812-4818.

International Conference on Science and Technology

ICONST 2018

5-9 September 2018 Prizren - KOSOVO

Energetic Assessment of A Transcritical Rankine Cycle Powered by Solar Energy

İsmail ÖZCAN[1*], Mehmet ALTINKAYNAK[2], Ahmet ÖZSOY[2], Arif Emre ÖZGÜR[2]

Özet: Günümüzde en önemli çevresel sorunlardan biri küresel ısınma gerçekliğidir. Dolayısıyla, temiz enerji kaynakları daha fazla önem kazanmaktadır. Güneş de bu temiz enerji kaynaklarından olup, elektrik üretimine uygulanmasının yanında güneş enerjisi ile çalışan kojenerasyon ve trijenerasyon uygulamaları da geliştirilmiştir. Bu çalışmada, bileşenleri CO_2 pompası, vakumlu güneş kolektörü, CO_2 türbini, CO_2 yoğuşmalı ünite ve boru hatları olan transkritik bir güç çevrimi sunulmuştur. Çevrim akışkanı olarak, mükemmel termofiziksel özelliklere, bununla birlikte küresel ısınma potansiyeli ve sıfır ozon tükenme potansiyeline sahip Rankin döngüleri için eşsiz bir alternatif çevrim sıvısı olan CO_2 tercih edilmiştir. Bu tercihin bir diğer önemli sebebi de literatürde sınırlı bir araştırma sayısı mevcut olmasına rağmen yapılan çalışmaların birçoğunda akışkan olarak kullanılan CO_2'in ısıl verimi önemli ölçüde arttırdığının gözlemlenmesi olmuştur. Çalışmada CO_2 pompası ile sıvı CO_2 basıncı arttırılmıştır. CO_2, yüksek basınçlı seviyelerde (9 MPa ila 12 MPa) vakumlu güneş kolektörlerinde buharlaşır. CO_2 'nin sıcaklığı 120 ºC ila 200 ºC arasında arttırılabilir. Bu durumda, CO_2 aşaması süper kritiktir. Süperkritik CO_2, güç üretmek için türbinde genişler. Türbinden sonra, CO_2 basıncı yaklaşık 5.7 MPa'dır. Bu basınçta, CO_2 yoğuşma ünitesinde soğutulur ve yoğuşturulur. Ayrıca yine bu çalışmada, transkritik CO_2 güneş enerjisi döngüsüne termodinamik analiz uygulanmıştır. Çeşitli kolektör basınçlarıyla analiz çalışması yapılmıştır. Bununla birlikte, CO_2 'nin sıcaklığı değişken bir parametre olarak belirlenmiştir. Analiz denklemlerini tanıtmak için bazı varsayımlar tanımlanmıştır. Parametrik analiz Engineering Equation Solver (EES) yazılımı kullanılarak yapılmış ve analiz sonuçları grafiklerle sunulmuştur.

Anahtar Kelimeler: CO_2, transkritik, Rankin çevrimi, güneş.

Abstract: Today, one of the most important environmental problems is global warming reality. So, clean energy resources gain more importance. The application of solar energy to electricity generation has received considerable attention. However cogeneration and trigeneration applications powered by solar energy have also been developed. In this study, a solar transcritical power cycle has been presented. Cycle components are CO_2 pump, evacuated solar collector, CO_2 turbine, CO_2 condensing unit and pipe lines. CO_2 has been selected cycle fluid. CO_2 has excellent thermophsical properties. However, CO_2 has unity global warming potential and zero ozone depletion potential. So, CO_2 is a unique alternative cycle fluid for Rankine cycles. Pressure of liquid CO_2 has been increased by CO_2 pump. CO_2 vaporizes in evacuated solar collectors at high pressure levels (9 MPa to 12 MPa). The temperature of CO_2 can be increased 120 ºC to 200 ºC. At this condition, phase of CO_2 is supercritical. Supercritic CO_2 expands in the turbine to produce power. After turbine, pressure of CO_2 is about 5.7 MPa. At this pressure, CO_2 is cooled and condensed in the condensing unit. In this study, thermodynamical analysis has been applied transcritical CO_2 solar power cycle. Analysis study has been made with various collector pressures. However, the temperature of CO_2 has been selected as a variable parameter. Some assumptions have been defined to introduce analysis equations. Parametric analysis has been made using software (Engineering Equation Solver – EES). The analysis results have been

[1]Isparta Applied Sciences University, Graduate Institute, Energy Syst. Eng. Dept., 32260, Isparta, TURKEY
[2]Isparta Applied Sciences University, Technology Faculty, Energy Syst. Eng. Dept., 32260, Isparta, TURKEY
*Corresponding author: isozcan84@gmail.com

presented with graphics. Power efficiency of cycle may exceed 20%. However, thermal efficiency of the system can be reaches higher than other solar thermal collecting units. Analysis results state that, transcritical CO_2 power cycle can be feasible way to produce power from solar energy.

Keywords: CO_2, transcritical, Rankine cycle, solar

Giriş

Güneş enerjisi yenilebilir enerji kaynağıdır ve daha yaygın olarak değerlendirilebilir. Günümüzde elektrik enerjisi üretimi, sıcak su hazırlanması ve kurutma gibi önemli uygulama alanlarında kullanılmaktadır. Bununla birlikte, elektrik üretiminde yaygın olarak kullanılan fotovoltaik sistemlerin verimleri nispeten düşüktür. Düzlemsel toplayıcılar ile elde edilecek akışkan sıcaklığında ise bir sınır vardır. Kurutma uygulamalarının da havalı düzlemsel toplayıcılar ile yapılması, birim kuru ürün için gerekli toplayıcı alanını arttırmaktadır. Dolayısıyla, güneş enerjisinin bu üç ana alanda, daha yüksek verim ile değerlendirilebileceği araştırma geliştirme çalışmaları sürmektedir.

CO_2 ise doğal bir akışkandır ve organik güç çevrimlerinde yaygınlaşmaktadır. Ülkemizin sahip olduğu güneş enerjisi potansiyelini, elektrik üretiminde, akışkan ısıtma uygulamalarında, kurutma gıda pastörizasyonu işlemlerinde daha yüksek verimlilik ile değerlendirebilmek adına bu araştırma konusu seçilmiştir. Literatürde sınırlı bir araştırma sayısı mevcut olmasına rağmen yapılan çalışmaların bir çoğunda akışkan olarak kullanılan CO_2'in ısıl verimi önemli ölçüde arttırdığı gözlemlenmiştir. Örneğin;

Yamaguchi vd. tarafından 2006 yılında yapılan bir çalışmada, 38 mm iç çapa sahip vakum tüpler içinde 4 mm çapa sahip U boru yapısı olan CO_2'li bir güneş toplayıcısının ısıl verimini ve elektrik enerjisi üretim verimini incelemişlerdir. 165 ºC CO_2 çıkış sıcaklığı, % 65 ısıl verim ve % 25 elektriksel enerji üretim veriminin elde edilebileceğini hesaplamışlardır. (Yamaguchi vd., 2006)

Yamaguchi vd. 2010 yılında yaptıkları bir araştırmada, vakum tüplü U borulu transkritik CO_2'li güneş toplayıcısının ısıl verimini araştırmışlar ve % 66 maksimum toplayıcı ısıl verim değeri elde etmişlerdir. Çalışmalarında standart kanatçık yapısı kullanılmıştır. (Yamaguchi vd., 2010)

Zhang X. R. ve Yamaguchi H., 2008 yılında yaptıkları çalışmada güneş kolektöründe akışkan olarak süperkritik CO_2 kullanmışlar ve güneş kolektörünün temel özelliklerini deneysel olarak incelemişler ve testlerin çoğunda, günlük ağırlık bazında, günlük ortalama toplayıcı verimliliği % 50.0'nin üstünde ve yıllık ortalama kolektör verimliliği % 60.0 olarak ölçülmüştür ve bunun çalışma sıvısı olarak su kullanan toplayıcıdan daha yüksek bir verim olduğunu ortaya koymuşlardır. (Zhang ve Yamaguchi., 2008)

Bu çalışmada, bileşenleri CO_2 pompası, vakumlu güneş kolektörü, CO_2 türbini, CO_2 yoğuşmalı ünite ve boru hatları olan transkritik bir güç çevrimi sunulmuştur. Çevrim akışkanı olarak CO seçilmiştir. CO_2, mükemmel termofiziksel özelliklere sahiptir. Bununla birlikte, CO_2, küresel ısınma potansiyeli ve sıfır ozon tükenme potansiyeline sahiptir. Dolayısıyla, CO_2 Rankine döngüleri için eşsiz bir alternatif çevrim sıvısıdır.

CO_2 pompası ile sıvı basıncı arttırılmıştır. CO_2, yüksek basınçlı seviyelerde (9 MPa ila 12 MPa) vakumlu güneş kolektörlerinde buharlaşır. CO_2 'nin sıcaklığı 120 ºC ila 200 ºC arasında arttırılabilir. Bu durumda, CO_2 aşaması süper kritiktir. Süperkritik CO, güç üretmek için türbinde genişler. Türbinden sonra, CO_2 basıncı yaklaşık 5.7 MPa'dır. Bu basınçta, CO_2 kondenserde soğutulur ve yoğuşturulur.

Materyal ve Yöntem

Şekil 1.'de kullanılacak olan sistemin şematik çizimi verilmiştir**.**

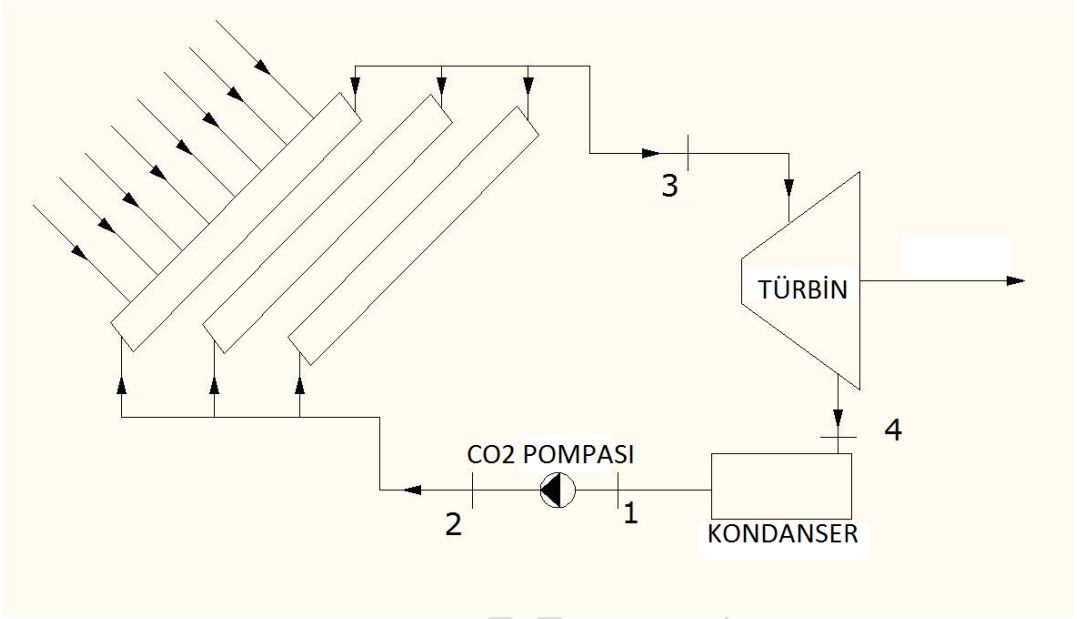

Şekil 1. Sistemin şematik çizimi

1 ile 2 noktaları arasındaki proseste sıvılaştırılmış CO_2'nin basıncı, CO_2 pompası ile arttırılmıştır. 2 ile 3 noktaları arası süreçte CO_2, yüksek basınçlı seviyelerde (9 MPa ila 12 MPa) vakumlu güneş kolektörlerinde buharlaşır. CO_2 'nin sıcaklığı 120 ^{o}C ila 200 ^{o}C arasında arttırılabilir. Bu durumda, CO_2 aşaması süper kritiktir. Çevrimin 3 ile 4 noktaları arasında ise CO_2, güç üretmek için türbinde genişler ve elektrik gücü kullanılabilir hale gelir. 4 ile 1 noktaları arasındaki süreçte ise Türbinden sonra, CO_2 basıncı yaklaşık 5.7 MPa'dır. Bu basınçta, CO_2 kondenserde soğutulur ve yoğuşturulur. İşlemden elde edilen ısı enerjisi, suyun ısıtılması veya diğer işlemler için etkili bir şekilde kullanılabilir. Bu sistemin önemli kılan, güneş enerjisi ile aynı anda elektrik enerjisi ve ısı enerjisi üretmesidir.

Termodinamik Analiz

Bu çalışmada, transkritik CO_2 güneş enerjisi döngüsüne termodinamik analiz uygulanmıştır. Çeşitli kollektör basınçlarıyla analiz çalışması yapılmıştır. Bununla birlikte, CO_2'in sıcaklığı değişken bir parametre olarak seçilmiştir. Analiz denklemlerini tanıtmak için bazı varsayımlar tanımlanmıştır. Parametrik analiz "Engineering Equation Solver (EES)" yazılımı kullanılarak yapılmıştır. Referans basınç ve sıcaklık değerleri sırasıyla 100 kPa ve 25 ^{o}C alınmıştır. Basınç kayıpları, kinetik ve potansiyel enerjiler ihmal edilmiştir. Sistem sürekli rejim şartlarında incelenmiştir.

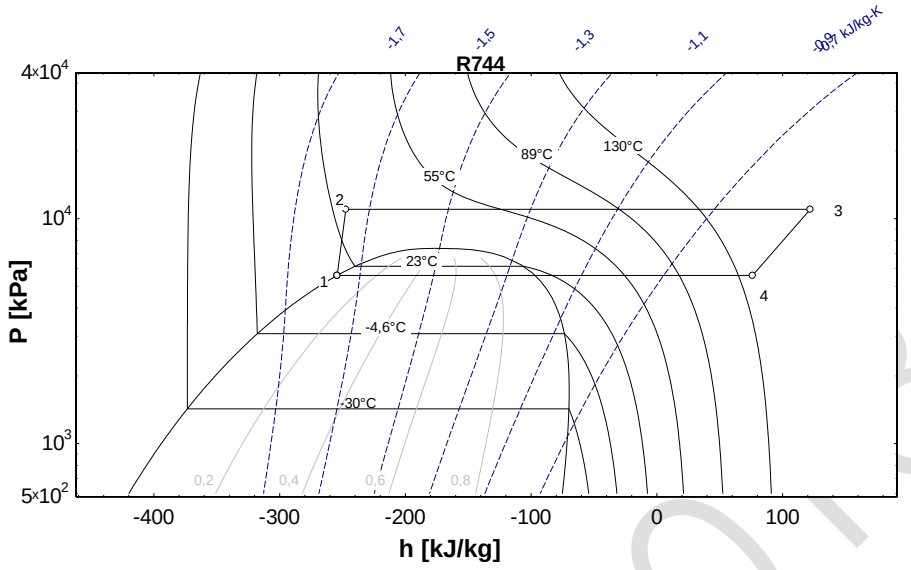

Şekil 2. Çevrimin CO_2 basınç – entalpi diyagramında gösterilmesi

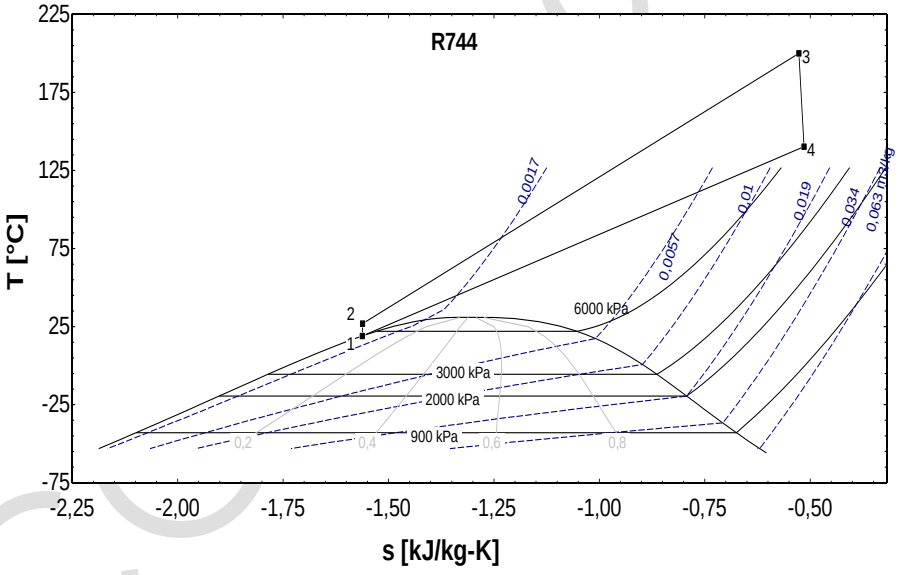

Şekil 3. Çevrimin CO_2 sıcaklık – entropi diyagramında gösterilmesi

Tablo 1.'de sistem bileşenlerinin birinci ve ikinci yasa analizleri verilmiştir.

Tablo 1. Sistem bileşenlerinin birinci ve ikinci yasa analizi (Dincer,2011;Dincer, 2013)

Bileşen	*Şematik Gösterimi*	*Kütle, Enerji, Ekserji Dengesi*
CO Pompası	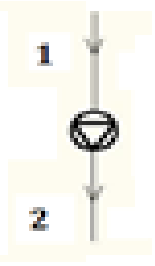	$\dot{m}_1 = \dot{m}_2$ $W_{pump} + \dot{m}_1 h_1 = \dot{m}_2 h_1$ $W_{pump} + \dot{m}_1 ex_1 = \dot{m}_2 ex_2 + \dot{E}x_{dest,pump}$
Güneş Kollektörü	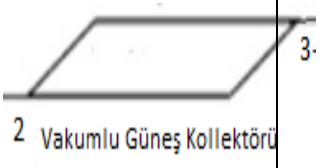	$\dot{m}_2 = \dot{m}_3$ $Q_{solar} + \dot{m}_2 h_2 = \dot{m}_3 h_3$ $\dot{E}x_{in,solar} = A_{total} I_{avg} (1 + \frac{1}{3}\left(\frac{T_0}{T_s}\right)^4 - \frac{4}{3}\left(\frac{T_0}{T_s}\right))$ $\dot{E}x_{in,solar} + \dot{m}_2 ex_2 = \dot{m}_3 ex_3 + \dot{E}x_{dest,solar}$
Türbin	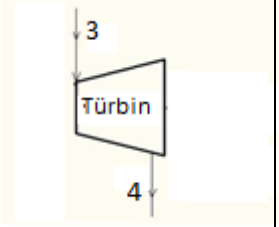	$\dot{m}_3 = \dot{m}_4$ $\dot{m}_3 ex_3 = \dot{m}_4 ex_4 + \dot{W}_{turbine} + \dot{E}x_{dest,turbine}$
Kondenser	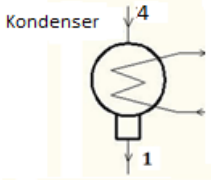	$\dot{m}_4 = \dot{m}_1$ $\dot{m}_4 h_4 = \dot{m}_1 h_1$ $\dot{m}_4 ex_4 = \dot{m}_1 ex_1 + \dot{E}x_{dest,condanser} + \left(1 - \frac{T_0}{T_s}\right) Q_{condanser}$

Bulgular

Analiz sonuçları aşağıda grafiklerle sunulmuştur. Döngünün güç verimliliği % 13'ü geçebilir. Bununla birlikte, sistemin termal verimliliği diğer güneş termal toplama ünitelerine göre daha yüksek olabilir. Analiz sonuçları, transkritik CO_2 güç döngüsünün güneş enerjisinden elektrik üretmek için uygun bir yol olabileceğini belirtmektedir.

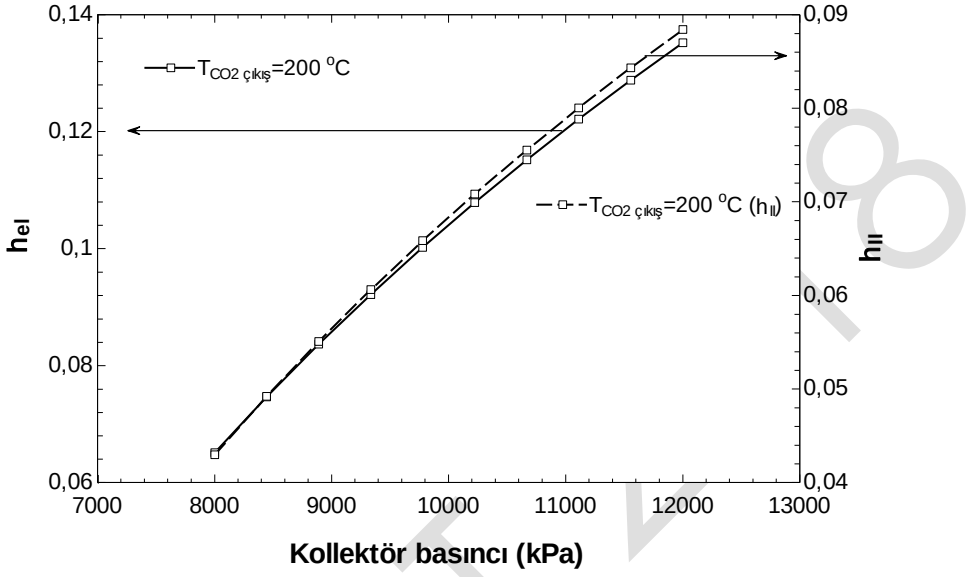

Şekil.4 Güç üretim verimi ve 2. yasa verimlerinin kollektör basıncıyla değişimi (η_{kol}=0.6, $\eta_{türbin}$=0.9, I_{ort}=800 W/m^2 ve 200 °C CO_2 çıkış sıcaklığı için)

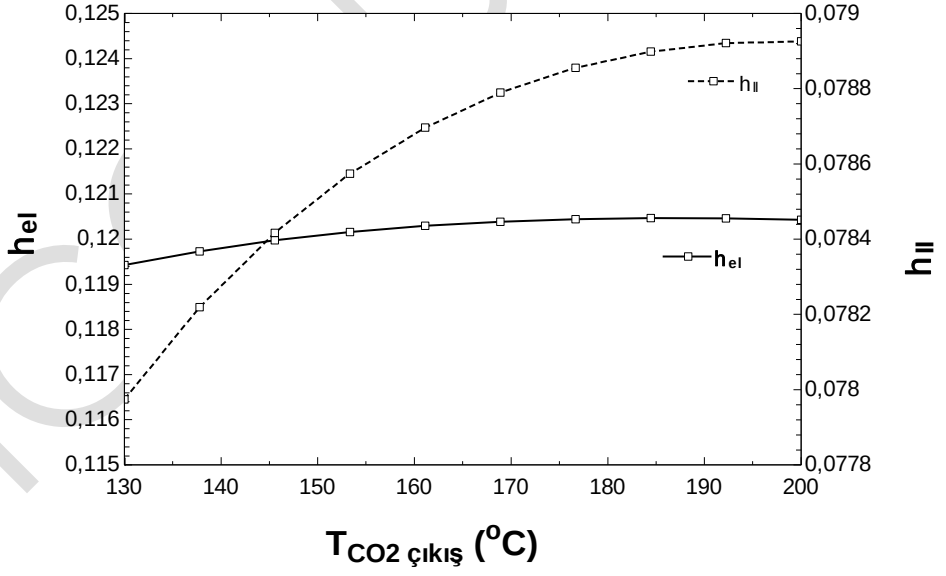

Şekil.5. Güç üretim verimi ve 2. yasa verimlerinin kollektör çıkış sıcaklığıyla değişimi (η_{kol}=0.6, $\eta_{türbin}$=0.9, I_{ort}=800 W/m^2 ve 11 MPa kollektör basıncı için)

Tartışma ve Sonuçlar

Bu çalışmada, CO_2 kullanılan vakum tüplü güneş kollektörleri ile çalıştırılan Rankine Güç Çevrimlerinin enerji ve ekserji verimleri incelenmiştir. Kollektör basıncının, hem enerji hem de ekserji verimi için kritik öneme sahip olduğu görülmüştür. Kollektör ısıl veriminin değişimi, sistemin güç ve ekserji verimi değişimleri açısından etkisi azdır. Kollektör ısıl verimi, sistem kapasitesinin değişimine etki etmektedir. Benzer şekilde CO_2'in kollektörden çıkış sıcaklığı da sistem kapasitesi için önem arz ederken, verimlilik üzerinde etkisi sınırlıdır. Literatürden elde edilen bilgilerde de, sistem verimliliğinin benzer şekilde değişimler gösterdiği gözlemlenmiştir.

Türbin çıkışında CO_2'in sıcaklığının kayda değer seviyede olması, buradaki ısı enerjisinin bazı uygulamalar ile değerlendirilmesini elzem kılmaktadır. Çoklu üretim uygulamalarının, transkritik güç çevrimleri için gerekli olduğu değerlendirilmiştir.

Kaynaklar

Dinçer, I., Zamfirescu C., Sustainable energy systems and applications, New York, NY: Springer, 2011.

Dincer, I., Rosen, M. A. Exergy: Energy, Environment and Sustainable Development, Elsevier, 225 Wyman Street, Waltham, MA 02451, USA, Second edition 2013.

Yamaguchi, H., Zhang, X. R., Fujima, K., Enomoto, M., Sawada, N., 2006. "Solar energy powered Rankine cycle using supercritical CO_2", Applied Thermal Engineering, 26, 2345–2354

Yamaguchi, H., Sawada, N., Suzuki, H., Ueda, H., Zhang, X. R., 2010. "Preliminary Study on a Solar Water Heater Using Supercritical Carbon Dioxide as Working Fluid", Author and Article Information J. Sol. Energy Eng, 132(1), 011010 (6 pages) doi:10.1115/1.4000350

Zhang, X. R., Yamaguchi, H., 2008. An Experimental Study on Evacuated Tube Solar Collector Using Supercritical CO_2. Applied Thermal Engineering 28, 1225–1233

International Conference on Science and Technology

ICONST 2018

5-9 September 2018 Prizren - KOSOVO

Mıtochondrıal Genome Analysıs and Haplo-group Determınatıon ın Human Skeletons

Nefize Ezgi ALTINIŞIK[1], Ercan ARICAN[2*]

Abstract: Molecular anthropology has been dramatically enhanced recently by the development of high-throughput next generation sequencing technologies. Significant findings have been obtained in respects of bio-cultural evolution of human under favour of ancient DNA researches in recent years. In Turkey, even if giving consequence to this field has been increased for five years, it is still limited.
aDNA isolations were performed from three human skeletons which uncovered from three different site - Karamattepe, Ballicaoluk and Baspinar- of Nif Mountain Excavations in İzmir, Turkey. Mitochondrial DNA *d-loop* regions of obtained aDNAs were amplified by "touchdown PCR" using eight primer pairs.
Amplified regions were sequenced by Sanger sequencing method and this three individuals haplo-groups were determined by using bioinformatic tools.
This study has importance to pave the way of ancient DNA researches that is going to conduct in the future in Turkey. This thesis that bears archeological and historical records out has also a potential to lead to interdiciplinary studies.

Keywords: Ancient DNA, mt-DNA, Bioinformatics, Anthropology

[1]Istanbul University, Institute of Science, Molecular Biology and Genetics Section, 34134, Vezneciler-Istanbul/Turkey
[2] Istanbul University, Science Faculty, Molecular Biology and Genetics Department, 34134, Vezneciler-Istanbul/Turkey
*Corresponding author: earican@istanbul.edu.tr

International Conference on Science and Technology

ICONST 2018

5-9 September 2018 Prizren - KOSOVO

The Usage of Strain Gauge in Tension, Torsion and Bending

Kerem Asmaz[1]*, Engin Erbayrak[2], Alparslan Solak[3]

Abstract: Strain calculation is important in determining mechanical properties of engineering. For this reason extensometer and strain gauge are mostly operated in strain measurement. Examples of applications of strain gauge are aircraft wings, turbine design, bridges and supports, load-bearing machine elements, and deformation calculations of various shapes. During the operation of mechanical systems, the amount of strain of the parts can be increased in undesirable situations such as fatigue and corrosion. In this case, the strain gauge offers the possibility of making the intervention to the user. Stress, force and deformation can also be calculated along with the strain calculation. The aim of this study is to investigate the strain behavior of the specified parts under various loads. Tensile, torsion and bending tests and finite element analysis were done.
Mild steel with modulus of elasticity of 207 MPa is used for the part material. The SM 1009 strain gauge was operated for strain calculation in the test environment. The CAD software SolidWorks was utilized for 3D modeling. Ansys Workbench was employed for numerical calculation.
Experimental results and numerical results were ascertained with the SM1009 Strain Gauge instrument and Ansys Workbench finite element program. The strain values in the determined regions of the parts were found at micron level. Half bridge was used in the tension test and 2 μ of strain was read when 1 kg is used. A quarter bridge was used in the bending test and the strain was found 12.5 μ when 50 gr is used at the moment distance of 420 mm. A full bridge was used in the torsion test and strain was computed 12 μ when a moment of 367.875 Nmm was applied. The numerical results support experimental results.
Tension, torsion and bending tests were performed to obtain strain values. Numerical strain values were found with using finite element program of Ansys Workbench. The experimental and numerical strain values are compared.

Keywords: Strain Gauge, Tension, Torsion, Bending

[1,3]Yildiz Technical University, Faculty of Mechanical Engineering, 34349, Istanbul, TURKEY
[2]Bayburt University, Faculty of Engineering, 69000, Bayburt, TURKEY
*Corresponding author: asmaz@yildiz.edu.tr

International Conference on Science and Technology

ICONST 2018

5-9 September 2018 Prizren - KOSOVO

Investigation of peroxidation kinetics in oil-in-water emulsions induced by Cu(II)

Temel Kan Bakır [1]*, Reyhan Arabacıoğlu[2], Fatma Kandemirli[3], İzzet Şener[4]

Abstract: In this study, peroxidation of olive oil, corn oil, sunflower oil, walnut oil, argan oil, rosehip oil emulsions was carried out in the presence of copper (II) ion at 37 ° C and pH 7 in a ventilated incubation environment.

Primer products (hydroperoxides) were monitored by Fe (III) SCN method and secondary products (malondialdehyde) were analyzed by TBARS analytical methods. In addition, GC-MS analysis were performed on the oils studied to identify compounds that behave as free radical scavengers or hydrogen donors.

Before preparation of the oil emulsions in water, iodine index determinations of the degrees of unsaturation in the oils were made and found to be 86.28, 128.12, 140.22, 164.97, 97.29 and 183.58 gI_2 / 100g for olive oil, corn oil, sunflower oil, walnut oil, argan oil and rosehip oil respectively. The rate constants were calculated $k_{walnut\ oil} > k_{argan\ oil} > k_{rosehip\ oil} > k_{sunflower\ oil} > k_{corn\ oil} > k_{olive\ oil}$ for FeSCN method and $k_{rosehip\ oil} > k_{walnut\ oil} > k_{argan\ oil} > k_{olive\ oil} > k_{sunflower\ oil} > k_{corn\ oil}$ for TBARS method, respectively.

As a result, pseudo first order kinetics of hydroperoxides and aldehydes were observed in copper-catalyzed oil emulsions at 37 ° C and pH 7, and the absorbance values obtained as a function of the incubation period gave sigmoidal curves. This study showed that the oxidation rates of fats are closely related to the conjugated fatty acids. It was thought that the kinetic data obtained could be used to accurately calculate the shelf life of oils used as food components.

Keywords: TBARS Method, Ferric Thiocyanate Method, Olive oil, Corn oil, Sunflower oil, Walnut oil, Argan oil, Rosehip oil, Lipid emulsion

Acknowledgement: This work was supported by Kastamonu University, Researchb Fund, KÜBAP Project No: KÜ-BAP01/2017-46. Dr. Bakır would like to thank Kastamonu University, Research Fund for these support.

[1] Kastamonu University, Faculty of Science and Letters, Department of Chemistry, 37150, Kastamonu, TURKEY
[2] Kastamonu University, Institute of Science (Msc Student), 37150, Kastamonu, Turkey
[3] Kastamonu University, Faculty of Engineering, Department of Biomedical Engineering, 37150, Kastamonu, TURKEY
[4] Kastamonu University, Faculty of Engineering, Department of Food Engineering, 37150, Kastamonu, TURKEY
*Corresponding author: temelkan@kastamonu.edu.tr, temelkan@hotmail.com

International Conference on Science and Technology

ICONST 2018

5-9 September 2018 Prizren - KOSOVO

Processing and Characterization of ZrC-SiC-Al_2O_3 Ceramic Composite

Ahmet Atasoy[1]*, Kenan Yıldız[2]

Abstract: In this study, silicon and zirconium carbides were produced by thermic process using zircon, petroleum coke and aluminum powders in presence of Ar flow at temperature between 1300-1450 ˚C. The carbides were characterized by scanning electron microscope and XRD/EDAX techniques. The results indicated that the decomposition of zircon and the formation of carbide phases were lowered by aluminothermic process. A reduction mechanism was proposed based on the reduction of zircon. First, the silicon carbide was formed and this accelerated the reduction of zirconia and the formation of zirconium carbide. The alumina formed in this process was removed from the reaction products by means of caustic soda leaching operation.

Keywords: Zircon, ZrC, SiC, High temperature ceramic, Thermic process

1. Introduction

Zircon consists of silica and zirconium dioxide (Abdelkader 2008). Each oxide is a very valuable component of oxide-based ceramics. It has wide range of application areas, such as abrasive (Atasoy 2009) and high temperature ceramic materials (Atasoy 2007). In addition, zircon is the only mineral in all zirconium compounds (Bharat 2003). Zirconium dioxide is one of the best structural ceramics for high temperature applications (Cho 2008) and it is also an oxide source for all boride, carbide or nitride of zirconium compounds. These compounds are major components for manufacturing high temperature materials and structural ceramics in nuclear applications. In addition, SiC is used as additive between 5-30% of matrix as it improves densification and oxidation resistance of high temperature materials. Zircon is the only source for the production of Zr and Si carbides. For the production of ZrC, the reaction temperature needs to be above 1700 °C from zirconia in conventional methods (Evans 1990Das 2004). Silica is the main raw material of silicon-based ceramics such as nitride (Habashi 1986, Garrido 2001, Kotic 2001) and carbides (Licheri R, et al. 2009) or traditional oxide materials (Mazzoni 1998).

Self-propagating process was applied as an alternative method in order to obtain silicon and zirconium carbide mixtures from the zircon in laboratory conditions (Merzhanov 1995, Moore 1995, Mariappan 2002). Both ZrC and SiC are excellent candidates for structural applications. They can be used alone or in combination with other oxides in high temperature applications (Panda 1999). On the other hand, productions of pure compounds are complex and expensive processing routes are required. There is a growing attention turned towards cheaper raw material sources, better mechanical properties and cleaner production route. As zircon consists of two oxides, the zirconium or silicon compounds such as carbide compounds can be directly synthesized from zircon (Toth 1971, Sorell 1983, Tsuchida 2007). Both compounds can be produced with

1Department of Research &Development-Arkel Elektrik ve Elektronik San. ve Tic. A.Ş. 34885,Istanbul, TURKEY
2Bilig Yenileşim San. Tic. Ltd. Şti.34906, Istanbul TURKEY
*Corresponding author: semihyuksel@yandex.com

high temperature processes. Reducing the metals such as Al, Mg, and Ca creates huge amount of heat that reduces reaction temperature of the process (Umebayashi 1977, Zhe X, et al. 2005). Conventionally, aluminum is one of the widely used metals in metallothermic processes in metallurgical applications (Zender H, et al. 1990).

The reliability of this study lies in the application of aluminothermic process for forming carbides from zircon under argon atmosphere. The main advantages of this process compared to other applications can be summarized as follows: the process conditions, gas atmosphere and the reaction temperature. Accordingly, it can be concluded regarding the aluminothermic reduction mechanism that it can be applied to develop and control the processing routes for manufacturing Si/Zr carbide compounds called as high temperature ceramics. The reaction products can be easily separated by a heavy medium liquid. Aluminothermic reduction process is highly exothermic and the addition of carbon can accelerate both the heat of formation and the carbide phase. The results obtained from the process and the reaction mechanisms were presented in this study. In this study, many relevant parameters and a combination of physical examination are addressed. In addition, analysis techniques were used in order to clarify the stages of the reaction mechanism.

2. Material and Method

In this study, the raw materials were zircon, carbon and metallic aluminum powders. The chemical analysis and some properties of the starting powders are shown in Table 1. The aluminum used in this study had 99.9% purity and was in a particle size smaller than 50 micron. In this study, argon was used as a flow gas during the experiments.

Table 1. Some properties of the starting powders

Oxides	Moisture	C %	Al	ZrO_2	SiO_2	ZrO_2/SiO_2	Particle size	Density
Zircon	1.5	--	--	66.8	32.5	2.05	10-50µm	4.2 g/cm^3
Al powder	-	--	99.9	--	--	--	d<50µm	2.45 g/cm^3
Carbon	2.5	98	--	--	--	--	d<50µm	350g/l

The starting mixture was ball-milled for 6 hours using acetone, as a liquid media, and zirconia ball in a planetary mill. After drying stage, 10 gr of the sample was placed into a graphite crucible and heat-treated at temperatures between 1300-1450 ˚C in presence of argon flow for different reducing times.

For determining the mineral in the starting powder and the reaction phases in the produced metallic beads, X-ray diffraction method (D/max Rigaku, Japan) was used under the condition of Cu Kα radiation (λ=0.15418 nm) with a step size of 0.02˚ (2θ) and a scanning rate of 2˚ min^{-1}. Energy dispersive analytical X-ray (EDAX) was also used for basic chemical analysis. Thermal analysis of the mixture was conducted with simultaneous thermal analysis (Netzsch STA 400, Germany). TG/DTA was carried out in an alumina crucible under nitrogen atmosphere in a temperature range of 20-1400 ˚C and at a heating rate of 10 ˚C/min. The microstructure and morphology of the samples were characterized by using a scanning electron microscope (SEM).

3. Results

The XRD pattern of the mixture of starting powders is shown in Figure 1. As seen in the table, the pattern showed a rapid change. The reducing and carburizing agents were identified and labelled on the pattern.

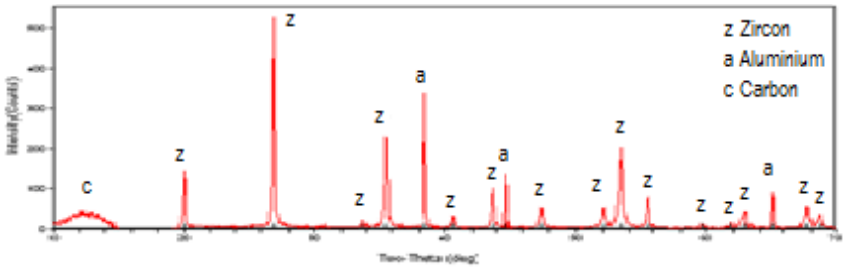

Figure 1. XRD pattern of the starting mixture

Scanning electron microscope (SEM) images of zircon powder are shown in Figure 2. It is evident that the particle size of the powder is very fine.

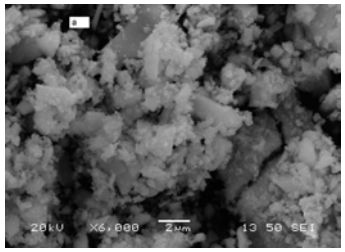

Figure 2. SEM micrograph of the zircon powder

As explained above, the sample consisted of zircon, aluminum and carbon powders. According to the Reaction 1, the presence of aluminum has changed the reaction mechanism of the mixture from solid-solid state to solid-liquid state that takes place below the melting point of its metallic content.

$Al_{(s)} \rightarrow Al_{(l)}$ (1)

Decomposition temperature of zircon is at around 1500 °C in air, but the process suggests that the aluminothermic reduction decreases this decomposition temperature. The second stage of the process is the decomposition of zircon into silica and zirconia according to the Reaction 2.

$SiZrO_{4(s)} \rightarrow SiO_{2(s)} + ZrO_{2(s)}$ (2)

In the third stage of the process, Aluminothermic reduction of silica and the formation of silicon carbide took place. It is well-known that silica is less stable than zirconia and its melting point is above 1700 °C. The silicon content of the zircon may be used as a source of metallic Si, carbide, silicide or Si compounds in the final product. The formation of SiO gas phase is also possible during the process. The heat of formation released through the aluminothermic process is enough to reduce silica under the experimental condition. Silica is highly reactive to Al and C to form SiC. The possible reduction of silica and the formation of silicon carbide were complex processes in presence of metallic reducing agent and carburizing agent.

The final stage of the process is the reduction of zirconia content of the mixture and the formation of zirconium carbide. However, before any formation of zirconium carbide reaction, there is simultaneous transformation reaction of monoclinic zirconia to tetragonal zirconia. In this study, it was observed that the partial conversion of m-ZrO_2 to t-ZO_2 took place very rapidly. The total quantity of zirconia was decreased by keeping the process time longer and increasing the temperature. It was assumed that the formation of silicon carbide was key to the formation of zirconium carbide.

Although the heating of the mixture was initiated by metallic aluminum, the second heat source was provided by carbon. It is a well-known process that after the reaction gas is formed, carbon dioxide is converted to two mole of carbon monoxide that acts as a reducing gas at above 700 °C. The carburization of silicon and zirconium occurs simultaneously in both of the carbon sources, the solid carbon and carbon monoxide gas, during the process. The formation of CO_2, the generation of CO and the CO/CO_2 ratio can determine the rate of reaction. It is also very important for the formation of carbide phases to reduce the partial pressure of oxygen throughout the process.

The reaction between aluminum and oxygen is very exothermic in the atmosphere, which is presented in the Reaction 3. The oxygen comes from the oxygen content of the reducible oxides in the system. Any reaction during the process occurs between the molten metal and the decomposed zircon and carbon.

$$Al_{(l)} + 3/2O_{2(g)} \rightarrow Al_2O_{3\,(s)} \quad (3)$$

$$SiZrO_{4(s)} + 3C_{(s)} + 2Al_{(l)} \rightarrow ZrC_{(s)} + SiC_{(s)} + Al_2O_{3(s)} + CO_{2(g)} \quad (4)$$

The Reaction 4 can be defined as the aluminothermic reduction and carburization of zircon, as an overall reaction.

After the process was completed, it was observed that there were some differences in the reaction products of the mixture of zircon, carbon and aluminum powders in argon. The XRD patterns of the reduced samples also revealed some differences in the shapes and intensities of the peaks and the phases. Some selected X-ray diffraction patterns of the samples are shown in Figures 3-5.

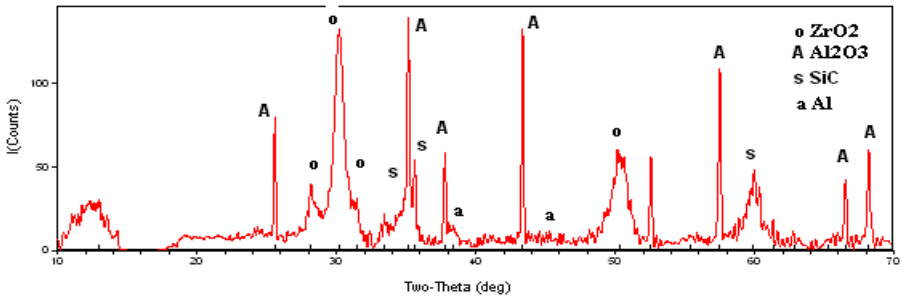

Figure 3. XRD pattern of the reduced mixture at 1400 °C for 2 h.

After the aluminothermic reduction and carburizing process at 1400 ˚C for 2 h, the reaction phases were identified and labelled as in Figure 3. As can be seen in Figure 3, m-ZrO2 and m-ZrO2 were determined in the reduced sample. In addition to these phases, there were alumina and silicon carbide and unreacted aluminum in the sample. At the same temperature but with longer waiting time, it was observed that some of the determined phases increased while especially the intensities of the m/t zirconium dioxide and aluminum decreased. Another significant point is that no ZrC phase was observed in both waiting times at this temperature. It indicates that the temperature and time were not enough for the formation of zirconium carbide. However, it was determined that the silicon carbide phase was dominant at this temperature. After decomposition of the zircon, silica was firstly reduced to oxide and then converted to stable form of the silicon carbide. The intermediate phase was formed before the carbide formation. There was a possibility of a reduction in silicon content of the final product as a result of the formation of silicon oxide gas phase and evaporation of it from the system.

At higher temperature and longer reaction times, there were some differences in the reaction product phases and their intensities. The XRD patterns of the reduced samples after the process at 1450 °C for 4 hoursare shown in Figures 4and 5. At 1400 °C, some crystalline phases of the zircon were determined such as m and t-ZrO_2, but at this temperature a new phase of zirconium was determined in the form of carbide phase. The results suggest that the formation of silicon carbide accelerated the formation of zirconium carbide and had a positive impact on the formation of zirconium carbide as a reducing agent. The exothermic heat released from the silicon carbide provides additional heat for the formation of zirconium carbide. However, there was still some portion of zirconia that was not converted to zirconium carbide. There was no silica peak at this temperature for both reaction times.

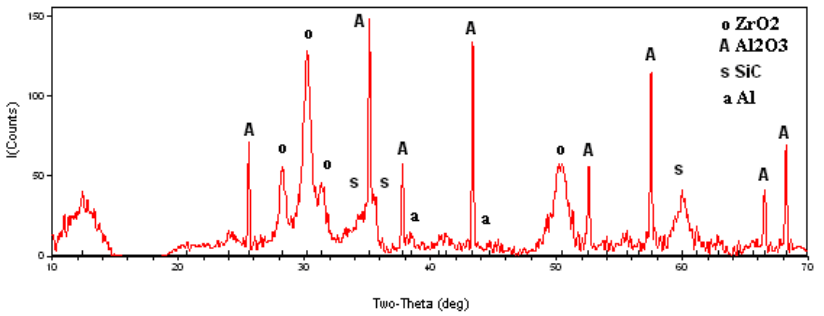

Figure 4. XRD pattern of the reduced mixture at 1400 ^{0}C for 4 h.

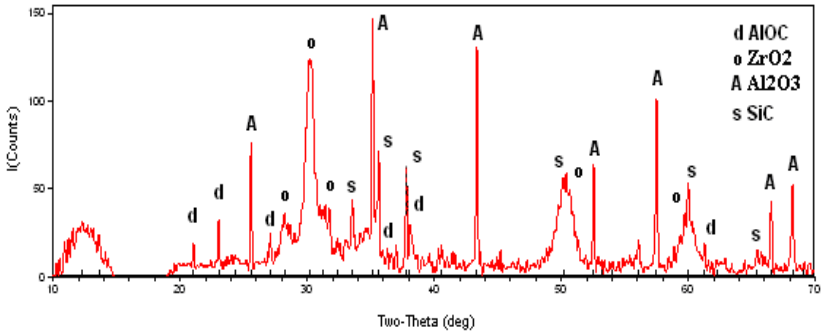

Figure 5. XRD pattern of the reduced sample at 1450 °C 4 h.

There was a huge difference between the peak intensities and forms as well as the phases between the XRD pattern of the starting mixture and the processed samples. The formation of new phases indicated that the process was feasible, the reduction started at 1300 °C. SiC, and Al_2O_3 and ZrC phases were successfully formed from the used mixture at this temperature.

The intensity ratio of ZrC/SiC was found to be 2.8. The intensity of ZrC was taken at 2 theta 33.15° and I_{SiC} was taken at 2theta 35.6°. Other phases of zirconia, such as t-ZrO_2 and m-ZrO_2 were determined in the samples. The formation of these phases indicates that zirconium dioxide content was not fully converted to carbide form of zirconium. In other words, there was unreacted zirconium oxide in the final powder. However, no silica was found in the reduced samples. This reveals that silica was converted to carbide form easier than zirconium oxide. There was also some background noise or amorphous structure on the X-ray patterns. As argon was used in other phases except alumina, it was not observed in the reaction product.

During the aluminothermic reduction-carburization process, there may be intermediate oxide phases, such as, SiO and ZrO. It can be said that t reaction products change depending on the reduction condition and atmosphere. In another words, the reduction mechanism of zircon to carbide forms is a complex process. Beside these reactions, the silica was reduced first and then silicon carbide phase was formed. The formation of silicon carbide can accelerate the reduction of zirconia. Subsequently, both exothermic reactions of aluminum and silicon carbide changed the rate so fast that it was difficult to distinguish their kinetics. The density of the sample was in the range of 4.2 - 5.2 g cm^3. The differences in the density of the samples may be explained with the effect of temperatures and reaction times. The results indicate that higher reaction temperature and longer waiting time led to the higher density of the products. The difference in the particle size scan be explained with the effect of reaction temperatures and times that resulted in the agglomeration of the sample. However, there was a uniform particle distribution in the product. The mean particle sizes of the powder were in the range of 20-30µm for alumina and 10-25µm for titanium carbide.

The non-isothermal aluminothermic reduction-carburizing of the mixture of zircon, aluminum and carbon powders was investigated using TGA in the range from room temperature to 1400 °C. The weight loss of the mixture is shown in Figure 6 between these temperature ranges. It was observed that the zircon started to lose weight by reacting with molten aluminum at temperature below the melting point of aluminum content and a

final weight loss was approximately 25% at 1400 °C. According to the slope of the TG curve, the weight loss can be divided into six stages which were presented as follows

1. Stage: 25-200 °C,
2. Stage: 200-400°C,
3. Stage: 400-1950°C,
4. Stage: 950-1100°C,
5. Stage: 1100-1300°C,
6. Stage: 1300°C -above

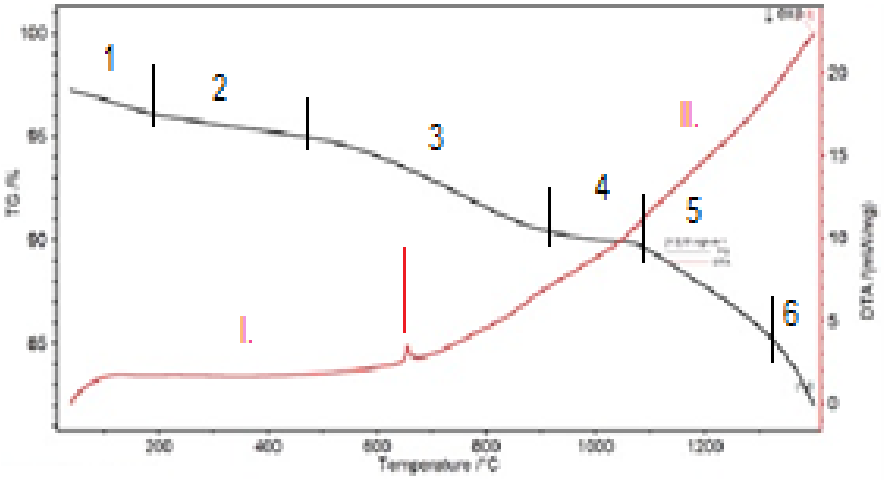

Figure 6. TG/DTA curves of the starting mixture

It was observed that approximately 25% of the weight of the starting sample was lost up to 1400 °C. There is a slow and sharp line on TG curve which corresponds to the removable part of the oxygen in the samples. The reaction among $SiZrO_4$, Al and C in the initial composition started at a temperature below the melting point of Al yielding the reaction products.

DTA curve of the sample is also shown in Figure 6 as a red line. It can be divided into two zones: the first one is up to melting point of metallic content and the second one is above the melting point of aluminum. The first exothermic reaction corresponds to the melting point of aluminum content, which is clear on the curve. The second one starts at this temperature and continues up to 1500 °C, which seems to be uncompleted huge exothermic peak in the mixture.

Solution-precipitation reaction sequences can be considered for the reaction mechanism of the formation of carbide powders from aluminothermic process. As described in another study [20], zircon is dissolved in the molten aluminum and it is followed by the formation of reaction products such as nitrides and carbides in the molten. The aluminothermic reduction and carburization of zircon is a complex procedure that can be divided into four stages:

1-from solid to liquid stage by melting the aluminum content,
2-decomposition of zircon,
3-aluminothermic reduction of silica and formation of SiC/Al_2O_3,
4-conversion of m→t ZrO_2, aluminothermic reduction of zirconia and formation of ZrC/Al_2O_3.

The produced powder has the composition of silicon carbide, zirconium carbide and alumina. These compounds are commercially the most important ceramic powders. The sample has very good specifications and characteristics for further applications and final use. The studies related to sintering composite powder and their mechanical properties are also in progress.

4. Discussion and Conclusion

It is believed that the composite materials will attract a great deal of attention in engineering ceramics in future. A composite based on ZrC-SiC can be a good candidate and compound for industrial applications. From this point of view, Zr-Si carbides can be prepared by the conventional ZrC/SiC production method under laboratory conditions by using aluminothermic reduction process.

It has been shown that the aluminothermic reduction and carburization of zircon can be used for the production of silicon-zirconium carbide compounds. Under the experimental conditions, there were a number of different crystalline phases such as SiC, ZrC, alumina, m-ZrO_2, t-ZrO_2 depending on the reaction temperature and time. According to the results of this study, it was determined that before any reduction process, decomposition of zircon occurred simultaneously with the reduction of silica to carbide phase. It was also determined that the resulting microstructure was consistent with a mechanism in which dissolution of zircon in the molten metal at the reaction temperatures led to formation of Si-Zr carbide phases. As a result of this study, it is suggested that further studies must be carried out for determining the mechanical properties of the composite powder.

Acknowledgements

This study was supported by the Scientific Research Project Unit of Sakarya University under the project no: 2011-50-01-055.

References

Abdelkader AM, Daher A. (2008) Novel decomposition method for zircon. J. Alloys Compd. 460:577-580.

Atasoy A. (2007) The growth and the reaction mechanism of Si_3N_4powder from silica. Mat. Sci. Forum. 554:157-162.

Atasoy A, Tümer M. (2009) Sinterability of silicon nitride powder produced by the CRN process. Solid State Phenomena. 147:896-901.

Bharat PD, P et al. (2003) Novel microwave route for the preparation of ZrC-SiC composite. J. Solid State Chem. 173:196-202.

Cho KH, et al. (2008) The size effect of zircon particles on the friction characteristic of brake lining materials. Wear, 264:291-297.

Das K, Bandyapadhay TK. (2004) Synthesis and characterization of ZrC reinforced iron based composite. Mat. Sci. Eng. 379:983-991.

Evans AG. (1990) Perspective on the development of high toughness ceramic. J. Am. Ceram. Soc. 73:187-194.

Garrido L B. (2001) Zircon based ceramic by colloidal processing. Ceram. Int. 27:491-502.

Habashi F. (1986) Principles of Extractive Metallurgy, New York, Gordon and Breach, v 3, 19

Kotic ZG. (2001) Optimal thermal plasma process for ZrC powder production from zircon concentrates. Ceram Int. 27:47-557.

Licheri R, et al. (2009) Spark plasma sintering of ZrB_2- and HfB_2-based Ultra High Temperature Ceramics prepared by SHS. Int. J. Self-Propag. High-Temp. Synth. 18:15-24

Mariappan L, *et al. (2002)* In situ synthesis of Al_2O_3-ZrO_2-SiCW ceramic matrix composites by carbothermal reduction of natural silicates. *Mat. Chem. and Physics. 75:284-290.*

Mazzoni AD, Aglietti EF. (1998) SiC-Si_3N_4 materials by nitriding of SiC and talc. Ceram Int. 24:327-332.
Merzhanov AG. (1995) History and development in SHS. Ceram. Int. 21:371-379.

Moore J, Feng H. (1995) Combustion synthesis of advanced materials. Prog. Mat. Sci. 39:243-273.

Panda PK, et al. (1999) Effect of various reaction parameters on carbo thermal reduction of kaolinite. Ceram Int. 25: 467-452.

Sorell C. (1983) Silicon nitride and related nitrogen ceramics. J Aust Ceram Soc. 19-2:48-67.

Tsuchida T, Yamamoto S. (2007) Spark plasma sintering of ZrB_2-ZrC powder mixtures synthesized by MA-SHS in air. J. Mat. Sci. 42: 772-778.
Toth LE. (1971) Refractory Materials, V7, Transition Metal Carbides, Academic Press, New York, 6-9

Umebayashi S, Kabayashi K. (1977) Direct preparation of dense Si-Al-O composites from silica and aluminium powders. Am. Ceram. Soc. Bull. 56: 578-579.

Zender H, et al. (1990) ZrO_2 materials for application in the ceramic industry. Ceram. Int. 39:33-39.

Zhe X, et al. (2005) Aluminothermic reduction of zirconia. J. Eur. Ceram. Soc. 25:695-702.

International Conference on Science and Technology

ICONST 2018

5-9 September 2018 Prizren - KOSOVO

Determination of Bicycle Routes in the Aspect of Landscape Planning in Antalya

Sibel Mansuroglu[1]*, Veysel Dag[2]

Abstract: Transportation facilities related to the use of non-motorized vehicles are developing in the world in recent years. Bicycles provide many economic and ecological benefits to society and individuals compared to other means of transportation. It is spreading the use of bicycles in short distances as being healthier, more economical and safer than motor vehicles. However, the use of bicycles is more limited in countries there is not enough infrastructure. Increasing transportation problems, short time proposals for solutions and increasing environmental problems and economic losses in the national dimension increase the need to work towards the expansion of bicycle transportation in our cities. The aim of this study is to determine the conditions of bicycle transportation in Antalya and to emphasize the importance of landscape planning approach

In cities such as Antalya, urbanization and motor vehicles are concentrated in certain centers. The research area is Antalya city center and have completed both urban development (Konyaalti, Muratpasa, Kepez) and still maintain rural characteristics (Dosemealti and Aksu) districts. The study consists of three stages. In the first stage, existing bicycle routes in the city of Antalya were examined and evaluated on the basis of international standards. In the second stage, natural features of the city center of Antalya (geology, geomorphology, soil, hydrology, climate, vegetation cover) were determined. At the last stage, the planning of bicycle routes in the city revealed the place and the importance of landscape planning, which is a holistic planning approach considering the natural, cultural and social characteristics of the city.

In Antalya, where the relation of existing bicycle routes is not good, the factors which affect bicycle usage in general were explained. The results were evaluated within the context of landscape planning principles. In Antalya, which is a tourism city, bicycle routes to be determined by landscape planning principles are considered from the point of view of tourism and the contributions to the city are emphasized.

As a result of the climate and topographical conditions of Antalya, bicycle is a suitable city for use as a means of transportation in the city. It was also emphasized that the use of bicycles in the city would be beneficial in terms of energy saving and prevention or reduction of some environmental problems and would contribute positively to the image of the city.

Keywords: Bicycle routes, Landscape planning, Antalya.

Acknowledgement: This study was supported by the Administration Unit of Scientific Research Projects of Akdeniz University (Project No: FBA-2018-3316).

[1]Akdeniz University, Faculty of Architecture, 07058, Antalya, TURKEY
[2]Akdeniz University, Faculty of Architecture, 07058, Antalya, TURKEY
*Corresponding author: smansur@akdeniz.edu.tr

International Conference on Science and Technology

ICONST 2018

5-9 September 2018 Prizren - KOSOVO

Evaluation of Landscape Potential of Tunceli/Ovacik District for Nature Conservation

Sibel Mansuroglu[1]*, Veysel Dag[2]

Abstract: Rapid population growth in recent years and the resulting urbanization have led to the loss of important habitats in urban areas. This change often leads to problems such as degradation of ecosystems. The destruction of basic ecological values is a barrier to the preservation and development of natural areas. It is important to protect natural/semi-natural areas for protection, this situation also contributes to the sustainability of nature and environmental protection . In this study, landscape features in Ovacik district were examined and values related to area and environment were evaluated in terms of nature conservation.
Ovacik district, the largest town of Tunceli, is located in the Eastern Anatolian, is the main material of this study. The study consists of three stages. In the first stage, is the literature survey on the study field and the subject. The historical, socio-demographic, natural and landscape characteristics of the area were determined. In the second stage, the natural values of the Ovacik have been revealed through ecologically important biotopes. At this stage, characteristic plant species, which represent ecological important biotopes have been identified, ecological important biotopes classified, mapping on Google Earth (2017). In the final stage of the study, the characteristics of the Ovacik were evaluated and a conclusion was reached regarding of the best protection status in terms of nature protection criteria.
There is no settlement, industry, transportation etc. that will negatively affect nature in the region. Due to the lack of population density and the lack of use of pastures and forests for security reasons, the appropriateness of organic farming for the area, the potential for pasture for livestock, the presence of all kinds of natural agricultural and animal products peculiar, experience and desire of local people to live together with nature, the potential for rural tourism and diversity of water resources, brings the existence of landscape into dominant position.
Protected areas created with fragmented understanding of Ovacık and its environs are not enough to protect their natural values. There is a need for a holistic understanding in which the region is treated holistically and the protection and targeting to protect it with the current natural situation can be done with international supports. More detailed work should be done in this regard. As a result of this study, where the natural, cultural and socio-economic characteristics of the region are evaluated, Ovacık and its surroundings are the result of the Biosphere Reserve Area.

Keywords: Landscape potential, Biotope mapping, Nature conservation, Tunceli/Ovacık

[1]Akdeniz University, Faculty of Architecture, 07058, Antalya, TURKEY
[2]Akdeniz University, Faculty of Architecture, 07058, Antalya, TURKEY
*Corresponding author: smansur@akdeniz.edu.tr

International Conference on Science and Technology

ICONST 2018

5-9 September 2018 Prizren - KOSOVO

Ophiolitic Nappe Emplacement between Tava Mount and Mount Murat (Kütahya)

Ali Kamil Yüksel[1]*, Meral Yılmaz[2]

Abstract: The studied area, composed of metamorphic rocks, carbonates, ophiolitic rocks and Neogen aged sedimentary, volcanic and plutonic rocks, is located in between Kütahya and Uşak in western Anatolia. The stratigraphically lowest part of the studied area is named as İkibaşlı Formation and it consists of Triassic metamorphic rocks and marble lenses. Metamorphic rocks of İkibaşlı Formation are composed of chloritoid schist, biotite-sericite schist, chlorite-sericite schist and sericite-quartz schist. Çiçeklikaya Formation, composed of Jurassic dolomitic limestones, conformably overlies İkibaşlı Formation. All these Mesozoic units are tectonically overthrusted by the ophiolitic nappe with a low-angle. Neotethyan ophiolitic rocks are represented by ultramafic rocks and a melange (volcanic-sedimantary rocks) in the study area. The ultramafic rocks contain serpentinized harzburgite and gabro. Emplacement of the ophiolites accompanied by the magmatism in the field. General trend of the all kind of lineations in the İkibaşlı Formation is NE-SW. This NE-SW trend suggests the ophiolite emplacement direction. S-shaped intrafolial fold and Z-shaped kink band were defined between Tava mount and mount Murat. These S shaped intrafolial fold and Z-shaped kink band structures also show top-to-the-northeast movement of the ophiolitic nappe during the tectonic transport. Asymmetric sigmoids in the outcrops and in the oriented thin sections are used for determining the sense of movement of the tectonic slices. These quartz sigmoids indicate top-to-the-NE sense of shear also. The shear band cleavages (S/C') parallel to the stretching lineation and perpendicular to the foliation indicates top-to-the-NE sense of shear. As a result, structural analysis in the study area between the Tava mount and mount Murat indicate top-to-the NE movement of the ophiolite emplacement.

Keywords: Ophiolite emplacement, Kinematic indicators, Tava mount, İkibaşlı Formation

Acknowledgement: This research has been supported by Balıkesir University Scientific Research Projects. Project Number: 2017/039

[1]Balıkesir University, Faculty of Engineering, Department of Geology, 10145, Çağış Campus, Balıkesir, TURKEY
[2]Balıkesir University, Institute of Science and Technology, 10145, Çağış Campus, Balıkesir, TURKEY
*Corresponding author: akyuksel@balikesir.edu.tr

International Conference on Science and Technology

ICONST 2018

5-9 September 2018 Prizren - KOSOVO

Ultrasound-assisted Bleaching of Canola Oil: Compare of Oxidative Effects According to Conventional Method

Necattin Cihat İÇYER[1,2]*, Muhammet Zeki DURAK[1]

Abstract: Edible oils are an indispensable part of daily meal all over the world. They are exposed to various refining process for improve quality. In bleaching phases, color pigments and other trace constituents formed during refining processes are removed by applying acid-activated earths. The aim of this study is to compare the oxidative effect of ultrasound method bleached canola oil with conventional methods.

The neutral canola oil exposed to degumming was obtained from a local oil processing company (Besler Gıda, Turkey). Analytical grade chemicals and bleaching earth were obtained from Merck and Süd Chemie A.G., (Germany). Especially, properties of bleached oil such as free fatty acids (FFAs), peroxides (PV), p-anisidine values (p-AV), conjugated diens and triens, TOTOX and fatty acid compositions have been considered.

The presence of these FFAs is an indication of oil oxidation. There is no significant difference between the ultrasonic and the conventional method samples in terms of FFAs. PVs indicate formations of hydroperoxides due to reaction of oxygen with oil during initial stages of lipid oxidation. The formation of secondary oxidation products is always observed through measurements of (p-AV). While on one hand the amount of PV is decreasing, on the other hand the value of p-AV is increasing. There is a statistically significant difference between ultrasonic and conventional methods. In this direction, TOTOX values are preferred since they represent PV and p-AV values that capture the whole oxidation status of oils. Although the TOTOX value decreased at the beginning, it increased as the contact time increased. The amount of conjugated dienes, which are related to hydro peroxides, decomposition of hydro peroxides may lead to formation of conjugated trienes having three conjugated double bonds. There is a statistically significant difference between the ultrasonic method and the conventional method with respect to conjugated diene and triene values. Bleaching of canola oil under different conditions did not result in a statistically significant difference in fatty acid composition.

The conventional or ultrasonic bleaching processes of oil increase the lipid oxidation depending on the contact time. It can be concluded that there is no meaningful difference between these two methods with respect to oxidative effect.

Keywords: Bleaching, Ultrasound, Oxidation

[1] Yildiz Technical University, Chemical and Metallurgical Engineering Faculty, 34210, Istanbul, Turkey
[2]Mus Alparslan Univesity, Faculty of Engineering and Architecture, 49100, Muş, TURKEY
*Corresponding author: ncicyer@yildiz.edu.tr

International Conference on Science and Technology

ICONST 2018

5-9 September 2018 Prizren - KOSOVO

Antioxidant, Oxidant and Oxidative Stress Levels of *Tricholomopsis rutilans*

Emel DEMİRBAĞ[1]*, Ömer F. ÇOLAK[1], Mustafa SEVİNDİK[2], Celal BAL[3]

Abstract: Mushrooms uses for food and therapeutic purposes since the early days of civilization. In this study, it was aimed to determine the TAS (Total Antioxidant Status), TOS (Total Oxidant Status) and OSI (Oxidative Stress Index) levels of *Tricholomopsis rutilans* (Schaeff.) Singer mushroom collected from Kütahya. After mushroom samples were identified, they were dried at 40 ^{0}C. Dried mushroom samples were pulverized with mechanical shredder and then their extracts removed with ethanol via soxhlet extractor. TAS, TOS and OSI levels of mushroom samples were analyzed by using Rel Assay Diagnostics kits. As a result of this study, it was detected that the TAS level was 1.102±0.062 mmol/L and TOS level was 9.379±0.213 µmol/L. OSI level, defined as the ratio of TOS levels to TAS levels, was 0.856±0.053. TAS of *T. rutilans* mushroom was at the normal levels but TOS was at high levels. OSI level which shows how antioxidant compounds tolerated oxidant compounds was found to be high.
Consequently, it is thought that *T. rutilans* collected from appropriate regions in terms of oxidative stress status can be used as an antioxidant source.

Keywords: *Trichomonas rutilans,* Antioxidant, Oxidant, Oxidative Stress

[1]Süleyman Demirel University, Vocational School of Health Services, Isparta, TURKEY
[2]Akdeniz University, Faculty of Science, Department of Biology, Antalya, TURKEY
[3]Gaziantep University, Oğuzeli Vocational School, Gaziantep, TURKEY
Corresponding author: emeldemirbag@sdu.edu.tr

International Conference on Science and Technology

ICONST 2018

5-9 September 2018 Prizren - KOSOVO

Antioxidant Potential of *Volvopluteus gloicephalus*

Emel DEMİRBAĞ[1]*, Ömer F. ÇOLAK[1], Mustafa SEVİNDİK[2], Celal BAL[3]

Abstract: The mushrooms that are found in many species on the world are also important in terms of being a natural source of medicine in addition to their nutritive properties. Mushrooms are organisms that are cosmopolitan distribution and they have become popular flavor in many countries and societies. In this study, it was aimed to determine the TAS (Total Antioxidant Status), TOS (Total Oxidant Status) and OSI (Oxidative Stress Index) levels of edible mushroom *Volvopluteus gloicephalus* (DC.) Vizzini, Contu & Justo collected from Köyceğiz (Muğla) region. The mushrooms samples collected during field studies were identified and then dried at 40 ^{0}C. Dried mushroom samples were pulverized with mechanical shredder and then their extracts removed with ethanol via soxhlet extractor. TAS, TOS and OSI levels of mushroom samples were analyzed by using Rel Assay Diagnostics kits. As a result of this study, it was detected that the TAS level was 3.716±0.138 mmol/L and TOS level was 2.317±0.069 µmol/L. OSI level, defined as the ratio of TOS levels to TAS levels, was 0.063±0.003. As a result of this study, it is thought that *V. gloicephalus* mushroom may be a natural antioxidant source because its TAS and TOS values are at appropriate levels. Besides the finding that OSI level which shows how antioxidant compounds tolerated oxidant compounds is low indicates that the adverse effects of oxidant compounds in consumption of this mushroom will also be minimal.
Consequently, it is identified that *V. gloicephalus* mushroom can be natural antioxidant source.

Keywords: *Volvopluteus gloicephalus*, Antioxidant, Oxidant, Oxidative Stress

[1]Süleyman Demirel University, Vocational School of Health Services, Isparta, TURKEY
[2]Akdeniz University, Faculty of Science, Department of Biology, Antalya, TURKEY
[3]Gaziantep University, Oğuzeli Vocational School, Gaziantep, TURKEY
Corresponding author: emeldemirbag@sdu.edu.tr

International Conference on Science and Technology

ICONST 2018

5-9 September 2018 Prizren - KOSOVO

Effects of Different Vegetable Oil on Egg Quality

Mustafa Öğütcü[1]*, Nazan Arifoğlu[2], Elif Dincer[2]

Abstract: Egg is not only nutritive food but also functional ingredients of processed food products. Egg is regarded as “reference protein source”, since egg has a digestibility of 95% and is rich in essential amino acids. Moreover, egg is rich in vitamins such as vitamin A, D, E, thiamine, riboflavin, biotin, choline, pantothenic acid and niacin and also is considered as good source of minerals such as sodium, potassium, chlorine, sulphur, magnesium, iron, copper, calcium, phosphorus and zinc. Recent research revealed that as it is for all living creatures, there is a relationship between growth, performance, quality and feeding. In order to egg composition changes, bioactive components, minerals amino acids, essential and vegetable oil are added to supplied fed. The aim of present study was to summarize effects of different vegetable oil addition to poultry feed on egg quality.

Keywords: Egg, Quality, Vegetable Oils, Cholesterol,

[1] Çanakkale Onsekiz Mart University, Faculty of Engineering, 17020, Çanakkale TURKEY
[2] Çanakkale Onsekiz Mart University, Çanakkale Applied Sciences College, 17020, Çanakkale, TURKEY
[3] Çanakkale Onsekiz Mart University, Bayramiç Vocational College, 17100, Çanakkale, Turkey
*Correspondingauthor: mogutcu@comu.edu.tr

International Conference on Science and Technology

ICONST 2018

5-9 September 2018 Prizren - KOSOVO

Sewage Sludge Solar Drying: Experiences from the Application in Polish Climate Conditions

Iwona Klosok-Bazan[1]*, Joanna Boguniewicz-Zablocka[1], Sybilla Raszka[2]

Abstract: Every year large quantities of sewage sludge are produced in wastewater treatment plants (WWTPs), at the same time regulations regarding sludge management increasingly strict. It is compulsory to improve new technical solutions which have to be environmentally friendly, cost-effective, getting an overall cost optimization, easy management and low cost of operation and maintenance as well as safety for operators. Solar sludge drying system meets all these requirements, but Polish climatic conditions are satisfactory for conducting such types of processes.

The effectiveness of drying sewage sludge in a solar dryer, by determining the dry matter content in raw and dryed sludge, has been carry out. In order to compare the dryer's operation, depending on the temperature change, the tests were carried out in two series, the first one was performed in the winter period, the second in the spring. Due to the slow evaporation of water from the sludge, in the winter the sludge sampling was performed every 3 weeks, whereas in the spring at elevated air temperature, sampling took place every 2 weeks. To minimize the measurement errors, each sample has been taken four times.

The results of the research indicate high efficiency of the system operation in the summer, in which the humidity of sewage sludge decrease over 60%. When the average air temperature increases to above 12° C, the drying rate of the sludge increased instantly. Unfortunately, in the winter period the dryer works with low efficiency, from November to March 2017 the sluge reduced its hydration by only 16.04%.

Sewage sludge contains water which can be reduced by common dewatering processes. After typical dewatering processes the sludge can be,wherein the energy that can be obtained from the burning may be equal to these one required to evaporate the water. Therefore, another reduction on water content is required. The use of a solar dryer in Polish conditions allows to obtain the mass contains until 90%, but it is only possible only in the period when the air temperature outside is higher than 12° C.

Keywords: Solar drying, Sludge, Sewage

[1]Opole University of Technology Prószkowska 76 Street 45-758 Opole POLAND
*Corresponding author: i.klosok-bazan@po.opole.pl or klosok@poczta.onet.pl

International Conference on Science and Technology

ICONST 2018

5-9 September 2018 Prizren - KOSOVO

Wastewater Management in Snack Food Industry – Case Study

Iwona Klosok-Bazan[1]*, Joanna Boguniewicz-Zablocka[1], Sybilla Raszka[2]

Abstract: Snack Food Industries manufacture various products therefore generated wastewater, varies on an hourly, daily and seasonal basis. Wastewater resulting from the manufacturing process contains significant amounts of suspended solids, suspended and dissolved organics (measured as COD and BOD_5), fats, oil and occasional high salinity. Those pollution can sediment and deposit in pipes, pumps and tanks at the municipal waste water system. The rules of company in the field of wastewater quality effluent are described in national regulations. The Regulation defines strictly parameters as allowable contamination indicator values in industrial wastewater effluent to wastewater system devices and the method of wastewater amount and quality control. It is therefore advisable to remove such contaminants on site to avoid problems and costly fees and fines.

The paper presents values of basic pollution indicators in wastewater treated using coagulation proces. Efficiency of preliminary treatment of snack food industry wastewater was evaluated. Physical and chemical analyses were conducted to obtain values of basic pollution indicators in total (raw) wastewater discharged from the production lines and pre-treated wastewater discharged into the municipal waste water system. Obtained results were compared with legal requirements.

Raw wastewater from the production lines entering the coagulation tank had very high concentrations of pollutants. The use of coagulation process reduced COD, BOD_5, total solids total suspended solids (TSS) and total nitrogen (TN) by 72, 47, 82 and 45 %, respectively.

Obtained results of wastewater quality discharged by analyzed snack food indudustry plant met most of the standards set for wastewater entering the municipal sewerage system. COD and BOD_5 values for pretreated wastewater only periodically exceeded the permissible values set in the water legal permit. The remaining parameters remained below the acceptable levels. New solutions have been proposed to improve the situation.

Keywords: Wastewater management, Food industry, Coagulation

[1] Opole University of Technology Prószkowska 76 Street 45-758 Opole POLAND
*Corresponding author: i.klosok-bazan@po.opole.pl or klosok@poczta.onet.pl

International Conference on Science and Technology

ICONST 2018

5-9 September 2018 Prizren - KOSOVO

Molecular Structural Analysıs of Cellulose Trıasetat II and Interactıon wıth Aspergıllus Niger Cellulase Enzyme

A. Demet DEMIRAG [1], Sefa CELIK [2], Aysen E. OZEL[1], Sevım AKYUZ[3]

Abstract: People have been forced to seek alternative sources because of the health problems created by the petrochemical products used in all areas of human life and the environmental problems they have caused because they remain unbroken for many years in the nature. CTA II is a cellulose triacetate polymorphism that reflects reversible and non-reversible crystal transformations. The transformation from Cellulose I to CTA II and from CTA I to CTA II is the case. The determination of the structure of this molecule is very important in terms of structure-activity relationship. Nighty two percent of the hydroxyl groups of the CTA II molecule were acetylated.

In this study, molecular structure analysis of Cellulose Triacetate II (CTA II) molecule obtained from cellulosic and acetate, which is the most usable material in nature, has been analyzed. The most stable molecular geometry of the cellulose triacetate II molecule was modeled by Density Function Theory using the Gaussian05 program. Scaled vibration wavenumbers of this optimized geometry are calculated using the Molvib program. These obtained wavenumbers are transformed into the theoretical spectrum in the Lorentzian distribution.

Aspergillus niger cellulase enzyme is an important enzyme that is active in cellulose digestion. Using the molecular docking method based on key-lock theory, the region with the highest binding activity of the enzyme and the groups that interacted at the molecular level were identified as a result of the molecular interaction between Aspergillus niger cellulase enzyme-cellulose triacetate II (CTA II).
Cellulose is an abundant and renewable biological source on the earth. Today, with the decline of organic food, these innovative studies will makes cellulose an important raw material for food, energy, fuel, drug design and industry in the future.

Keywords: Cellulose triasetat II , Molecular docking

[1] Istanbul University, Faculty of Science, Department of Physics, Vezneciler, 34134, Istanbul,
e-mail: dmtdemirag@gmail.com, aozel@istanbul.edu.tr
[2]Istanbul University-Cerrahpasa, Faculty of Engineering, Department of Electrical and Electronic Engineering, 34320 – Avcılar, İstanbul, Turkey
e-mail: scelik@istanbul.edu.tr
[3]Istanbul Kültür University, Faculty of Science and Letters , Department of Physics, 34156, Bakırköy-Istanbul,Turkey
e-mail: s.akyuz@iku.edu.tr

International Conference on Science and Technology

ICONST 2018

5-9 September 2018 Prizren - KOSOVO

Development of Chitosan Nanoparticles Loaded with Carvacrol Using Ionic Gelation Method by Central Composite Design

Muhammet Ali Çakır[1]*, Fatih Törnük[2]

Abstract: Bioactive compounds have take attention in recent years due to their health benefits and increasing negative perception against use of artificial food additives. Essential oils are obtained from aromatic plants and spices. For decades their antibacterial and antifungal properties have been known. Those functional properties of essential oil are mainly attributed to bioactive compounds such as carvacrol and thymol available in the volatile essential oil composition. Use of essential oils in food application is limited because of their weak solubility in water. Therefore, encapsulation is a productive method to increase application potential of essential oils by allowing them spread in water.

Chitosan (low molecul weight) from crab shells (85% deacylated), sodium tripolyphosphate (STPP, technical grade) and acetic acid (>99.7% purity) was purchased from Sigma Aldrich (Germany). Tween 80 and carvacrol (%98) were provided from Merck (Germany).

The aim of this study was to produce recent water-soluble and thermally stable chitosan nanoparticles loaded with level (0.5%) of carvacrol essential oil using ionic gelation method and to determine their characteristic properties. The response surface method (RSM) face centered central composite design (CCD) is created and parameters are optimized responses. Nanoparticles with diameters between from 350 nm to 400 nm were obtained at pH level of 4.6. Zeta potential values of these were found to be positive (+20.54 to +25.12 mV). Encapsulation efficiency was in the range of 30-40%.

The results of this study indicated that carvacrol could be encapsulated with chitosan to increase its use for food applications. In conclusion, carvacrol loaded chitosan nanoparticules that were highly adapted to environmental factors such as high pH and high temperature and with high bioactive properties were successfully produced useful for food processing and packaging applications.

Keywords: Essential oils, İonic gelation method, Carvacrol, chitosan

[1]Namık Kemal University, School of Health, 39100, Kırklareli, TURKEY
[2] Yildiz Technical University, Chemical and Metallurgical Engineering Faculty, 34210, Istanbul, Turkey
*Corresponding author: m.ali.cakir@klu.edu.tr

International Conference on Science and Technology

ICONST 2018

5-9 September 2018 Prizren - KOSOVO

Effects of Chitosan Applications on Melon Seedlings Quality and Growth

Nuray Akbudak[1]*, Melis Ergi[2]

Abstract: Chitosan is a modified and natural carbohydrate polymer which is obtained from the partial deacetylation of chitin and includes the copolymer of glucosamine and N-acetyl glucosamine. Chitosan has been used in seed as fertilizer and in controlled agrochemical release, to increase plant productivity, to protect plants against microorganisms and to stimulate plant growth.

This study was investigated to effects of chitosan applications on seedling quality and seedling growth on the melon plant. Chitosan was applied to seed (10 mg L-1) and foliage (0,60 mg L-1) to study effects on induced plant growth and seedling quality in melon (Cucumis melo), cvs. Kırkağaç 637 and Akhisar. Growth parameters of seedling (Radicle length, radicle fresh and dry weight, hypocotyl length, hypocotyl fresh and dry weight, stem diameter, seedling length, number of leaves, leaf relative water content and seedling quality parameters (number of leaves, leaf color, total chlorophyll content) were measured and conducted.

Seed applications were increased hypocotyl fresh weight, radicle dry and fresh weight. No significant increase in leaf number per plant was determined. Seedling length and stem diameter were no affected by the seed and seedling stage chitosan applications. Total chlorophyll content increased with seedling chitosan applications in both cultivar, whereas no difference was found between control and seed chitosan treatments plants. Data further suggest that chitosan has a promotional effect on leaf color of melon seedling.

The results indicated that chitosan solution may have a potential in seedling quality in melon.

Keywords: Chitosan, *Cucumis melo*, Seedling, Plant growth

[1]Uludag University, Faculty of Agriculture, Department of Horticulture,16059, Bursa, TURKEY
[2]Uludag University, Graduate School of Natural and Applied Science, 16059, Bursa, TURKEY
*Corresponding author: nakbudak@uludag.edu.tr

International Conference on Science and Technology

ICONST 2018

5-9 September 2018 Prizren - KOSOVO

Effects of Zinc Oxide Nanoparticles Supplementation on the Growth Performance of Holstein Calves during Preweaning Period

İsmail ÜLGER [1]*, Fatih Doğan KOCA[2], Mahmut KALİBER[1]

Abstract: Nanoparticles, small than 100 nm, have unique properties such as antimicrobial, antifungal, anticancer etc. In this study, the effects of green synthesis zinc oxide nanoparticles (ZnO-NPs) on the growth performance of Holstein calves during pre-weaning period were examined.

For this purpose, a total of 30 male calves were allocated to 3 equal groups and colostrum was supplied to experimental calves for 3 days after the birth. After 3 days, the live weights of the calves were recorded and fresh milk was offered to control group calves, while treatment groups were consuming 20 mg/kg ZnO-NPs and 40 mg/kg ZnO-NPs supplemented milk daily in 2 meals till weaning. All calves consumed a total of 212 liters milk throughout 8 weeks of milk-feeding period. Calves were housed in individual pens throughout the experiment and clean drinking water, calf starter feed and dry alfalfa hay were supplied ad libitum in addition to milk from the 7th day of birth till weaning. Calves were weighed in every two weeks with an electronic scale to calculate live weight gains, also feeds (calf starter and alfalfa hay) were weighed weekly to determine feed consumption of the calves.

Higher weaning live weight values were observed in ZnO-NPs supplemented milk consuming calves than the control group ($P<0.05$) and, parallel to this, ZnO-NPs supplementation increased daily live weight gain of experimental calves ($P<0.05$). Feed consumption of ZnO-NPs supplemented milk consuming calves was 2% higher than control calves ($P>0.05$), but still better feed conversion ratios were observed from ZnO-NPs supplemented milk consuming calves ($P<0.05$).

Finally, it can be concluded that ZnO-NPs supplementation to fresh milk during preweaning period improved the growth performance according to weaning live weights, daily live weight gains and feed conversion ratios of the experimental calves.

Keywords: Calf, Nanoparticle, Green synthesis, Zinc oxide, Performance

1Erciyes University, Faculty of Agriculture, Department of Animal Science, Kayseri, Turkey
2Erciyes University, Faculty of Veterinary Medicine, Department of Aquatic Animal Diseases, Kayseri, Turkey
*Corresponding Author: i_ulger@hotmail.com

International Conference on Science and Technology

ICONST 2018

5-9 September 2018 Prizren - KOSOVO

Multivariate Statistical Methods for Spatial Characterization of Surface Water Quality

Virgjina Lipoveci[1], Mirjana Čurlin[2*]

Abstract: The aim of this work is focused on spatial water quality classification based on the monitoring dataset for different location. Dataset for spatial classification of surface water consist of physico chemical water quality parameters monitored in monthly periods for seven locations.
For handling the dataset different chemometrics methods were employed, such as basic statistical methods, Pearson`s correlation coefficients, the principal component analysis (PCA) and cluster analysis (CA).
The obtained results show and explain the value movement of quality indicators in relation to the maximum permissible concentration prescribed in the Regulations as well as some significant correlation of individual variables for a specified period.
This study allows drawing out new information from the monitoring datasets such as patterns of similarity between different locations, sesonal behaviour of physico-chemical contents and time trends. The implementation of these analyses is necessary in the preliminary study for water usage and healthcare protection of population in the region.

Keywords: Water quality, Statistical methods, Pearson`s correlations, Cluster analysis (CA), Principal component analysis (PCA).

[1]National Centre of Labour Medicine in Gjakova, Kosovo
[2*]University of Zagreb, Faculty of Food Technology and Biotechnology, Department of Process Engineering, Section for Fundamental of Engineering Pierottijeva 6, 10000 Zagreb
*Corresponding author: mcurlin@pbf.hr

iconst
www.iconst.org

www.iconst.org
info@iconst.org

KUTBİLGE
Association of Academicians
organized by

bilge
sci

http://dergipark.gov.tr/bilgesci
kutbilgescience@gmail.com